

BNL-113876-2017-FORE

Proceedings of RIKEN BNL Research Center Workshop:Saturation: Recent Developments, New Ideas and measurements

T. Lappi, V. Skokov

May 2017

Physics Department

Brookhaven National Laboratory

U.S. Department of Energy

USDOE Office of Science (SC),

USDOE Office of Science (SC), Nuclear Physics (NP) (SC-26)

Notice: This manuscript has been authored by employees of Brookhaven Science Associates, LLC under Contract No. DE-SC0012704 with the U.S. Department of Energy. The publisher by accepting the manuscript for publication acknowledges that the United States Government retains a non-exclusive, paid-up, irrevocable, world-wide license to publish or reproduce the published form of this manuscript, or allow others to do so, for United States Government purposes.

DISCLAIMER

This report was prepared as an account of work sponsored by an agency of the United States Government. Neither the United States Government nor any agency thereof, nor any of their employees, nor any of their contractors, subcontractors, or their employees, makes any warranty, express or implied, or assumes any legal liability or responsibility for the accuracy, completeness, or any third party's use or the results of such use of any information, apparatus, product, or process disclosed, or represents that its use would not infringe privately owned rights. Reference herein to any specific commercial product, process, or service by trade name, trademark, manufacturer, or otherwise, does not necessarily constitute or imply its endorsement, recommendation, or favoring by the United States Government or any agency thereof or its contractors or subcontractors. The views and opinions of authors expressed herein do not necessarily state or reflect those of the United States Government or any agency thereof..

BNL-113876-2017

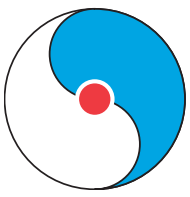
RIKEN/RBRC Workshop

Saturation: Recent Developments, New Ideas and Measurements

April 26-28, 2017

Proceedings of RIKEN BNL Research Center Workshop

Volume 129



RBRC

RIKEN BNL Research Center

Disclaimer

This work was prepared as an account of work sponsored by an agency of the United States Government. Neither the United States Government nor any agency thereof, nor any of their employees, nor any of their contractors, subcontractors or their employees, makes any warranty, express or implied, or assumes any legal liability or responsibility for the accuracy, completeness, or any third party's use or the results of such use of any information, apparatus, product, or process disclosed, or represents that its use would not infringe privately owned rights. Reference herein to any specific commercial product, process, or service by trade name, trademark, manufacturer, or otherwise, does not necessarily constitute or imply its endorsement, recommendation, or favoring by the United States Government or any agency thereof or its contractors or subcontractors. The views and opinions of authors expressed herein do not necessarily state or reflect those of the United States Government or any agency thereof.

Notice: This manuscript has been authored by employees of Brookhaven Science Associates, LLC under Contract No. DE-SC0012704 with the U.S. Department of Energy. The publisher by accepting the manuscript for publication acknowledges that the United States Government retains a non-exclusive, paid-up, irrevocable, world-wide license to publish or reproduce the published form of this manuscript, or allow others to do so, for United States Government purposes.

Preface to the Series

The RIKEN BNL Research Center (RBRC) was established in April 1997 at Brookhaven National Laboratory*. It is funded by RIKEN, "Rikagaku Kenkyusho", of Japan and the U. S. Department of Energy's Office of Science. The Memorandum of Understanding between RIKEN and BNL, initiated in 1997, has been renewed in 2002, 2007 and 2012. The Center is dedicated to the study of strong interactions, including spin physics, lattice QCD, and RHIC physics through the nurturing of a new generation of young physicists.

The RBRC has theory, lattice gauge computing and experimental components. In experimental physics RBRC is presently conducting R&D for a silicon tracking system to be used in sPHENIX a major upgrade to PHENIX for the completion of the RHIC program in 5 or 6 years. The RBRC experimental group is led by Yasuyuki Akiba and Abhay Deshpande. In theoretical physics RBRC is exploring collaboration in chiral condensed matter with BNL's Condensed Matter and Material Sciences Department and RIKEN's Center for Emergent Matter Science. RBRC theory group is led by Dmitri Kharzeev and Robert Pisarski. In computational physics RBRC is developing, in collaboration with Columbia University, BNL and others, next-generation computing architecture for next-generation lattice gauge calculations and is led by Taku Izubuchi.

RBRC comprise a total of 41 researchers. Positions include the following: full time RBRC Fellow, half-time RHIC Physics Fellow, and full-time post-doctoral Research Associate. The RHIC Physics Fellows hold joint appointments with RBRC and other institutions and have tenure track positions at their respective institutions. To date, RBRC has over 111 graduates (Fellows and Post-docs) of whom approximately 74 have already attained tenure positions at major institutions worldwide.

Beginning in 2001 the RIKEN Spin Program (RSP) category was implemented at RBRC. RSP appointments are joint RBRC-RIKEN positions in theory and experiment, including: RSP Researchers, RSP Research Associates, and Young Researchers, who are mentored by senior RBRC Scientists. A number of RIKEN Jr. Research Associates and Visiting Scientists also contribute to the physics program at the Center.

RBRC has an active workshop program on strong interaction physics with each workshop focused on a specific physics problem. For most of these workshops all the talks are made available on the RBRC website. To date there are over 137 proceedings volumes available.

In 2017 RBRC cerebrates its 20th anniversary since its inauguration in 1997. This is also the year of the 100th anniversary of RIKEN. RBRC is well matured and moves into the new generation with dismantling of the PHENIX detector and construction of the new sPHENIX detector at RHIC. We are on track with growth plans in place. On April 1st 2017, Hideto En'yo, Director of RIKEN Nishina Center for Accelerator-Based Science, was named Acting Director of the RBRC, preceded by Samuel Aronson, Nicholas Samios and T.D. Lee.

Hideto En'yo, Director
May 2017

*Work performed under the auspices of U.S.D.O.E. Contract No. DE-SC0012704.

Introduction

The focus of this workshop is to discuss all aspects of gluon saturation, encompassing theoretical advances, phenomenological studies, experimental status, and future prospects at current and planned facilities.

In recent years, major advances have been made in our understanding of the small x physics and gluon saturation. Extensive theoretical research has led to a significant development in such fields as: gluon correlations in the Colored Glass Condensate and Glasma; low x evolution beyond leading order; hadron production at NLO and forward physics in dA/pA; first analytical results on saturation corrections for nucleus-nucleus collisions; the helicity evolution towards small x and theoretical understanding of the proton spin; hadron wave function at small x and fluctuations of multiplicity; TMD evolution from small to moderate x; the structure of chromo-magnetic fields and topological transitions in the Glasma; and thermalization from first principles of QCD.

An active study of these theoretical puzzles induced parallel research directions into many phenomenological issues including di-photon and di-hadron correlations, heavy meson production in dA/pA, initial azimuthal anisotropy and long range correlations (the so-called ridge), the non-equilibrium chiral magnetic effect, etc. At the same time, there are many striking experimental results obtained recently that are to be explained. For example, measurements in collisions of small systems at RHIC and LHC showed that the emerging pattern of the long-range azimuthal correlations is similar to the one in AA collisions.

A major goal of the workshop is to discuss theory, phenomenology and experimental issues in the context of the future facility — the Electron Ion Collider (EIC). This high precision experiment will give us the possibility to study nuclear matter at high energy and reveal saturation effects with a high level of accuracy.

Specific topics we plan to address include:

- Small x evolution and hadron production in NLO
- Spin at small x
- TMD evolution
- Small-x physics in e+p and e+A DIS
- Heavy meson production in pA
- Topological transitions and thermalization in the early stages

Contents

Presentations:

I. Balitsky.....*Higher-twist corrections to gluon TMD factorization*

G. Beuf .....*Full NLO corrections for DIS structure functions in the dipole factorization formalism*

S. Caron-Huot .....*Linear and nonlinear small-x evolution in perturbation theory*

S. Caron-Huot .....*Nuclear Theory/RIKEN Seminar: Analyticity in Spin and Causality in Conformal Theories*

G. Chirilli.....*Rapidity factorization of high-energy scattering processes at NLO*

A. Dumitru.....*Fluctuations of the gluon distribution at small-x: correlation of multiplicity and transverse momentum fluctuations*

K. Dusling.....*Collectivity from the initial state: four-particle correlations in proton-nucleus collisions*

K. Fukushima .....*Particle production in CGC*

E. Iancu .....*Particle production in proton-nucleus collisions beyond leading order*

J. Jia .....*Flow in small systems*

D. Kharzeev.....*Deep inelastic scattering as a probe of entanglement*

Y. Kovchegov.....*Small-x asymptotics of the quark helicity distribution*

A. Kovner.....*Exploring correlations in the CGC wave function: odd azimuthal anisotropy*

M. Lublinsky .....*From light-cone wave function to NLO JIMWLK*

D. Neill .....*Finding small-x like evolution in QCD final state dynamics: the problem of non-global logarithms*

P. Newman.....*Low-x physics and saturation studies for the Large Hadron Electron Collider*

A. Ogawa.....*Polarized p+A physics at forward rapidity at STAR*

R. Paatelainen .....*Toward higher-order accuracy in LCPT*

T. Peitzmann.....*Opportunities for forward photon measurements in ALICE at the LHC*

A. Rezaeian.....*Elliptic flow from color-dipole orientation in pp and pA collisions*

C. Royon.....*Forward jets at HERA and Mueller-Navelet and jet gap jet events at Tevatron and LHC*

B. Schenke.....*Subnucleonic fluctuations, diffraction, and small-x evolution*

S. Schlichting.....*Event-by-event pre-equilibrium dynamics — from gluon saturation toward the onset of hydrodynamics*

M. Sievert.....*Quark helicity evolution at small-x*

A. Stasto.....*Low-x physics and prompt neutrino production*

D. Tapia-Takaki.....*Studying gluon saturation and nuclear effects using forward heavy-ion probes and UPCs at LHC*

R. Venugopalan .....*Ridge-like correlations in small systems: status and problems*

Agenda

List of Registered Participants

Additional RIKEN BNL Research Center Proceeding Volumes

Presentations

Higher-twist corrections to gluon TMD factorization

I. Balitsky (in collaboration with A. Tarasov)

JLAB & ODU

Saturation 2017 BNL, 27 April 2017

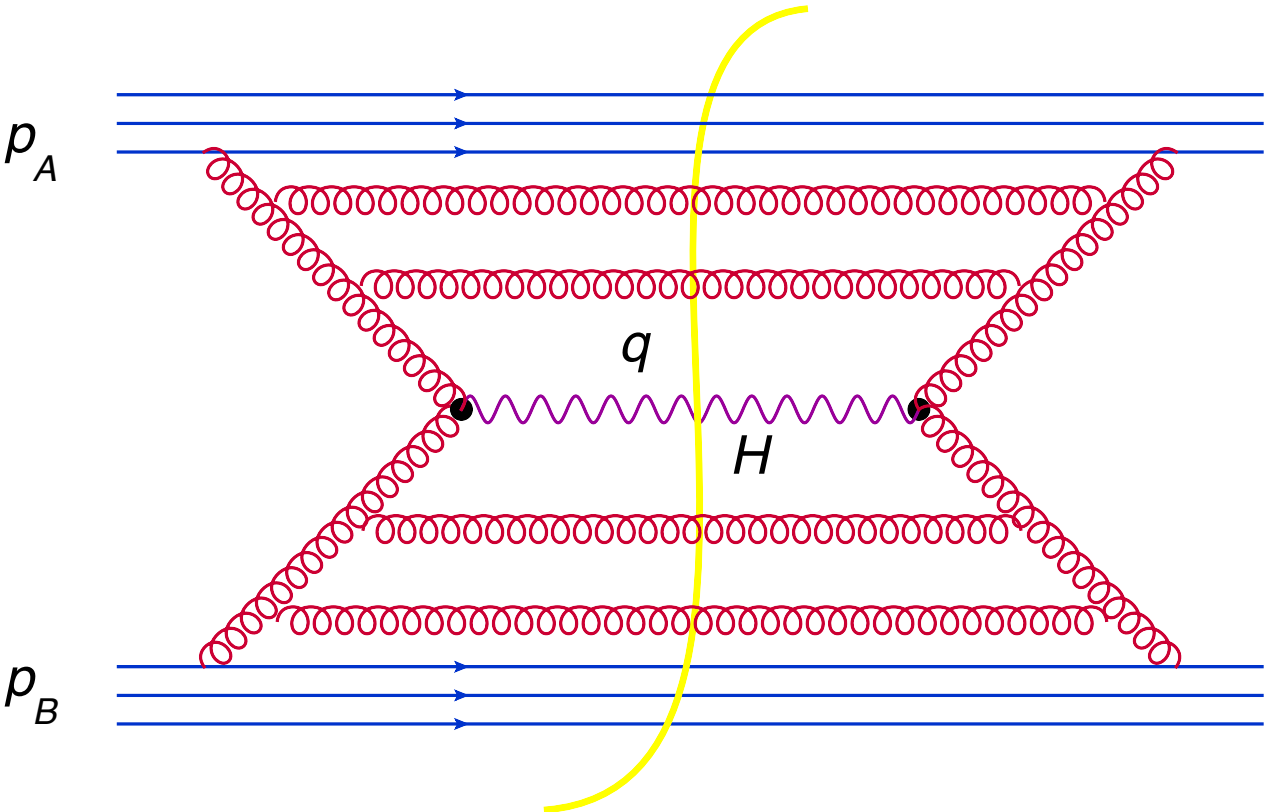
Particle production by gluon fusion in pp scattering

Suppose we produce a scalar particle (e.g. Higgs) in a gluon-gluon fusion.

For simplicity, assume the vertex is local:

$$\mathcal{L}_\Phi \;=\; g_\Phi \int dz\; \Phi(z) F^2(z), \qquad F^2 \equiv F^a_{\mu\nu} F^{\mu\nu}_a$$

.



$$s >> Q^2 >> Q_\perp^2$$

$$q^2 = Q^2 = M_H^2$$

Matrix element between hadron states $\Rightarrow \sum_X = 1$

"Hadronic tensor"

$$W(p_A,p_B,q) \stackrel{\text{def}}{=} \sum_X \int d^4x\, e^{-iqx} \langle p_A,p_B|F^2(x)|X\rangle\langle X|F^2(0)|p_A,p_B\rangle$$
$$= \int d^4x\, e^{-iqx} \langle p_A,p_B|F^2(x)F^2(0)|p_A,p_B\rangle$$

Double functional integral for W

$$W(p_A,p_B,q) = \sum_X \int d^4x\, e^{-iqx} \langle p_A,p_B|F^2(x)|X\rangle\langle X|F^2(0)|p_A,p_B\rangle$$
$$= \lim_{\substack{t_f\to\infty \\ t_i\to-\infty}} \int d^4x\, e^{-iqx} \int^{\tilde{A}(t_f)=A(t_f)} D\tilde{A}_\mu DA_\mu \int^{\tilde{\psi}(t_f)=\psi(t_f)} D\bar{\tilde{\psi}} D\tilde{\psi} D\bar{\psi} D\psi\ \Psi^*_{p_A}(\vec{\tilde{A}}(t_i),\tilde{\psi}(t_i))$$
$$\times\ \Psi^*_{p_B}(\vec{\tilde{A}}(t_i),\tilde{\psi}(t_i)) e^{-iS_{\rm QCD}(\tilde{A},\tilde{\psi})} e^{iS_{\rm QCD}(A,\psi)} \tilde{F}^2(x)F^2(y)\Psi_{p_A}(\vec{A}(t_i),\psi(t_i))\Psi_{p_B}(\vec{A}(t_i),\psi(t_i))$$

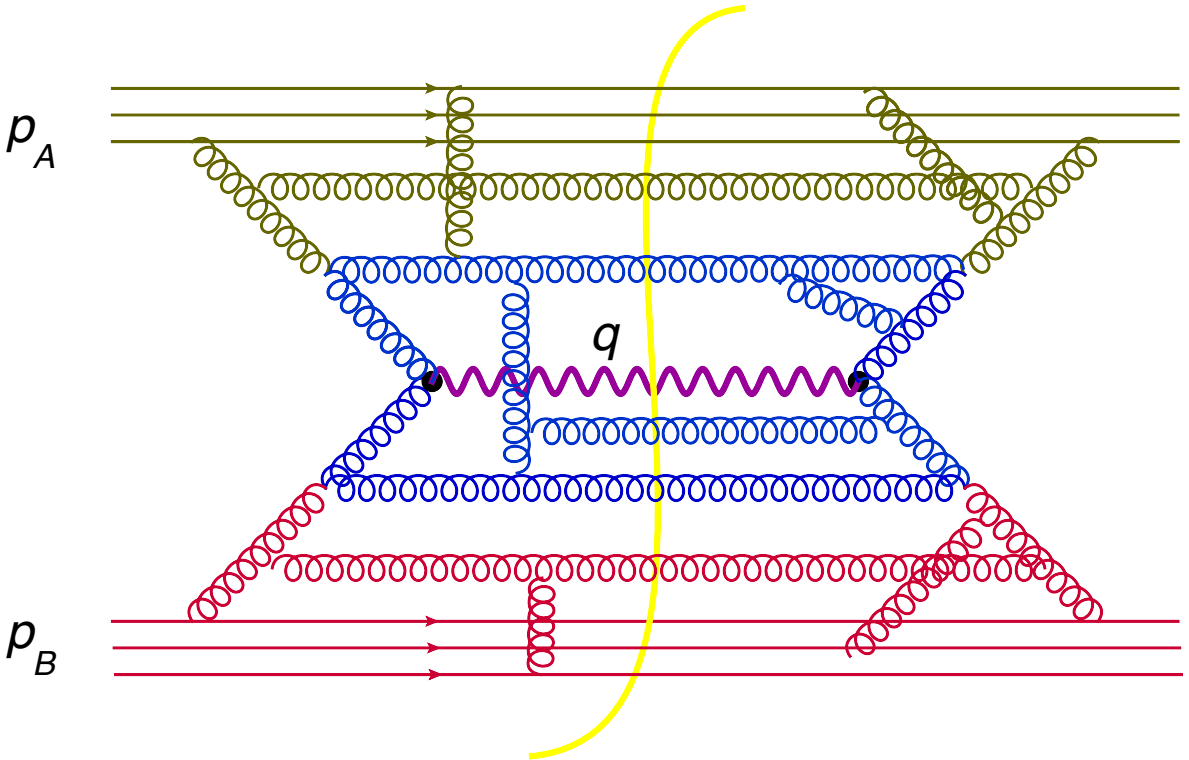
"Left" A,ψ fields correspond to the amplitude $\langle X|F^2(0)|p_A,p_B\rangle$,
"right" fields $\tilde{A},\tilde{\psi}$ correspond to amplitude $\langle p_A,p_B|F^2(x)|X\rangle$
The boundary conditions $\tilde{A}(t_f)=A(t_f)$ and $\tilde{\psi}(t_f)=\psi(t_f)$ reflect the sum over intermediate states X.

Rapidity factorization for particle production

Sudakov variables:

$$p = \alpha p_1 + \beta p_2 + p_\perp, \qquad p_1 \simeq p_A, \quad p_2 \simeq p_B, \quad p_1^2 = p_2^2 = 0$$

$$x_* \equiv p_2 \cdot x = \sqrt{\frac{s}{2}} x^+, \qquad x_\bullet \equiv p_1 \cdot x = \sqrt{\frac{s}{2}} x^-$$



"Projectile'' fields: $|\beta| < b$

"Central'' fields

"Target'' fields: $|\alpha| < a$

We integrate over "central" fields in the background of projectile and target fields.

Rapidity factorization for particle production

After integration over C fields

$$
\begin{aligned}
& W(p_A, p_B, q) \\
&= \int d^4x\, e^{-iqx} \int^{\tilde{A}(t_f)=A(t_f)} D\tilde{A}_\mu DA_\mu \int^{\tilde{\psi}_a(t_f)=\psi_a(t_f)} D\bar{\psi}_a D\psi_a D\bar{\tilde{\psi}}_a D\tilde{\psi}_a \\
&\quad \times e^{-iS_{\rm QCD}(\tilde{A},\tilde{\psi}_a)} e^{iS_{\rm QCD}(A,\psi_a)} \Psi^*_{p_A}(\vec{\tilde{A}}(t_i), \tilde{\psi}_a(t_i)) \Psi_{p_A}(\vec{A}(t_i), \psi(t_i)) \\
&\quad \times \int^{\tilde{B}(t_f)=B(t_f)} D\tilde{B}_\mu DB_\mu \int^{\tilde{\psi}_b(t_f)=\psi_b(t_f)} D\bar{\psi}_b D\psi_b D\bar{\tilde{\psi}}_b D\tilde{\psi}_b \\
&\quad \times e^{-iS_{\rm QCD}(\tilde{B},\tilde{\psi}_b)} e^{iS_{\rm QCD}(B,\psi_b)} \Psi^*_{p_B}(\vec{\tilde{B}}(t_i), \tilde{\psi}_b(t_i)) \Psi_{p_B}(\vec{B}(t_i), \psi_b(t_i)) \\
&\quad \times e^{S_{\rm eff}(U,V,\tilde{U},\tilde{V})} \mathcal{O}(q, x, y; A, \psi_a, \tilde{A}, \tilde{\psi}_a; B, \psi_b, \tilde{B}, \tilde{\psi}_b)
\end{aligned}
$$

$\mathcal{O}$ - sum of the *connected* diagrams for $F^2(x)F^2(0)$ in the background fields

$S_{\rm eff}$ - effective action (sum of disconnected diagrams = $e^{S_{\rm eff}}$).

Approximations for projectile and target fields

At the tree level $\beta = 0$ for $A, \tilde{A}$ fields and $\alpha = 0$ for $B, \tilde{B}$ fields $\Leftrightarrow$
$A = A(x_\bullet, x_\perp),\ \tilde{A} = \tilde{A}(x_\bullet, x_\perp)$ and $B = B(x_*, x_\perp),\ \tilde{B} = \tilde{B}(x_\bullet, x_\perp)$.

NB: because of boundary conditions $\tilde{A}(t_f) = A(t_f)$ and $\tilde{\psi}(t_f) = \psi(t_f)$ for the purpose of calculating the integral over central fields one can set

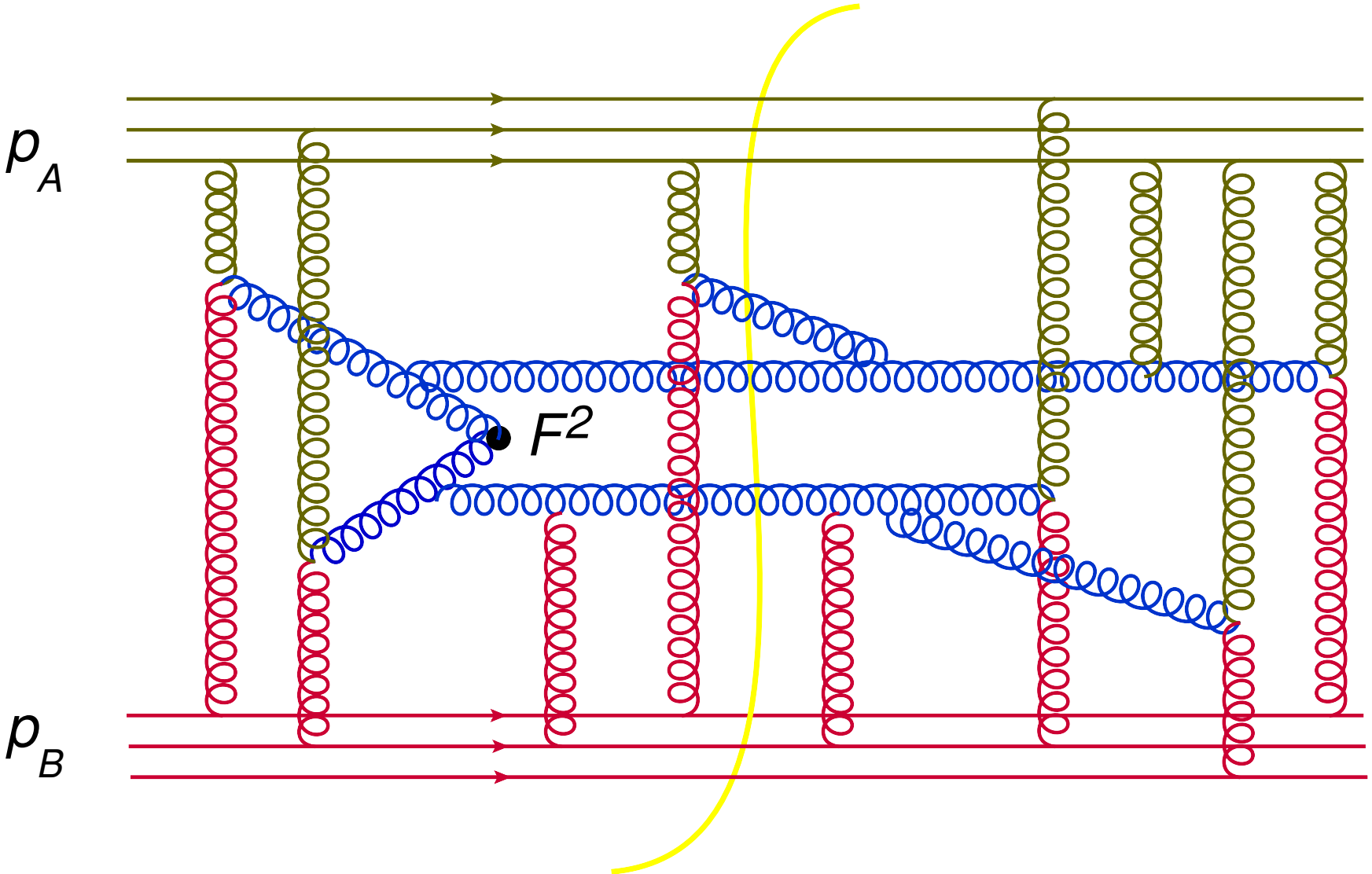
$$A(x_\bullet, x_\perp) = \tilde{A}(x_\bullet, x_\perp), \quad \psi_a(x_\bullet, x_\perp) = \tilde{\psi}_a(x_\bullet, x_\perp)$$

and

$$B(x_*, x_\perp) = \tilde{B}(x_*, x_\perp), \quad \psi_b(x_*, x_\perp) = \tilde{\psi}_b(x_*, x_\perp).$$

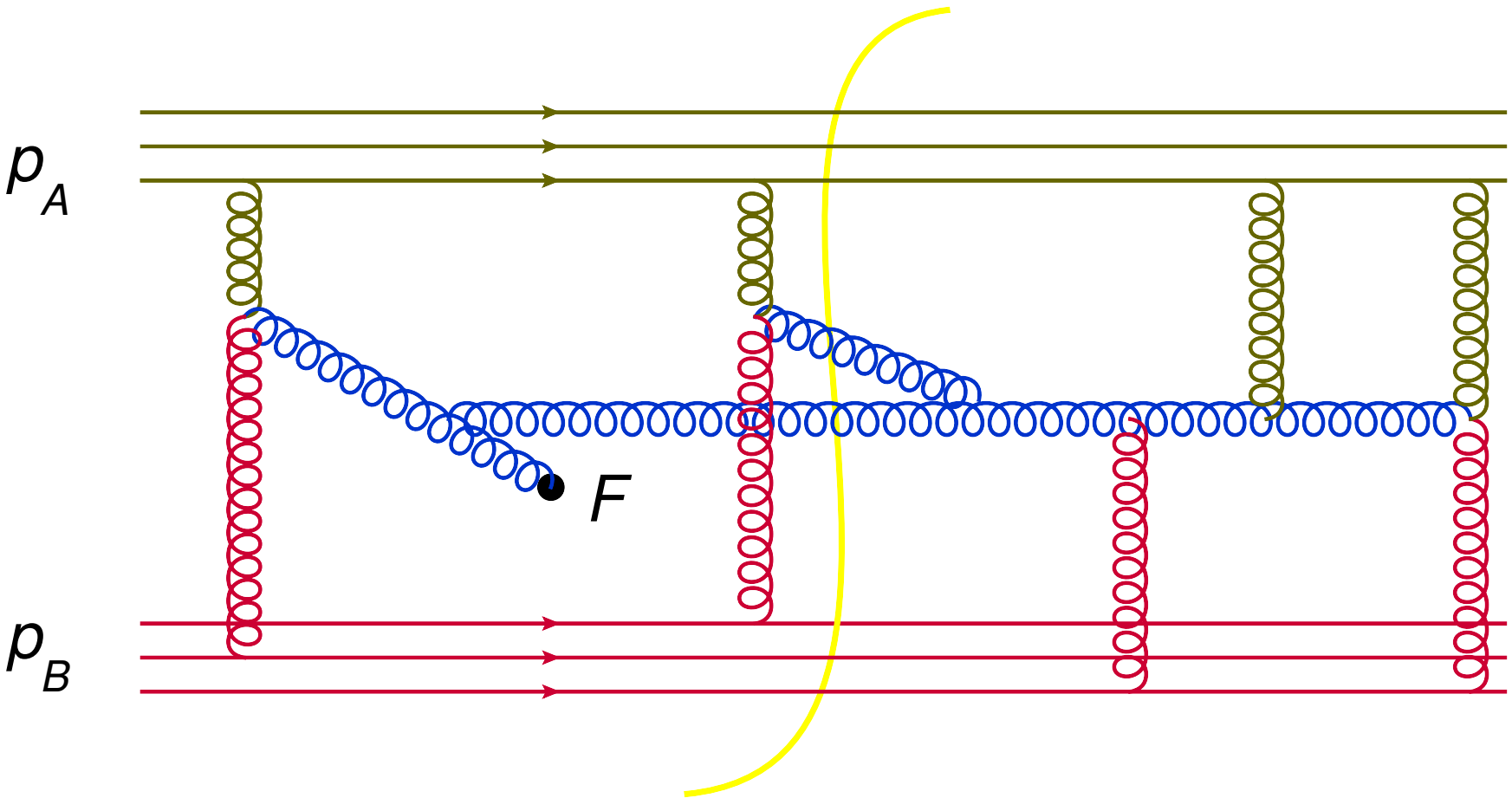
The fields A, ψ and $\tilde{A}, \tilde{\psi}$ do not depend on $x_* \Rightarrow$
if they coincide at $x_* = \infty \Rightarrow$ they coincide everywhere.
Similarly,
B, ψ_b and $\tilde{B}, \tilde{\psi}_b$ do not depend on $x_\bullet \Rightarrow$
if they coincide at $x_\bullet = \infty$ they should be equal.

$F^2_{\mu\nu}(C)$ in the tree approximation



$F_{\mu\nu}(C)$ = sum of tree diagrams in external A and B fields

$F_{\mu\nu}(C)$ in the tree approximation



$F_{\mu\nu}(C)$ = sum of tree diagrams in external $\tilde{A}, A$ and $\tilde{B}, B$ fields with sources $\tilde{J}_\mu = D^\mu F_{\mu\nu}(\tilde{A} + \tilde{B})$ and $J_\mu = D^\mu F_{\mu\nu}(A + B)$

$F_{\mu\nu}(C)$ in the tree approximation

Since $\tilde{A} = A$ and $\tilde{B} = B$ the sources and background fields are the same to the left and to the right of the cut

$\Rightarrow$

$F_{\mu\nu}(C)$ is a sum of diagrams with *retarded* Green functions

(F. Gelis, R. Venugopalan)

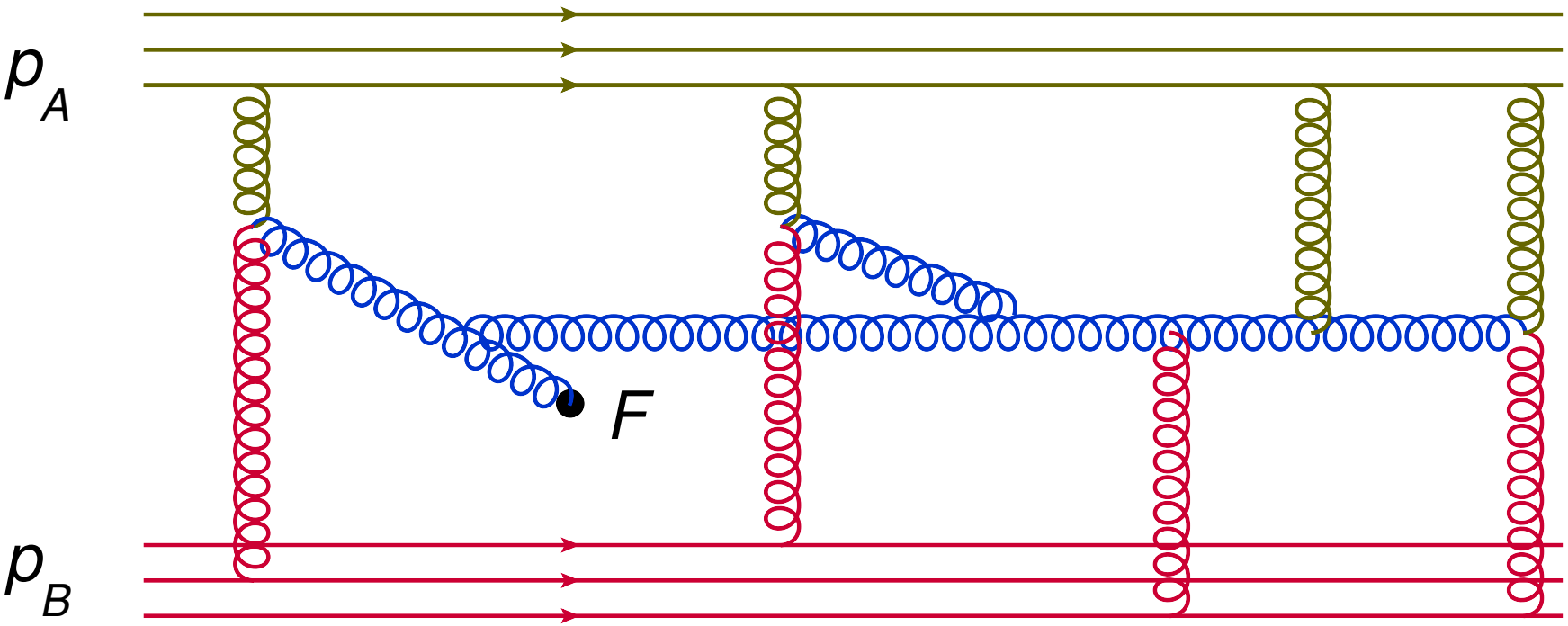
$F_{\mu\nu}(C)$ in the tree approximation

Since $\tilde{A} = A$ and $\tilde{B} = B$ the sources and background fields are the same to the left and to the right of the cut

$\Rightarrow$

$F_{\mu\nu}(C)$ is a sum of diagrams with *retarded* Green functions

(F. Gelis, R. Venugopalan)



Classical solution

The sum of diagrams with retarded Green functions $\Leftrightarrow$ solution of classical YM equations

$$D^\nu F^a_{\mu\nu} = \sum_f g\bar{\psi}^f t^a \gamma_\mu \psi^f, \quad (\not{P} + m_f)\psi^f = 0$$

with boundary conditions

$$A_\mu(x) \overset{x_* \to -\infty}{=} \bar{A}_\mu(x_\bullet, x_\perp), \quad \psi(x) \overset{x_* \to -\infty}{=} \psi_a(x_\bullet, x_\perp)$$
$$A_\mu(x) \overset{x_\bullet \to -\infty}{=} \bar{B}_\mu(x_*, x_\perp), \quad \psi(x) \overset{x_\bullet \to -\infty}{=} \psi_b(x_*, x_\perp)$$

following from $C_\mu, \psi_c \overset{t \to -\infty}{\to} 0$.
The projectile and target fields satisfy YM equations

$$D^\nu F^a_{\mu\nu} = \sum_f g\bar{\psi}^f_a t^a \gamma_\mu \psi^f_a, \quad (\not{P} + m_f)\psi^f_a = 0$$
$$D^\nu F^a_{\mu\nu} = \sum_f g\bar{\psi}^f_b t^a \gamma_\mu \psi^f_b, \quad (\not{P} + m_f)\psi^f_b = 0$$

Method of solution: start with $\bar{A}_\mu + \bar{B}_\mu$ and correct by computing Feynman diagrams (with retarded propagators) with a source $J_\nu = D^\mu F^{\mu\nu}(U + V)$

Power counting for background fields

To get the relative strength of Lorentz components of background $A(x_\bullet, x_\perp)$ and $B(x_*, x_\perp)$ fields, we compare the typical term in the leading contribution to possible higher-twist corrections

Leading-twist operator

$$\langle p_A | U_*^{mi}(x_\bullet, x_\perp) U_*^{mj}(0) | p_A \rangle \sim s^2 \left(g_{ij}^\perp + \frac{x_i^\perp x_j^\perp}{x_\perp^2} \right)$$

$$U_{*i}^a(z_\bullet, z_\perp) \equiv \left([-\infty_\bullet, z_\bullet]_z^{\bar{A}_*} \right)^{ab} \bar{A}_{*i}^b(z_\bullet, z_\perp)$$

Higher-twist operator

$$d^{mnl} \langle p_A | U_*^{mi}(x_\bullet, x_\perp) U_*^{nk}(x'_\bullet, x_\perp) U_*^{lj}(0) | p_A \rangle$$

$$\sim s^3 \left(g_{ij}^\perp \frac{x^k}{x_\perp^2} + g_{ik}^\perp \frac{x^j}{x_\perp^2} + g_{jk}^\perp \frac{x^i}{x_\perp^2} + \frac{x_i^\perp x_j^\perp x^k}{x_\perp^2} \right)$$

$\Rightarrow U_{*k} \sim s \frac{x_k}{x_\perp^2} \sim s m_\perp$. Similarly, $V_{\bullet k} \sim s \frac{x_k}{x_\perp^2} \sim s m_\perp$

(For the purpose of power counting $m_\perp \sim q_\perp, m_N$)

Power counting for background fields

In this way we get the relative strength of the background gluon fields in projectile and target:

$$A_*(x_\bullet, x_\perp) \sim s, \quad A_\bullet(x_\bullet, x_\perp) \sim m_\perp^2, \quad A_i(x_\bullet, x_\perp) \sim m_\perp,$$
$$B_*(x_*, x_\perp) \sim m_\perp^2, \quad B_\bullet(x_*, x_\perp) \sim s, \quad B_i(x_*, x_\perp) \sim m_\perp$$

for the gluon fields and

$$\hat{p}_1\psi_a(x_\bullet, x_\perp) \sim m_\perp^{5/2}, \quad \gamma_i\psi_a(x_\bullet, x_\perp) \sim m_\perp^{3/2}, \quad \hat{p}_2\psi_a(x_\bullet, x_\perp) \sim s\sqrt{m_\perp},$$
$$\hat{p}_1\psi_b(x_\bullet, x_\perp) \sim s\sqrt{m_\perp}, \quad \gamma_i\psi_b(x_\bullet, x_\perp) \sim m_\perp^{3/2}, \quad \hat{p}_2\psi_b(x_\bullet, x_\perp) \sim m_\perp^{5/2}$$

for quark fields.

We see that there large background fields $A_*, B_\bullet \sim s$ so the linear term $J_\nu \sim D^\mu F_{\mu\nu}(A+B) \sim s^2 \Rightarrow$ the expansion in powers of J_ν is bad.

Way out: gauge transformation

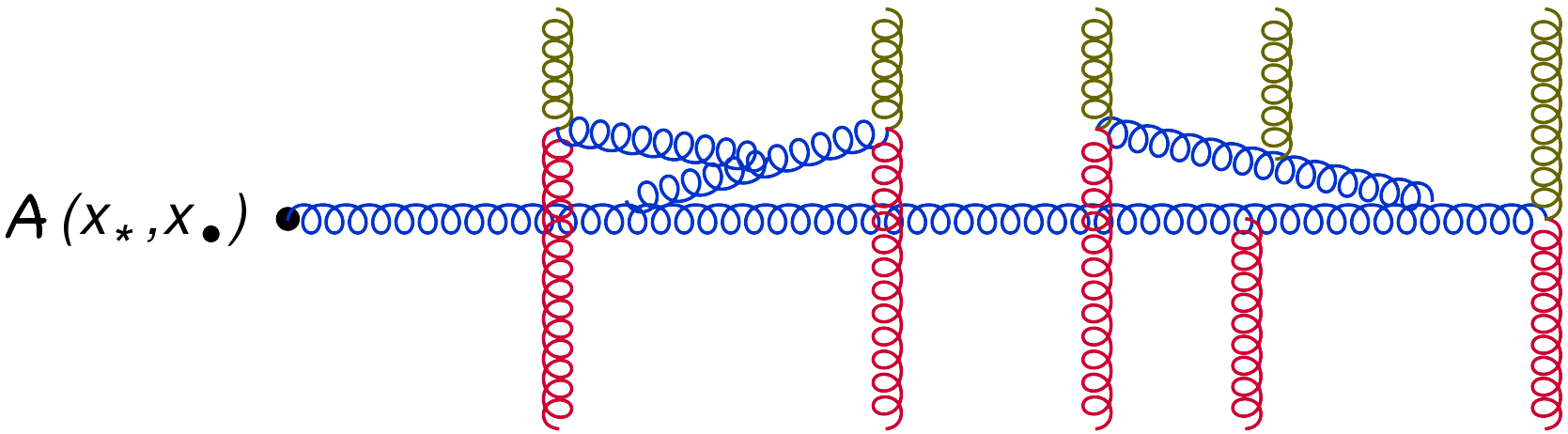
Gauge transformation with a matrix $\Omega(x)$ such that

$$\Omega(x_*, x_\bullet, x_\perp) \overset{x_* \to -\infty}{\to} [x_\bullet, -\infty_\bullet]_x^{\bar{A}_*}, \qquad \Omega(x_*, x_\bullet, x_\perp) \overset{x_\bullet \to -\infty}{\to} [x_*, -\infty_*]_x^{\bar{B}_\bullet}$$

The matrix Ω is obtained in a following way:

$$\mathcal{A}_\mu(x_*, x_\bullet) \;=\; \Omega^\dagger(x_*, x_\bullet)\partial_\mu\Omega(x_*, x_\bullet)$$

is a solution of our YM equation in 2 longitudinal dimensions.



Way out: gauge transformation

Gauge transformation with a matrix $\Omega(x)$ such that

$$\Omega(x_*, x_\bullet, x_\perp) \overset{x_* \to -\infty}{\to} [x_\bullet, -\infty_\bullet]_x^{\bar{A}_*}, \qquad \Omega(x_*, x_\bullet, x_\perp) \overset{x_\bullet \to -\infty}{\to} [x_*, -\infty_*]_x^{\bar{B}_\bullet}$$

The initial conditions turn to

$$A_\mu(x) \overset{x_* \to -\infty}{=} U_\mu(x_\bullet, x_\perp), \qquad \psi(x) \overset{x_* \to -\infty}{=} \Sigma_a(x_\bullet, x_\perp)$$
$$A_\mu(x) \overset{x_\bullet \to -\infty}{=} V_\mu(x_*, x_\perp), \qquad \psi(x) \overset{x_\bullet \to -\infty}{=} \Sigma_b(x_*, x_\perp)$$

where

$$U_\mu(x_\bullet, x_\perp) \equiv \frac{2}{s} p_{2\mu} U_\bullet(x_\bullet, x_\perp) + U_{\mu_\perp}(x_\bullet, x_\perp),$$
$$V_\mu(x_*, x_\perp) \equiv \frac{2}{s} p_{1\mu} V_*(x_*, x_\perp) + V_{\mu_\perp}(x_*, x_\perp),$$
$$U_i(x_\bullet, x_\perp) \equiv \frac{2}{s} \int_{-\infty}^{x_\bullet} dx'_\bullet \; U_{*i}(x'_\bullet, x_\perp), \qquad V_i(x_*, x_\perp) \equiv \frac{2}{s} \int_{-\infty}^{x_*} dx'_* \; V_{\bullet i}(x'_*, x_\perp)$$
$$\Sigma_a(z_\bullet, z_\perp) \equiv [-\infty_\bullet, z_\bullet]_z \psi(z_\bullet, z_\perp), \qquad \Sigma_b(z_*, z_\perp) \equiv [-\infty_*, z_*]_z \psi(z_*, z_\perp)$$

New initial conditions look like the projectile fields in the light-like gauge $p_2^\mu A_\mu = 0$ and target fields in the light-like gauge $p_1^\mu A_\mu = 0$

Classical solution with new background fields

Now all background fields are $\sim m_\perp$

$$U_i(x_\bullet, x_\perp) \sim m_\perp, \quad U_\bullet(x_\bullet, x_\perp) \sim m_\perp^2, \quad U_* = 0$$
$$V_i(x_*, x_\perp) \sim m_\perp^2, \quad V_*(x_*, x_\perp) \sim m_\perp^2, \quad V_\bullet = 0$$

and we have to solve

$$D^\nu F^a_{\mu\nu} = \sum_f g\bar{\psi}^f t^a \gamma_\mu \psi^f, \quad (\not{P} + m_f)\psi^f = 0$$

with boundary conditions

$$A_\mu(x) \overset{x_* \to -\infty}{=} U_\mu(x_\bullet, x_\perp), \quad \psi(x) \overset{x_* \to -\infty}{=} \Sigma_a(x_\bullet, x_\perp)$$
$$A_\mu(x) \overset{x_\bullet \to -\infty}{=} V_\mu(x_*, x_\perp), \quad \psi(x) \overset{x_\bullet \to -\infty}{=} \Sigma_b(x_*, x_\perp)$$

Now we start with $U_\mu + V_\mu$ and computie Feynman diagrams (with retarded propagators) with a source $J_\nu = D^\mu F^{\mu\nu}(A + B) \sim m_\perp^3$

Expansion at small momentum transfer

The solution of YM equations in general case (scattering of two "color glass condensates") is yet unsolved problem.
Fortunately, for our case of particle production with $\frac{q_\perp}{Q} \ll 1$ we can use this small parameter and construct the approximate solution as a series in $\frac{q_\perp}{Q}$.

Example:

$$A_\bullet = U_\bullet + \int dz (x| \frac{1}{p^2 + i\epsilon p_0} p_\bullet |z) [U_j, V^j](z) = U_\bullet + \frac{1}{2} \int dz (x| \frac{1}{\alpha - \frac{p_\perp^2}{\beta s} + i\epsilon} |z) [U_j, V^j](z)$$

The characteristic $\alpha \geq \alpha_q$ and $\beta \geq \beta_q$ so $\alpha \gg \frac{p_\perp^2}{\beta s}$

$$\Rightarrow (x| \frac{1}{\alpha - \frac{p_\perp^2}{\beta s} + i\epsilon} |z) = (x| \frac{1}{\alpha + i\epsilon} |z) + (x| \frac{1}{\alpha + i\epsilon} \frac{p_\perp^2}{\beta s} \frac{1}{\alpha + i\epsilon} |z) + \ldots$$

and in the leading order in $p_\perp / p_{||}$ we get

$$A_\bullet(x) = U_\bullet(x_\bullet, x_\perp) + \frac{1}{2} \int dz (x| \frac{1}{\alpha + i\epsilon} |z) [U_j, V^j](z)$$
$$= U_\bullet(x_\bullet, x_\perp) - \frac{i}{2} \int_{-\infty}^{x_\bullet} dx'_\bullet \, [U_j(x'_\bullet, x_\perp), V^j(x_*, x_\perp)]$$

Gluon fields in the leading order in $p_\perp^2/p_\parallel^2 \sim q_\perp^2/Q^2$

With the expansion

$$\frac{1}{p^2+i\epsilon p_0} = \frac{1}{p_\parallel^2 - p_\perp^2 + i\epsilon p_0} = \frac{1}{p_\parallel^2} - \frac{1}{p_\parallel^2 + i\epsilon p_0} p_\perp^2 \frac{1}{p_\parallel^2 + i\epsilon p_0} + \dots$$

the dynamics in transverse space is trivial.

Gluon fields :

$$\begin{aligned}
F_{\bullet i}^{(-1)} &= V_{\bullet i}, \quad F_{*i}^{(-1)} = U_{*i}, \\
F_{*\bullet}^{(-1)} &= U_{*\bullet} + V_{*\bullet} - \frac{is}{2} U_j^{ab} V^{bj} \\
F_{\bullet i}^{(0)a} &= U_{\bullet i}^a - iU_\bullet^{ab} V_i^b - \frac{i}{2(\alpha+i\epsilon)} \tilde{L}_i^{(0)} - \mathcal{D}_i^{ab} V_j^{bc} \frac{1}{2(\alpha+i\epsilon)} U^{cj}, \\
F_{*i}^{(0)a} &= V_{*i}^a - iV_*^{ab} U_i^b - \frac{i}{2(\beta+i\epsilon)} \tilde{L}_i^{(0)} - \mathcal{D}_i^{ab} U_j^{bc} \frac{1}{2(\beta+i\epsilon)} V^{cj}, \\
F_{ik}^{(0)} &= U_{ik} + V_{ik} - i[U_i, V_k] - i[V_i, U_k],
\end{aligned}$$

where

$$\begin{aligned}
L_i^{(0)a} &= -iU^{jab} V_{ji} - iV^{jab} U_{ji} - i\mathcal{D}_j^{ab} (U^{jbc} V_i^c + V^{jbc} U_i^c) \\
&\quad - \frac{2i}{s} \left(U_{*\bullet}^{ab} V_i^b - V_{*\bullet}^{ab} U_i \right) + \bar{\Sigma}_a t^a \gamma_i \Sigma_b + \bar{\Sigma}_b t^a \gamma_i \Sigma_a
\end{aligned}$$

Gluon fields in the leading order in $p_\perp^2/p_\parallel^2 \sim q_\perp^2/Q^2$

With the expansion

$$\frac{1}{p^2+i\epsilon p_0} = \frac{1}{p_\parallel^2 - p_\perp^2 + i\epsilon p_0} = \frac{1}{p_\parallel^2} - \frac{1}{p_\parallel^2 + i\epsilon p_0} p_\perp^2 \frac{1}{p_\parallel^2 + i\epsilon p_0} + \dots$$

the dynamics in transverse space is trivial.

Gluon fields :

$$F_{\bullet i}^{(-1)} = V_{\bullet i}, \quad F_{*i}^{(-1)} = U_{*i},$$

$$F_{*\bullet}^{(-1)} = U_{*\bullet} + V_{*\bullet} - \frac{is}{2} U_j^{ab} V^{bj}$$

$$F_{\bullet i}^{(0)a} = U_{\bullet i}^a - iU_\bullet^{ab} V_i^b - \frac{i}{2(\alpha+i\epsilon)} \tilde{L}_i^{(0)} - \mathcal{D}_i^{ab} V_j^{bc} \frac{1}{2(\alpha+i\epsilon)} U^{cj},$$

$$F_{*i}^{(0)a} = V_{*i}^a - iV_*^{ab} U_i^b - \frac{i}{2(\beta+i\epsilon)} \tilde{L}_i^{(0)} - \mathcal{D}_i^{ab} U_j^{bc} \frac{1}{2(\beta+i\epsilon)} V^{cj},$$

$$F_{ik}^{(0)} = U_{ik} + V_{ik} - i[U_i, V_k] - i[V_i, U_k],$$

We integrate over α without cutoff $\alpha > \sigma$ since the contour over α can be removed from the pole to the region of large α (if there is no pinch). Similarly, we integrate over all β's.

(Different from SCET where they keep the cutoffs $\alpha > \sigma_b$ and $\beta > \sigma_a$).

TMD factorization with power corrections

At the tree level

$$F^2(x) \;=\; \frac{8}{s} U^{ai}_*(x) V^a_{\bullet i}(x) + 2 f^{mac} f^{mbd} \Delta^{ij,kl} U^a_i(x) U^b_j(x) V^c_k(x) V^d_l(x) \;+\; \ldots$$

$$\Delta^{ij,kl} \;\equiv\; g^{ij} g^{kl} - g^{ik} g^{jl} - g^{il} g^{jk}$$

$\Rightarrow$ in the region $s \gg Q^2 \gg Q^2_\perp$

$$W(p_A, p_B, q) \;=\; \frac{64/s^2}{N_c^2 - 1} \int d^2 x_\perp \; e^{i(q,x)_\perp} \frac{2}{s} \int dx_\bullet dx_* \; e^{-i\alpha_q x_\bullet - i\beta_q x_*}$$

$$\times \Big\{ \langle p_A | U^{mi}_*(x_\bullet, x_\perp) U^{mj}_*(0) | p_A \rangle \langle p_B | \mathcal{F}^n_{\bullet i}(x_*, x_\perp) \mathcal{F}^n_{\bullet j}(0) | p_B \rangle$$

$$- \frac{N_c^2}{N_c^2 - 4} \frac{\Delta^{ij,kl}}{Q^2} \int_{-\infty}^{x_\bullet} d\frac{2}{s} x'_\bullet \; d^{abc} \langle p_A | U^a_{*i}(x_\bullet, x_\perp) U^b_{*j}(x'_\bullet, x_\perp) U^c_{*r}(0) | p_A \rangle$$

$$\times \int_{-\infty}^{x_\bullet} d\frac{2}{s} x'_* \; d^{mnl} \langle p_B | V^m_{\bullet k}(x_*, x_\perp) V^n_{\bullet l}(x'_*, x_\perp) V^n_{\bullet r}(0) | p_B \rangle \;+\; x \leftrightarrow 0 \Big\}$$

The correction is $\sim \frac{Q^2_\perp}{Q^2}$ (easy to see e.g. on a quark target).

Conclusions and outlook

1. Conclusions
   - Higher-twist power correction to particle production by gluon fusion at $s \gg q^2 \gg q_\perp^2$ is calculated
2. Outlook
   - Power corrections to Drell-Yan and SIDIS
   - Factorization at the one-loop level (and match to evolution equations for gluon TMDs).

Conclusions and outlook

1. Conclusions
   - Higher-twist power correction to particle production by gluon fusion at $s \gg q^2 \gg q_\perp^2$ is calculated
2. Outlook
   - Power corrections to Drell-Yan and SIDIS
   - Factorization at the one-loop level (and match to evolution equations for gluon TMDs).

Thank you for attention!

Full NLO corrections for DIS structure functions in the dipole factorization formalism

Guillaume Beuf

ECT*, Trento

Saturation: Recent Developments, New Ideas and Measurements
RBRC workshop, Brookhaven Nat. Lab., 26-28 april 2017

Outline

- Introduction: dipole factorization for DIS at low x_{Bj}
- One-loop correction to the $\gamma^*_{T,L} \to q\bar{q}$ light-front wave-functions:

  Direct calculation

  G.B., PRD94 (2016)
- DIS at NLO in the dipole factorization :

  Detailed calculation for γ^*_L case

  Cancellation of the UV divergences between the $q\bar{q}$ and $q\bar{q}g$ terms

  Results for γ^*_T case

  G.B., *in preparation*

Introduction

At low x_{Bj}, many DIS observables can be expressed within dipole factorization, including gluon saturation $\rightarrow$ rich phenomenology.

In particular: Dipole amplitude obtained from fits of HERA data for DIS structure functions in the dipole factorization at LO+LL with rcBK
Albacete *et al.*, PRD80 (2009); EPJC71 (2011)
Kuokkanen *et al.*, NPA875 (2012);
Lappi, Mäntysaari, PRD88 (2013)

$\Rightarrow$ The fitted dipole amplitude can then be used for pp, pA, AA, as well as other DIS observables.

Introduction

At low x_{Bj}, many DIS observables can be expressed within dipole factorization, including gluon saturation $\rightarrow$ rich phenomenology.

In particular: Dipole amplitude obtained from fits of HERA data for DIS structure functions in the dipole factorization at LO+LL with rcBK
Albacete *et al.*, PRD80 (2009); EPJC71 (2011)
Kuokkanen *et al.*, NPA875 (2012);
Lappi, Mäntysaari, PRD88 (2013)

$\Rightarrow$ The fitted dipole amplitude can then be used for pp, pA, AA, as well as other DIS observables.

In the last 10 years, many theoretical (including numerical) progresses towards NLO/NLL accuracy for gluon saturation/CGC.

Obviously, DIS structure functions at NLO in the dipole factorization are required to push the fits beyond LO+LL accuracy.

DIS at NLO: previous results

2 independent calculations had been performed earlier for NLO corrections to photon impact factor and/or DIS cross-section:

1. Balitsky, Chirilli, PRD83 (2011); PRD87 (2013)
   Using covariant perturbation theory. Results provided as
   - Current correlator in position space
   - Impact factor for $k_\perp$ factorization $\rightarrow$ Good for BFKL phenomenology

2. G.B., PRD85 (2012)
   Using light-front perturbation theory. Results provided as
   - DIS structure functions in dipole factorization
     $\rightarrow$ Good for gluon saturation phenomenology

DIS at NLO: previous results

2 independent calculations had been performed earlier for NLO corrections to photon impact factor and/or DIS cross-section:

1. Balitsky, Chirilli, PRD83 (2011); PRD87 (2013)
   Using covariant perturbation theory. Results provided as
   - Current correlator in position space
   - Impact factor for $k_\perp$ factorization $\rightarrow$ Good for BFKL phenomenology

2. G.B., PRD85 (2012)
   Using light-front perturbation theory. Results provided as
   - DIS structure functions in dipole factorization
     $\rightarrow$ Good for gluon saturation phenomenology

However, in both papers only the $q\bar{q}g$ contribution was calculated explicitly, whereas NLO corrections to the $q\bar{q}$ contribution were guessed.
Methods used for that:
In Balitsky, Chirilli, PRD83 (2011):
Matching with earlier vacuum results

DIS at NLO: previous results

2 independent calculations had been performed earlier for NLO corrections to photon impact factor and/or DIS cross-section:

1. Balitsky, Chirilli, PRD83 (2011); PRD87 (2013)
   Using covariant perturbation theory. Results provided as
   - Current correlator in position space
   - Impact factor for $k_\perp$ factorization $\rightarrow$ Good for BFKL phenomenology

2. G.B., PRD85 (2012)
   Using light-front perturbation theory. Results provided as
   - DIS structure functions in dipole factorization
     $\rightarrow$ Good for gluon saturation phenomenology

However, in both papers only the $q\bar{q}g$ contribution was calculated explicitly, whereas NLO corrections to the $q\bar{q}$ contribution were guessed.
Methods used for that:
In G.B., PRD85 (2012):
Unitary argument

DIS at NLO: previous results

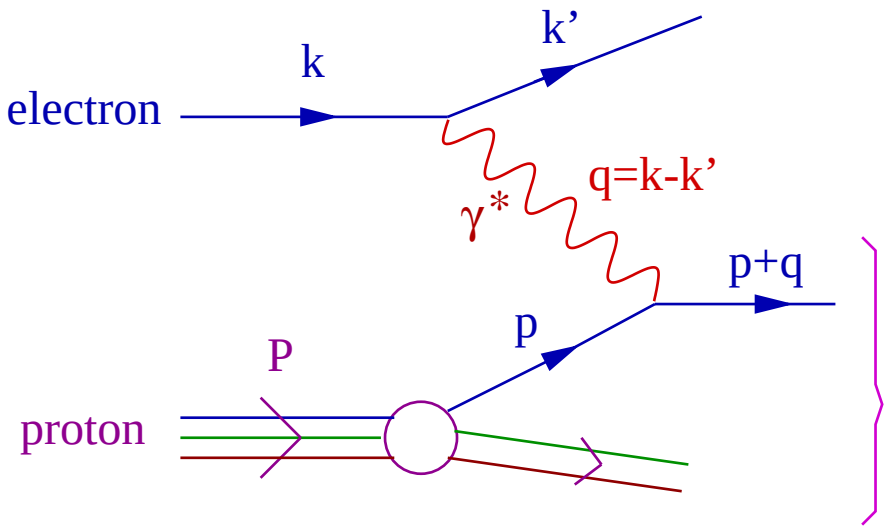
2 independent calculations had been performed earlier for NLO corrections to photon impact factor and/or DIS cross-section:

1. Balitsky, Chirilli, PRD83 (2011); PRD87 (2013)
   Using covariant perturbation theory. Results provided as
   - Current correlator in position space
   - Impact factor for $k_\perp$ factorization $\rightarrow$ Good for BFKL phenomenology

2. G.B., PRD85 (2012)
   Using light-front perturbation theory. Results provided as
   - DIS structure functions in dipole factorization
     $\rightarrow$ Good for gluon saturation phenomenology

However, in both papers only the $q\bar{q}g$ contribution was calculated explicitly, whereas NLO corrections to the $q\bar{q}$ contribution were guessed.
Methods used for that:
In G.B., PRD85 (2012):
Unitary argument $\rightarrow$ wrong: missed photon finite WF renormalization
$\Rightarrow$ NLO $q\bar{q}$ terms needs to be calculated separately in LFPT

Kinematics for Deep Inelastic Scattering (DIS)



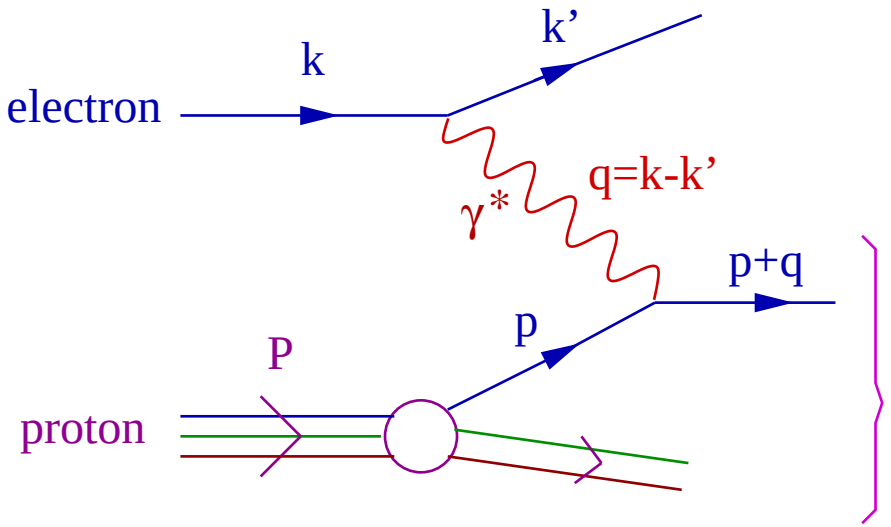
$$\frac{d\sigma^{ep\to e+X}}{dx_{Bj}\,d^2Q} = \frac{\alpha_{em}}{\pi x_{Bj} Q^2}\left[\left(1-y+\frac{y^2}{2}\right)\sigma_T^{\gamma}(x_{Bj},Q^2)+(1-y)\,\sigma_L^{\gamma}(x_{Bj},Q^2)\right]$$

Photon virtuality: $Q^2 \equiv -q^2 > 0$

Bjorken x variable: $x_{Bj} \equiv \frac{Q^2}{2P\cdot q} \in [0,1]$

Inelasticity: $y \equiv \frac{2P\cdot q}{(P+k)^2} = \frac{2P\cdot q}{s} \in [0,1]$ $\qquad x_{Bj}\,y\,s = Q^2$

Kinematics for Deep Inelastic Scattering (DIS)



$$\frac{d\sigma^{ep\to e+X}}{dx_{Bj}\,d^2Q} = \frac{\alpha_{em}}{\pi x_{Bj} Q^2}\left[\left(1-y+\frac{y^2}{2}\right)\sigma_T^{\gamma}(x_{Bj},Q^2)+(1-y)\,\sigma_L^{\gamma}(x_{Bj},Q^2)\right]$$

Other equivalent parametrization: structure functions F_i

$$\begin{aligned}\sigma_{T,L}^{\gamma}(x_{Bj},Q^2) &= \frac{(2\pi)^2\alpha_{em}}{Q^2}\,F_{T,L}(x_{Bj},Q^2)\\ F_2 &= F_T+F_L \;\text{ and }\; 2x_{Bj}\,F_1 = F_T\end{aligned}$$

Dipole factorization for eikonal DIS

Total cross section for (virtual) photon scattering on a gluon shockwave background, in light-front perturbation theory:

$$\begin{aligned}\sigma_\lambda^\gamma &= 2N_c \widetilde{\sum_{q_0\bar{q}_1 \text{ F. states}}} \frac{2\pi\delta(k_0^+ + k_1^+ - q^+)}{2q^+} \left|\widetilde{\psi}_{\gamma_\lambda \to q_0\bar{q}_1}\right|^2 \mathrm{Re}\left[1 - \mathcal{S}_{01}\right] \\ &+ 2N_c C_F \widetilde{\sum_{q_0\bar{q}_1 g_2 \text{ F. states}}} \frac{2\pi\delta(k_0^+ + k_1^+ + k_2^+ - q^+)}{2q^+} \\ &\times \left|\widetilde{\psi}_{\gamma_\lambda \to q_0\bar{q}_1 g_2}\right|^2 \mathrm{Re}\left[1 - \mathcal{S}_{012}^{(3)}\right] + \cdots\end{aligned}$$

$\widetilde{\psi}_{\gamma_\lambda \to f}$: color-stripped light-front wavefunctions of the incoming photon for the Fock-state decomposition in mixed-space $(k^+, \mathbf{x})$

Dipole factorization for eikonal DIS

Total cross section for (virtual) photon scattering on a gluon shockwave background, in light-front perturbation theory:

$$\sigma_\lambda^\gamma = 2N_c \widetilde{\sum_{q_0\bar{q}_1 \text{ F. states}}} \frac{2\pi\delta(k_0^+ + k_1^+ - q^+)}{2q^+} \left|\widetilde{\psi}_{\gamma_\lambda \to q_0\bar{q}_1}\right|^2 \mathrm{Re}\left[1 - \mathcal{S}_{01}\right]$$

$$+ 2N_c C_F \widetilde{\sum_{q_0\bar{q}_1 g_2 \text{ F. states}}} \frac{2\pi\delta(k_0^+ + k_1^+ + k_2^+ - q^+)}{2q^+}$$

$$\times \left|\widetilde{\psi}_{\gamma_\lambda \to q_0\bar{q}_1 g_2}\right|^2 \mathrm{Re}\left[1 - \mathcal{S}_{012}^{(3)}\right] + \cdots$$

Dipole operator: $\mathcal{S}_{01} \equiv \frac{1}{N_c}\mathrm{Tr}\left(U_F(\mathbf{x}_0)\, U_F^\dagger(\mathbf{x}_1)\right)$

"Tripole" operator: $\mathcal{S}_{012}^{(3)} \equiv \frac{1}{N_c\, C_F}\mathrm{Tr}\left(t^b U_F(\mathbf{x}_0)\, t^a U_F^\dagger(\mathbf{x}_1)\right) U_A(\mathbf{x}_2)_{ba}$

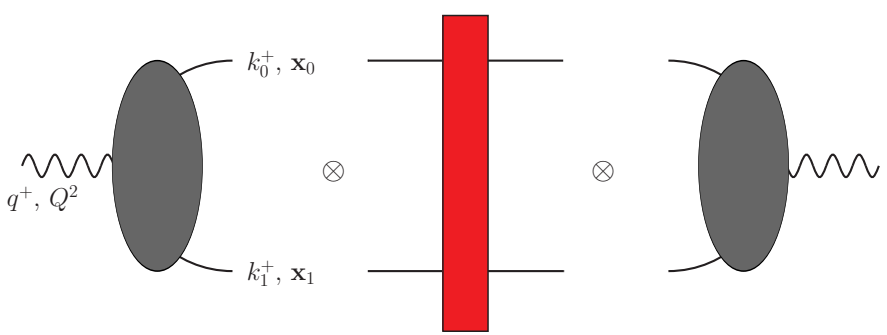
Dipole factorization for eikonal DIS

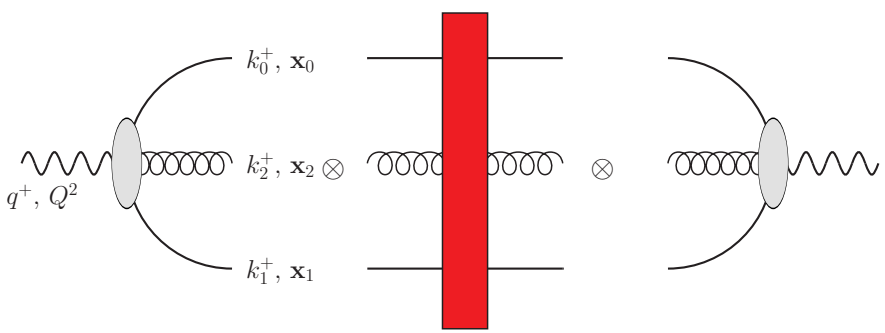
Total cross section for (virtual) photon scattering on a gluon shockwave background, in light-front perturbation theory:

$$\sigma_\lambda^\gamma = 2N_c \widetilde{\sum_{q_0\bar{q}_1 \text{ F. states}}} \frac{2\pi\delta(k_0^+ + k_1^+ - q^+)}{2q^+} \left|\widetilde{\psi}_{\gamma_\lambda \to q_0\bar{q}_1}\right|^2 \mathrm{Re}\left[1 - \mathcal{S}_{01}\right]$$

$$+ 2N_c C_F \widetilde{\sum_{q_0\bar{q}_1 g_2 \text{ F. states}}} \frac{2\pi\delta(k_0^+ + k_1^+ + k_2^+ - q^+)}{2q^+}$$

$$\times \left|\widetilde{\psi}_{\gamma_\lambda \to q_0\bar{q}_1 g_2}\right|^2 \mathrm{Re}\left[1 - \mathcal{S}_{012}^{(3)}\right] + \cdots$$





Calculation of the $\gamma_{T,L} \to q\bar{q}$ LF wave-functions at NLO

- Calculation done in Light-front perturbation theory for QCD+QED
- Cut-off k^+_{min} introduced to regulate the small k^+ divergences

  $\Rightarrow$ associated with low-x leading logs to be resummed with BK/JIMWLK evolution at the end
- UV divergences from various tensor transverse integrals, but no UV renormalization at this order.

  $\Rightarrow$ UV divergences (and finite regularization artifacts) have to cancel at cross-section level

  $\Rightarrow$ Use (Conventional) Dimensional Regularization, and pay attention to rational terms in $(D-4)/(D-4)$

Diagrams for the $\gamma_T \to q\bar{q}$ LF wave-function only

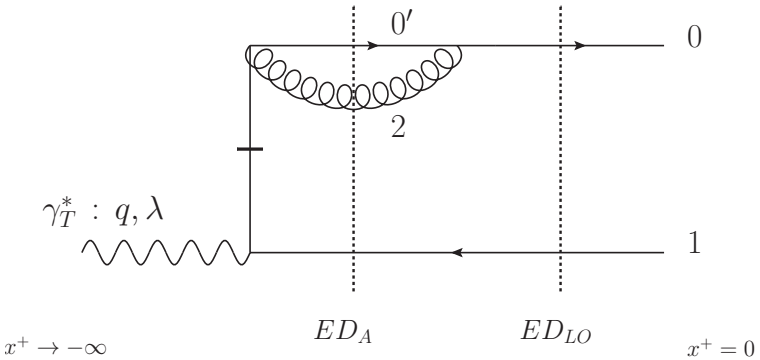


Diagram A'

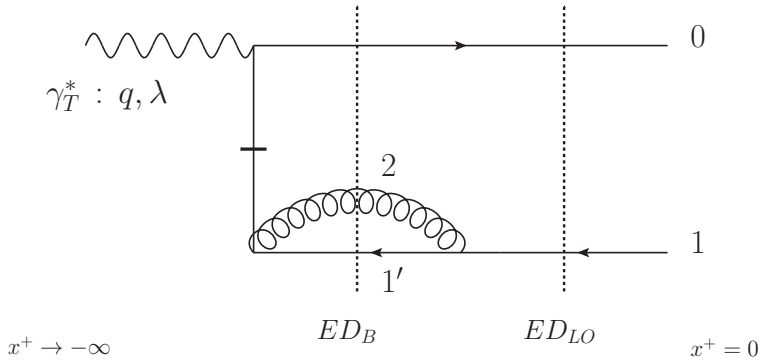


Diagram B'

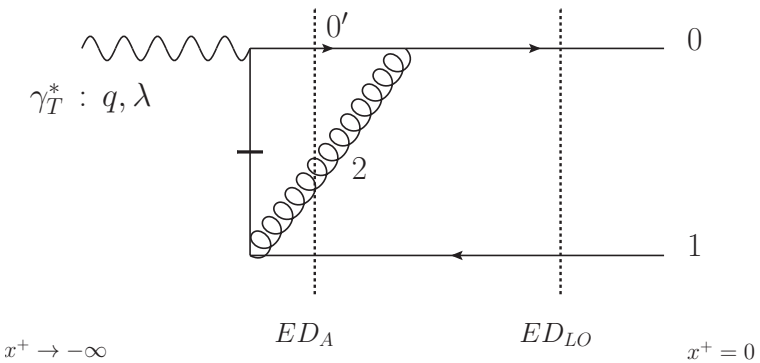


Diagram 1'

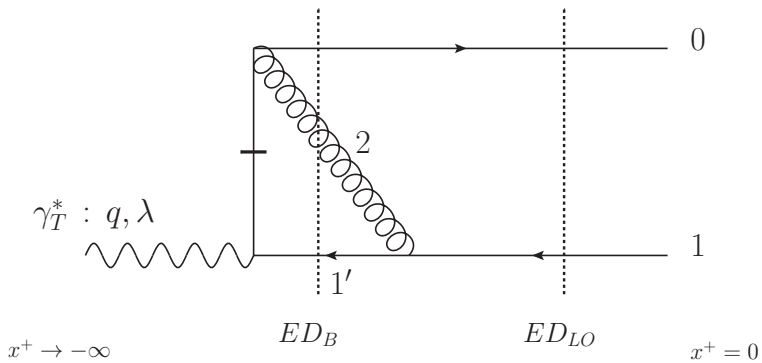


Diagram 2'

Diagrams for the $\gamma_T \to q\bar{q}$ LF wave-function only

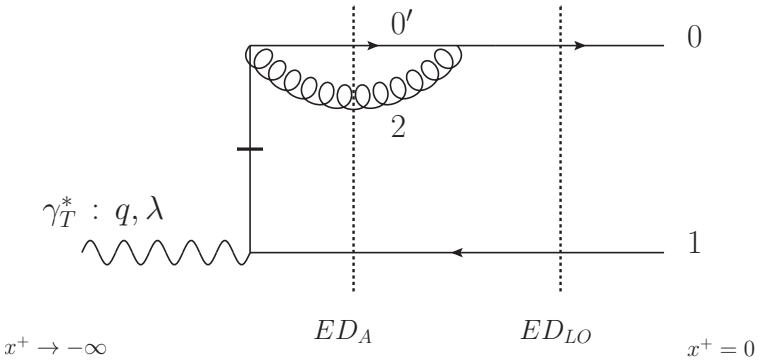


Diagram A'

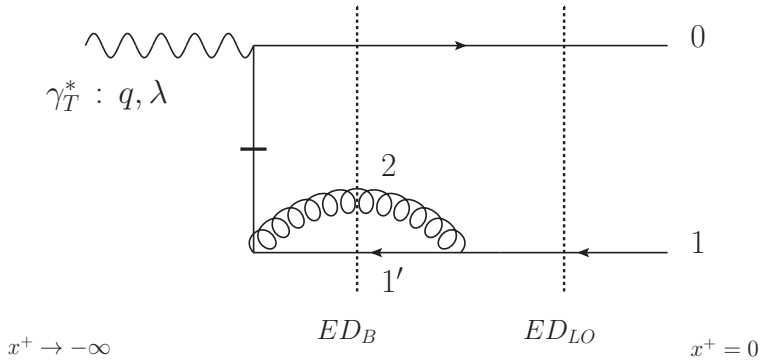


Diagram B'

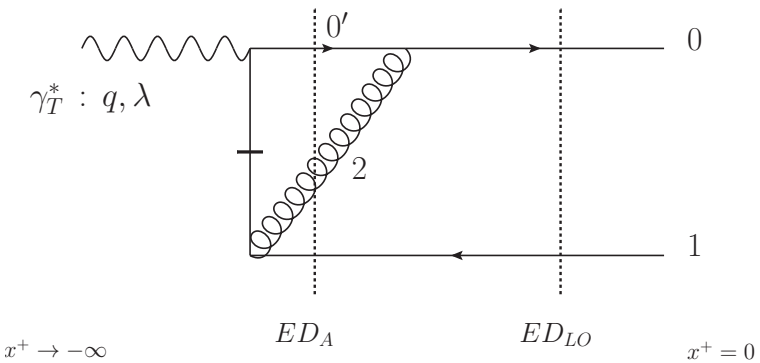


Diagram 1'

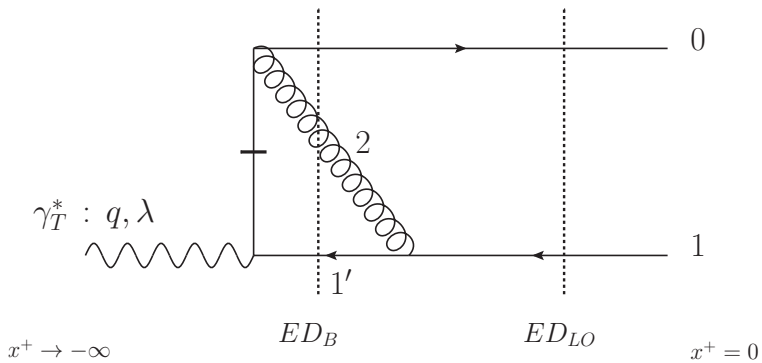


Diagram 2'

All four vanish due to Lorentz symmetry!

Diagrams for γ_T and γ_L LFWFs: 3 steps graphs

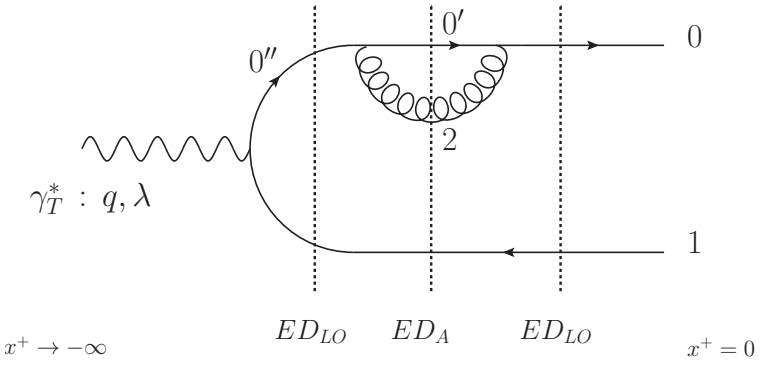


Diagram A

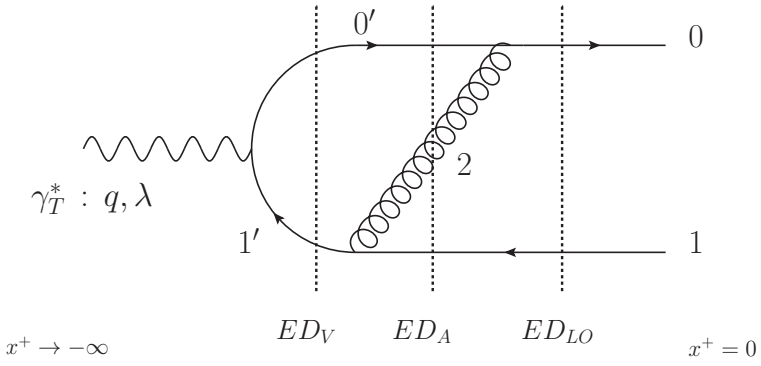


Diagram 1

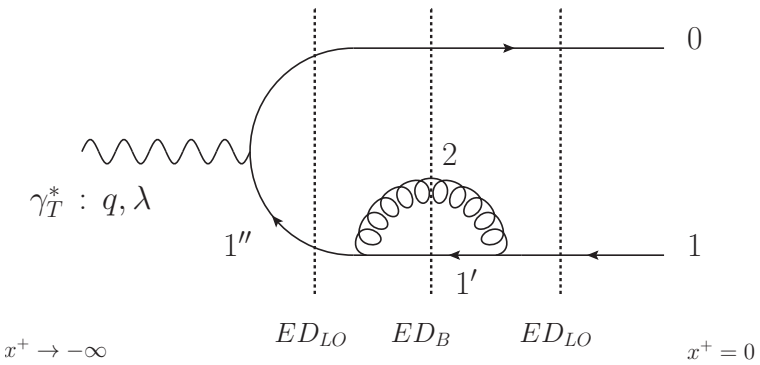


Diagram B

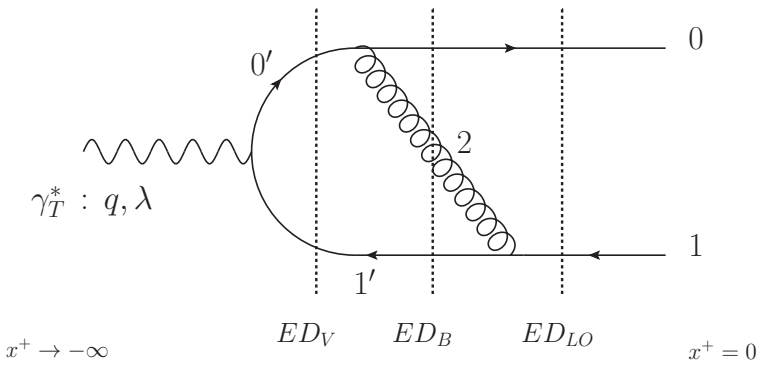


Diagram 2

Diagrams for γ_T and γ_L LFWFs: 2 steps graph

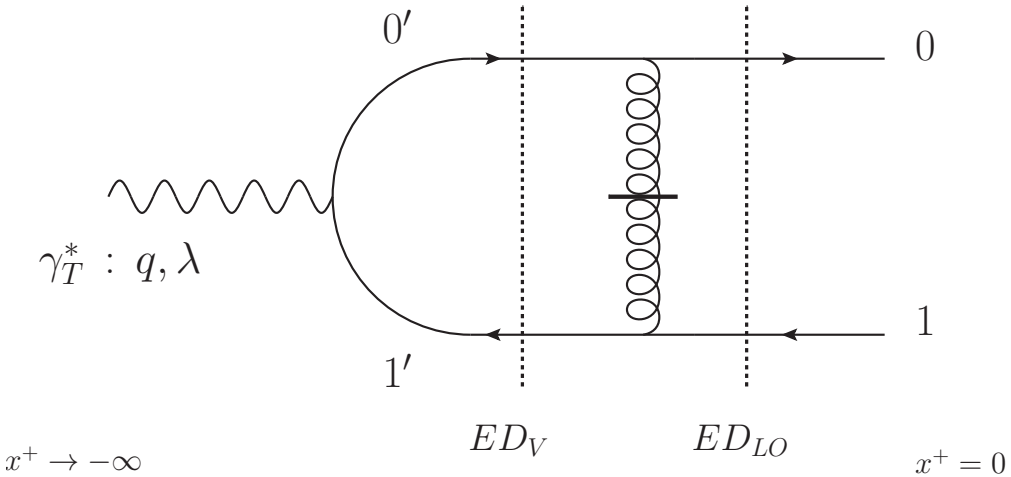


Diagram 3

- In the γ_T case: vanishes due to Lorentz symmetry
- In the γ_L case: non-zero, and cancels the unphysical power-like small k^+ divergence of the other vertex correction graphs.

Results for NLO $\gamma_{T,L} \to q\bar{q}$ LFWFs in momentum space

$$\psi_{\gamma^*_{T,L}\to q_0\bar{q}_1} = \left[1+\left(\frac{\alpha_s\, C_F}{2\pi}\right)\,\mathcal{V}^{T,L}\right]\,\psi^{\rm tree}_{\gamma^*_{T,L}\to q_0\bar{q}_1} + \mathcal{O}(e\,\alpha_s^2)$$

$$\mathcal{V}^L = 2\left[\log\left(\frac{k^+_{\rm min}}{\sqrt{k_0^+ k_1^+}}\right)+\frac{3}{4}\right]\left[\Gamma\left(2-\frac{D}{2}\right)\left(\frac{\overline{Q}^2}{4\pi\,\mu^2}\right)^{\frac{D}{2}-2} - 2\log\left(\frac{\mathbf{P}^2+\overline{Q}^2}{\overline{Q}^2}\right)\right]$$
$$+\frac{1}{2}\left[\log\left(\frac{k_0^+}{k_1^+}\right)\right]^2 - \frac{\pi^2}{6} + 3 + O\left(D-4\right)$$

$$\mathcal{V}^T = \mathcal{V}^L + 2\left[\log\left(\frac{k^+_{\rm min}}{\sqrt{k_0^+ k_1^+}}\right)+\frac{3}{4}\right]\left(\frac{\mathbf{P}^2+\overline{Q}^2}{\mathbf{P}^2}\right)\log\left(\frac{\mathbf{P}^2+\overline{Q}^2}{\overline{Q}^2}\right) + O\left(D-4\right)$$

Notations: $\overline{Q}^2 \equiv \frac{k_0^+ k_1^+}{(q^+)^2}\,Q^2$,

and relative transverse momentum: $\mathbf{P} \equiv \mathbf{k}_0 - \frac{k_0^+}{q^+}\,\mathbf{q} = -\mathbf{k}_1 + \frac{k_1^+}{q^+}\,\mathbf{q}$

Remark: results consistent with the ones of Boussarie, Grabovsky, Szymanowski and Wallon, JHEP11(2016)149

Results for NLO $\gamma_{T,L} \to q\bar{q}$ LFWFs in mixed space

$$\widetilde{\psi}_{\gamma^*_{T,L}\to q_0\bar{q}_1} = \left[1+\left(\frac{\alpha_s\, C_F}{2\pi}\right)\,\widetilde{\mathcal{V}}^{T,L}\right]\,\widetilde{\psi}^{\rm tree}_{\gamma^*_{T,L}\to q_0\bar{q}_1} + \mathcal{O}(e\,\alpha_s^2)$$

$$\begin{aligned}\widetilde{\mathcal{V}}^{T} &= \widetilde{\mathcal{V}}^{L} + O\,(D-4)\\ &= 2\left[\log\left(\frac{k^+_{\rm min}}{\sqrt{k_0^+\,k_1^+}}\right)+\frac{3}{4}\right]\left[\frac{1}{\left(2-\frac{D}{2}\right)}-\Psi(1)+\log\left(\pi\,\mu^2\,{\mathbf{x}_{01}}^2\right)\right]\\ &\quad +\frac{1}{2}\left[\log\left(\frac{k_0^+}{k_1^+}\right)\right]^2-\frac{\pi^2}{6}+3+O\,(D-4)\end{aligned}$$

- In mixed space: NLO corrections $\Rightarrow$ rescaling of the LO $\gamma_{T,L} \to q\bar{q}$ LFWFs by a factor independent of the photon polarization and virtuality !
- Leftover logarithmic UV and low k^+ divergences to be dealt with at cross-section level.

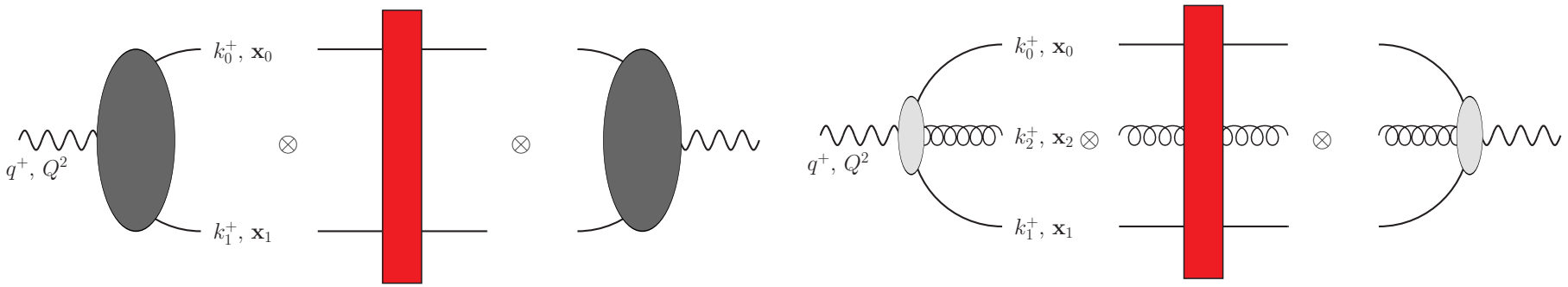
Results for NLO $\gamma_{T,L} \to q\bar{q}$ LFWFs in mixed space

$$\widetilde{\psi}_{\gamma^*_{T,L}\to q_0\bar{q}_1} = \left[1+\left(\frac{\alpha_s\, C_F}{2\pi}\right)\,\widetilde{\mathcal{V}}^{T,L}\right]\,\widetilde{\psi}^{\rm tree}_{\gamma^*_{T,L}\to q_0\bar{q}_1} + \mathcal{O}(e\,\alpha_s^2)$$

$$\begin{aligned}\widetilde{\mathcal{V}}^{T} &= \widetilde{\mathcal{V}}^{L} + O\,(D-4)\\ &= 2\left[\log\left(\frac{k^+_{\rm min}}{\sqrt{k_0^+\,k_1^+}}\right)+\frac{3}{4}\right]\left[\frac{1}{\left(2-\frac{D}{2}\right)}-\Psi(1)+\log\left(\pi\,\mu^2\,{\mathbf{x}_{01}}^2\right)\right]\\ &\quad +\frac{1}{2}\left[\log\left(\frac{k_0^+}{k_1^+}\right)\right]^2-\frac{\pi^2}{6}+\frac{5}{2}+\frac{1}{2}+O\,(D-4)\end{aligned}$$

- In mixed space: NLO corrections $\Rightarrow$ rescaling of the LO $\gamma_{T,L} \to q\bar{q}$ LFWFs by a factor independent of the photon polarization and virtuality !
- $(D-4)/(D-4)$ rational term $1/2$: from γ^μ algebra in D dimensions $\Rightarrow$ UV regularization scheme dependent!

From LFWFs to DIS cross-section



$\widetilde{\psi}^{\gamma^*_{T,L}}_{\gamma^*_{T,L}\to\bar{q}}$ now known at NLO accuracy in Dim Reg.

$\Rightarrow$ Need to be combined with the $q\bar{q}g$ contribution in the dipole factorization formula at NLO

$\Rightarrow$ $\widetilde{\psi}_{\gamma^*_{T,L}q\bar{q}g}$ is required also in Dim Reg, in order to cancel UV divergences as well as scheme dependent artifacts.

Only the derivation of σ_L^γ will be discussed in detail in the following for simplicity.

$q\bar{q}$ contribution to σ_L^γ at NLO in dim. reg.

$$\widetilde{\psi}^{\text{tree}}_{\gamma_L^*\to q_0\bar{q}_1} = -e\,e_f\,\mu^{2-\frac{D}{2}}\,(2\pi)^{1-\frac{D}{2}}\,2Q\,\frac{k_0^+k_1^+}{(q^+)^2}\left(\frac{\overline{Q}}{|\mathbf{x}_{01}|}\right)^{\frac{D}{2}-2}\,\mathrm{K}_{\frac{D}{2}-2}\left(|\mathbf{x}_{01}|\,\overline{Q}\right)\,\overline{u_G}(0)\,\gamma^+ v_G(1)$$

$$\sigma_L^\gamma\Big|_{q\bar{q}} = 2N_c\sum_{q_0\bar{q}_1\ \text{F. states}}\frac{2\pi\delta(k_0^+ + k_1^+ - q^+)}{2q^+}\left|\widetilde{\psi}^{\text{tree}}_{\gamma_L\to q_0\bar{q}_1}\right|^2\,\mathrm{Re}\left[1-\mathcal{S}_{01}\right]$$
$$\times\left[1+\left(\frac{\alpha_s\,C_F}{2\pi}\right)\,\widetilde{\mathcal{V}}^L\right]^2 + O(\alpha_{em}\,\alpha_s^2)$$

$$\sigma_L^\gamma\Big|_{q\bar{q}} = 4N_c\,\alpha_{em}\sum_f e_f^2\int\frac{\mathrm{d}^{D-2}\mathbf{x}_0}{2\pi}\int\frac{\mathrm{d}^{D-2}\mathbf{x}_1}{2\pi}\int_0^{+\infty}dk_0^+\int_0^{+\infty}dk_1^+\,\delta(k_0^+ + k_1^+ - q^+)$$
$$\times\frac{4Q^2}{(q^+)^5}\,(k_0^+k_1^+)^2\left[\frac{\overline{Q}^2}{(2\pi)^2\mu^2x_{01}^2}\right]^{\frac{D}{2}-2}\left[\mathrm{K}_{\frac{D}{2}-2}\left(|\mathbf{x}_{01}|\,\overline{Q}\right)\right]^2$$
$$\times\left[1+\left(\frac{\alpha_s\,C_F}{\pi}\right)\,\widetilde{\mathcal{V}}^L\right]\,\mathrm{Re}\left[1-\mathcal{S}_{01}\right] + O(\alpha_{em}\,\alpha_s^2)$$

Tree-level diagrams for $\gamma_L \to q\bar{q}g$ LFWFs

2 diagrams contribute to $\gamma_L \to q\bar{q}g$ (and 4 to $\gamma_T \to q\bar{q}g$):

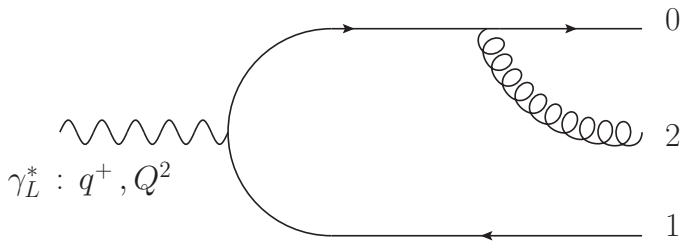


Diagram (a)

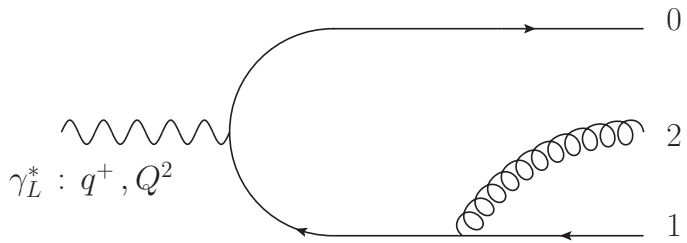


Diagram (b)

$\to$ Standard calculation in momentum space using LFPT rules, but to be done in dimensional regularization

Then: Fourier transform to mixed space

$\gamma_L \to q\bar{q}g$ LFWF in mixed space

Result:

$$\widetilde{\psi}^{\mathrm{Tree}}_{\gamma_L^* \to q_0 \bar{q}_1 g_2} = e\, e_f\, g\, \varepsilon^{j*}_{\lambda_2}\, \frac{2Q}{(q^+)^2}$$

$$\times \Bigg\{ k_1^+ \;\; \overline{u_G}(0)\gamma^+ \Big[(2k_0^+ + k_2^+)\delta^{jm} + \tfrac{k_2^+}{2}\,[\gamma^j, \gamma^m]\Big] v_G(1) \;\; \mathcal{I}^m\Big(\mathbf{x}_{0+2;1}, \mathbf{x}_{20}; \overline{Q}^2_{(a)}, \mathcal{C}_{(a)}\Big)$$

$$- k_0^+ \;\; \overline{u_G}(0)\gamma^+ \Big[(2k_1^+ + k_2^+)\delta^{jm} - \tfrac{k_2^+}{2}\,[\gamma^j, \gamma^m]\Big] v_G(1) \;\; \mathcal{I}^m\Big(\mathbf{x}_{0;1+2}, \mathbf{x}_{21}; \overline{Q}^2_{(b)}, \mathcal{C}_{(b)}\Big) \Bigg\}$$

with the notations:

$$\overline{Q}^2_{(a)} = \frac{k_1^+(q^+ - k_1^+)}{(q^+)^2}\, Q^2 \quad \text{and} \quad \overline{Q}^2_{(b)} = \frac{k_0^+(q^+ - k_0^+)}{(q^+)^2}\, Q^2$$

$$\mathcal{C}_{(a)} = \frac{q^+\, k_0^+\, k_2^+}{k_1^+(k_0^+ + k_2^+)^2} \quad \text{and} \quad \mathcal{C}_{(b)} = \frac{q^+\, k_1^+\, k_2^+}{k_0^+(k_1^+ + k_2^+)^2}$$

And parent dipole vectors defined as:

$$\mathbf{x}_{n+m;p} \;\; = \;\; -\mathbf{x}_{p;n+m} \equiv \left(\frac{k_n^+ \mathbf{x}_n + k_m^+ \mathbf{x}_m}{k_n^+ + k_m^+}\right) - \mathbf{x}_p$$

$q\bar{q}g$ contribution to σ_L^γ at NLO in dim. reg.

$$\sigma_L^\gamma|_{q\bar{q}g} = 2N_c C_F \widetilde{\sum_{q_0\bar{q}_1 g_2 \text{ F. states}}} \frac{2\pi\delta(k_0^+ + k_1^+ + k_2^+ - q^+)}{2q^+} \left|\widetilde{\psi}_{\gamma_L \to q_0\bar{q}_1 g_2}\right|^2 \text{Re}\left[1 - \mathcal{S}_{012}^{(3)}\right]$$

$$= 4N_c\,\alpha_{em} \sum_f e_f^2 \int_0^{+\infty} dk_0^+ \int_0^{+\infty} dk_1^+ \int_{k_{\text{min}}^+}^{+\infty} \frac{dk_2^+}{k_2^+}\,\delta(k_0^+ + k_1^+ + k_2^+ - q^+)$$

$$\times 2\alpha_s C_F \int \mathrm{d}^{D-2}\mathbf{x}_0 \int \mathrm{d}^{D-2}\mathbf{x}_1 \int \mathrm{d}^{D-2}\mathbf{x}_2\, \text{Re}\left[1 - \mathcal{S}_{012}^{(3)}\right] \frac{4Q^2}{(q^+)^5}$$

$$\times \Big\{ (k_1^+)^2 \left[2k_0^+(k_0^+ + k_2^+) + \frac{(D-2)}{2}\left(k_2^+\right)^2\right] \left|\mathcal{I}^m\left((a)\right)\right|^2$$

$$+ (k_0^+)^2 \left[2k_1^+(k_1^+ + k_2^+) + \frac{(D-2)}{2}\left(k_2^+\right)^2\right] \left|\mathcal{I}^m\left((b)\right)\right|^2$$

$$- k_0^+ k_1^+ \left[2(k_0^+ + k_2^+)k_1^+ + 2k_0^+(k_1^+ + k_2^+) - (D-4)(k_2^+)^2\right]$$

$$\times \text{Re}\Big(\mathcal{I}^m\left((a)\right)^* \mathcal{I}^m\left((b)\right)\Big)\Big\} + O(\alpha_{em}\,\alpha_s^2)$$

UV divergences of the $q\bar{q}g$ contribution to σ_L^γ

UV divergences :

- At $\mathbf{x}_2 \to \mathbf{x}_0$ for $|(a)|^2$ contribution
- At $\mathbf{x}_2 \to \mathbf{x}_1$ for $|(b)|^2$ contribution

UV divergences of the $q\bar{q}g$ contribution to σ_L^γ

UV divergences :

- At $\mathbf{x}_2 \to \mathbf{x}_0$ for $|(a)|^2$ contribution
- At $\mathbf{x}_2 \to \mathbf{x}_1$ for $|(b)|^2$ contribution

Traditional method to deal with these UV divergences:

1. Make the subtraction $\left[1 - \mathcal{S}^{(3)}_{012}\right] \to \left[1 - \mathcal{S}^{(3)}_{012}\right] - \left[1 - \mathcal{S}_{01}\right]$ in $\sigma_L^\gamma|_{q\bar{q}g}$
2. Add the corresponding term to $\sigma_L^\gamma|_{q\bar{q}}$

It works for the divergences, but it is far from optimal in the present case!
$\Rightarrow$ Let us present an improvement of that method.

Properties of the Fourier integral

$$\mathcal{I}^m\left(\mathbf{r},\mathbf{r}';\overline{Q}^2,\mathcal{C}\right) \equiv (\mu^2)^{2-\frac{D}{2}} \int \frac{d^{D-2}\mathbf{P}}{(2\pi)^{D-2}} \int \frac{d^{D-2}\mathbf{K}}{(2\pi)^{D-2}} \frac{\mathbf{K}^m\, e^{i\mathbf{K}\cdot\mathbf{r}'}\, e^{i\mathbf{P}\cdot\mathbf{r}}}{\left[\mathbf{P}^2+\overline{Q}^2\right]\left\{\mathbf{K}^2+\mathcal{C}\left[\mathbf{P}^2+\overline{Q}^2\right]\right\}}$$

Introducing Schwinger variables:

$$\begin{aligned}\mathcal{I}^m\left(\mathbf{r},\mathbf{r}';\overline{Q}^2,\mathcal{C}\right) &= \mathbf{r}'^m \left(\mathbf{r}'^2\right)^{1-\frac{D}{2}} \frac{i}{2}(2\pi)^{2-D} \left(\mu^2\right)^{2-\frac{D}{2}} \\ &\quad \times \int_0^{+\infty} d\sigma\, \sigma^{1-\frac{D}{2}}\, e^{-\sigma\overline{Q}^2}\, e^{-\frac{\mathbf{r}^2}{4\sigma}}\, \Gamma\left(\frac{D}{2}-1, \frac{\mathbf{r}'^2\mathcal{C}}{4\sigma}\right)\end{aligned}$$

Properties of the Fourier integral

$$\mathcal{I}^m\left(\mathbf{r},\mathbf{r}';\overline{Q}^2,\mathcal{C}\right) \equiv (\mu^2)^{2-\frac{D}{2}} \int \frac{d^{D-2}\mathbf{P}}{(2\pi)^{D-2}} \int \frac{d^{D-2}\mathbf{K}}{(2\pi)^{D-2}} \frac{\mathbf{K}^m\, e^{i\mathbf{K}\cdot\mathbf{r}'}\, e^{i\mathbf{P}\cdot\mathbf{r}}}{\left[\mathbf{P}^2+\overline{Q}^2\right]\left\{\mathbf{K}^2+\mathcal{C}\left[\mathbf{P}^2+\overline{Q}^2\right]\right\}}$$

Introducing Schwinger variables:

$$\begin{aligned}\mathcal{I}^m\left(\mathbf{r},\mathbf{r}';\overline{Q}^2,\mathcal{C}\right) &= \mathbf{r}'^m \left(\mathbf{r}'^2\right)^{1-\frac{D}{2}} \frac{i}{2}(2\pi)^{2-D} \left(\mu^2\right)^{2-\frac{D}{2}} \\ &\quad \times \int_0^{+\infty} d\sigma\, \sigma^{1-\frac{D}{2}}\, e^{-\sigma\overline{Q}^2}\, e^{-\frac{\mathbf{r}^2}{4\sigma}}\, \Gamma\left(\frac{D}{2}-1, \frac{\mathbf{r}'^2\mathcal{C}}{4\sigma}\right)\end{aligned}$$

For $D = 4$:

$$\mathcal{I}^m\left(\mathbf{r},\mathbf{r}';\overline{Q}^2,\mathcal{C}\right) = \frac{i}{(2\pi)^2}\left(\frac{\mathbf{r}'^m}{\mathbf{r}'^2}\right) \mathrm{K}_0\left(\overline{Q}\sqrt{\mathbf{r}^2+\mathcal{C}\,\mathbf{r}'^2}\right)$$

Properties of the Fourier integral

$$\mathcal{I}^m\left(\mathbf{r},\mathbf{r}';\overline{Q}^2,\mathcal{C}\right) \equiv (\mu^2)^{2-\frac{D}{2}} \int \frac{d^{D-2}\mathbf{P}}{(2\pi)^{D-2}} \int \frac{d^{D-2}\mathbf{K}}{(2\pi)^{D-2}} \frac{\mathbf{K}^m\, e^{i\mathbf{K}\cdot\mathbf{r}'}\, e^{i\mathbf{P}\cdot\mathbf{r}}}{\left[\mathbf{P}^2+\overline{Q}^2\right]\left\{\mathbf{K}^2+\mathcal{C}\left[\mathbf{P}^2+\overline{Q}^2\right]\right\}}$$

Introducing Schwinger variables:

$$\begin{aligned}\mathcal{I}^m\left(\mathbf{r},\mathbf{r}';\overline{Q}^2,\mathcal{C}\right) &= \mathbf{r}'^m \left(\mathbf{r}'^2\right)^{1-\frac{D}{2}} \frac{i}{2}(2\pi)^{2-D} \left(\mu^2\right)^{2-\frac{D}{2}} \\ &\quad \times \int_0^{+\infty} d\sigma\, \sigma^{1-\frac{D}{2}}\, e^{-\sigma\overline{Q}^2}\, e^{-\frac{\mathbf{r}^2}{4\sigma}}\, \Gamma\left(\frac{D}{2}-1, \frac{\mathbf{r}'^2\mathcal{C}}{4\sigma}\right)\end{aligned}$$

For $D=4$:

$$\mathcal{I}^m\left(\mathbf{r},\mathbf{r}';\overline{Q}^2,\mathcal{C}\right) = \frac{i}{(2\pi)^2}\left(\frac{\mathbf{r}'^m}{\mathbf{r}'^2}\right) \mathrm{K}_0\left(\overline{Q}\sqrt{\mathbf{r}^2+\mathcal{C}\,\mathbf{r}'^2}\right)$$

UV behavior: For $|\mathbf{r}'|\to 0$: $\mathcal{I}^m\left(\mathbf{r},\mathbf{r}';\overline{Q}^2,\mathcal{C}\right) \sim \mathcal{I}^m_{UV}\left(\mathbf{r},\mathbf{r}';\overline{Q}^2\right)$

$$\mathcal{I}^m_{UV}\left(\mathbf{r},\mathbf{r}';\overline{Q}^2\right) \equiv \mathbf{r}'^m \left(\mathbf{r}'^2\right)^{1-\frac{D}{2}} \frac{i}{(2\pi)^2}\Gamma\left(\frac{D}{2}-1\right)\left(\frac{2\overline{Q}}{(2\pi)^2\mu^2|\mathbf{r}|}\right)^{\frac{D}{2}-2} \mathrm{K}_{\frac{D}{2}-2}\left(\overline{Q}\,|\mathbf{r}|\right)$$

Building the UV subtraction terms

Next attempt to deal with the UV divergences : make the subtraction

$$\left\{ \left| \mathcal{I}^m\left((a)\right) \right|^2 \mathrm{Re}\left[1 - \mathcal{S}^{(3)}_{012}\right] - \left| \mathcal{I}^m_{UV}\left(\mathbf{x}_{01}, \mathbf{x}_{20}; \overline{Q}^2_{(a)}\right) \right|^2 \mathrm{Re}\left[1 - \mathcal{S}_{01}\right] \right\}$$

Cancels indeed the UV divergence at $\mathbf{x}_2 \to \mathbf{x}_0$, but produces an IR divergence at $|\mathbf{x}_{20}| \to +\infty$, absent in the original term!

Building the UV subtraction terms

Final idea: subtract the IR divergence from the UV subtraction term, as

$$\left\{ \left| \mathcal{I}^m \left((a) \right) \right|^2 \mathrm{Re}\left[1 - \mathcal{S}^{(3)}_{012} \right] - \left[\left| \mathcal{I}^m_{UV} \left(\mathbf{x}_{01}, \mathbf{x}_{20}; \overline{Q}^2_{(a)} \right) \right|^2 \right. \right.$$
$$\left. \left. - \mathrm{Re}\left(\mathcal{I}^{m*}_{UV} \left(\mathbf{x}_{01}, \mathbf{x}_{20}; \overline{Q}^2_{(a)} \right) \mathcal{I}^m_{UV} \left(\mathbf{x}_{01}, \mathbf{x}_{21}; \overline{Q}^2_{(a)} \right) \right) \right] \mathrm{Re}\left[1 - \mathcal{S}_{01} \right] \right\}$$

This difference leads to a UV and IR finite integral in $\mathbf{x}_2$.

Building the UV subtraction terms

Final idea: subtract the IR divergence from the UV subtraction term, as

$$\left\{ \left| \mathcal{I}^m \left((a) \right) \right|^2 \mathrm{Re}\left[1 - \mathcal{S}^{(3)}_{012} \right] - \left[\left| \mathcal{I}^m_{UV} \left(\mathbf{x}_{01}, \mathbf{x}_{20}; \overline{Q}^2_{(a)} \right) \right|^2 \right.\right.$$
$$\left.\left. - \mathrm{Re}\left(\mathcal{I}^{m*}_{UV} \left(\mathbf{x}_{01}, \mathbf{x}_{20}; \overline{Q}^2_{(a)} \right) \mathcal{I}^m_{UV} \left(\mathbf{x}_{01}, \mathbf{x}_{21}; \overline{Q}^2_{(a)} \right) \right) \right] \mathrm{Re}\left[1 - \mathcal{S}_{01} \right] \right\}$$

This difference leads to a UV and IR finite integral in $\mathbf{x}_2$.
$\Rightarrow$ The $D \to 4$ limit is now safe to take:

$$\to \left\{ \frac{1}{(2\pi)^4} \frac{1}{\mathbf{x}^2_{20}} \left[\mathrm{K}_0 \left(Q\, X_{012} \right) \right]^2 \mathrm{Re}\left[1 - \mathcal{S}^{(3)}_{012} \right] \right.$$
$$\left. - \frac{1}{(2\pi)^4} \left[\frac{\mathbf{x}_{20}}{\mathbf{x}^2_{20}} \cdot \left(\frac{\mathbf{x}_{20}}{\mathbf{x}^2_{20}} - \frac{\mathbf{x}_{21}}{\mathbf{x}^2_{21}} \right) \right] \left[\mathrm{K}_0 \left(\overline{Q}^2_{(a)} \left| \mathbf{x}_{01} \right| \right) \right]^2 \mathrm{Re}\left[1 - \mathcal{S}_{01} \right] \right\}$$

$$Q^2 X^2_{012} \equiv \frac{Q^2}{(q^+)^2} \left[k_0^+ k_1^+ x^2_{01} + k_0^+ k_2^+ x^2_{02} + k_1^+ k_2^+ x^2_{12} \right] = \frac{q\bar{q}g \text{ form. time}}{\gamma^* \text{ life time}}$$

UV-subtracted $q\bar{q}g$ contribution to σ_L^γ

Subtracting both UV divergences this way:

$$\sigma_L^\gamma|_{q\bar{q}g} - \sigma_L^\gamma|_{UV,|(a)|^2} - \sigma_L^\gamma|_{UV,|(b)|^2} \quad = \quad \sigma_L^\gamma|_{q\to g} + \sigma_L^\gamma|_{\bar{q}\to g}$$

where

$$\sigma_L^\gamma|_{q\to g} \quad = \quad 4N_c\,\alpha_{em}\sum_f e_f^2 \int_0^{+\infty} dk_0^+ \int_0^{+\infty} dk_1^+ \int_{k_{\min}^+}^{+\infty} \frac{dk_2^+}{k_2^+}\,\delta(k_0^+ + k_1^+ + k_2^+ - q^+)$$

$$\times \frac{\alpha_s C_F}{\pi}\,\frac{4Q^2\,(k_1^+)^2}{(q^+)^5} \int \frac{\mathrm{d}^2\mathbf{x}_0}{2\pi} \int \frac{\mathrm{d}^2\mathbf{x}_1}{2\pi} \int \frac{\mathrm{d}^2\mathbf{x}_2}{2\pi}$$

$$\times \left\{ \left[2k_0^+(k_0^+ + k_2^+) + \left(k_2^+\right)^2\right] \left[\frac{\mathbf{x}_{20}}{x_{20}^2}\cdot\left(\frac{\mathbf{x}_{20}}{x_{20}^2} - \frac{\mathbf{x}_{21}}{x_{21}^2}\right)\right] \left[\left(\mathrm{K}_0(QX_{012})\right)^2 \mathrm{Re}\left(1 - \mathcal{S}_{012}^{(3)}\right) - \left(\mathbf{x}_2 \to \mathbf{x}_0\right)\right] \right.$$

$$\left. + \left(k_2^+\right)^2 \frac{(\mathbf{x}_{20}\cdot\mathbf{x}_{21})}{x_{20}^2 x_{21}^2} \left(\mathrm{K}_0(QX_{012})\right)^2 \mathrm{Re}\left(1 - \mathcal{S}_{012}^{(3)}\right) \right\}$$

UV-subtracted $q\bar{q}g$ contribution to σ_L^γ

Subtracting both UV divergences this way:

$$\sigma_L^\gamma|_{q\bar{q}g} - \sigma_L^\gamma|_{UV,|(a)|^2} - \sigma_L^\gamma|_{UV,|(b)|^2} \quad = \quad \sigma_L^\gamma|_{q\to g} + \sigma_L^\gamma|_{\bar{q}\to g}$$

where

$$\sigma_L^\gamma|_{q\to g} \quad = \quad 4N_c\,\alpha_{em}\sum_f e_f^2 \int_0^{+\infty} dk_0^+ \int_0^{+\infty} dk_1^+ \int_{k_{\min}^+}^{+\infty} \frac{dk_2^+}{k_2^+}\,\delta(k_0^+ + k_1^+ + k_2^+ - q^+)$$

$$\times \frac{\alpha_s C_F}{\pi}\,\frac{4Q^2\,(k_1^+)^2}{(q^+)^5} \int \frac{\mathrm{d}^2\mathbf{x}_0}{2\pi} \int \frac{\mathrm{d}^2\mathbf{x}_1}{2\pi} \int \frac{\mathrm{d}^2\mathbf{x}_2}{2\pi}$$

$$\times \left\{ \left[2k_0^+(k_0^+ + k_2^+) + (k_2^+)^2\right] \left[\frac{\mathbf{x}_{20}}{x_{20}^2}\cdot\left(\frac{\mathbf{x}_{20}}{x_{20}^2} - \frac{\mathbf{x}_{21}}{x_{21}^2}\right)\right] \left[\Big(\mathrm{K}_0(QX_{012})\Big)^2 \mathrm{Re}\Big(1 - \mathcal{S}_{012}^{(3)}\Big) - \Big(\mathbf{x}_2 \to \mathbf{x}_0\Big)\right] \right.$$

$$\left. + (k_2^+)^2\,\frac{(\mathbf{x}_{20}\cdot\mathbf{x}_{21})}{x_{20}^2 x_{21}^2}\Big(\mathrm{K}_0(QX_{012})\Big)^2 \mathrm{Re}\Big(1 - \mathcal{S}_{012}^{(3)}\Big) \right\}$$

And $\sigma_L^\gamma|_{\bar{q}\to g}$: integrand obtained by exchanging the quark and antiquark: $(k_0^+, \mathbf{x}_0) \leftrightarrow (k_1^+, \mathbf{x}_1)$

$\Rightarrow \sigma_L^\gamma|_{\bar{q}\to g} = \sigma_L^\gamma|_{q\to g}$

UV-subtracted $q\bar{q}g$ contribution to σ_L^γ

Hence:

$$\sigma_L^\gamma|_{q\bar{q}g} - \sigma_L^\gamma|_{UV,|(a)|^2} - \sigma_L^\gamma|_{UV,|(b)|^2} \quad = \quad 2\,\sigma_L^\gamma|_{q\to g}$$

Changing variable to momentum fractions:

$$\sigma_L^\gamma|_{q\to g} \quad = \quad 4N_c\,\alpha_{em}\sum_f e_f^2 \int_0^1 dz\, 4Q^2z^2(1-z)^2\,\frac{\alpha_s C_F}{\pi}\int_{\frac{k^+_{\min}}{zq^+}}^1 d\xi \int\frac{\mathrm{d}^2\mathbf{x}_0}{2\pi}\int\frac{\mathrm{d}^2\mathbf{x}_1}{2\pi}\int\frac{\mathrm{d}^2\mathbf{x}_2}{2\pi}$$

$$\times\left\{\frac{\left[1+(1-\xi)^2\right]}{\xi}\left[\frac{\mathbf{x}_{20}}{x_{20}^2}\cdot\left(\frac{\mathbf{x}_{20}}{x_{20}^2}-\frac{\mathbf{x}_{21}}{x_{21}^2}\right)\right]\left[\left(\mathrm{K}_0(QX_{012})\right)^2\mathrm{Re}\left(1-\mathcal{S}^{(3)}_{012}\right)-\left(\mathbf{x}_2\to\mathbf{x}_0\right)\right]\right.$$

$$\left.+\xi\,\frac{(\mathbf{x}_{20}\cdot\mathbf{x}_{21})}{x_{20}^2x_{21}^2}\left(\mathrm{K}_0(QX_{012})\right)^2\mathrm{Re}\left(1-\mathcal{S}^{(3)}_{012}\right)\right\}$$

with now:

$$X_{012}^2 = (1-\xi)z(1-z)x_{01}^2 + \xi(1-\xi)z^2x_{20}^2 + \xi z(1-z)x_{21}^2$$

Combining the UV terms with the $q\bar{q}$ contribution to σ_L^γ

In dim. reg., the UV subtraction terms can be written as

$$\sigma_L^\gamma|_{UV,|(a)|^2} + \sigma_L^\gamma|_{UV,|(b)|^2}$$

$$= 4N_c\,\alpha_{em}\sum_f e_f^2 \int \frac{\mathrm{d}^{D-2}\mathbf{x}_0}{2\pi} \int \frac{\mathrm{d}^{D-2}\mathbf{x}_1}{2\pi} \int_0^{+\infty} dk_0^+ \int_0^{+\infty} dk_1^+\,\delta(k_0^+ + k_1^+ - q^+)$$

$$\times \frac{4Q^2}{(q^+)^5}\,(k_0^+ k_1^+)^2 \left[\frac{\overline{Q}^2}{(2\pi)^2\mu^2 x_{01}^2}\right]^{\frac{D}{2}-2} \left[\mathrm{K}_{\frac{D}{2}-2}\left(|\mathbf{x}_{01}|\,\overline{Q}\right)\right]^2$$

$$\times \left(\frac{\alpha_s\,C_F}{\pi}\right) \left[\widetilde{\mathcal{V}}^L_{UV,|(a)|^2} + \widetilde{\mathcal{V}}^L_{UV,|(b)|^2}\right] \mathrm{Re}\left[1 - \mathcal{S}_{01}\right]$$

Combining the UV terms with the $q\bar{q}$ contribution to σ_L^γ

In dim. reg., the UV subtraction terms can be written as

$$\sigma_L^\gamma|_{UV,|(a)|^2} + \sigma_L^\gamma|_{UV,|(b)|^2}$$
$$= 4N_c\,\alpha_{em}\sum_f e_f^2 \int \frac{\mathrm{d}^{D-2}\mathbf{x}_0}{2\pi} \int \frac{\mathrm{d}^{D-2}\mathbf{x}_1}{2\pi} \int_0^{+\infty} dk_0^+ \int_0^{+\infty} dk_1^+\,\delta(k_0^+ + k_1^+ - q^+)$$
$$\times \frac{4Q^2}{(q^+)^5}\,(k_0^+ k_1^+)^2 \left[\frac{\overline{Q}^2}{(2\pi)^2\mu^2 x_{01}^2}\right]^{\frac{D}{2}-2} \left[\mathrm{K}_{\frac{D}{2}-2}\left(|\mathbf{x}_{01}|\,\overline{Q}\right)\right]^2$$
$$\times \left(\frac{\alpha_s\,C_F}{\pi}\right) \left[\widetilde{\mathcal{V}}^L_{UV,|(a)|^2} + \widetilde{\mathcal{V}}^L_{UV,|(b)|^2}\right] \mathrm{Re}\left[1-\mathcal{S}_{01}\right]$$

With:

$$\widetilde{\mathcal{V}}^L_{UV,|(a)|^2} = \Gamma\left(\frac{D}{2}-2\right)\,(\pi\mu^2\mathbf{x}_{01}^2)^{2-\frac{D}{2}}\left[\log\left(\frac{k^+_{\mathrm{min}}}{k_0^+}\right) + \frac{3}{4} - \frac{(D-4)}{8}\right]$$

Combining the UV terms with the $q\bar{q}$ contribution to σ_L^γ

In dim. reg., the UV subtraction terms can be written as

$$\sigma_L^\gamma|_{UV,|(a)|^2} + \sigma_L^\gamma|_{UV,|(b)|^2}$$
$$= 4N_c\,\alpha_{em}\sum_f e_f^2 \int \frac{\mathrm{d}^{D-2}\mathbf{x}_0}{2\pi} \int \frac{\mathrm{d}^{D-2}\mathbf{x}_1}{2\pi} \int_0^{+\infty} dk_0^+ \int_0^{+\infty} dk_1^+\,\delta(k_0^+ + k_1^+ - q^+)$$
$$\times \frac{4Q^2}{(q^+)^5}\,(k_0^+ k_1^+)^2 \left[\frac{\overline{Q}^2}{(2\pi)^2\mu^2 x_{01}^2}\right]^{\frac{D}{2}-2} \left[\mathrm{K}_{\frac{D}{2}-2}\left(|\mathbf{x}_{01}|\,\overline{Q}\right)\right]^2$$
$$\times \left(\frac{\alpha_s\,C_F}{\pi}\right) \left[\widetilde{\mathcal{V}}^L_{UV,|(a)|^2} + \widetilde{\mathcal{V}}^L_{UV,|(b)|^2}\right] \mathrm{Re}\left[1-\mathcal{S}_{01}\right]$$

With:

$$\widetilde{\mathcal{V}}^L_{UV,|(b)|^2} = \Gamma\left(\frac{D}{2}-2\right)\,(\pi\mu^2\mathbf{x}_{01}^2)^{2-\frac{D}{2}}\left[\log\left(\frac{k^+_{\mathrm{min}}}{k_1^+}\right) + \frac{3}{4} - \frac{(D-4)}{8}\right]$$

Combining the UV terms with the $q\bar{q}$ contribution to σ_L^γ

Expanding around $D = 4$:

$$\widetilde{\mathcal{V}}^L_{UV,|(a)|^2} + \widetilde{\mathcal{V}}^L_{UV,|(b)|^2} = -2\left[\frac{1}{\left(2-\frac{D}{2}\right)} - \Psi(1) + \log\left(\pi\,\mathbf{x}_{01}{}^2\,\mu^2\right)\right] \times \left[\log\left(\frac{k^+_{\min}}{\sqrt{k_0^+ k_1^+}}\right) + \frac{3}{4}\right] - \frac{1}{2} + O(D-4)$$

Combining the UV terms with the $q\bar{q}$ contribution to σ_L^γ

Expanding around $D = 4$:

$$\widetilde{\mathcal{V}}^L_{UV,|(a)|^2} + \widetilde{\mathcal{V}}^L_{UV,|(b)|^2} = -2\left[\frac{1}{\left(2-\frac{D}{2}\right)} - \Psi(1) + \log\left(\pi\,\mathbf{x}_{01}{}^2\,\mu^2\right)\right] \times \left[\log\left(\frac{k^+_{\min}}{\sqrt{k_0^+ k_1^+}}\right) + \frac{3}{4}\right] - \frac{1}{2} + O(D-4)$$

But in the $q\bar{q}$ contribution to σ_L^γ:

$$\widetilde{\mathcal{V}}^L = 2\left[\frac{1}{\left(2-\frac{D}{2}\right)} - \Psi(1) + \log\left(\pi\,\mathbf{x}_{01}{}^2\,\mu^2\right)\right]\left[\log\left(\frac{k^+_{\min}}{\sqrt{k_0^+ k_1^+}}\right) + \frac{3}{4}\right] + \frac{1}{2}\left[\log\left(\frac{k_0^+}{k_1^+}\right)\right]^2 - \frac{\pi^2}{6} + \frac{5}{2} + \frac{1}{2} + O(D-4)$$

$\Rightarrow$ Cancelation of:

- the UV divergence
- the $k^+_{\min}$ dependence
- the $\pm 1/2$ rational term : strong hint of UV regularization scheme independence

Combining the UV terms with the $q\bar{q}$ contribution to σ_L^γ

Total contribution for the dipole-like terms:

$$\sigma_L^\gamma|_{\rm dipole} = \sigma_L^\gamma|_{q\bar{q}} + \sigma_L^\gamma|_{UV,|(a)|^2} + \sigma_L^\gamma|_{UV,|(b)|^2}$$

$$= 4N_c\,\alpha_{em}\sum_f e_f^2 \int \frac{{\rm d}^2\mathbf{x}_0}{2\pi}\int \frac{{\rm d}^2\mathbf{x}_1}{2\pi}\int_0^{+\infty} dk_0^+ \int_0^{+\infty} dk_1^+\,\delta(k_0^+ + k_1^+ - q^+)\,\frac{4Q^2}{(q^+)^5}$$

$$\times (k_0^+ k_1^+)^2 \left[{\rm K}_0\left(|\mathbf{x}_{01}|\,\overline{Q}\right)\right]^2 \left[1 + \left(\frac{\alpha_s\,C_F}{\pi}\right)\,\widetilde{\mathcal{V}}^L_{\rm reg.}\right]\,\,{\rm Re}\left[1 - \mathcal{S}_{01}\right]$$

With:

$$\widetilde{\mathcal{V}}^L_{\rm reg.} \equiv \widetilde{\mathcal{V}}^L + \widetilde{\mathcal{V}}^L_{UV,|(a)|^2} + \widetilde{\mathcal{V}}^L_{UV,|(b)|^2}$$

$$= \frac{1}{2}\left[\log\left(\frac{k_0^+}{k_1^+}\right)\right]^2 - \frac{\pi^2}{6} + \frac{5}{2}$$

Combining the UV terms with the $q\bar{q}$ contribution to σ_L^γ

Total contribution for the dipole-like terms:

$$\sigma_L^\gamma|_{\rm dipole} = \sigma_L^\gamma|_{q\bar{q}} + \sigma_L^\gamma|_{UV,|(a)|^2} + \sigma_L^\gamma|_{UV,|(b)|^2}$$

$$= 4N_c\,\alpha_{em}\sum_f e_f^2\int_0^1 dz\,4Q^2z^2(1-z)^2\int\frac{{\rm d}^2\mathbf{x}_0}{2\pi}\int\frac{{\rm d}^2\mathbf{x}_1}{2\pi}\,{\rm Re}\left[1-\mathcal{S}_{01}\right]$$

$$\times\left[{\rm K}_0\left(Q\sqrt{z(1-z)}|\mathbf{x}_{01}|\right)\right]^2\left\{1+\left(\frac{\alpha_s\,C_F}{\pi}\right)\left[\frac{1}{2}\left[\log\left(\frac{z}{1-z}\right)\right]^2-\frac{\pi^2}{6}+\frac{5}{2}\right]\right\}$$

Full NLO result (fixed order) for σ_L^γ:

$$\begin{aligned}\sigma_L^\gamma &= \sigma_L^\gamma|_{q\bar{q}} + \sigma_L^\gamma|_{q\bar{q}g}\\ &= \sigma_L^\gamma|_{\rm dipole} + \sigma_L^\gamma|_{q\to g} + \sigma_L^\gamma|_{\bar{q}\to g}\\ &= \sigma_L^\gamma|_{\rm dipole} + 2\,\sigma_L^\gamma|_{q\to g}\end{aligned}$$

Transverse photon case: result for σ_T^γ at NLO

- Cancellation of UV divergence follow the same pattern in the γ_T case
- Results can be expressed in the same form:

$$\begin{aligned}\sigma_T^\gamma &= \sigma_T^\gamma|_{q\bar{q}} + \sigma_T^\gamma|_{q\bar{q}g} \\ &= \sigma_T^\gamma|_{\text{dipole}} + \sigma_T^\gamma|_{q\to g} + \sigma_T^\gamma|_{\bar{q}\to g} \\ &= \sigma_T^\gamma|_{\text{dipole}} + 2\,\sigma_T^\gamma|_{q\to g}\end{aligned}$$

where:

$$\begin{aligned}\sigma_T^\gamma|_{\text{dipole}} = {} & 4N_c\,\alpha_{em}\sum_f e_f^2\int_0^1 dz\, z(1-z)\int\frac{\mathrm{d}^2\mathbf{x}_0}{2\pi}\int\frac{\mathrm{d}^2\mathbf{x}_1}{2\pi}\,\mathrm{Re}\left[1-\mathcal{S}_{01}\right] \\ & \times\left[z^2+(1-z)^2\right]\,Q^2\left[\mathrm{K}_1\left(Q\sqrt{z(1-z)}|\mathbf{x}_{01}|\right)\right]^2 \\ & \times\left\{1+\left(\frac{\alpha_s\,C_F}{\pi}\right)\left[\frac{1}{2}\left[\log\left(\frac{z}{1-z}\right)\right]^2-\frac{\pi^2}{6}+\frac{5}{2}\right]\right\}\end{aligned}$$

Transverse photon case: result for σ_T^γ at NLO

Main complication: diagrammatic calculations lead to a cumbersome expression for the contributions to $\sigma_L^\gamma|_{q\bar{q}g}$, see: G.B., PRD85 (2012)

However, after lengthy algebraic manipulations, the results can be simplified into:

$$\sigma_T^\gamma|_{q\to g} = 4N_c\,\alpha_{em}\sum_f e_f^2\int_0^1 dz\, z(1-z)\,\frac{\alpha_s C_F}{\pi}\int_{\frac{k^+_{\min}}{zq^+}}^1 d\xi\int\frac{\mathrm{d}^2\mathbf{x}_0}{2\pi}\int\frac{\mathrm{d}^2\mathbf{x}_1}{2\pi}\int\frac{\mathrm{d}^2\mathbf{x}_2}{2\pi}$$

$$\times\Bigg\{\left[z^2+(1-z)^2\right]\frac{\left[1+(1-\xi)^2\right]}{\xi}\left[\frac{\mathbf{x}_{20}}{x_{20}^2}\cdot\left(\frac{\mathbf{x}_{20}}{x_{20}^2}-\frac{\mathbf{x}_{21}}{x_{21}^2}\right)\right]$$

$$\times\left[Q^2\Big(\mathrm{K}_1\left(QX_{012}\right)\Big)^2\mathrm{Re}\Big(1-\mathcal{S}_{012}^{(3)}\Big)-\Big(\mathbf{x}_2\to\mathbf{x}_0\Big)\right]$$

$$+\xi\left[\left[z^2+(1-z)^2\right]\frac{(\mathbf{x}_{20}\cdot\mathbf{x}_{21})}{x_{20}^2x_{21}^2}+2z(1-z)(1-\xi)\frac{(\mathbf{x}_{20}\cdot\mathbf{x}_{21})}{x_{20}^2X_{012}^2}-\frac{z(1-\xi)}{X_{012}^2}\right]$$

$$\times Q^2\Big(\mathrm{K}_1\left(QX_{012}\right)\Big)^2\mathrm{Re}\Big(1-\mathcal{S}_{012}^{(3)}\Big)\Bigg\}$$

Final step: BK/JIMWLK resummation

1. Assign k^+_{min} to the scale set by the target: $k^+_{\text{min}} = \frac{Q_0^2}{2x_0\,P^-} = \frac{x_{Bj}\,Q_0^2}{x_0\,Q^2}\,q^+$
2. Choose a factorization scale $k_f^+ \lesssim k_0^+, k_1^+$, corresponding to a range for the high-energy evolution $Y_f^+ \equiv \log\left(\frac{k_f^+}{k^+_{\text{min}}}\right) = \log\left(\frac{x_0\,Q^2\,k_f^+}{x_{Bj}\,Q_0^2\,q^+}\right)$
3. In the LO term in the observable, make the replacement

$$\langle \mathcal{S}_{01}\rangle_0 \quad = \quad \langle \mathcal{S}_{01}\rangle_{Y_f^+} - \int_0^{Y_f^+} dY^+ \left(\partial_{Y^+}\langle \mathcal{S}_{01}\rangle_{Y^+}\right)$$

   with both terms calculated with the same evolution equation
4. Combine the second term with the NLO correction to cancel its k^+_{min} dependence and the associated large logs.

$\Rightarrow$ Works straightforwardly in the case of

- the naive LL BK equation
- the kinematically improved LL BK equation as implemented in G.B., PRD89 (2014)

Should also work with the other implementation (Iancu *et al.*, PLB744 (2015)), but might require a bit more work.

Conclusion

1. Direct calculation of $\gamma_{T,L} \to q\bar{q}$ LFWFs at one-gluon-loop order, both in momentum and in mixed space

2. Full NLO corrections to F_L and F_T from the combination of the $q\bar{q}$ and $q\bar{q}g$ contributions, with improved method to cancel UV divergences

Phenomenology outlook : All ingredients soon available for fits to HERA data at NLO+LL accuracy, and hopefully NLO+NLL accuracy, in the dipole factorization, including gluon saturation.

Theory outlook :

- Application of the NLO $\gamma_{T,L} \to q\bar{q}(g)$ LFWFs to calculate other DIS observables at NLO?
- Extension to the case of massive quarks?
- Comparison to other calculations of photon impact factor at NLO ?
  Bartels et al.(2001-2004); Balitsky, Chirilli (2011-2013)

Linear and non-linear small-x evolution in pQCD

Simon Caron-Huot

(McGill University)

Based on: 1501.03754
1604.07417 (w/ Matti Herranen)

RBRC saturation workshop, Brookhaven, April. 27th 2017

Motivations

I'll be discussing higher-order perturbative corrections.

1. BFKL convergence is slow:

[~'98]

attributed to DGLAP physics -> resum.

[Salam; Ball,Forte ~'00,… Iancu,Mueller et al '14]

theoretically, this fits one data point.
⇒how well does it predict 3-loop?

Further Motivations

2. Multi-loops are standard in many QCD contexts

(β: 4(5) loops; DGLAP: 3 loops; Higgs σ: 3loops,…)

Q_s^2 in saturation physics never that big…

3. Purely theoretical:

-partonic amplitudes in Regge limit:
unique insight into scattering at high loops

-generally interesting limit (pomeron→graviton in AdS CFT,…)

-new qualitative features @NNLL(non-planar pomeron loop…)

Outline

1. New duality between rapidity & soft evolution
   [cf Duff Neill's talk!]

2. Rapidity-Soft duality as a computation tool
   -What is needed at NLO
   -Why do they match even in QCD?

3. Outline of NNLO (so far, N=4 SYM)
   -test 1: integrability
   -test 2: collinear limits& DGLAP

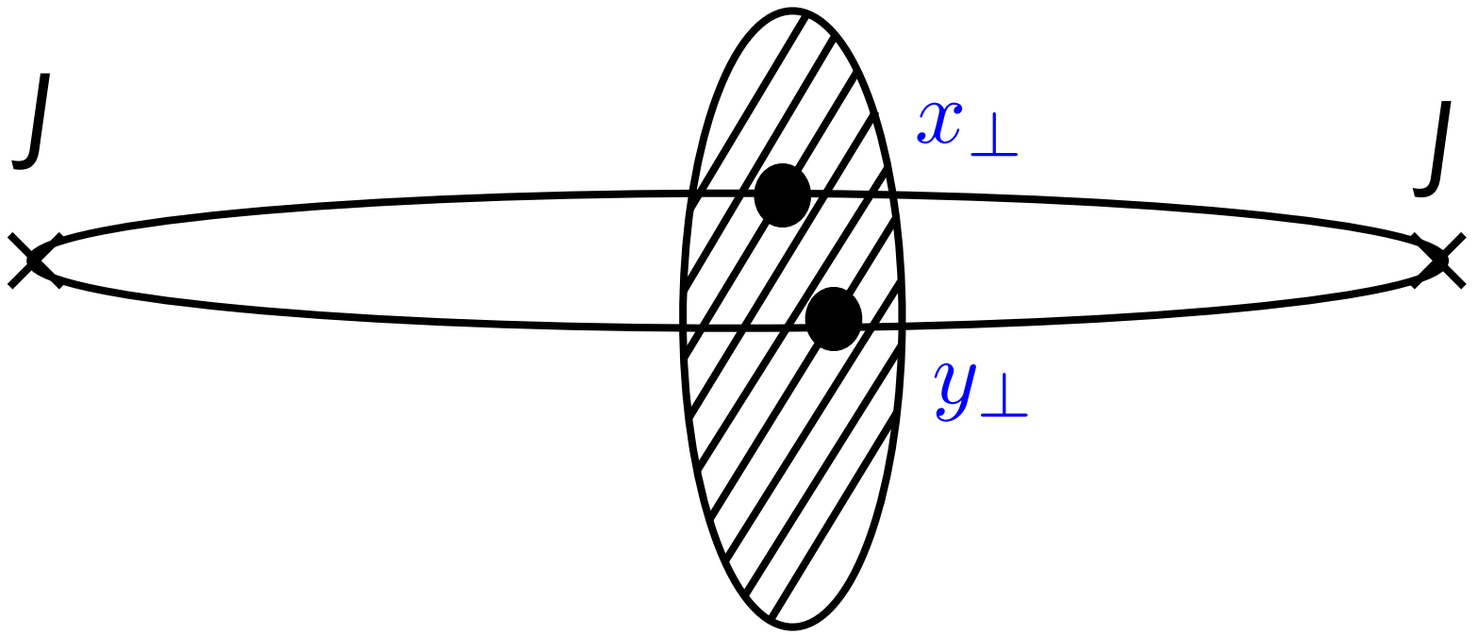
NLO BFKL&BK ('98,'07)
were hard to compute

A different formulation
would be nice

- Consider amplitude (like others in this workshop):

$$\sigma_{\rm DIS} \propto \mathrm{Im}\, A(\gamma^* p \to \gamma^* p)$$

- Dipole picture: $\to \int d^2x d^2y\, \rho(x-y)\, \langle U_{xy} \rangle_{\rm target}$

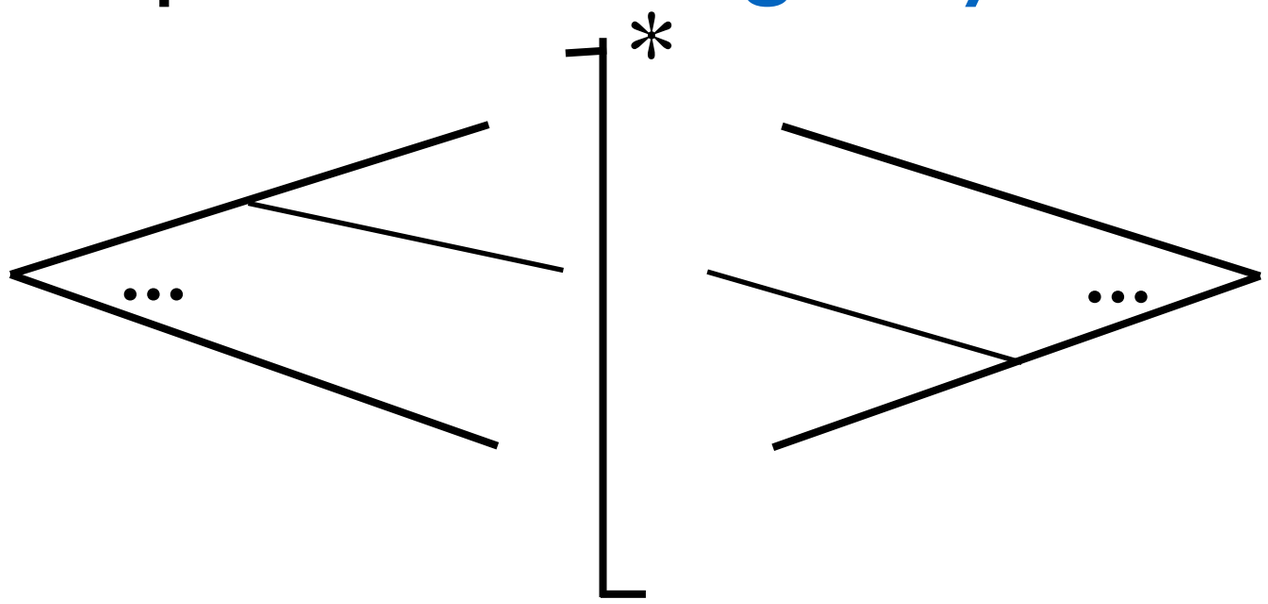


[Mueller; Balitsky; Kovchegov; JIMWLK,…]

Small dipole: transparent $(U \to 1)$

Large dipole: opaque $(U \to 0)$

- General (semi-exclusive) jet observables can be phrased analogously



$$\sigma = \sum_n \int d\mathrm{Lips}_n(\{p_i\})\, u(\{\theta_i\}, \{E_i\})\, |A_n|^2$$

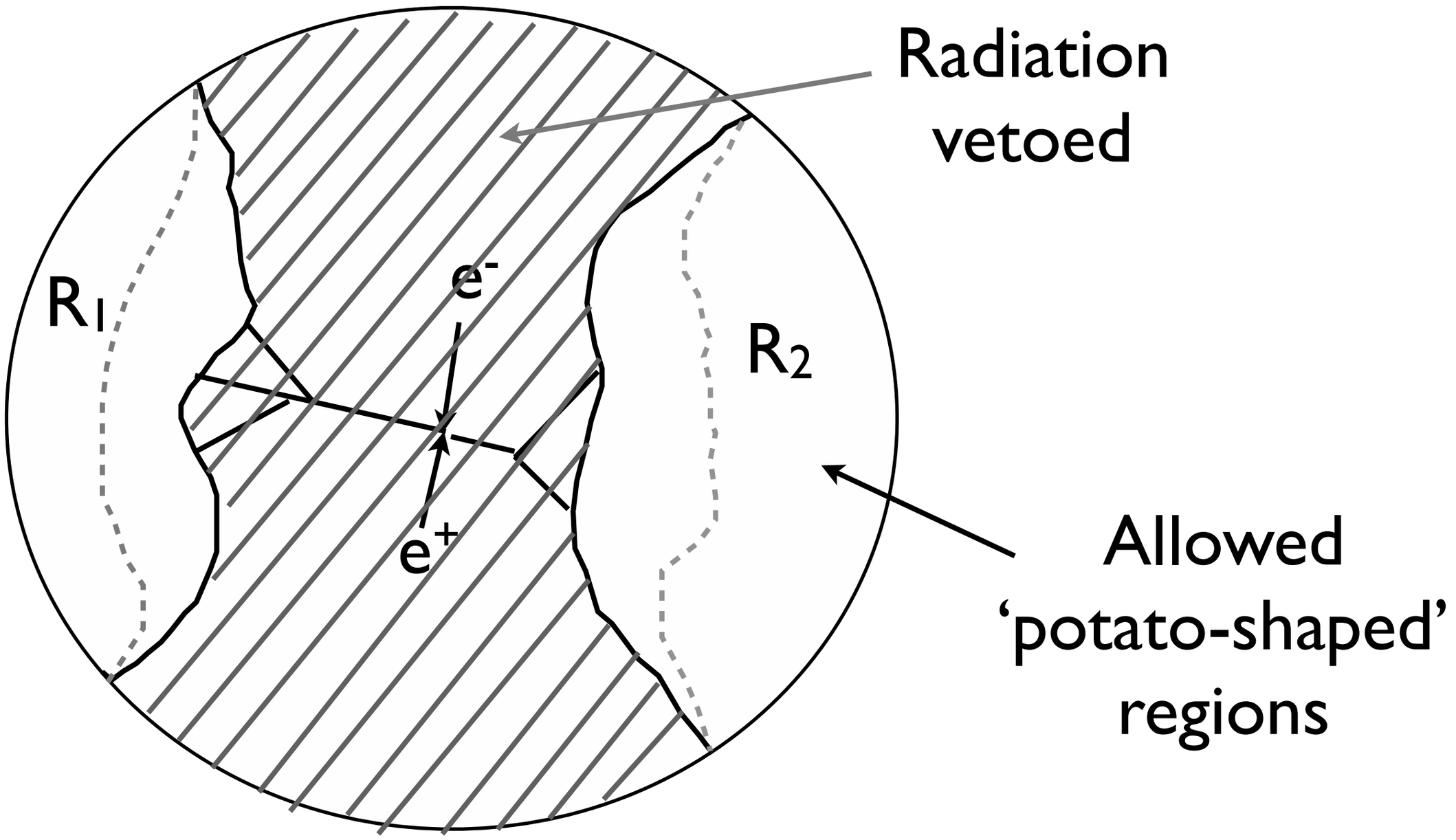
measurement ‘u’ encodes all the experimental cuts

Forward scattering ⇔ jet observables

Target	Measurement
Transparent	Allowed region
Opaque	Veto region
Rapidity Y	?

Non-global logs

Q: Cross-section for $e^+e^- \to X$, with 'X' energy smaller than E_0 outside some region R



- Archetype for some actually interesting questions ('how much energy inside a fixed cone',…)

- Suppressed by large soft* logs

$$\exp(-\#\alpha_s \log(Q/E_{\rm cut})$$

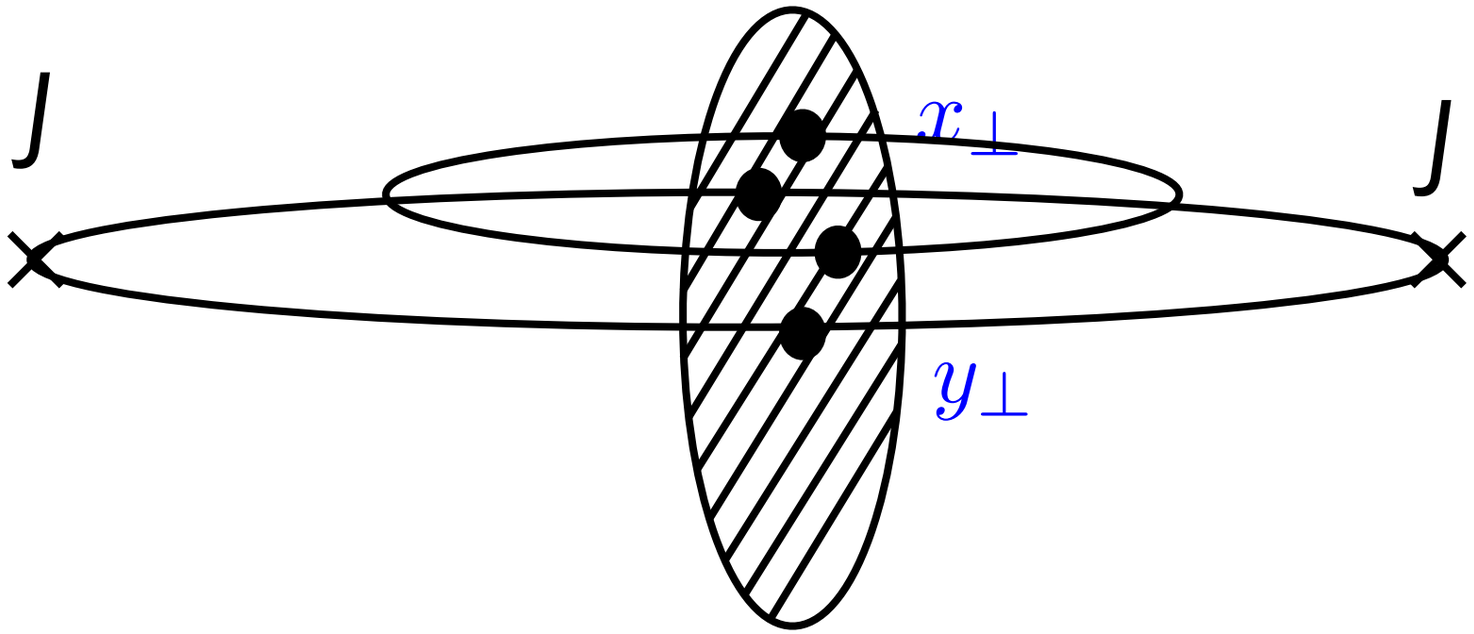
[Salam&Dasupta '01
Banfi, Salam& Dasgupta '03]

- angles not 'globally integrated'

- Difficulty: need to keep track of all radiation in allowed region! [color&angle]

*'soft'=GeV<E_{cut}<<TeV

In forward scattering we also keep all radiation

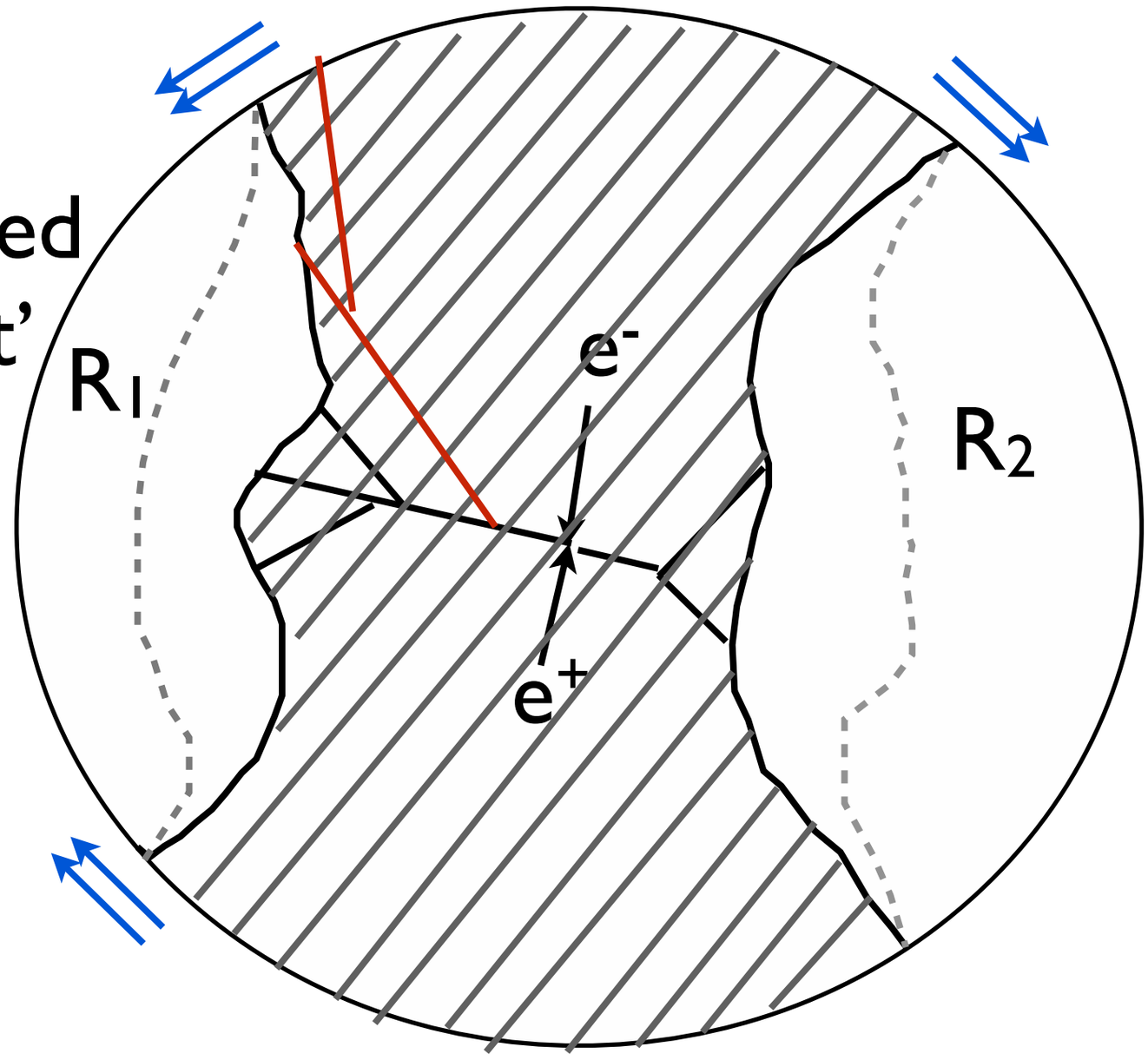


More and more dipoles
become saturated (opaque) at high rapidity

With increased energy, near-boundary jets less likely

Effective allowed
='transparent'
shrinks

veto region 'opaque':
effectively grows



Rapidity evolution (small x amplitude)	⇔	Soft evolution (small E cross-section)
Transparent		Allowed region
Opaque		Vetoed region
Rapidity Y		Soft veto
smaller dipoles		effective veto
saturate		region grows

- Both controlled by soft gluons
- Care not about energies, but about color
- Promote measurement functions to matrices

$$u(\theta, E) \to U_j^i(\theta)$$

(can be viewed as Wilson lines which will source softer radiation)

- Quantitative equivalence:

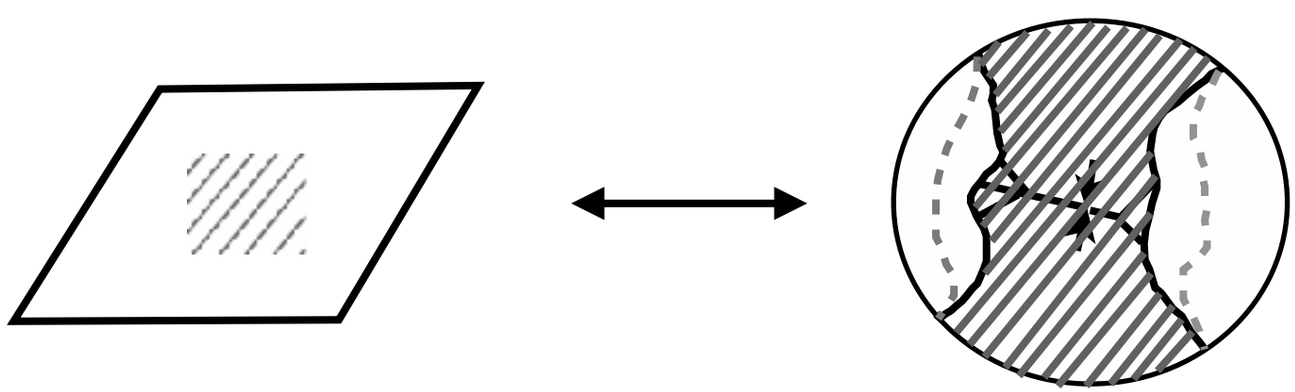
BK: $$\frac{d}{d\eta}U_{12} = \frac{\lambda}{8\pi^2}\int \frac{d^2z_0}{\pi}\frac{z_{12}^2}{z_{10}z_{02}}\left(U_{10}U_{02}-U_{12}\right)$$ Rapidity evolution

BMS: $$E\frac{d}{dE}U_{12} = \frac{\lambda}{8\pi^2}\int \frac{d^2\Omega_0}{4\pi}\frac{\alpha_{12}}{\alpha_{10}\alpha_{02}}\left(U_{10}U_{02}-U_{12}\right)$$ Soft evolution

- Conformal (stereographic) transformation:

$$\alpha_{ij} \equiv \frac{1-\cos\theta_{ij}}{2} \to z_{ij}^2 \equiv (z_i - z_j)^2, \qquad \frac{d\Omega}{4\pi} \to \frac{d^2z}{\pi}$$

[Weigert '03; Hatta '08-…]



Outline

1. New duality between rapidity & soft evolution

2. Rapidity-Soft duality as a computation tool
   -What is needed at NLO
   -Why does it work even in QCD?

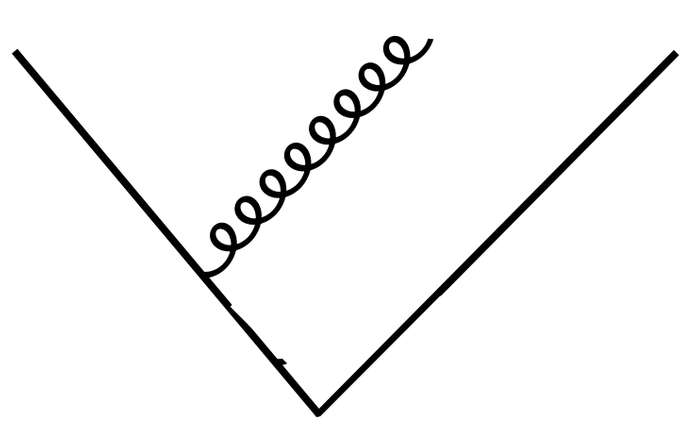
3. Outline of NNLO (so far, N=4 SYM)
   -test 1: integrability
   -test 2: collinear limits& DGLAP

Computing non-global logs

- Soft gluon amplitude is universal:

[Weinberg]

$$\lim_{p_0 \to 0} M_{n+1} = \sum_i \frac{\epsilon \cdot p_i}{p_0 \cdot p_i} g T_i^a \times M_n$$



- For a parent dipole:

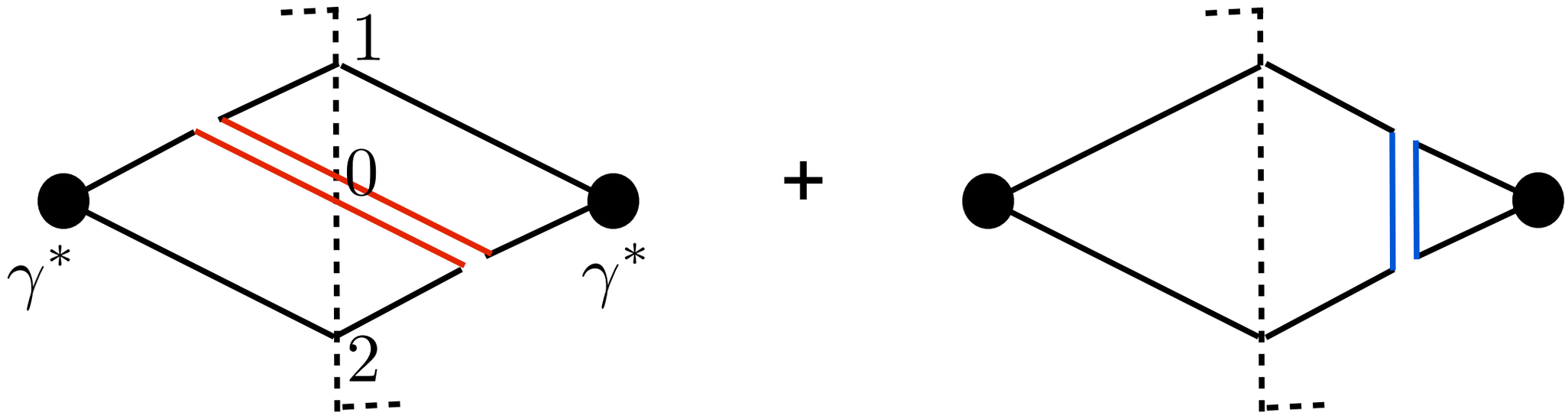
$$|M_3|^2 \simeq \frac{s_{12}}{s_{10} s_{02}} |M_2|^2$$

- Energy logs from usual IR divergent phase space:

$$\int d\mathrm{Lips}(p_0)|M_3|^2 \to |M_2|^2 \int_{E_0}^{Q} \frac{dp_0}{p_0} \int \frac{d\Omega}{4\pi} \frac{\alpha_{12}}{\alpha_{10}\alpha_{02}}$$

$\sim \log(Q/E_{\mathrm{cut}})$

- Radiated gluon will induce softer radiation at later steps: dress with a Wilson line

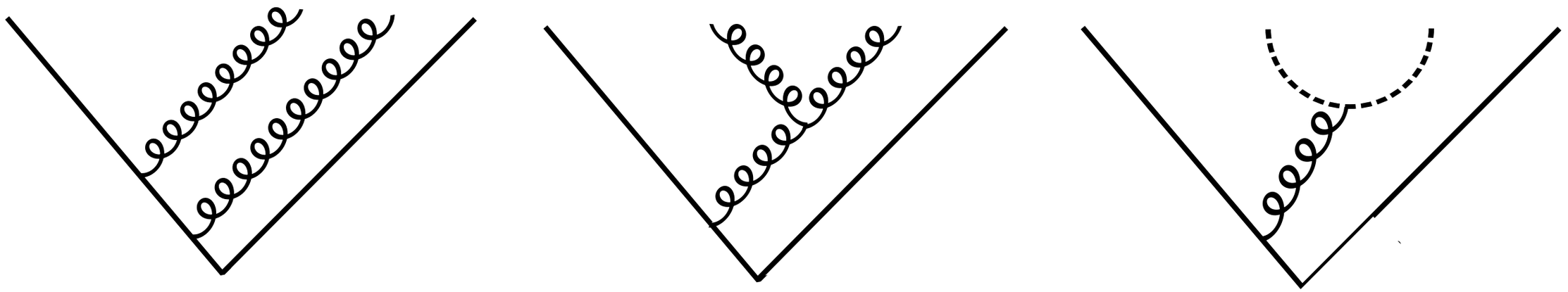


- Similar to textbook computation of IR divergences, except angular integral ‘not global’!

$$E\frac{d}{dE}U_{12} = \frac{\lambda}{8\pi^2}\int\frac{d^2\Omega_0}{4\pi}\frac{\alpha_{12}}{\alpha_{10}\alpha_{02}}\left(U_{10}U_{02}-U_{12}\right)$$ [BMS eq] ✔

- Real& virtual related by KLN [cancel for U=1]

NLO:



[Catani&Grazzini '99]

Square of tree-level soft current relatively simple:

$$|\mathcal{S}|^2 = \frac{s_{12}}{s_{10}s_{00'}s_{0'2}}\left[1+\frac{s_{12}s_{00'}+s_{10}s_{0'2}-s_{10'}s_{20}}{2(s_{10}+s_{10'})(s_{02}+s_{0'2})}\right]$$

N=4SYM

$$+(n_F-4)\frac{s_{12}}{s_{00'}(s_{10}+s_{10'})(s_{20}+s_{20'})}$$

$$+(2+n_s-2n_F)\frac{(s_{10}s_{20'}-s_{10'}s_{20'})^2}{2s_{00'}^2(s_{10}+s_{10'})^2(s_{20}+s_{20'})^2}$$

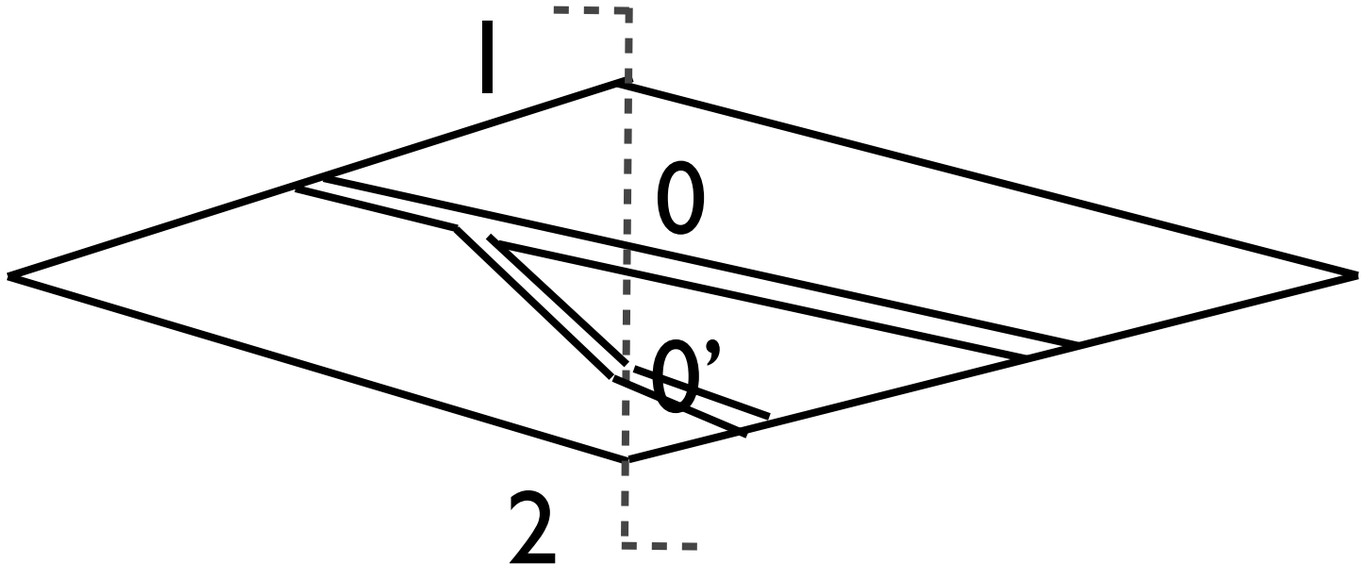
← general gauge thy

[SCH, '15]

- Crucial: two soft gluons not independent

$$|\mathcal{S}|^2 = \frac{s_{12}}{s_{10}s_{00'}s_{0'2}}\left[1+\frac{s_{12}s_{00'}+s_{10}s_{0'2}-s_{10'}s_{20}}{2(s_{10}+s_{10'})(s_{02}+s_{0'2})}\right]$$

- Amplitude depends on ratio of soft gluon energies
- NLO is basically the integral over that ratio

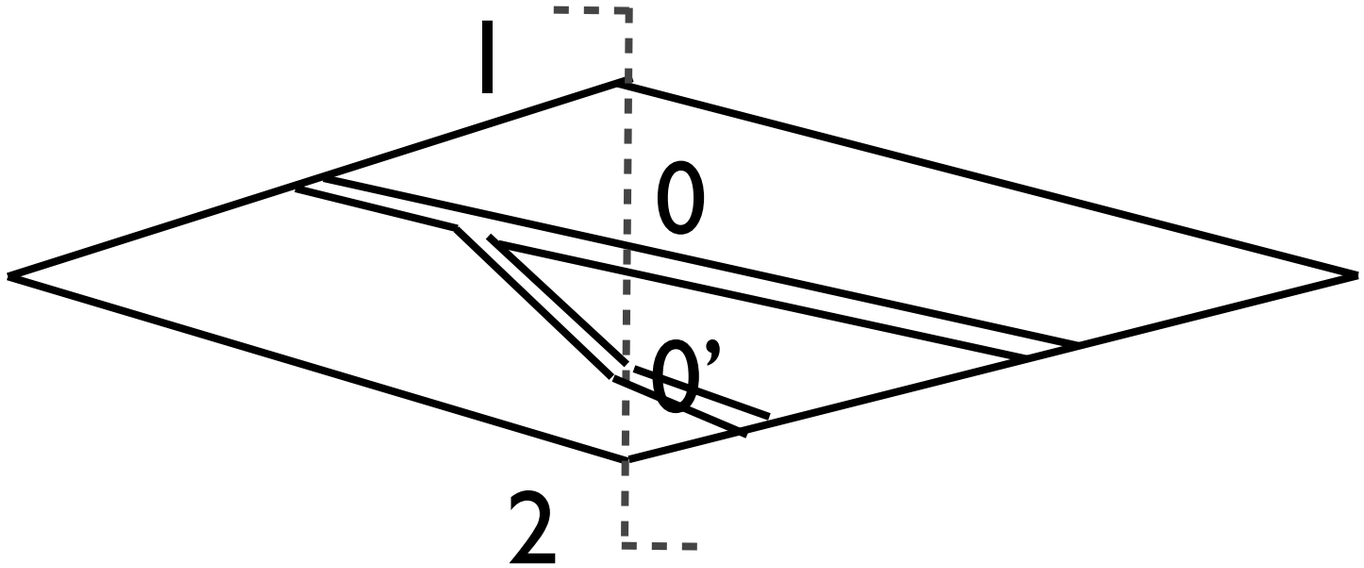


Pull out angular integrals:

$$E\frac{d}{dE}U_{12} \supset \int \frac{d^2\Omega_0}{4\pi}\frac{d^2\Omega_{0'}}{4\pi} K_{[1\,00'\,2]} U_{10}U_{00'}U_{0'2}$$

Integrate over relative energies:

$$K_{[1\,00'\,2]} = \int_0^\infty \tau d\tau \left[\left| \mathcal{S}(\tau\beta_0, \beta_{0'}) \right|^2 \right]$$



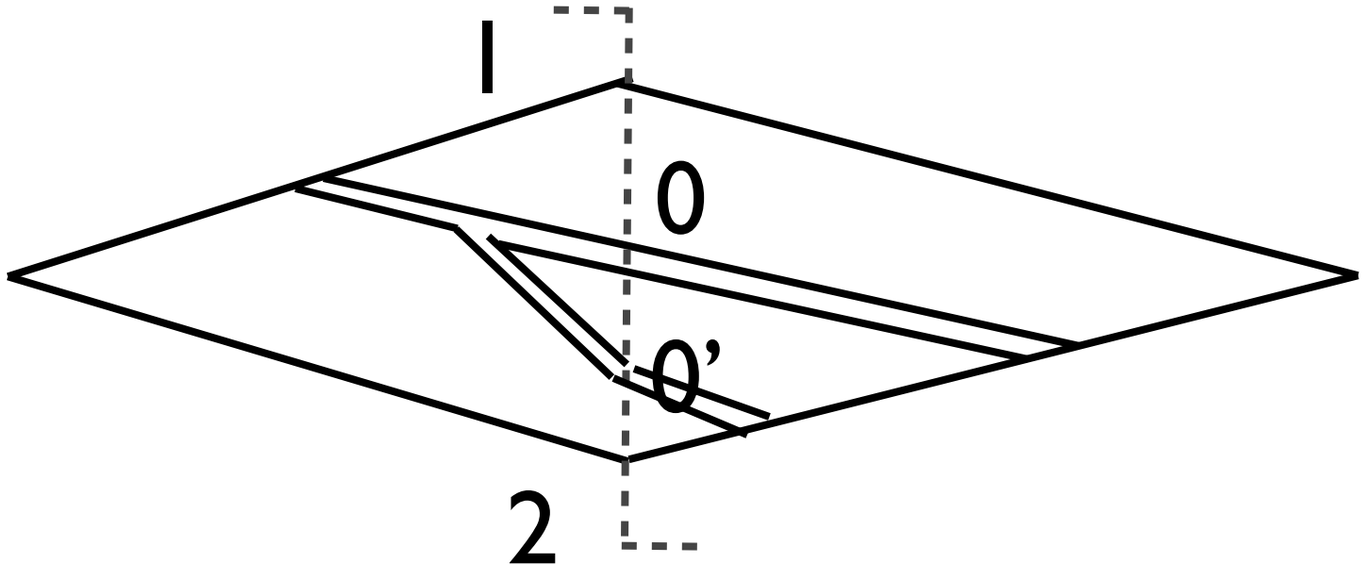
Pull out angular integrals:

$$E\frac{d}{dE}U_{12} \supset \int \frac{d^2\Omega_0}{4\pi}\frac{d^2\Omega_{0'}}{4\pi} K_{[1\,00'\,2]} U_{10}U_{00'}U_{0'2}$$

Integrate over relative energies:

$$K_{[1\,00'\,2]} = \int_0^\infty \tau d\tau \left[\left|\mathcal{S}(\tau\beta_0, \beta_{0'})\right|^2 - \Big|_{\tau\to 0}\theta(\tau{<}1) - \Big|_{\tau\to\infty}\theta(\tau{>}1)\right]$$

Subtract iterations of LO



Pull out angular integrals:

$$E\frac{d}{dE}U_{12} \supset \int \frac{d^2\Omega_0}{4\pi}\frac{d^2\Omega_{0'}}{4\pi} K_{[1\,00'\,2]} U_{10}U_{00'}U_{0'2}$$

Integrate over relative energies:

$$K_{[1\,00'\,2]} = \int_0^\infty \tau d\tau \left[\begin{array}{l} \left|\mathcal{S}(\tau\beta_0, \beta_{0'})\right|^2 \\ -\big|_{\tau\to 0}\theta(Q^2_{[1\tau 00']} < Q^2_{[10'2]}) \\ -\big|_{\tau\to\infty}\theta(Q^2_{[00'2]} < Q^2_{1\tau 02]}) \end{array} \right]$$

Best: order w/Lorentz-invariant trans. mom $Q^2_{[i0j]} \equiv \dfrac{s_{i0}s_{0j}}{s_{ij}}$

- That's basically it! NLO (planar) evolution:

$$K^{(2)}U_{12} = \int_{\beta_0,\beta_{0'}} \frac{\alpha_{12}}{\alpha_{10}\alpha_{00'}\alpha_{0'2}} K^{(2)}_{[1\,00'\,2]} \left(U_{10}U_{02}+U_{10'}U_{0'2}-2U_{10}U_{00'}U_{0'2}\right) + \gamma_K^{(2)} K^{(1)}U_{12}$$

$$K^{(2)}_{[1\,00'\,2]} = 2\log\frac{\alpha_{12}\alpha_{00'}}{\alpha_{10'}\alpha_{02}} + \left(1+\frac{\alpha_{12}\alpha_{00'}}{\alpha_{10}\alpha_{0'2}-\alpha_{10'}\alpha_{02}}\right)\log\frac{\alpha_{10}\alpha_{0'2}}{\alpha_{10'}\alpha_{02}}$$



- Precisely Balitsky&Chirilli's (N=4) result!!!

[Balistky&Chirilli '07,'08]

- Eigenvalues match 'Pomeron trajectory'

[Fadin&Lipatov(&Kotikov) '98;
Ciafaloni&Gamici '98]

- Full non-planar NLO result also available (N=4&QCD)

$$
\begin{aligned}
K^{(2)} = & \int_{i,j,k}\int \frac{d^2\Omega_0}{4\pi}\frac{d^2\Omega_{0'}}{4\pi} K^{(2)\ell}_{ijk;00'} i f^{abc}\left(L^a_{i;0}L^b_{j;0'}R^c_k - R^a_{i;0}R^b_{j;0'}L^c_k\right) \\
& + \int_{i,j}\int \frac{d^2\Omega_0}{4\pi}\frac{d^2\Omega_{0'}}{4\pi} K^{(2)N=4,\ell}_{ij;00'}\left(f^{abc}f^{a'b'c'}U^{bb'}_0 U^{cc'}_{0'} - \frac{C_A}{2}(U^{aa'}_0 + U^{aa'}_{0'})\right)(L^a_i R^{a'}_j + R^{a'}_i L^a_j) \\
& + \int_{i,j}\int \frac{d^2\Omega_0}{4\pi}\frac{\alpha_{ij}}{\alpha_{0i}\alpha_{0j}}\gamma^{(2)}_K\left(R^a_{i;0}L^a_j + L^a_{i;0}R^a_j\right) + K^{(2)N\neq 4}. \qquad (3.32)
\end{aligned}
$$

known

[SCH '15]

$$
L^a_{i;0} \equiv (L^{a'}_i U^{a'a}_0 - R^a_i)
$$

$$
\begin{aligned}
\alpha_{0i}\alpha_{0'j}K^{(2)\ell}_{ijk;00'} = & \frac{\alpha_{ij}}{\alpha_{00'}}\log\frac{\alpha_{0'i}\alpha_{0'j}\alpha^2_{0k}}{\alpha_{0i}\alpha_{0j}\alpha^2_{0'k}} + \frac{\alpha_{ik}\alpha_{jk}}{\alpha_{0k}\alpha_{0'k}}\log\frac{\alpha_{ik}\alpha_{0'j}\alpha_{0k}}{\alpha_{jk}\alpha_{0i}\alpha_{0'k}} + \frac{\alpha_{0'i}\alpha_{jk}}{\alpha_{00'}\alpha_{0'k}}\log\frac{\alpha_{jk}\alpha_{0i}\alpha_{00'}\alpha_{0'k}}{\alpha^2_{0k}\alpha_{0'i}\alpha_{0'j}} \\
& - \frac{\alpha_{ik}\alpha_{0j}}{\alpha_{0k}\alpha_{00'}}\log\frac{\alpha_{ik}\alpha_{0'j}\alpha_{00'}\alpha_{0k}}{\alpha^2_{0'k}\alpha_{0i}\alpha_{0j}} + \frac{\alpha_{ik}\alpha_{0'j}}{\alpha_{0'k}\alpha_{00'}}\log\frac{\alpha_{ik}\alpha_{00'}}{\alpha_{0k}\alpha_{0'i}} - \frac{\alpha_{0i}\alpha_{jk}}{\alpha_{0k}\alpha_{00'}}\log\frac{\alpha_{jk}\alpha_{00'}}{\alpha_{0'k}\alpha_{0j}} \\
K^{(2)N=4,\ell}_{ij;00'} = & \frac{\alpha_{ij}}{\alpha_{0i}\alpha_{00'}\alpha_{0'j}}\left(2\log\frac{\alpha_{ij}\alpha_{00'}}{\alpha_{0'i}\alpha_{0j}} + \left[1 + \frac{\alpha_{ij}\alpha_{00'}}{\alpha_{0i}\alpha_{0'j} - \alpha_{0'i}\alpha_{0j}}\right]\log\frac{\alpha_{0i}\alpha_{0'j}}{\alpha_{0'i}\alpha_{0j}}\right). \qquad (3.33)
\end{aligned}
$$

Precisely the same as NLO B-JIMWLK result ✔

[Kovner,Mulian&Lublinski '14,
(cf's Lublinski's talk) Balitsky&Chirilli '14]

Upshots:

- Use building blocks that are standard within the pQCD/amplitudes community: soft currents



- (Already known to two-loops)

- All steps Lorentz-invariant
  (=SL2(C) conformal symmetry of transverse plane)

- No Fourier transform step: $\theta \leftrightarrow x_\perp$

- Agreement is both:
  -check on duality
  -check on recent NLO results



Wait. They look different!

$$
\begin{aligned}
H^{NLO\ JIMWLK} &= \int_{x,y} K_{2,0}(x,y)\ [J_L^a(x)\,J_L^a(y)\ +\ J_R^a(x)\,J_R^a(y)] \\
&- 2\int_{x,y,z} K_{2,1}(x,y,z)\,J_L^a(x)\,S_A^{ab}(z)\,J_R^b(y) \\
&+ \int_{x,y,z,z'} K_{2,2}(x,y;z,z')\ \Big[f^{abc}\,f^{def}\,J_L^a(x)\,S_A^{be}(z)\,S_A^{cf}(z')\,J_R^d(y)\ -\ N_c\,J_L^a(x)\,S_A^{ab}(z)\,J_R^b(y)\Big] \\
&+ \int_{w,x,y,z,z'} K_{3,2}(w;x,y;z,z') f^{acb}\Big[J_L^d(x)\,J_L^e(y)\,S_A^{dc}(z)\,S_A^{eb}(z')\,J_R^a(w) \\
&\qquad\qquad - J_L^a(w)\,S_A^{cd}(z)\,S_A^{be}(z')\,J_R^d(x)\,J_R^e(y)\Big] \\
&+ \int_{w,x,y,z} K_{3,1}(w;x,y;z)\,f^{bde}\Big[J_L^d(x)\,J_L^e(y)\,S_A^{ba}(z)\,J_R^a(w)\ -\ J_L^a(w)\,S_A^{ab}(z)\,J_R^d(x)\,J_R^e(y)\Big] \\
&+ \int_{w,x,y} K_{3,0}(w,x,y) f^{bde}\Big[J_L^d(x)\,J_L^e(y)\,J_L^b(w)\ -\ J_R^d(x)\,J_R^e(y)\,J_R^b(w)\Big]\ . \qquad (2.7)
\end{aligned}
$$

[Kovner,Lublinsky&Mulian '14]

- there are relations between real&virtual

$$K_{3,0}(w,x,y)\ =\ -\frac{1}{3}\left[\int_{z,z'} K_{3,2}(w,x,y;z,z')\ +\ \int_z K_{3,1}(w,x,y;z)\right]$$

- Upshot: grouping in previous slide: all convergent

Wait. QCD is not conformal!

- QCD non-global logs in the same way
- Regge and Soft kernels don't quite agree:

$$K_{Regge} - K_{Soft} = (11C_A - 4n_F T_F - n_S T_S) \int \left(\frac{z_{ij}^2}{z_{0i}^2 z_{0j}^2} \log(\mu^2 z_{ij}^2) + \frac{z_{0j}^2 - z_{0i}^2}{z_{0i}^2 z_{0j}^2} \log \frac{z_{0i}^2}{z_{0j}^2} \right)$$

- diff prop to β = conformal breaking, as expected!

  $\Rightarrow$ difference computable from matter loops!

Rapidity vs Soft divergences

- Work in d=4-2ε dimensions:

K_{Soft} does not depend on ε

$K_{Regge}(\epsilon)$ does

- In the conformal dimension, they are equal!

$$K_{Regge}(2\epsilon = -\beta(\alpha_s)) = K_{soft}$$

- Given the ε-dependence at lower loops, they are equivalent to each other!!!

[Vladimirov '16]

A slide from Ian Balitsky's talk (@Edinburgh):

NLO evolution of composite "conformal" dipoles in QCD

I. B. and G. Chirilli

$$a\frac{d}{da}[\mathrm{tr}\{U_{z_1}U^\dagger_{z_2}\}]^{\mathrm{comp}}_a = \frac{\alpha_s}{2\pi^2}\int d^2z_3\Big([\mathrm{tr}\{U_{z_1}U^\dagger_{z_3}\}\mathrm{tr}\{U_{z_3}U^\dagger_{z_2}\}-N_c\mathrm{tr}\{U_{z_1}U^\dagger_{z_2}\}]^{\mathrm{comp}}_a$$

$$\times\frac{z_{12}^2}{z_{13}^2z_{23}^2}\Big[1+\frac{\alpha_sN_c}{4\pi}\Big(b\ln z_{12}^2\mu^2+b\frac{z_{13}^2-z_{23}^2}{z_{13}^2z_{23}^2}\ln\frac{z_{13}^2}{z_{23}^2}+\frac{67}{9}-\frac{\pi^2}{3}\Big)\Big]$$

=O(eps)term in LO BK

$$+\frac{\alpha_s}{4\pi^2}\int\frac{d^2z_4}{z_{34}^4}\Big\{\Big[-2+\frac{z_{23}^2z_{23}^2+z_{24}^2z_{13}^2-4z_{12}^2z_{34}^2}{2(z_{23}^2z_{23}^2-z_{24}^2z_{13}^2)}\ln\frac{z_{23}^2z_{23}^2}{z_{24}^2z_{13}^2}\Big]$$

$$\times[\mathrm{tr}\{U_{z_1}U^\dagger_{z_3}\}\mathrm{tr}\{U_{z_3}U^\dagger_{z_4}\}\{U_{z_4}U^\dagger_{z_2}\}-\mathrm{tr}\{U_{z_1}U^\dagger_{z_3}U_{z_4}U^\dagger_{z_2}U_{z_3}U^\dagger_{z_4}\}-(z_4\to z_3)]$$

'conformal QCD' bit

$$+\frac{z_{12}^2z_{34}^2}{z_{13}^2z_{24}^2}\Big[2\ln\frac{z_{12}^2z_{34}^2}{z_{23}^2z_{23}^2}+\Big(1+\frac{z_{12}^2z_{34}^2}{z_{13}^2z_{24}^2-z_{23}^2z_{23}^2}\Big)\ln\frac{z_{13}^2z_{24}^2}{z_{23}^2z_{23}^2}\Big]$$

$$\times[\mathrm{tr}\{U_{z_1}U^\dagger_{z_3}\}\mathrm{tr}\{U_{z_3}U^\dagger_{z_4}\}\mathrm{tr}\{U_{z_4}U^\dagger_{z_2}\}-\mathrm{tr}\{U_{z_1}U^\dagger_{z_4}U_{z_3}U^\dagger_{z_2}U_{z_4}U^\dagger_{z_3}\}-(z_4\to z_3)]\Big\}$$

N=4 bit

$$b=\tfrac{11}{3}N_c-\tfrac{2}{3}n_f$$

$K_{\mathrm{NLO\ BK}}$ = Running coupling part + Conformal "non-analytic" (in j) part
+ Conformal analytic ($\mathcal{N}=4$) part

Linearized $K_{\mathrm{NLO\ BK}}$ reproduces the known result for the forward NLO BFKL kernel.

Outline

1. New duality between rapidity & soft evolution

2. Rapidity-Soft duality as a computation tool
   -What is needed at NLO
   -Why does it work even in QCD?

3. Outline of NNLO (so far, N=4 SYM)
   -test 1: integrability
   -test 2: collinear limits& DGLAP

NNLO

[Herranen+SCH, '16]

- Triple soft current at tree-level

  ⇒ extract from known 4-particle integrand ✓

- Double soft current at one-loop

  ⇒ extract from known one-loop 6-point ✓ [~'94]

- Single soft current at two-loops

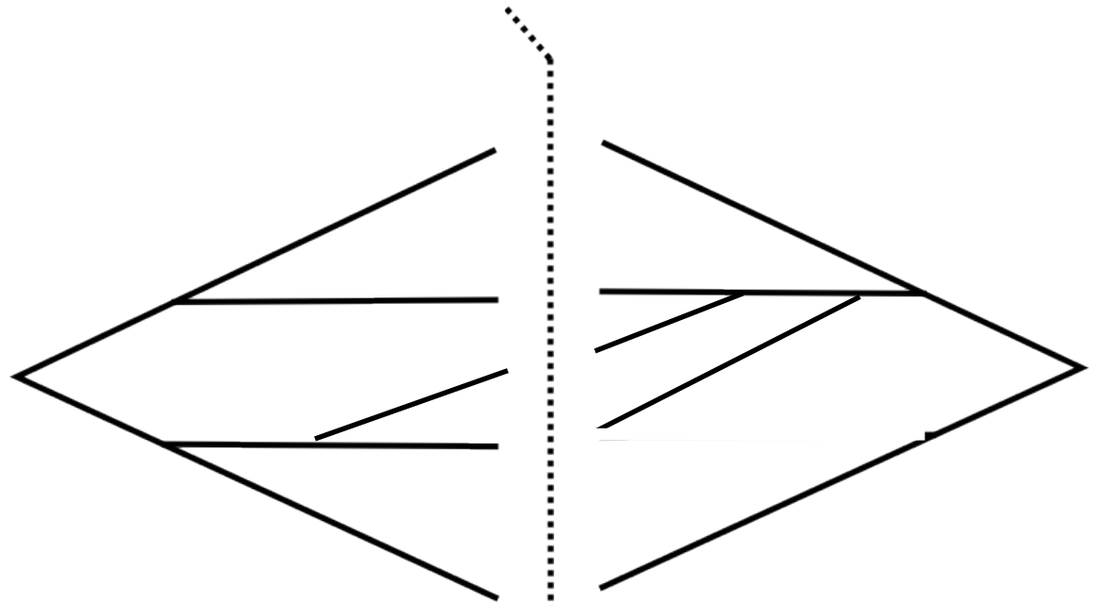
  ⇒ not needed: contribution really just $\gamma_K^{(3)}$ ✓

- Fully virtual IR divergences at three-loops

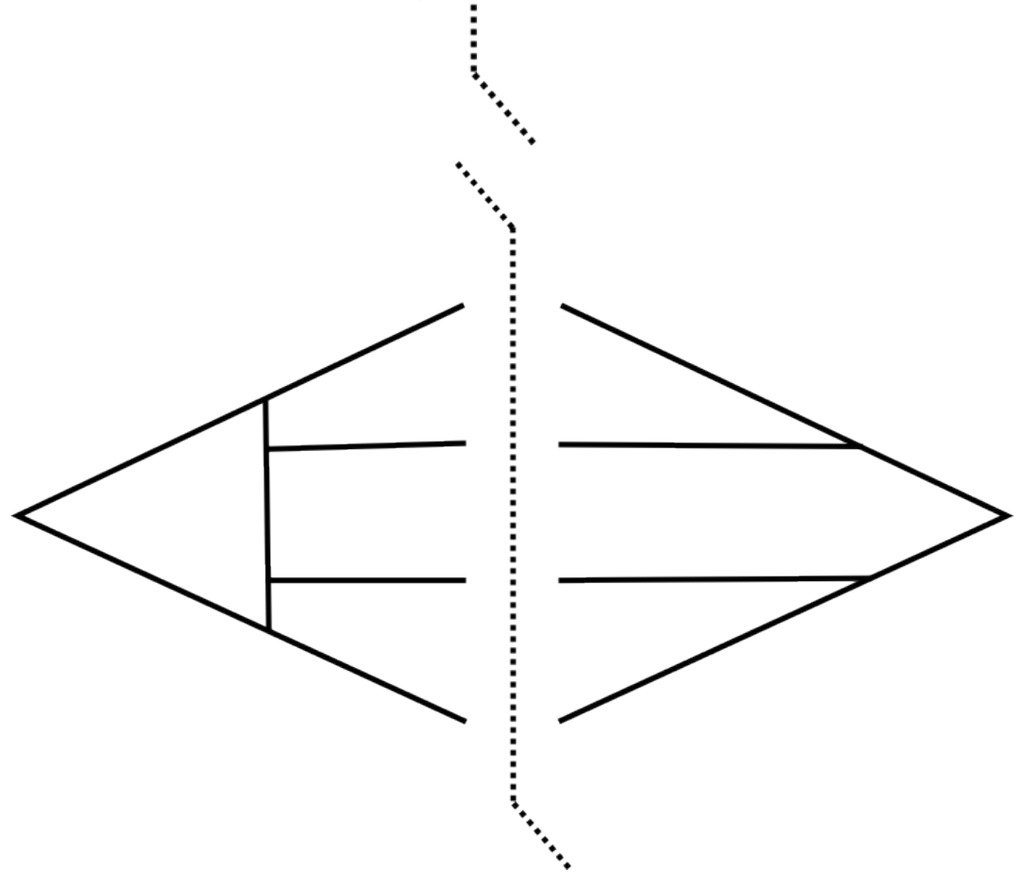
  ⇒ not needed: KLN fixes it from rest ✓

- Sample graphs we computed/borrowed:

triple soft emission (squared) at tree-level



double soft emission: tree/one-loop interference



- Recursive subtraction of subdivergences:

$$F^{\rm sub}_{[1\,0\,2]} \equiv F_{[1\,0\,2]} = 1, \tag{4.20a}$$

$$F^{\rm sub}_{[1\,00'\,2]} \equiv F_{[1\,00'\,2]} - [1\,0\,0'][1\,0'\,2] - [0\,0'\,2][1\,0\,2], \tag{4.20b}$$

$$\begin{aligned} F^{\rm sub}_{[1\,00'0''\,2]} \equiv\ & F_{[1\,00'0''\,2]} - [1\,0\,0'][1\,0'0''\,2] - [0\,0'\,0''][1\,00''\,2] - [0'\,0''\,2][1\,00'\,2] \\ & - [1\,00'\,0''][1\,0''\,2] - [0\,0'0''\,2][1\,0\,2] \\ & - [1\,0\,0'][1\,0'\,0''][1\,0''\,2] - [0'\,0''\,2][0\,0'\,2][1\,0\,2] - [0\,0'\,0''][1\,0\,0''][1\,0''\,2] \\ & - [0\,0'\,0''][0\,0''\,2][1\,0\,2] - [1\,0\,0'][0'\,0''\,2][1\,0'\,2] - [0'\,0''\,2][1\,0\,0'][1\,0'\,2]. \end{aligned} \tag{4.20c}$$

energy step functions

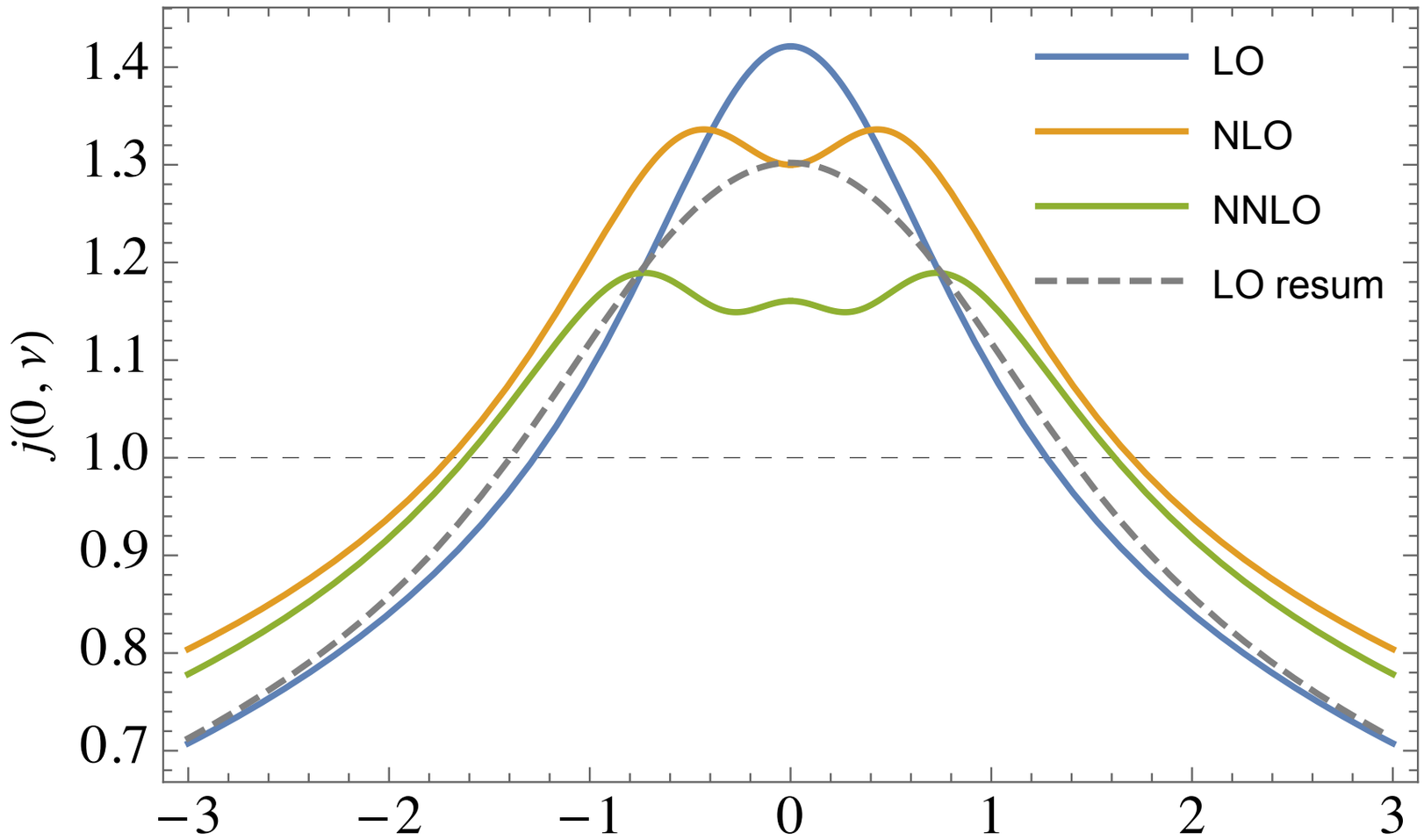
- Cleanly removes iterations of lower-loop evolution ✓

We computed only finite absolutely convergent integrals result:

$$
\begin{aligned}
K^{(3)}_{[1\,00'\,2]} = &\left(1-\frac{u}{1-v}\right)\log v\left[\log u\log\frac{v}{u}-\frac{1}{3}\log^2 v-4\zeta_2\right]+2(1+v-u)\left(\zeta_2\log\frac{u}{v}-2\zeta_3\right)\\
&+\left(\frac{2u}{1-v}+v-u-1\right)\left[4\mathrm{Li}_3\left(1-\frac{1}{v}\right)+2\mathrm{Li}_2\left(1-\frac{1}{v}\right)\log\frac{v}{u}\right]-\frac{5}{6}\log^3 u\\
&+4\big(\mathrm{Li}_3(x)+\mathrm{Li}_3(\bar{x})-2\zeta_3\big)-2\big(\mathrm{Li}_2(x)+\mathrm{Li}_2(\bar{x})+2\zeta_2\big)\log u\,. \qquad (4.35)
\end{aligned}
$$

$$
\begin{aligned}
K^{(3)}_{[1\,00'0''\,2]} = &\left(1-\frac{u_3}{1-v_1v_2}\right)\left[\begin{array}{l}2\mathrm{Li}_2\left(1-\frac{1}{v_1v_2}\right)-2\mathrm{Li}_2\left(1-\frac{1}{v_1}\right)-2\mathrm{Li}_2\left(1-\frac{1}{v_2}\right)\\+\log v_1\log v_2+\log(v_1v_2)\big(\log(u_1u_2)-\frac{3}{2}\log u_3\big)\end{array}\right]\\
&+(u_1u_2-u_1v_2-u_2v_1+v_1+v_2-u_1-u_2+u_3)\left[\mathrm{Li}_2\left(1-\frac{1}{v_1v_2}\right)-\zeta_2\right]\\
&+3\log u_1\log u_2-\tfrac{3}{2}\log^2 u_3+(1+P)(f+f_1), \qquad (4.23)
\end{aligned}
$$

Fast to evaluate, attached in computer-friendly format to arXiv submission.



- Pomeron trajectory = linearized eigenvalue

$$U_{ij} = 1 - \frac{1}{N_c}\mathcal{U}_{ij}$$

for eigenfunction: $\mathcal{U}_{m,\nu} = |z_i - z_j|^{i\nu} e^{im\arg(z_i - z_j)}$

$$\frac{d}{d\eta}\mathcal{U}_{m,\nu} = \big[j(m,\nu) - 1\big]\mathcal{U}_{m,\nu} \qquad (\Delta = 2 + i\nu)$$

[see Brower,Polchinski,Strassler&Tan]

Tests

- Collinear limit $\nu \to \pm i$ controlled by small-x limit of DGLAP

[Jaroscewicz '83; Ball, Falgari, Forte, Marzani… 07]

$$\omega^{(3)} \to +g^6\left(\frac{1024}{\gamma^5}-\frac{512}{\gamma^3}\zeta_2+\frac{576}{\gamma^2}\zeta_3-\frac{464}{\gamma}\zeta_4+840\zeta_5+64\zeta_2\zeta_3+\gamma\left(-40{\zeta_3}^2-373\zeta_6\right)\right.$$
$$\left.+\gamma^2\left(-8\zeta_2\zeta_5-86\zeta_3\zeta_4+\frac{1001}{4}\zeta_7\right)\right). \qquad (21)$$

✔

[Velizhanin '15]

- Analytic expression for m=0 conjectured using Integrability of planar N=4

$$\frac{F^{(3)}_{0,\nu}}{32} = -S_5+2S_{-4,1}-S_{-3,2}+2S_{-2,3}-S_{2,-3}-2S_{3,-2}+4S_{-3,1,1}+4S_{1,-3,1}+2S_{1,-2,2}$$
$$+2S_{1,2,-2}+2S_{2,1,-2}-8S_{1,-2,1,1}+\zeta_2\big(S_1S_2-3S_{-3}+2S_{-2,1}-4S_{1,-2}\big)-\tfrac{49}{2}\zeta_4S_1$$
$$+7\zeta_3\big(2S_{1,-1}+2(S_1-S_{-1})\log 2-S_{-2}-\log^2 2\big)+(8\zeta_{-3,1}-17\zeta_4)\big(S_{-1}-S_1+\log 2\big)$$
$$-\tfrac{1}{2}\zeta_3S_2+4\zeta_5-6\zeta_2\zeta_3+8\zeta_{-3,1,1}\,. \qquad (C.3)$$

✔

[new result for m>0]

[Gromov,Levkovich-Maslyuk&Sizov, '15]

[more on DGLAP vs BFKL: use *dimensions* instead of γ]

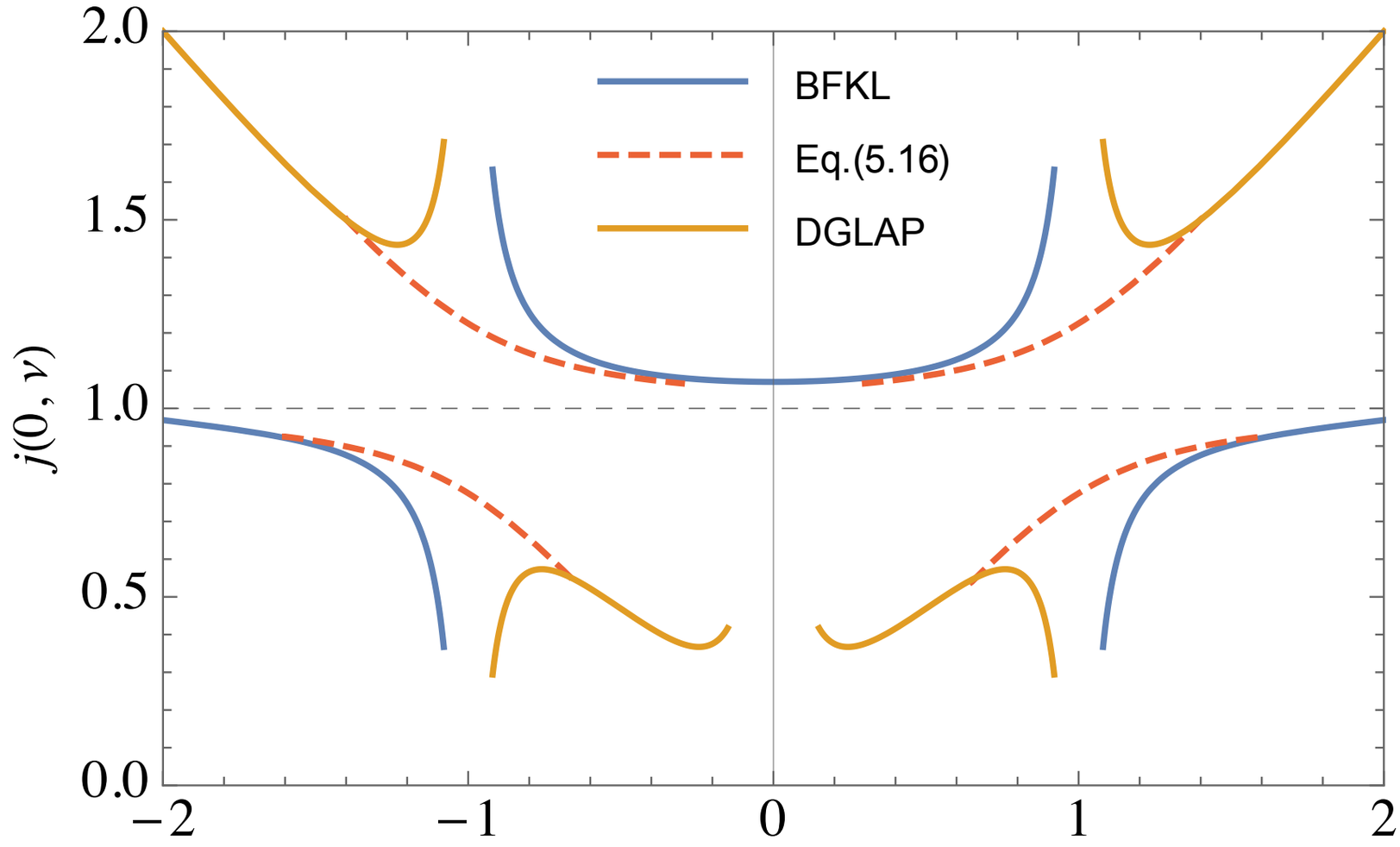


Figure 6. Level repulsion between the Pomeron and DGLAP trajectories for $m = 0$ as a function of scaling dimension, illustrating the $\nu = \pm i$ singularities. (LO expressions plotted with $\lambda = g^2_{\rm YM} N_c = 1$.)

$$j \approx 1 + \frac{\Delta - 3 \pm \sqrt{(\Delta-3)^2 + 32 g^2}}{2}, \qquad \Delta = 2 + i\nu. \tag{5.16}$$

[for polarized PDFs: level crossing is at ν=0]

Bartels, Ermolaev&Ryskin '96]

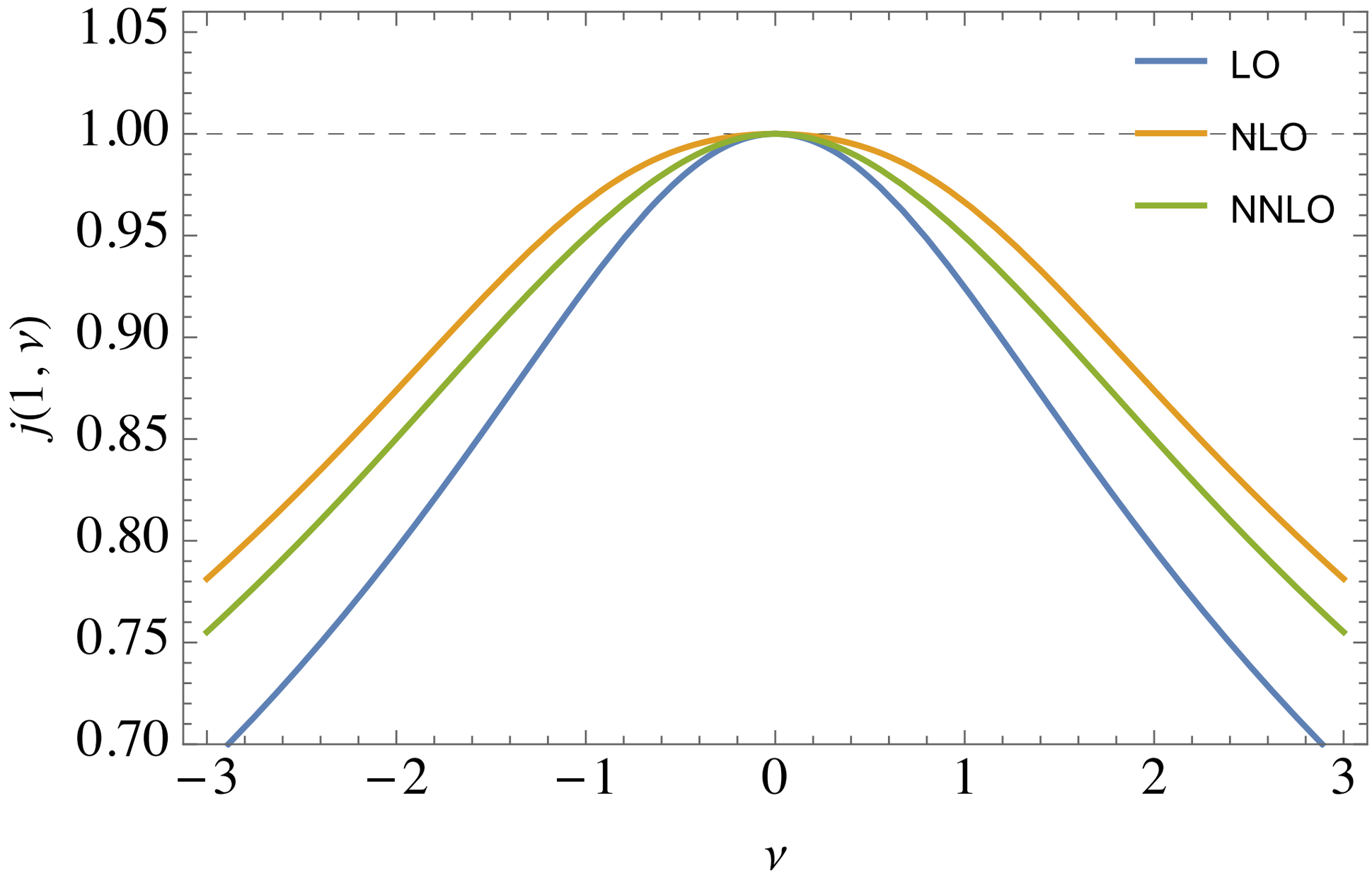
[cf Sievert & Kovchegov's talks]

Conclusions

- Established equivalence between two evolutions:
  Rapidity ⇔ Soft (in pQCD)

- NNLL Evolution now known in planar N=4 SYM:
  -linear eigenvalue for all m=0,1,2,3,…
  -include nonlinear interactions
- QCD now in sight
- Study convergence& resummations?
- Extend duality to impact factors?

m=1 (leading Odderon trajectory)



note: Odderon intercept=1 to all orders in λ.

Agrees with strong coupling!

[Tan et al '14]

On the Odderon intercept

- m=1,ν=0 is a very special wavefunction:

$$\mathcal{U}_{12} = 1 - \frac{1}{N_c}(z_1 - z_2)$$

- Strings of dipoles in planar limit telescope:

$$\mathcal{U}_{10}\mathcal{U}_{02} = 1 - \frac{1}{N_c}((z_1 - z_0) + (z_0 - z_2)) + O(1/N_c^2)$$
$$= 1 - \frac{1}{N_c}(z_1 - z_2) = \mathcal{U}_{12}$$
$$\mathcal{U}_{10}\mathcal{U}_{00'2}\mathcal{U}_{0'2} = \mathcal{U}_{12}$$
$$\dots$$

- Cancel in evolution. Thm: Odderon intercept vanishes to all order in λ in planar limit

matter loop contributions to NGLs:

$$
\begin{aligned}
K^{(2)N\neq 4} = & \int_{i,j}\int \frac{d\Omega_0}{4\pi}\frac{d\Omega_{0'}}{4\pi}\frac{1}{\alpha_{00'}}\left[\frac{\alpha_{ij}\log\frac{\alpha_{0i}\alpha_{0'j}}{\alpha_{0'i}\alpha_{0j}}}{\alpha_{0i}\alpha_{0'j}-\alpha_{0'i}\alpha_{0j}}\right](L_i^a R_j^{a'}+R_i^{a'}L_j^a) \\
& \times\Big\{2n_F\mathrm{Tr}_R\big[T^a U_0 T^{a'}U_{0'}^\dagger\big]-4f^{abc}f^{a'b'c'}U_0^{bb'}U_{0'}^{cc'}-(n_F T_R-2C_A)(U_0^{aa'}+U_{0'}^{aa'})\Big\} \\
+ & \int_{i,j}\int \frac{d\Omega_0}{4\pi}\frac{d\Omega_{0'}}{4\pi}\frac{1}{2\alpha_{00'}^2}\left[\frac{\alpha_{0i}\alpha_{0'j}+\alpha_{0'i}\alpha_{0j}}{\alpha_{0i}\alpha_{0'j}-\alpha_{0'i}\alpha_{0j}}\log\frac{\alpha_{0i}\alpha_{0'j}}{\alpha_{0'i}\alpha_{0j}}-2\right](L_i^a R_j^{a'}+R_i^{a'}L_j^a) \\
& \times\left\{\begin{array}{c}2(n_S-2n_F)\mathrm{Tr}_R\big[T^a U_0 T^{a'}U_{0'}^\dagger\big]+2f^{abc}f^{a'b'c'}U_0^{bb'}U_{0'}^{cc'} \\ -((n_S-2n_F)T_R+C_A)(U_0^{aa'}+U_{0'}^{aa'})\end{array}\right\} \\
+ & \int_{i,j} 2\pi i b_0\log(\alpha_{ij})\big(L_i^a L_j^a-R_i^a R_j^a\big). \qquad (3.34)
\end{aligned}
$$

Analyticity in Spin and Causality in Conformal Theories

(based on 1703.00278)

Simon Caron-Huot

McGill University

[Nuclear Theory]/RIKEN seminar, Brookhaven, April 18th 2017

Outline

The aim of this talk will be to present a formula…

1. Why conformal Regge theory?
   -Conformal bootstrap and large spin physics
   -AdS/CFT and bulk locality

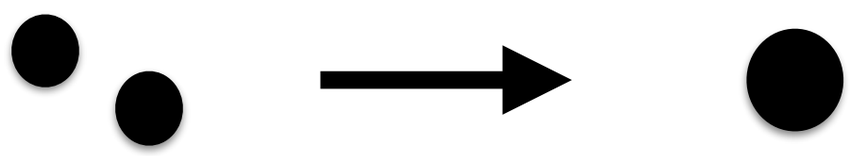
2. CFT Froissart-Gribov formula
   -Why operators are analytic in spin
   -New ingredients in CFT (ANEC&bound on chaos)

3. Applications:
   -operators of large spin
   -CFTs dual to gravity: causality&bulk locality

Conformal bootstrap

- Input: Operator Product Expansion

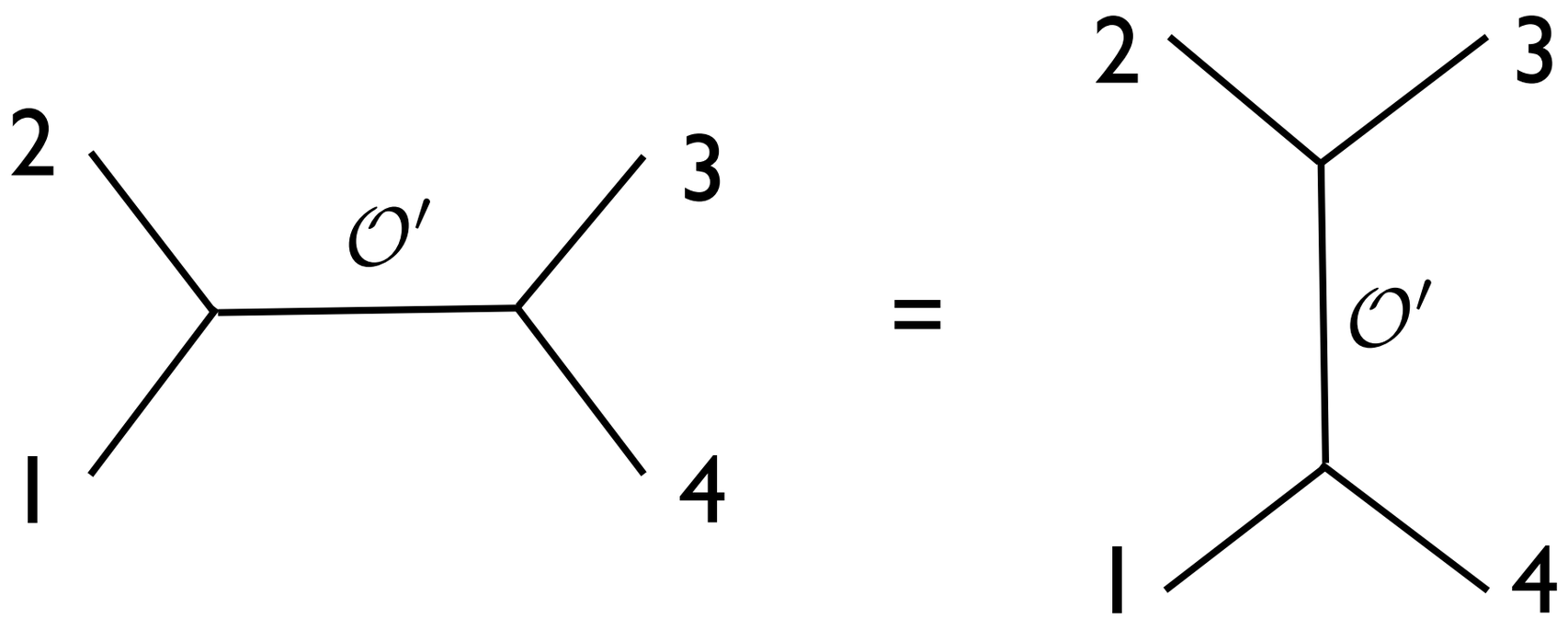
$$\lim_{y\to x}\mathcal{O}(x)\mathcal{O}(y)=\sum_{\mathcal{O}'}f_{\mathcal{O}\mathcal{O}\mathcal{O}'}(x-y)^{\#}\mathcal{O}'(x)\quad(+\text{derivatives})$$



- Converges in finite radius
- In CFT, operator have scaling exponents:

$$\#=\Delta_{\mathcal{O}'}-2\Delta_{\mathcal{O}}$$

- Dynamics: Crossing Equation



$$\sum_{\mathcal{O}'} f^2_{\mathcal{O}\mathcal{O}\mathcal{O}'}(x_{12}x_{34})^{\#} = \sum_{\mathcal{O}'} f^2_{\mathcal{O}\mathcal{O}\mathcal{O}'}(x_{23}x_{14})^{\#}$$

(+derivatives) (+derivatives)

Why is it constraining?

Imagine points are slightly closer to one limit:

$$\sum_{\mathcal{O}'} f^2_{\mathcal{O}\mathcal{O}\mathcal{O}'}(\text{smaller}) = \sum_{\mathcal{O}'} f^2_{\mathcal{O}\mathcal{O}\mathcal{O}'}(\text{bigger})$$

$$\Rightarrow\ 0 = \sum_{\mathcal{O}'} f^2_{\mathcal{O}\mathcal{O}\mathcal{O}'}(\text{bigger} - \text{smaller})$$

Naively, no solution!! (since f^2's are positive)

Why is it constraining?

Imagine points are slightly closer to one limit:

$$\sum_{\mathcal{O}'} f^2_{\mathcal{O}\mathcal{O}\mathcal{O}'}(\text{smaller}) = \sum_{\mathcal{O}'} f^2_{\mathcal{O}\mathcal{O}\mathcal{O}'}(\text{bigger})$$

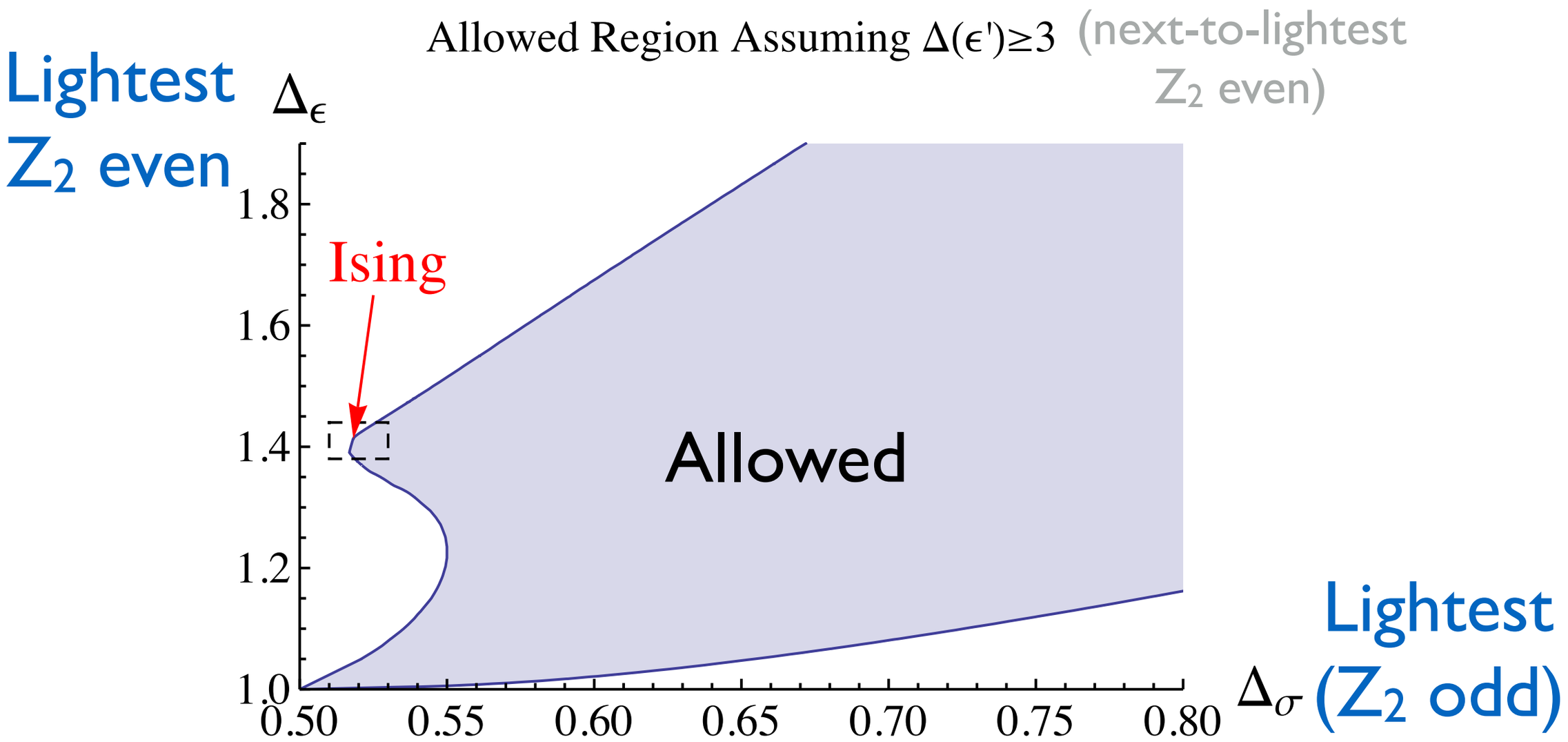
$$\Longrightarrow\ 0 = \sum_{\mathcal{O}'} f^2_{\mathcal{O}\mathcal{O}\mathcal{O}'}(\text{bigger} - \text{smaller})$$

Naively, no solution!! (since f^2's are positive)

But: first few terms go the other way: $(\# = \Delta_{\mathcal{O}'} - 2\Delta_{\mathcal{O}})$

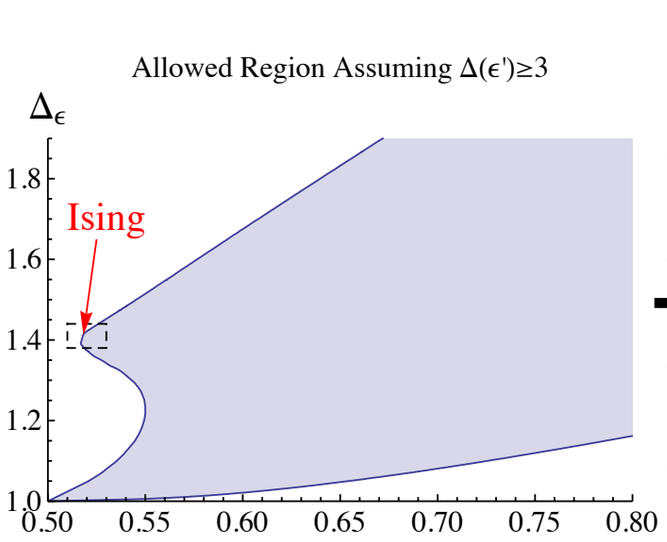
$$\Longrightarrow \sum_{\text{first few}} f^2_{\mathcal{O}\mathcal{O}\mathcal{O}'}(\text{positive}) = \sum_{\text{rest}} f^2_{\mathcal{O}\mathcal{O}\mathcal{O}'}(\text{positive})$$

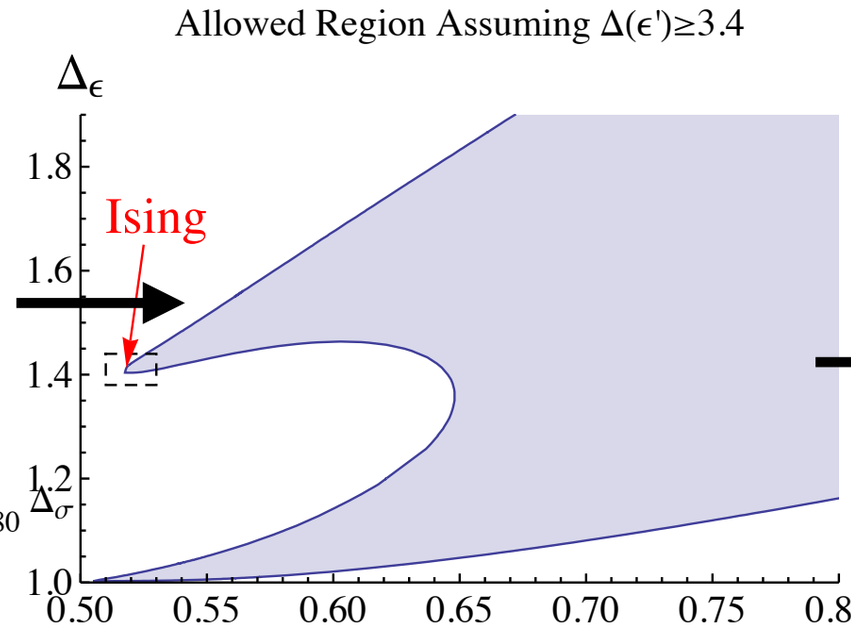
Numerical exclusion plots: the 3D Ising CFT

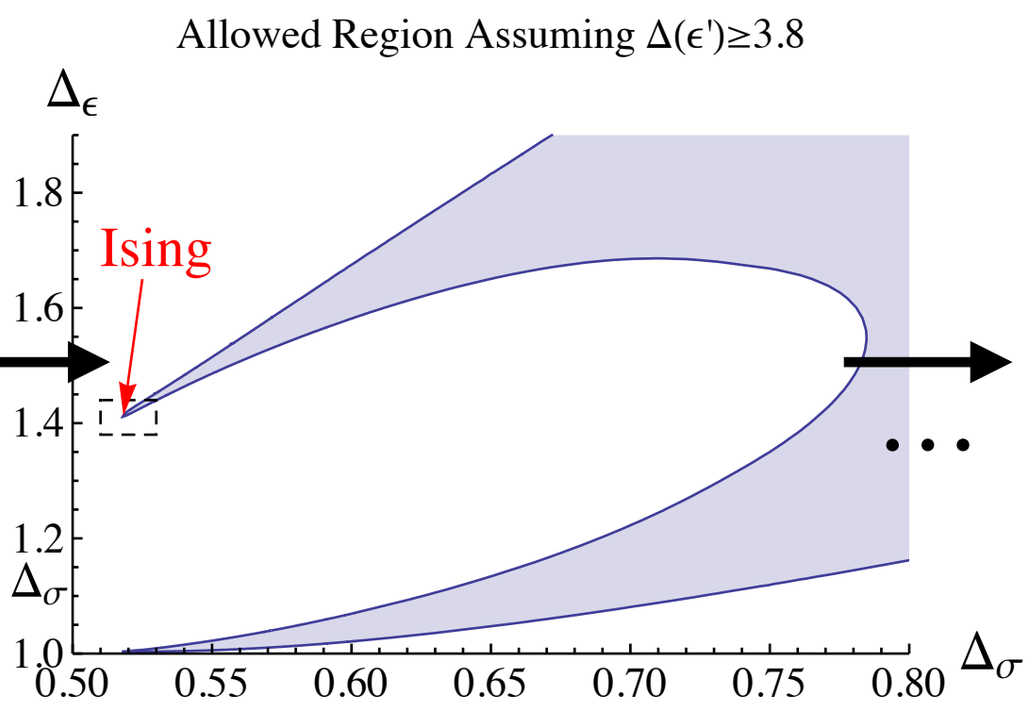


[From: El-Showk,Paulos,Poland, Rychkov,Simmons-Duffin&Vichi '12]

As one learns more about next-to-lightest op, an island is carved out







The `tip' which can't be excluded, must be the theory we're looking for!

Computer algorithm to solve multiple inequalities:
semidefinite programming [Poland,Simmons-Duffin&Vichi '11]

Leads to precise, quantitative critical exponents,
in various CFTs. Ex: 3D Ising:

spin & $\mathbb{Z}_2$	name	Δ	OPE coefficient
$\ell = 0,\ \mathbb{Z}_2 = -$	σ	$0.518154(15)$	
$\ell = 0,\ \mathbb{Z}_2 = +$	ϵ	$1.41267(13)$	$f^2_{\sigma\sigma\epsilon} = 1.10636(9)$
	ϵ'	$3.8303(18)$	$f^2_{\sigma\sigma\epsilon'} = 0.002810(6)$
$\ell = 2,\ \mathbb{Z}_2 = +$	T	3	$c/c_{\text{free}} = 0.946534(11)$
	T'	$5.500(15)$	$f^2_{\sigma\sigma T'} = 2.97(2) \times 10^{-4}$

[El-Showk,Paulos,Poland,
Rychkov,Simmons-Duffin&Vichi '14]

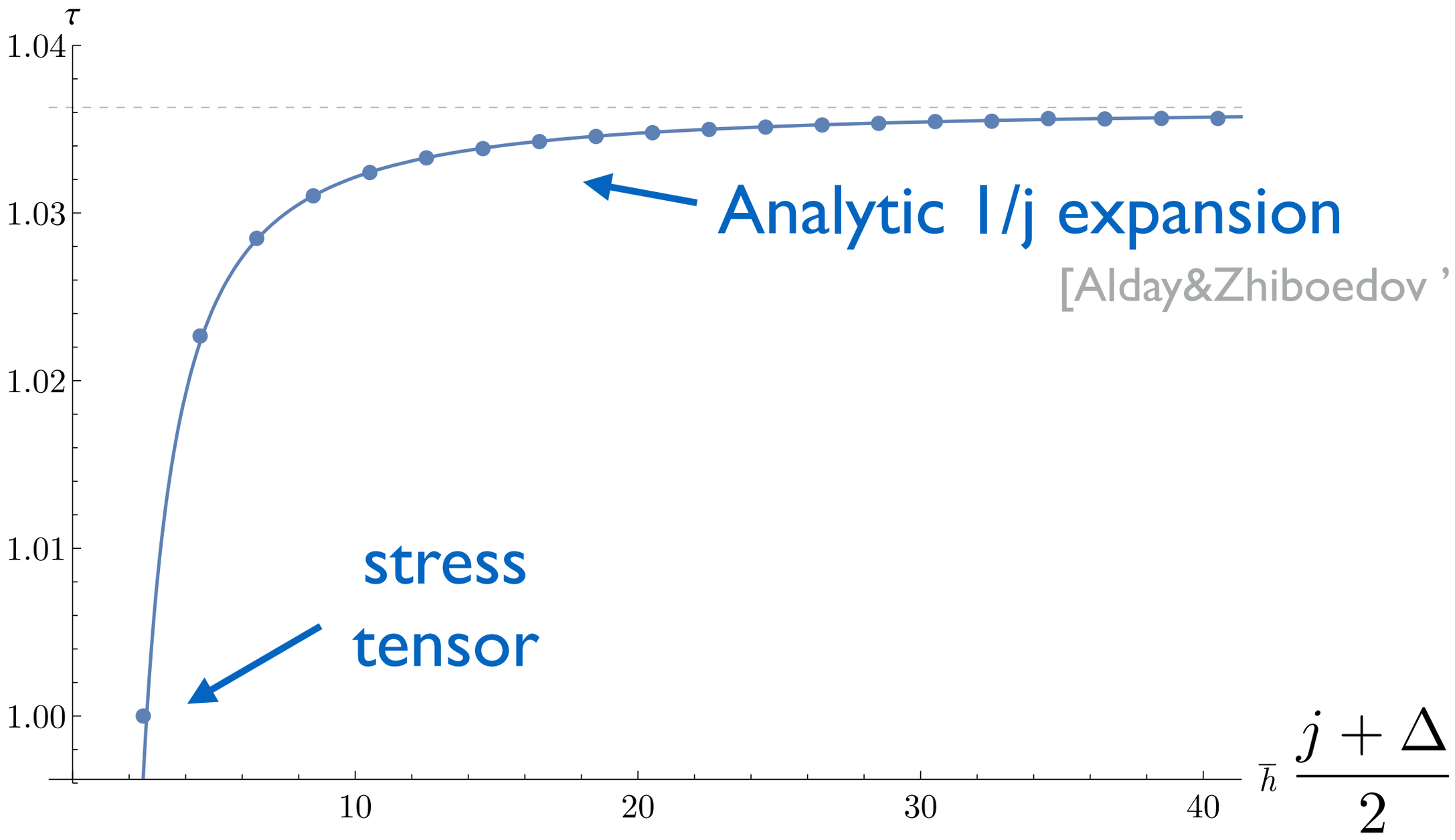
Why CFTs?

- CFTs are interesting:
  - Critical exponents in phase transitions
  - Many interesting theories are near-conformal
    (e.g. QCD at high energies)
  - Any theory of gravity in AdS is dual to a CFT

- CFTs are simpler:
  - 4-pt function depends on only 2 cross-ratios
    (compare with 6 distances: x_{ij}^2/ℓ_0^2 !)
  - total derivatives not independent operators

Empirical observation: operators lie in smooth families

$$\tau_{[\sigma\sigma]_0}(\overline{h}) \qquad = \Delta - j$$



[Plot from Simmons-Duffin '16]

Why Conformal Regge Theory?

To explain why operators organize into families ('Regge trajectories')

Quantitatively, a Froissart-Gribov inversion formula:

$$f^2_{\mathcal{O}\mathcal{O}\mathcal{O}'} = \int dz d\bar{z}\,(\ldots)\,\text{“Im}\,\mathcal{M}\text{”}$$

In AdS/CFT, this formula will know about bulk locality !

Second motivation

Conjecture:

Any large-N CFT with a large gap of operator dimension has an AdS dual, down to lengths $\ell_{\rm AdS}/\Delta_{\rm gap}$

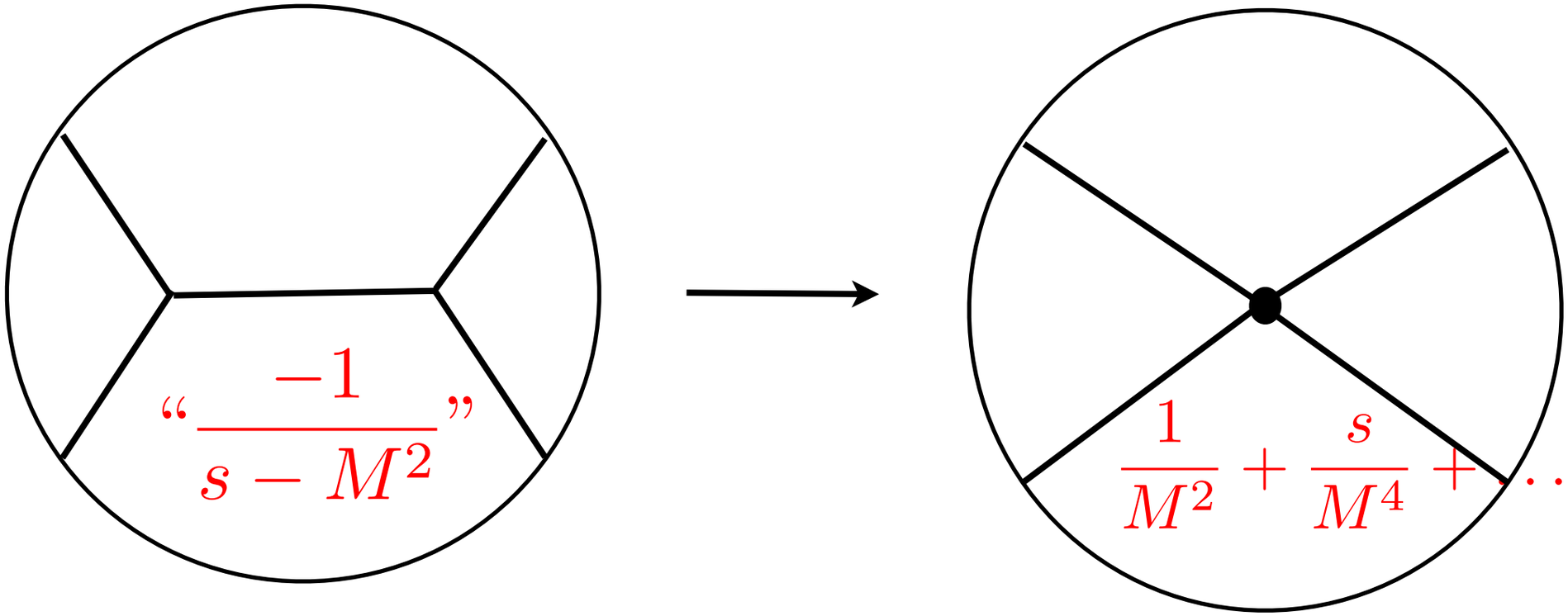
[Heemskerk,Penedones,Polchinski& Sully '09]

They proved: solutions to crossing in large-N CFTs w/gap

$\longleftrightarrow$ local interactions in AdS

But why are higher-dim interactions suppressed by powers of Δ_{gap}?

Effective field theory in AdS:



In string theory, for example, $M \sim M_{\rm string} \gg 1/R_{\rm AdS}$

Suppression would be clear from a 'dispersion relation in the flat space limit of AdS':



$$\mathcal{M}(s) \sim \int_{M^2}^{\infty} \frac{ds'}{s'-s} \mathrm{Im}\mathcal{M}(s') \sim \frac{1}{M^2} + \frac{s}{M^4} + \ldots$$

Sigh, if only a CFT formula existed that read like this!

Why Conformal Regge Theory?

To explain why operators organize into families ('Regge trajectories')

Quantitatively, a Froissart-Gribov inversion formula:

$$f^2_{\mathcal{O}\mathcal{O}\mathcal{O}'} = \int dz d\bar{z}\,(\ldots)\,\text{“Im}\,\mathcal{M}\text{”}$$



In AdS/CFT, this formula will know about bulk locality !

Outline

1. Why conformal Regge theory?
   -Conformal bootstrap and large spin physics ✔
   -AdS/CFT and bulk locality

2. CFT Froissart-Gribov formula
   -Why operators are analytic in spin
   -New ingredients in CFT (ANEC&bound on chaos)

3. Applications:
   -operators of large spin
   -CFTs dual to gravity: causality&bulk locality

Why is physics analytic in spin?

Short answer:

because Euclidean physics has to resum into something sensible at high energies

- Toy model: single-variable power series

$$f(x) = \sum_{j=1}^{\infty} f_j x^j$$ ('Euclidean OPE')

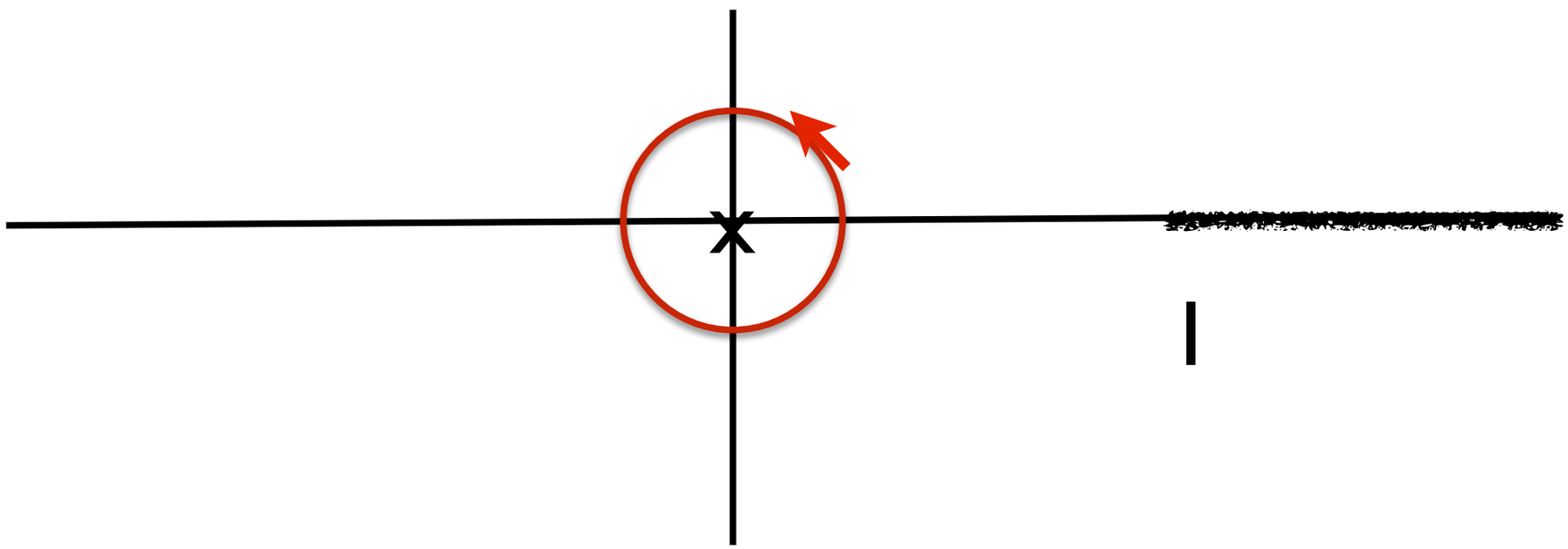
- Assume:
  - f(x) is analytic in cut plane C\[1,∞)
  - |f(x)/x| → 0 at infinity

(large x= 'large energy')

⇒ What does this tell us about the f_j's?

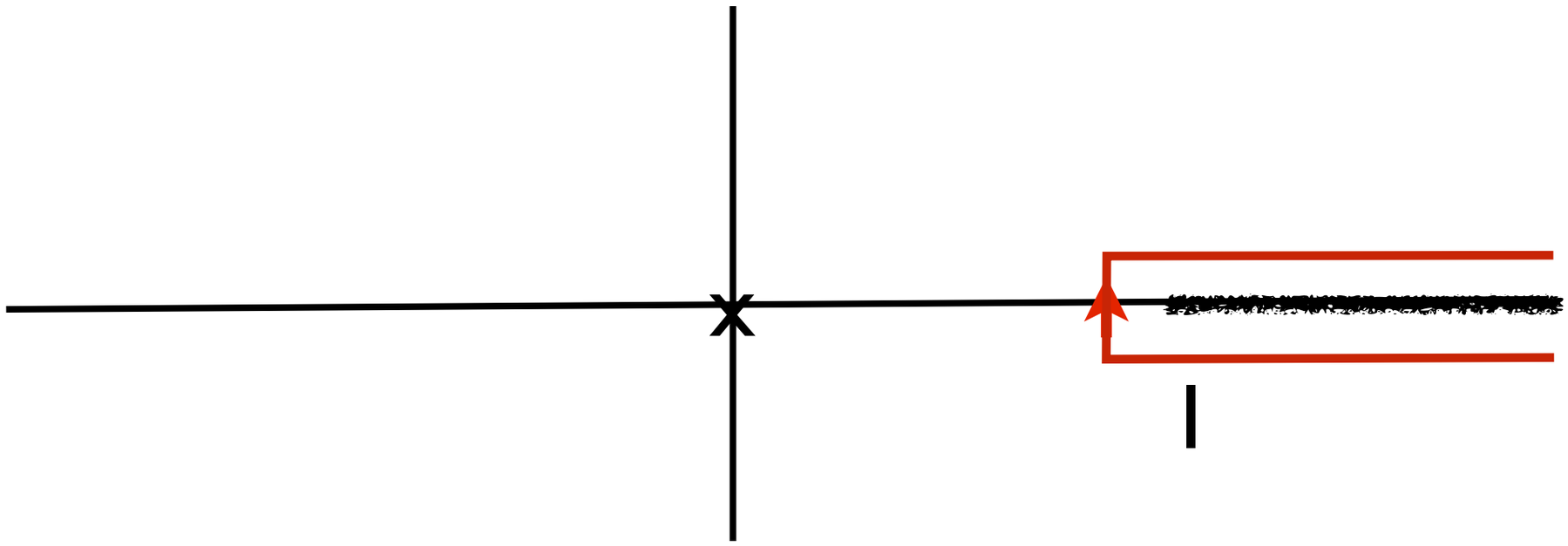
- Q: How to extract f_j from f(x) ?
- A: Cauchy

$$f_j(x) = \frac{1}{2\pi i} \oint \frac{dx}{x}\, x^{-j}\, f(x)$$



- Q: How to extract f_j from f(x) ?
- A: Cauchy

Deform the contour:



$$\Rightarrow \quad f_j = \frac{1}{2\pi i}\int_1^\infty \frac{dx}{x} x^{-j}\,\mathrm{Disc}\, f(x) \qquad (j \geq 1)$$

Basic inversion formula

$$f_j = \int_1^\infty \frac{dx}{x} x^{-j} \frac{\text{Disc}\, f(x)}{2\pi i}$$

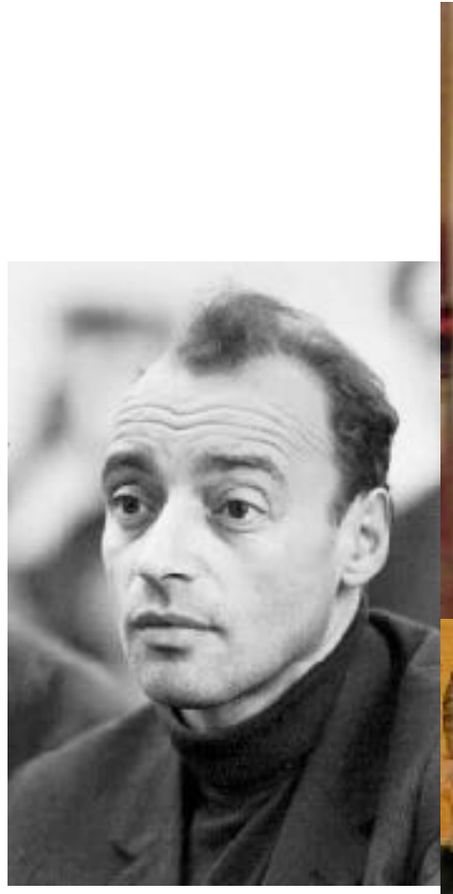
(Sanity check: $f(x) = -\log(1-x) \Rightarrow \frac{\text{Disc}\, f(x)}{2\pi i} = 1$)

$\Rightarrow f_j = 1/j$ ✔

⇒ Good high-energy behavior leads to:

- Taylor coefficients are analytic for Re[j] ≥ 1 !
- Determined by imaginary part of amplitude

Froissart-Gribov formula







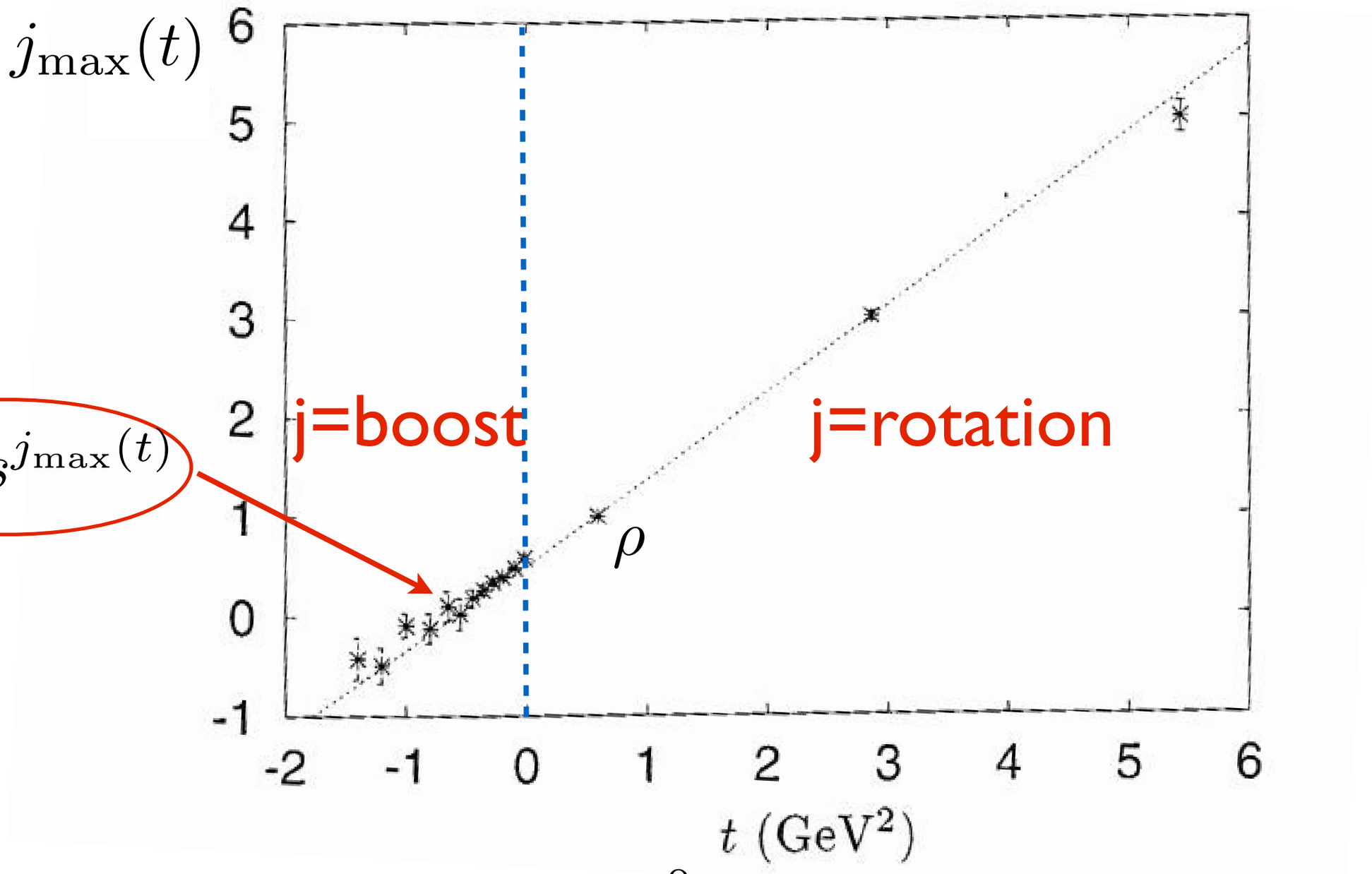
inverts Legendre polynomials:

$$A(s,\cos\theta) = \sum_{j=0}^{\infty} a_j(s) P_j(\cos\theta)$$

$$\Leftrightarrow a_j^{(t)} = \int_{\eta_0}^{\infty} d\eta\, Q_j(\cosh\eta)\, \mathrm{Disc}\, A(\cosh(\eta)) + (-1)^j [\text{t-channel}]$$

- Explains why S-matrix can be decomposed into analytic-in-spin partial waves
- Foundation of Regge theory

Classic application to QCD



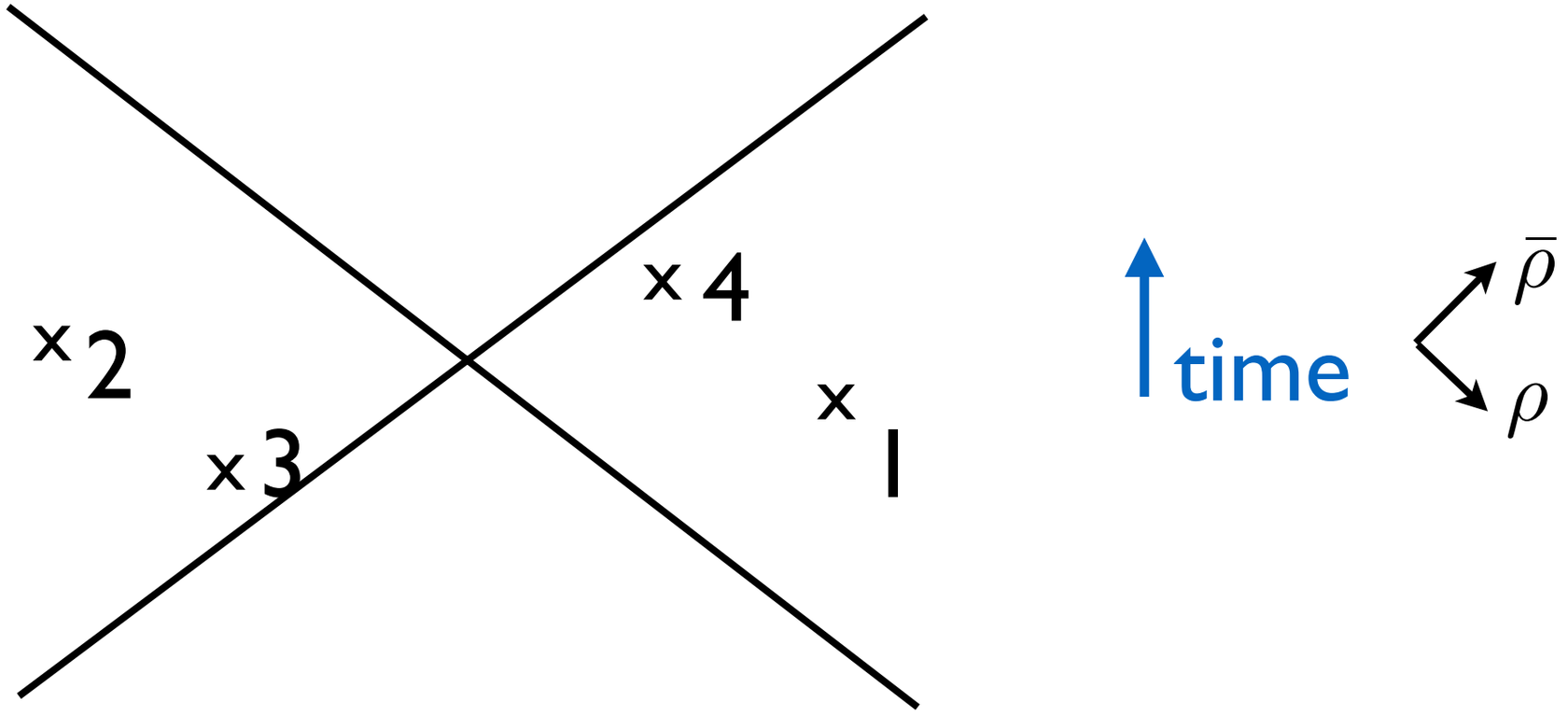
t<0 obtained from $\pi^- p \to \pi^0 n$ **data,** (@3.6,5.85&13.3GeV/c)

[from Donnachie, Dosch,Landshoff&Nachtmann]

Suppose we had a Froissart-Gribov formula in CFT

What should be '$\mathrm{Im}\,\mathcal{M}$' ?

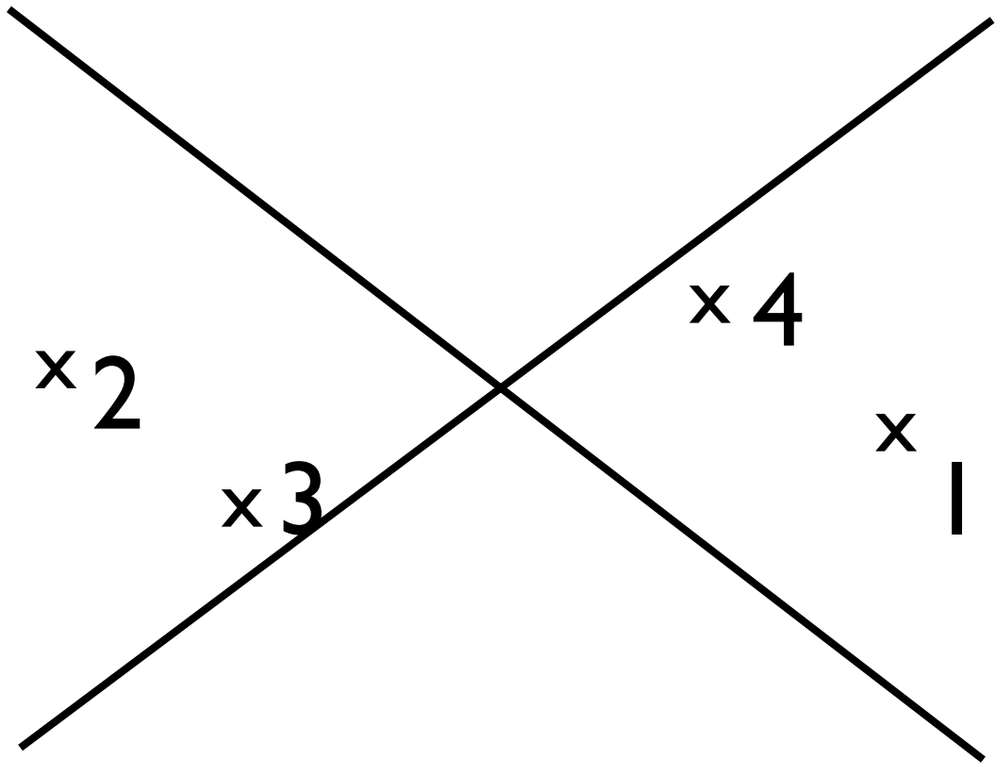
- We consider 4-point correlator in CFT_d



- Symmetrical param. within Rindler wedges:

$$-\rho_2 = \rho_1 = 1$$
$$-\rho_3 = \rho_4 \equiv \rho$$

- We consider 4-point correlator in CFT_d

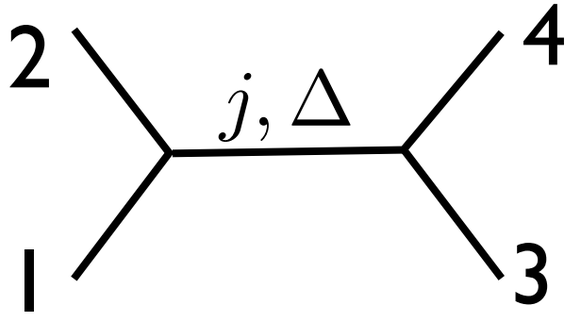




$$-\rho_2 = \rho_1 = 1$$
$$-\rho_3 = \rho_4 \equiv \rho$$

- at small ρ, s-channel OPE:

$$G(\rho, \bar{\rho}) = \sum_{j,\Delta} c_{j,\Delta} \rho^{\frac{\Delta - j}{2}} \bar{\rho}^{\frac{\Delta + j}{2}} \quad =$$



(one normally replaces power series by 'blocks' which include derivatives of primary operators:

$$G_{J,\Delta}(z,\bar{z}) = \frac{k_{\Delta-J}(z)k_{\Delta+J}(\bar{z}) + k_{\Delta+J}(z)k_{\Delta-J}(\bar{z})}{1+\delta_{J,0}} \qquad (d=2)\,,$$

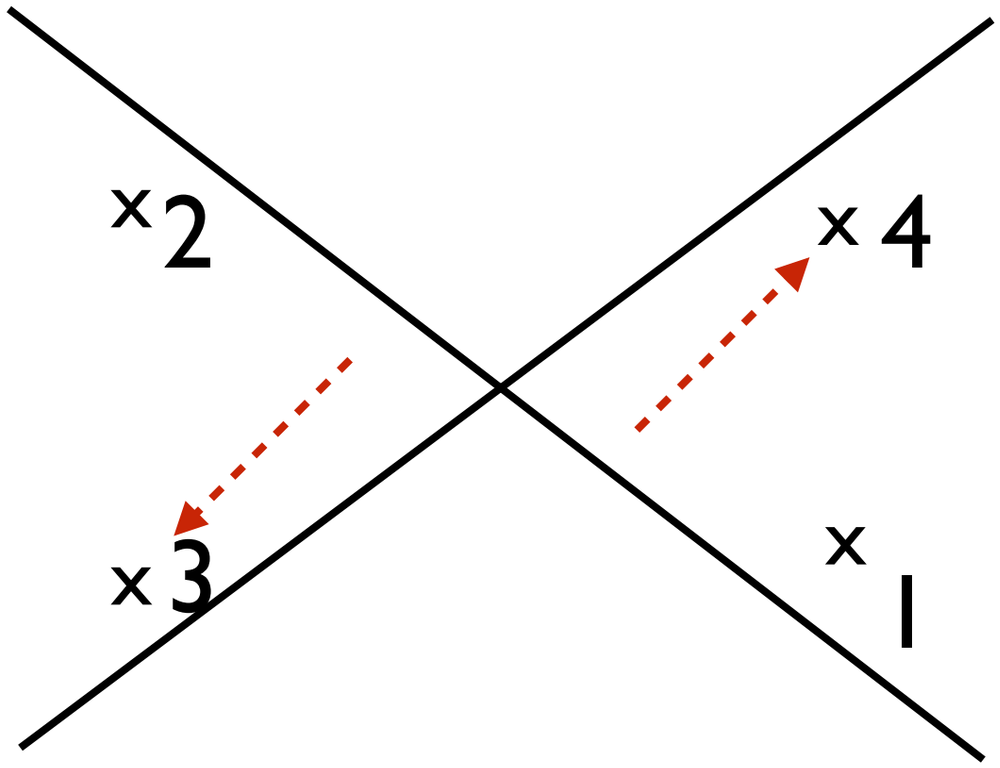
$$G_{J,\Delta}(z,\bar{z}) = \frac{z\bar{z}}{\bar{z}-z}\left[k_{\Delta-J-2}(z)k_{\Delta+J}(\bar{z}) - k_{\Delta+J}(z)k_{\Delta-J-2}(\bar{z})\right] \qquad (d=4)\,.$$

where

$$k_\beta(z) = z^{\beta/2}{}_2F_1(\beta/2,\beta/2,\beta,z) \qquad z = \frac{4\rho}{(1+\rho)^2}$$

This will be important below,
but Taylor series will suffice for now.)

- Take x_{41} and x_{23} time-like:



- Certainly looks like a ‘scattering amplitude’
- Claim:

$$S \equiv \frac{G}{G_{\rm Eucl}} \quad \text{satisfies} \quad |S| \leq 1$$

proof

- s-channel OPE diverges upon entering light-cone

- Use OPE around t-channel (timelike one)

$$G(\rho,\bar\rho)=\sum_{j,\Delta} c_{j,\Delta}\left(\frac{1-\sqrt{\rho}}{1+\sqrt{\rho}}\right)^{\Delta-j}\left(\frac{1-\sqrt{\bar\rho}}{1+\sqrt{\bar\rho}}\right)^{\Delta+j}$$

[Hogervorst&Rychkov '13]

- For timelike, $\rho>1$, only get extra phases:

$$\begin{aligned}\left|G(\rho,\bar\rho)\right| &= \left|\sum(\text{positive})e^{i\pi(\Delta-j)}\right| \\ &\le \sum(\text{positive}) = G(1/\rho,\bar\rho)\equiv G_{\text{Eucl}}\end{aligned}$$

This means that an 'imaginary part' is positive:

$$\begin{array}{c} S = 1 + i\mathcal{M} \\ |S| \leq 1 \end{array} \quad \Rightarrow \mathrm{Im}\,\mathcal{M} > 0$$

Since S contains the 'I', this is *double discontinuity*:

$$G_{\mathrm{Eucl}} \propto 1$$
$$G_{\mathrm{below}} \propto 1 + i\mathcal{M}$$
$$G_{\mathrm{above}} \propto 1 - i\mathcal{M}^*$$

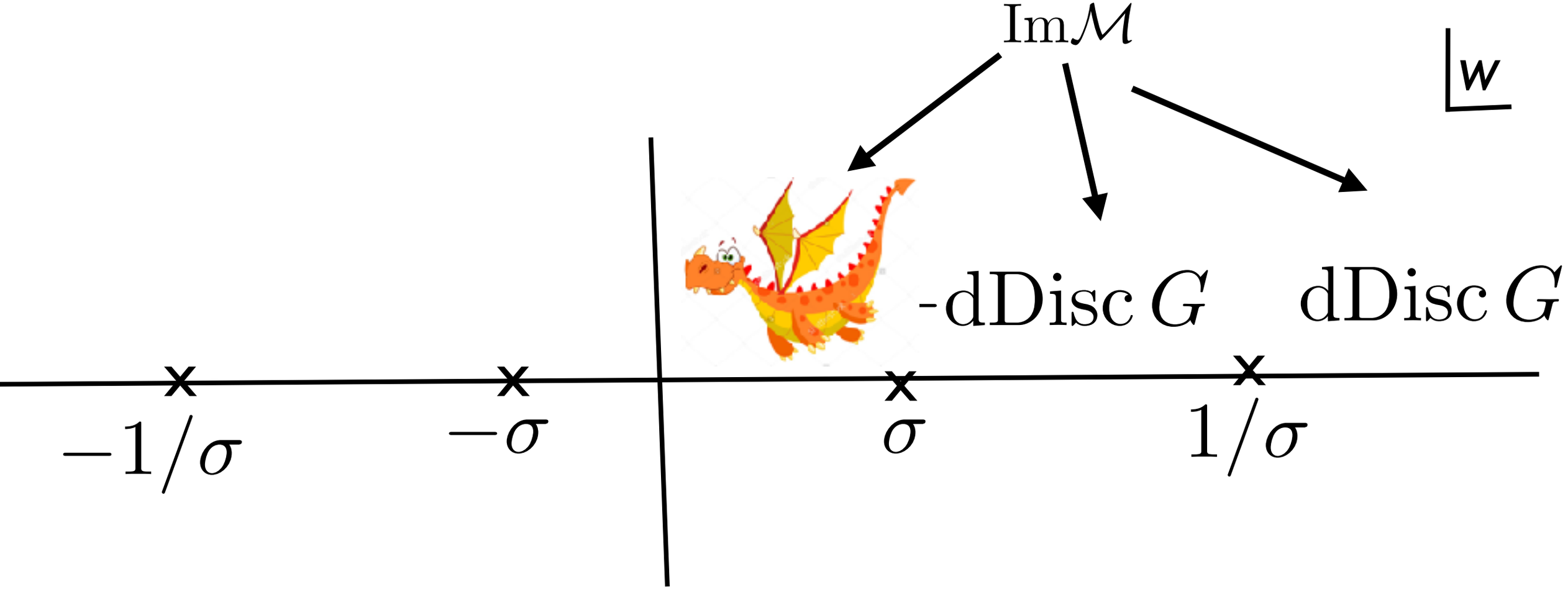
$$\Rightarrow 2\mathrm{Im}\,\mathcal{M} \propto 2G_{\mathrm{Eucl}} - G_{\mathrm{above}} - G_{\mathrm{below}}$$
$$\equiv \mathrm{dDisc}\,G$$
$$> 0$$

Writing M from Im M: 'dispersion relation'

This doesn't quite work because analytic structure in coordinate space is weird

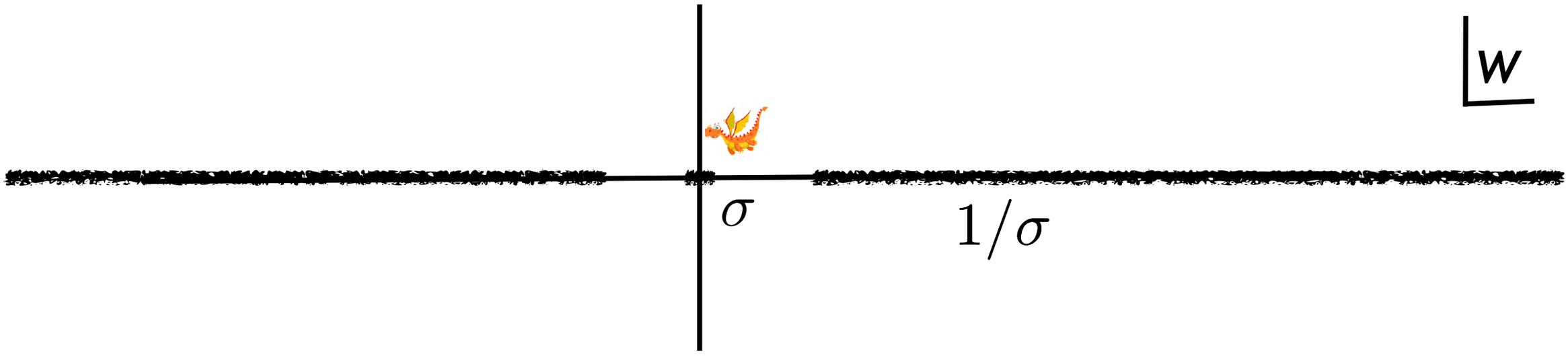
For example, fix $\rho\bar{\rho}$: $\rho = \sigma w$

$\bar{\rho} = \sigma / w$



The dragons shrink in the Regge limit

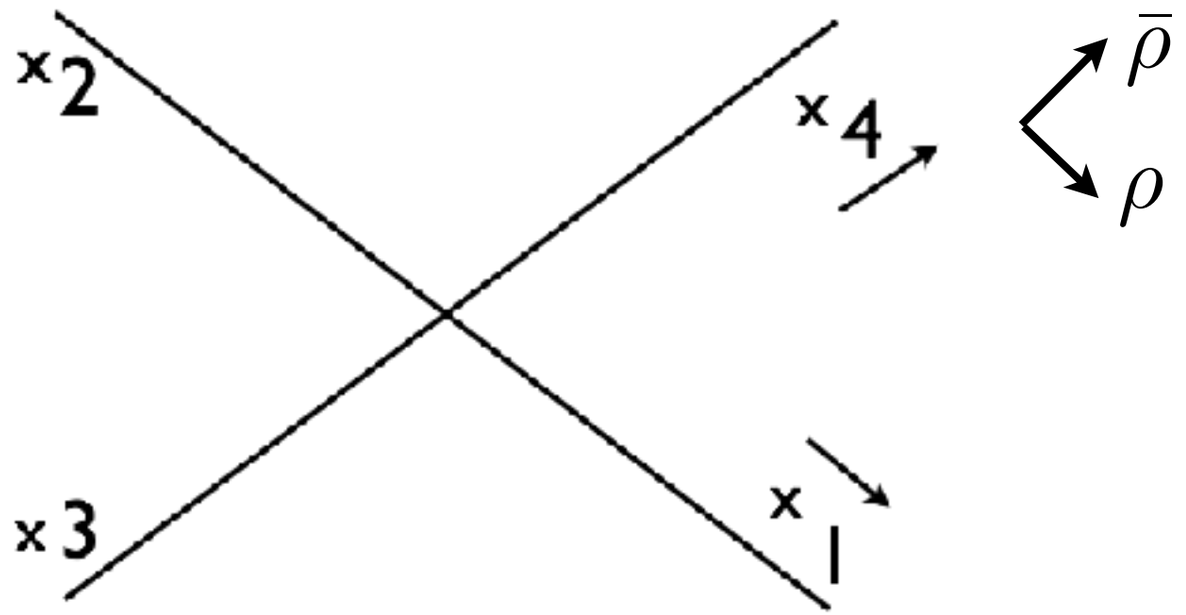
$$w \to \infty$$



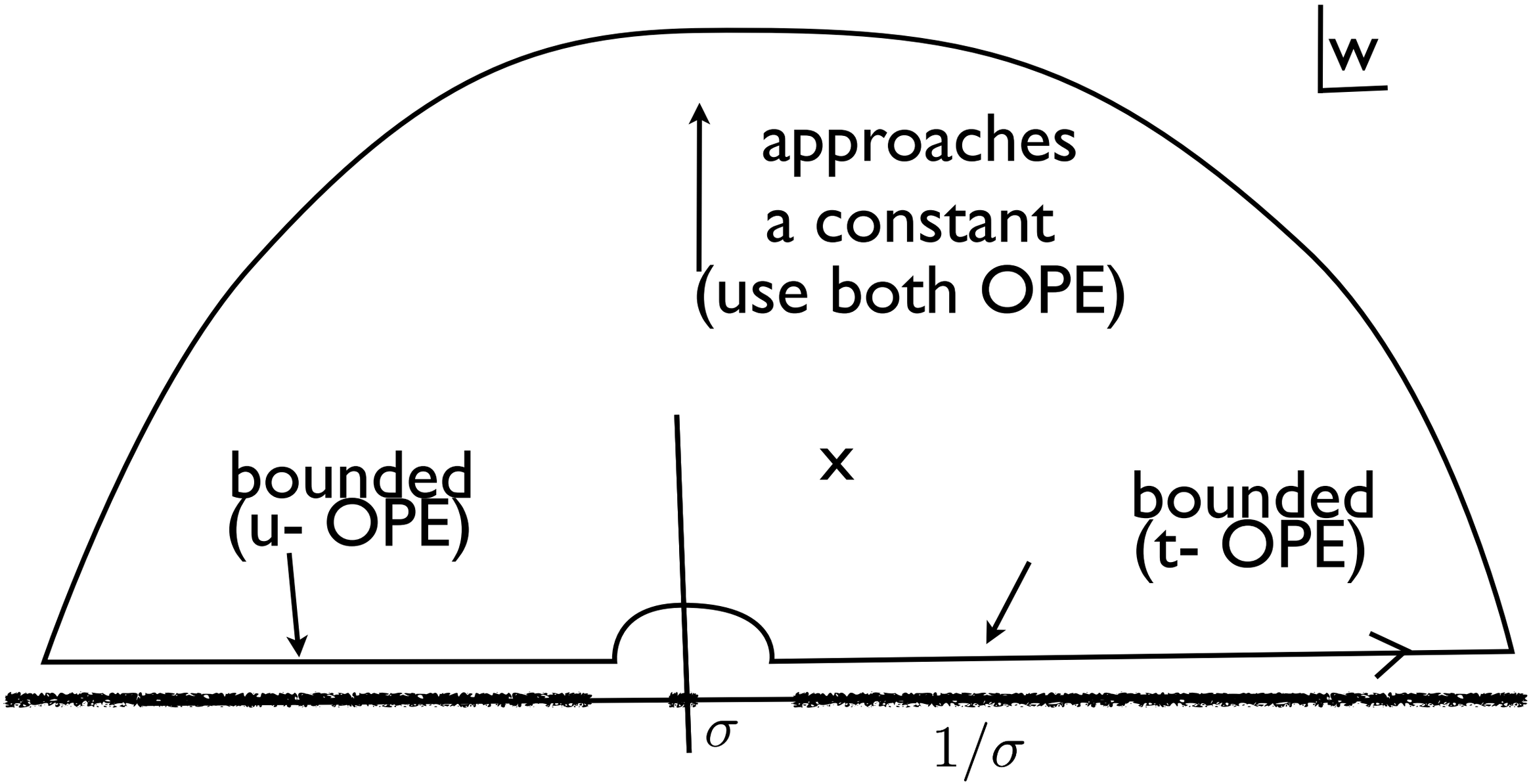
This corresponds to a boosted coordinates:

$$\rho = \sigma w$$

$$\bar{\rho} = \sigma / w$$



Regge limit dispersion relation:



$$\mathcal{M}(E) = C + \frac{1}{\pi}\int_{-\infty}^{\infty} \frac{dE' \mathrm{Im}\,\mathcal{M}(E')}{E - E'}$$

[Hartman,Kundu&Tajdini '16]

Some implications of the dispersion relation:

Look in upper-half-plane:

$$\mathrm{Im}\,\mathcal{M}(x+iy) = \int \frac{y\,dx'\,\mathrm{Im}\mathcal{M}(x')}{(x'-x)^2+y^2} > 0$$

⇒Proof of ANEC:

$$\mathcal{M}(w) \approx w\langle \int_{-\infty}^{\infty} dx^+ T_{++}\rangle_{34} \;\Rightarrow \langle \int dx^+ T_{++}\rangle > 0$$

[Hartman,Kundu&Tajdini '16]

(ANEC was proved just a few month earlier using entanglement entropy inequalities)

[Faulkner,Leigh,Parrikar&Wang, '16]

Derivative of dispersion relation:

$$(y\partial_y - 1)\Big[\log \mathrm{Im}\mathcal{M}(x+iy)\Big] = -2\frac{\int \frac{dx'\, y^2\, \mathrm{Im}\mathcal{M}(x')}{((x'-x)^2+y^2)^2}}{\int \frac{dx'\, \mathrm{Im}\mathcal{M}(x')}{(x'-x)^2+y^2}} \leq 0$$

$\Rightarrow$ can't grow faster than linear in energy!

This proves that the Pomeron intercept $j \leq 2$ in CFT

when converted to Rindler time $w=e^{t/(2\pi T)}$, this is the CFT case of the 'bound on chaos' (Lyapunov $\lambda < 2\pi T$)

[Maldacena,Shenker&Stanford '15]

$\Rightarrow$ Dispersion relation encodes much nice physics!

Because of the ‘dragons’ at low-energy, this dispersion relation doesn’t fully reconstruct the correlator

Following the Froissart-Gribov logic, we’ll instead obtain a dispersion relation for OPE coefficients

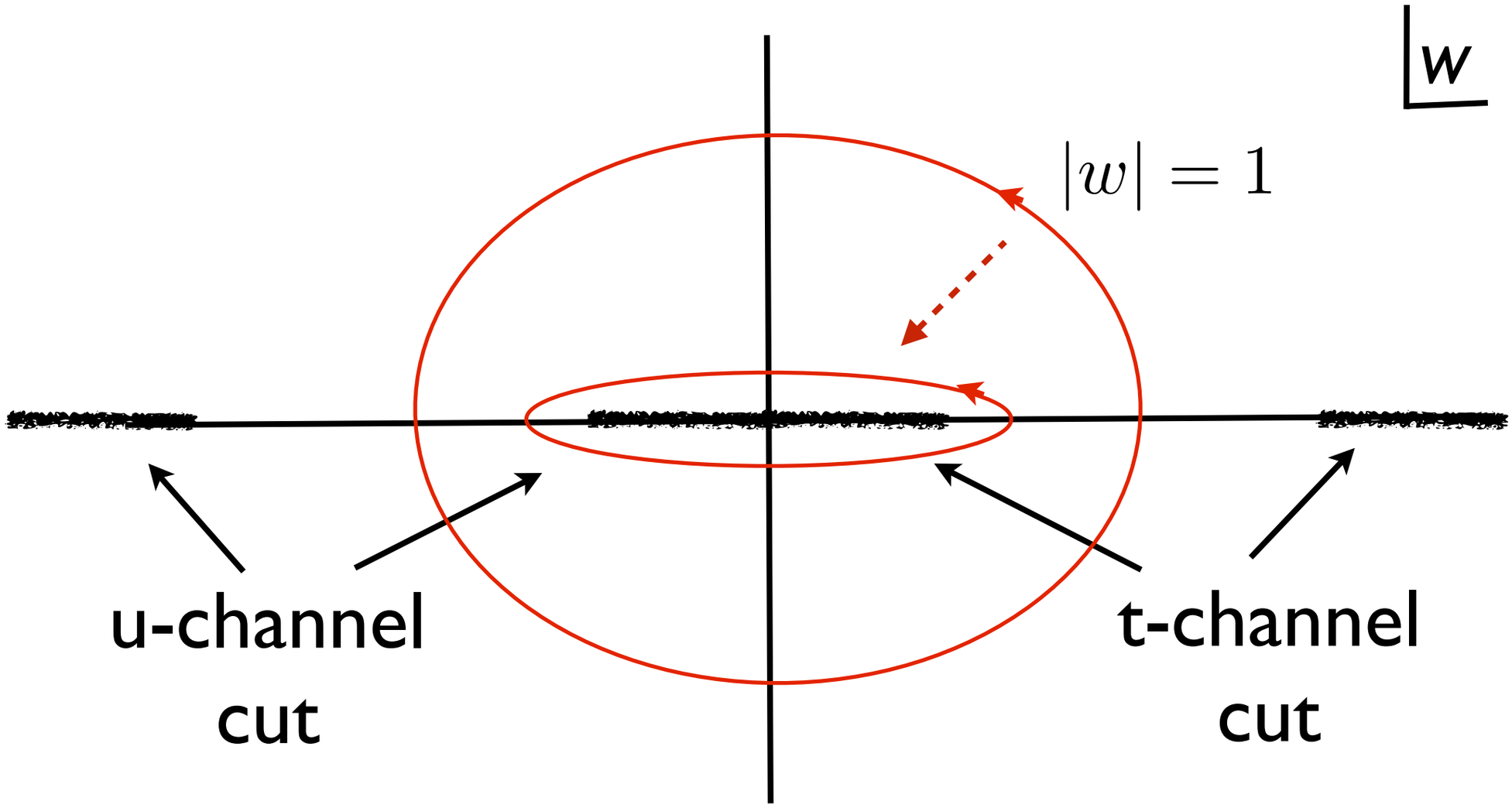
Froissart-Gribov: how to invert $f(\cos\theta) = \sum_{j=0}^{\infty} f_j \cos(j\theta)$?

A: Start from Euclidean inverse, use variable: $w = e^{i\theta}$

$$f_j \sim \int_0^{2\pi} d\theta \cos(j\theta) f(\cos\theta)$$

$$= \oint \frac{dw}{w} (w^j + w^{-j}) f(\cos\theta)$$

Trick is to close the contour on cut:



Result: integral over cut

$$f_j^{(t)} \sim \int_{\eta_0}^{\infty} d\eta\, e^{-j\eta}\, \mathrm{Disc}\, f(\cosh(\eta))$$

$$+(-1)^j [\text{u-channel}]$$

CFT steps are the same: Euclidean OPE:

$$G(z,\bar{z}) = \sum_{j,\Delta} f^2_{j,\Delta} G_{j,\Delta}(z,\bar{z})$$

- Actually, we first have to make Δ continuous:

$$G(z,\bar{z}) = \delta_{12}\delta_{34} + \sum_{j=0}^{\infty} \int_{d/2-i\infty}^{d/2+i\infty} \frac{d\Delta}{2\pi i}\, c(j,\Delta)\, F_{j,\Delta}(z,\bar{z}).$$

✓

$$F_{j,\Delta} = g_{j,\Delta} + g_{j,d-\Delta}$$

[Costa,Goncalves&Penedones'12]

[see also: Mazac'16 Hogervorst&van Rees '17, Gadde '17]

= single-valued, needed for self-adjointness of Casimir

[Simmons-Duffin '12]

- Contour like a Mellin transform

- OPE reproduced if c has correct poles:

$$c(j,\Delta') \approx \frac{f^2_{OO\to j,\Delta}}{\Delta - \Delta'}$$

step 1. Invert the Euclidean OPE (SO(d+1,1)):

- To extract the coefficients, invoke orthogonality and integrate against block (+shadow):

$$c(j,\Delta) = \#(j,\Delta) \int d^2z\, \mu(z,\bar{z})\, G(z,\bar{z})\, F_{j,\Delta}(z,\bar{z})\,.$$

- Still a Euclidean integral: integer spin, not yet what we want

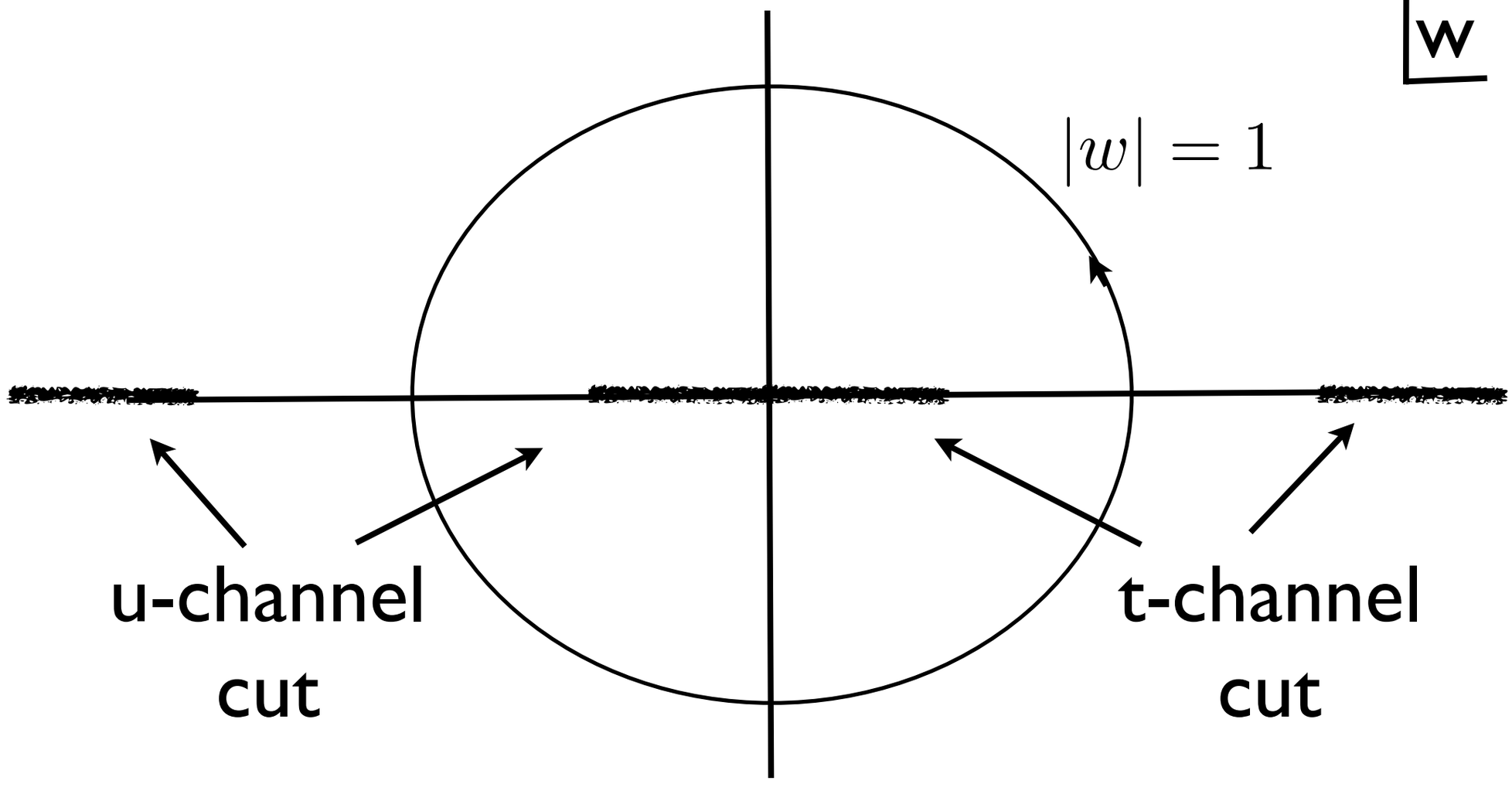
step 2

- Contour deformation. Use clever variables

[Hogervorst&Rychkov '13]

$$z = \frac{4\rho}{(1+\rho)^2} \qquad w = \sqrt{\rho/\bar{\rho}} = e^{i\theta}$$

$$\int d^2 z \to \int_0^1 d|\rho| \oint \frac{dw}{w}$$



The tricky part is to split the block(+shadow) into bits that are nice in individual Regge limits:

$$2\cos(j\theta) = e^{ij\theta} + e^{-ij\theta}$$
$$= w^j + w^{-j}$$

That is, we want:

$$F_{j,\Delta}(z,\bar{z}) = F^{(+)}_{j,\Delta} + F^{(-)}_{j,\Delta}$$

$\sim w^j$ $(w \to 0)$

$\sim w^{-j}$ $(w \to \infty)$

- tricky because there are 8 basic solutions to conformal Casimirs diff eqs.: (quadratic and quartic)

$$g^{\rm pure}_{j,\Delta}(z,\bar{z}) \sim z^{\frac{\Delta-j}{2}}\,\bar{z}^{\frac{\Delta+j}{2}} \qquad (0 \ll z \ll \bar{z} \ll 1)$$

- Solutions related by symmetries:

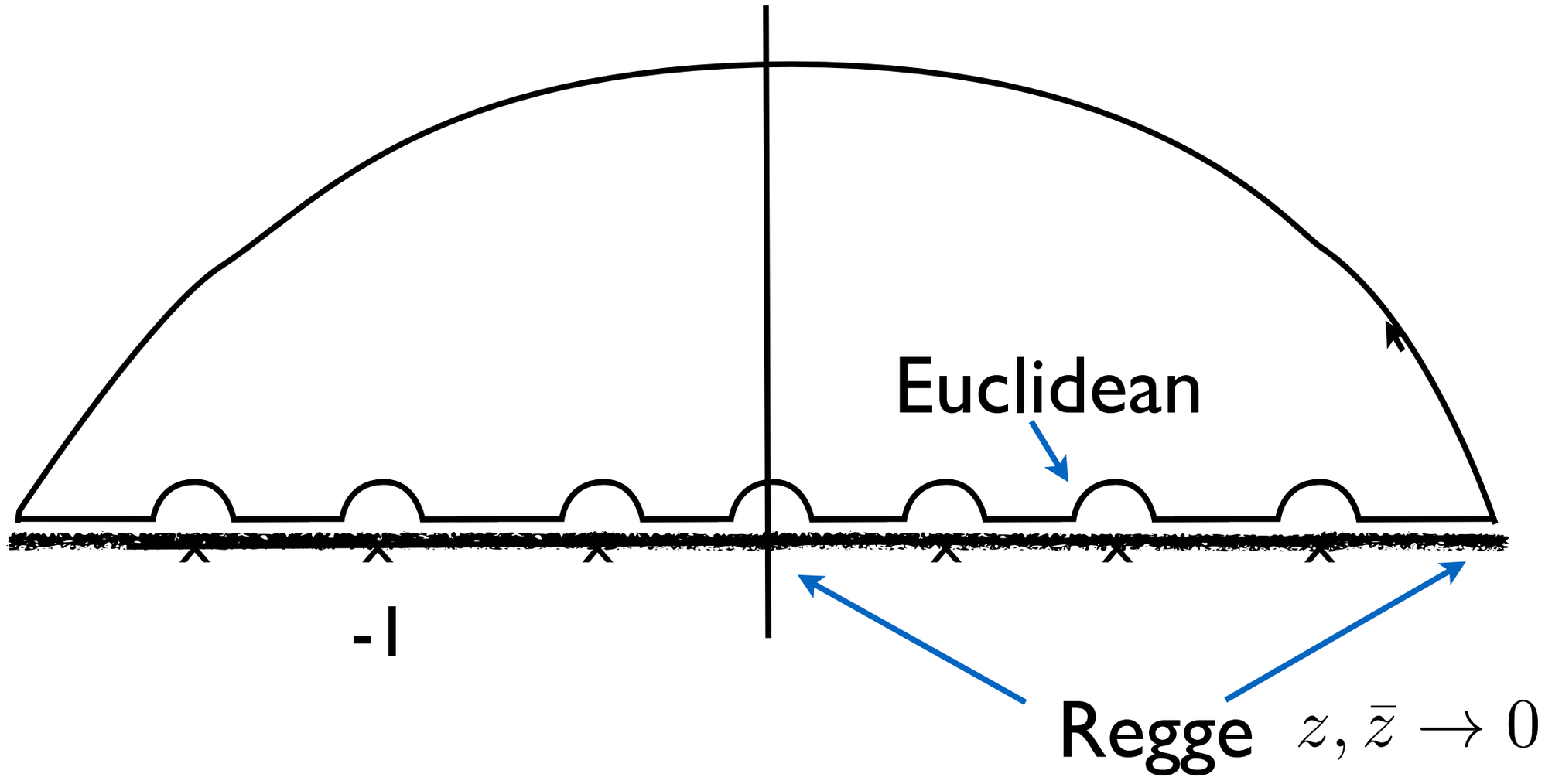
$$j \longleftrightarrow 2-d-j, \qquad \Delta \longleftrightarrow d-\Delta, \qquad \Delta \longleftrightarrow 1-j\,.$$

- Only 2 are nice (convergent) in Regge limit:

$$g^{\rm pure}_{\Delta+1-d,j+d-1}, \qquad g^{\rm pure}_{1-\Delta,j+d-1} \sim (z\bar{z})^{j/2}$$

- So we have 4 parameters and 8 constraints

- The constraints are on different sheets:



(all 8 solutions mix under continuation:)

$$g^{\text{pure}}_{j,\Delta}(z,\bar{z})^{\circlearrowleft} = g^{\text{pure}}_{j,\Delta}(z,\bar{z}) \left[1 - 2i\frac{e^{-i\pi(a+b)}}{\sin(\pi\beta)}\sin(\pi(\beta/2+a))\sin(\pi(\beta/2+b))\right]$$
$$- g^{\text{pure}}_{1-\Delta,1-j}(z,\bar{z})\, 2\pi i \frac{e^{-i\pi(a+b)}\Gamma(\Delta+j-1)\Gamma(\Delta+j)}{\Gamma\left(\frac{\Delta+j}{2}-a\right)\Gamma\left(\frac{\Delta+j}{2}+a\right)\Gamma\left(\frac{\Delta+j}{2}-b\right)\Gamma\left(\frac{\Delta+j}{2}+b\right)}\,.$$

4 parameters, 8 constraints,
fingers crossed…

Result: CFT Froissart-Gribov formula

$$c(J,\Delta) = c^t(J,\Delta) + (-1)^J c^u(J,\Delta)$$

$$c^t(J,\Delta) = \frac{\kappa_{J+\Delta}}{4} \int_0^1 dz d\bar{z}\, \mu(z,\bar{z})\, G_{\Delta+1-d,J+d-1}(z,\bar{z})\, \mathrm{dDisc}\left[G(z,\bar{z})\right]$$

Result: CFT Froissart-Gribov formula

$$c(J,\Delta) = \int_{\diamondsuit} \Big[\text{Inverse block}\Big] \times \Big[\text{dDisc}\, G\Big]$$

s-channel
OPE coefficients

convergent
t-channel sum

Result: CFT Froissart-Gribov formula

$$c(J,\Delta) = \int_{\diamond} [\text{Inverse block}] \times [\text{dDisc}\, G]$$

s-channel
OPE coefficients

block with
j and Δ
exchanged

convergent
t-channel sum

converges for j>1 (Regge limit bounds)

A (boring) test: 2D Ising

$$G(\rho,\bar\rho)=\left|\frac{1}{(1-\rho^2)^{1/4}}\right|^2+\left|\frac{\sqrt{\rho}}{(1-\rho^2)^{1/4}}\right|^2$$

- Double discontinuity:

$$\frac{1-\frac{1}{\sqrt{2}}(\sqrt{\rho}+\sqrt{\bar\rho})+\sqrt{\rho\bar\rho}}{(1-\rho^2)^{1/4}(1-\bar\rho^2)^{1/4}}>0$$

- Integral against 2d (global) blocks: factorize

$$c_{j,\Delta}=f_0(j+\Delta)f_0(j+2-\Delta)-\tfrac{1}{2}f_{1/4}(j+\Delta)f_0(j+2-\Delta)+\dots$$

$$f_p(\alpha)=2^{a-3+2p}\frac{\Gamma(\frac{7}{4})\Gamma(p+\frac{\alpha-2}{4})}{\Gamma(p+\frac{\alpha+5}{4})}{}_3F_2\left(\tfrac{1}{2},\tfrac{\alpha}{2},p+\tfrac{\alpha-2}{4};\tfrac{a+1}{2},p+\tfrac{\alpha+5}{4};1\right). \qquad \text{(B.6)}$$

- Residues at all poles do match global OPE!*

$$C_{j,\Delta} = -K_{j,\Delta}\mathrm{Res}_{\Delta'=\Delta}c(j,\Delta')$$

$$C_{0,1} = \frac{1}{4}, \qquad C_{2,2} = \frac{1}{64}, \qquad C_{4,4} = \frac{9}{40960}, \qquad C_{0,4} = \frac{1}{4096}$$
$$C_{4,5} = \frac{1}{65536}, \qquad C_{6,6} = \frac{35}{3670016} \qquad C_{2,6} = \frac{9}{2621440}, \qquad C_{6,7} = \frac{1}{1310720}, \ldots$$

* Including (predicted) spurious poles for $\Delta - j - d = 0, 1, 2 \ldots$

$$\frac{(-1)^{m+1}\Gamma(1+a+\frac{m}{2})\Gamma(1+b+\frac{m}{2})}{m!(m+1)!\Gamma(a-\frac{m}{2})\Gamma(b-\frac{m}{2})} \times$$
$$\times K_{j+1+m,j+d-1}c(j+1+m, j+d-1)$$

**And: never trust Mathematica's Residue on 3F2.....

Outline

The aim of this talk will be to present a formula…

1. Context: the conformal bootstrap ✔
2. An inverse OPE formula:
   -Why operators are analytic in spin
   -building it up: SO(2),SO(3),SO(2,1)…SO(d,2) ✔
3. Applications:
   -operators of large spin
   -CFTs dual to gravity: causality&bulk locality

Large spin operators

- Physical intuition: take two operators and put many derivatives between them:

$$\mathcal{O}_{\#} = \mathcal{O}_1 \partial^{\#} \mathcal{O}_2$$

- Should make them 'far' and decoupled:

$$\Delta_{\#} \approx \Delta_1 + \Delta_2 + (\#\ \text{derivatives})$$ (as in free theory!)

- **Actually, twist is more useful:** $\tau = \Delta - j$

$$\tau_{[12]_n} \approx \tau_1 + \tau_2 + 2n$$

Large spin expansions

large spin in s-channel ← low twist in t-channel

standard story: double-light-cone limit $(z, \bar{z}) \to (0, 1)$

non-analytic behaviour in $(1 - \bar{z})$needs large spin:

$$\sum_j \frac{1}{j^\alpha} F_j(\bar{z}) = (1 - \bar{z})^{\alpha/2} + \text{regular}$$

⇒ Solve OPE in asymptotic series in 1/j

[Komargodski&Zhiboedov,
Fitzpatrick,Kaplan,Poland&Simmons-Duffin,
Alday&Bissi&…,
,Kaviraj,Sen,Sinha&…,
Alday,Bissi,Perlmutter&Aharony,…]

- New: start instead from Froissart-Gribov formula:

$$c(j,\Delta) \sim \int_0^1 dz d\bar{z}\, z^{j-\Delta}\, \bar{z}^{j+\Delta} F_{j+\Delta}(\bar{z}) \mathrm{dDisc} G(z,\bar{z})$$

- Recall, OPE data encoded in Δ-poles: $z \to 0$

if $G(z,\bar{z}) \to z^{\tau} G_{\tau}(\bar{z})$,

$$c(j,\Delta) = \frac{1}{j-\Delta-\tau} \times \int_0^1 d\bar{z}\, \bar{z}^{j+\Delta} F_{j+\Delta}(\bar{z}) \mathrm{dDisc} G_{\tau}(\bar{z})$$

- Large j+Δ and low twist pushes to (0,1) corner

- Analytic result for collinear integral of power:

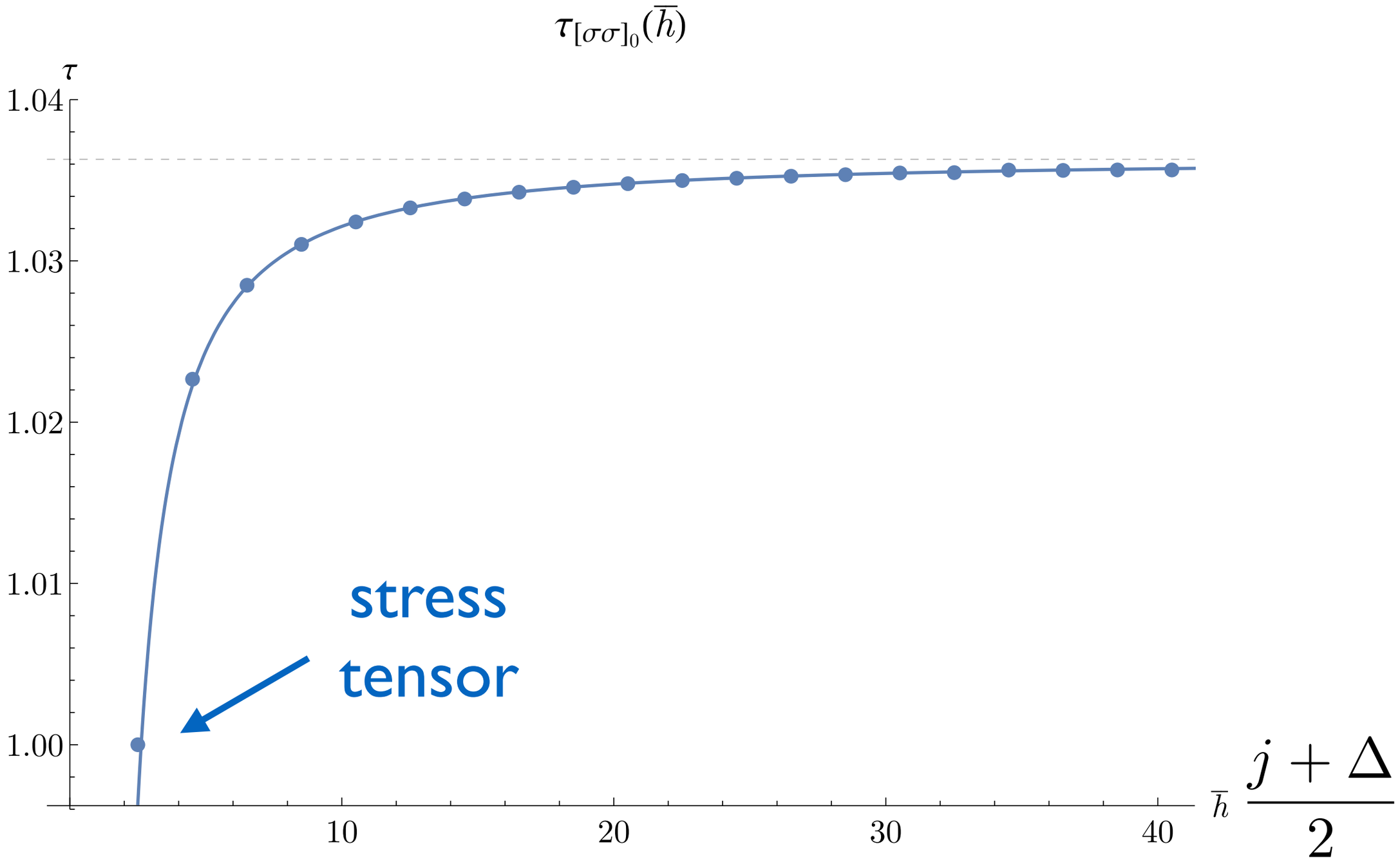
$$I^{a,b}_{\tau'}(\bar{h}) \equiv \int_0^1 \frac{d\bar{z}}{\bar{z}^2}(1-\bar{z})^{a+b}\kappa_{\bar{h}}k_{\bar{h}}(\bar{z})\,\mathrm{dDisc}\left[\left(\frac{1-\bar{z}}{\bar{z}}\right)^{\frac{\tau'}{2}-b}(\bar{z})^{-b}\right] \tag{4.7}$$

$$= \frac{1}{\Gamma(-\frac{\tau'}{2}-a)\Gamma(-\frac{\tau'}{2}+b)} \times \frac{\Gamma(\bar{h}-a)\Gamma(\bar{h}+b)}{\Gamma(2\bar{h}-1)} \times \frac{\Gamma(\bar{h}-\frac{\tau'}{2}-1)}{\Gamma(\bar{h}+\frac{\tau'}{2}+1)}\,.$$

$\sim 1/\bar{h}^{\tau'}$ $\qquad (\bar{h} = \frac{j+\Delta}{2})$

- Earlier results reproduced by: 'expand cross-channel OPE in $\frac{1-\bar{z}}{\bar{z}}$ and integrate termwise using (4.7)'
- Conceptually, no need to expand in 1/j
  (=why earlier expansions were asymptotic) [Alday&Zhiboedov '15; Simmons-Duffin '16]

Asymptotic series in 3D Ising



[Plot from Simmons-Duffin '16; see Alday&Zhiboedov '15]

What's new:

- Asymptotic expansion ⇒ convergent sum
  (no need to expand in $(1-\bar{z})/\bar{z}$)
- Control over individual spins, not only averages over many spins ('no stick-out')
- Can try to bound errors

AdS/CFT:
Why dDisc is awesome

In theories with large-N factorization, saturated by single-traces

$$G_{\rm conn} \sim \sum_{\rm single\,trace} c_j |1-z|^{\Delta_j} + \sum_{\rm double\,trace} c_i |1-z|^{\gamma_i^{(1)}/N}$$

Leading connected order $\sim \log(1-\bar{z})$

$$c_{j,\Delta} \sim \int \mathrm{dDisc}\, G$$

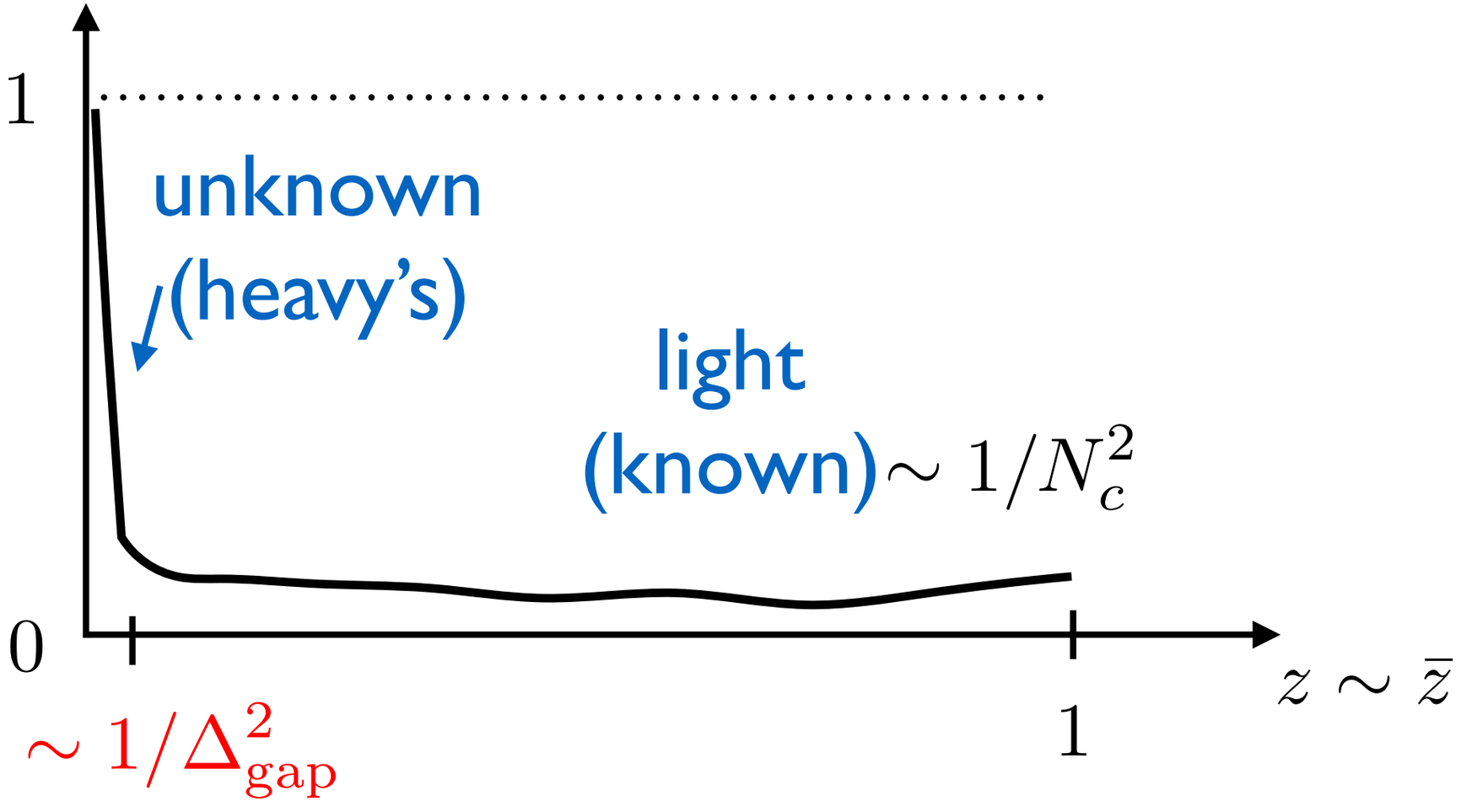
single+double traces

single trace

Theories with gravity dual have few light single-traces: the graviton ($T^{\mu\nu}$), a few scalars,… up to $\Delta_{\rm gap}$

Heavy's in cross-channel can be bounded:

$$\left(\frac{1-\sqrt{\rho}}{1+\sqrt{\rho}}\right)^{\Delta_{\rm gap}} \leq e^{-2\sqrt{\rho}\Delta_{\rm gap}}$$



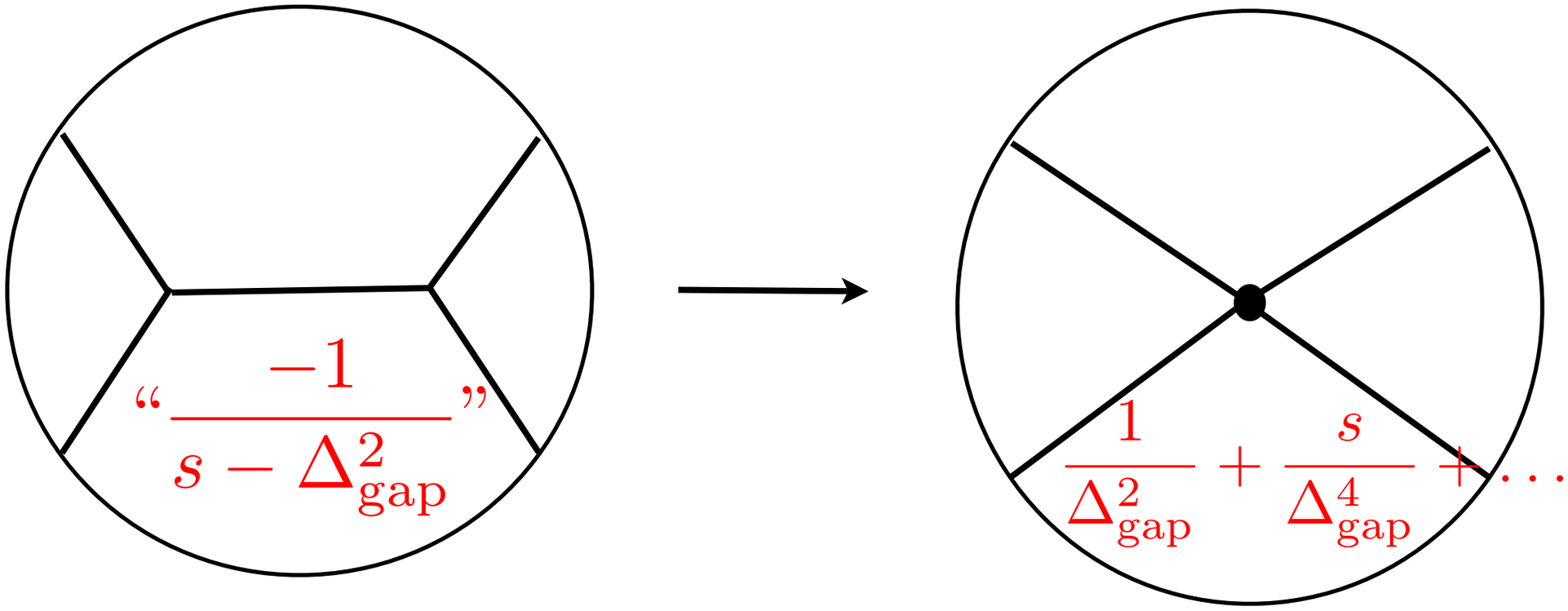
s-channel OPE coefficients ~ weighted areas

$$c(j, \tfrac{d}{2}+i\nu) \sim \int_0^1 d(z\bar{z})(z\bar{z})^{j/2-1} e^{-(\sqrt{z}+\sqrt{\bar{z}})\Delta_{\rm gap}} \times \int d(z/\bar{z})(\ldots)$$

$$\propto \frac{1}{(\Delta^2_{\rm gap})^{j-1}}$$

Area itself is (inverse) stress-tensor two-point function

$$\Rightarrow \quad \left|c(j, \tfrac{d}{2}+i\nu)_{\rm heavy}\right| \leq \frac{1}{c_T} \frac{\#}{(\Delta^2_{\rm gap})^{j-2}}$$



- AdS/CFT expectation: EFT coefficients suppressed by dimension: $(\partial^{2k})\phi^4$ down by $1/\Delta_{\rm gap}^{2k}$

- What this shows: down by spin $1/\Delta_{\rm gap}^{2(j-2)}$

- Same as 'causality bound' conjectured recently (equivalent to existence of dispersion relation in the bulk)
[Maldacena,Simmons-Duffin&Zhiboedov '15]

- What was known from CFT:
  Solutions to crossing symmetry in a large-N CFT with large gap = Witten diagrams

  [Heemskerk,Penedones, Polchinski& Sully '09]

  For given light spectrum, solutions are ambiguous by contact interactions

- What we learn:
  analyticity in spin (good Regge behavior) singles out a unique, 'causal' solution, up to errors:

  $$< 1/(\Delta^2_{\rm gap})^{j-2}$$

- key step toward AdS/CFT from CFT!

(Spin versus dimension)

- Some sporadic few-derivative interactions remain unconstrained
- Consider an AdS interaction with flat-space limit:

$$stu$$

- This has spin two in the Regge limit in all channels:

$$stu = st(s+t) \sim s^2 \equiv s^j \qquad (s \to \infty, t \,\text{fixed})$$

- All interactions with more derivative, however, must have small coefficients

Conclusion

- Novel formula: *(Froissart-Gribov-like)*

$$c(j,\Delta) \equiv \int_0^1 dz d\bar{z}\, g_{\Delta,j}\, \mathrm{dDisc}\, G$$

s-channel t-channel

- Valid in any unitary CFT_D. Regge behavior ensures convergence; ounds derivative interactions in AdS
- Opens the way for AdS/CFT beyond gravity
- Outlook:
  -Numerical bootstrap: bound errors using convergent 1/j expansion?
  -Higher points?

& much more!

Interpretation of Q_j

- Legendre polys P_j: finite dim representations, with J_z = -j…j:

Ex: $$P_4(\cos\theta) \propto 35e^{4i\theta} + 20e^{2i\theta} + 18 + 20e^{-2i\theta} + 35e^{-4i\theta}$$

- Q_j functions associated with infinite-dim highest-weight reps:

$$Q_j(\cosh\eta) = e^{-(j+1)\eta} + \#e^{-(j+3)\eta} + \#'e^{-(j+5)\eta} + \ldots$$

- Q_j = second solution to Legendre diff eq.

Rapidity factorization of high-energy scattering processes at NLO

Giovanni Antonio Chirilli

University of Regensburg

Saturation: Recent Developments, New Ideas and Measurements
Upton - NY, USA 26 - 28 April, 2017

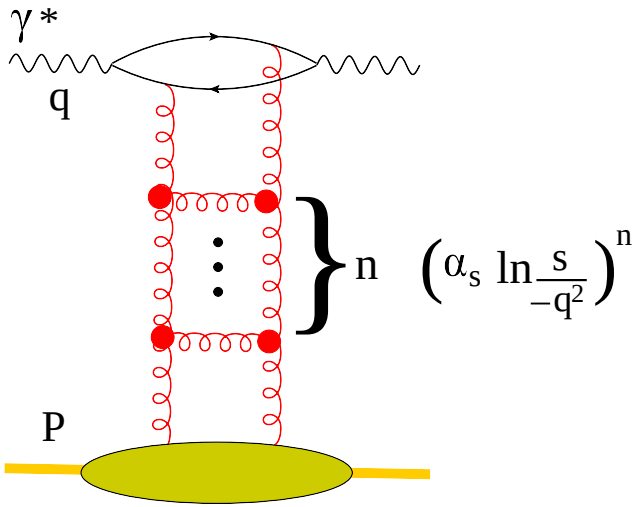
Outline

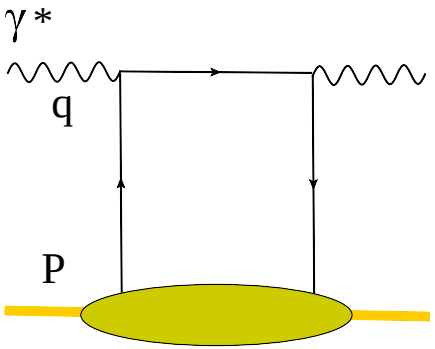
- High-energy Operator Product Expansion: factorization in rapidity space.
- Evolution equation and background field method.
- NLO impact factor and composite Wilson line operators.
- Application of high-energy OPE at NLO: $\gamma^*\gamma^*$ scattering at NLO.
- Role of the composite Wilson line operators in $\gamma^*\gamma^*$ and DIS amplitudes and the $\gamma \to 1-\gamma$ symmetry.
- Conclusions.

Leading Log Approximation in scatt. process at high energy

electron-proton/nucleus Deep Inelastic Scattering (DIS) $s = (q+P)^2$

$$\langle P|\mathrm{T}\, j^{\mu}(x) j^{\nu}(y)|P\rangle$$

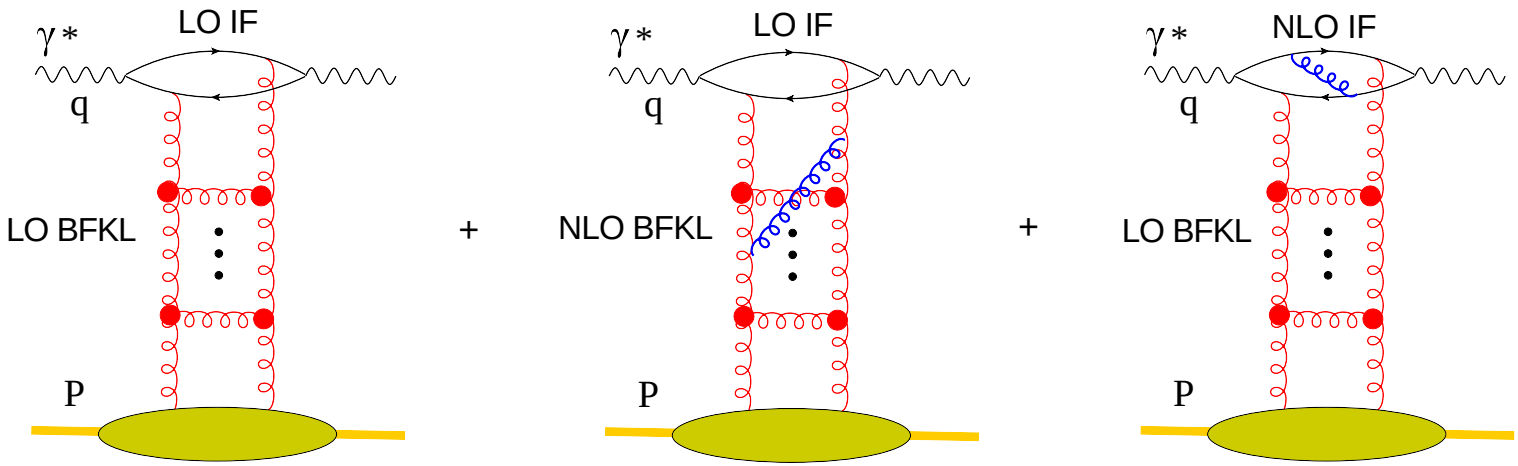




energy suppressed

- BFKL resum $\left(\alpha_s \ln \frac{s}{-q^2}\right)^n$
- Dynamics is linear and it describes proliferation of gluons
  $\Rightarrow$ Violation of Unitarity

NLO DIS with BFKL dynamics

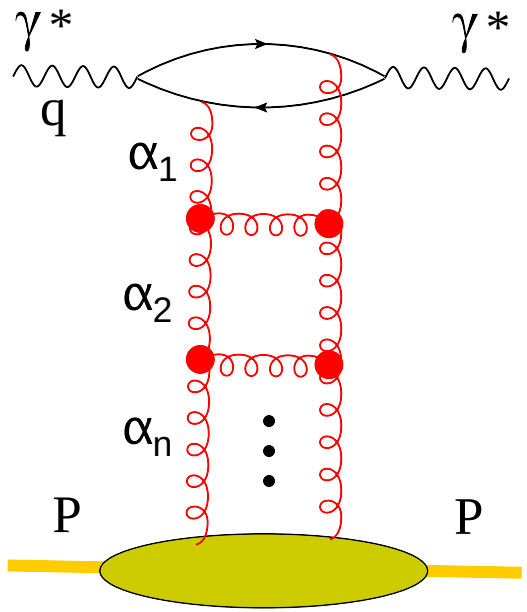


- NLO BFKL: $\alpha_s \left(\alpha_s \ln \frac{1}{x_B}\right)^n$
- NLO Impact factor contains contributions prop. to $\alpha_s \ln \frac{1}{x_B}$ which can be included in the LLA.
- Need systematics of perturbation theory
  $\Rightarrow$ Operator Product Expansion formalism can be the solution.

Semi-classical approach: Background field method

p_1^μ , p_2^μ light-cone vectors $\Rightarrow k^\mu = \alpha p_1^\mu + \beta p_2^\mu + k_\perp^\mu$

$\alpha_1 \gg \alpha_2 \ldots \gg \alpha_n$

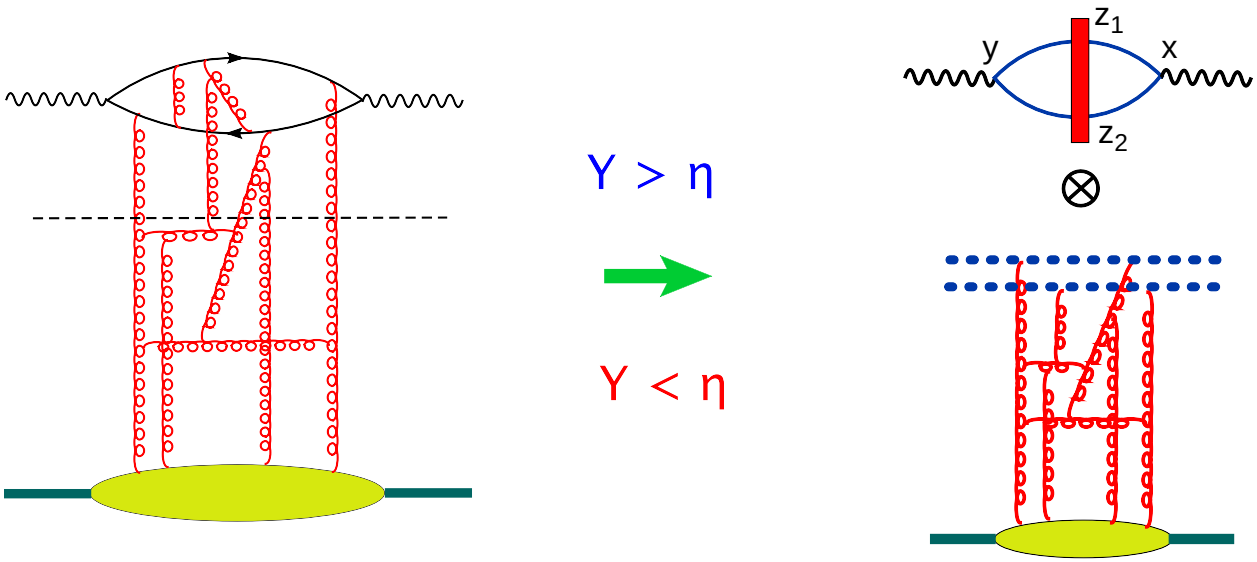


Fields are ordered in their rapidities $\Rightarrow$

- fast fields are treated as quantum fields
- slow fields are treated as classical fields

High-Energy Operator Product Expansion

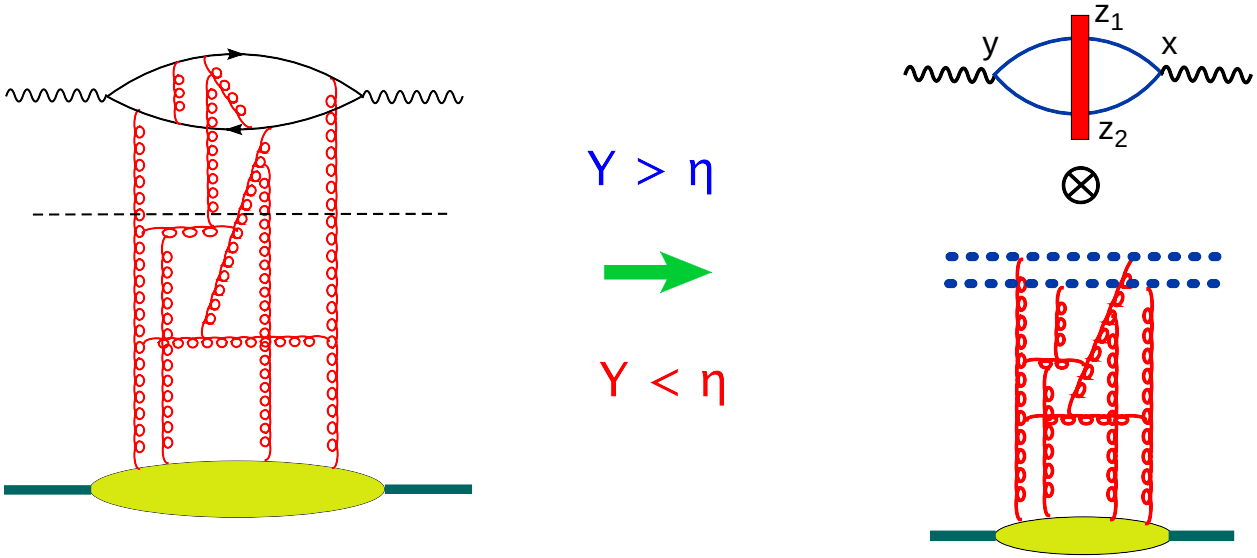
DIS amplitude is factorized in rapidity: η



$|B\rangle$ is the target state.

$$\langle B|T\{\hat{j}_\mu(x)\hat{j}_\nu(y)\}|B\rangle = \int \frac{d^2z_1 d^2z_2}{z_{12}^4}\, I^{\rm LO}_{\mu\nu}(x,y;z_1,z_2)\langle B|{\rm tr}\{\hat{U}^\eta_{z_1}\hat{U}^{\dagger\eta}_{z_2}\}|B\rangle + \dots$$

High-Energy Operator Product Expansion

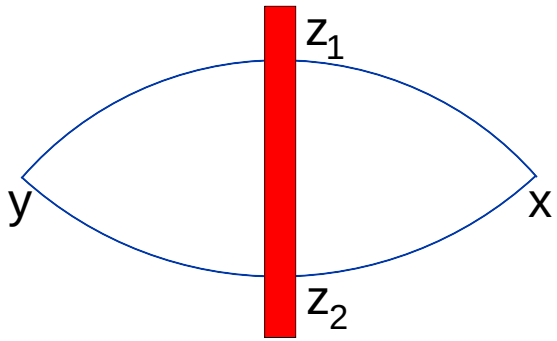


$$\langle B|T\{\hat{j}_\mu(x)\hat{j}_\nu(y)\}|B\rangle = \int \frac{d^2z_1 d^2z_2}{z_{12}^4} I^{\rm LO}_{\mu\nu}(x,y;z_1,z_2)\langle B|{\rm tr}\{\hat{U}^\eta_{z_1}\hat{U}^{\dagger\eta}_{z_2}\}|B\rangle + \dots$$

- If we use a model to evaluate $\langle B|{\rm tr}\{\hat{U}^\eta_{z_1}\hat{U}^{\dagger\eta}_{z_2}\}|B\rangle$ we can calculate the DIS cross-section.
- If we want to include energy dependence to the DIS cross section, we need to find the evolution of $\langle B|{\rm tr}\{\hat{U}^\eta_{z_1}\hat{U}^{\dagger\eta}_{z_2}\}|B\rangle$ with respect to the rapidity parameter η.

LO Impact Factor

Conformal invariance: $(x^+, x_\perp)^2 = -x_\perp^2 \Rightarrow$ after the inversion $x_\perp \to x_\perp/x_\perp^2$ and $x^+ \to x^+/x_\perp^2$



Conformal vectors:

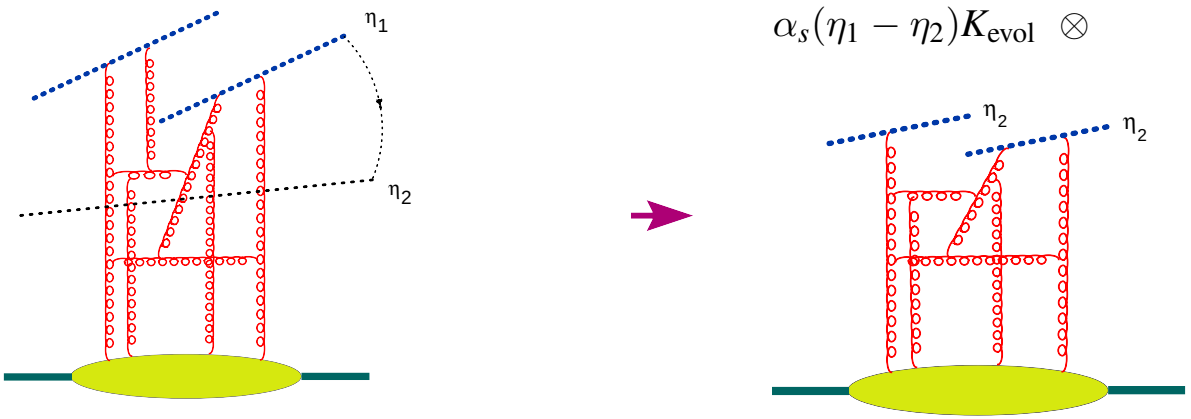
$$\kappa = \frac{\sqrt{s}}{2x_*}\left(\frac{p_1}{s} - x^2 p_2 + x_\perp\right) - \frac{\sqrt{s}}{2y_*}\left(\frac{p_1}{s} - y^2 p_2 + y_\perp\right)$$

$$\zeta_1 = \left(\frac{p_1}{s} + z_{1\perp}^2 p_2 + z_{1\perp}\right), \qquad \zeta_2 = \left(\frac{p_1}{s} + z_{2\perp}^2 p_2 + z_{2\perp}\right)$$

$\sqrt{\frac{s}{2}}x^+ = x_* \equiv x_\mu p_2^\mu$ (similarly for y); $\mathcal{R} = \frac{\kappa^2(\zeta_1\cdot\zeta_2)}{2(\kappa\cdot\zeta_1)(\kappa\cdot\zeta_2)}$

$$I_{\mu\nu}^{\rm LO}(z_1, z_2) = \frac{\mathcal{R}^2}{\pi^6(\kappa\cdot\zeta_1)(\kappa\cdot\zeta_2)} \frac{\partial^2}{\partial x^\mu \partial y^\nu}\left[(\kappa\cdot\zeta_1)(\kappa\cdot\zeta_2) - \frac{1}{2}\kappa^2(\zeta_1\cdot\zeta_2)\right]$$

Evolution Equation



- Separate fields in quantum and classical according to low and large rapidity. Formally we may write:

$$\langle B|\mathcal{O}^{\eta_1}|B\rangle \to \langle\mathcal{O}^{\eta_1}\rangle_A \to \langle\mathcal{O}'^{\eta_2}\otimes\mathcal{O}'^{\eta_1}\rangle_A$$

- Integrate over the quantum fields and get one-loop rapidity evolution of the operator $\mathcal{O}$

$$\langle\mathcal{O}^{\eta_1}\rangle_A = \alpha_s(\eta_1-\eta_2)K_{\rm evol}\otimes\langle\mathcal{O}'^{\eta_2}\rangle_A$$

- Where in principle $\mathcal{O}$ and $\mathcal{O}'$ are different operators.

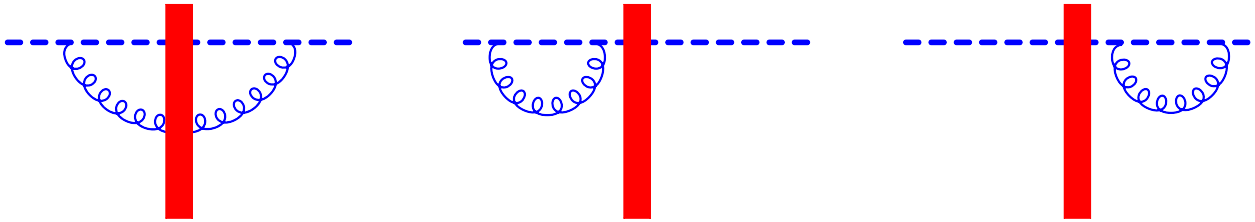
Non-linear evolution equation

- Linear case $\mathcal{O}^{\eta_1} = \alpha_s \Delta\eta \, K_{\text{evol}} \otimes \mathcal{O}^{\eta_2}$

Non-linear evolution equation

- Linear case $\mathcal{O}^{\eta_1} = \alpha_s \Delta\eta \, K_{\text{evol}} \otimes \mathcal{O}^{\eta_2}$
- Non-linear case $\mathcal{O}^{\eta_1} = \alpha_s \Delta\eta \, K_{\text{evol}} \otimes \{\mathcal{O}^{\eta_2} \mathcal{O}^{\eta_2}\}$

Non-linear evolution equation

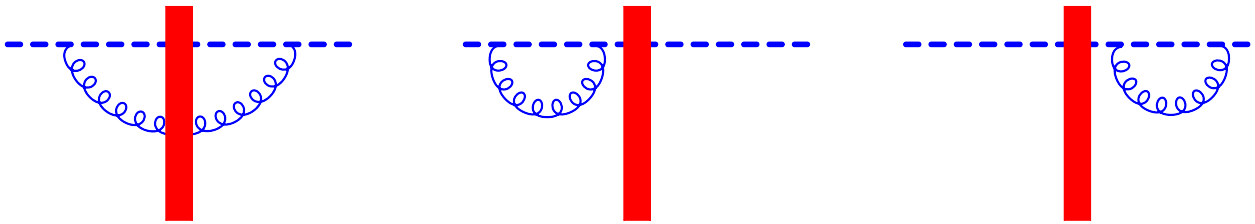


$$\langle \{U_x^{\eta_1}\}_{ij} \rangle_A = \frac{\alpha_s}{2\pi^2} \Delta\eta \int \frac{d^2 z_\perp}{(x-z)_\perp^2} \left[\langle \mathrm{tr}\{U_x^{\eta_2} U_z^{\eta_2 \dagger}\} \{U_z^{\eta_2}\}_{ij} \rangle_A - \langle \frac{1}{N_c} \{U_x^{\eta_2}\}_{ij} \rangle_A \right]$$

$\Delta = \eta_1 - \eta_2$

$$\{U_x^{\dagger \eta_1}\}_{ij}, \quad \{U_x^{\eta_1} U_y^{\eta_1}\}_{ij}, \quad \{U_x^{\eta_1} U_y^{\dagger \eta_1}\}_{ij}, \quad \{U_x^{\dagger \eta_1} U_y^{\dagger \eta_1}\}_{ij}$$

Non-linear evolution equation



$$\langle\{U_x^{\eta_1}\}_{ij}\rangle_A = \frac{\alpha_s}{2\pi^2}\Delta\eta\int\frac{d^2z_\perp}{(x-z)_\perp^2}\left[\langle \mathrm{tr}\{U_x^{\eta_2}U_z^{\eta_2\dagger}\}\{U_z^{\eta_2}\}_{ij}\rangle_A - \langle\frac{1}{N_c}\{U_x^{\eta_2}\}_{ij}\rangle_A\right]$$

$\Delta = \eta_1 - \eta_2$

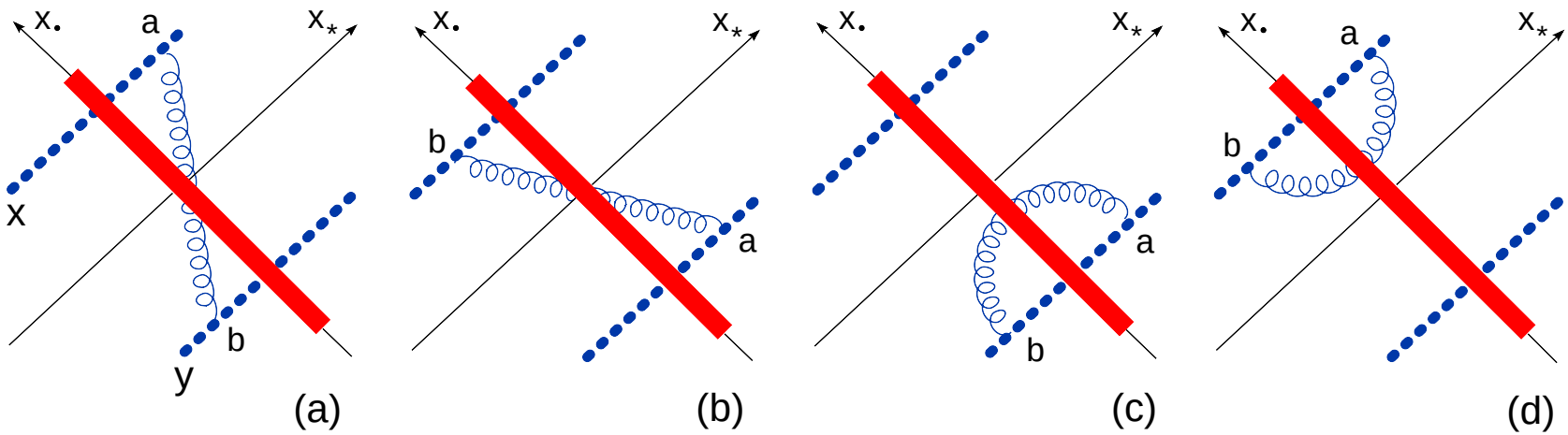
$$\{U_x^{\dagger\eta_1}\}_{ij},\quad \{U_x^{\eta_1}U_y^{\eta_1}\}_{ij},\quad \{U_x^{\eta_1}U_y^{\dagger\eta_1}\}_{ij},\quad \{U_x^{\dagger\eta_1}U_y^{\dagger\eta_1}\}_{ij}$$

- Obtain a set of rules that allow one to get the LO evolution of any trace or product of traces of Wilson lines
- Hierarchy of evolution equation: B-JIMWLK equation.

Leading order evolution equation

$$\frac{d}{d\eta}\mathrm{tr}\{\hat{U}_x\hat{U}_y^\dagger\} = K_{\mathrm{LO}}\mathrm{tr}\{\hat{U}_x\hat{U}_y^\dagger\} + \ldots \quad \Rightarrow$$

$$\frac{d}{d\eta}\langle \mathrm{tr}\{\hat{U}_x\hat{U}_y^\dagger\}\rangle_{\mathrm{shockwave}} = \langle K_{\mathrm{LO}}\mathrm{tr}\{\hat{U}_x\hat{U}_y^\dagger\}\rangle_{\mathrm{shockwave}}$$



$$x_\bullet = \sqrt{\tfrac{s}{2}}x^- \qquad x_* = \sqrt{\tfrac{s}{2}}x^+$$

Non-linear evolution equation: Balitsky-Kovchegov equation

$$\hat{\mathcal{U}}(x,y) \equiv 1 - \frac{1}{N_c}\mathrm{tr}\{\hat{U}(x_\perp)\hat{U}^\dagger(y_\perp)\}$$

$$\frac{d}{d\eta}\hat{\mathcal{U}}(x,y) \;=\; \frac{\alpha_s N_c}{2\pi^2}\int \frac{d^2z\,(x-y)^2}{(x-z)^2(y-z)^2}\Big\{\hat{\mathcal{U}}(x,z)+\hat{\mathcal{U}}(z,y)-\hat{\mathcal{U}}(x,y)-\hat{\mathcal{U}}(x,z)\hat{\mathcal{U}}(z,y)\Big\}$$

Non-linear evolution equation: Balitsky-Kovchegov equation

$$\hat{\mathcal{U}}(x,y) \equiv 1 - \frac{1}{N_c}\mathrm{tr}\{\hat{U}(x_\perp)\hat{U}^\dagger(y_\perp)\}$$

$$\frac{d}{d\eta}\hat{\mathcal{U}}(x,y) = \frac{\alpha_s N_c}{2\pi^2}\int \frac{d^2z\,(x-y)^2}{(x-z)^2(y-z)^2}\left\{\hat{\mathcal{U}}(x,z) + \hat{\mathcal{U}}(z,y) - \hat{\mathcal{U}}(x,y) - \hat{\mathcal{U}}(x,z)\hat{\mathcal{U}}(z,y)\right\}$$

- LLA for DIS in pQCD $\Rightarrow$ BFKL
  - (LLA: $\alpha_s \ll 1, \alpha_s\eta \sim 1$): describes proliferation of gluons.

Non linear evolution equation: Balitsky-Kovchegov equation

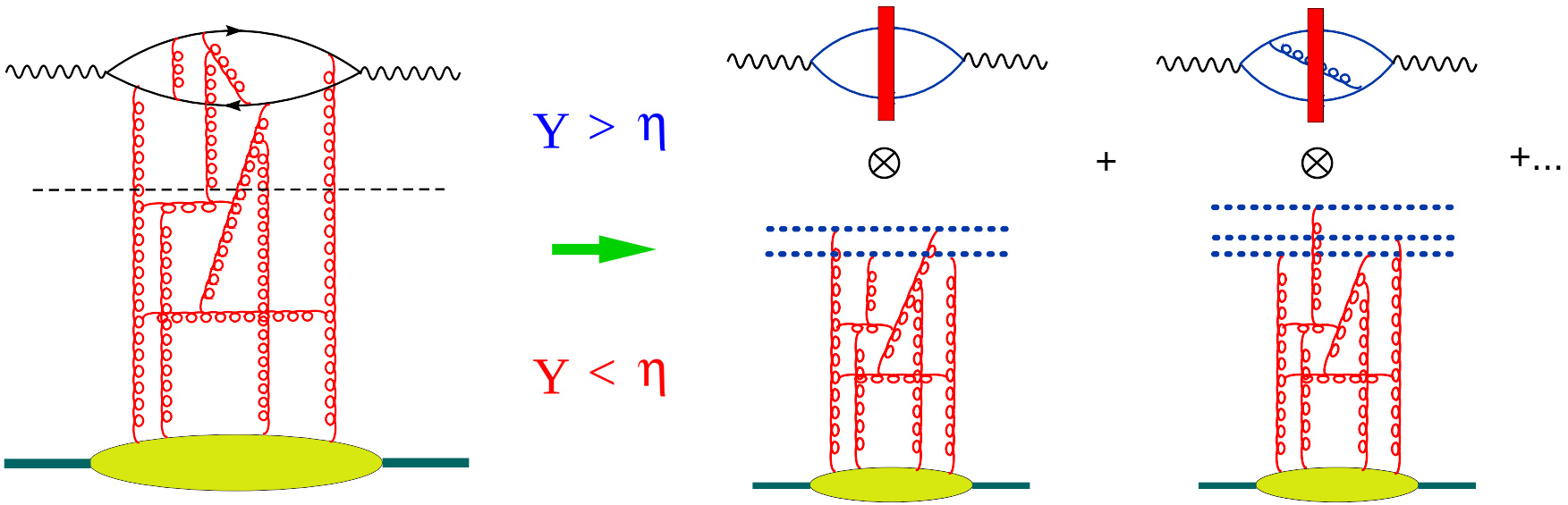
$$\hat{\mathcal{U}}(x,y) \equiv 1 - \frac{1}{N_c}\mathrm{tr}\{\hat{U}(x_\perp)\hat{U}^\dagger(y_\perp)\}$$

$$\frac{d}{d\eta}\hat{\mathcal{U}}(x,y) = \frac{\alpha_s N_c}{2\pi^2}\int \frac{d^2z\,(x-y)^2}{(x-z)^2(y-z)^2}\Big\{\hat{\mathcal{U}}(x,z) + \hat{\mathcal{U}}(z,y) - \hat{\mathcal{U}}(x,y) - \hat{\mathcal{U}}(x,z)\hat{\mathcal{U}}(z,y)\Big\}$$

- LLA for DIS in pQCD $\Rightarrow$ BFKL
  - (LLA: $\alpha_s \ll 1, \alpha_s\eta \sim 1$): describes proliferation of gluons.

- LLA for DIS in semi-classical-QCD $\Rightarrow$ BK eqn
  - background field method: describes recombination process.

High-energy expansion in color dipoles at the NLO



The high-energy operator expansion is

$$T\{\hat{j}_\mu(x)\hat{j}_\nu(y)\} = \int d^2z_1 d^2z_2\; I^{\rm LO}_{\mu\nu}(z_1,z_2,x,y)\,{\rm Tr}\{\hat{U}^\eta_{z_1}\hat{U}^{\dagger\eta}_{z_2}\}$$

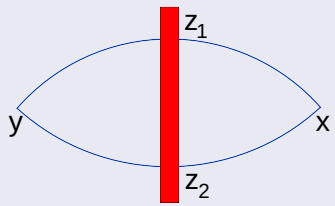
$$+\int d^2z_1 d^2z_2 d^2z_3\; I^{\rm NLO}_{\mu\nu}(z_1,z_2,z_3,x,y)\,[{\rm tr}\{\hat{U}^\eta_{z_1}\hat{U}^{\dagger\eta}_{z_3}\}{\rm tr}\{\hat{U}^\eta_{z_3}\hat{U}^{\dagger\eta}_{z_2}\} - N_c\,{\rm tr}\{\hat{U}^\eta_{z_1}\hat{U}^{\dagger\eta}_{z_2}\}]$$

LO and NLO Impact Factor

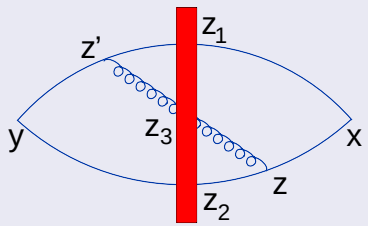
$$T\{\hat{j}_\mu(x)\hat{j}_\nu(y)\} = \int d^2z_1 d^2z_2\, I^{\rm LO}_{\mu\nu}(z_1,z_2,x,y)\mathrm{Tr}\{\hat{U}^\eta_{z_1}\hat{U}^{\dagger\eta}_{z_2}\}$$

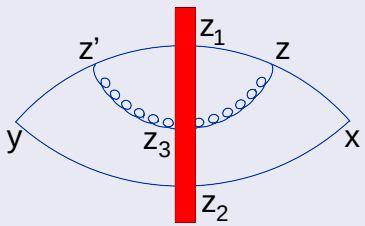
$$+\int d^2z_1 d^2z_2 d^2z_3\, I^{\rm NLO}_{\mu\nu}(z_1,z_2,z_3,x,y)[\mathrm{tr}\{\hat{U}^\eta_{z_1}\hat{U}^{\dagger\eta}_{z_3}\}\mathrm{tr}\{\hat{U}^\eta_{z_3}\hat{U}^{\dagger\eta}_{z_2}\} - N_c\mathrm{tr}\{\hat{U}^\eta_{z_1}\hat{U}^{\dagger\eta}_{z_2}\}]$$

LO Impact Factor diagram: $I^{\rm LO}$



NLO Impact Factor diagrams: $I^{\rm NLO}$





NLO Photon Impact Factor

$$\left[\langle T\{\hat{j}_\mu(x)\hat{j}_\nu(y)\}\rangle_A\right]^{\rm LO} = \int \frac{d^2z_1 d^2z_2}{z_{12}^4}\, I^{\rm LO}_{\mu\nu}(x,y;z_1,z_2)\langle {\rm tr}\{\hat{U}^\eta_{z_1}\hat{U}^{\dagger\eta}_{z_2}\}\rangle_A$$

$$\left[\langle T\{\hat{j}_\mu(x)\hat{j}_\nu(y)\}\rangle_A\right]^{\rm NLO} = \int \frac{d^2z_1 d^2z_2}{z_{12}^4} d^2z_3 \left[I_1^{\mu\nu}(z_1,z_2,z_3) + I_2^{\mu\nu}(z_1,z_2,z_3)\right] \times\left[{\rm tr}\{U_{z_1}U^\dagger_{z_3}\}{\rm tr}\{U_{z_3}U^\dagger_{z_2}\} - N_c{\rm tr}\{U_{z_1}U^\dagger_{z_2}\}\right]$$

where $I_2^{\mu\nu}(z_1,z_2,z_3)$ is finite and conformal, while

$$I_1^{\mu\nu}(z_1,z_2,z_3) = \frac{\alpha_s}{2\pi^2} I^{\rm LO}_{\mu\nu}\frac{z_{12}^2}{z_{13}^2 z_{23}^2}\int_0^{+\infty}\frac{d\alpha}{\alpha}\, e^{i\frac{s\alpha}{4}z_3}$$

is rapidity divergent.

How to get the NLO Impact factor

$$\langle T\{\hat{j}_\mu(x)\hat{j}_\nu(y)\}\rangle_A = \int \frac{d^2z_1 d^2z_2}{z_{12}^4}\, I^{\rm LO}_{\mu\nu}(x,y;z_1,z_2)\langle {\rm tr}\{\hat{U}^\eta_{z_1}\hat{U}^{\dagger\eta}_{z_2}\}\rangle_A$$

$$+ \int \frac{d^2z_1 d^2z_2}{z_{12}^4} d^2z_3\; I^{\rm NLO}_{\mu\nu}(x,y;z_1,z_2,z_3;\eta)[{\rm tr}\{U_{z_1}U^\dagger_{z_3}\}{\rm tr}\{U_{z_3}U^\dagger_{z_2}\} - N_c{\rm tr}\{U_{z_1}U^\dagger_{z_2}\}] + \dots$$

$$\Rightarrow$$

$$\left[\langle T\{\hat{j}_\mu(x)\hat{j}_\nu(y)\}\rangle_A\right]^{\rm NLO} - \int \frac{d^2z_1 d^2z_2}{z_{12}^4}\, I^{\rm LO}_{\mu\nu}(x,y;z_1,z_2)\left[\langle {\rm tr}\{\hat{U}^\eta_{z_1}\hat{U}^{\dagger\eta}_{z_2}\}\rangle_A\right]^{\rm LO}$$

$$= \int \frac{d^2z_1 d^2z_2}{z_{12}^4} d^2z_3\; I^{\rm NLO}_{\mu\nu}(x,y;z_1,z_2,z_3;\eta)[{\rm tr}\{U_{z_1}U^\dagger_{z_3}\}{\rm tr}\{U_{z_3}U^\dagger_{z_2}\} - N_c{\rm tr}\{U_{z_1}U^\dagger_{z_2}\}]$$

$$\left[\langle {\rm tr}\{\hat{U}^\eta_{z_1}\hat{U}^{\dagger\eta}_{z_2}\}\rangle_A\right]^{\rm LO} = \frac{\alpha_s}{2\pi^2}\frac{z_{12}^2}{z_{13}^2 z_{23}^2}[{\rm tr}\{U_{z_1}U^\dagger_{z_3}\}{\rm tr}\{U_{z_3}U^\dagger_{z_2}\} - N_c{\rm tr}\{U_{z_1}U^\dagger_{z_2}\}]\int_0^{e^\eta}\frac{d\alpha}{\alpha}$$

How to get the NLO Impact factor

$$\int \frac{d^2z_1 d^2z_2}{z_{12}^4} d^2z_3 \; I^{\rm NLO}_{\mu\nu}(x,y;z_1,z_2,z_3;\eta)[{\rm tr}\{U_{z_1}U^\dagger_{z_3}\}{\rm tr}\{U_{z_3}U^\dagger_{z_2}\} - N_c{\rm tr}\{U_{z_1}U^\dagger_{z_2}\}]$$

$$= \int \frac{d^2z_1 d^2z_2}{z_{12}^4} d^2z_3 \left\{ I_2^{\mu\nu}(z_1,z_2,z_3) + \frac{\alpha_s}{2\pi^2} I^{\rm LO}_{\mu\nu} \frac{z_{12}^2}{z_{13}^2 z_{23}^2} \left[\int_0^{+\infty} \frac{d\alpha}{\alpha} \; e^{i\frac{s\alpha}{4}\mathcal{Z}_3} - \int_0^{e^\eta} \frac{d\alpha}{\alpha} \right] \right\}$$
$$\times [{\rm tr}\{U_{z_1}U^\dagger_{z_3}\}{\rm tr}\{U_{z_3}U^\dagger_{z_2}\} - N_c{\rm tr}\{U_{z_1}U^\dagger_{z_2}\}]$$

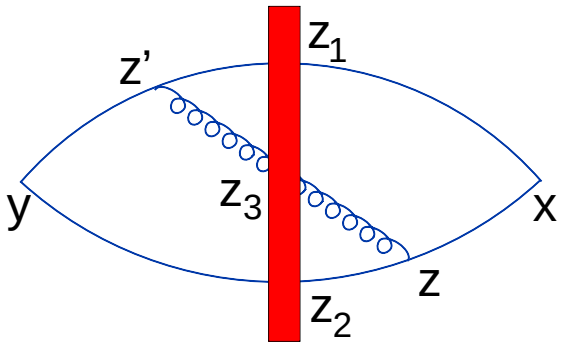
$$\left[\int_0^{+\infty} \frac{d\alpha}{\alpha} \; e^{i\frac{s\alpha}{4}\mathcal{Z}_3} - \int_0^{e^\eta} \frac{d\alpha}{\alpha} \right] \to -\ln\frac{\sigma s}{4}\mathcal{Z}_3 - \frac{i\pi}{2} + C$$

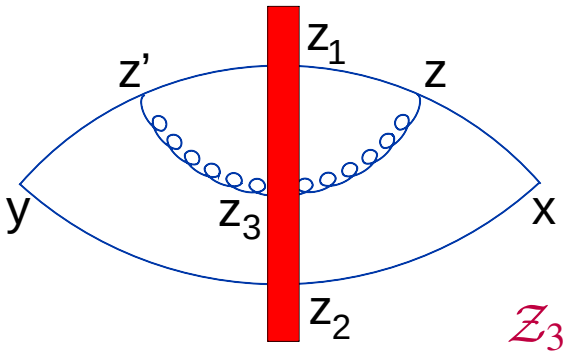
where $\sigma = e^\eta$ and C is the Euler constant

$$\mathcal{Z}_3 \equiv \frac{(x-z_3)^2_\perp}{x^+} - \frac{(y-z_3)^2_\perp}{y^+}$$

$\mathcal{Z}_3$ is not conformal invariant in the transverse 2-d coordinate space, but QCD at tree level has to be conformal invariant.

NLO Impact Factor





$$\mathcal{Z}_3 \equiv \frac{(x-z_3)^2_\perp}{x^+} - \frac{(y-z_3)^2_\perp}{y^+}$$

$$I^{\rm NLO}_{\mu\nu}(x,y;z_1,z_2,z_3;\eta) \;=\; -\,I^{\rm LO}_{\mu\nu}\times\frac{\alpha_s}{2\pi}\frac{z_{13}^2}{z_{12}^2 z_{23}^2}\ln\frac{\sigma s}{4}\mathcal{Z}_3 \;+\; \text{conf.}$$

The NLO impact factor is not Möbius invariant $\Rightarrow$ the color dipole with the cutoff $\eta = \ln\sigma$ is not invariant.

Conformal Composite Operator

Define a composite operator

$$[\mathrm{Tr}\{\hat{U}^{\eta}_{z_1}\hat{U}^{\dagger\eta}_{z_2}\}]^{\mathrm{conf}} = \mathrm{Tr}\{\hat{U}^{\eta}_{z_1}\hat{U}^{\dagger\eta}_{z_2}\}$$
$$+\frac{\alpha_s}{4\pi^2}\int d^2z_3\,\frac{z_{12}^2}{z_{13}^2 z_{23}^2}[\mathrm{tr}\{\hat{U}^{\eta}_{z_1}\hat{U}^{\dagger\eta}_{z_3}\}\mathrm{tr}\{\hat{U}^{\eta}_{z_3}\hat{U}^{\dagger\eta}_{z_2}\} - N_c\mathrm{Tr}\{\hat{U}^{\eta}_{z_1}\hat{U}^{\dagger\eta}_{z_2}\}]\ln\frac{4\,a\,z_{12}^2}{\sigma^2\,s\,z_{13}^2 z_{23}^2} + O(\alpha_s^2)$$

(a - analog of μ^{-2} for usual OPE)

the impact factor becomes conformal at the NLO.

Conformal Composite Operator

Define a composite operator

$$[\mathrm{Tr}\{\hat{U}^{\eta}_{z_1}\hat{U}^{\dagger\eta}_{z_2}\}]^{\mathrm{conf}} = \mathrm{Tr}\{\hat{U}^{\eta}_{z_1}\hat{U}^{\dagger\eta}_{z_2}\}$$
$$+\frac{\alpha_s}{4\pi^2}\int d^2z_3\,\frac{z_{12}^2}{z_{13}^2 z_{23}^2}[\mathrm{tr}\{\hat{U}^{\eta}_{z_1}\hat{U}^{\dagger\eta}_{z_3}\}\mathrm{tr}\{\hat{U}^{\eta}_{z_3}\hat{U}^{\dagger\eta}_{z_2}\} - N_c\mathrm{Tr}\{\hat{U}^{\eta}_{z_1}\hat{U}^{\dagger\eta}_{z_2}\}]\ln\frac{4\,a\,z_{12}^2}{\sigma^2\,s\,z_{13}^2 z_{23}^2} + O(\alpha_s^2)$$

(a - analog of μ^{-2} for usual OPE)

the impact factor becomes conformal at the NLO.

$$[\mathrm{Tr}\{\hat{U}^{\eta}_{z_1}\hat{U}^{\dagger\eta}_{z_2}\}]^{\mathrm{conf}} = \mathrm{Tr}\{\hat{U}^{\eta}_{z_1}\hat{U}^{\dagger\eta}_{z_2}\} + BK_{\mathrm{LO}}\ln\sqrt{\frac{4\,a\,z_{12}^2}{\sigma^2\,s\,z_{13}^2 z_{23}^2}} + O(\alpha_s^2)$$

Conformal Composite Operator

Define a composite operator

$$[\mathrm{Tr}\{\hat{U}^{\eta}_{z_1}\hat{U}^{\dagger\eta}_{z_2}\}]^{\mathrm{conf}} = \mathrm{Tr}\{\hat{U}^{\eta}_{z_1}\hat{U}^{\dagger\eta}_{z_2}\}$$
$$+\frac{\alpha_s}{4\pi^2}\int d^2z_3\,\frac{z_{12}^2}{z_{13}^2 z_{23}^2}[\mathrm{tr}\{\hat{U}^{\eta}_{z_1}\hat{U}^{\dagger\eta}_{z_3}\}\mathrm{tr}\{\hat{U}^{\eta}_{z_3}\hat{U}^{\dagger\eta}_{z_2}\} - N_c\mathrm{Tr}\{\hat{U}^{\eta}_{z_1}\hat{U}^{\dagger\eta}_{z_2}\}]\ln\frac{4\,a\,z_{12}^2}{\sigma^2\,s\,z_{13}^2 z_{23}^2} + O(\alpha_s^2)$$

(a - analog of μ^{-2} for usual OPE)
the impact factor becomes conformal at the NLO.

$$[\mathrm{Tr}\{\hat{U}^{\eta}_{z_1}\hat{U}^{\dagger\eta}_{z_2}\}]^{\mathrm{conf}} = \mathrm{Tr}\{\hat{U}^{\eta}_{z_1}\hat{U}^{\dagger\eta}_{z_2}\} + BK_{\mathrm{LO}}\ln\sqrt{\frac{4\,a\,z_{12}^2}{\sigma^2\,s\,z_{13}^2 z_{23}^2}} + O(\alpha_s^2)$$

$$[\mathrm{Tr}\{\hat{U}^{\eta}_{z_1}\hat{U}^{\dagger\eta}_{z_2}\}]^{\mathrm{conf}} = \mathrm{Tr}\{\hat{U}^{\eta}_{z_1}\hat{U}^{\dagger\eta}_{z_2}\} + BK_{\mathrm{LO}}\int_0^{\sqrt{\frac{a\,z_{12}^2}{z_{13}^2 z_{23}^2}}}\frac{d\alpha}{\alpha} + O(\alpha_s^2)$$

(cf. Caron-Huot's talk)

Conformal Composite Operator

$$[\mathrm{Tr}\{\hat{U}_{z_1}\hat{U}^\dagger_{z_2}\}]^{\mathrm{conf}}_{a,\eta}$$

$$= \mathrm{Tr}\{\hat{U}^\eta_{z_1}\hat{U}^{\dagger\eta}_{z_2}\} + \frac{\alpha_s}{4\pi^2}\int d^2z_3\,\frac{z_{12}^2}{z_{13}^2 z_{23}^2}[\mathrm{tr}\{\hat{U}^\eta_{z_1}\hat{U}^{\dagger\eta}_{z_3}\}\mathrm{tr}\{\hat{U}^\eta_{z_3}\hat{U}^{\dagger\eta}_{z_2}\} - N_c\mathrm{Tr}\{\hat{U}^\eta_{z_1}\hat{U}^{\dagger\eta}_{z_2}\}]\ln\frac{4\,a\,z_{12}^2}{\sigma^2\,s\,z_{13}^2 z_{23}^2} + O(\alpha_s^2)$$

choose a rapidity-dependent constant $a \to ae^{-2\eta} \Rightarrow [\mathrm{Tr}\{\hat{U}^\sigma_{z_1}\hat{U}^{\dagger\sigma}_{z_2}\}]^{\mathrm{conf}}_{a}$
does not depend on $\eta = \ln\sigma$ and all the rapidity dependence is encoded into a-dependence:

$$[\mathrm{Tr}\{\hat{U}_{z_1}\hat{U}^\dagger_{z_2}\}]^{\mathrm{conf}}_{a}$$

$$= \mathrm{Tr}\{\hat{U}^\eta_{z_1}\hat{U}^{\dagger\eta}_{z_2}\} + +\frac{\alpha_s}{4\pi^2}\int d^2z_3\,\frac{z_{12}^2}{z_{13}^2 z_{23}^2}[\mathrm{tr}\{\hat{U}^\eta_{z_1}\hat{U}^{\dagger\eta}_{z_3}\}\mathrm{tr}\{\hat{U}^\eta_{z_3}\hat{U}^{\dagger\eta}_{z_2}\} - N_c\mathrm{Tr}\{\hat{U}^\eta_{z_1}\hat{U}^{\dagger\eta}_{z_2}\}]\ln\frac{4\,a\,z_{12}^2}{\sigma^2\,s\,z_{13}^2 z_{23}^2} + O(\alpha_s^2)$$

Using the leading-order evolution equation

$$\frac{d}{d\eta}\mathrm{Tr}\{\hat{U}^\eta_{z_1}\hat{U}^{\dagger\eta}_{z_2}\} = \frac{\alpha_s}{2\pi^2}\int d^2z_3\,\frac{z_{12}^2}{z_{13}^2 z_{23}^2}[\mathrm{tr}\{\hat{U}^\eta_{z_1}\hat{U}^{\dagger\eta}_{z_3}\}\mathrm{tr}\{\hat{U}^\eta_{z_3}\hat{U}^{\dagger\eta}_{z_2}\} - N_c\mathrm{Tr}\{\hat{U}^\eta_{z_1}\hat{U}^{\dagger\eta}_{z_2}\}]$$

$\Rightarrow \frac{d}{d\eta}[\mathrm{Tr}\{\hat{U}_{z_1}\hat{U}^\dagger_{z_2}\}]^{\mathrm{conf}}_{a} = 0$ (with $O(\alpha_s^2)$ accuracy).

$$2a\frac{d}{da}[\mathrm{Tr}\{\hat{U}_{z_1}\hat{U}^\dagger_{z_2}\}]^{\mathrm{conf}}_{a} = \frac{\alpha_s}{2\pi^2}\int d^2z_3\,\frac{z_{12}^2}{z_{13}^2 z_{23}^2}[\mathrm{tr}\{\hat{U}^\eta_{z_1}\hat{U}^{\dagger\eta}_{z_3}\}\mathrm{tr}\{\hat{U}^\eta_{z_3}\hat{U}^{\dagger\eta}_{z_2}\} - N_c\mathrm{Tr}\{\hat{U}^\eta_{z_1}\hat{U}^{\dagger\eta}_{z_2}\}]$$

Operator expansion in conformal dipoles

$$T\{\hat{j}_\mu(x)\hat{j}_\nu(y)\} = \int d^2z_1 d^2z_2\, I^{\rm LO}_{\mu\nu}(z_1,z_2,x,y)\,{\rm tr}[\{\hat{U}^\eta_{z_1}\hat{U}^{\dagger\eta}_{z_2}\}]^{\rm conf}$$

$$+\int d^2z_1 d^2z_2 d^2z_3\, I^{\rm NLO}_{\mu\nu}(z_1,z_2,z_3,x,y)[\frac{1}{N_c}{\rm tr}\{\hat{U}^\eta_{z_1}\hat{U}^{\dagger\eta}_{z_3}\}{\rm tr}\{\hat{U}^\eta_{z_3}\hat{U}^{\dagger\eta}_{z_2}\}-{\rm tr}\{\hat{U}^\eta_{z_1}\hat{U}^{\dagger\eta}_{z_2}\}]$$

$$I^{\rm NLO}_{\mu\nu} = -\,I^{\rm LO}_{\mu\nu}\,\frac{\alpha_s N_c}{4\pi}\int dz_3\,\frac{z_{12}^2}{z_{13}^2 z_{23}^2}\,\ln\frac{z_{12}^2 e^{2\eta} as^2}{z_{13}^2 z_{23}^2}\,\mathcal{Z}_3^2 + {\rm conf.}$$

The new NLO impact factor is conformally invariant.

In conformal $\mathcal{N}=4$ SYM theory one can construct the composite conformal dipole operator order by order in perturbation theory.

NLO structure functions for DIS off a large nucleus

$$(x-y)^4 T\{\bar{\hat{\psi}}(x)\gamma^\mu\hat{\psi}(x)\bar{\hat{\psi}}(y)\gamma^\nu\hat{\psi}(y)\} = \int \frac{d^2z_1 d^2z_2}{z_{12}^4}\Big\{ I^{\mu\nu}_{\rm LO}(z_1,z_2)\Big[1+\frac{\alpha_s}{\pi}\Big][{\rm tr}\{\hat{U}_{z_1}\hat{U}^\dagger_{z_2}\}]_{a_0}$$

$$+\int d^2z_3\Big[\frac{\alpha_s}{4\pi^2}\frac{z_{12}^2}{z_{13}^2 z_{23}^2}\Big(\ln\frac{\kappa^2(\zeta_1\cdot\zeta_3)(\zeta_1\cdot\zeta_3)}{2(\kappa\cdot\zeta_3)^2(\zeta_1\cdot\zeta_2)}-2C\Big)I^{\mu\nu}_{\rm LO}+I^{\mu\nu}_2\Big]$$

$$\times[{\rm tr}\{\hat{U}_{z_1}\hat{U}^\dagger_{z_3}\}{\rm tr}\{\hat{U}_{z_3}\hat{U}^\dagger_{z_2}\}-N_c{\rm tr}\{\hat{U}_{z_1}\hat{U}^\dagger_{z_2}\}]_{a_0}\Big\}$$

where

$$(I_2)_{\mu\nu}(z_1,z_2,z_3) = \frac{\alpha_s}{16\pi^8}\frac{\mathcal{R}^2}{(\kappa\cdot\zeta_1)(\kappa\cdot\zeta_2)}\Big\{\frac{(\kappa\cdot\zeta_2)}{(\kappa\cdot\zeta_3)}\frac{\partial^2}{\partial x^\mu\partial y^\nu}\Big[-\frac{(\kappa\cdot\zeta_1)^2}{(\zeta_1\cdot\zeta_3)}+\frac{(\kappa\cdot\zeta_1)(\kappa\cdot\zeta_2)}{(\zeta_2\cdot\zeta_3)}$$

$$+\frac{(\kappa\cdot\zeta_1)(\kappa\cdot\zeta_3)(\zeta_1\cdot\zeta_2)}{(\zeta_1\cdot\zeta_3)(\zeta_2\cdot\zeta_3)}-\frac{\kappa^2(\zeta_1\cdot\zeta_2)}{(\zeta_2\cdot\zeta_3)}\Big]+\frac{(\kappa\cdot\zeta_2)^2}{(\kappa\cdot\zeta_3)^2}\frac{\partial^2}{\partial x^\mu\partial y^\nu}\Big[\frac{(\kappa\cdot\zeta_1)(\kappa\cdot\zeta_3)}{(\zeta_2\cdot\zeta_3)}-\frac{\kappa^2(\zeta_1\cdot\zeta_3)}{2(\zeta_2\cdot\zeta_3)}\Big]$$

$$+(\zeta_1\leftrightarrow\zeta_2)\Big\}$$

NLO evolution of composite "conformal" dipoles in QCD

$$2a\frac{d}{da}[\mathrm{tr}\{\hat{U}_{z_1}U^{\dagger}_{z_2}\}]^{\mathrm{conf}} = \frac{\alpha_s}{2\pi^2}\int d^2z_3\,\Big([\mathrm{tr}\{\hat{U}_{z_1}\hat{U}^{\dagger}_{z_3}\}\mathrm{tr}\{\hat{U}_{z_3}\hat{U}^{\dagger}_{z_2}\} - N_c\mathrm{tr}\{\hat{U}_{z_1}\hat{U}^{\dagger}_{z_2}\}]^{\mathrm{conf}}$$

$$\times\frac{z_{12}^2}{z_{13}^2z_{23}^2}\Big[1+\frac{\alpha_sN_c}{4\pi}\Big(b\ln z_{12}^2\mu^2 + b\frac{z_{13}^2-z_{23}^2}{z_{13}^2z_{23}^2}\ln\frac{z_{13}^2}{z_{23}^2}+\frac{67}{9}-\frac{\pi^2}{3}\Big)\Big]$$

$$+\frac{\alpha_s}{4\pi^2}\int\frac{d^2z_4}{z_{34}^4}\Big\{\Big[-2+\frac{z_{14}^2z_{23}^2+z_{24}^2z_{13}^2-4z_{12}^2z_{34}^2}{2(z_{14}^2z_{23}^2-z_{24}^2z_{13}^2)}\ln\frac{z_{14}^2z_{23}^2}{z_{24}^2z_{13}^2}\Big]$$

$$\times[\mathrm{tr}\{\hat{U}_{z_1}\hat{U}^{\dagger}_{z_3}\}\mathrm{tr}\{\hat{U}_{z_3}\hat{U}^{\dagger}_{z_4}\}\{\hat{U}_{z_4}\hat{U}^{\dagger}_{z_2}\} - \mathrm{tr}\{\hat{U}_{z_1}\hat{U}^{\dagger}_{z_3}\hat{U}_{z_4}\hat{U}^{\dagger}_{z_2}\hat{U}_{z_3}\hat{U}^{\dagger}_{z_4}\} - (z_4\to z_3)]$$

$$+\frac{z_{12}^2z_{34}^2}{z_{13}^2z_{24}^2}\Big[2\ln\frac{z_{12}^2z_{34}^2}{z_{14}^2z_{23}^2}+\Big(1+\frac{z_{12}^2z_{34}^2}{z_{13}^2z_{24}^2-z_{14}^2z_{23}^2}\Big)\ln\frac{z_{13}^2z_{24}^2}{z_{14}^2z_{23}^2}\Big]$$

$$\times[\mathrm{tr}\{\hat{U}_{z_1}\hat{U}^{\dagger}_{z_3}\}\mathrm{tr}\{\hat{U}_{z_3}\hat{U}^{\dagger}_{z_4}\}\mathrm{tr}\{\hat{U}_{z_4}\hat{U}^{\dagger}_{z_2}\} - \mathrm{tr}\{\hat{U}_{z_1}\hat{U}^{\dagger}_{z_4}\hat{U}_{z_3}\hat{U}^{\dagger}_{z_2}\hat{U}_{z_4}\hat{U}^{\dagger}_{z_3}\} - (z_4\to z_3)]\Big\}$$

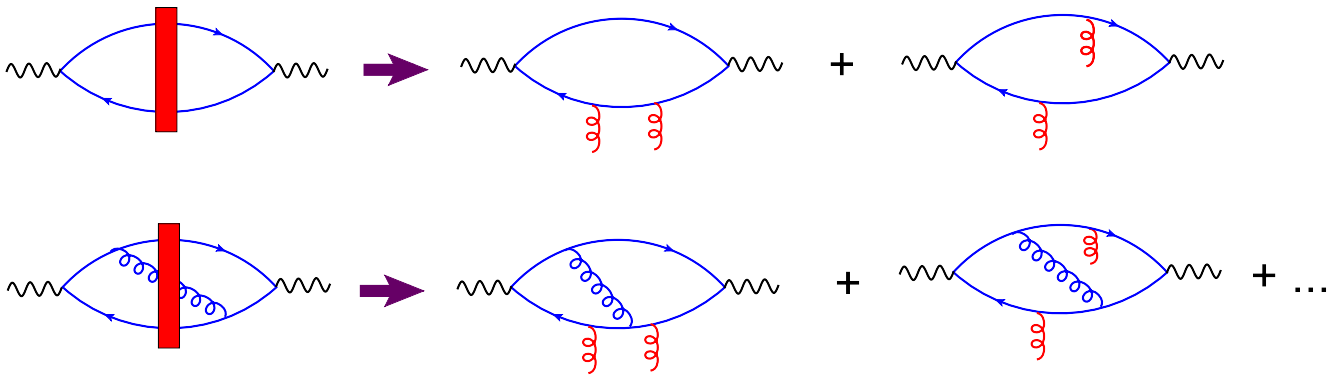
$$b=\tfrac{11}{3}N_c-\tfrac{2}{3}n_f$$

I. Balitsky and G.A.C

$K_{\mathrm{NLO\ BK}}$ = Running coupling part + Conformal "non-analytic" (in j) part + Conformal analytic ($\mathcal{N}=4$) part

Linearized $K_{\mathrm{NLO\ BK}}$ reproduces the known result for the forward NLO BFKL kernel Fadin and Lipatov (1998).

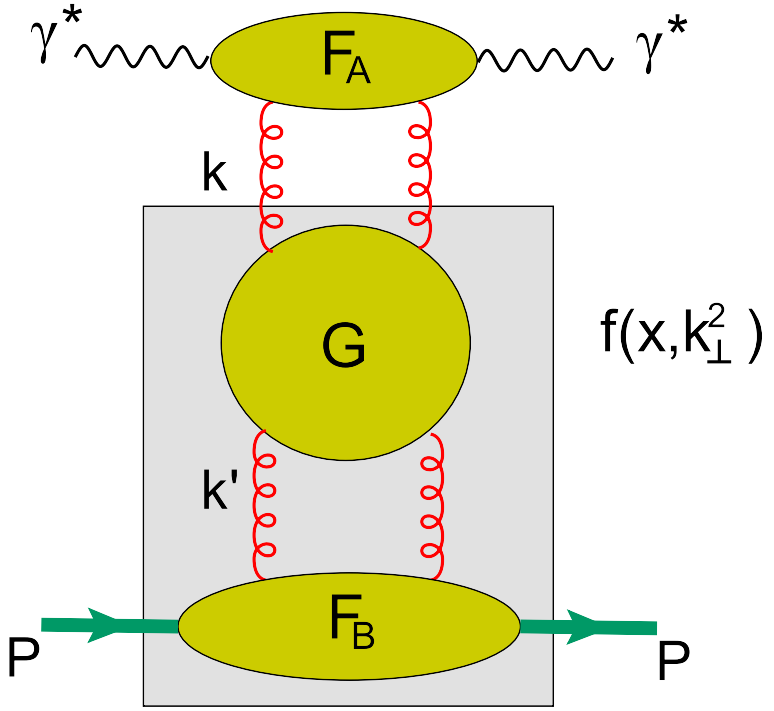
2-gluon approx. and BFKL pomeron in DIS



$$I^{\mathrm{LO}}\hat{\mathcal{U}}(x_\perp, y_\perp)$$
$$I^{\mathrm{NLO}}\left\{\hat{\mathcal{U}}(x,z)+\hat{\mathcal{U}}(z,y)-\hat{\mathcal{U}}(x,y)\right\}$$

where $\mathcal{U}(x,y) = 1 - \frac{1}{N_c}\mathrm{tr}\{U_x U_y^\dagger\}$ and we neglected the non-linear term $\hat{\mathcal{U}}(x,z)\hat{\mathcal{U}}(z,y)$

NLO DIS in the k_T factorization form



- $f(x,k_\perp^2) \propto \int \frac{d^2k'}{k'^2_\perp} F_B(k'^2_\perp)\, k_\perp^2\, G(x,k_\perp,k'_\perp)$
- $\mathcal{V}(z) \equiv z^{-2}\mathcal{U}(z)$

$$2a\frac{d}{da}\mathcal{V}_a(z) \;=\; \frac{\alpha_s N_c}{2\pi^2}\int d^2z'\,\left[\frac{2\mathcal{V}_a(z')}{(z-z')^2} - \frac{z^2\mathcal{V}_a(z)}{z'^2(z-z')^2}\right]$$

$$\int d^4x\, e^{iqx}\langle p|T\{\hat{j}_\mu(x)\hat{j}_\nu(0)\}|p\rangle \;=\; \frac{s}{2}\int\frac{d^2k_\perp}{k_\perp^2}\, I_{\mu\nu}(q,k_\perp)\mathcal{V}_{a_m=x_B}(k_\perp)$$

NLO Evolution of the unintegrated gluon distribution

$$
\begin{aligned}
2a\frac{d}{da}\mathcal{V}_a(k) \;=\; & \frac{\alpha_s N_c}{\pi^2}\int d^2k'\Big\{\Big[\frac{\mathcal{V}_a(k')}{(k-k')^2}-\frac{(k,k')\mathcal{V}_a(k)}{k'^2(k-k')^2}\Big] \\
& \times\Big(1+\frac{\alpha_s b}{4\pi}\Big[\ln\frac{\mu^2}{k^2}+\frac{N_c}{b}\Big(\frac{67}{9}-\frac{\pi^2}{3}-\frac{10n_f}{9N_c}\Big)\Big]\Big)-\frac{b\alpha_s}{4\pi} \\
& \times\Big[\frac{\mathcal{V}_a(k')}{(k-k')^2}\ln\frac{(k-k')^2}{k'^2}-\frac{k^2\mathcal{V}_a(k)}{k'^2(k-k')^2}\ln\frac{(k-k')^2}{k^2}\Big] \\
& +\frac{\alpha_s N_c}{4\pi}\Big[-\frac{\ln^2(k^2/k'^2)}{(k-k')^2}+F(k,k')+\Phi(k,k')\Big]\mathcal{V}_a(k')\Big\} \\
& +3\frac{\alpha_s^2 N_c^2}{2\pi^2}\zeta(3)\mathcal{V}_a(k)
\end{aligned}
$$

I. Balitsky and G.A.C.

Unintegrated Dipole Gluon Distribution

$$\mathcal{V}_{x_B}(z_\perp,\mu) \;=\; \frac{4\pi^2 x_B}{N_c}\alpha_s(\mu)\mathcal{D}(x_B,z_\perp,\mu)$$

where

$$\mathcal{D}(x_B,z_\perp,\mu) \equiv \frac{4}{s^2}\int\frac{dz_*}{\pi x_B}\langle p|\mathrm{Tr}\Big\{\Big[\infty p_1+z_\perp,\frac{2}{s}z_* p_1+z_\perp\Big]$$

$$\hat{F}_{\bullet\xi}\Big(\frac{2}{s}z_* p_1+z_\perp\Big)\Big[\frac{2}{s}x_* p_1+z_\perp,-\infty p_1+z_\perp\Big][-\infty p_1,0]\hat{F}_{\bullet}^{\ \xi}(0)[0,\infty p_1]\Big\}|p\rangle^{a_m=x_B}$$



Photon Impact Factor for BFKL pomeron in momentum space

k_T-factorization form

I. Balitsky and G.A.C.

$$
\begin{aligned}
&I^{\mu\nu}(q,k_\perp)\\
&=\frac{N_c}{32}\int\frac{d\nu}{\pi\nu}\frac{\sinh\pi\nu}{(1+\nu^2)\cosh^2\pi\nu}\left(\frac{k_\perp^2}{Q^2}\right)^{\frac{1}{2}-i\nu}\Big\{\Big[\Big(\frac{9}{4}+\nu^2\Big)\Big(1+\frac{\alpha_s}{\pi}+\frac{\alpha_s N_c}{2\pi}\mathcal{F}_1(\nu)\Big)P_1^{\mu\nu}\\
&+\Big(\frac{11}{4}+3\nu^2\Big)\Big(1+\frac{\alpha_s}{\pi}+\frac{\alpha_s N_c}{2\pi}\mathcal{F}_2(\nu)\Big)P_2^{\mu\nu}\Big]\\
&+\frac{\frac{1}{4}+\nu^2}{2k_\perp^2}\Big(1+\frac{\alpha_s}{\pi}+\frac{\alpha_s N_c}{2\pi}\mathcal{F}_3(\nu)\Big)\left[\tilde{P}^{\mu\nu}\bar{k}^2+\bar{P}^{\mu\nu}\tilde{k}^2\right]\Big\}
\end{aligned}
$$

$$
\begin{aligned}
P_1^{\mu\nu} &= g^{\mu\nu}-\frac{q_\mu q_\nu}{q^2}\\
P_2^{\mu\nu} &= \frac{1}{q^2}\Big(q^\mu-\frac{p_2^\mu q^2}{q\cdot p_2}\Big)\Big(q^\nu-\frac{p_2^\nu q^2}{q\cdot p_2}\Big)\\
\bar{P}^{\mu\nu} &= \big(g^{\mu 1}-ig^{\mu 2}-p_2^\mu\frac{\bar{q}}{q\cdot p_2}\big)\big(g^{\nu 1}-ig^{\nu 2}-p_2^\nu\frac{\bar{q}}{q\cdot p_2}\big)\\
\tilde{P}^{\mu\nu} &= \big(g^{\mu 1}+ig^{\mu 2}-p_2^\mu\frac{\tilde{q}}{q\cdot p_2}\big)\big(g^{\nu 1}+ig^{\nu 2}-p_2^\nu\frac{\tilde{q}}{q\cdot p_2}\big)
\end{aligned}
$$

Photon Impact Factor for BFKL pomeron in momentum space

k_T-factorization form

I. Balitsky and G.A.C.

$$\mathcal{F}_{1(2)}(\nu) = \Phi_{1(2)}(\nu) + \chi_\gamma \Psi(\nu), \quad \mathcal{F}_3(\nu) = F_6(\nu) + \left(\chi_\gamma - \frac{1}{\bar\gamma\gamma}\right)\Psi(\nu),$$

$$\Psi(\nu) \equiv \psi(\bar\gamma) + 2\psi(2-\gamma) - 2\psi(4-2\gamma) - \psi(2+\gamma),$$

$$F_6(\gamma) = F(\gamma) - \frac{2C}{\bar\gamma\gamma} - 1 - \frac{2}{\gamma^2} - \frac{2}{\bar\gamma^2} - 3\frac{1+\chi_\gamma - \frac{1}{\gamma\bar\gamma}}{2+\bar\gamma\gamma},$$

$$\Phi_1(\nu) = F(\gamma) + \frac{3\chi_\gamma}{2+\bar\gamma\gamma} + 1 + \frac{25}{18(2-\gamma)} + \frac{1}{2\bar\gamma} - \frac{1}{2\gamma} - \frac{7}{18(1+\gamma)} + \frac{10}{3(1+\gamma)^2}$$

$$\Phi_2(\nu) = F(\gamma) + \frac{3\chi_\gamma}{2+\bar\gamma\gamma} + 1 + \frac{1}{2\bar\gamma\gamma} - \frac{7}{2(2+3\bar\gamma\gamma)} + \frac{\chi_\gamma}{1+\gamma} + \frac{\chi_\gamma(1+3\gamma)}{2+3\bar\gamma\gamma},$$

$$F(\gamma) = \frac{2\pi^2}{3} - \frac{2\pi^2}{\sin^2\pi\gamma} - 2C\chi_\gamma + \frac{\chi_\gamma - 2}{\bar\gamma\gamma}$$

where $\gamma = \frac{1}{2} + i\nu$

No symmetry $\gamma \to 1-\gamma$

Comparing with NLO BFKL

two gluons in the dipole $\mathcal{U}(k)$ come with extra g^2 factor $\Rightarrow$

$$\mathcal{L}(k) \;=\; \frac{1}{g^2(k)}\mathcal{V}(k)$$

$$\begin{aligned}
2a\frac{d}{da}\mathcal{L}_a(k) \;=\; & \frac{\alpha_s(k^2)N_c}{\pi^2}\int d^2k'\Big\{\Big[\frac{\mathcal{L}_a(k')}{(k-k')^2} \\
& - \frac{(k,k')\mathcal{L}_a(k)}{k'^2(k-k')^2}\Big]\Big[1+\frac{\alpha_s N_c}{4\pi}\Big(\frac{67}{9}-\frac{\pi^2}{3}-\frac{10n_f}{9N_c}\Big)\Big] - \\
& - \frac{b\alpha_s}{4\pi}\Big[\frac{\mathcal{L}_a(k')}{(k-k')^2}-\frac{k^2\mathcal{L}_a(k)}{k'^2(k-k')^2}\Big]\ln\frac{(k-k')^2}{k^2} \\
& + \frac{\alpha_s N_c}{4\pi}\Big[-\frac{\ln^2(k^2/k'^2)}{(k-k')^2}+F(k,k')+\Phi(k,k')\Big]\,\mathcal{L}_a(k')\Big\} \\
& + 3\frac{\alpha_s^2N_c^2}{2\pi^2}\zeta(3)\mathcal{L}_a(k)
\end{aligned}$$

Eigenvalues (LO eigenfunctions) coincide with NLO BFKL eq.

BFKL equation in the $\mathcal{N}$=4 SYM case

- In $\mathcal{N} = 4$ SYM theory the coupling constant does not run.
- $\Rightarrow (k^2)^{-\frac{1}{2}+i\nu}$ are eigenfunctions at any order.

$$K(q,k) = \alpha_{\rm SYM} K^{\rm LO}(q,k) + \alpha_{\rm SYM}^2 K^{\rm NLO}(q,k) + \dots$$

BFKL equation in the $\mathcal{N}$=4 SYM case

- In $\mathcal{N}=4$ SYM theory the coupling constant does not run.
- $\Rightarrow (k^2)^{-\frac{1}{2}+i\nu}$ are eigenfunctions at any order.

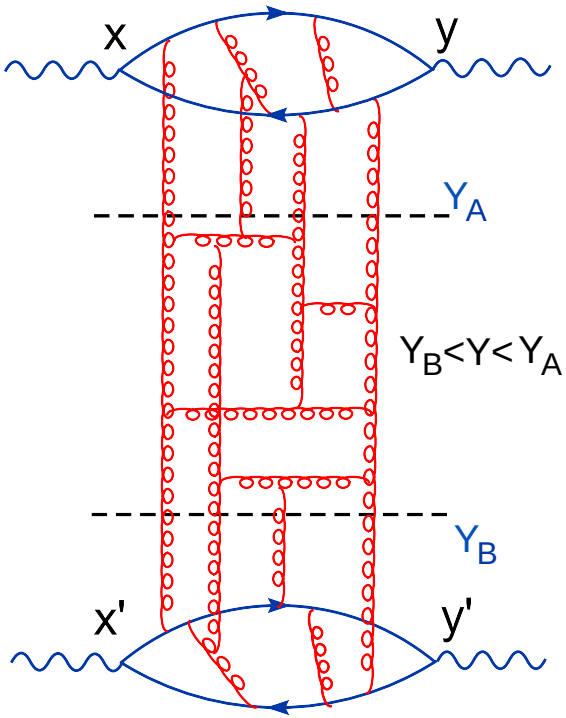
$$K(q,k) = \alpha_{\rm SYM} K^{\rm LO}(q,k) + \alpha_{\rm SYM}^2 K^{\rm NLO}(q,k) + \dots$$

$$\int d^2q\, K(q,k)\, (q^2)^{-\frac{1}{2}+i\nu} = \left[\alpha_{\rm SYM}\chi_0(\nu) + \alpha_{\rm SYM}^2\chi_1(\nu)\dots\right](k^2)^{-\frac{1}{2}+i\nu}$$

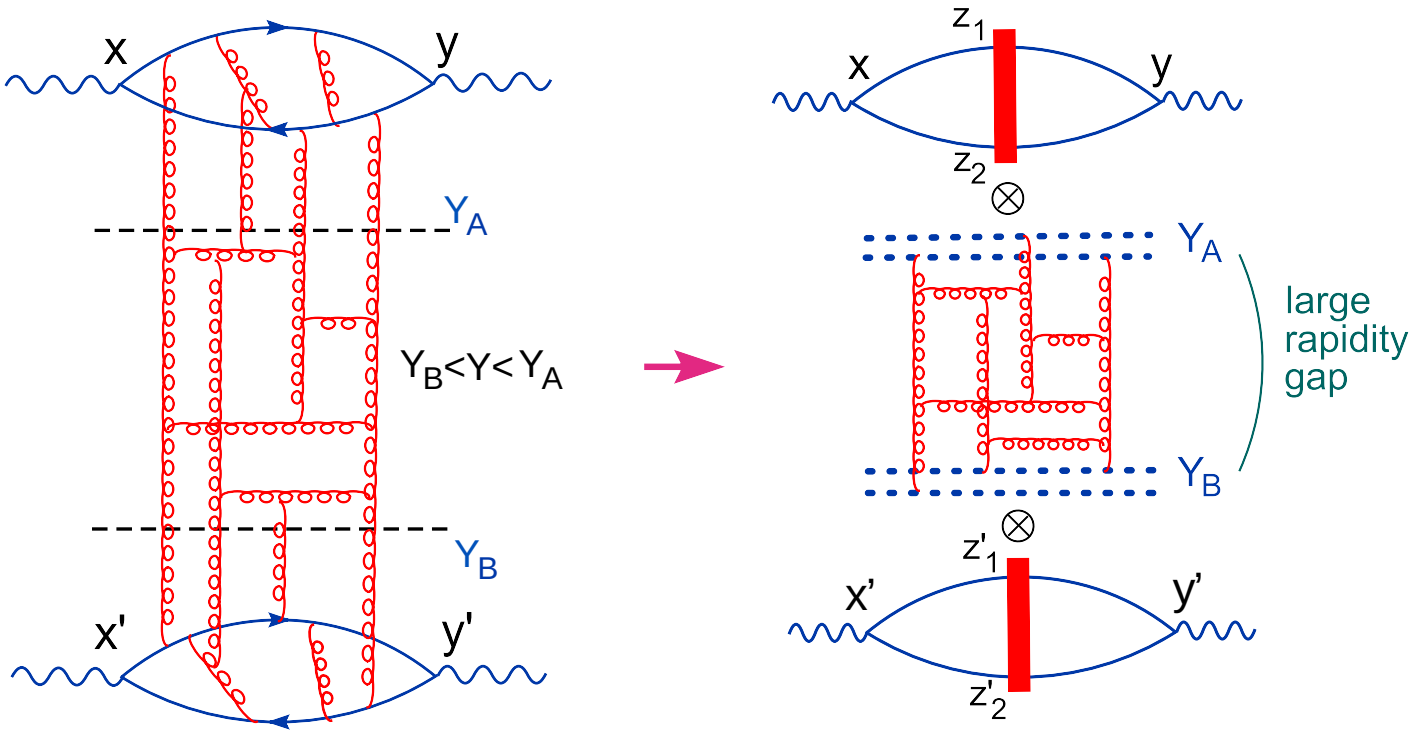
$$G(k,k',Y) = \int \frac{d\nu}{2\pi^2 k\, k'}\, e^{\left[\alpha_{\rm SYM}\chi_0(\nu)+\alpha_{\rm SYM}^2\chi_1(\nu)\dots\right]} \left(\frac{k^2}{k'^2}\right)^{i\nu}$$

- The eigenvalues $\bar{\alpha}_\mu\, \chi_0(\nu) + \bar{\alpha}_\mu^2\, \chi_1^{\rm SYM}(\nu) + \dots$ are real and symmetric for $\nu \leftrightarrow -\nu$.
- NLO Impact Factor in $\mathcal{N}$=4 is symmetric for $\nu \leftrightarrow -\nu$.

$\gamma^*\gamma^*$ scattering cross-section at LO

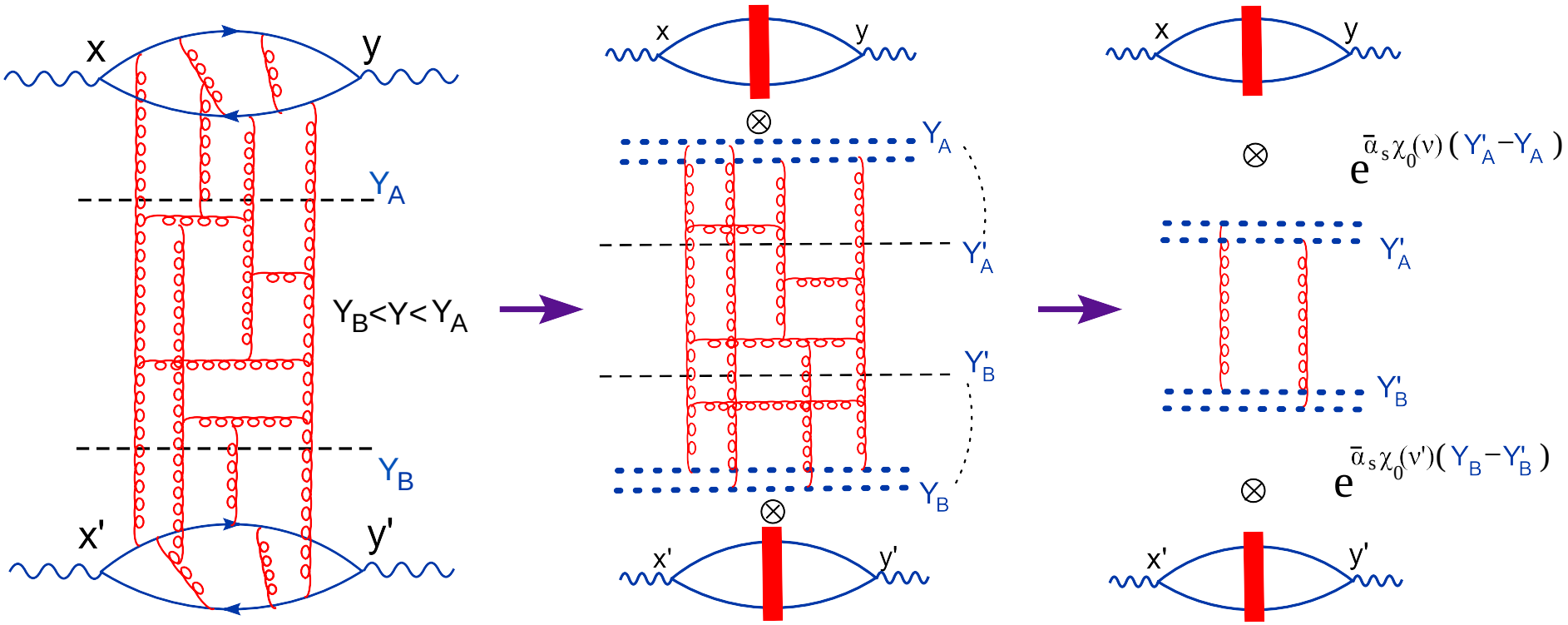


$\gamma^*\gamma^*$ scattering cross-section at LO



$$\langle j^{\alpha}(x) j^{\beta}(y) j^{\rho}(x') j^{\lambda}(y') \rangle \propto I_A^{\alpha\beta}(x, y; z_1, z_2)\, I_B^{\rho\lambda}(x', y'; z_1', z_2') \otimes \langle \mathrm{tr}\{U_{z_1} U_{z_2}^{\dagger}\}^{Y_A} \mathrm{tr}\{U_{z_3} U_{z_4}^{\dagger}\}^{Y_B} \rangle$$

$\gamma^*\gamma^*$ scattering cross-section at LO



$$\langle j^\alpha(x) j^\beta(y) j^\rho(x') j^\lambda(y')\rangle \propto I_A^{\alpha\beta}(x,y;z_1,z_2)\, I_B^{\rho\lambda}(x',y';z_1',z_2') \otimes \langle \mathrm{tr}\{U_{z_1}U_{z_2}^\dagger\}^{Y_A}\rangle_A \langle \mathrm{tr}\{U_{z_3}U_{z_4}^\dagger\}^{Y_B}\rangle_A$$

$\gamma^*\gamma^*$ scattering cross-section at LO

$$U_x = \mathrm{Pexp}\left\{ ig \int_{-\infty}^{+\infty} dx^+ A^-(x^+ + x_\perp) \right\}$$

$$\mathcal{A}^{\alpha\beta\,\rho\lambda}(q_1,q_2) \propto i\frac{\alpha_s^2}{Q_1 Q_2} \int d\nu\, I_{\mathrm{LO}}^{\alpha\beta}(\nu)\, I_{\mathrm{LO}}^{\rho\lambda}(\nu) \left(\frac{Q_1^2}{Q_2^2}\right)^{i\nu} e^{\bar{\alpha}_\mu\, \chi_0(\nu)\,(Y_A - Y_B)}$$

$$Y_A = \frac{1}{2}\ln\frac{s}{Q_1^2}, \qquad Y_B = -\frac{1}{2}\ln\frac{s}{Q_2^2}, \qquad s = (q_1+q_2)^2$$

$$\mathcal{A}^{\alpha\beta\,\rho\lambda}(q_1,q_2) \propto i\frac{\alpha_s^2}{Q_1 Q_2} \int d\nu\, I_{\mathrm{LO}}^{\alpha\beta}(\nu)\, I_{\mathrm{LO}}^{\rho\lambda}(\nu) \left(\frac{Q_1^2}{Q_2^2}\right)^{i\nu} e^{\bar{\alpha}_\mu\, \chi_0(\nu)\, \ln\frac{s}{Q_1 Q_2}}$$

What about NLO?

- Can we repit the steps performed at LO also at NLO?
- Problems to be solved:
  - Solve NLO BFKL equation G.A.C and Yu. Kovchegov
  - Calculate NLO Impact Factor I. Balitsky and G.A.C.
  - NLO Impact Factor has to be conformal invariant;
  - $\Rightarrow$ Energy dependence of NLO Impact Factor needs to be eliminated;
  - $\Rightarrow$ Composite Wilson line operators I. Balisky and G.A.C.

BFKL equation at NLO in QCD

$$K^{\rm LO+NLO}(k,q) \equiv \bar{\alpha}_\mu\, K^{\rm LO}(k,q) + \bar{\alpha}_\mu^2\, K^{\rm NLO}(k,q)$$

$$\int d^2q\, K^{\rm LO+NLO}(k,q)\; q^{2\gamma-2} = \left[\bar{\alpha}_\mu\, \chi_0(\gamma) - \bar{\alpha}_\mu^2\, \beta_2\, \chi_0(\gamma)\, \ln\frac{k^2}{\mu^2} + \bar{\alpha}_\mu^2\, \frac{\delta(\gamma)}{4}\right] k^{2\gamma-2}$$

$$\bar{\alpha}_\mu = \frac{\alpha_\mu N_c}{\pi}, \qquad \beta_2 = \frac{11\, N_c - 2\, N_f}{12\, N_c}$$

BFKL equation at NLO in QCD

$$K^{\rm LO+NLO}(k,q) \equiv \bar{\alpha}_\mu\, K^{\rm LO}(k,q) + \bar{\alpha}_\mu^2\, K^{\rm NLO}(k,q)$$

$$\int d^2q\, K^{\rm LO+NLO}(k,q)\; q^{2\gamma-2} = \left[\bar{\alpha}_\mu\, \chi_0(\gamma) - \bar{\alpha}_\mu^2\, \beta_2\, \chi_0(\gamma)\, \ln\frac{k^2}{\mu^2} + \bar{\alpha}_\mu^2\, \frac{\delta(\gamma)}{4}\right] k^{2\gamma-2}$$

$$\bar{\alpha}_\mu = \frac{\alpha_\mu N_c}{\pi}, \qquad \beta_2 = \frac{11\, N_c - 2\, N_f}{12\, N_c}$$

- $-\bar{\alpha}_\mu^2\, \beta_2\, \chi_0(\gamma)\, \ln\frac{k^2}{\mu^2}$ 1-loop running coupling.
- $\delta(\gamma) = -2\,\beta_2\,\chi_0'(\gamma) + 4\,\chi_1(\gamma)$ Fadin-Lipatov (1998)
- $\chi_1(\gamma)$ Real and symmetric in $\gamma \leftrightarrow 1-\gamma$ $\gamma = \frac{1}{2} + i\nu$.
- $\frac{d}{d\gamma}\chi_0(\gamma) \equiv \chi_0'(\gamma)$ imaginary and NOT symmetric in $\gamma \leftrightarrow 1-\gamma$.

Solution of NLO BFKL equation

- NLO eigenfunctions: perturbation around the conformal LO eigenfunctions

$$H_{\frac{1}{2}+i\,\nu}(k) = k^{-1+2\,i\,\nu}\,\left[1+\bar{\alpha}_\mu\,\beta_2\left(i\,\frac{\chi_0(\nu)}{2\,\chi_0'(\nu)}\,\ln^2\frac{k^2}{\mu^2}+\frac{1}{2}\left(\frac{\partial}{\partial\nu}\frac{\chi_0(\nu)}{\chi_0'(\nu)}\right)\ln\frac{k^2}{\mu^2}\right)\right]$$

- NLO eigenvalues $\quad \Delta(\nu) = \bar{\alpha}_\mu\,\chi_0(\nu) + \bar{\alpha}_\mu^2\,\chi_1(\nu)$

Solution of NLO BFKL equation

- NLO eigenfunctions: perturbation around the conformal LO eigenfunctions

$$H_{\frac{1}{2}+i\,\nu}(k) = k^{-1+2\,i\,\nu}\,\left[1+\bar{\alpha}_\mu\,\beta_2\left(i\,\frac{\chi_0(\nu)}{2\,\chi_0'(\nu)}\,\ln^2\frac{k^2}{\mu^2}+\frac{1}{2}\left(\frac{\partial}{\partial\nu}\frac{\chi_0(\nu)}{\chi_0'(\nu)}\right)\ln\frac{k^2}{\mu^2}\right)\right]$$

- NLO eigenvalues $\Delta(\nu) = \bar{\alpha}_\mu\,\chi_0(\nu) + \bar{\alpha}_\mu^2\,\chi_1(\nu)$

Solution of NLO BFKL equation **G.A.C. and Yu. Kovchegov**

$$G(k,k',Y) = \int_{-\infty}^{\infty}\frac{d\nu}{2\pi^2}\,e^{\left[\bar{\alpha}_\mu\,\chi_0(\nu)+\bar{\alpha}_\mu^2\,\chi_1(\nu)\right]\,Y}\,H_{\frac{1}{2}+i\,\nu}(k)\,\left[H_{\frac{1}{2}+i\,\nu}(k')\right]^*$$

- The perturbative expansion is in both the exponent and in the eigenfunctions (contrary to DGLAP case and $\mathcal{N}$=4 BFKL).

μ-independence of the NLO solution

- The $H_\gamma(k)$ eigenfunctions diagonalize the LO+NLO BFKL kernel

$$\bar{\alpha}_\mu \, K^{\rm LO}(k,q) + \bar{\alpha}_\mu^2 \, K^{\rm NLO}(k,q) = \int_{\frac{1}{2}-i\infty}^{\frac{1}{2}+i\infty} \frac{d\gamma}{2\,\pi^2\,i}\,\Delta(\gamma)\,H_\gamma(k) H^*_\gamma(q)$$

- LO+NLO BFKL kernel is μ-independent up to $\mathcal{O}(\alpha_\mu^3)$ $\Rightarrow$
- So is its diagonalization through $H_\gamma(k)$ eigenfunctions.

μ-independence of the NLO solution

$$
\begin{aligned}
G(k,k',Y) &= \int_{-\infty}^{\infty} \frac{d\nu}{2\pi^2\, k\, k'}\, e^{\left[\bar{\alpha}_\mu\, \chi_0(\nu)+\bar{\alpha}_\mu^2\, \chi_1(\nu)\right] Y}\, H_\gamma(k) H^*_\gamma(q) \\
&= \int_{-\infty}^{\infty} \frac{d\nu}{2\pi^2\, k\, k'}\, e^{\left[\bar{\alpha}_\mu\, \chi_0(\nu)+\bar{\alpha}_\mu^2\, \chi_1(\nu)\right] Y} \left(\frac{k^2}{k'^2}\right)^{i\,\nu} \left(1-\bar{\alpha}_\mu^2\, \beta_2\, \chi_0(\nu)\, Y\, \ln\frac{k k'}{\mu^2}\right)
\end{aligned}
$$

- $\Rightarrow$ $G(k,k',Y)$ is μ-independent up to order $\mathcal{O}(\alpha_\mu^3)$.

μ-independence of the NLO solution

$$G(k,k',Y) = \int_{-\infty}^{\infty} \frac{d\nu}{2\pi^2\, k\, k'}\, e^{\left[\bar{\alpha}_\mu\, \chi_0(\nu)+\bar{\alpha}_\mu^2\, \chi_1(\nu)\right] Y}\, H_\gamma(k) H^*_\gamma(q)$$

$$= \int_{-\infty}^{\infty} \frac{d\nu}{2\pi^2\, k\, k'}\, e^{\left[\bar{\alpha}_\mu\, \chi_0(\nu)+\bar{\alpha}_\mu^2\, \chi_1(\nu)\right] Y} \left(\frac{k^2}{k'^2}\right)^{i\,\nu} \left(1 - \bar{\alpha}_\mu^2\, \beta_2\, \chi_0(\nu)\, Y\, \ln\frac{k k'}{\mu^2}\right)$$

- $\Rightarrow$ $G(k,k',Y)$ is μ-independent up to order $\mathcal{O}(\alpha_\mu^3)$.
- At NLO we may write the solution as (the structure is the same as NLO $\mathcal{N}$=4 SYM)

$$G(k,k',Y) = \int_{-\infty}^{\infty} \frac{d\nu}{2\pi^2\, k\, k'}\, e^{\left[\bar{\alpha}_s(k\,k')\, \chi_0(\nu)+\bar{\alpha}_s^2(k\,k')\, \chi_1(\nu)\right] Y} \left(\frac{k^2}{k'^2}\right)^{i\,\nu}$$

- At this order the scale $\bar{\alpha}_s^{\lambda}(k^2)\, \bar{\alpha}_s^{\lambda}(k'^2) \bar{\alpha}_s^{1-2\lambda}(k\,k')$ (for real λ) works as well.

General Form of the Solution of All-Order BFKL equation

Ansatz

$$G(k,k',Y) = \int_{-\infty}^{\infty} \frac{d\nu}{2\pi^2}\, e^{\left[\bar{\alpha}_s(k\,k')\,\chi_0(\nu)+\bar{\alpha}_s^2(k\,k')\,\chi_1(\nu)+\bar{\alpha}_s^3(k\,k')\,\chi_2(\nu)+\ldots\right] Y} \left(\frac{k^2}{k'^2}\right)^{i\,\nu}$$

- $\chi_2(\nu)$ and higher-order coefficients indicated by the ellipsis in the exponent are the scale-invariant (conformal) $(\nu \leftrightarrow -\nu)$-even (real-valued) parts of the prefactor function generated by the action of the next-to-next-to-leading-order (NNLO) (and higher-order) kernels on the LO eigenfunctions.

General Form of the Solution of All-Order BFKL equation

Ansatz

$$G(k,k',Y) = \int_{-\infty}^{\infty} \frac{d\nu}{2\pi^2}\, e^{\left[\bar{\alpha}_s(k\,k')\,\chi_0(\nu)+\bar{\alpha}_s^2(k\,k')\,\chi_1(\nu)+\bar{\alpha}_s^3(k\,k')\,\chi_2(\nu)+\ldots\right] Y} \left(\frac{k^2}{k'^2}\right)^{i\,\nu}$$

- To check the ansatz we have to plug it in the evolution eq. and we need the two-loop beta-function β_3:

$$\mu^2 \frac{d\bar{\alpha}_\mu}{d\mu^2} = -\beta_2 \bar{\alpha}_\mu^2 + \beta_3 \bar{\alpha}_\mu^3$$

and

$$\int d^2q\, K^{\rm LO+NLO+NNLO}(k,q)\; q^{-1+2i\nu} = \left\{ \bar{\alpha}_\mu\, \chi_0(\nu) \left[1 - \bar{\alpha}_\mu\, \beta_2\, \ln\frac{k^2}{\mu^2} + \bar{\alpha}_\mu^2 \beta_2^2\, \ln^2\frac{k^2}{\mu^2} + \bar{\alpha}_\mu^2\, \beta_3\, \ln\frac{k^2}{\mu^2}\right] \right.$$
$$\left. + \bar{\alpha}_\mu^2 \left[\frac{i}{2}\,\beta_2\,\chi_0'(\nu) + \chi_1(\nu)\right] \left[1 - 2\,\bar{\alpha}_\mu\,\beta_2\,\ln\frac{k^2}{\mu^2}\right] + \bar{\alpha}_\mu^3\,\left[\chi_2(\nu) + i\,\delta_2(\nu)\right] \right\} k^{-1+2i\nu}$$

General Form of the Solution of All-Order BFKL equation

- The ansatz does not work, but it allows us to recover the structure of the NNLO solution

$$G(k,k',Y) = \int_{-\infty}^{\infty} \frac{d\nu}{2\pi^2 k\,k'}\, e^{\left[\bar{\alpha}_s(k\,k')\,\chi_0(\nu)+\bar{\alpha}_s^2(k\,k')\chi_1(\nu)+\bar{\alpha}_s^3(k\,k')\,\chi_2(\nu)\right]Y} \left(\frac{k^2}{k'^2}\right)^{i\,\nu}$$

$$\times \left\{1 + (\bar{\alpha}_\mu\beta_2)^2 \left[-\frac{1}{24}(\bar{\alpha}_\mu Y)^3\chi_0(\nu)^2\chi_0''(\nu) + \frac{1}{4}(\bar{\alpha}_\mu Y)^2\chi_0(\nu)\left(\frac{\chi_0'(\nu)^2}{2\chi_0(\nu)} - \chi_0''(\nu)\right) + \bar{\alpha}_\mu Y\frac{\chi_0''(\nu)}{4}\right]\right\}$$

provided that the imaginary part $i\delta_2(\gamma)$ is

$$i\delta_2(\nu) = -\frac{i}{2}\chi_0'(\nu)\beta_3 + i\chi_1'(\nu)\beta_2$$

This solution satisfies also the initial condition: the solution is unique so it is the right one.

General Form of the Solution of All-Order BFKL equation

- The ansatz does not work, but it allows us to recover the structure of the NNLO solution

$$G(k,k',Y) = \int_{-\infty}^{\infty} \frac{d\nu}{2\pi^2 k\,k'}\, e^{\left[\bar{\alpha}_s(k\,k')\,\chi_0(\nu)+\bar{\alpha}_s^2(k\,k')\chi_1(\nu)+\bar{\alpha}_s^3(k\,k')\,\chi_2(\nu)\right]Y} \left(\frac{k^2}{k'^2}\right)^{i\,\nu}$$

$$\times \left\{1 + (\bar{\alpha}_\mu\beta_2)^2 \left[-\frac{1}{24}(\bar{\alpha}_\mu Y)^3\chi_0(\nu)^2\chi_0''(\nu) + \frac{1}{4}(\bar{\alpha}_\mu Y)^2\chi_0(\nu)\left(\frac{\chi_0'(\nu)^2}{2\chi_0(\nu)} - \chi_0''(\nu)\right) + \bar{\alpha}_\mu Y\frac{\chi_0''(\nu)}{4}\right]\right\}$$

provided that the imaginary part $i\delta_2(\gamma)$ is

$$i\delta_2(\nu) = -\frac{i}{2}\chi_0'(\nu)\beta_3 + i\chi_1'(\nu)\beta_2$$

This solution satisfies also the initial condition: the solution is unique so it is the right one.

- The imaginary part $i\delta_2(\nu)$ has to be confirmed from the explicit calculation of the NNLO eigenfunction.
- Part of $\chi_2(\nu)$ has been already calculated: it is the NNLO BFKL in planar $\mathcal{N}$=4 SYM
  - Gromov, Levkovich-Maslyuka, Sizov (2015); Velizhanin (2015)

General Form of the Solution of All-Order BFKL equation

The eigenfunction of the NNLO BFKL equation is

$$H_{\frac{1}{2}+i\,\nu}(k) = k^{-1+2\,i\,\nu}\left[1 \;+\; \bar{\alpha}_\mu\,\beta_2\left(i\,\frac{\chi_0(\nu)}{2\,\chi_0'(\nu)}\,\ln^2\frac{k^2}{\mu^2} + \frac{1}{2}\left(\frac{\partial}{\partial\nu}\frac{\chi_0(\nu)}{\chi_0'(\nu)}\right)\ln\frac{k^2}{\mu^2}\right) + \;\bar{\alpha}_\mu^2 f_2\left(\frac{k}{\mu},\nu\right) + \ldots\right]$$

- The function $f_2(k/\mu,\nu)$ denotes the NNLO corrections to the eigenfunctions.
- Ansatz for $f_2(k/\mu,\nu)$:

$$f_2(k/\mu,\nu) = c_0^{(2)}(\nu) + c_1^{(2)}(\nu)\,\ln\frac{k^2}{\mu^2} + c_2^{(2)}(\nu)\ln^2\frac{k^2}{\mu^2} + c_3^{(2)}(\nu)\ln^3\frac{k^2}{\mu^2} + \ldots$$

- We have completely determined the $c_0^{(2)}(\nu), c_1^{(2)}(\nu), c_2^{(2)}(\nu), c_3^{(2)}(\nu)$ and confirmed the ansatz for the structure of the NNLO solution of the NNLO BFKL equation.

Structure of the NNLO BFKL Solution

- From explicit calculation of $f_2(\gamma)$ we not only confirm the imaginary part

$$i\delta_2(\nu) = -\frac{i}{2}\chi_0'(\nu)\beta_3 + i\chi_1'(\nu)\beta_2$$

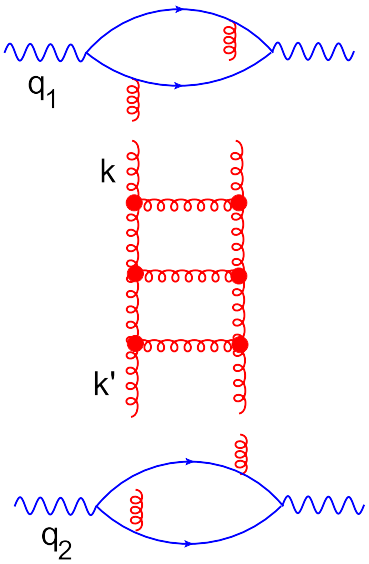
- but also confirm the structure of the NNLO BFKL solution obtained above in an indirect way

$$G(k,k',Y) = \int\limits_{-\infty}^{\infty} \frac{d\nu}{2\pi^2\, k\, k'}\, e^{\left[\bar{\alpha}_s(k\,k')\,\chi_0(\nu)+\bar{\alpha}_s^2(k\,k')\,\chi_1(\nu)+\bar{\alpha}_s^3(k\,k')\,\chi_2(\nu)\right] Y} \left(\frac{k^2}{k'^2}\right)^{i\,\nu}$$

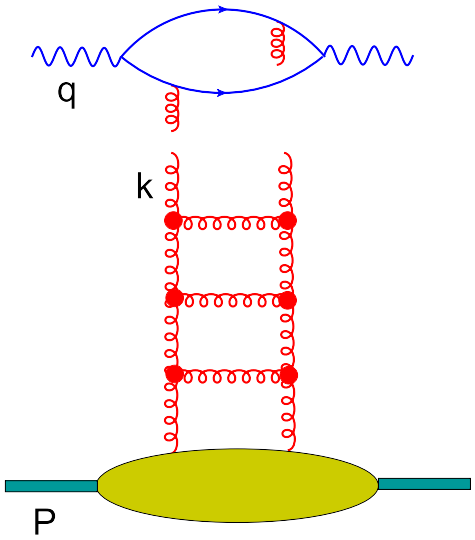
$$\times \left\{1 + (\bar{\alpha}_\mu\beta_2)^2 \left[-\frac{1}{24}(\bar{\alpha}_\mu\, Y)^3\chi_0(\nu)^2\chi_0''(\nu) + \frac{1}{4}(\bar{\alpha}_\mu\, Y)^2\chi_0(\nu)\left(\frac{\chi_0'(\nu)^2}{2\chi_0(\nu)} - \chi_0''(\nu)\right) + \bar{\alpha}_\mu Y\frac{\chi_0''(\nu)}{4}\right]\right\}$$

- It looks like QCD is not just conformal part and running coupling contributions.

BFKL at NNLO and higher orders

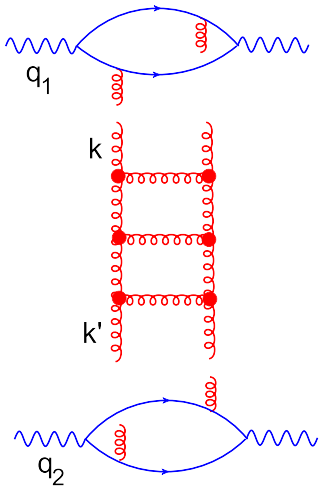


VS.



- At NNLO there are Pomeron loop contributions which are inevitable in the symmetric case of γ^*-γ^* case $\Rightarrow$ a simple generalization of BFKL at NNLO (and higher) does not exist unless we consider large N_c limit.
- In the asymmetric case of DIS, there are no pomeron loops. $\Rightarrow$ Linearization (with large N_c limit) of the Balitsky-Kovchegov equation at any order provides a systematic procedure to consistently define a BFKL type of evolution equation at any order.
- BFKL to all order: linearization of all order BK equation in large N_c limit.

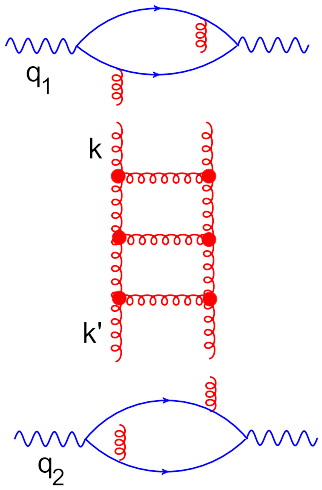
BFKL equation in DIS case



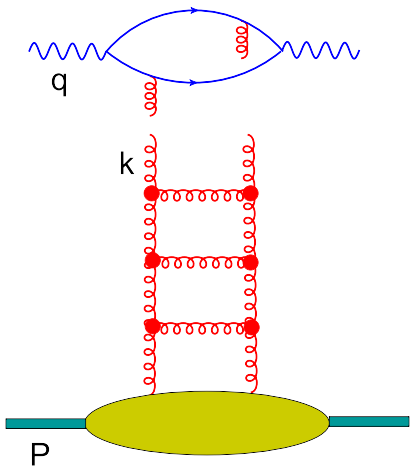
K_{BFKL} is $k \leftrightarrow k'$ symmetric

$$Y^{\text{sym}} = \ln \frac{s}{k\,k'}$$

BFKL equation in DIS case



VS.



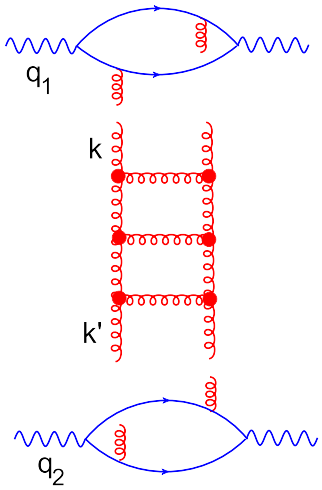
$K_{\rm BFKL}$ is $k \leftrightarrow k'$ symmetric

$Y^{\rm sym} = \ln \dfrac{s}{k\,k'}$

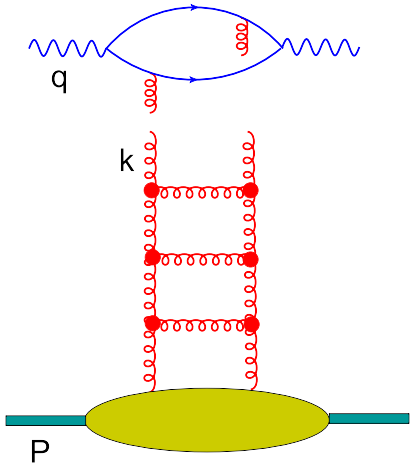
NLO $K^{\rm DIS}_{\rm BFKL}$ is not Symmetric

$Y^{\rm DIS} = \ln \dfrac{s}{k^2} \simeq \ln \dfrac{1}{x_{\rm B}}$

BFKL equation in DIS case



VS.



$K_{\rm BFKL}$ is $k \leftrightarrow k'$ symmetric

$Y^{\rm sym} = \ln \dfrac{s}{k\,k'}$

NLO $K^{\rm DIS}_{\rm BFKL}$ is not Symmetric

$Y^{\rm DIS} = \ln \dfrac{s}{k^2} \simeq \ln \dfrac{1}{x_{\rm B}}$

$$K^{\rm DIS}_{\rm NLO} = K^{\rm sym}_{\rm NLO} - \frac{1}{2}\int d^{D-2}q'\, K_{\rm LO}(q_1,q')\ln\frac{q'^2}{q^2}\,K_{\rm LO}(q,q_2) \qquad \text{Fadin}-\text{Lipatov}(1998)$$

- $K^{\rm DIS}_{BFKL}$ is not symmetric $\Rightarrow$ eigenvalues not $\gamma \leftrightarrow 1-\gamma$ symmetric.
- $\Rightarrow$ Eigenvalues get an extra term: $\Delta^{\rm DIS}(\gamma) = \Delta^{\rm sym}(\gamma) - \frac{1}{2}\,\bar{\alpha}_\mu^2\,\chi_0(\gamma)\chi'(\gamma)$
- Reproduced lower order and predicted (and later confirmed) the 3-loop DGLAP anomalous dimension (Fadin-Lipatov (1998))

DGLAP anomalous dimension from NLO BFKL solution

$$G(k,k',Y) = \int_{-\infty}^{\infty} \frac{d\nu}{2\pi^2}\, e^{\left[\bar{\alpha}_\mu\,\chi_0(\nu)+\bar{\alpha}_\mu^2\,\chi_1(\nu)\right](Y^{\rm DIS}+\ln\frac{k}{k'})}\, H_{\frac{1}{2}+i\nu}(k)\, \left[H_{\frac{1}{2}+i\nu}(k')\right]^*$$

$$\simeq \int_{-\infty}^{\infty} \frac{d\nu}{2\pi^2}\, e^{\left[\bar{\alpha}_\mu\,\chi_0(\nu)+\bar{\alpha}_\mu^2\,\chi_1(\nu)\right]Y^{\rm DIS}}\, H_{\frac{1}{2}+i\nu}(k) \left[H_{\frac{1}{2}+i\nu}(k')\right]^* \left(1+\bar{\alpha}_\mu\chi_0(\nu)\ln\frac{k}{k'}\right)$$

$\Rightarrow$ perform partial integration and exponentiate the $Y^{\rm DIS}$-dependent terms $\Rightarrow$

$$G(k,k',Y^{\rm DIS}) = \int_{-\infty}^{\infty} \frac{d\nu}{2\pi^2}\, e^{\left[\bar{\alpha}_\mu\,\chi_0(\nu)+\bar{\alpha}_\mu^2\,\left(\chi_1(\nu)+2\,i\,\chi_0(\nu)\chi_0'(\nu)\right)\right]Y^{\rm DIS}}\, H_{\frac{1}{2}+i\nu}(k) \left[H_{\frac{1}{2}+i\nu}(k')\right]^*$$
$$\times \left(1+\frac{i}{2}\,\bar{\alpha}_\mu\,\chi_0'(\nu)\right)$$

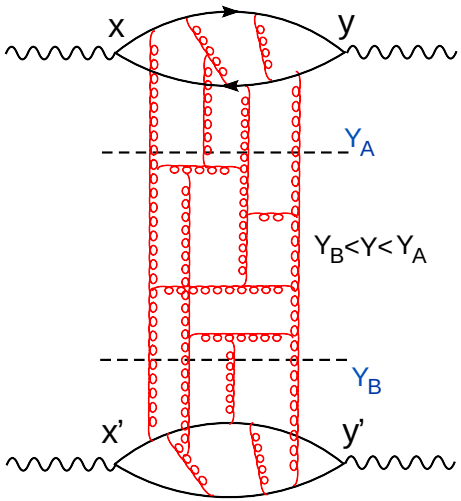
- $\Rightarrow \quad \Delta^{\rm DIS}(\gamma) = \bar{\alpha}_\mu\,\chi_0(\gamma) + \bar{\alpha}_\mu^2\,\chi_1(\gamma) - \frac{1}{2}\,\bar{\alpha}_\mu^2\,\chi_0(\gamma)\chi_0'(\gamma)$

DGLAP anomalous dimension from NLO BFKL solution

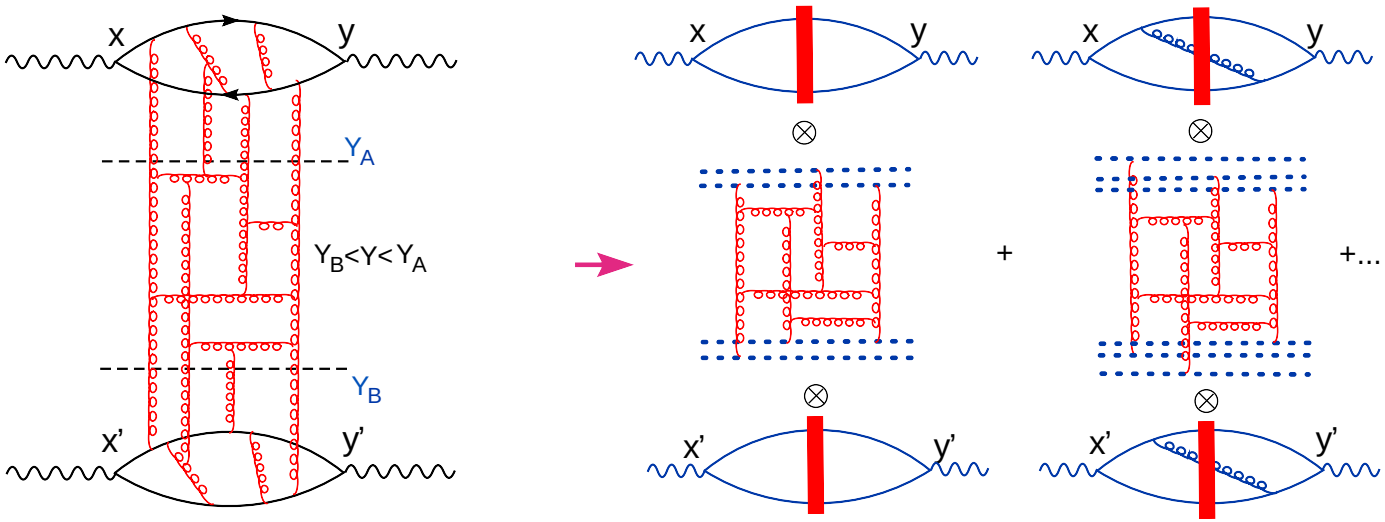
$$G(k,k',Y^{\rm DIS}) = \int\limits_{-\infty}^{\infty} \frac{d\nu}{2\pi^2}\, e^{\left[\bar\alpha_\mu\,\chi_0(\nu)+\bar\alpha_\mu^2\,\left(\chi_1(\nu)+2\,i\,\chi_0(\nu)\chi_0'(\nu)\right)\right]\,Y^{\rm DIS}} H_{\frac12+i\,\nu}(k)\,\left[H_{\frac12+i\,\nu}(k')\right]^*$$
$$\times\left(1+\frac{i}{2}\,\bar\alpha_\mu\,\chi_0'(\nu)\right)$$

- $\Rightarrow \qquad \Delta^{\rm DIS}(\gamma) = \bar\alpha_\mu\,\chi_0(\gamma) + \bar\alpha_\mu^2\,\chi_1(\gamma) - \frac12\,\bar\alpha_\mu^2\,\chi_0(\gamma)\chi_0'(\gamma)$
- Agrees with DGLAP 3-loop anomalous dimension.
- DIS eigenvalues are not symmetric in $\gamma \to 1-\gamma$

$\gamma^*\gamma^*$ scattering cross-section at NLO

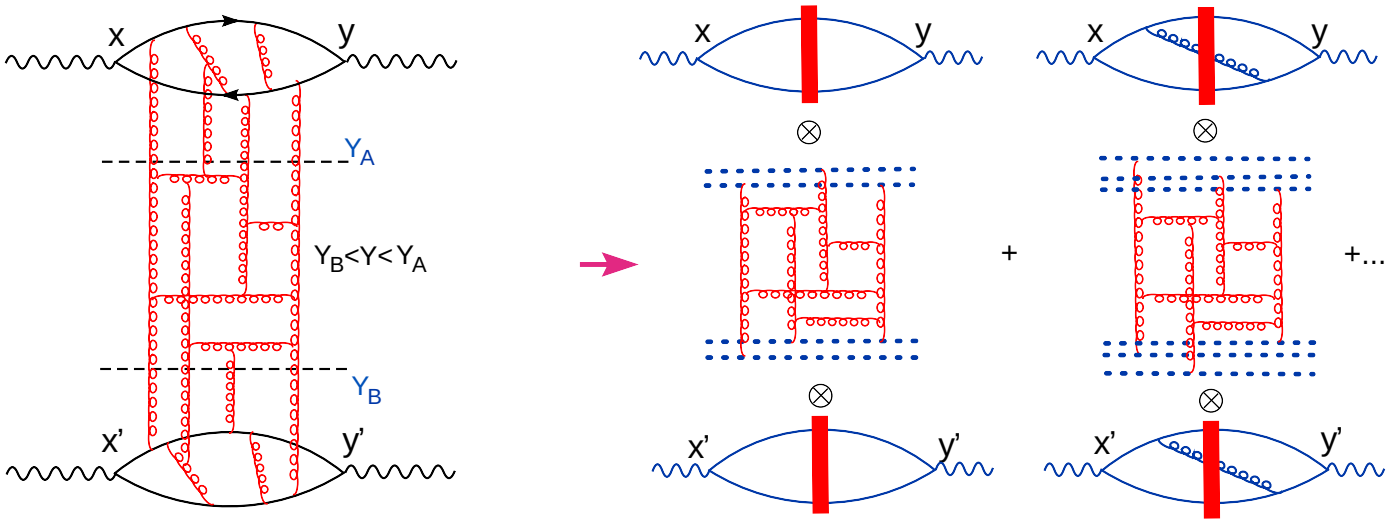


$\gamma^*\gamma^*$ scattering cross-section at NLO



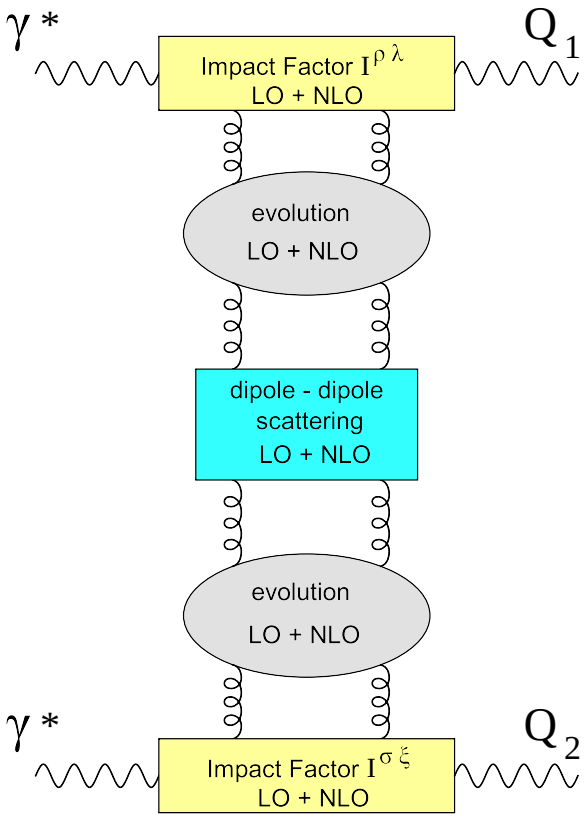
Using high-energy Operator Product Expansion in composite Wilson line operators we get NLO Impact Factor that does not scale with energy.

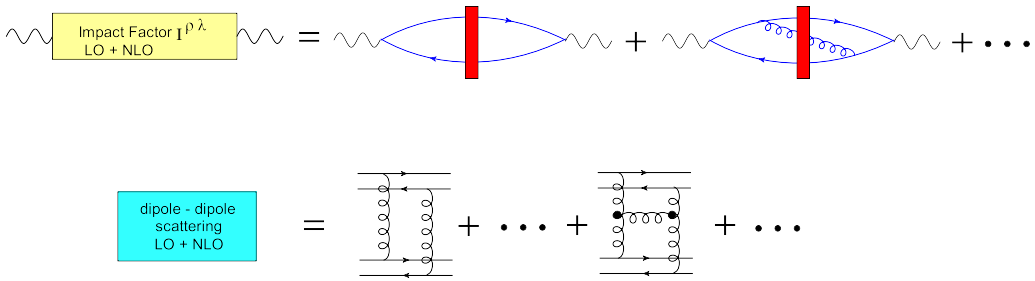
$\gamma^*\gamma^*$ scattering cross-section at NLO

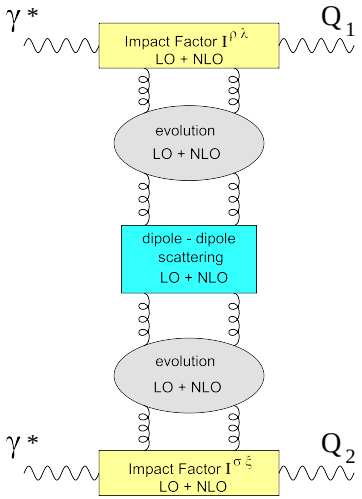


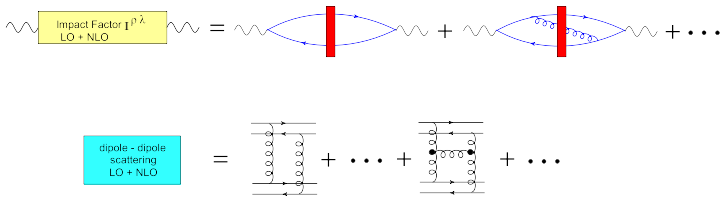
Composite Wilson line operators — I. Balitsky and G.A.C.

$$[\mathrm{tr}\{\hat{U}^{\eta}_{z_1}\hat{U}^{\dagger\eta}_{z_2}\}]^{\mathrm{conf}} = \mathrm{tr}\{\hat{U}^{\eta}_{z_1}\hat{U}^{\dagger\eta}_{z_2}\}$$
$$+\frac{\alpha_s}{4\pi^2}\int d^2z_3\,\frac{z_{12}^2}{z_{13}^2 z_{23}^2}[\mathrm{tr}\{\hat{U}^{\eta}_{z_1}\hat{U}^{\dagger\eta}_{z_3}\}\mathrm{tr}\{\hat{U}^{\eta}_{z_3}\hat{U}^{\dagger\eta}_{z_2}\} - N_c\mathrm{tr}\{\hat{U}^{\eta}_{z_1}\hat{U}^{\dagger\eta}_{z_2}\}]\ln\frac{az_{12}^2}{z_{13}^2 z_{23}^2} + O(\alpha_s^2)$$


γ *
Q 1
Impact Factor I ρ λ
LO + NLO
evolution
LO + NLO
dipole - dipole
scattering
LO + NLO
evolution
LO + NLO
γ *
Q 2
Impact Factor I σ ξ
LO + NLO


Impact Factor I ρ λ
LO + NLO
=
+
+ • • •
dipole - dipole
scattering
LO + NLO
=
+ • • •
+
+ • • •





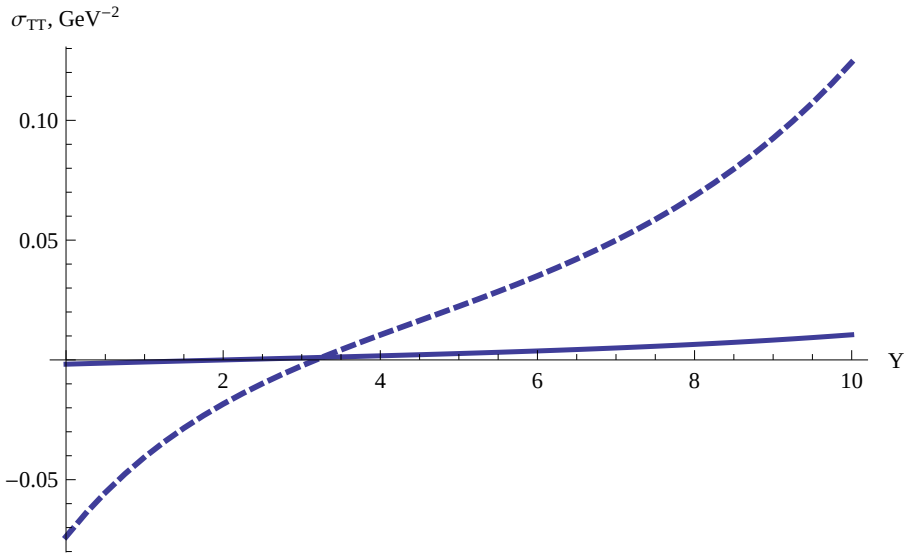
$$\sigma^{\gamma^*\gamma^*}_{\rm LO+NLO}(TT) = \frac{1}{4}\sum_{\lambda_1,\lambda_2=\pm 1} 32\pi^6 \varepsilon^{\lambda_1 *}_{\rho_1}(q_1)\varepsilon^{\lambda_1}_{\sigma_1}(q_1)\varepsilon^{\lambda_2 *}_{\rho_2}(q_2)\varepsilon^{\lambda_2}_{\sigma_2}(q_2)\frac{N_c^2-1}{N_c^2}\frac{\alpha_s(Q_1^2)\alpha_s(Q_2^2)}{Q_1 Q_2}$$
$$\times \int_{-\infty}^{\infty} d\nu \left(\frac{Q_1^2}{Q_2^2}\right)^{i\nu} \left(\frac{s}{Q_1 Q_2}\right)^{\bar\alpha_s(Q_1Q_2)\,\chi_0(\nu)+\bar\alpha_s^2(Q_1Q_2)\chi_1(\nu)} \tilde I^{\rho_1\sigma_1}_{\rm LO+NLO}(q_1,\nu)\tilde I^{\rho_2\sigma_2}_{\rm LO+NLO}(q_2,-\nu)$$
$$\times\left[1+\bar\alpha_s(Q_1Q_2){\rm Re}[F(\nu)]\right]$$

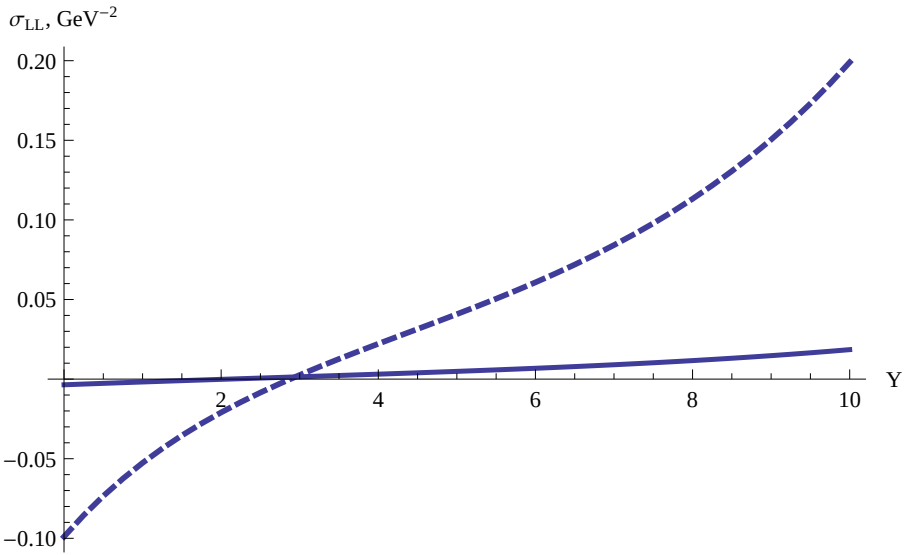
${\rm Re}[F(\nu)]$ is the NLO dipole-dipole scattering projected on the LO eigenfunctions.

$$\sigma^{\gamma^*\gamma^*}_{\rm LO+NLO}(TT) = \frac{1}{4}\sum_{\lambda_1,\lambda_2=\pm 1} 32\pi^6 \varepsilon^{\lambda_1 *}_{\rho_1}(q_1)\varepsilon^{\lambda_1}_{\sigma_1}(q_1)\varepsilon^{\lambda_2 *}_{\rho_2}(q_2)\varepsilon^{\lambda_2}_{\sigma_2}(q_2)\frac{N_c^2-1}{N_c^2}\frac{\alpha_s(Q_1^2)\alpha_s(Q_2^2)}{Q_1 Q_2}$$
$$\times \int_{-\infty}^{\infty} d\nu \left(\frac{Q_1^2}{Q_2^2}\right)^{i\nu}\left(\frac{s}{Q_1 Q_2}\right)^{\bar\alpha_s(Q_1Q_2)\,\chi_0(\nu)+\bar\alpha_s^2(Q_1Q_2)\chi_1(\nu)} \tilde I^{\rho_1\sigma_1}_{\rm LO+NLO}(q_1,\nu)\tilde I^{\rho_2\sigma_2}_{\rm LO+}$$
$$\times\left[1+\bar\alpha_s(Q_1Q_2){\rm Re}[F(\nu)]\right]$$

- NLO Impact factor is not symmetric in $\gamma \to 1-\gamma$
  BUT the full amplitude is!

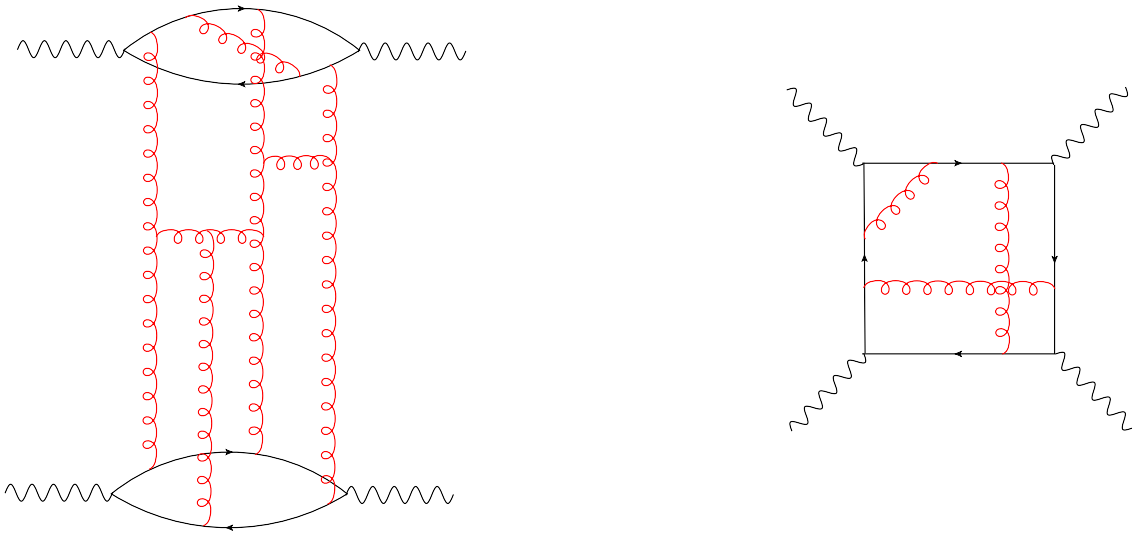
Numerical results





- NLO $\gamma^*\gamma^*$ cross section with $Q_1 = Q_2 = 5$ GeV (dashed line) and $Q_1 = Q_2 = 10$ GeV (solid line) plotted as functions of rapidity Y.

Numerical results



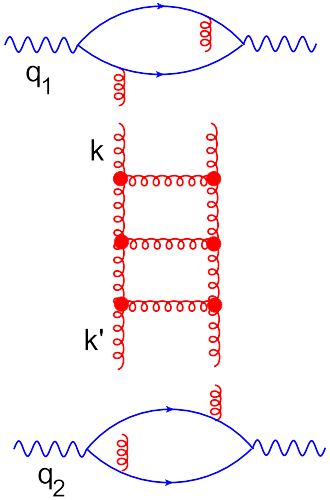
a) b)

- Left panel depicts a Feynman diagram that contributes to the high-energy asymptotics of $\gamma^*\gamma^*$ scattering. The right panel shows an example of the "box" diagram that are suppressed at high energies by a power of energy and, therefore, can be neglected. However, such types of diagrams become relevant, and therefore not anymore negligible at low rapidity where energy is not high enough to suppress such contributions.

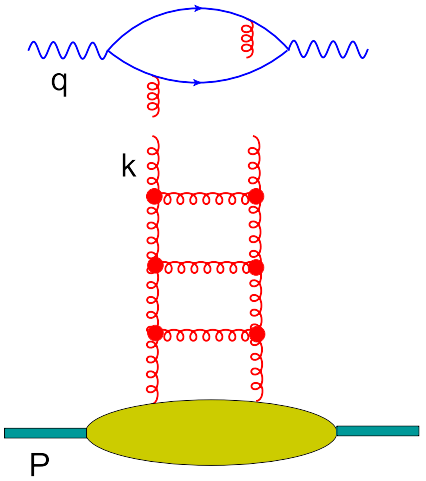
NLO DIS with composite Wilson lines operator

- $\Delta^{\rm DIS}(\gamma) = \bar{\alpha}_\mu\, \chi_0(\gamma) + \bar{\alpha}_\mu^2\, \chi_1(\gamma) - \frac{1}{2}\, \bar{\alpha}_\mu^2\, \chi_0(\gamma)\chi_0'(\gamma)$

DIS eigenvalues are not symmetric in $\gamma \to 1-\gamma$



VS.



$K_{\rm BFKL}$ is $k \leftrightarrow k'$ symmetric

$$Y^{\rm sym} = \ln \frac{s}{k\,k'}$$

NLO $K^{\rm DIS}_{\rm BFKL}$ is not Symmetric

$$Y^{\rm DIS} = \ln \frac{s}{k^2} \simeq \ln \frac{1}{x_{\rm B}}$$

- NLO Impact Factor in front of the composite Wilson lines operator is not symmetric in $\gamma \to 1-\gamma$ either!
- So, evolution equation of composite Wilson lines operator is suitable for both $\gamma^*\gamma^*$ and DIS scattering processes!

Conclusions

- Guiding line for the systematics of the high-energy OPE is conformal invariance in 2-d coordinates space order by order.
- The NLO Impact Factor obtained through the OPE in terms of composite Wilson lines operators is conformal invariant and energy independent.
- NLO Impact factor for pomeron exchange in momentum space has been obtained (aloso available in coordinate space and Mellin space).
- To get the DIS cross section at NLO at highe energy one has to convolute the NLO impact factor with the evolution equation of $\mathrm{tr}\{U_{x_1}U^{\dagger}_{x_2}\}\mathrm{tr}\{U_{x_3}U^{\dagger}_{x_4}\}$ at LO and the LO Impact factor with NLO BK equation.

Conclusions

- Is the symmetry $\gamma \to 1-\gamma$ related to conformal invariance? Probably not. It seems to be related to the *intrinsic* symmetry of the amplitude
  - $\gamma^*\gamma^*$ amplitude is upside down symmetric: it has $\gamma \to 1-\gamma$ symmetry.
  - DIS amplitude is not upside down symmetric: it does not have $\gamma \to 1-\gamma$ symmetry.

- Evolution equation of composite Wilson lines operator is suitable for both $\gamma^*\gamma^*$ and DIS scattering processes!

- It looks like QCD is not just conformal part and running coupling contributions...

Fluctuations of the gluon distribution at small x: correlation of multiplicity and transverse momentum fluctuations

Adrian Dumitru
Baruch College
(City Univ. of NY)

Saturation: Recent Developments,
New Ideas and Measurements
April 2017
BNL

based on A.D. & V. Skokov,
arXiv:1704.05917

Observables at small x

average over stochastic small-x color fields:

$$\langle O[A^+]\rangle = \frac{1}{Z}\int \mathcal{D}A^+\, W[A^+]\, O[A^+]$$

$W[A^+]$: JIMWLK weight functional

In the MV model:

$$W[A^+] = e^{-S[A^+]},$$

$$S[A^+] = \int dx^- d^2x_\perp \frac{\mathrm{tr}\,\nabla_\perp^2 A^+(x^-,x_\perp)\nabla_\perp^2 A^+(x^-,x_\perp)}{2\mu^2(x^-)}$$

Examples:

- $O[A^+] = g^2\,\mathrm{tr}\,A^+(x_\perp)A^+(y_\perp)$ (cov. gauge) gluon distribution
- $O[A^+] = g^2\,\mathrm{tr}\,A^i(x_\perp)A^i(y_\perp)$ (L.C. gauge) WW gluon distribution
- $O[A^+] = \frac{1}{N_c}\,\mathrm{tr}\,V(x_\perp)V^\dagger(y_\perp)$ dipole forw. scatt. amplitude

$$V(x_\perp) = \mathcal{P}e^{-ig\int dx^- A^+(x^-,x_\perp)}$$

Idea: integrate out fluctuations which do not affect observable O[A^+]

→ obtain effective action / potential for that observable

(we work directly with MV / JIMWLK action w/o introducing “dipole picture”)

$$e^{-V_{\rm eff}[X(q)]} = \int \mathcal{D}A^+(q)\, W[A^+(q)]\, \delta(X(q) - O[A^+(q)])$$

$$\frac{\delta V_{\rm eff}[X(k)]}{\delta X(q)} = 0 \to X_s(q) \equiv \langle X(q) \rangle$$

(at large Nc; or else do proper Legendre transform)

$$\text{for } O[A^+] = g^2\, \mathrm{tr}\, |A^+(q)|^2 \text{ in MV model :}$$

$$V_{\rm eff}[X(q)] = \int \frac{d^2q}{(2\pi)^2} \left[\frac{q^4}{g^4\mu^2} X(q) - \frac{1}{2} A_\perp N_c^2 \log X(q) \right]$$

$$X_s(q) = \frac{1}{2} N_c^2 A_\perp \frac{g^4\mu^2}{q^4} \quad \checkmark$$

(cov. gauge gluon distribution at q>Qs)

same result for non-local Gaussian model by Iancu, Itakura & McLerran (approx. to JIMWLK), provided

at q > Q_s : $\mu^2 \to \mu_0^2 \left(\frac{q^2}{Q_s^2} \right)^{1-\gamma}$

γ = 0.63, BFKL anom. dim. in presence of absorptive (saturation) boundary (Mueller & Triantafyllopoulos)

Aside: constrained effective potential introduced originally to compute potential for Polyakov loop in YM at T>0:

$$\exp(-V\mathcal{V}(\ell)) = \int \mathcal{D}A_\mu \, \delta(\ell - \frac{1}{N}\mathrm{tr}\,\overline{\mathbf{L}}) \, \exp(-\frac{1}{g^2}S(A))$$

for Higgs:

L. O'Raifeartaigh, A. Wipf and H. Yoneyama: Nucl. Phys. B 271 (1986) 653

for Polyakov loop:

C. Korthals Altes: Nucl. Phys. B 420 (1994) 637

to two loops and general eigenvalues:

A. Dumitru, Y. Guo and C. P. Korthals Altes: Phys. Rev. D 89, 016009 (2014)

Fluctuations:

instead of $X(q) = X_s(q) + \delta X(q)$,

$$\Delta V_{\rm eff}[\delta X(q)] = \frac{1}{2}\int \frac{d^2l}{(2\pi)^2}\frac{d^2k}{(2\pi)^2}\,\delta X(l)\left\{\frac{\delta}{\delta X(l)}\frac{\delta}{\delta X(k)}V_{\rm eff}[\delta X(q)]\right\}\delta X(k)$$

$$= \frac{1}{2}\int \frac{d^2q}{(2\pi)^2}\frac{\delta X(q)^2}{X_s(q)^2}\frac{1}{2}N_c^2 A_\perp$$

$$Z_{1\ \rm loop} = \int \mathcal{D}\,\delta X(q)\; e^{-V_{\rm eff}[\delta X(q)]} = e^{-\frac{1}{2}\,\mathrm{tr}\,\log\left(\frac{1}{2}\frac{N_c^2 A_\perp}{X_s(q)^2}\right)}$$

let's go with $X(q) = X_s(q)\,\eta(q)$ (canonical dim. of η is zero)

$$\Delta V_{\rm eff}[\eta(q)] \equiv V_{\rm eff}[\eta(q)] - V_{\rm eff}[\eta(q)=1]$$

$$= \frac{1}{2}N_c^2 A_\perp \int \frac{d^2q}{(2\pi)^2}\,[\eta(q) - 1 - \log\eta(q)]$$

- field redefinition φ = log η yields Liouville action/potential (in q space!) with R<0

Fluctuations: correlation of gluon number and transv. momentum

$$\Delta N_g[\eta(q)] = \int \frac{d^2q}{(2\pi)^2} q^2 X_s(q)\ [\eta(q) - 1]$$

$$\Delta\overline{q^2}[\eta(q)] = \frac{\Delta N_g[\eta(q)]}{\int \frac{d^2q}{(2\pi)^2} X_s(q)\eta(q)}$$

Ansatz: $$\eta(q > Q_s) = 1 + \eta_0 \left(\frac{Q_s^2}{q^2}\right)^a \Theta\left(Q^2 - q^2\right)$$

$$\Delta N_g \simeq N_c A_\perp \Delta\overline{q^2}$$

for small amplitude fluctuations

ΔN_g increases with $\Delta\overline{q^2}$

- a > 0: fluctuation "know" about scale Q_s
- a → 0: scale invariant fluctuation

maximize ΔN_g (and $\Delta\overline{q^2}$), minimize "penalty" $\Delta S[\eta(q)] \equiv \Delta V_{\rm eff}[\eta(q)]$

→ MV model: 0<a<1
(because for *a=0*: $\Delta N_g \sim \log Q^2$, $\Delta S \sim Q^2$)

IIM model (anom. dim.) a ≈ 0
→ Mueller picture where Qs corresponds to an absorptive boundary

$$\eta_0 \sim \Delta S \frac{\left(Q^2/Q_s^2\right)^a}{N_c^2 A_\perp Q^2}$$

(ΔS ~ log p^{-1} where p is probability of fluctuation)

MC simulation:

- MV: generate random configurations of $A^+(x^-,x_\perp)$ according to $S_{MV}[A^+]$
- JIMWLK: stochastic evolution (at fixed α_s) of associated Wilson line to $\alpha_s Y=1$

$$X(q) = \int d^2b \int d^2r\, e^{-iqr}\, \mathrm{tr}\left[V_Y\left(b-\frac{r}{2}\right)V_Y^\dagger\left(b+\frac{r}{2}\right)-1\right]$$

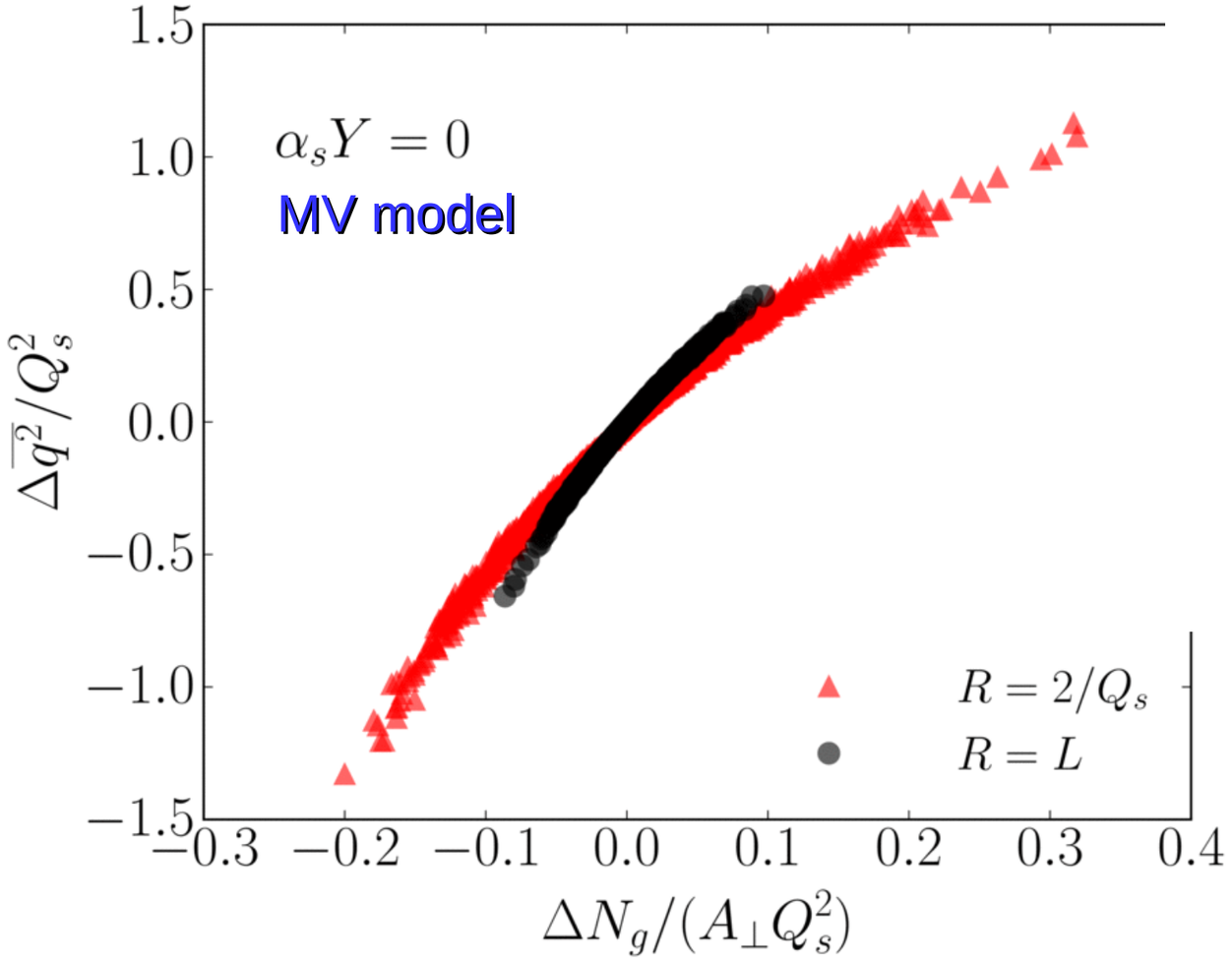
(integrated over entire 2d lattice)

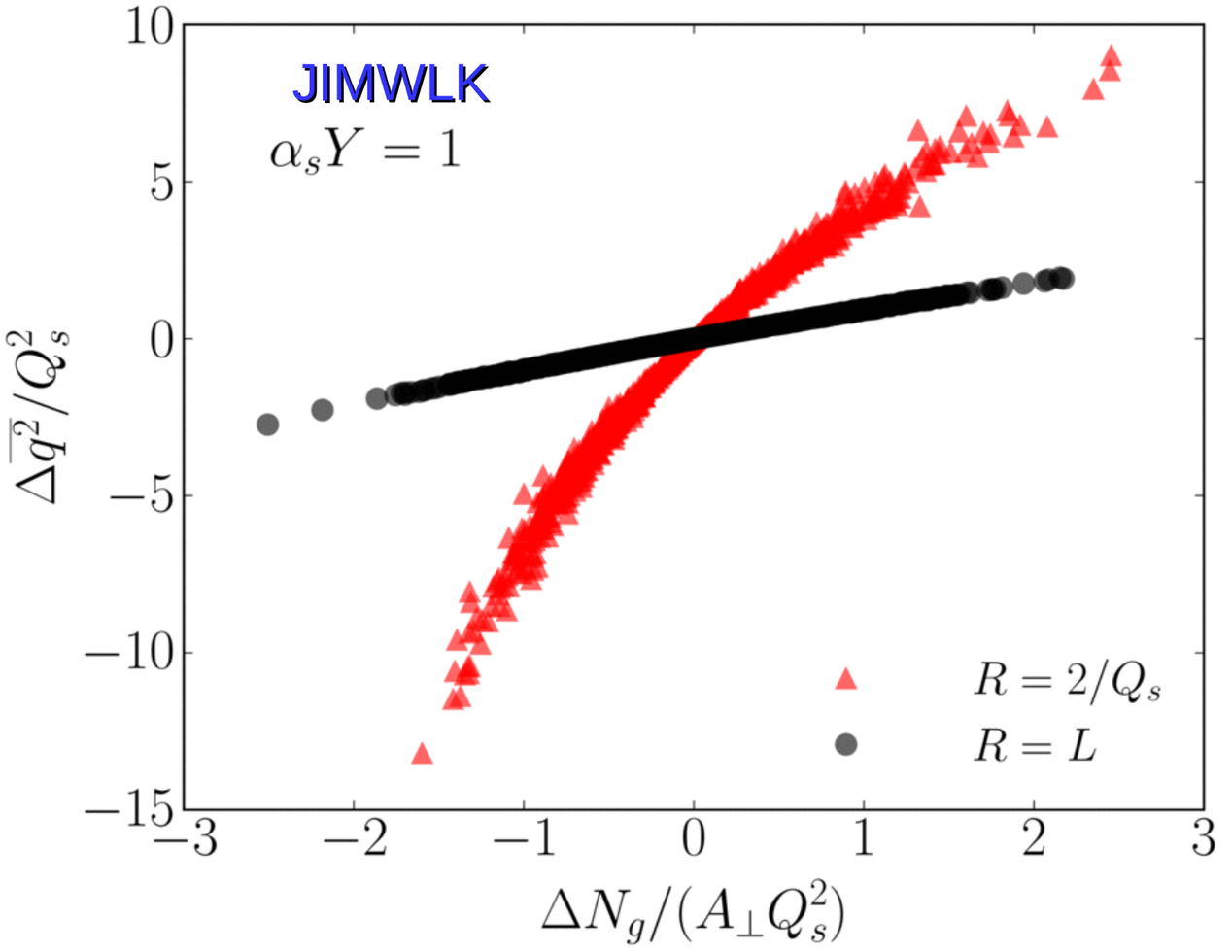
$$X_R(q,b) = \int d^2x \int d^2y\, e^{-iq(y-x)}\, e^{-\frac{(b-x)^2}{2R^2}}\, e^{-\frac{(b-y)^2}{2R^2}}\, \mathrm{tr}\left[V_Y(x)V_Y^\dagger(y)-1\right]$$

("local" distribution at b;
similar to "smeared" Wigner distr.)

$$R=\frac{2}{Q_s}$$

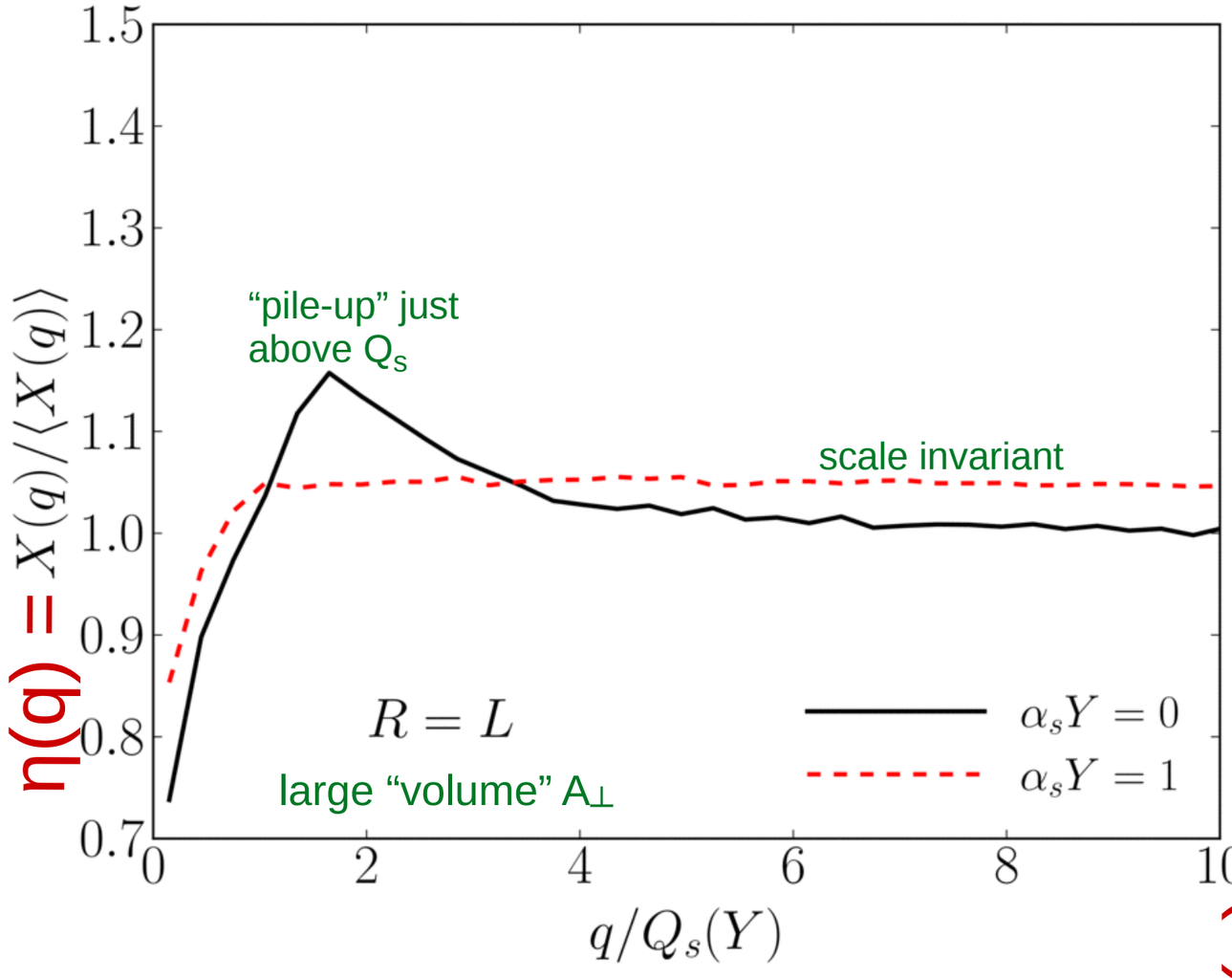
Correlation of transv. momentum and multiplicity fluctuations

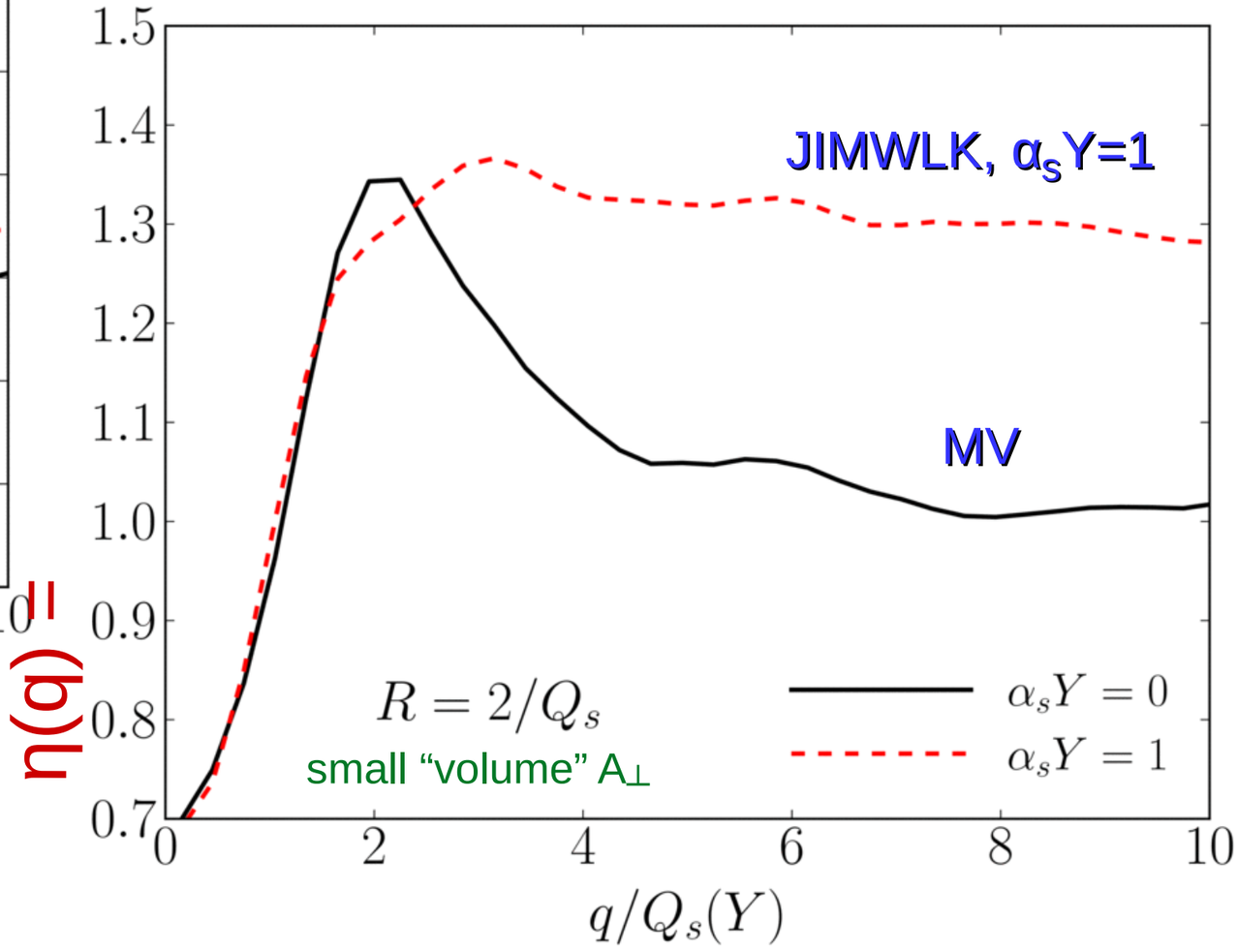




- ΔN_g ~ 10 – 100 for A = 0.1 fm^2, Q_s^2 = (1-2.5 GeV)^2
- tight correlation (~ single curve, few outliers)
- JIMWLK shows correlations in b-space
- strong increase of Δq^2 with ΔN_g in small area “patches”

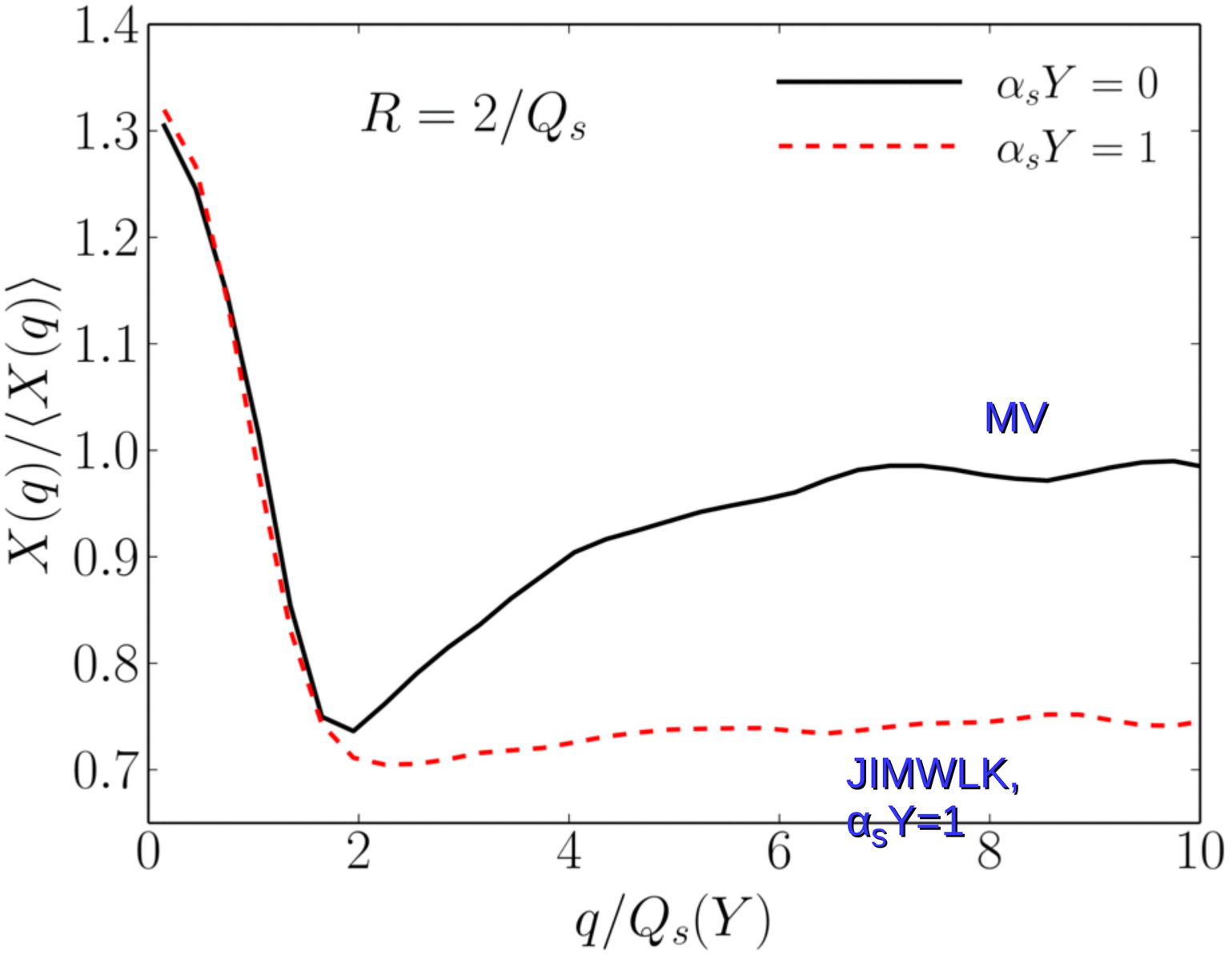
Spectral shape of high multiplicity fluctuations





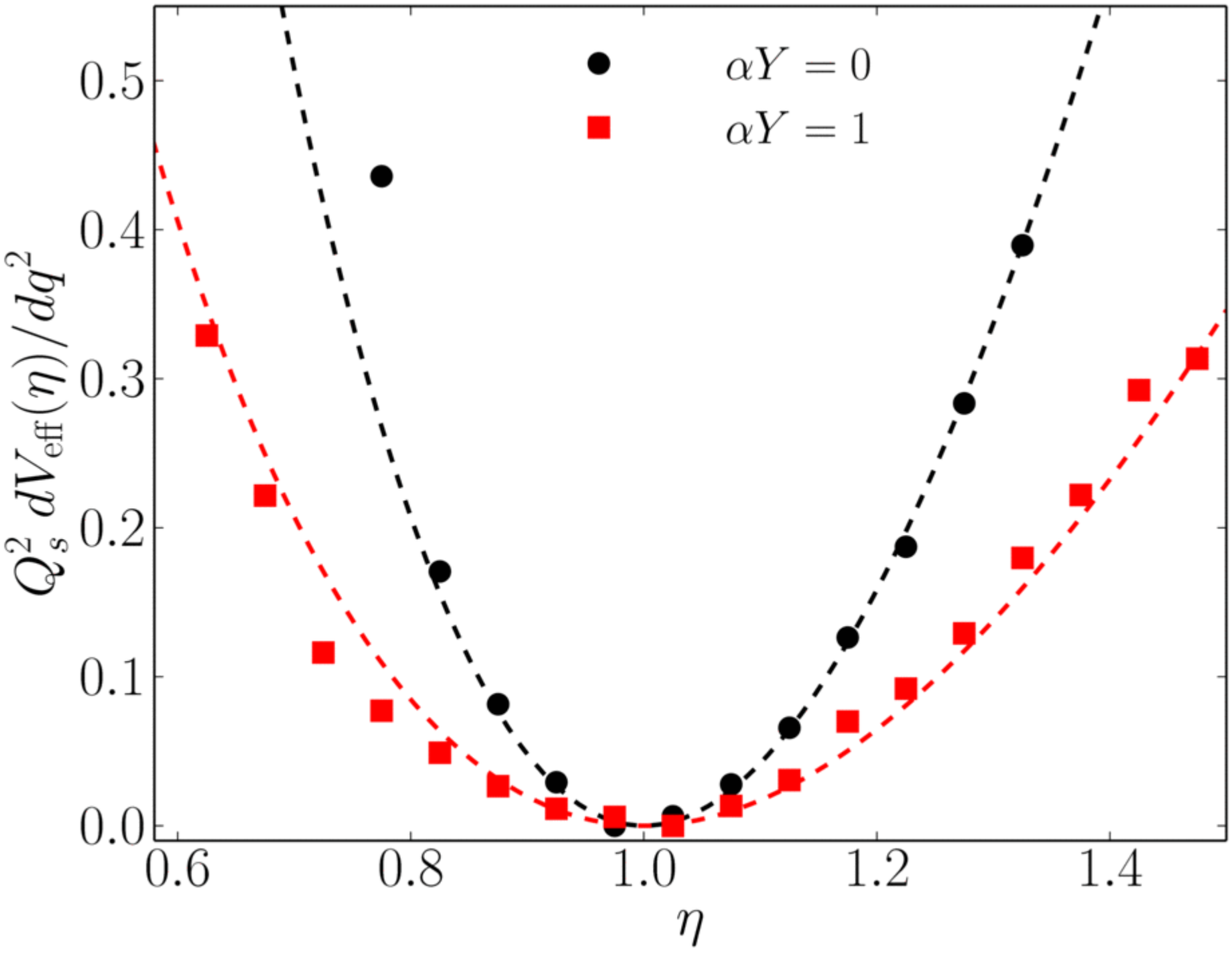
- evolution modifies spectrum of fluctuations
- MV model piles up addtl gluons around Qs
- perturbative evolution with scale invariant kernel → flat spectral shape above 'absorptive boundary' (canonical dimension of η(q) is 0)

Spectral shape of low multiplicity fluctuations



$V_{eff}[\eta]$ extracted from MC (histogram of fluctuations etc)

- linear minus log indeed appears to work ✓
- prefactor (curvature) ~ $N_c^2 A_\perp Q_s^2$, effective area of fluct. appears to decrease with Y (i.e. $A_\perp Q_s^2$ decreases with Y)



WW (light cone gauge) gluon distribution $g^2 \mathrm{tr}\, A^i(q) A^j(-q)$

at order $(gA^+)^4$

$$\delta^{ij}\, g^2 \mathrm{tr}\, A^i(q) A^j(-q) = \frac{1}{2} q^2 g^2 A^{+a}(q) A^{+a}(-q) - \frac{g^4}{8} f^{abe} f^{cde} \left(\delta^{lm} - \frac{q^l q^m}{q^2}\right) \int \frac{d^2k}{(2\pi)^2} \frac{d^2p}{(2\pi)^2} k^l p^m A^{+a}(q-k) A^{+b}(k) A^{+c}(-q-p) A^{+d}(p)$$

$$\left(2\frac{q^i q^j}{q^2} - \delta^{ij}\right) g^2 \mathrm{tr}\, A^i(q) A^j(-q) = \frac{1}{2} q^2 g^2 A^{+a}(q) A^{+a}(-q) + \frac{g^4}{8} f^{abe} f^{cde} \left(\delta^{lm} - \frac{q^l q^m}{q^2}\right) \int \frac{d^2k}{(2\pi)^2} \frac{d^2p}{(2\pi)^2} k^l p^m A^{+a}(q-k) A^{+b}(k) A^{+c}(-q-p) A^{+d}(p)$$

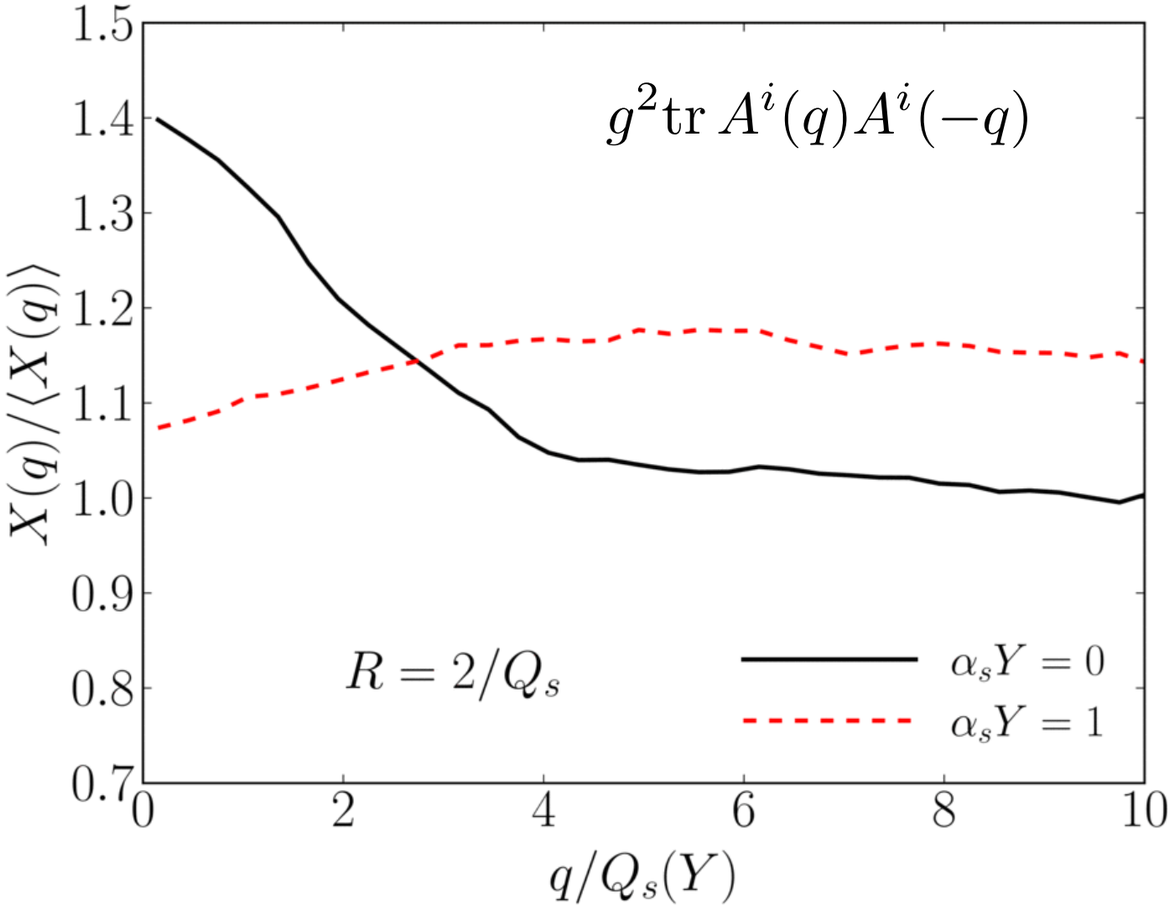
* not “diagonal” in q, analytic calculation of $V_{eff}[X(q)]$ more complicated
* numerical MC computation is no problem though,
  (to all orders in gA^+: $A^i = (i/g)\, U[A^+]\, \partial^i\, U^\dagger[A^+]$)

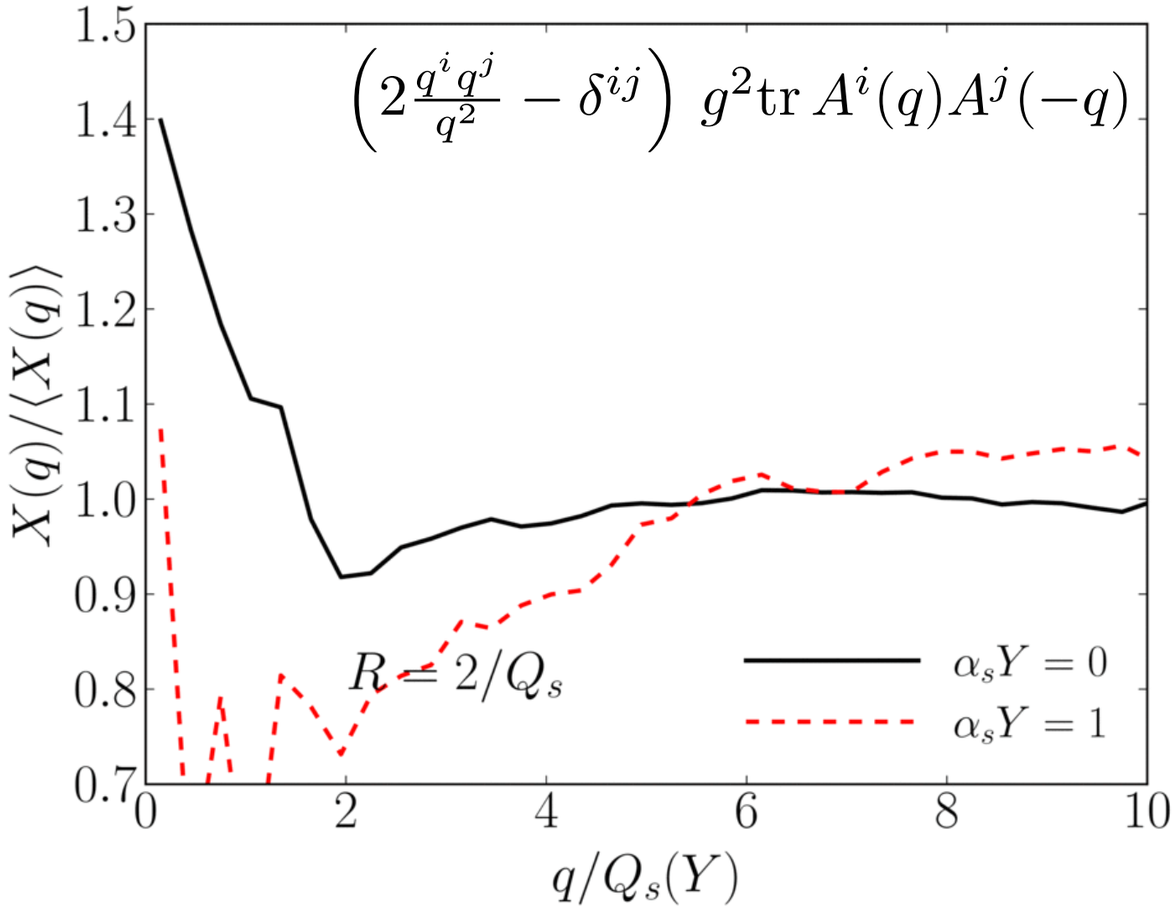
Summary

- effective potential for observable $O[A^+]$:
  integrate out "orthogonal" fluctuations of A^+ from MV / JIMWLK action
- for $O[A^+] = g^2\ \mathrm{tr}\ |A^+(q)|^2$ we obtained $V_{\mathrm{eff}}[\eta]$ analytically & numerically: linear minus log
  $\eta(q) \equiv X(q) / X_s(q)$ describes fluctuations of cov. gauge gluon distribution
- tight correlation of gluon number and transverse momentum fluctuations
- strong increase of Δq^2 with ΔN_g, especially in small transv. area
- evolution modifies the spectrum of fluctuations:
  MV: gluon pile-up near Qs;
  JIMWLK: scale invariant fluctuation $\eta(q)$ (for fixed coupl. kernel !)
  above absorptive boundary

Backup Slides

MC results for WW (light cone gauge) gluon distribution





high multiplicity configurations via

$$\Delta N_g[\eta(q)] = \int \frac{d^2q}{(2\pi)^2} [X(q) - X_s(q)]$$

←X(q)

Resummation of boost-invariant quantum fluctuations (JIMWLK):

classical ensemble at Y = log x_0/x = 0:

$$P[\rho] \sim e^{-S_{\rm cl}[\rho]} \ , \quad S_{\rm MV} \quad = \quad \int d^2x_\perp \, \frac{1}{2\mu^2} \rho^a \rho^a \ , \qquad V(x_\perp) = \mathcal{P} \exp \ ig^2 \int dx^- \frac{1}{\nabla_\perp^2} \rho(x_\perp)$$

quantum evolution to Y>0: random walk in space of Wilson lines

$$\partial_Y V(x_\perp) = V(x_\perp) \, it^a \left\{ \int d^2y_\perp \, \varepsilon_k^{ab}(x_\perp, y_\perp) \, \xi_k^b(y_\perp) + \sigma^a(x_\perp) \right\} \ .$$

$$\varepsilon_k^{ab} = \left(\frac{\alpha_s}{\pi} \right)^{1/2} \ \frac{(x_\perp - y_\perp)_k}{(x_\perp - y_\perp)^2} \ \left[1 - U^\dagger(x_\perp) U(y_\perp) \right]^{ab}$$

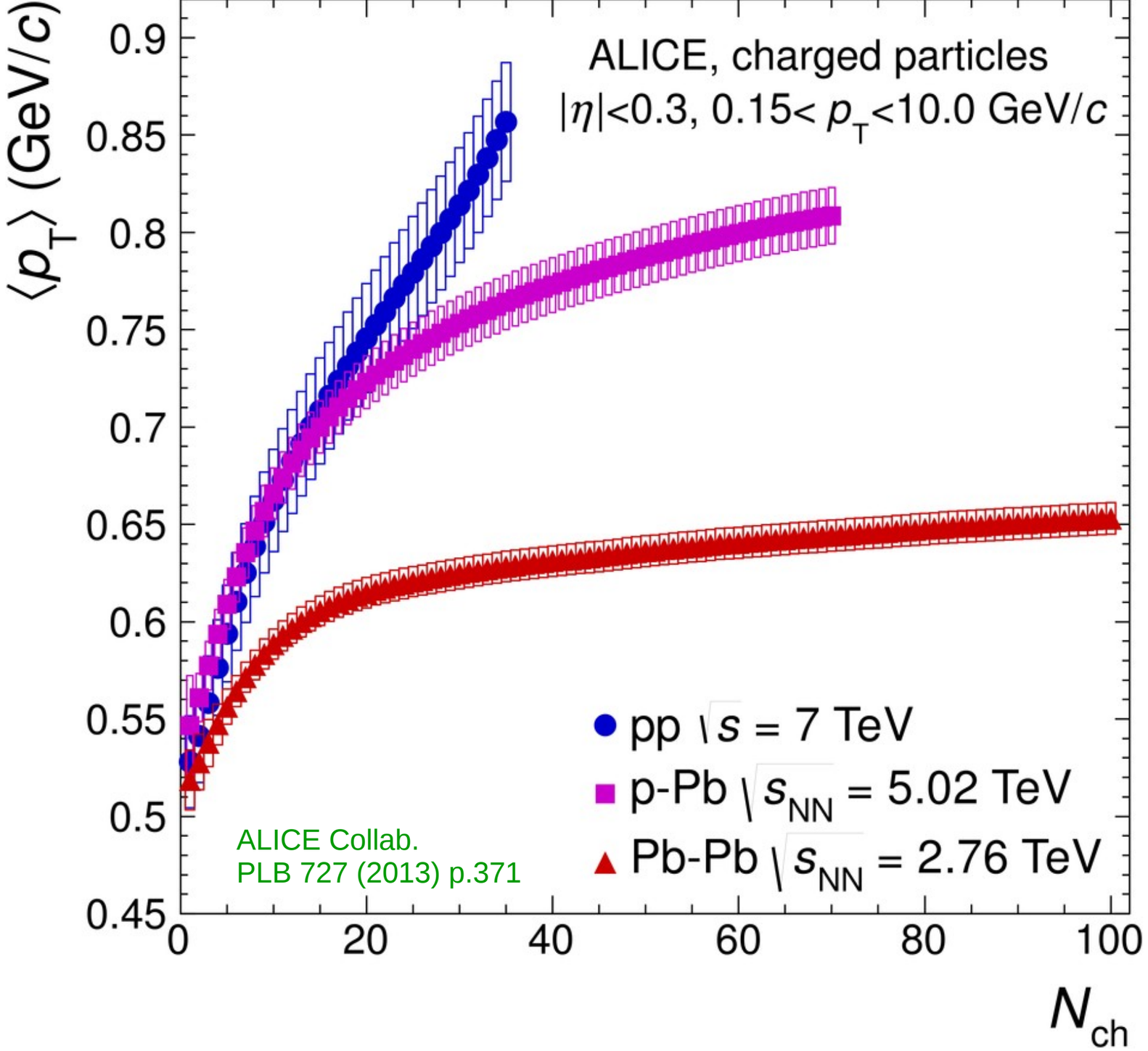
$$t^b U_{ab}(x_\perp) = {\rm tr} \ (V(x_\perp) t^a V^\dagger(x_\perp))$$

$$\langle \xi_i^a(x_\perp) \, \xi_j^b(y_\perp) \rangle = \delta^{ab} \delta_{ij} \delta^{(2)}(x_\perp - y_\perp)$$ (Gaussian white noise)

$$\sigma^a(x_\perp) = -i \frac{\alpha_{\rm s}}{2\pi^2} \int d^2z_\perp \, \frac{1}{(x_\perp - z_\perp)^2} {\rm tr} \ \left(T^a U^\dagger(x_\perp) \, U(z_\perp) \right)$$ (drag term)

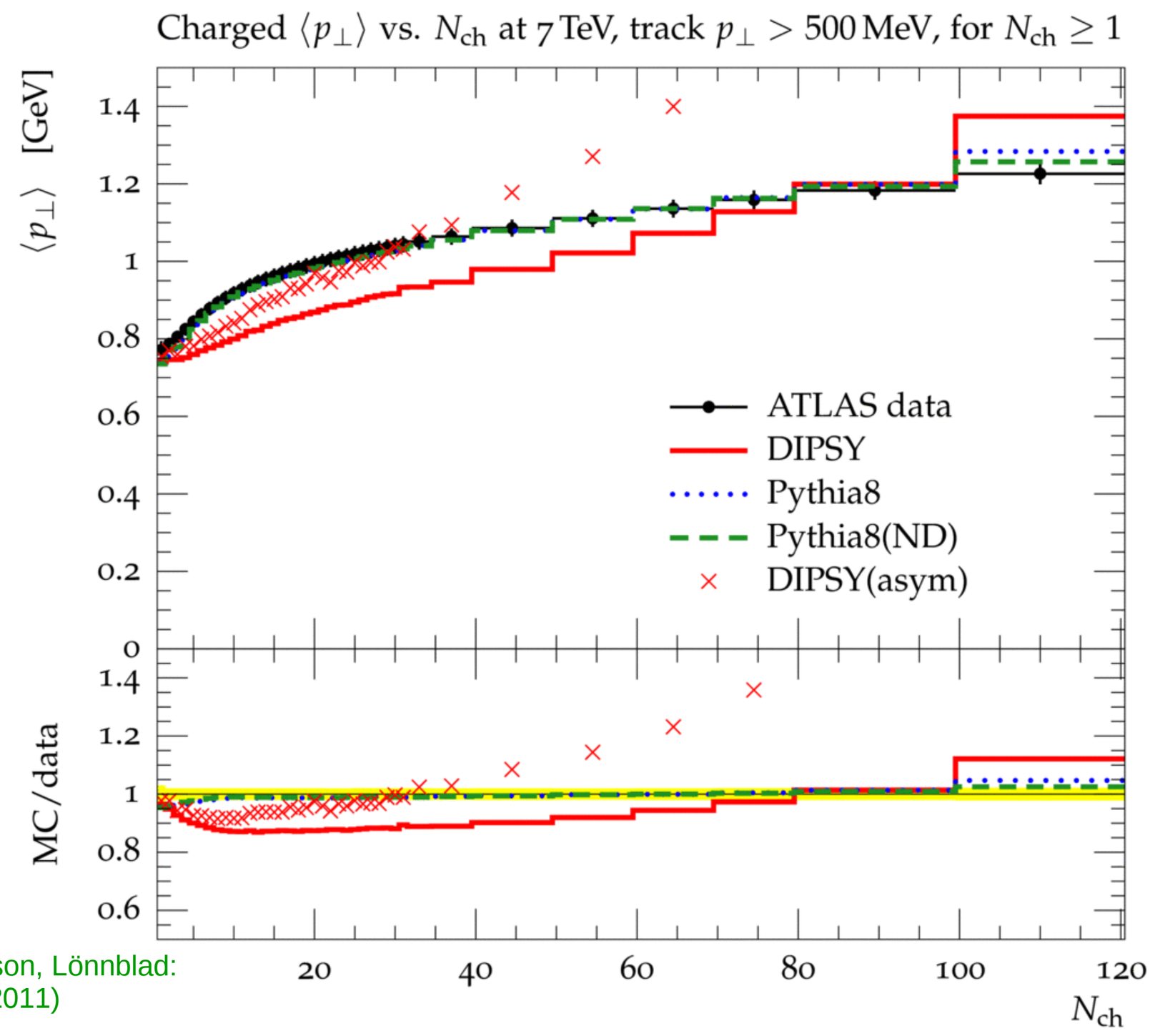
Increase of <pT>
in p+p, p+Pb collisions
with event multiplicity

?



<p_T> vs. N_{ch}: ATLAS data vs. models

- PYTHIA8 virtually perfect
- DIPSY qualitatively ok
- can one relate this to B-JIMWLK W[A^+] ?



Flensburg, Gustafson, Lönnblad:
JHEP 1108, 103 (2011)

Collectivity from the initial state:

Four-particle correlations in proton-nucleus collisions

A work in progress with

Mark Mace (Stony Brook / Brookhaven)
Raju Venugopalan (Brookhaven)

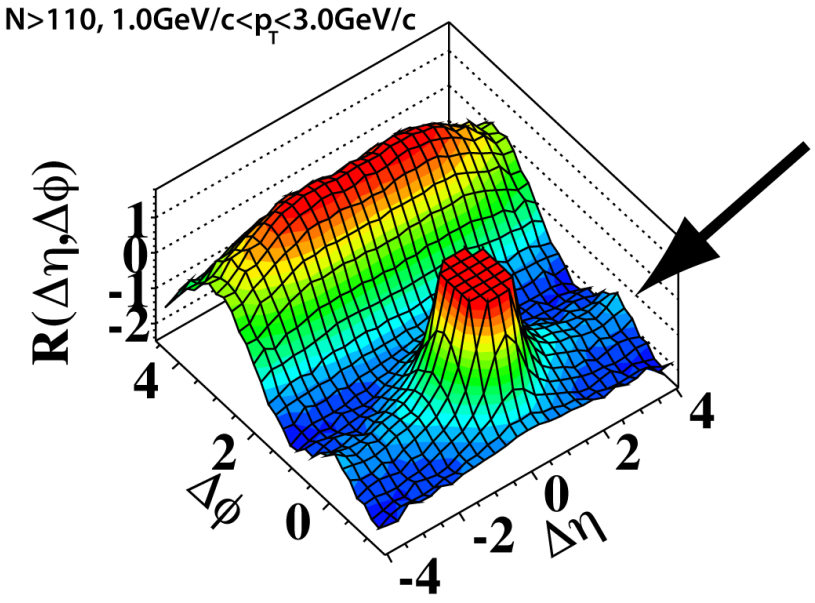
Contents

- Background / Motivation
- Particle production in proton-nucleus collisions
- Beyond the dipole: n-point correlators in the MV model
- Results

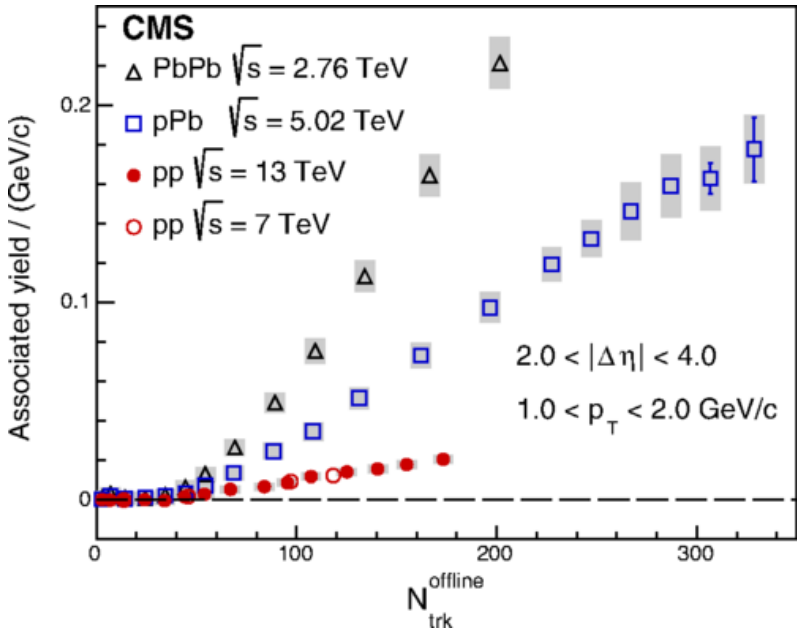
BACKGROUND / MOTIVATION

Background 1: Collectivity in small systems

V. Khachatryan et al. (CMS Collaboration)
JHEP, 1009:091, 2010.

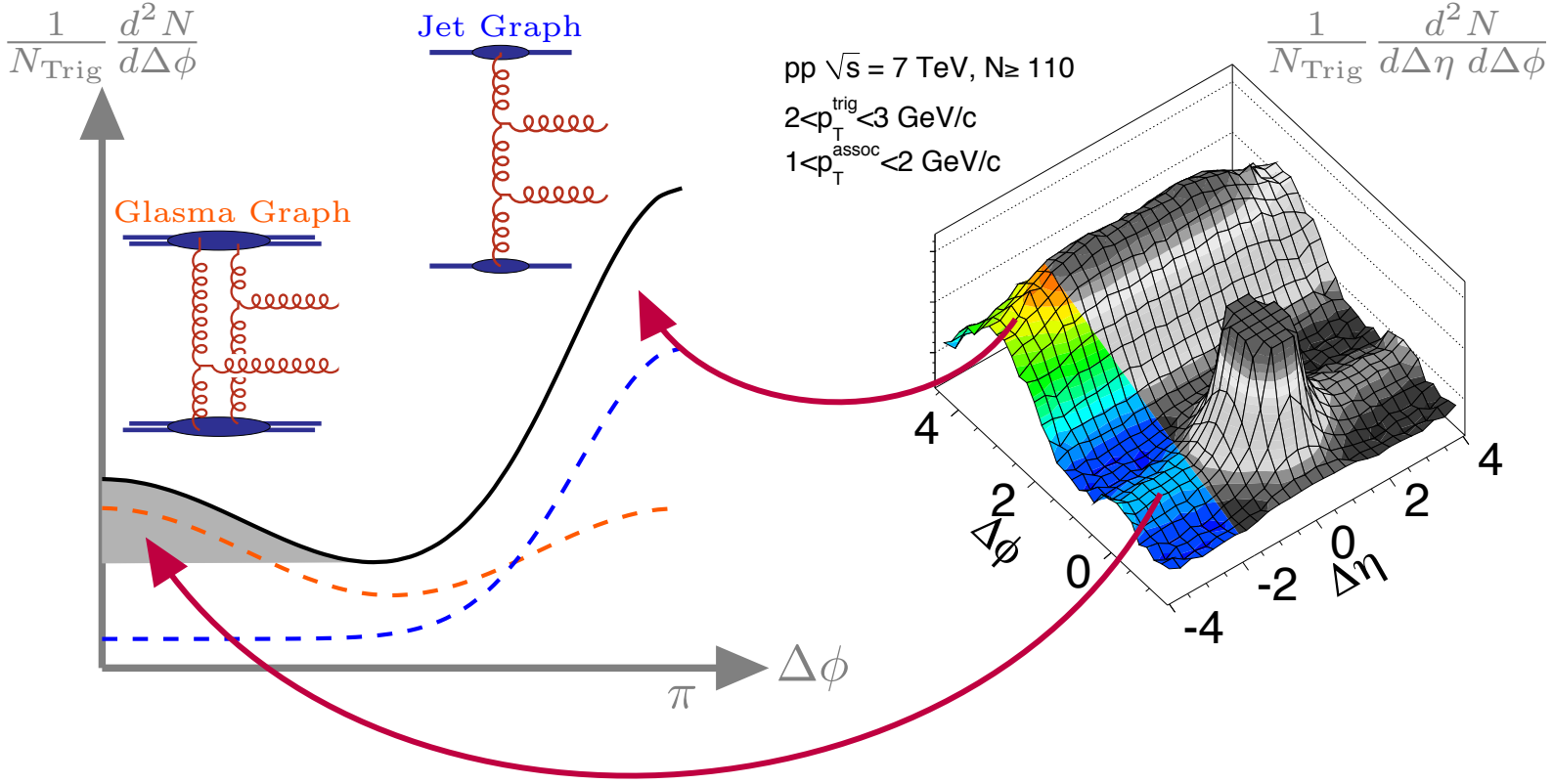


V. Khachatryan et al. (CMS Collaboration)
Phys. Rev. Lett., 116(17):172302, 2016.



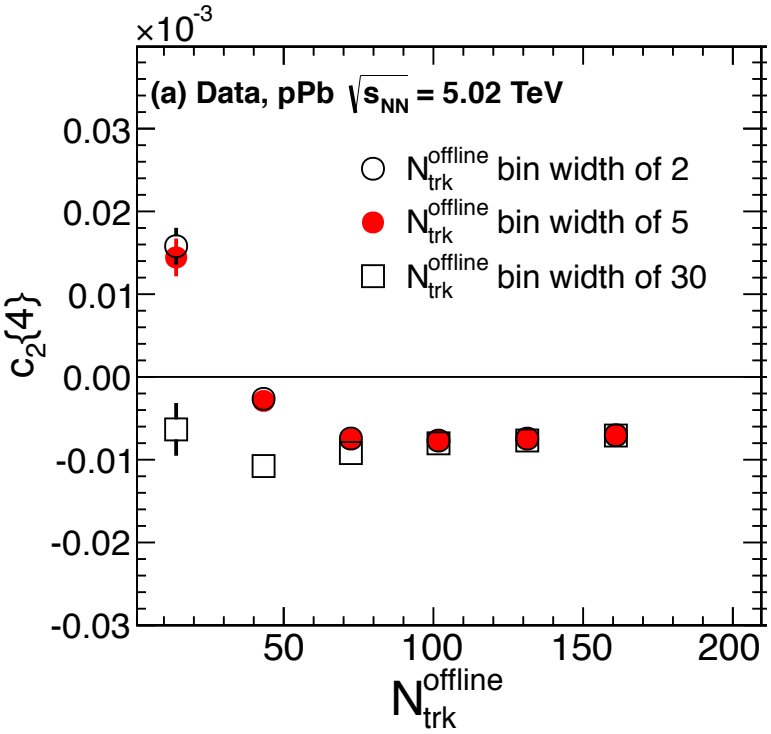
K. Dusling, W. Li, and B. Schenke
Novel collective phenomena in high-energy proton–proton and proton–nucleus collisions
Int. J. Mod. Phys., E25(01):1630002, 2016. [arXiv:1509.07939]

Background II: Glasma-graphs

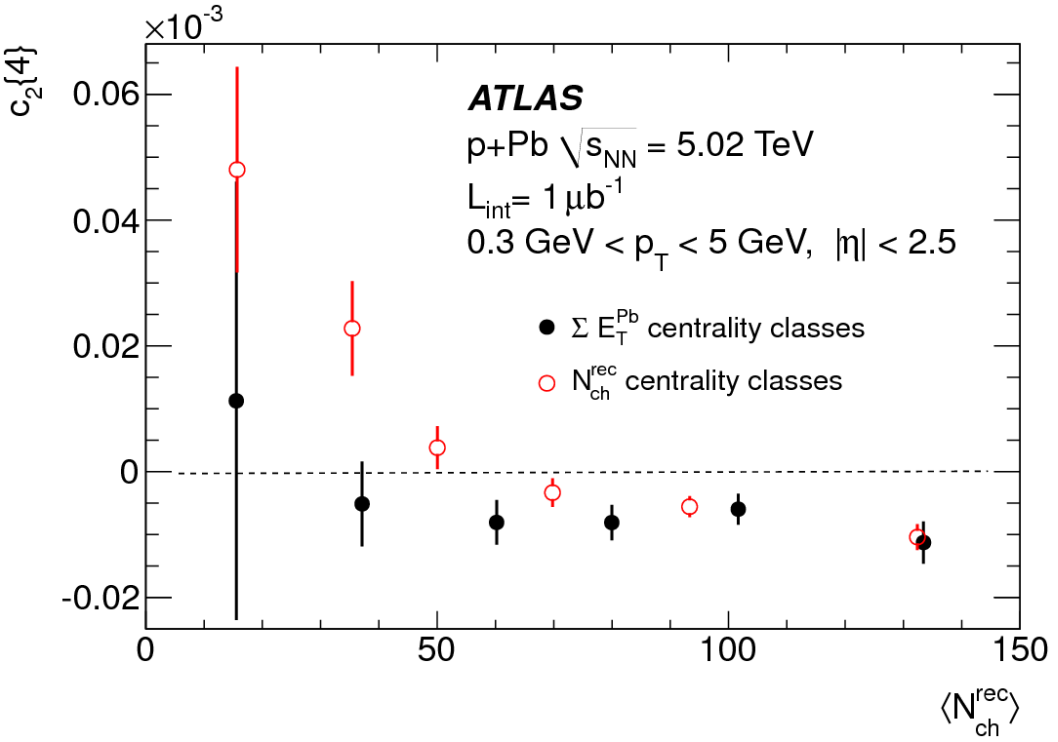


Dusling, Tribedy, Venugopalan, Phys.Rev. D93 (2016) no.1, 014034
Dusling, Venugopalan, PRD87 094034, PRD87 054014, PRD87 051502, PRL 108 262001
Dumitru, Dusling, Gelis, Jalilian-Marian, Lappi, Venugopalan, Phys.Lett. B697 (2011) 21-25

Motivation I: Four-particle cumulants



CMS Collaboration
Phys. Lett., B724 (2013) 213–240.



ATLAS Collaboration
Phys. Lett. B725 (2013) 60-78.

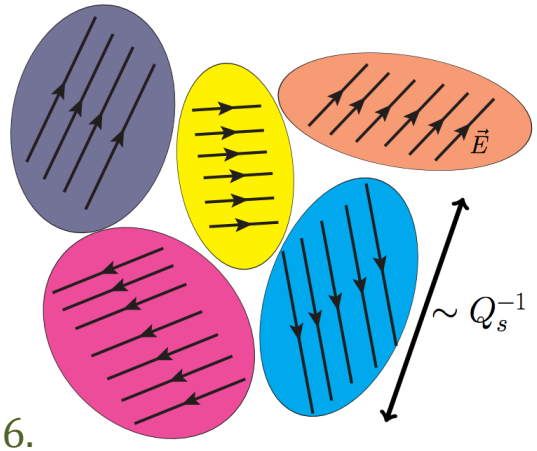
Motivation II: The color domain model

- Gaussian correlation of E-fields will produce particles isotropically

$$\frac{g^2}{N_c}\left\langle E_i^a(b_1)E_j^b(b_2)\right\rangle = \frac{1}{(N_c^2-1)}\delta^{ab}\delta_{ij}Q_s^2\Delta(b_1-b_2)$$

- Consider sub-class of events with a predefined orientation:

$$\frac{g^2}{N_c}\left\langle E_i^a(b_1)E_j^b(b_2)\right\rangle = \frac{1}{(N_c^2-1)}\delta^{ab}Q_s^2\Delta(b_1-b_2)\left(\delta_{ij}+2\mathcal{A}\left[\hat{a}_i\hat{a}_j-\frac{1}{2}\delta_{ij}\right]\right)$$

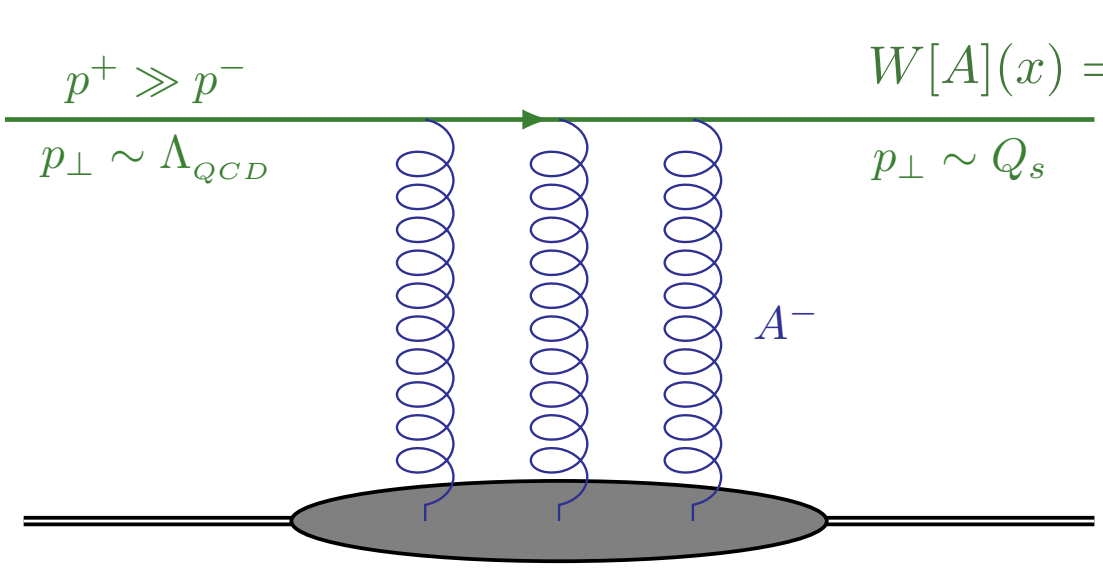


A. Kovner and M. Lublinsky,Phys.Rev., D84:094011, 2011.
A. Dumitru and A. V. Giannini, Nucl. Phys., A933:212–228, 2015.
A. Dumitru, L. McLerran, and V. Skokov, Phys. Lett., B743:134–137, 2015.
A. Dumitru and V. Skokov, Phys. Rev., D91(7):074006, 2015.
T. Lappi, B. Schenke, S. Schlichting, and R. Venugopalan. JHEP, 01:061, 2016.

PARTICLE PRODUCTION IN PROTON-NUCLEUS COLLISIONS

The hybrid framework

- Consider eikonal scattering of quark from a dense target



$$W[A](x) = \mathcal{P} \exp\left[ig \int dz^+ A_a^-(z^+, x)\right]$$

- Differential cross-section for quark scattering on a nucleus

$$\frac{dN}{d^2p} \simeq \frac{1}{\pi B_p} \int_{x\bar{x}} e^{-(x^2+\bar{x}^2)/2B_p} \left\langle \frac{1}{N_c} \mathrm{Tr}\left[W(x)W^\dagger(\bar{x})\right] \right\rangle e^{ip\cdot(x-\bar{x})}$$

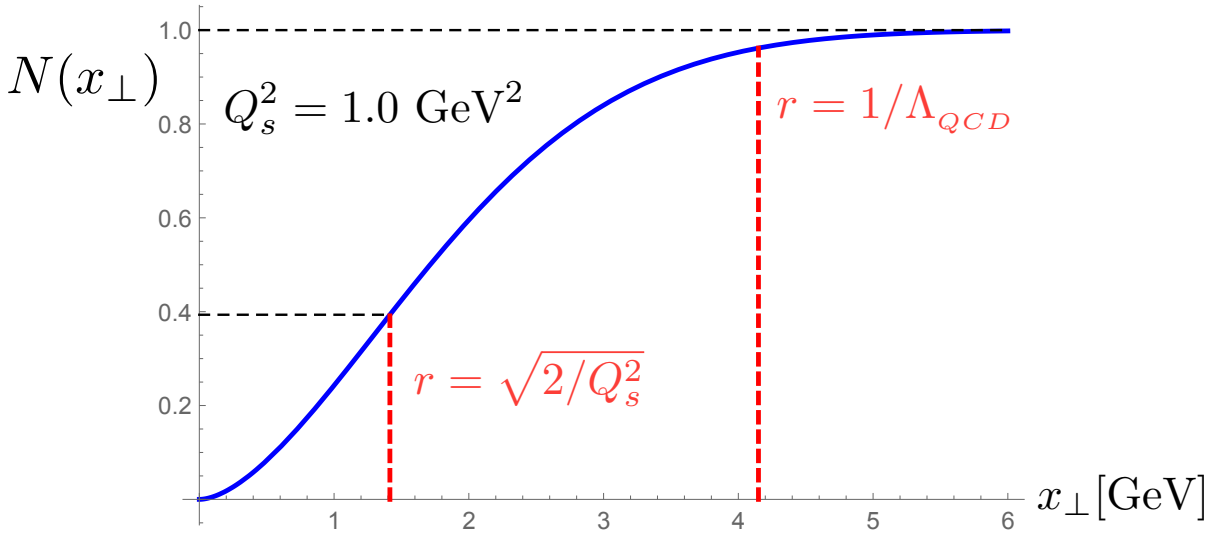
A. Dumitru and J. Jalilian-Marian, Phys. Rev. Lett., 89:022301, 2002.
J. D. Bjorken, J. B. Kogut, and D. E. Soper, Phys. Rev., D3:1382, 1971.

Multiple-scattering in the CGC

- Dipole correlator is evaluated in the MV model whereby averaging over the color field of the nucleus

$$g^2 \left\langle A_a^-(x) A_b^-(y) \right\rangle = \delta^{ab} L_{xy} \qquad L_{xy} = -\frac{g^4 \mu^2}{16\pi} |x-y|^2 \ln \frac{1}{\Lambda |x-y|}$$

- results in $D(x,\bar{x}) = \frac{1}{N_c} \mathrm{Tr}\left[W(x) W^\dagger(\bar{x})\right] = \exp(C_F L_{x\bar{x}})$



Multi-particle production

- Single quark scattering:

$$\frac{dN}{d^2p} \simeq \frac{1}{\pi B_p} \int_{x\bar{x}} e^{-(x^2+\bar{x}^2)/2B_p} \left\langle \frac{1}{N_c} \mathrm{Tr}\left[W(x)W^\dagger(\bar{x})\right] \right\rangle e^{ip\cdot(x-\bar{x})}$$

- Two quark scattering:

$$\frac{d^2N}{d^2p_1 d^2p_2} \simeq \frac{1}{(\pi B_p)^2} \int_{x\bar{x}y\bar{y}} e^{-(x^2+\bar{x}^2)/2B_p}\ e^{-(y^2+\bar{y}^2)/2B_p} e^{ip_1\cdot(x-\bar{x})} e^{ip_2\cdot(y-\bar{y})} \times \left\langle \frac{1}{N_c} \mathrm{Tr}\left[W(x)W^\dagger(\bar{x})\right] \frac{1}{N_c} \mathrm{Tr}\left[W(y)W^\dagger(\bar{y})\right] \right\rangle$$

- Four quark scattering:

$$d^4N \sim \int \left\langle \mathrm{Tr}\left[W(w)W^\dagger(\bar{w})\right] \mathrm{Tr}\left[W(x)W^\dagger(\bar{x})\right] \mathrm{Tr}\left[W(y)W^\dagger(\bar{y})\right] \mathrm{Tr}\left[W(z)W^\dagger(\bar{z})\right] \right\rangle$$

BEYOND THE DIPOLE

n-point correlators in the MV model

Multiple-scattering in the CGC

- Start with the dipole scattering matrix: $\langle D(x,\bar{x})\rangle_W = \frac{1}{N_c}\left\langle \mathrm{Tr}\left[W(x)W^\dagger(\bar{x})\right]\right\rangle$

- Expand out the last slice in rapidity:

$$W(x) \equiv \mathcal{P}\exp\left[ig\int dz^+ A_a^-(z^+,x)\right] \simeq V(x)\left[1+igA_a^-(\xi,x)T^a+\cdots\right]$$

- Take all two-point functions:

$$\langle D(x,\bar{x})\rangle_W \simeq \langle D(x,\bar{x})\rangle_V + \underbrace{g^2\left\langle A_a^-(x)A_b^-(\bar{x})\right\rangle}_{\delta^{ab}L_{x\bar{x}}}\frac{1}{N_c}\underbrace{\mathrm{Tr}\left[V(x)T^aT^bV^\dagger(\bar{x})\right]}_{\frac{\delta^{ab}}{2}\mathrm{Tr}\left[V(x)V^\dagger(\bar{x})\right]}$$

- And re-exponentiate:

$$\langle D(x,\bar{x})\rangle_W = \exp\left(C_F\, L_{x\bar{x}}\right)$$

- As before expand out all Wilson lines:

$$W(x) \equiv \mathcal{P} \exp\left[ig \int dz^+ A_a^-(z^+, x)\right] \simeq V(x)\left[1 + igA_a^-(\xi, x)T^a + \cdots\right]$$

- Four point function: $\langle D_{x\bar{x}} D_{y\bar{y}} \rangle_W \simeq \alpha_{x\bar{x}y\bar{y}} \langle D_{x\bar{x}} D_{y\bar{y}} \rangle_V + \beta_{xy\bar{x}\bar{y}} \langle Q_{x\bar{y}y\bar{x}} \rangle_V$

$$\begin{pmatrix} \langle D_{x\bar{x}} D_{y\bar{y}} \rangle \\ \langle Q_{x\bar{y}y\bar{x}} \rangle \end{pmatrix}_W = \begin{pmatrix} \alpha_{x\bar{x}y\bar{y}} & \beta_{xy\bar{x}\bar{y}} \\ \beta_{xy\bar{y}\bar{x}} & \alpha_{x\bar{y}y\bar{x}} \end{pmatrix} \begin{pmatrix} \langle D_{x\bar{x}} D_{y\bar{y}} \rangle \\ \langle Q_{x\bar{y}y\bar{x}} \rangle \end{pmatrix}_V$$

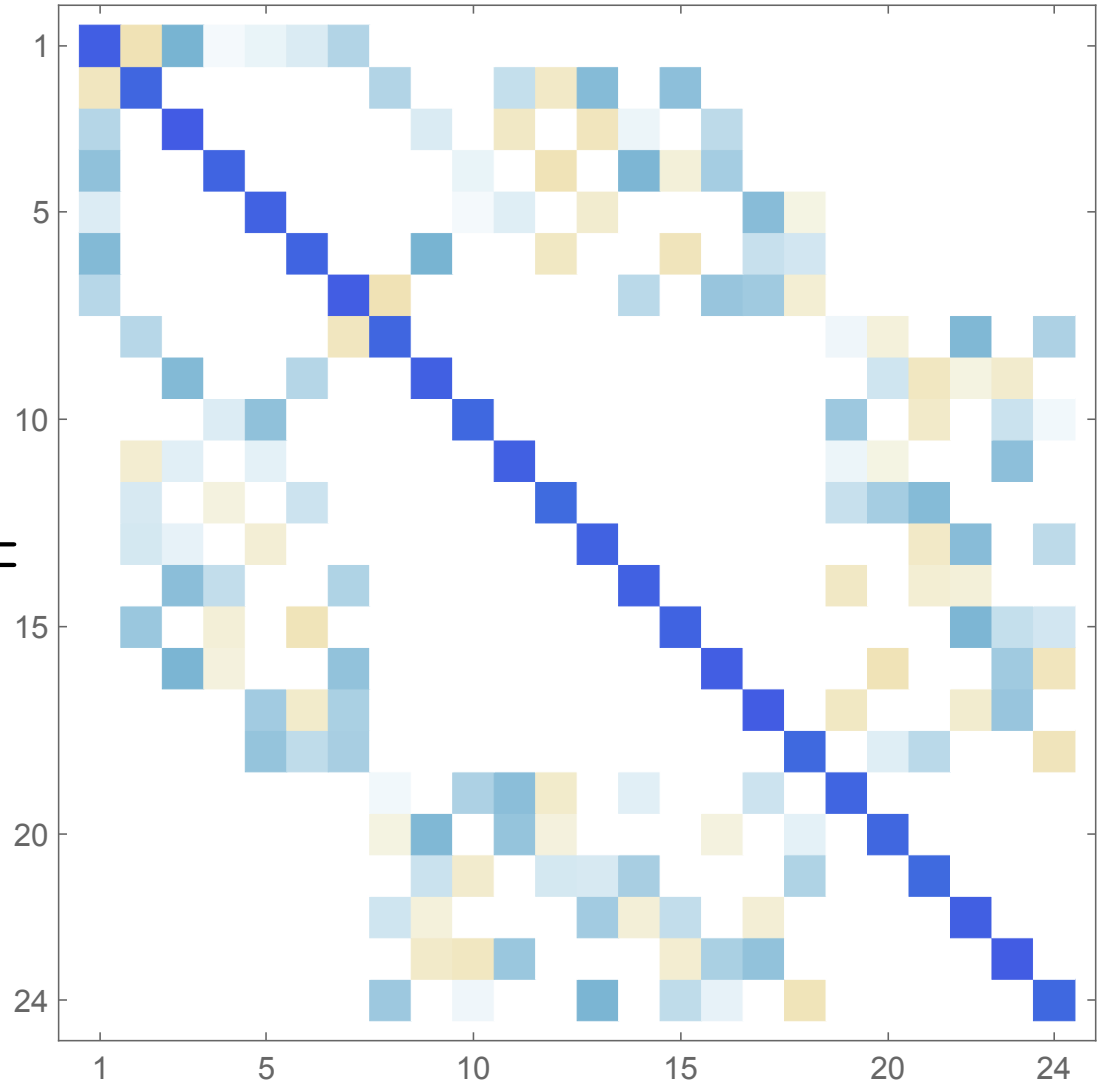
- Eight point function:

$$\begin{aligned} \langle D_{w\bar{w}} D_{x\bar{x}} D_{y\bar{y}} D_{z\bar{z}} \rangle_W \simeq{}& \alpha_{w\bar{w}x\bar{x}y\bar{y}z\bar{z}} \langle D_{w\bar{w}} D_{x\bar{x}} D_{y\bar{y}} D_{z\bar{z}} \rangle_V \\ &+ \beta_{wx\bar{w}\bar{x}} \langle Q_{x\bar{w}w\bar{x}} D_{y\bar{y}} D_{z\bar{z}} \rangle_V + \beta_{wy\bar{w}\bar{y}} \langle Q_{y\bar{w}w\bar{y}} D_{x\bar{x}} D_{z\bar{z}} \rangle_V \\ &+ \beta_{wz\bar{w}\bar{z}} \langle Q_{z\bar{w}w\bar{z}} D_{x\bar{x}} D_{y\bar{y}} \rangle_V + \beta_{xy\bar{x}\bar{y}} \langle Q_{y\bar{x}x\bar{y}} D_{w\bar{w}} D_{z\bar{z}} \rangle_V \\ &+ \beta_{xz\bar{x}\bar{z}} \langle Q_{z\bar{x}x\bar{z}} D_{w\bar{w}} D_{y\bar{y}} \rangle_V + \beta_{yz\bar{y}\bar{z}} \langle Q_{z\bar{y}y\bar{z}} D_{w\bar{w}} D_{x\bar{x}} \rangle_V \end{aligned}$$

Kovner and U. A. Wiedemann. Phys. Rev., D64:114002, 2001.
H. Fujii.. Nucl. Phys., A709:236–250, 2002.
J. P. Blaizot, F. Gelis, and R. Venugopalan. Nucl. Phys., A743:57–91, 2004.
F. Dominguez, C. Marquet, and B. Wu, Nucl. Phys., A823:99–119, 2009.

Correlator of eight Wilson lines

$$
\begin{bmatrix}
\langle D_{w\bar{w}} D_{x\bar{x}} D_{y\bar{y}} D_{z\bar{z}} \rangle \\
\langle Q_{w\bar{w}x\bar{x}} D_{y\bar{z}} D_{z\bar{y}} \rangle \\
\langle Q_{w\bar{w}x\bar{y}} D_{y\bar{x}} D_{z\bar{z}} \rangle \\
\langle Q_{w\bar{w}x\bar{y}} D_{y\bar{z}} D_{z\bar{x}} \rangle \\
\langle Q_{w\bar{w}x\bar{z}} D_{y\bar{x}} D_{z\bar{y}} \rangle \\
\langle Q_{w\bar{w}x\bar{z}} D_{y\bar{y}} D_{z\bar{x}} \rangle \\
\langle Q_{w\bar{x}x\bar{w}} D_{y\bar{y}} D_{z\bar{z}} \rangle \\
\langle Q_{w\bar{x}x\bar{w}} Q_{y\bar{z}z\bar{y}} \rangle \\
\langle Q_{w\bar{x}x\bar{y}} Q_{y\bar{w}z\bar{z}} \rangle \\
\langle Q_{w\bar{x}x\bar{y}} Q_{y\bar{z}z\bar{w}} \rangle \\
\langle S_{w\bar{x}x\bar{z}y\bar{w}} D_{z\bar{y}} \rangle \\
\langle S_{w\bar{x}x\bar{z}y\bar{y}} D_{z\bar{w}} \rangle \\
\langle S_{w\bar{y}x\bar{w}y\bar{x}} D_{z\bar{z}} \rangle \\
\langle S_{w\bar{y}x\bar{w}y\bar{z}} D_{z\bar{x}} \rangle \\
\langle S_{w\bar{y}x\bar{x}y\bar{w}} D_{z\bar{z}} \rangle \\
\langle S_{w\bar{y}x\bar{x}y\bar{z}} D_{z\bar{w}} \rangle \\
\langle S_{w\bar{y}x\bar{z}y\bar{w}} D_{z\bar{x}} \rangle \\
\langle S_{w\bar{y}x\bar{z}y\bar{x}} D_{z\bar{w}} \rangle \\
\langle O_{w\bar{z}x\bar{w}y\bar{x}z\bar{y}} \rangle \\
\langle O_{w\bar{z}x\bar{w}y\bar{y}z\bar{x}} \rangle \\
\langle O_{w\bar{z}x\bar{x}y\bar{w}z\bar{y}} \rangle \\
\langle O_{w\bar{z}x\bar{x}y\bar{y}z\bar{w}} \rangle \\
\langle O_{w\bar{z}x\bar{y}y\bar{w}z\bar{x}} \rangle \\
\langle O_{w\bar{z}x\bar{y}y\bar{x}z\bar{w}} \rangle
\end{bmatrix}_W
=
\begin{bmatrix}
\langle D_{w\bar{w}} D_{x\bar{x}} D_{y\bar{y}} D_{z\bar{z}} \rangle \\
\langle Q_{w\bar{w}x\bar{x}} D_{y\bar{z}} D_{z\bar{y}} \rangle \\
\langle Q_{w\bar{w}x\bar{y}} D_{y\bar{x}} D_{z\bar{z}} \rangle \\
\langle Q_{w\bar{w}x\bar{y}} D_{y\bar{z}} D_{z\bar{x}} \rangle \\
\langle Q_{w\bar{w}x\bar{z}} D_{y\bar{x}} D_{z\bar{y}} \rangle \\
\langle Q_{w\bar{w}x\bar{z}} D_{y\bar{y}} D_{z\bar{x}} \rangle \\
\langle Q_{w\bar{x}x\bar{w}} D_{y\bar{y}} D_{z\bar{z}} \rangle \\
\langle Q_{w\bar{x}x\bar{w}} Q_{y\bar{z}z\bar{y}} \rangle \\
\langle Q_{w\bar{x}x\bar{y}} Q_{y\bar{w}z\bar{z}} \rangle \\
\langle Q_{w\bar{x}x\bar{y}} Q_{y\bar{z}z\bar{w}} \rangle \\
\langle S_{w\bar{x}x\bar{z}y\bar{w}} D_{z\bar{y}} \rangle \\
\langle S_{w\bar{x}x\bar{z}y\bar{y}} D_{z\bar{w}} \rangle \\
\langle S_{w\bar{y}x\bar{w}y\bar{x}} D_{z\bar{z}} \rangle \\
\langle S_{w\bar{y}x\bar{w}y\bar{z}} D_{z\bar{x}} \rangle \\
\langle S_{w\bar{y}x\bar{x}y\bar{w}} D_{z\bar{z}} \rangle \\
\langle S_{w\bar{y}x\bar{x}y\bar{z}} D_{z\bar{w}} \rangle \\
\langle S_{w\bar{y}x\bar{z}y\bar{w}} D_{z\bar{x}} \rangle \\
\langle S_{w\bar{y}x\bar{z}y\bar{x}} D_{z\bar{w}} \rangle \\
\langle O_{w\bar{z}x\bar{w}y\bar{x}z\bar{y}} \rangle \\
\langle O_{w\bar{z}x\bar{w}y\bar{y}z\bar{x}} \rangle \\
\langle O_{w\bar{z}x\bar{x}y\bar{w}z\bar{y}} \rangle \\
\langle O_{w\bar{z}x\bar{x}y\bar{y}z\bar{w}} \rangle \\
\langle O_{w\bar{z}x\bar{y}y\bar{w}z\bar{x}} \rangle \\
\langle O_{w\bar{z}x\bar{y}y\bar{x}z\bar{w}} \rangle
\end{bmatrix}_V
$$



RESULTS

Quantities of interest

- Particle spectra:

$$\frac{d^n N}{d^2 p \cdots} \sim \int \overbrace{e^{-(x^2+\bar{x}^2)/2B_p \cdots}}^{B_p = 4\ \mathrm{GeV}^{-2}} \left\langle \overbrace{\frac{1}{N_c} \mathrm{Tr}\left[W(x) W^\dagger(\bar{x})\right] \cdots}^{Q_s^2 \sim 2\ \mathrm{GeV}^2} \right\rangle e^{ip\cdot(x-\bar{x})\cdots}$$

- Two-particle cumulants:

$$c_n\{2\} = \frac{\kappa_n\{2\}}{\kappa_0\{2\}}, \quad v_n\{2\} = \sqrt{c_n\{2\}}$$

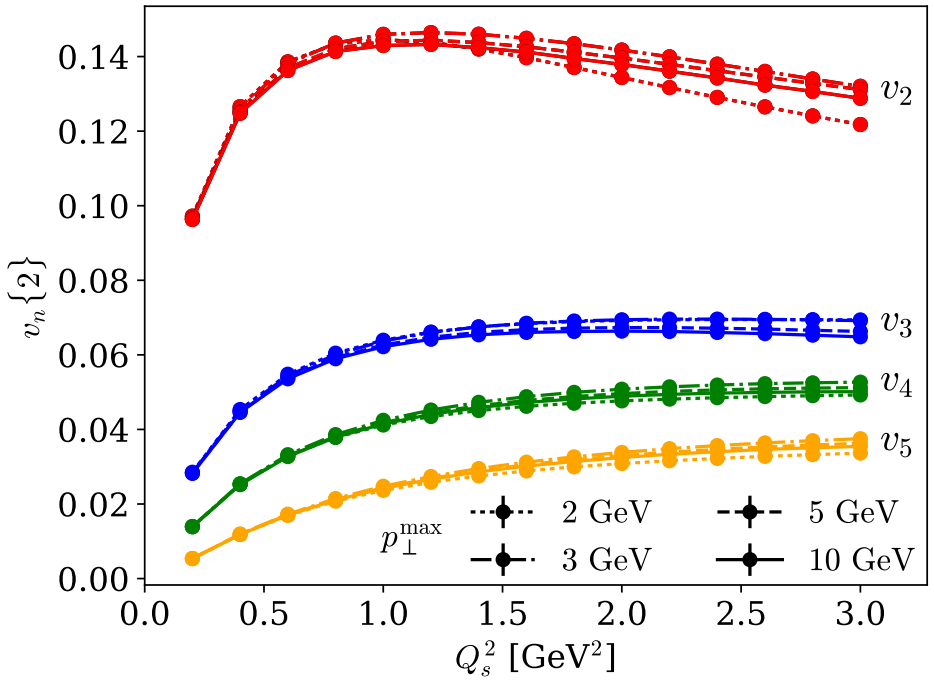
$$\kappa_n\{2\} \equiv \int d^2p_1 d^2p_2 \ \cos\left[n\left(\phi_{p_1} - \phi_{p_2}\right)\right] \frac{d^2N}{d^2p_1 d^2p_2}$$

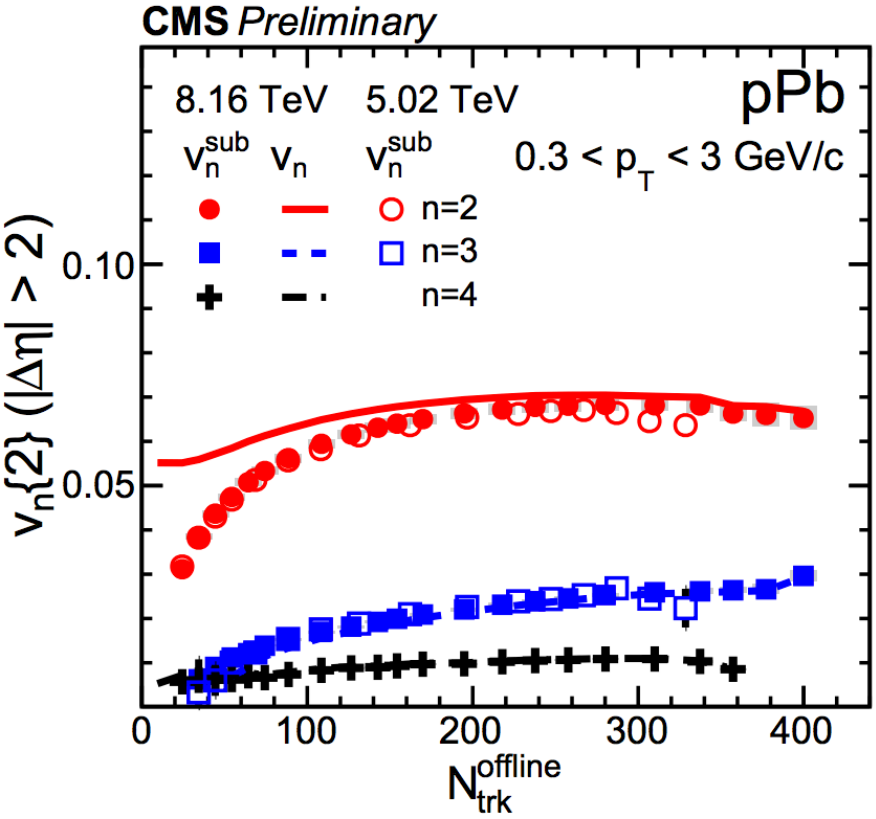
- Four-particle cumulants:

$$\kappa_n\{4\} \equiv \int d^2p_1 d^2p_2 d^2p_3 d^2p_4 \ \cos\left[n\left(\phi_{p_1} + \phi_{p_2} - \phi_{p_3} - \phi_{p_4}\right)\right] \frac{d^4N}{d^2p_1 d^2p_2 d^2p_3 d^2p_4}$$

$$c_n\{4\} = \frac{\kappa_n\{4\}}{\kappa_0\{4\}} - 2\left(\frac{\kappa_n\{2\}}{\kappa_0\{0\}}\right)^2, \qquad v_n\{4\} = \left(-c_n\{4\}\right)^{1/4}$$

Integrated elliptic flow

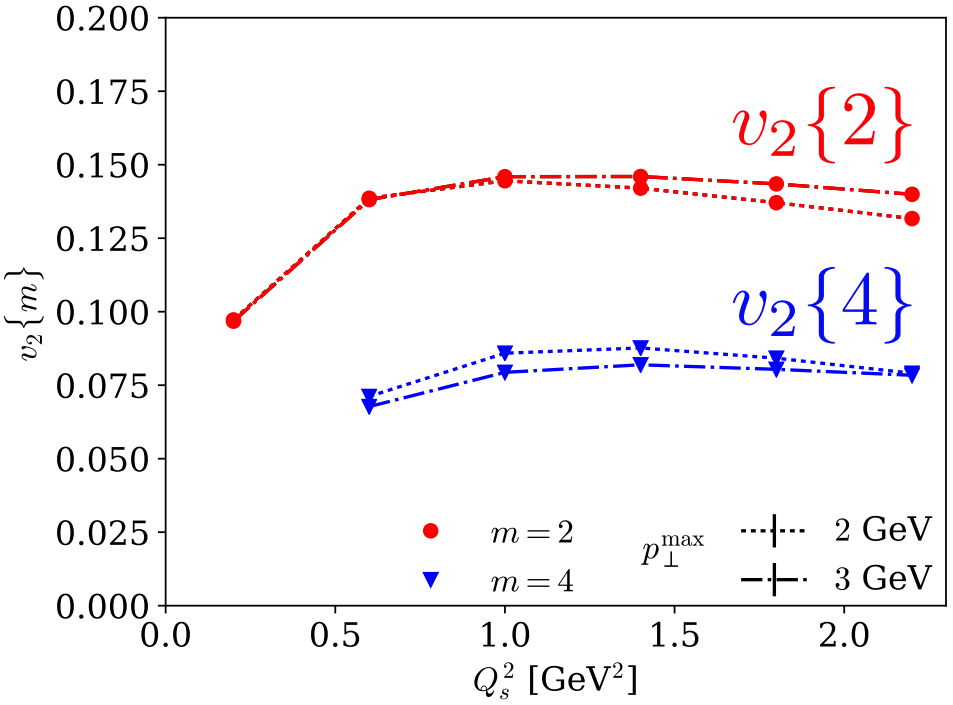


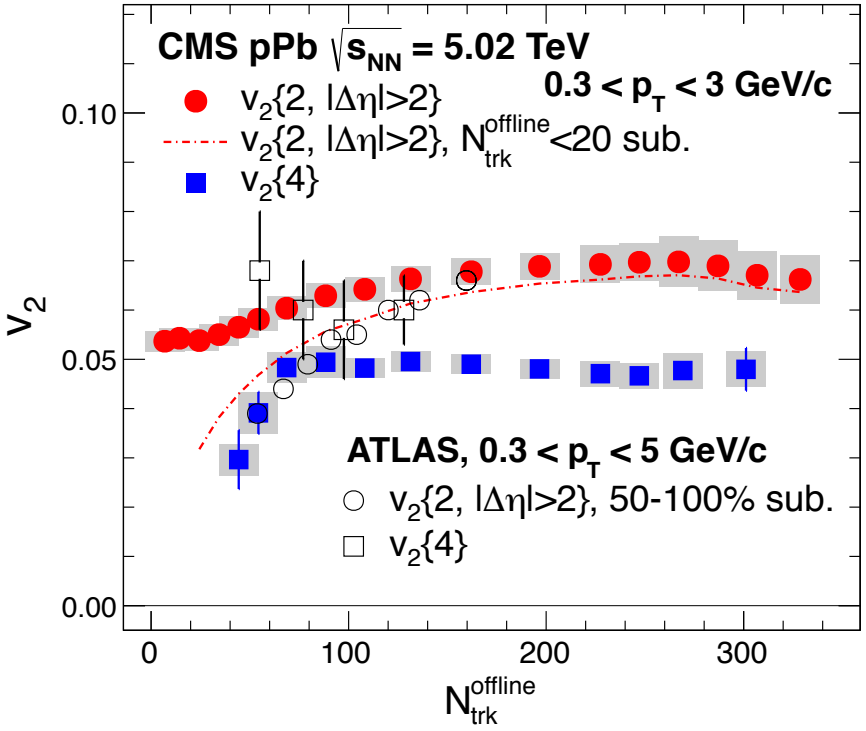


T. Lappi, Phys. Lett., B744:315–319, 2015.

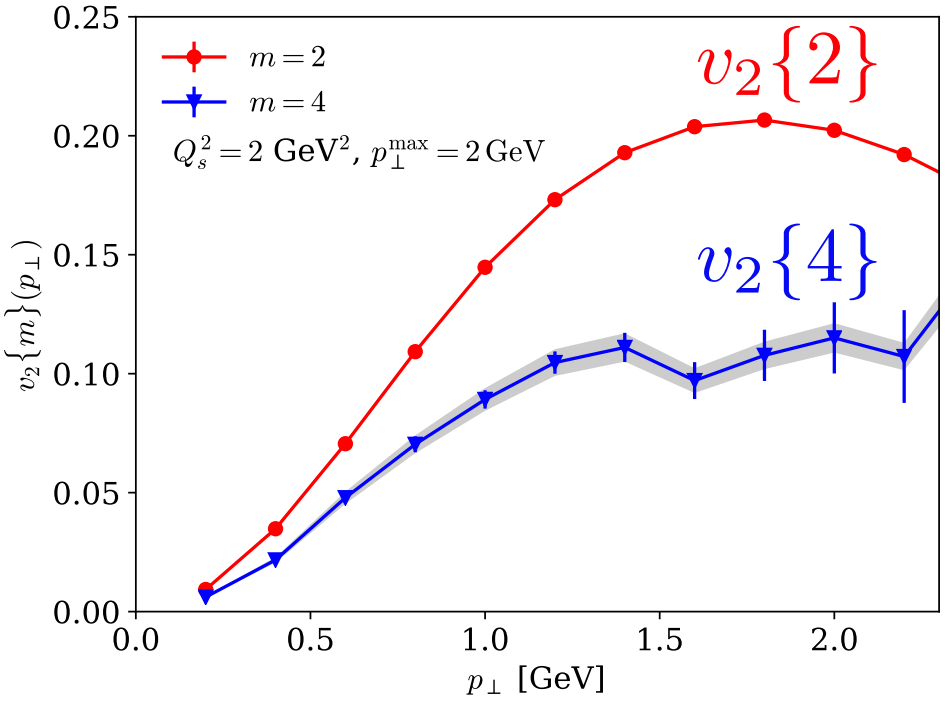
T. Lappi, B. Schenke, S. Schlichting, and R. Venugopalan. JHEP, 01:061, 2016.

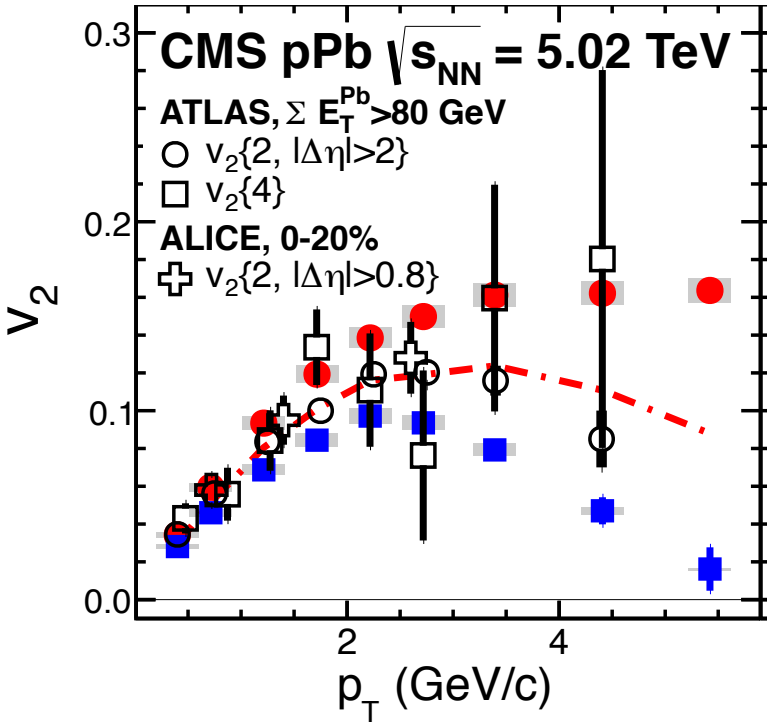
Integrated elliptic flow





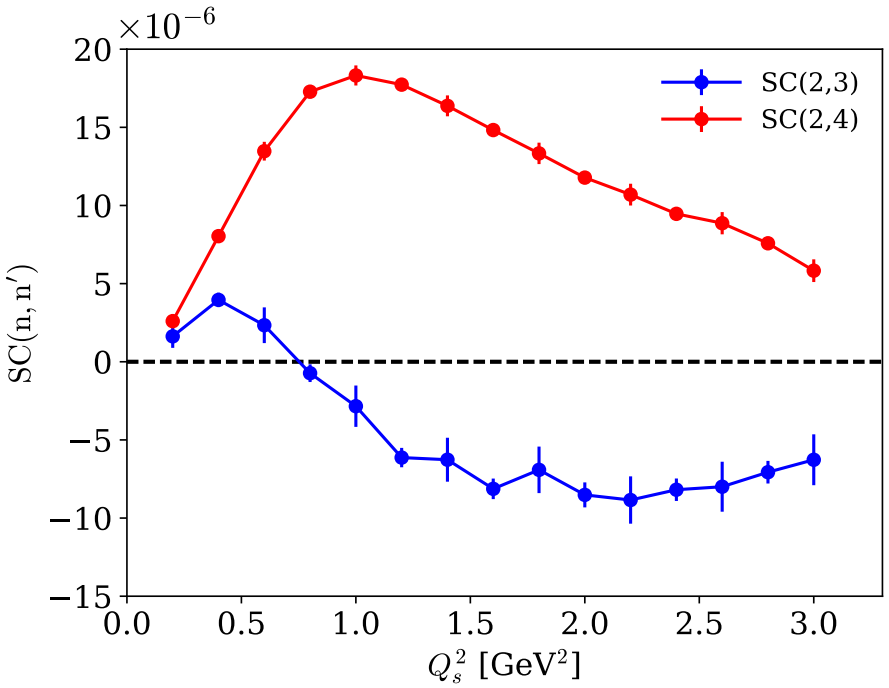
Differential flow

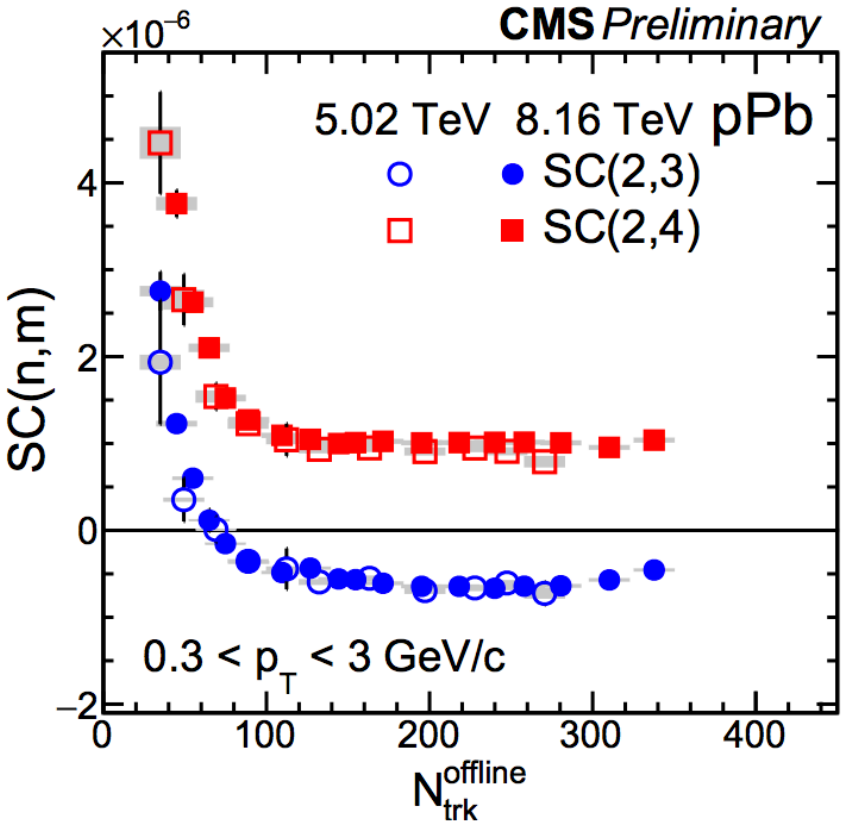




Symmetric cumulants

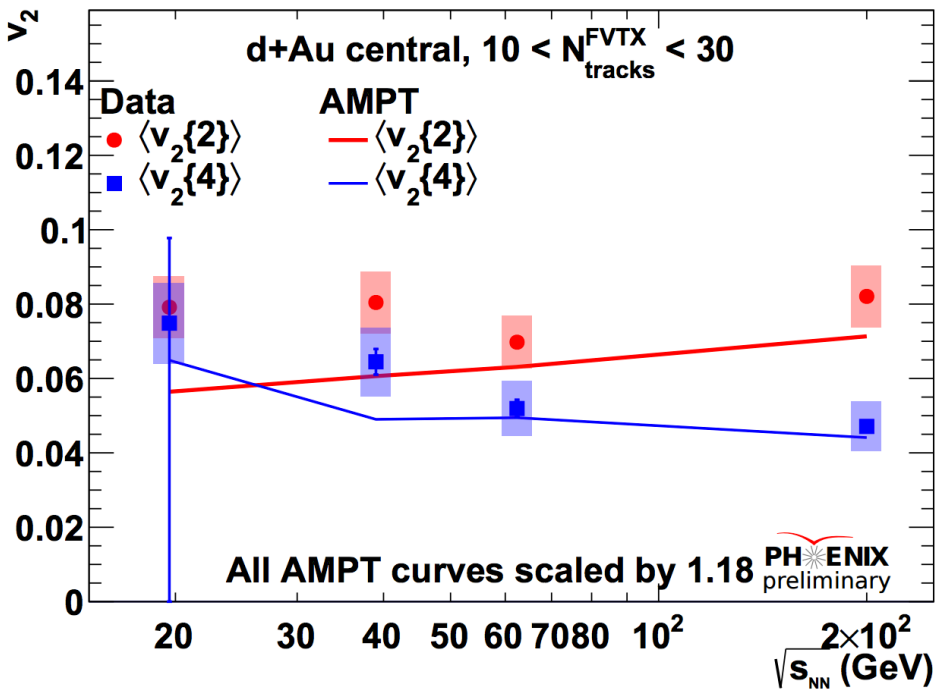
$$SC(m,n) = \langle v_m^2 v_n^2 \rangle - \langle v_m^2 \rangle \langle v_n^2 \rangle$$

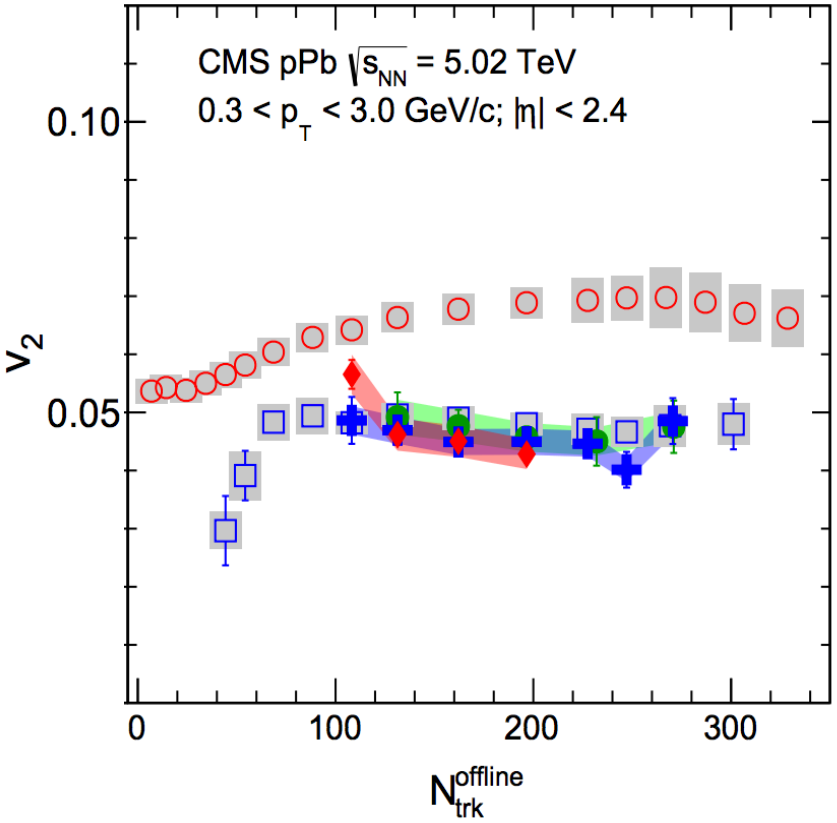




A random event having $v_2 > \langle v_2 \rangle$ will be more likely to have a $v_4 > \langle v_4 \rangle$.

Further thoughts…





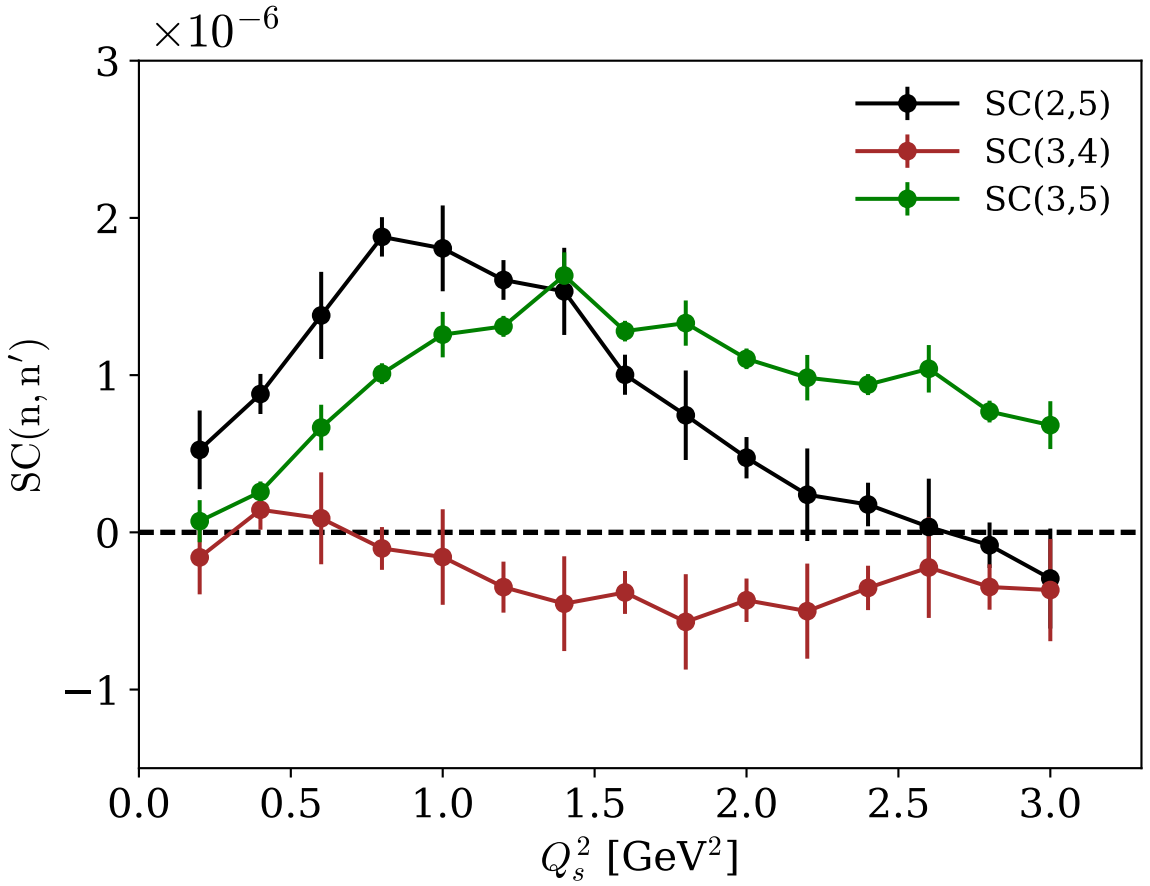
Conclusions

- Developed the machinery to compute correlators of six and eight fundamental Wilson lines at finite N_c

- Modulo many caveats qualitative features of the measured four-particle correlations are understood by non-linear classical fields

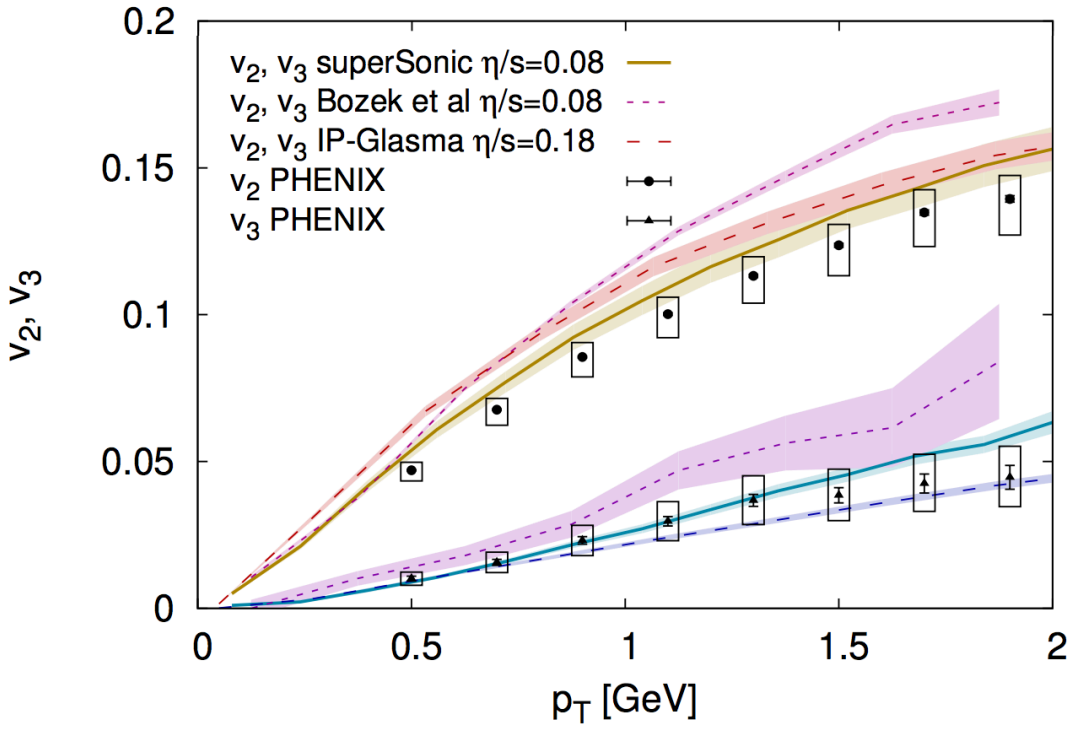
BACKUP

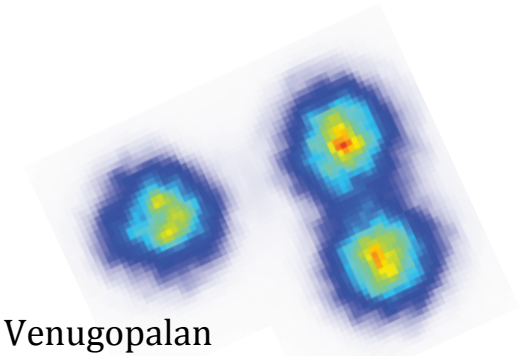
Symmetric cumulants



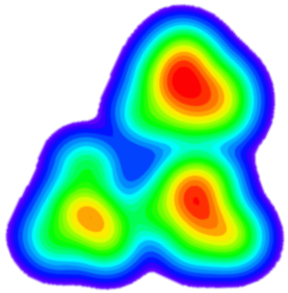
Background II: Collectivity

A. Adare et al. (PHENIX Collaboration)
Phys. Rev. Lett. 115, 142301 (2015)

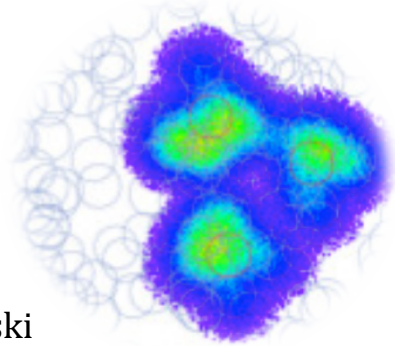




Schenke, Venugopalan
Nucl. Phys. A931 (2014) 1039-1044



J.L. Nagle, et al.
Phys. Rev. Lett. 113, 112301



Bożek, Broniowski
Physics Letters B 747 (2015) 135–138

Particle Production in CGC

Kenji Fukushima

The University of Tokyo

Based on works with
S. Benic, O. Garcia-Montero, R. Venugopalan
N. Tanji

— Saturation: Recent developments, new ideas and Measurements —

Talk Plan

Photons in *pA* at high energies

- Leading-order — Bremsstrahlung (***quarks***)

  Gelis-Jalilian-Marian hep-ph/0205037

- Next-leading-order — Annihilation/Bremsstrahlung (***gluons***)

  Benic-Fukushima arXiv:1602.01989

  Benic-Fukushima-Garcia-Montero-Venugopalan arXiv:1609.09424

  Semi-CGC regime where the latter is overwhelming!

Quarks in *AA* at small proper time

- Proper-time expansion (glasma)

  Fries-Kapusta-Li nucl-th/0604054 / arXiv:1602.09060

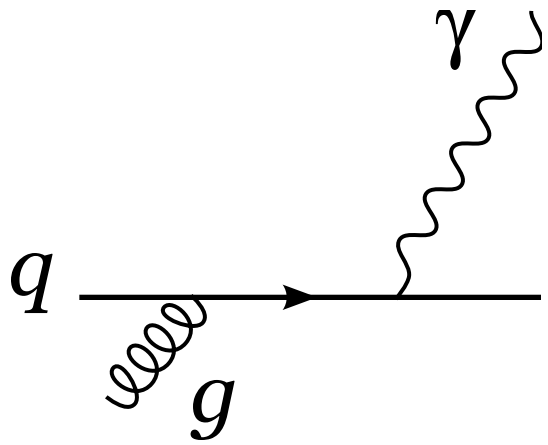
  Fukushima-Fujii-Hidaka arXiv:0811.0437

- Quark sector — quark production / **chirality** production

  Gelis-Tanji arXiv:1506.03327 / Fukushima-Tanji ?????

Photon Production

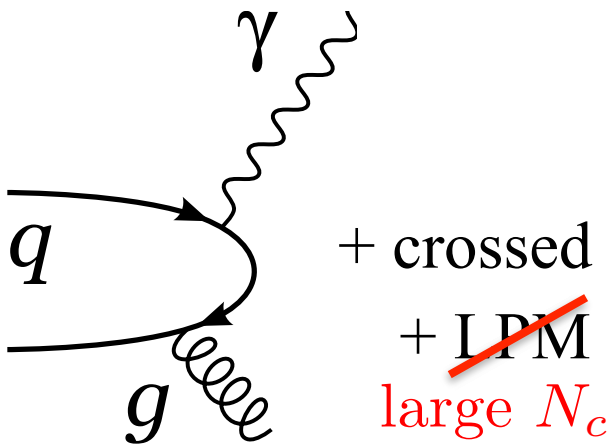
Compton Scattering



$$\propto \alpha_e \alpha_s \, n_q (1 - n_q) n_g$$

$$(qg \rightarrow q\gamma)$$

Annihilation

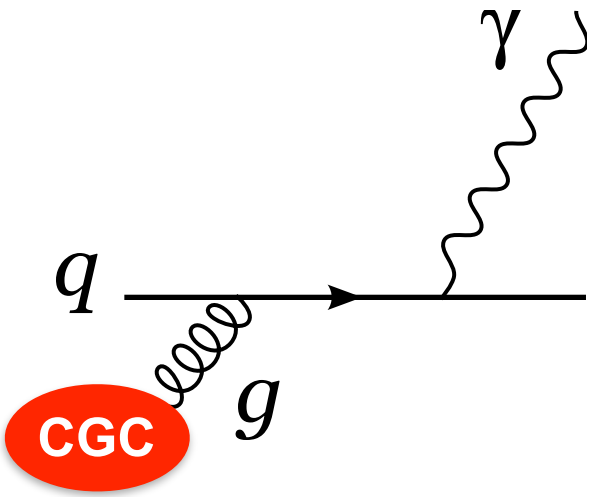


$$\propto \alpha_e \alpha_s \, n_q n_{\bar{q}} (1 + n_g)$$

$$(q\bar{q} \rightarrow g\gamma)$$

Photon Production with CGC

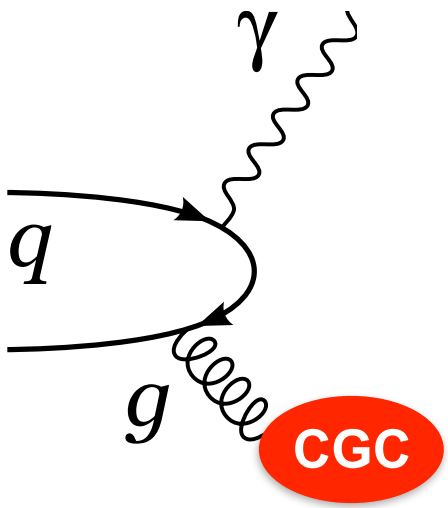
Compton Scattering



$$\propto \alpha_e \alpha_s \, n_q(1-n_q)\alpha_s^{-1}$$

$$\sim \alpha_e n_q(1-n_q)$$

Annihilation

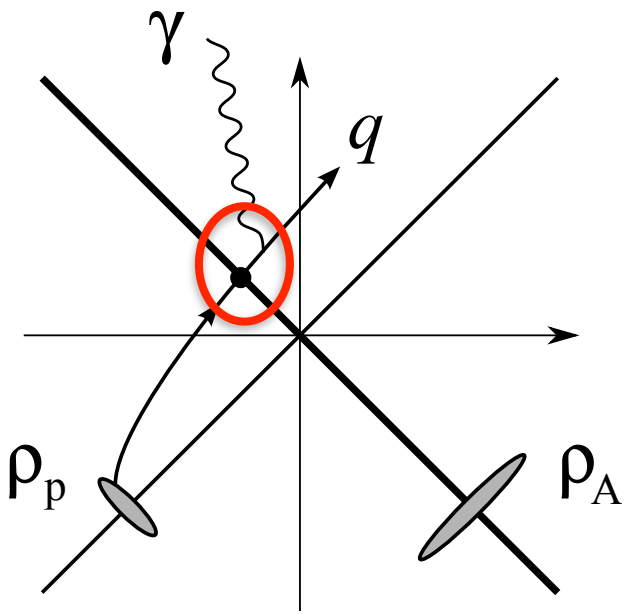


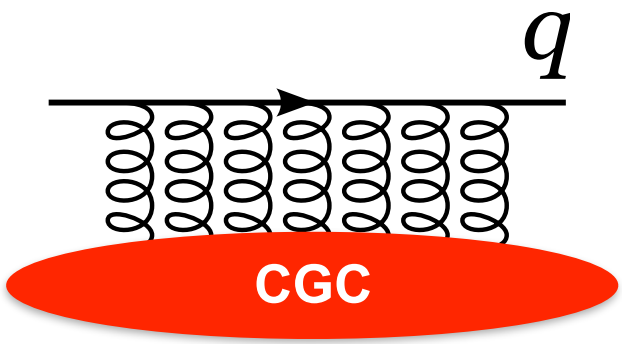
$$\propto \alpha_e \alpha_s \, n_q n_{\bar{q}} \alpha_s^{-1}$$

$$\sim \alpha_e n_q n_{\bar{q}}$$

Photon Production with CGC

Gauge choice: $A \sim \rho_{\mathrm{A}} \sim \delta(x^+)$ **Gelis-Mehtar-Tani (2006)**

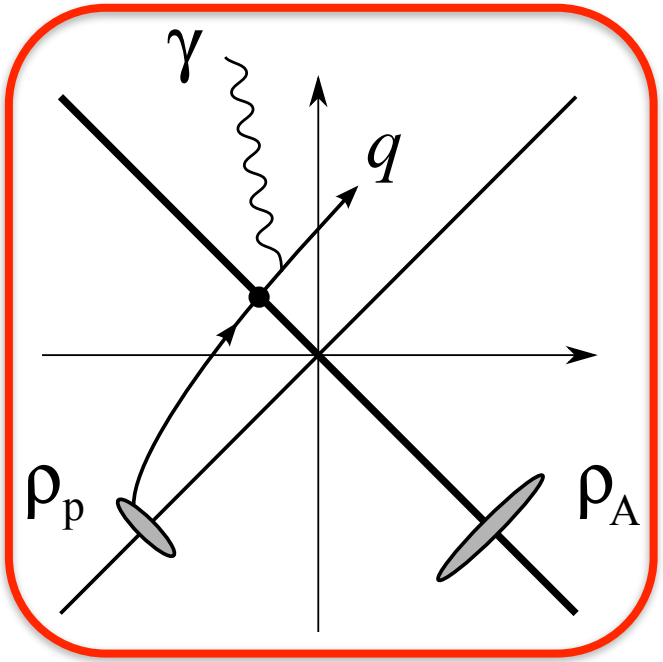




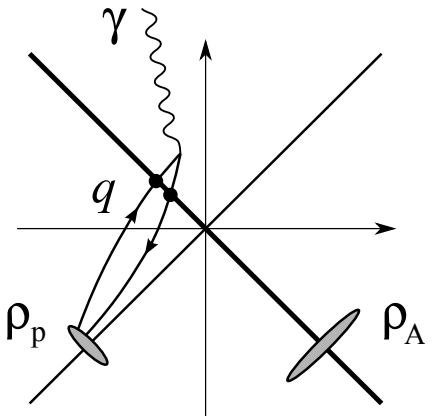
$$U \sim 1 + igA + \frac{1}{2}(igA)^2 + \cdots$$

Leading-order Process

Gelis-Jalilian-Marian (2002)



$$\sim \alpha_e n_q \langle UU^\dagger \rangle$$



$$\sim \alpha_e n_q n_{\bar{q}} \langle UU^\dagger UU^\dagger \rangle$$

Suppressed by quark distribution

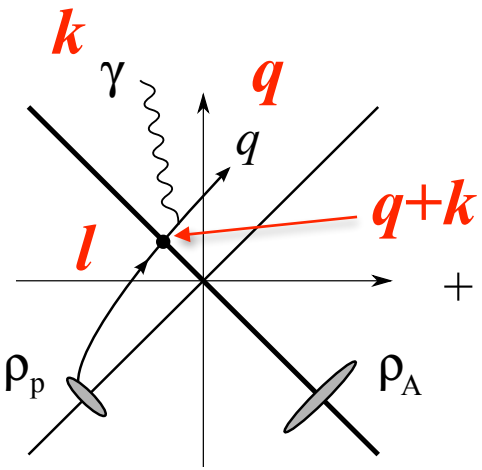
Multiple Scattering with CGC

Leading-order Process

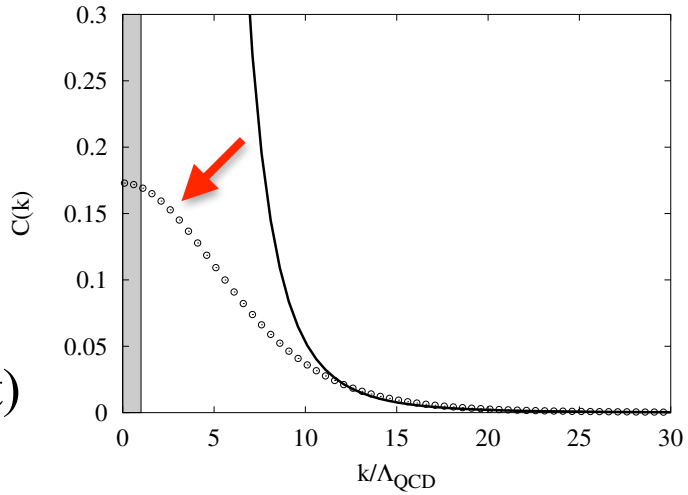
$$\frac{1}{A_\perp}\frac{d\sigma^{q\to q\gamma}}{d^2\boldsymbol{k}_\perp} = \frac{2\alpha_e}{(2\pi)^4\boldsymbol{k}_\perp^2}\int_0^1 dz\frac{1+(1-z)^2}{z}\int d^2\boldsymbol{l}_\perp \frac{\boldsymbol{l}_\perp^2 C(\boldsymbol{l}_\perp)}{(\boldsymbol{l}_\perp-\boldsymbol{k}_\perp/z)^2}$$

$$C(\boldsymbol{l}_\perp)\equiv\int d^2\boldsymbol{x}_\perp e^{i\boldsymbol{l}_\perp\cdot\boldsymbol{x}_\perp}e^{-B_2(\boldsymbol{x}_\perp)} = \int d^2\boldsymbol{x}_\perp e^{i\boldsymbol{l}_\perp\cdot\boldsymbol{x}_\perp}\left\langle U(0)U^\dagger(\boldsymbol{x}_\perp)\right\rangle_\rho$$

$$B_2(\boldsymbol{x}_\perp-\boldsymbol{y}_\perp) \equiv Q_s^2\int d^2\boldsymbol{z}_\perp[G_0(\boldsymbol{x}_\perp-\boldsymbol{z}_\perp)-G_0(\boldsymbol{y}_\perp-\boldsymbol{z}_\perp)]^2$$

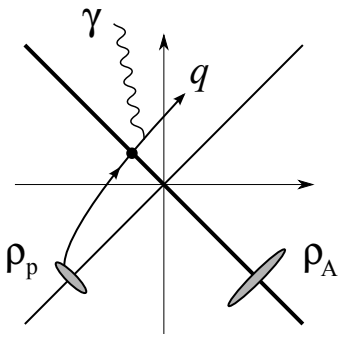


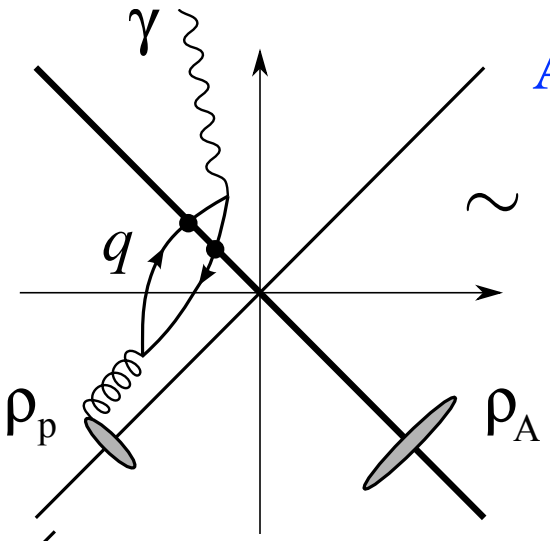
+ crossed diagram
(photon emitted first)



Gelis-Jalilian-Marian (2002)

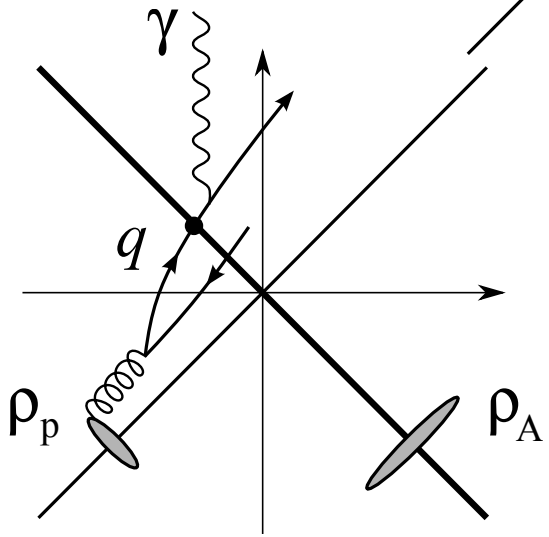
"Higher"-order Processes





Annihilation

$$\sim \alpha_e \langle (g\rho_p)^2 \rangle \langle UU^\dagger UU^\dagger \rangle$$



Bremsstrahlung

$$\sim \alpha_e \delta n_q \langle UU^\dagger \rangle \quad \text{(evolution)}$$

$$\sim \alpha_e \langle (g\rho_p)^2 \rangle \langle UU^\dagger UU^\dagger \rangle$$

"Higher"-order Processes

LO: $\sim \alpha_e n_q \langle UU^\dagger \rangle$

NLO: $\sim \alpha_e \langle (g\rho_p)^2 \rangle \langle UU^\dagger UU^\dagger \rangle$

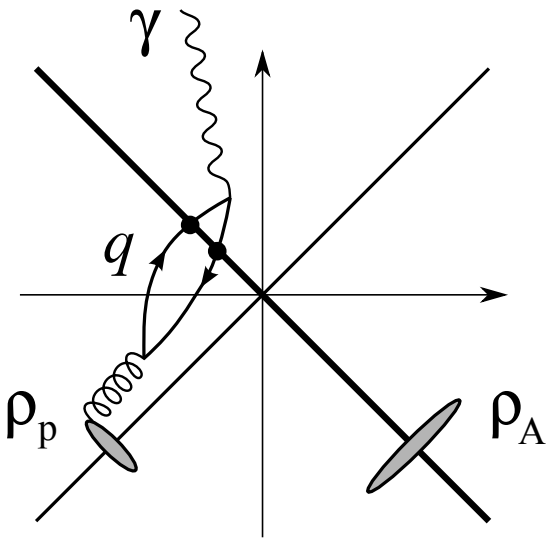
$$(g\rho_p)^2 < g\rho_p \sim n_q$$

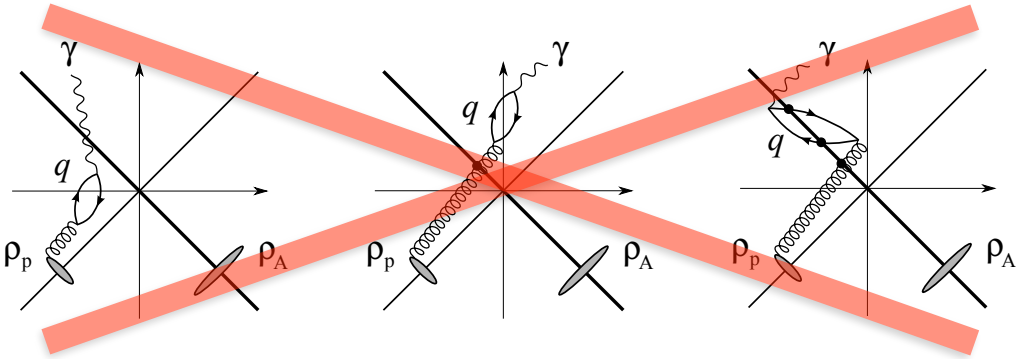
NLO is overwhelming but the pA expansion still works

Systematic calculations feasible
Not small corrections but dominant at high energies
pA photon (hopefully) coming very soon

Annihilation Diagram

Benic-Fukushima (2016)





$$\mathcal{M}_\lambda(\boldsymbol{k}) \equiv \langle \boldsymbol{k}, \lambda | \Omega \rangle = eg \int d^4x\, d^4y\, e^{ik\cdot x}\, \mathrm{Tr}\left[\not{\epsilon}(\boldsymbol{k}, \lambda) S(x,y) \not{A}_{(1)}(y) S(y,x) \right]$$

Known

$$\sim S_F\, \gamma^+ U\, S_F$$

ρ_p + propagator

Annihilation Diagram

Benic-Fukushima (2016)

✔ Ward identity:

$$\mathcal{M}_\lambda(\boldsymbol{k}) = \frac{eg^2}{4\pi^3}\int_0^1 dx \int d^2\boldsymbol{u}_\perp\, d^2\boldsymbol{v}_\perp \int \frac{d^2\boldsymbol{p}_\perp}{(2\pi)^2}\, e^{-i(\boldsymbol{k}_\perp-\boldsymbol{p}_\perp)\cdot[\boldsymbol{v}_\perp+a(x)\boldsymbol{u}_\perp]}$$
$$\times \frac{\rho_p^a(\boldsymbol{p}_\perp)}{p_\perp^2}\,\mathrm{Tr}_c\left[U\left(\boldsymbol{v}_\perp+\frac{\boldsymbol{u}_\perp}{2}\right)T_F^a U^\dagger\left(\boldsymbol{v}_\perp-\frac{\boldsymbol{u}_\perp}{2}\right)\right]$$
$$\times \left[\hat{u}_\lambda p_\perp \Psi_1(\boldsymbol{p}_\perp,\boldsymbol{u}_\perp,x)+p_\lambda\Psi_2(\boldsymbol{p}_\perp,\boldsymbol{u}_\perp,x)\right],$$

Looks complicated but the structure is intuitive

$$\Psi_1(\boldsymbol{p}_\perp,\boldsymbol{u}_\perp,x) \equiv -4ia(x)b(x)p_\perp K_0(m_p(x)u_\perp)mK_1(mu_\perp)$$
$$+4b(x)\hat{\boldsymbol{p}}_\perp\cdot\hat{\boldsymbol{u}}_\perp m_p(x)K_1(m_p(x)u_\perp)mK_1(mu_\perp)$$
$$\Psi_2(\boldsymbol{p}_\perp,\boldsymbol{u}_\perp,x) \equiv mK_1(mu_\perp)m_p(x)K_1(m_p(x)u_\perp)$$
$$+m^2K_0(mu_\perp)K_0(m_p(x)u_\perp)\,.$$

$$a(x)\equiv x-\tfrac{1}{2}$$
$$b(x)\equiv x(1-x)$$
$$m_p^2(x)\equiv m^2+b(x)p_\perp^2$$

Annihilation Diagram

Benic-Fukushima (2016)

$$S(\boldsymbol{y}_\perp, \boldsymbol{z}_\perp, \boldsymbol{y}'_\perp, \boldsymbol{z}'_\perp) \equiv \frac{1}{N_c}\left\langle \mathrm{Tr}_c\left[U(\boldsymbol{y}_\perp)T_F^a U^\dagger(\boldsymbol{z}_\perp)\right]\mathrm{Tr}_c\left[U(\boldsymbol{z}'_\perp)T_F^a U^\dagger(\boldsymbol{y}'_\perp)\right]\right\rangle$$

Master formula **Fukushima-Hidaka arXiv:0704.2806**

$$\left\langle U(\boldsymbol{x}_{1\perp})_{\beta_1\alpha_1} U(\boldsymbol{x}_{2\perp})_{\beta_2\alpha_2} \cdots U(\boldsymbol{x}_{n\perp})_{\beta_n\alpha_n}\right\rangle = \exp[-(H_0+V)]_{\beta_1\cdots\beta_n;\alpha_1\cdots\alpha_n}$$

$$H_0 = Q_{\mathrm{s}}^2 \frac{2N_{\mathrm{c}}}{N_{\mathrm{c}}^2-1}\left(\sum_{k=1}^{n} t_k^a\right)^2 L(0,0)$$

$$V = -Q_{\mathrm{s}}^2 \frac{2N_{\mathrm{c}}}{N_{\mathrm{c}}^2-1}\sum_{i>j} t_i^a\, t_j^a\; \Gamma(\boldsymbol{x}_{i\perp}, \boldsymbol{x}_{j\perp})$$

Annihilation Diagram

Benic-Fukushima (2016)

$$S(\boldsymbol{y}_\perp, \boldsymbol{z}_\perp, \boldsymbol{y}'_\perp, \boldsymbol{z}'_\perp) \equiv \frac{1}{N_c}\left\langle \mathrm{Tr}_c\left[U(\boldsymbol{y}_\perp)T_F^a U^\dagger(\boldsymbol{z}_\perp)\right]\mathrm{Tr}_c\left[U(\boldsymbol{z}'_\perp)T_F^a U^\dagger(\boldsymbol{y}'_\perp)\right]\right\rangle$$

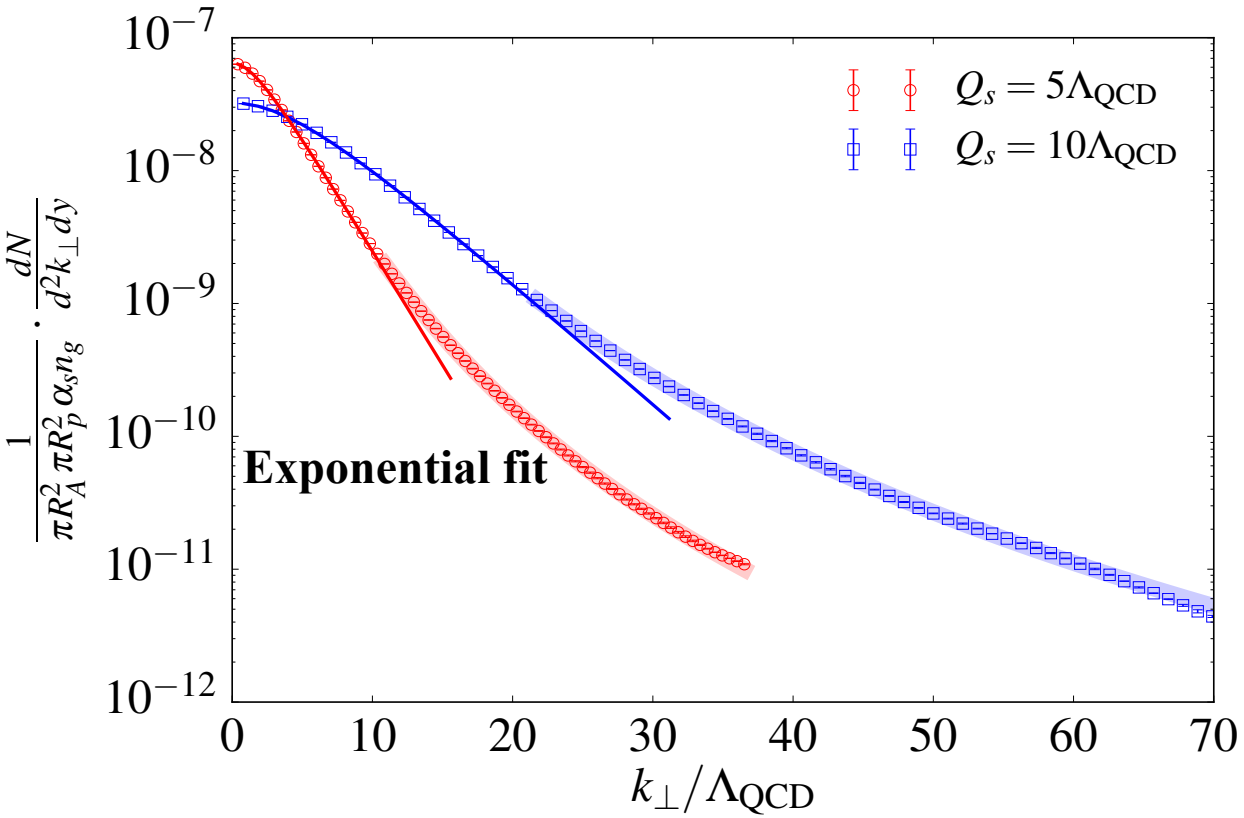
Color average in MV

$$\frac{1}{N_c}\frac{(N_c^2-1)(\beta-\alpha)}{\sqrt{N_c^2(\alpha-\gamma)^2-4(\alpha-\beta)(\beta-\gamma)}} \times \exp\left[-\frac{2\beta+(N_c^2-2)(\alpha+\gamma)}{N_c^2-1}\right] \times \sinh\left[\frac{N_c}{N_c^2-1}\sqrt{N_c^2(\alpha-\gamma)^2-4(\alpha-\beta)(\beta-\gamma)}\right]$$

α, β, γ : combinations of $\dfrac{1}{2\pi}\dfrac{Q_s^2}{\Lambda_{\mathrm{QCD}}^2}\left[1-x_\perp\Lambda_{\mathrm{QCD}}K_1(x_\perp\Lambda_{\mathrm{QCD}})\right]$

Annihilation Diagram

Benic-Fukushima (2016)



8-dim numerical integration (Monte-Carlo)

UV tail behaves numerically like:

$$(k^2 + (1.3Q_s)^2)^{-2.4}$$

Caveat

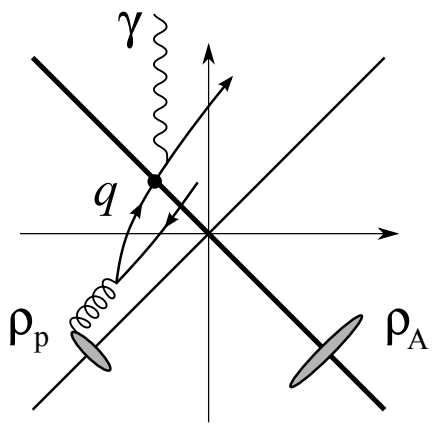
Caveat

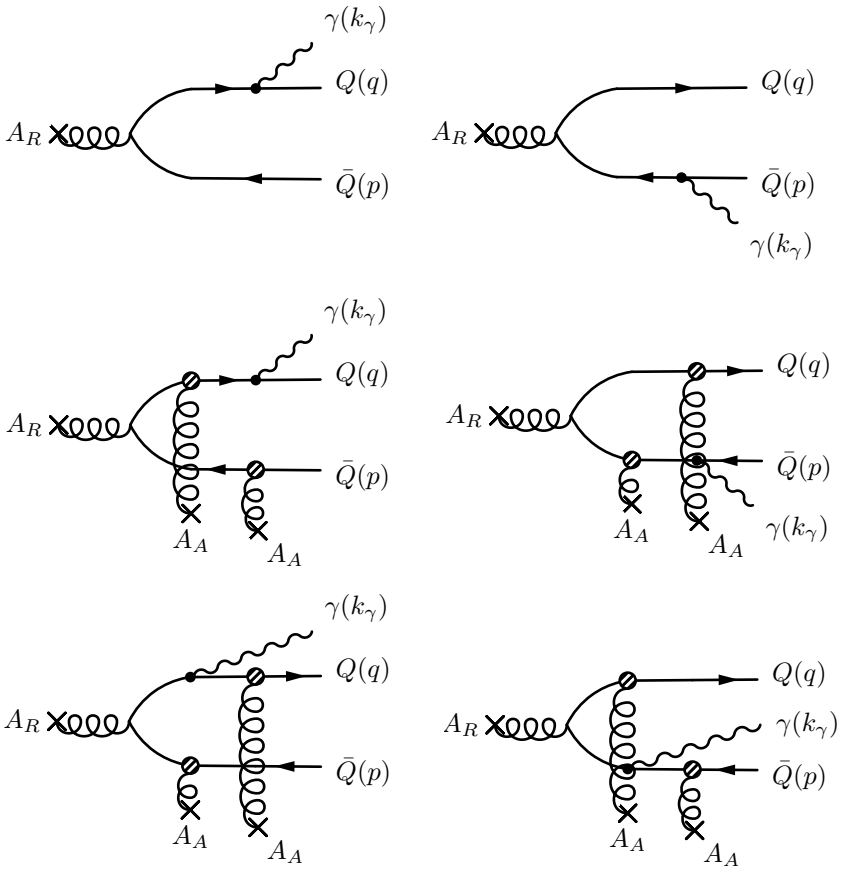
Loops vanish for *u*, *d*, *s* quarks

$$q_u + q_d + q_s = 0$$

Bremsstrahlung Diagram

Benic-Fukushima-Garcia-Montero-Venugopalan (2016)



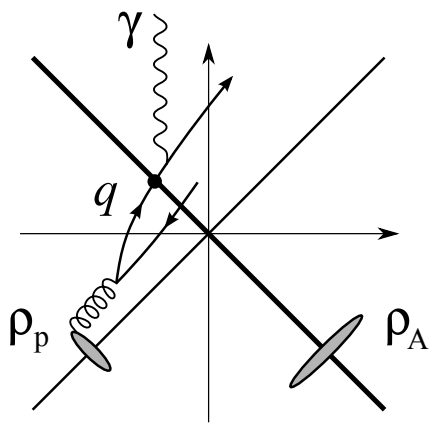


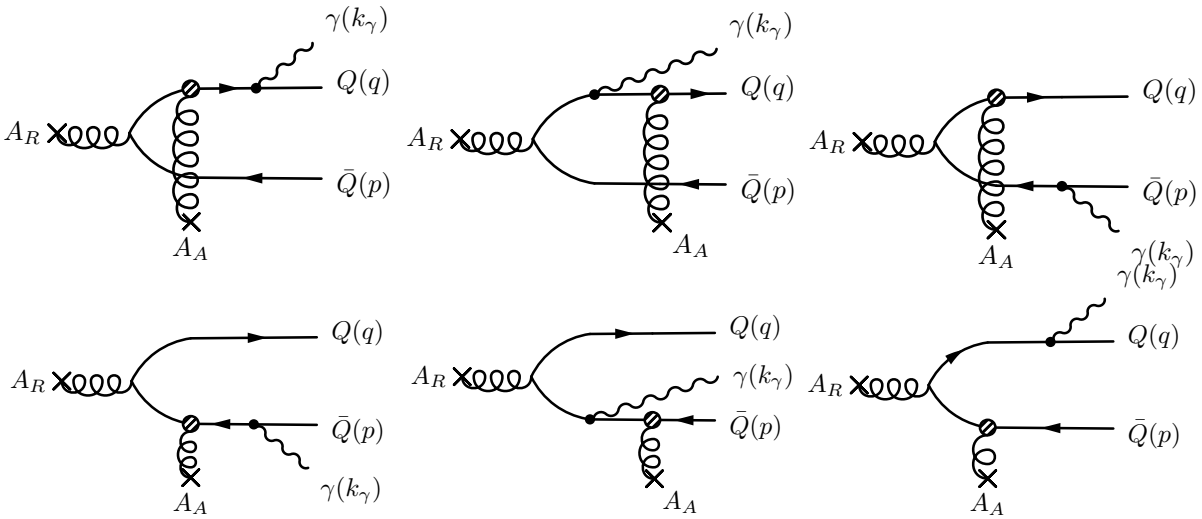
$\sim U_{ad}$

$\sim U t^a U^\dagger$

Bremsstrahlung Diagram

Benic-Fukushima-Garcia-Montero-Venugopalan (2016)

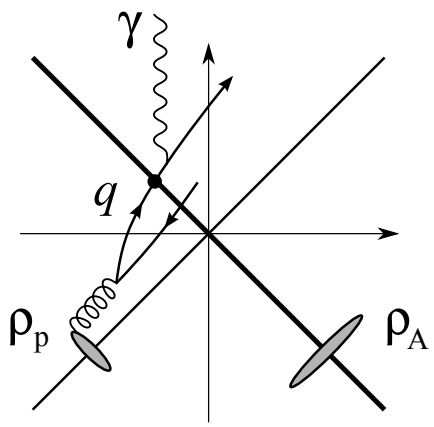


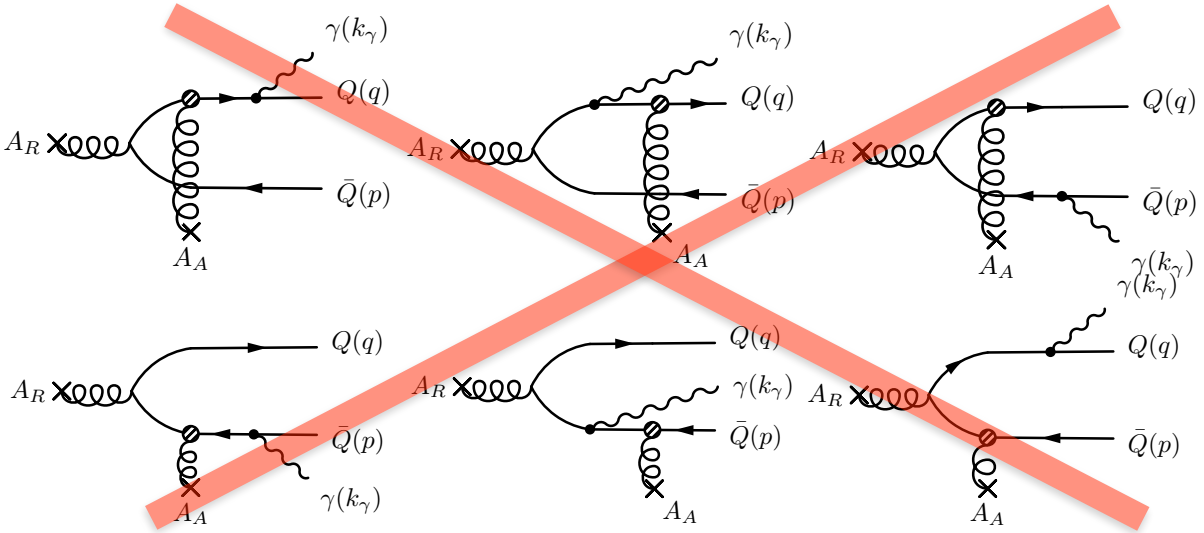


$$\sim U,\ U^\dagger$$

Bremsstrahlung Diagram

Benic-Fukushima-Garcia-Montero-Venugopalan (2016)





$$\sim U,\ U^\dagger$$

Bremsstrahlung Diagram

Benic-Fukushima-Garcia-Montero-Venugopalan (2016)

$$\mathcal{M}^{\mu}(\boldsymbol{p},\boldsymbol{q},\boldsymbol{k}_{\gamma}) = -q_f e g^2 \int_{\boldsymbol{k}_{\perp},\boldsymbol{k}_{1\perp}} \int_{\boldsymbol{x}_{\perp}\boldsymbol{y}_{\perp}} \frac{\rho_p^a(\boldsymbol{k}_{1\perp})}{\boldsymbol{k}_{1\perp}^2} \mathrm{e}^{\mathrm{i}\boldsymbol{k}_{\perp}\cdot\boldsymbol{x}_{\perp}+\mathrm{i}(\boldsymbol{P}_{\perp}-\boldsymbol{k}_{\perp}-\boldsymbol{k}_{1\perp})\cdot\boldsymbol{y}_{\perp}}$$
$$\times\, \bar{u}(\boldsymbol{q})\big\{T_g^{\mu}(\boldsymbol{k}_{1\perp})U(\boldsymbol{x}_{\perp})^{ba}t^b + T_{q\bar{q}}^{\mu}(\boldsymbol{k}_{\perp},\boldsymbol{k}_{1\perp})\tilde{U}(\boldsymbol{x}_{\perp})t^a\tilde{U}^{\dagger}(\boldsymbol{y}_{\perp})\big\}v(\boldsymbol{p})$$

Structure is simple but the full expression is…

Necessary conditions for correctness

- ✔ Gauge invariance (Coulomb/Light-cone)
- ✔ Ward identity: $k_{\gamma\mu}\mathcal{M}^{\mu}(\boldsymbol{p},\boldsymbol{q},\boldsymbol{k}_{\gamma}) = 0$ satisfied separately for T_g and T_{qq}
- ✔ Leading-twist (perturbative)
- ✔ Soft-photon limit (Low-Burnett-Kroll theorem)

Bremsstrahlung Diagram

Parametric form of the final expression

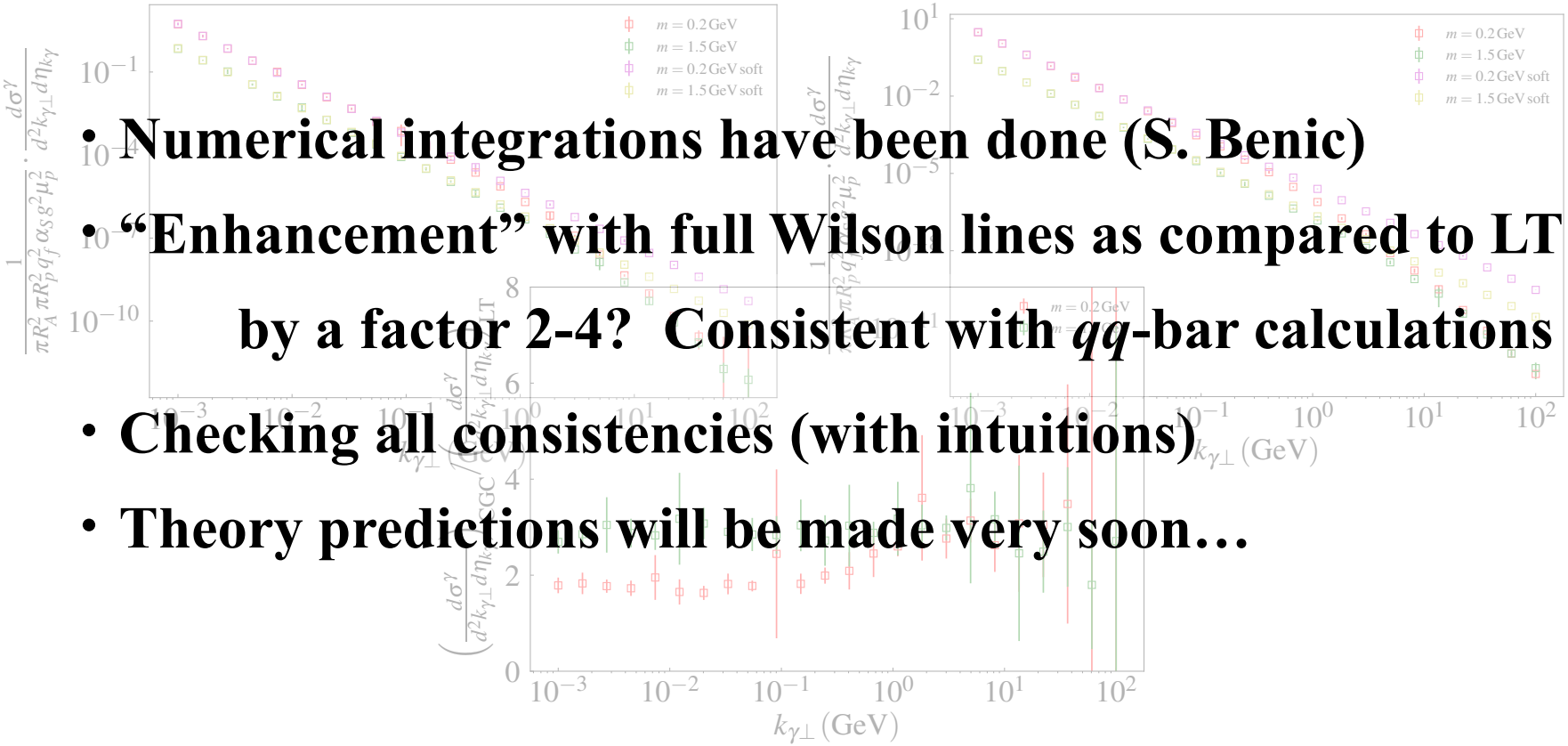
$$\frac{\mathrm{d}\sigma^{\gamma}}{\mathrm{d}^2\boldsymbol{k}_{\gamma\perp}\mathrm{d}\eta_{k_\gamma}} = \frac{\alpha_e\alpha_S^2 q_f^2}{16\pi^4 C_F}\int_0^\infty \frac{\mathrm{d}q^+}{q^+}\frac{\mathrm{d}p^+}{p^+}\int_{\boldsymbol{k}_{1\perp}\boldsymbol{k}_{2\perp}\boldsymbol{q}_\perp\boldsymbol{p}_\perp}(2\pi)^2\delta^{(2)}(\boldsymbol{P}_\perp-\boldsymbol{k}_{1\perp}-\boldsymbol{k}_{2\perp})\,\frac{\varphi_p(\boldsymbol{k}_{1\perp})}{\boldsymbol{k}_{1\perp}^2\boldsymbol{k}_{2\perp}^2}$$
$$\times\left\{\tau_{g,g}(\boldsymbol{k}_{1\perp};\boldsymbol{k}_{1\perp})\phi_A^{g,g}(\boldsymbol{k}_{2\perp})+\int_{\boldsymbol{k}_\perp}2\mathrm{Re}\left[\tau_{g,q\bar{q}}(\boldsymbol{k}_{1\perp};\boldsymbol{k}_\perp,\boldsymbol{k}_{1\perp})\right]\phi_A^{q\bar{q},g}(\boldsymbol{k}_\perp,\boldsymbol{k}_{2\perp}-\boldsymbol{k}_\perp;\boldsymbol{k}_{2\perp})\right.$$
$$\left.+\int_{\boldsymbol{k}_\perp\boldsymbol{k}'_\perp}\tau_{q\bar{q},q\bar{q}}(\boldsymbol{k}_\perp,\boldsymbol{k}_{1\perp};\boldsymbol{k}'_\perp,\boldsymbol{k}_{1\perp})\,\phi_A^{q\bar{q},q\bar{q}}(\boldsymbol{k}_\perp,\boldsymbol{k}_{2\perp}-\boldsymbol{k}_\perp;\boldsymbol{k}'_\perp,\boldsymbol{k}_{2\perp}-\boldsymbol{k}'_\perp)\right\}.$$

Leading twist → k_t-factorized form

$$\frac{\mathrm{d}\sigma^{\gamma}}{\mathrm{d}^6K_\perp\mathrm{d}^3\eta_K} = \frac{\alpha_e\alpha_S^2 q_f^2}{256\pi^8 N_c(N_c^2-1)}\int_{\boldsymbol{k}_{1\perp}\boldsymbol{k}_{2\perp}}(2\pi)^2\delta^{(2)}(\boldsymbol{P}_\perp-\boldsymbol{k}_{1\perp}-\boldsymbol{k}_{2\perp})\,\frac{\varphi_p(Y_p,\boldsymbol{k}_{1\perp})\varphi_A(Y_A,\boldsymbol{k}_{2\perp})}{\boldsymbol{k}_{1\perp}^2\boldsymbol{k}_{2\perp}^2}\,\Theta(\boldsymbol{k}_{1\perp},\boldsymbol{k}_{2\perp})$$

Bremsstrahlung Diagram

Benic-Fukushima-Garcia-Montero-Venugopalan (2016)

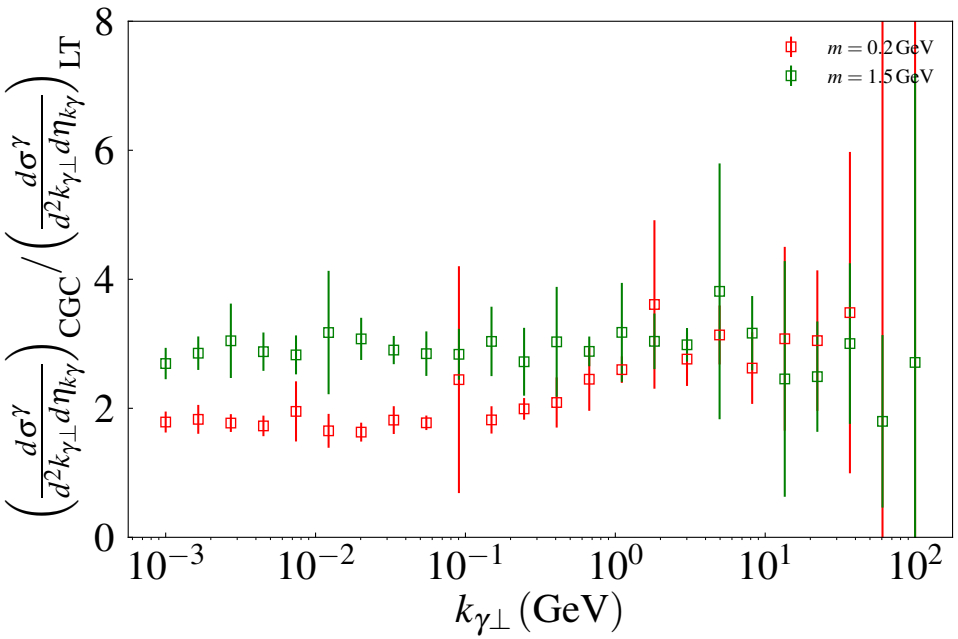


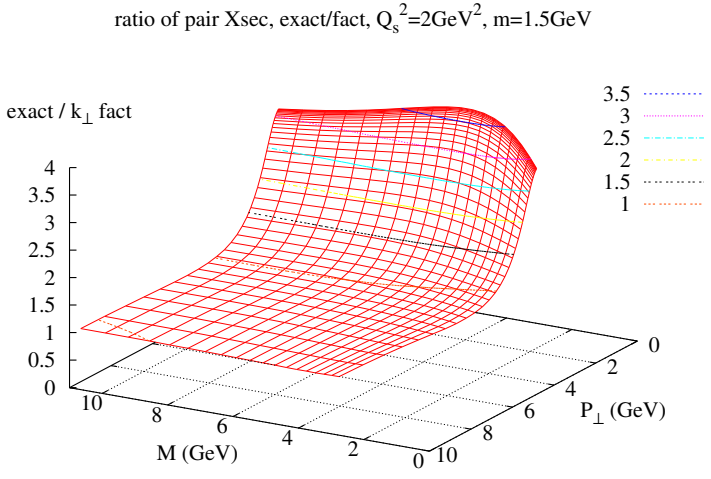
- **Numerical integrations have been done (S. Benic)**
- **"Enhancement" with full Wilson lines as compared to LT by a factor 2-4? Consistent with *qq*-bar calculations**
- **Checking all consistencies (with intuitions)**
- **Theory predictions will be made very soon…**

Bremsstrahlung Diagram

Benic-Fukushima-Garcia-Montero-Venugopalan (2016)

Preliminary





Fujii-Gelis-Venugopalan (2006)

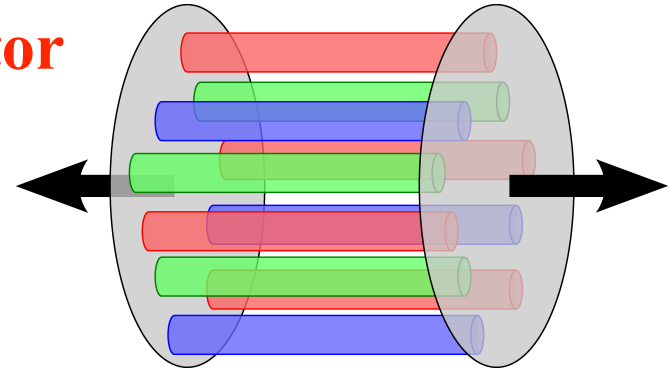
Quarks in AA

Analytically calculable up to $\tau = 0^+$

Initial condition for the gluon sector

$$A_{i(0)} = \alpha_i^{(1)} + \alpha_i^{(2)} \ , \qquad A_{\eta(0)} = 0$$

$$E^i_{(0)} = 0 \ , \qquad E^\eta_{(0)} = ig\left[\alpha_i^{(1)}, \alpha_i^{(2)}\right]$$



Kovner-McLerran-Weigert (1995)

What do we know about quarks on CGC?

Initial condition for the quark sector
How μ_5 distributes (anomalous hydro)?

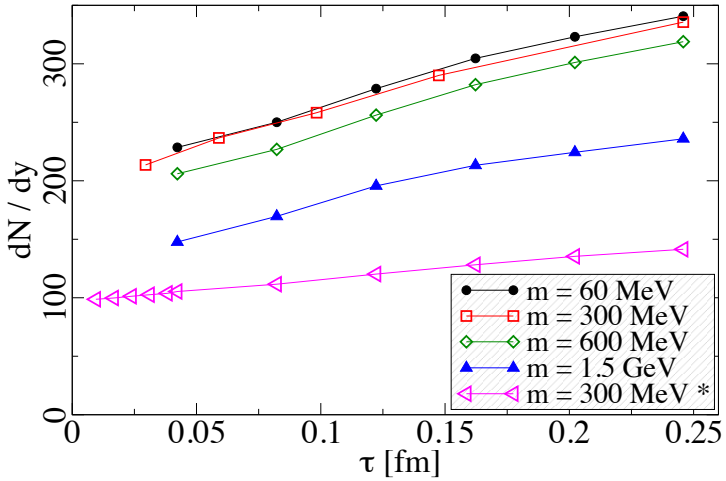
Quarks in AA

Gelis-Kajantie-Lappi (2005)

$$M_\tau(p,q) \equiv \int \frac{\tau \mathrm{d}z \mathrm{d}^2\mathbf{x}_T}{\sqrt{\tau^2+z^2}} \phi^\dagger_{\mathbf{p}}(\tau,\mathbf{x}) \gamma^0\gamma^\tau \psi_{\mathbf{q}}(\tau,\mathbf{x})$$

Amplitude from *anti-particles* to *particles*

$$\frac{dN}{dy} = \int \frac{\mathrm{d}y_p \mathrm{d}^2\mathbf{p}_T}{2\,(2\pi)^3} \frac{\mathrm{d}y_q \mathrm{d}^2\mathbf{q}_T}{2\,(2\pi)^3} \delta(y-y_p)\,|M_\tau(p,q)|^2$$



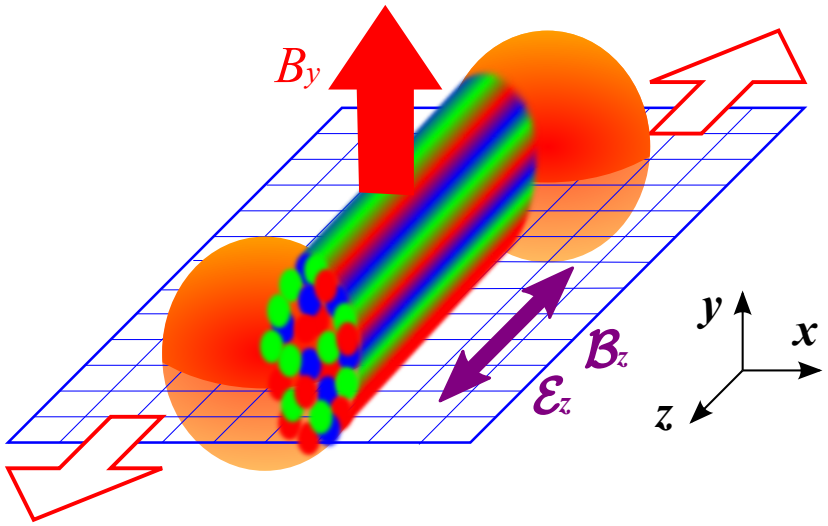
$$\psi_{\mathbf{q}}(t \to -\infty, \mathbf{x}) = e^{iq\cdot x} v(q)$$

$$\phi_{\mathbf{p}}(x) = e^{-ip\cdot x} u(p)$$

Quarks in AA

A substantial portion of particle production at $\tau = 0^+$?

If this is true, and if the glasma is true (color fluxtubes), chirality fluctuations (local parity violation) at $\tau = 0^+$?

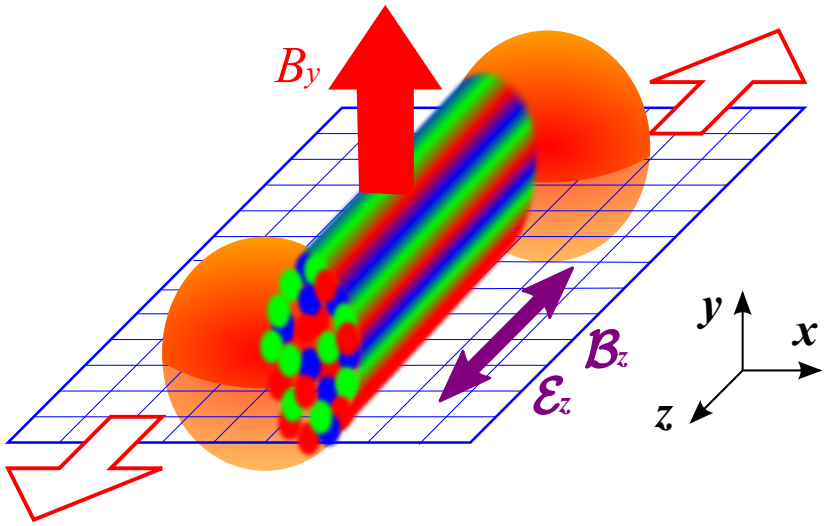


Fukushima-Kharzeev-Warringa (2009)

Quarks in AA

A substantial portion of particle production at $\tau = 0^+$?

If this is true, and if the glasma is true (color fluxtubes), chirality fluctuations (local parity violation) at $\tau = 0^+$?



Fukushima-Kharzeev-Warringa (2009)

The answer is negative

$$\text{Chirality} \sim \sqrt{\tau} \text{ at most}$$

Fukushima-Tanji (coming soon)

Quarks in AA

Gelis-Tanji (2015)

Anti-particle mode functions

$$\widetilde{\psi}^{-}_{\boldsymbol{k}_\perp \nu s a}(\tau \to 0^+) = -\frac{e^{i\pi/4}}{\sqrt{M_{\boldsymbol{k}}}} \int \frac{d^2\boldsymbol{p}_\perp}{(2\pi)^2} \frac{e^{i\boldsymbol{p}_\perp\cdot\boldsymbol{x}_\perp}}{M_{\boldsymbol{p}}}$$

$$\times \left[e^{\pi\nu/2} \left(\frac{M_{\boldsymbol{p}}^2\tau}{2M_{\boldsymbol{k}}}\right)^{i\nu} \Gamma(-i\nu+\tfrac{1}{2}) U_2^\dagger(\boldsymbol{x}_\perp) U_2(\boldsymbol{p}_\perp+\boldsymbol{k}_\perp)\gamma^+ \right.$$

$$\left. + e^{-\pi\nu/2} \left(\frac{M_{\boldsymbol{p}}^2\tau}{2M_{\boldsymbol{k}}}\right)^{-i\nu} \Gamma(i\nu+\tfrac{1}{2}) U_1^\dagger(\boldsymbol{x}_\perp) U_1(\boldsymbol{p}_\perp+\boldsymbol{k}_\perp)\gamma^- \right]$$

$$\times (p^i\gamma^i + m) v_s(\boldsymbol{k}_\perp, y_k = 0)$$

Quarks in AA

Gelis-Tanji (2015)

Anti-particle mode functions

$$\widetilde{\psi}^{-}_{\boldsymbol{k}_\perp \nu s a}(\tau \to 0^+) = -\frac{e^{i\pi/4}}{\sqrt{M_{\boldsymbol{k}}}} \int \frac{d^2\boldsymbol{p}_\perp}{(2\pi)^2} \frac{e^{i\boldsymbol{p}_\perp\cdot\boldsymbol{x}_\perp}}{M_{\boldsymbol{p}}}$$

$$\times \left[e^{\pi\nu/2} \left(\frac{M_{\boldsymbol{p}}^2\tau}{2M_{\boldsymbol{k}}}\right)^{i\nu} \Gamma(-i\nu+\tfrac{1}{2}) U_2^\dagger(\boldsymbol{x}_\perp) U_2(\boldsymbol{p}_\perp+\boldsymbol{k}_\perp)\gamma^+ \right.$$

$$\left. + e^{-\pi\nu/2} \left(\frac{M_{\boldsymbol{p}}^2\tau}{2M_{\boldsymbol{k}}}\right)^{-i\nu} \Gamma(i\nu+\tfrac{1}{2}) U_1^\dagger(\boldsymbol{x}_\perp) U_1(\boldsymbol{p}_\perp+\boldsymbol{k}_\perp)\gamma^- \right]$$

$$\times (p^i\gamma^i + m) v_s(\boldsymbol{k}_\perp, y_k = 0)$$

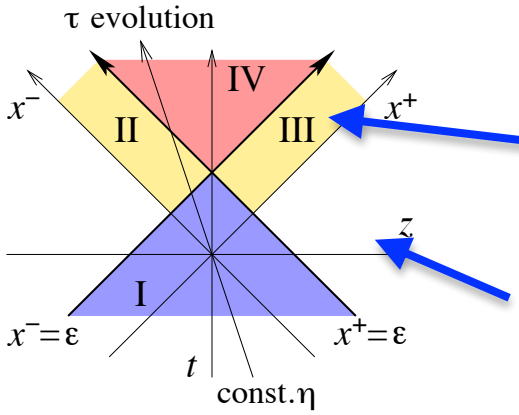
Quarks in AA

$$\widetilde{\psi}^{-}_{\boldsymbol{k}_\perp \nu s a}(\tau \to 0^+) = -\frac{e^{i\pi/4}}{\sqrt{M_{\boldsymbol{k}}}} \int \frac{d^2\boldsymbol{p}_\perp}{(2\pi)^2} \frac{e^{i\boldsymbol{p}_\perp \cdot \boldsymbol{x}_\perp}}{M_{\boldsymbol{p}}}$$

$$\times \left[e^{\pi\nu/2} \left(\frac{M_{\boldsymbol{p}}^2 \tau}{2M_{\boldsymbol{k}}} \right)^{i\nu} \Gamma(-i\nu + \tfrac{1}{2}) U_2^\dagger(\boldsymbol{x}_\perp) U_2(\boldsymbol{p}_\perp + \boldsymbol{k}_\perp) \gamma^+ \right.$$

$$\left. + e^{-\pi\nu/2} \left(\frac{M_{\boldsymbol{p}}^2 \tau}{2M_{\boldsymbol{k}}} \right)^{-i\nu} \Gamma(i\nu + \tfrac{1}{2}) U_1^\dagger(\boldsymbol{x}_\perp) U_1(\boldsymbol{p}_\perp + \boldsymbol{k}_\perp) \gamma^- \right]$$

$$\times (p^i \gamma^i + m) v_s(\boldsymbol{k}_\perp, y_k = 0)$$



Eikonal *approx* → Color rotation
canceled from LC to FS

Pure-gauge → Gauge rotation (*full*)

Quarks in AA

Expectation values

$$\phi_{\boldsymbol{p}}^{(1)} = e^{-\frac{\pi\nu}{2}} \left(\frac{M_{\boldsymbol{p}}^2\tau}{2M_{\boldsymbol{k}}}\right)^{-i\nu} \Gamma(i\nu+\tfrac{1}{2}) U_1^\dagger(\boldsymbol{x}_\perp)\widetilde{U}_1(\boldsymbol{p}_\perp+\boldsymbol{k}_\perp)$$

$$\phi_{\boldsymbol{p}}^{(2)} = e^{\frac{\pi\nu}{2}} \left(\frac{M_{\boldsymbol{p}}^2\tau}{2M_{\boldsymbol{k}}}\right)^{i\nu} \Gamma(-i\nu+\tfrac{1}{2}) U_2^\dagger(\boldsymbol{x}_\perp)\widetilde{U}_2(\boldsymbol{p}_\perp+\boldsymbol{k}_\perp)$$

$$\langle 0|\overline{\widehat{\Psi}}(x) M \widehat{\Psi}(x)|0\rangle$$

$$= \frac{1}{2(2\pi)^2}\int d\nu \int_{\boldsymbol{k}_\perp} \frac{1}{M_{\boldsymbol{k}}} \int_{\boldsymbol{p}_\perp} \frac{1}{M_{\boldsymbol{p}}} \int_{\boldsymbol{q}_\perp} \frac{1}{M_{\boldsymbol{q}}} e^{-i(\boldsymbol{p}_\perp-\boldsymbol{q}_\perp)\cdot\boldsymbol{x}_\perp}$$

$$\times \mathrm{tr}\left[(q^i\gamma^i+m)(M_{\boldsymbol{k}}\gamma^0 - k^j\gamma^j - m)(p^l\gamma^l+m)\left(\phi_{\boldsymbol{p}}^{(2)\,\dagger}\gamma^+ + \phi_{\boldsymbol{p}}^{(1)\,\dagger}\gamma^-\right) M \left(\phi_{\boldsymbol{q}}^{(2)}\gamma^+ + \phi_{\boldsymbol{q}}^{(1)}\gamma^-\right)\right]$$

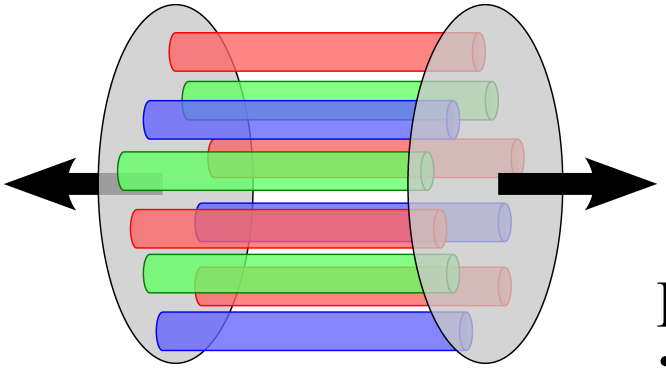
Easily shown:

Chirality / Longitudinal Current → Zero for any U_1, U_2

Transverse Currents → Non-zero for non-trivial U_1, U_2

Momentum kicks only on the transverse plane

Quarks in AA



Quarks at $\tau = 0^+$ do not feel any glasma fields at all…

Eikonal approximation is insensitive to the longitudinal fields

Eikonal approximation is "exact" in the thin pancake limit and in the $\tau = 0^+$ limit…

Transverse momentum dependent terms (higher twists) contribute to the chirality that grows as $\sim \sqrt{\tau}$

Summary

Photons in *pA* at high energies

- LO / NLO-Annihilation / NLO-Bremsstrahlung
- Numerical calculations partially done:
  CGC affects LO in IR
  CGC enhances NLO-Bremsstrahlung (**dominant**)
- Full predictions are coming very soon

Quarks in *AA* at small proper time

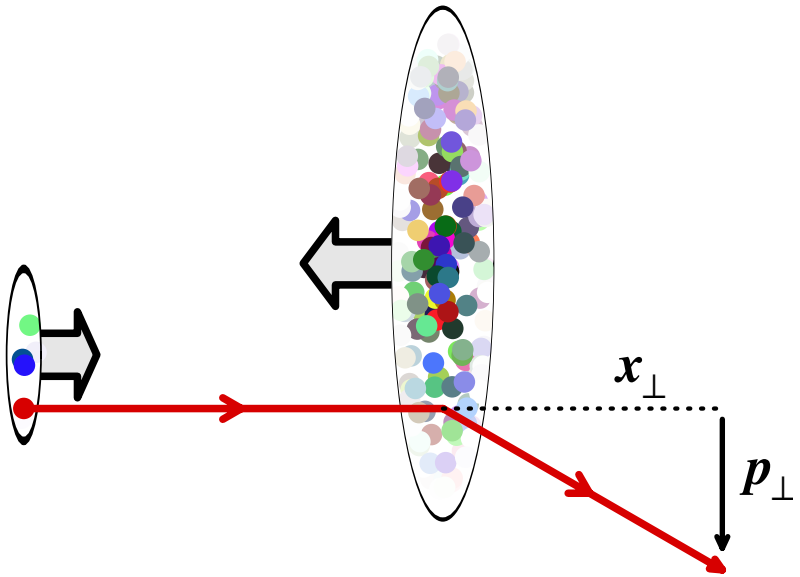
- Particle production not well-defined (unreliable)
- **Chirality production from higher twist effects at finite time** (vanishing at zero proper time)
- Fluctuations (current/chirality) still calculable (*B* dep?)

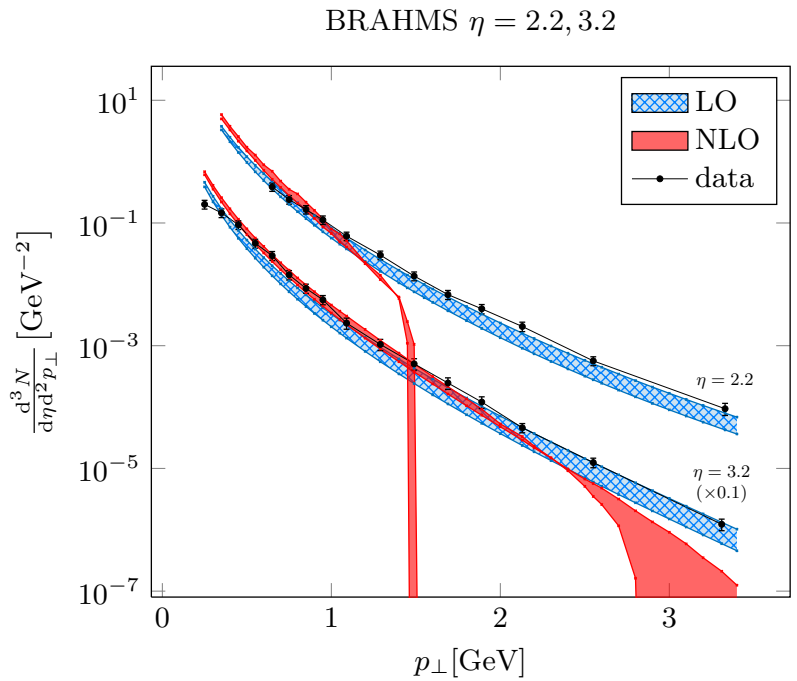
Particle production in pA collisions beyond leading order

Edmond Iancu

IPhT Saclay & CNRS

w/ A.H. Mueller and D.N. Triantafyllopoulos, arXiv:1608.05293



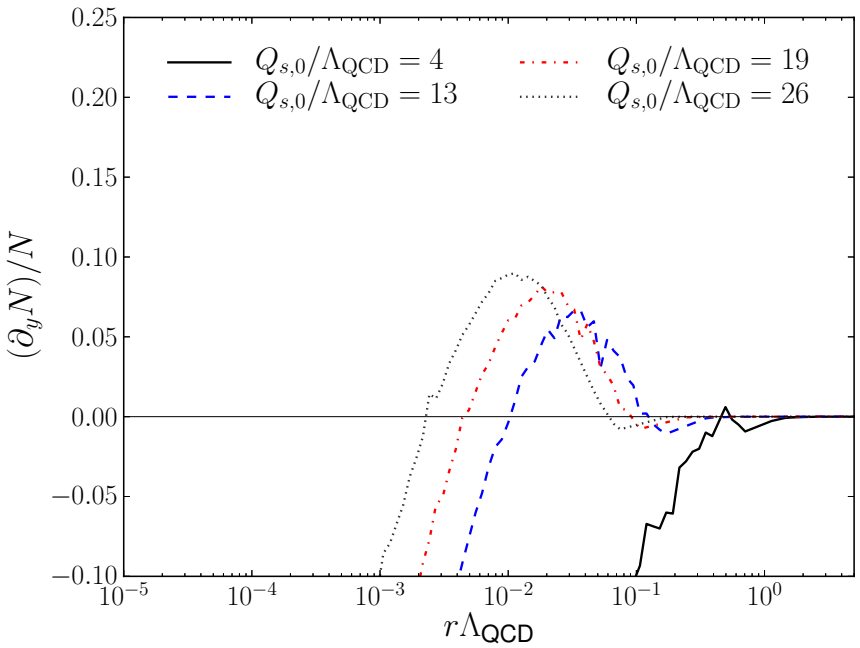


Introduction

- Particle production in pp and pA collisions at forward rapidities explores the physics of high gluon densities at small-x
  - non-linear phenomena: gluon saturation, multiple scattering
  - resummations based on the eikonal approximation (Wilson lines)
  - non-linear evolution equations: BK, B-JIMWLK
- Effective theory derived in pQCD: Color Glass Condensate
- The CGC formalism is now being promoted to NLO
  - NLO versions for the BK and B-JIMWLK equations
    (Balitsky and Chirilli, 2008, 2013; Kovner, Lublinsky, and Mulian, 2013)
  - NLO impact factor for particle production in pA collisions
    (Chirilli, Xiao, and Yuan, 2012; Mueller and Munier, 2012)
- But the strict NLO approximations turned out to be problematic

NLO BK evolution

- "Negative growth" of the dipole scattering amplitude



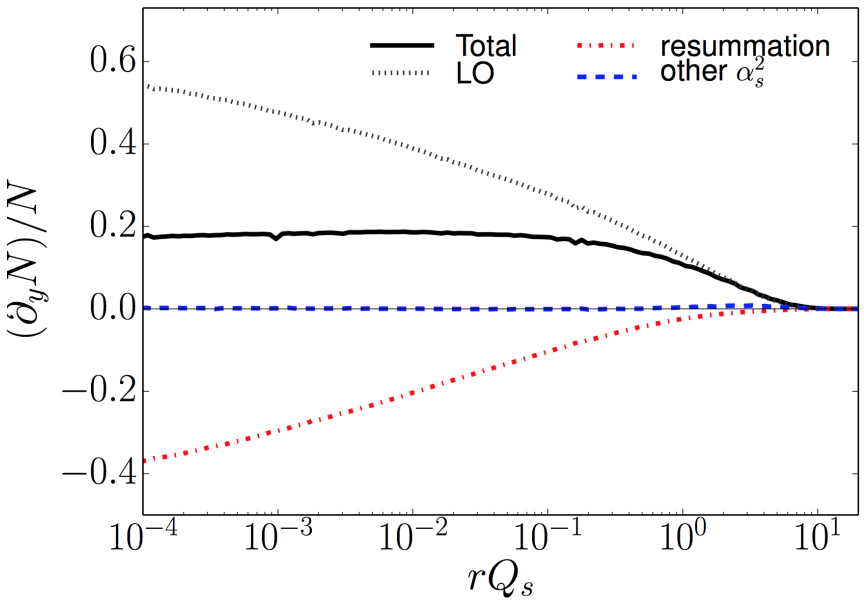
Lappi, Mäntysaari, arXiv:1502.02400

- Not really a surprise
  - similar problems for NLO BFKL
  - large transverse logarithms
  - collinear resummations
  - Mellin representation

(Salam, Ciafaloni, Colferai, Stasto, 98-03; Altarelli, Ball, Forte, 00-03)

NLO BK evolution

- "Negative growth" of the dipole scattering amplitude



Lappi, Mäntysaari, arXiv:1601.06598

- Not really a surprise
  - similar problems for NLO BFKL
  - large transverse logarithms
  - collinear resummations
  - Mellin representation

(Salam, Ciafaloni, Colferai, Stasto, 98-03; Altarelli, Ball, Forte, 00-03)

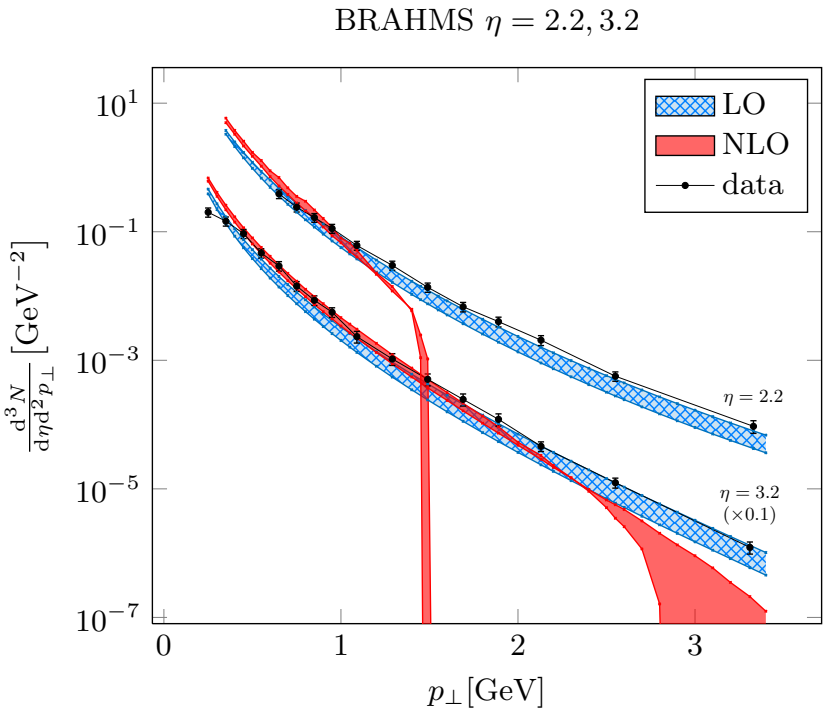
- Collinear improvement for NLO BK (transverse coordinates)

  (E.I., J. Madrigal, A. Mueller, G. Soyez, and D. Triantafyllopoulos, 2015)

- Evolution becomes stable with promising phenomenology
  - excellents fits to DIS *(Iancu et al, 2015; Albacete, 2015)*

Particle production in d+Au collisions (RHIC)

- Very good agreement at low $p_\perp$ ☺ ... but negative at larger $p_\perp$ ☹

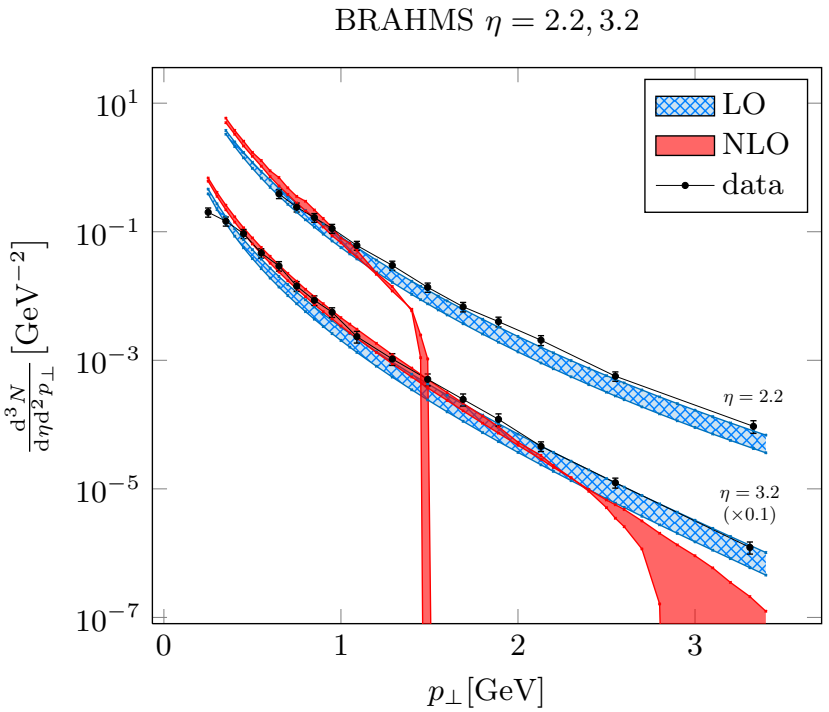


Stasto, Xiao, and Zaslavsky, arXiv:1307.4057

- Is this a real problem ?
  - "small-x resummations do not apply at large $p_\perp$"
  - but $p_\perp \sim Q_s$ is not that large !
- Likely related to the rapidity subtraction in NLO impact factor

Particle production in d+Au collisions (RHIC)

- Very good agreement at low $p_\perp$ ☺ ... but negative at larger $p_\perp$ ☹



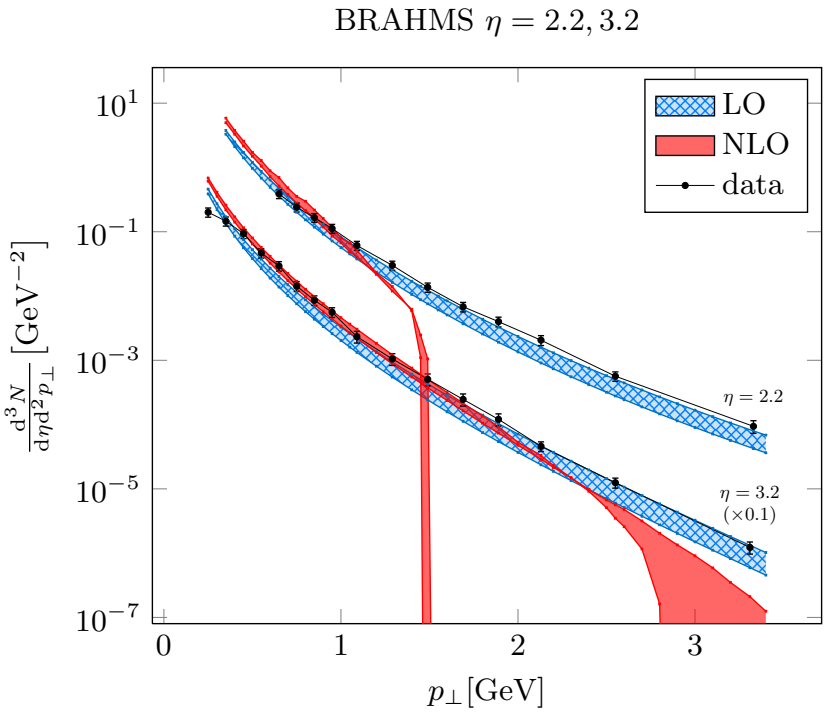
Stasto, Xiao, and Zaslavsky, arXiv:1307.4057

- Is this a real problem ?
  - "small-x resummations do not apply at large $p_\perp$"
  - but $p_\perp \sim Q_s$ is not that large !
- Likely related to the rapidity subtraction in NLO impact factor

- Various proposals which alleviate the problem (pushed to higher $p_\perp$)
  - *Kang, Vitev, and Xing, arXiv:1403.5221*
  - *Altinoluk, Armesto, Beuf, Kovner, and Lublinsky, arXiv:1411.2869*
  - *Ducloué, Lappi, and Zhu, arXiv:1604.00225*

Particle production in d+Au collisions (RHIC)

- Very good agreement at low $p_\perp$ ☺ ... but negative at larger $p_\perp$ ☹



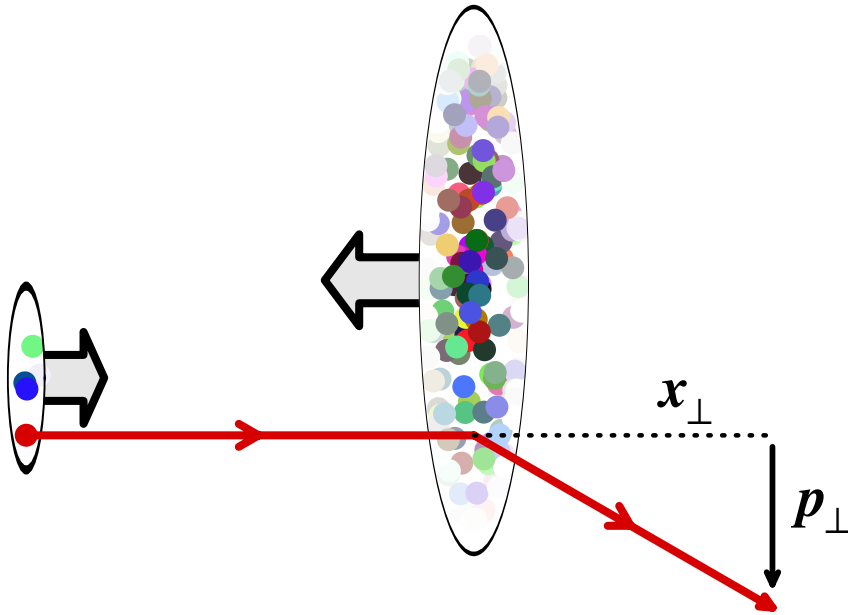
- Is this a real problem ?
  - "small-x resummations do not apply at large $p_\perp$"
  - but $p_\perp \sim Q_s$ is not that large !
- Likely related to the rapidity subtraction in NLO impact factor

Stasto, Xiao, and Zaslavsky, arXiv:1307.4057

- A reorganization of the perturbative expansion which avoids the rapidity subtraction *(E.I., A. Mueller and D. Triantafyllopoulos, 2016)*
- Sensible numerical results (positive cross-section)... and a new puzzle *(Ducloué, Lappi, and Zhu, arXiv:1703.04962)*

Forward quark production in pA collisions

- A quark initially collinear with the proton acquires a transverse momentum $p_\perp$ via multiple scattering off the saturated gluons



$$x_p \equiv \frac{p^+}{q^+} = \frac{p_\perp}{\sqrt{s}}\,\mathrm{e}^{\eta}$$

$$X_g \equiv \frac{p^-}{P^-} = \frac{p_\perp}{\sqrt{s}}\,\mathrm{e}^{-\eta}$$

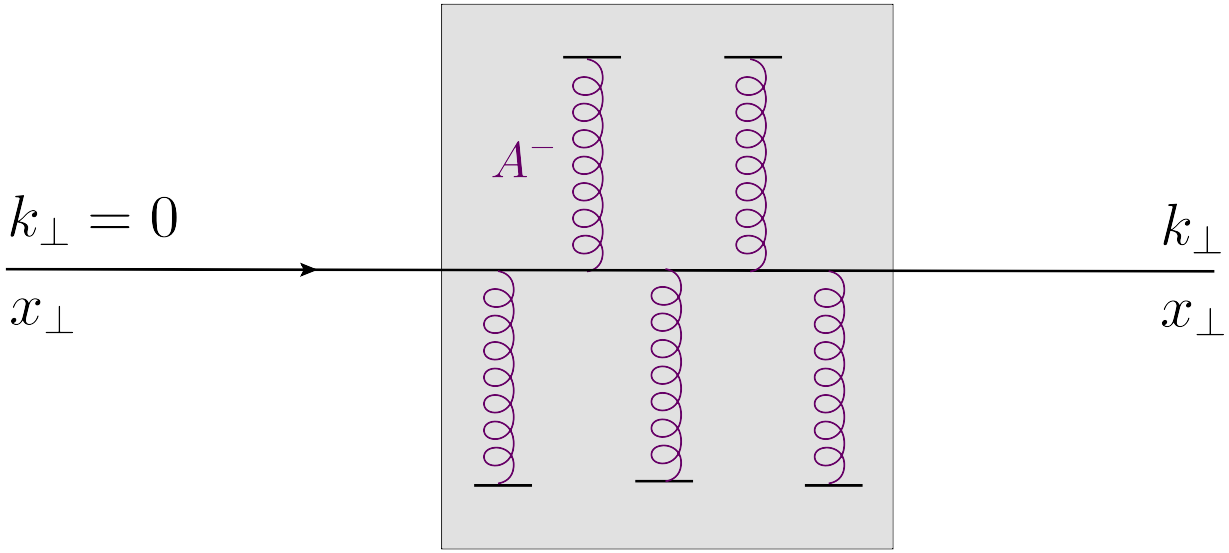
$X_g \ll x_p$ when $\eta > 0$

  - η : quark rapidity in the COM frame
  - x_p : longitudinal fraction of the quark in the proton
  - X_g : longitudinal fraction of the gluon in the target

- Gluons in the nucleus have a typical transverse momentum $k_\perp \sim Q_s(X_g)$

Multiple scattering

- Eikonal approximation $\Longrightarrow$ the transverse coordinate representation

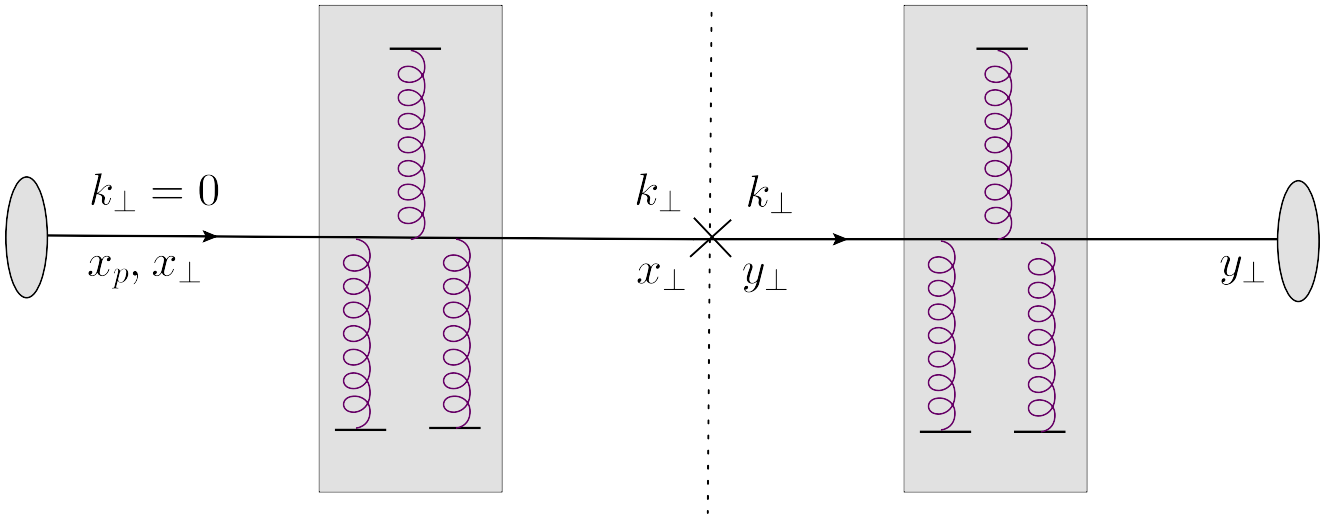


Amplitude: $$\mathcal{M}_{ij}(\boldsymbol{k}_\perp) \equiv \int \mathrm{d}^2\boldsymbol{x}_\perp \, \mathrm{e}^{-i\boldsymbol{x}_\perp\cdot\boldsymbol{k}_\perp} \, V_{ij}(\boldsymbol{x}_\perp)$$

Wilson line: $$V(\boldsymbol{x}_\perp) = \mathrm{P}\exp\left\{\mathrm{i}g\int \mathrm{d}x^+ A_a^-(x^+,\boldsymbol{x}_\perp)t^a\right\}$$

- A_a^- : color field representing small-x gluons in the nucleus

Multiple scattering



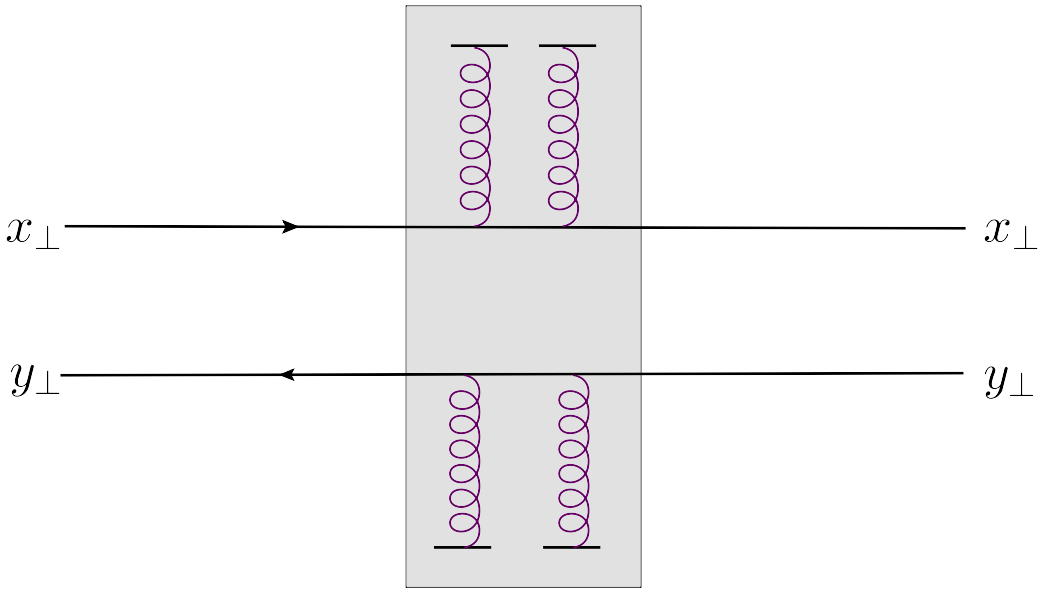
Amplitude: $$\mathcal{M}_{ij}(\boldsymbol{k}_\perp) \equiv \int \mathrm{d}^2\boldsymbol{x}_\perp \, \mathrm{e}^{-i\boldsymbol{x}_\perp\cdot\boldsymbol{k}_\perp} \, V_{ij}(\boldsymbol{x}_\perp)$$

Cross-section: $$\frac{\mathrm{d}\sigma}{\mathrm{d}\eta \mathrm{d}^2\boldsymbol{k}_\perp} \simeq x_p q(x_p, Q^2) \, \frac{1}{N_c} \left\langle \sum_{ij} |\mathcal{M}_{ij}(\boldsymbol{k}_\perp)|^2 \right\rangle_{X_g}$$

- Average over the color fields A^- in the target (CGC)
- Two Wilson lines at different transverse coordinates, traced over color

Dipole picture

- Equivalently: the elastic S-matrix for a $q\bar{q}$ color dipole



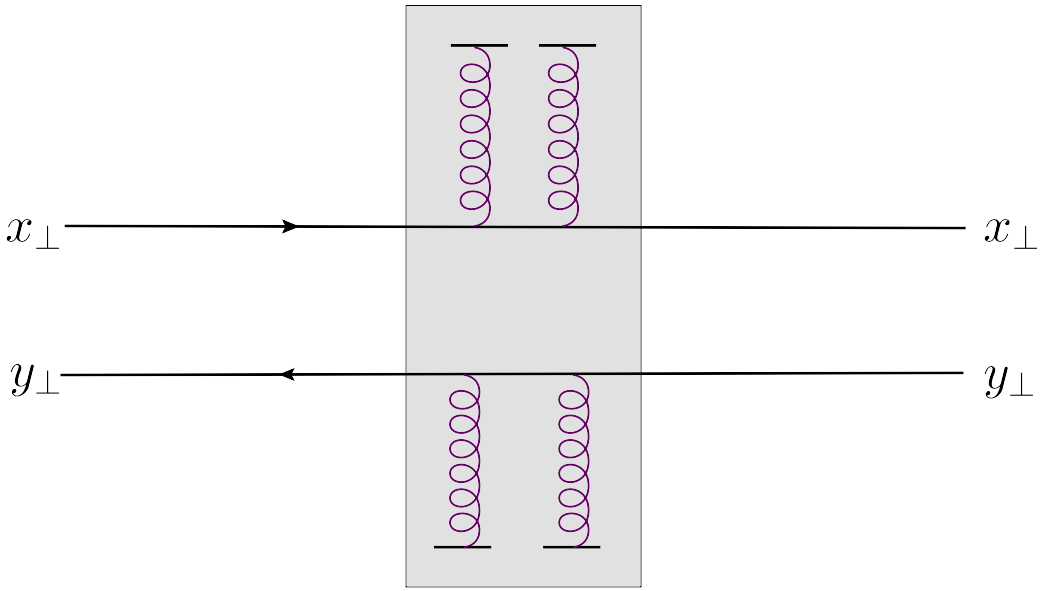
$$S(\boldsymbol{x},\boldsymbol{y};X_g) \equiv \frac{1}{N_c}\left\langle \mathrm{tr}\left[V(\boldsymbol{x})V^\dagger(\boldsymbol{y})\right]\right\rangle_{X_g}$$

$$\frac{\mathrm{d}\sigma}{\mathrm{d}\eta \mathrm{d}^2\boldsymbol{k}} \simeq x_p q(x_p) \int_{\boldsymbol{x},\boldsymbol{y}} \mathrm{e}^{-\mathrm{i}(\boldsymbol{x}-\boldsymbol{y})\cdot\boldsymbol{k}}\, S(\boldsymbol{x},\boldsymbol{y};X_g)$$

- The Fourier transform $\mathcal{S}(\boldsymbol{k},X_g)$: "unintegrated gluon distribution"

Dipole picture

- Equivalently: the elastic S-matrix for a $q\bar{q}$ color dipole



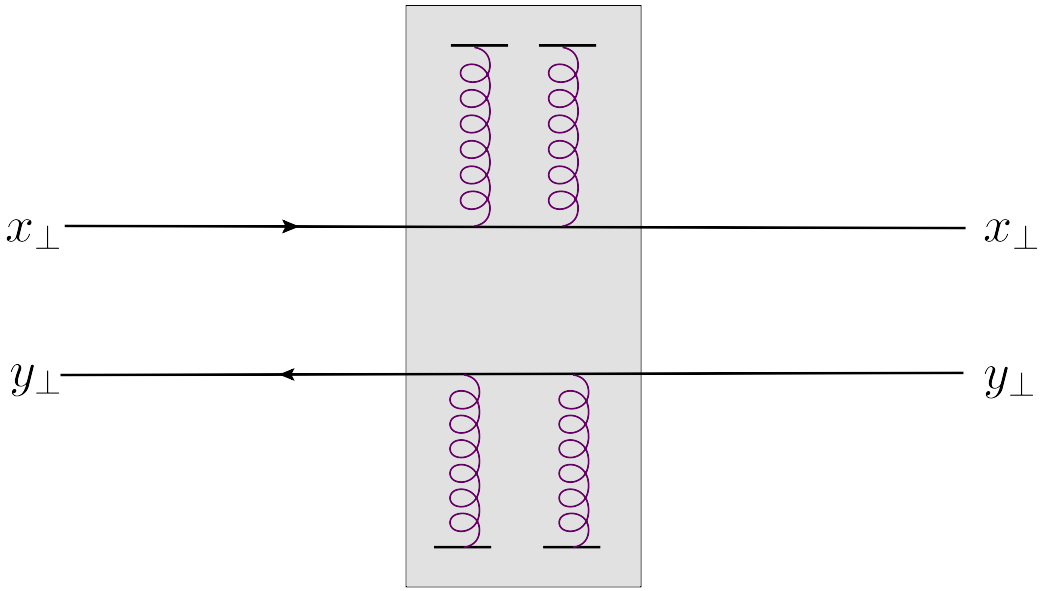
$$S(\boldsymbol{x},\boldsymbol{y};X_g) \equiv \frac{1}{N_c}\left\langle \mathrm{tr}\left[V(\boldsymbol{x})V^\dagger(\boldsymbol{y})\right]\right\rangle_{X_g}$$

$$\frac{\mathrm{d}\sigma}{\mathrm{d}\eta\mathrm{d}^2\boldsymbol{k}} \simeq x_p q(x_p)\int_{\boldsymbol{x},\boldsymbol{y}} \mathrm{e}^{-\mathrm{i}(\boldsymbol{x}-\boldsymbol{y})\cdot\boldsymbol{k}}\, S(\boldsymbol{x},\boldsymbol{y};X_g)$$

- 'Hybrid factorization': collinear fact. for p & CGC fact. for A *(Dumitru, Hayashigaki, and Jalilian-Marian, arXiv:hep-ph/0506308)*.

Dipole picture

- Equivalently: the elastic S-matrix for a $q\bar{q}$ color dipole



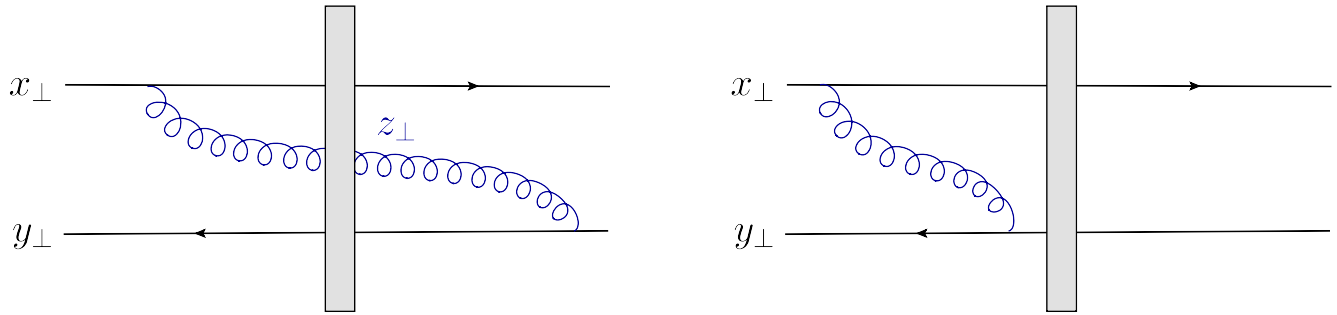
$$S(\boldsymbol{x},\boldsymbol{y};X_g) \equiv \frac{1}{N_c}\left\langle \mathrm{tr}\left[V(\boldsymbol{x})V^\dagger(\boldsymbol{y})\right]\right\rangle_{X_g}$$

$$\frac{\mathrm{d}\sigma}{\mathrm{d}\eta \mathrm{d}^2\boldsymbol{k}} \simeq x_p q(x_p) \int_{\boldsymbol{x},\boldsymbol{y}} \mathrm{e}^{-\mathrm{i}(\boldsymbol{x}-\boldsymbol{y})\cdot\boldsymbol{k}}\, S(\boldsymbol{x},\boldsymbol{y};X_g)$$

- The dipole picture is preserved by the high-energy evolution up to NLO *(Kovchegov and Tuchin, 2002; Mueller and Munier, 2012)*

BK equation *(leading order)*

- Probability $\sim \alpha_s \ln \frac{1}{x}$ to radiate a soft gluon with $x \equiv \frac{p^+}{k^+} \ll 1$



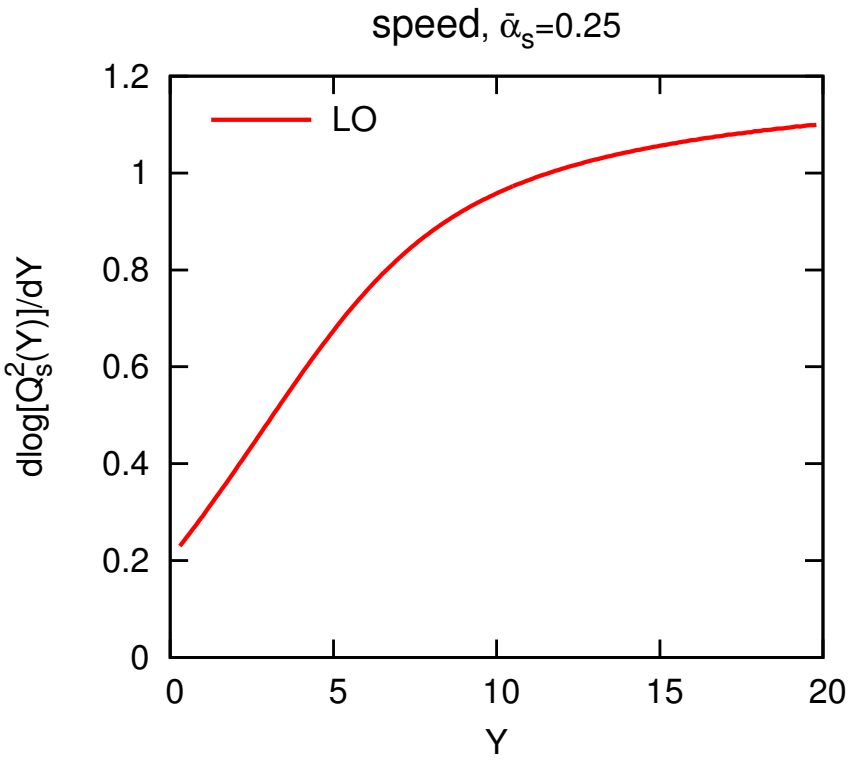
- When $\alpha_s \ln \frac{1}{x} \sim 1$: resummation to all orders (part of LO)
- Evolution equation for the dipole S–matrix $S_{\boldsymbol{xy}}(Y)$ with $Y \equiv \ln(1/x)$

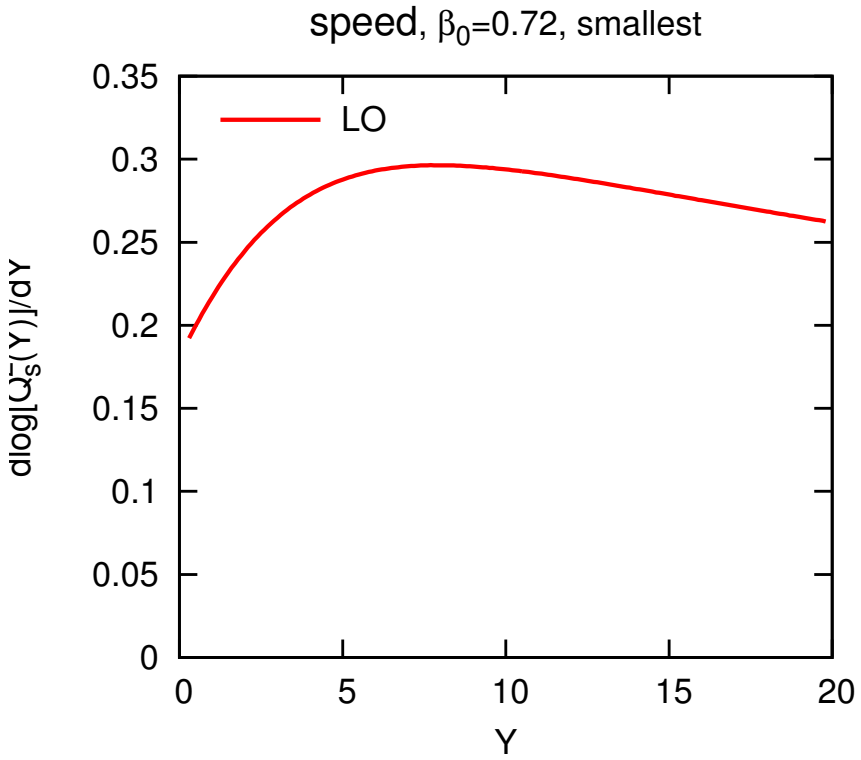
$$\frac{\partial S_{\boldsymbol{xy}}}{\partial Y} = \frac{\bar{\alpha}_s}{2\pi} \int \mathrm{d}^2\boldsymbol{z}\, \frac{(\boldsymbol{x}-\boldsymbol{y})^2}{(\boldsymbol{x}-\boldsymbol{z})^2(\boldsymbol{y}-\boldsymbol{z})^2} \left[S_{\boldsymbol{xz}} S_{\boldsymbol{zy}} - S_{\boldsymbol{xy}}\right]$$

  - dipole kernel: probability for the dipole to emit a soft gluon at $\boldsymbol{z}$
  - large-N_c approximation to the Balitsky-JIMWLK hierarchy
  - saturation momentum $Q_s(Y)$: $S(r, Y) = 0.5$ when $r = 1/Q_s(Y)$

Adding running coupling: rcBK

- The evolution speed: saturation exponent $\lambda_s \equiv \mathrm{d}\ln Q_s^2/\mathrm{d}Y$
- At LO, $\lambda_s \sim 1$ is way too large: $\lambda_{\mathrm{HERA}} = 0.2 \div 0.3$

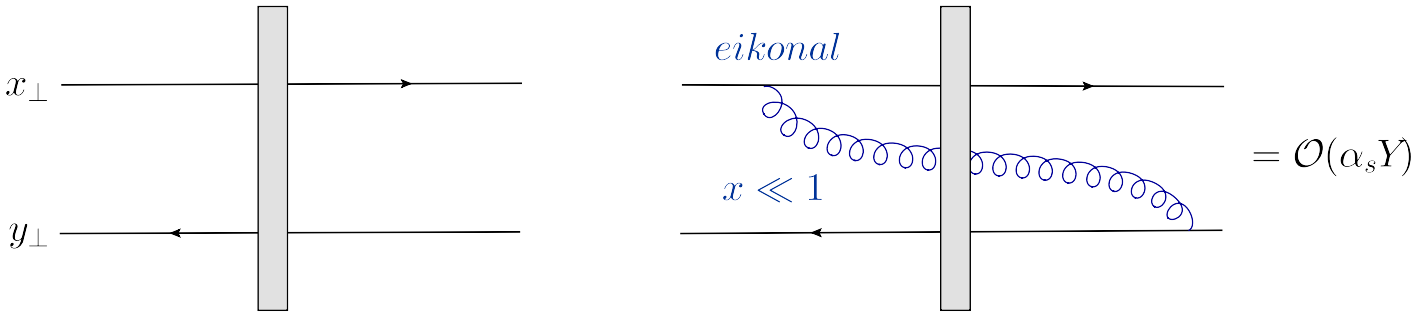




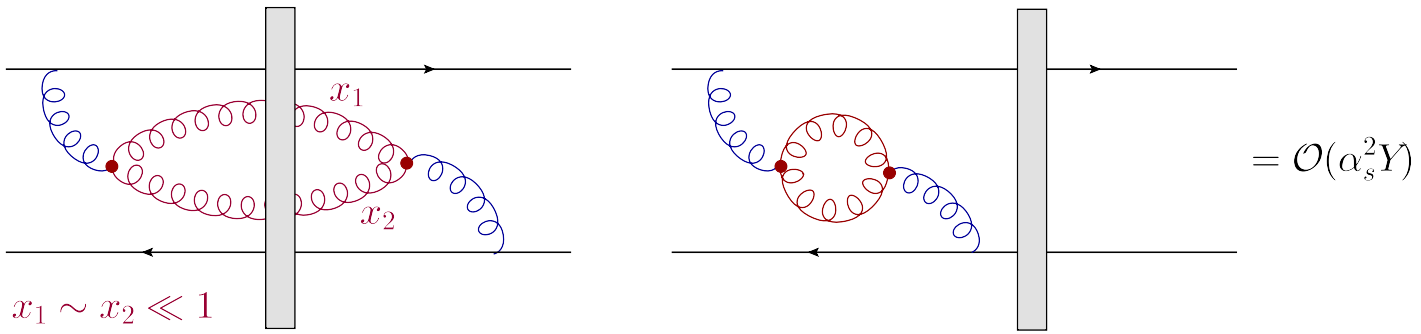
- Including running coupling dramatically slows down the evolution
- ... but there are other, equally important, NLO corrections !

Particle production beyond leading order

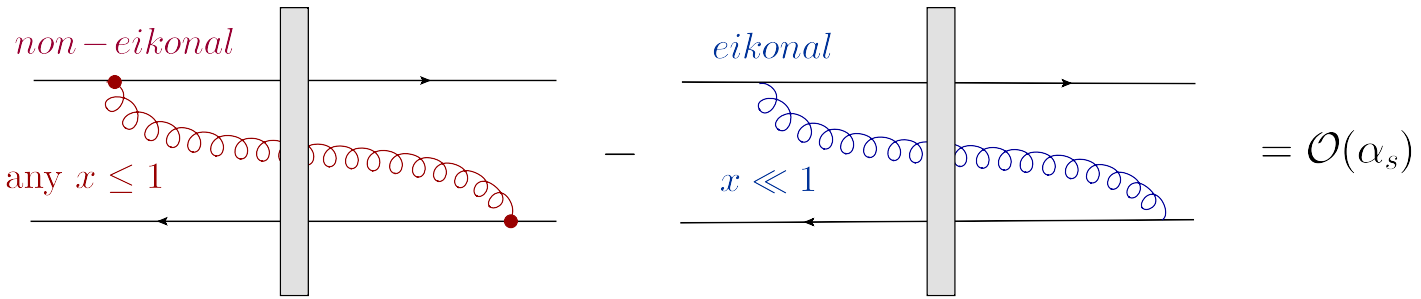
- LO approximation: any number $n \geq 0$ of soft emissions $\Longrightarrow (\alpha_s Y)^n$



- NLO corrections to the evolution: 2 soft gluons, with similar values of x

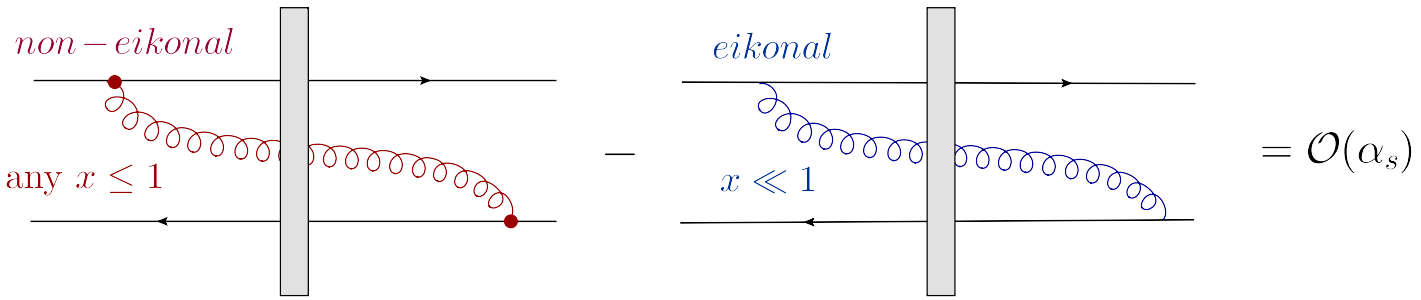


- NLO correction to impact factor: the first gluon can be hard



Towards NLO factorization in pA

- The first gluon contributes both to the evolution (when $x \ll 1$) and to the NLO impact factor (generic x) : How to avoid over counting ?
- $k_\perp$-factorization : use a 'rapidity subtraction'



  - the method used by *Chirilli, Xiao, and Yuan (arXiv:1203.6139)*
  - leads to a negative cross-section at semi-hard $k_\perp$
- Our proposal *(E.I., A. Mueller and D. Triantafyllopoulos, arXiv:1608.05293)*
  - separate the first gluon emission from the evolution and compute it with the exact kinematics
- The integral representation of the BK equation is useful in that sense

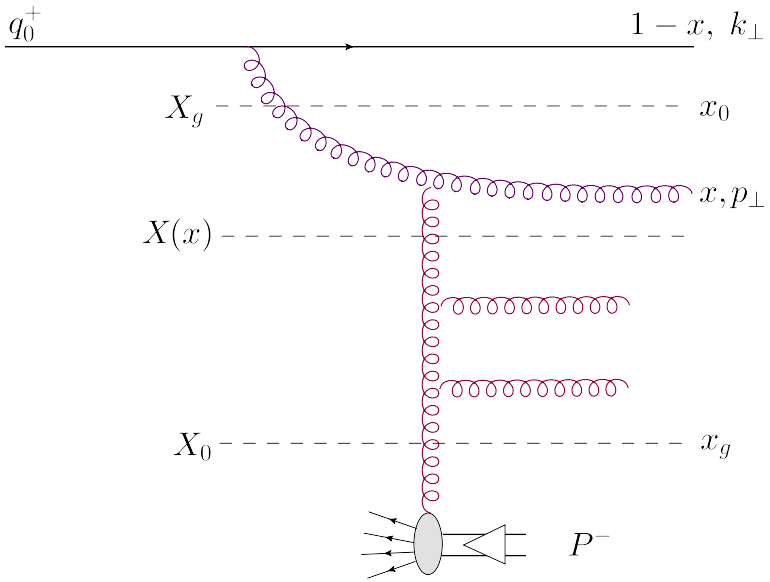
LO BK evolution in integral form

$$\left.\frac{\mathrm{d}N}{\mathrm{d}\eta \mathrm{d}^2\boldsymbol{k}}\right|_{\mathrm{LO}} = x_p q(x_p)\, \mathcal{S}(\boldsymbol{k}, X_g)\,, \qquad \mathcal{S}(\boldsymbol{k}, X_g) = \int \mathrm{d}^2\boldsymbol{r}\, \mathrm{e}^{-\mathrm{i}\boldsymbol{k}\cdot\boldsymbol{r}} S(\boldsymbol{r}, X_g)$$

- $S(\boldsymbol{r}, X_g)$ is the solution to the LO BK equation and can be written as

$$S_{\boldsymbol{xy}}(X_g) = S_{\boldsymbol{xy}}(X_0) + \bar{\alpha}_s \int_{X_g}^1 \frac{\mathrm{d}x}{x} \int_{\boldsymbol{z}} \frac{(\boldsymbol{x}-\boldsymbol{y})^2}{(\boldsymbol{x}-\boldsymbol{z})^2(\boldsymbol{y}-\boldsymbol{z})^2} \Big[S_{\boldsymbol{xz}} S_{\boldsymbol{zy}} - S_{\boldsymbol{xy}}\Big]\big(X(x)\big)$$

- Except for the first gluon, the evolution is associated with the nucleus



- $X(x)$: energy fraction in the target

$$X(x) \simeq \frac{k_\perp^2}{xs} = \frac{X_g}{x}$$

$$X \leq 1 \Longrightarrow x \geq X_g$$

LO BK evolution in integral form

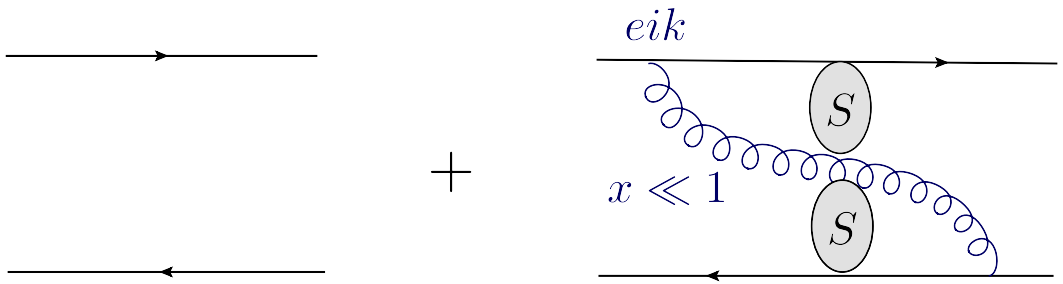
$$\left.\frac{\mathrm{d}N}{\mathrm{d}\eta \mathrm{d}^2\boldsymbol{k}}\right|_{\mathrm{LO}} = x_p q(x_p)\, \mathcal{S}(\boldsymbol{k}, X_g)\,, \qquad \mathcal{S}(\boldsymbol{k}, X_g) = \int \mathrm{d}^2\boldsymbol{r}\, \mathrm{e}^{-\mathrm{i}\boldsymbol{k}\cdot\boldsymbol{r}} S(\boldsymbol{r}, X_g)$$

- $S(\boldsymbol{r}, X_g)$ is the solution to the LO BK equation and can be written as

$$S_{\boldsymbol{xy}}(X_g) = S_{\boldsymbol{xy}}(X_0) + \bar{\alpha}_s \int_{X_g}^1 \frac{\mathrm{d}x}{x} \int_{\boldsymbol{z}} \frac{(\boldsymbol{x}-\boldsymbol{y})^2}{(\boldsymbol{x}-\boldsymbol{z})^2(\boldsymbol{y}-\boldsymbol{z})^2} \Big[S_{\boldsymbol{xz}} S_{\boldsymbol{zy}} - S_{\boldsymbol{xy}}\Big]\big(X(x)\big)$$

- In more compact, but formal, notations

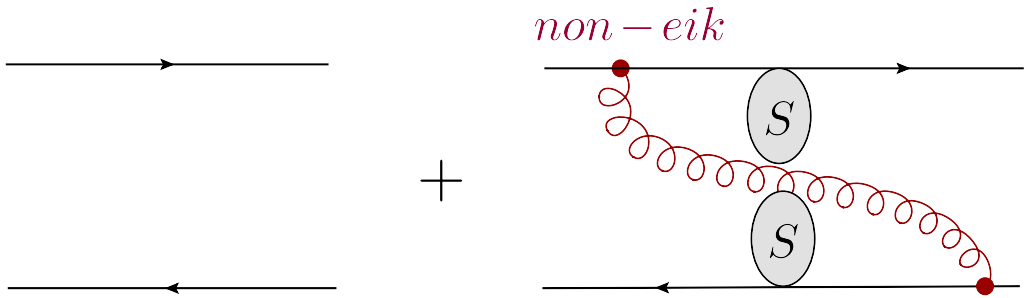
$$\mathcal{S}(\boldsymbol{k}, X_g) \,=\, \mathcal{S}_0(\boldsymbol{k}) + \bar{\alpha}_s \int_{X_g}^1 \frac{\mathrm{d}x}{x}\, \mathcal{K}(\boldsymbol{k}; 0)\, \mathcal{S}\big(\boldsymbol{k}, X(x)\big)\,; \quad X(x) \equiv \frac{X_g}{x}$$



$\mathcal{S}$ *(solution to LO BK equation)*

Adding the NLO impact factor

- Compute (only) the first gluon emission with the exact kinematics



$$\frac{\mathrm{d}N}{\mathrm{d}\eta \mathrm{d}^2\boldsymbol{k}} = \mathcal{S}_0(\boldsymbol{k}) + \bar{\alpha}_s \int_{X_g}^1 \frac{\mathrm{d}x}{x}\, \mathcal{K}(\boldsymbol{k};x)\, \mathcal{S}\big(\boldsymbol{k}, X(x)\big)\,; \quad X(x) \simeq \frac{X_g}{x}$$

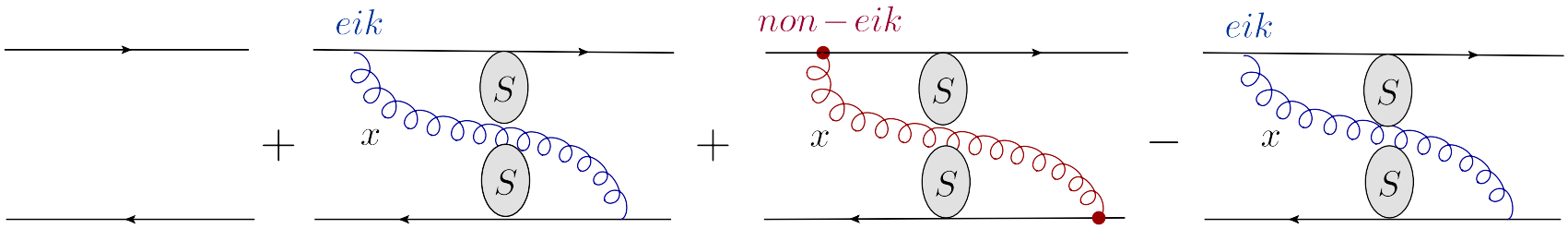
- $\mathcal{K}(\boldsymbol{k};x)$: kernel for emitting a gluon with exact kinematics ($x \leq 1$)

  (Chirilli, Xiao, and Yuan, arXiv:1203.6139)

- This cross-section is (almost) manifestly positive definite
- LO evolution + NLO impact factor are mixed with each other
- To recover the LO result: $\mathcal{K}(\boldsymbol{k};x) \to \mathcal{K}(\boldsymbol{k};0)$ (eikonal limit)

Recovering $k_\perp$-factorization

- Add and subtract the LO result:



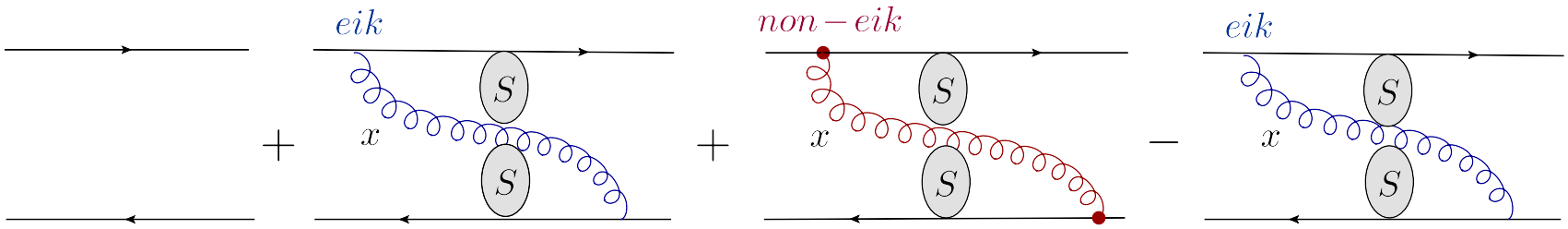
$\mathcal{S}$ *(solution to BK equation)* $\qquad$ $\mathcal{NLO}$ *correction to impact factor*

$$\frac{\mathrm{d}N}{\mathrm{d}\eta \mathrm{d}^2\boldsymbol{k}} = \mathcal{S}(\boldsymbol{k}, X_g) + \bar{\alpha}_s \int_{X_g}^1 \frac{\mathrm{d}x}{x} \left[\mathcal{K}(x) - \mathcal{K}(0)\right] \mathcal{S}\big(\boldsymbol{k}, X(x)\big)$$

- To NLO accuracy, one can perform additional approximations:
  - replace $\mathcal{S}\big(X(x)\big) \simeq \mathcal{S}(X_g)$ (since integral dominated by $x \sim 1$)
  - ... and set $X_g \to 0$ in the lower limit ('plus prescription')
- Local in rapidity : $k_\perp$-factorization in the form presented by CXY *(Chirilli, Xiao, and Yuan, arXiv:1203.6139)*

Recovering $k_\perp$-factorization

- Add and subtract the LO result:



$\mathcal{S}$ (solution to $\mathcal{BK}$ equation) $\mathcal{NLO}$ correction to impact factor

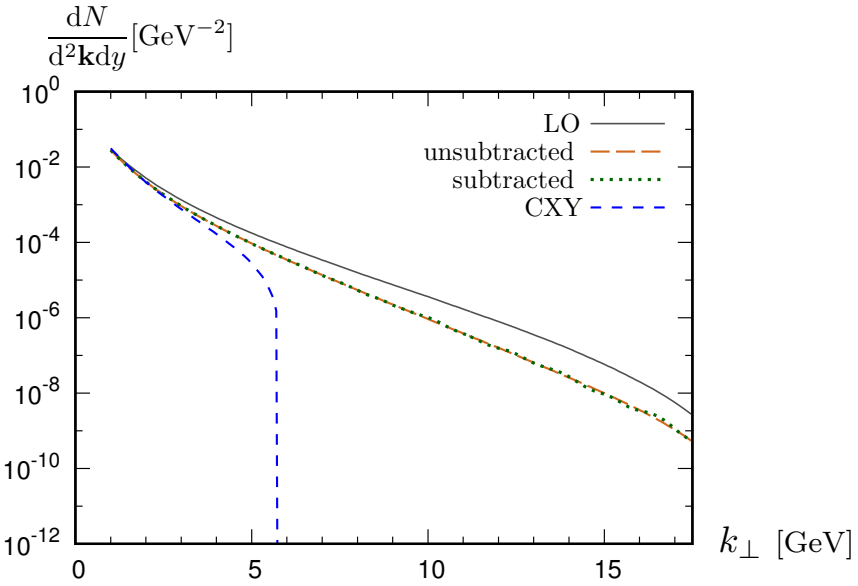
$$\frac{\mathrm{d}N}{\mathrm{d}\eta \mathrm{d}^2\boldsymbol{k}} = \mathcal{S}(\boldsymbol{k}, X_g) + \bar{\alpha}_s \int_0^1 \frac{\mathrm{d}x}{x} \left[\mathcal{K}(x) - \mathcal{K}(0)\right] \mathcal{S}\big(\boldsymbol{k}, X_g\big)$$

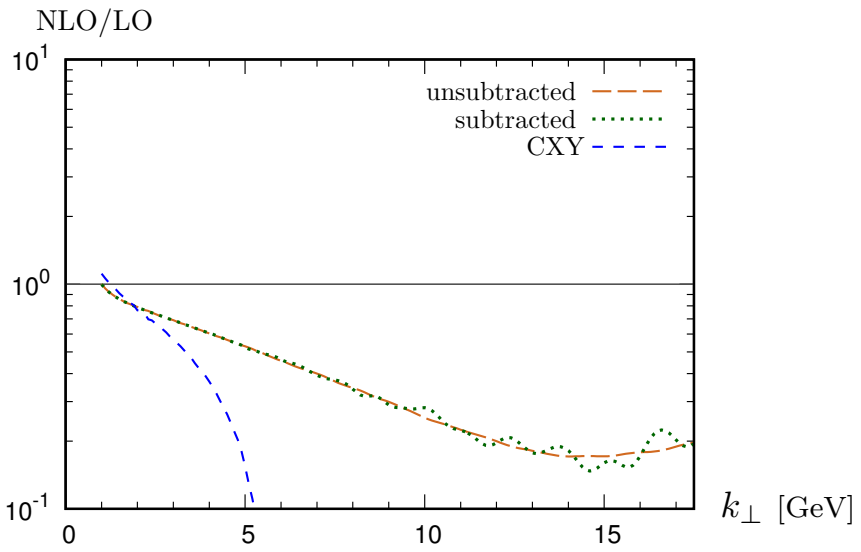
- To NLO accuracy, one can perform additional approximations:
  - replace $\mathcal{S}\big(X(x)\big) \simeq \mathcal{S}(X_g)$ (since integral dominated by $x \sim 1$)
  - ... and set $X_g \to 0$ in the lower limit ('plus prescription')
- Local in rapidity : $k_\perp$-factorization in the form presented by CXY

(Chirilli, Xiao, and Yuan, arXiv:1203.6139)

Numerical results: Fixed coupling

(Ducloué, Lappi, and Zhu, arXiv:1703.04962)

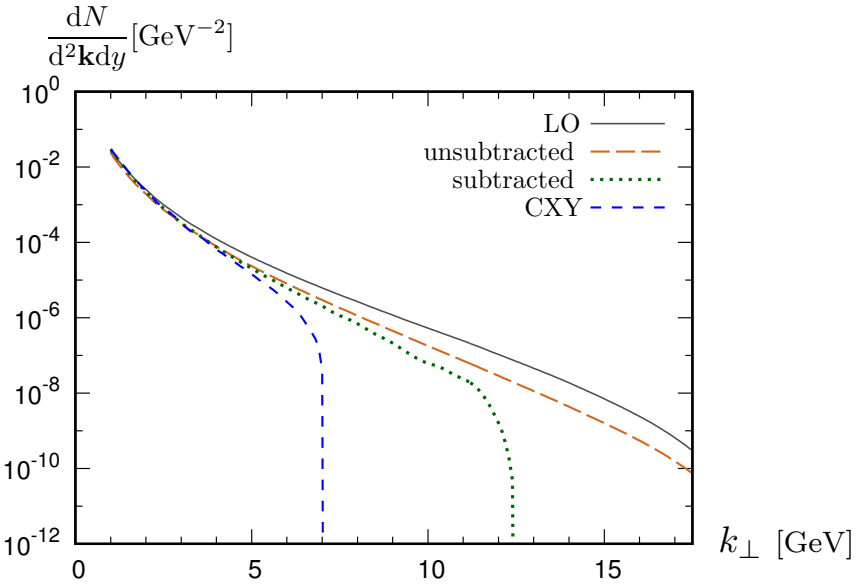


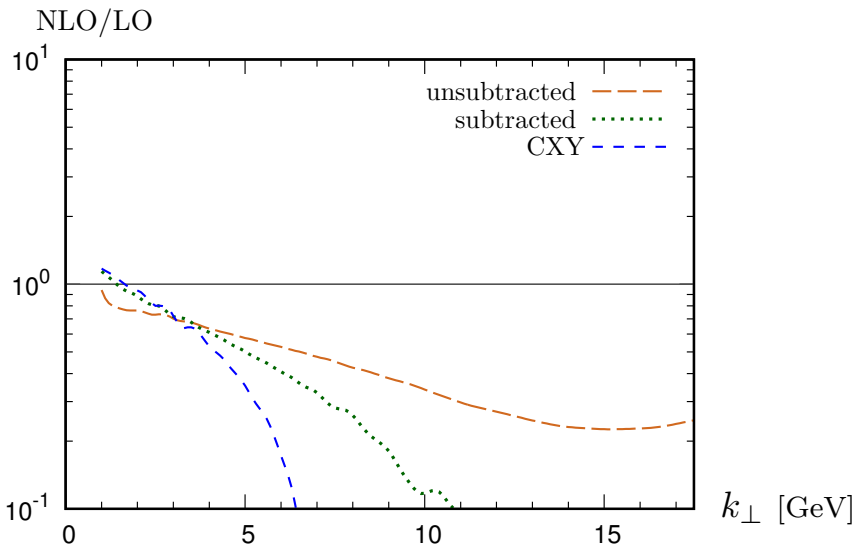


- Large NLO correction: $\gtrsim 50\,\%$ for $k_\perp \geq 5$ GeV
- The same results with and without subtraction (of the LO result)
- "A mathematical identity" ... sure, but tricky in practice !
  - one adds and subtracts a large, LO, contribution
  - small oscillations in "subtracted" due to numerical errors
- Strict $k_\perp$-factorization rapidly becomes negative : over-subtraction

Numerical results: Running coupling

(Ducloué, Lappi, and Zhu, arXiv:1703.04962)





- The running of the coupling renders the problem even more subtle:
  - already the "subtracted" result becomes negative
  - the "CXY" curve becomes negative even faster
- Mismatch between the running coupling prescriptions used ...
  - in coordinate space (for solving the BK equation)
  - ... and in momentum space (for computing the NLO impact factor)

Adding a running coupling

- The NLO impact factor is generally computed in momentum space
  - natural to use a running coupling $\bar{\alpha}_s(k_\perp^2)$ (at least for $k_\perp^2 \gtrsim Q_s^2$)

$$\frac{\mathrm{d}N}{\mathrm{d}\eta \mathrm{d}^2\boldsymbol{k}} = \mathcal{S}_0(\boldsymbol{k}) + \bar{\alpha}_s(k_\perp^2) \int_{X_g}^1 \frac{\mathrm{d}x}{x}\, \mathcal{K}(\boldsymbol{k};x)\, \mathcal{S}\big(\boldsymbol{k}, X(x)\big)$$

  - more generally: $\bar{\alpha}_s(k^2_{\mathrm{max}})$

- Dipole S-matrix is computed by solving rcBK in coordinate space

$$S_{\boldsymbol{xy}}(X_g) = S_{\boldsymbol{xy}}(X_0) + \int_{X_g}^1 \frac{\mathrm{d}x}{x} \int_{\boldsymbol{z}} \bar{\alpha}_s(r^2_{\mathrm{min}}) \frac{(\boldsymbol{x}-\boldsymbol{y})^2}{(\boldsymbol{x}-\boldsymbol{z})^2(\boldsymbol{y}-\boldsymbol{z})^2} \Big[S_{\boldsymbol{xz}} S_{\boldsymbol{zy}} - S_{\boldsymbol{xy}}\Big]$$

  - $r_{\mathrm{min}} \equiv \min\big\{|\boldsymbol{x}-\boldsymbol{y}|, |\boldsymbol{x}-\boldsymbol{z}|, |\boldsymbol{y}-\boldsymbol{z}|\big\}$

- Running coupling and Fourier transform do not "commute" with each other

Towards a new puzzle ?

- The FT transform $\mathcal{S}(\boldsymbol{k}, X)$ does not obey the expected integral equation in momentum space

$$\mathcal{S}(\boldsymbol{k}, X_g) \neq \mathcal{S}_0(\boldsymbol{k}) + \bar{\alpha}_s(k_\perp^2) \int_{X_g}^1 \frac{\mathrm{d}x}{x} \mathcal{K}(\boldsymbol{k}; 0)\, \mathcal{S}\big(\boldsymbol{k}, X(x)\big)$$

  - subtracting the LO result is not an identity anymore
  - mismatch between "subtracted" and "unsubtracted" results

- Our prescription *(E.I., Mueller, Triantafyllopoulos, arXiv:1608.05293)*
  - use the "unsubtracted" result with momentum-space RC $\bar{\alpha}_s(k_\perp^2)$
  - reasonable numerical results: positive definite

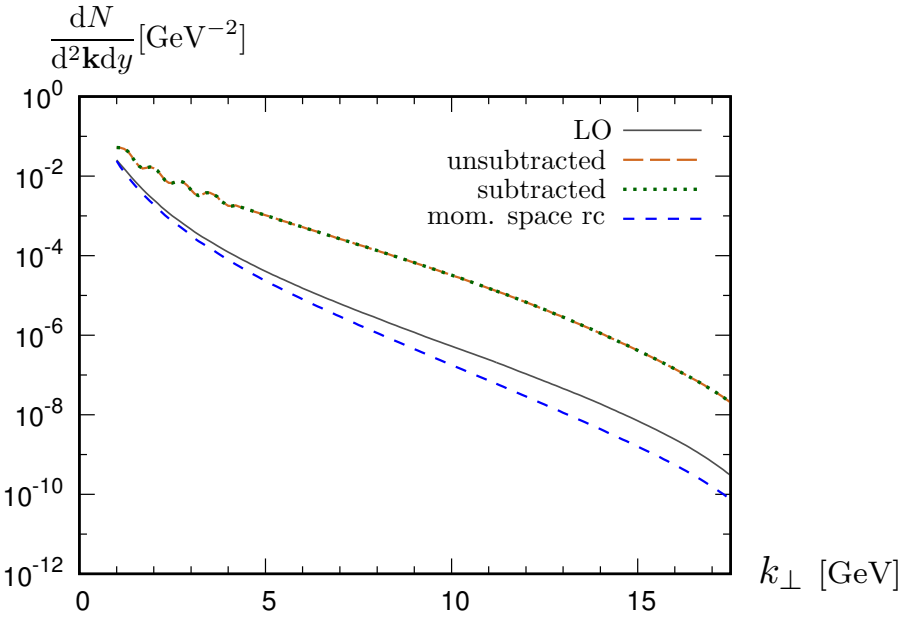
- But how sensitive are these results upon the choice of a scheme ?

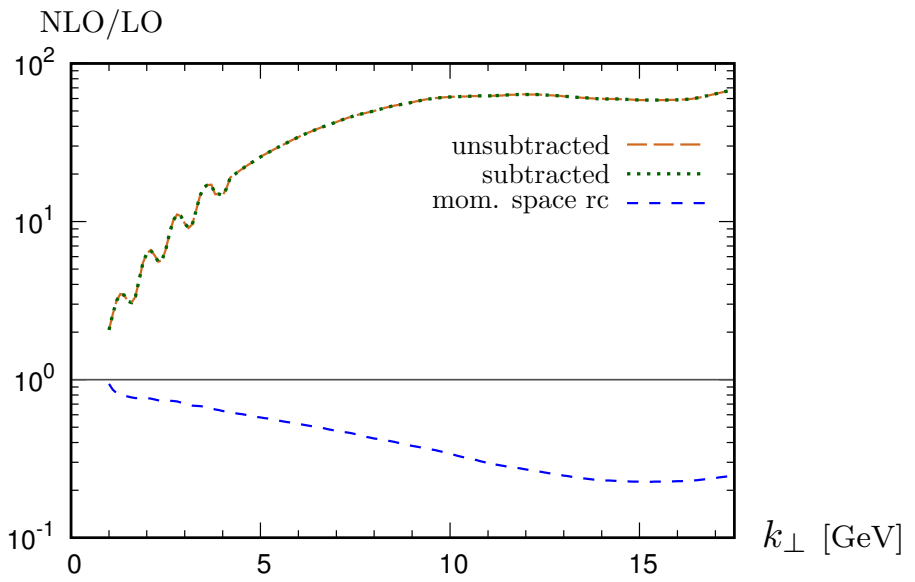
- Alternative scheme: compute the NLO impact factor fully in coordinate space and make the FT at the very end

  (Ducloué, Lappi, and Zhu, arXiv:1703.04962)

Numerical results: Coordinate space with RC

(Ducloué, Lappi, and Zhu, arXiv:1703.04962 – see the Appendix)



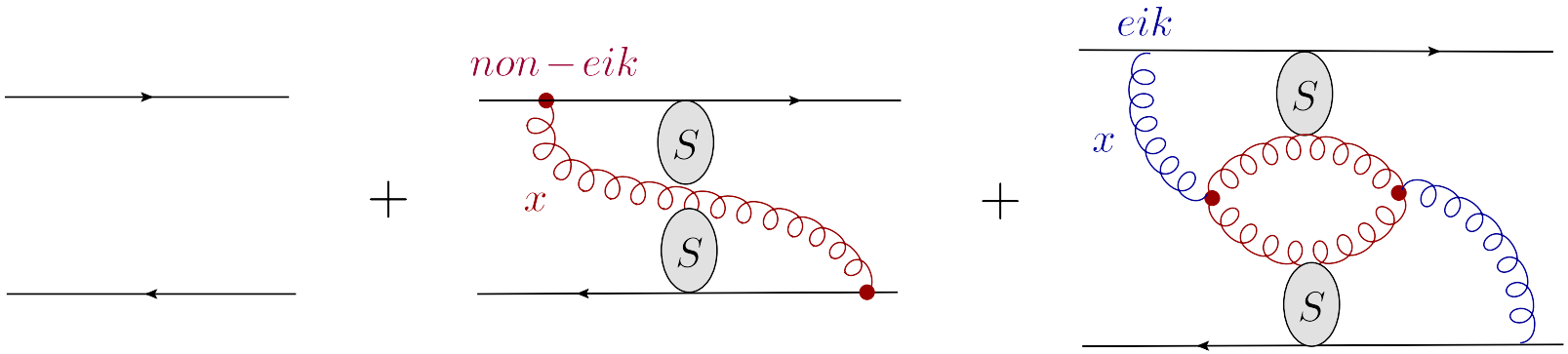


- "Unsubtracted" and "subtracted" results coincide with each other ☺
  - calculations systematically done in coordinate space
  - subtraction performed in coordinate space before the final FT
- ... but they are larger than the LO result by a factor ~ 100 !
- The mismatch with the "momentum-space scheme" is spectacular, but so far we do not understand its origin

Completing the NLO evolution

(E.I., A. Mueller and D. Triantafyllopoulos, arXiv:1608.05293)

- Recall: the NLO BK evolution also involves 2-loop graphs



$$\frac{\mathrm{d}N}{\mathrm{d}\eta \mathrm{d}^2\boldsymbol{k}} = \mathcal{S}_0 + \bar{\alpha}_s \int_{X_g}^1 \frac{\mathrm{d}x}{x}\, \mathcal{K}(x)\, \mathcal{S}\big(X(x)\big) + \bar{\alpha}_s^2 \int_{X_g}^1 \frac{\mathrm{d}x}{x}\, \mathcal{K}_2(0)\, \mathcal{S}\big(X(x)\big)$$

- $\mathcal{K}_2(0)$: NLO correction to the BK kernel with collinear improvement

  (Balitsky and Chirilli, 2008; Iancu et al, 2015)

Conclusions

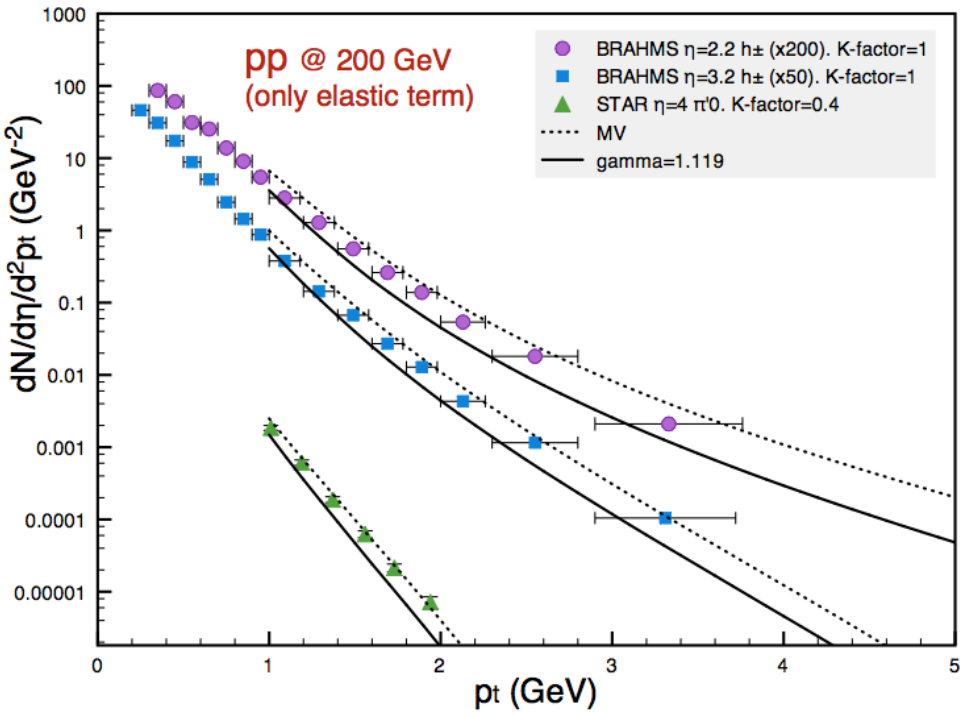
- The usual $k_\perp$-factorization at high energy (local in rapidity) can provide unphysical results at NLO
  - the strict separation between a 'LO result' and 'NLO corrections' involves a high degree of fine tuning, leading to instabilities in the presence of seemingly innocuous additional approximations
- A more general factorization has been proposed to circumvent this problem
  - no explicit separation between LO and NLO
  - non-local in rapidity
- Sensible physical results: positive cross-section, but smaller than at LO
  - at fixed coupling
  - with running coupling, but using a mixed scheme
- A fully coordinate-space calculation with RC leads to new difficulties
- Next step: attempt a fully momentum-space calculation with RC

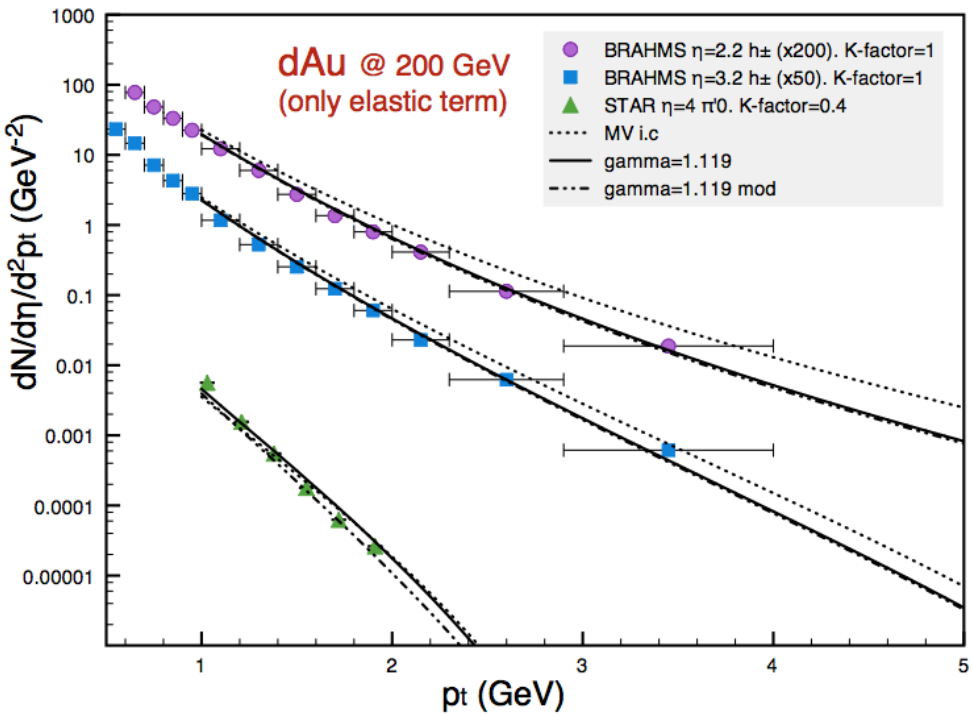
Back-up Slides

LO phenomenology (rcBK)

(Albacete, Dumitru, Fujii, Nara, arXiv:1209:2001)

- Fit parameters: initial condition for the rcBK equation + K-factors

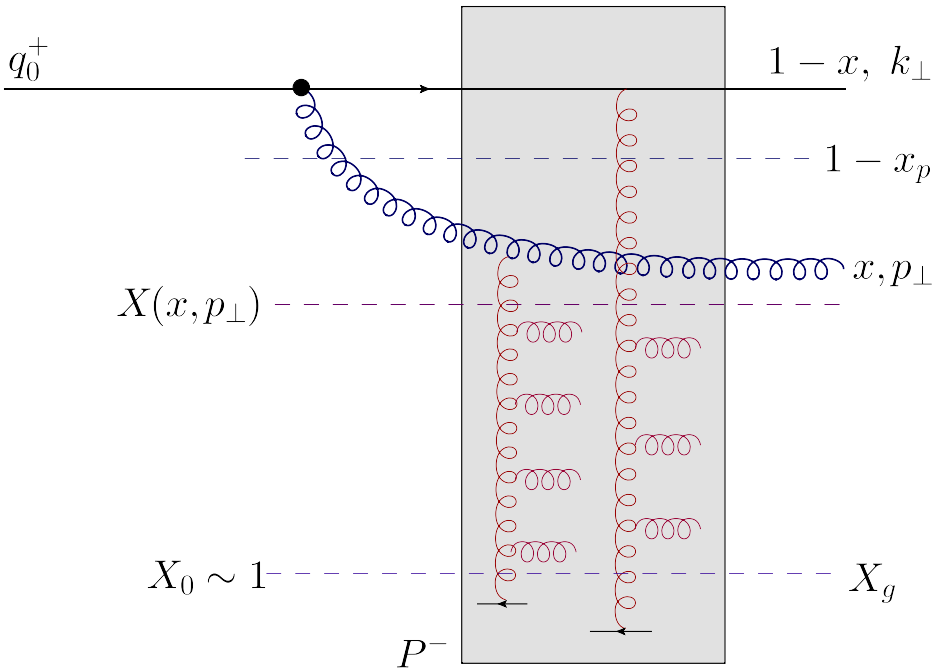




$$\left.\frac{\mathrm{d}N}{\mathrm{d}\eta \mathrm{d}^2\boldsymbol{k}}\right|_{\mathrm{LO}} = K^h \int_{x_p}^1 \frac{\mathrm{d}z}{z^2}\, \frac{x_p}{z} q\left(\frac{x_p}{z}\right)\, \mathcal{S}\left(\frac{\boldsymbol{k}}{z}, X_g\right)\, D_{h/q}(z)$$

Exact kinematics for target evolution

- 'Real amplitude' : the gluon is produced in the final state



- LC energy conservation:

$$\frac{k_\perp^2}{2(1-x)q_0^+} + \frac{p_\perp^2}{2xq_0^+} = XP^-$$

- $\Longrightarrow \quad X = X(x, p_\perp)$
- simplifies when $k_\perp \simeq p_\perp \gg Q_s$

$$X(x) \simeq \frac{k_\perp^2}{xs} = \frac{X_g}{x}$$

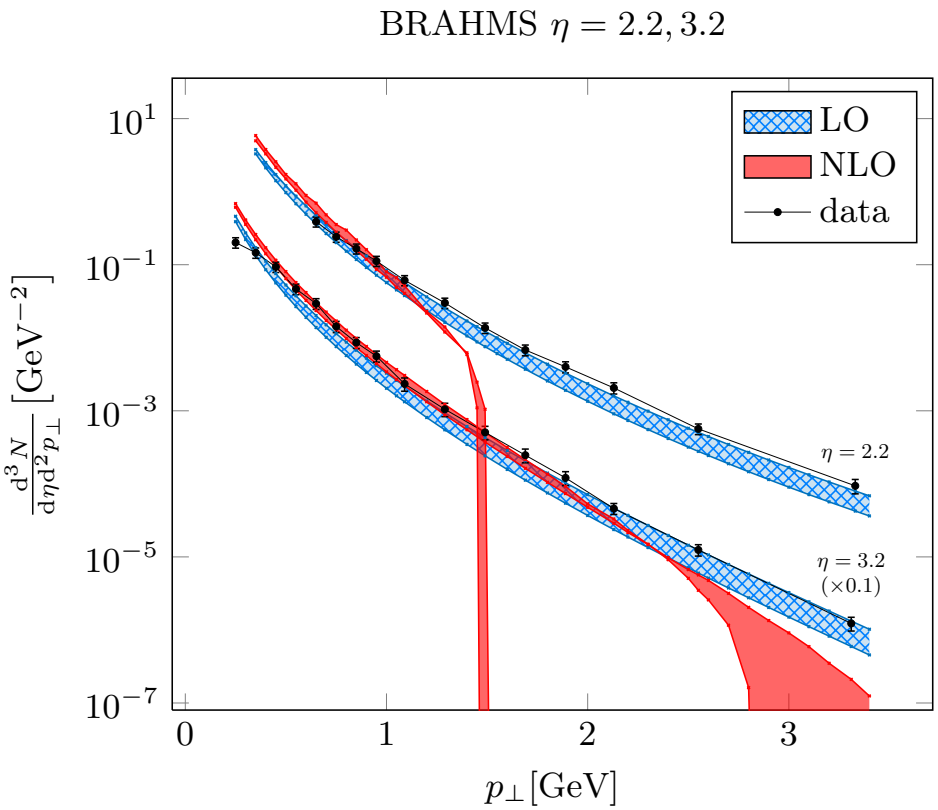
- $X \leq 1 \Longrightarrow x \geq X_g$

- Equivalently: gluon lifetime should be larger than the target width
- The same condition holds for the 'virtual' corrections
  - non-trivial cancellations required by probability conservation

The negativity problem

(Stasto, Xiao, and Zaslavsky, arXiv:1307.4057)

- Sudden drop in the numerical estimate at momenta $p_\perp$ of order Q_s



- "NLO evolution is notoriously unstable"
- Sure, but in this calculation $\mathcal{S} \approx \mathcal{S}_{\mathrm{rcBK}}$
  - rcBK evolution is well behaved
  - the actual "LO approx" in practice

$$\left.\frac{\mathrm{d}N}{\mathrm{d}y\,\mathrm{d}^2\boldsymbol{k}}\right|_{\mathrm{LO}} = \mathcal{S}_{\mathrm{rcBK}}(\boldsymbol{k}, X_g)$$

- The NLO correction to the impact factor is negative (not a real surprise) ... and dominates over the LO result at sufficiently large $k_\perp$

Some proposals to solve the problem

- General idea: the 'subtracted' term performs an ... over-subtraction
- Strategy: reduce the longitudinal (x) phase-space for the 'hard' gluon
  - factorization scale x_0 separating 'evolution' from 'impact factor'
    (Kang, Vitev, and Xing, arXiv:1403.5221)

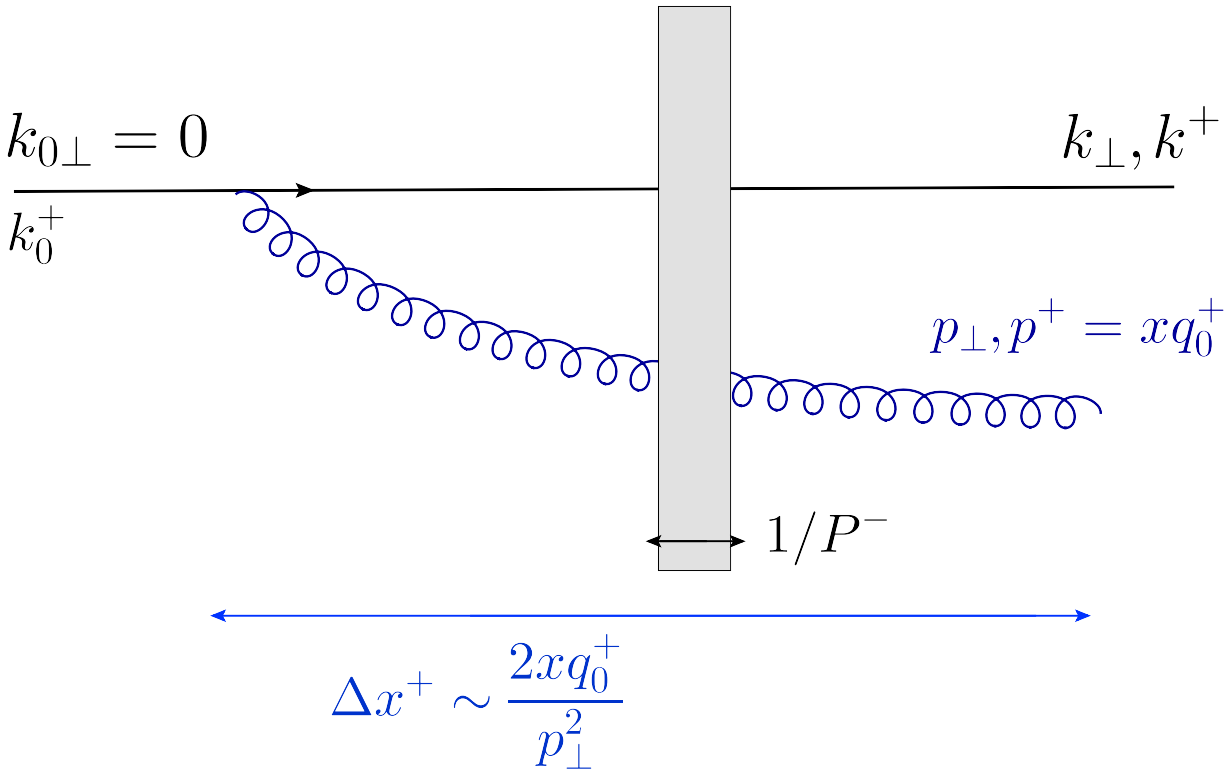
$$\int_0^1 \frac{\mathrm{d}x}{x}\left[\mathcal{K}(x)-\mathcal{K}(0)\right] \Longrightarrow \int_0^{x_0} \frac{\mathrm{d}x}{x}\left[\mathcal{K}(x)-\mathcal{K}(0)\right]$$

  - x_0 can depend upon $k_\perp$, say to account for 'time-ordering'
    (Ducloué, Lappi, and Zhu, arXiv:1604.00225)
- In principle, it shouldn't matter that much
  - the x_0–dependence must cancel in a complete calculation
- In practice, it only pushes the problem up to somewhat higher $k_\perp$
  - also, strongly dependent upon the precise implementation of x_0

Energy conservation *("Ioffe's time")*

(Altinoluk, Armesto, Beuf, Kovner, and Lublinsky, arXiv:1411.2869)

- x cannot be arbitrarily small since constrained by energy conservation



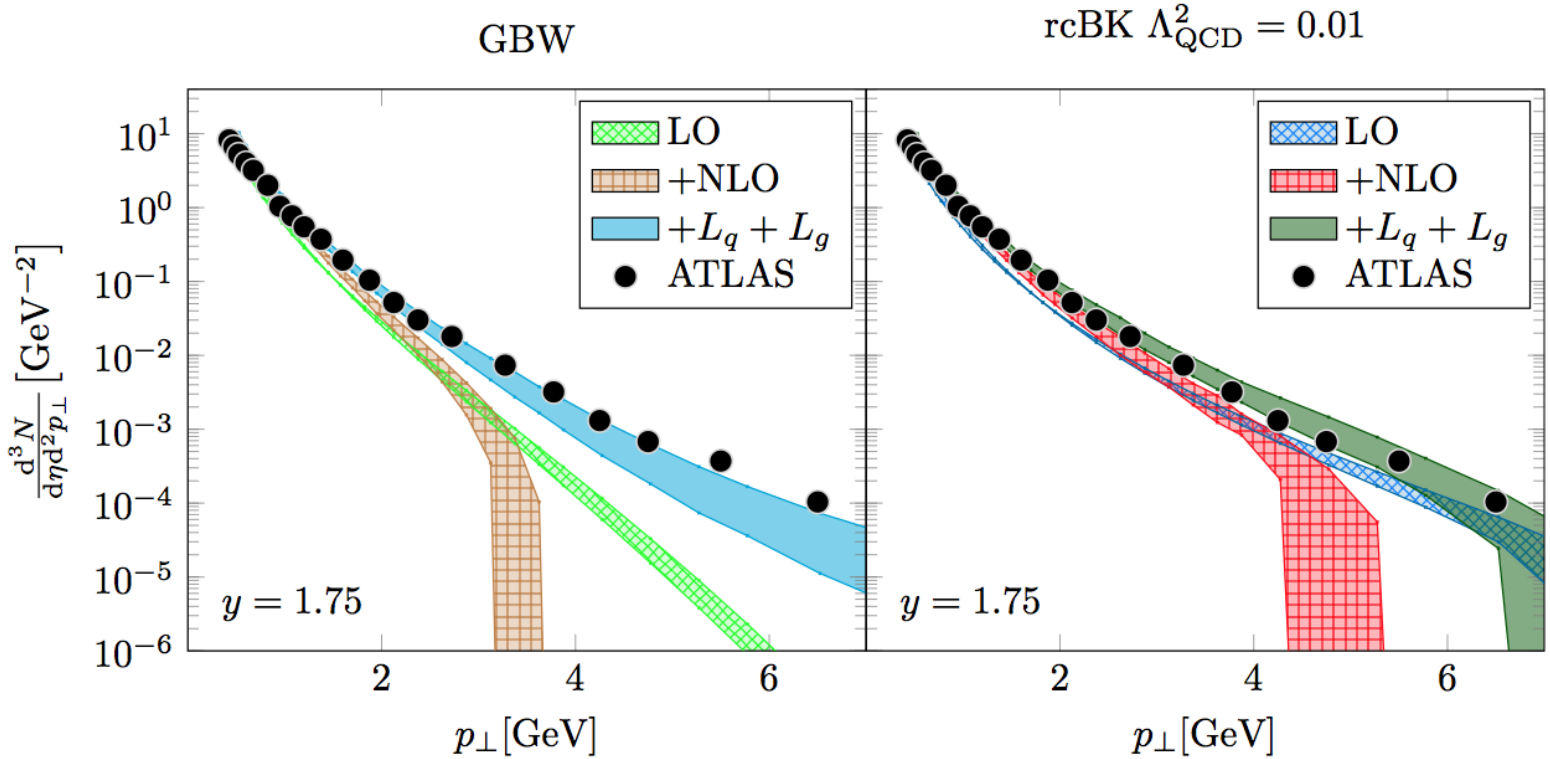
- Gluon lifetime should be larger than the target width

$$\frac{2xq_0^+}{p_\perp^2} > \frac{1}{P^-} \Longrightarrow x > \frac{p_\perp^2}{s}$$

Implementing the constraint

(Watanabe, Xiao, Yuan, and Zaslavsky, arXiv:1505:05183)

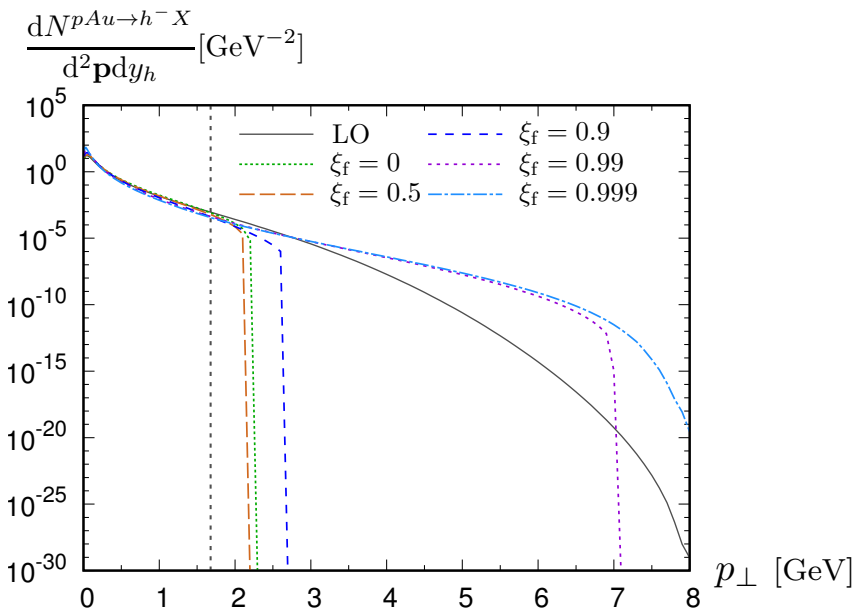
- It matters for the subtraction scheme only if $k_\perp \gg p_\perp$

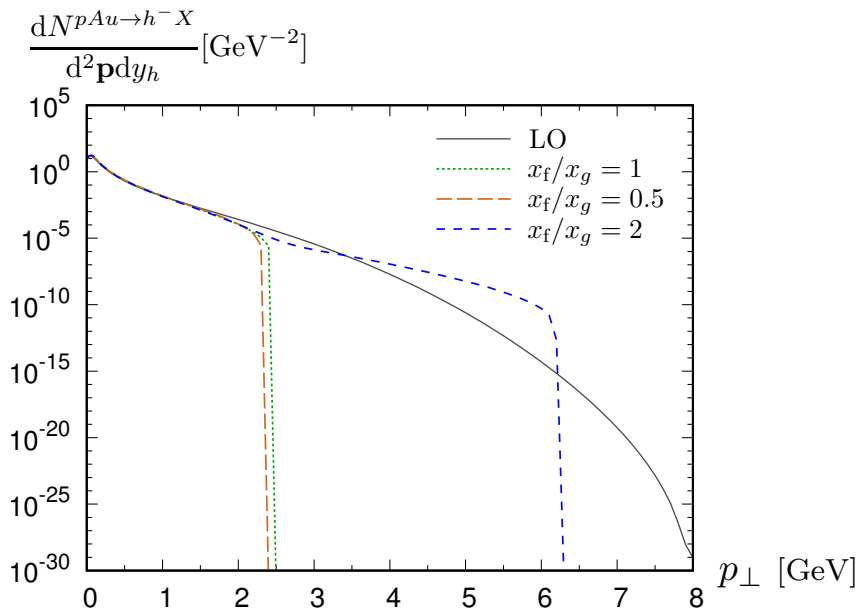


- Once again, it pushes the problem to higher $k_\perp$
  - ... and strongly dependent upon the model/evolution chosen for $\mathcal{S}$

Why is this a problem ?

- An extreme example: GBW saturation model $\mathcal{S}_{\rm GBW}(\boldsymbol{k}, X) \propto \mathrm{e}^{-\frac{k_\perp^2}{Q_s^2}}$
  - the 'added' piece is exponentially suppressed at $k_\perp \gg Q_s$
  - the 'subtracted' piece develops a power-law tail $\propto 1/k_\perp^4$
  - the overall result becomes negative at sufficiently large $k_\perp$





(Ducloué, Lappi, and Zhu, arXiv:1604.00225)

Stony Brook University | The State University of New York

"Long-range collectivity" in small systems

Jiangyong Jia, BNL and Stony Brook University

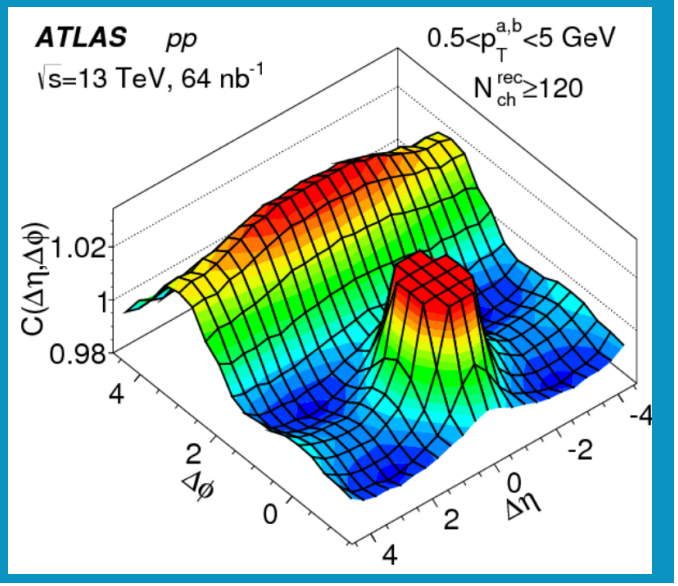
- What is collectivity?
- How to distinguish initial vs final state effects?

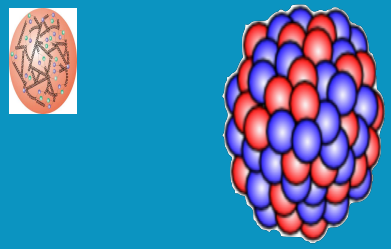


Long-range collectivity in different systems

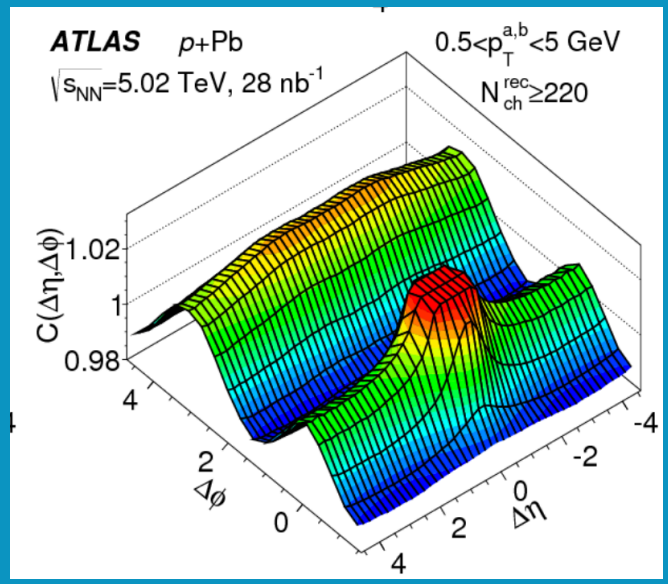


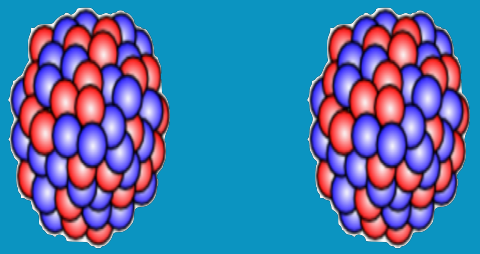
p+p



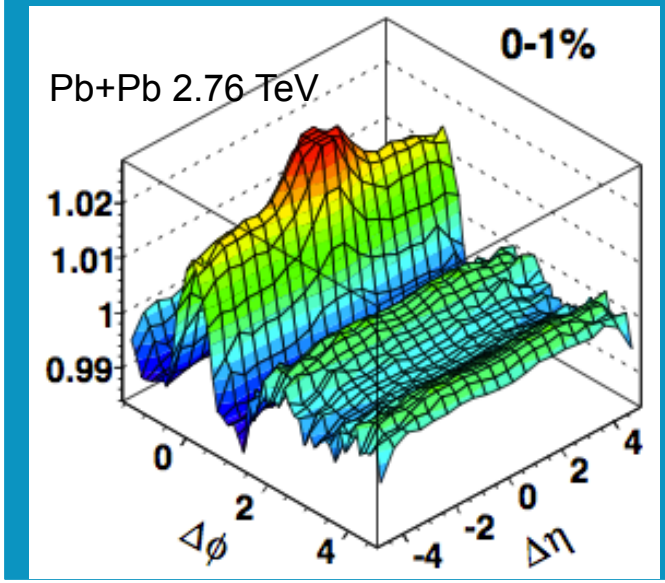


p+Pb





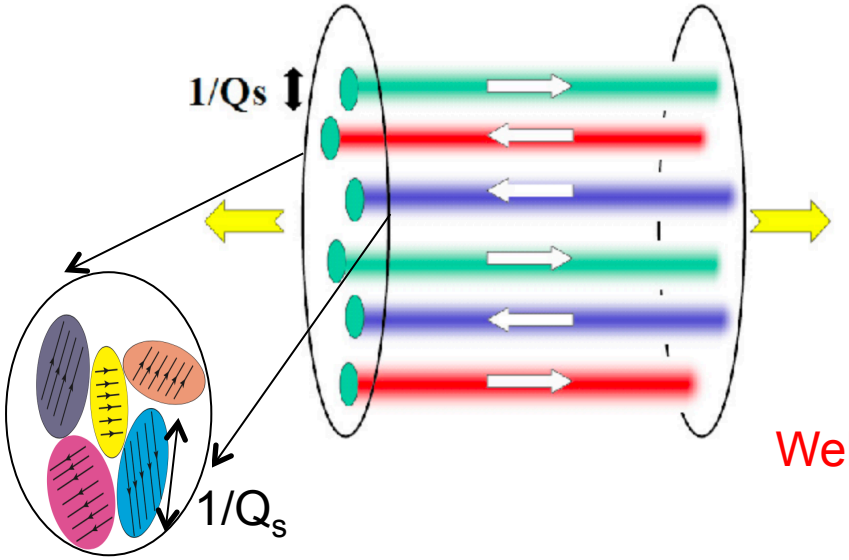
Pb+Pb



- Long-range correlation in momentum space comes
  - directly from early time t~0 (CGC)
  - or it is a final state response to spatial fluctuation at t=0 (hydro).

Examples of initial vs final state scenarios

CGC



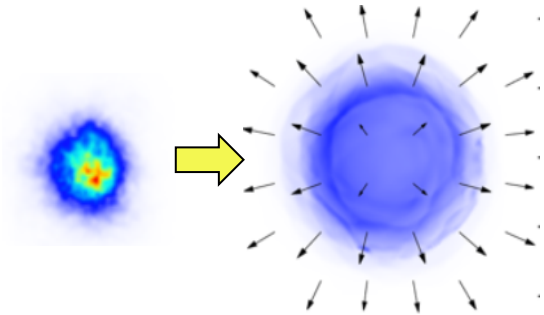
Domain of color fields of size $1/Q_s$, each produce multi-particles correlated across full η.

Uncorr. between domains, strong fluct. in Q_s

More domains, smaller v_n, more Q_s fluct, stronger v_n

Well motivated model framework, need systematic treatment

Hydro



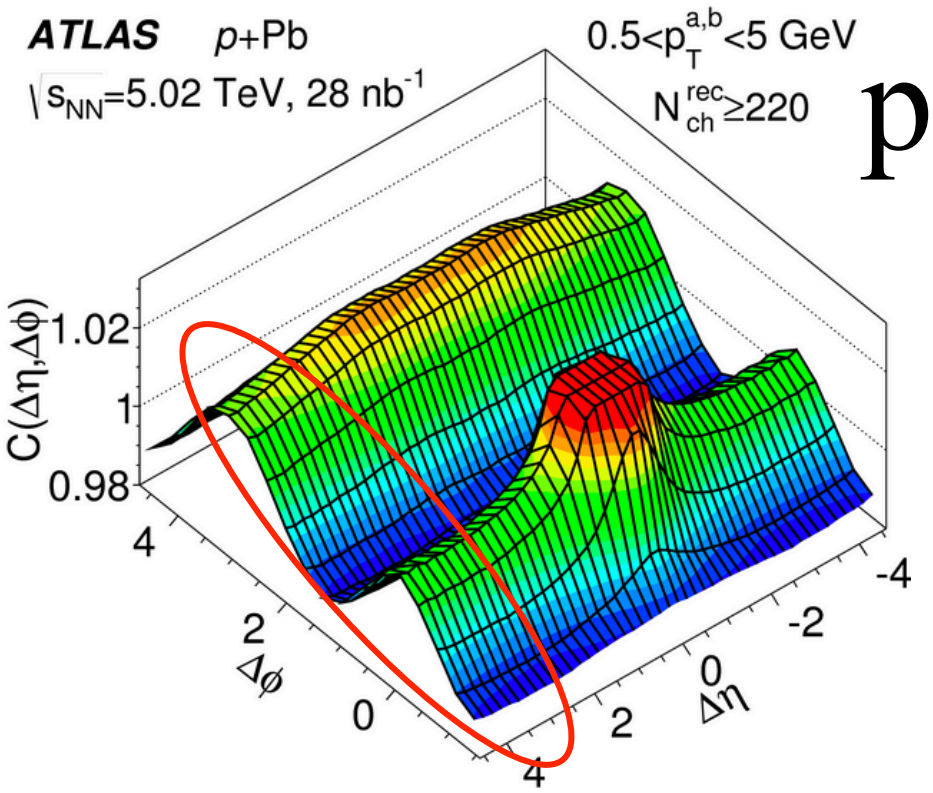
Hot spots (domains) in transverse plane e.g IP-plasma, boost-invariant geometry shape

Expansion and interaction of hot spots generate collectivity

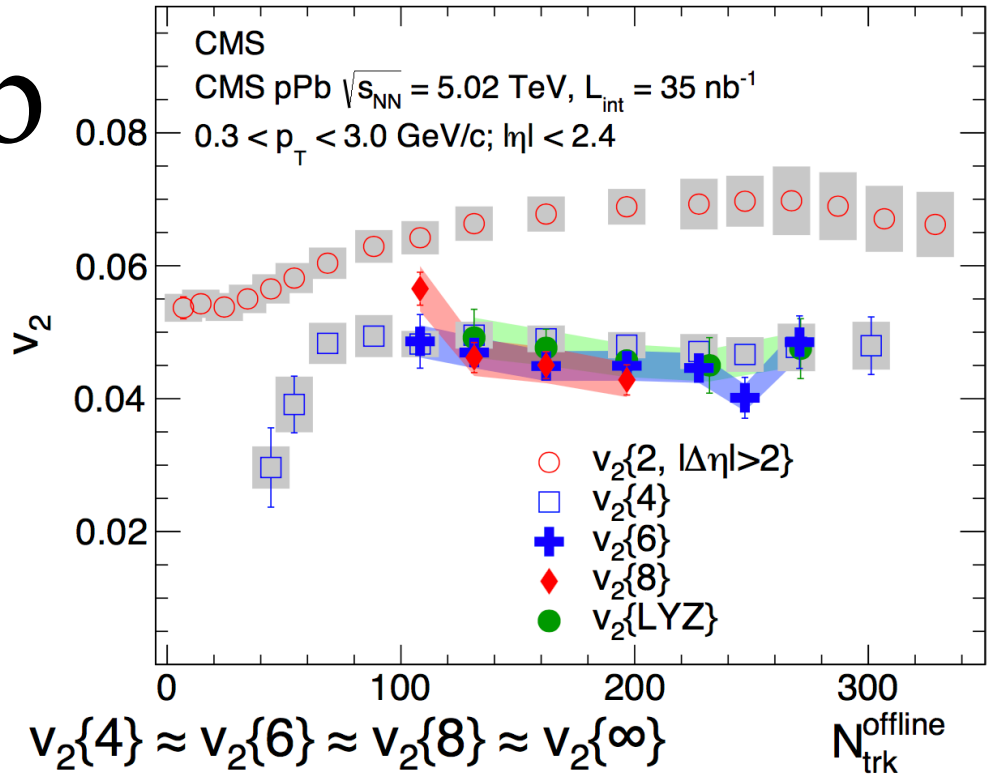
v_n depends on distribution of hot spots (ε_n) and transport properties.

Ongoing debate whether hydro is applicable in small systems

Features of collectivity in HM pPb



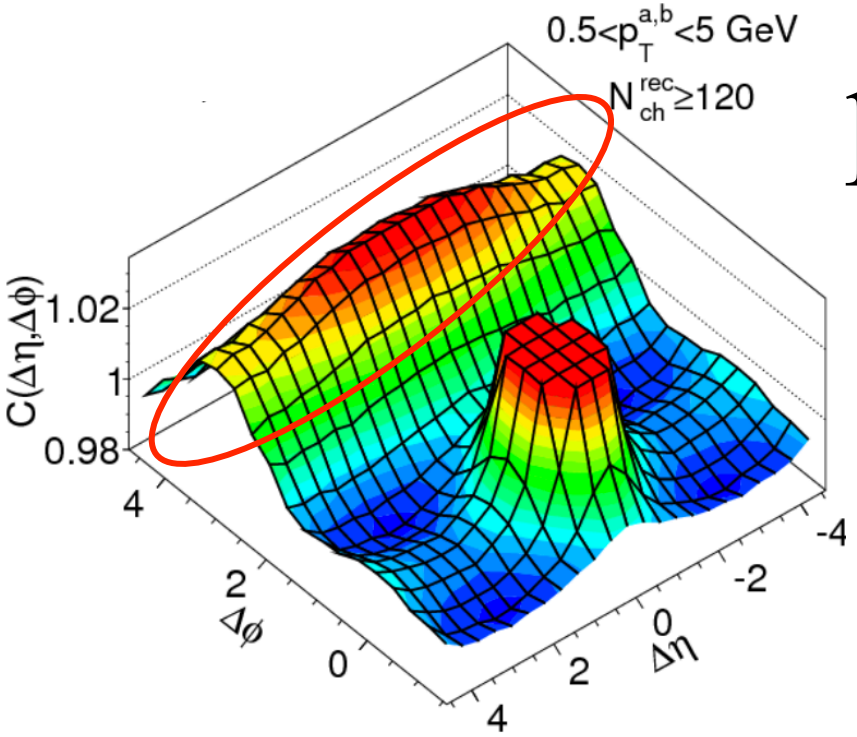
pPb



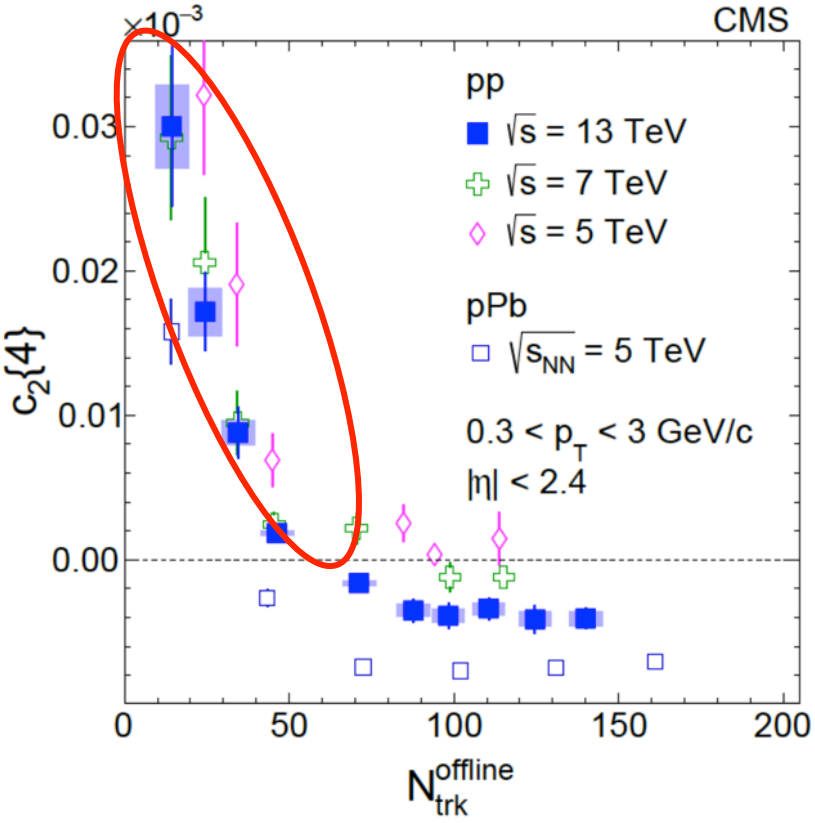
Long-range in η

Multi-particle signals

Features of collectivity in HM pp



pp



Long-range in η

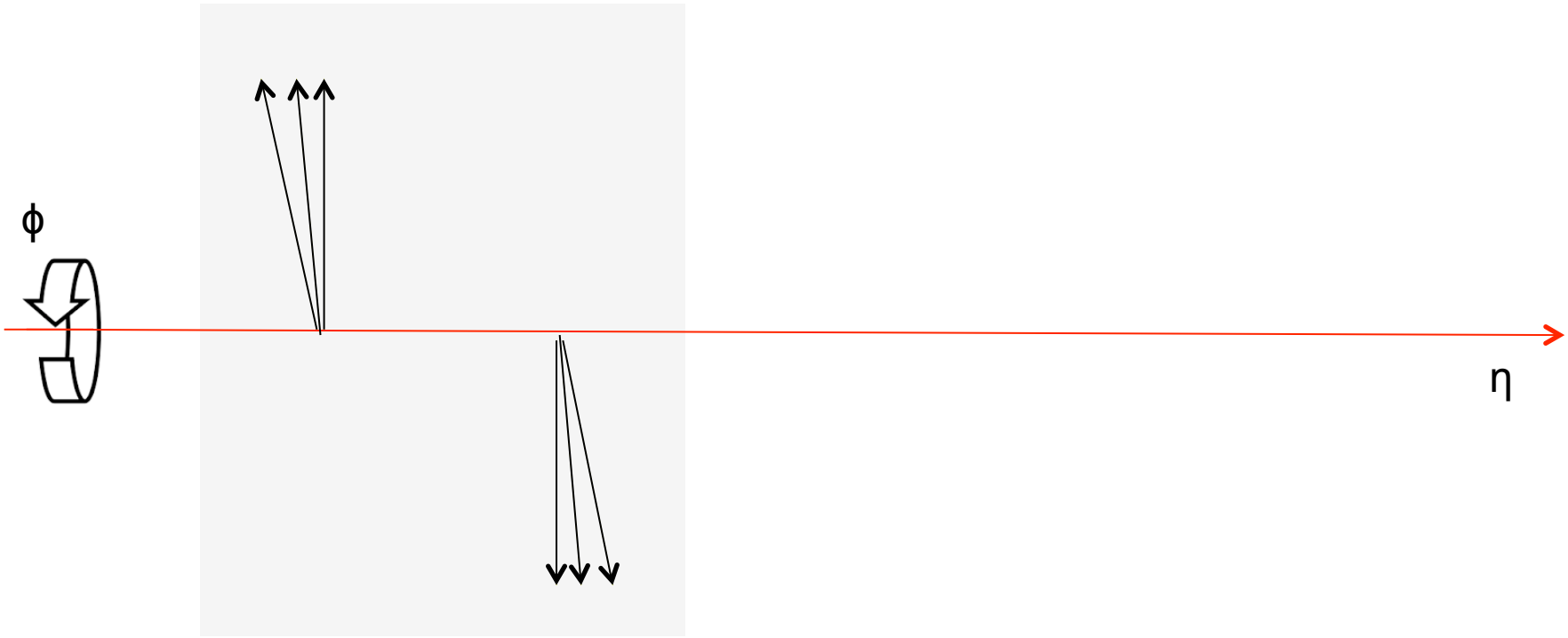
Multi-particle signals

Non-flow can generate long-range (away-jet) or multi-particle correlation (fragmentation) but not both

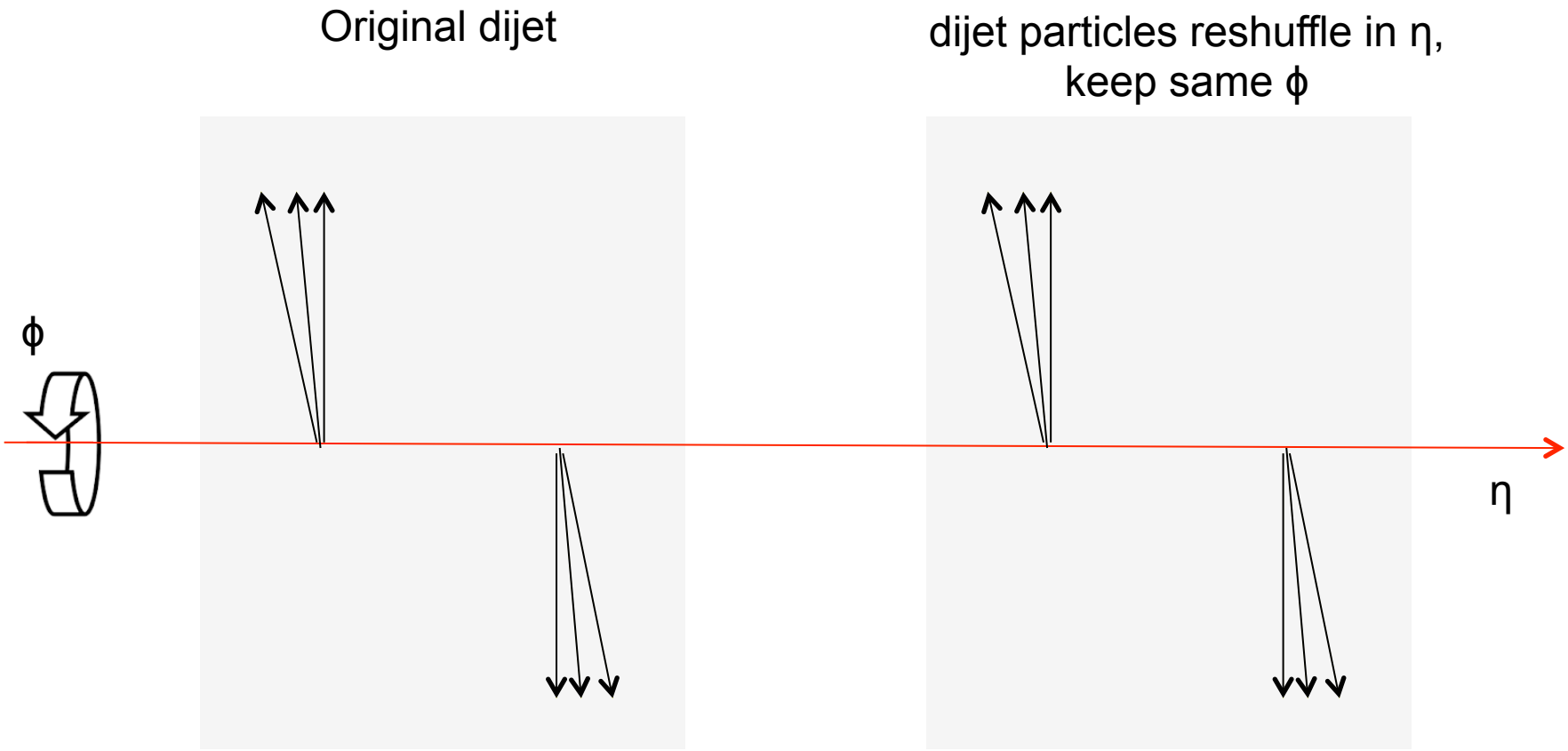
Collectivity must mean both

Azimuthal correlation from collectivity

Original dijet



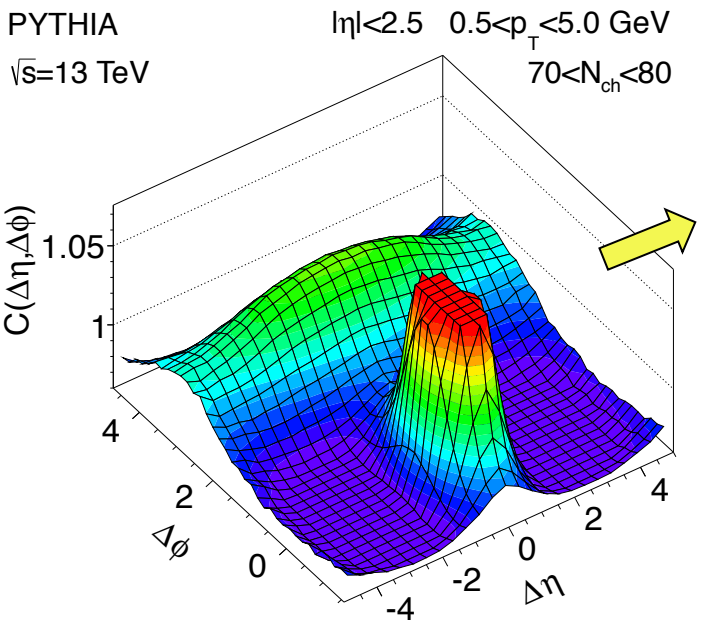
Azimuthal correlation from collectivity

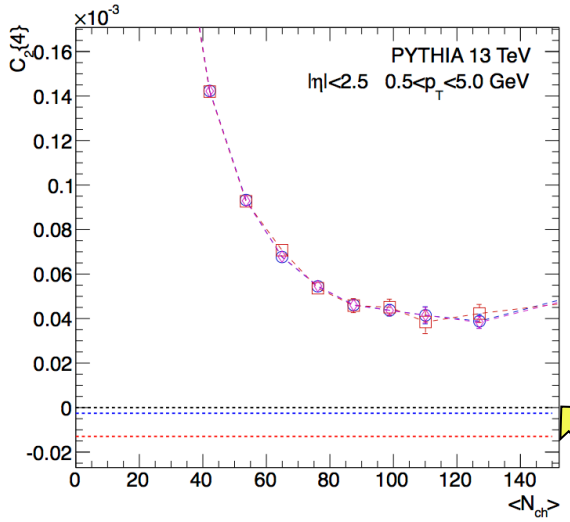


They give the same flow coefficient $c_n\{4\}$ and $v_n\{4\}$, although clearly the first case is non-flow and the second case would be classified as flow

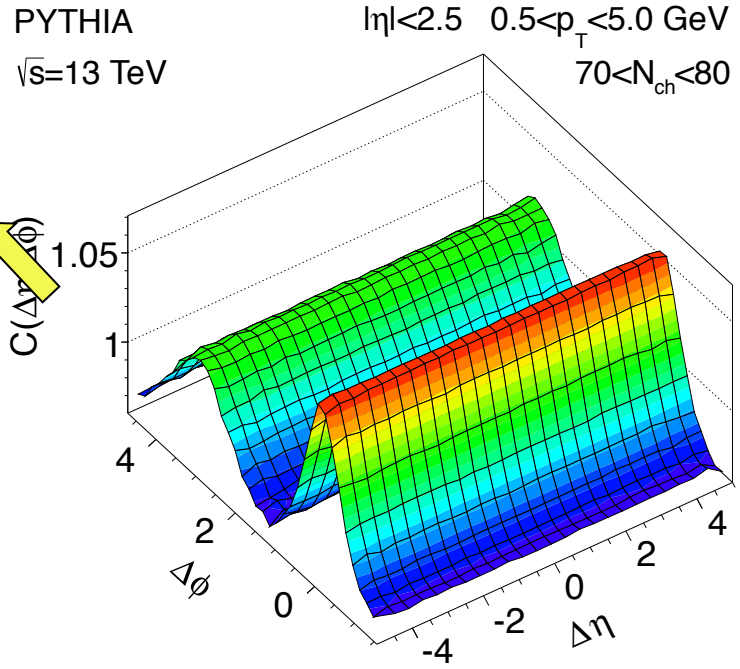
Azimuthal correlation from collectivity

original





η reshuffled



By mingliang Zhou

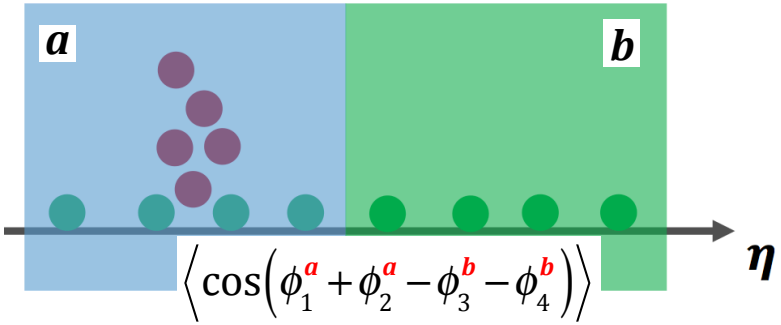
They give the same flow coefficient $c_n\{4\}$ and $v_n\{4\}$, although clearly the first case is non-flow and the second case would be classified as flow

Azumuthal corr. alone can't distinguish flow & non-flow.

Long-range collectivity via subevent cumulants

arXiv:1701.03830

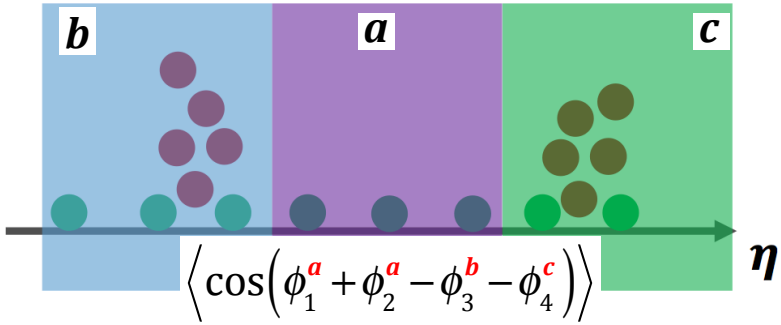
Event with jet



2 sub-event

removes intra-jet correlations

Event with dijet



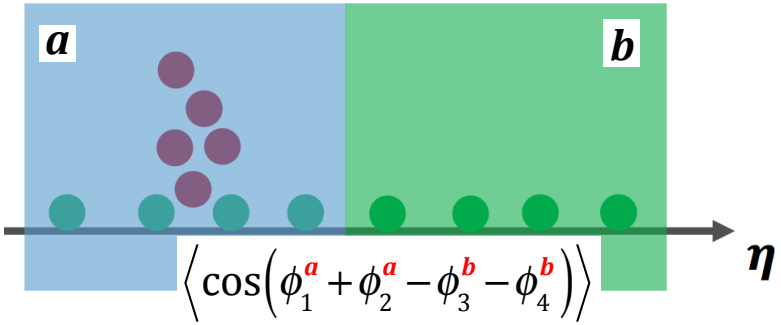
3 sub-event

removes inter-jet correlations

Long-range collectivity via subevent cumulants

arXiv:1701.03830

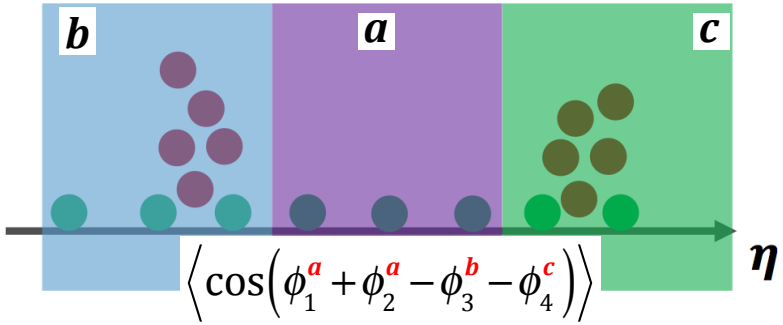
Event with jet



2 sub-event

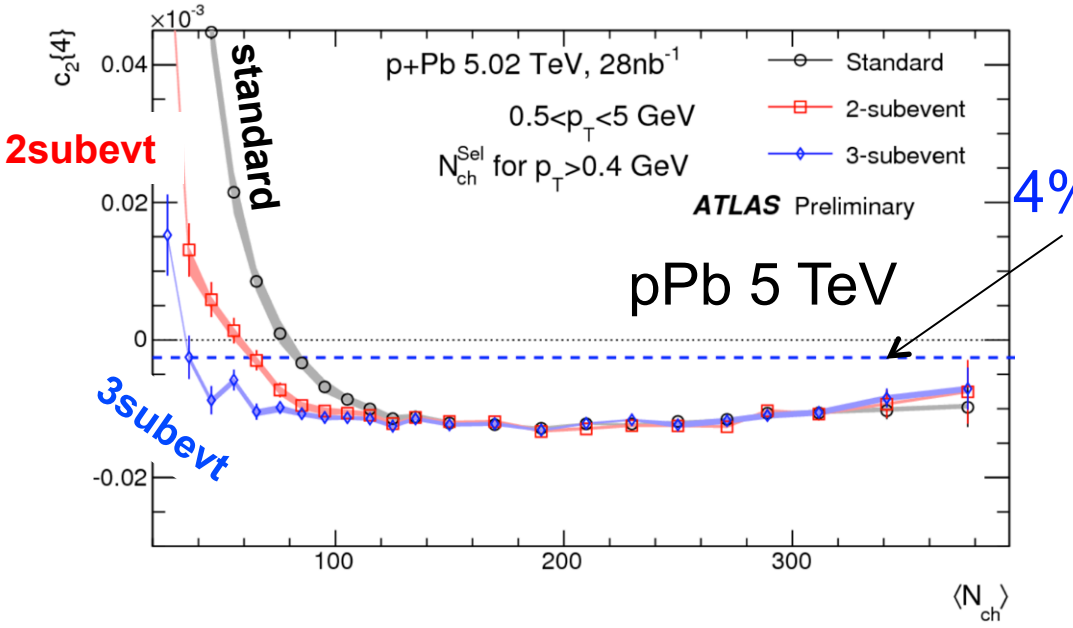
removes intra-jet correlations

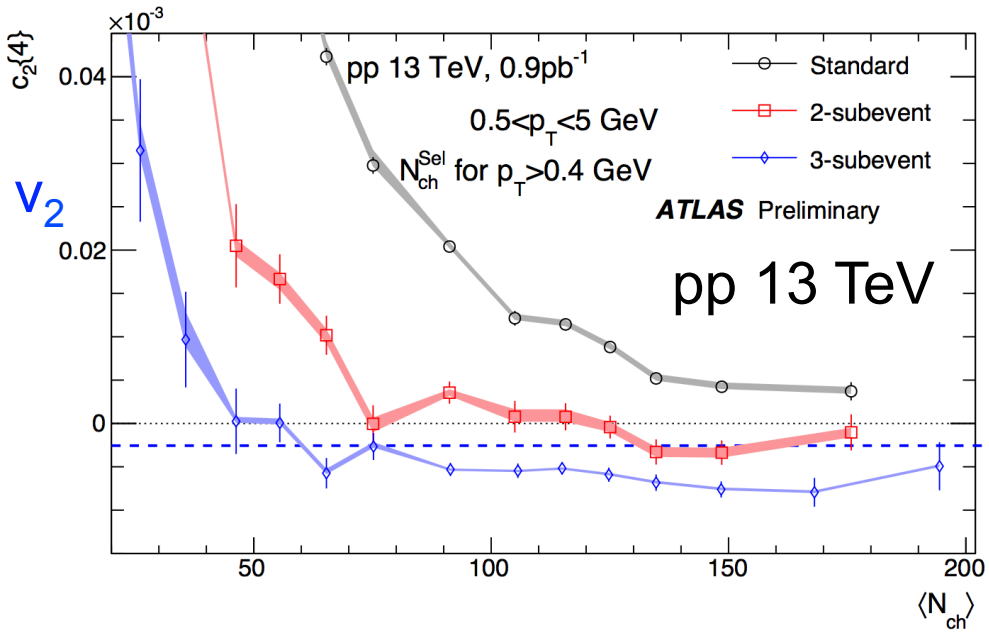
Event with dijet



3 sub-event

removes inter-jet correlations



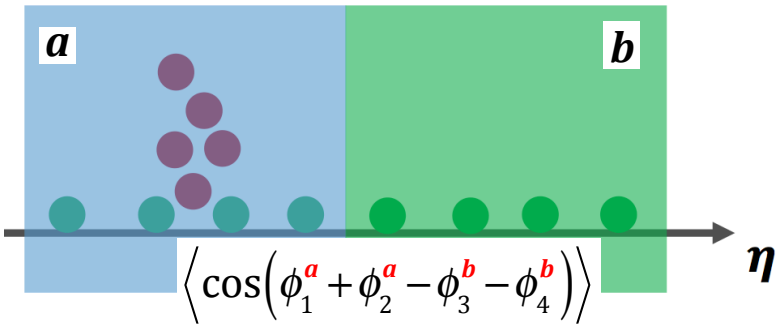


pPb: methods consistent for N_{ch}>100, but split below that

Long-range collectivity via subevent cumulants

arXiv:1701.03830

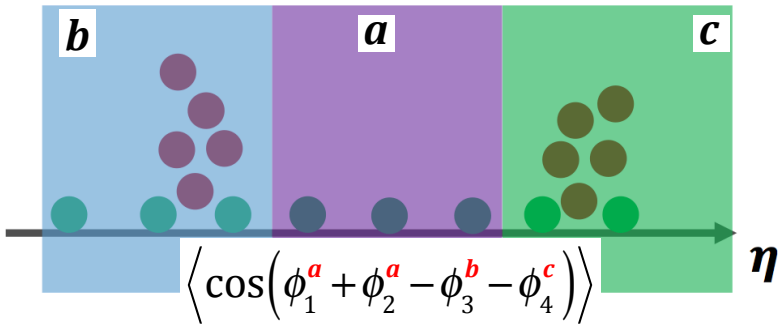
Event with jet



2 sub-event

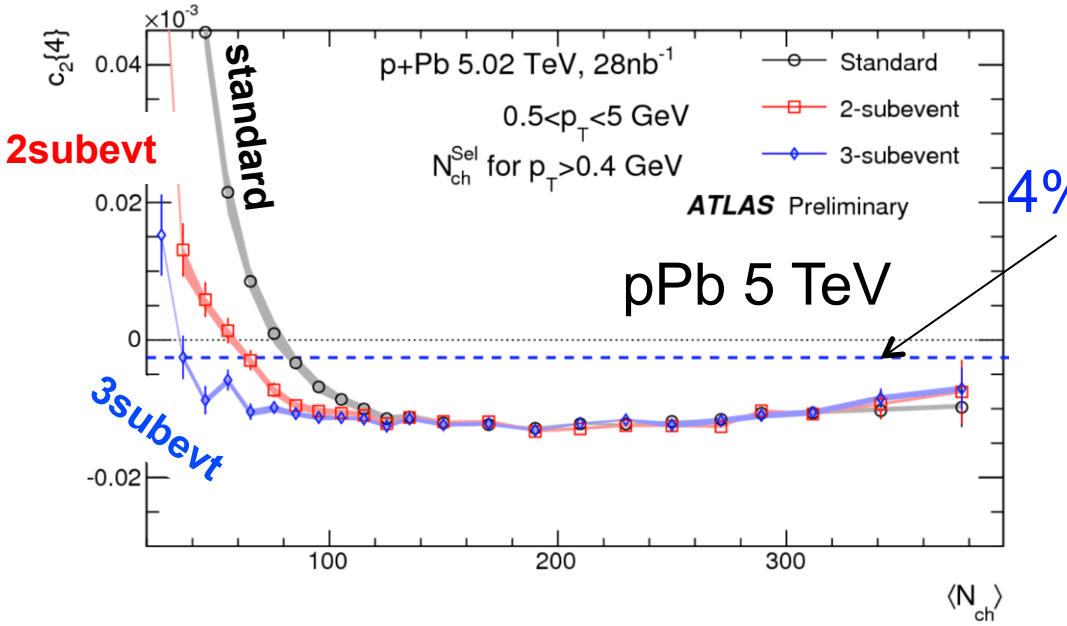
removes intra-jet correlations

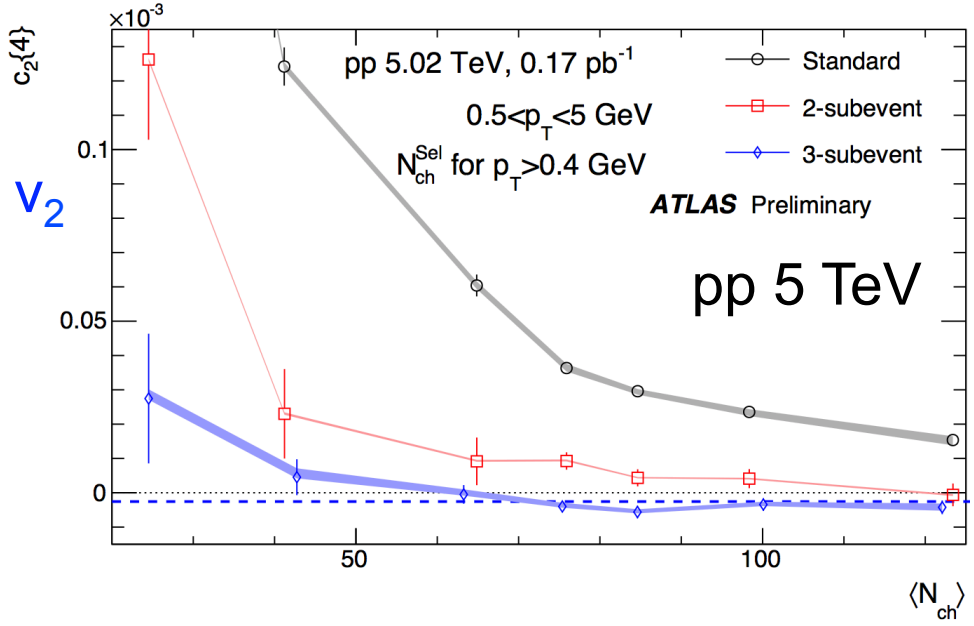
Event with dijet



3 sub-event

removes inter-jet correlations





pPb: methods consistent for N_{ch}>100, but split below that

Only subevent method gives negative $c_2\{4\}$ in broad range of N_{ch}

Sign-change of $c_2\{4\}$

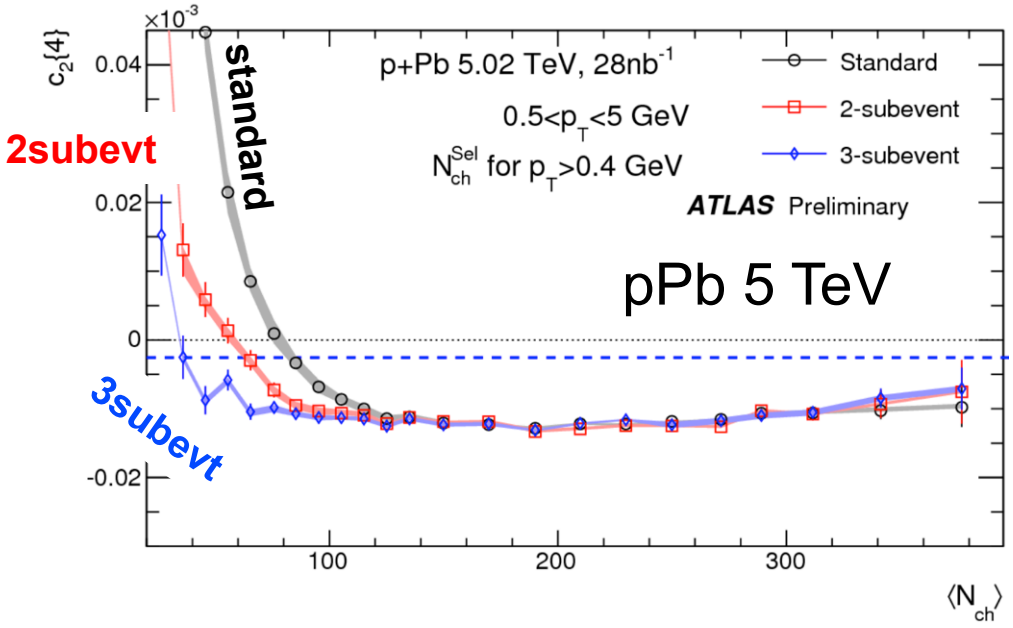
- Most positive $c_2\{4\}$ in standard cumulants are jets and dijets.
  - Remaining positive $c_2\{4\}$in 3-subevent due to residual dijets.
- CGC expect sign change at low N_{ch}

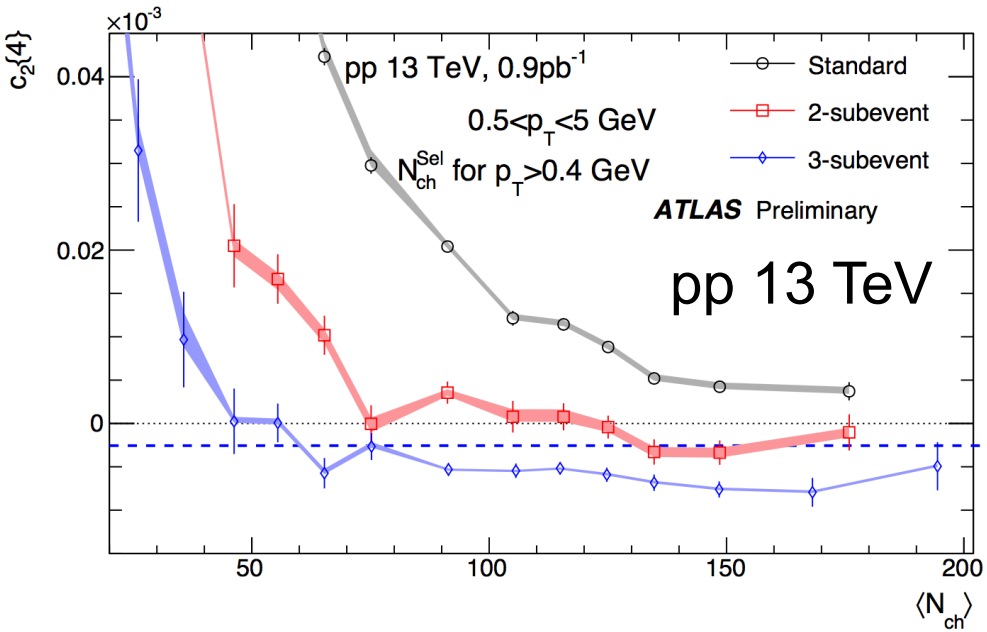
Dumitru,McLerran,Skokov

$$c_2\{4\} = \frac{1}{N_D^3}\left(\frac{1}{4(N_c^2-1)^3} - A^4\right)$$

Glasma diagram

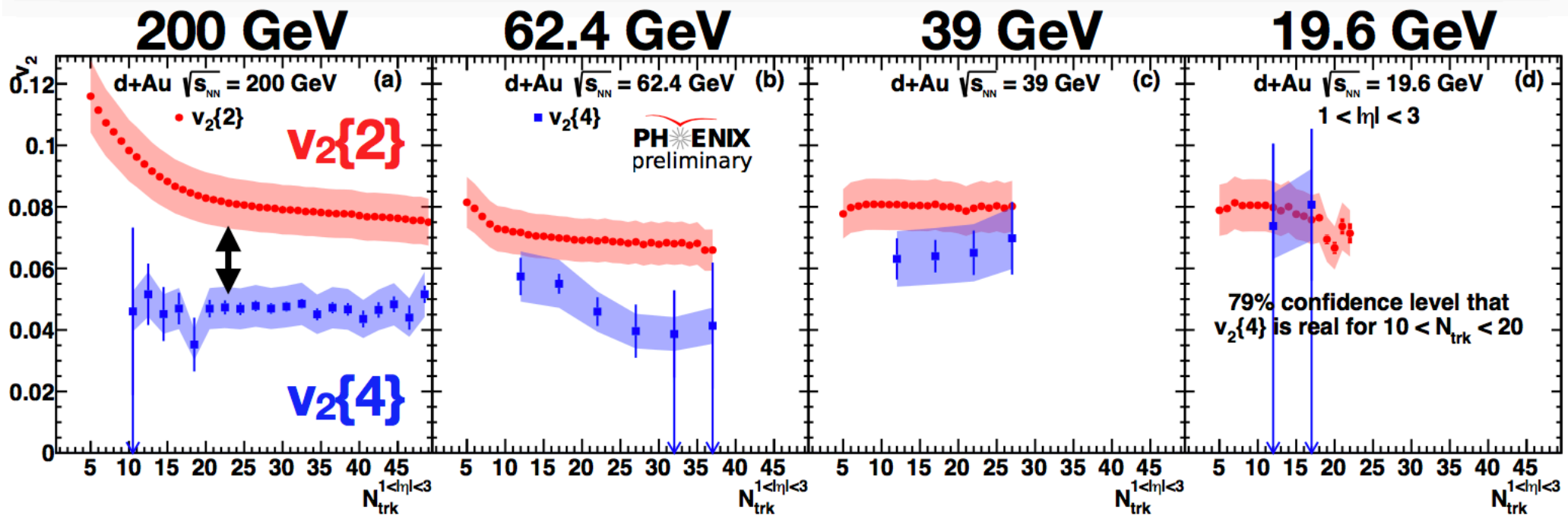
non-linear/non-Gaussian effects





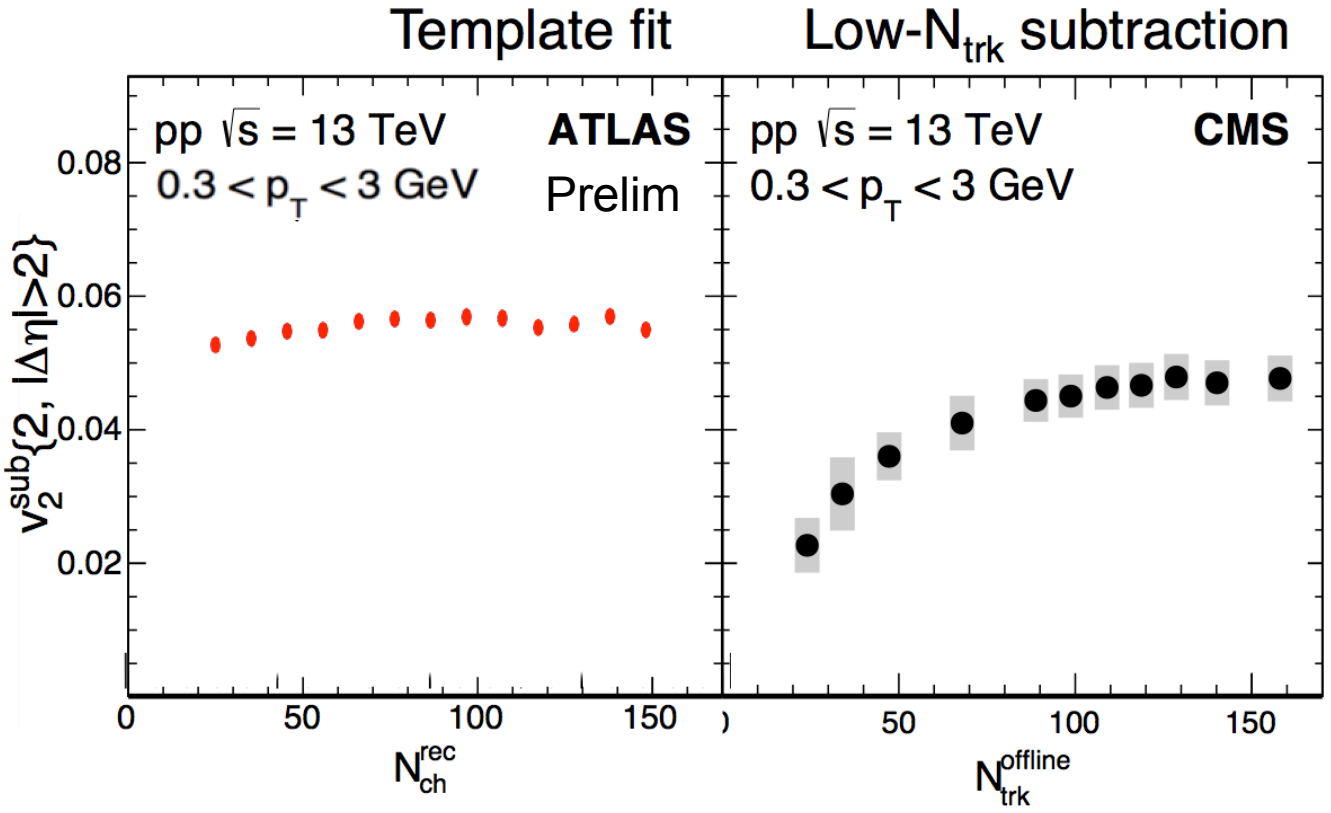
Glasma diagram contribution is small?

√s dependence of $c_2\{4\}$ at RHIC



- Surprising features: $v_2\{4\}$ larger at lower √s, reaching $v_2\{2\}$.
- Difficult to describe in both CGC and hydro
- Important to understand non-flow in standard cumulant method

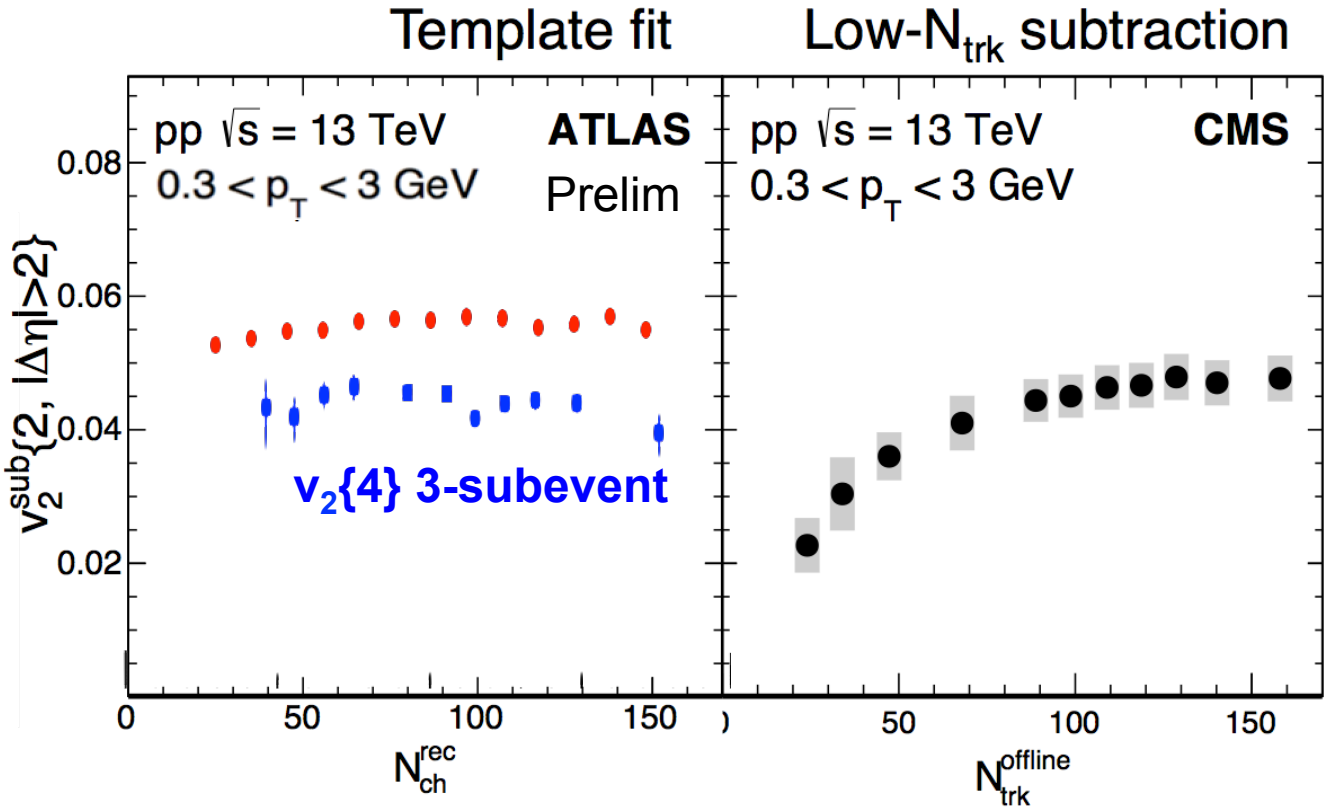
Does collectivity turn off at low N_{ch}?



peripheral subtraction including peripheral pedestal (assuming the peripheral also has flow)
→so called template fit

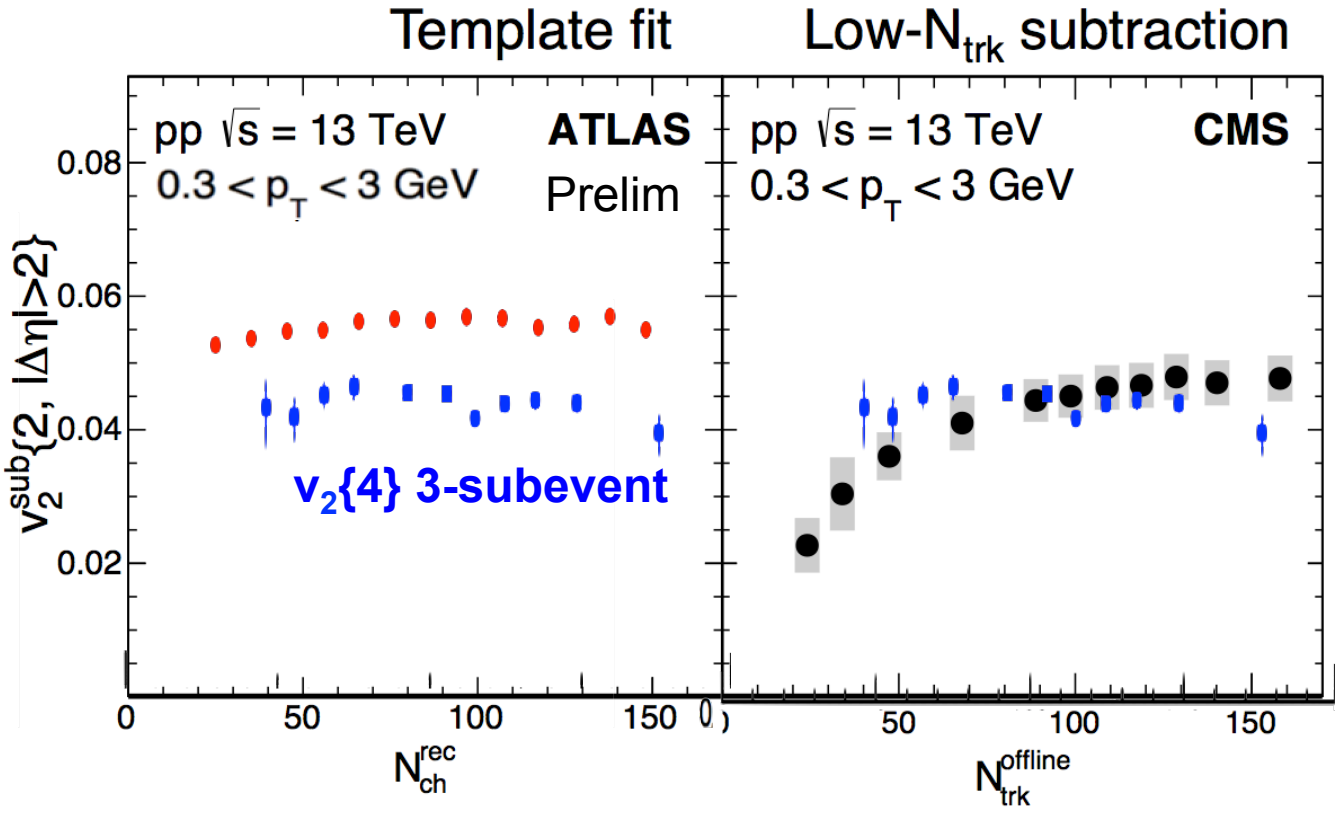
peripheral subtraction not including peripheral pedestal (assuming the peripheral has no flow)
→ so call peripheral sub.

Does collectivity turn off at low N_{ch}?



- $v_2\{4\}$ from 3-subevent show no dependence on N_{ch}.

Does collectivity turn off at low N_{ch}?



- $v_2\{4\}$ from 3-subevent show no dependence on N_{ch}.
- Why $v_2\{2\}_{\text{peri. sub}} \approx v_2\{4\}$ in pp? surprising because:

$$v_n\{2\}^4 - v_n\{4\}^4 = \langle v_n^4 \rangle - \langle v_n^2 \rangle^2 = \langle (v_n^2 - \langle v_n^2 \rangle)^2 \rangle \geq 0$$

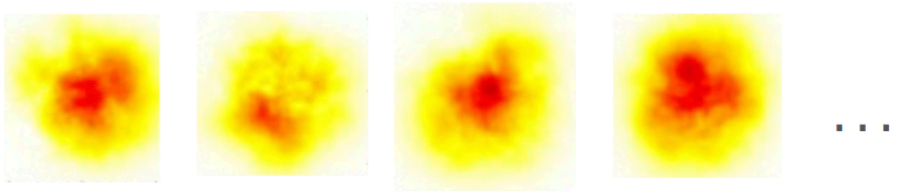
$v_2\{4\}$ also show No hint of collectivity turning-off at low N_{ch}!

Challenge both CGC and standard hydro?

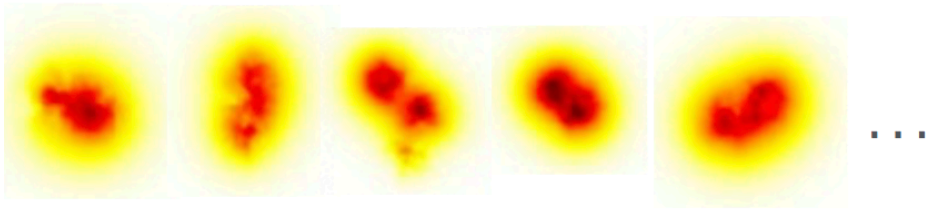
Role of initial geometry is very different

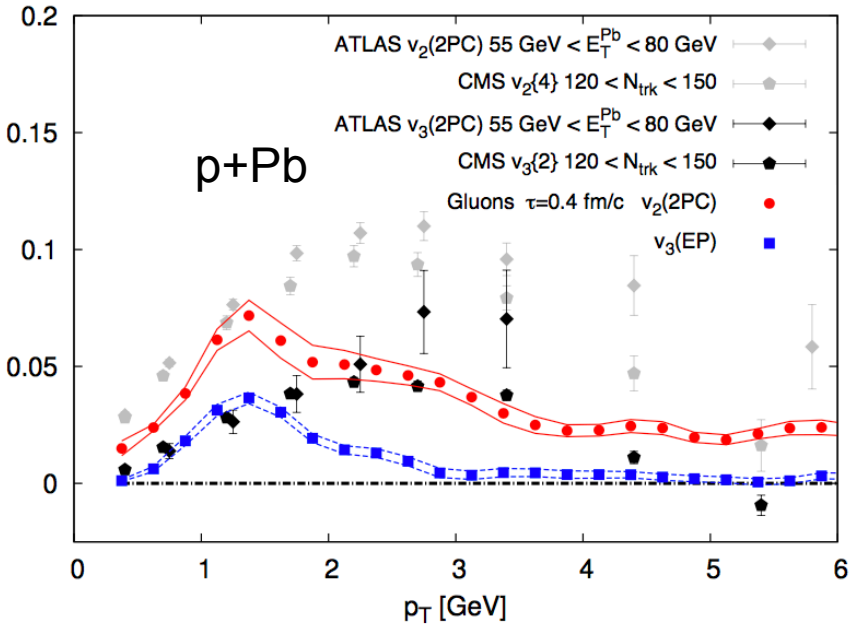
From Schenke, Schlichting, Venugopalan,

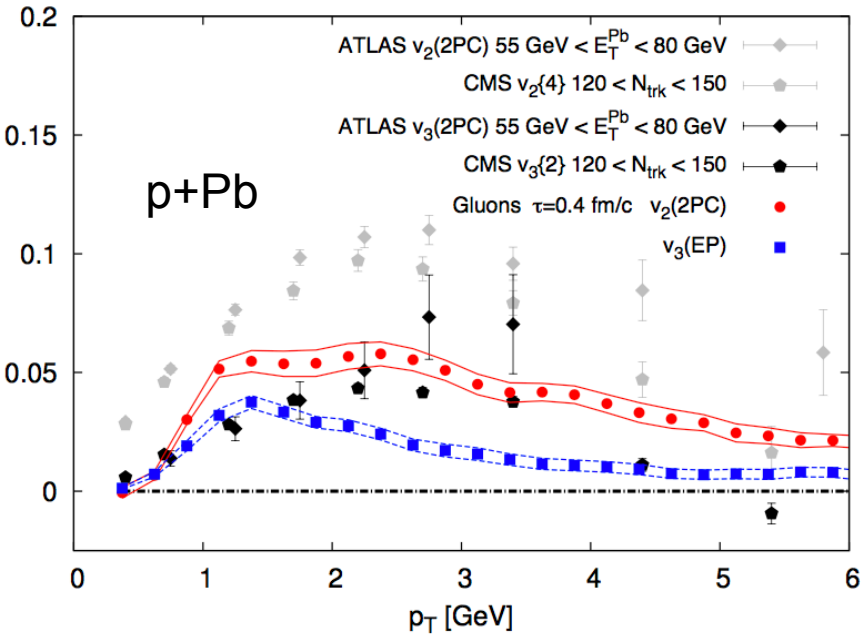
'Spherical' proton



'Eccentric' proton





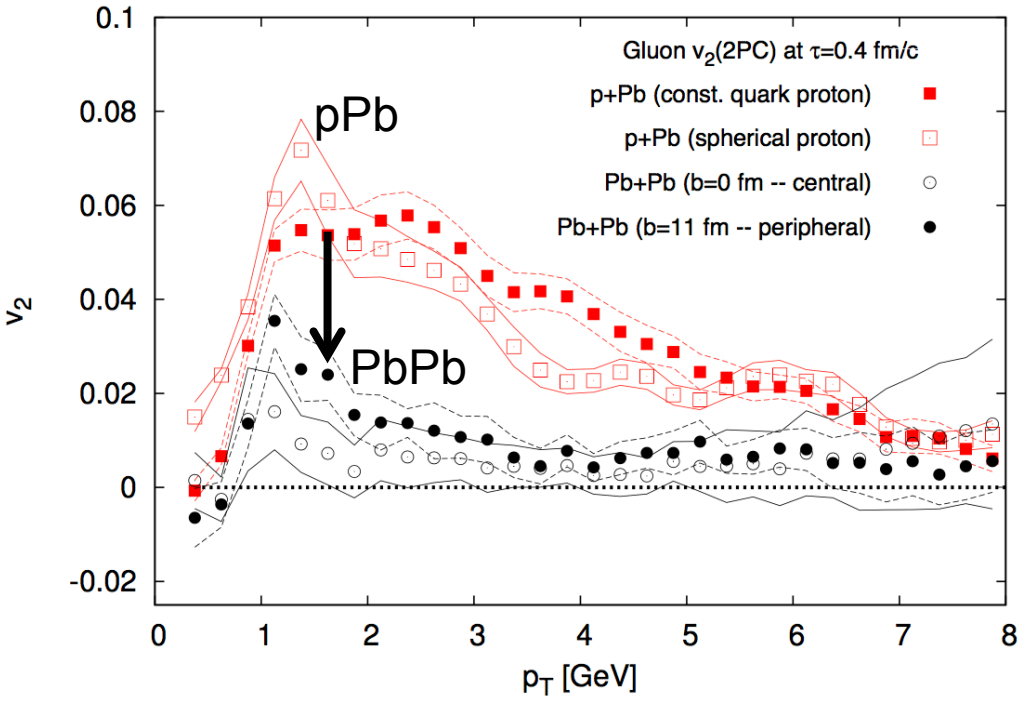


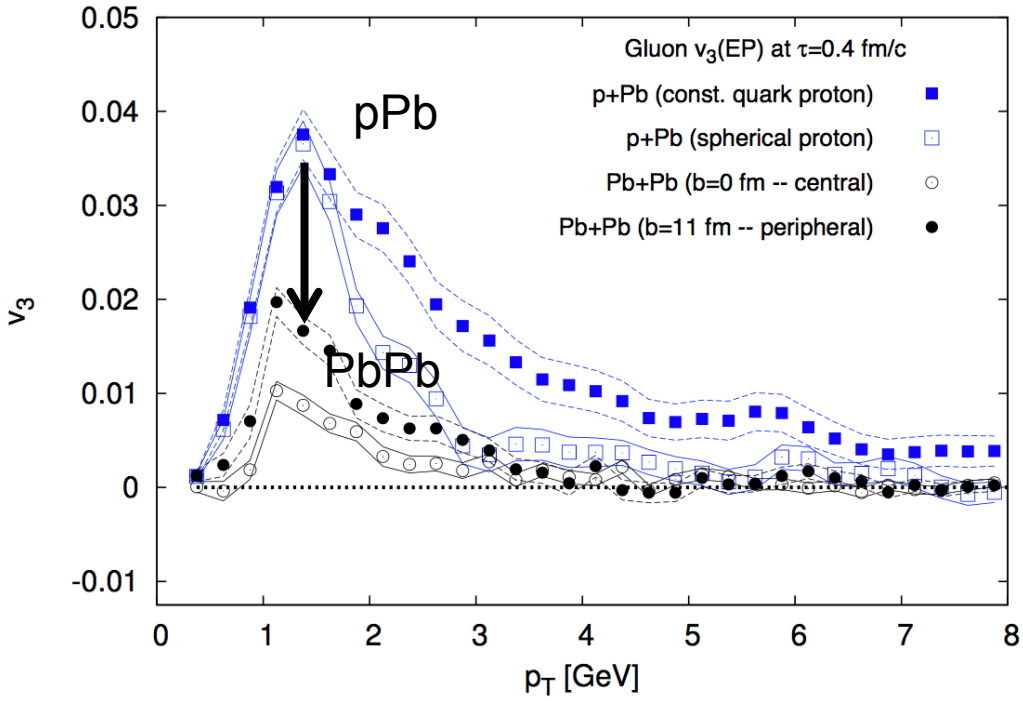
The orientation of collectivity is unrelated to initial eccentricity

→Very different from hydrodynamics

Role of initial geometry is very different

From Schenke, Schlichting, Venugopalan,



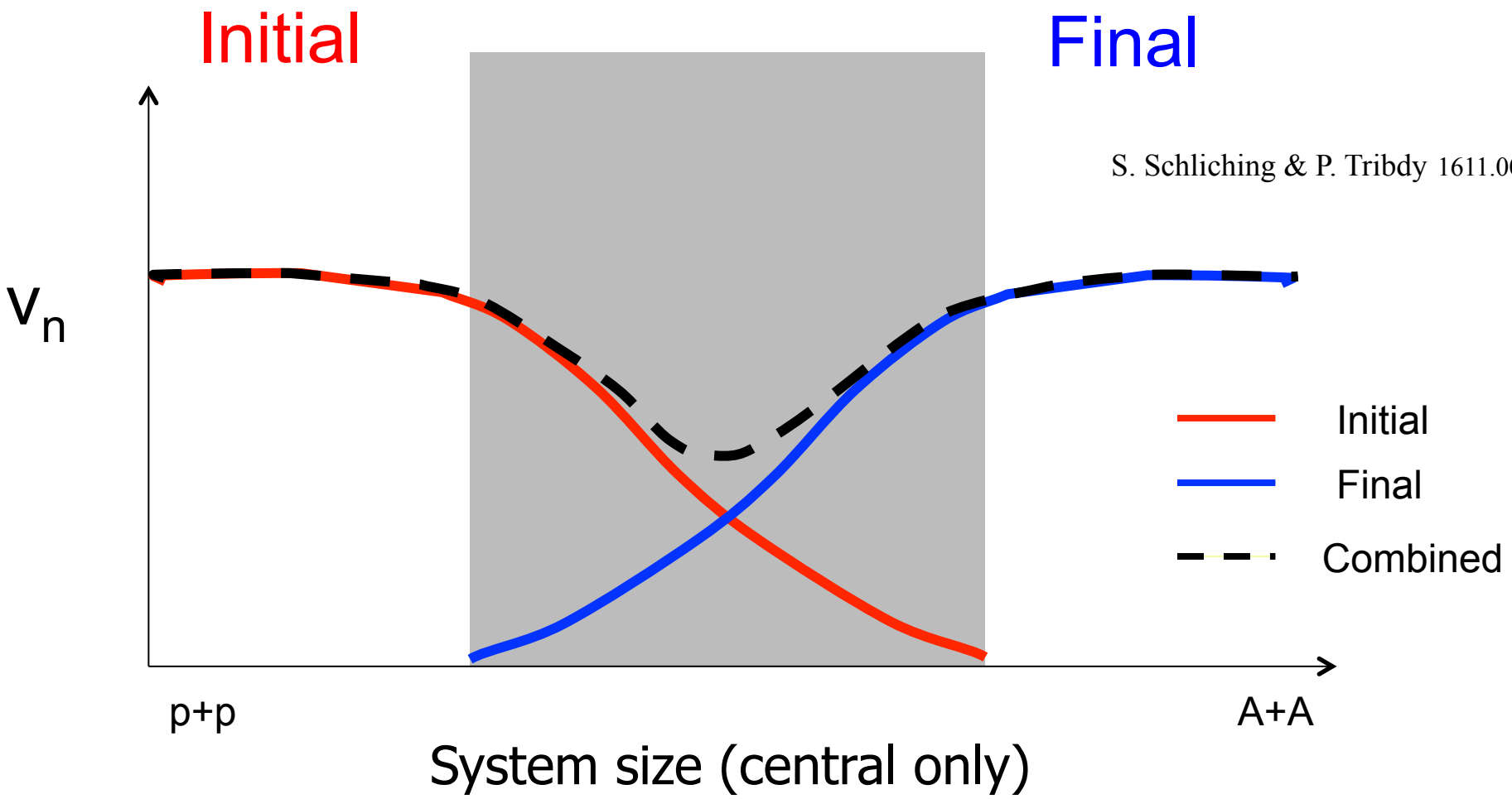


The orientation of collectivity is unrelated to initial eccentricity

→Very different from hydrodynamics

Expect contribution diminish as system size is increased

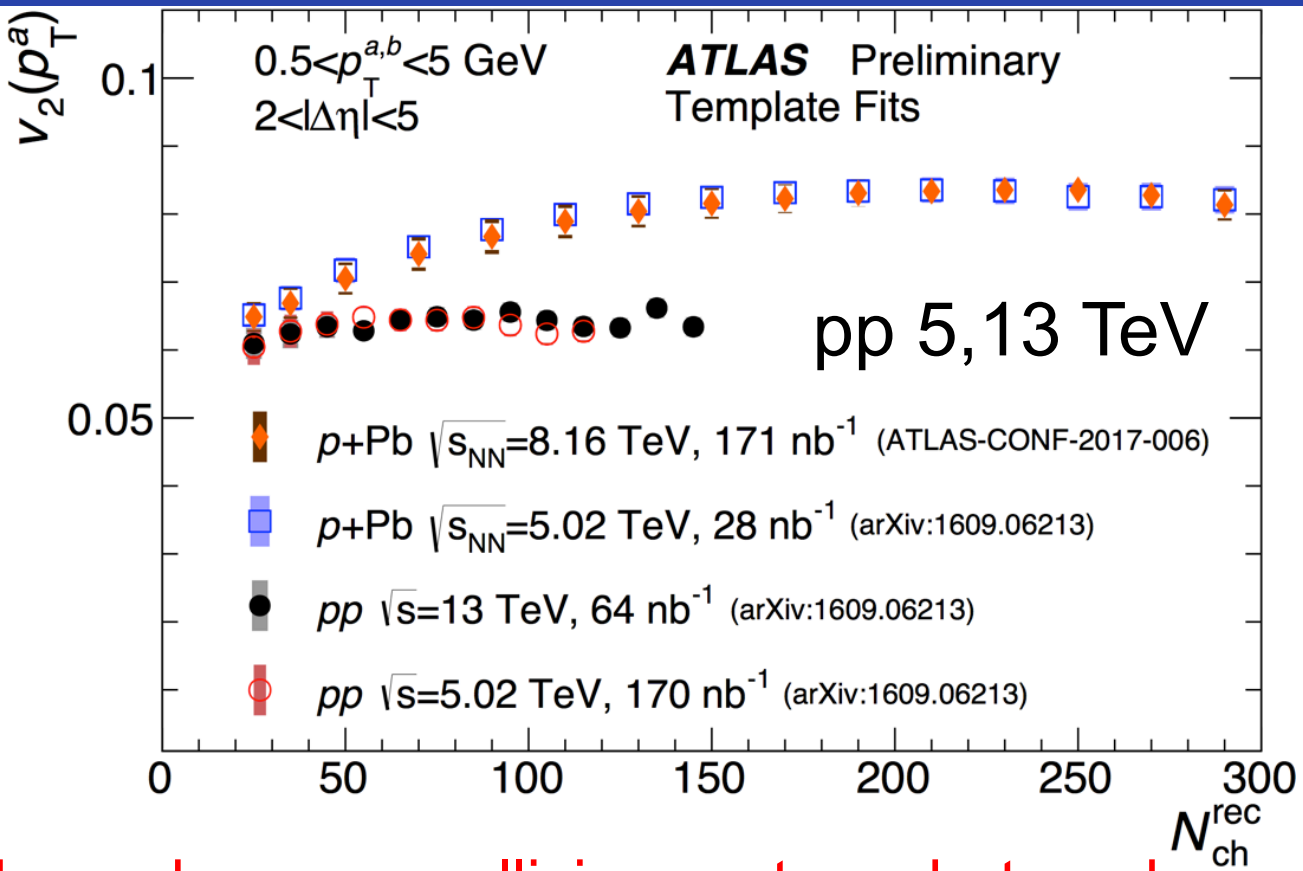
Presence of both initial and final state scenarios?



Phases of collectivity from CGC and hydro are unrelated

→ a minimum of total v_n at certain system size?

System size dependence

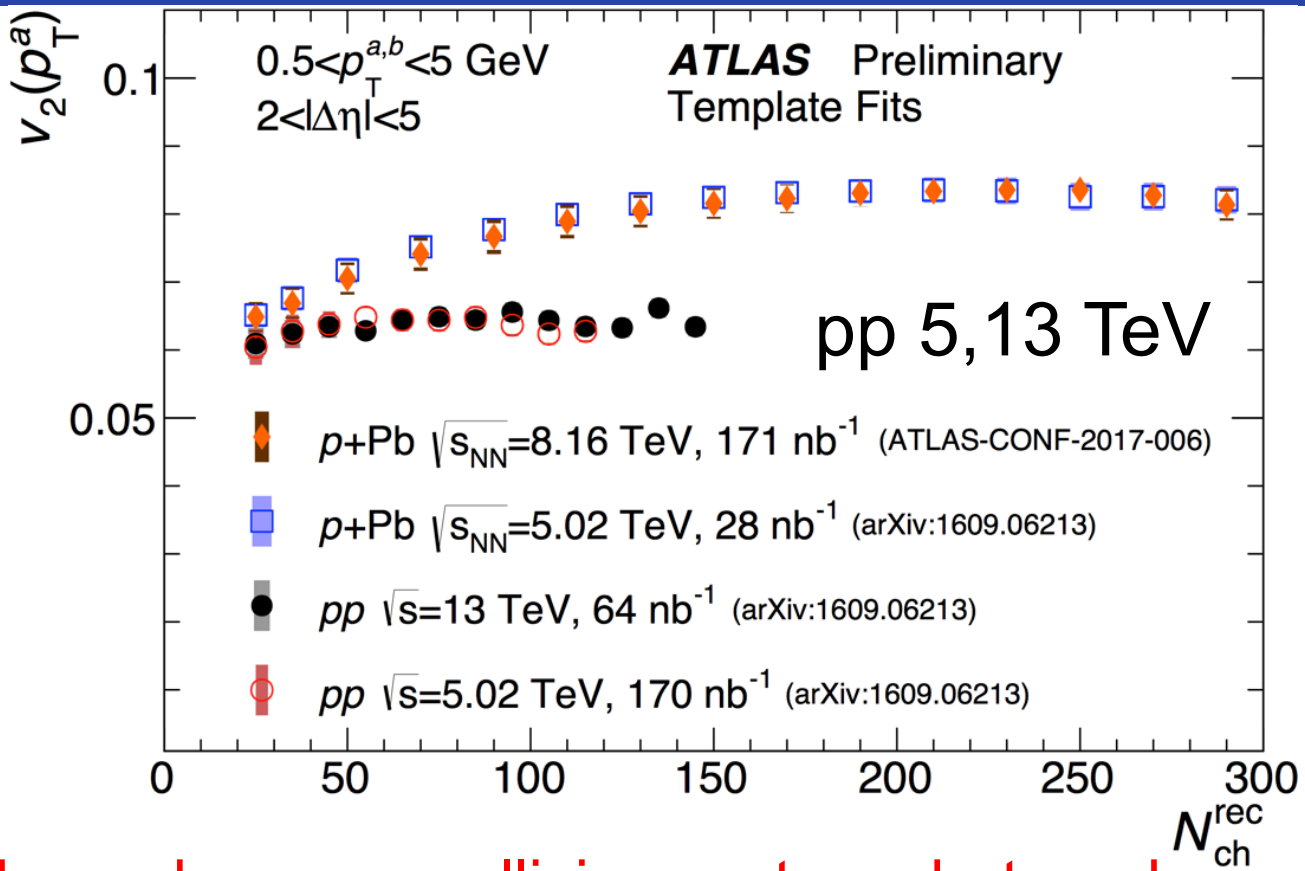


pPb 5,8 TeV

Clear dependence on collision systems but no dependence on √s

v_2^{pp} (high-mul)<v_2^{pPb}(low-mul)!

System size dependence



pPb 5,8 TeV

Clear dependence on collision systems but no dependence on √s

v_2^{pp} (high-mul)<v_2^{pPb}(low-mul)!

CGC — Unclear if the pp/pPb hierarchy is expected.

Hydro — Interplay between viscous damping and initial ε_n
pPb: may seen an average geometry effect
pp: geometry maybe poorly correlated with N_{ch}.

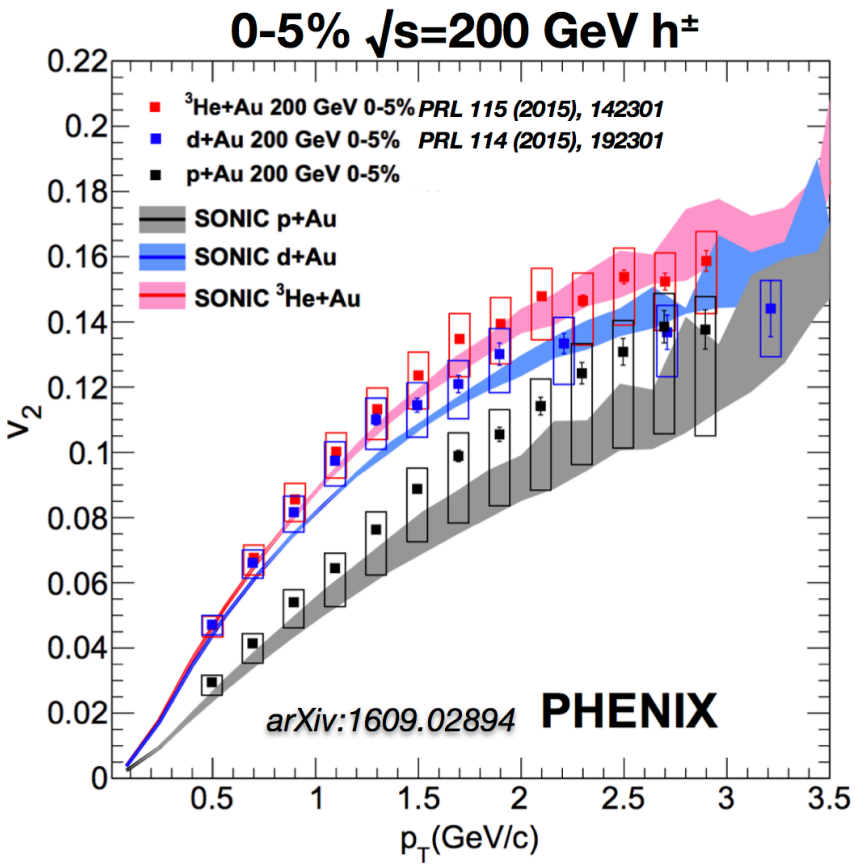
Kevin Welsh, Jordan Singer, and Ulrich Heinz 1605.09418

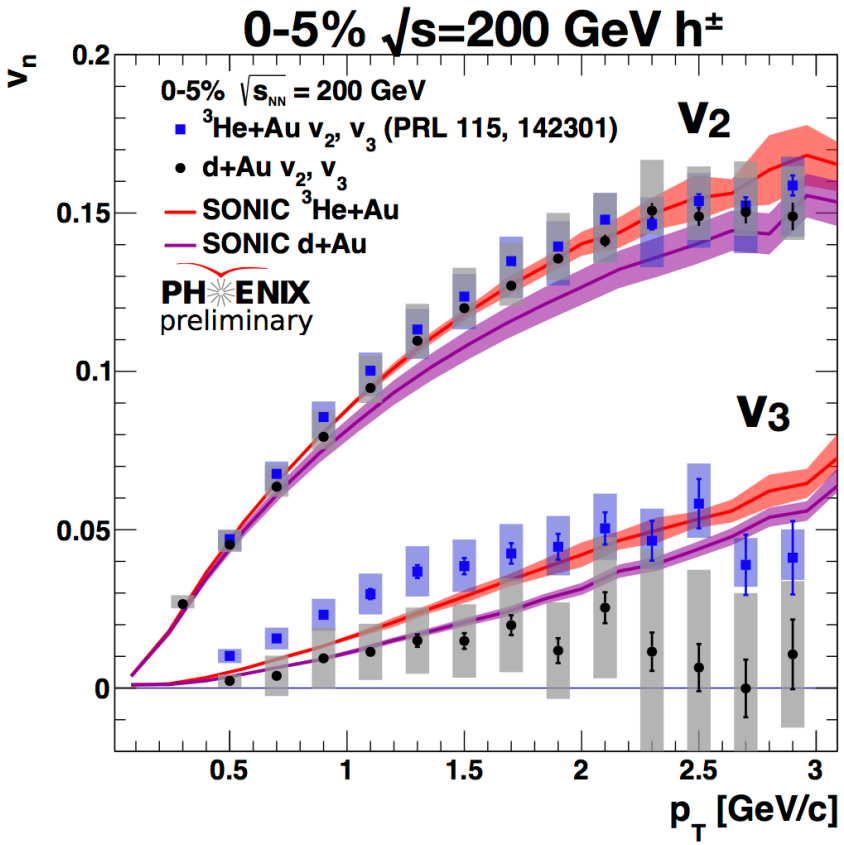
Geometry scan at RHIC

p+Au 2015

d+Au 2016

^{3}He+Au 2014





$v_2^{pAu} < v_2^{dAu} \leq v_2^{HeAu}$

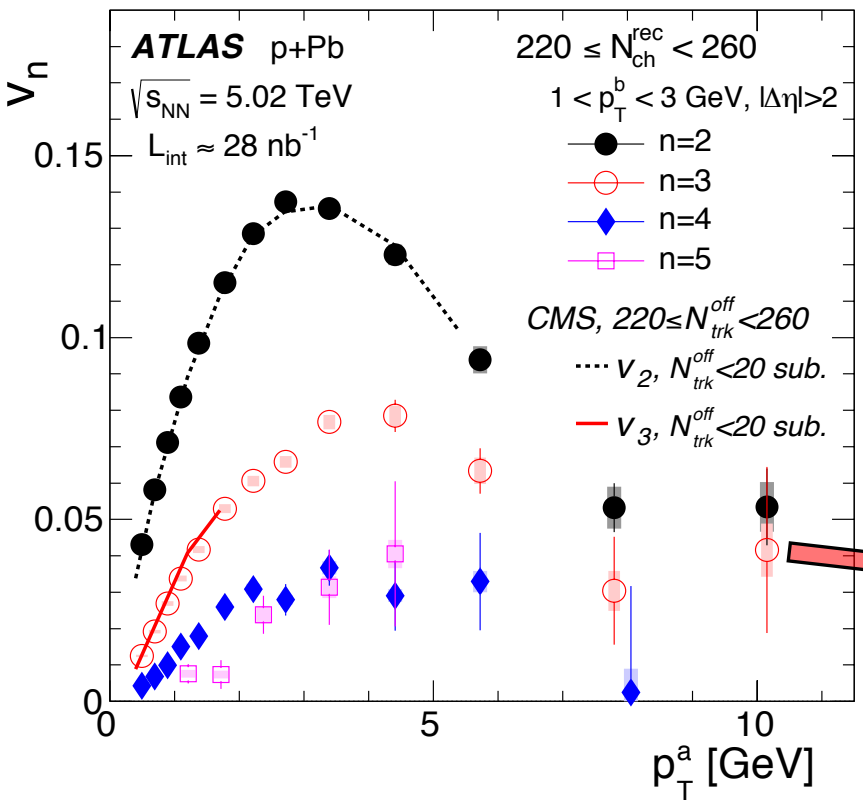
$v_3^{dAu} < v_3^{HeAu}$

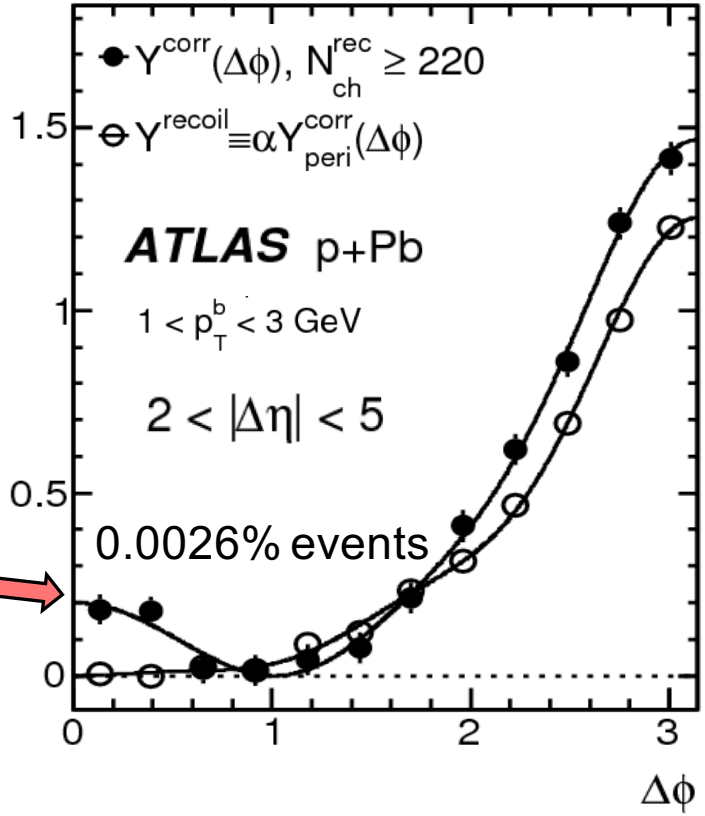
Hierarchy compatible with initial geometry + final state effects

Look forward to the CGC predictions

Original of high-p_T v_2?

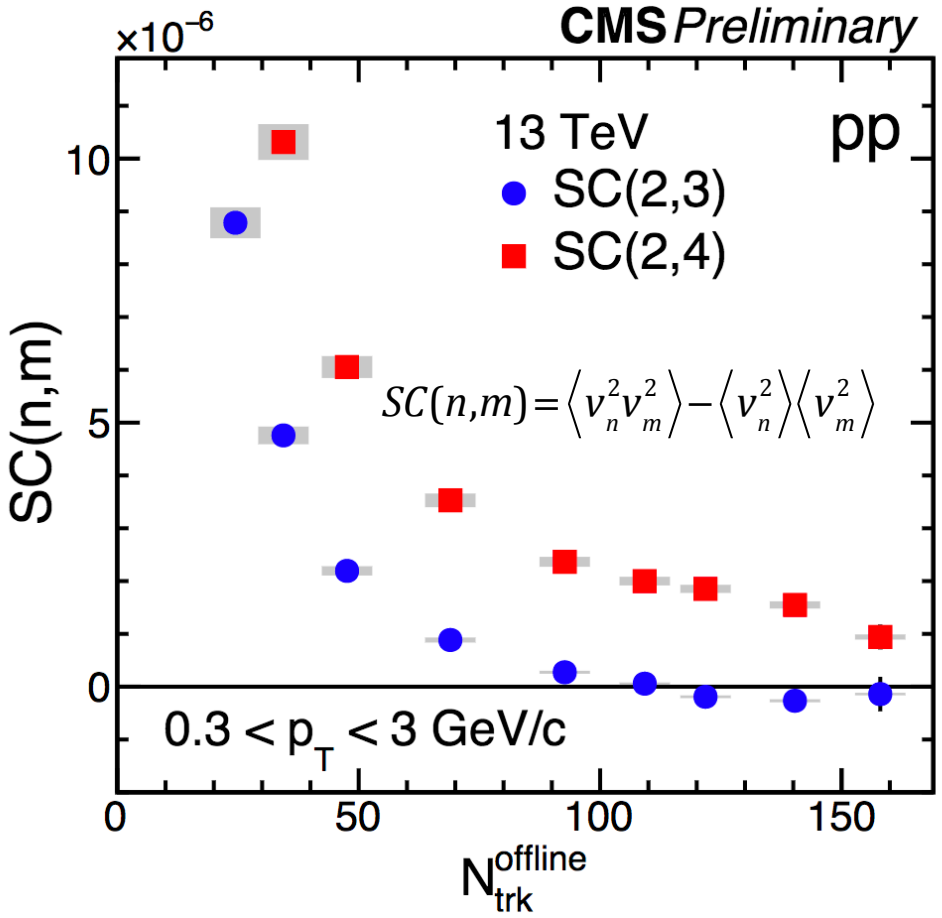
- Ridge seen directly at 10 GeV or 5% v_2 in pPb
  - →final state effects, e.g. jet quenching (better observable than R_{AA})?
  - →initial state effects, rare Q_s fluctuation?

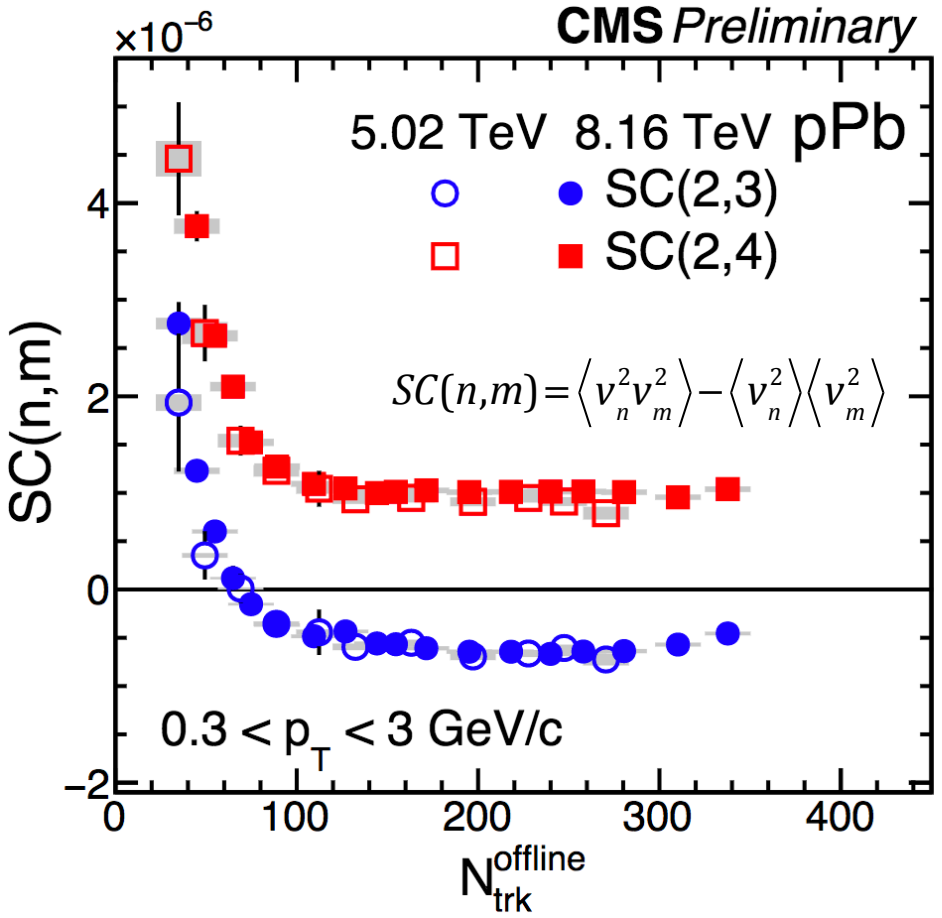




Outlook: more precision and higher p_T with 8 TeV pPb data

Symmetric cumulants





- Influence of non-flow need to be taken out, but see anti-correlation between v_2 v_3 and correlation between v_2 v_4.
- Naturally understood in hydrodynamics
  - v_2v_3 reflects $\varepsilon_2\varepsilon_3$ correlation, v_2v_4 correlation reflects mode-mixing effects
- Are these correlations expected in CGC? see K. Dusling talk tomorrow

More ways of distinguishing initial and final

- More small collision system scan at same √s
  - Increase the final state effects, while only change initial state contribution slightly
- $p(v_n)$, constraining the nature of EbyE fluctuations
  - Doable in pPb collisions.
- Event-plane correlations, e.g. $\langle V_2^2 V_4^* \rangle$, complementary information to symmetric cumulants.
- Soft-hard event-shape engineering
  - Increase the low-p_T v_2 and see how the high-p_T v_2 respond.

Summary of collectivity in small system

- Collectivity associated with ridge must involve many particles in multiple η ranges → access via subevent cumulant methods

Challenge for both initial & final state scenarios?

- LHC v_2 associated with ridge does not turn off at low N_{ch}.
- RHIC $v_2\{4\}$ increases and approach $v_2\{2\}$ at lower $\sqrt{s}$

Challenge (or not) for initial state only scenarios?

- LHC $v_2^{pp} < v_2^{pPb}$ in all N_{ch} and all $\sqrt{s}$.
- LHC $c_2\{4\} < 0$ down to very low N_{ch} and more negative at higher p_T.
- RHIC geometry scan suggest ordering of v_n follows that of ε_n.
- LHC 5% v_2 at $p_T \sim 10$ GeV.
- LHC symmetric cumulants SC(2,3), SC(2,4) similar to PbPb

Coexistence of initial state & final state scenarios?

Key issue: How to constrain timescales for onset of collectivity?

RIKEN-BNL Research Center Workshop "Saturation: Recent Developments, New Ideas, and Measurements", April 26-28, 2017

Deep Inelastic Scattering as a probe of entanglement

D. Kharzeev

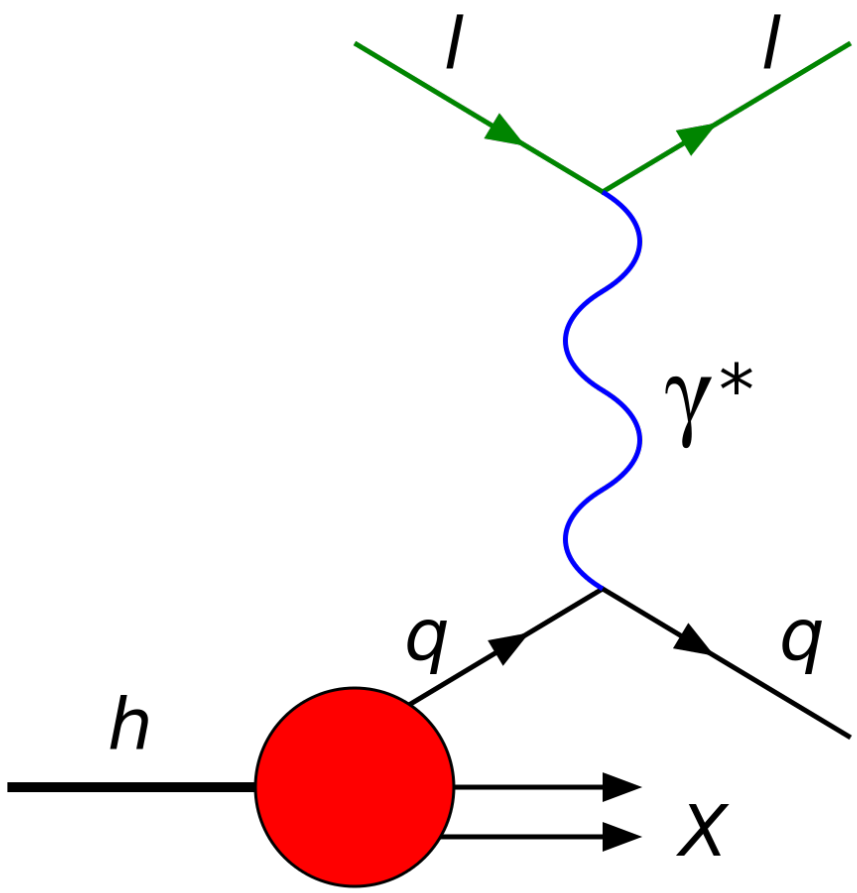
Based on DK, E. Levin, arXiv:1702.03489

Stony Brook University
RIKEN BNL Research Center
BROOKHAVEN NATIONAL LABORATORY
U.S. DEPARTMENT OF ENERGY | Office of Science

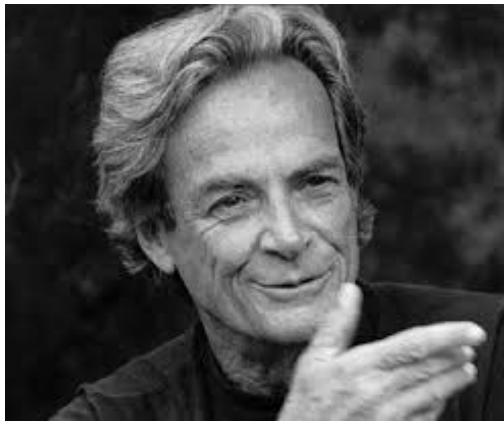
Outline

1. The puzzle of the parton model
2. Quantum mechanics of partons and entanglement
3. Entanglement entropy from QCD evolution
4. Proton at small x as a maximally entangled state
5. Relation between the entanglement entropy and the structure function
6. New experimental observables in DIS and pp collisions: from RHIC to EIC

The parton model: 50 years of success



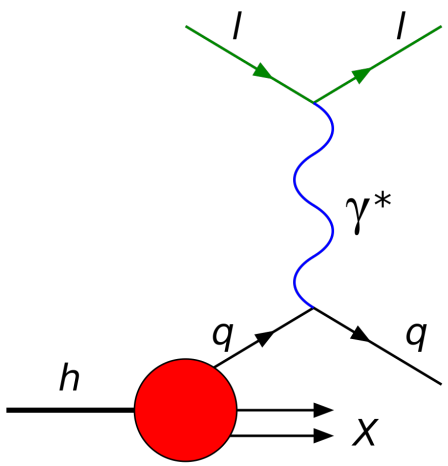






In almost fifty years that have ensued after the birth of the parton model, it has become an indispensable building block of high energy physics

The parton model: basic assumptions



In parton model, the proton is pictured as a collection of point-like quasi-free partons that are frozen in the infinite momentum frame due to Lorentz dilation.

The DIS cross section is given by the incoherent sum of cross sections of scattering off individual partons.

How to reconcile this with quantum mechanics?

DIS and entanglement

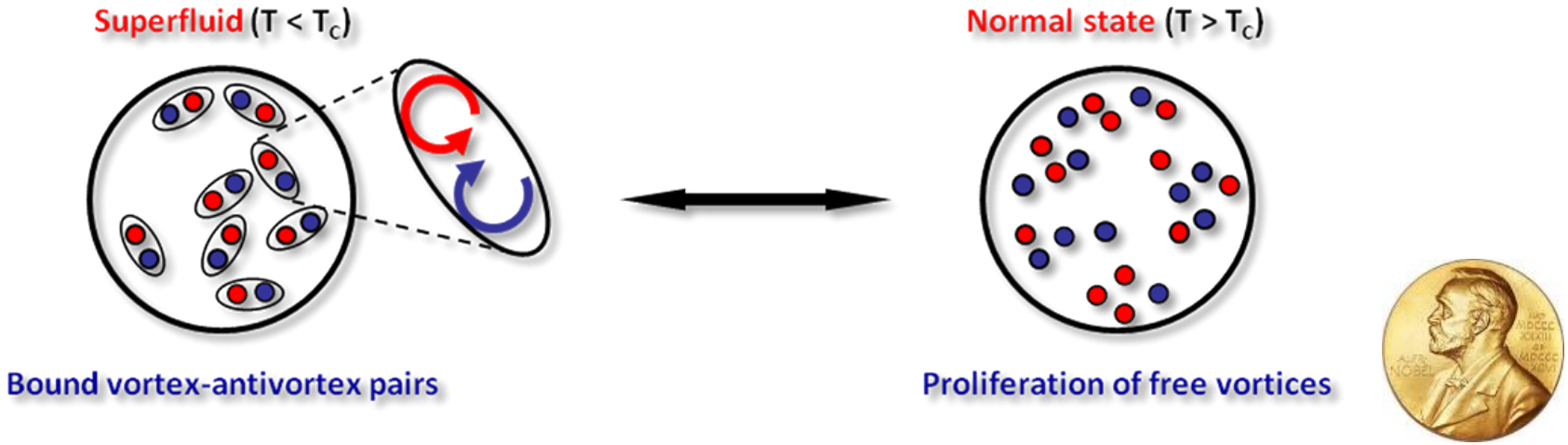
“...we never experiment with just one electron or atom or (small) molecule. In thought experiments, we sometimes assume that we do; this invariably entails ridiculous consequences ... .”



Erwin Schrödinger, 1952

The puzzle of the parton model

In quantum mechanics, the proton is a pure state with zero entropy. Yet, a collection of free partons does possess entropy… Boosting to the infinite momentum frame does not help, as a Lorentz boost cannot transform a pure state into a mixed one.



The crucial importance of entropy in (2+1)D systems: BKT phase transition (Nobel prize 2016)

Entanglement Entropy in quantum theory:

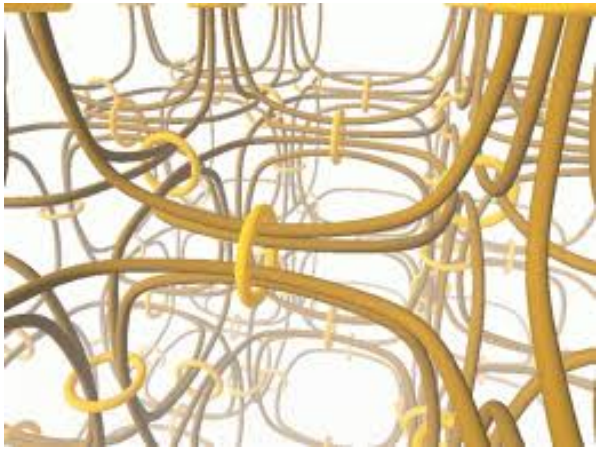
light



black holes



topological phases
of matter



The quantum mechanics of partons and entanglement

Our proposal: the key to solving this apparent paradox is entanglement.

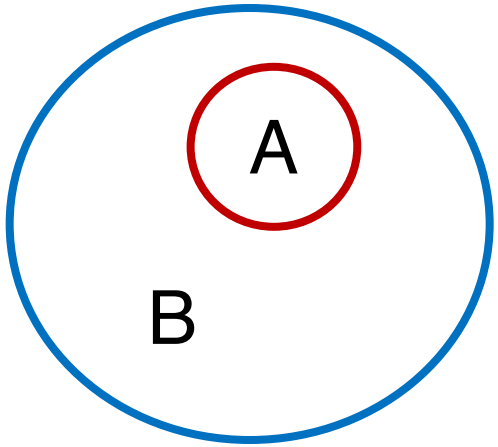
DK, E. Levin, arXiv:1702.03489

DIS probes only a part of the proton's wave function (region A). We sum over all hadronic final states; in quantum mechanics, this corresponds to accessing the density matrix of a mixed state

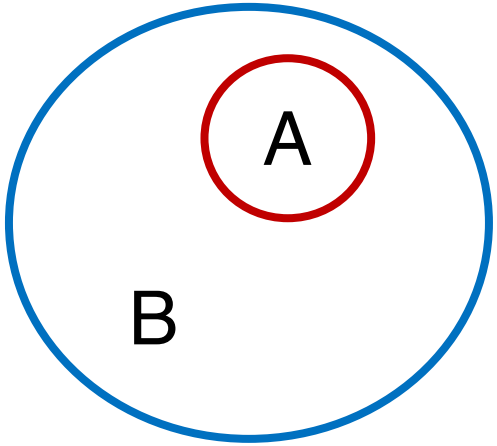
$$\hat{\rho}_A = \mathrm{tr}_B \hat{\rho}$$

with a non-zero entanglement entropy

$$S_A = -\mathrm{tr}\left[\hat{\rho}_A \ln \hat{\rho}_A\right]$$



The quantum mechanics of partons and entanglement



The proton is described by a vector

$$|\Psi_{AB}\rangle = \sum_{i,j} c_{ij} \; |\varphi_i^A\rangle \otimes |\varphi_j^B\rangle$$

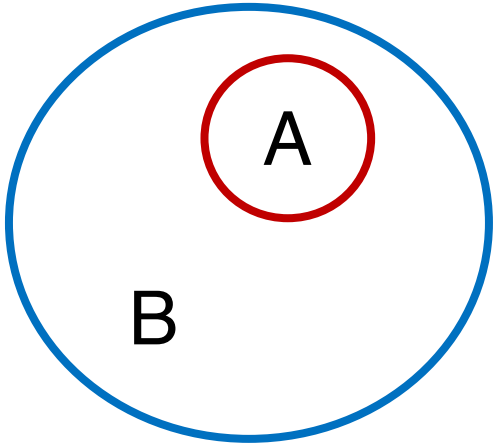
in Hilbert space $\mathcal{H}_A \otimes \mathcal{H}_B$

If $|\Psi_{AB}\rangle = |\varphi^A\rangle \otimes |\varphi^B\rangle$ only one term

contributes, then the state is separable (not our case!). Otherwise, the state is **entangled**.

The quantum mechanics of partons and entanglement

The Schmidt decomposition theorem:



$$|\Psi_{AB}\rangle = \sum_n \alpha_n |\Psi_n^A\rangle |\Psi_n^B\rangle$$

There exist the orthonormal states $|\Psi_n^A\rangle$ and $|\Psi_n^B\rangle$ for which the pure state can be represented as a single sum with real and positive coefficients α_n

If only one term (Schmidt rank one), then the state is separable. Otherwise, it is **entangled**; but no interference between different n's.

The quantum mechanics of partons and entanglement

We assume that the Schmidt basis $|\Psi_n^A\rangle|\Psi_n^B\rangle$ corresponds to the states with different numbers of partons n; since it represents a relativistic quantum field theory (QCD), the Schmidt rank is in general infinite.

The density matrix is now given by

$$\rho_A = \mathrm{tr_B}\ \rho_{\mathrm{AB}} = \sum_{\mathrm{n}} \alpha_{\mathrm{n}}^2\ |\Psi_{\mathrm{n}}^{\mathrm{A}}\rangle\langle\Psi_{\mathrm{n}}^{\mathrm{A}}|$$

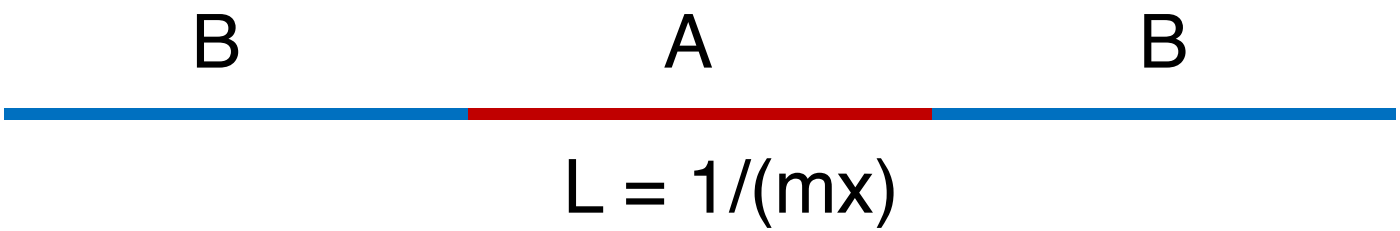
where $\alpha_n^2 \equiv p_n$ is the probability of a state with n partons

The entanglement entropy

The entanglement entropy is now given by the von Neumann's formula

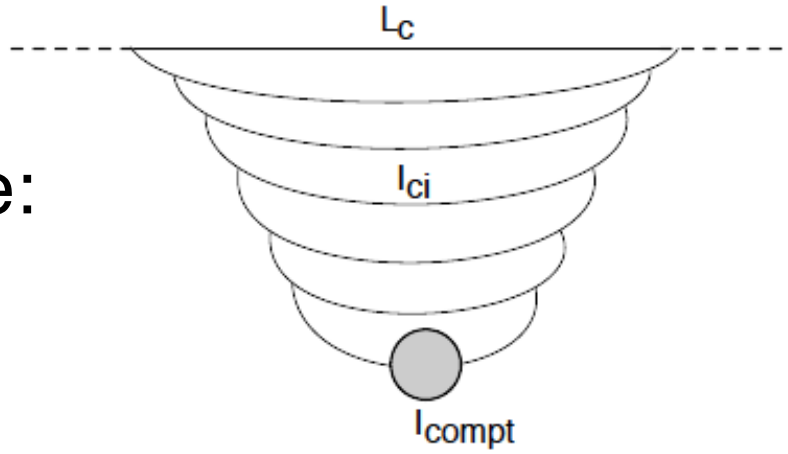
$$S = -\sum_n p_n \ln p_n$$

and can be evaluated by using the QCD evolution equations.
Let us start with a (1+1) case, followed by (3+1).



The entanglement entropy from QCD evolution

Space-time picture
in the proton's rest frame:



The evolution equation:

$$\frac{dP_n(Y)}{dY} = -\Delta n\, P_n(Y) + (n-1)\Delta P_{n-1}(Y)$$

The entanglement entropy from QCD evolution

$$\frac{dP_n(Y)}{dY} = -\Delta n\, P_n(Y) + (n-1)\Delta P_{n-1}(Y)$$

Solve by using the generating function method (A.H.Mueller '94; E.Levin, M.Lublinsky '04):

$$P_n(Y) = e^{-\Delta Y}(1 - e^{-\Delta Y})^{n-1}.$$

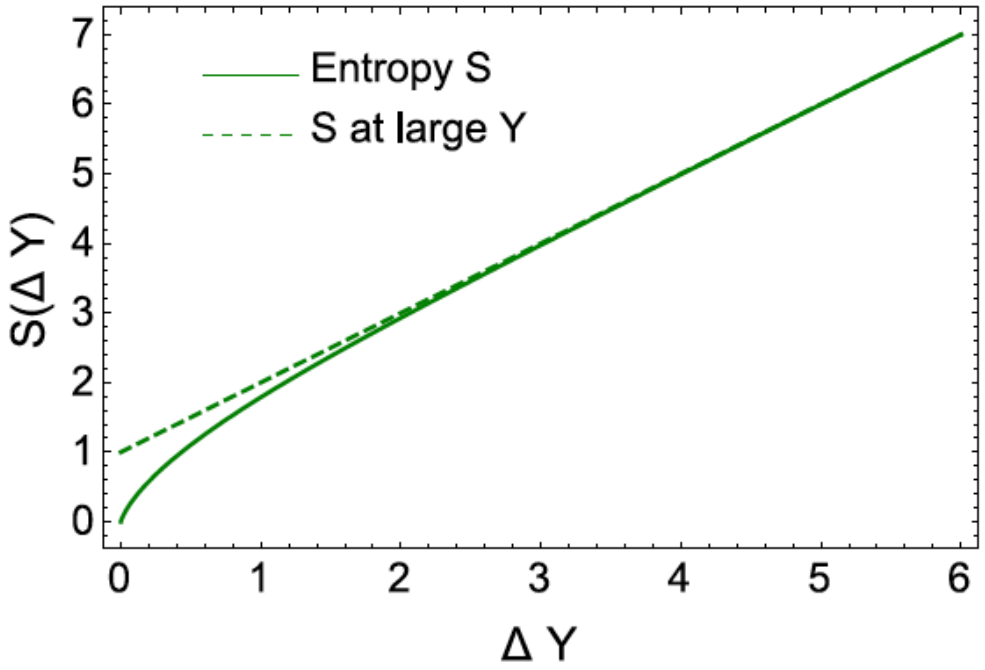
The resulting von Neumann entropy is

$$S(Y) = \ln(e^{\Delta Y} - 1) + e^{\Delta Y} \ln\left(\frac{1}{1 - e^{-\Delta Y}}\right)$$

The entanglement entropy from QCD evolution

At large ΔY , the entropy becomes

$$S(Y) \to \Delta Y$$



This "asymptotic" regime starts rather early, at

$$\Delta Y \simeq 2$$

The entanglement entropy from QCD evolution

At large ΔY (x ~ 10^{-3}) the relation between the entanglement entropy and the structure function

$$xG(x) = \langle n \rangle = \sum_n n P_n(Y) = \left(\frac{1}{x}\right)^{\Delta}$$

becomes very simple:

$$S = \ln[xG(x)]$$

The entanglement entropy from QCD evolution

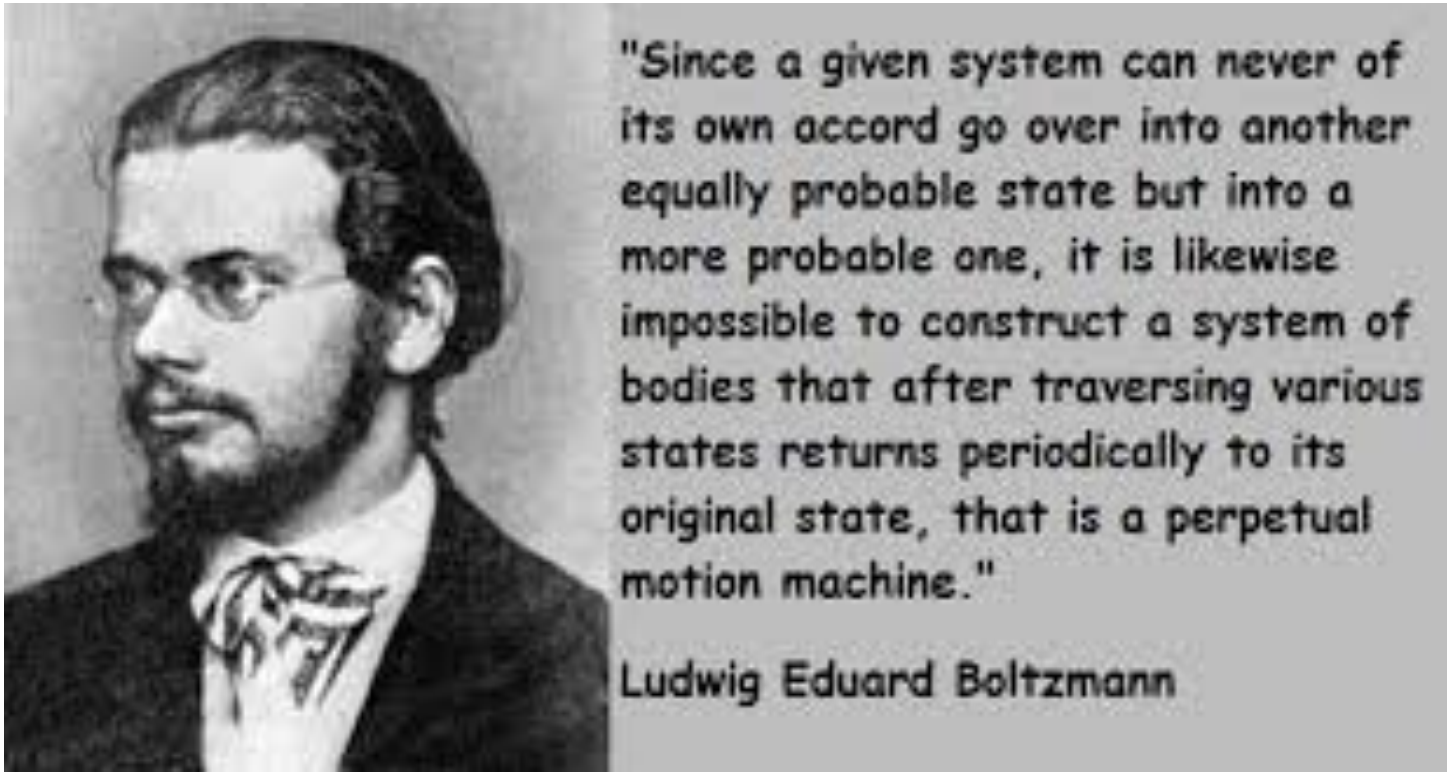
The (3+1) case is cumbersome, but the result is the same, with $\Delta = \bar{\alpha}_s \ln(r^2 Q_s^2)$

What is the physics behind this relation?

$$S = \ln[xG(x)]$$

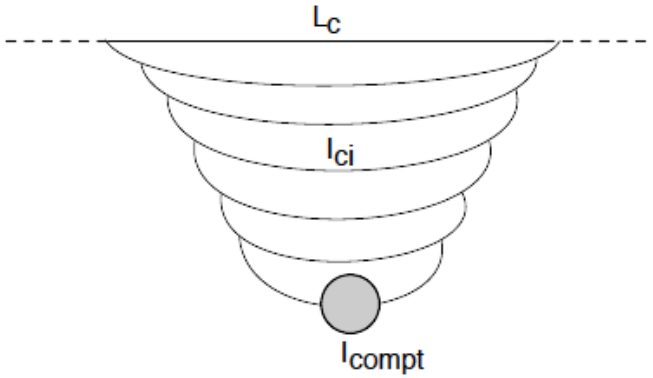
It signals that all $\exp(\Delta Y)$ partonic states have about equal probabilities $\exp(-\Delta Y)$ – in this case the **entanglement entropy is maximal**, and the proton is a **maximally entangled state** (a new look at the parton saturation and CGC?)

L. Boltzmann:



the system is driven to the most probable state with the largest entropy

Possible relation to CFT



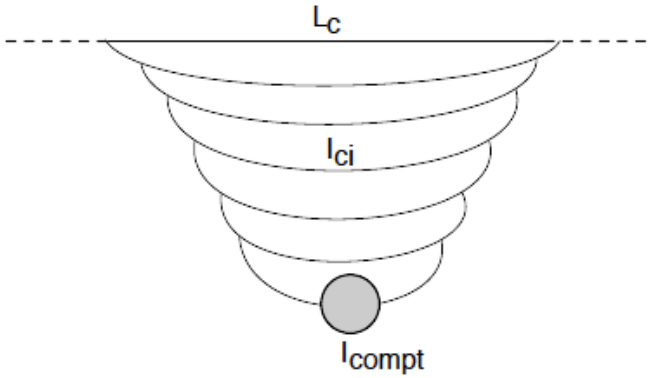
The small x formula $S = \ln[xG(x)]$

yields $S(x) = \Delta \ln[1/x] = \Delta \ln \frac{L}{\epsilon}$

where $L = (mx)^{-1}$

is the longitudinal length probed in DIS (in the target rest frame), and $\epsilon \equiv 1/m$ is the proton's Compton wavelength

Possible relation to CFT



This formula

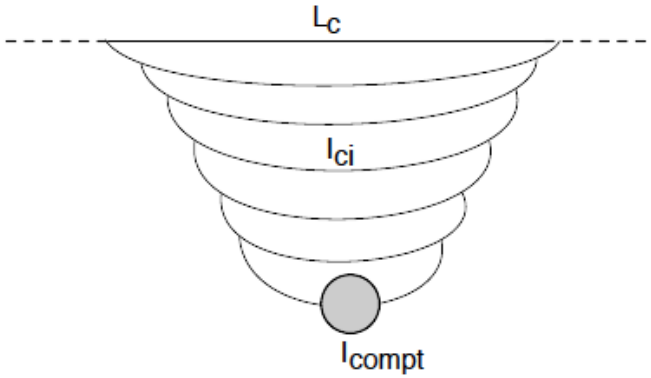
$$S(x) = \Delta \ln[1/x] = \Delta \ln \frac{L}{\epsilon}$$

looks very similar to the well-known (1+1) CFT result (Holzhey, Larsen, Wilczek '94; Calabrese, Cardy '05):

$$S_E = \frac{c}{3} \ln \frac{L}{\epsilon}$$

where c is the central charge of the CFT, and ε is the resolution scale

Possible relation to CFT



If this is not a mere coincidence:
the central charge $c \leq 1$:

$$c = 1 - \frac{6}{m(m+1)}, \quad m = 3, 4, ..., \infty$$

c=1 corresponds to free bosonic theory.
This means that $\Delta \leq 1/3$;
a bound on the growth of the structure function!

$$xG(x) \leq \text{const} \ \frac{1}{x^{1/3}}$$

The Second Law for entanglement entropy?

If the Second Law applies to entanglement entropy (EE) (a number of indications, e.g. from black hole physics), then the entropy of hadronic final state in DIS has to be equal or larger than the EE of the initial state measured through the structure function:

$$S_{\rm hadrons} \geq S_{EE}(x)$$

Indications from holography that the entropy does not increase at strong coupling; this leads to

$$S_{\rm hadrons} \simeq S_{EE}(x)$$ **parton liberation** ?

Future directions

- The entanglement entropy (EE) can be defined and computed for any value of the coupling – generalization of parton distribution to strong coupling? holography
- The EE is a non-local order parameter in topologically ordered phases – relation of parton distributions to QCD topology?
- Elucidate connections to CFT
- Reformulate parton evolution in terms of EE (momentum space entanglement? – Kovner, Lublinsky ‘15)
- A new look at thermalization

Physics at EIC:

supplement the measurements of
structure functions by the studies of hadronic final state
(especially in the target fragmentation region).

Testing the Second Law for the Entanglement entropy is fundamentally important;

extracting the entropy of the final hadronic state will require event-by-event measurements.

This can be started at RHIC! Combine measurements of “hard” cross sections with the e-by-e measurements of associated hadron multiplicity

Summary

1. Entanglement entropy (EE) provides a viable solution to the apparent contradiction between the parton model and quantum mechanics.
2. The use of EE allows to generalize the notion of parton distribution to any value of the coupling, and possibly to elucidate the role of topology.
3. If the connection to CFT is confirmed, it will put a bound on the growth of parton distributions at small x (no other bound exists; unitarity does not provide a bound).
4. Measuring hadronic final states at EIC will allow to test the Second Law for the EE.

Small x Asymptotics of the Quark Helicity Distribution

Yuri Kovchegov

The Ohio State University

work with Dan Pitonyak and Matt Sievert,
arXiv:1610.06188 [hep-ph]

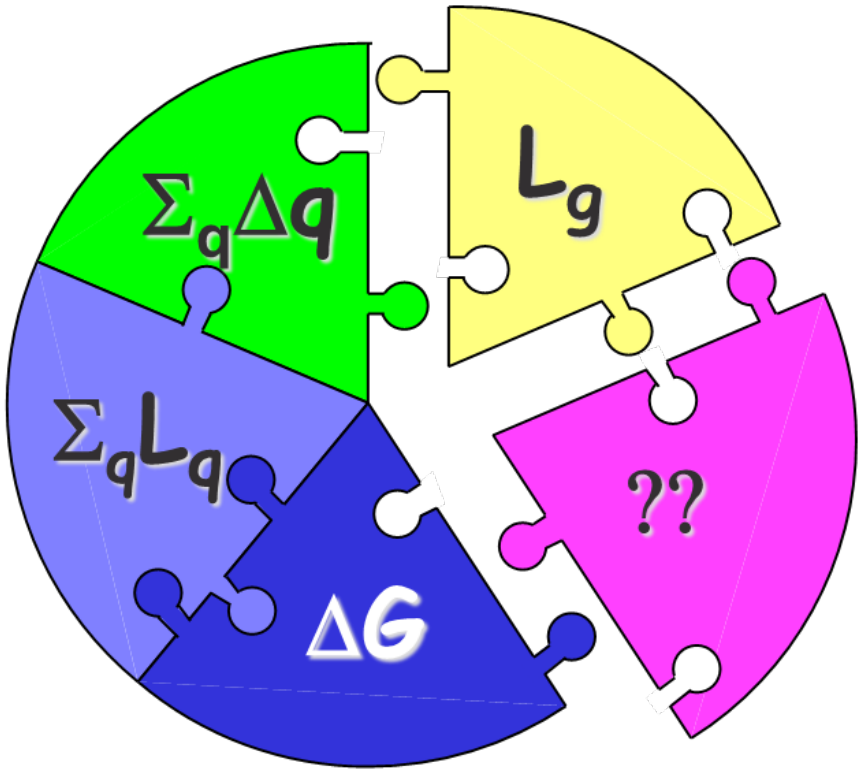
arXiv:1703.05809 [hep-ph]

Outline

- Goal: understanding the proton spin coming from small x
- Small-x helicity evolution:
  - Observables: quark helicity TMD & PDF at small-x, g_1 structure function
  - Small-x evolution for the "polarized dipole": large-N_C limit
- Numerical solution of the large-N_C evolution equations:
  - small-x asymptotics of the g_1 structure function, quark hPDFs and helicity TMDs
  - impact on proton spin
- Analytic solution of the large-N_C evolution equations:
  - Pure joy

Our Goal: Proton Spin at Small x

Proton Spin Pie Chart



- The proton spin carried by the quarks is estimated to be (for $0.001 < x < 1$)

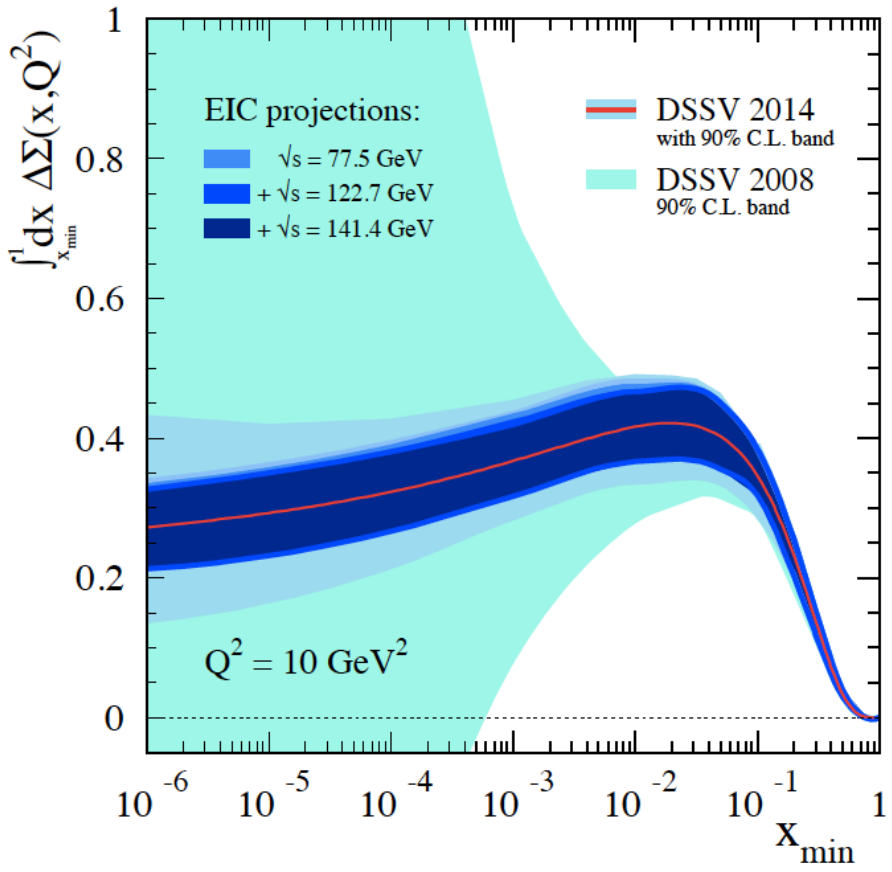
$$S_q(Q^2 = 10\,\mathrm{GeV}^2) \approx 0.15 \div 0.20$$

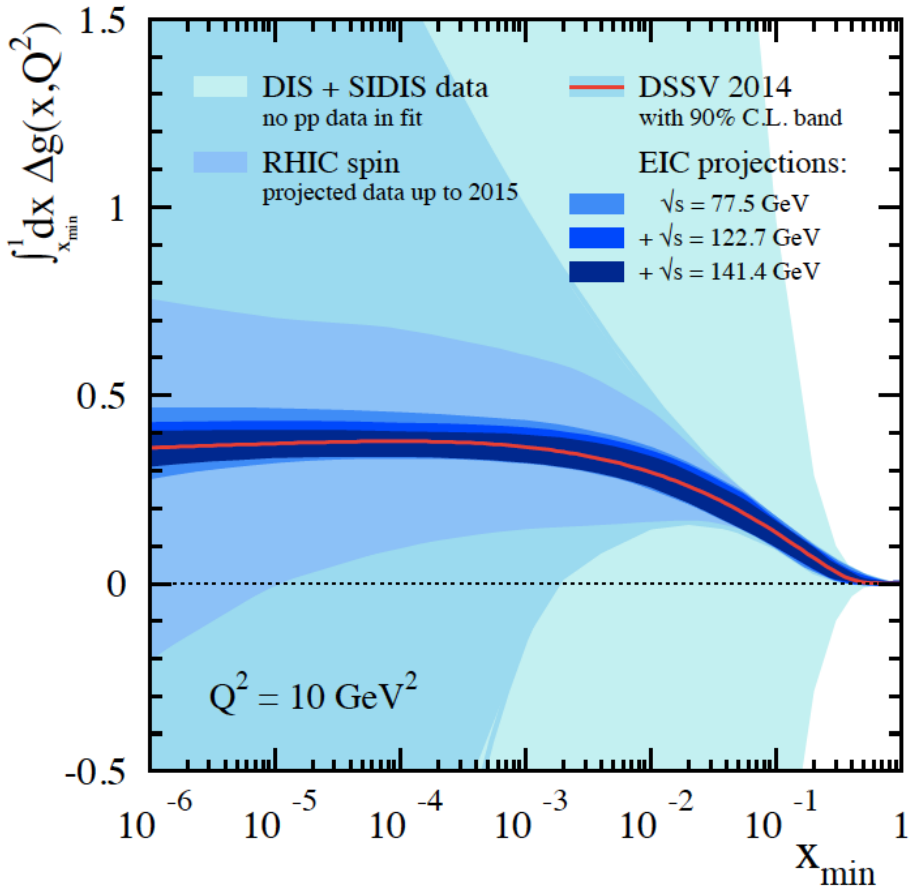
- The proton spin carried by the gluons is (for $0.05 < x < 1$)

$$S_G(Q^2 = 10\,\mathrm{GeV}^2) \approx 0.13 \div 0.26$$

- Unfortunately the uncertainties are large. Note also that the x-ranges are limited, with more spin (positive or negative) possible at small x.

How much spin is at small x?





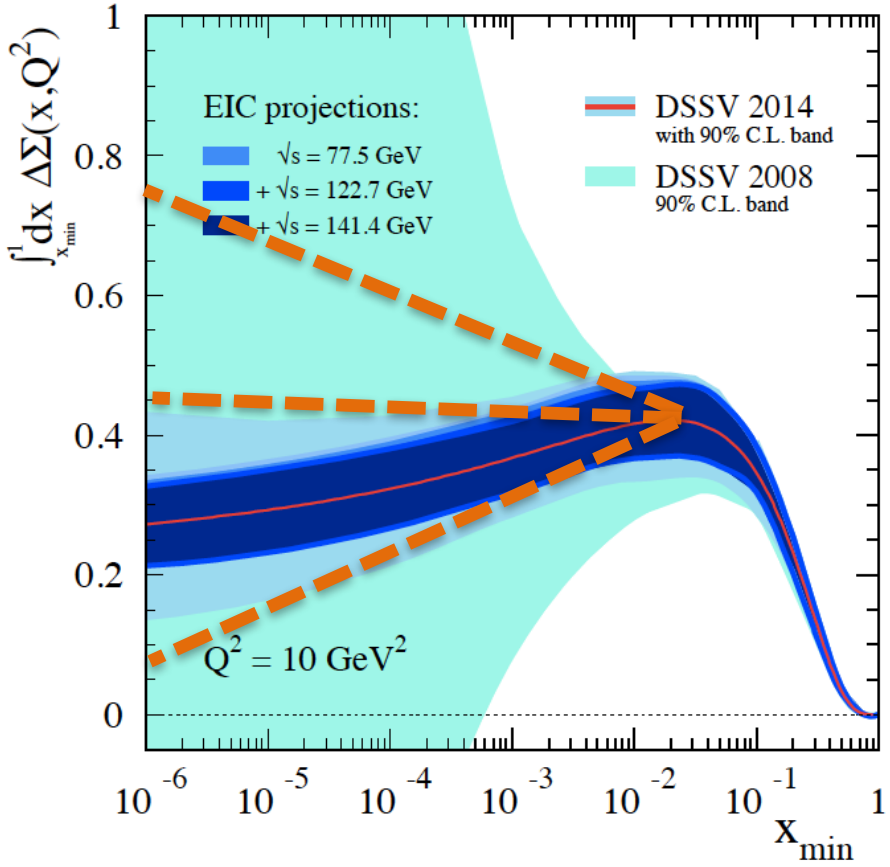
- E. Aschenaur et al, **arXiv:1509.06489 [hep-ph]**
- Uncertainties are very large at small x!

Spin at small x

- The goal of this project is to provide theoretical understanding of helicity PDF's at very small x.

- Our work would provide guidance for future hPDF's parametrizations of the existing and new data (e.g., the data to be collected at EIC).

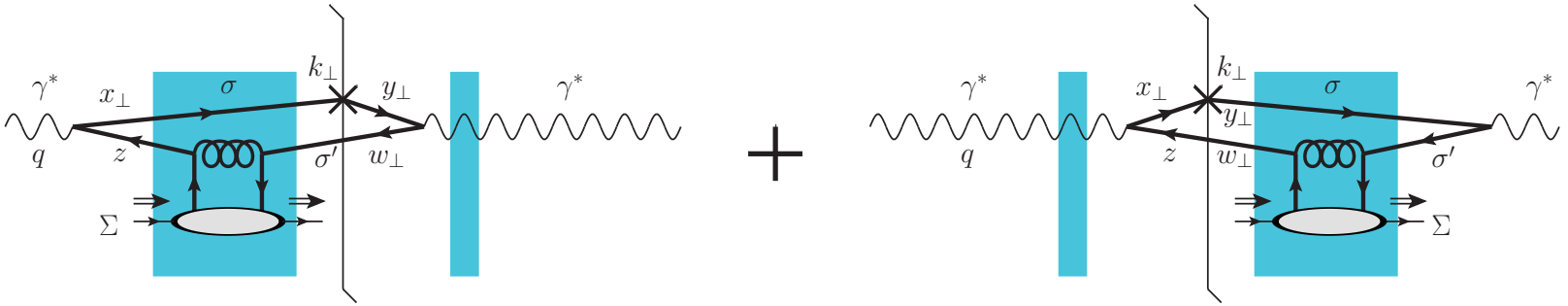
- Strictly-speaking we only talk about quark helicity, but most likely our analysis applies to gluon hPDF's as well.



Helicity Evolution Equations at Small x
flavor-singlet case

Yu.K., M. Sievert, arXiv:1505.01176 [hep-ph]
Yu.K., D. Pitonyak, M. Sievert, arXiv:1511.06737 [hep-ph],
arXiv:1610.06197 [hep-ph]

Quark Helicity Observables at Small x



- One can show that the g_1 structure function and quark helicity PDF (Δq) and TMD at small-x can be expressed in terms of the polarized dipole amplitude (flavor singlet case):

$$g_1^S(x,Q^2) = \frac{N_c\,N_f}{2\,\pi^2\alpha_{EM}} \int\limits_{z_i}^{1} \frac{dz}{z^2(1-z)} \int dx_{01}^2 \left[\frac{1}{2}\sum_{\lambda\sigma\sigma'} |\psi^T_{\lambda\sigma\sigma'}|^2_{(x_{01}^2,z)} + \sum_{\sigma\sigma'} |\psi^L_{\sigma\sigma'}|^2_{(x_{01}^2,z)}\right] G(x_{01}^2,z),$$

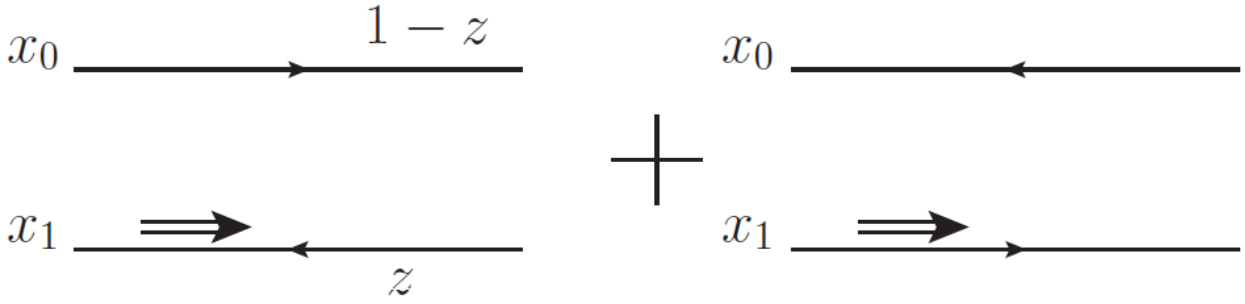
$$\Delta q^S(x,Q^2) = \frac{N_c\,N_f}{2\pi^3} \int\limits_{z_i}^{1} \frac{dz}{z} \int\limits_{\frac{1}{zs}}^{\frac{1}{zQ^2}} \frac{dx_{01}^2}{x_{01}^2}\, G(x_{01}^2,z),$$

$$g_{1L}^S(x,k_T^2) = \frac{8\,N_c\,N_f}{(2\pi)^6} \int\limits_{z_i}^{1} \frac{dz}{z} \int d^2x_{01}\, d^2x_{0'1}\, e^{-i\underline{k}\cdot(\underline{x}_{01}-\underline{x}_{0'1})}\, \frac{\underline{x}_{01}\cdot\underline{x}_{0'1}}{x_{01}^2 x_{0'1}^2}\, G(x_{01}^2,z)$$

- Here s is cms energy squared, $z_i=\Lambda^2/s$, $G(x_{01}^2,z) \equiv \int d^2b\, G_{10}(z)$

Polarized Dipole

- All flavor singlet small-x helicity observables depend on one object, "polarized dipole amplitude":



$$G_{10}(z) \equiv \frac{1}{2N_c}\left\langle\!\!\left\langle \mathrm{tr}\left[V_{\underline{0}} V_{\underline{1}}^{pol\,\dagger}\right] + \mathrm{tr}\left[V_{\underline{1}}^{pol} V_{\underline{0}}^{\dagger}\right] \right\rangle\!\!\right\rangle(z)$$

unpolarized quark

polarized quark: eikonal propagation, non-eikonal spin-dependent interaction

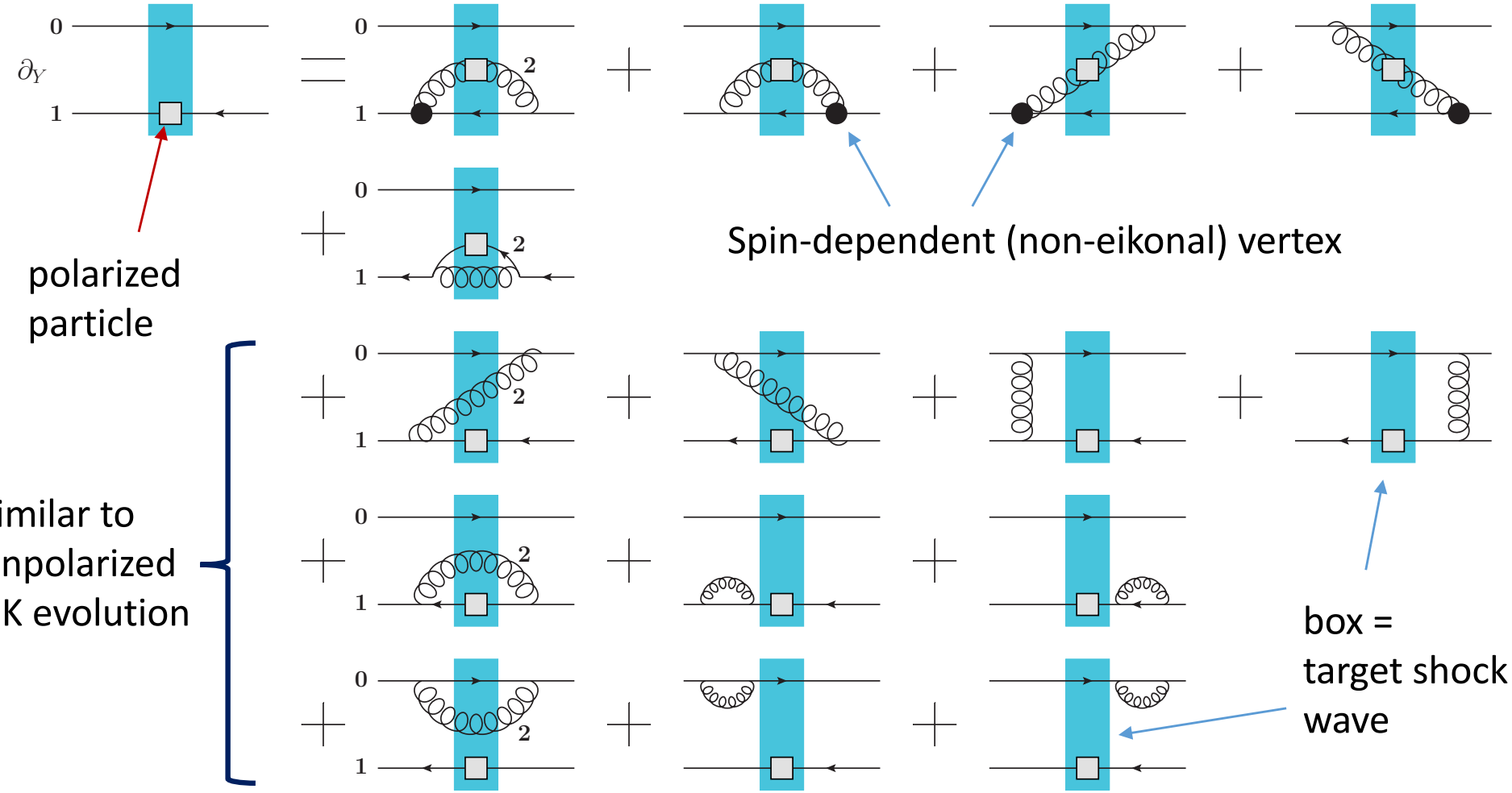
$$V_{\underline{x}} \equiv \mathcal{P}\exp\left[ig\int_{-\infty}^{\infty} dx^+ A^-(x^+, 0^-, \underline{x})\right]$$

- Double brackets denote an object with energy suppression scaled out:

$$\left\langle\!\!\left\langle \mathcal{O} \right\rangle\!\!\right\rangle(z) \equiv zs \left\langle \mathcal{O} \right\rangle(z)$$

Evolution for Polarized Quark Dipole

One can construct an evolution equation for the polarized dipole:



Resummation Parameter

- For helicity evolution the resummation parameter is different from BFKL, BK or JIMWLK, which resum powers of leading logarithms (LLA)

$$\alpha_s \ln(1/x)$$

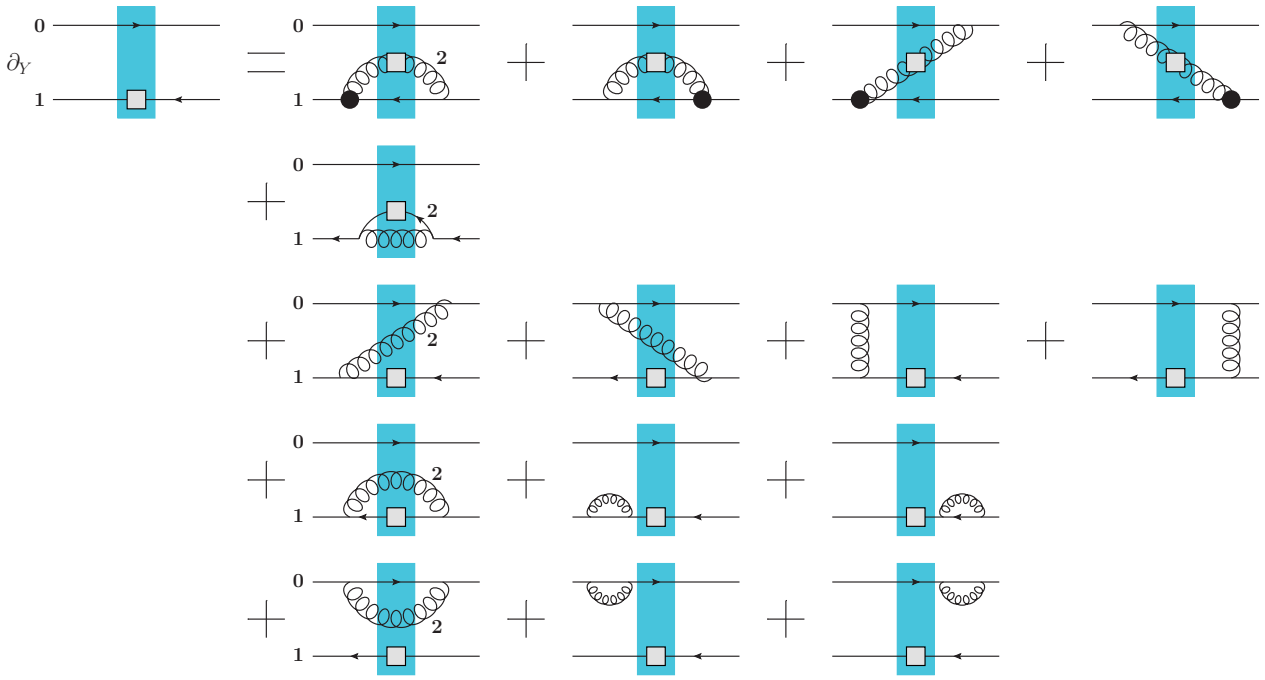
- Helicity evolution resummation parameter is double-logarithmic (DLA):

$$\alpha_s \ln^2 \frac{1}{x}$$

- The second logarithm of x arises due to transverse momentum integration being logarithmic both in UV and IR.

- This was known before: Kirschner and Lipatov ’83; Kirschner ’84; Bartels, Ermolaev, Ryskin ‘95, ‘96; Griffiths and Ross ’99; Itakura et al ’03; Bartels and Lublinsky ‘03.

Evolution for Polarized Quark Dipole



$$\langle\langle \ldots \rangle\rangle = \frac{1}{z\, s} \langle \ldots \rangle$$

$$\rho'^{\,2} = \frac{1}{z'\, s}$$

$$\frac{1}{N_c} \left\langle\!\!\left\langle \mathrm{tr}\left[V_0^{unp}\, V_1^{pol\,\dagger} \right] \right\rangle\!\!\right\rangle (z) = \frac{1}{N_c} \left\langle\!\!\left\langle \mathrm{tr}\left[V_0^{unp}\, V_1^{pol\,\dagger} \right] \right\rangle\!\!\right\rangle_0 (z) + \frac{\alpha_s}{2\pi^2} \int_{z_i}^{z} \frac{dz'}{z'} \int_{\rho'^2} \frac{d^2x_2}{x_{21}^2}$$

$$\times \left\{ \theta(x_{10} - x_{21})\, \frac{2}{N_c} \left\langle\!\!\left\langle \mathrm{tr}\left[t^b\, V_0^{unp}\, t^a\, V_1^{unp\,\dagger} \right] U_2^{pol\,ba} \right\rangle\!\!\right\rangle (z') \right.$$

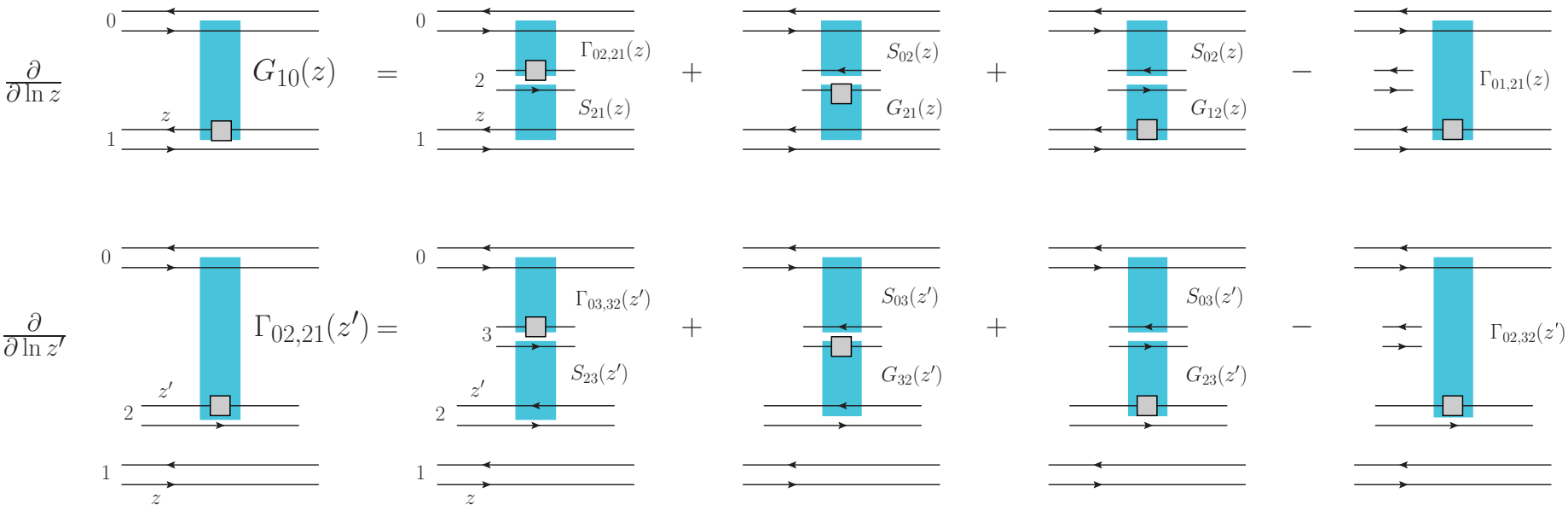
$$+ \theta(x_{10}^2 z - x_{21}^2 z')\, \frac{1}{N_c} \left\langle\!\!\left\langle \mathrm{tr}\left[t^b\, V_0^{unp}\, t^a\, V_2^{pol\,\dagger} \right] U_1^{unp\,ba} \right\rangle\!\!\right\rangle (z')$$

$$\left. + \theta(x_{10} - x_{21})\, \frac{1}{N_c} \left[\left\langle\!\!\left\langle \mathrm{tr}\left[V_0^{unp}\, V_2^{unp\,\dagger} \right] \mathrm{tr}\left[V_2^{unp}\, V_1^{pol\,\dagger} \right] \right\rangle\!\!\right\rangle (z') - N_c \left\langle\!\!\left\langle \mathrm{tr}\left[V_0^{unp}\, V_1^{pol\,\dagger} \right] \right\rangle\!\!\right\rangle (z') \right] \right\}$$

Equation does not close!

Polarized Dipole Evolution in the Large-N_c Limit

In the large-N_c limit the equations close, leading to a system of 2 equations:



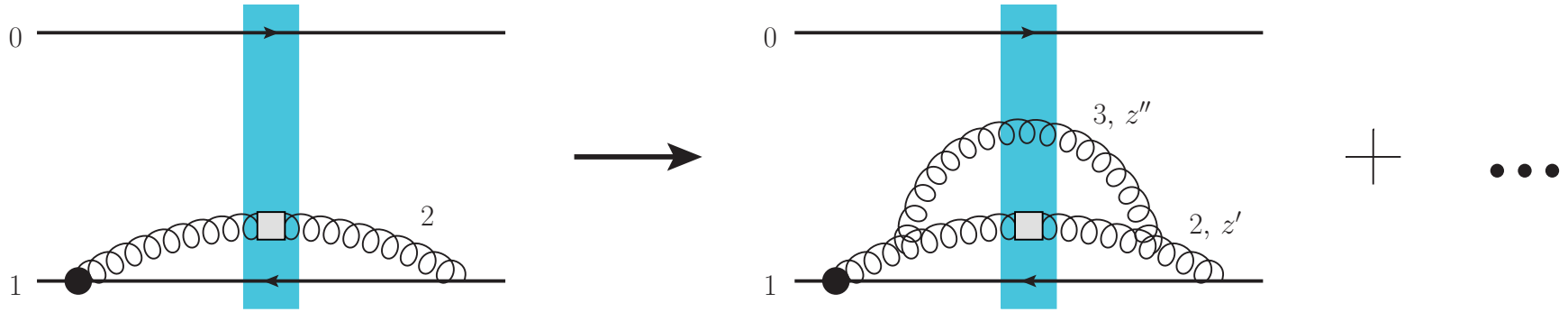
$$G_{10}(z) = G_{10}^{(0)}(z) + \frac{\alpha_s\, N_c}{2\pi} \int_{z_i}^{z} \frac{dz'}{z'} \int_{\rho'^2}^{x_{10}^2} \frac{dx_{21}^2}{x_{21}^2} \left[2\,\Gamma_{02,\,21}(z')\, S_{21}(z') + 2\, G_{21}(z')\, S_{02}(z') + G_{12}(z')\, S_{02}(z') - \Gamma_{01,\,21}(z')\right]$$

$$\Gamma_{02,\,21}(z') = \Gamma_{02,\,21}^{(0)}(z') + \frac{\alpha_s\, N_c}{2\pi} \int_{z_i}^{z'} \frac{dz''}{z''} \int_{\rho''^2}^{\min\{x_{02}^2,\, x_{21}^2\, z'/z''\}} \frac{dx_{32}^2}{x_{32}^2} \left[2\,\Gamma_{03,\,32}(z'')\, S_{23}(z'') + 2\, G_{32}(z'')\, S_{03}(z'') + G_{23}(z'')\, S_{03}(z'') - \Gamma_{02,\,32}(z'')\right]$$

S = found from BK/JIMWLK, it is LLA

You friendly “neighborhood” dipole

- There is a new object in the evolution equation – **the neighbor dipole**.
- This is specific for the DLA evolution. Gluon emission may happen in one dipole, but, due to transverse distance ordering, may ’know’ about another dipole:



$$x_{21}^2\, z' \gg x_{32}^2\, z''$$

- We denote the evolution in the neighbor dipole 02 by $\Gamma_{02,\,21}(z')$

Large-N_c Evolution: Strict DLA Limit

- In the strict DLA limit we neglect the LLA evolution (put S=1) and get:

$$G(x_{10}^2,z) = G^{(0)}(x_{10}^2,z) + \frac{\alpha_s\, N_c}{2\pi} \int\limits_{\frac{1}{x_{10}^2 s}}^{z} \frac{dz'}{z'} \int\limits_{\frac{1}{z' s}}^{x_{10}^2} \frac{dx_{21}^2}{x_{21}^2} \left[\Gamma(x_{10}^2, x_{21}^2, z') + 3\, G(x_{21}^2, z')\right]$$

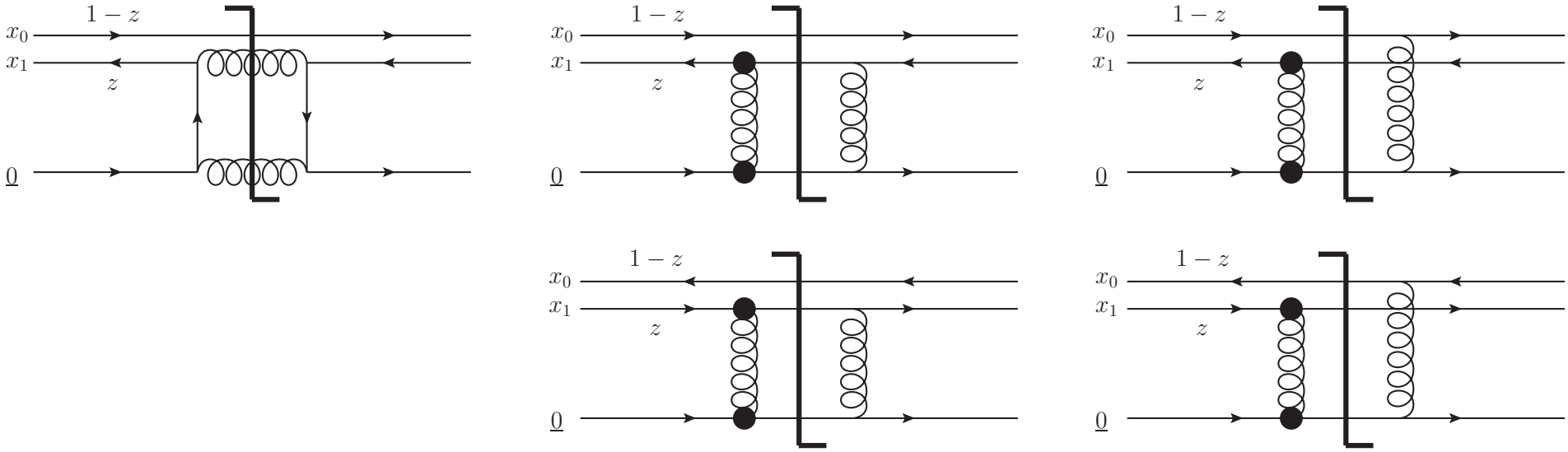
$$\Gamma(x_{10}^2, x_{21}^2, z') = \Gamma^{(0)}(x_{10}^2, x_{21}^2, z') + \frac{\alpha_s\, N_c}{2\pi} \int\limits_{\frac{1}{x_{10}^2 s}}^{z'} \frac{dz''}{z''} \int\limits_{\frac{1}{z'' s}}^{\min\left\{x_{10}^2, x_{21}^2 \frac{z'}{z''}\right\}} \frac{dx_{32}^2}{x_{32}^2} \left[\Gamma(x_{10}^2, x_{32}^2, z'') + 3\, G(x_{32}^2, z'')\right]$$

- The initial conditions are given by Born-level graphs, for which

$$\Gamma^{(0)}(x_{10}^2, x_{21}^2, z) = G^{(0)}(x_{10}^2, z)$$

Initial Conditions

- Initial conditions for all our evolution equations should be given by Born-level interactions ("dressed" by multiple rescatterings in the saturation case):



$$G^{(0)}(x_{10}^2, z) = \frac{\alpha_s^2 C_F}{N_c}\pi \left[C_F \ln \frac{zs}{\Lambda^2} - 2\,\ln(zs\,x_{10}^2)\right]$$

Large-N_c Equations: Numerical Solution

Yu.K., D. Pitonyak, M. Sievert, arXiv:1610.06188 [hep-ph]

Prior Results

- Small-x DLA evolution for the g_1 structure function was first considered by Bartels, Ermolaev and Ryskin (BER) in '96.

- Including the mixing of quark and gluon ladders, they obtained

$$\Delta\Sigma \sim g_1 \sim \left(\frac{1}{x}\right)^{z_s \sqrt{\frac{\alpha_s N_c}{2\pi}}}$$

with z_s = 3.45 for 4 quark flavors and z_S=3.66 for pure glue.

$$S_q(Q^2) = \frac{1}{2}\int_0^1 dx\, \Delta\Sigma(x, Q^2)$$

- The power is large: it becomes larger than 1 for the realistic strong coupling of the order of α_s = 0.2 − 0.3, resulting in polarized PDFs which actually grow with decreasing x fast enough for the integral of the PDFs over the low-x region to be (potentially) large (infinite).

Large-N_C Equations

- We want to find the numerical solution of the large-N_c DLA evolution equations (linearized, without saturation corrections):

$$G_{01}(z) = G_{01}^{(0)}(z) + \frac{\alpha_s\, N_c}{2\pi} \int\limits_{z_i}^{z} \frac{dz'}{z'} \int\limits_{\rho'^2}^{x_{10}^2} \frac{dx_{21}^2}{x_{21}^2}\, \left[\Gamma_{02,\,21}(z') + 3\, G_{21}(z')\right],$$

$$\Gamma_{02,\,21}(z') = \Gamma_{02,\,21}^{(0)}(z') + \frac{\alpha_s\, N_c}{2\pi} \int\limits_{z_i}^{z'} \frac{dz''}{z''} \int\limits_{\rho''^2}^{\min\left\{x_{02}^2, x_{21}^2\, z'/z''\right\}} \frac{dx_{32}^2}{x_{32}^2}\, \left[\Gamma_{03,\,32}(z'') + 3\, G_{23}(z'')\right]$$

- First we define new variables:

$$\eta = \sqrt{\frac{\alpha_s N_c}{2\pi}}\, \ln\frac{zs}{\Lambda^2} \qquad\qquad s_{10} = \sqrt{\frac{\alpha_s N_c}{2\pi}}\, \ln\frac{1}{x_{10}^2\, \Lambda^2}$$

Large-N_C Equations

- In terms of the new variables the equations become

$$G(s_{10},\eta) = G^{(0)}(s_{10},\eta) + \int_{s_{10}}^{\eta} d\eta' \int_{s_{10}}^{\eta'} ds_{21}\ [\Gamma(s_{10},s_{21},\eta') + 3\,G(s_{21},\eta')]$$

$$\Gamma(s_{10},s_{21},\eta') = \Gamma^{(0)}(s_{10},s_{21},\eta') + \int_{s_{10}}^{\eta'} d\eta'' \int_{\max\{s_{10},s_{21}+\eta''-\eta'\}}^{\eta''} ds_{32}\,[\Gamma(s_{10},s_{32},\eta'') + 3\,G(s_{32},\eta'')]\,.$$

$$\eta = \sqrt{\frac{\alpha_s N_c}{2\pi}}\ \ln\frac{zs}{\Lambda^2} \qquad\qquad s_{10} = \sqrt{\frac{\alpha_s N_c}{2\pi}}\ \ln\frac{1}{x_{10}^2\,\Lambda^2}$$

- The initial conditions are

$$G^{(0)}(s_{10},\eta) = \Gamma^{(0)}(s_{10},s_{21},\eta) = \alpha_s^2\pi\tfrac{C_F}{N_c}[C_F\,\eta - 2(\eta - s_{10})]$$

Numerical Solution

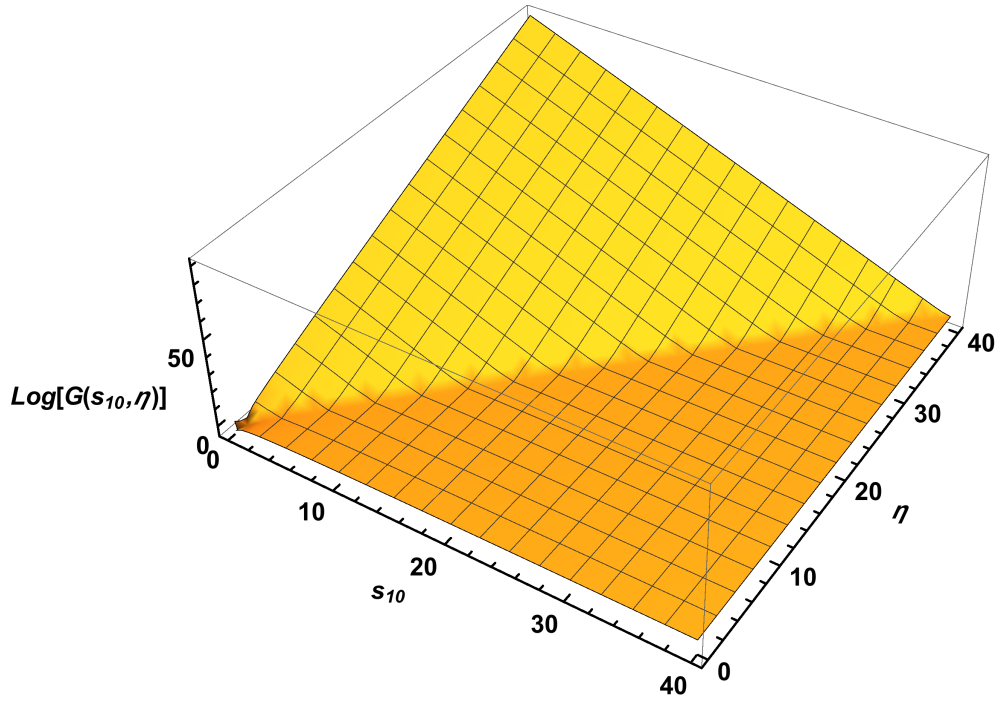
- We discretize the equations

$$G_{ij} = G_{ij}^{(0)} + \Delta\eta\,\Delta s \sum_{j'=i}^{j-1} \sum_{i'=i}^{j'} \left[\Gamma_{ii'j'} + 3\,G_{i'j'}\right],$$

$$\Gamma_{ikj} = \Gamma_{ikj}^{(0)} + \Delta\eta\,\Delta s \sum_{j'=i}^{j-1} \sum_{i'=\max\{i,k+j'-j\}}^{j'} \left[\Gamma_{ii'j'} + 3\,G_{i'j'}\right]$$

and solve them by progressively populating each fixed-η row in s.

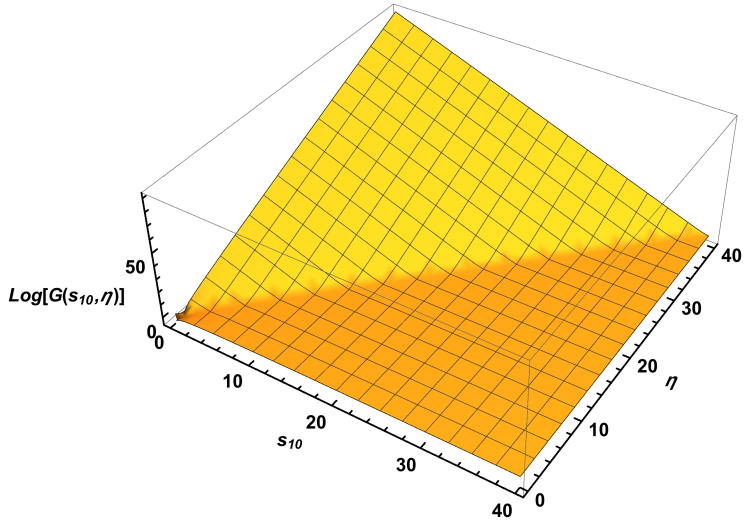
- The solution for G looks like this:



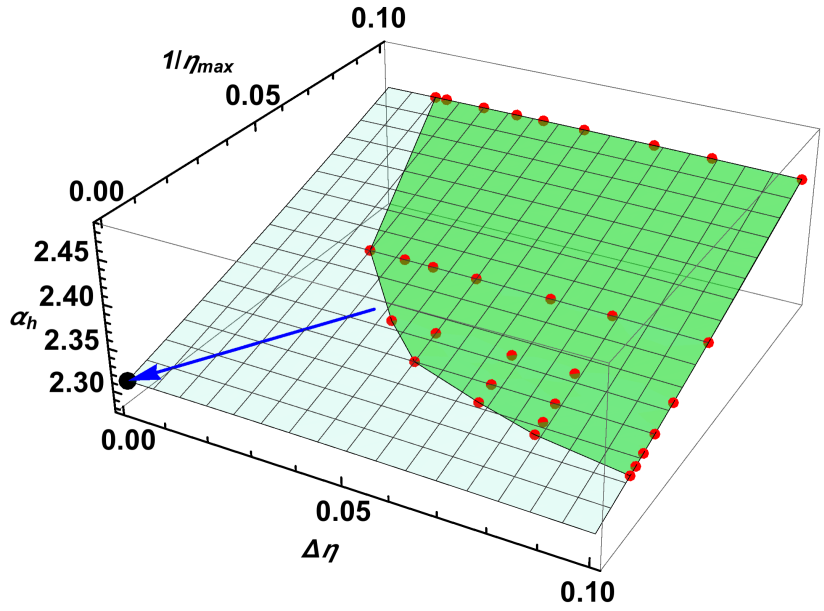
$$\eta = \sqrt{\frac{\alpha_s N_c}{2\pi}}\,\ln\frac{zs}{\Lambda^2} \qquad s_{10} = \sqrt{\frac{\alpha_s N_c}{2\pi}}\,\ln\frac{1}{x_{10}^2\,\Lambda^2}$$

Extracting the intercept

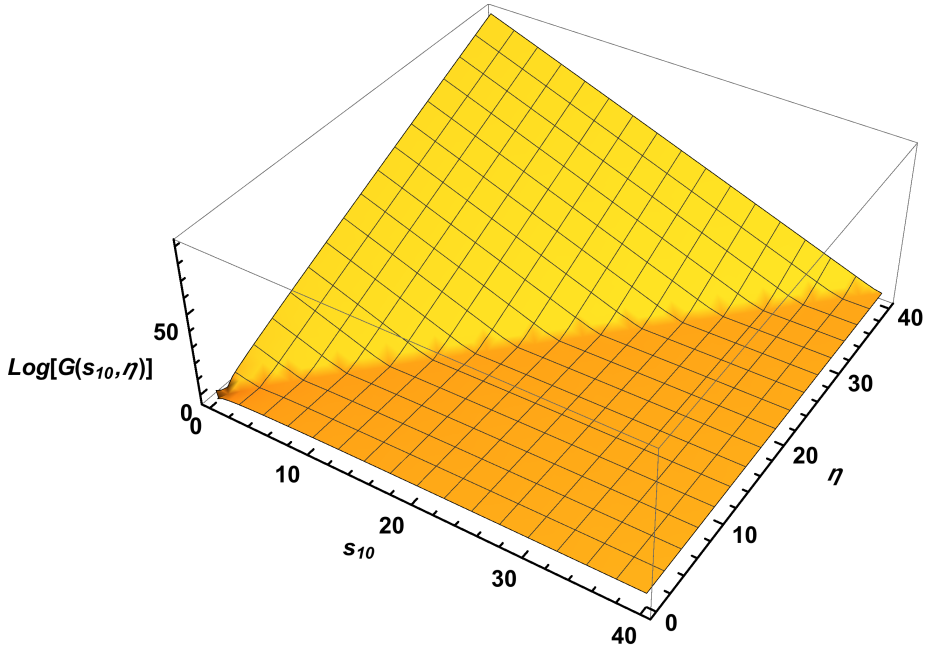
- The solution for G grows exponentially with rapidity η:



- We read off the "intercept" (the slope of ln G vs η) for different-size lattices and step sizes, and extrapolate the intercept to the continuum:



Solution of the large-N_C Equations



$$\alpha_h \approx 2.31 \sqrt{\frac{\alpha_s N_c}{2\pi}}$$

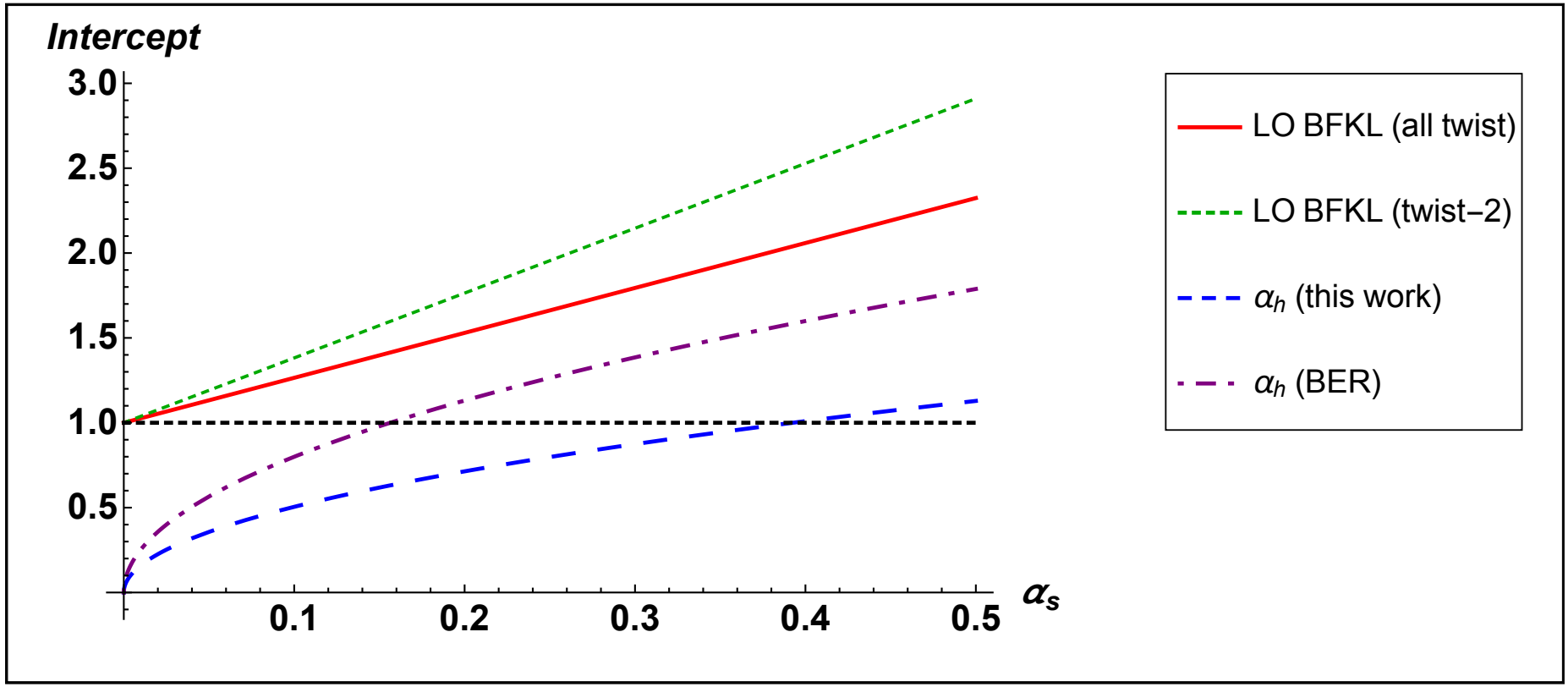
- The resulting small-x asymptotics is

$$g_1^S(x,Q^2) \sim \Delta q^S(x,Q^2) \sim g_{1L}^S(x,k_T^2) \sim \left(\frac{1}{x}\right)^{\alpha_h} \approx \left(\frac{1}{x}\right)^{2.31\sqrt{\frac{\alpha_s N_c}{2\pi}}}$$

- Our result, 2.31, is about 35% smaller than BER's 3.66 any-N_C pure glue.

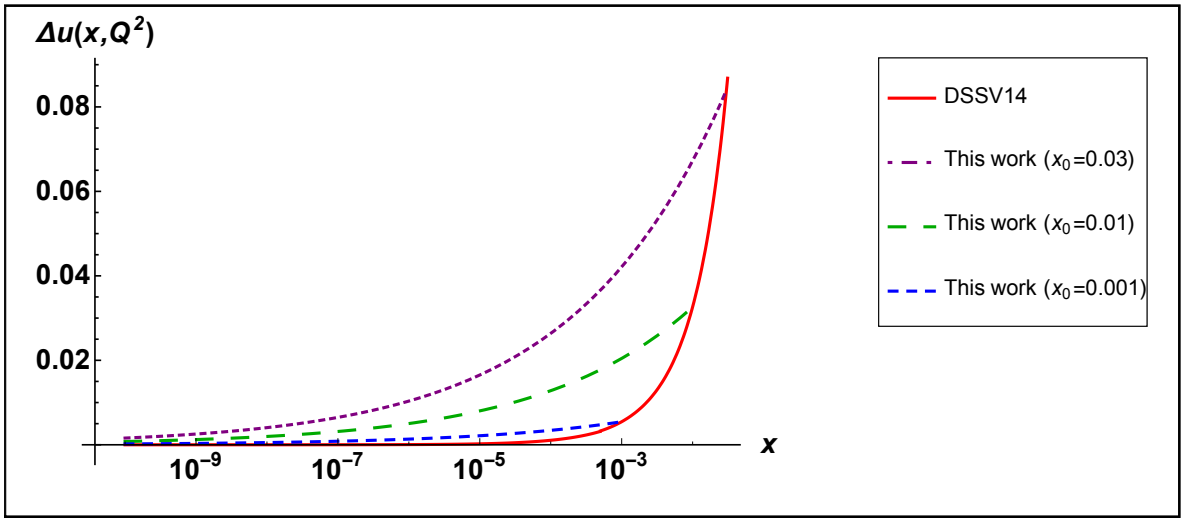
Intercepts

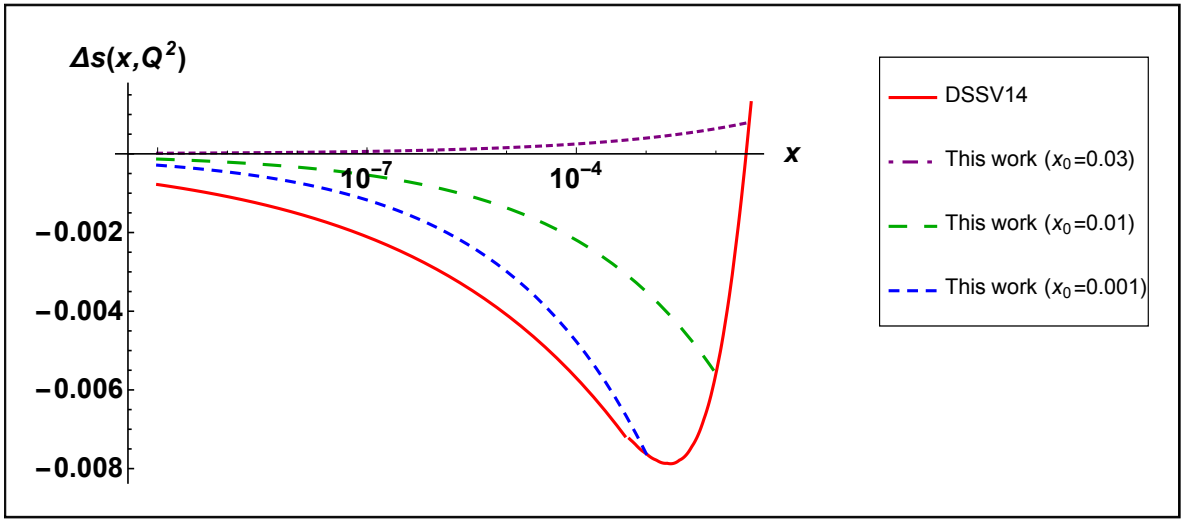
Here we plot our (flavor-singlet) helicity intercept as a function of the coupling.
We show BER result and LO BFKL (all twist and leading twist) for comparison.



Impact on proton spin

- We have attached a $\Delta\tilde{\Sigma}(x,Q^2) = N\,x^{-\alpha_h}$ curve to the existing hPDF's fits at some ad hoc small value of x labeled x_0 :

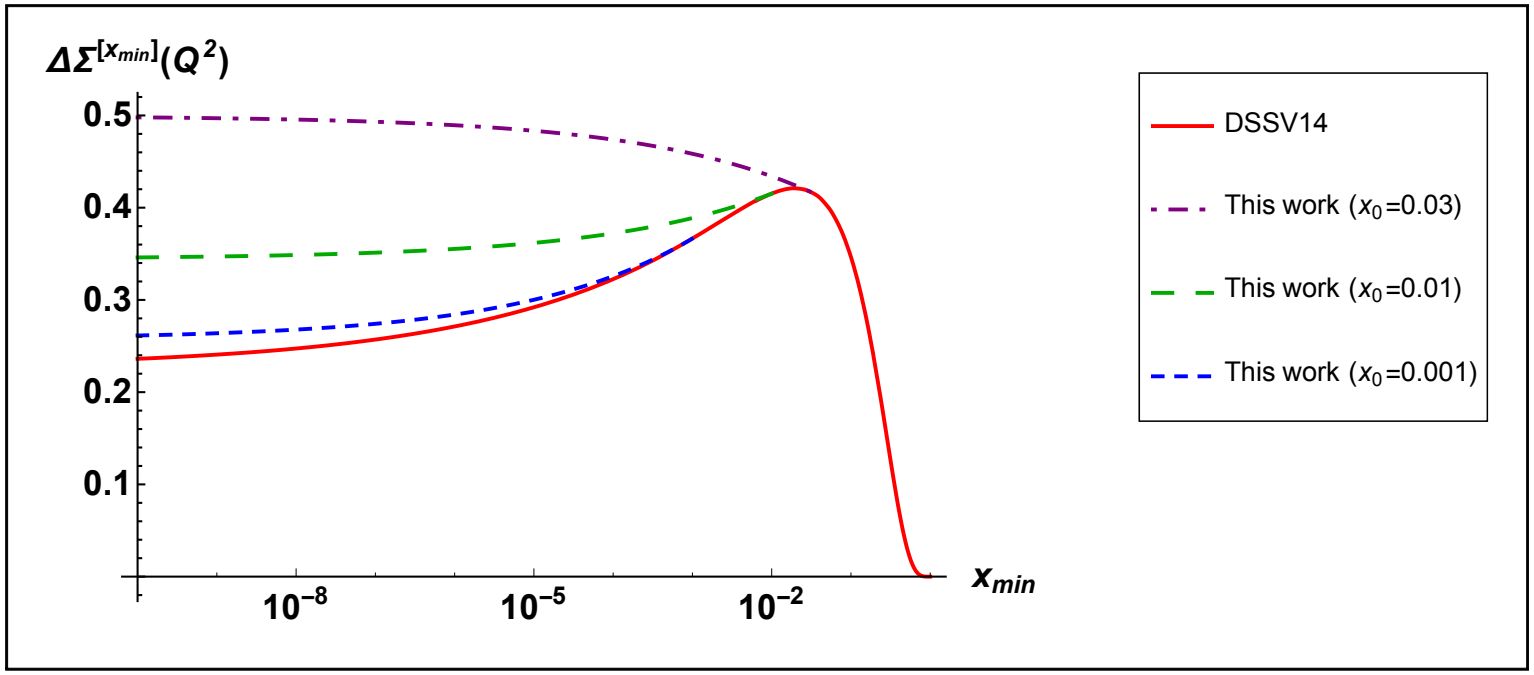




"ballpark" phenomenology

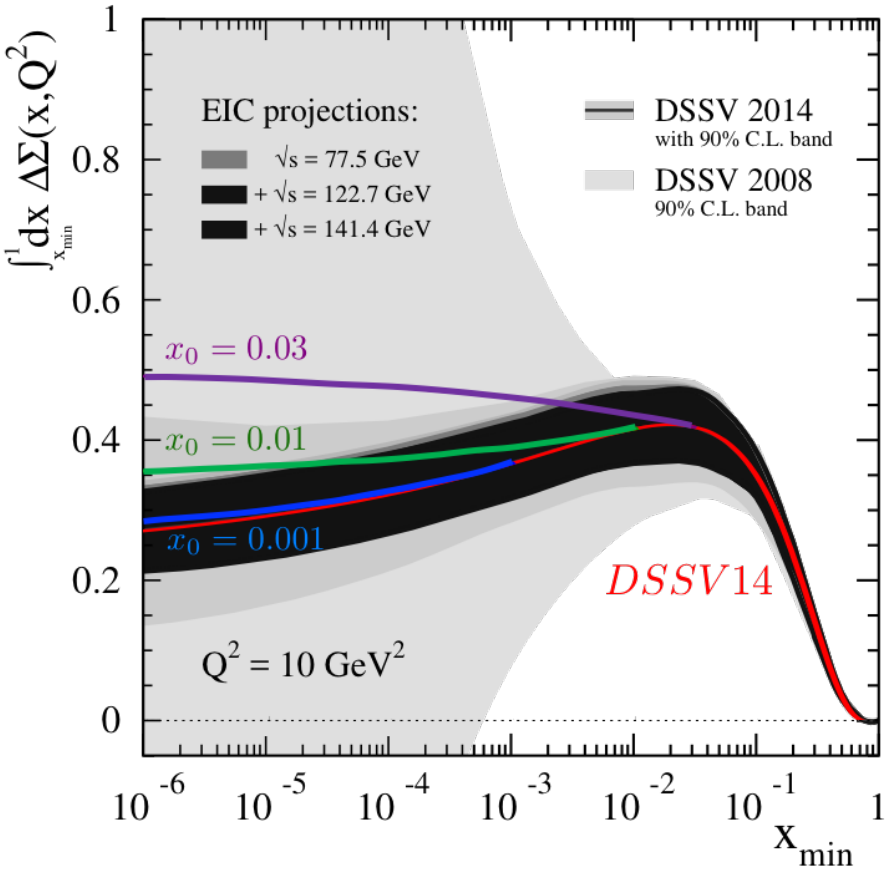
Impact on proton spin

- Defining $\Delta\Sigma^{[x_{min}]}(Q^2) \equiv \int_{x_{min}}^{1} dx\, \Delta\Sigma(x, Q^2)$ we plot it for x_0=0.03, 0.01, 0.001:



- We observe a moderate to significant enhancement of quark spin.
- More detailed phenomenology is needed in the future.

Impact on proton spin



- Here we compare our results with DSSV, now including the error band.
- We observe consistency of our lower two curves with DSSV.
- Our upper curve disagrees with DSSV, but agrees with NNPDF (Nocera, Santopinto, ‘16).
- Better phenomenology is needed. EIC would definitely play a role.

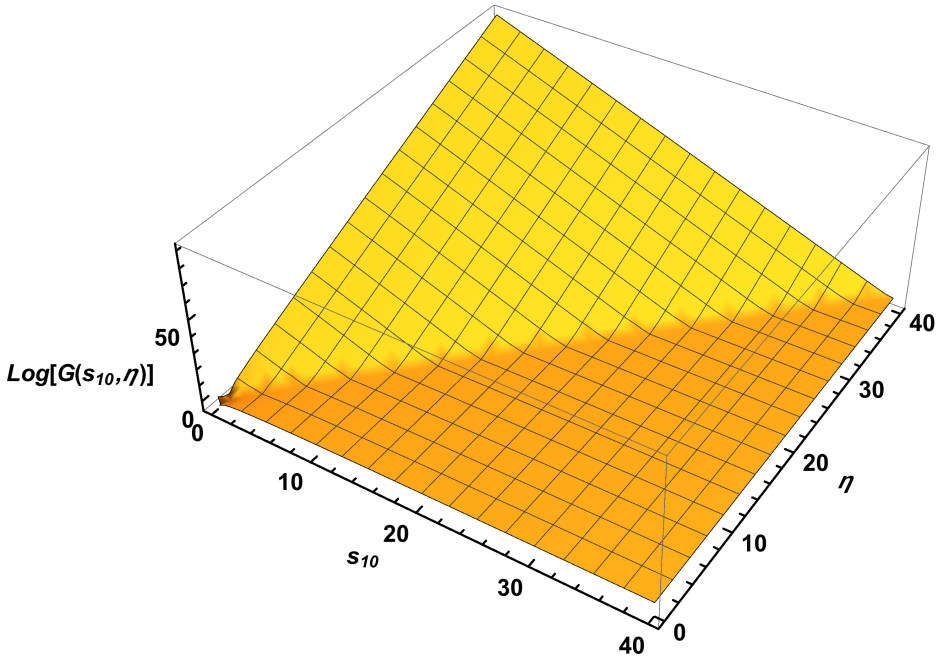
Large-N_c Equations: Analytic Solution

Yu.K., D. Pitonyak, M. Sievert, arXiv:1703.05809 [hep-ph]

Scaling

- Consider our numerical solution again

$$\eta = \sqrt{\frac{\alpha_s N_c}{2\pi}}\,\ln\frac{zs}{\Lambda^2} \qquad s_{10} = \sqrt{\frac{\alpha_s N_c}{2\pi}}\,\ln\frac{1}{x_{10}^2\,\Lambda^2}$$



- It is well approximated by

$$G(s_{10},\eta) \propto e^{2.31\,(\eta - s_{10})}$$

- This motivated us to look for the solution in the following scaling form:

$$G(s_{10},\eta) = G(\eta - s_{10})$$
$$\Gamma(s_{10},s_{21},\eta') = \Gamma(\eta' - s_{10},\eta' - s_{21})$$

Scaling Equations

- The large-N_c evolution equations can be rewritten in terms of the scaling variables (not a trivial property, does not work for the large-N_c&N_f equations):

$$G(\zeta) = 1 + \int_0^\zeta d\xi \int_0^\xi d\xi' \; [\Gamma(\xi, \xi') + 3\, G(\xi')] \,,$$

$$\Gamma(\zeta, \zeta') = 1 + \int_0^{\zeta'} d\xi \int_0^\xi d\xi' \; [\Gamma(\xi, \xi') + 3\, G(\xi')]$$

$$+ \int_{\zeta'}^\zeta d\xi \int_0^{\zeta'} d\xi' \, [\Gamma(\xi, \xi') + 3\, G(\xi')]$$

- For simplicity, pick the following initial conditions:

$$G(0) = 1, \quad \Gamma(\zeta', \zeta') = G(\zeta')$$

Analytic Solution

- These scaling equations can be solved exactly via Laplace transform + a few clever tricks, yielding

$$G(\zeta) = \int \frac{d\omega}{2\pi i}\, e^{\omega\,\zeta + \frac{\zeta}{\omega}}\; \frac{\omega^2 - 1}{\omega\,(\omega^2 - 3)},$$

$$\Gamma(\zeta, \zeta') = 4 \int \frac{d\omega}{2\pi i}\, e^{\omega\,\zeta' + \frac{\zeta}{\omega}}\; \frac{\omega^2 - 1}{\omega\,(\omega^2 - 3)}$$

$$- 3 \int \frac{d\omega}{2\pi i}\, e^{\omega\,\zeta' + \frac{\zeta'}{\omega}}\; \frac{\omega^2 - 1}{\omega\,(\omega^2 - 3)}.$$

- As usual, the high-energy asymptotics is given by the right-most pole in the complex ω-plane: the pole is at $\omega = +\sqrt{3}$.

Analytic Solution and Intercept

- The contribution of the pole at $\omega = +\sqrt{3}$ is

$$G(\zeta) \approx \frac{1}{3} e^{\frac{4}{\sqrt{3}}\zeta}$$

$$\Gamma(\zeta, \zeta') \approx \frac{1}{3} e^{\frac{4}{\sqrt{3}}\zeta'} \left(4e^{\frac{\zeta - \zeta'}{\sqrt{3}}} - 3 \right)$$

$$= G(\zeta') \left(4e^{\frac{\zeta - \zeta'}{\sqrt{3}}} - 3 \right)$$

- The corresponding helicity intercept is

$$\alpha_h = \frac{4}{\sqrt{3}} \sqrt{\frac{\alpha_s N_c}{2\pi}} \approx 2.3094 \sqrt{\frac{\alpha_s N_c}{2\pi}}$$

- This is in complete agreement with the numerical solution!

$$\alpha_h \approx 2.31 \sqrt{\frac{\alpha_s N_c}{2\pi}}$$

Conclusions

- We have constructed new DLA evolution equations for the polarized dipole operator, which allow us to find the small-x asymptotics of the quark helicity TMDs and PDFs and of the g_1 structure function.

- Like the B-JIMWLK hierarchy, our equations do not close in general. They close in the large-N_C and large-N_C&N_f limits.

- Solution of the flavor singlet evolution equations at large-N_C gives

$$g_1^S(x,Q^2) \sim \Delta q^S(x,Q^2) \sim g_{1L}^S(x,k_T^2) \sim \left(\frac{1}{x}\right)^{\alpha_h} = \left(\frac{1}{x}\right)^{\frac{4}{\sqrt{3}}\sqrt{\frac{\alpha_s N_c}{2\pi}}}$$

  which may potentially generate a solid amount of spin at small-x.

- Future work includes gluon helicity TMD at small x (coming soon) and may involve including running coupling and saturation corrections + solving the large-N_C&N_f equations.

Backup Slides

Polarized “Wilson line”

- Our polarized “Wilson line” is defined as (for purely gluonic exchanges with the target)

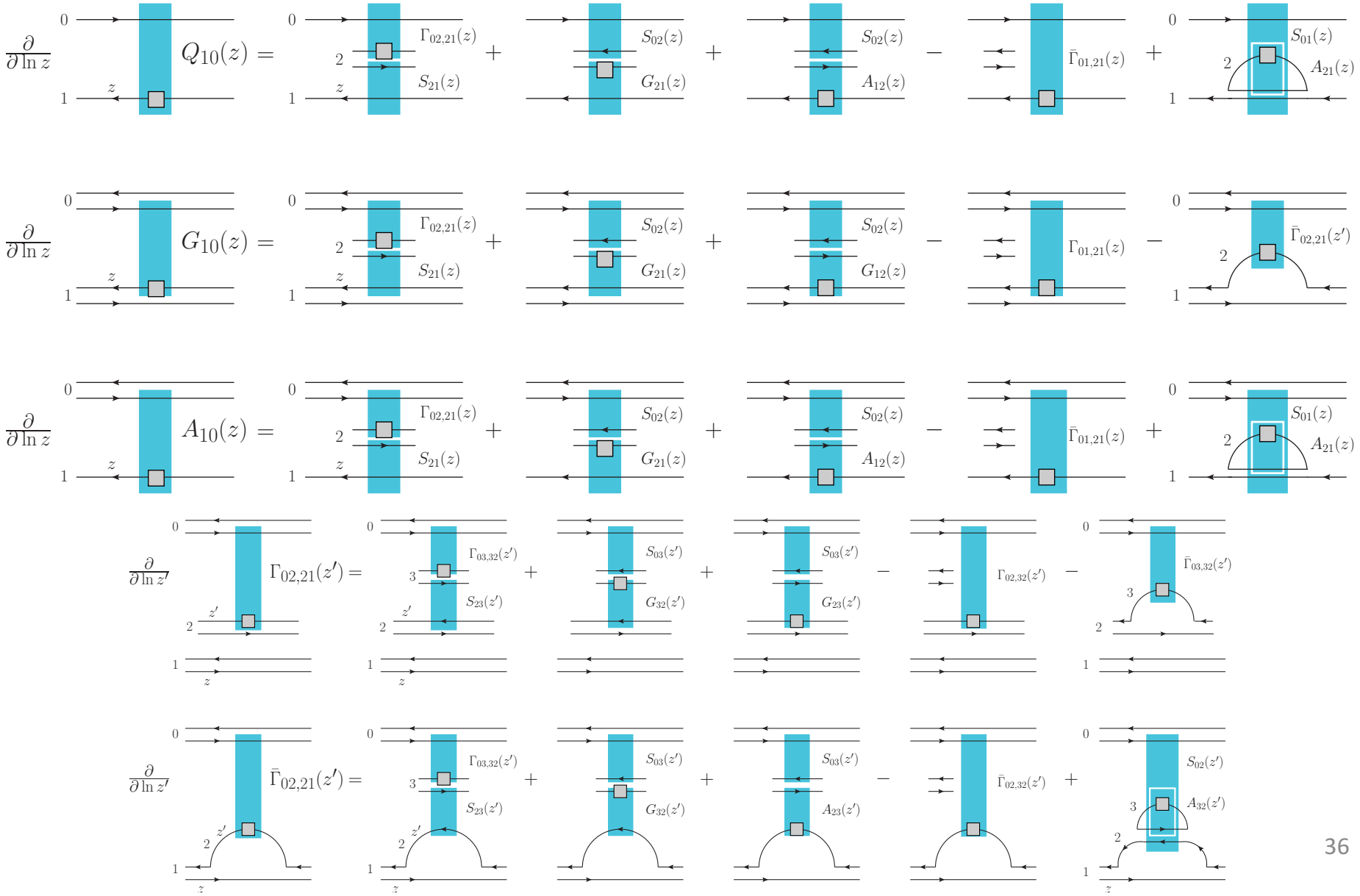
$$V^{pol}_{\underline{x}} = \frac{1}{2\,s}\int\limits_{-\infty}^{\infty} dx^- \,\mathrm{P}\exp\left\{ig\int\limits_{x^-}^{\infty} dx'^-\, A^+(x'^-,\underline{x})\right\} ig\,\underline{\nabla}\times\underline{\tilde{A}}(x^-,\underline{x})\,\mathrm{P}\exp\left\{ig\int\limits_{-\infty}^{x^-} dx'^-\, A^+(x'^-,\underline{x})\right\}$$

where $\underline{A}_{\Sigma}(x^-,\underline{x}) = \dfrac{\Sigma}{2p_1^+}\,\underline{\tilde{A}}(x^-,\underline{x})$ is the spin-dependent gluon field of the plus-direction moving target. (A^+ is the unpolarized eikonal field.)

- In preparation…

Polarized Dipole Evolution in the Large-N_c&N_f Limit

In the large-N_c&N_f limit the equations close too, leading to a closed system of 5 equations:



Large-N_c&N_f Evolution

- The evolution equations read (in the strict DLA limit, S=1):

$$Q_{01}(z) = Q_{01}^{(0)}(z) + \frac{\alpha_s N_c}{2\pi^2}\int_{z_i}^{z}\frac{dz'}{z'}\int_{\rho'^2}\frac{d^2x_2}{x_{21}^2}\,\theta(x_{10}-x_{21})\,\left[G_{12}(z')+\Gamma_{02,21}(z')+A_{21}(z')-\bar{\Gamma}_{01,21}(z')\right]$$

$$+\frac{\alpha_s N_c}{4\pi^2}\int_{z_i}^{z}\frac{dz'}{z'}\int_{\rho'^2}\frac{d^2x_2}{x_{21}^2}\,\theta(x_{10}^2 z - x_{21}^2 z')\,A_{21}(z'),$$

$$G_{10}(z) = G_{10}^{(0)}(z) + \frac{\alpha_s N_c}{2\pi^2}\int_{z_i}^{z}\frac{dz'}{z'}\int_{\rho'^2}\frac{d^2x_2}{x_{21}^2}\,\theta(x_{10}-x_{21})\,\left[\Gamma_{02,21}(z')+3\,G_{12}(z')\right]$$

$$-\frac{\alpha_s N_f}{4\pi^2}\int_{z_i}^{z}\frac{dz'}{z'}\int_{\rho'^2}\frac{d^2x_2}{x_{21}^2}\,\theta(x_{10}^2 z - x_{21}^2 z')\,\bar{\Gamma}_{02,21}(z'),$$

$$A_{01}(z) = A_{01}^{(0)}(z) + \frac{\alpha_s N_c}{2\pi^2}\int_{z_i}^{z}\frac{dz'}{z'}\int_{\rho'^2}\frac{d^2x_2}{x_{21}^2}\,\theta(x_{10}-x_{21})\,\left[G_{12}(z')+\Gamma_{02,21}(z')+A_{21}(z')-\bar{\Gamma}_{01,21}(z')\right]$$

$$+\frac{\alpha_s N_c}{4\pi^2}\int_{z_i}^{z}\frac{dz'}{z'}\int_{\rho'^2}\frac{d^2x_2}{x_{21}^2}\,\theta(x_{10}^2 z - x_{21}^2 z')\,A_{12}(z').$$

$$\Gamma_{02,21}(z') = \Gamma_{02,21}^{(0)}(z') + \frac{\alpha_s N_c}{2\pi}\int_{z_i}^{z'}\frac{dz''}{z''}\int_{\rho''^2}^{\min\{x_{02}^2,\,x_{21}^2\,z'/z''\}}\frac{dx_{32}^2}{x_{32}^2}\,\left[\Gamma_{03,32}(z'')+3\,G_{23}(z'')\right]$$

$$-\frac{\alpha_s N_f}{4\pi}\int_{z_i}^{z'}\frac{dz''}{z''}\int_{\rho''^2}^{x_{21}^2\,z'/z''}\frac{dx_{32}^2}{x_{32}^2}\,\bar{\Gamma}_{03,32}(z'),$$

$$\bar{\Gamma}_{02,21}(z') = \bar{\Gamma}_{02,21}^{(0)}(z') + \frac{\alpha_s N_c}{2\pi}\int_{z_i}^{z'}\frac{dz''}{z''}\int_{\rho''^2}^{\min\{x_{02}^2,\,x_{21}^2\,z'/z''\}}\frac{dx_{32}^2}{x_{32}^2}\,\left[\Gamma_{03,32}(z'')+G_{23}(z'')+A_{23}(z'')-\bar{\Gamma}_{02,32}(z'')\right]$$

$$+\frac{\alpha_s N_c}{4\pi}\int_{z_i}^{z'}\frac{dz''}{z''}\int_{\rho''^2}^{x_{21}^2\,z'/z''}\frac{dx_{32}^2}{x_{32}^2}\,A_{32}(z').$$

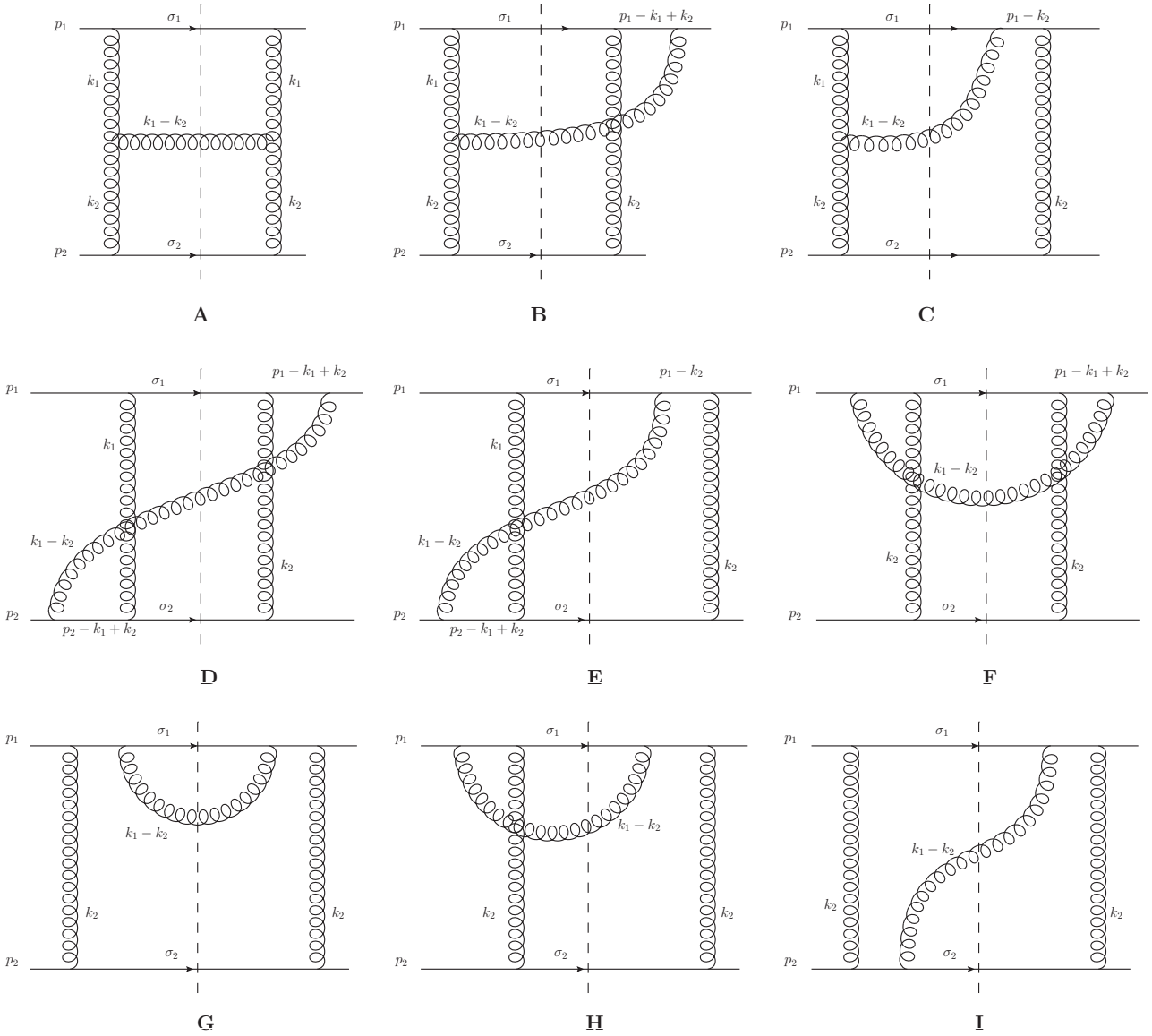
Intercepts

- We can summarize some LO intercepts, including the ones we found, in the following table:

Observable	Evolution	Intercept	$Q^2 = 3$ GeV^2 $\alpha_s = 0.343$	$Q^2 = 10$ GeV^2 $\alpha_s = 0.249$	$Q^2 = 87$ GeV^2 $\alpha_s = 0.18$
Unpolarized flavor singlet structure function F_2	LO BFKL Pomeron	$1 + \frac{\alpha_s N_c}{\pi} 4 \ln 2$	1.908	1.659	1.477
Unpolarized flavor non-singlet structure function F_2	Reggeon	$\sqrt{\frac{2\,\alpha_s C_F}{\pi}}$	0.540	0.460	0.391
Flavor singlet structure function g_1^S	us (Pure Glue)	$2.31\sqrt{\frac{\alpha_s N_c}{2\pi}}$	0.936	0.797	0.678
	BER (Pure Glue)	$3.66\sqrt{\frac{\alpha_s N_c}{2\pi}}$	1.481	1.262	1.073
	BER ($N_f = 4$)	$3.45\sqrt{\frac{\alpha_s N_c}{2\pi}}$	1.400	1.190	1.011
Flavor non-singlet structure function g_1^{NS}	BER and us (large-N_c)	$\sqrt{\frac{\alpha_s N_c}{\pi}}$	0.572	0.488	0.415

$$\alpha_h^{BER} = \sqrt{\frac{17+\sqrt{97}}{2}}\sqrt{\frac{\alpha_s N_c}{2\pi}} \approx 3.66\sqrt{\frac{\alpha_s N_c}{2\pi}}$$

Comparison with BER



To better understand BER work, we tried calculating one (real) step of DLA helicity evolution for the qq->qq scattering.

It appears that we have identified the $k_2 >> k_1$ (or $k_1 >> k_2$) regime in which diagrams A, B, C, D, E, I are DLA, which was not considered by BER for B, C, … I.

Helicity Evolution at Small x

flavor non-singlet case

Yu.K., D. Pitonyak, M. Sievert, arXiv:1610.06197 [hep-ph]

Flavor Non-Singlet Observables

- In the flavor non-singlet case, all helicity observables again depend on the polarized dipole amplitude:

$$g_1^{NS}(x,Q^2) = \frac{N_c}{2\,\pi^2\alpha_{EM}} \int\limits_{z_i}^{1} \frac{dz}{z^2(1-z)} \int dx_{01}^2 \left[\frac{1}{2}\sum_{\lambda\sigma\sigma'} |\psi^T_{\lambda\sigma\sigma'}|^2_{(x_{01}^2,z)} + \sum_{\sigma\sigma'} |\psi^L_{\sigma\sigma'}|^2_{(x_{01}^2,z)}\right] G^{NS}(x_{01}^2,z),$$

$$\Delta q^{NS}(x,Q^2) = \frac{N_c}{2\pi^3} \int\limits_{z_i}^{1} \frac{dz}{z} \int\limits_{\frac{1}{zs}}^{\frac{1}{zQ^2}} \frac{dx_{01}^2}{x_{01}^2}\, G^{NS}(x_{01}^2,z),$$

$$g_{1L}^{NS}(x,k_T^2) = \frac{8\,N_c}{(2\pi)^6} \int\limits_{z_i}^{1} \frac{dz}{z} \int d^2x_{01}\, d^2x_{0'1}\, e^{-i\underline{k}\cdot(\underline{x}_{01}-\underline{x}_{0'1})}\, \frac{\underline{x}_{01}\cdot\underline{x}_{0'1}}{x_{01}^2 x_{0'1}^2}\, G^{NS}(x_{01}^2,z)$$

- Polarized dipole amplitude is different (difference instead of sum):

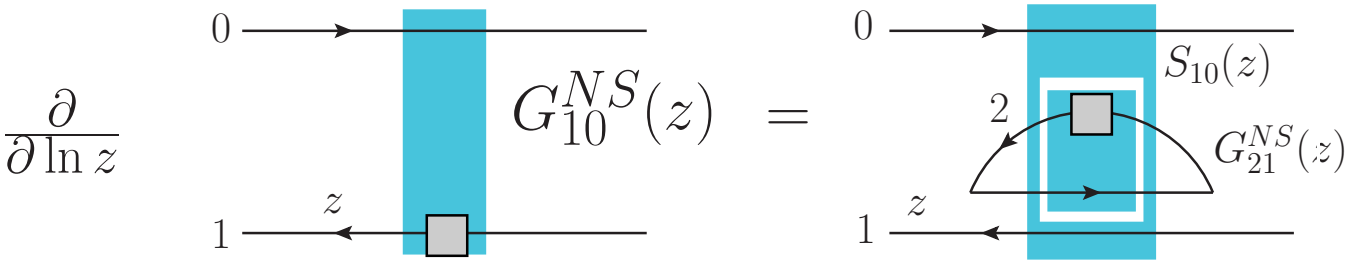
$$G_{10}^{NS}(z) \equiv \frac{1}{2N_c}\left\langle\!\!\left\langle \mathrm{tr}\left[V_{\underline{0}} V_{\underline{1}}^{pol\,\dagger}\right] - \mathrm{tr}\left[V_{\underline{1}}^{pol} V_{\underline{0}}^{\dagger}\right] \right\rangle\!\!\right\rangle(z)$$

- This is related to the definition

$$\Delta q^{NS}(x,Q^2) \equiv \Delta q^f(x,Q^2) - \Delta\bar{q}^f(x,Q^2)$$

Flavor Non-Singlet Evolution

- Evolution equations end up being much simpler in the non-singlet case:



$$G_{10}^{NS}(z) = G_{10}^{NS\,(0)}(z) + \frac{\alpha_s N_c}{4\pi} \int_{\frac{\Lambda^2}{s}}^{z} \frac{dz'}{z'} \int_{\frac{1}{z's}}^{x_{10}^2 \frac{z}{z'}} \frac{dx_{21}^2}{x_{21}^2}\, S_{10}(z')\, G_{21}^{NS}(z')$$

- Analytical solution (in the DLA case, S=1) leads to (in agreement with Bartels et al, '95)

$$g_1^{NS}(x,Q^2) \sim \Delta q^{NS}(x,Q^2) \sim g_{1L}^{NS}(x,k_T^2) \sim \left(\frac{1}{x}\right)^{\alpha_h^{NS}} \approx \left(\frac{1}{x}\right)^{\sqrt{\frac{\alpha_s N_c}{\pi}}}$$

- The resulting intercept is smaller than the flavor-singlet intercept.

Exploring correlations in the CGC wave function.

Alex Kovner

University of Connecticut

April 28, 2017

[with M. Lublinsky and V. Skokov, arXiv:1612.07790 [hep-ph]]

Motivation

Correlations in pA: who is responsible?

Do they come from collective effects in the final state?

Is p-A collisions really hydro? Even up to $p_T \approx 10 Gev$?

Or do they come from correlated structure of the initial wave function?

The Ridge in Double Inclusive Hadron Production in p-p.

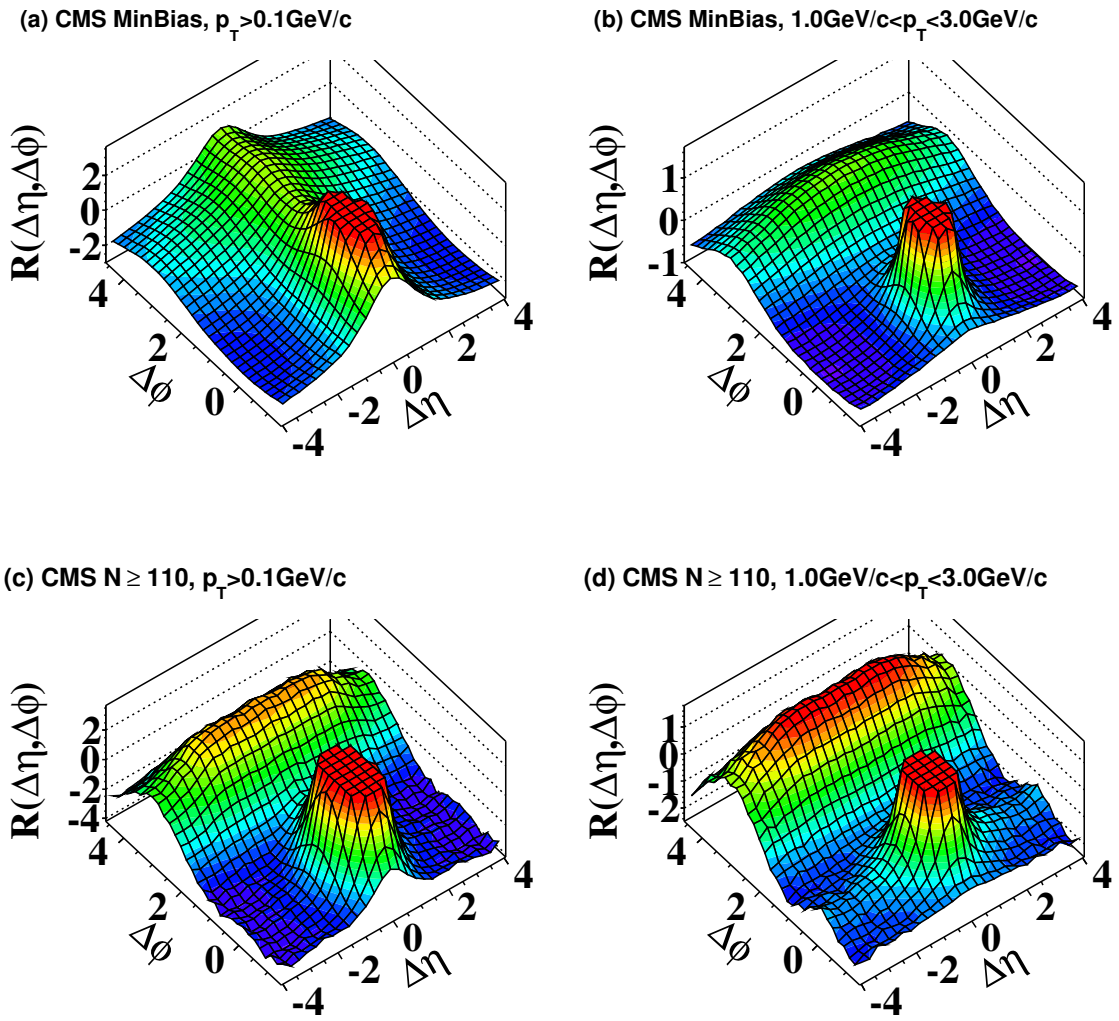


Figure: Ridge in p-p at CMS circa 2010, $\sim 10^{-6}$ events

Ridge in p-Pb.

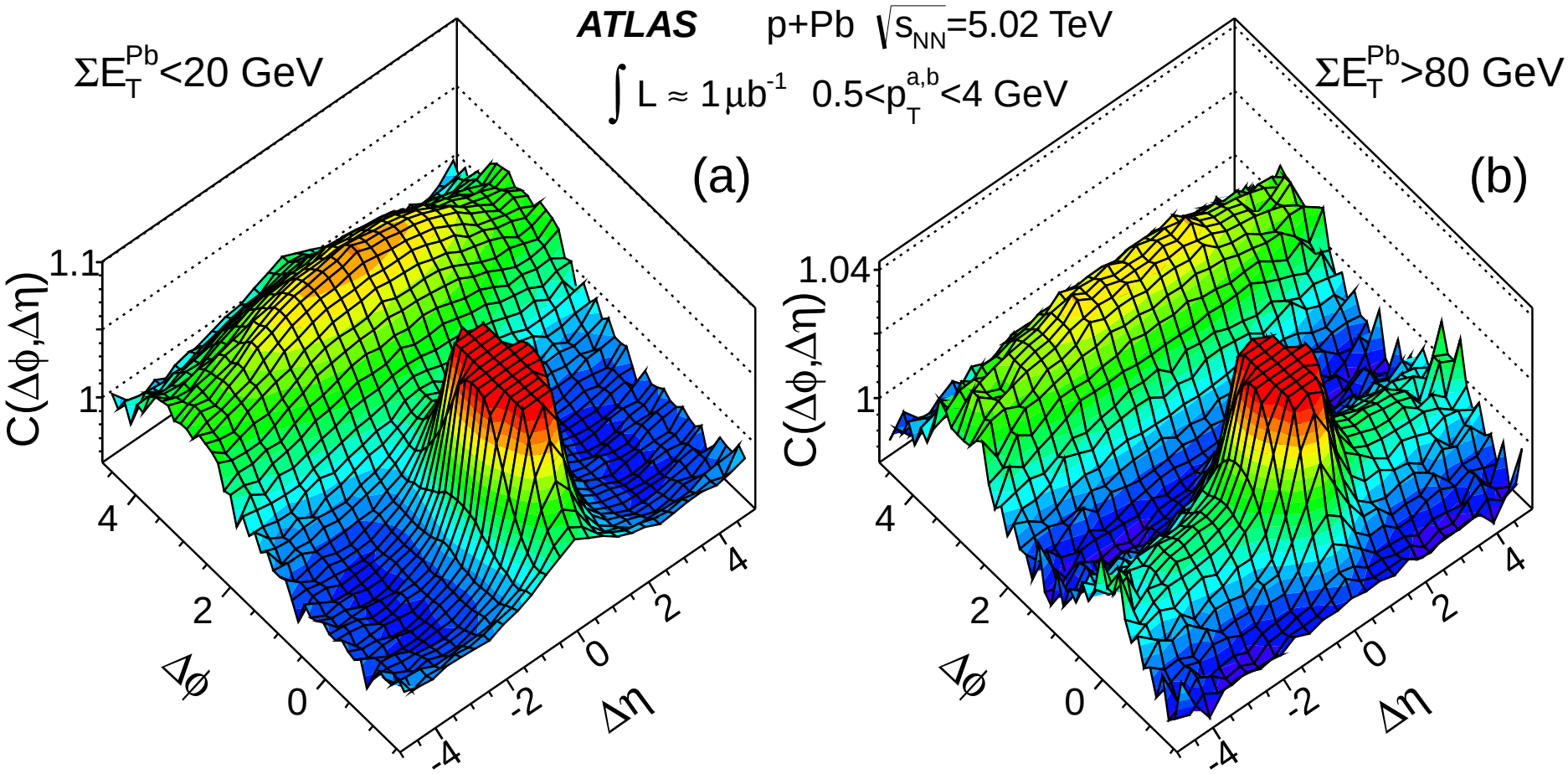
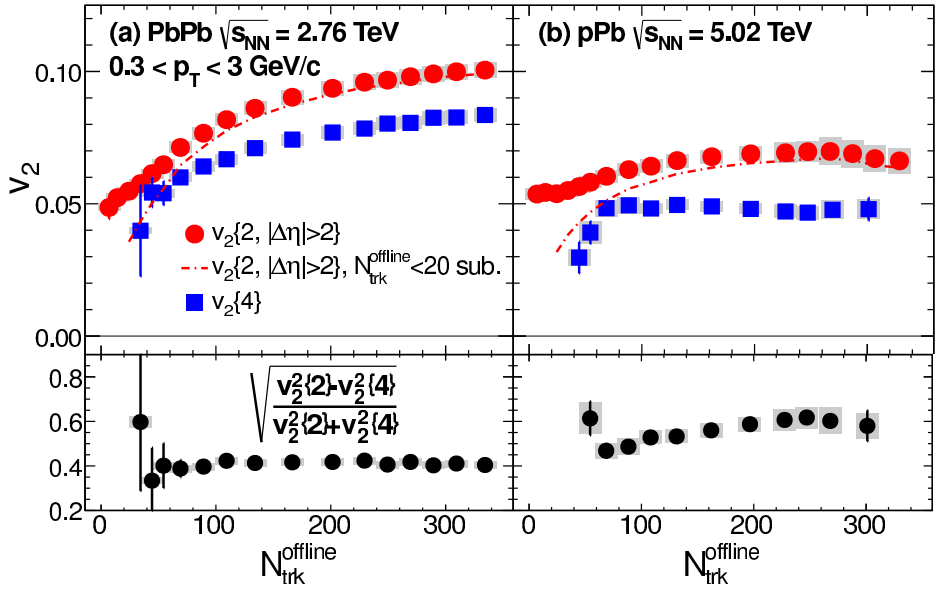
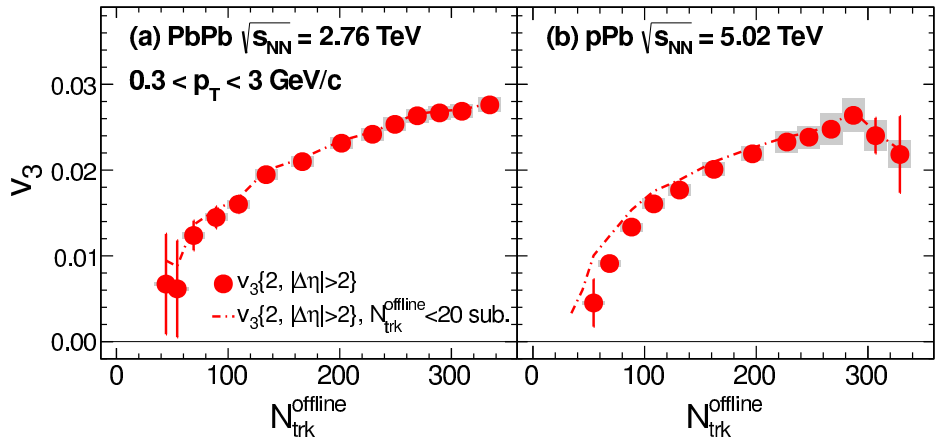


Figure: Ridge in p-Pb at ATLAS, $\sim 10^{-2}$ events

Things got more interesting.

The correlations point to collective, or at least quasi collective behavior.





"Flow coefficients" measure correlations between the emitted particles, and are believed to encode collectivity of the final state. For double inclusive spectrum

$$\frac{d^2N}{d^2p_1 d^2p_2} \propto 1 + \sum_{n=1}^{\infty} 2V_n(\mathbf{p_1}, \mathbf{p_2}) \cos(n\Delta\phi)$$

$$v_n^2 = \frac{V_n(p_T, p_T^{ref})}{\sqrt{V_n(p_T^{ref}, p_T^{ref})}}; \quad n = 2, 3$$

Analogously for v_2^4 - from four particle inclusive spectrum.
Hydro codes seem to describe the data on v_n.
But: the produced system is small, the momenta involved are quite large $\sim 8 Gev$, so that hydro is suspect.

Even more exciting: recent CMS and ATLAS analysis of p-p at LHC - ridge persists even in MIN. BIAS events, and below.

Does the ridge and v_n data necessarily require strong final state interactions?
Is it possible that nontrivial initial state correlations mimic collectivity (quasi collectivity)?

Saturation?

Initially ridge was found in small fraction, high multiplicity events: "rare" proton configurations with high density. Perhaps saturation is at play?

Several possible mechanisms to generate correlations from initial state.

G. Levin and A. Rezaeian - density profile variation;
A.K nd M. Lublinsky - local anisotropy of target fields;
The one explored phenomenologically:
"Glasma graphs" $\equiv$ gluon Bose enhancement Dumitru, Gelis, Jalilian-Marian, Lappi: Phys.Lett. B697 (2011) 21 (arXiv:1009.5295)
Followed by a quantitative effort to describe data: Dusling and Venugopalan Phys.Rev.Lett. 108 (2012) 262001 (arXiv:1201.2658); arXiv:1302.7018
In the calculation - no final state interctions. Correlations are "inherited" from the initial state.

Where is v_3?

All the approaches invariably lead to "symmetry"

$$\sigma(p_T, k_T) = \sigma(p_T, -k_T)$$

It is NOT a symmetry of QCD: it is "acccidental".

E.G: It is broken by final state interactions: L.McLerran and V. Skokov : arXiv:1611.09870; B.Schenke, S. Schlichting, R. Venugopalan Phys.Lett. B747 (2015) 76-82,

Is the "dilute" CGC state we are using good enough?

Better approximation to the CGC state?

The CGC hadron wave function.

High energy factorization: the fast partons are dressed by the soft gluon cloud.

Fast partons: color charge density in the transverse plane $\rho^a(x_\perp)$.

Soft gluons: the Weiszacker-Williams cloud.

Soft gluon wave function **in dilute limit**:

$$\Psi[A] = e^{i\int_{x_\perp} b_i[\rho]A_i(x_\perp)}|0\rangle$$

Solution of classical Yang-Mills equation:

$$\partial_i b_i^a(x_\perp) = g\rho^a(x_\perp)$$

ρ has to be averaged over with some weight functional, e.g. simplest Gaussian: McLerran-Venugopalan model.

Denser is better?

The inspiration: The Old Kharzeev-Levin-McLerran argument.

A single high p_T parton in the wave function is most likely accompanied by several lower p_T partons, who collectively balance the transverse momentum.

This is kinda like flow: many particles move along an axis, which is determined by a fluctuation.

But coherent state does not do that!

But it is also true that Coherent state is not the whole story: it is only dilute limit of the CGC wave function.

A better CGC state.

The first "dense" correction to the CGC wave function (T.Altinoluk,A.K., M. Lublinsky, J. Peressutti, JHEP 0903 (2009) 109)

$$\Psi_{CGC}[\phi] = \mathcal{N}\, e^{i\sqrt{2}\int_k b_{\alpha i}(-k)\left[a^\dagger_{\alpha i}(k)\,+\,a_{\alpha i}(-k)\right]}\times$$

$$e^{-\frac{1}{4}\int_{k,p} B^{-1}_{\alpha\beta ij}(k,p)\left[a^\dagger_{\alpha i}(k)+a_{\alpha i}(-k)\right]\left[a^\dagger_{\beta j}(p)+a_{\beta j}(-p)\right]}$$

The WW field $b_{\alpha i}$:

$$\partial_i b_{\alpha i}(x) = g\rho_\alpha(x)$$

The operator B:

$$B = (1 - I - L)^2 = 1 - I - L + [I, L]_+$$

where

$$I^{\alpha\beta}_{ij}(x,y) \equiv \delta^{\alpha\beta}\frac{\partial_i\partial_j}{\partial^2}(x,y); \qquad L^{\alpha\beta}_{ij}(x,y) = U^{\alpha\gamma}(x)\frac{\partial_i\partial_j}{\partial^2}(x,y)U^{\dagger\,\gamma\beta}(y)$$

Gluon correlations in the wave function.

The first question: is there "accidental" symmetry in the wave function?

Answer: No!

$$\frac{1}{2}(f(k,p)-f(k,-p))=\frac{1}{2}\left(b(k)\tilde{B}(-k,p)b(-p)+b(-k)\tilde{B}(k,-p)b(p)\right)$$

$$-\frac{1}{2}\left(b(k)\tilde{B}(-k,-p)b(p)+b(-k)\tilde{B}(k,p)b(-p)\right),$$

Important thing for now: it does not vanish. More later.

Particle production.

Scatter this projectile wave function on a target eikonally. Things fundamentally do not change: the antisymmetric part of the production does not vanish.

$$\frac{1}{2}(\sigma(k,p)-\sigma(k,-p)) = \frac{\mathbb{C}(k)}{2}\frac{\mathbb{A}\mathbb{A}^T(-k,p)-\delta(p-k)}{2}\frac{\mathbb{C}(-p)}{2}$$
$$+\frac{\mathbb{C}(-k)}{2}\frac{\mathbb{A}\mathbb{A}^T(k,-p)-\delta(p-k)}{2}\frac{\mathbb{C}(p)}{2}$$
$$-\frac{\mathbb{C}(k)}{2}\frac{\mathbb{A}\mathbb{A}^T(-k,-p)-\delta(p+k)}{2}\frac{\mathbb{C}(p)}{2}$$
$$-\frac{\mathbb{C}(-k)}{2}\frac{\mathbb{A}\mathbb{A}^T(k,p)-\delta(p+k)}{2}\frac{\mathbb{C}(-p)}{2}$$

$\mathbb{A}$ and $\mathbb{C}$ depend on the WW field b and the eikonal scattering matrix S.

The letters:

$$\mathbb{A} \stackrel{\text{def}}{=} \bar{\Gamma}^{-1} S \Gamma \,,$$
$$\mathbb{C} \stackrel{\text{def}}{=} 2\bar{\Gamma}^{T}(Sb - \bar{b})\,.$$

with

$$\Gamma \equiv (\mathfrak{t} - \mathfrak{l})(1 - \mathfrak{l} - L); \quad \bar{b} \equiv b[S\rho]; \qquad \bar{L} = L[\bar{b}]$$

Some drastic approximations.

The crucial question: **what is the sign of the coefficient of the third harmonic** $V_3 \cos 3\phi$)**?** $v_3 = \sqrt{V_3}$

Let's try to get an idea what our long expressions mean.

A. High transverse momentum:
$p_T,\ k_T \gg Q_S^P \approx g^4\mu^2$; $p_T,\ k_T \gg Q_T^P \approx g^4\lambda^2$

B. McLerran-Venugopalan model for the projectile - expand to leading order in μ.

C. Operator product expansion on the target side.

Correlated production can be expressed in terms of "condensates" of the eikonal factors $< \partial S \partial S^\dagger ... >$

The Odderon rules.

At high k_T the leading term in the operator product expansion is the Odderon. At leading order in $1/k_T$:

$$\propto \frac{\mu^4}{p^4 k^4} \Lambda_{st}(k,p) \Big[f^{acd} S^{de} \partial_t S^{\dagger eb} f^{cbf} S^{fg} \partial_s S^{\dagger ga} - (S \to S^\dagger) \Big]$$

C- conjugation odd, i. e. Oddeon.

We do not have a well motivated model for Odderon - so at this order the sign of the correlated contribution is not fixed.

But the Odderon is subleading at high energies.

Target averaging.

At short distances we can write without approximation:

$$S(x) = \exp\{iT^a E_i^a x_i\}$$

which leads to

$$\partial_s S(x) \to iT^a E_s^a; \qquad \partial_r \partial_s S(x) \to -\frac{1}{2}\{T^a, T^b\} E_s^a E_t^b; \qquad etc.$$

We then assume Wick factorization of averages with

$$\langle E_i^a E_j^b \rangle = \lambda^2 \delta^{ab} \delta_{ij}$$

The answer.

This is our correlated yield:

$$g^2 N_c^5 A \frac{\mu^4 \lambda^4}{k^4 p^4} \Bigg\{ -\frac{29}{4}\frac{k\cdot p}{k^2 p^2} - 3\frac{(k\cdot p)^3}{k^4 p^4} + \frac{15}{2}\frac{k\cdot(k-p)p\cdot(k-p)}{k^2 p^2 (k-p)^2}$$
$$+\frac{k\cdot p(p\cdot(k-p))^2}{k^2 p^4 (k-p)^2} + \frac{k\cdot p(k\cdot(k-p))^2}{k^4 p^2 (k-p)^2}$$
$$+\frac{1}{4}\frac{(k\cdot(k-p))^2}{k^2(k-p)^2}\left(\frac{5}{k^2}-\frac{7}{p^2}\right) + \frac{1}{4}\frac{(p\cdot(k-p))^2}{p^2(k-p)^2}\left(\frac{5}{p^2}-\frac{7}{k^2}\right)$$
$$+\frac{7}{2}\left(\frac{1}{k^2}+\frac{1}{p^2}\right)\frac{k\cdot pk\cdot(k-p)p\cdot(k-p)}{k^2 p^2 (k-p)^2}$$
$$+\frac{3}{8}\left[\frac{k\cdot(k-p)}{k^2(k-p)^2} - \frac{p\cdot(k-p)}{p^2(k-p)^2}\right]\Bigg\}$$

But what does it mean?

Correlation function.

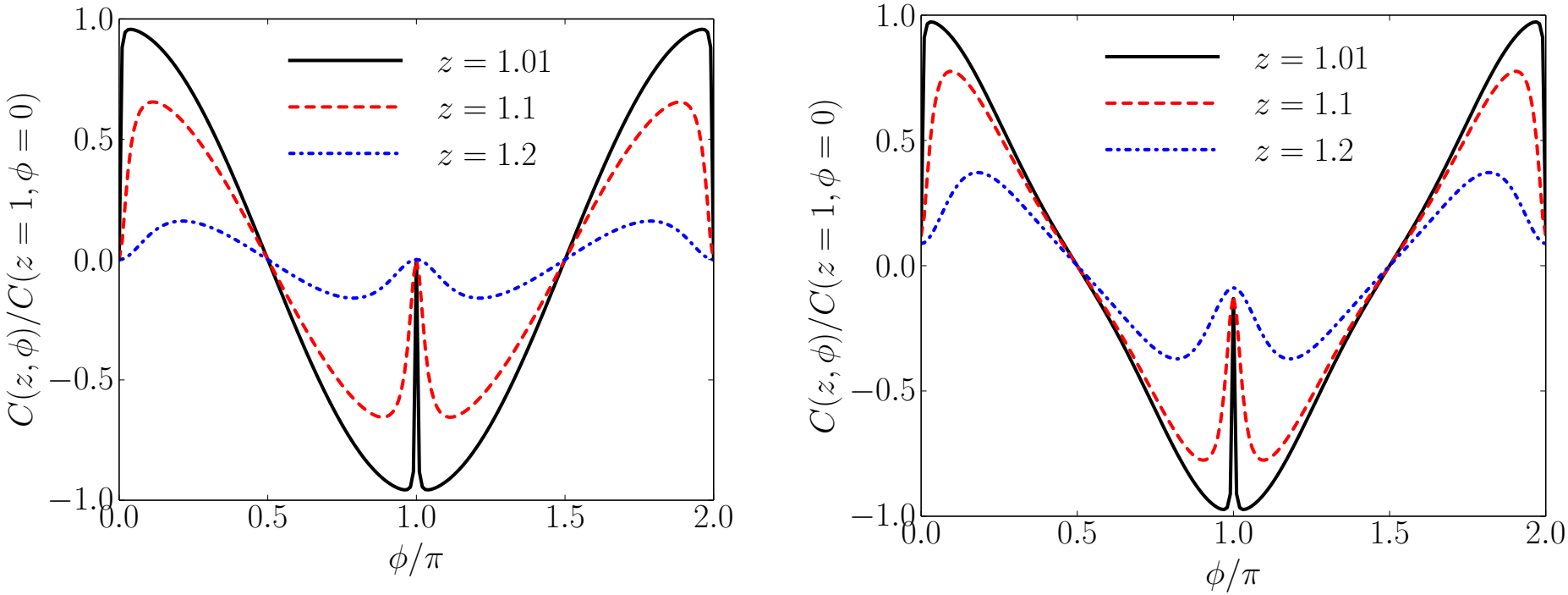
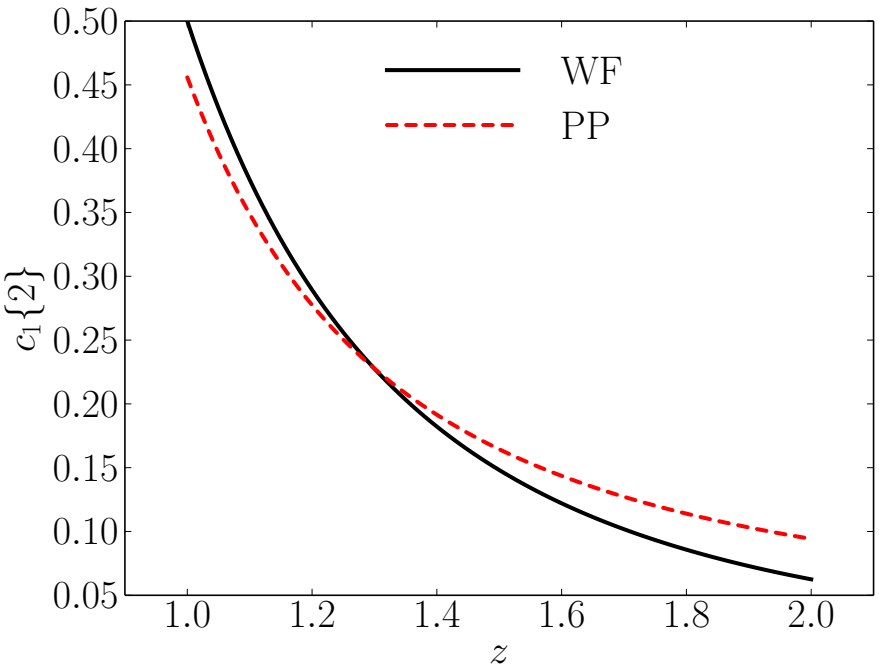


Figure: The correlation function as a function of the azimuthal angle, ϕ for different values of $z = p/k$. Left panel: in the projectile wave function. Right panel: double gluon inclusive roduction. The correlation functions are normalized by $C(z = 1, \phi = 0)$.

The odd harmonics.



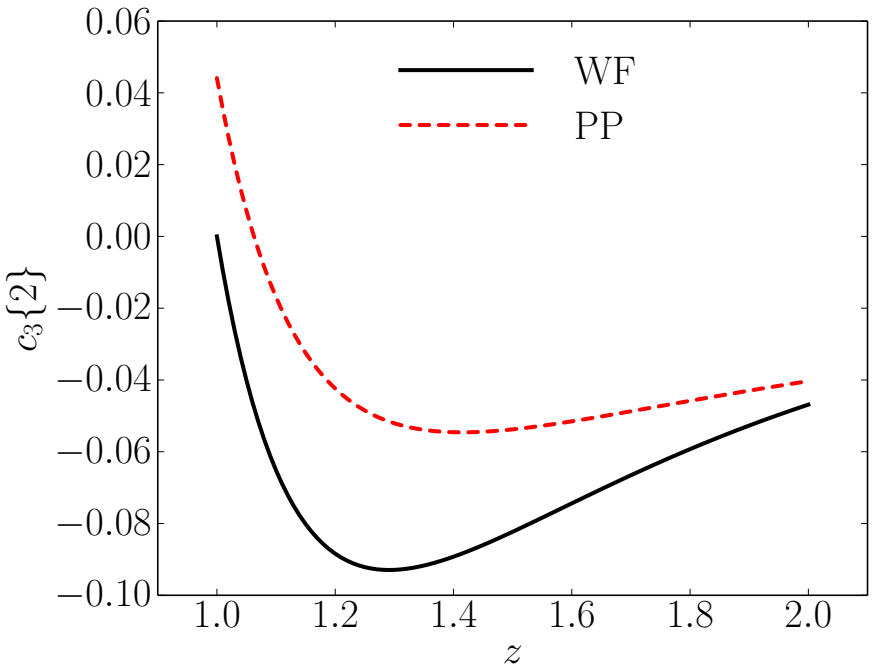


Figure: The first and the third cumulants as a function of $z = p/k$.

Conclusions.

1. The absence of odd harmonics in dilute-dense scattering is accidental: a denser projectile generates odd harmonics. The squeezed state has wider applicability parametrically: $N = O(1)$ rather than $N = O(g^2)$.

2. Relative to correlated piece from glasma graphs: our production cross section is $O(\alpha_s N_c)$ - so coupling suppressed but N_c enhanced.

3. The sign of V_3 is only positive for $1.1 > p/k > .9$. Keep momentum of trigger fixed, increase the momentum of associated particle, the v_3 should decrease pretty fast. Some sign of this in the data, although not clear that momenta large enough to trust our approximations.

4. Either way, our understanding of the proton wave function is quite rudimentary. We have a lot of work to do.

From light-cone wave function to NLO JIMWLK

Michael Lublinsky

Ben-Gurion University of the Negev
(Israel)

Alex Kovner, ML, and Yair Mulian
arXiv:1310.0378 (PRD), arXiv:1401.0374 (JHEP), arXiv:1405.0418 (JHEP)

ML and Yair Mulian, arXiv:1610.03453 (JHEP)

High Energy Scattering

Target (ρ^t) **Projectile (ρ^p)**

$$\langle \mathbf{T}| \quad \rightarrow \qquad\qquad \leftarrow \quad |\mathbf{P}\rangle$$

S-matrix:

$$\mathbf{S(Y)} \;=\; \langle \mathbf{T}\, \langle\, \mathbf{P}|\;\; \hat{\mathbf{S}}(\rho^{\mathrm{t}},\, \rho^{\mathrm{p}})\;\; |\mathbf{P}\rangle\, \mathbf{T}\rangle$$

or, more generally, any observable $\hat{\mathcal{O}}(\rho^{\mathrm{t}},\, \rho^{\mathrm{p}})$

$$\langle \hat{\mathcal{O}} \rangle_{\mathbf{Y}} \;=\; \langle \mathbf{T}\, \langle\, \mathbf{P}|\;\; \hat{\mathcal{O}}(\rho^{\mathrm{t}},\, \rho^{\mathrm{p}})\;\; |\mathbf{P}\rangle\, \mathbf{T}\rangle$$

The question we pose is how these averages change with increase in energy of the process

Projectile averaged S-matrix:

$$\mathbf{\Sigma(Y)} \equiv \langle \mathbf{P}| \hat{\mathbf{S}}(\rho^{\mathrm{t}},\, \rho^{\mathrm{p}}) \,|\mathbf{P}\rangle \;=\; \int \mathbf{D}\rho^{\mathrm{p}}\;\; \mathbf{S}(\rho^{\mathrm{t}},\, \rho^{\mathrm{p}})\;\; \mathbf{W}^{\mathrm{p}}_{\mathbf{Y}}[\rho^{\mathrm{p}}]$$

evolve with rapidity as $\mathbf{H}$ $\rightarrow$ **the HE effective Hamiltonian**

$$\mathbf{\Sigma(Y+\delta Y)} \;=\; \int \mathbf{D}\rho^{\mathrm{p}}\;\; \mathbf{e}^{-\delta \mathbf{Y}\,\mathbf{H}}\;\; \mathbf{S}(\rho^{\mathrm{t}},\, \rho^{\mathrm{p}})\;\; \mathbf{W}^{\mathrm{p}}_{\mathbf{Y}}[\rho^{\mathrm{p}}]$$

Spectrum of $\mathbf{H}$ **defines energy dependence of the observables.**

$$\mathbf{e}^{-\delta \mathbf{Y}\,\mathbf{H}} \;\simeq\; \mathbf{1} \;-\; \delta\mathbf{Y}\,\mathbf{H} \;+\; \frac{\mathbf{1}}{\mathbf{2}}\,\delta\mathbf{Y}^{\mathbf{2}}\,\mathbf{H}^{\mathbf{2}} \;\ldots$$

$$\mathbf{H} \;=\; \mathbf{H}^{\mathbf{LO}}(\alpha_{\mathrm{s}}) \;+\; \mathbf{H}^{\mathbf{NLO}}(\alpha_{\mathrm{s}}^{\mathbf{2}}) \;+\; \ldots\,; \qquad\qquad \mathbf{H} \;=\; \mathbf{H}[\rho^{\mathrm{t}},\, \delta/\delta\rho^{\mathrm{t}}]$$

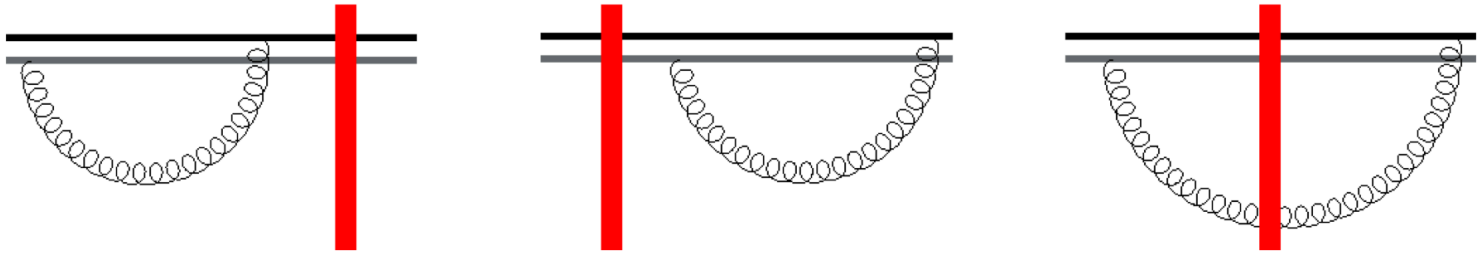
Charge densities ρ **are important parameters (define dilute or dense limits)**

LO JIMWLK Hamiltonian

Jalilian Marian, Iancu, McLerran, Weigert, Leonidov, Kovner (1997-2002)

The JIMWLK Hamiltonian is a limit of H for dilute partonic system ($\rho^{\mathrm{p}} \to 0$) which scatters on a dense target. It accounts for linear gluon emission + multiple rescatterings.

$$H_{LO}^{JIMWLK} = \frac{\alpha_s}{2\pi^2} \int_{x,y,z} \frac{(x-z)_i (y-z)_i}{(x-z)^2 (y-z)^2} \left\{ J_L^a(x) J_L^a(y) + J_R^a(x) J_R^a(y) - 2 J_L^a(x) S_A^{ab}(z) J_R^b(y) \right\}$$



Here $\rho^{\mathrm{p}} \to \mathbf{J_L}$ and $\hat{\mathbf{S}}\rho^{\mathrm{p}} \to \mathbf{J_R}$ are left and right SU(N) generators:

$$\mathbf{J_L^a(x) S_A^{ij}(z) = (T^a S_A(z))^{ij}\, \delta^2(x-z)} \qquad \mathbf{J_R^a(x) S_A^{ij}(z) = (S_A(z) T^a)^{ij}\, \delta^2(x-z)}$$

- $\mathbf{H^{JIMWLK}}$ **contains all the LO BFKL / BKP / TPV physics**

JIMWLK Hamiltonian @ NLO

Alex Kovner, ML and Yair Mulian (2013)

$$H^{NLO\ JIMWLK} = \int_{x,y,z} K_{JSJ}(x,y;z)\left[J^a_L(x)J^a_L(y) + J^a_R(x)J^a_R(y) - 2J^a_L(x)S^{ab}_A(z)J^b_R(y)\right]$$

$$+\int_{x\,y\,z\,z'} K_{JSSJ}(x,y;z,z')\left[f^{abc}f^{def}J^a_L(x)S^{be}_A(z)S^{cf}_A(z')J^d_R(y) - N_c J^a_L(x)S^{ab}_A(z)J^b_R(y)\right]$$

$$+\int_{x,y,z,z'} K_{q\bar{q}}(x,y;z,z')\left[2\,J^a_L(x)\,tr[S^\dagger_F(z)\,t^a\,S_F(z')t^b]\,J^b_R(y) - J^a_L(x)\,S^{ab}_A(z)\,J^b_R(y)\right]$$

$$+\int_{w,x,y,z,z'} K_{JJSSJ}(w;x,y;z,z')f^{acb}\left[J^d_L(x)\,J^e_L(y)\,S^{dc}_A(z)\,S^{eb}_A(z')\,J^a_R(w)\right.$$

$$\left. - J^a_L(w)\,S^{cd}_A(z)\,S^{be}_A(z')\,J^d_R(x)\,J^e_R(y)\right]$$

$$+\int_{w,x,y,z} K_{JJSJ}(w;x,y;z)\,f^{bde}\left[J^d_L(x)\,J^e_L(y)\,S^{ba}_A(z)\,J^a_R(w) - J^a_L(w)\,S^{ab}_A(z)\,J^d_R(x)\,J^e_R(y)\right]$$

$$+\int_{w,x,y} K_{JJJ}(w;x,y)f^{deb}\left[J^d_L(x)\,J^e_L(y)\,J^b_L(w) - J^d_R(x)\,J^e_R(y)\,J^b_R(w)\right].$$

Symmetries: $\mathbf{SU_L(N)} \times \mathbf{SU_R(N)}$ **CPT,** **Unitarity**

Shortcuts to the Kernels

Step 1: Compute evolution of 3-quark Wilson loop operator in SU(3) (baryon)

$$\mathbf{B(u,v,w)} = \epsilon^{\mathbf{ijk}}\epsilon^{\mathbf{lmn}}\mathbf{S_F^{il}(u)S_F^{jm}(v)S_F^{kn}(w)}$$

$$\partial_{\mathbf{Y}}\,\mathbf{B(u,v,w)} = -\mathbf{H}^{\mathbf{NLO\,JIMWLK}}\,\mathbf{B(u,v,w)}$$

and compare with Grabovsky (hep-ph/1307.5414) $\rightarrow$ $\mathbf{K_{JJSSJ}}$, $\mathbf{K_{JJSJ}}$

Step 2: Compute evolution of quark dipole operator

$$\mathbf{s(u,v)} = \mathbf{tr}[\mathbf{S_F(u)S_F^{\dagger}(v)}]/\mathbf{N_c}$$

$$\partial_{\mathbf{Y}}\,\mathbf{s(u,v)} = -\mathbf{H}^{\mathbf{NLO\,JIMWLK}}\,\mathbf{s(u,v)}$$

and compare with Balitsky and Chirilli (hep-ph/0710.4330) $\rightarrow$ $\mathbf{K_{JSSJ}}$, $\mathbf{K_{JSJ}}$, $\mathbf{K_{qq}}$

NLO Kernels (for gauge invariant operators)

$$K_{JJSSJ}(w;x,y;z,z') = -i\frac{\alpha_s^2}{2\,\pi^4}\left(\frac{X_i Y'_j}{X^2 Y'^2}\right)$$
$$\times\Big(\frac{\delta_{ij}}{2(z-z')^2}+\frac{(z'-z)_i W'_j}{(z'-z)^2 W'^2}+\frac{(z-z')_j W_i}{(z-z')^2 W^2}-\frac{W_i W'_j}{W^2 W'^2}\Big)\ln\frac{W^2}{W'^2}$$

$$K_{JJSJ}(w;x,y;z) \;=\; -\,i\,\frac{\alpha_s^2}{4\,\pi^3}\Big[\frac{X\cdot W}{X^2\,W^2}\;-\;\frac{Y\cdot W}{Y^2\,W^2}\Big]\ln\frac{Y^2}{(x-y)^2}\,\ln\frac{X^2}{(x-y)^2},$$

$$K_{q\bar{q}}(x,y;z,z') = -\frac{\alpha_s^2\,n_f}{8\,\pi^4}\Big\{\frac{X'^2Y^2+Y'^2X^2-(x-y)^2(z-z')^2}{(z-z')^4(X^2Y'^2-X'^2Y^2)}\ln\frac{X^2Y'^2}{X'^2Y^2}-\frac{2}{(z-z')^4}\Big\}$$

$$X = x-z,\quad X' = x-z',\quad Y = y-z,\quad Y' = y-z',\quad W = w-z$$

$$K_{JSSJ}(x,y;z,z') = \frac{\alpha_s^2}{16\,\pi^4}\Bigg[-\frac{4}{(z-z')^4} + \Big\{2\frac{X^2Y'^2 + X'^2Y^2 - 4(x-y)^2(z-z')^2}{(z-z')^4[X^2Y'^2 - X'^2Y^2]}$$

$$+\frac{(x-y)^4}{X^2Y'^2 - X'^2Y^2}\Big[\frac{1}{X^2Y'^2}+\frac{1}{Y^2X'^2}\Big]+\frac{(x-y)^2}{(z-z')^2}\Big[\frac{1}{X^2Y'^2}-\frac{1}{X'^2Y^2}\Big]\Big\}\ln\frac{X^2Y'^2}{X'^2Y^2}\Bigg] + \tilde{K}(x,y,z,z').$$

$$K_{JSJ}(x,y;z) = -\frac{\alpha_s^2}{16\pi^3}\frac{(x-y)^2}{X^2Y^2}\Big[b\ln(x-y)^2\mu^2 - b\frac{X^2-Y^2}{(x-y)^2}\ln\frac{X^2}{Y^2} + (\frac{67}{9}-\frac{\pi^2}{3})N_c - \frac{10}{9}n_f\Big]$$

$$-\frac{N_c}{2}\int_{z'}\tilde{K}(x,y,z,z').$$

Here μ is the normalization point, $b = \frac{11}{3}N_c - \frac{2}{3}n_f$

$$\tilde{K}(x,y,z,z') = \frac{i}{2}\Big[K_{JJSSJ}(x;x,y;z,z') - K_{JJSSJ}(y;x,y;z,z') - K_{JJSSJ}(x;y,x;z,z')$$

$$+K_{JJSSJ}(y;y,x;z,z')\Big]$$

The kernels are not unique though...

NLO Kernels for color non-singlets

"By inspection" of Balitsky and Chirilli (arXiv:1309.7644 [hep-ph])

$$K_{JSJ}(x,y,z) \to \bar{K}_{JSJ}(x,y,z) \equiv K_{JSJ}(x,y,z) + \\ + \frac{\alpha_s^2}{16\pi^3}\left\{\left[\frac{1}{X^2}+\frac{1}{Y^2}\right]\left[\left(\frac{67}{9}-\frac{\pi^2}{3}\right)N_c - \frac{10}{9}n_f\right] + \frac{b}{X^2}\ln X^2\mu^2 + \frac{b}{Y^2}\ln Y^2\mu^2\right\};$$

$$K_{JSSJ}(x,y;z,z') \to \bar{K}_{JSSJ}(x,y;z,z') + \\ \equiv K_{JSSJ}(x,y;z,z') + \frac{\alpha_s^2}{8\pi^4}\left[\frac{4}{(z-z')^4} - \frac{I(x,z,z')}{(z-z')^2} - \frac{I(y,z,z')}{(z-z')^2}\right];$$

$$K_{q\bar{q}}(x,y;z,z') \to \bar{K}_{q\bar{q}}(x,y;z,z') \equiv K_{q\bar{q}}(x,y;z,z') - \frac{\alpha_s^2 n_f}{8\pi^4}\left[\frac{I_f(x,z,z')}{(z-z')^2} + \frac{I_f(y,z,z')}{(z-z')^2}\right],$$

$$I(x,z,z') = \frac{1}{X^2-(X')^2}\ln\frac{X^2}{(X')^2}\left[\frac{X^2+(X')^2}{(z-z')^2} - \frac{X\cdot X'}{X^2} - \frac{X\cdot X'}{(X')^2} - 2\right];$$

$$I_f(x,z,z') = \frac{2}{(z-z')^2} - \frac{2X\cdot X'}{(z-z')^2(X^2-(X')^2)}\ln\frac{X^2}{(X')^2}.$$

Comparing with Balitsky and Chirilli (arXiv:1309.7644 [hep-ph])

Compute evolution of Wilson lines with open color indices:

$$\partial_Y \left[\mathbf{S}^{\mathbf{ab}}(\mathbf{x})\right] = -\mathbf{H}^{\mathbf{NLO\,JIMWLK}} \left[\mathbf{S}^{\mathbf{ab}}(\mathbf{x})\right]$$

$$\partial_Y \left[\mathbf{S}^{\mathbf{ab}}(\mathbf{x})\mathbf{S}^{\mathbf{cd}}(\mathbf{y})\right] = -\mathbf{H}^{\mathbf{NLO\,JIMWLK}} \left[\mathbf{S}^{\mathbf{ab}}(\mathbf{x})\mathbf{S}^{\mathbf{cd}}(\mathbf{y})\right]$$

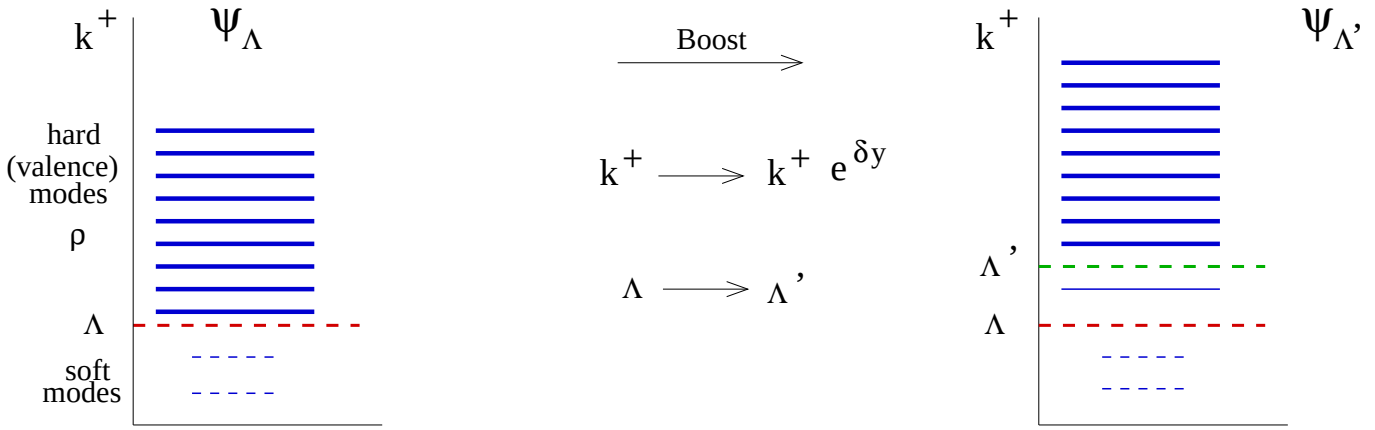
$$\partial_Y \left[\mathbf{S}^{\mathbf{ab}}(\mathbf{x})\mathbf{S}^{\mathbf{cd}}(\mathbf{y})\mathbf{S}^{\mathbf{ef}}(\mathbf{z})\right] = -\mathbf{H}^{\mathbf{NLO\,JIMWLK}} \left[\mathbf{S}^{\mathbf{ab}}(\mathbf{x})\mathbf{S}^{\mathbf{cd}}(\mathbf{y})\mathbf{S}^{\mathbf{ef}}(\mathbf{z})\right]$$

100% agreement!

Light Cone Wave Function

$$\mathbf{H_{LC\,QCD}}\,|\Psi\rangle \;=\; \mathbf{E}\,|\Psi\rangle$$

Born-Oppenheimer adiabatic approximation



Hard particles with $k^+ > \Lambda$ scatter of the target. Hard (valence) modes are described by the valence density $\rho(x_\perp)$ (shock wave).

The boost opens a window above Λ with the width $\sim \delta y$. The window is populated by soft modes, which became hard after the boost. These newly created hard modes do scatter off the target.

In the dilute limit $\rho \sim 1$; gluon emission $\sim \alpha_s\,\rho$, LO = one gluon, NLO = 2 gluons/quarks

Denote soft glue (quark) creation and annihilation operators as $\mathbf{a}$ and $\mathbf{a}^\dagger$.

$$\mathbf{H_{LC\,QCD}} \;=\; \mathbf{H}[\rho,\,\mathbf{a},\,\mathbf{a}^\dagger] \;=\; \mathbf{H_V}[\rho] \;+\; \mathbf{H_{free}}[\mathbf{a},\,\mathbf{a}^\dagger] \;+\; \mathbf{H_{int}}[\rho,\,\mathbf{a},\,\mathbf{a}^\dagger]$$

LCWF with no soft gluons

$$\mathbf{H_V}\,|\mathbf{v},\,\mathbf{0_a}\rangle \;=\; \mathbf{E_0}\;|\mathbf{v},\,\mathbf{0_a}\rangle\,; \qquad\qquad \mathbf{a}\,|\mathbf{v},\,\mathbf{0_a}\rangle \;=\; \mathbf{0}\,; \qquad\qquad \mathbf{E_0} \;=\; \mathbf{0}$$

LCWF with soft gluon/quark dressing

$$|\mathbf{\Psi}\rangle \;=\; \mathbf{\Omega}(\rho,\,\mathbf{a},\,\mathbf{a}^\dagger)\,|\mathbf{v},\,\mathbf{0_a}\rangle\,; \qquad\qquad \mathbf{\Omega}^\dagger\;\mathbf{H_{LC\,QCD}}\;\mathbf{\Omega} \;=\; \mathbf{H_{diagonal}}$$

Find Ω in perturbation theory

- **Dilute limit ($\rho \to 0$) – usual perturbation theory in H_{int}**
- **Dense limit ($\rho \sim 1/\alpha_s$) – all order resummation in a strong background field**

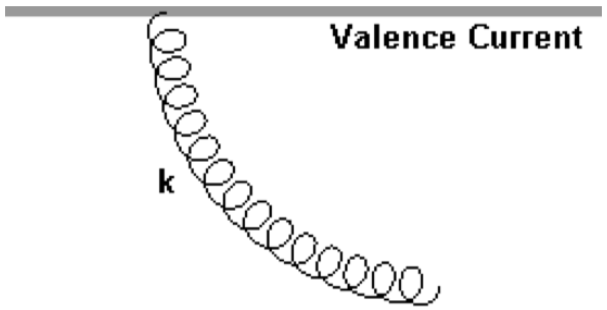
LCWF at LO

First order (g) perturbation theory

$$|\Psi_{\rm LO}\rangle \;=\; \mathcal{N}\,|0_{\rm a}\rangle \;-\; \sum_{\rm i}\,|{\rm i}\rangle\,\frac{\langle {\rm i}|\,{\rm H_{int}}\,|0_{\rm a}\rangle}{\rm E_i} \qquad\qquad \langle\Psi_{\rm LO}|\Psi_{\rm LO}\rangle \;=\; 1 \;\to\; \mathcal{N}$$

Eikonal coupling between valence and soft gluons due to separation of scales

$$\mathbf{H_{int}} \;=\; -\int \frac{\mathbf{dk^+}}{\mathbf{2\pi}}\frac{\mathbf{d^2k_\perp}}{\mathbf{(2\pi)^2}}\frac{\mathbf{g\,k_i}}{\mathbf{\sqrt{2}\,|k^+|^{3/2}}}\;\Big[\mathbf{a_i^{\dagger a}(k^+,\,k_\perp)}\;\rho^{\rm a}(-\mathbf{k_\perp})\;+\;\mathbf{a_i^{a}(k^+,\,-k_\perp)}\;\rho^{\rm a}(\mathbf{k_\perp})\Big]$$



A cloud of WW gluons dressing the valence ones

ρ are operators on the valence Hilbert space

SU(N) algebra: $\quad[\rho^{\rm a},\,\rho^{\rm b}] \;=\; {\rm if}^{\rm abc}\,\rho^{\rm c}$

$$\Omega_Y(\rho \to 0) \equiv C_Y = \mathrm{Exp}\left\{ i \int d^2z\, b_i^a(z) \int_{e^{Y_0}\Lambda}^{e^Y \Lambda} \frac{dk^+}{\pi^{1/2}|k^+|^{1/2}} \left[a_i^a(k^+, z) + a_i^{\dagger a}(k^+, z)) \right] \right\}$$

The classical Weizsaker-Williams field

$$b_i^a(z) = \frac{g}{2\pi} \int d^2x \frac{(z-x)_i}{(z-x)^2} \rho^a(x)$$

The operator C dresses the valence charges by a cloud of the WW gluons

The LCWF is a starting point for numerous semi-inclusive calculations, such as single/double inclusive particle production.

$$\Sigma^{LO} = \langle \Psi_{LO} | \hat{S} | \Psi_{LO} \rangle = \langle \rho,\, 0_a |\, C^\dagger \hat{S}\, C\, | \rho, 0_a \rangle \to \text{LO JIMWLK}$$

LCWF at NLO

ML and Yair Mulian, arXiv:1610.03453

- g^3 + normalisation at g^4

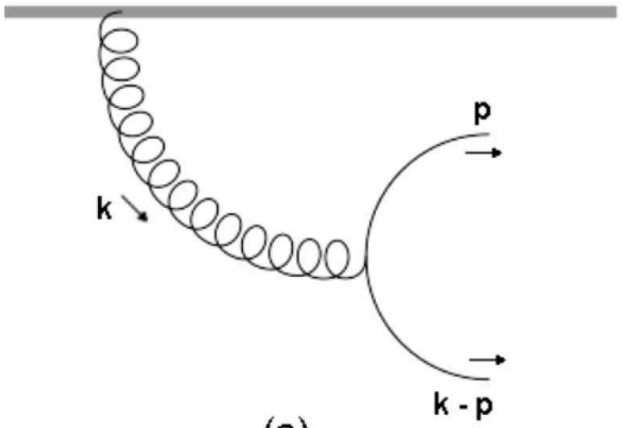
$$|\Psi_{\rm NLO}\rangle = \mathcal{N}\,|0\rangle + \sum_{\rm i} |{\rm i}\rangle \left[-\frac{\langle {\rm i}|\,{\rm H_{int}}\,|0\rangle}{\rm E_i} + \frac{\langle {\rm i}|\,{\rm H_{int}}\,|{\rm j}\rangle\,\langle {\rm j}|\,{\rm H_{int}}\,|0\rangle}{\rm E_i\,E_j} + \right.$$
$$\left. + \frac{\langle {\rm i}|\,{\rm H_{int}}\,|0\rangle\,\langle {\rm j}|\,{\rm H_{int}}\,|0\rangle^2\,({\rm 2\,E_j} - {\rm E_i})}{\rm 2\,E_i^2\,E_j^2} - \frac{\langle {\rm i}|\,{\rm H_{int}}\,|{\rm j}\rangle\,\langle {\rm j}|\,{\rm H_{int}}\,|{\rm k}\rangle\,\langle {\rm k}|\,{\rm H_{int}}\,|0\rangle}{\rm E_i\,E_j\,E_k} \right]$$

i runs over one gluon, two gluons, and two quarks

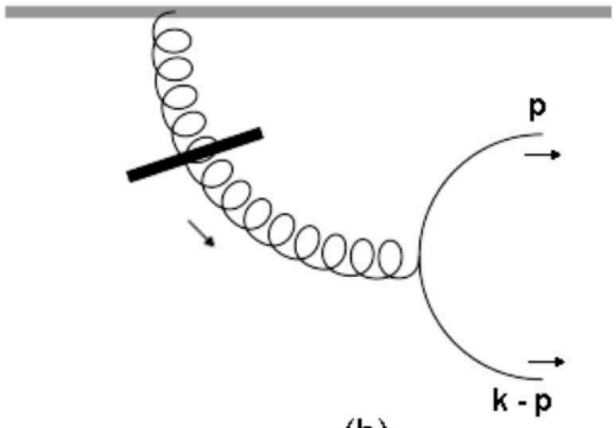
Operator valued matrix elements

Accounts for first non-linear/saturation effects in the projectile

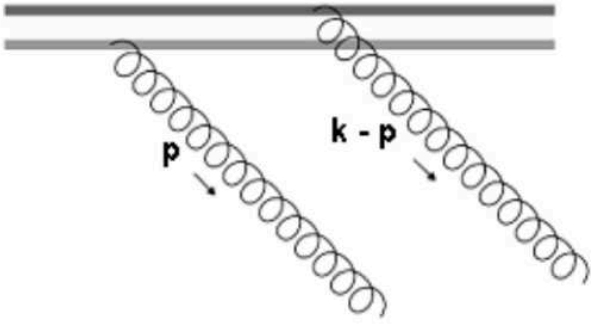
$$\langle \Psi_{\rm NLO}|\Psi_{\rm NLO}\rangle = 1 \rightarrow |\mathcal{N}|\,; \qquad \mathcal{N} = |\mathcal{N}|\,{\rm e}^{{\rm i}\phi}$$



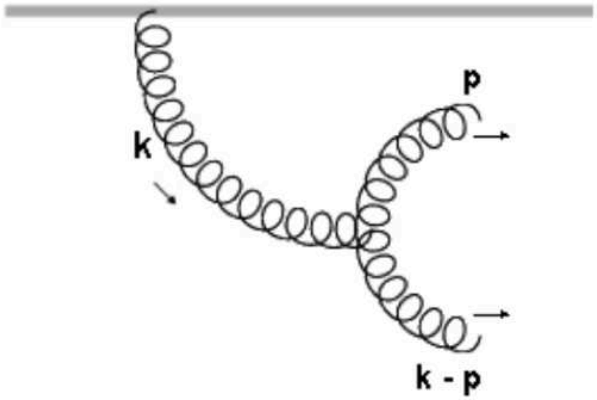
(a)



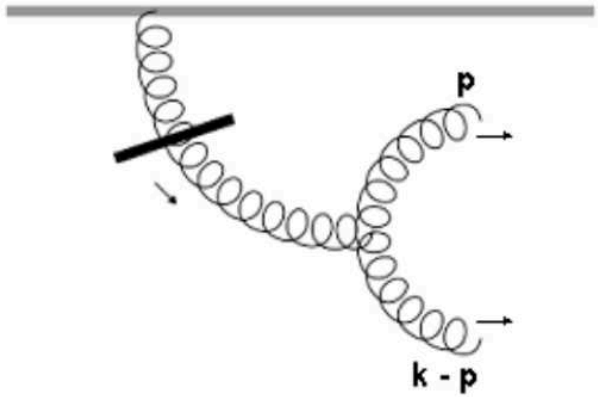
(b)



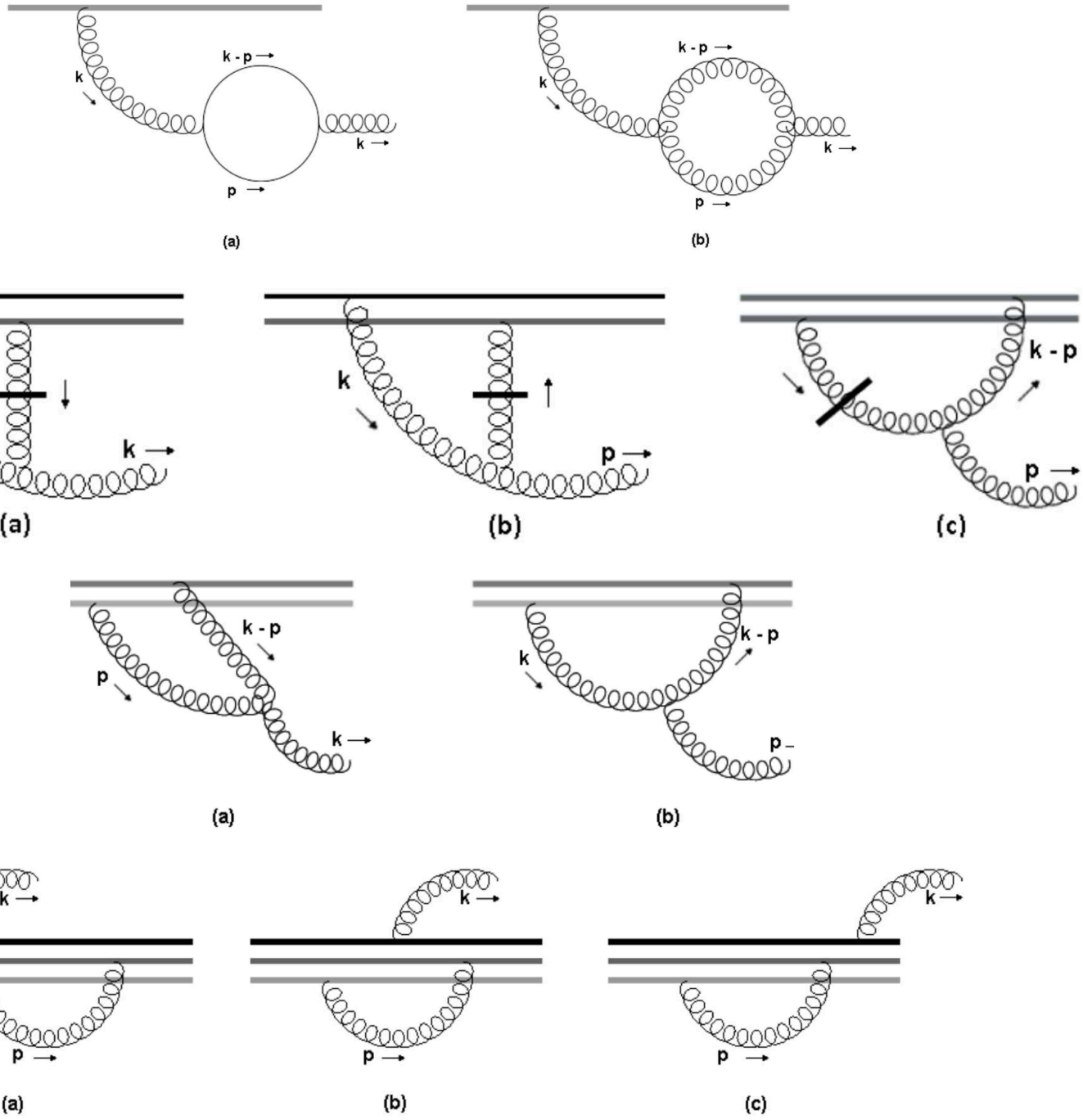
(a)



(b)



(c)


k - p
k
k
p
(a)
k - p
k
k
p
(b)
p
k
(a)
k
p
(b)
k - p
p
k
(c)
k - p
k
(a)
k - p
k
p
(b)
k
p
(a)
k
p
(b)
k
p
(c)

Phase of the LCWF @ NLO

$$\mathcal{N} \;=\; |\mathcal{N}|\, \mathbf{e}^{\mathbf{i}\phi}$$

Beyond perturbation theory: Born-Oppenheimer adiabatic approximation

$$\langle \mathbf{v}| \otimes \langle \psi|\, \mathbf{H_V}\, |\psi\rangle \otimes |\mathbf{v}\rangle \;\simeq\; \langle \mathbf{v}|\, \mathbf{H_V}\, |\mathbf{v}\rangle \qquad \textbf{or} \qquad \langle \psi|\; \mathbf{H_V}\; |\psi\rangle_{\mathbf{soft}} \;\simeq\; \mathbf{0}$$

the dynamics of the soft modes does not significantly affect that of the valence.

Berry connection

$$\langle \psi|\; \frac{\delta}{\delta \rho^{\mathbf{d}}(\mathbf{w})}\; |\psi\rangle \;=\; \mathbf{0} \qquad \rightarrow\; \phi$$

JIMWLK Hamiltonian @ NLO (again)

$$\mathbf{\Sigma} = \left\langle \psi^{\mathbf{NLO}} \right| \hat{\mathbf{S}} \left| \psi^{\mathbf{NLO}} \right\rangle = \langle \rho,\, \mathbf{0_a}|\, \mathbf{\Omega}^\dagger\, \hat{\mathbf{S}}\, \mathbf{\Omega}\, |\rho, \mathbf{0_a}\rangle$$

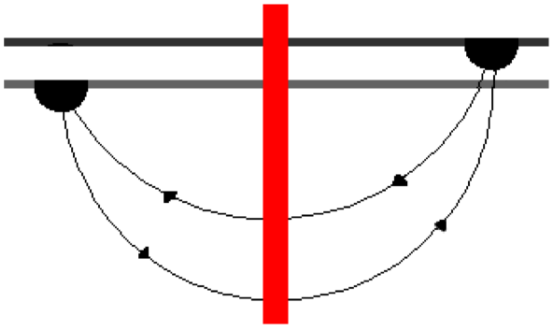
$$= \Sigma^{LO} + \Sigma_{q\bar{q}} + \Sigma_{JJSSJ} + \Sigma_{JSSJ} + \Sigma_{JJSJ} + \Sigma_{JSJ} + \Sigma_{JJSSJJ} + \Sigma_{JJJSJ} + \Sigma_{virtual}.$$

$$\mathbf{\Sigma}_{\dots} = \mathbf{\Sigma}^{\mathbf{NLO}}_{\dots}(\delta \mathrm{Y}) + \mathbf{\Sigma}^{(\delta \mathrm{Y})^{\mathbf{2}}}_{\dots}$$

$$\mathbf{\Sigma}^{(\delta \mathrm{Y})^{\mathbf{2}}} = \frac{\mathbf{1}}{\mathbf{2}} \left(\delta \mathbf{Y}\, \mathbf{H}^{\mathbf{LO}}_{\mathbf{JIMWLK}}\right)^{\mathbf{2}}$$

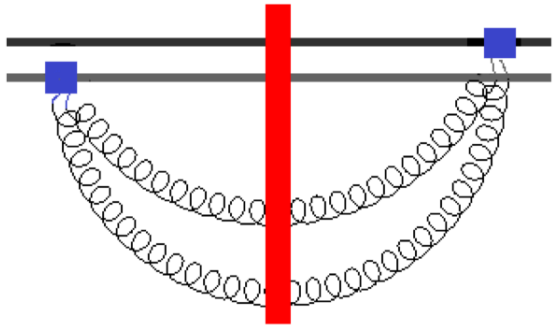
$$\mathbf{\Sigma}^{\mathbf{NLO}}(\delta \mathrm{Y}) \rightarrow \mathbf{H}^{\mathbf{NLO\,JIMWLK}}$$

Σ_{qq}



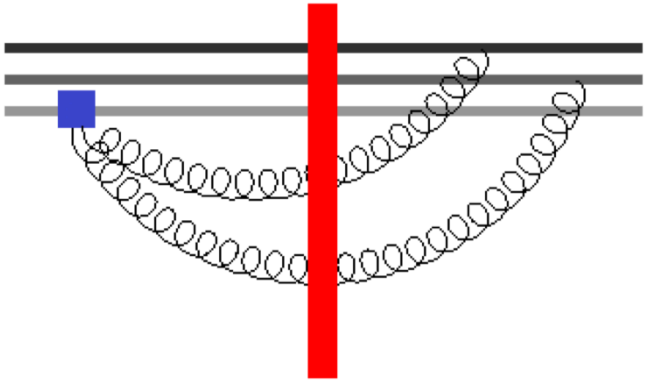
(a)

Σ_{JSSJ}

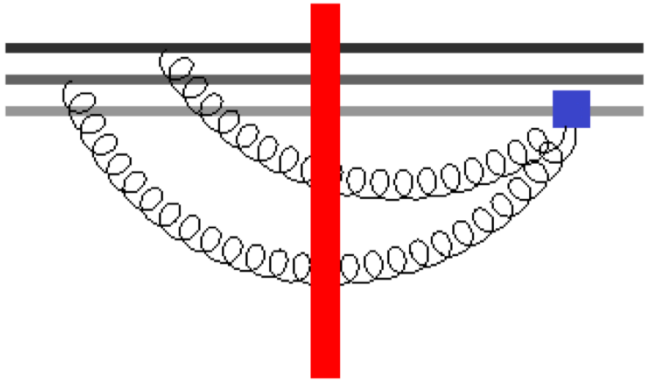


(b)

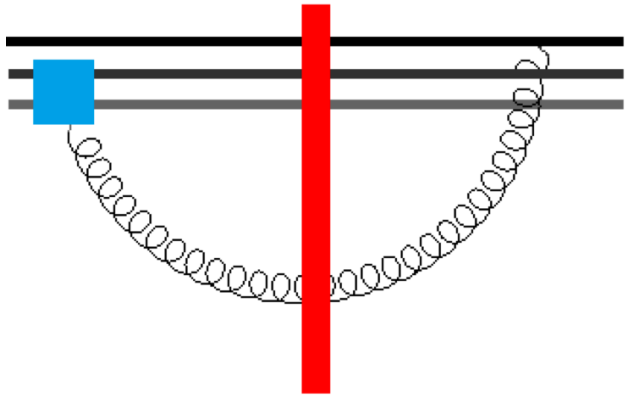
Σ_{JJSSJ}



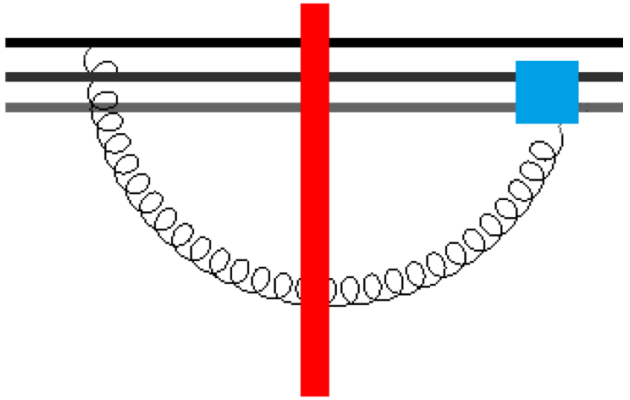
Σ_{JJSSJ}



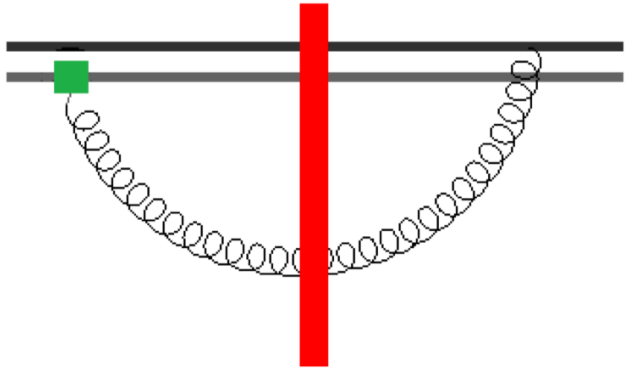
Σ_{JJSJ}



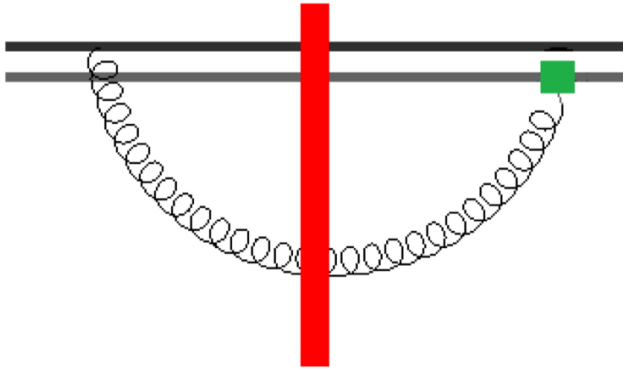
Σ_{JJSJ}



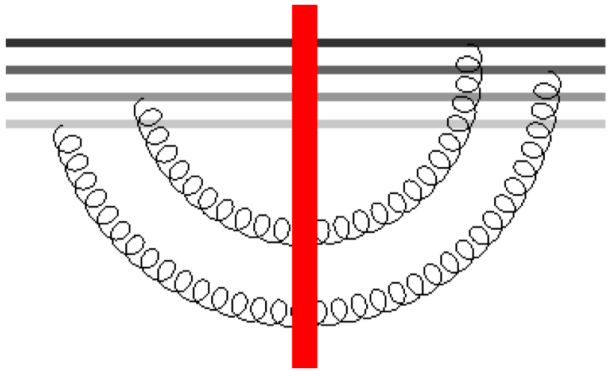
Σ_{JSJ}



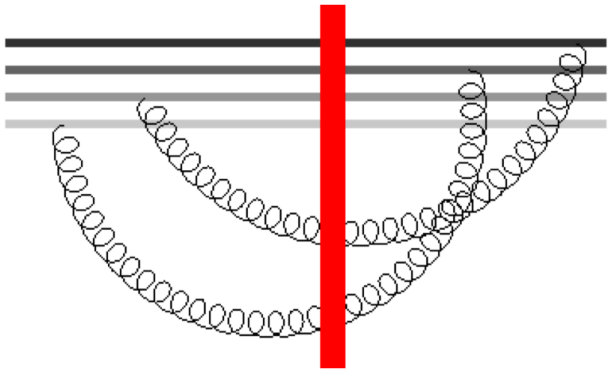
Σ_{JSJ}



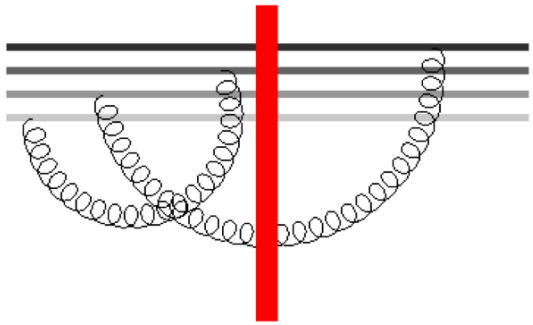
$\Sigma_{\mathbf{JJSSJJ}}$

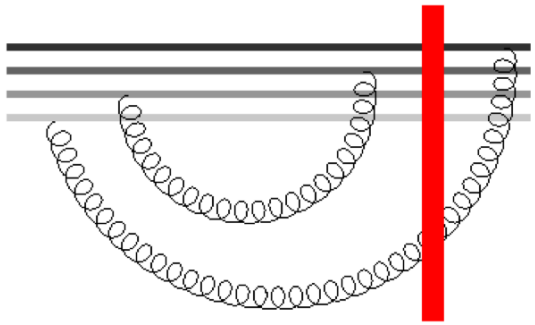


$\Sigma_{\mathbf{JJSSJJ}}$

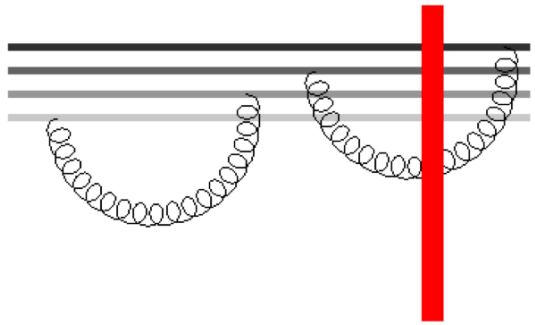


$\Sigma_{\mathbf{JJJSJ}}$





$\Sigma_{\mathbf{JJJSJ}}$



And also $\Sigma_{\mathbf{virtual}}$ **;** $\phi \rightarrow J\,J\,J$

Is the JIMWLK Hamiltonian Conformally invariant?

Alex Kovner, ML and Yair Mulian (2014)

Scale invariance is trivial. Lets focus on inversion. Introduce $\mathbf{x}_\pm = \mathbf{x_1} \pm \mathbf{i}\,\mathbf{x_2}$

$$\textbf{Inversion transformation}: \quad x_+ \to 1/x_- \,; \qquad\qquad x_- \to 1/x_+$$

A "naive" representation $\mathcal{I}_0$ of the inversion transformation is

$$\mathcal{I}_0: \quad \mathbf{S}(\mathbf{x}_+,\mathbf{x}_-) \to \mathbf{S}(\mathbf{1}/\mathbf{x}_-,\mathbf{1}/\mathbf{x}_+)\;, \qquad \mathbf{J_{L,R}}(\mathbf{x}_+,\mathbf{x}_-) \to \frac{\mathbf{1}}{\mathbf{x}_+\mathbf{x}_-}\,\mathbf{J_{L,R}}(\mathbf{1}/\mathbf{x}_-,\mathbf{1}/\mathbf{x}_+)\,.$$

Conformal invariance (in the gauge invariant sector) @LO:

$$\mathcal{I}_0\;\mathbf{H}^{\text{LO JIMWLK}}\;\mathcal{I}_0 \;=\; \mathbf{H}^{\text{LO JIMWLK}}$$

No (naive) Conformal invariance @NLO:

$$\mathcal{I}_0\;\mathbf{H}^{\text{NLO JIMWLK}}\;\mathcal{I}_0 \;=\; \mathbf{H}^{\text{NLO JIMWLK}} + \mathcal{A}$$

QCD is not conformally invariant beyond tree level, but $\mathcal{N}=4$ SUSY is.

JIMWLK Hamiltonian IS conformally invariant! (in $\mathcal{N}=4$)

S **forms a non-trivial representation of the conformal group:**

$$\mathcal{I} : S(x) \to S(1/x) + \delta S(x)\,, \qquad \mathcal{I} : H^{LO} \to H^{LO} - \mathcal{A}$$

Here δS is of order α_s. The condition is that the net anomaly cancels:

$$\mathcal{I}\,(\mathbf{H^{LO}} + \mathbf{H^{NLO}})\,\mathcal{I} \;=\; \mathbf{H^{LO}} + \mathbf{H^{NLO}}$$

We have constructed $\mathcal{I}$ perturbatively: $\qquad \mathcal{I} \;=\; (\mathbf{1} + \mathcal{C})\,\mathcal{I}_\mathbf{0}\,.$

$$\mathcal{C} \;=\; -\,\frac{\mathbf{1}}{\mathbf{2}}\,\frac{\alpha_\mathbf{s}}{\mathbf{2}\pi^\mathbf{2}}\int_{\mathbf{x,y,z}} \ln\left[\frac{(\mathbf{x}-\mathbf{y})^\mathbf{2}\mathbf{a}^\mathbf{2}}{(\mathbf{x}-\mathbf{z})^\mathbf{2}(\mathbf{y}-\mathbf{z})^\mathbf{2}}\right]\times$$

$$\times\frac{(\mathbf{x}-\mathbf{y})^\mathbf{2}}{(\mathbf{x}-\mathbf{z})^\mathbf{2}(\mathbf{y}-\mathbf{z})^\mathbf{2}}\left\{\mathbf{J}^\mathbf{a}_\mathbf{L}(\mathbf{x})\mathbf{J}^\mathbf{a}_\mathbf{L}(\mathbf{y}) + \mathbf{J}^\mathbf{a}_\mathbf{R}(\mathbf{x})\mathbf{J}^\mathbf{a}_\mathbf{R}(\mathbf{y}) - \mathbf{2}\mathbf{J}^\mathbf{a}_\mathbf{L}(\mathbf{x})\mathbf{S}^\mathbf{ab}_\mathbf{A}(\mathbf{z})\mathbf{J}^\mathbf{b}_\mathbf{R}(\mathbf{y})\right\}$$

For an arbitrary operator $\mathcal{O}$ (s, B, H^{JIMWLK},...) we define its conformal extension:

$$\mathcal{O}^{conf} \;=\; \mathcal{O} + \frac{1}{2}\,[\mathcal{C},\,\mathcal{O}]\,; \qquad [s^{conf} \text{ by Balitsky and Chirilli (arXiv : 0903.5326)}]$$

CONCLUSIONS

- We have computed the LCWF@NLO. Apart of leading to JIMWLK equation, it can be used to compute semi-inclusive observables @NLO.

- We have first constructed and then independently derived the JIMWLK Hamiltonian at NLO. It fully reproduces and generalises (all?) previously known low x evolution equations at NLO, including Balitsky's hierarchy at NLO

- We have proven the conformal invariance of the NLO JIMWLK Hamiltonian (in $\mathcal{N} = 4$). For any operator, we can construct its perturbative extension, such that the resulting operator evolves with conformal kernels.

- Once expanded in the dilute limit, the NLO JIMWLK makes it possible to study evolution of any multi-gluon BKP state and transition vertices at NLO.

QCD

QCD Lagrangian

$$\mathcal{L} \;=\frac{1}{4}\, G_{\mu\nu}\, G^{\mu\nu} \;+\; \overline{\psi}\,(i\;\not{\partial} \;-\; g\,\not{A} - m)\;\psi$$

The field strength

$$G_a^{\mu\nu} \;=\; \partial^\mu\, A_a^\nu \;-\; \partial^\nu\, A_a^\mu \;-\; g\, f^{abc}\, A_b^\mu\, A_c^\nu$$

Equations of motion:

Maxwell equation:

$$\partial_\mu\, G^{\mu\nu} \;=\; g\, J^\nu\,; \qquad\qquad J_a^\nu \;=\; \bar{\psi}\,\gamma^\nu\,\tau^a\,\psi \;-\; f^{abc}\, G_b^{\nu\mu}\, A_c^\mu$$

Dirac equation

$$(i\,\gamma^\mu\, D_\mu \;-\; m)\,\psi \;=\; 0$$

Light Cone

LC time $x^+ = (t + z)/\sqrt{2}$ $\qquad\qquad$ $x^- = (t - z)/\sqrt{2}$

LC gauge

$$A^+ = \frac{1}{\sqrt{2}}\,(A^0 + A^3) = 0$$

The Gauss law constraint

$$\partial_\mu\, G^{\mu\,+} = g\, J^+$$

is solved for the A^- **field**

$$-\,(\partial^+)^2\, A^-_a + \partial^+ \partial_i\, A^i_a = g\, J^+_a$$

$$A^-_a = -\frac{\partial^i}{\partial^+}\, A^i_a + \frac{g}{(\partial^+)^2}\, J^+_a$$

Same story with quarks

Light Cone Hamiltonian

Canonical variables: $A^i, \quad \Pi^i = \frac{\delta L}{\delta(\partial^- A^i)} = G^{+i} = \partial^+ A^i$

Light Cone Hamiltonian:

$$H^{LC} = \int dx^- d^2x_\perp \left[\Pi^i \, \partial^- A^i - L\right] = H_E + H_M$$

The electric and magnetic parts

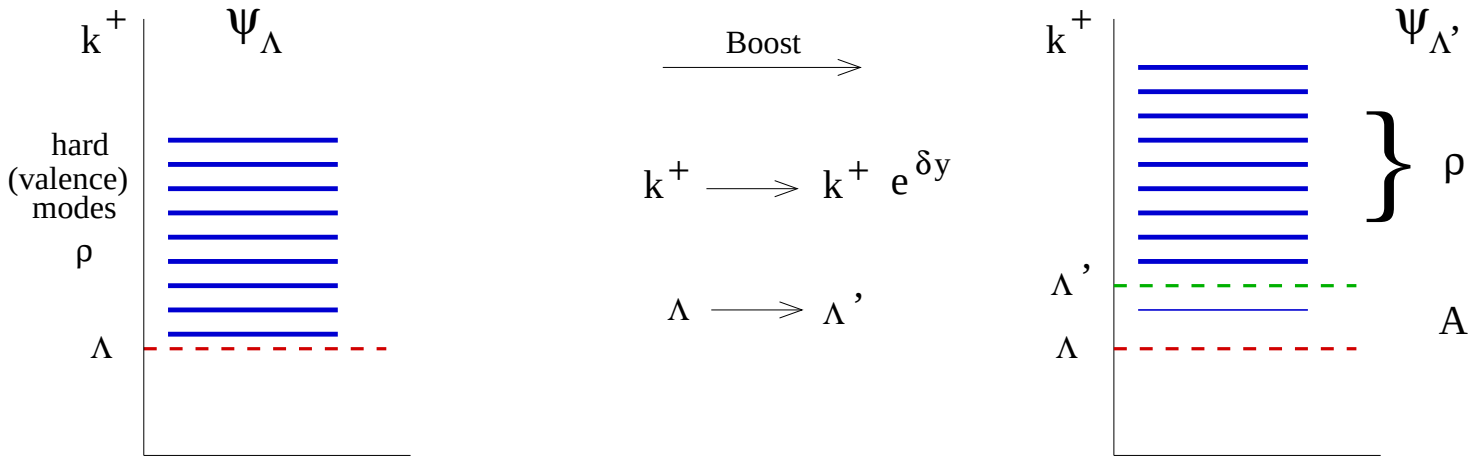
$$H_E = \frac{1}{2} \int \frac{dk^+}{(2\,\pi)} d^2x \;\; \Pi_a^-(k^+, x)\, \Pi_a^-(-k^+, x)$$

$$H_M = \frac{1}{4} \int \frac{dk^+}{(2\,\pi)} d^2x \;\; G_{ij}^a(k^+, x)\, G_{ij}^a(-k^+, x)$$

The chromoelectric field

$$\Pi_a^-(k^+, x) = \partial^+ A^- = -\,\partial^i A_i^a + \frac{g}{\partial^+} J_a^+$$

We split the modes into hard and soft: The hard modes act as an external current $j_a^+ = \delta(x^-)\,\rho^a$ for the soft modes. $J^+ = j^a + g\,A\,A + (quark\ current)$



$$H^{LC} = H_A^{LC} + H_\rho^{LC}\,; \qquad H_\rho^{LC}\,|\Psi_\Lambda\rangle = E\,|\Psi_\Lambda\rangle\,; \qquad H^{LC}\,|\Psi_{\Lambda'}\rangle = E'\,|\Psi_{\Lambda'}\rangle$$

$|\Psi_\Lambda\rangle$ is a vacuum of the soft modes A.

$$H_A^{LC} = H_0 + \delta H^\rho + g\,AAA + \ldots\,; \qquad \delta H^\rho \sim g\,\rho\,A$$

Quantization

$$A_i^a(x^-,\mathbf{x}_\perp) = \int_0^\infty \frac{dk^+}{2\pi}\frac{1}{\sqrt{2k^+}}\left\{ a_i^a(k^+,\mathbf{x})\, e^{-ik^+x^-} + a_i^{a\,\dagger}(k^+,\mathbf{x})\, e^{ik^+x^-}\right\}$$

$$\left[a_i^a(k^+,k), a_j^{b\,\dagger}(p^+,p)\right] = (2\pi)^3\,\delta^{ab}\,\delta_{ij}\,\delta^3(k-p)$$

The free part of the LCH

$$H_0 \;=\; \int_{k^+>0} \frac{dk^+}{2\pi}\frac{d^2k_\perp}{(2\pi)^2}\frac{k_\perp^2}{2k^+}\; a_i^{\dagger a}(k^+,k_\perp)\; a_i^a(k^+,k_\perp)$$

The vacuum of the LCH is simply the Fock space vacuum of the operators a

$$a_q|0\rangle = 0\,; \qquad\qquad E_0 \;=\; 0$$

The one particle state

$$|k,a,i\rangle \;=\; \frac{1}{(2\pi)^{3/2}}\, a_i^{a\,\dagger}(k^+,k)\,|0\rangle \qquad\qquad E_g \;=\; k^- \;=\; \frac{k_\perp^2}{2k^+}$$

Perturbation Theory

$$\delta H^{\rho} \;=\; -\int \frac{dk^{+}}{2\pi}\frac{d^{2}k_{\perp}}{(2\pi)^{2}}\frac{g\,k_{i}}{\sqrt{2}\,|k^{+}|^{3/2}}\;\Big[a_{i}^{\dagger a}(k^{+},\,k_{\perp})\;\hat{\rho}^{a}(-k_{\perp})\;+\;a_{i}^{a}(k^{+},\,-k_{\perp})\;\;\hat{\rho}^{a}(k_{\perp})\Big]$$

The first order perturbation theory

$$|\theta\rangle \;=\; \beta\,|0\rangle \;-\; \sum_{i}\,|i\rangle\,\frac{\langle i|\,\delta H^{\rho}\,|0\rangle}{E_{i}} \qquad\qquad \langle\theta|\theta\rangle \;=\; 1 \;\to\; \beta$$

This Hamiltonian creates only one particle state from the vacuum

$$\langle 1\,gluon|\,\delta H^{\rho}\,|0\rangle \;=\; \langle k_{\perp},k^{+},a,i|\,\delta H^{\rho}\,|0\rangle \;=\; \frac{g\,k_{i}}{4\,\pi^{3/2}\,|k^{+}|^{3/2}}\,\rho^{a}(-k_{\perp})$$

We can write the soft gluon vacuum state to the first order in the coupling as

$$|\theta\rangle \;=\; C_{\delta Y}\,|0\rangle\,; \qquad\qquad |\Psi_{\Lambda'}\rangle \;=\; C_{\delta Y}\,|\Psi_{\Lambda}\rangle$$

Finding small-x physics in final state jets

Duff Neill

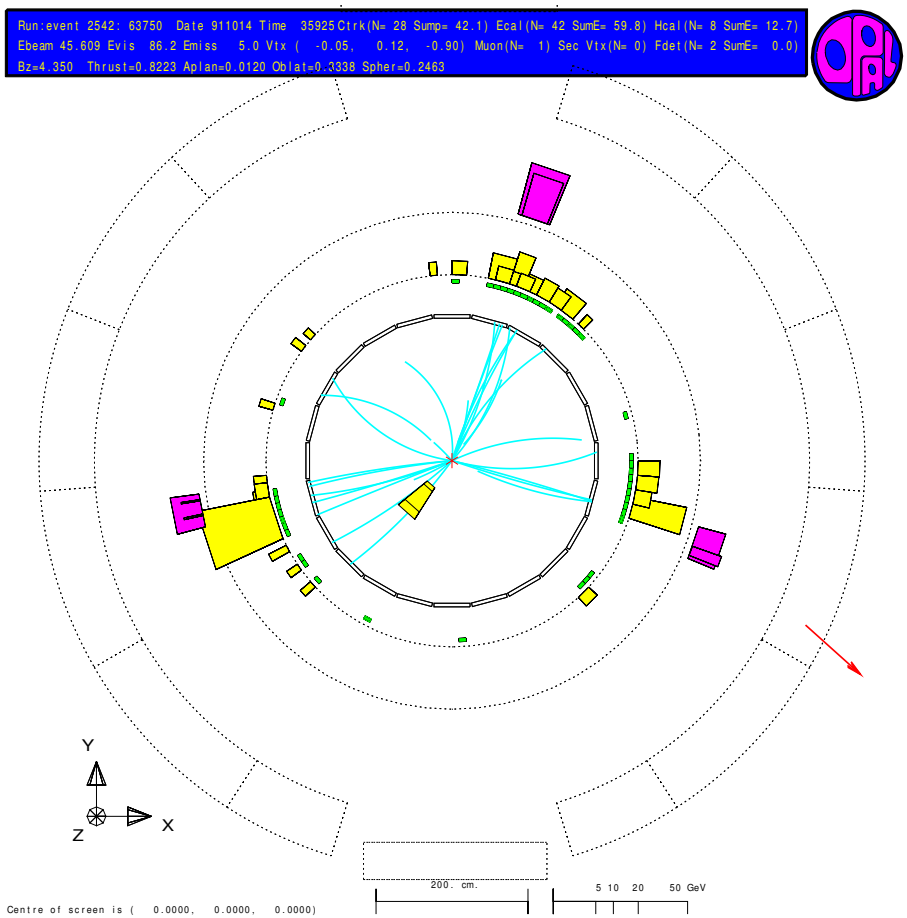
LANL
arXiv: 1501.04596, 1508.07568, 1609.04011, 1610.02031

BNL/RIKEN Saturation Workshop
April 26, 2017

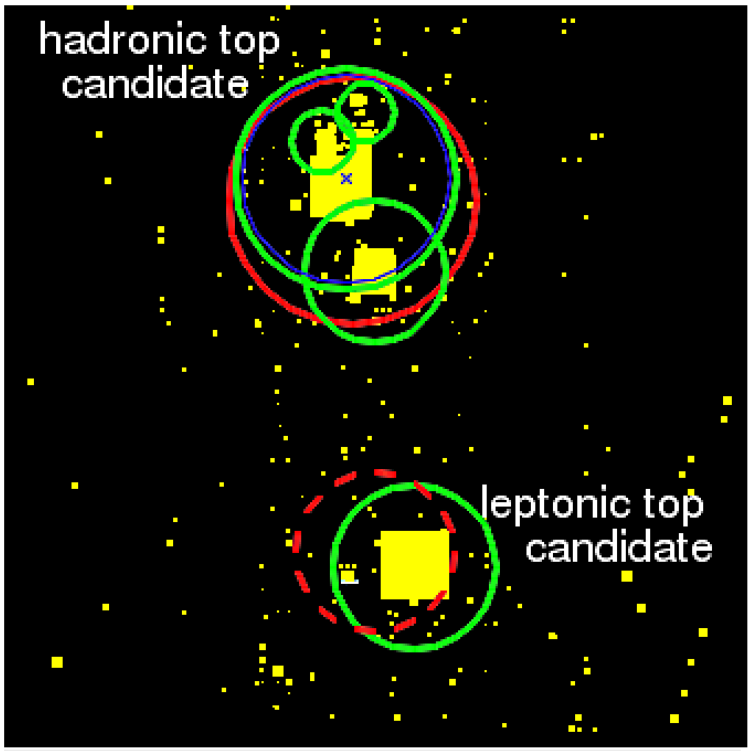
Outline

- Jet Physics
- What is an NGL?
- Banfi-Marchesini-Smye Equation.
- Conformal Mappings and the BK Equation.
- Asymptotics of NGLs and Saturation physics.
- Conclusions.

Question: Given a hard process at $t = 0$, what is the pattern of radiation at $t = \infty$ on S^2?



[ATLAS]



Is it a top quark or QCD gluon jet?

Scattering in QFT

- Hard interaction = scattering amplitude.
- Massive particles $\rightarrow$ small-space-time interaction region.
- Interactions stop for $\Delta x^2 \gg m_{gap}^{-2}$

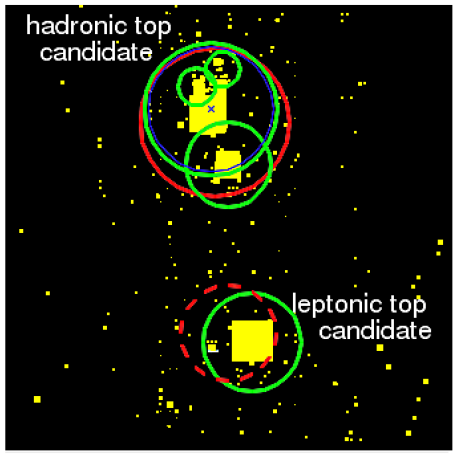
LSZ Recipe:

- Few particles emerge from scattering.
- Well defined mass poles or narrow resonances, definable perturbatively.
- Measure masses and angles and energies.

$$\begin{aligned}\text{Isolated Jet} &\approx \text{tight group of hadrons} \\ &\approx \text{off-shell parton+splittings} \\ &\approx \text{particle}\end{aligned}$$

LSZ ?

No. States are never (perturbatively) asymptotically isolated.



Continuous spectrum and long range-interactions.

On-shell Momentum Regions by power counting:

$$p = (\bar{n} \cdot p, n \cdot p, p_\perp)$$

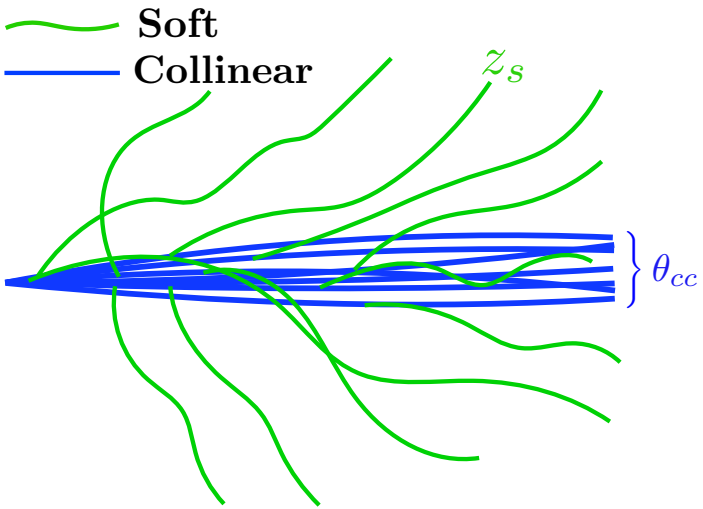
$$p_c \sim Q(1, \theta_{cc}^2, \theta_{cc}) \qquad p_s \sim Q(z_s, z_s, z_s)$$

Dispersion relations with homogeneous scaling:

$$\textbf{Collinear: } p_c^2 = \bar{n} \cdot p_c n \cdot p_c - p_{c\perp}^2 \sim Q^2 \theta_{cc}^2$$

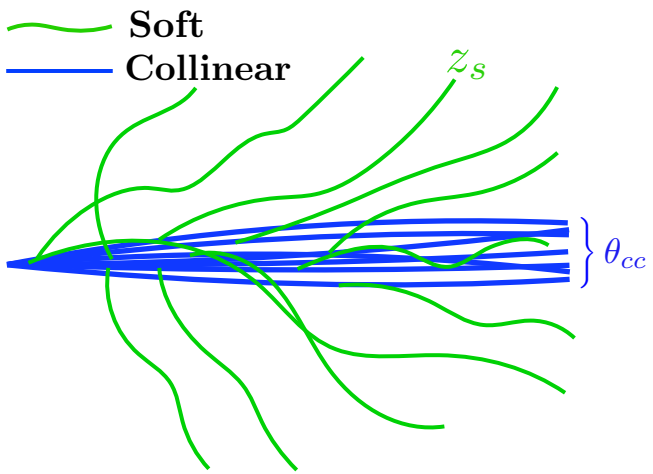
$$\textbf{Soft: } p_s^2 = \bar{n} \cdot p_s n \cdot p_s - p_{s\perp}^2 \sim Q^2 z_s^2$$

$\theta_{cc}, z_s \to 0$ recovers on-shell partons.



$$m_{ab}^2 = (p_a + p_b)^2 \sim Q^2 z_a z_b \theta_{ab}^2$$

The Soft and The Collinear: Factorization



These contributions factorize from each other:

- Collinears sensitive only to *total* momentum contributions from soft radiation.
- Softs sensitive only direction and total charge of collinear regions.
- This factorization is as close to LSZ we get.

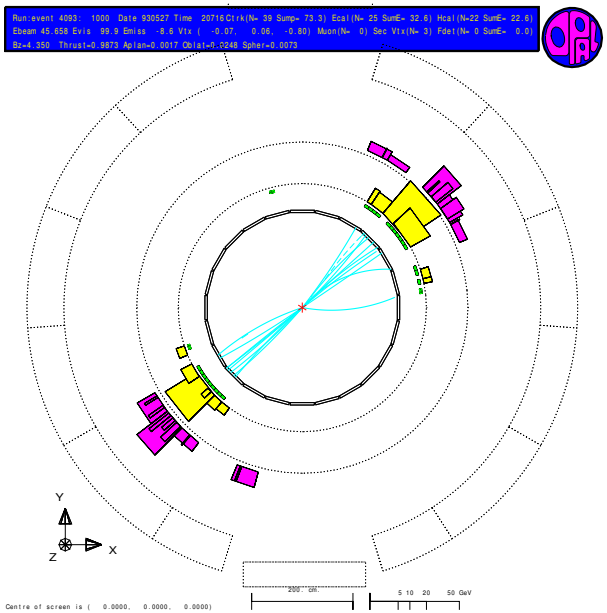
$$\mathcal{A}(i \to f) = C_H\left(\{p_j\}_{j=1}^N\right) \otimes \mathcal{A}_S(i_s \to f_s) \otimes \prod_{i=j}^{N} \mathcal{A}_j(i_{\|j} \to f_{\|j})$$

Global Event Shapes

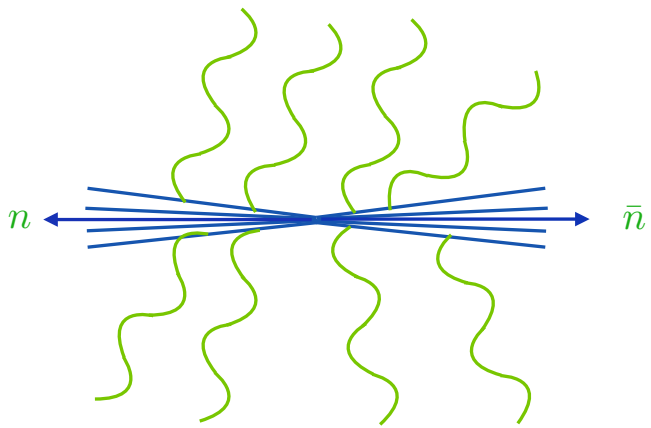
- Paradigmatic example: $e^+e^- \to hadrons$, measure thrust.
- One vetos the production of additional jets anywhere in phase space.

Find axis $\hat{n}$ maximizing momentum flow parallel.

$$T = \max_{\hat{n}} \sum_{i \in \text{event}} \frac{|\hat{n} \cdot \vec{p}_i|}{Q}, \quad \text{and} \quad \tau = 1 - T$$



$\tau \ll 1$



Global Logarithms

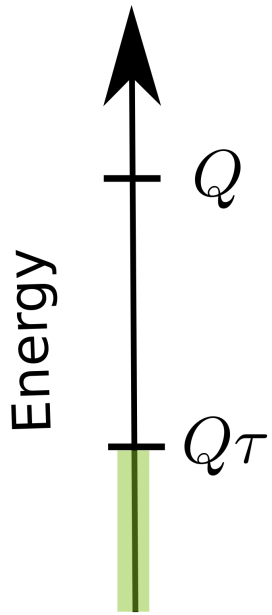
- How? Soft-Collinear Effective Field Theory: final state degrees of freedom precisely known.
- $\theta_{cc} \sim \sqrt{\tau}$
- $z_s \sim \tau$

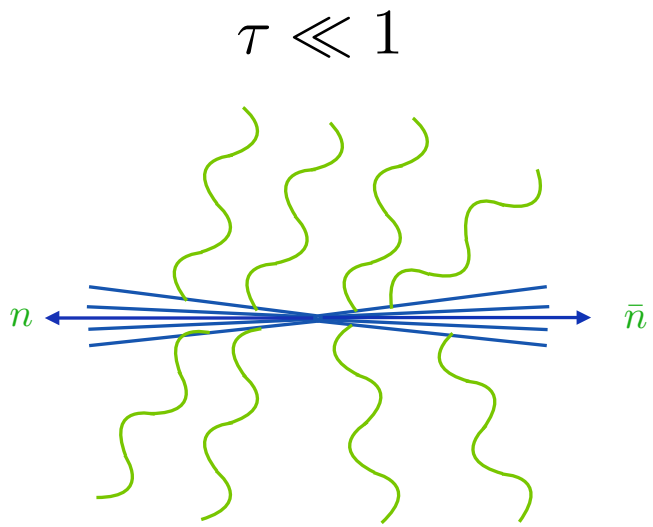
Global Event Shapes

Factorize cross-section into distinct objects:

$$\frac{d\sigma}{d\tau} = H\Big(Q,\mu\Big)\, J_n\Big(\tau,\mu\Big) \otimes J_{\bar{n}}\Big(\tau,\mu\Big) \otimes S_{n\bar{n}}\Big(\tau,\mu\Big) + \ldots$$

$$\tau = \tau_n + \tau_{\bar{n}} + \tau_s$$





- Nothing happens between Q and thrust value $Q\tau$.

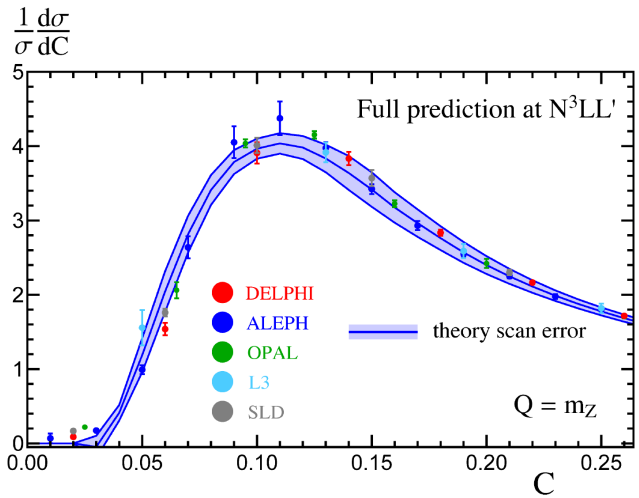
Global Logarithms

- Nothing happens (no on-shell final states emitted) between $q\bar{q}$ production at Q and thrust value $Q\tau$.

$\alpha_s \ln\tau$ resummed thru RG evolution:

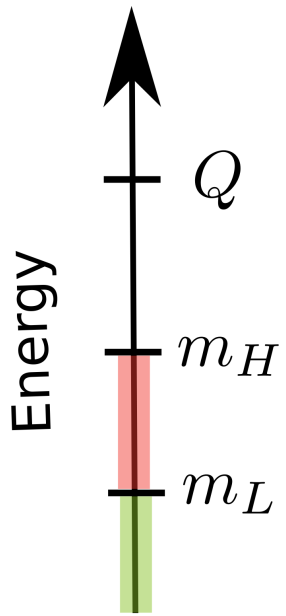
$$\mu \frac{d}{d\mu} F(\mu) = \gamma(\mu) \otimes F(\mu)$$

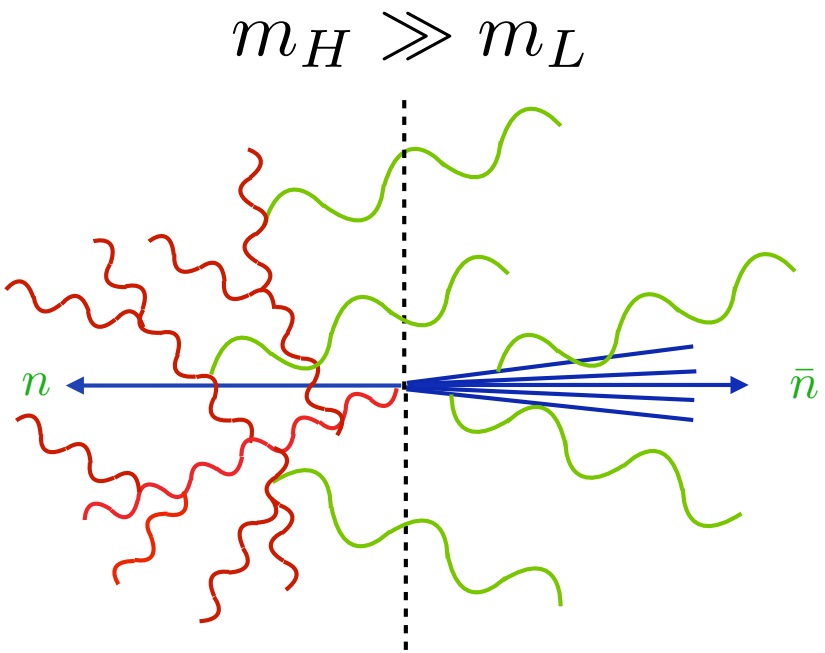
γ and F computable to high orders in fixed order perturbation theory.



Non-Global Measurements

Measure each jets mass independently:



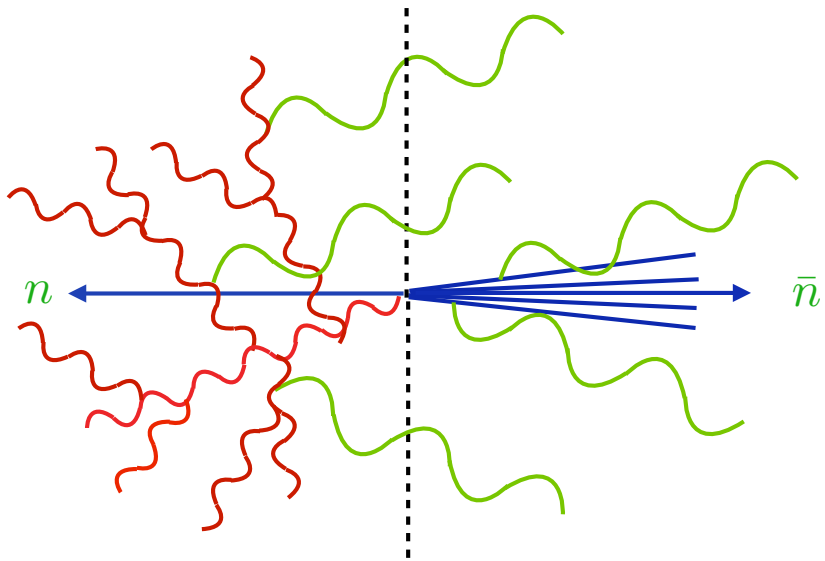


Between the scale m_H and m_L we can have active jet production. [Dasgupta, Salam]

- Distribution in m_L entangled with the "on-shell" branching history below m_H.

Non-Global Logarithms: The Global Factorization

$$m_H \gg m_L$$



$$\frac{d\sigma}{dm_H dm_L} = H\Big(Q,\mu\Big) J_n\Big(m_H,\mu\Big) J_{\bar{n}}\Big(m_L,\mu\Big) \otimes S_{n\bar{n}}\Big(m_H,m_L,\mu\Big) + \ldots$$

- Simulate arbitrarily complicated secondary branching.
- Linear evolution equations no longer sufficient for all logarithms. [Banfi, et. al.; Wiegert]

Non-Global Logarithms

- The final state degrees of freedom *not* precisely known.
- $\theta_{cc} \sim \sqrt{\frac{m_L}{Q}}$ or $\sqrt{\frac{m_H}{Q}}$?
- $z_s \leq \frac{m_H}{Q}$
- The heavier hemisphere $\rightarrow$ more jets at the light-jet "clustering" scale.
- Position of these jets are integrated over.

Banfi-Marchesini-Smye Equation

- Calculate the production of additional jets given jets already produced.
- Use full eikonal approximation for each step.
- Jets = Eikonal lines.
- Jet energies are ordered.

Note: This is at the heart of all modern parton-showers: ARIADNE, VINCIA, DEDUCTOR, DIRE, dipole versions of HERWIGG and SHERPA, etc.

BMS equation at large N_c

Soft function expressable in terms of color dipole functions:

Non-global Log:

$$L = \frac{C_A}{\pi} \int_{m_L}^{m_H} \frac{d\mu}{\mu} \alpha_s(\mu)$$

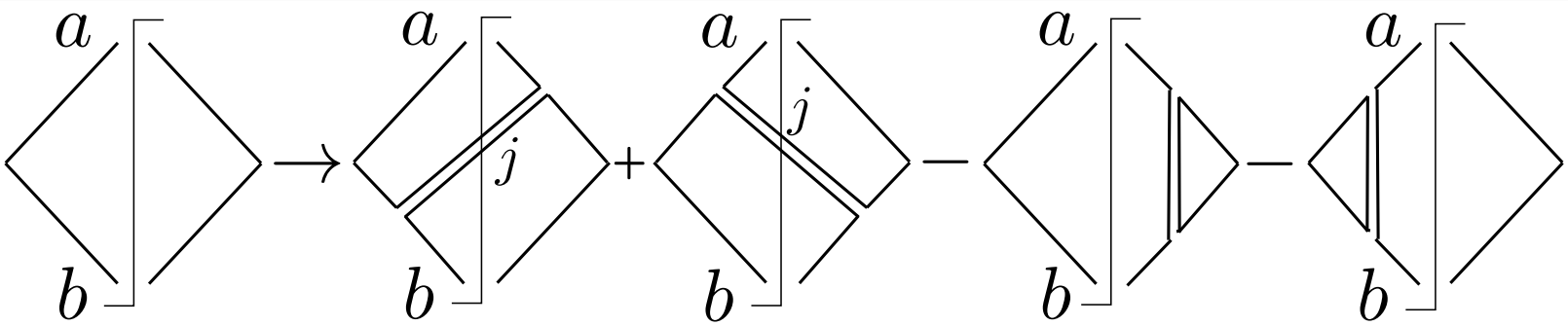
$$S_{ab}(m_H, m_L; \mu) \sim V_{ab}(\mu, m_H, m_L) g_{ab}(L)$$

- S_{ab}: soft function appearing in dijet factorization with eikonal lines $a = (1, \hat{n}_a)$ and $b = (1, \hat{n}_b)$.

$$S_{ab}(m_H, m_L) \propto \mathrm{tr}\langle 0|T\{S_a S_b\}\theta(m_H - \hat{E}\theta_J)\theta(m_L - \hat{E}\theta_{S^2/J})\bar{T}\{S_a S_b\}|0\rangle$$

- g_{ab}: color dipole function with **global** or **Sudakov** evolution factored out.
- A measurable distribution.

BMS equation at large N_c



Evolution of Color Dipoles:

$$\partial_L g_{ab} = \int_J \frac{d\Omega_j}{4\pi} W_{ab}(j) \left(U_{abj}(L) g_{aj} g_{jb} - g_{ab} \right)$$

$$W_{ab}(j) = \frac{a \cdot b}{a \cdot j \; j \cdot b}, \; j = (1, \hat{n}_j)$$

$$U_{abj}(L) = \exp\left(L \int_{S^2/J} \frac{d\Omega_q}{4\pi} W_{aj}(q) + W_{jb}(q) - W_{ab}(q) \right)$$

- Full color evolution $\rightarrow$ reduced density matrix [Wiegert, Caron-Huot, Nagy-Soper, Hatta et al.].
- EFT interpretation and small R[Becher et. al.].
- Evolution equation related to factorization for jet substructure [Larkoski, DN, Moult; DN].

BMS eqn. is (almost) the BK eqn.

If $J = S^2$ and the theory is conformal, and ignore initial conditions, then

- $U_{abj} \to 1$.

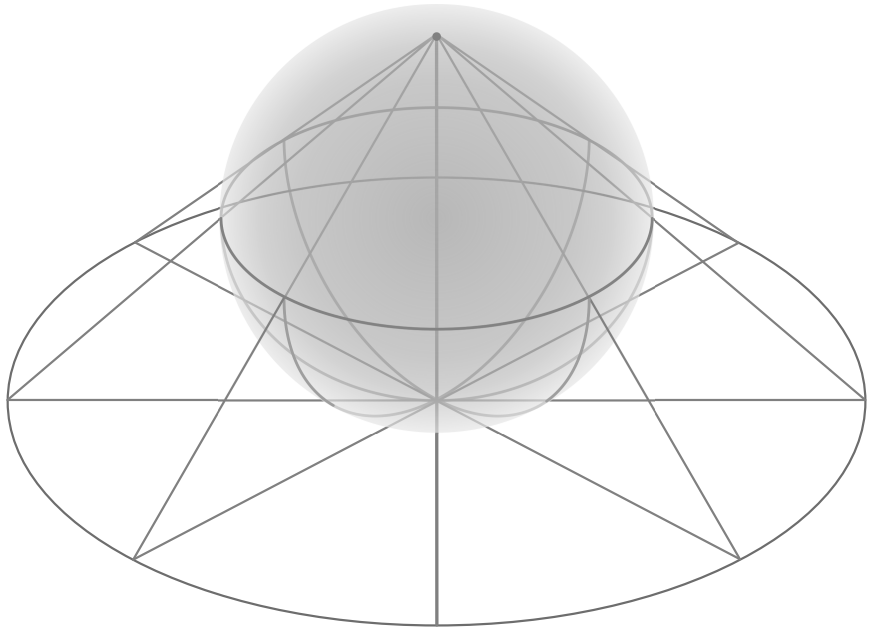
$$\partial_L g_{ab} = \int_{S^2} \frac{d\Omega_j}{4\pi} \frac{a \cdot b}{a \cdot j \; j \cdot b} \left(g_{aj} g_{jb} - g_{ab} \right)$$

$$\leftrightarrow$$

$$\partial_Y S_{\vec{a}\vec{b}} = \frac{\alpha_s C_A}{\pi} \int_{\mathbb{R}^2} \frac{d\Omega_j}{2\pi} \frac{x^2_{\vec{a}\vec{b}}}{x^2_{\vec{a}\vec{j}} x^2_{\vec{j}\vec{b}}} \left(S_{\vec{a}\vec{j}} S_{\vec{j}\vec{b}} - S_{\vec{a}\vec{b}} \right)$$

BMS eqn. is (almost) the BK eqn.

Why? Stereographic projection of $S^2 \to \mathbb{R}^2$



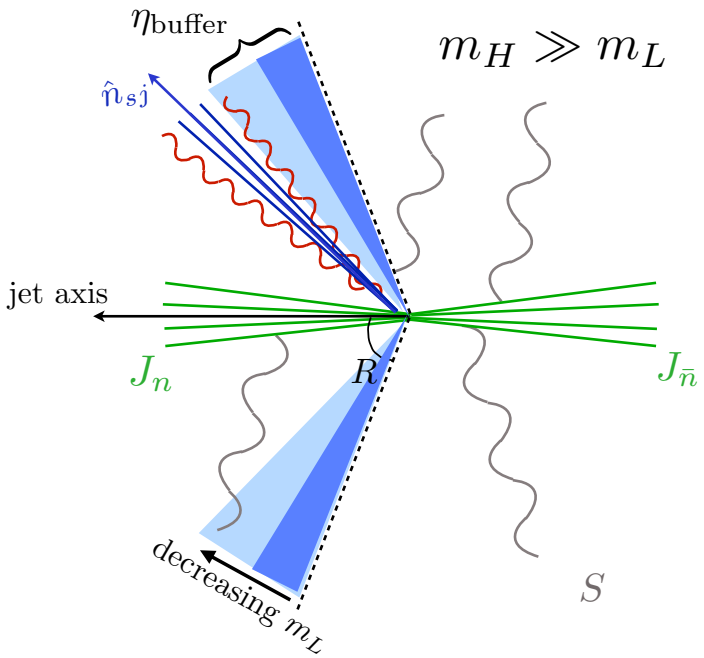
[Hatta et. al.]

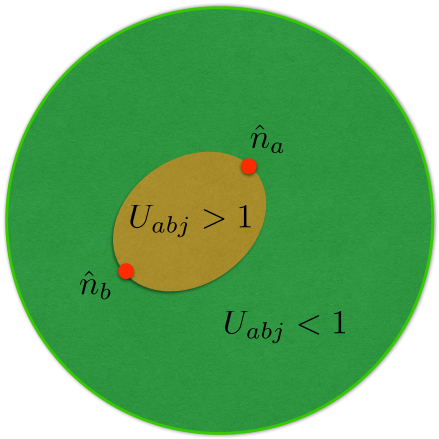
- Checked at NLO, used at NNLO to calculate BK in $N = 4$ SYM [Caron-Huot et. al.].

But Jet Physics is not Small-x

- Jet physics is manifestly dilute.
- At small $L \ll 1$ to moderate $L \sim 1$, the jet physics (J, U_{abj}) parts of BMS eqn. the most important.

The Buffer Region and Phenomonolgy of Soft jets





- Resummation of Sudakov Effects:
  $$U_{abj} \propto \left(1 - \frac{\tan^2 \frac{\theta_{sj}}{2}}{\tan^2 \frac{R}{2}}\right)^L$$
- Cross-section for production of a jet at the boundary vanishes!
- "Buffer Region" noticed in Monte Carlo by [Dasgupta,Salam].
- Existence implies finite region of convergence ($L = 1$) for LL series [DN et. al.].

The Importance of the Buffer Region

However, one can show that irrespective of the differences, BK and BMS equations imply the same asymptotics.

Key: The asymptotic behavior of the buffer region.

[DN]

Buffer Region Beyond $L = 1$

Intuition: suppression of soft gluon production at large angles is moderate for $L \leq 1$, driven by U_{abj}.

- Recall:

$$\partial_L g_{ab} = \int_J \frac{d\Omega_j}{4\pi} W_{ab}(j) \left(U_{abj}(L) g_{aj} g_{jb} - g_{ab} \right)$$

However, what happens to buffer region as $L \to \infty$?

- If g_{ab} dies off, then non-linear term dies off twice as fast.
- Truncate:

$$\lim_{L\to\infty} \partial_L g_{ab} =_? - \left(\int_J \frac{d\Omega_j}{4\pi} W_{ab}(j) \right) g_{ab}$$

Collinearly Regulated BMS

Add collinear regulator to make truncation possible:

- $$\partial_L g^\delta_{ab} = \int_J \frac{d\Omega_j}{4\pi} W^\delta_{ab}(j) \Big(U_{abj}(L) g^\delta_{aj} g^\delta_{jb} - g^\delta_{ab} \Big)$$
$$W^\delta_{ab}(j) = \frac{a \cdot b}{(a \cdot j + \delta^2)(j \cdot b + \delta^2)}$$
- Comparison Theorem For Diff Eq.:
$$\ln g^\delta_{ab} \geq - \int_0^L d\ell \gamma_{ab}\Big(\delta(\ell)\Big)$$
$$\gamma_{ab}(\delta) = \int_J \frac{d\Omega_j}{4\pi} W^\delta_{ab}(j)$$

Idea: For large L, virtual correction dominates BMS equation except for small collinear region of size $\delta(L)$.

Asymptotic to Full Solution

Now choose $\delta(L)$ such that:

$$g_{ab}\Big(\gamma(\delta)\Big) = \mathrm{Exp}\Big(-\int_0^L d\ell \gamma_{ab}(\delta(\ell))\Big)$$

Asymptotically solves *full* BMS:

$$\lim_{L\to\infty} \partial_L g_{ab}\big(\gamma(\delta)\big) = \int_J \frac{d\Omega_j}{4\pi} W_{ab}(j)\Big(U_{abj}(L) g_{aj}\big(\gamma(\delta)\big) g_{jb}\big(\gamma(\delta)\big) - g_{ab}\big(\gamma(\delta)\big)\Big)$$

This would be trivial, except for collinear regions!

Complication in Collinear Regions

Collinear safety of BMS equation demands:

$$g_{ab} \to 1, a \parallel b, \forall L$$

So expand BMS equation about limit $a \parallel b \parallel j$:

$$g_{ab} = 1 + \Phi_{ab} + ...$$

$$\lim_{L\to\infty} \partial_L \Phi_{ab} = \int_0^\infty d\theta_j \int_0^{2\pi} \frac{d\phi_j}{2\pi} \frac{\theta_{ab}^2}{\theta_{aj}^2 \theta_{jb}^2} \Big(\Phi_{aj} + \Phi_{jb} - \Phi_{ab} \Big) + O(\Phi^2)$$

This is the position space BFKL equation for color dipoles. [Marchesini, Mueller]

NOTE: Jet region dependence is lost in collinear limits!
U_{abj} contributions are power suppressed.

Complication in Collinear Regions

Simply matter to write solutions in terms of eigenfunctions:

$$\Phi^{\nu}_{ab} = A\Big(\frac{\theta^2_{ab}}{\theta^2_c(L)}\Big)^{\nu}$$

$$\theta_c(L) = \mathrm{Exp}\Big(-\frac{\chi(\nu)}{2\nu}L\Big)$$

Note that the earlier anzats has small angle behavior:

$$g_{ab}\Big(\gamma(\delta)\Big) = 1 - \int_0^L d\ell \frac{\theta^2_{ab}}{4\delta^2(\ell)} + ...$$

$\nu = 2$ is a pole! Must use BFKL solution in collinear regions.

Returning to Asymptotic Condition

Suppose only a leg in active jet region:

$$\lim_{L\to\infty} \partial_L g_{ab}\big(\gamma(\delta)\big) = \int_J \frac{d\Omega_j}{4\pi} W_{ab}(j) \Big(U_{abj}(L) g_{aj}\big(\gamma(\delta)\big) g_{jb}\big(\gamma(\delta)\big) - g_{ab}\big(\gamma(\delta)\big) \Big)$$

$$= \int_{J,\theta_{aj}\leq\theta_c} \frac{d\Omega_j}{4\pi} W_{ab}(j) \Big(U_{abj}(L) g_{aj}\big(\gamma(\delta)\big) g_{jb}\big(\gamma(\delta)\big) - g_{ab}\big(\gamma(\delta)\big) \Big)$$

$$+ \int_{J,\theta_{aj}\geq\theta_c} \frac{d\Omega_j}{4\pi} W_{ab}(j) \Big(U_{abj}(L) g_{aj}\big(\gamma(\delta)\big) g_{jb}\big(\gamma(\delta)\big) - g_{ab}\big(\gamma(\delta)\big) \Big)$$

First term, use BFKL solution.
In second term use buffer region anzats.
Consistency requires:

$$\delta(L) = \theta_c(L) = \mathrm{Exp}\Big(-\frac{\chi(\nu)}{2\nu} L \Big)$$

Asymptotic NGL distribution

- At small cut-off $\gamma_{ab}(\delta)$ is dominated by universal collinear poles.
- Only geometry dependence is the number of radiators in the active jet!

$$\ln g_{ab}\big(\gamma(\delta)\big)\Big|_{\text{in-out}} = +\int_0^L d\ell\, \ln\delta(\ell) + \ldots = -\frac{\chi(\nu)}{4\nu} L^2 + \ldots$$

$$\ln g_{ab}\big(\gamma(\delta)\big)\Big|_{\text{in-in}} = +2\int_0^L d\ell\, \ln\delta(\ell) + \ldots = -\frac{\chi(\nu)}{2\nu} L^2 + \ldots$$

Slowest possible decay: $\frac{\chi(\nu_{\min})}{4\nu_{\min}} \approx 1.22$

In some sense this is "topological," since the location within and the shape of jet region is irrelevant.

Buffer Region = Saturation Region

Yet this may be obvious for the small-x acolytes:

$$Q_s(Y) = Q_0 \exp\left(\frac{\chi(\nu_{\min})}{\nu_{\min}}\bar{\alpha}_s Y - \frac{3}{2\nu_{\min}}\ln\left(\bar{\alpha}_s Y\right) + \ldots\right)$$

$$Q_s^{-1}(Y) \leftrightarrow \delta(L)$$

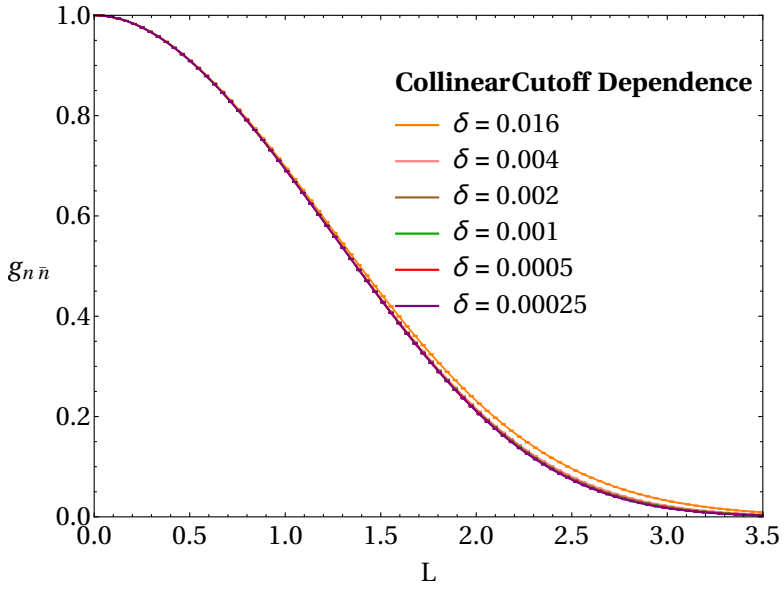
$$g_{ab}\big(\gamma(\delta)\big) \leftrightarrow \text{Levin-Tuchin Black Disc for BK}$$

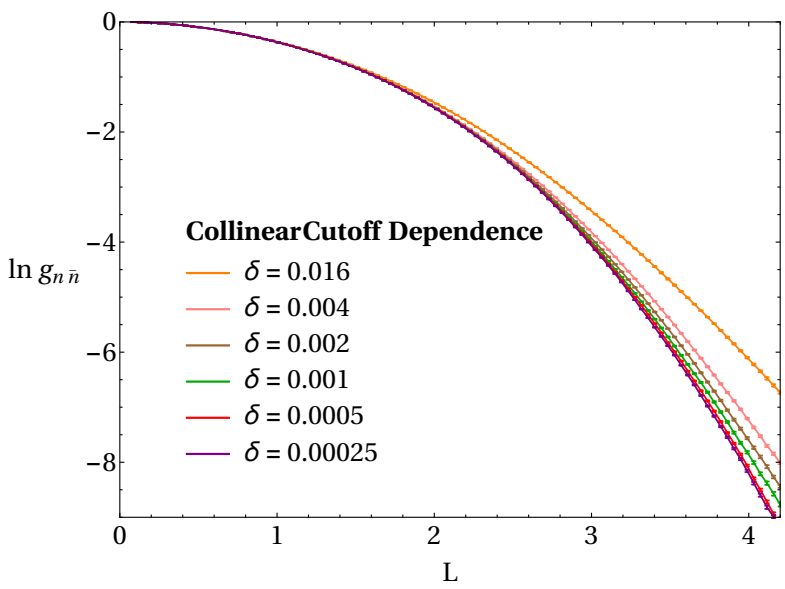
But the physical interpretation is distinct:
In the buffer region, there are no real emissions.
In the saturation region, there are lots of wee partons.

Numerical Check

Inspired by saturation, fit log of tail to Dasgupta-Salam MC:

$$M(L) = aL^2 + bL\ln L + cL, \qquad 1.5 \geq L \geq 4$$

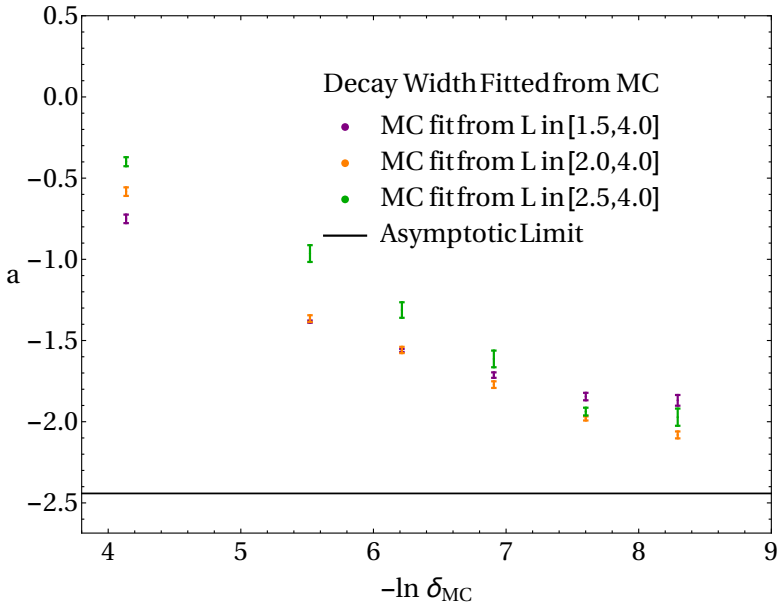


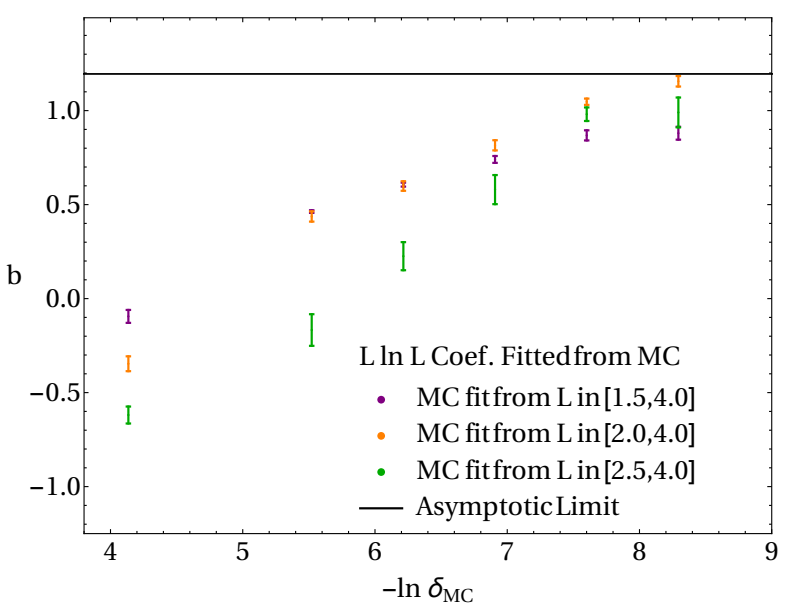


MC runs with collinear cutoff on all emmissions.
Must extrapolate to zero.

Numerical Check

Extrapolate to zero cutoff.





Consistent with slowest possible decay: $\frac{\chi(\nu_{\min})}{4\nu_{\min}} \approx 1.22$

Conclusions

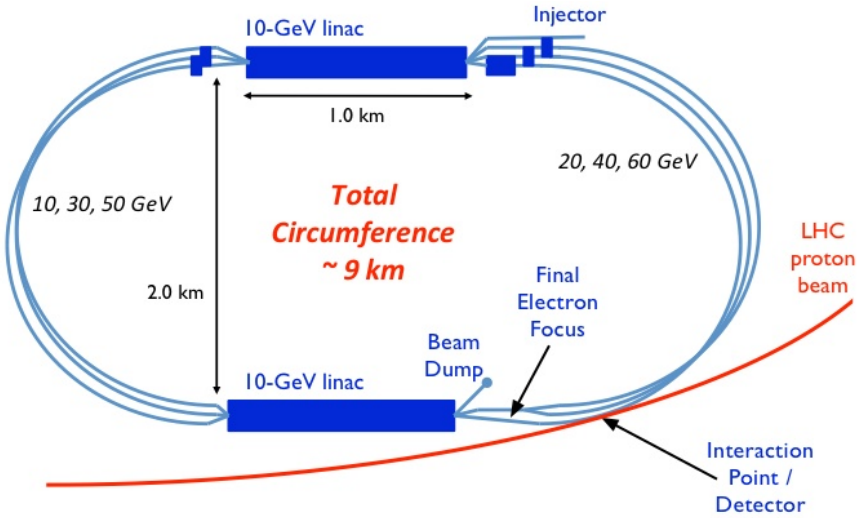
- *BFKL is the ultimate controlling equation for the asymptotics of pQCD, both in initial and final state distributions.*
- Asymptotics of NGLs is "topological": count number of initial hard emitters in active region.
- Angular size of buffer region directly maps to saturation scale.

Puzzles:

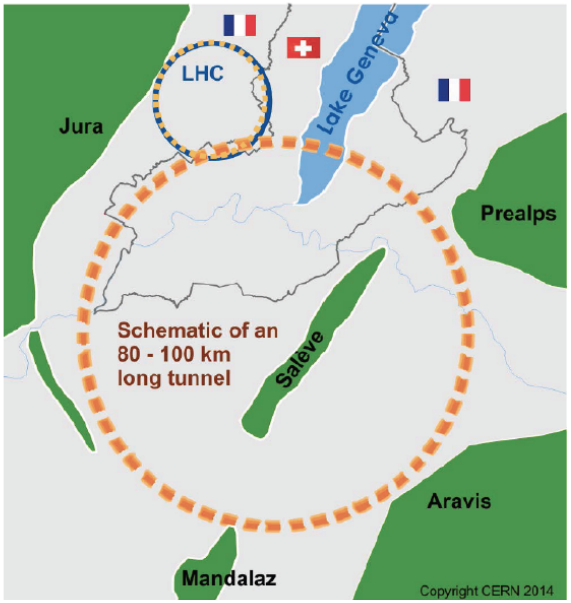
- BMS equation built upon soft branching only, but asymptotics governed by a *collinear* limit.
- Must we consider the full parton shower, even for purely soft-sensitive observables?

Low x Physics and Saturation: From HERA to Future DIS and the LHeC

Paul Newman
Birmingham University









Low x Physics at HERA: the "Pathological" Gluon

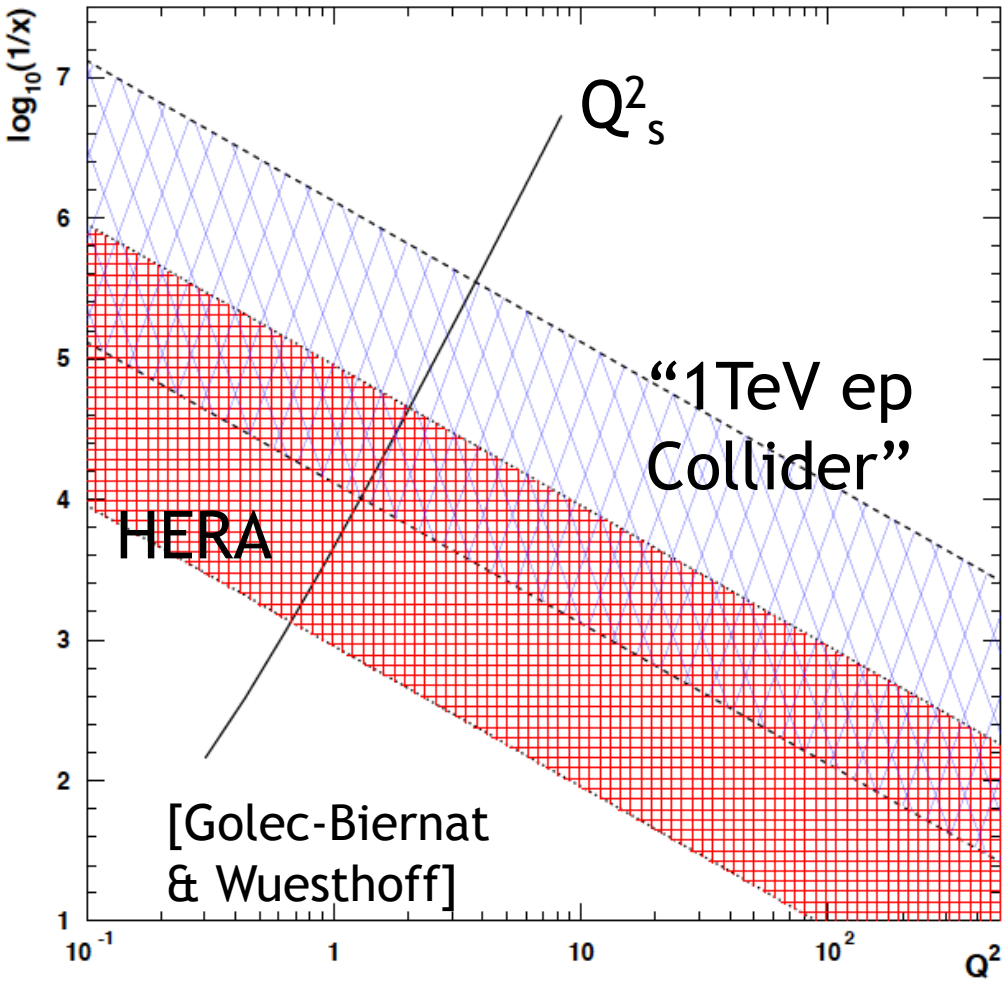
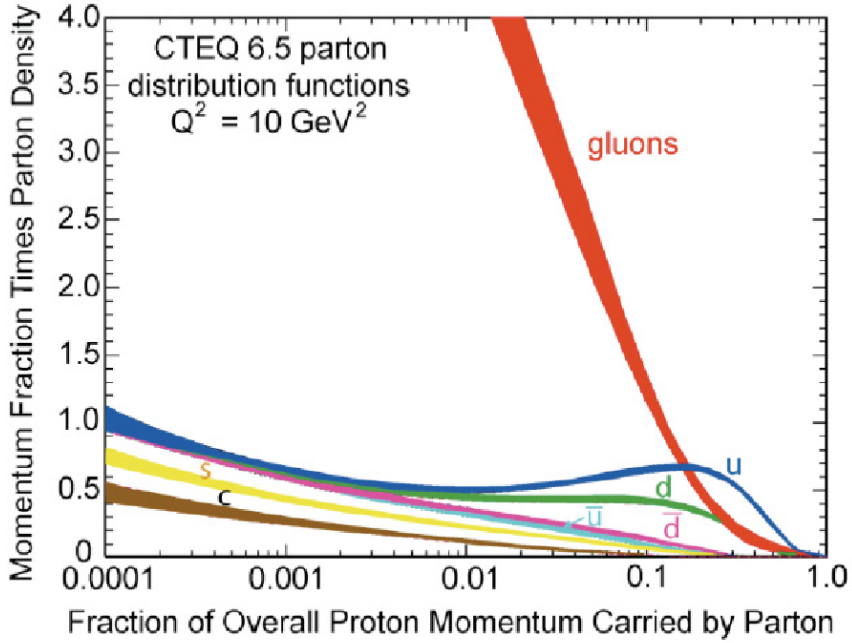


Figure 5: The position of the critical line in the (x, Q^2)-plane. The narrow hatched area corresponds to the acceptance region of HERA. The wide hatched region indicates the range for a future 1 TeV ep-collider. The boundaries are lines of constant y.

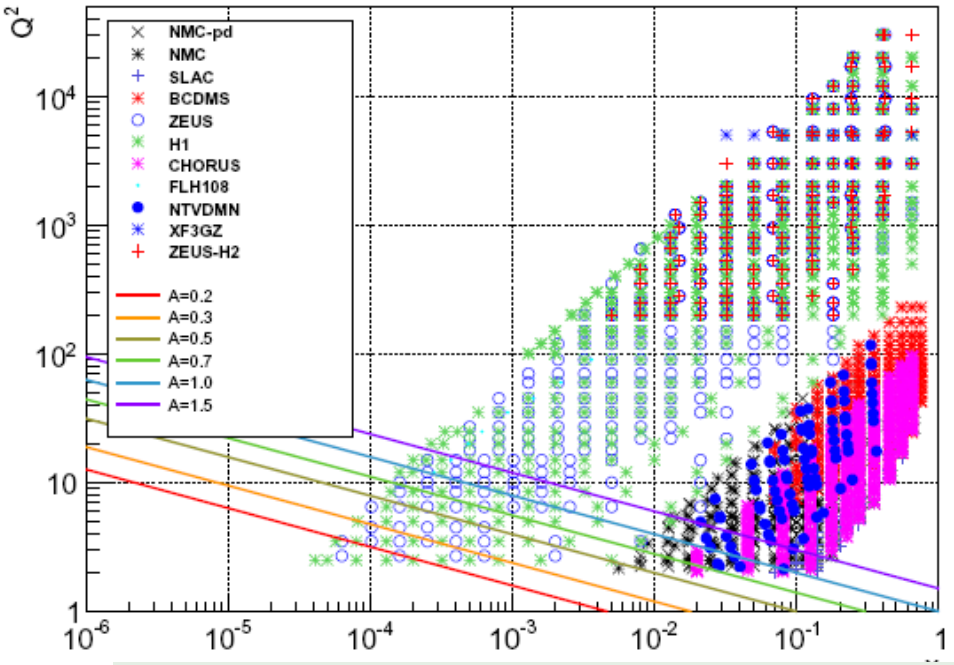


1998: Low x HERA data are well fitted in (dipole) models that include saturation effects
- x dependent "saturation scale", $Q^2_s(x)$

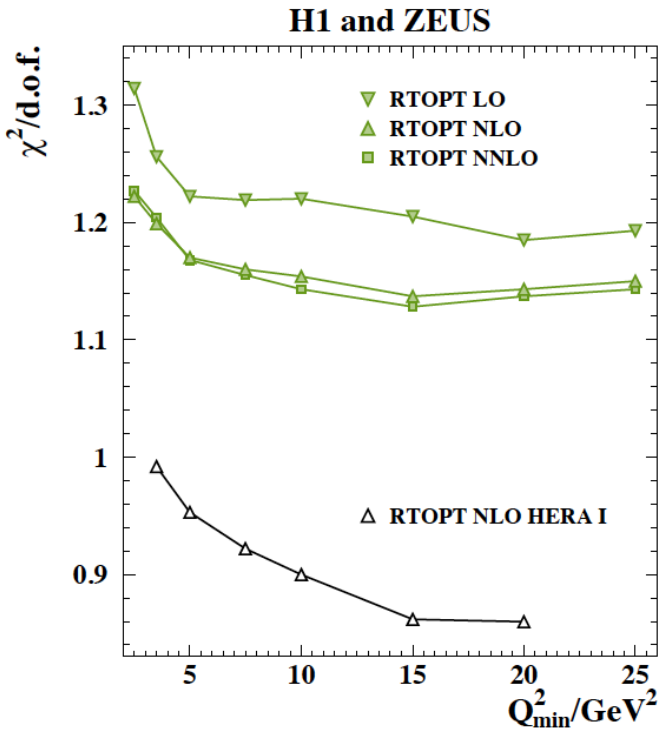
$$\frac{xG_A(x,Q_s^2)}{\pi R_A^2 Q_s^2} \sim 1 \Longrightarrow Q_s^2 \propto A^{1/3} x^{\sim -0.3}$$

Saturation and DGLAP PDF fits

e.g. NNPDF: NLO DGLAP description deteriorates when adding data in lines $Q^2 > Ax^{-0.3}$ parallel to 'saturation' curve in x/Q^2.



A	$\chi^2_{\text{without cuts}}/d.o.f.$	$\chi^2_{\text{cut}}/d.o.f$
0.5	$19.68/25 = 0.79$	$106.22/25 = 4.25$
1.0	$54.41/44 = 1.24$	$138.24/44 = 3.14$
1.5	$62.31/59 = 1.06$	$860.65/59 = 14.6$



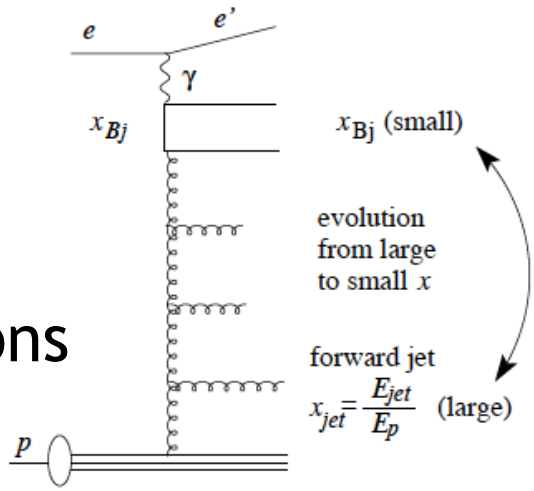
Final HERA-2 Combined PDF Paper:
"some tension in fit between low & medium Q^2 data… not attributable to particular x region" (though kinematic correlation)

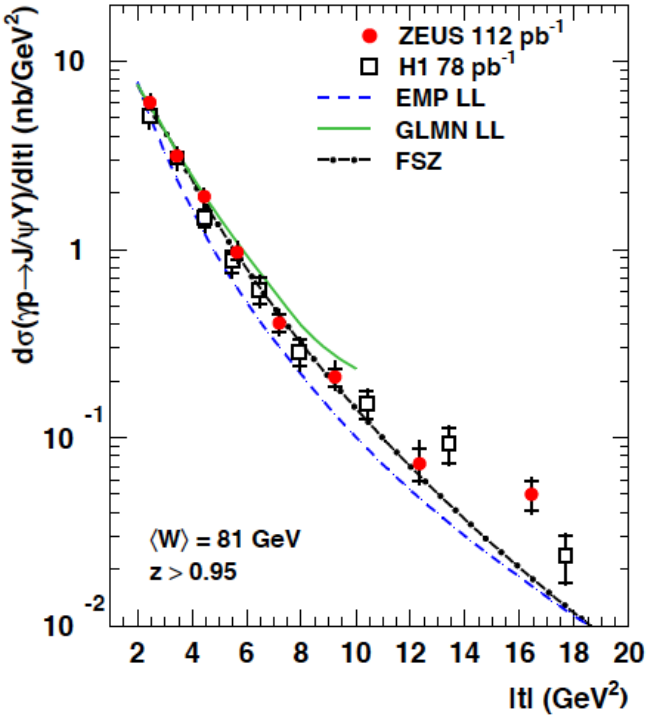
… something happens, but interpretation?

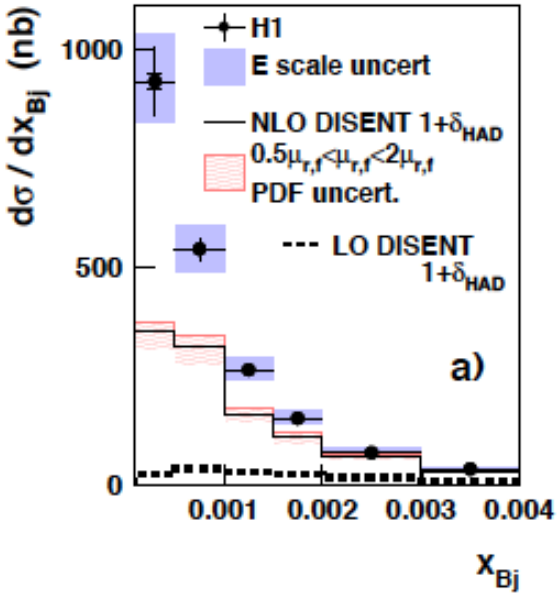
Hadronic Final State Observables

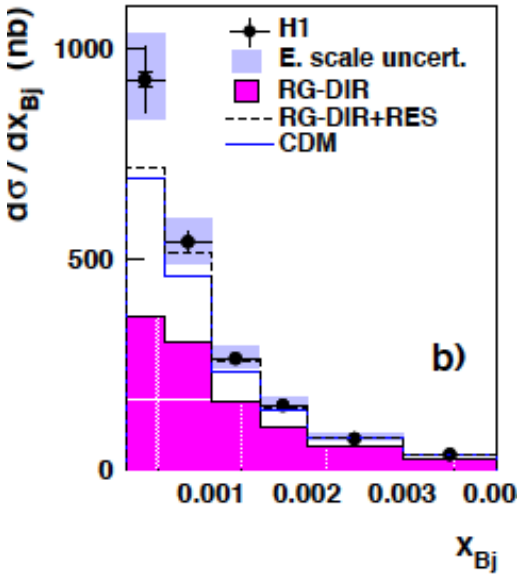
Inventive new observables to search for deviations from p_T ordering in the parton cascade …

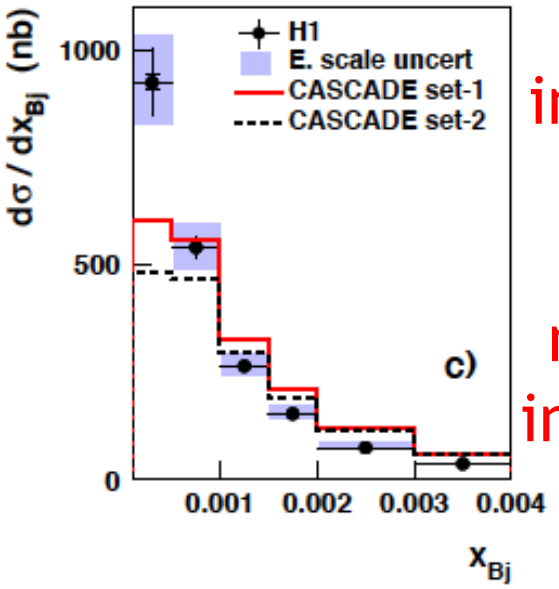
- Forward jets
- Azimuthal decorrelations
- High |t| p-diss J/Ψ…





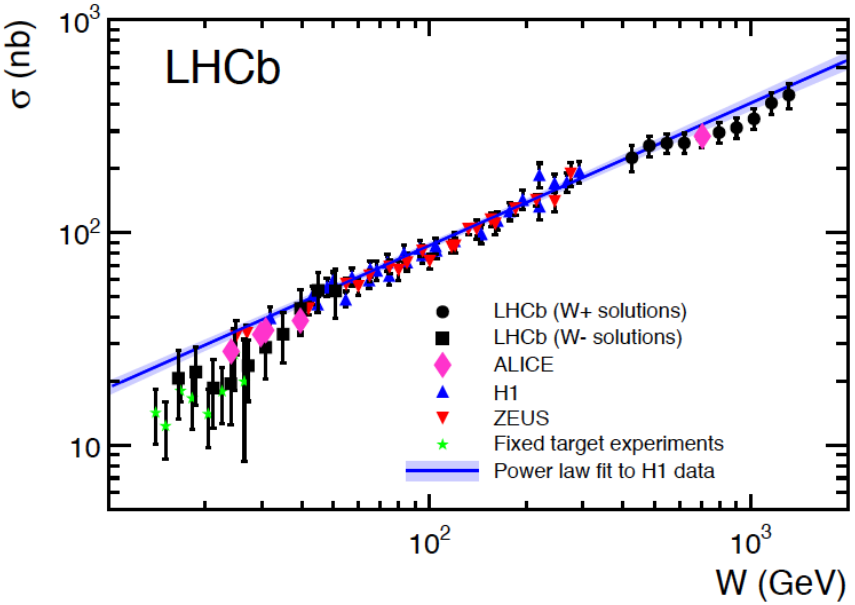


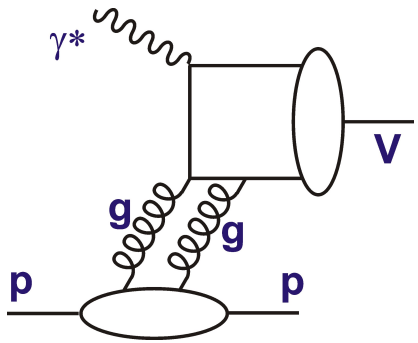




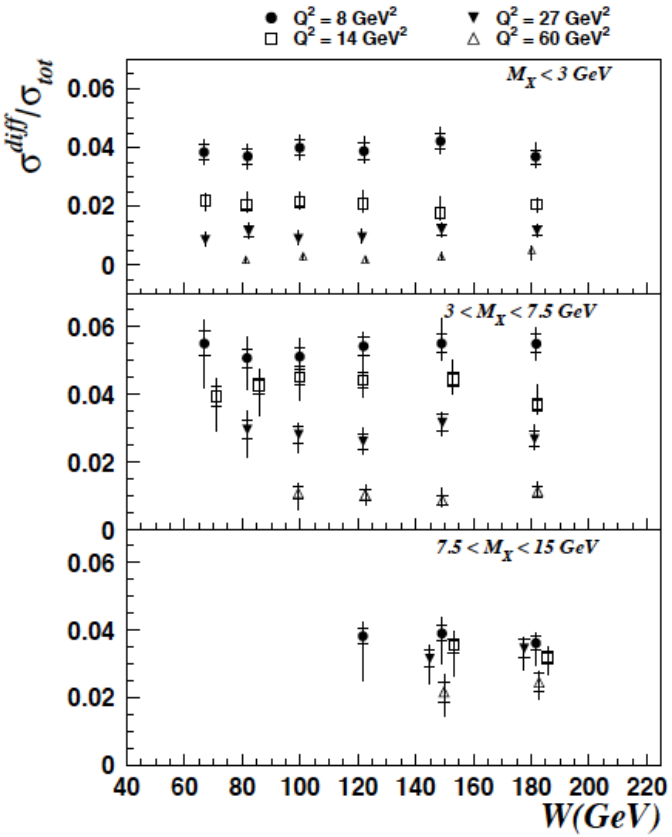
Some interesting effects … not easily interpreted

Low x Saturation in Diffractive Data?





- **Elastic J/Ψ in γp …**
- No evidence for change in shape at high W (i.e. low x), even at LHC (t dependence yet to be exploited)

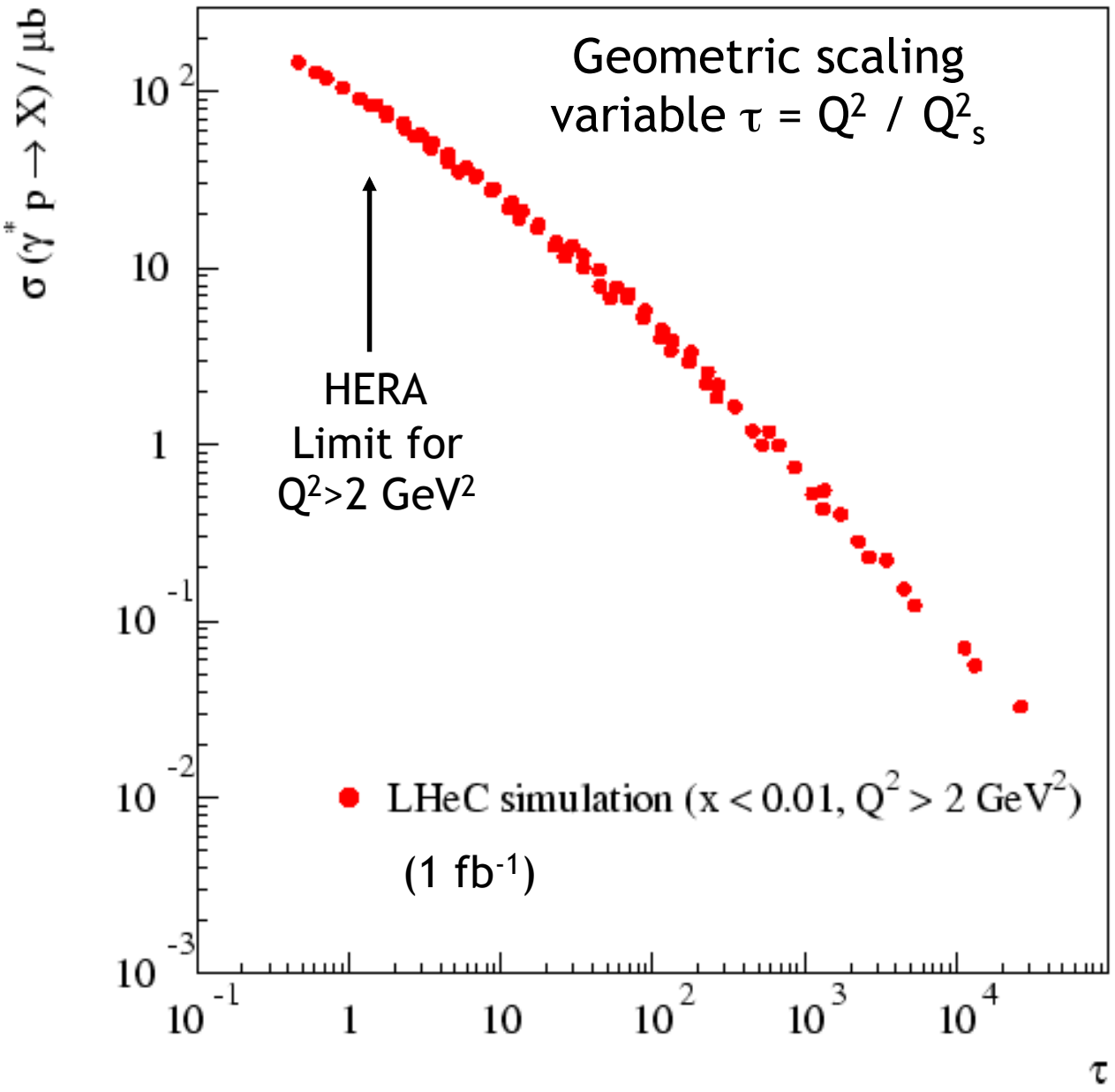


- **Rather flat diffractive/inclusive ratio**

and failure of diffractive PDF fits to data below Q^2 ~ 5 GeV^2 best described by dipole models incorporating saturation …

BOTTOM LINE … HERA not conclusive on location or dynamics of onset and LHC has not given greater clarity

Problem of Inclusive Data in 1 Dimension



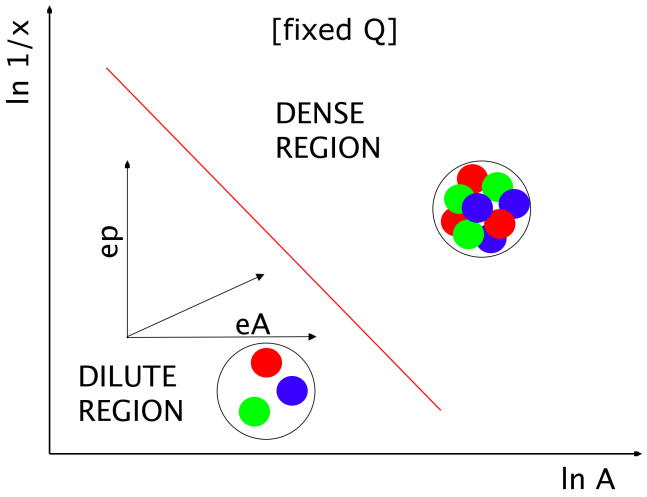
… HERA had very limited aceptance for $\tau<1$ … **saturation effects depend mainly on data with $0.045 < Q^2 < 1$ GeV²**

LHeC reaches $\tau \sim 0.15$ for $Q^2=1$ GeV² and $\tau \sim 0.4$ for $Q^2=2$ GeV²

Can also be enhanced with nuclei.

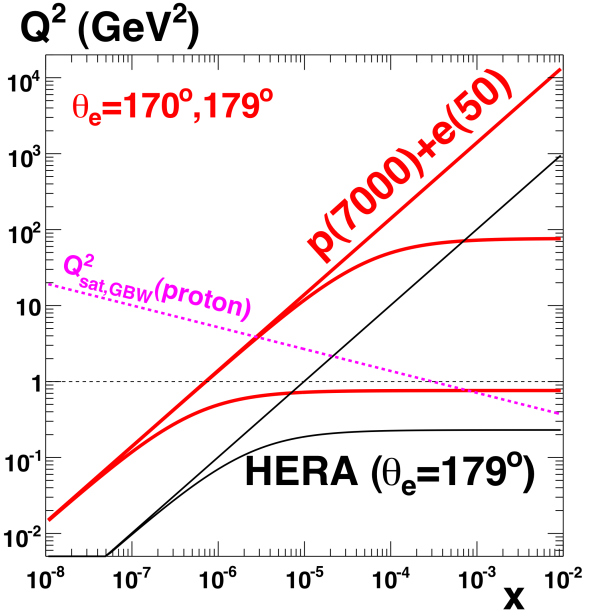
Accessing saturation region at large Q^2

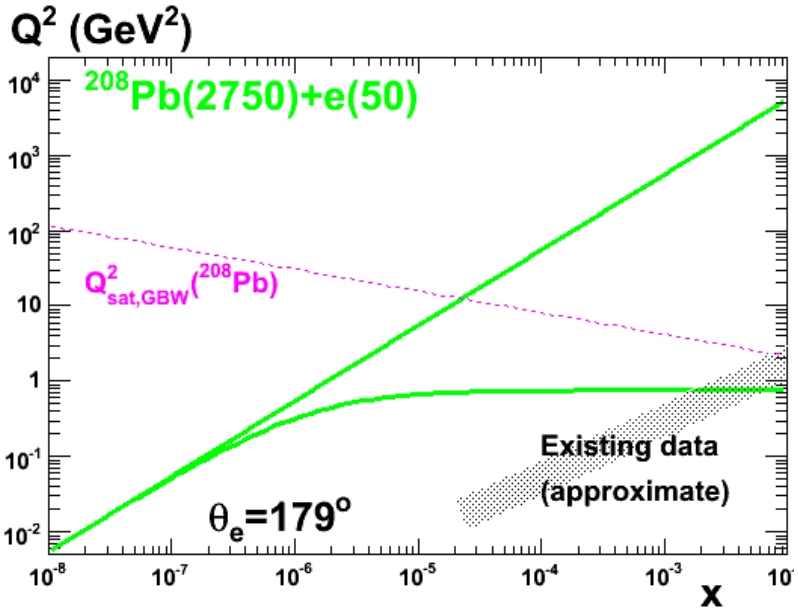
2-pronged approach: EIC and LHeC



Enhance target `blackness' by:

1) Probing lower x at fixed Q^2 in ep
   [evolution of a single source]
2) Increasing target matter in eA
   [overlapping many sources at fixed kinematics …
   Density ~ $A^{1/3}$ ~ 6 for Pb … worth 2 orders of magnitude in x]





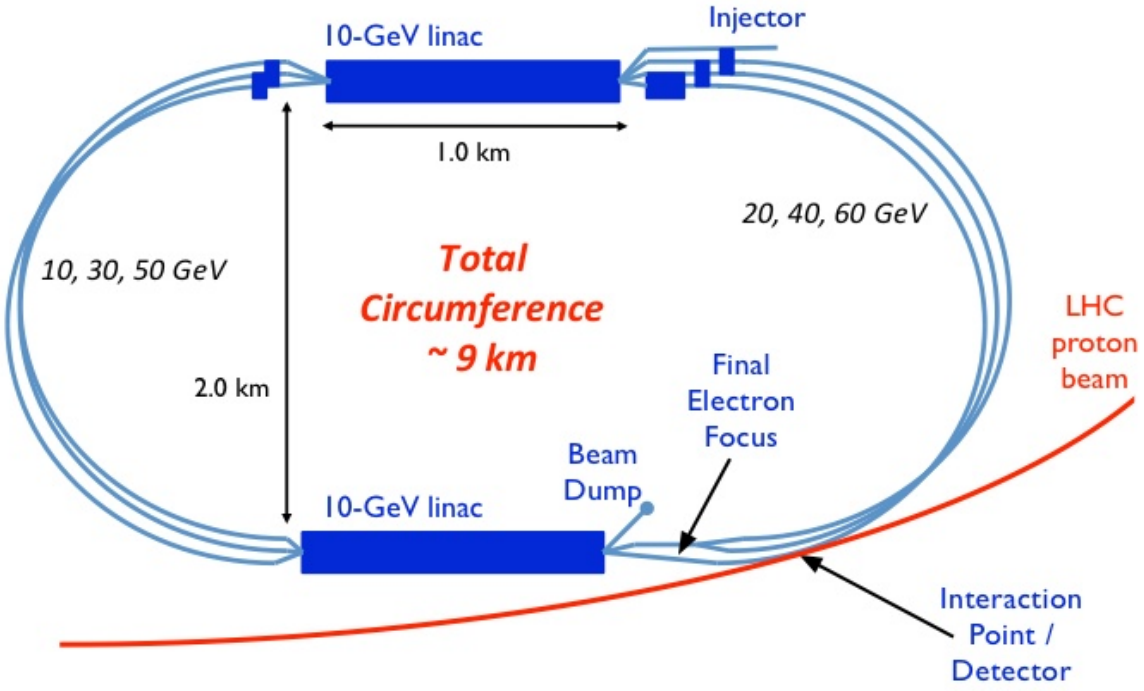
… e.g. LHeC reaches saturated region in both ep & eA inclusive data according to models

Baseline Design (Electron "Linac")

- Design constraint: power consumption < 100 MW → E_e = 60 GeV

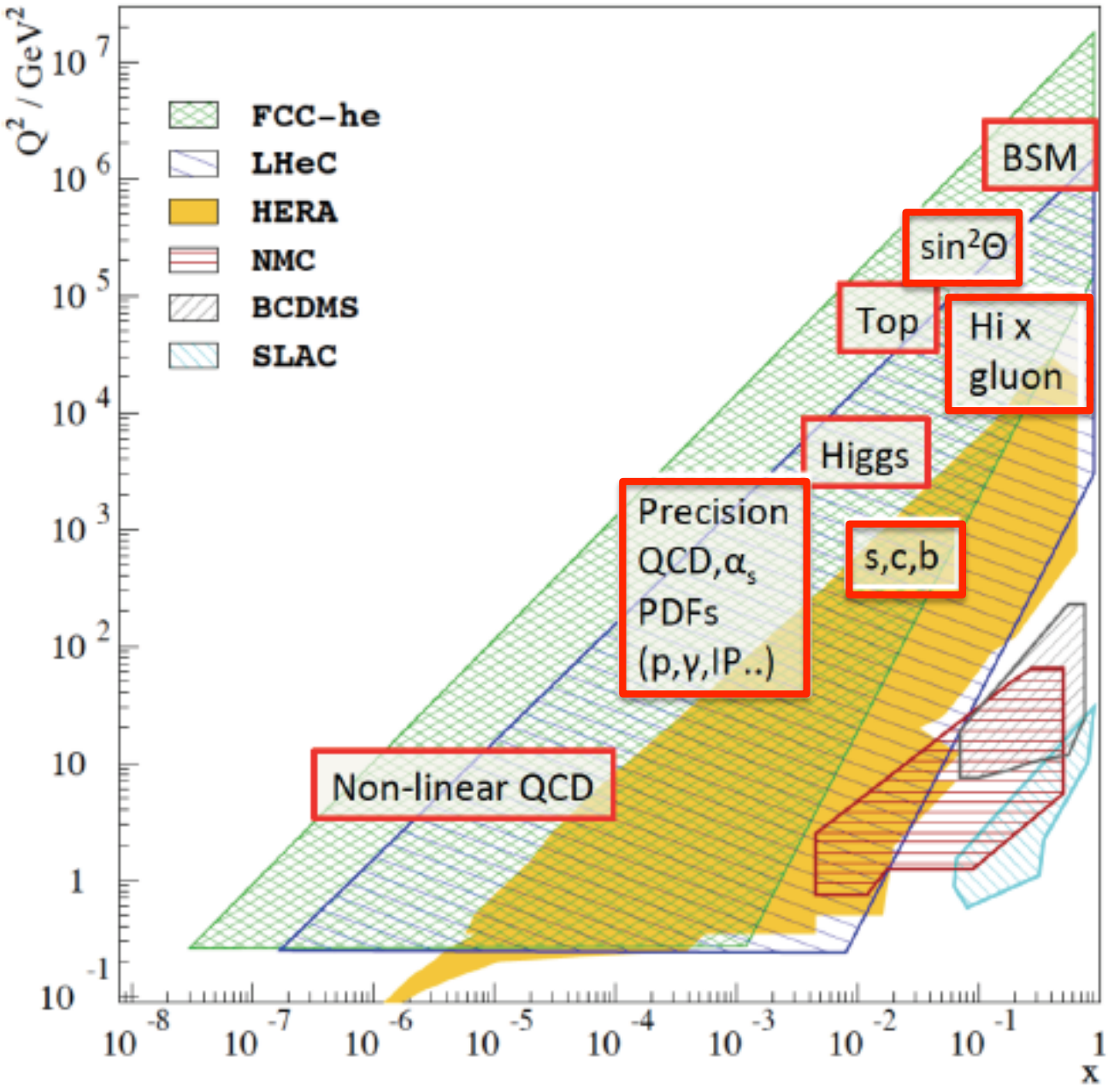
- Colliding with E_p = 7 TeV from LHC (or even 50 TeV from FCC) and equivalent ion beams

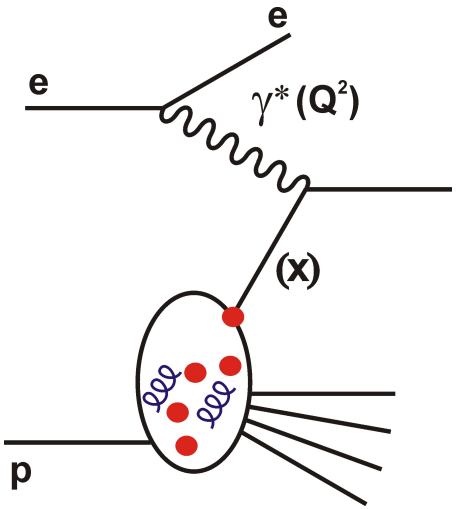
• Two 10 GeV linacs,
• 3 returns, 20 MV/m
• Energy recovery in same structures
[Energy recovery Linac prototype planned @ Orsay]



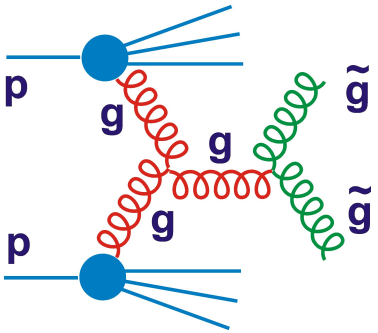
• ep lumi → 10^{34} cm^{-2} s^{-1}
→ ~100 fb^{-1} per year →~1 ab^{-1} total
• **eD and eA collisions have always been integral to programme**
• **e-nucleon Lumi estimates ~ 10^{31} (10^{32}) cm^{-2} s^{-1} for eD (ePb)**

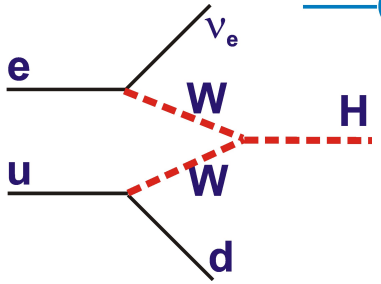
LHeC Physics at 10^{34} cm^{-2}s^{-1}





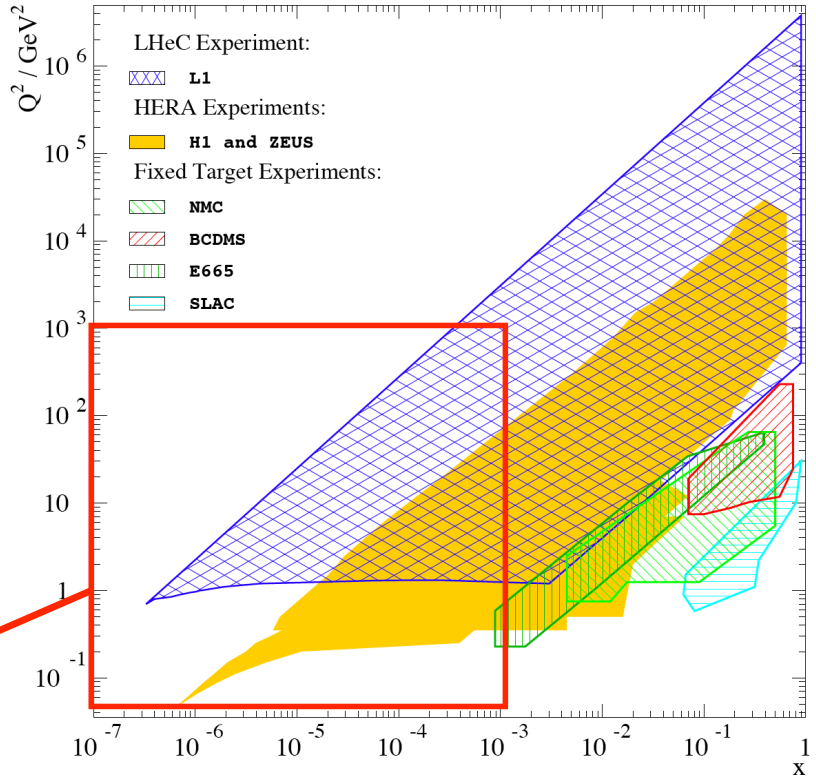
Diverse physics goals require precision throughout wide accessible kinematic region.

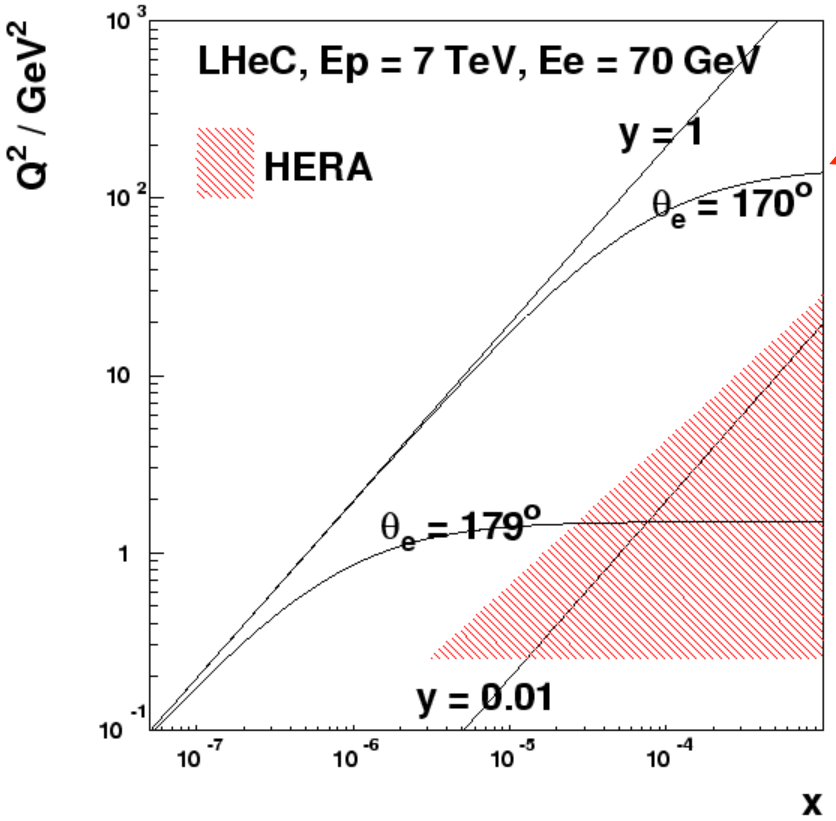




LHeC Kinematic Detector Requirements

Access to Q^2=1 GeV^2 in ep mode for all $x > 5 \times 10^{-7}$ requires scattered electron acceptance to 179^o



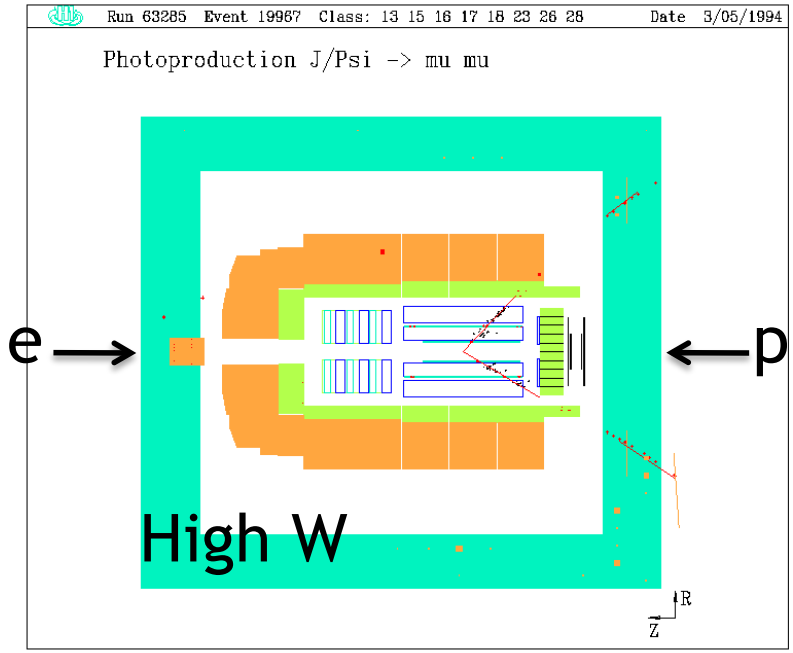


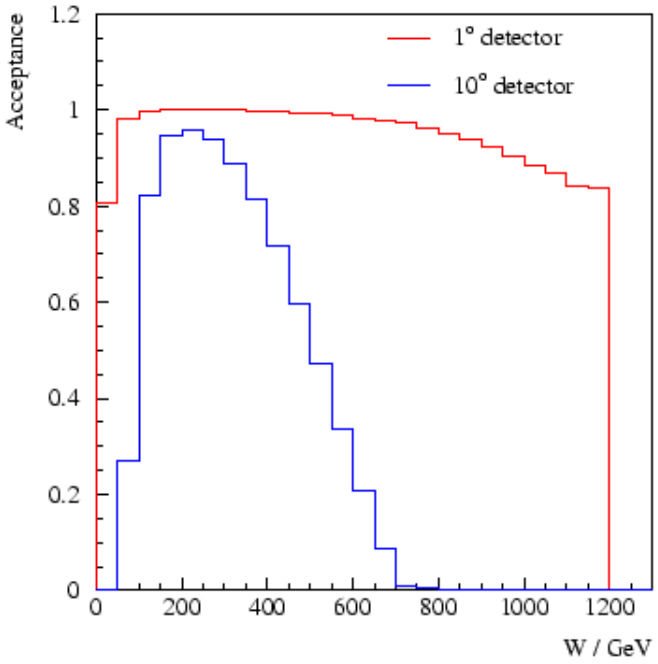
Also need 1^o acceptance in proton direction to contain hadrons for kinematic reconstruction, Mueller-Navelet jets, maximise acceptance for new massive particles …

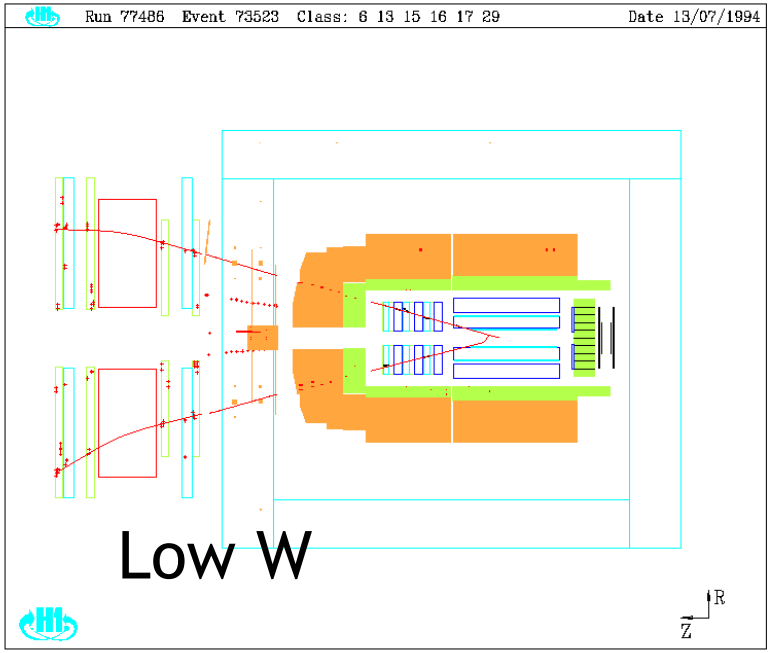
Elastic J/Ψ Kinematics

- At fixed $\sqrt{s}$, decay muon direction is determined by $W = \sqrt{s_{\gamma p}}$

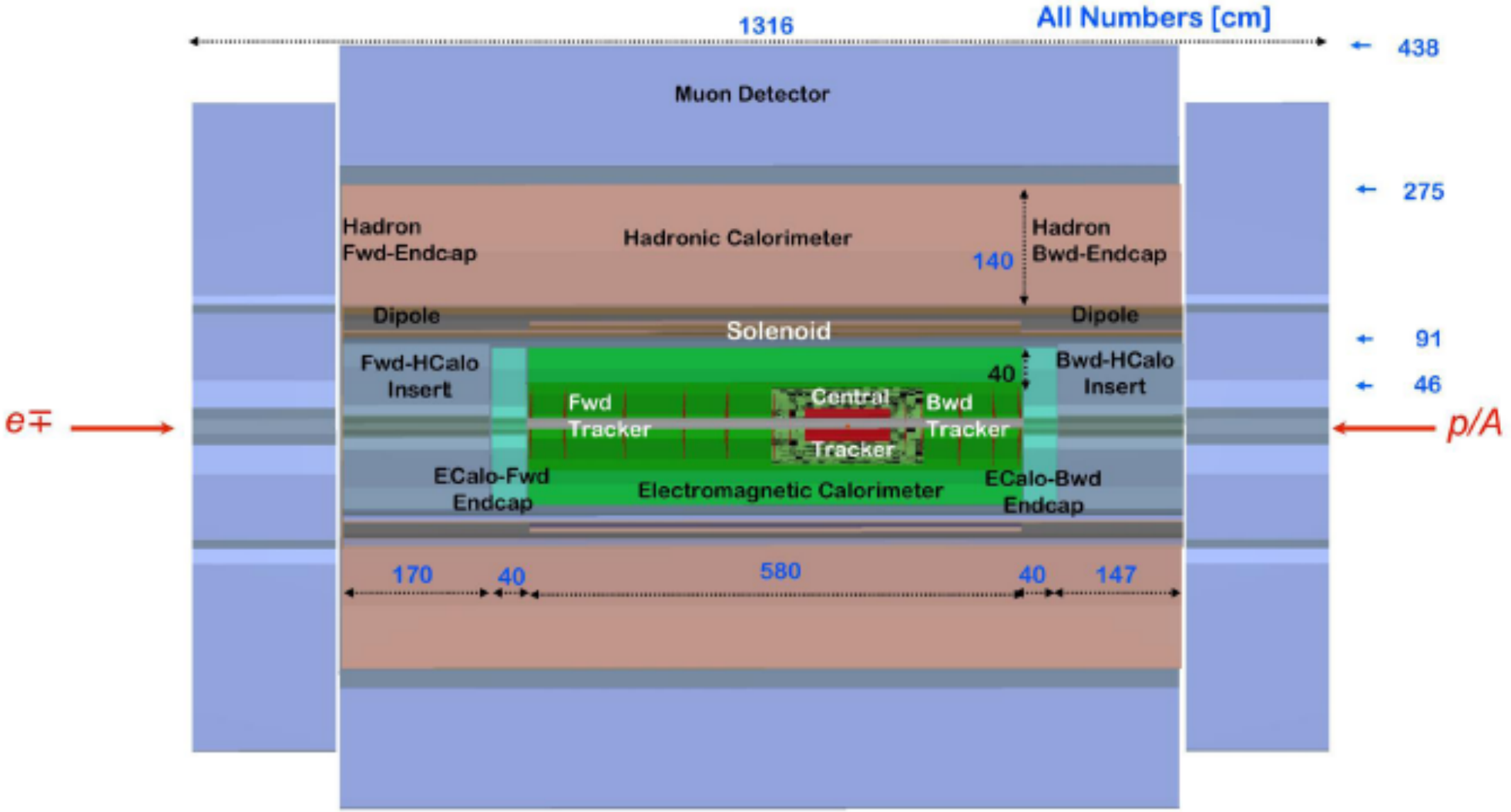
- To access highest W, acceptance in outgoing electron beam direction crucial





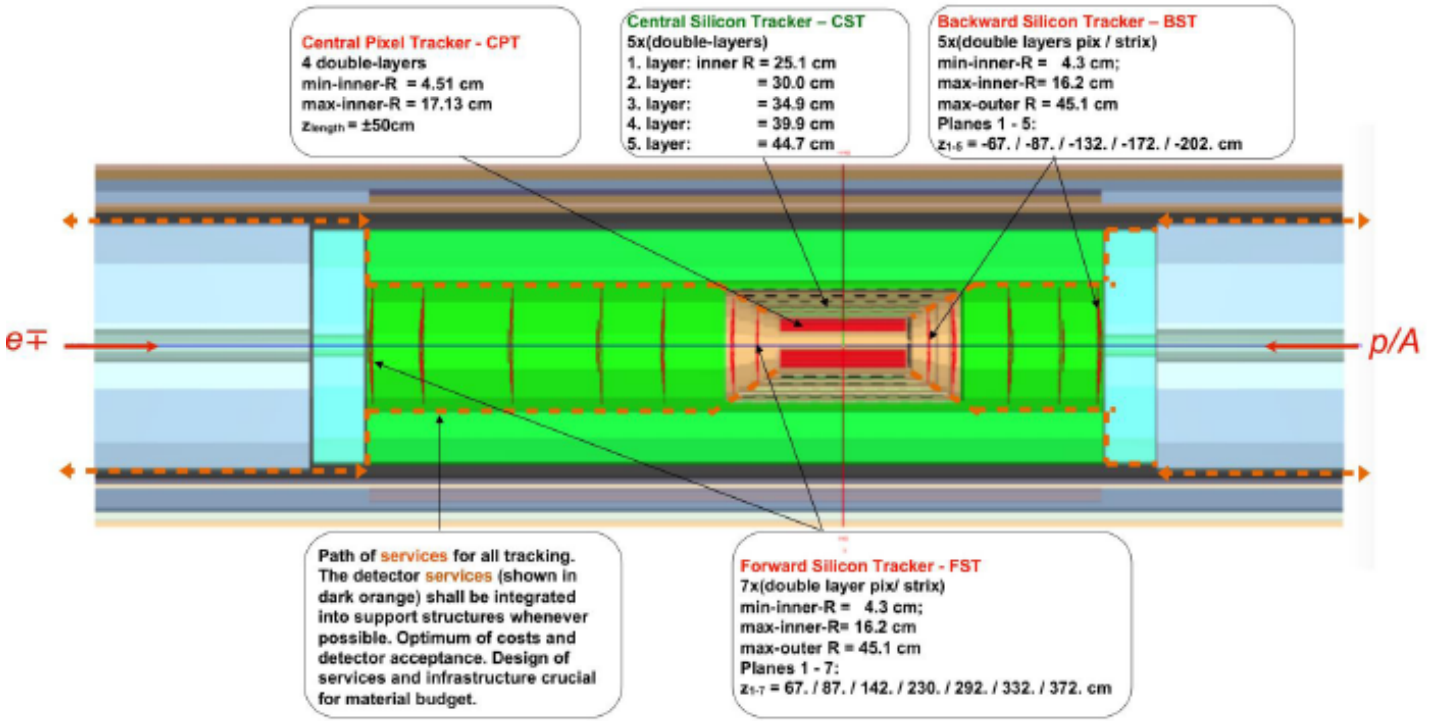


LHeC Detector Design Overview



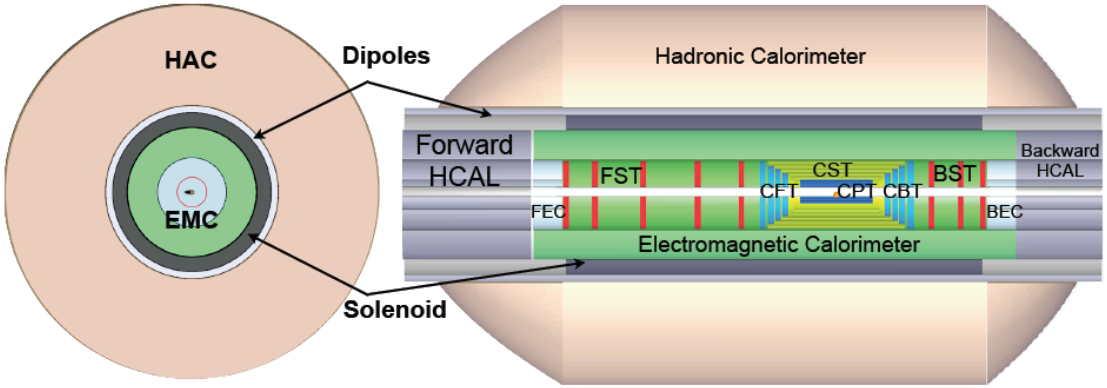
- Present size 13m x 9m (c.f. CMS 21m x 15m, ATLAS 45m x 25m)
- Forward / backward asymmetry reflecting beam energies
- Demanding tracking → high fraction of pixels, wide acceptance

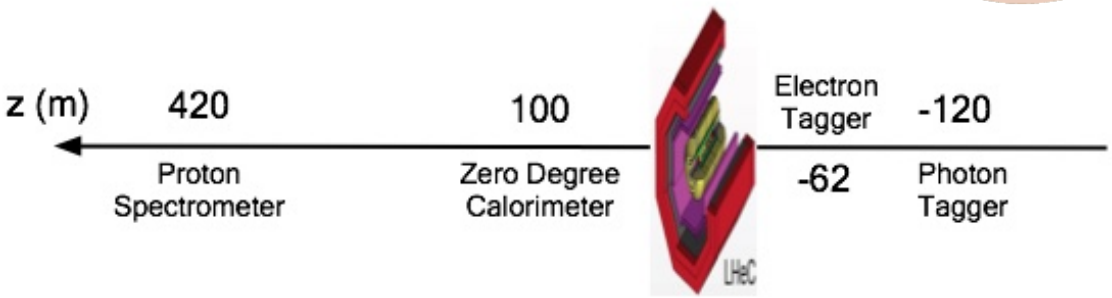
Detector Details



- Long tracking region (pixels + strips) → 1° electron hits 2 tracker planes

- Lar / Tile calorimeter leaning heavily on LHC experience

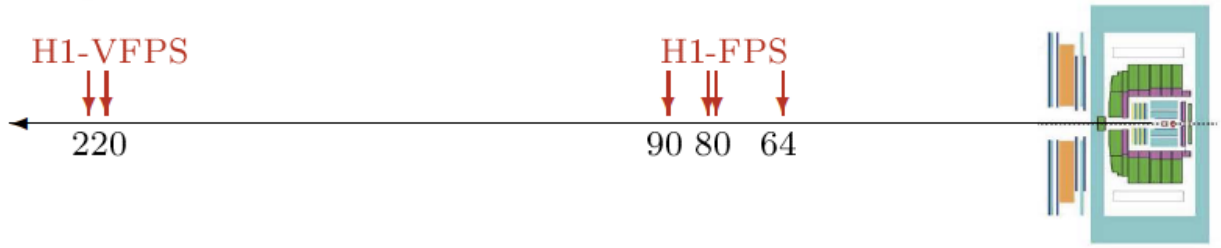




- Beamline insrumentation considered from outset.

Intact Proton Selection Methods beyond HERA

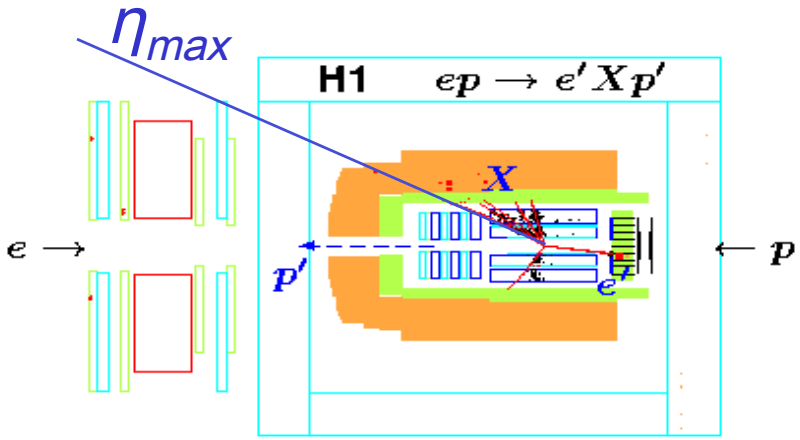
1) Measure scattered Proton in Roman Pots



- Allows t measurement, but limited by stats, p- tagging systs

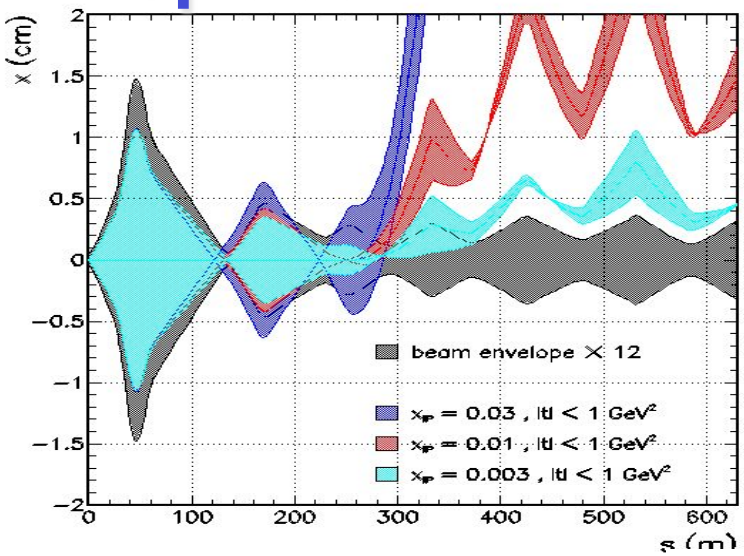
2) Select Large Rapidity Gaps

-Limited by control over proton dissociation contribution



- Methods have very different systematics → complementary
- In practice, method 2 yielded lasting HERA results, because of statistical and kinematic range limitations of Roman pots
- Roman pots mainly contsrained t distributions
- **LHeC & EIC different → higher lumi + pot design from outset**

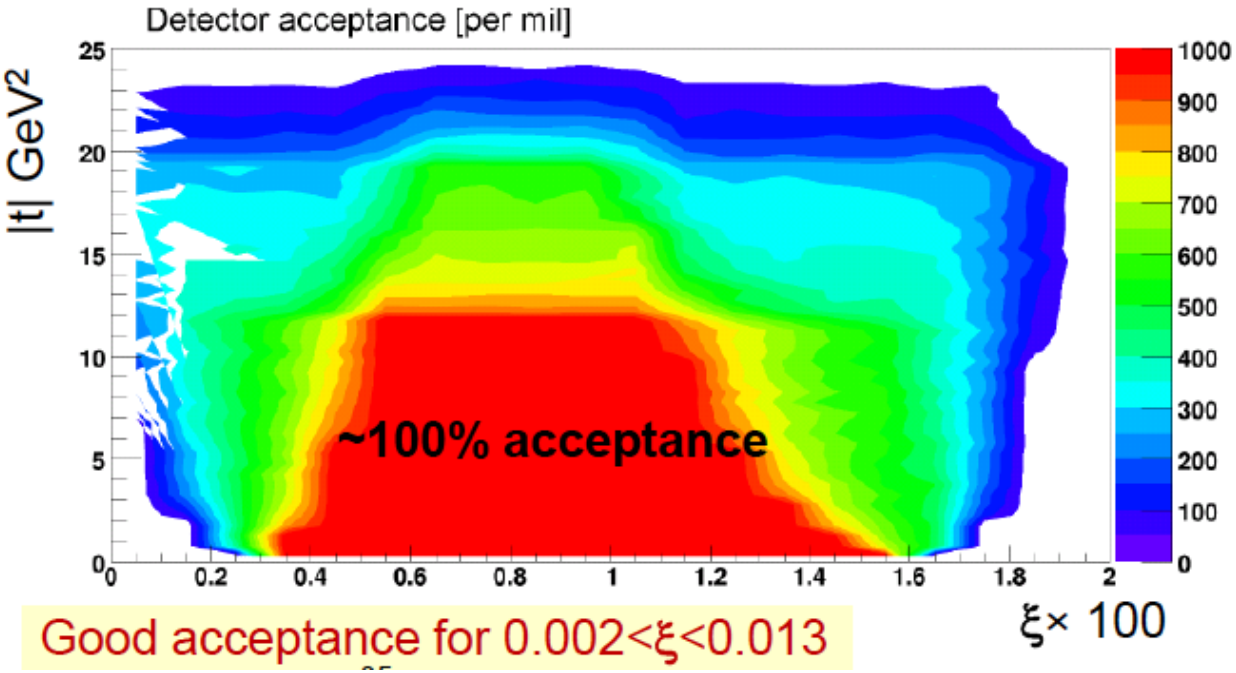
Forward Proton Spectrometer



- Proton spectrometer uses outcomes of FP420 project (proposal for low ξ Roman pots at ATLAS / CMS – not yet adopted)
-
- Approaching beam to 12σ (~250 μm) tags elastically scattered protons with high acceptance over a wide x_{IP}, t range

-These detectors came of age at LHC (TOTEM, AFP) …

- We should build full acceptance forward detector systems with them



(NEW) DGLAP PDF Fits to LHeC Pseudo-Data

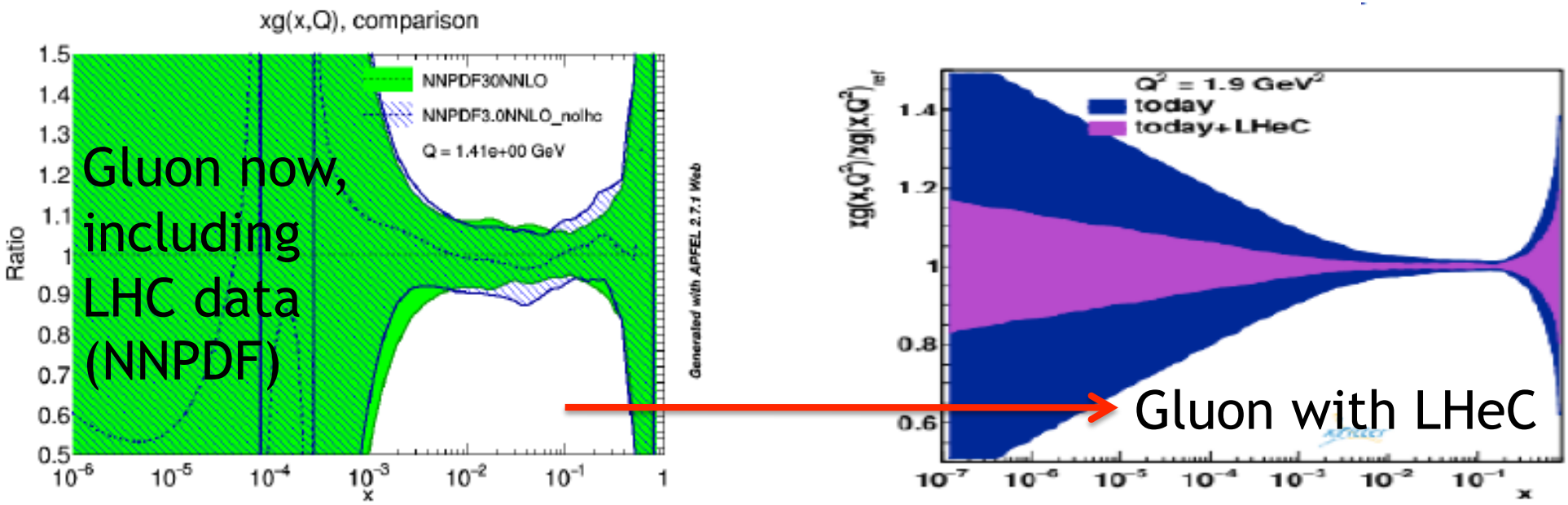
-Simulated NC, CC `pseudo-data' with reasonable assumptions on systematics (typically 2x better than H1 and ZEUS at HERA).

- NEW: Luminosity increased since CDR → up to $1ab^{-1}$
- NEW: Fitting framework → as for HERAPDF 2.0 at NLO

source of uncertainty	error on the source or cross section
scattered electron energy scale $\Delta E'_e/E'_e$	0.1 %
scattered electron polar angle	0.1 mrad
hadronic energy scale $\Delta E_h/E_h$	0.5 %
calorimeter noise (only $y < 0.01$)	1-3 %
radiative corrections	0.3%
photoproduction background (only $y > 0.5$)	1 %
global efficiency error	0.7 %

- NLO DGLAP fit using HERAPDF2.0, including:
  - LHeC NC and CC e^+p and e^-p cross sections
  - NEW: HERA-1 and HERA-2 final combined H1+ZEUS data
  - Fixed target BCDMS data with W>15 GeV
  - NEW: HERA jet and various Tevatron / LHC data

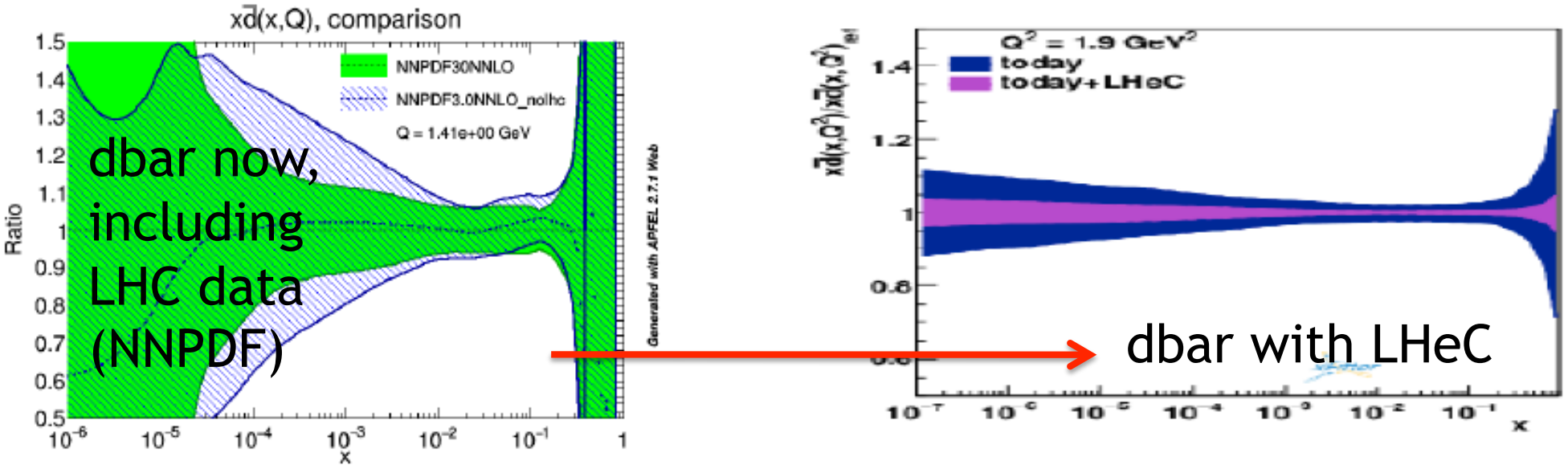
Low x Gluon with LHC, with and without LHeC



Standard LHC channels do not help much:

- ATLAS and CMS constraints as currently included in PDF fits (jets, top) don't extend below $x \sim 10^{-3}$.
- Other channels may help if theoretical issues can be overcome (LHCb c,b, maybe even exclusive J/Ψ)
- Current knowledge basically comes from HERA: stops at $x \sim 5.10^{-4}$
- LHeC gives constraints to $x \sim 10^{-6}$ from scaling violations and F_L

Low x Sea with LHC, with and without LHeC



LHC channels help, but not on same level as LHeC:

- ATLAS and CMS low mass Drell-Yan data have an impact
- Also potentially LHCb Drell-Yan
- Other channels may help (see eg ALICE direct photon / FOCAL)
- LHeC goes to x~10^{-6}, directly from F_2

… this is what DIS does best …

FCC-eh Data have also been included

NC/CC	E_e [GeV]	E_p [TeV]	P(e)	charge	lumi. [fb^{-1}]
NC	60 (60)	50 (7)	−0.8	−1	1000
CC	60 (60)	50 (7)	−0.8	−1	1000
NC	60 (60)	50 (7)	+0.8	−1	300
CC	60 (60)	50 (7)	+0.8	−1	300
NC	60 (60)	50 (7)	0	+1	100
CC	60 (60)	50 (7)	0	+1	100
NC	20 (60)	7 (1)	0	−1	100
CC	20 (60)	7 (1)	0	−1	100

e−, neg. pol.

e−, pos. pol.

e+, unpol.

low energy

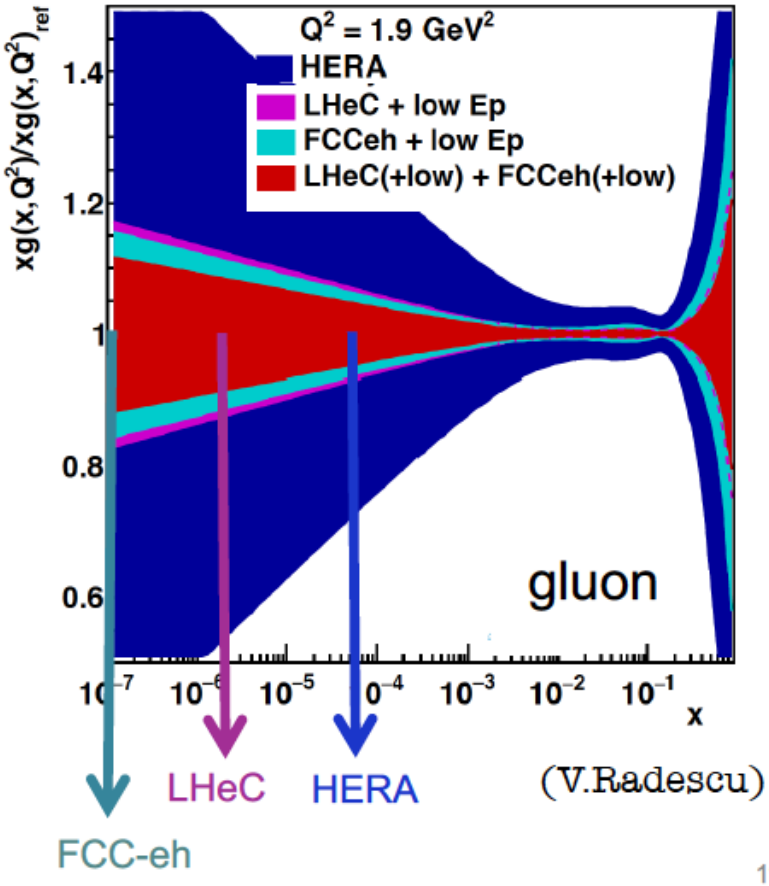
* second and third columns show FCC-eh (LHeC)

(M.Klein)

error assumptions:
elec. scale: 0.1%; hadr. scale 0.5%
radcor: 0.3%; γp at high y: 1%
uncorrelated extra eff. 0.5%

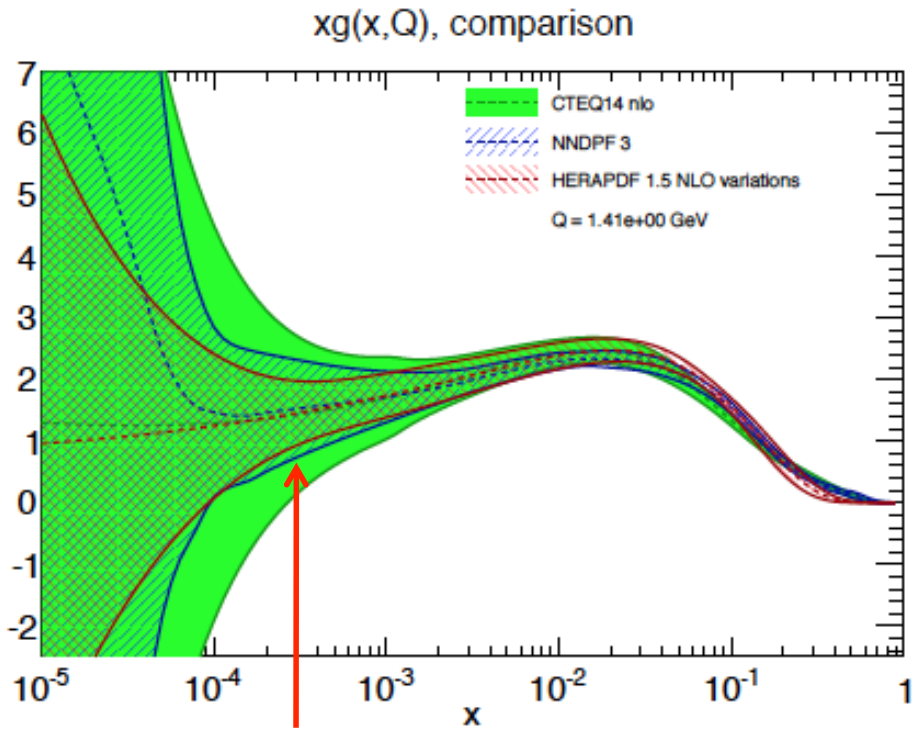
Some improvement in precision

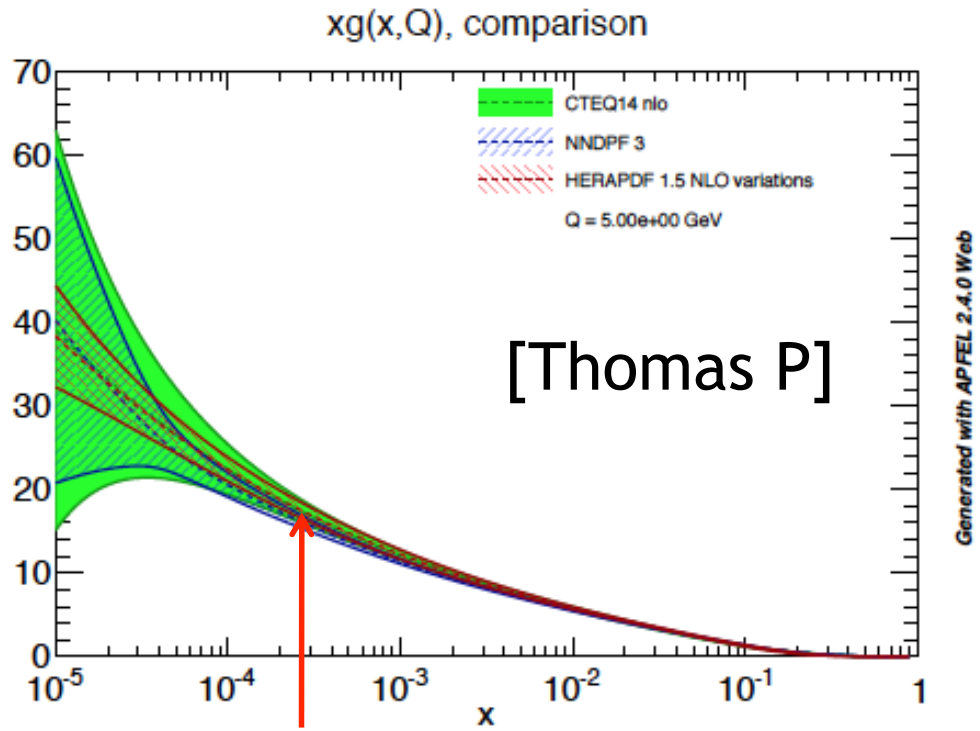
Main impact is direct coverage with data down to $x=10^{-7}$.



Why this is already dangerous at the LHC

- Use of PDFs based purely on DGLAP Q^2 evolution at low(ish) x, high Q^2 at the LHC will give incorrect results if there are saturation effects in the low x, low Q2 data …





[Thomas P]

Constrained by data

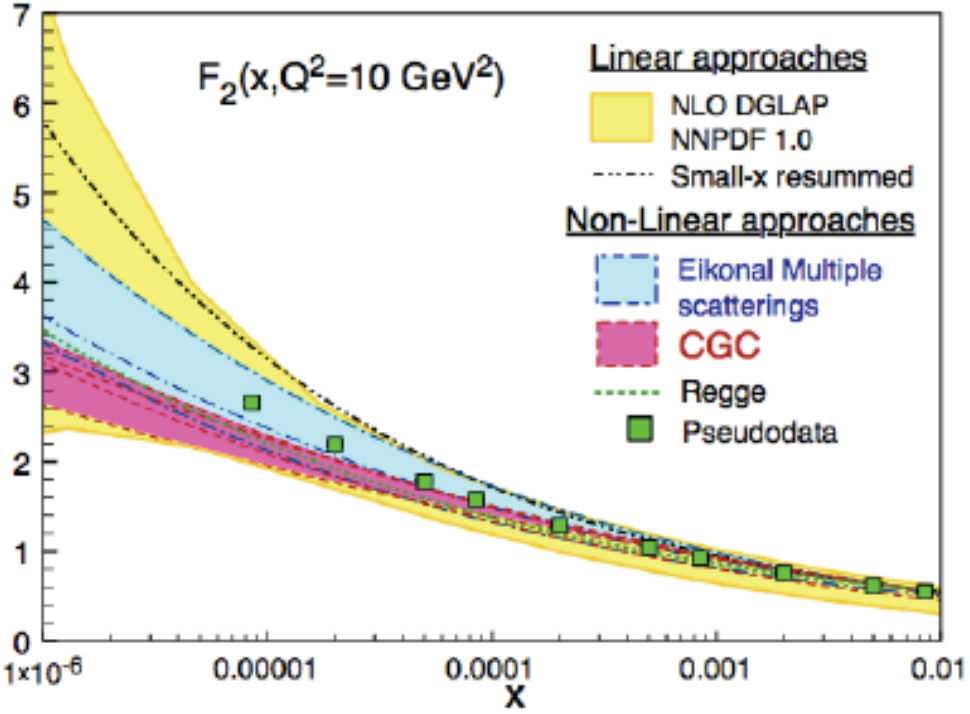
Unconstrained by data

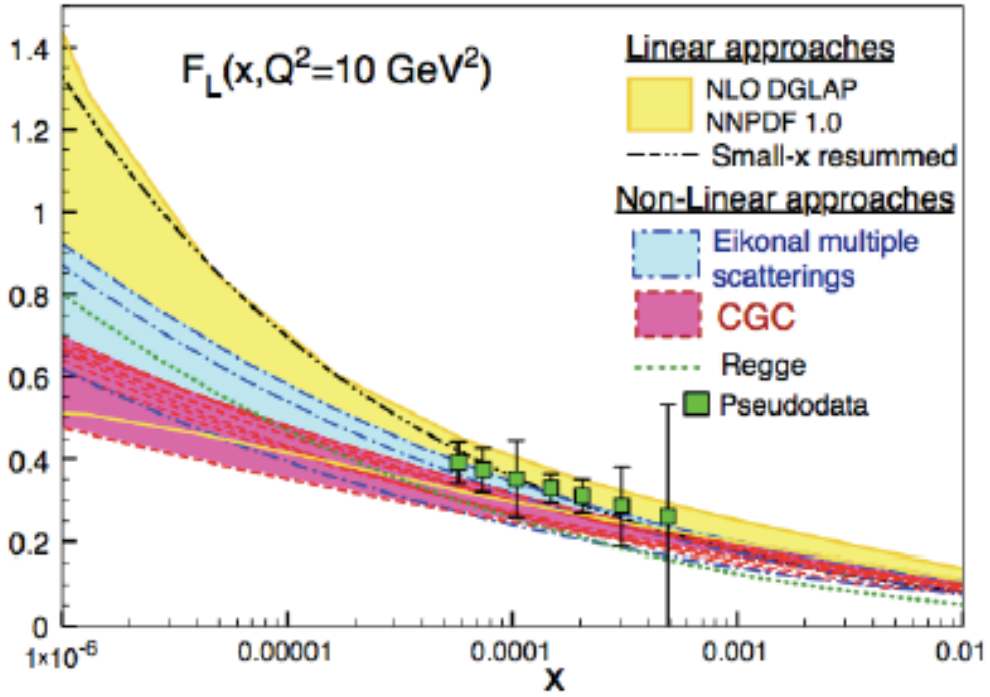
- Convergent solutions after DGLAP evolution can already be misleading at the LHC … worse at lower x → LHeC, FCC-eh …

LHeC Sensitivity to Different Saturation Models

With 1 fb^{-1} (1 month at 10^{33} cm^{-2} s^{-1}), F_2 stat. < 0.1%, syst, 1-3%
F_L measurement to 8% with 1 year of varying E_e or E_p

F_2 and F_L pseudodata at Q^2 = 10 GeV^2



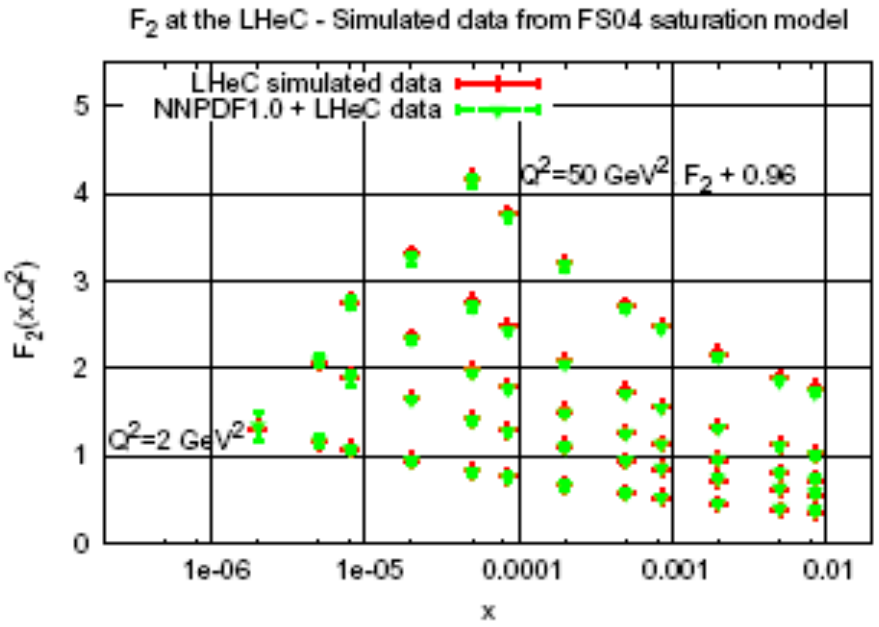


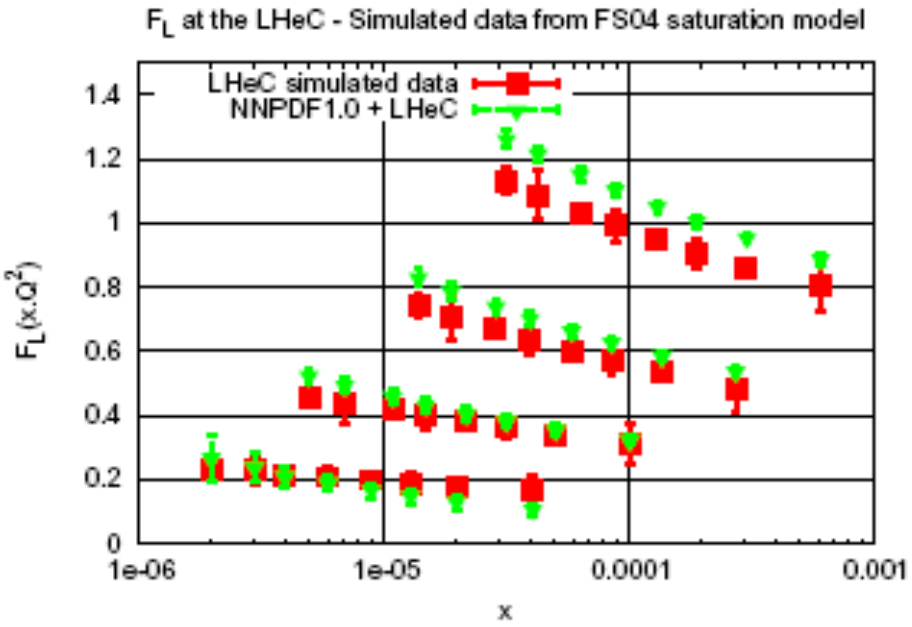
• LHeC can distinguish between different QCD-based models for the onset of non-linear dynamics

… but can sat^n effects hide in standard fit parameterisations?

Can Parton Saturation be Established in ep @ LHeC?

Simulated LHeC F_2 and F_L data based on an (old) dipole model containing low x saturation (FS04-sat)… Try to fit in NLO DGLAP … NNPDF (also HERA framework) DGLAP QCD fits work OK if only F_2 is fitted, but cannot accommodate saturation effects if F_2 and F_L both fitted

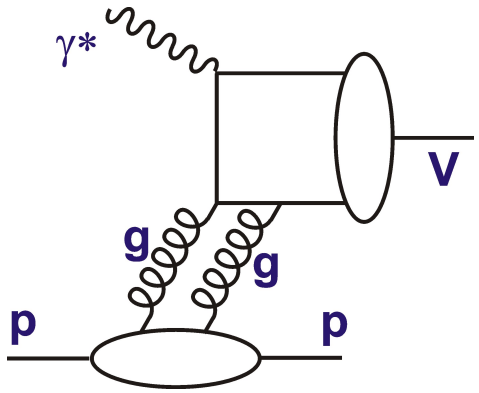




• Unambiguous observation of saturation will be based on tension between different observables e.g. F_2 v F_L in ep or F_2 in ep v eA

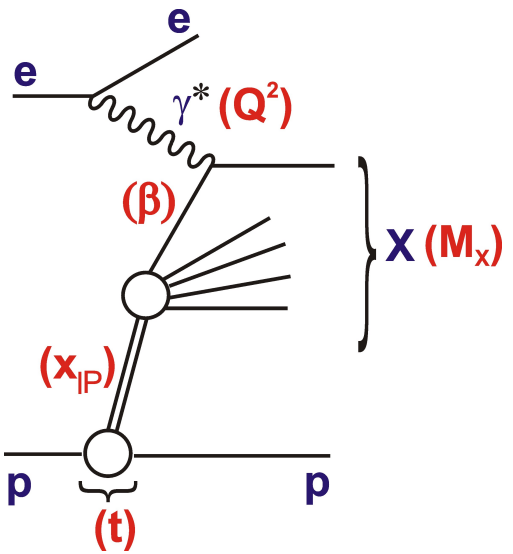
Exclusive / Diffractive Channels and Saturation

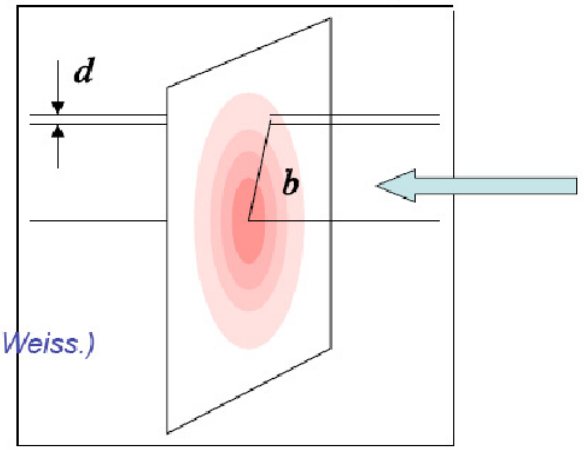
1) [Low-Nussinov] interpretation as 2 gluon exchange enhances sensitivity to low x gluon



2) Additional variable t gives access to impact parameter (b) dependent amplitudes

→ Large t (small b) probes densest packed part of proton?

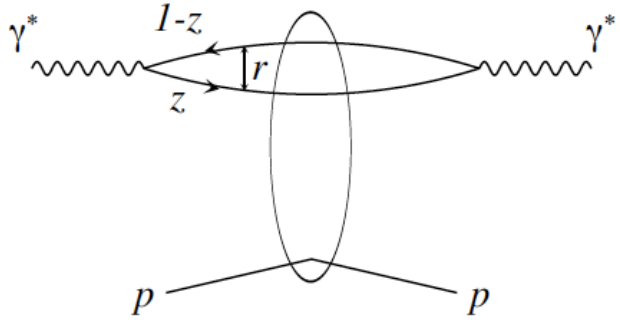




(figure from C. Weiss.)

Central black region growing with decrease of x.

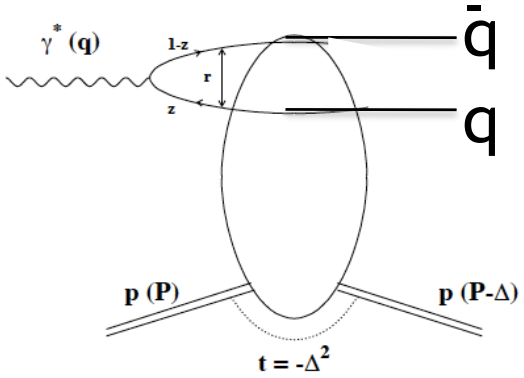
Advantage of Diffractive DIS: Dipole Language



Inclusive Cross Section

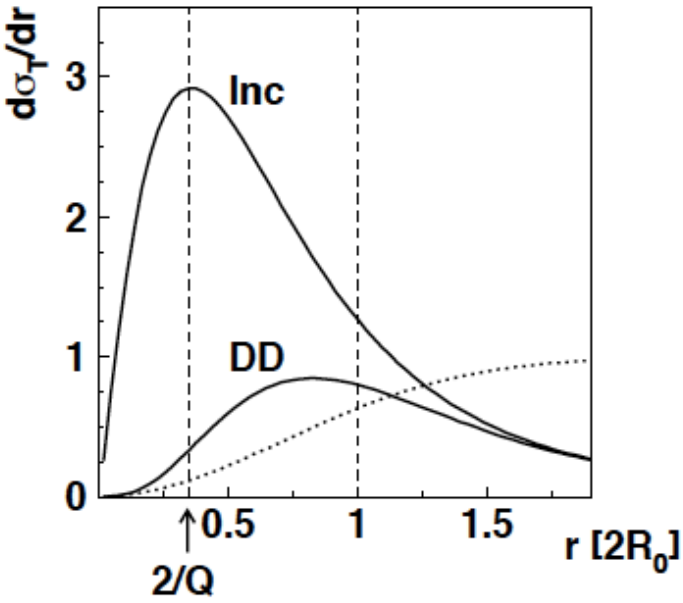
$$\sigma_{T,L}(x,Q^2) = \int d^2\mathbf{r} \int_0^1 d\alpha \, |\Psi_{T,L}(\alpha,\mathbf{r})|^2 \, \hat{\sigma}(x,r^2)$$

Diffractive DIS



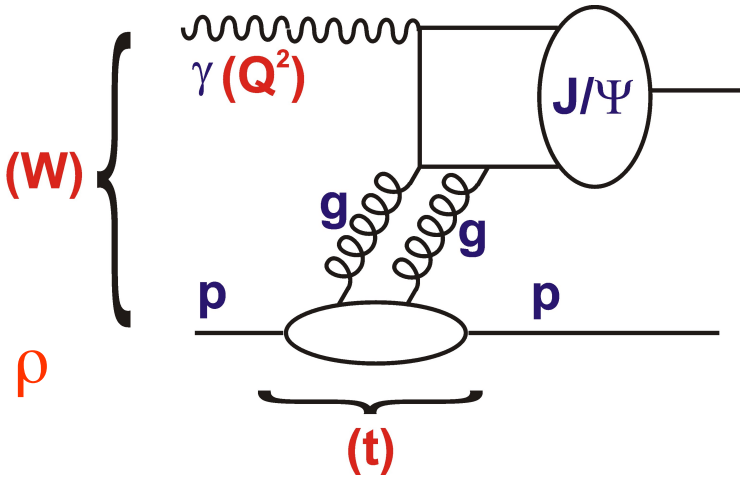
$$\left.\frac{d\sigma^D_{T,L}}{dt}\right|_{t=0} = \frac{1}{16\pi} \int d^2\mathbf{r} \int_0^1 d\alpha \, |\Psi_{T,L}(\alpha,\mathbf{r})|^2 \, \hat{\sigma}^2(x,r^2)$$

3) Extra factor of dipole cross section weights DDIS cross section towards larger dipole sizes → enhanced sensitivity to saturation effects.



Test Case: Elastic J/Ψ Photoproduction

• `Cleanly' interpreted as hard 2g exchange coupling to qqbar dipole



• c and c-bar share energy equally, simplifying VM wavefunction relative to ρ

• Clean experimental signature (just 2 leptons)

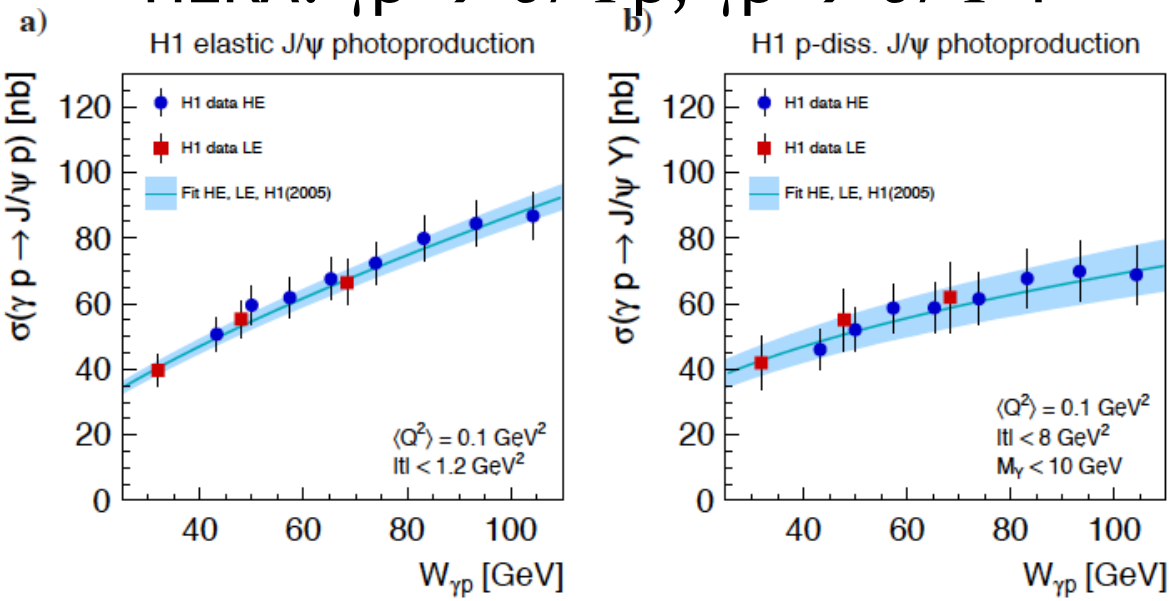
• Scale $\overline{Q^2} \sim (Q^2 + M_V^2) / 4 >\sim 3\ GeV^2$ ideally suited to reaching Lowest possible x whilst remaining in perturbative regime

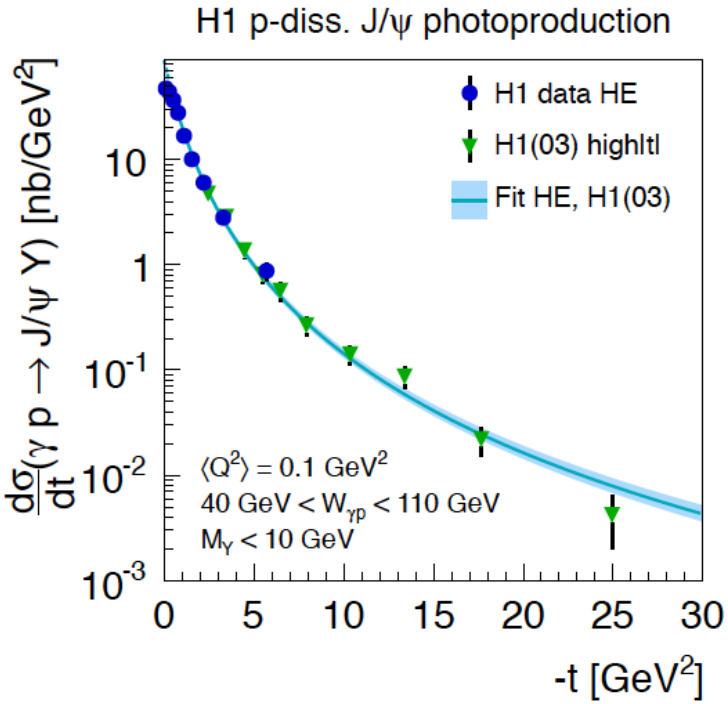
… eg LHeC reach extends to: $x_g \sim (Q^2 + M_V^2) / (Q^2 + W^2) \sim 5.10^{-6}$

• Simulations (DIFFVM) of elastic J/Ψ → μμ photoproduction
→ scattered electron untagged, 1° acceptance for muons
(similar method to H1 and ZEUS)

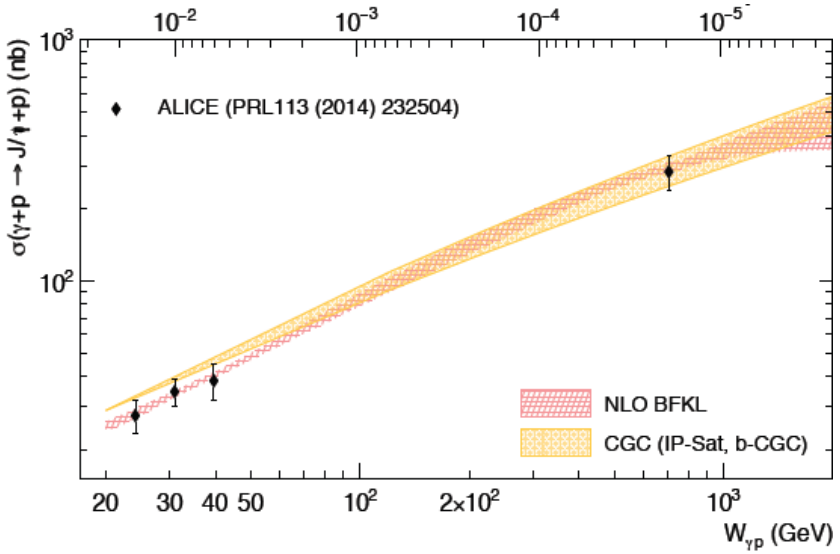
Existing Diffractive J/Ψ Photoproduction Data

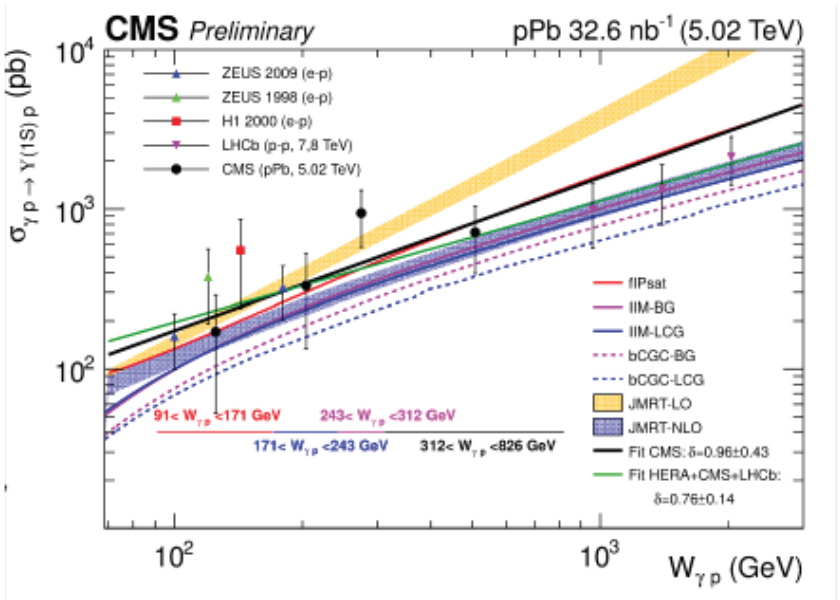
HERA: γp → J/Ψp, γp → J/Ψ Y





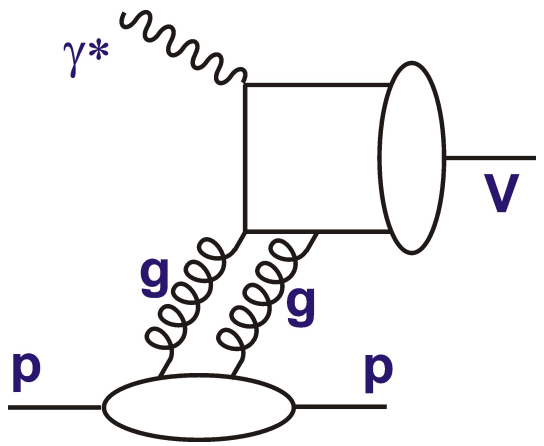
UPC at LHC: γp → J/Ψp

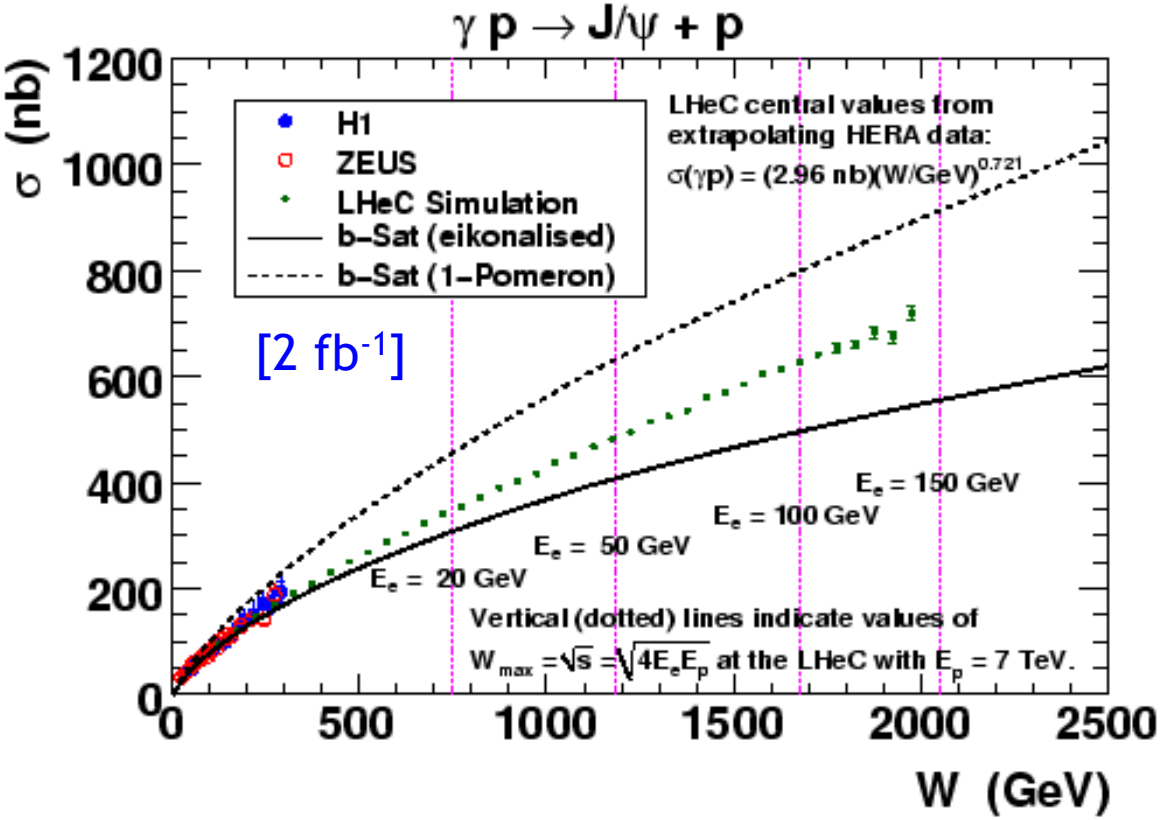




Comparison with Dipole model Predictions

e.g. “b-Sat” Dipole model
- “eikonalised”: with impact-parameter dependent saturation
- “1 Pomeron”: non-saturating

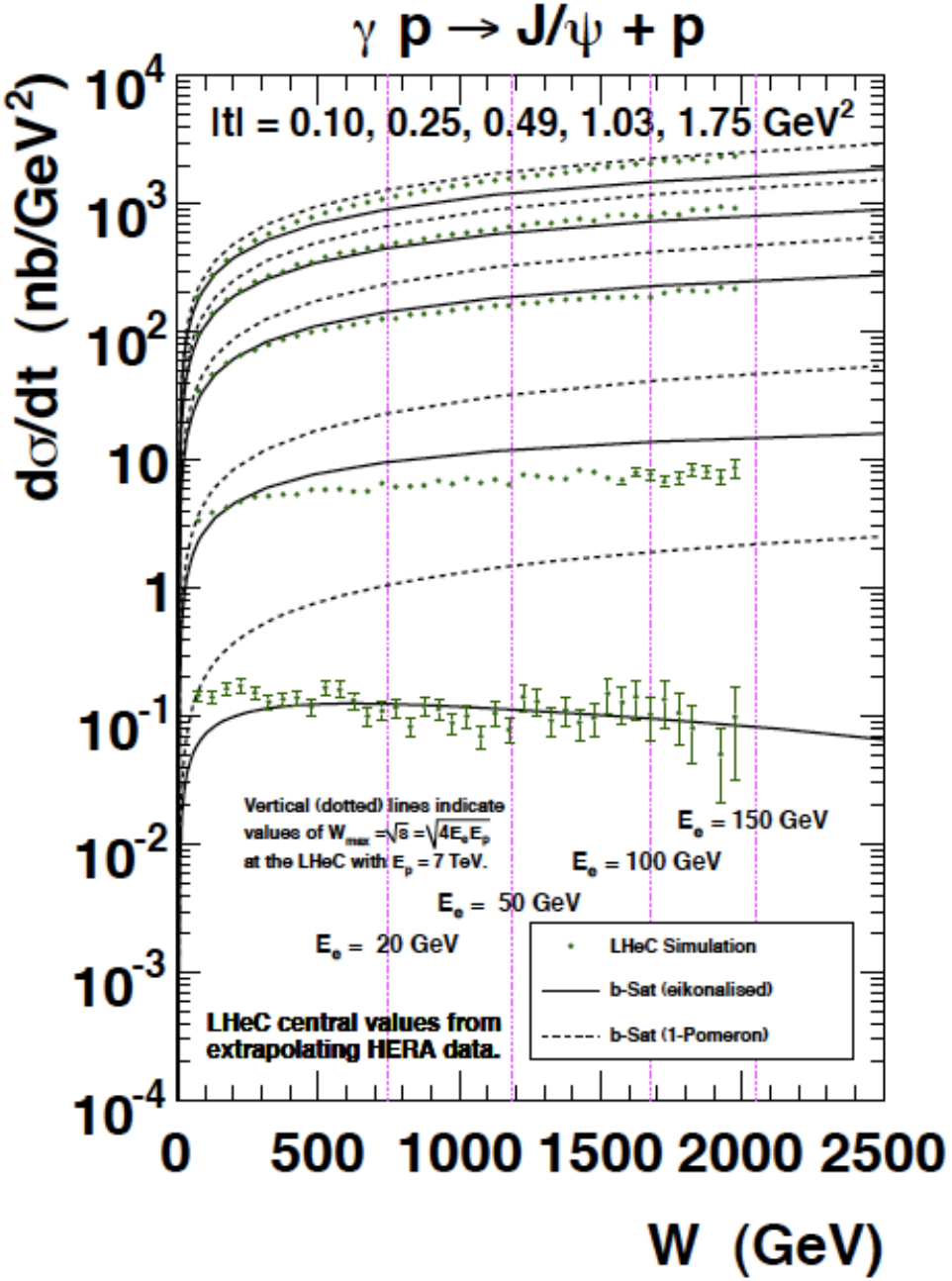




- Significant non-linear effects expected in LHeC kinematic range.

With detailed exploration of ep and eA, including t dependences, this becomes a powerful probe!...

t Dependence of Elastic J/ψ Photoproduction



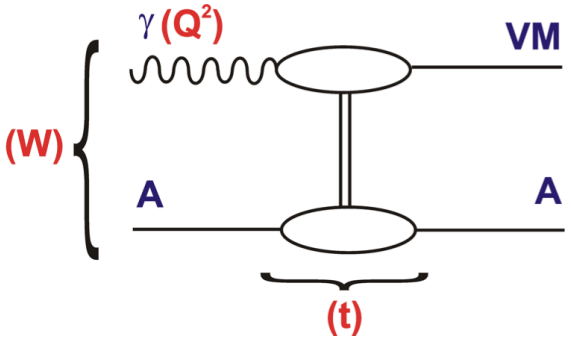
- Precise t measurement from decay μ tracks over wide W range extends to $|t| \sim 2$ GeV^2 and enhances sensitivity to saturation effects

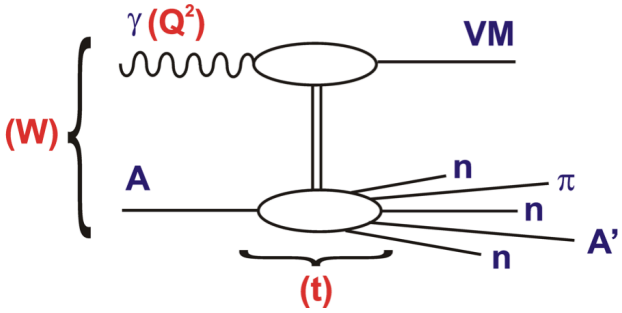
- Measurements also possible in multiple Q^2 bins

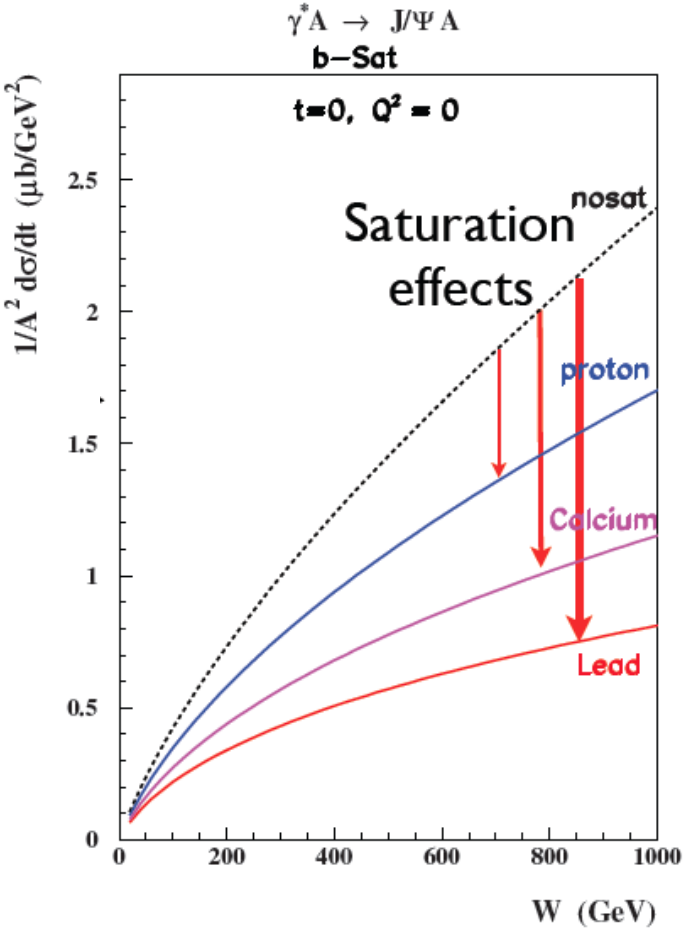
- Level of precision from ep and eA unlikely to be matched in UPC
- Incoherent ep diffraction still needs to be studied

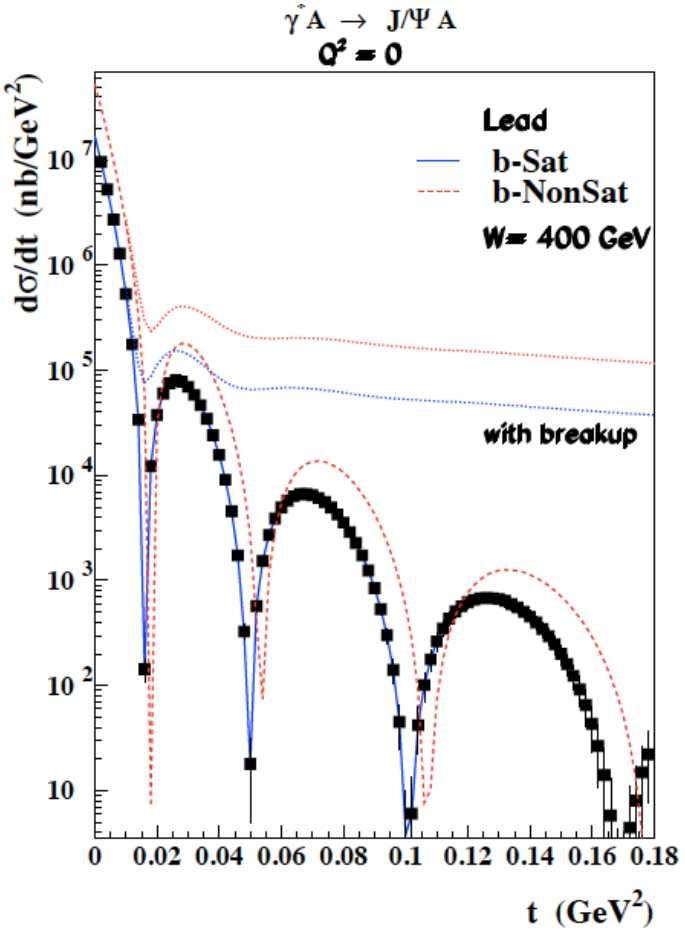
Exclusive Diffraction in eA

Experimentally clear signatures and theoretically cleanly calculable saturation effects in coherent diffraction case (eA → eVA)



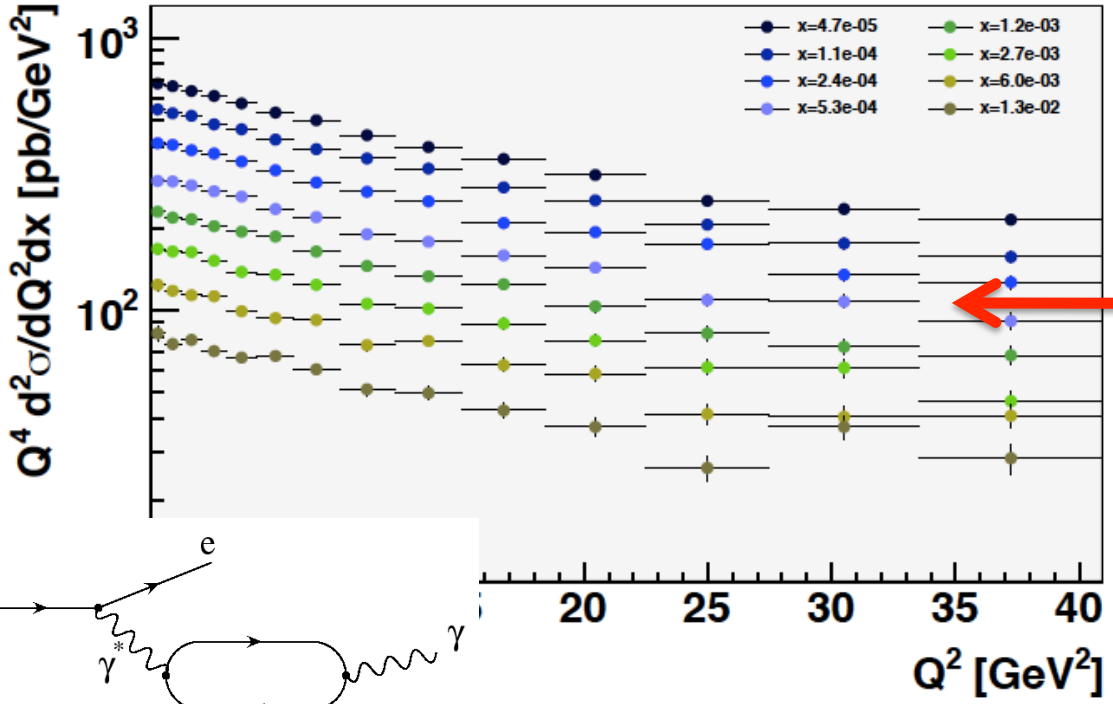




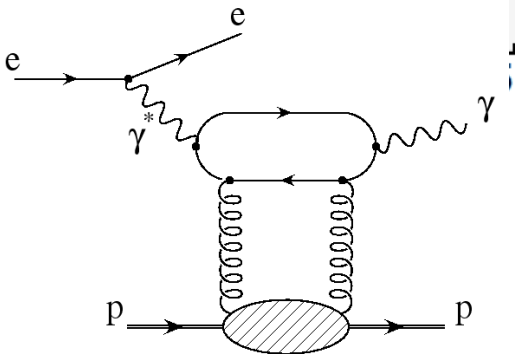


Experimental separation of incoherent diffraction based mainly on ZDC

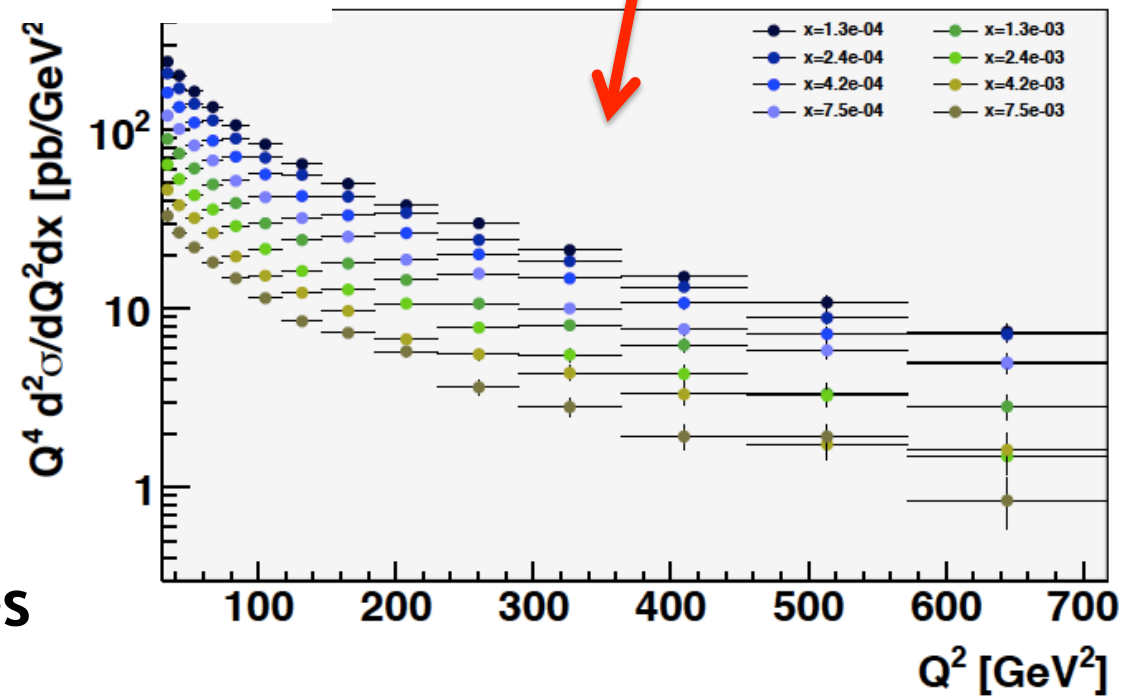
DVCS (MILOU simulation)



1 fb^{-1}, E_e = 50 GeV,
1° acc'nce, p_T^γ > 2 GeV



100 fb^{-1}, E_e = 50 GeV,
10° acc'nce, p_T^γ > 5 GeV

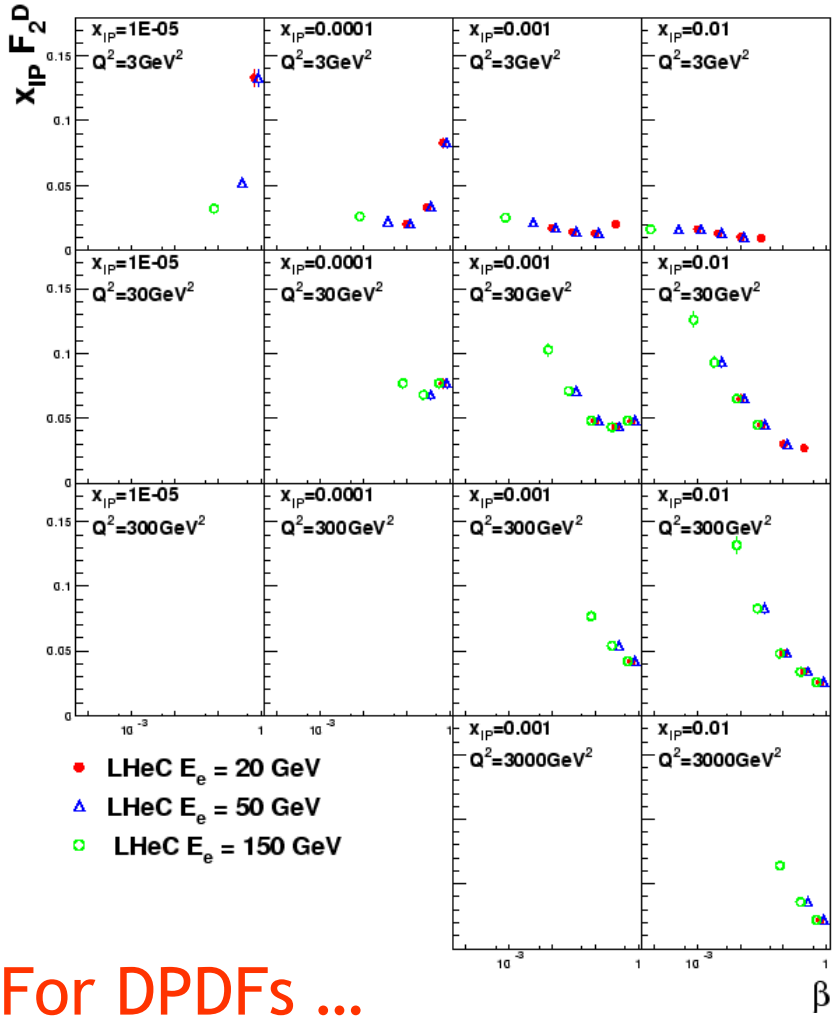


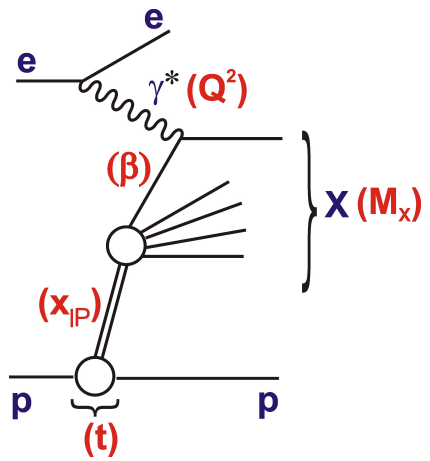
Precise data with
$W \rightarrow 1$ TeV, $Q^2 \rightarrow 700$ GeV^2,
$x \rightarrow 5.10^{-5}$

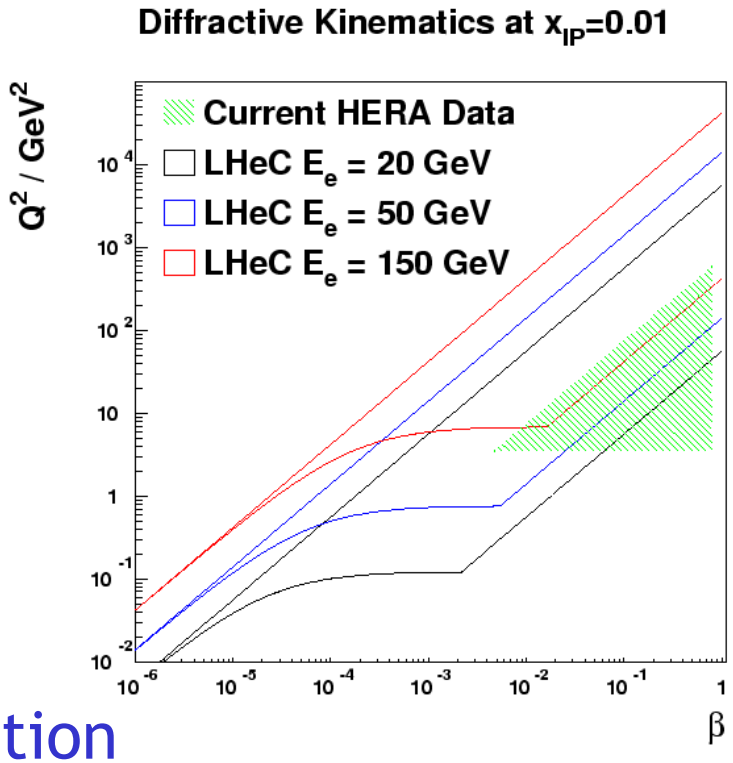
Still to do:

- **Beam charge asymmrtries**
- **Sensitivity to GPDs**

Inclusive Diffraction / Diffractive PDFs at LHeC







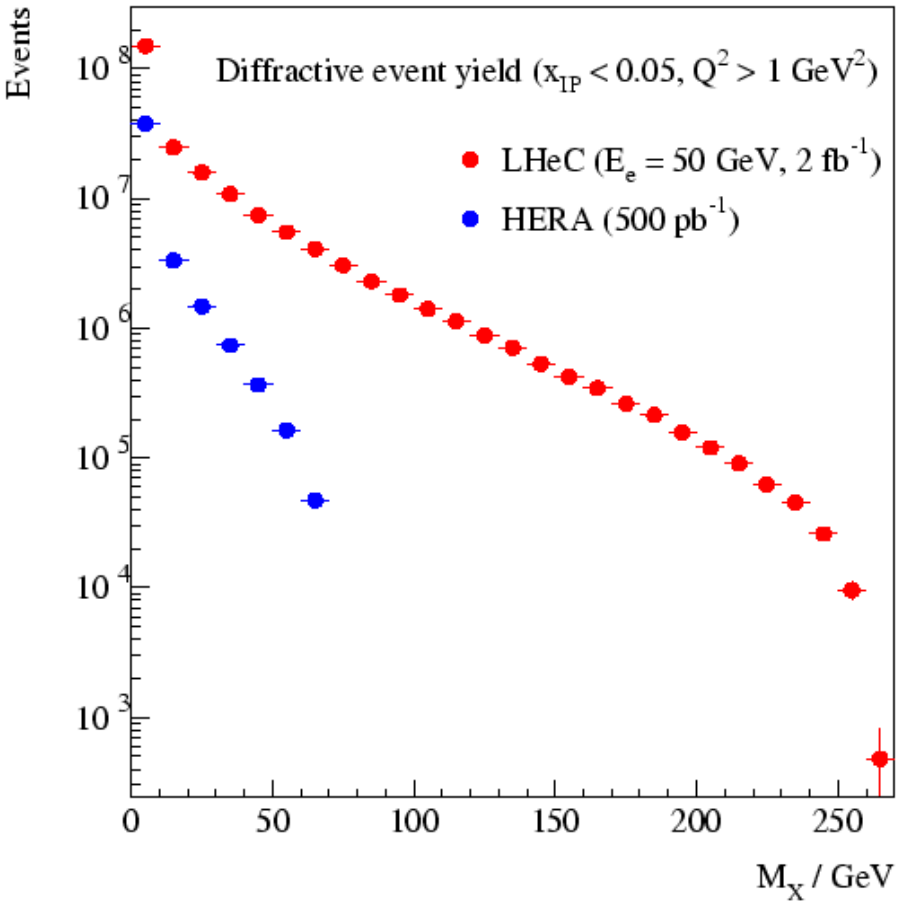
For DPDFs …

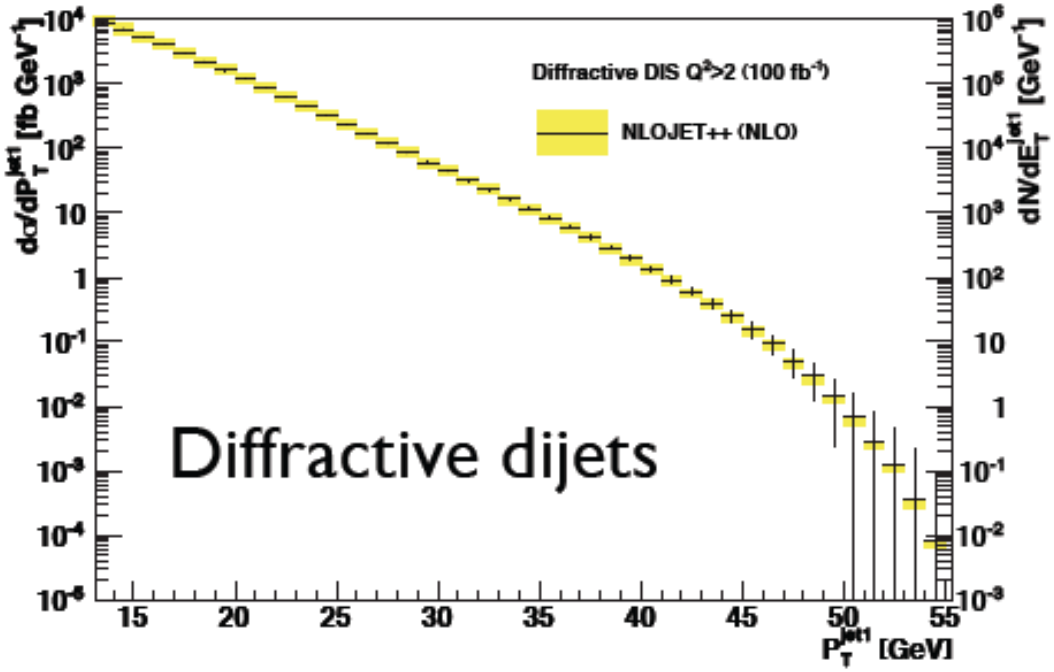
- Low x_{IP} → cleanly separate diffraction
- Low β → Novel low x DPDF effects /non-linear dynamics?
- High Q^2 → Lever-arm for gluon, Flavour separation via EW

Still to do: detailed DPDF sensitivity study

New Region of Large Diffractive Masses

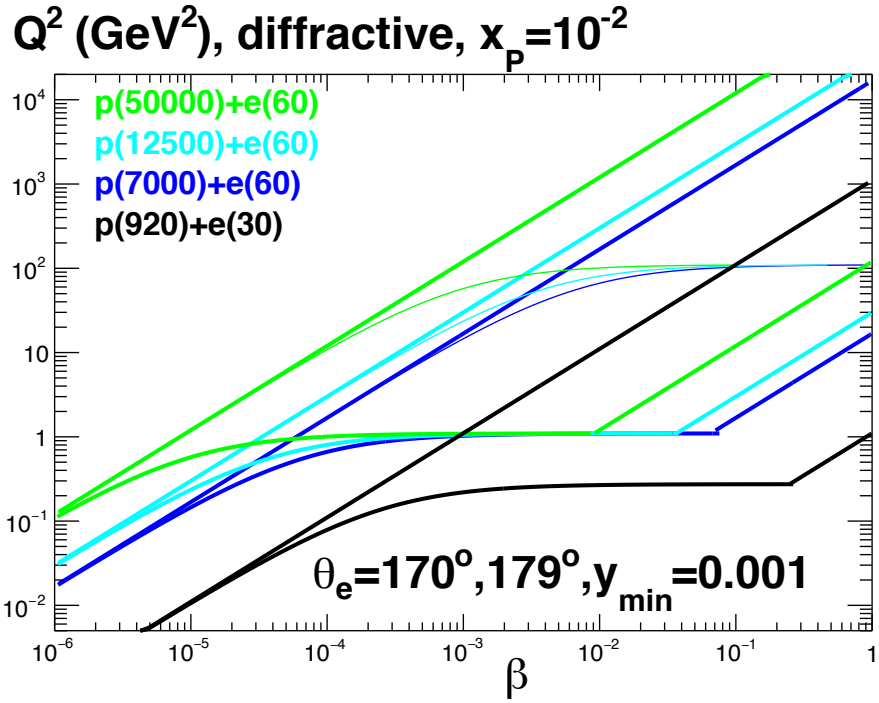
Large x_{IP} region highly correlated with large Mx





- `Proper' QCD (e.g. large E_T) with jets and charm accessible
- New diffractive channels … beauty, W / Z bosons
- Unfold quantum numbers / precisely measure new 1^- states

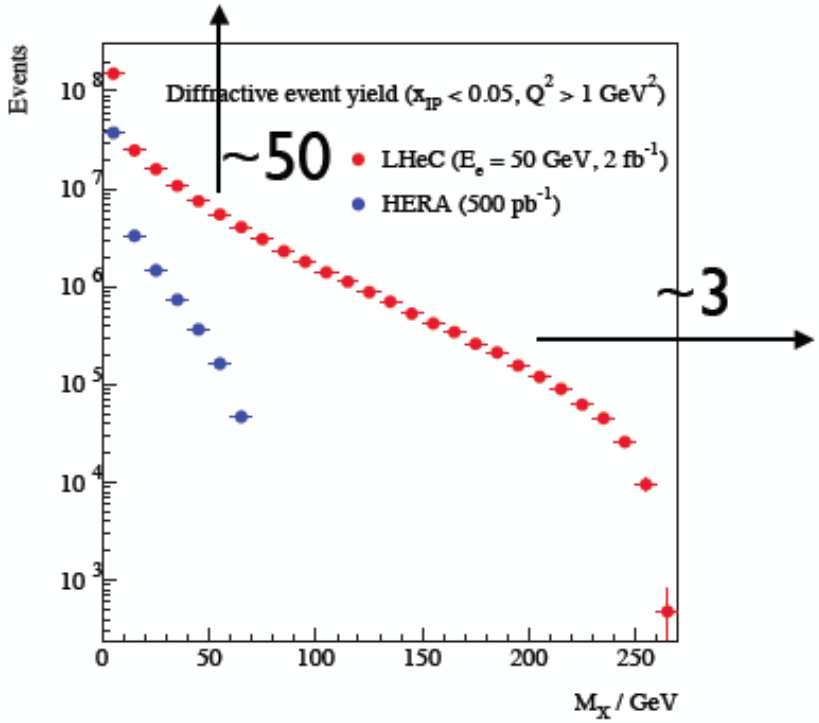
The More Distant Future: ep at a CERN Future Circular Collider



FCC-eh kinematics sensitive to diffractive structure in larger (β,Q^2) range than (x,Q^2) range sampled for the proton @ HERA!

-Similarly for masses and transverse momenta of jets.

- W range for VMs → multi-TeV

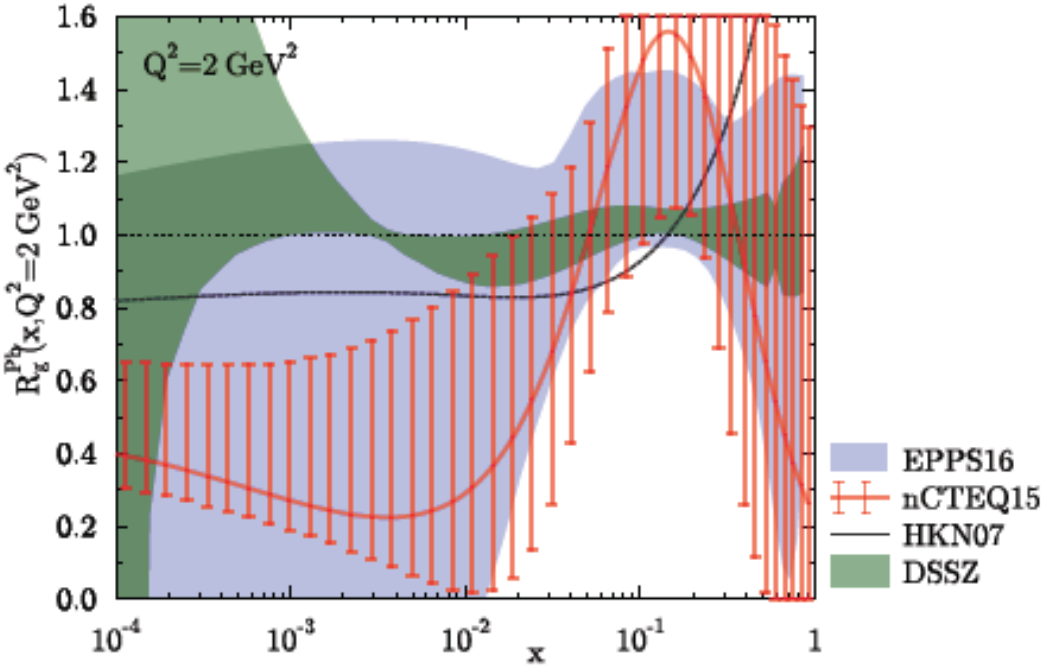


Current Status of Nuclear Parton Densities

- Significant uncertainties in the nuclear PDFs (nPDFs)

$$R_g^A(x, Q^2) = f_g^{\mathrm{p},A}(x, Q^2)/f_g^{\mathrm{p}}(x, Q^2),$$

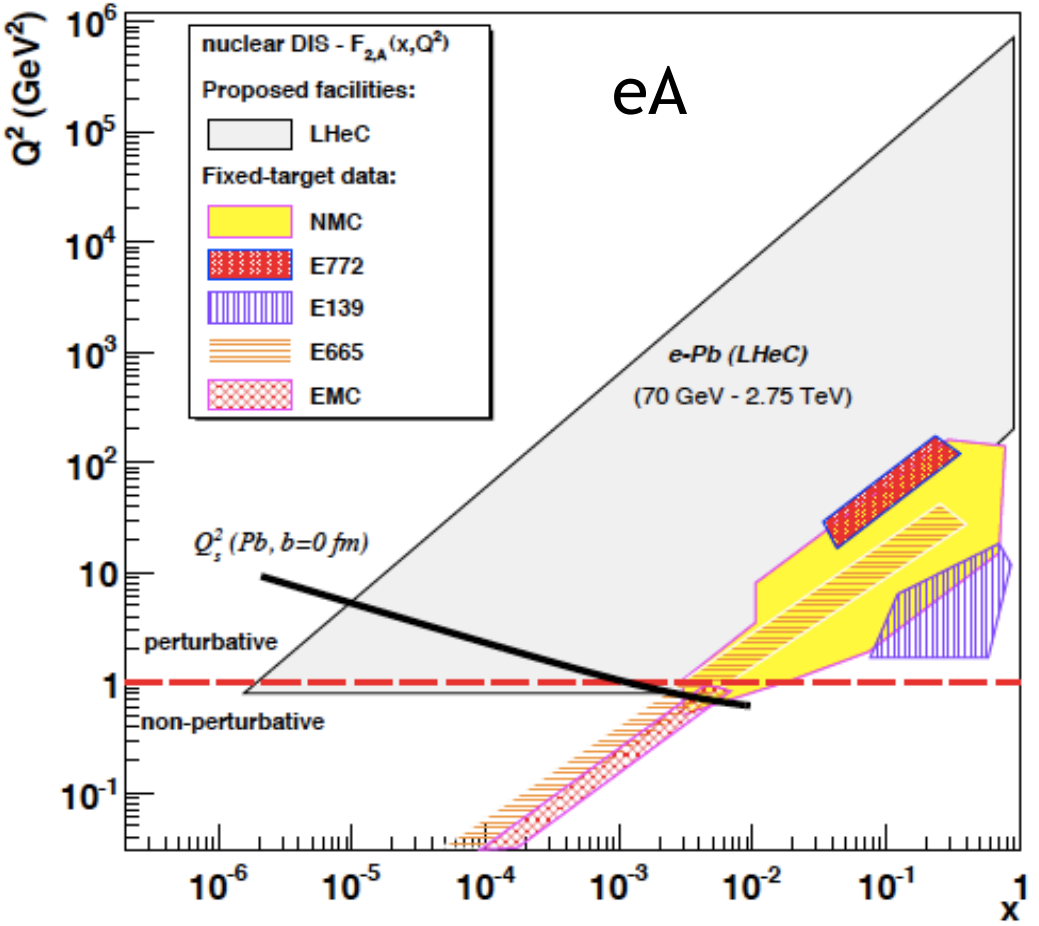
[Slide from Hannu Paukkunen]

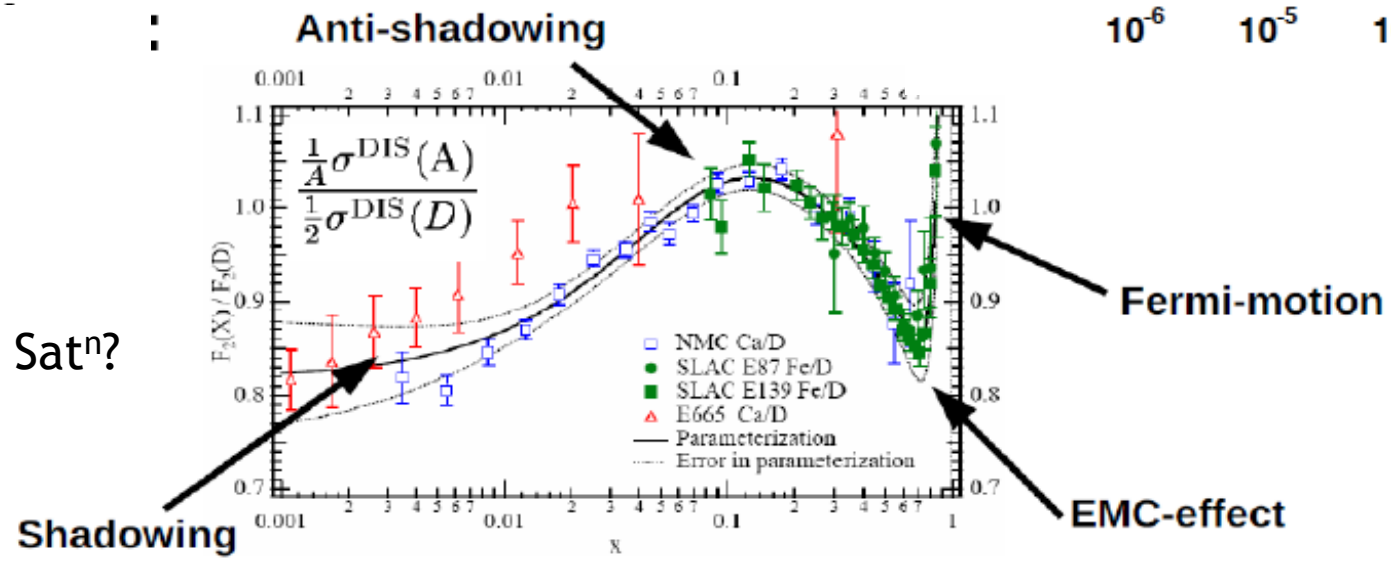


- Especially the small-x (here, $x \lesssim 10^{-2}$) behaviour of nPDFs at smallish Q^2 are largely unknown — may become a bottleneck e.g. in
  - distinguishing effects of non-linear evolution
  - precision studies of phenomena in heavy-ion collisions
  - calculations of cosmic-ray interactions in the air

EPPS Input Data

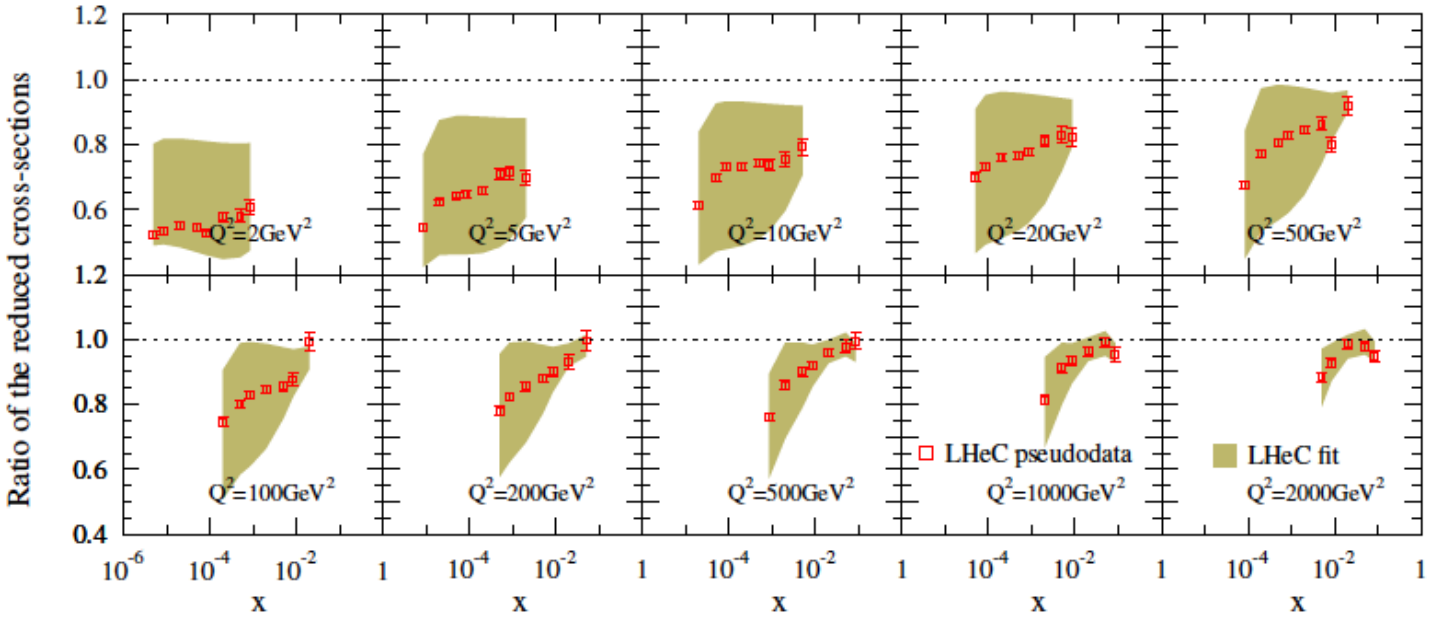
- Exciting phenomenology not matched by DIS data
- EPPS16 also uses various Drell-Yan, semi-inclusive π^0 in PHENIX dAu, W,Z, dijets in ATLAS and CMS
- Direct γ, B, D mesons at LHC promising if theoretical understanding sufficient





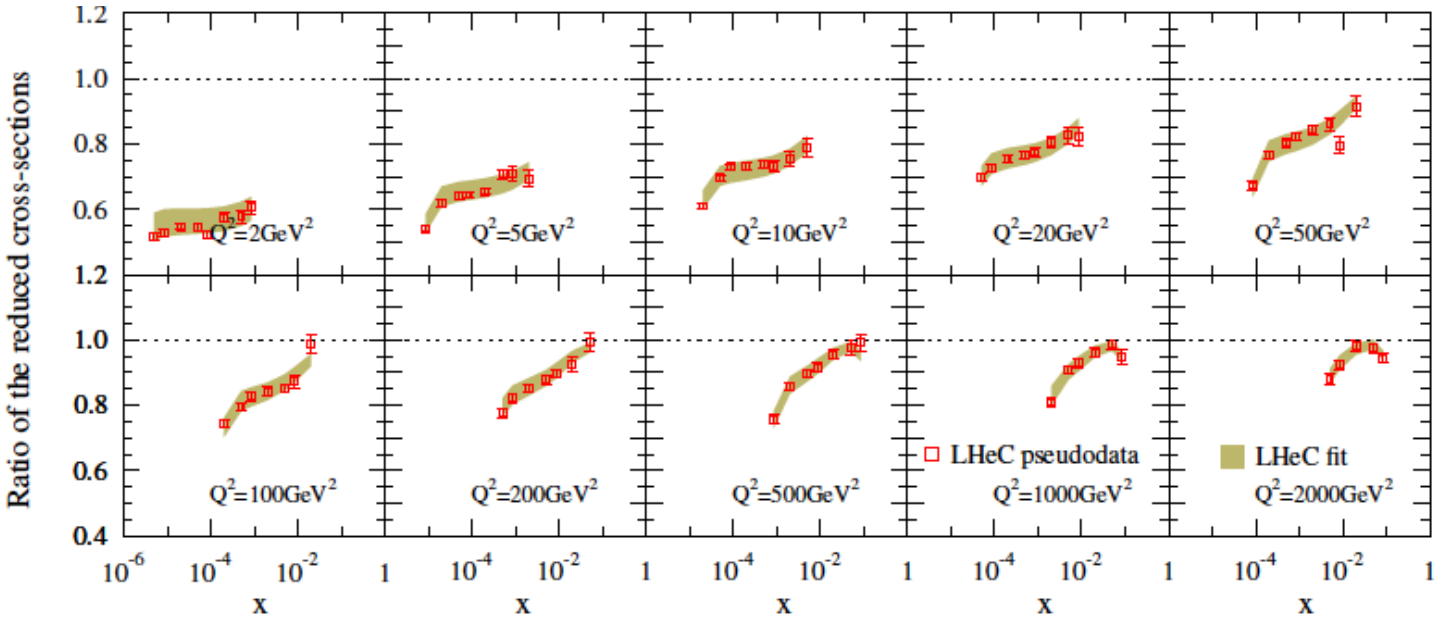
LHeC: Four orders of magnitude Increase in kinematic range over previous DIS experiments.

Influence of 1fb^{-1} A^{-1} LHeC ePb data on EPPS16

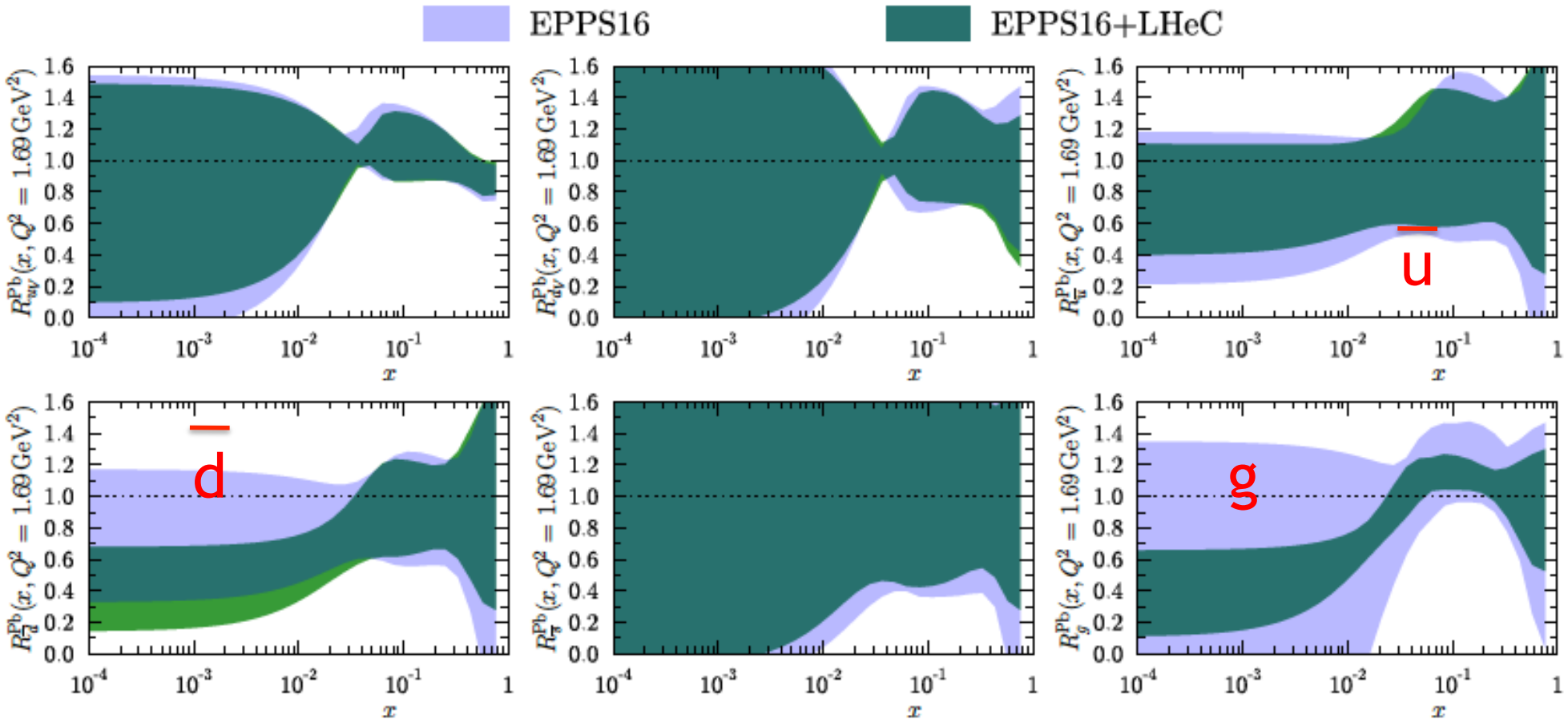


LHeC NC pseudodata before inclusion in EPPS16

EPPS16 after including LHeC pseudodata

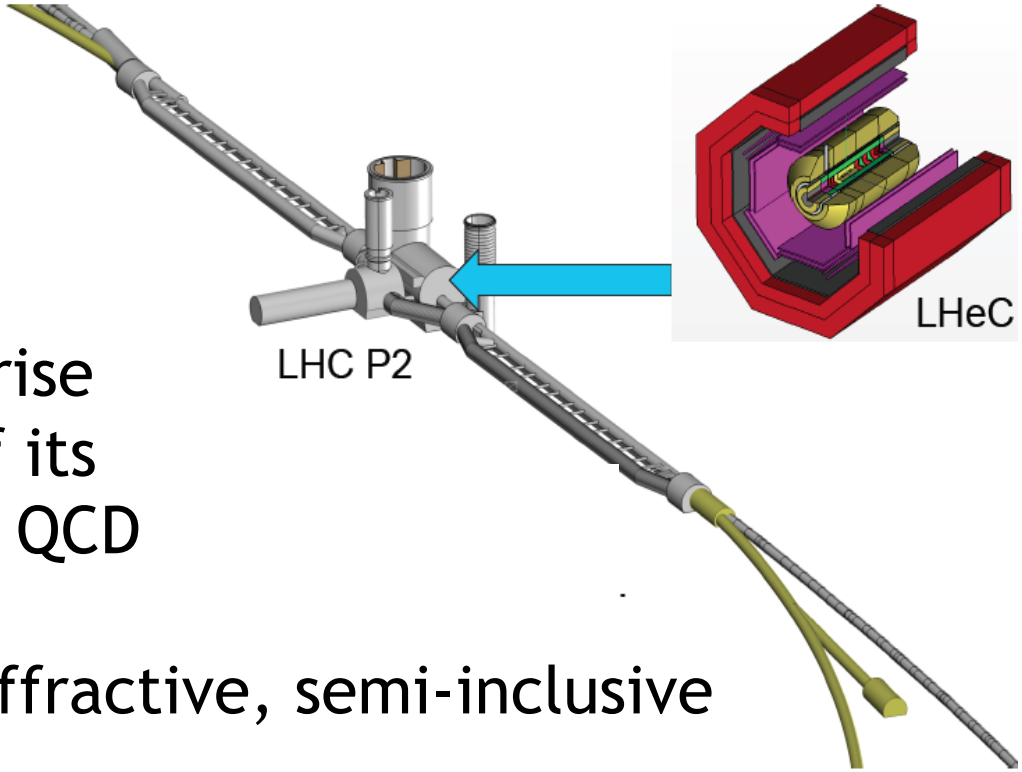


Improvement in EPPS16 nPDFs



[Probably understates full impact – still some Parameterisation bias in EPPS16 without future eA]

Summary



• Future DIS facilities are vital to fully establish and characterise saturation and the dynamics of its onset → the energy frontier of QCD

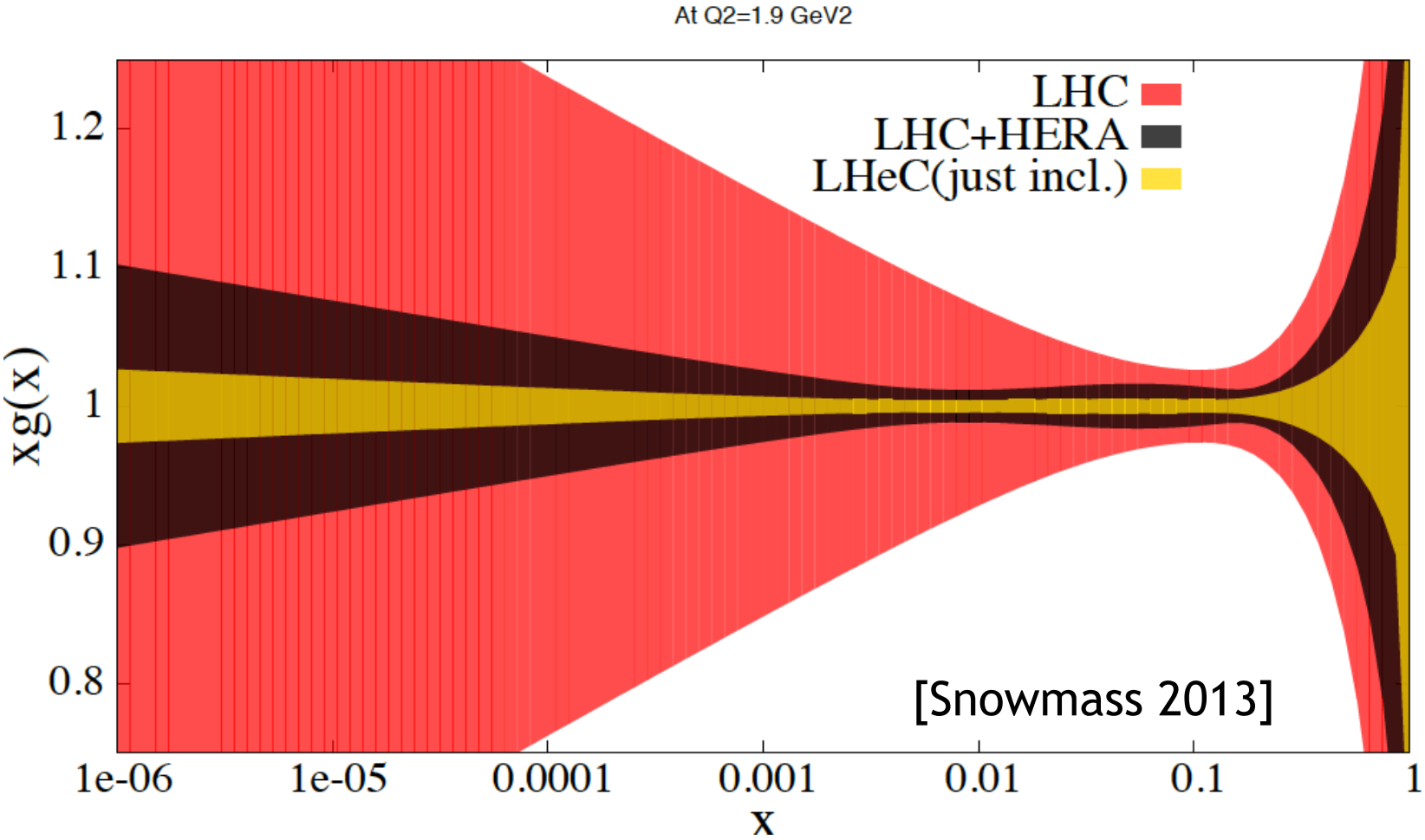
• Needs ep and eA inclusive, diffractive, semi-inclusive over a range of energies

• Complementarity beween EIC and LHeC

• LHeC working towards next CERN Council European Strategy exercise (2020) with a view to running in later stages of LHC (post-LS4, from ~2031) … lots to do!

Back-Ups Follow

What can be done with LHC alone?

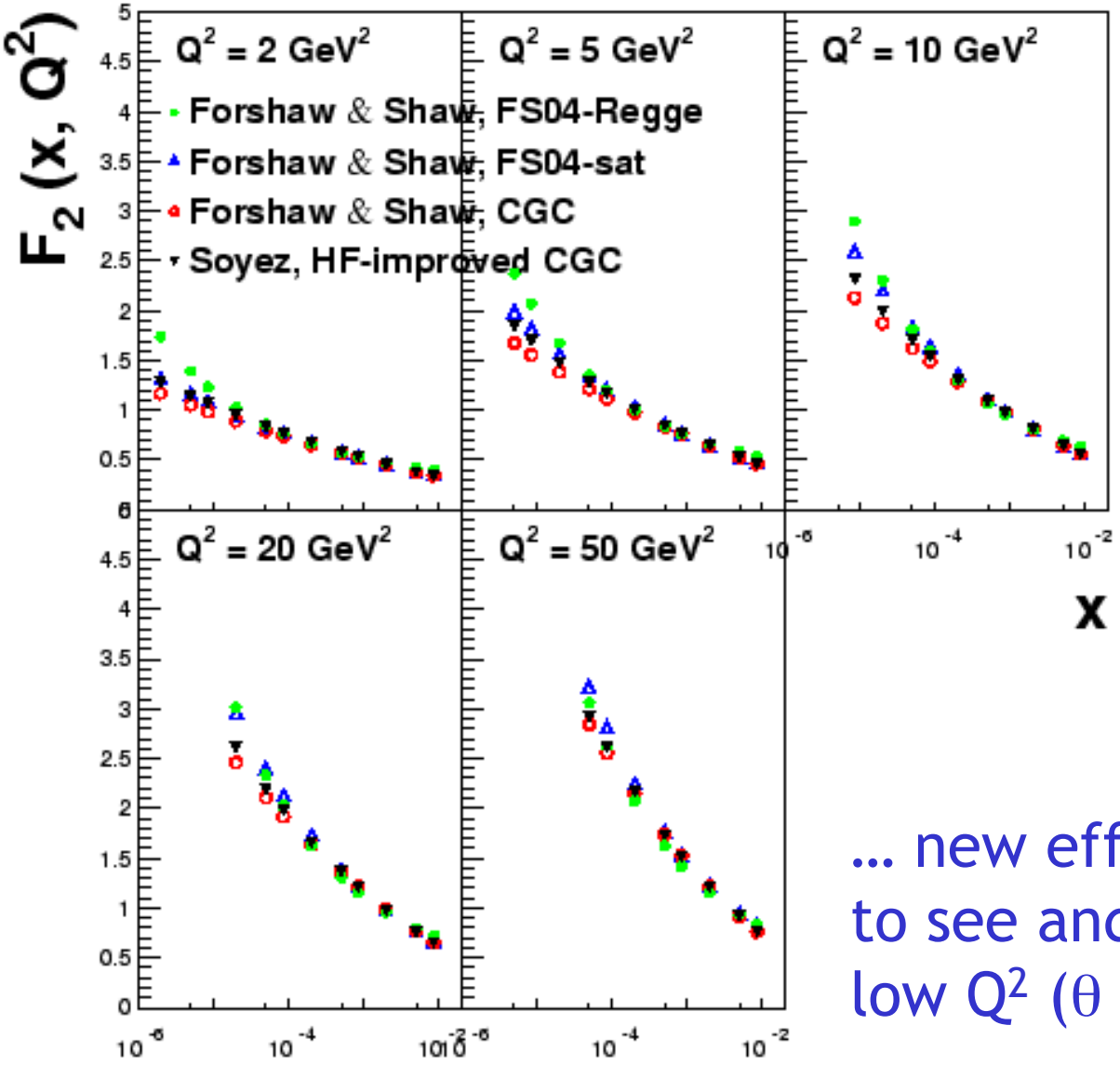


- LHC = current LHC W, Z and jet data
- Remarkable what can be achieved with LHC data alone
- Can we improve substantially? – Often already systs limited

Some models of low x F_2 with LHeC Data

With 1 fb^{-1} (1 year at 10^{33} cm^{-2} s^{-1}), 1º detector:
stat. precision < 0.1%, syst, 1-3%

[Forshaw, Klein, PN, Soyez]



Precise data in LHeC region, x > ~10^{-6}

- Extrapolated HERA dipole models …
- FS04, CGC models including saturation suppressed at low x & Q^2 relative to non-sat FS04-Regge

… new effects may not be easy to see and will certainly need low Q^2 ($\theta \rightarrow 179^o$) region …

F_L Simulation

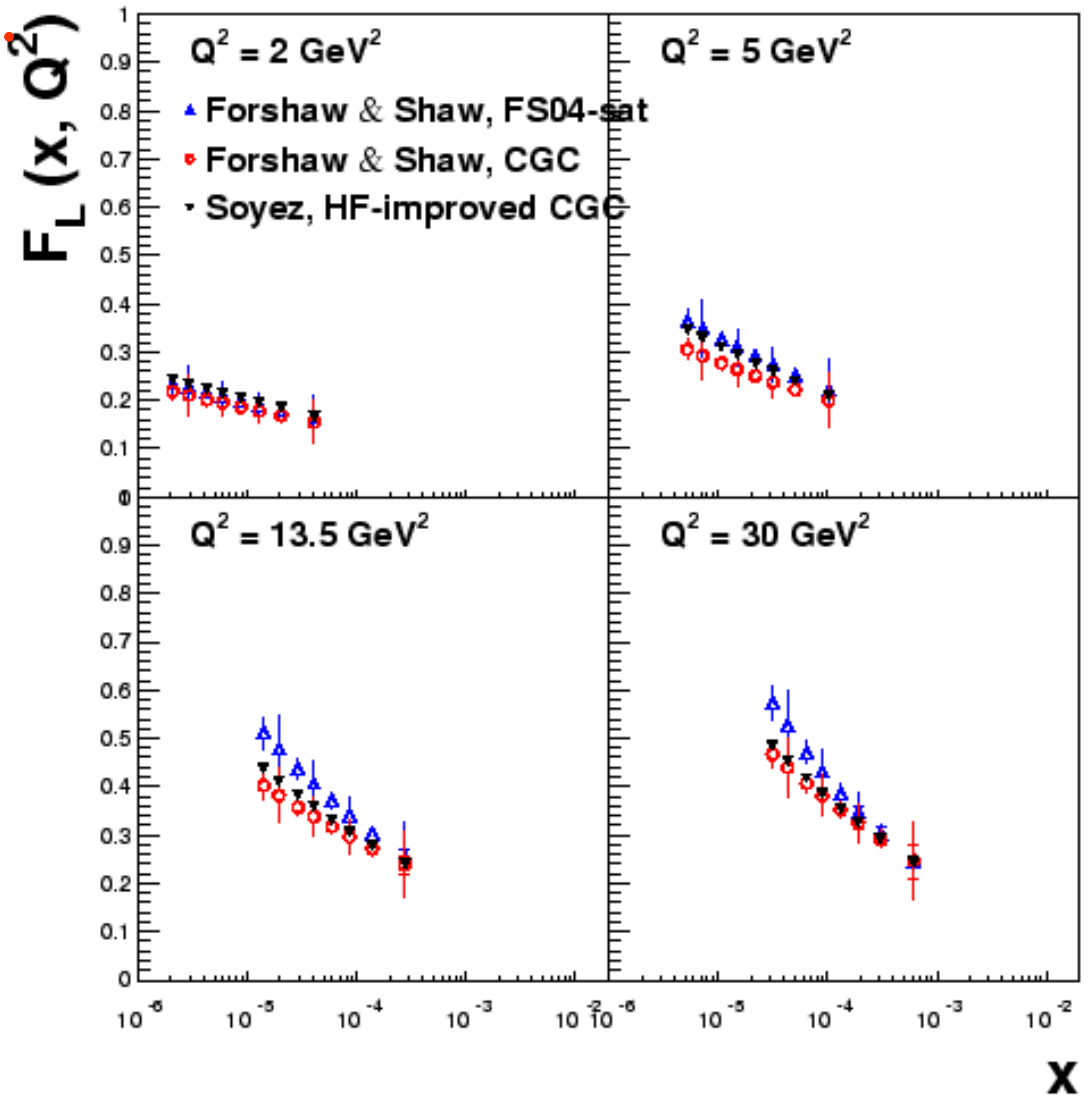
Vary proton beam energy
as recently done at HERA ?...
'direct' gluon measurement ...

E_p (TeV)	Lumi (fb^{-1})
7	1
4	0.8
2	0.2
1	0.05
[0.45	0.01]

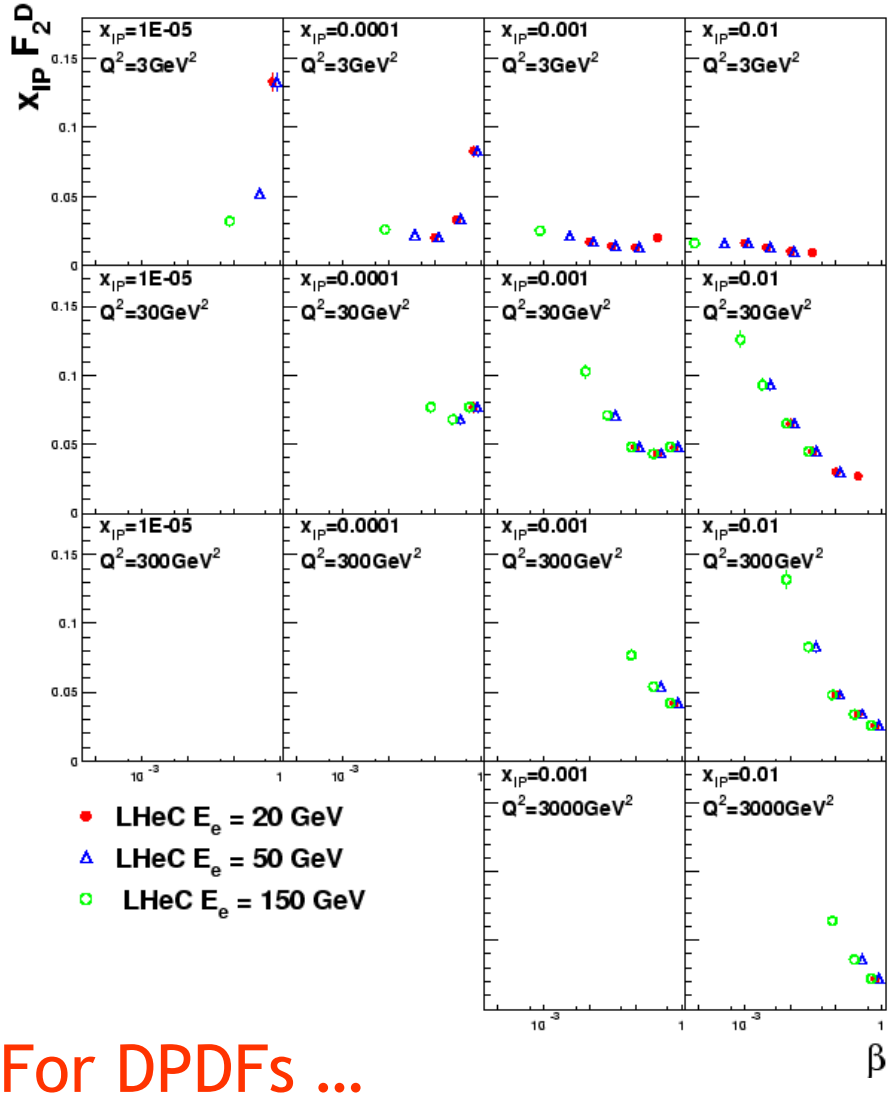
... precision typically 5%
... stats limited for
$Q^2 > 1000\ GeV^2$
... could also vary E_e ...

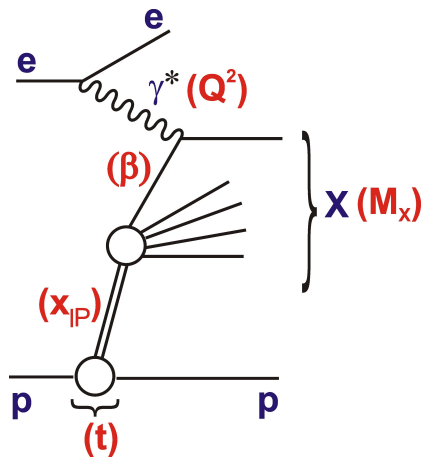
... selected lowest x data
compared with 3 dipole
models including saturation ...

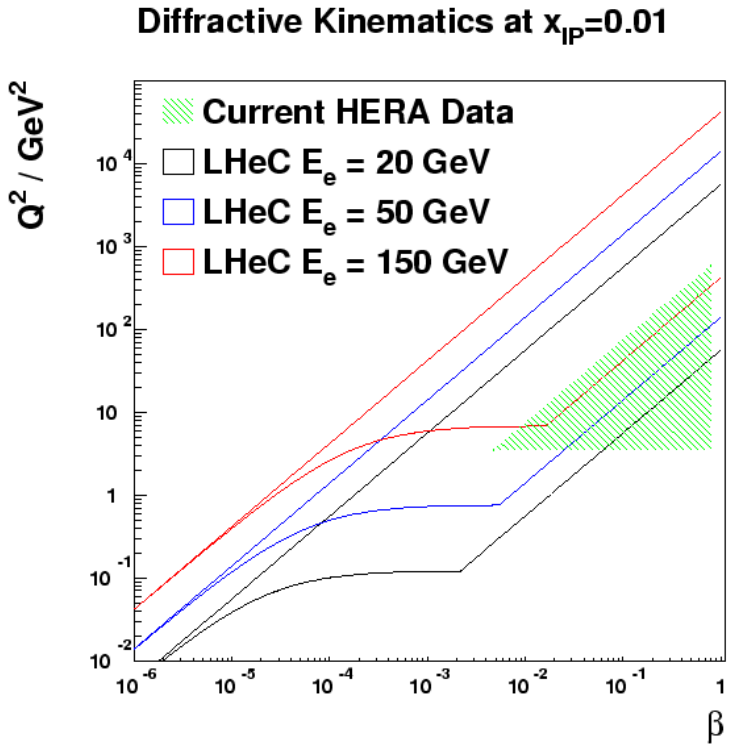
[Forshaw, Klein, PN, Soyez]



Inclusive Diffraction / Diffractive PDFs







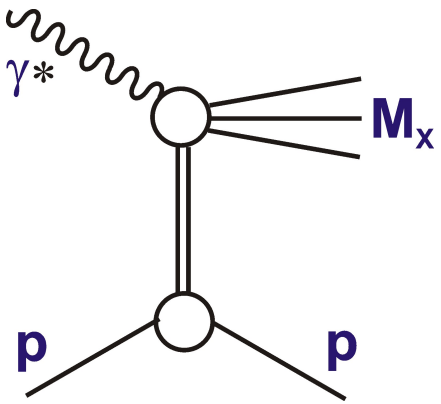
For DPDFs …

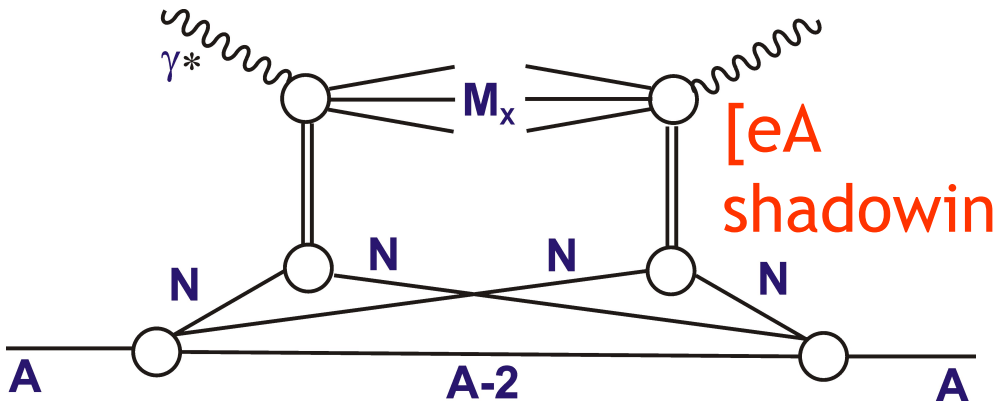
- Low x_{IP} → cleanly separate diffraction
- Low β → Novel low x DPDF effects /non-linear dynamics?
- High Q^2 → Lever-arm for gluon, Flavour separation via EW

F_2^D and Nuclear Shadowing

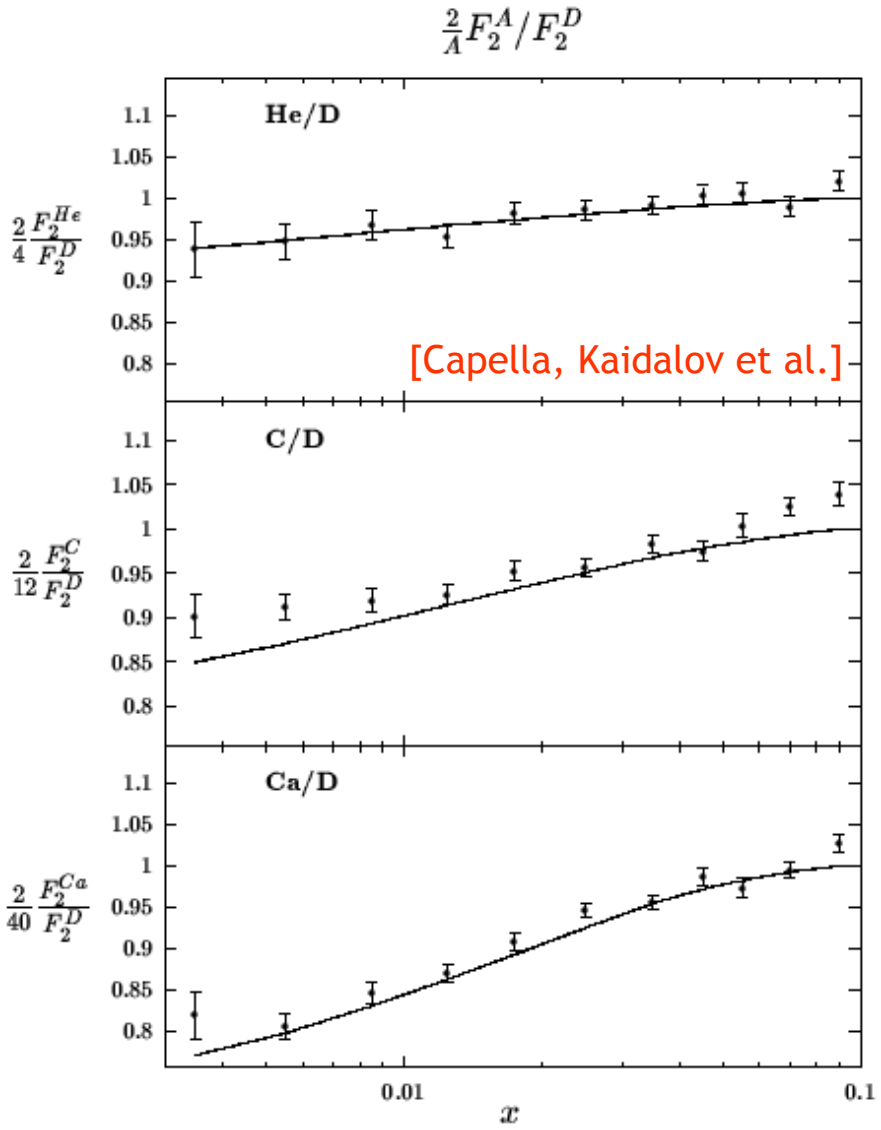
Nuclear shadowing can be described (Gribov-Glauber) as multiple interactions, starting from ep DPDFs

[Diff DIS]



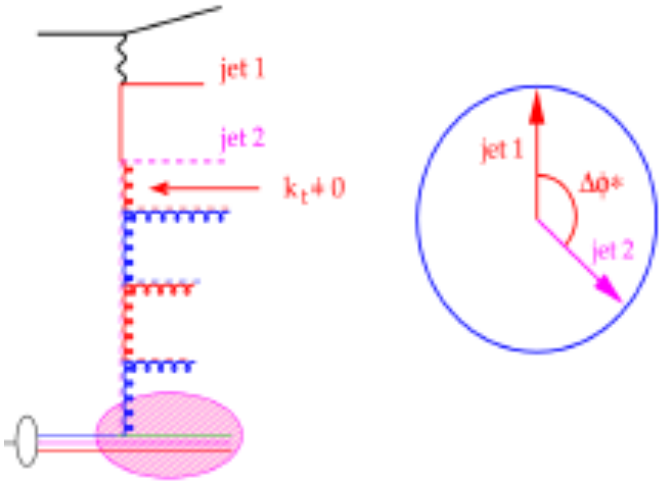


[eA shadowing]



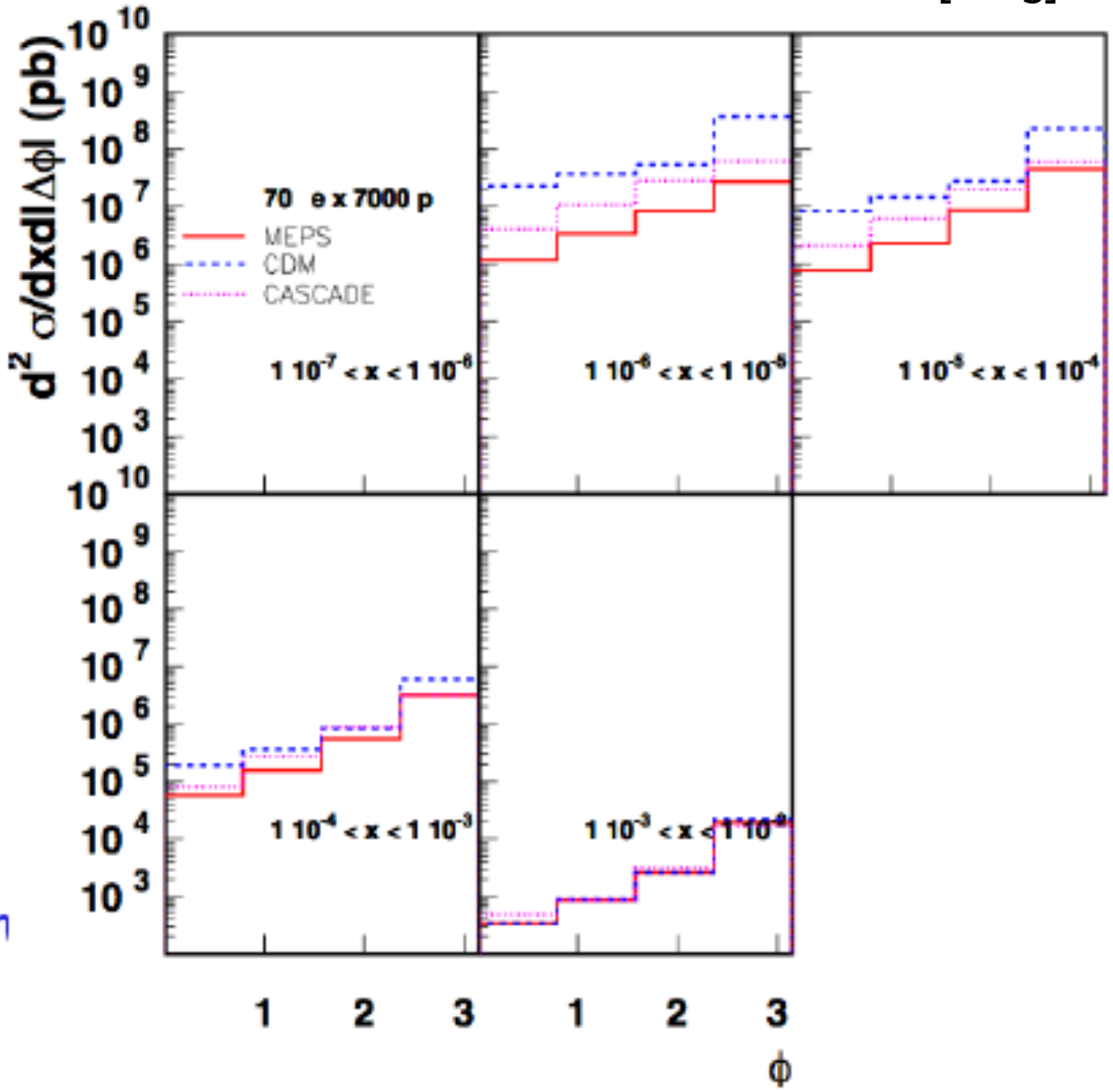
… starting point for extending precision LHeC studies into eA collisions

Azimuthal (de)correlations between Jets

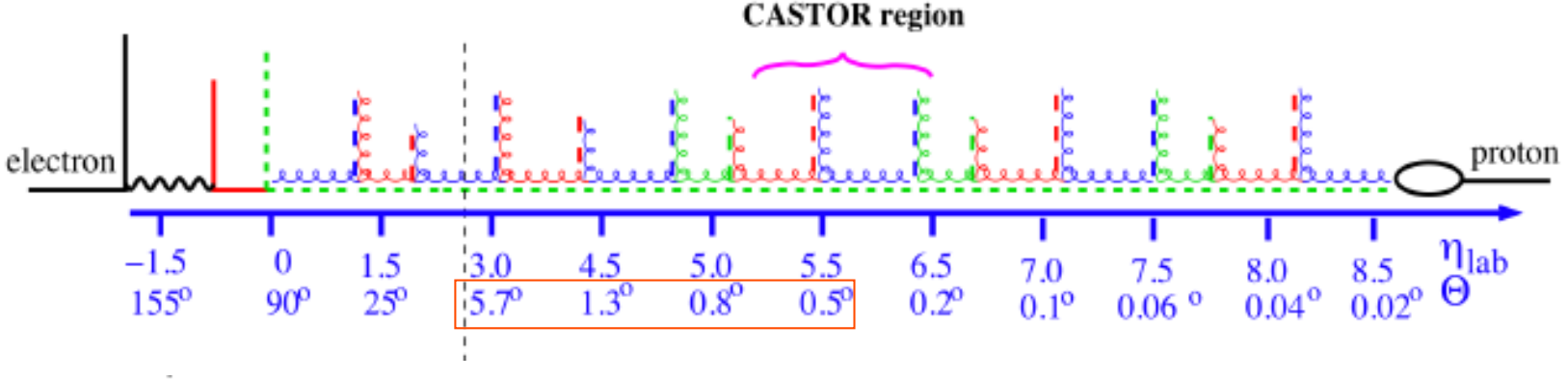


- $5 < Q^2 < 100\ \mathrm{GeV}^2$
  $-1 < \eta < 2.5$
  $E_T > 5\ \mathrm{GeV}$
- small $k_t \rightarrow \Delta\phi \sim 180$
- large k_t from evolution

[Jung]



Forward Instrumentation and Jets



[Jung]

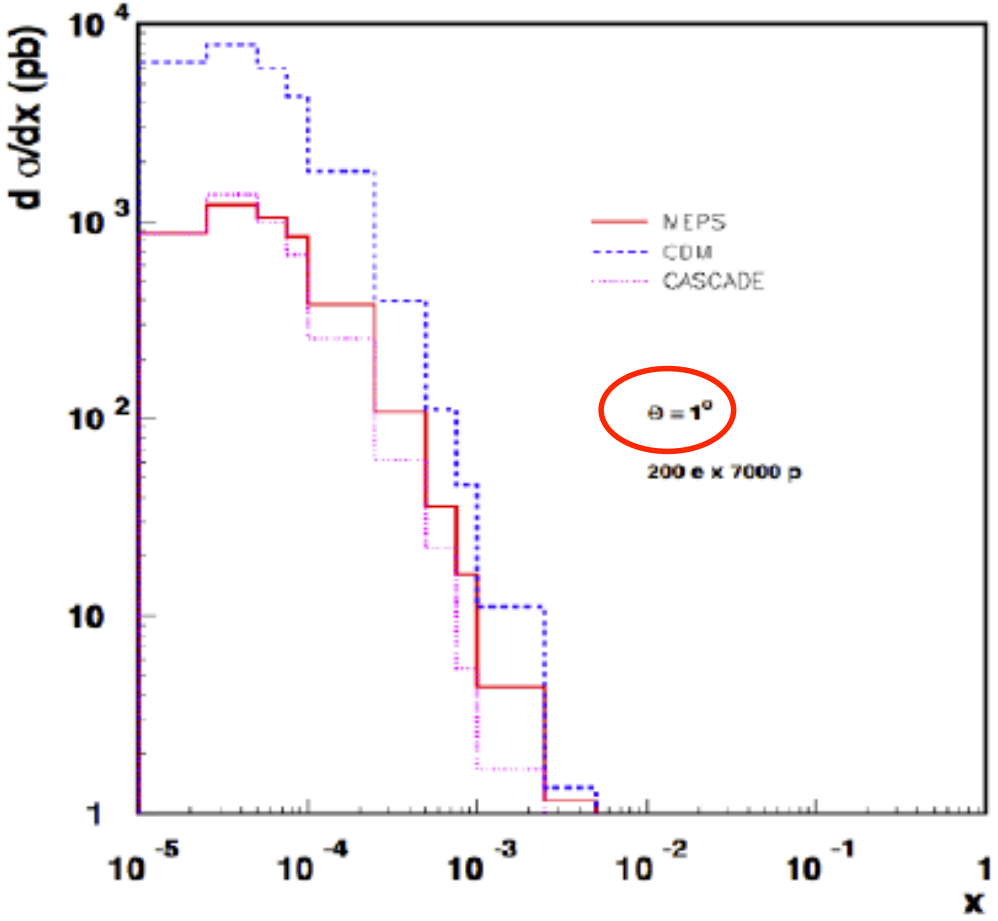
- DIS and forward jet:

$$x_{jet} > 0.03$$

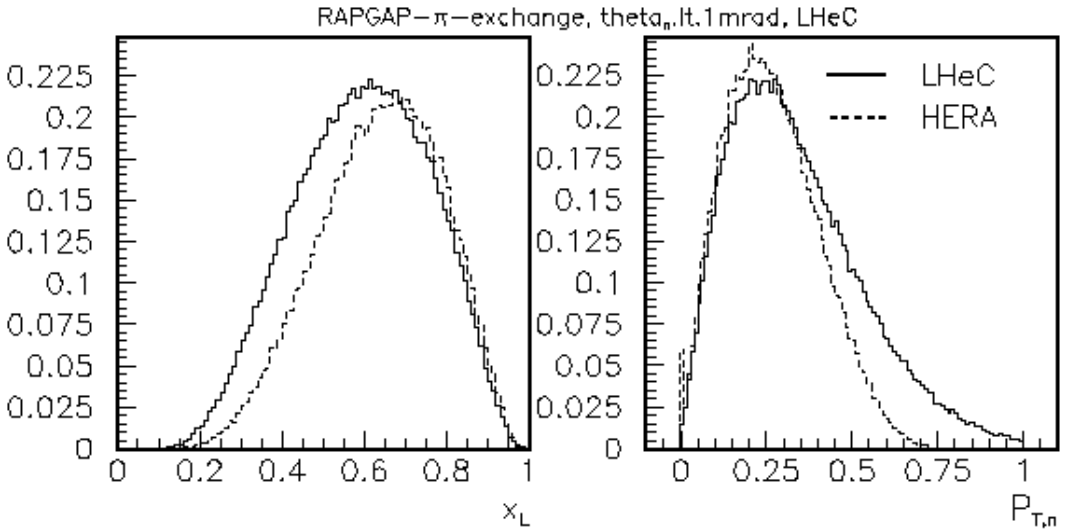
$$0.5 < \frac{p_{t\,jet}^2}{Q^2} < 2$$

x range (and sensitivity to novel QCD effects) strongly depend on θ cut

Similar conclusions for Δϕ decorrelations between jets

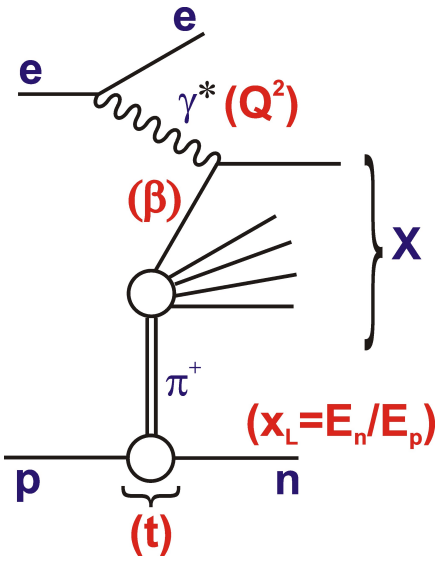


π Structure with Leading Neutrons



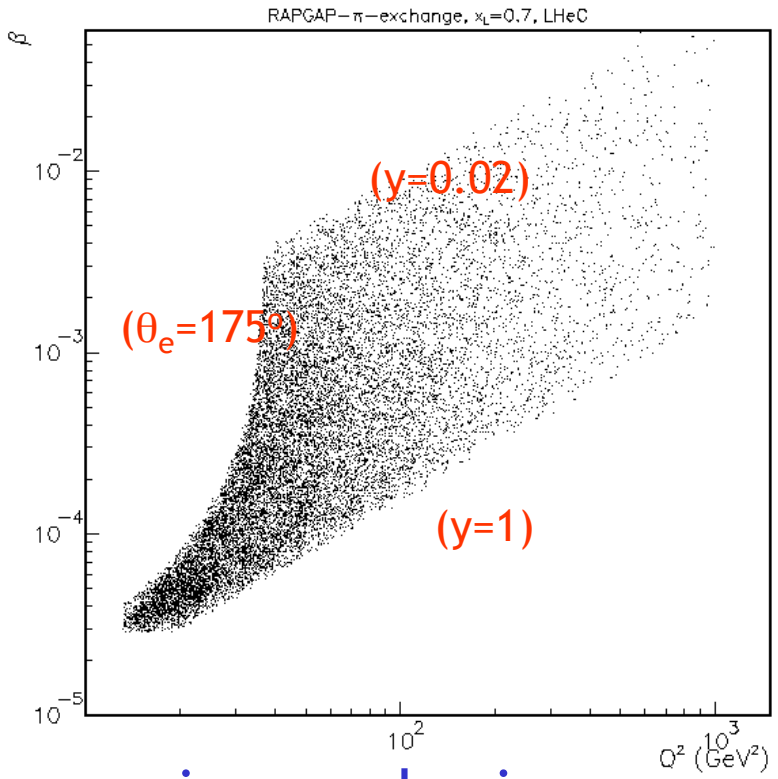
[Bunyatyan]

(RAPGAP MC model, E_p=7TeV, E_e=70GeV)



- With θ_n < 1 mrad, similar x_L and p_t ranges to HERA (a bit more p_t lever-arm for π flux).

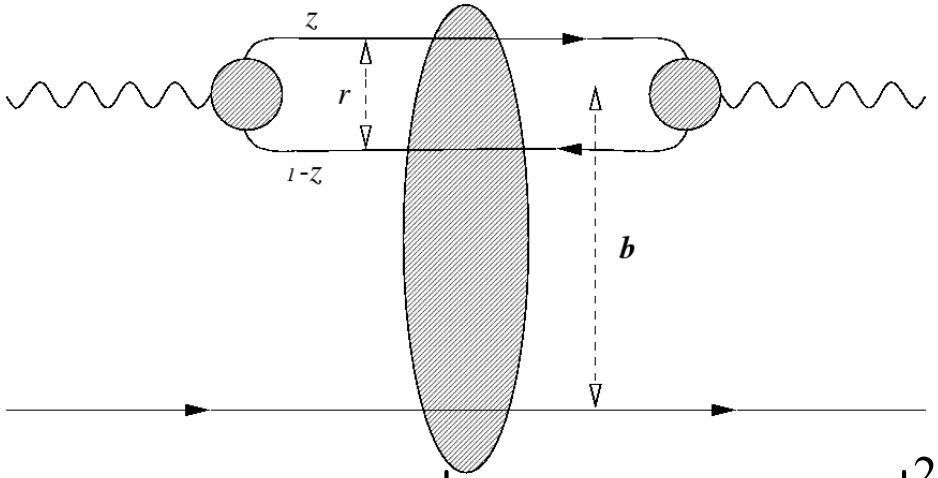
- Extentions to lower β and higher Q^2 as in leading proton case. → F_2^{π}
At $\beta<5.10^{-5}$ (cf HERA reaches $\beta\sim10^{-3}$)



Also relevant to absorptive corrections, cosmic ray physics …

Reminder : Dipole models

- Unified description of low x region, including region where Q^2 small and partons not appropriate degrees of freedom …

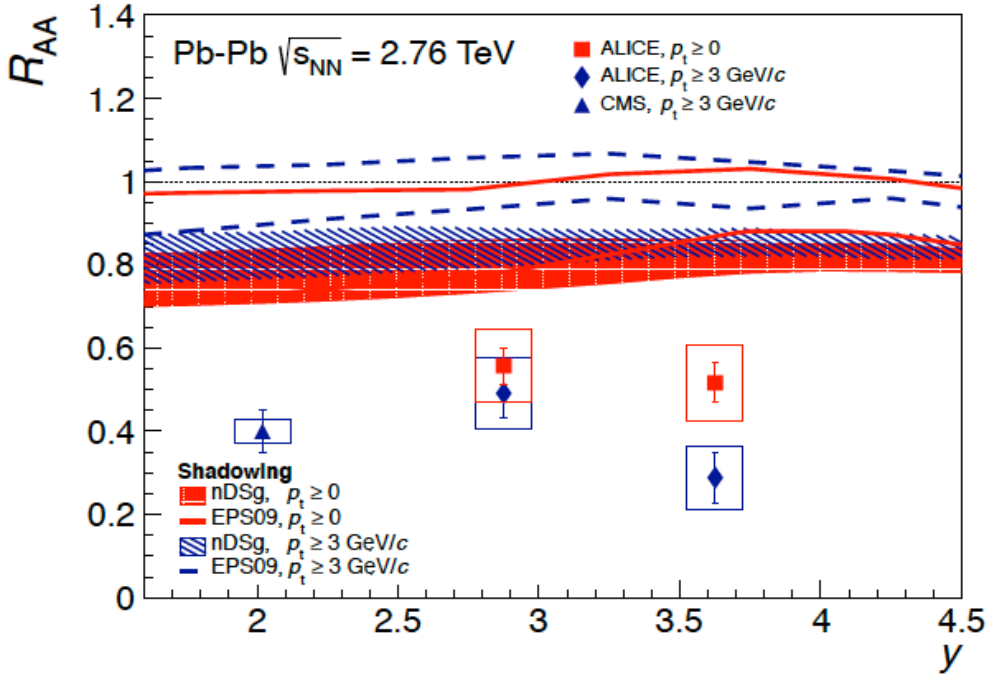


$$\sigma^{T,L}_{\gamma^* p}(x,Q^2) \sim \int \mathrm{d}z\, \mathrm{d}^2 r \left|\psi^{T,L}_{\gamma^*}(z,r,Q^2)\right|^2 \sigma_{dipole}(x,r,z)$$

- Simple unified picture of many inclusive and exclusive processes … strong interaction physics in (universal) dipole cross section σ_{dipole}. Process dependence in wavefunction Ψ Factors
- qqbar-g dipoles also needed to describe inclusive diffraction

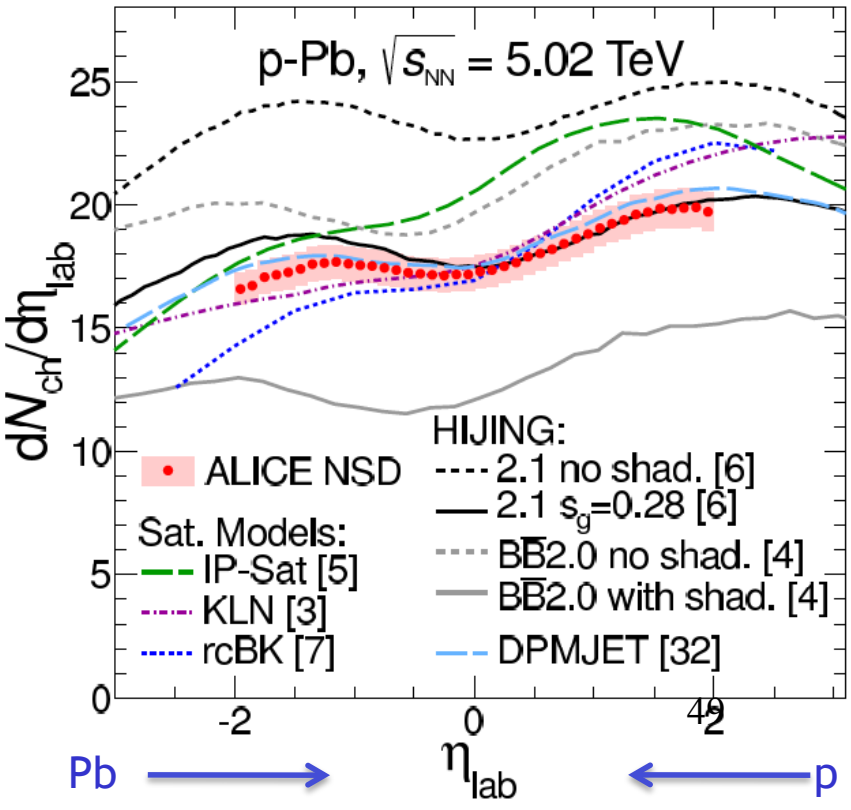
Current Low x Understanding in LHC Ion Data

Inclusive J/Ψ AA data



Uncertainties in low-x nuclear PDFs preclude precision statements on medium produced in AA (e.g. extent of screening of c-cbar potential)

Minimum Bias pA data

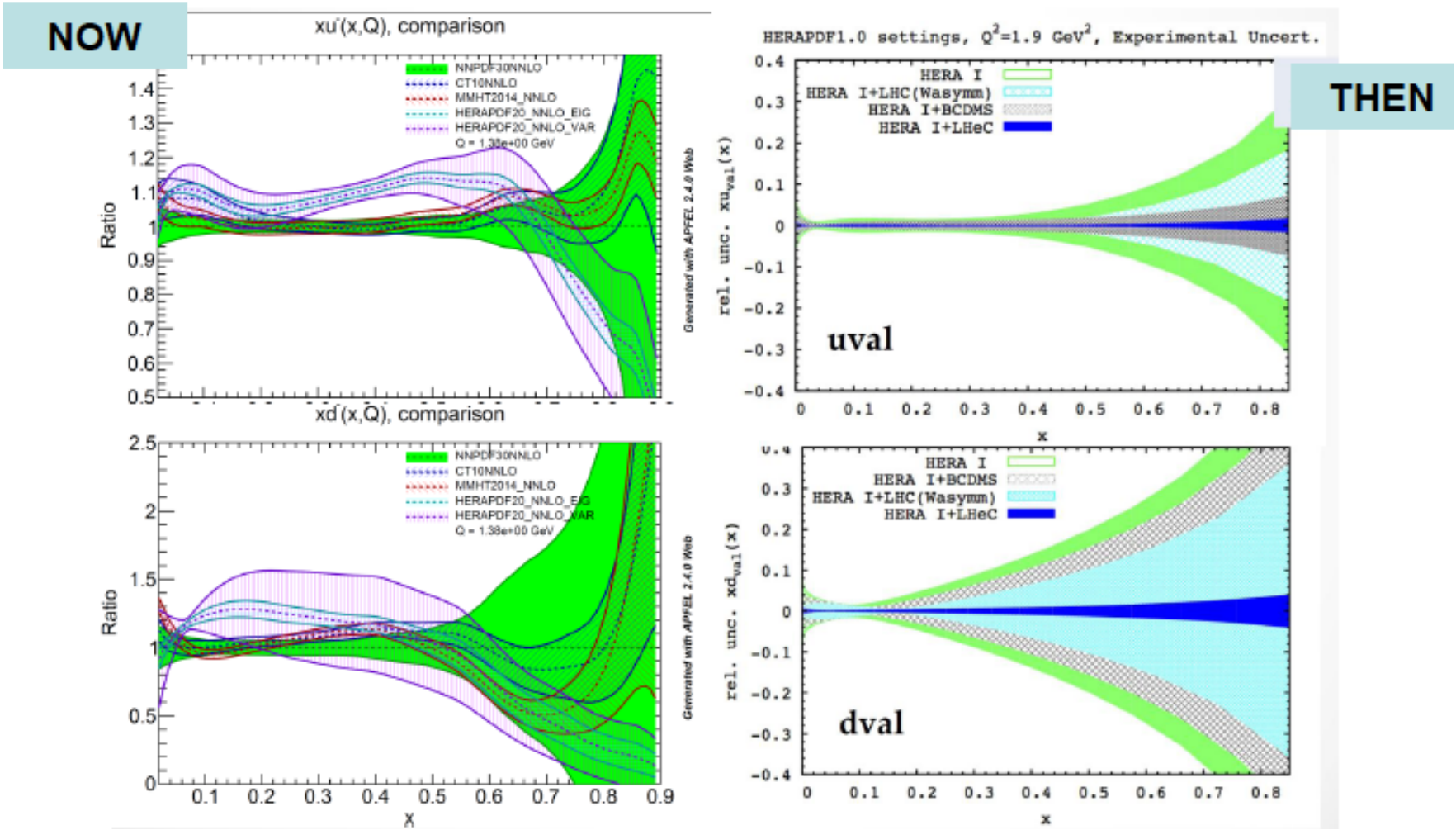


η dependence of pPb charged particle spectra best described by shadowing-only models (saturation models too steep?)

… progress with pPb, but uncertainties still large, detailed situation far from clear

Valence Quarks at LHeC

Disentangle sea and valence through CC, xF_3 etc



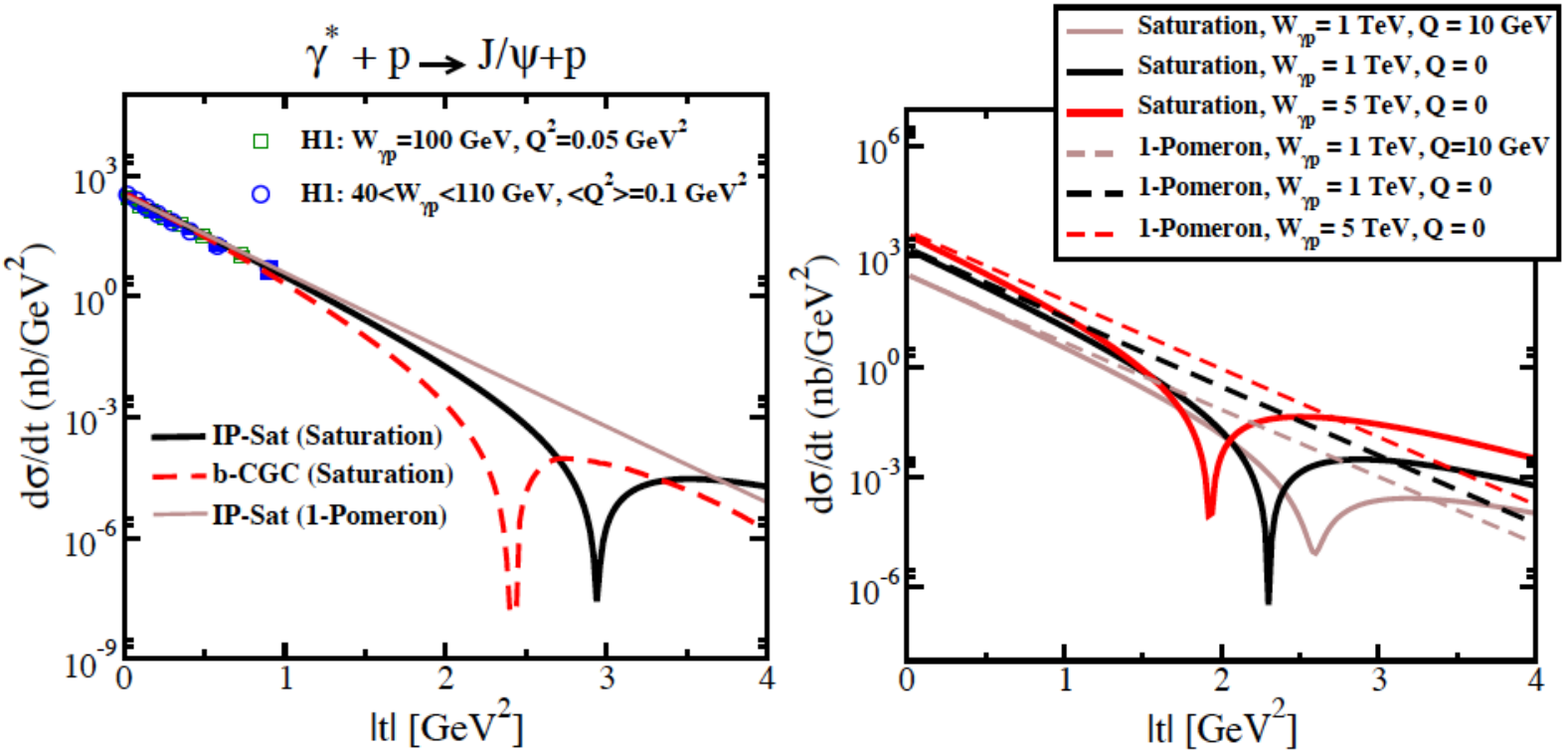
- Also, precision light quark axial / vector couplings, weak mixing angle, α_s and full flavour decomposition …

Signals in t Dependences: e.g. J/ψ Photoproduction

t dependences measure Fourier transform of impact parameter distribution. → Unusual features can arise from deviations from Gaussian matter distribution

e.g. Characteristic dips in model by Rezaeian et al,

(just) within LHeC sensitive t range.



Leading Neutrons

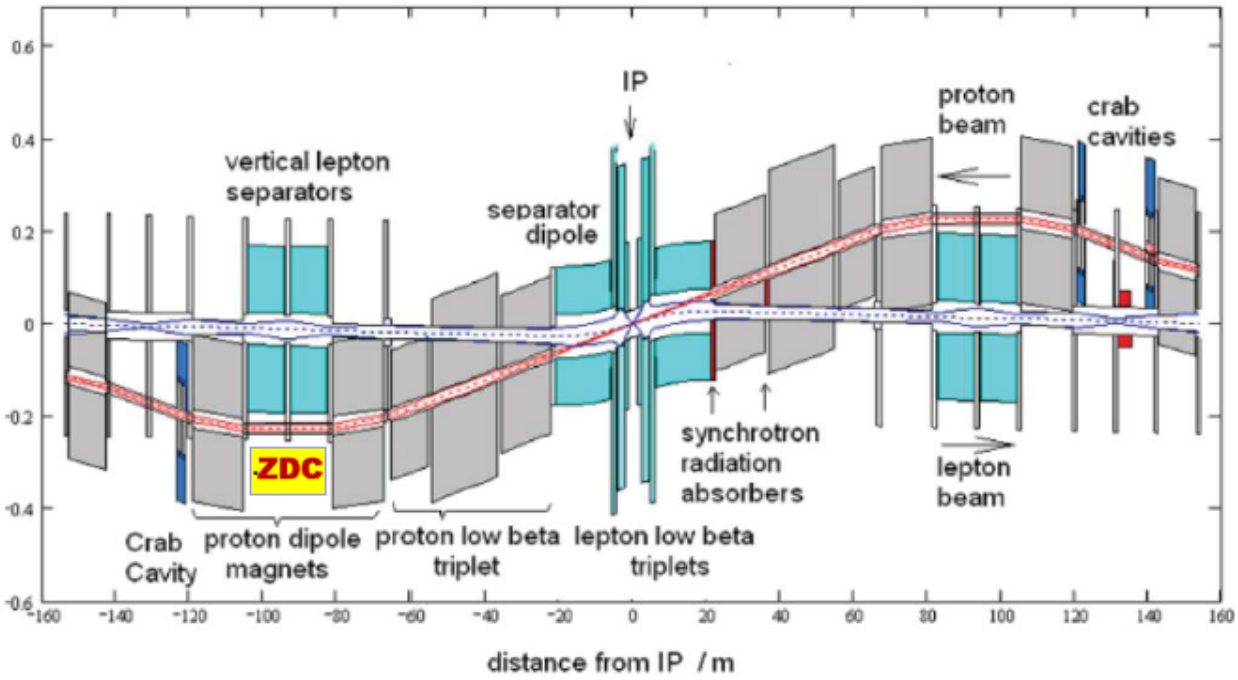
- Crucial in eA, to determine whether nucleus remains intact e.g. to distinguish coherent from incoherent diffraction

- Crucial in ed, to distinguish scattering from p or n

- Forward γ and n cross sections relevant to cosmic ray physics

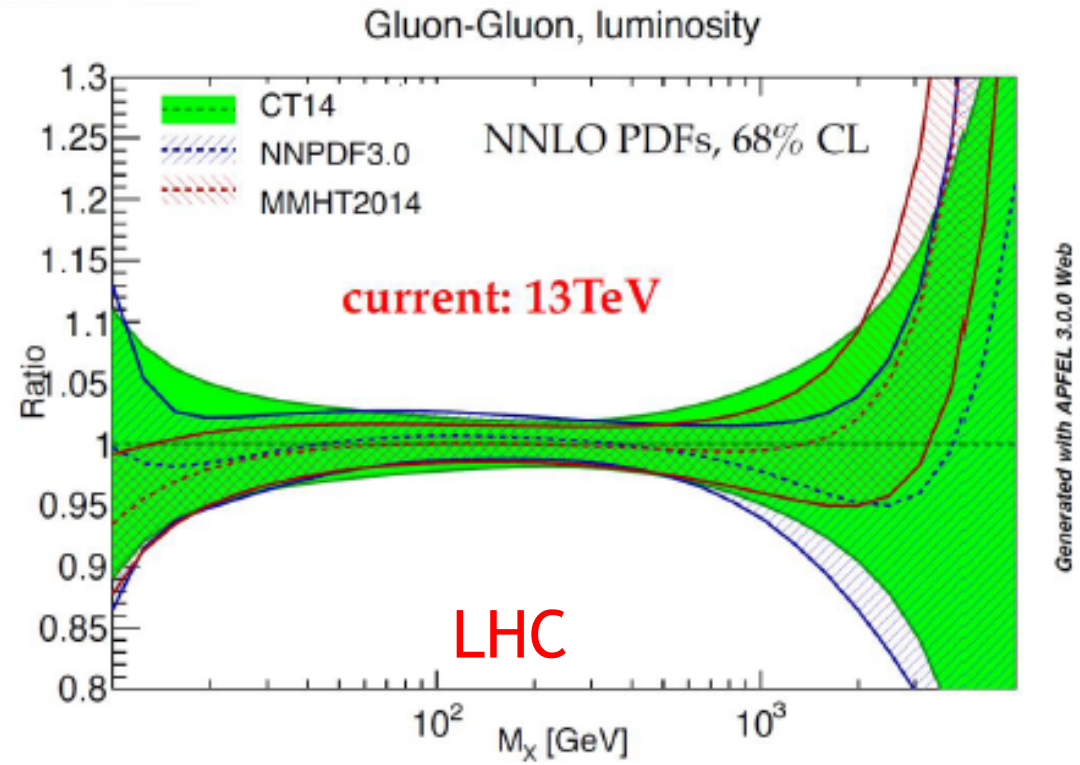
- Has previously been used in ep to study π structure function

Possible space at
z ~ 100m (also possibly for proton calorimeter)

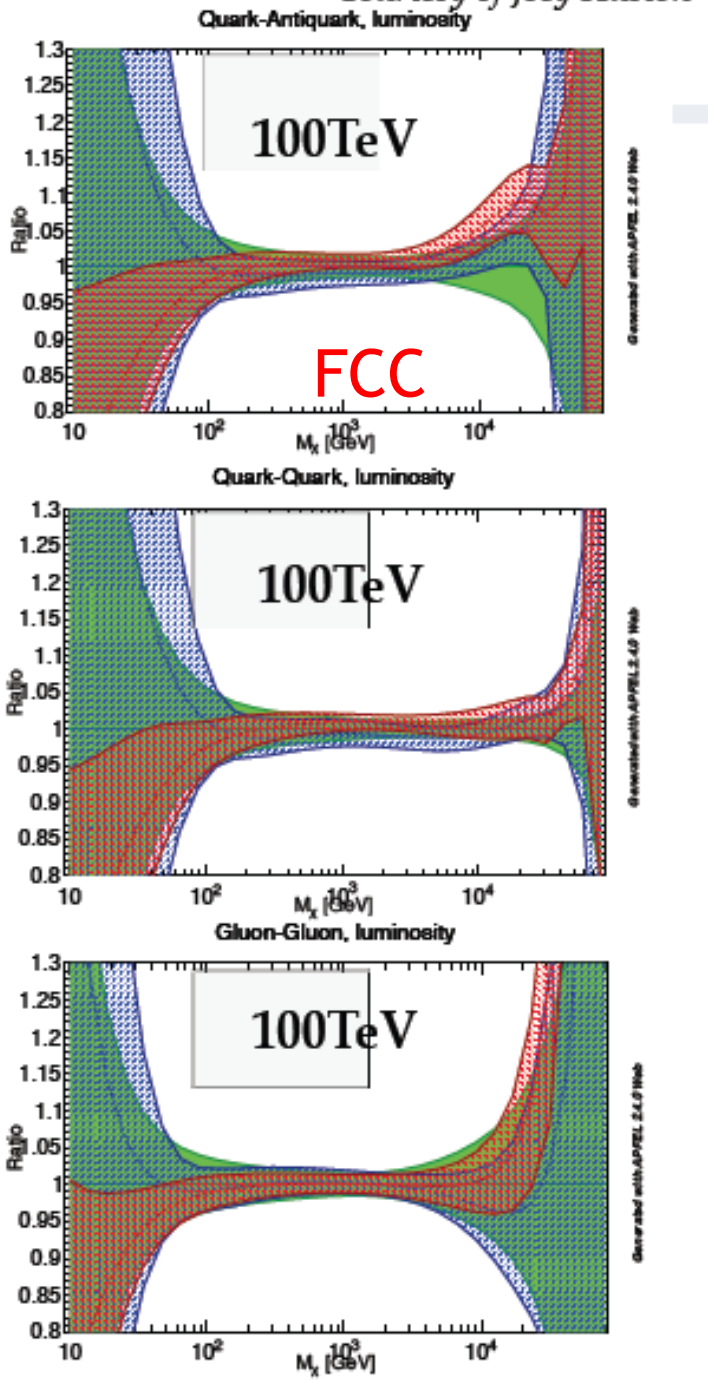


… to be further investigated

Current PDF Uncertainties



Courtesy of Joey Huston



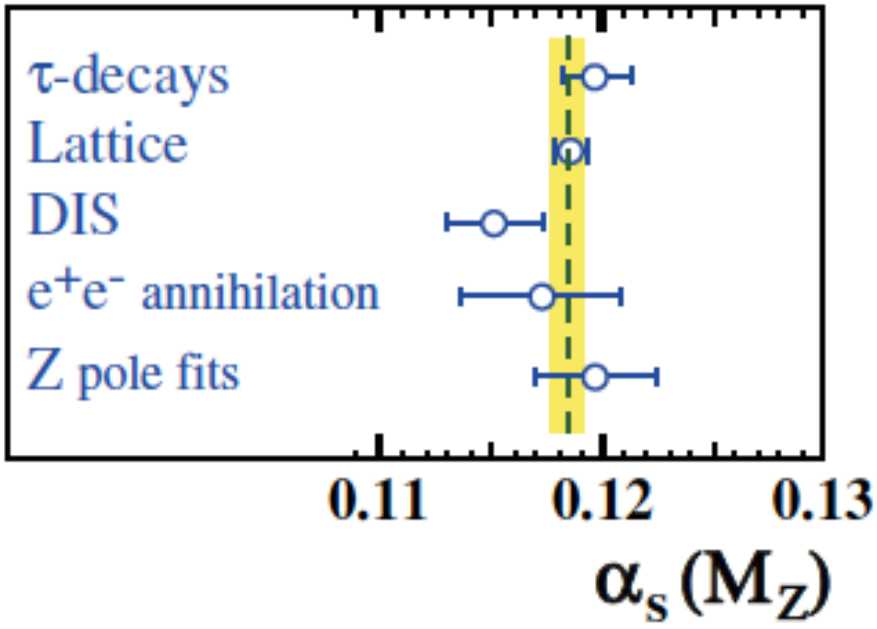
Low x / M_x → novel QCD / unitarity

Medium x / M_x → precision H and EW

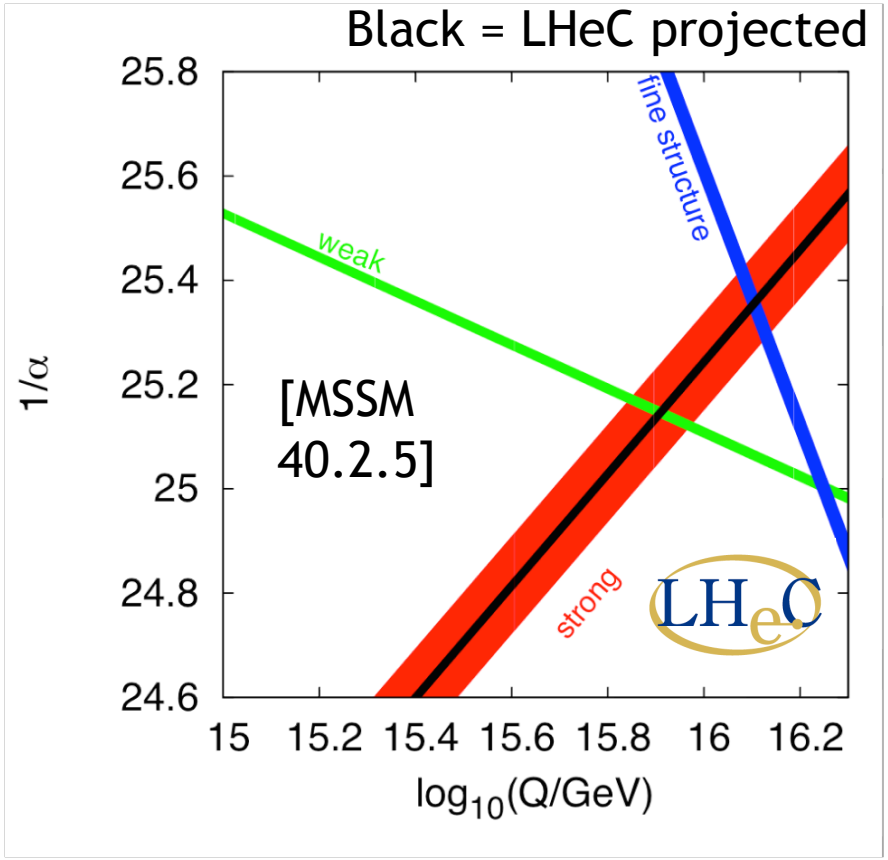
High x / M_x → new particle mass frontier

Precision α_s

- Least constrained fundamental coupling by far (known to ~1%)
- Do coupling constants unify (with a little help from SUSY)?
- (Why) is DIS result historically low?



Red = current world average
Black = LHeC projected



- Simulated LHeC precision from fitting inclusive data
→ per-mille (experimental)
→ also requires improved theory

Context of Precision α_s

Snowmass13 report – arXiv:1310.5189

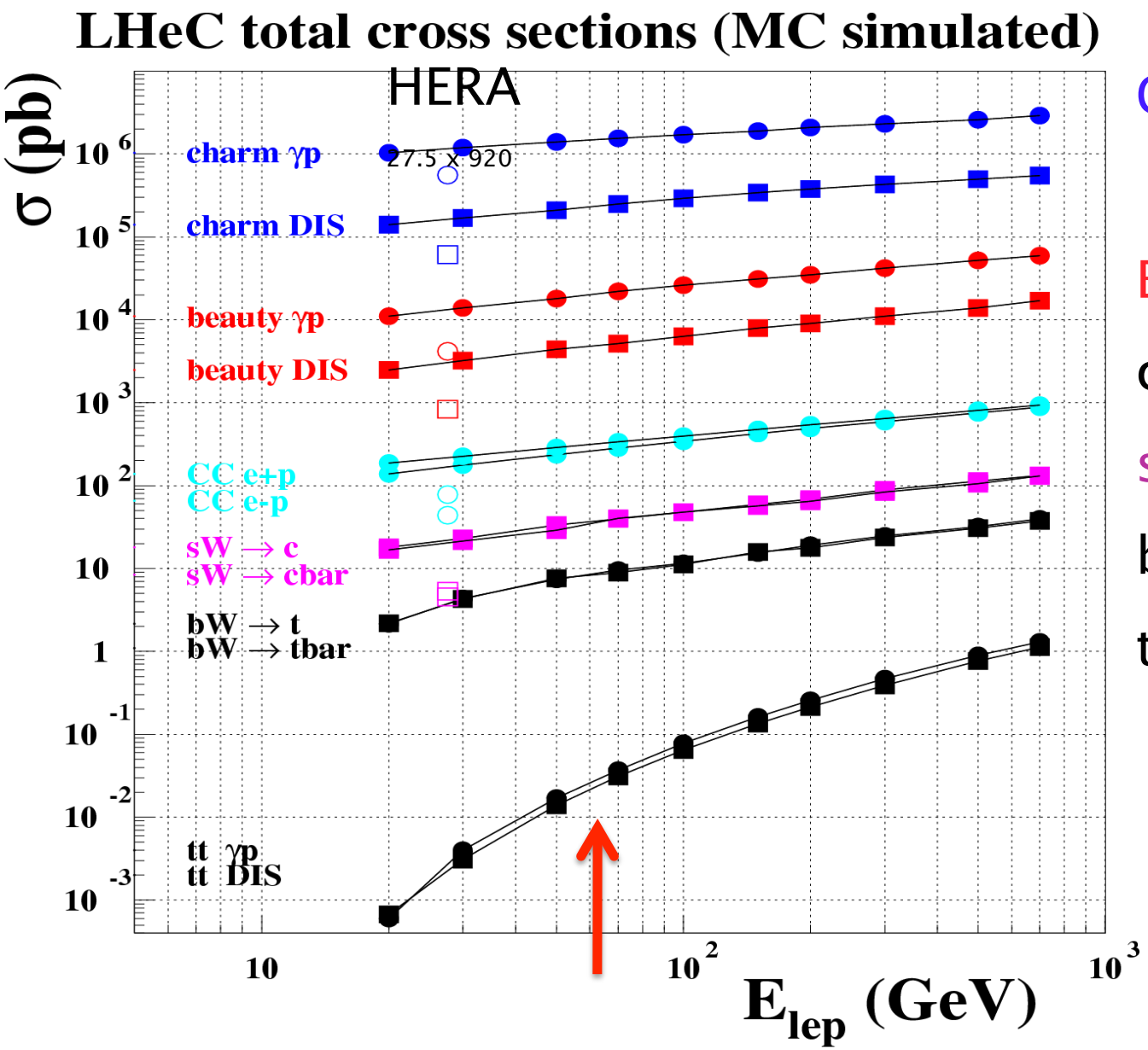
Method	Current relative precision	Future relative precision
e^+e^- evt shapes	expt $\sim$ 1% (LEP) thry $\sim$ 1–3% (NNLO+up to N^{3}LL, n.p. signif.) [27]	$<$ 1% possible (ILC/TLEP) $\sim$ 1% (control n.p. via Q^2-dep.)
e^+e^- jet rates	expt $\sim$ 2% (LEP) thry $\sim$ 1% (NNLO, n.p. moderate) [28]	$<$ 1% possible (ILC/TLEP) $\sim$ 0.5% (NLL missing)
precision EW	expt $\sim$ 3% (R_Z, LEP) thry $\sim$ 0.5% (N^{3}LO, n.p. small) [9,29]	0.1% (TLEP [10]), 0.5% (ILC [11]) $\sim$ 0.3% (N^{4}LO feasible, $\sim$ 10 yrs)
τ decays	expt $\sim$ 0.5% (LEP, B-factories) thry $\sim$ 2% (N^{3}LO, n.p. small) [8]	$<$ 0.2% possible (ILC/TLEP) $\sim$ 1% (N^{4}LO feasible, $\sim$ 10 yrs)
ep colliders	$\sim$ 1–2% (pdf fit dependent) [30,31], (mostly theory, NNLO) [32,33]	0.1% (LHeC + HERA [23]) $\sim$ 0.5% (at least N^{3}LO required)
hadron colliders	$\sim$ 4% (Tev. jets), $\sim$ 3% (LHC $t\bar{t}$) (NLO jets, NNLO $t\bar{t}$, gluon uncert.) [17,21,34]	$<$ 1% challenging (NNLO jets imminent [22])
lattice	$\sim$ 0.5% (Wilson loops, correlators, ...) (limited by accuracy of pert. th.) [35–37]	$\sim$ 0.3% ($\sim$ 5 yrs [38])

per mille

per mille

… tensions between lattice and DIS α_s results as a sensitive probe of new physics?...

Cross Sections and Rates for Heavy Flavours



Charm [10^{10} / 10 fb^{-1}]

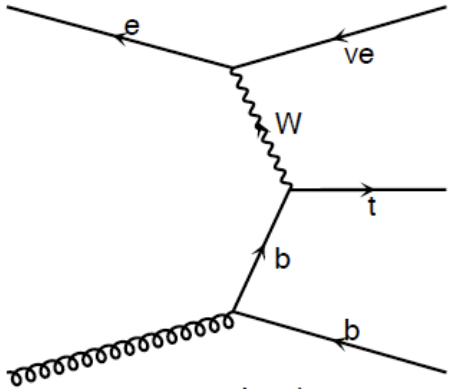
Beauty [10^{8} / 10 fb^{-1}]

cc

sW → c [4.10^{5} / 10 fb^{-1}]

bW → t [10^{5} / 10 fb^{-1}]

ttbar [10^{3} / 10 fb^{-1}]



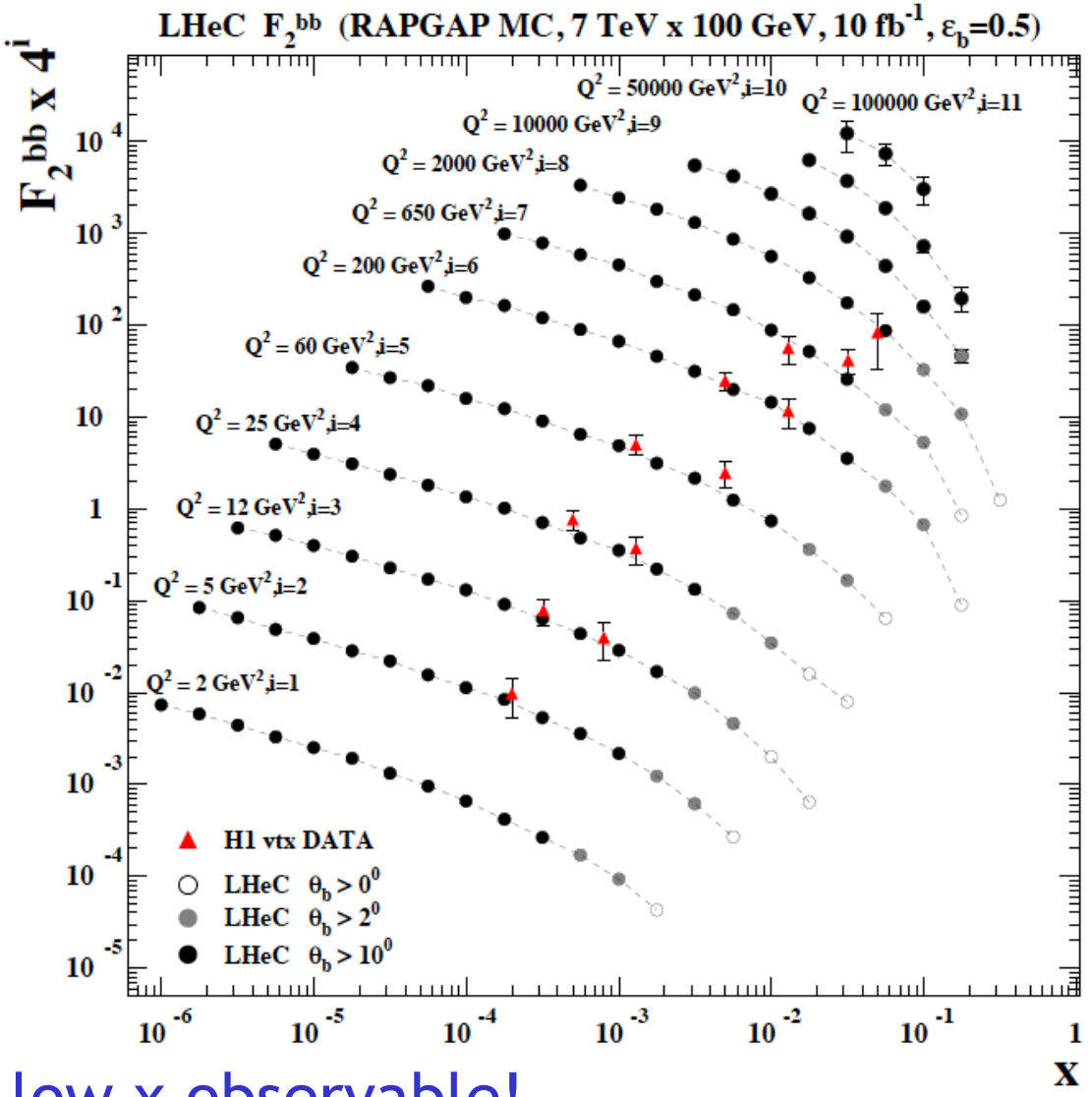
c.f. luminosity of ~10-100 fb^{-1} per year

e.g. Beauty Production

Precise c, b measurements from impact parameter distributions (modern Si trackers, beam spot 15 * 35 μm^2 , increased HF rates at higher scales).

(Assumes 10 fb^{-1} and
- 50% beauty, 10% charm efficiency
- 1% uds → c mistag probability.
- 10% c → b mistag)

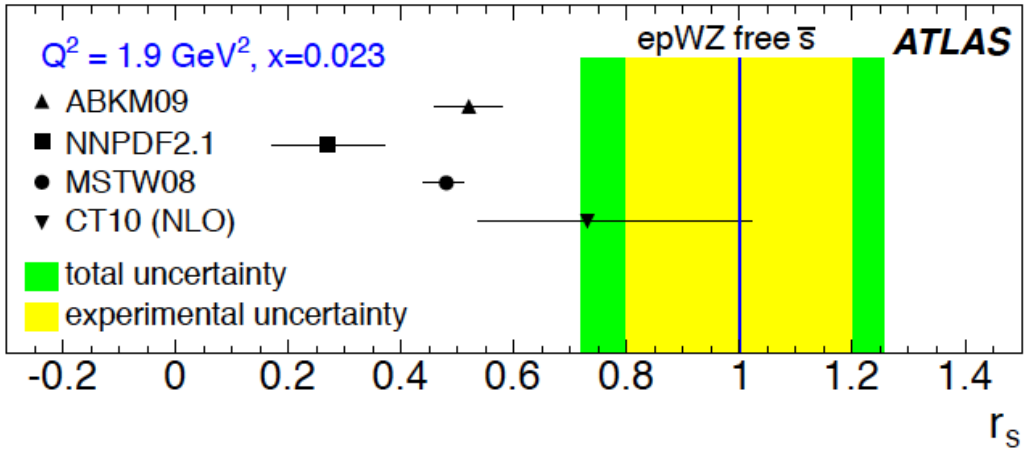
Systematics at 10% level

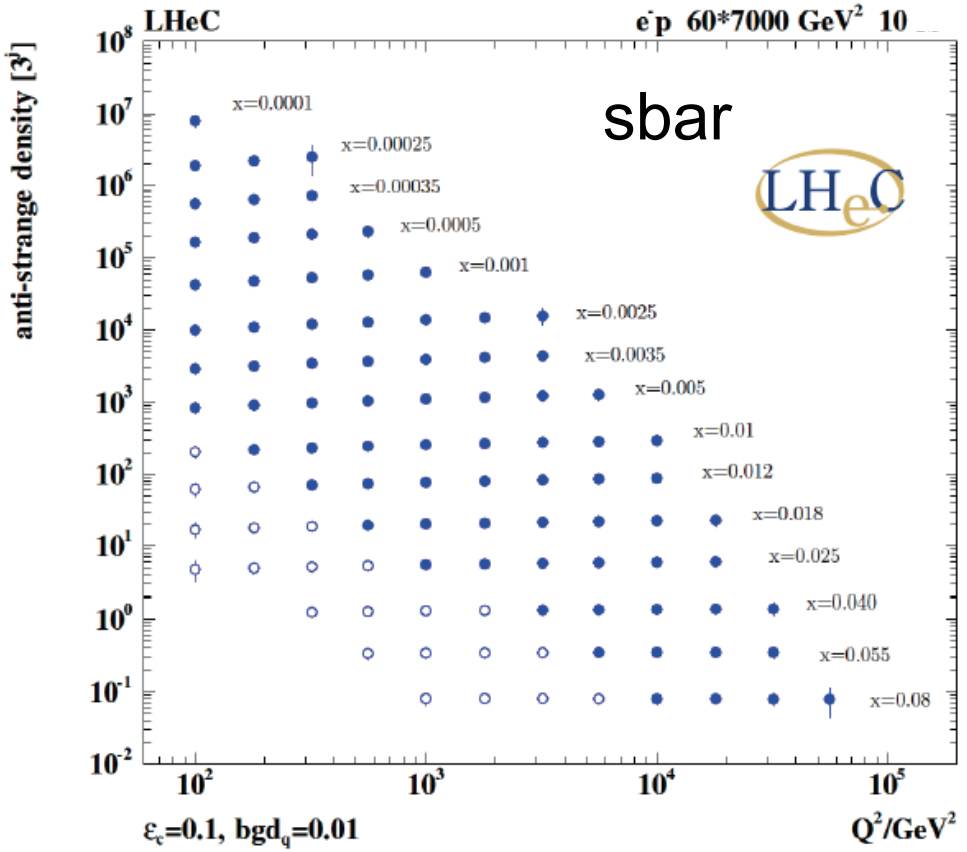


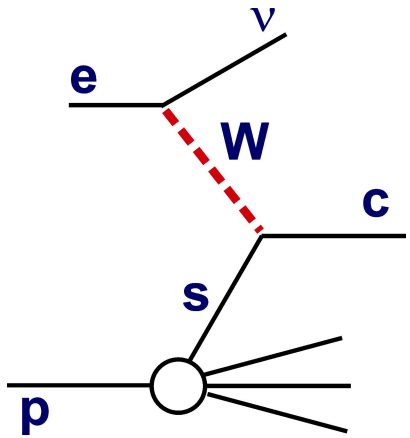
→beauty as a low x observable!

e.g. Strange and Anti-strange Quarks

Evidence from LHC that strange density is larger than thought: SU(3) symmetric sea?...



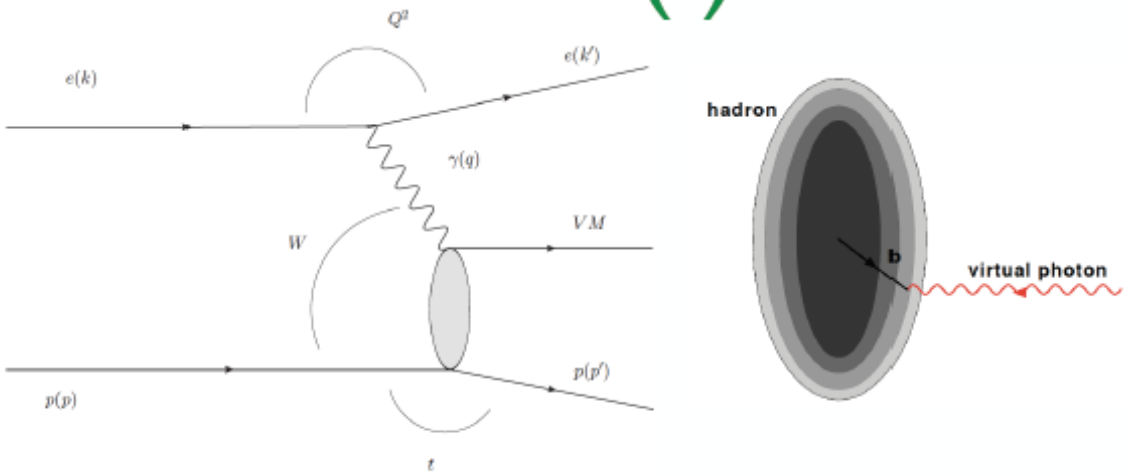


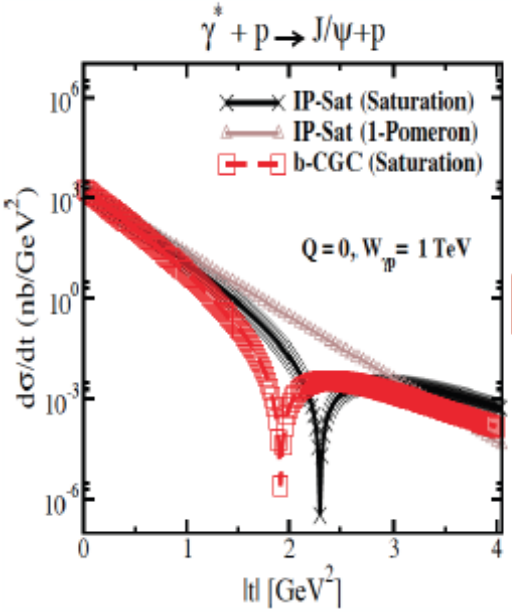


Assuming 10% charm tagging efficiency, 1% light quark background

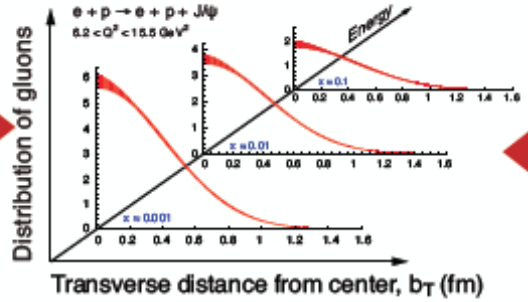
Transverse structure (I):

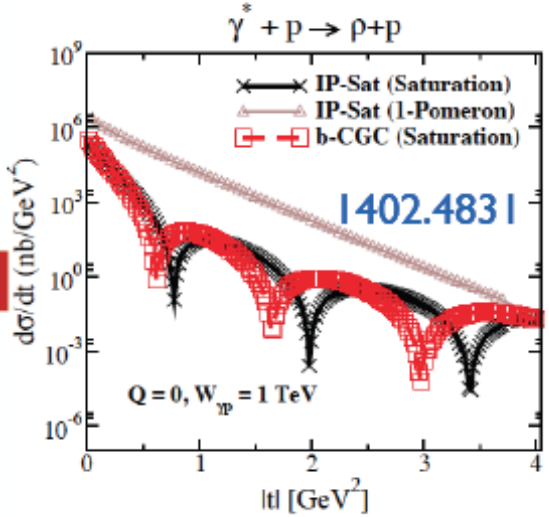
- Exclusive VM meson production/DVCS provides a transverse scan of the partonic structure of the hadron, may also be sensitive to dynamics:





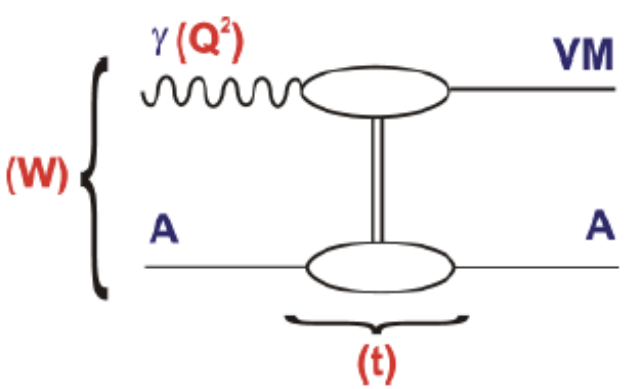
Rezaeian

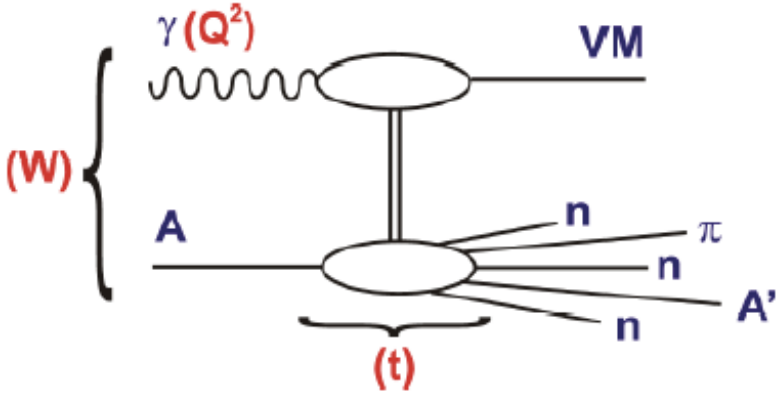


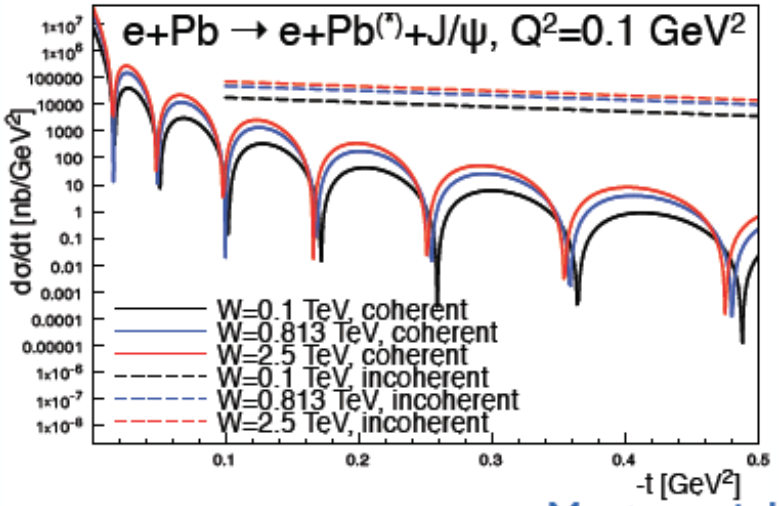


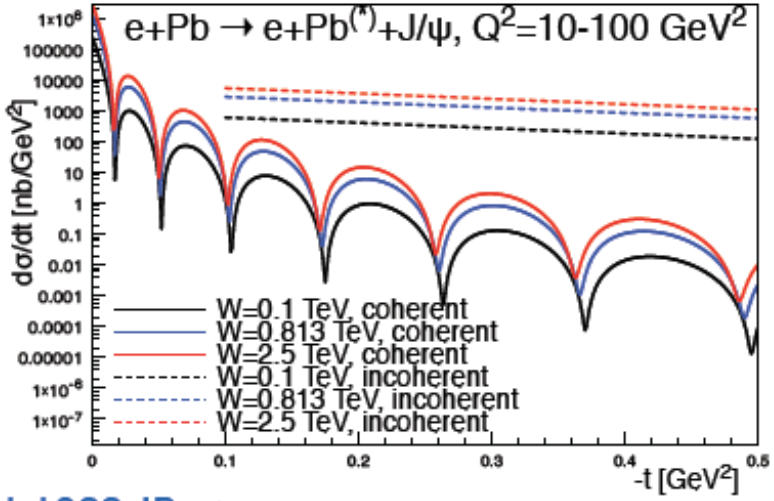
Transverse structure (II):

- Coherent versus incoherent diffraction may help to solve the issue of the existence/number of hot spots in p and A, relevant for fluctuations, azimuthal asymmetries, definition of MPIs,…









Mantysaari, 1011.1988, IPsat

The LHeC pseudodata

- Assume $\mathcal{L}_{\mathrm{ep}} = 10\,\mathrm{fb}$, $\mathcal{L}_{\mathrm{ePb}} = 1\,\mathrm{fb}$ (per nucleon)
- Considered energy configs: $\sqrt{s_{\mathrm{p}}} = 7\,\mathrm{TeV}$, $\sqrt{s_{\mathrm{Pb}}} = 2.75\,\mathrm{TeV}$ (per nucleon) on $E_e = 60\,\mathrm{GeV}$ electrons.
- The pseudodata are here obtained from ratios of reduced cross sections σ^i_{ePb}, σ^i_{ep} and relative point-to-point ($\delta^i_{\mathrm{uncor.}}$) and normalization ($\delta^i_{\mathrm{uncor.}}$) uncertainties as

$$R_i = R_i(EPS09) \times \left[1 + \delta^i_{\mathrm{uncor.}} r^i + \delta_{\mathrm{norm.}} r^{\mathrm{norm.}}\right]$$

  where

$$R_i(EPS09) = \frac{\sigma^i_{\mathrm{ePb}}(CTEQ6.6 + EPS09)}{\sigma^i_{\mathrm{ep}}(CTEQ6.6)},$$

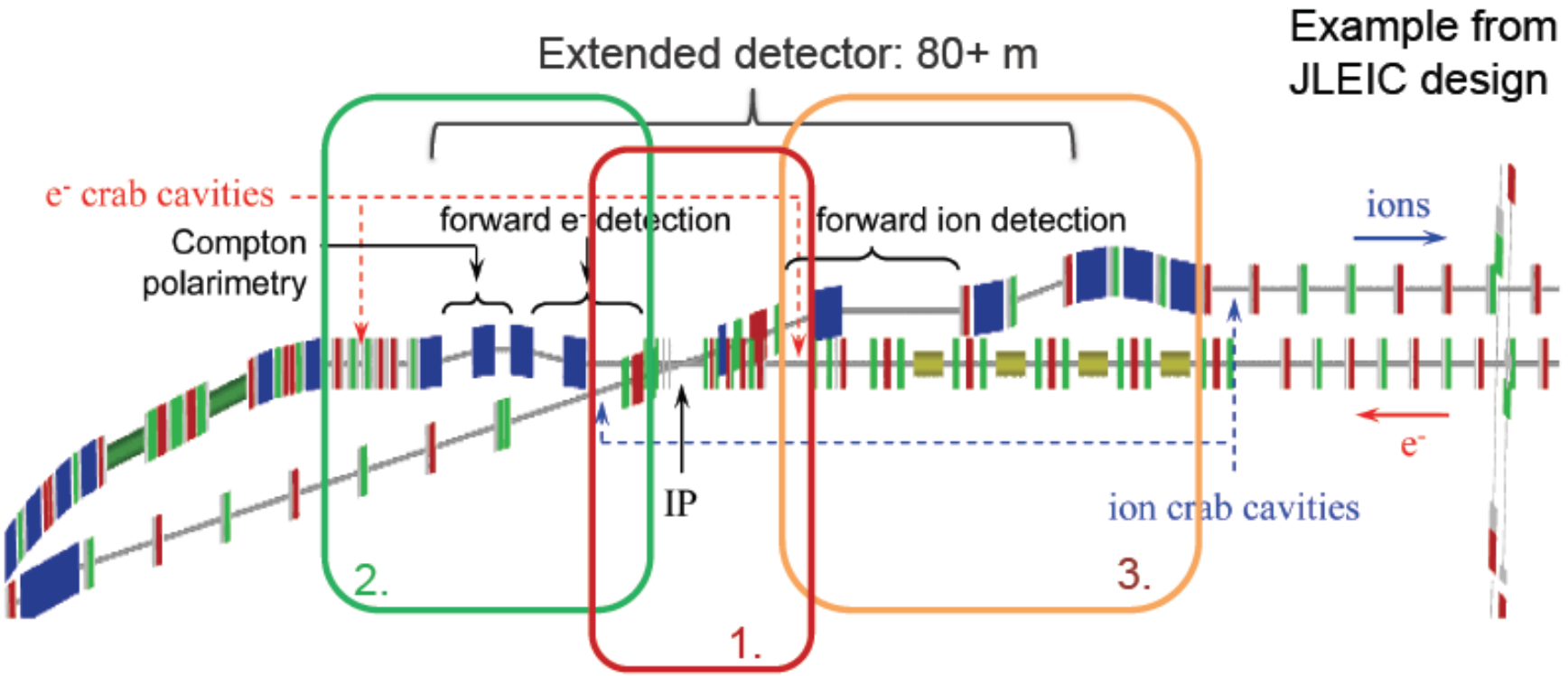
  and r^i and $r^{\mathrm{norm.}}$ are Gaussian random numbers.
- In EPS09 $R_{u_{\mathrm{V}}} \approx R_{d_{\mathrm{V}}}$, $R_{\overline{u}} \approx R_{\overline{d}} \approx R_{\overline{s}}$ (free in EPPS16, but would not expect large deviations from this)
- EPS09 and CTEQ6.6 used only in generating the pseudodata.

EIC Forward Proton Spectrometer

- Beamline instrumentation intrinsic to design from outset
- Many possible access points:

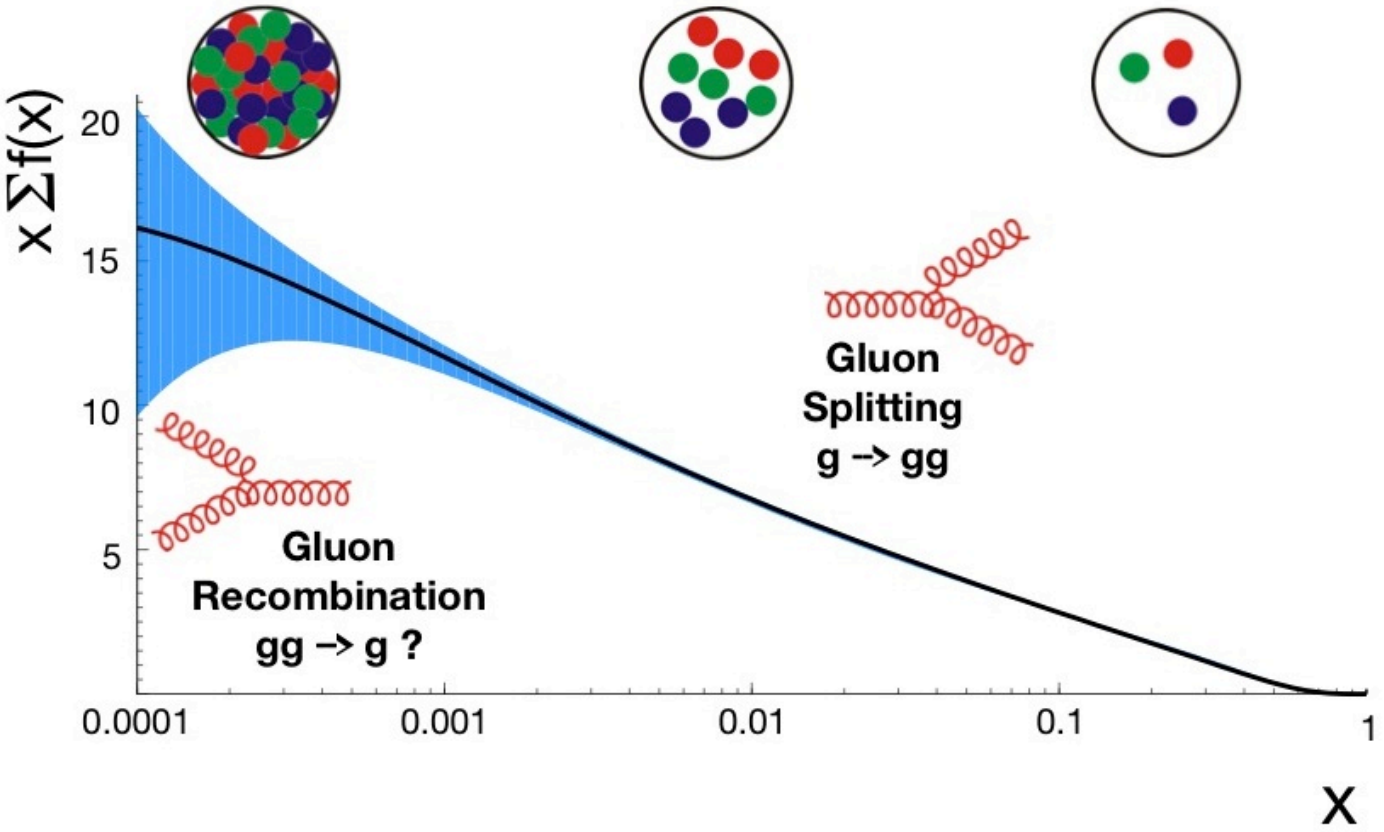
  4m , 18m, 38m at eRHIC

  12m – 45m at JLEIC



Low-x Physics and Parton Saturation

• Somewhere & somehow, the low x growth of cross sections must be tamed to satisfy unitarity … non-linear effects

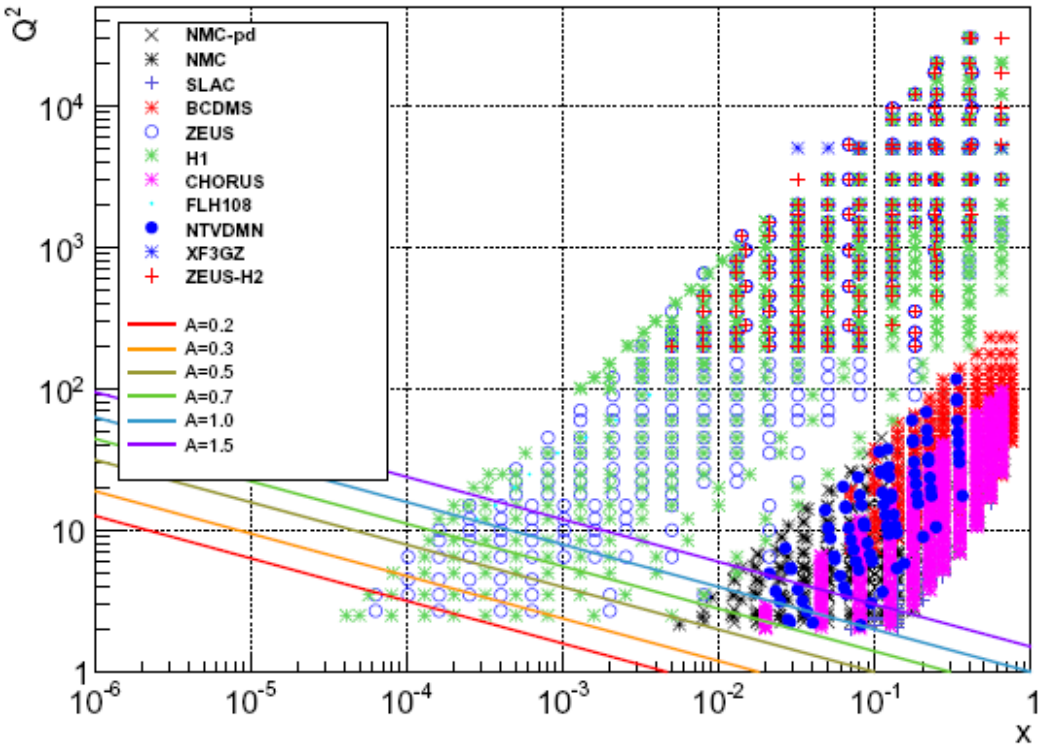


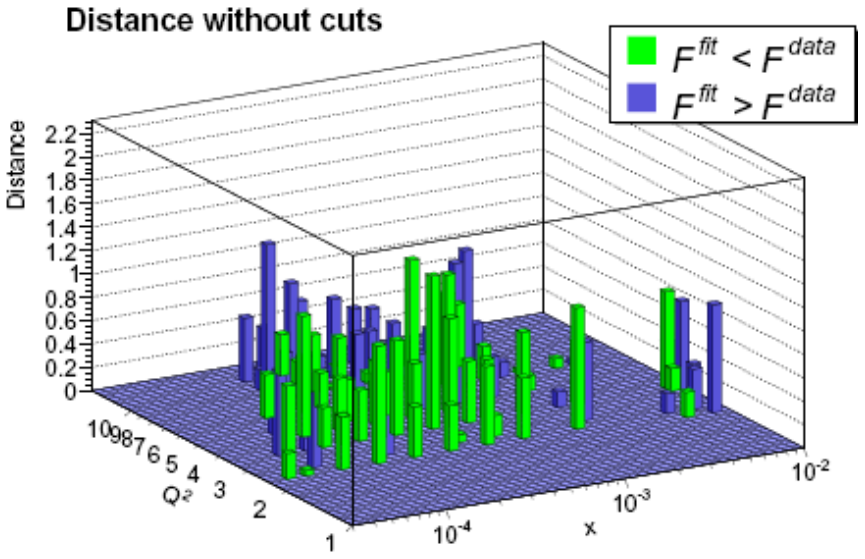
→new high density, small coupling parton regime of non-linear parton evolution dynamics

• x dependent "saturation scale", $Q^2_s(x)$ and dynamics of onset not well known theoretically:

$$\frac{xG_A(x,Q_s^2)}{\pi R_A^2 Q_s^2} \sim 1 \Longrightarrow Q_s^2 \propto A^{1/3} x^{\sim -0.3}$$

e.g. NNPDF study of low Q^2 NLO DGLAP



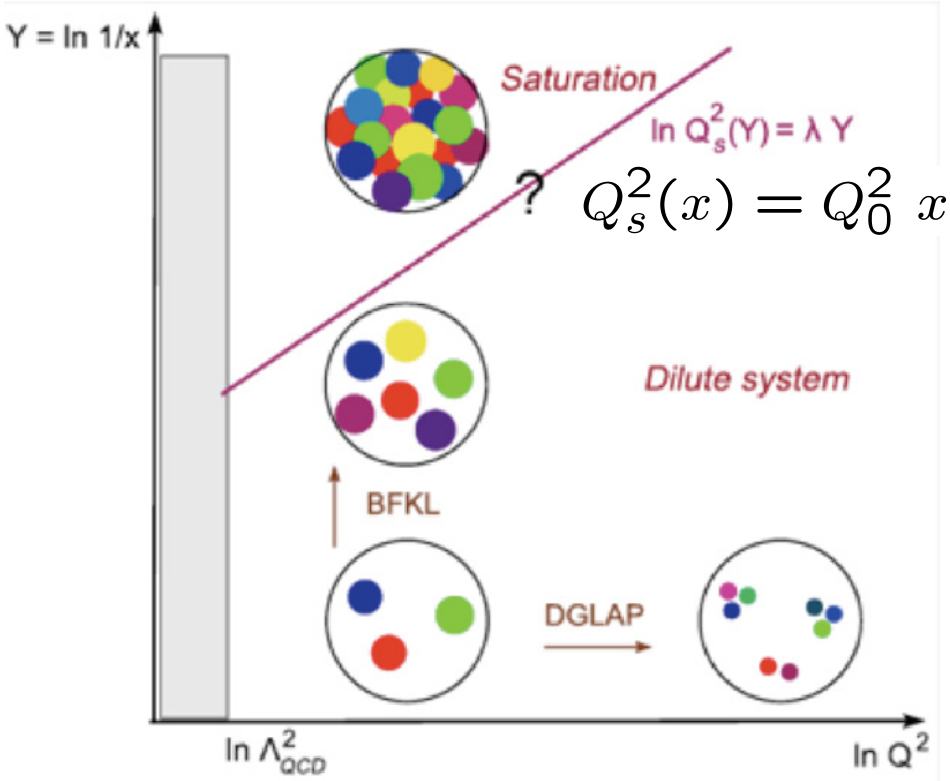


- Fit HERA data in limited regions above lines of $Q^2 > Ax^{-0.3}$
  → backwards evolve to lower scales and compare χ^2
- Signed pulls show backward evolution consistently above data

… something happens, but not easily interpreted …

A	$\chi^2_{\text{without cuts}}/d.o.f.$	$\chi^2_{\text{cut}}/d.o.f$
0.5	$19.68/25 = 0.79$	$106.22/25 = 4.25$
1.0	$54.41/44 = 1.24$	$138.24/44 = 3.14$
1.5	$62.31/59 = 1.06$	$860.65/59 = 14.6$

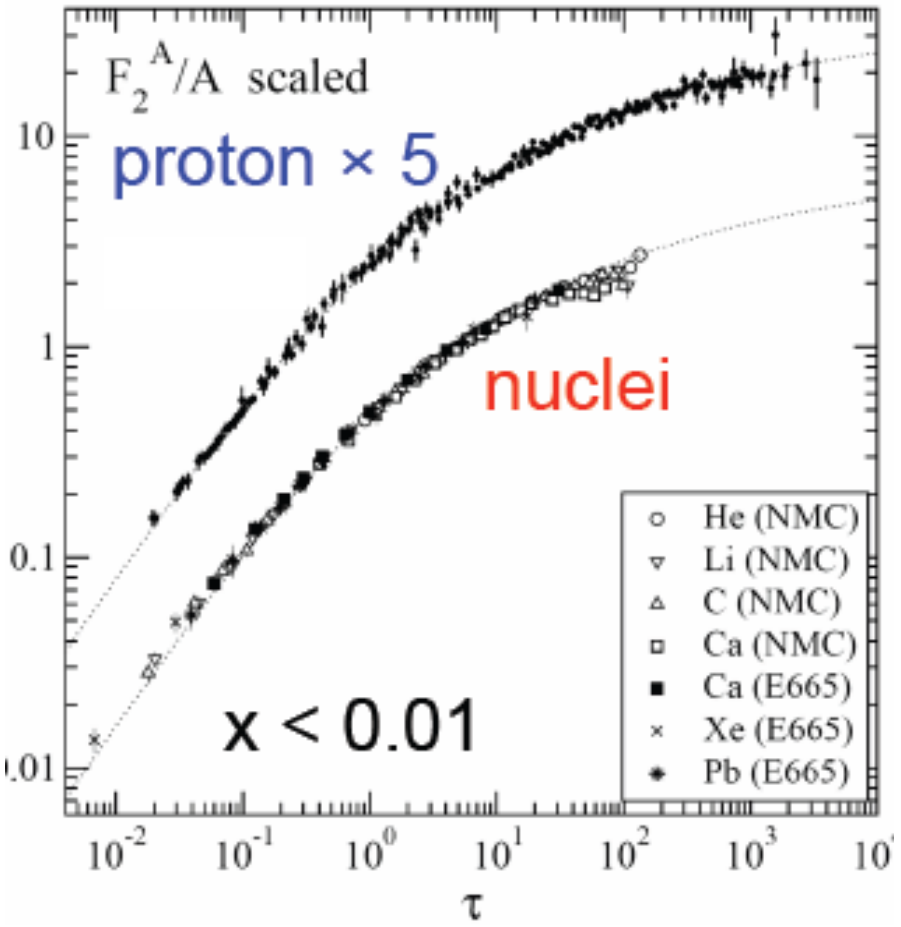
Non-linear effects in HERA and eA Data?



$$Q_s^2(x) = Q_0^2\ x^{-\lambda}$$

Lines of constant 'blackness' diagonal … scattering cross section appears constant along them … "Geometric Scaling"

$$\sigma_{tot}^{\gamma^* h \to X}(x, Q^2) = \sigma_{tot}^{\gamma^* h \to X}(Q^2/Q_s^2(x))$$

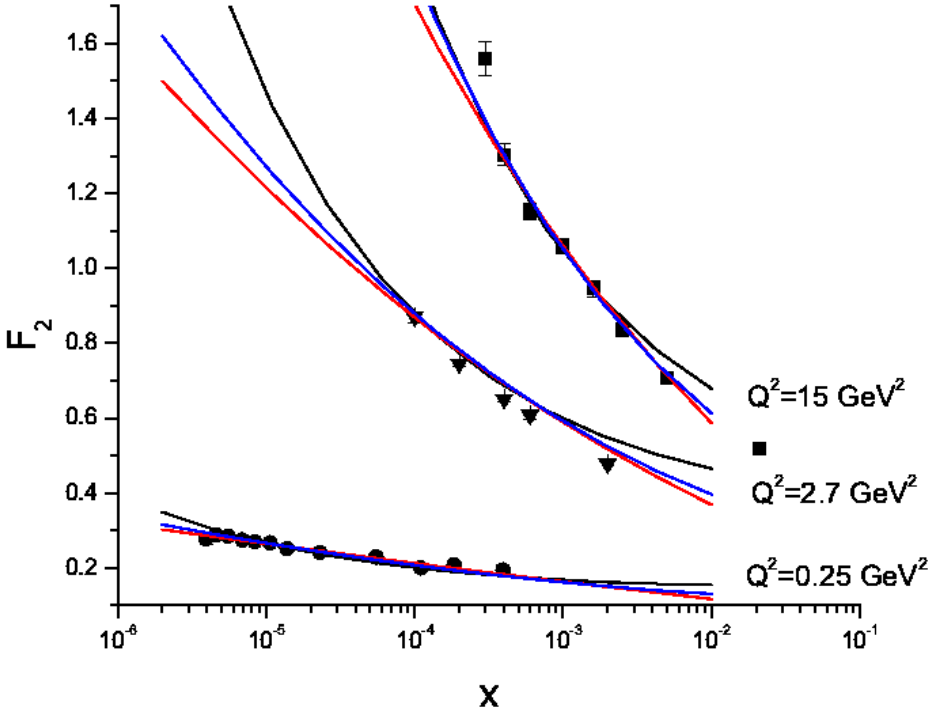


Something appears to happen around $\tau = Q^2/Q^2_s = 1$
(confirmed in many analyses)
BUT … Q^2 small for τ <~ 1
… not easily interpreted in QCD

Parton Saturation after HERA?

e.g. Forshaw, Sandapen, Shaw
hep-ph/0411337,0608161
… used for illustrations here

Fit inclusive HERA data
using dipole models
with and without parton
saturation effects

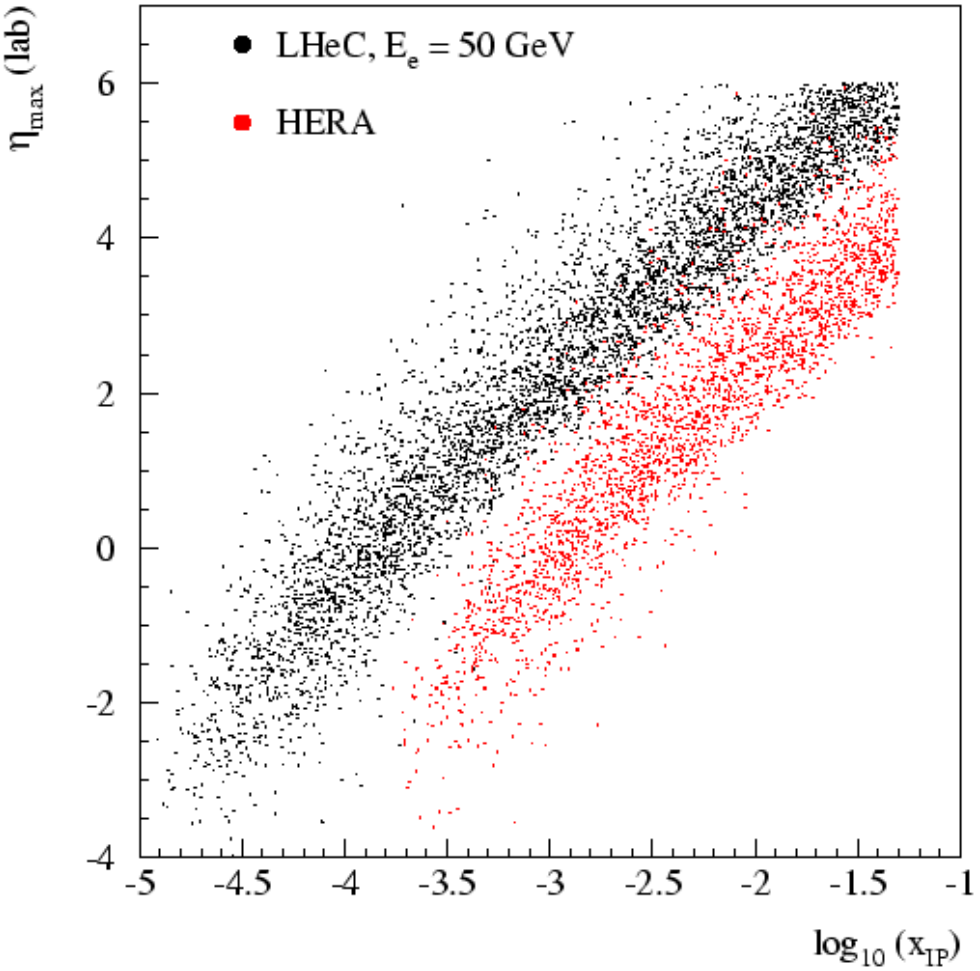


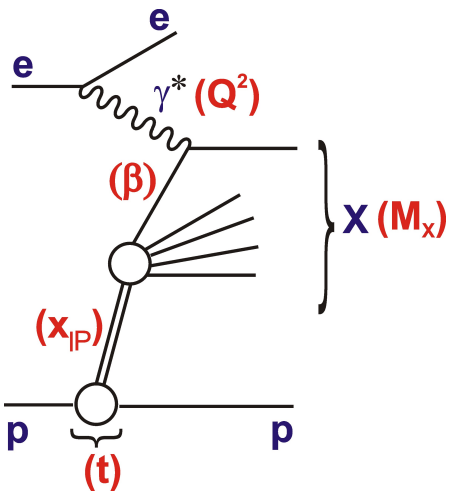
FS04 Regge (~FKS): 2 pomeron model, no saturation
FS04 Satn: Simple implementation of saturation
CGC: Colour Glass Condensate version of saturation

- All three models can describe data with $Q^2 > 1\text{GeV}^2$, $x < 0.01$
- Only versions with saturation work for $0.045 < Q^2 < 1\ \text{GeV}^2$

… any saturation at HERA not easily interpreted partonically

Rapidity Gap Selection

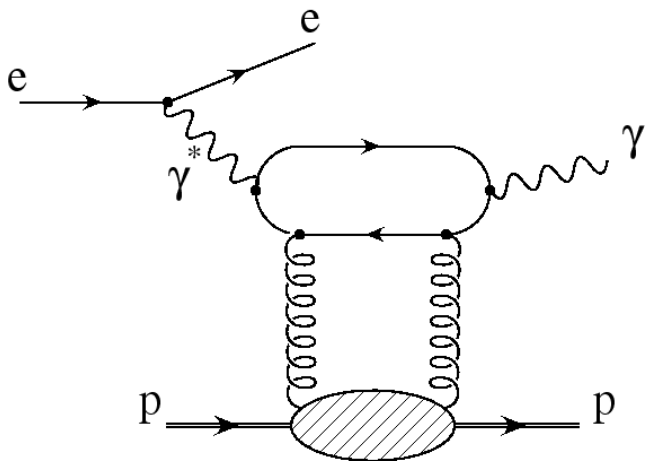




– η_{max} v ξ correlation entirely determined by proton beam energy

- Cut around $\eta_{max} \sim 3$ selects events with $x_{IP} <\sim 10^{-3}$ at LHeC (cf $x_{IP} <\sim 10^{-2}$ at HERA

Deeply Virtual Compton Scattering



- No vector meson wavefunction complications

- Cross sections suppressed by photon coupling

→ limited precision at HERA

→ would benefit most from high lumi of LHeC and EIC

LHeC Simulations based on FFS model in MILOU generator

→ Double differential distributions in (x, Q^2) with

1^o and 10^o cuts for scattered electron

→Kinematic range determined largely by cut on p_T^{γ}

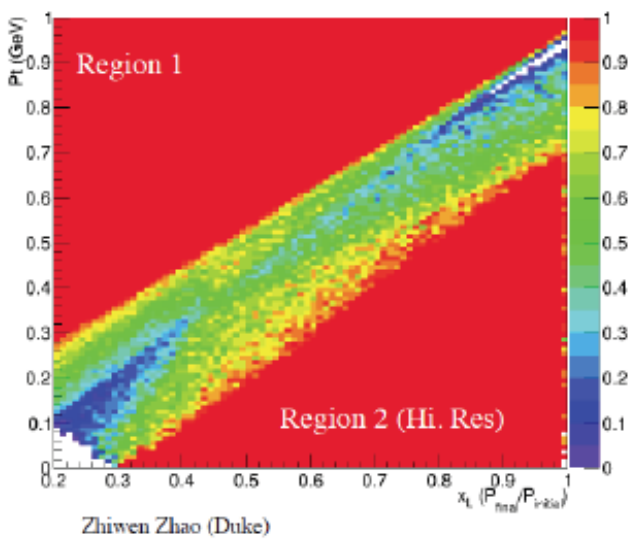
(relies on ECAL performance / linearity at low energies)

EIC Forward Proton Spectrometer

Full Acceptance for Forward Physics!

Example: acceptance for p' in e + p → e' + p' + X

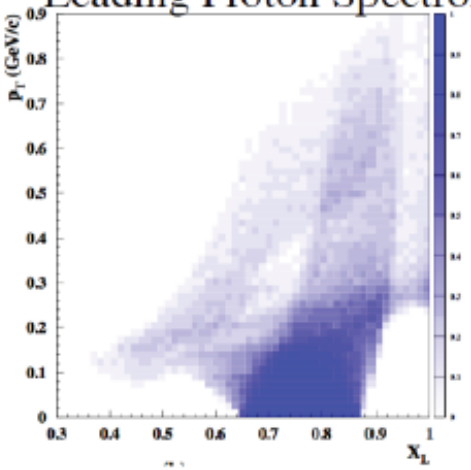
JLEIC acceptance



Zhiwen Zhao (Duke)

ZEUS

Leading Proton Spectrometer

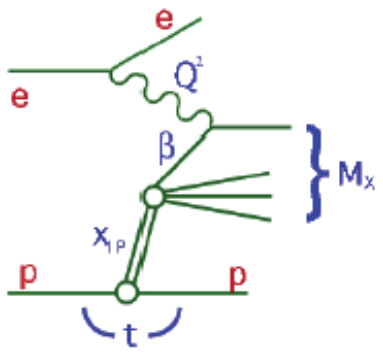


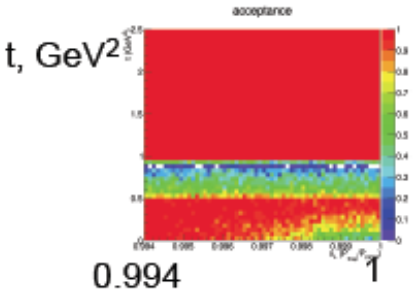
Acceptance in diffractive peak (X_L>~.98)

ZEUS: ~2%

JLEIC: ~100% (also covers much higher X_L than ZEUS)

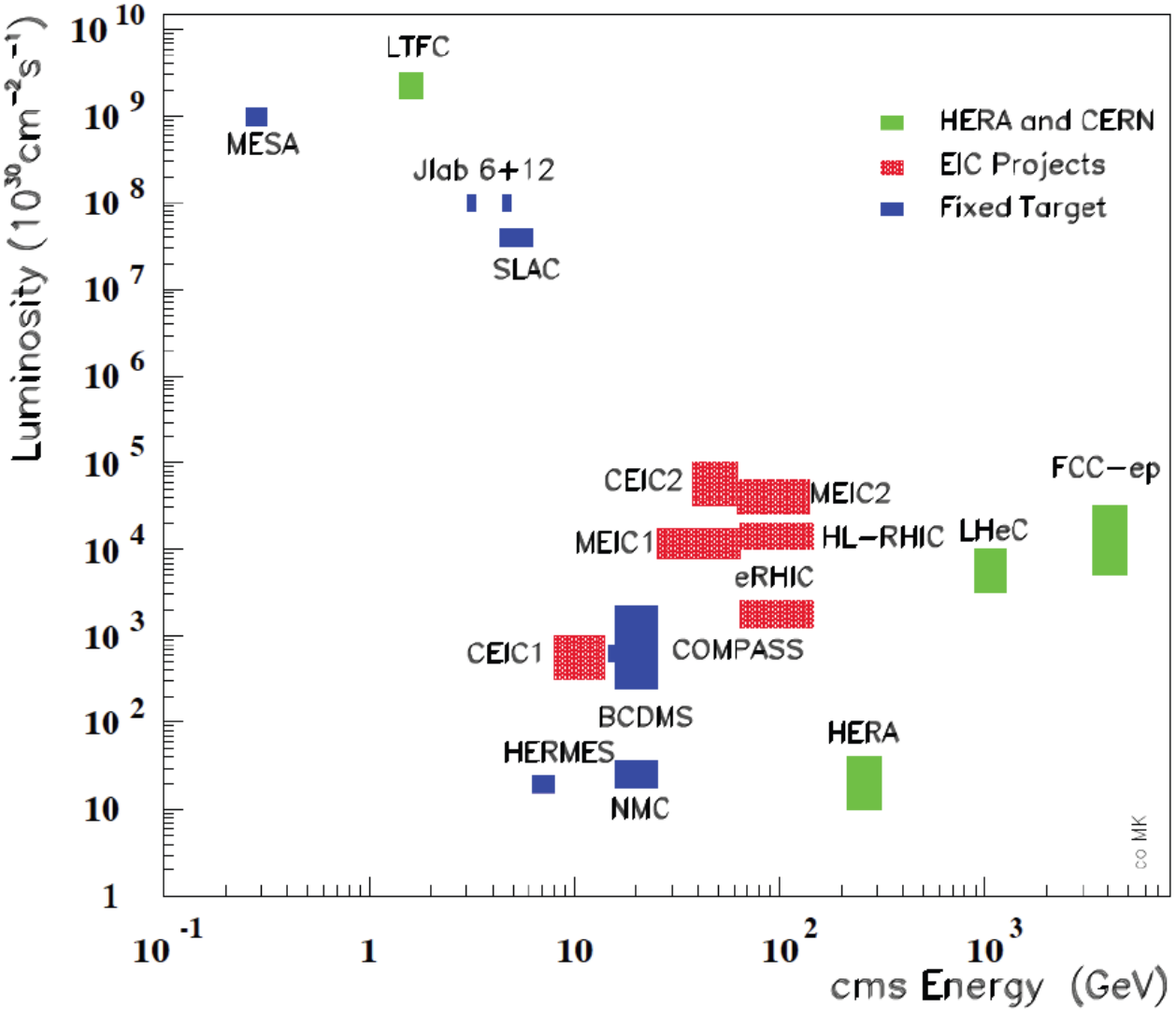
Diffraction





These detectors came of age at LHC: we should be ambitious

LHeC / FCC-he Context



Main weakness: No polarised hadrons

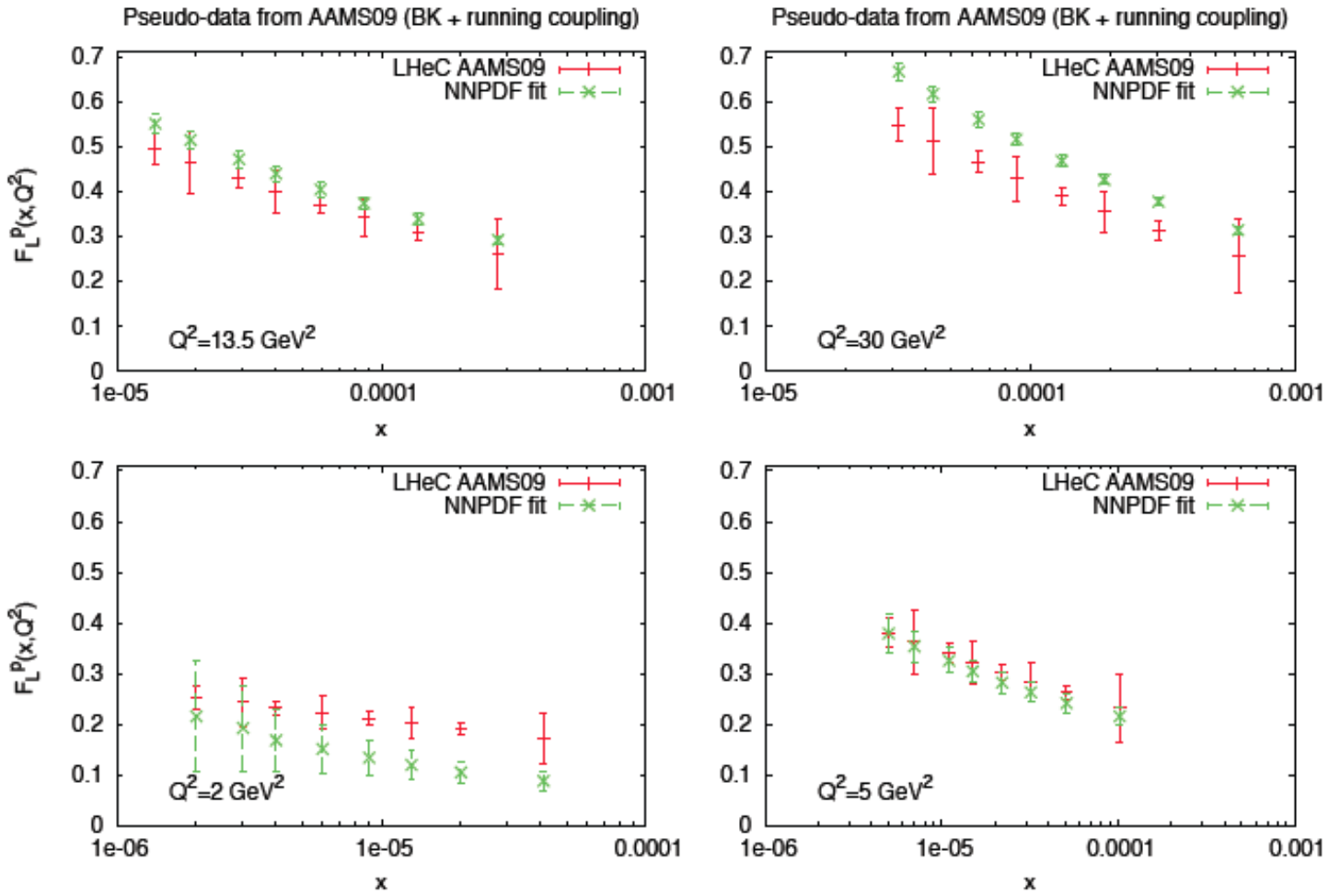
Lepton-hadron scattering at the TeV scale …

LHeC: 60 GeV electrons x LHC protons & ions
→ 10^{34} cm^{-2} s^{-1}
→ Simultaneous running with ATLAS / CMS sometime in HL-LHC period

FCC-he: 60 GeV electrons x 50 TeV protons (and corresponding ions) from FCC

Establishing Saturation in Inclusive Data

(Lack of) quality of NNPDF fit to F_2 and F_L pseudodata with saturation effects included …



• Unambiguous observation of saturation will be based on tension between different observables e.g. F_2 v F_L in ep or F_2 in ep v eA

Polarized p+A Physics at Forward Rapidity at STAR









Akio Ogawa for the STAR collaboration
Brookhaven National Laboratory

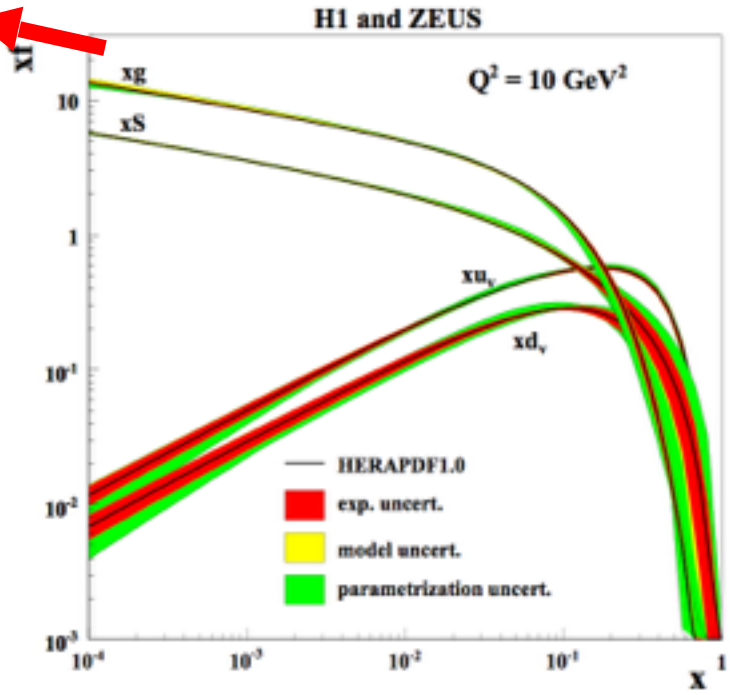
2017 April 26
RBRC workshop @ BNL

Contents

1. Introduction - Gluon saturation and RHIC pA
2. STAR Forward Calorimeter
3. Results - Single Spin Asymmetry at pA
4. Status – Di-hadron azimuthal correlation
5. Summary and outlook

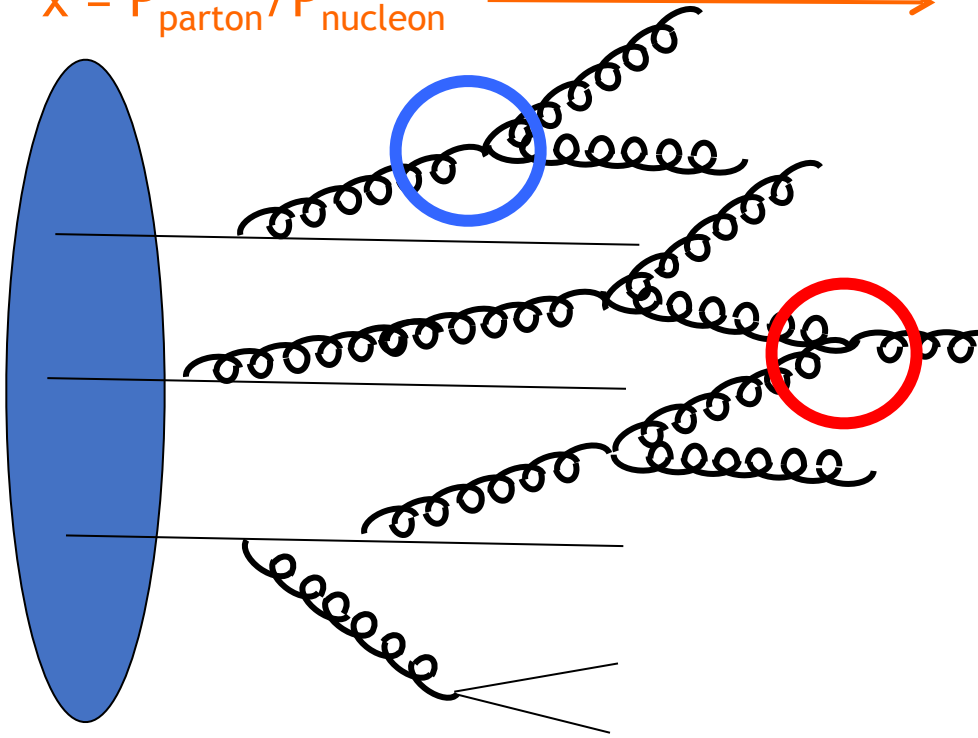
Gluon Density at Low x

Gluon density can't grow forever



JHEP 1001:109,2010 H1 and Zeus

$x = P_{parton}/P_{nucleon}$ small x



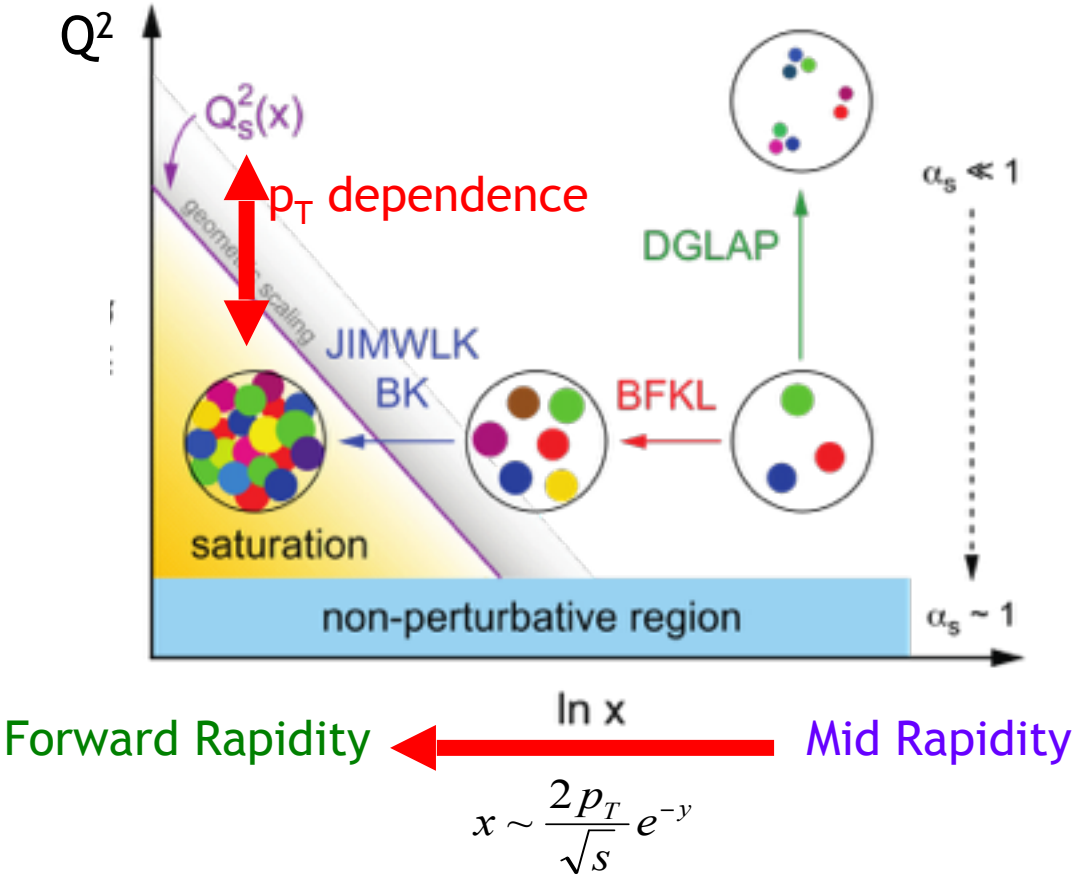
Bremsstrahlung
~ $s_s \ln(1/x)$

Recombination
~ $\sigma_s \rho$

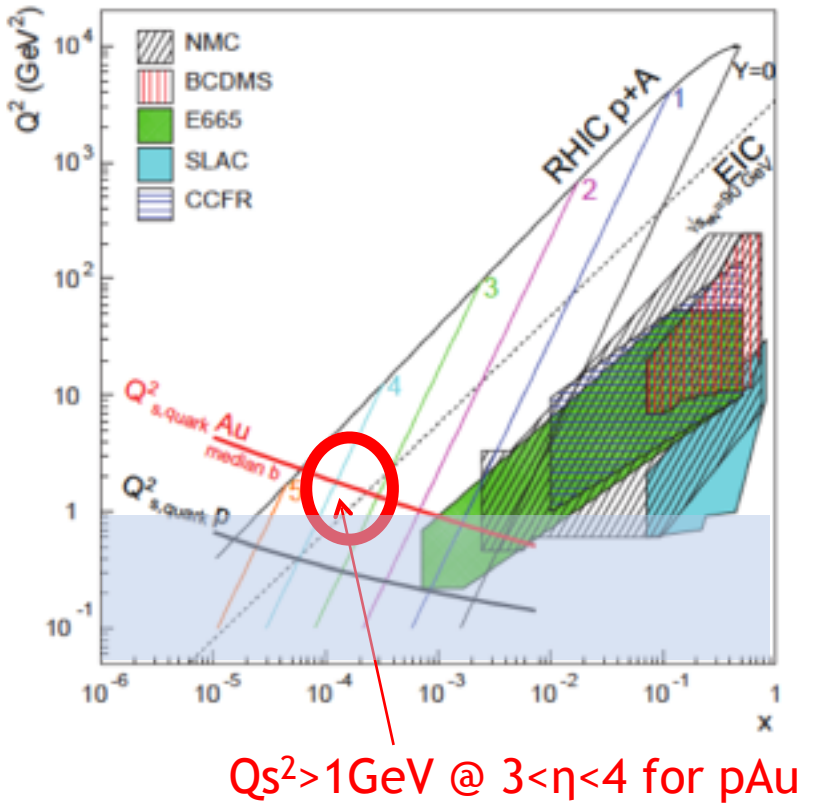
Rapid rise in gluon density described by linear DGLAP & BFKL pQCD evolution

But saturation must set in at low-x when gluons start to overlap and when recombination becomes important

Gluon Saturation



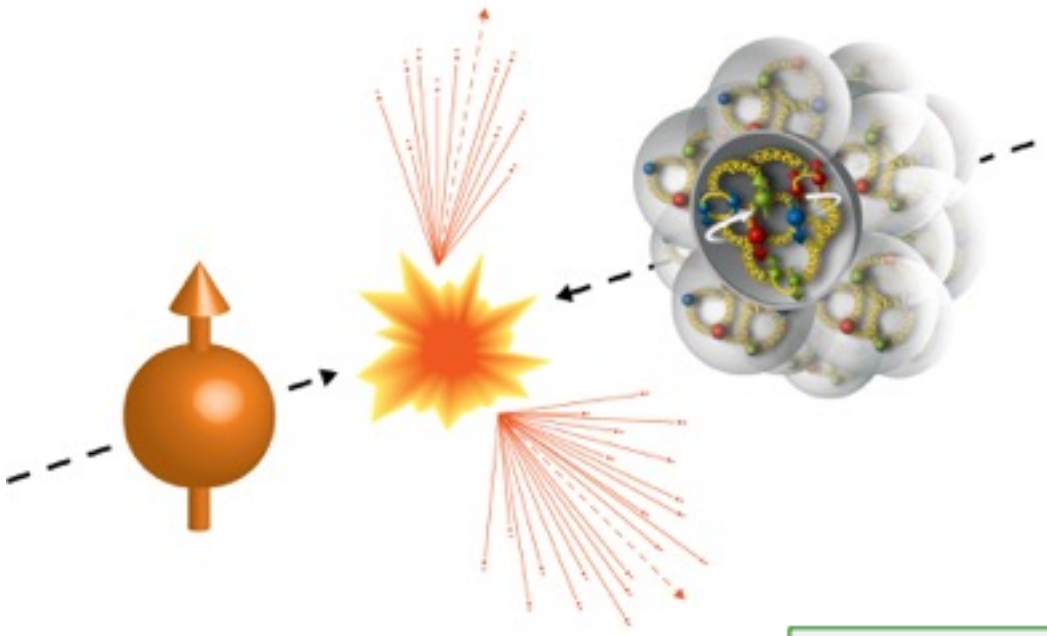
$$x \sim \frac{2p_T}{\sqrt{s}} e^{-y}$$



Qs^2>1GeV @ 3<η<4 for pAu

- Non-linear pQCD evolution equations provide a natural way to tame this growth and lead to a saturation of gluons, characterized by the saturation scale $Q_s^2(x)$
- RHIC can reach in pA collisions the saturation region at forward rapidity
- p_T scan and rapidity/x scan may allow to cross saturation scale $Q_s^2(x)$

Polarized p+A @ RHIC



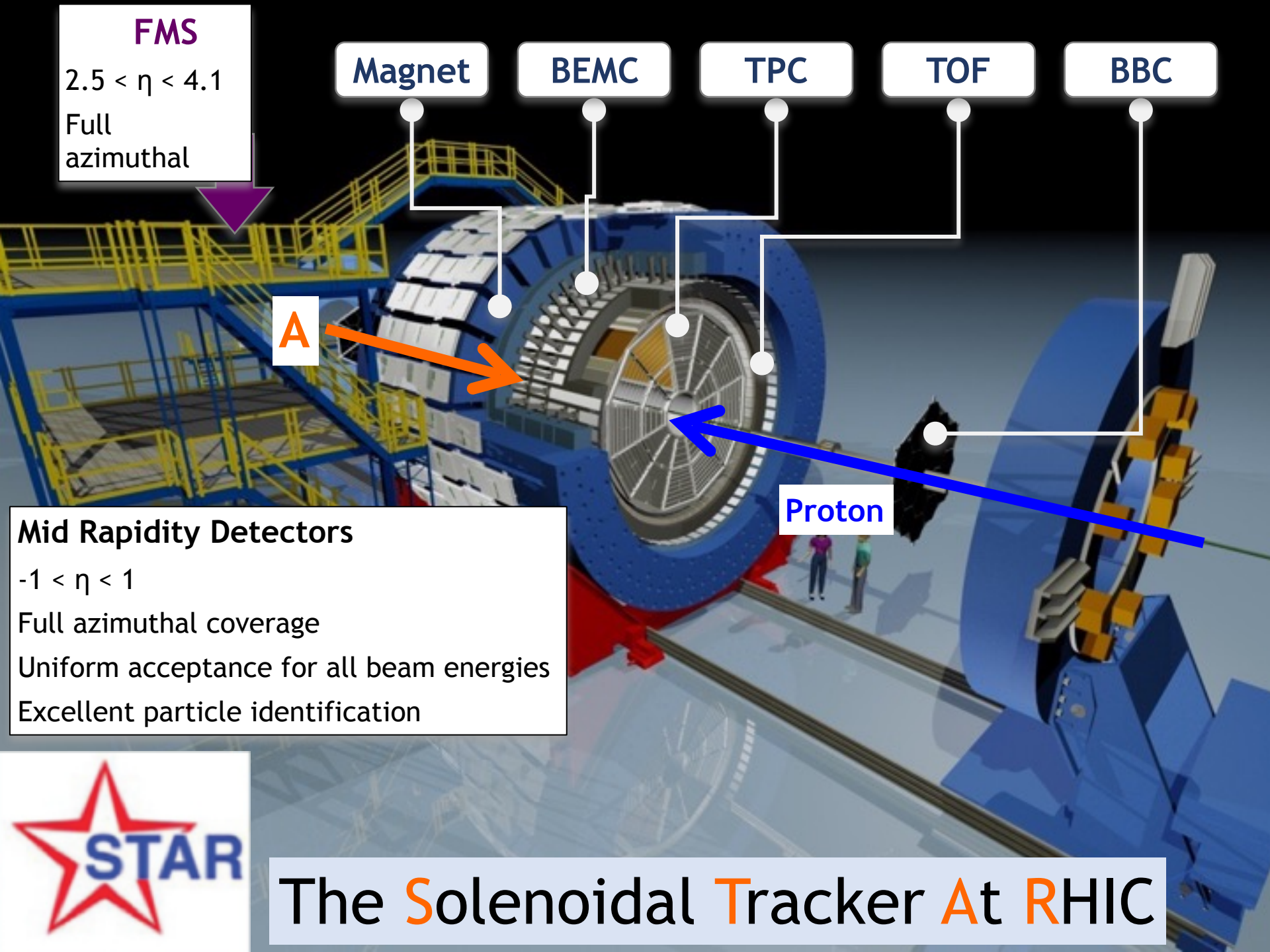
- Polarized protons
- Scanning A → Au, Al, …
- Forward rapidity hadron production
  - can access to low-x gluons
  - with highly polarized & high-x quark probe

Transverse Spin

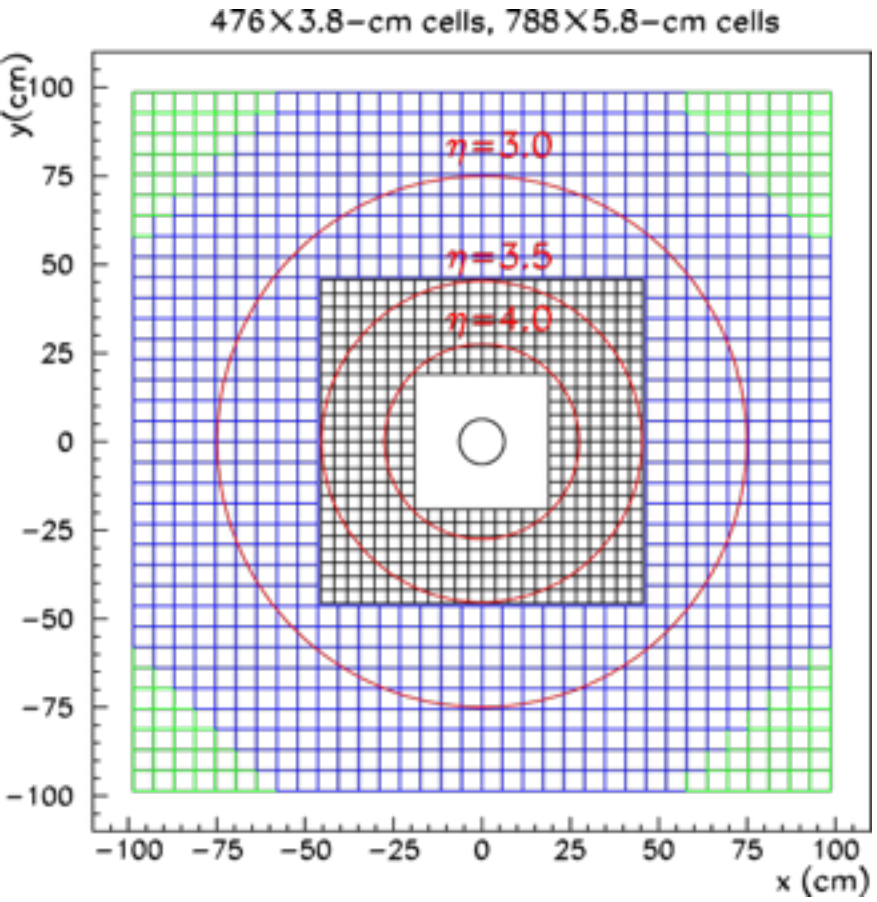
RHIC 2015

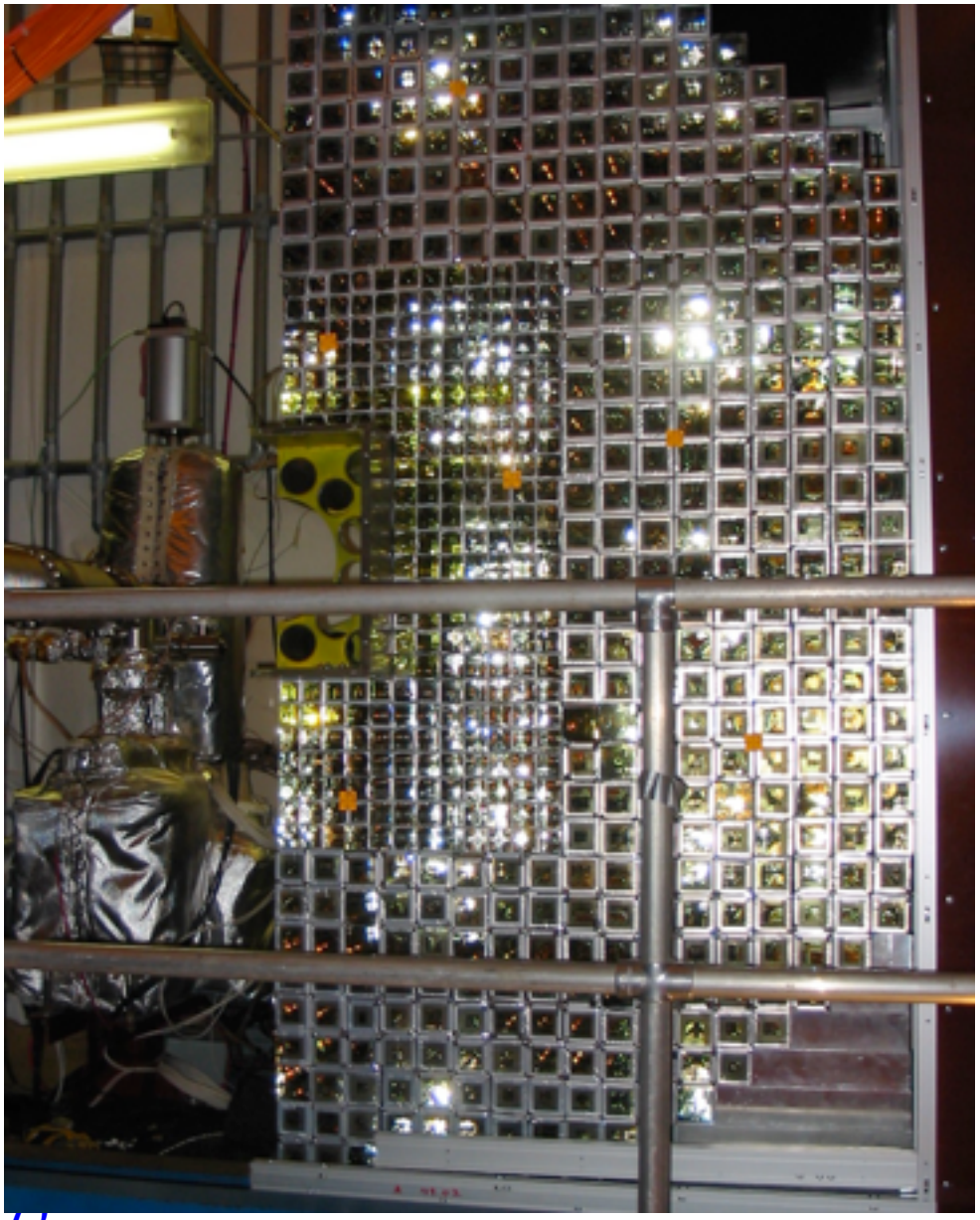
- $\vec{p} + p, L_{\text{int}} = 40 + 50\ \text{pb}^{-1}$
- $\vec{p} + Al, L_{\text{int}} = 1.0\ \text{pb}^{-1}$
- $\vec{p} + Au, L_{\text{int}} = 0.45\ \text{pb}^{-1}$

RHIC offers unique opportunities to study low-x gluon and gluon saturation signatures in transverse single spin asymmetries A_N


FMS
2.5 < η < 4.1
Full azimuthal
Magnet
BEMC
TPC
TOF
BBC
A
Proton
Mid Rapidity Detectors
-1 < η < 1
Full azimuthal coverage
Uniform acceptance for all beam energies
Excellent particle identification
STAR
The Solenoidal Tracker At RHIC

STAR Forward Calorimetry: FMS





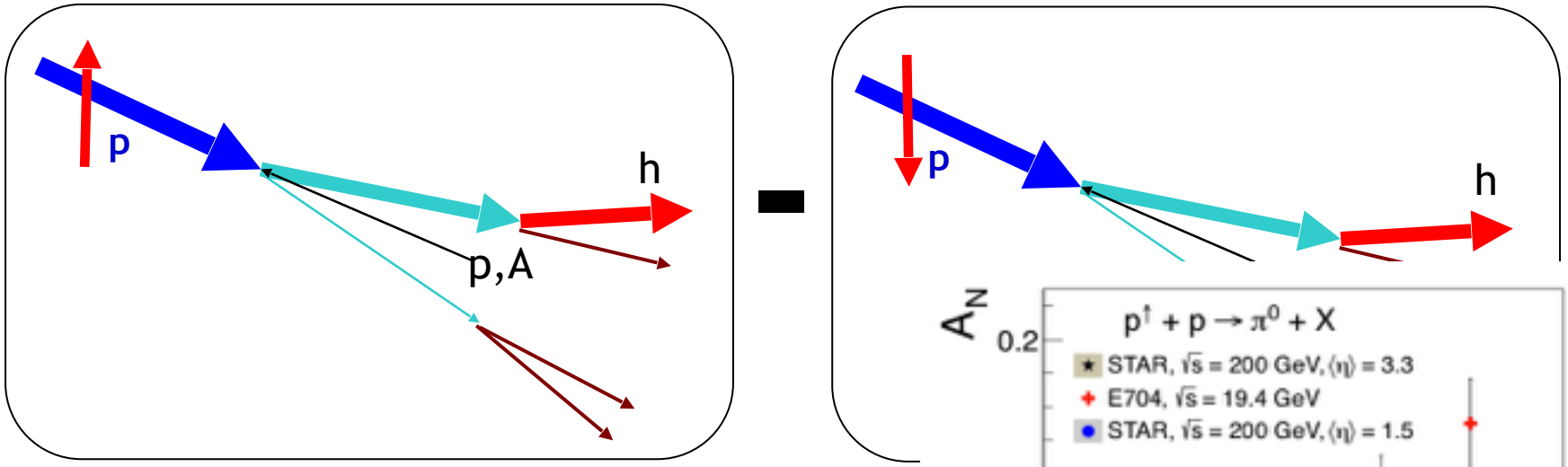
>1400 Pb glass towers with PMT readout

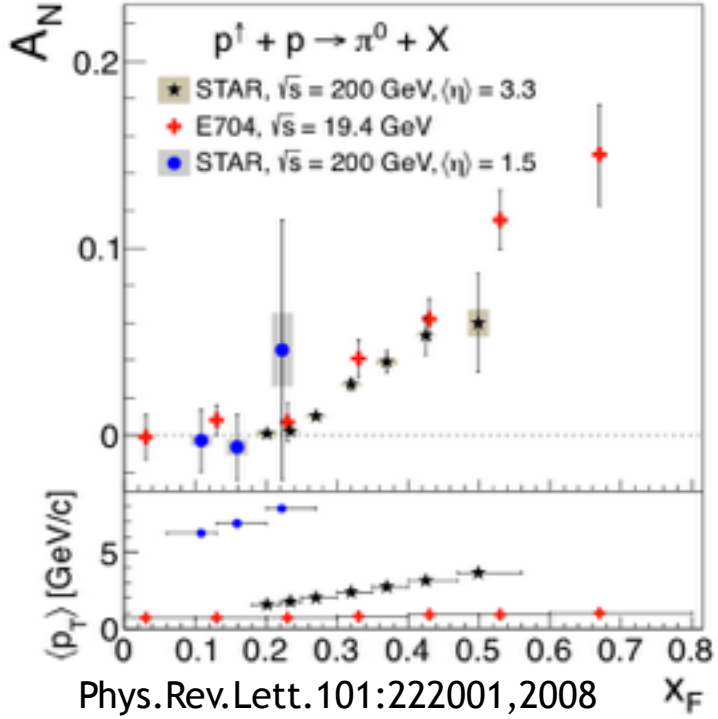
- Neutral pions / eta / EM-jet
- Direct photons with Pre-shower(2015)
- J/ψ and Drell-Yan with Post-shower(2017)

Transverse Single Spin Asymmetry (SSA) A_N at p+p

$$A_N = \frac{\sigma^{\uparrow} - \sigma^{\downarrow}}{\sigma^{\uparrow} + \sigma^{\downarrow}}$$

Left-Right Asymmetry
cos(ϕ) modulation





Phys.Rev.Lett.101:222001,2008

It requires k_T to left or right with respect t
polarization direction generated from

Initial State Effect
Nucleon Spin → Parton k_T → Hadron k_T

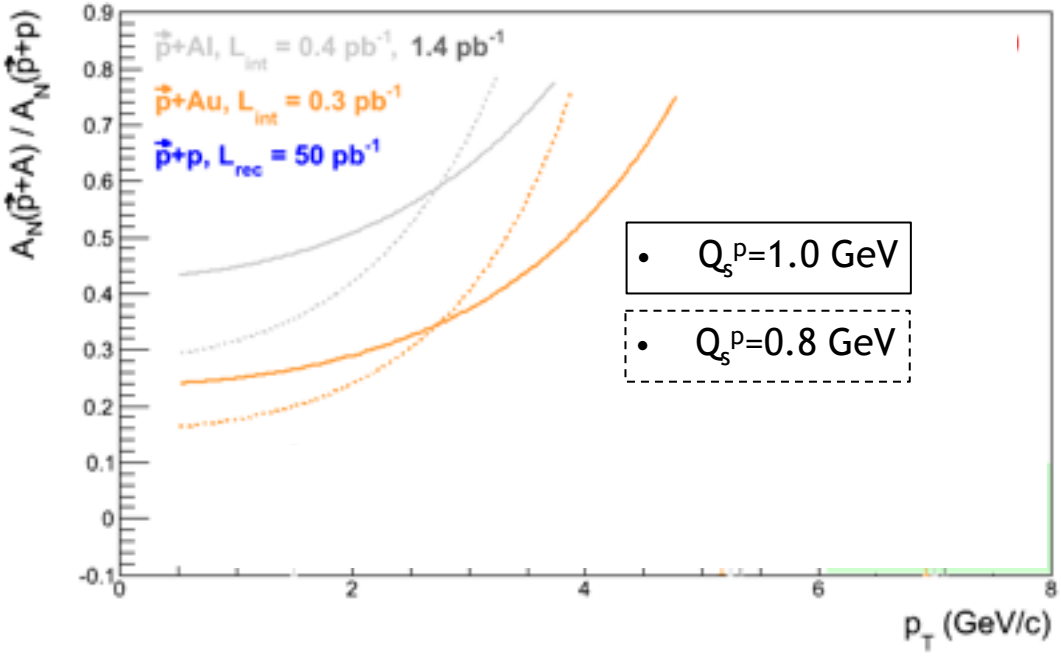
Final State Effect
Nucleon spin → Parton Spin → Hadron k_T

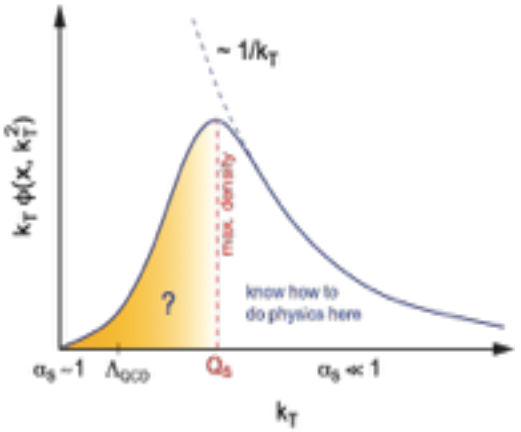
Transverse Single Spin Asymmetry (SSA) A_N at p+A

Hybrid Approach Yoshitaka Hattaa,et al, Phys. Rev. D 95, 014008 (2017)

Initial state effect in p + k_T un-integrated gluon distribution in Au + Final State effect

Odderon exchange Yuri V. Kovchegov, Matthew D. Sievert, PhysRevD.86.034028



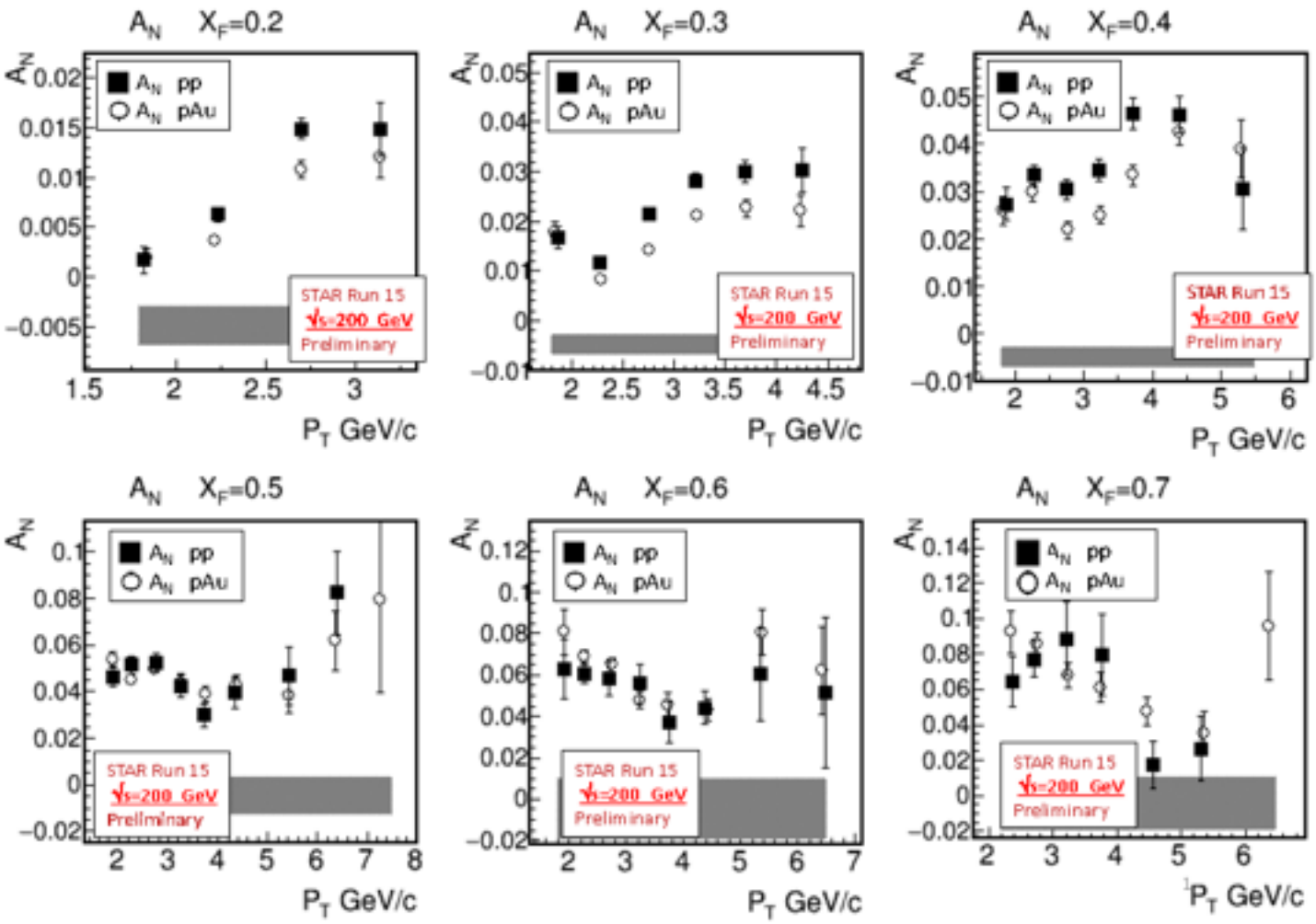


$$Q_s^A = A^{1/3} Q_s^p$$

Both models predict gluon saturation suppresses A_N by ~$A^{1/3}$

Suppression of A_N in $p^{\uparrow}$+A provides sensitivity to Q_s PhysRevD.84.034019, PhysRevD. 86.034028

First results from Polarized p+Au

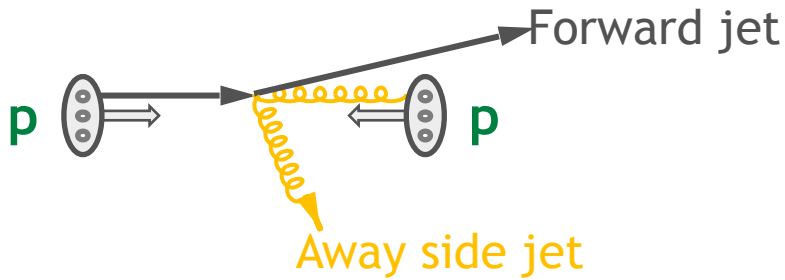


Shaded bands represent systematic uncertainty, dominated by dependence of A_N on observed BBC multiplicity → central vs. peripheral collisions

Small to no suppression is observed

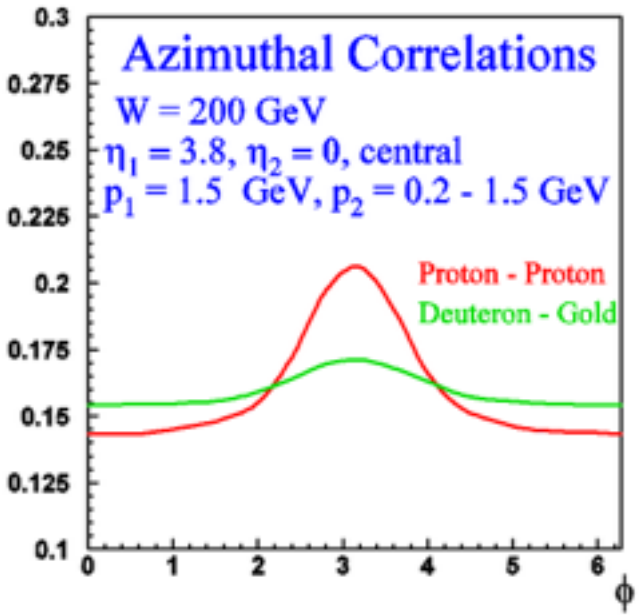
Back-to-back Angular Correlations

pQCD 2➔2 process = back-to-back di-jet (Works well for p+p)



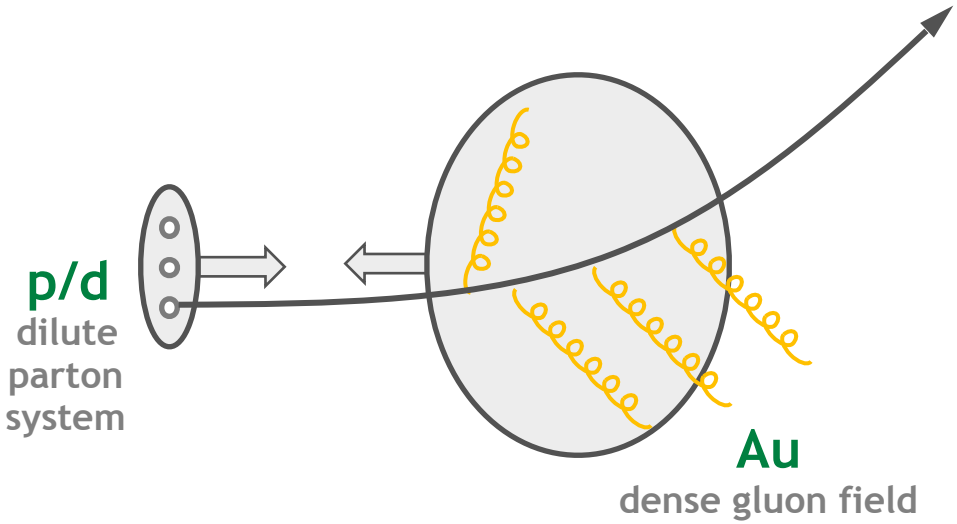
Kharzeev, Levin, McLerran

(NPA748, 627)



With high gluon density

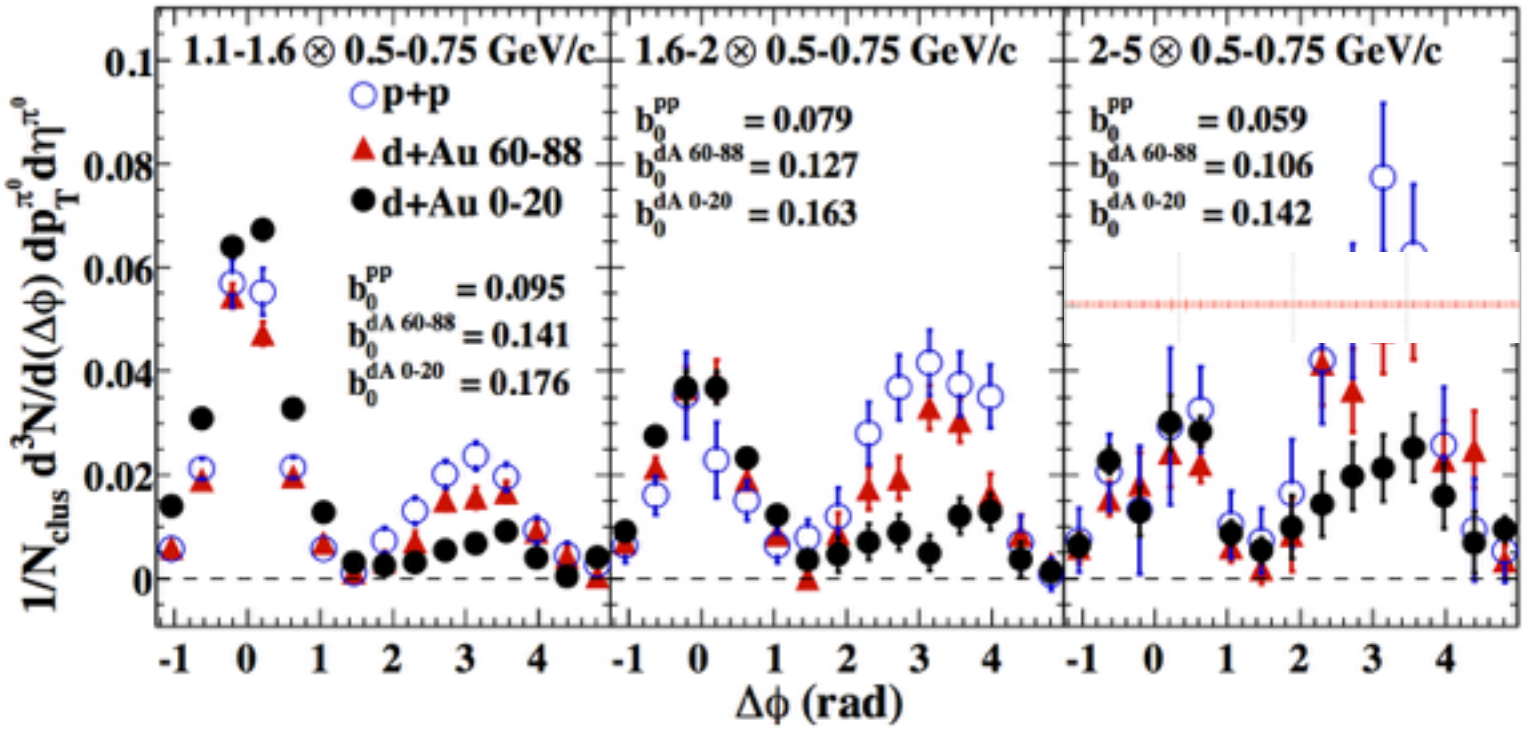
2➔1 (or 2➔many) process = Mono-jet



CGC predicts suppression of back-to-back

Back-to-back Angular Correlations

Phys. Rev. Lett. 107, 172301 (2011)



PHENIX

Cluster analysis

Run15 pA statistic

STAR year 2015 data being analyzed for

- π^0-π^0 and EM jet-EM jet correlations
- p+p, p+Al, p+Au (d+Au in 2016)
- p_T^{Trig} dependence from 1GeV ~ 3GeV
- $p_T^{Associated}$ dependence from 1GeV ~ 3GeV
- Centrality / N_{coll} dependence

We are still working on

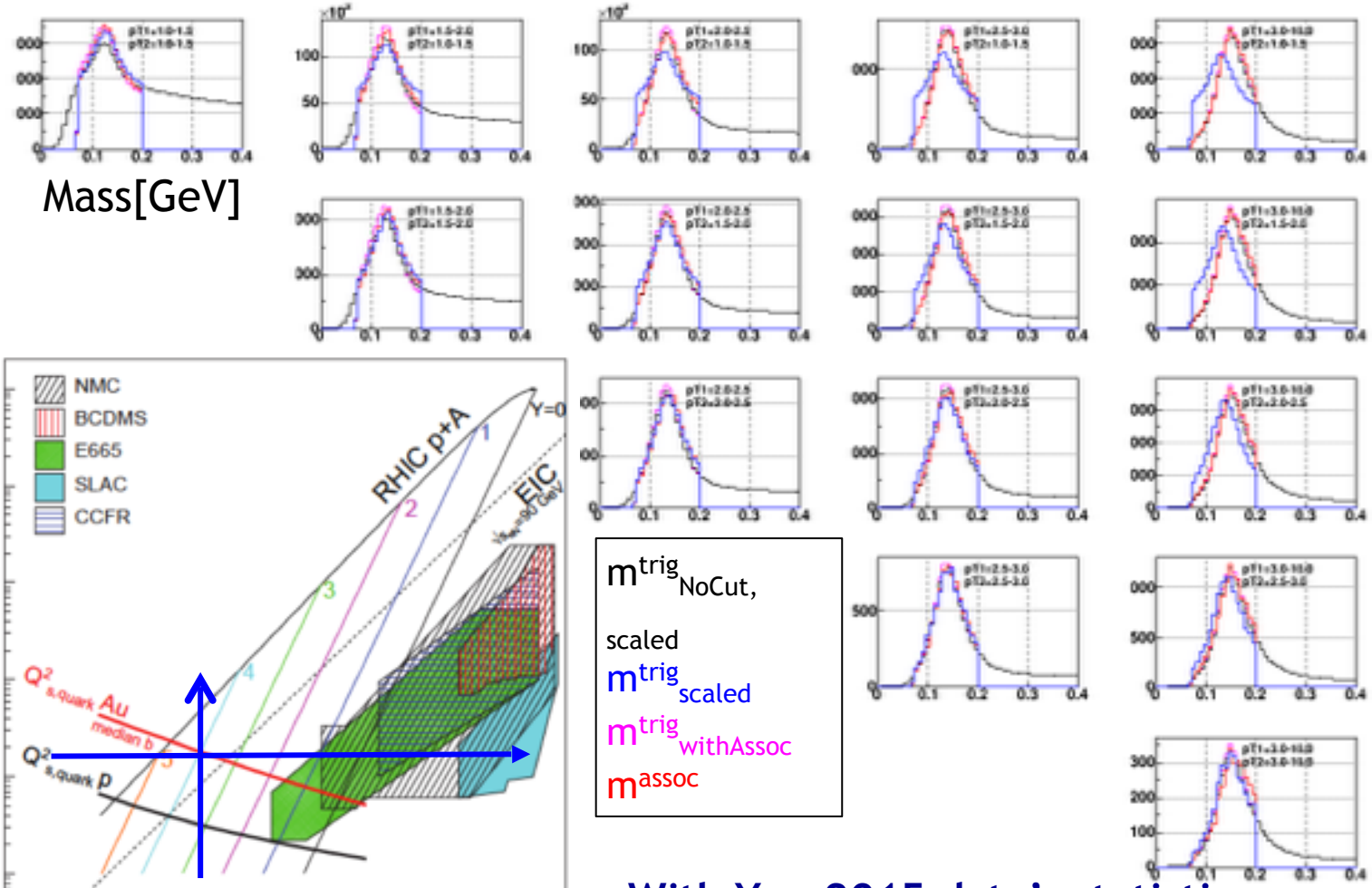
- Gain uniformity and stability
  - (This cancels out in A_N)
- STAR common Centrality / N_{coll}

Scanning in p_T and xπ^0 mass peaks in different p_T bins

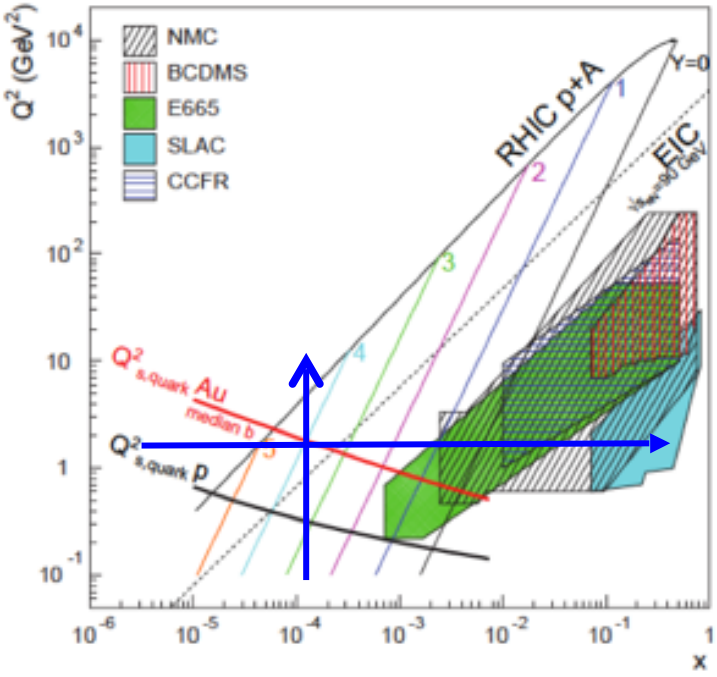
1GeV → p_T^{trig} → >3GeV

Counts

Mass[GeV]



1GeV → p_T^{assoc} → >3GeV



m^{trig}_{NoCut},

scaled

m^{trig}_{scaled}

$m^{trig}_{withAssoc}$

m^{assoc}

With Year2015 data's statistics,

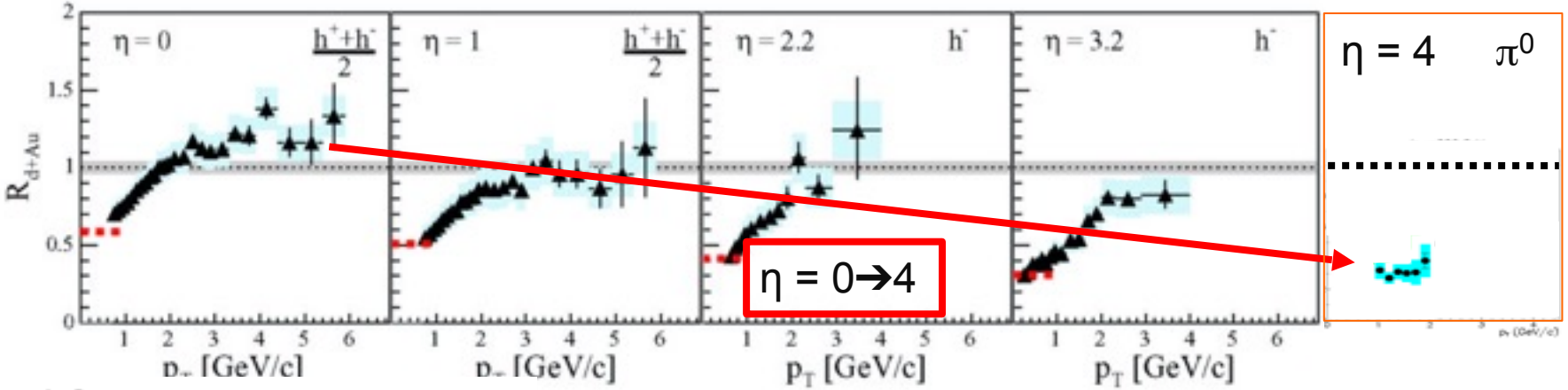
STAR can study evolution of Q_s^2 (x) with A

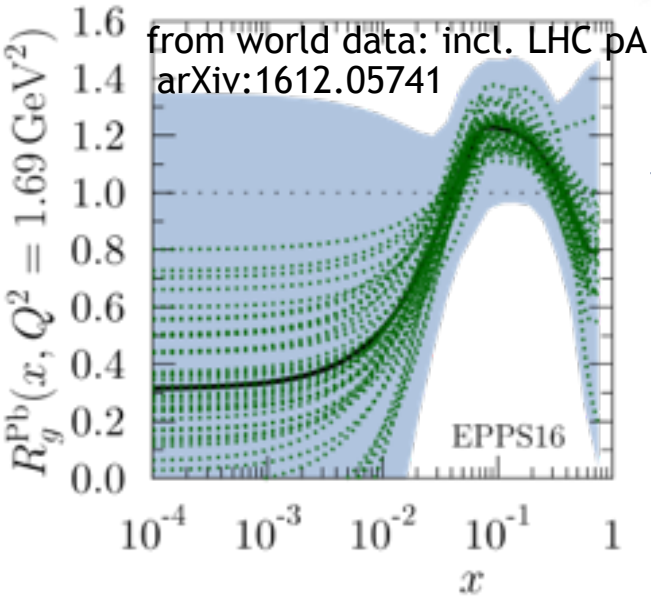
Suppression in Forward Hadron Production

$$R_{dAu} = \frac{1}{2*197}\frac{\sigma_{dAu}}{\sigma_{pp}}$$

BRAHMS PRL 93, 242303

STAR PRL 97, 152302





Observe significant rapidity dependence consistent with expectation from the CGC

World data on nuclear gluon PDF has large uncertain

Work in progress for R_{pA} from Year 2015 data

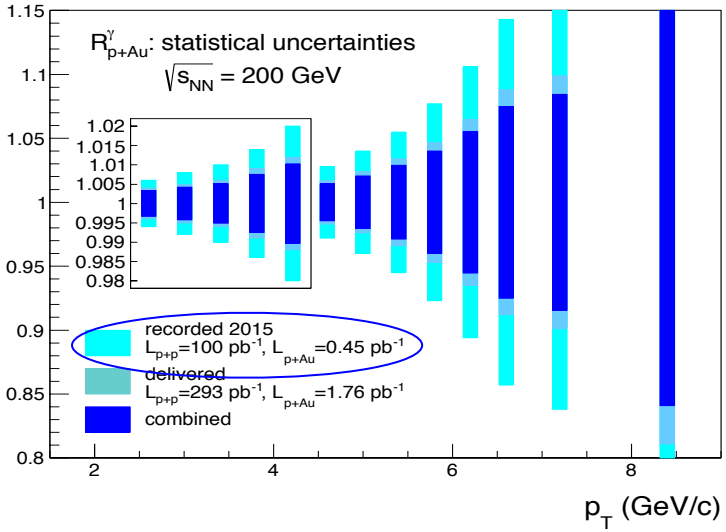
- R_{pAu} and R_{pAl}
- Pi0 and photon final state
- eta 2.7 to 3.9

Leading and Higher Twist Shadowing

STAR ideal experiment to separate
leading twist → nPDF
from higher twist shadowing → CGC
without the complication of fragmentation

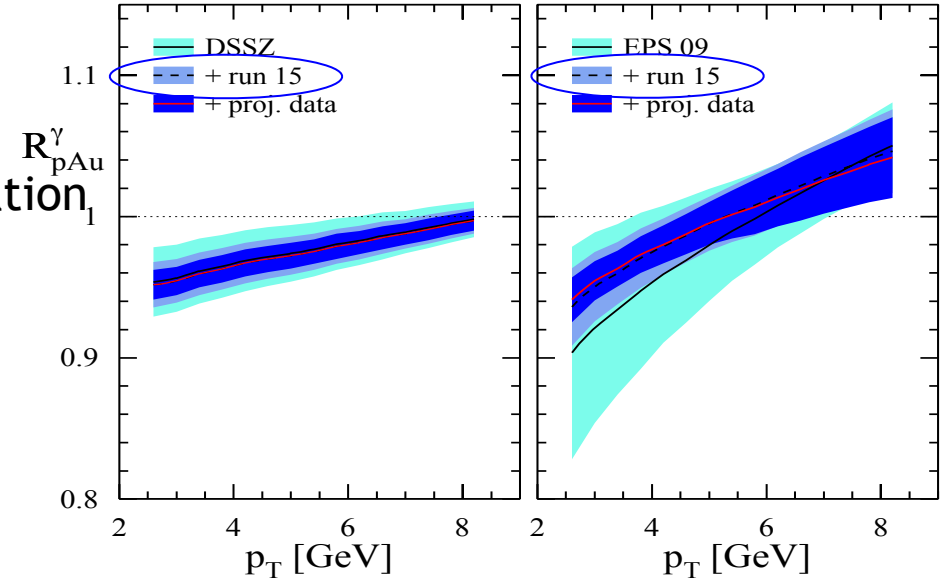
FMS + FPS: R_{pA} for direct photons

Direct photon @ $2.8 < \eta < 4.0$



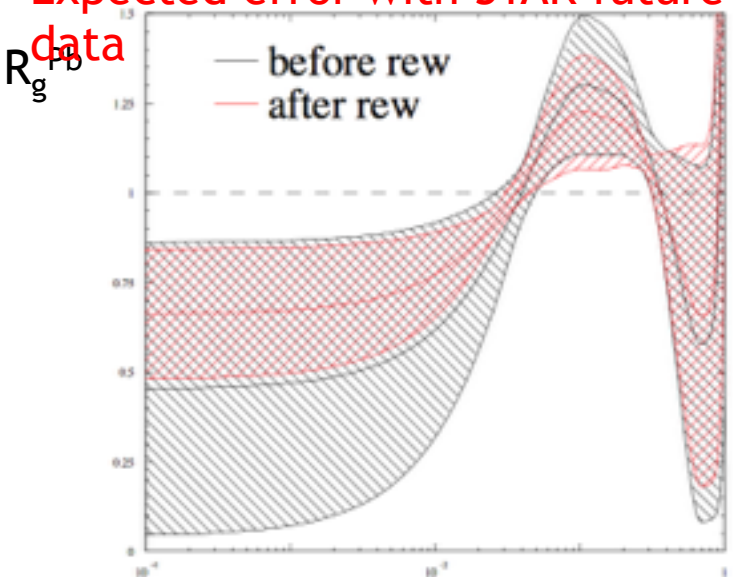
The STAR forward upgrade will allow R_{pA} for DY to constrain sea quarks

Impact on nPDFs: → mainly on gluon



EPS09 (1.3GeV)

Expected error with STAR future photon data



RHIC Cold QCD Plan and STAR forward upgrade

2015 | 2017 | ≧2021 | ≧ 2025

➢ wide accepta

➢ forward rapi

,p)

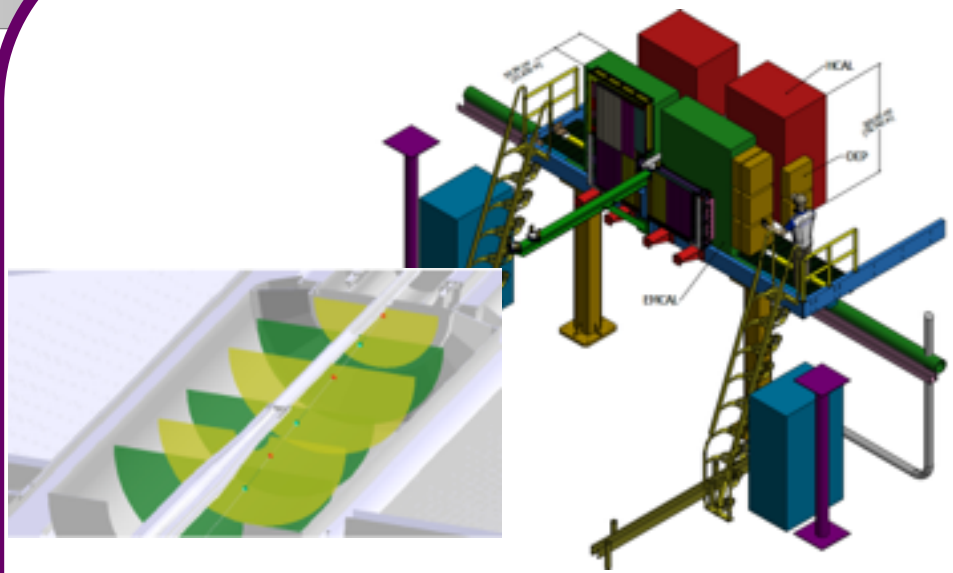
ntification

longitudinal & transverse

- p↑+Au/Al 200 GeV transverse

Goal:

- $\Delta g(x,Q^2)$
- transverse spin structure of the p
- Search for exotics
- Spin effects in diffraction
- J/Ψ in UPC →GPD E_g
- nPDF: $g(x,Q^2)$
- Saturation



Add to existing STAR at rapidity
$2.5 < \eta < 4.5$

Ecal:
reuse PHENIX Ecal

Hcal:
STAR fHCal and EIC fHCal

Tracking:
4-6 Si strip-disks



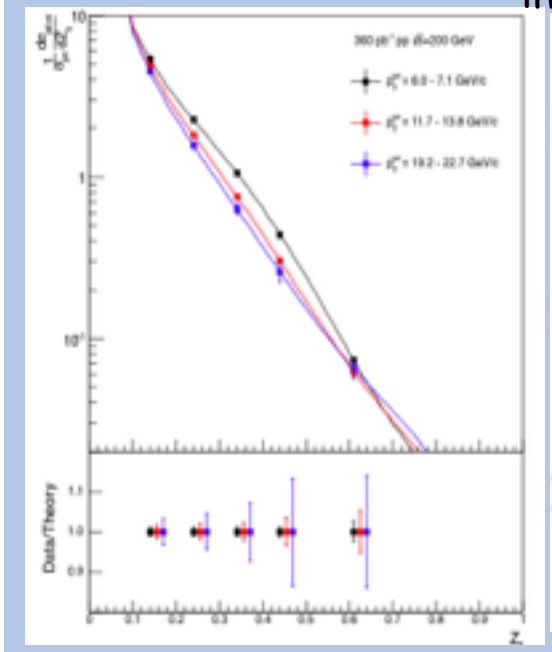
602.03922 [nucl-ex]

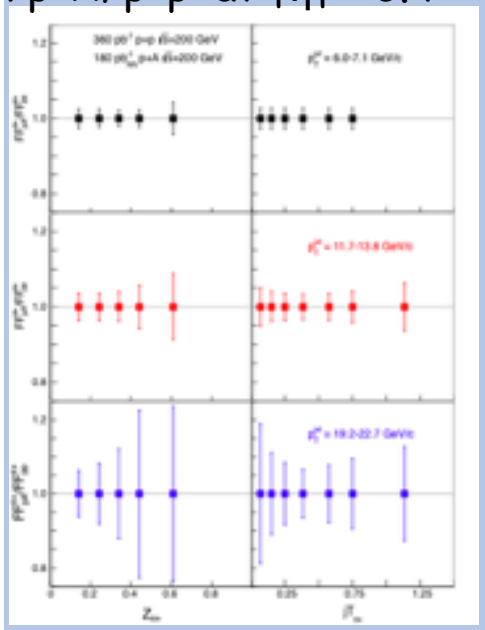
Run2023+ Physics Opportunities

	Year	$\sqrt{s}$ (GeV)	Delivered Luminosity	Scientific Goals	Observable	Required Upgrade
Scheduled RHIC running	2017	p↑p @ 510	400 pb^{-1} 12 weeks	Sensitive to Sivers effect non-universality through TMDs and Twist-3 $T_{q,F}(x,x)$ Sensitive to sea quark Sivers or ETQS function Evolution in TMD and Twist-3 formalism	A_N for γ, $W^{\pm}$, Z^0, DY	A_N^{DY}: Postshower to FMS@STAR
				Transversity, Collins FF, linear pol Gluons, Gluon Sivers in Twist-3	$A_{UT}^{\sin(\phi_s-2\phi_h)}$ $A_{UT}^{\sin(\phi_s-\phi_h)}$ modulations of $h^{\pm}$ in jets, $A_{UT}^{\sin(\phi_s)}$ for jets	None
				First look on GPD Eg	A_{UT} for J/Ψ in UPC	None
	2023	p↑p @ 200	300 pb^{-1} 8 weeks	subprocess driving the large A_N at high x_F and η	A_N for charged hadrons and flavor enhanced jets	Yes Forward instrum.
				properties and nature of the diffractive exchange in p+p collisions	A_N for diffractive events	None
	2023	p↑Au @ 200	1.8 pb^{-1} 8 weeks	What is the nature of the initial state and hadronization in nuclear collisions	R_{pAu} direct photons and DY	R_{pAu}(DY):Yes Forward instrum.
				Nuclear dependence of TMDs and nFF	$A_{UT}^{\sin(\phi_s-\phi_h)}$ modulations of $h^{\pm}$ in jets, nuclear FF	None
				Clear signatures for Saturation	Dihadrons, γ-jet, h-jet, diffraction	Yes Forward instrum.
	2023	p↑Al @ 200	12.6 pb^{-1} 8 weeks	A-dependence of nPDF,	R_{pAl}: direct photons and DY	R_{pAl}(DY): Yes Forward instrum.
				A-dependence of TMDs and nFF	$A_{UT}^{\sin(\phi_s-\phi_h)}$ modulations of $h^{\pm}$ in jets, nuclear FF	None
				A-dependence for Saturation	Dihadrons, γ-jet, h-jet, diffraction	Yes Forward instrum.
Potential future running	202X	p↑p @ 510	1.1 fb^{-1} 10 weeks	TMDs at low and high x	A_{UT} for Collins observables, i.e. hadron in jet modulations at $\eta > 1$ and mid-rapidity	Yes Forward instrum.
				quantitative comparisons of the validity and the limits of factorization and universality in lepton-proton and proton-proton collisions		None
	202X	$\vec{p}\vec{p}$ @ 510	1.1 fb^{-1} 10 weeks	$\Delta g(x)$ at small x	A_{LL} for jets, di-jets, h/γ-jets at $\eta > 1$	Yes Forward instrum.

p+p FF π+

fragmentation functions in p+A/p+p at $|\eta| < 0.4$



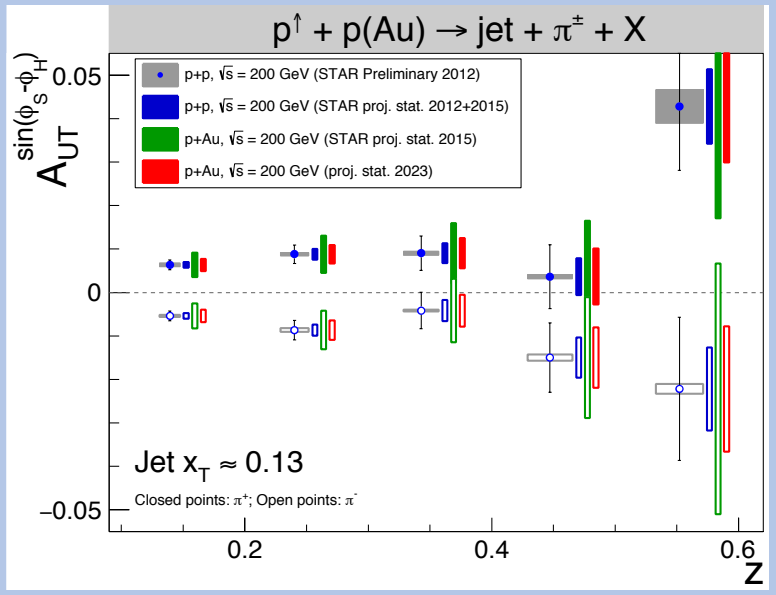


Critical to have π,K,p PID

Opportunities

	Observable	Required Upgrade
...rough TMDs	A_N for γ, $W^{\pm}$, Z^0, DY	A_N^{DY}: Postshower to FMS@STAR
...function ...alism		
...luons,	$A_{UT}^{\sin(\phi_s-2\phi_h)}$ $A_{UT}^{\sin(\phi_s-\phi_h)}$ modulations of h^+ in jets, $A_{UT}^{\sin(\phi_s)}$ for jets	None
	A_{UT} for J/Ψ in UPC	None
x_F and η	A_N for charged hadrons and flavor	Yes

First measurement of nuclear spin effects polarized FF → nCollins

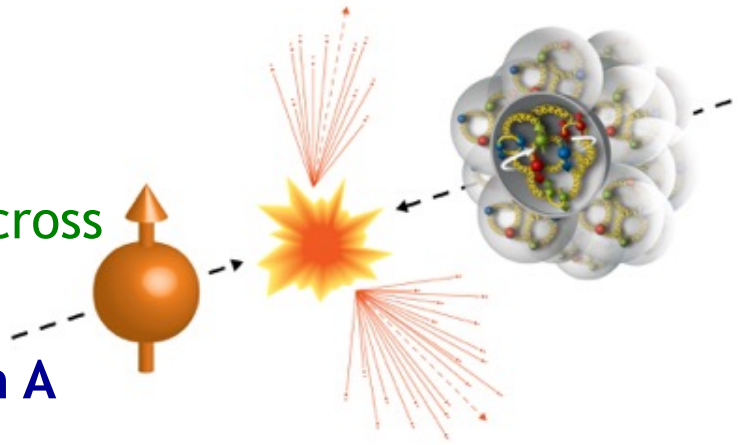


only at RHIC!

	2023	p↑Al @ 200	12.6 pb^{-1} 8 weeks	A-dependence of nPDF, A-dependence of TMDs and A-dependence for Saturati
Potential future running	202X	p↑p @ 510	1.1 fb^{-1} 10 weeks	TMDs at low and high x; quantitative comparisons of the validity factorization and universality in lepton-p proton collisions
	202X	$\vec{p}\vec{p}$ @ 510	1.1 fb^{-1} 10 weeks	$\Delta g(x)$ at small x

Summary and Outlook

- STAR @ RHIC can reach the saturation region at forward rapidity in p+A
- Polarized protons
- Scanning A ➔ Au, Al, …
- p_T scan and rapidity/x scan may allow to cross saturation scale Q_s^2 (x)



STAR can study evolution of $Q^2_s(x)$ with A

- First results on Transverse Single Spin Asymmetry A_N
  - Small to no suppression in p+Au
- Results coming soon for
  - Di-hadron angular correlation
  - R_{pA} for π^0 and photons

RHIC 2015

- $\vec{p} + p, L_{\text{int}} = 40 + 50\ \text{pb}^{-1}$
- $\vec{p} + Al, L_{\text{int}} = 1.0\ \text{pb}^{-1}$
- $\vec{p} + Au, L_{\text{int}} = 0.45\ \text{pb}^{-1}$

- Future forward upgrade at STAR is proposed, including saturation/pA physics at forward and mid-rapidity

STAR at RHIC offers unique opportunities to study low-x gluon

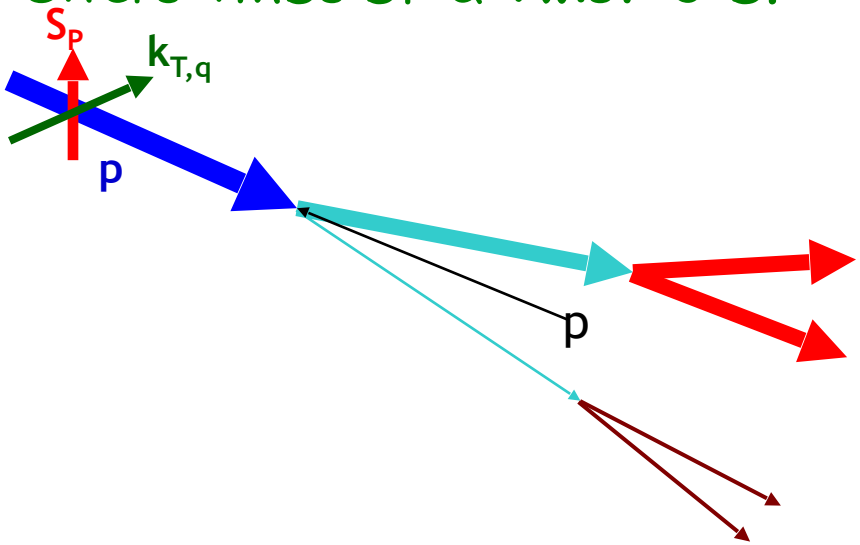
Backup

Transverse Single Spin Asymmetry (SSA) : A_N

Transverse Momentum Dependent (TMD) or Twist-3 DF or FF required

Initial State

Sivers TMDs DF & Twist-3 DF



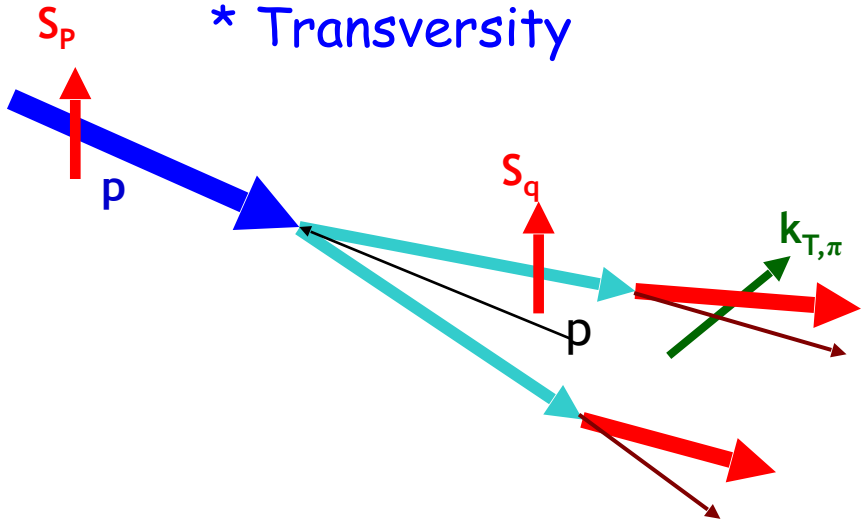
Sensitive to correlations between **proton spin** & parton **transverse motion**

Not universal (sign change) between SIDIS & pp

$$-\int d^2k_\perp \frac{|k_\perp^2|}{M} f_{1T}^{\perp q}(x,k_\perp^2)|_{SIDIS} = T_{q,F}(x,x)$$

Final State

Collins TMD FF & Twist-3 FF * Transversity



Sensitive to quark transverse spin and **spin-dependent** fragmentation function

Universal between SIDIS & pp & e+e-

Or something else…

Transverse Single Spin Asymmetry (SSA) : A_N

p+p

Initial State	Final State
Nucleon Spin ➔ Parton k_T	Nucleon spin ➔ Parton Spin ➔ Hadron k_T
Sivers TMD PDF	Transversity * Collins TMD Frag.Func.
$-\int d^2k_\perp \frac{\lvert k_\perp^2 \rvert}{M} f_{1T}^{\perp q}(x,k_\perp^2)\rvert_{SIDIS} = T_{q,F}(x,x)$	Only one part
Twist-3 PDF	Twist-3 Frag.Func = "Collins" + 3 Parton Corr.

p+A

Dominant in p+p, and NOT suppressed at p+A

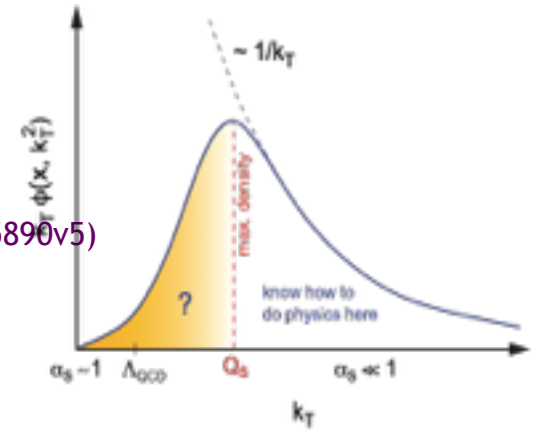
Yoshitaka Hattaa,et al, Phys. Rev. D 95, 014008 (2017)

Leonard Gamberg, Zhong-Bo Kang, Daniel Pitonyak, Alexei Prokudin arXiv:1701.09170v1

Hybrid Approach (Yoshitaka Hattaa,et al, arXiv:1611.04746v1)

Twist-3 + k_T un-integrated gluon distribution

Odderon exchange (Yuri V. Kovchegov, Matthew D. Sievert, arXiv:1201.5890v5)



Both predict A_N suppression for p+A

Towards higher-order accuracy in LCPT

Risto Paatelainen
University of Jyväskylä

BNL saturation workshop - April 28. 2017

In collaboration with

Tuomas Lappi (*University of Jyväskylä)*

Work in progress

see also T. Lappi, RP **Annals of Physics** (2017) 379, 34-66
arXiv:1611.00497

Motivation

Hamiltonian perturbation theory in the light-cone form (LCPT)

- A standard tool for calculations of small-x dilute-dense scattering processes in the CGC picture
- LCPT calculations in CGC slowly approaching the NLO level
  - the inclusive DIS cross sections (G. Beuf arXiv:1606.00777)
  - small-x evolution equations (I. Balitsky, G. Chirilli arXiv:0710.4330)

Problem:

- Perturbative computation of wavefunctions is quite tedious (hard to automatize)

Solution:
We introduce a new helicity formulation for LCPT

- Perturbative (NLO) computation of wavefunctions is easy and can be fully automatized

LCPT in a nutshell

QCD Hamiltonian: $T^{\mu\nu}_{\rm QCD}$, LC gauge $A^+_a = 0$ & EOMs

$$\mathcal{H}_{\rm QCD} = \frac{1}{2}\int {\rm d}x^- {\rm d}^2\mathbf{x}\left(\bar{\tilde{\Psi}}\gamma^+\frac{m^2+(i\nabla_\perp)^2}{i\partial^+}\tilde{\Psi} + \tilde{A}^\mu_a (i\nabla_\perp)^2 \tilde{A}^a_\mu\right)$$
$$+ g\int {\rm d}x^- {\rm d}^2\mathbf{x}\tilde{J}^\mu_a \tilde{A}^a_\mu$$
$$+ \frac{g^2}{2}\int {\rm d}x^- {\rm d}^2\mathbf{x}\left(\tilde{J}^+_a \frac{1}{(i\partial^+)^2}\tilde{J}^{+a} + \bar{\tilde{\Psi}}\gamma_\mu \tilde{A}^\mu_a t^a \frac{\gamma^+}{i\partial^+}\gamma_\nu \tilde{A}^\nu_b t^b \tilde{\Psi}\right)$$
$$+ \frac{g^2}{4}\int {\rm d}x^- {\rm d}^2\mathbf{x}\tilde{B}^{\mu\nu}_a \tilde{B}^a_{\mu\nu} = \mathcal{H}_0 + \mathcal{H}_{\rm I}$$

- $\tilde{J}^\mu_a = \bar{\tilde{\Psi}}\gamma^\mu t_a \tilde{\Psi} + f^{abc}\partial^\mu \tilde{A}^\nu_b \tilde{A}_{\nu c}$ & $\tilde{B}^{\mu\nu}_a = f^{abc}\tilde{A}^\mu_b \tilde{A}^\nu_c$

Note: in the $A^+_a = 0$ gauge

- positive: gluons have only two physical transverse degrees of freedom
- negative: breaking of manifest rotational invariance

Quantizing the $\mathcal{H}_{\rm QCD}$ by expanding field at $x^+ = 0$

$$\tilde{A}^\mu_c(x^-, \mathbf{x}) = \sum_{\lambda=\pm 1} \int \widetilde{\mathrm{d}k} \Big[a^c_\lambda \varepsilon^\mu_\lambda e^{-ik\cdot x} + \text{h.c.} \Big], \qquad \lambda \text{ gluon polarization}$$

$$\tilde{\Psi}(x^-, \mathbf{x}) = \sum_{h=\pm\frac{1}{2}} \int \widetilde{\mathrm{d}k} \Big[b_h u_h e^{-ik\cdot x} + \text{h.c.} \Big], \qquad h \text{ quark helicity}$$

- operators $(b_h), a^c_\lambda$... satisfy the standard (anti)commutation relations
- the integral measure in the LC coordinates is

$$\int \widetilde{\mathrm{d}k} = \int \frac{\mathrm{d}^4 k}{(2\pi)^4} (2\pi)\delta(k^2 - m^2) = \int \frac{\mathrm{d}k^+ \mathrm{d}^2\mathbf{k}}{(2\pi)^3 2k^+}, \quad k^+ > 0$$

- In the LC gauge $\varepsilon^+ = 0$ and $k \cdot \varepsilon_\lambda(k) = 0$

$$\varepsilon^\mu_\lambda(k) = (0, \frac{\mathbf{k}\cdot\epsilon_\lambda}{k^+}, \epsilon_\lambda), \quad \text{physical 2d transverse pol.} \quad \epsilon_\lambda = \frac{1}{\sqrt{2}}(1, \pm i)$$

The x^+-ordered LCPT theory = familiar perturbative expansion in QM

- Express the full physical incoming particle state $|\Psi\rangle_{\rm int}$ as a perturbative Fock state decomposition (in momentum space)

$$|\Psi\rangle_{\rm int} = |\Psi\rangle + \sum_{n_1} \frac{|n_1\rangle\langle n_1|\mathcal{H}_{\rm I}|\Psi\rangle}{\Delta^-_{1\Psi}} + \sum_{n_1,n_2} \frac{|n_2\rangle\langle n_2|H_{\rm I}|n_1\rangle\langle n_1|\mathcal{H}_{\rm I}|\Psi\rangle}{\Delta^-_{2\Psi}\Delta^-_{1\Psi}} + \dots$$

- LC energy denominators

$$\Delta^-_{n\Psi} = \sum_{\Psi} p^-_{\Psi} - \sum_{n} p^-_{n} + i0_+$$

- Note: only $\vec{p} = (p^+, \mathbf{p})$ is conserved!

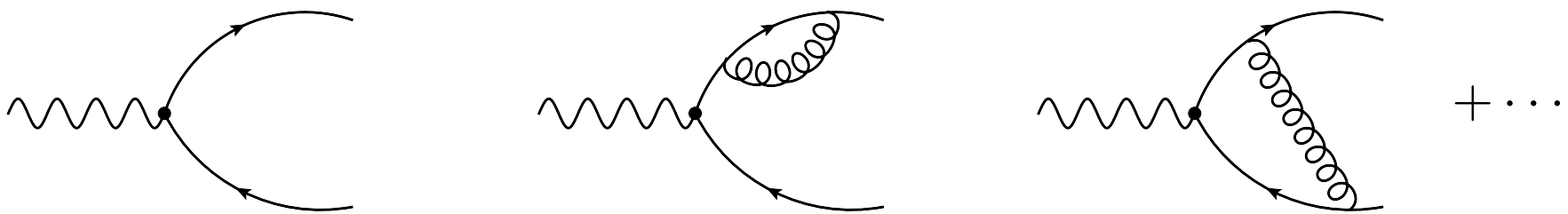
Consider now the DIS process $\gamma^* \to q\bar{q}$ (talk by G. Beuf)

$$|\gamma^*(\vec{q})\rangle_{\rm int} = \sqrt{Z_{\gamma^*}(q^+)}\Big[|\gamma^*(\vec{q})\rangle + \int \widetilde{\mathrm{d}p'}\widetilde{\mathrm{d}q}(2\pi)^3\delta^{(3)}(\vec{q}-\vec{p}-\vec{p}\,') \times \psi^{\gamma^*_{\rm T/L}\to q\bar{q}}|q(\vec{p})\bar{q}(\vec{p}\,')\rangle + \ldots\Big]$$

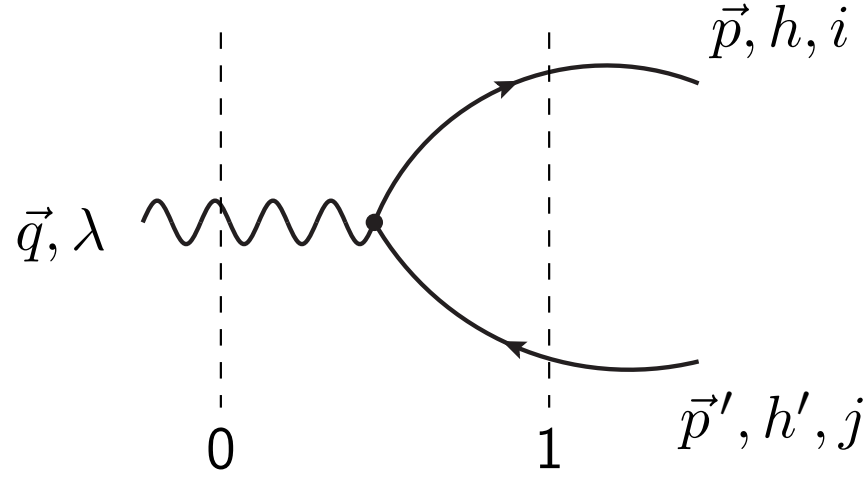
This expression **defines** the LC wavefunctions

$$\psi^{\gamma^*_{\rm T/L}\to q\bar{q}}, \quad \psi^{\gamma^*_{\rm T/L}\to q\bar{q}g}, \ldots$$

e.g. in NLO: $\mathcal{O}(g^2)$ QCD virtual corrections



Leading-order $\psi_{\rm LO}^{\gamma_{\rm T}^*\to q\bar{q}}$ wavefunction (for transverse γ^*)



- The WF (without overall momentum conservation $\vec{q} = \vec{p} + \vec{p}'$)

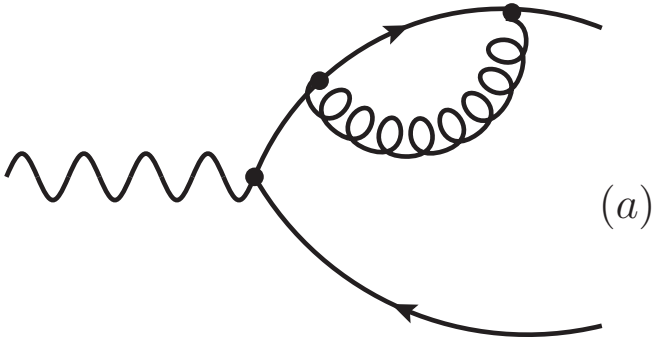
$$\psi_{\rm LO}^{\gamma_{\rm T}^*\to q\bar{q}} = (-ee_f)\delta_{ij}\frac{\bar{u}_h(p)\not{\epsilon}_\lambda(q)v_{h'}(p')}{\Delta_{01}^-}$$

- The LO LC energy denominator (frame $\mathbf{q} = \mathbf{0}$)

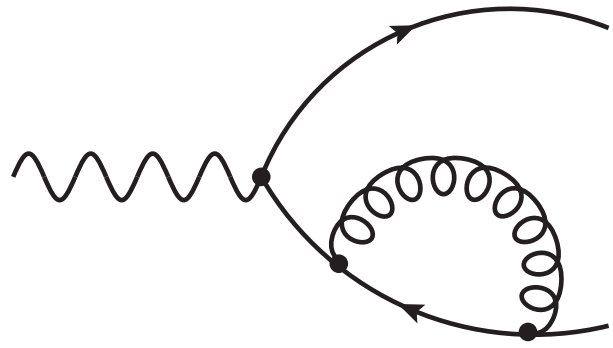
$$\Delta_{01}^- = q^- - (p^- + p'^-) = \frac{\mathbf{q}^2 - Q^2}{2q^+} - \left(\frac{\mathbf{p}^2}{2p^+} + \frac{(\mathbf{q}-\mathbf{p})^2}{2p'^+}\right)$$

$$= \frac{-q^+}{2p^+p'^+}\left(\mathbf{p}^2 + \overline{Q}^2\right), \quad \text{where} \quad \overline{Q}^2 = \frac{p^+p'^+}{(q^+)^2}Q^2 > 0$$

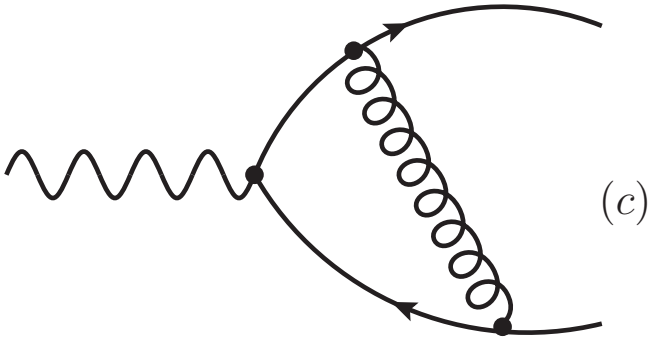
One-loop $\mathcal{O}(g^2)$ QCD corrections to the $\psi^{\gamma^*_{\rm T}\to q\bar{q}}$



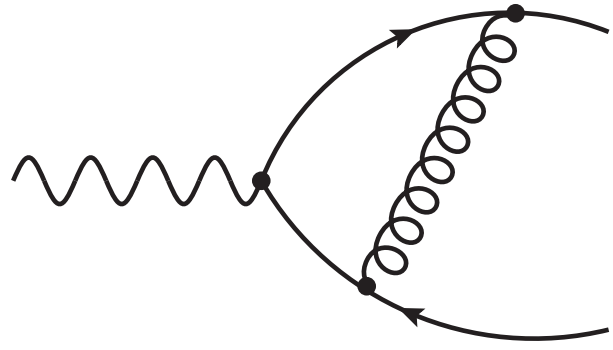
(a)



(b)



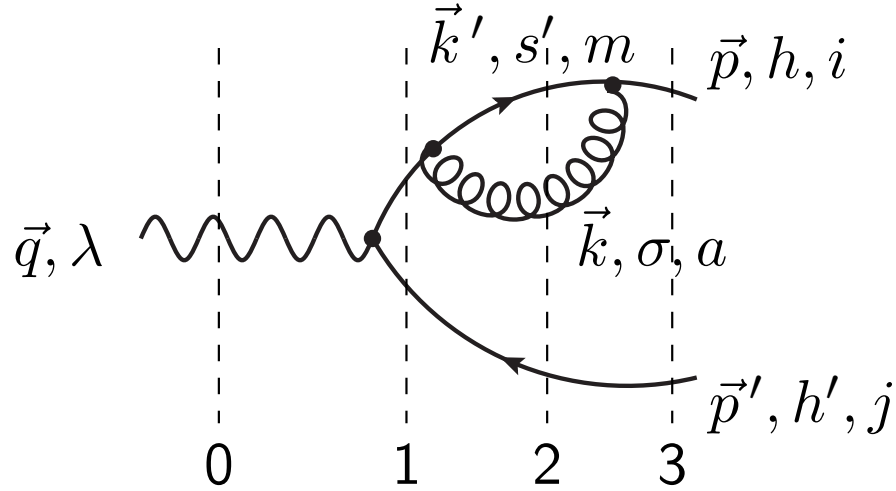
(c)



(d)

+ instantaneous diagrams (goes to zero in dim.reg)

One-loop quark self-energy correction (a) (for $\gamma_{\rm T}^*$)



- The WF

$$\psi_{(a)}^{\gamma_{\rm T}^*\to q\bar{q}} = -ee_f g^2 C_{\rm F}\delta^{ij}\int_0^{q^+}\frac{{\rm d}k^+}{2k^+}\int\frac{{\rm d}^2\mathbf{k}}{(2\pi)^3}\frac{1}{4p^+k'^+}\frac{{\rm num}|_a}{\Delta_{01}^-\Delta_{02}^-\Delta_{03}^-}$$

- The LC energy denominators

$$\Delta_{01}^- = \Delta_{03}^- = \frac{-q^+}{2p^+p'^+}\left(\mathbf{p}^2+\overline{Q}^2\right)$$

$$\Delta_{02}^- = -\frac{p^+}{2k^+k'^+}\left[(\mathbf{k}-\frac{k^+}{p^+}\mathbf{p})^2+\frac{k^+k'^+q^+}{(p^+)^2p'^+}(\mathbf{p}^2+\overline{Q}^2)\right]$$

- and the numerator

$$\mathrm{num}|_a = \sum_\sigma \varepsilon_\sigma^\mu(k)\varepsilon_\sigma^{*\nu}(k)\left[\bar{u}_h(p)\gamma_\mu \not{k}'\gamma_\nu \not{p}\not{\varepsilon}_\lambda(q)v_{h'}(p')\right]$$

To evaluate the (UV & col. IR divergent) transverse integrals and numerators we need some regularization framework

- **Conventional Dim. Reg.** (CDR) scheme: both observed and unobserved particles and momenta are continued to d dimension

- **Four Dimensional Helicity** (FDH) scheme: momenta of unobserved particles is continued to $d > 4$ and observed particles are kept in 4d
  - all unobserved internal states are treated as $d_s > d$ dim. and should be distinct from the dim. d
  - once the spin and Lorentz algebra is done the limit $d_s \to 4$ can be taken

$$\int \frac{\mathrm{d}^2\mathbf{k}}{(2\pi)^2} \frac{k^i k^j}{k^2 + M} \xrightarrow[\text{FDH}]{\text{CDR}} \frac{\delta^{ij}_{(d)}}{d} \int \frac{\mathrm{d}^{d-2}\mathbf{k}}{(2\pi)^{d-2}} \frac{\mathbf{k}^2}{\mathbf{k}^2 + M}$$

The longitudinal k^+ (soft IR divergent) integrals are regulated with the momentum cut-off

$$k^+ > \alpha q^+, \quad \text{where} \quad \alpha > 0$$

CDR scheme result for (a) (G. Beuf Phys. Rev. D 94 (2016) 054016)

$$\psi_{(a)}^{\gamma_{\mathrm{T}}^{*}\to q\bar{q}}\Big|_{\mathrm{CDR}} = \psi_{\mathrm{LO}}^{\gamma_{\mathrm{T}}^{*}\to q\bar{q}}(\mathbf{p},z)\left(\frac{g_{\mathrm{R}}^{2}C_{\mathrm{F}}}{8\pi^{2}}\right)\left\{\left[\frac{3}{2}+2\log\left(\frac{\alpha}{z}\right)\right]C_{a}-\log^{2}\left(\frac{\alpha}{z}\right) - \frac{\pi^{2}}{3}+3+\frac{1}{2}\right\}+\mathcal{O}(\varepsilon)$$

where $z = p^{+}/q^{+}$ with $0 < z < 1$ and

$$C_{a} = \frac{1}{\varepsilon_{\overline{\mathrm{MS}}}} + \log\left(\frac{\mu^{2}}{\overline{Q}^{2}}\right) - \log\left(\frac{\mathbf{p}^{2}+\overline{Q}^{2}}{\overline{Q}^{2}}\right) + \log(1-z)$$

Note: the factor $\frac{1}{2}$ is scheme dependent

Full (= (a) + (b) + (c) + (d)) CDR scheme result (G. Beuf Phys. Rev. D 94 (2016) 054016)

$$\psi^{\gamma_{\mathrm{T}}^{*}\to q\bar{q}}_{(\mathrm{full})}\Big|_{\mathrm{CDR}} = \psi^{\gamma_{\mathrm{T}}^{*}\to q\bar{q}}_{\mathrm{LO}}(\mathbf{p},z)\left(\frac{g_{\mathrm{R}}^{2}C_{\mathrm{F}}}{8\pi^{2}}\right)\left\{\left[\frac{3}{2}+\log\left(\frac{\alpha}{z}\right)+\log\left(\frac{\alpha}{1-z}\right)\right]C_{\mathrm{full}} + \frac{1}{2}\log^{2}\left(\frac{z}{1-z}\right)-\frac{\pi^{2}}{3}+\frac{5}{2}+\frac{1}{2}\right\}+\mathcal{O}(\varepsilon)$$

where

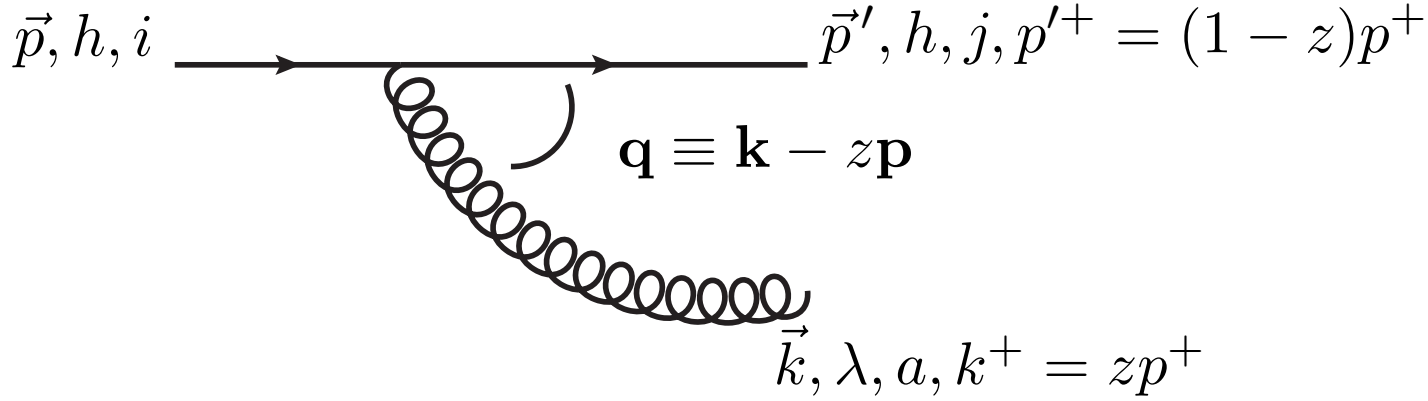
$$C_{\mathrm{full}} = \frac{1}{\varepsilon_{\overline{\mathrm{MS}}}}+\log\left(\frac{\mu^{2}}{\overline{Q}^{2}}\right)+\left(\frac{\overline{Q}^{2}-\mathbf{p}^{2}}{\mathbf{p}^{2}}\right)\log\left(\frac{\mathbf{p}^{2}+\overline{Q}^{2}}{\overline{Q}^{2}}\right)$$

Notes:

- complicated "brute force" calculation
  - in LCPT framework "covariant style" helicity algebra is difficult to automatize

New Helicity Approach (T. Lappi & RP in preparation)

The QCD light-cone vertices can be very compactly expressed in the helicity basis (**independent of spinor representation**)

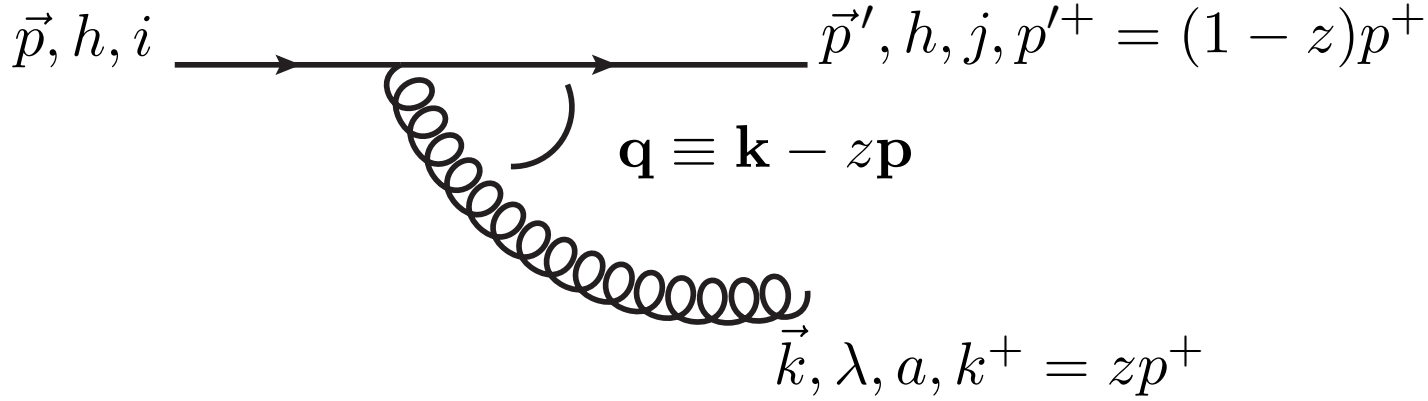


$$-gt^a_{ji}\bar{u}_h(p')\not{\epsilon}^*_\lambda(k)u_h(p) = \frac{-2gt^a_{ji}}{z\sqrt{1-z}}\left[\left(1-\frac{z}{2}\right)\delta^{ij} + ih\frac{z}{2}\epsilon^{ij}\right]\mathbf{q}^i\epsilon^{*j}_\lambda$$
$$= V^{i;j,a}_{\lambda,h}(\mathbf{q},z)$$

Note: Our FDH formulation in (arXiv:1611.00497) was incorrect

New Helicity Approach (T. Lappi & RP in preparation)

The QCD light-cone vertices can be very compactly expressed in the helicity basis (**independent of spinor representation**)



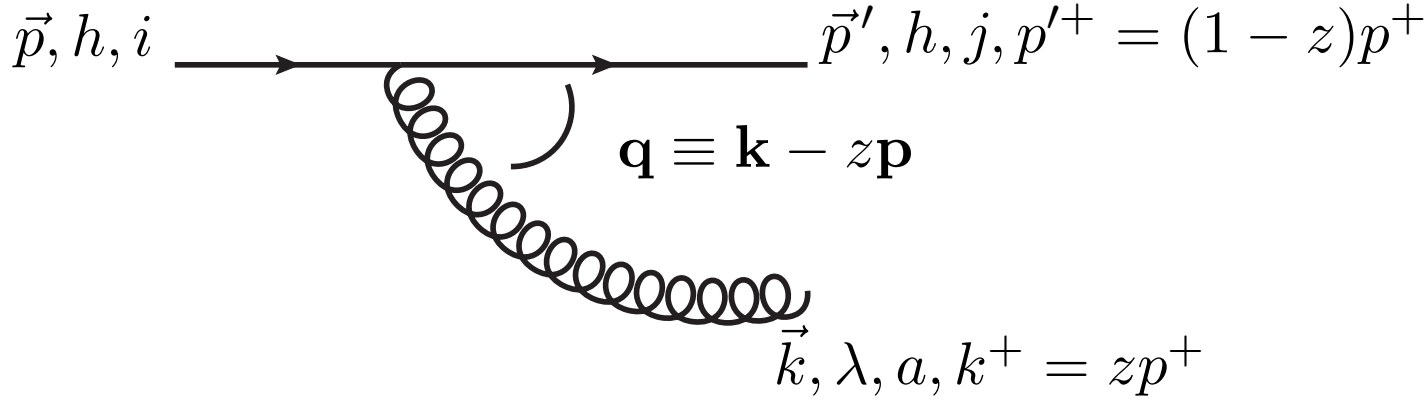
$$-gt^a_{ji}\bar{u}_h(p')\not{\epsilon}^*_\lambda(k)u_h(p) = \frac{-2gt^a_{ji}}{z\sqrt{1-z}}\left[\left(1-\frac{z}{2}\right)\delta^{ij} + ih\frac{z}{2}\epsilon^{ij}\right]\mathbf{q}^i\epsilon^{*j}_\lambda$$
$$= V^{i;j,a}_{\lambda,h}(\mathbf{q},z)$$

- $+$ and transverse momentum conservation implemented automatically

Note: Our FDH formulation in (arXiv:1611.00497) was incorrect

New Helicity Approach (T. Lappi & RP in preparation)

The QCD light-cone vertices can be very compactly expressed in the helicity basis (**independent of spinor representation**)



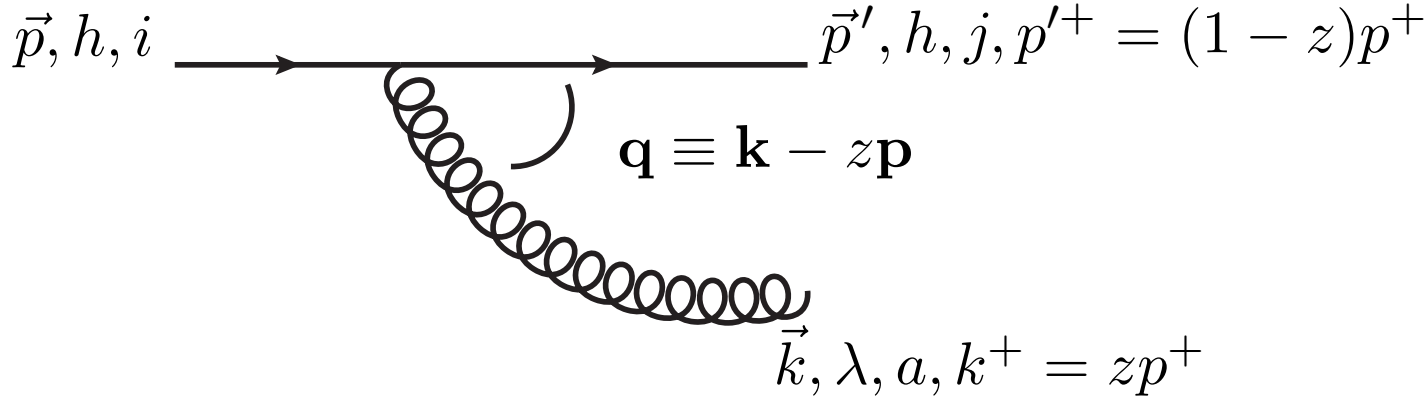
$$-gt^a_{ji}\bar{u}_h(p')\not{\epsilon}^*_\lambda(k)u_h(p) = \frac{-2gt^a_{ji}}{z\sqrt{1-z}}\left[\left(1-\frac{z}{2}\right)\delta^{ij} + ih\frac{z}{2}\epsilon^{ij}\right]\mathbf{q}^i\epsilon^{*j}_\lambda$$
$$= V^{i;j,a}_{\lambda,h}(\mathbf{q},z)$$

- $+$ and transverse momentum conservation implemented automatically
- all particles have exactly two helicity states $\Rightarrow$ FDH scheme

Note: Our FDH formulation in (arXiv:1611.00497) was incorrect

New Helicity Approach (T. Lappi & RP in preparation)

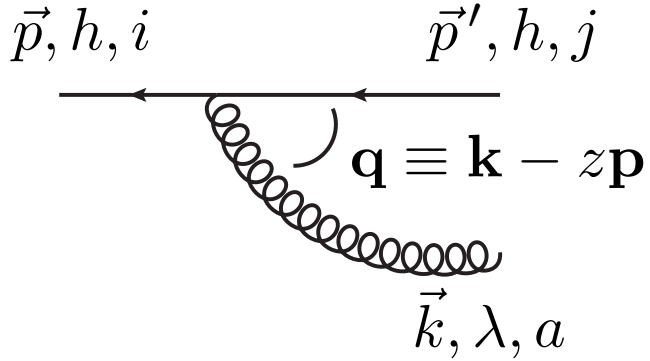
The QCD light-cone vertices can be very compactly expressed in the helicity basis (**independent of spinor representation**)



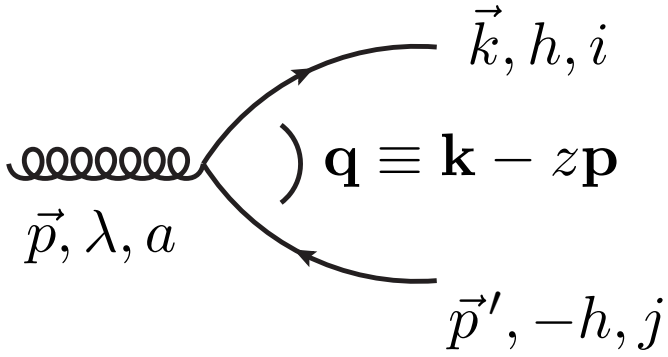
$$-gt^a_{ji}\bar{u}_h(p')\not{\epsilon}^*_\lambda(k)u_h(p) = \frac{-2gt^a_{ji}}{z\sqrt{1-z}}\left[\left(1-\frac{z}{2}\right)\delta^{ij} + ih\frac{z}{2}\epsilon^{ij}\right]\mathbf{q}^i\epsilon^{*j}_\lambda$$
$$= V^{i;j,a}_{\lambda,h}(\mathbf{q},z)$$

- $+$ and transverse momentum conservation implemented automatically
- all particles have exactly two helicity states $\Rightarrow$ FDH scheme
- enables a very efficient computation of NLO WFs (easy to automatize)

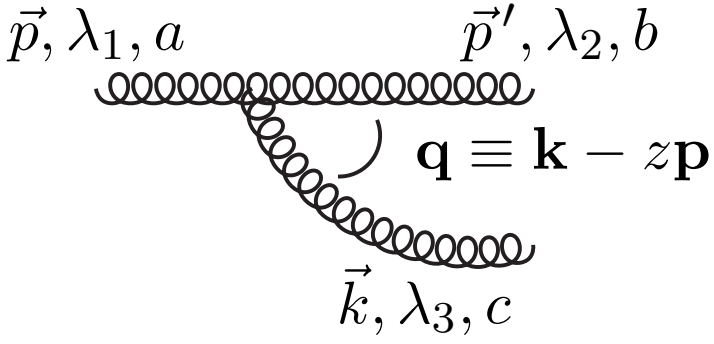
Note: Our FDH formulation in (arXiv:1611.00497) was incorrect



- $\overline{V}^{i;j,a}_{\lambda,h}(\mathbf{q}, z) =$
$\frac{+2gt^a_{ji}}{z\sqrt{1-z}}\left[\left(1-\frac{z}{2}\right)\delta^{ij} + ih\frac{z}{2}\epsilon^{ij}\right]\mathbf{q}^i\epsilon^{*j}_\lambda$



- $A^{a;j,i}_{\lambda,h}(\mathbf{q}, z) =$
$\frac{-2gt^a_{ij}}{\sqrt{z(1-z)}}\left[\left(z-\frac{1}{2}\right)\delta^{ij} - ih\frac{1}{2}\epsilon^{ij}\right]\mathbf{q}^i\epsilon^j_\lambda$



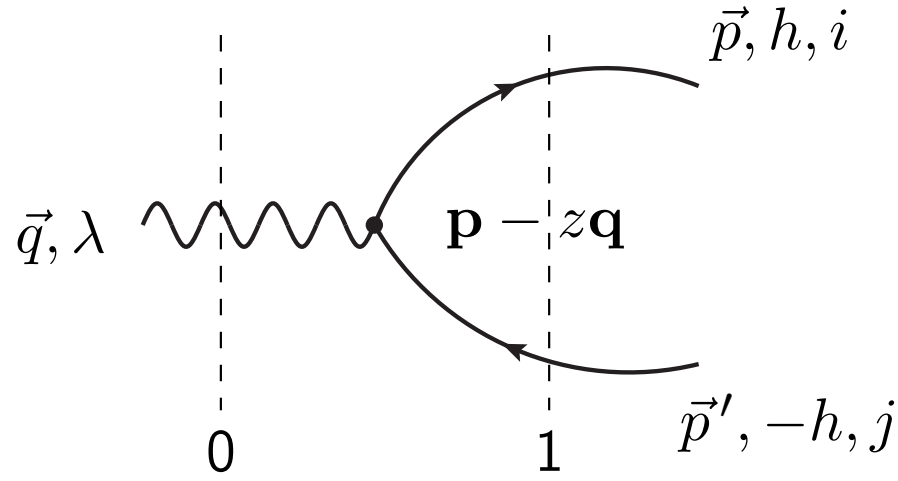
- $\Gamma^{a;b,c}_{\lambda_1,\lambda_2,\lambda_3}(\mathbf{q}, z) =$
$-2igf^{abc}\left[\frac{\boldsymbol{\varepsilon}^{*j}_{\lambda_2}\boldsymbol{\varepsilon}^{*k}_{\lambda_3}\boldsymbol{\varepsilon}^{l}_{\lambda_1}}{1-z} + \frac{\boldsymbol{\varepsilon}^{*j}_{\lambda_3}\boldsymbol{\varepsilon}^{*k}_{\lambda_2}\boldsymbol{\varepsilon}^{l}_{\lambda_1}}{z} - \boldsymbol{\varepsilon}^{j}_{\lambda_1}\boldsymbol{\varepsilon}^{*k}_{\lambda_3}\boldsymbol{\varepsilon}^{*l}_{\lambda_2}\right]\delta^{ij}\delta^{kl}\mathbf{q}^i$

+complex conjugates & 4-gluon vertex & instantaneous vertices!

LO WF $\psi_{\rm LO}^{\gamma_{\rm T}^*\to q\bar{q}}$ (Helicity approach)

$p^+ = zq^+$

$p'^+ = (1-z)q^+$



- The LO WF (frame $\mathbf{q} = \mathbf{0}$)

$$\psi_{\rm LO}^{\gamma_{\rm T}^*\to q\bar{q}} = \delta_{ij}\frac{A_{\lambda,h}^{\gamma_{\rm T}^*}(\mathbf{p},z)}{\Delta_{01}^-},$$

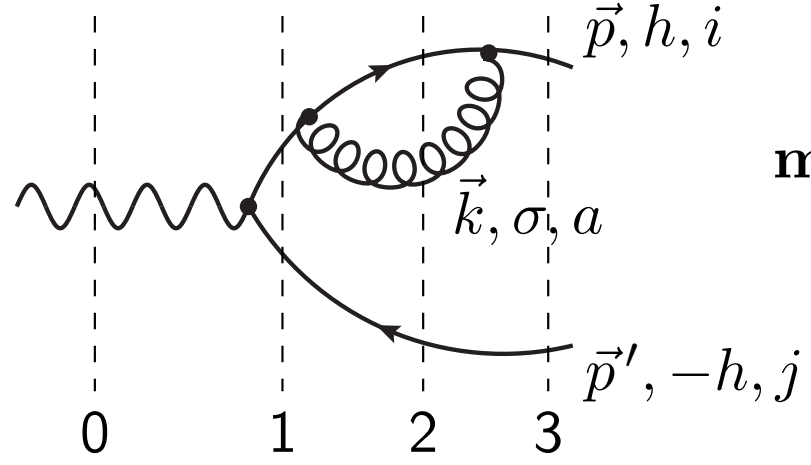
where (QCD $\to$ QED vertex: $gt^a \to ee_f$)

$$A_{\lambda,h}^{\gamma_{\rm T}^*}(\mathbf{p},z) = \frac{-2ee_f}{\sqrt{z(1-z)}}\left[\left(z-\frac{1}{2}\right)\delta^{ij} - ih\frac{1}{2}\epsilon^{ij}\right]\mathbf{p}^i\epsilon_\lambda^j$$

- The LO LC energy denominator

$$\Delta_{01}^- = \frac{1}{(-2q^+)z(1-z)}\left(\mathbf{p}^2 + \overline{Q}^2\right), \quad \text{where} \quad \overline{Q}^2 = z(1-z)Q^2 > 0$$

$$k^+ = z'q^+$$
$$p^+ = zq^+$$
$$p'^+ = (1-z)q^+$$



$$\mathbf{m} = \mathbf{k} - \frac{z'}{z}\mathbf{p}$$

- The WF (without overall momentum conservation $\vec{q} = \vec{p} + \vec{p}'$)

$$\psi_{(a)}^{\gamma_{\mathrm{T}}^* \to q\bar{q}} = \frac{1}{16\pi(q^+)^2} \int_0^z \frac{\mathrm{d}z'}{zz'(z-z')} \int \frac{\mathrm{d}^{d-2}\mathbf{m}}{(2\pi)^{d-2}} \frac{\mathrm{num}|_a}{\Delta_{01}^- \Delta_{02}^- \Delta_{03}^-}$$

- The LC energy denominators

$$\Delta_{01}^- = \Delta_{03}^- = \frac{1}{(-2q^+)z(1-z)} \left(\mathbf{p}^2 + \overline{Q}^2\right)$$

$$\Delta_{02}^- = \frac{z}{(-2q^+)z'(z-z')} \left[\mathbf{m}^2 + \frac{z'(z-z')}{z^2(1-z)}(\mathbf{p}^2 + \overline{Q}^2)\right]$$

- and the numerator

$$\mathrm{num}|_a = \sum_\sigma A_{\lambda,h}^{\gamma_{\mathrm{T}}^*}(\mathbf{p}, z) V_{\sigma,h}^{j;m,a}(\mathbf{m}, z'/z) V_{\sigma,h}^{m,a;i}(\mathbf{m}, z'/z)$$

now the algebra in the numerator is trivial

$$\mathrm{num}|_a = A^{\gamma_{\mathrm{T}}^*}_{\lambda,h}(\mathbf{p},z)\frac{4g_{\mathrm{R}}^2 C_{\mathrm{F}}\delta^{ij}}{z^2(1-z)}\sum_\sigma \epsilon^{*j}_\sigma \epsilon^\ell_\sigma \left[\left(1-\frac{z'}{2z}\right)\delta^{ij}_{(d_s)} + ih\frac{z'}{2z}\epsilon^{ij}_{(d_s)}\right]$$
$$\times \left[\left(1-\frac{z'}{2z}\right)\delta^{k\ell}_{(d_s)} - ih\frac{z'}{2z}\epsilon^{k\ell}_{(d_s)}\right]\mathbf{m}^i\mathbf{m}^k$$

using (remember $d_s > d$)

$$\sum_\sigma \epsilon^{*j}_\sigma \epsilon^\ell_\sigma = \delta^{j\ell}_{(d_s)} \qquad \text{and} \qquad \mathbf{m}^i\mathbf{m}^k = \frac{\delta^{ik}_{(d)}}{d}\mathbf{m}^2$$

and

$$\epsilon^{jj}_{(d_s)} = 0, \qquad \epsilon^{ij}_{(d_s)}\epsilon^{k\ell}_{(d_s)} = \delta^{ik}_{(d_s)}\delta^{j\ell}_{(d_s)} - \delta^{i\ell}_{(d_s)}\delta^{jk}_{(d_s)} \qquad \text{(Fierz identity)}$$

we get (remember $h^2 = 1$)

$$\mathrm{num}|_a = A^{\gamma_{\mathrm{T}}^*}_{\lambda,h}(\mathbf{p},z)\frac{4g_{\mathrm{R}}^2 C_{\mathrm{F}}\delta^{ij}}{z^2(1-z)}\left[\left(1-\frac{z'}{2z}\right)^2 + \left(\frac{z'}{2z}\right)^2(d_s-1)\right]\mathbf{m}^2$$

Taking limit $d_s \to 2$ & integrating over $\mathbf{m}$ and z' we find for (a)

$$\left.\psi_{(a)}^{\gamma_{\rm T}^*\to q\bar{q}}\right|_{\rm FDH} = \psi_{\rm LO}^{\gamma_{\rm T}^*\to q\bar{q}}(\mathbf{p},z)\left(\frac{g_{\rm R}^2 C_{\rm F}}{8\pi^2}\right)\left\{\left[\frac{3}{2}+2\log\left(\frac{\alpha}{z}\right)\right]C_a - \log^2\left(\frac{\alpha}{z}\right) - \frac{\pi^2}{3}+3\right\}+\mathcal{O}(\varepsilon)$$

where $z = p^+/q^+$ with $0 < z < 1$ and

$$C_a = \frac{1}{\varepsilon_{\overline{\rm MS}}} + \log\left(\frac{\mu^2}{\overline{Q}^2}\right) - \log\left(\frac{\mathbf{p}^2+\overline{Q}^2}{\overline{Q}^2}\right) + \log(1-z)$$

For comparison the CDR scheme result was

$$\left.\psi_{(a)}^{\gamma_{\rm T}^*\to q\bar{q}}\right|_{\rm CDR} = \psi_{\rm LO}^{\gamma_{\rm T}^*\to q\bar{q}}(\mathbf{p},z)\left(\frac{g_{\rm R}^2 C_{\rm F}}{8\pi^2}\right)\left\{\left[\frac{3}{2}+2\log\left(\frac{\alpha}{z}\right)\right]C_a - \log^2\left(\frac{\alpha}{z}\right) - \frac{\pi^2}{3}+3+\frac{1}{2}\right\}+\mathcal{O}(\varepsilon)$$

For the full correction ((a) + (b) + (c) + (d)) we find

$$\psi^{\gamma_{\rm T}^*\to q\bar{q}}_{\rm (full)}\Big|_{\rm FDH} = \psi^{\gamma_{\rm T}^*\to q\bar{q}}_{\rm LO}(\mathbf{p},z)\left(\frac{g_{\rm R}^2 C_{\rm F}}{8\pi^2}\right)\left\{\left[\frac{3}{2}+\log\left(\frac{\alpha}{z}\right)+\log\left(\frac{\alpha}{1-z}\right)\right]C_{\rm full} + \frac{1}{2}\log^2\left(\frac{z}{1-z}\right)-\frac{\pi^2}{3}+\frac{5}{2}-\log(z(1-z))\right\}+\left(\frac{g_{\rm R}^2 C_{\rm F}}{8\pi^2}\right)\times\Pi+\mathcal{O}(\varepsilon)$$

where

$$C_{\rm full} = \frac{1}{\varepsilon_{\overline{\rm MS}}}+\log\left(\frac{\mu^2}{\overline{Q}^2}\right)+\left(\frac{\overline{Q}^2-\mathbf{p}^2}{\mathbf{p}^2}\right)\log\left(\frac{\mathbf{p}^2+\overline{Q}^2}{\overline{Q}^2}\right)$$

$$\Pi = \delta^{ij}\frac{-2ee_f}{\Delta_{03}^-}\frac{(z-\frac{1}{2})}{\sqrt{z(1-z)}}(\mathbf{p}\cdot\epsilon_\lambda)\log(z(1-z))$$

For comparison the full CDR scheme result was

$$\psi^{\gamma_{\rm T}^*\to q\bar{q}}_{\rm (full)}\Big|_{\rm CDR} = \psi^{\gamma_{\rm T}^*\to q\bar{q}}_{\rm LO}(\mathbf{p},z)\left(\frac{g_{\rm R}^2 C_{\rm F}}{8\pi^2}\right)\left\{\left[\frac{3}{2}+\log\left(\frac{\alpha}{z}\right)+\log\left(\frac{\alpha}{1-z}\right)\right]C_{\rm full} + \frac{1}{2}\log^2\left(\frac{z}{1-z}\right)-\frac{\pi^2}{3}+\frac{5}{2}+\frac{1}{2}\right\}+\mathcal{O}(\varepsilon)$$

Conclusion and Outlook

- Formulation of LCPT rules for massless QCD in helicity space independently of spinor representation
  - replace the complicated γ-algebra and spin sums by simple metric tensor algebra (easy to automatize - FORM)
  - full NLO corrections to WFs can be calculated by using the helicity approach
- To-Do List:
  - include the mass corrections
  - transition rules from FDH scheme to CDR scheme
  - full NLO computations to DIS and other processes
  - higher-order (NNLO) corrections (?)

BACKUP SLIDE:

T. Lappi, RP arXiv:1611.00497:

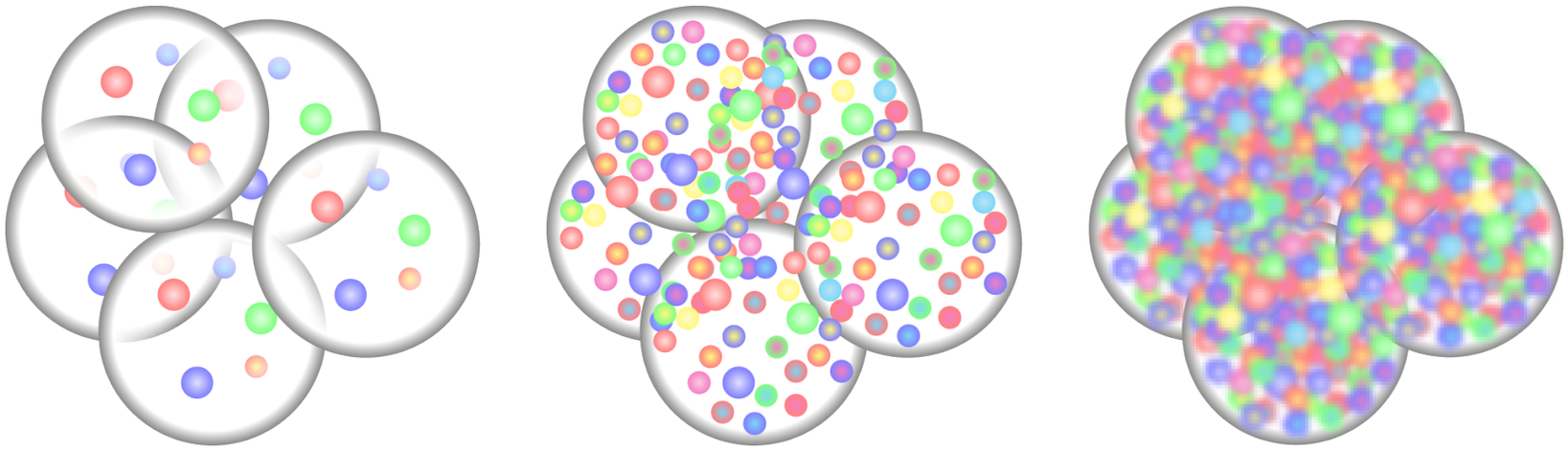
$$-gt^a_{ji}\bar{u}_h(p')\not{\epsilon}^*_\lambda(k)u_h(p) = \frac{-2gt^a_{ji}}{z\sqrt{1-z}}\left[\delta_{\lambda,h} + (1-z)\delta_{\lambda,-h}\right]\mathbf{q}\cdot\epsilon^*_\lambda$$

Rewriting this as

$$-gt^a_{ji}\bar{u}_h(p')\not{\epsilon}^*_\lambda(k)u_h(p) = \frac{-2gt^a_{ji}}{z\sqrt{1-z}}\left[\left(1-\frac{z}{2}\right) + \lambda h\frac{z}{2}\right]\mathbf{q}^i\epsilon^{*i}_\lambda$$

and using $\lambda\varepsilon^*_\lambda = i\epsilon\times\varepsilon^*_\lambda$ where ϵ is rank-2 levi-civita tensor,

$$-gt^a_{ji}\bar{u}_h(p')\not{\epsilon}^*_\lambda(k)u_h(p) = \frac{-2gt^a_{ji}}{z\sqrt{1-z}}\left[\left(1-\frac{z}{2}\right)\delta^{ij} + ih\frac{z}{2}\epsilon^{ij}\right]\mathbf{q}^i\epsilon^{*j}_\lambda$$



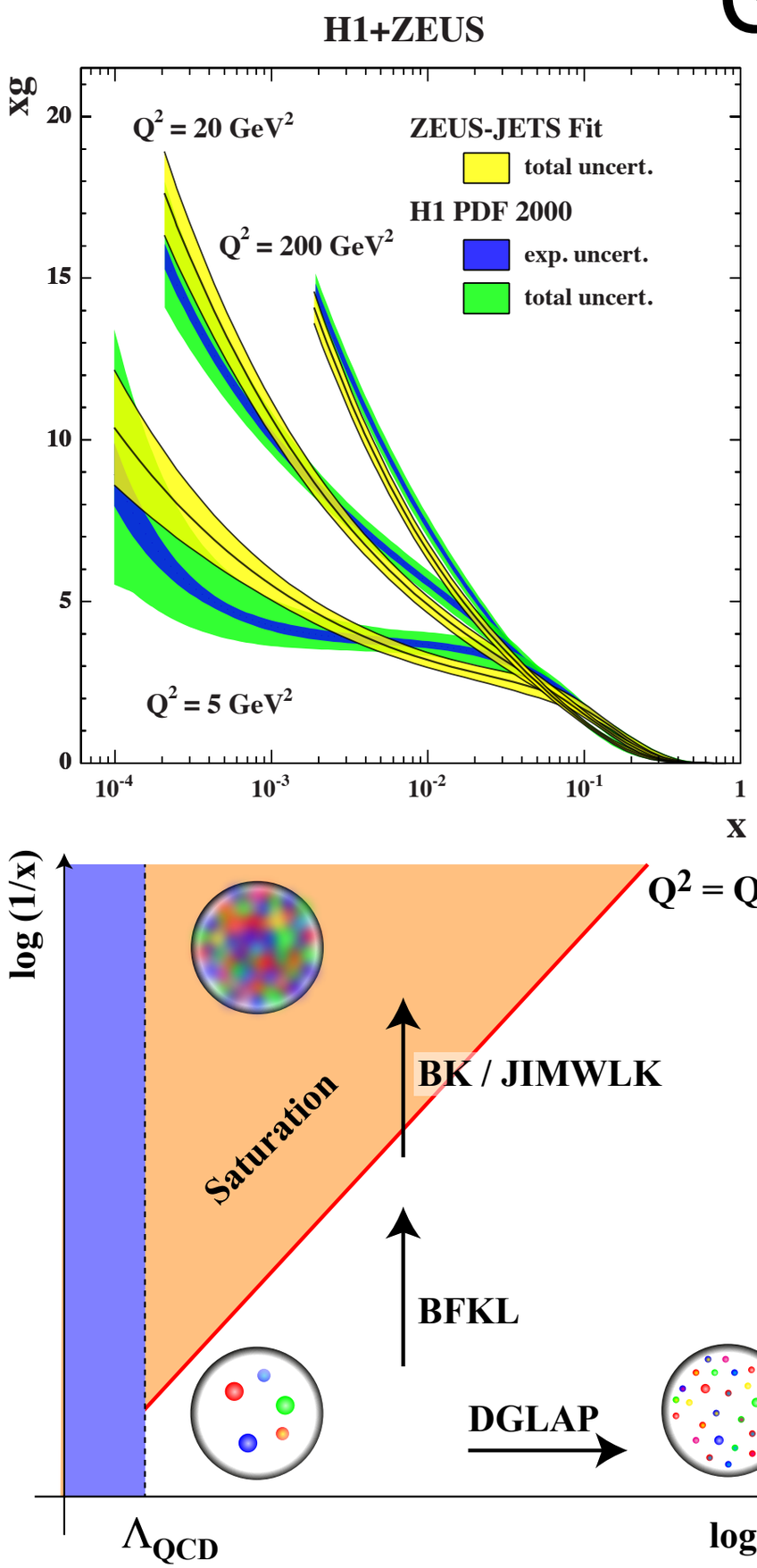
Opportunities for Forward Photon Measurements in ALICE at the LHC

T. Peitzmann (Utrecht University/Nikhef)

Outline

- Introduction
  - low-x physics, gluon saturation
  - first results from LHC
- Saturation signals
  - PDF uncertainties?
  - range of validity of saturation models?
  - charm vs photons?
- FoCal - an ALICE upgrade proposal
  - baseline design: performance studies
  - progress on detector R&D
- Summary

Gluon Saturation

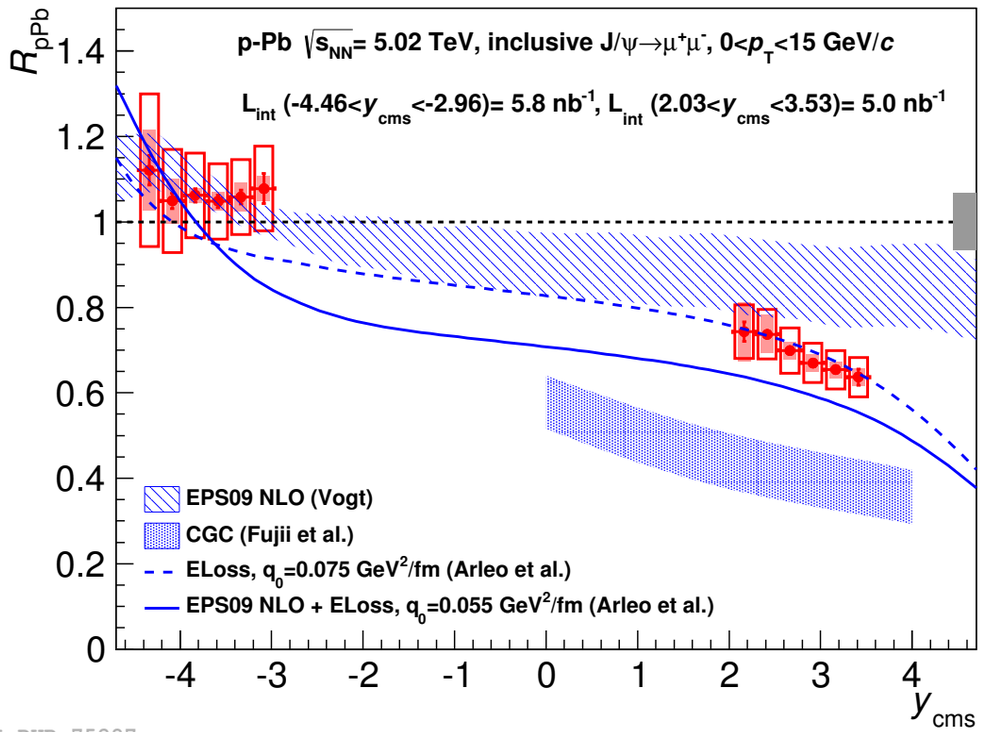


- from evolution equations (DGLAP, BFKL):
  - gluon density increases with Q^2 and 1/x
    - leads to very high gluon density
    - problems with unitarity(?)
- for high density non-linear processes become important
- gluon saturation below saturation scale
  - enhanced in nuclei

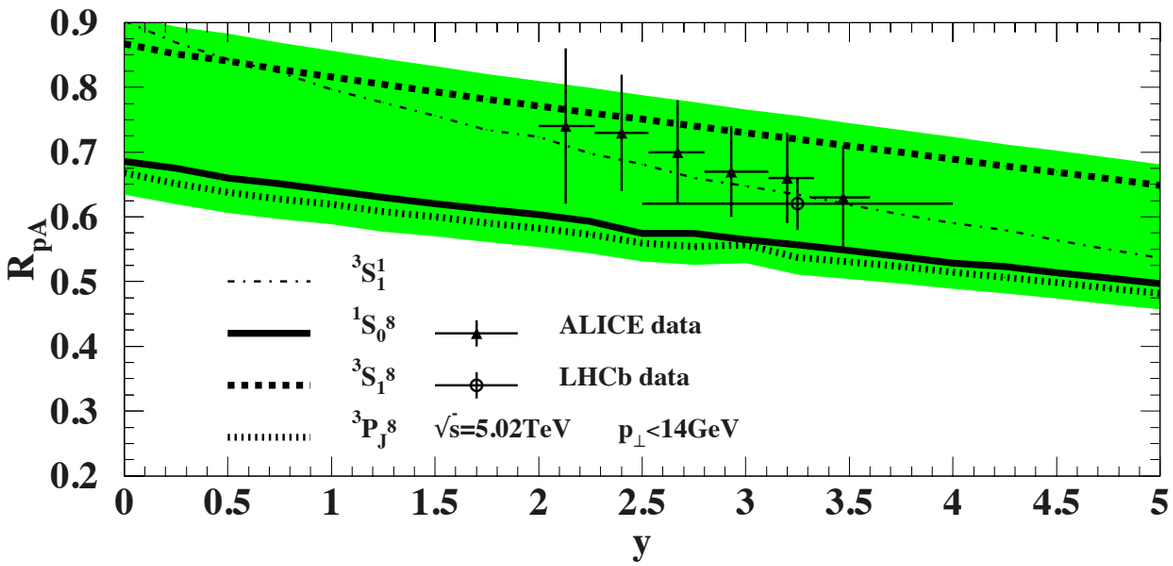
$$Q_s^2(x) \approx \frac{\alpha_S}{\pi R^2} x G(x, Q^2) \propto A^{1/3} \cdot x^{-\lambda}$$

Results from p-Pb at LHC (1)

ALICE, JHEP02 (2014) 073



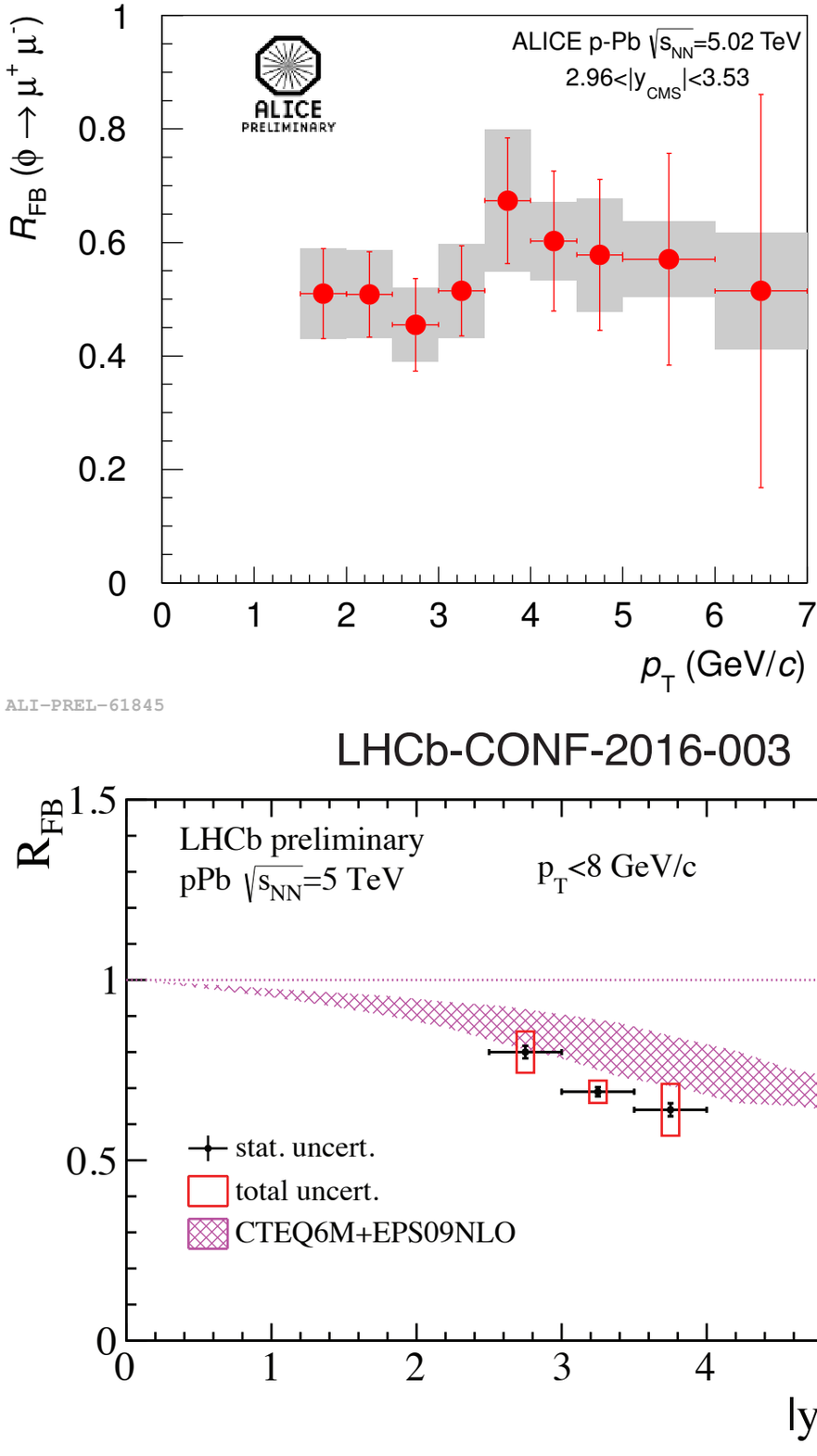
Ma, Venugopalan, Zhang, arXiv:1503.07772



$$R_{pA} = \frac{dN/dp_T(pA)}{< N_{coll}(pA) > dN/dp_T(pp)}$$

- nuclear modification factor RpPb for charmonium
- J/ψ suppressed at forward rapidity
  - consistent with shadowing (EPS09)
  - not described by one CGC calculation (state of the art?)
- description by CGC
  - needs refined calculations
  - uncertainties due to population of different quantum states
- not conclusive

Results from p-Pb at LHC (2)



- forward/backward ratio R_{FB}

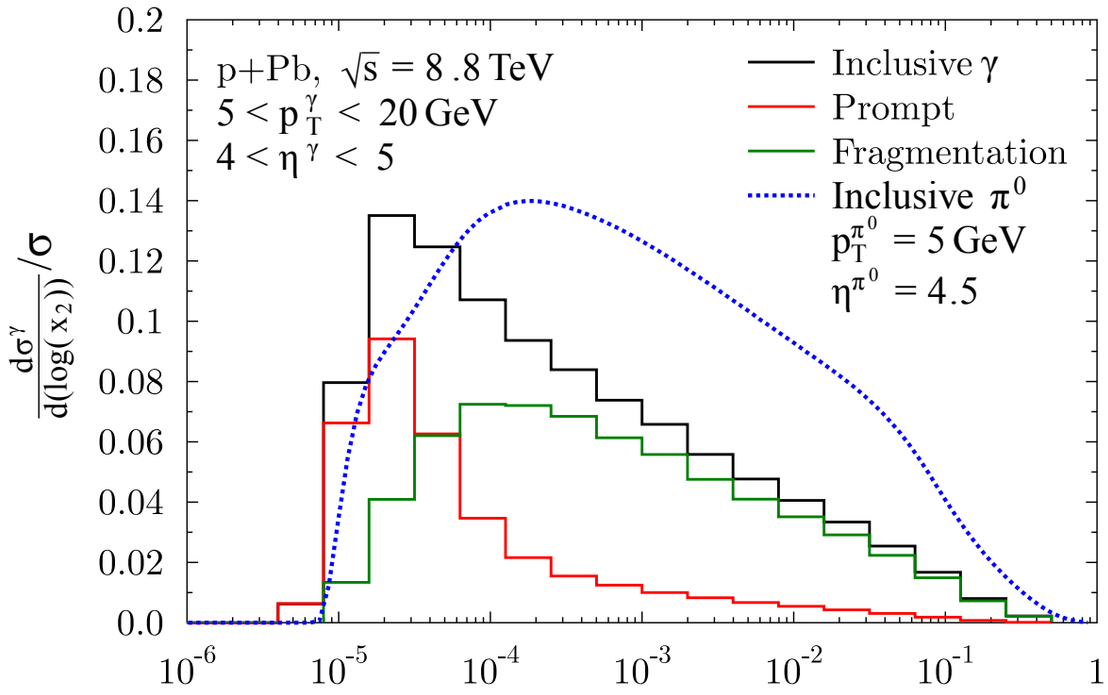
$$R_{FB} = \frac{dN/dp_T(\mathrm{p-going})}{dN/dp_T(\mathrm{Pb-going})}$$

for ϕ-mesons in ALICE (dimuons) and for open charm in LHCb

- ϕ strongly suppressed at forward rapidity
  - interpretation unclear
- prompt D^0 suppressed
  - comparison with shadowing (EPS09): consistent, but data slightly more suppressed

Signals of Saturation?

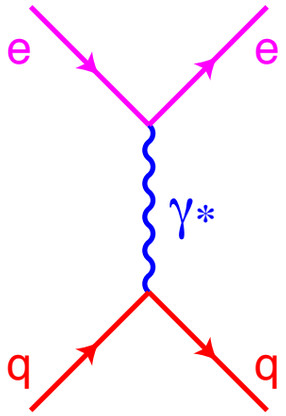
- cleaner observables: EM probes (direct photons, Drell-Yan)
  - no final state interaction
  - well-understood production process
  - well-defined kinematics
- advantage of direct photons: large cross section
  - forward p–A measurement of DY likely not possible with expected luminosity



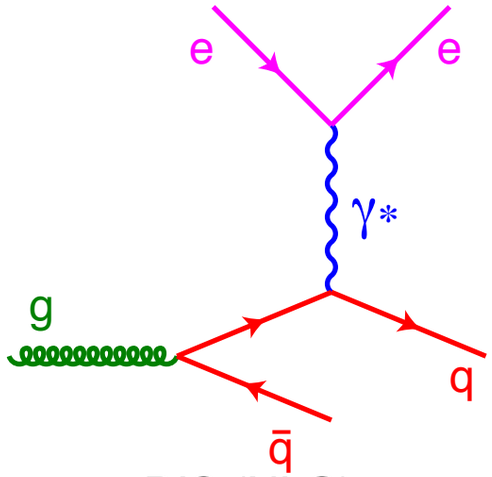
NLO pQCD calculations with shadowing (EPS09)
Helenius, Eskola, Paukkunen, arXiv:1406.1689

- interpretation of hadronic observables remains inconclusive
  - final state modifications in p–A collisions?
  - production process not fully understood for many hadrons
  - kinematic relation to Bjorken-x uncertain (e.g. fragmentation)
- best alternative candidate: open charm
  - direct sensitivity to gluons
  - final state interactions?

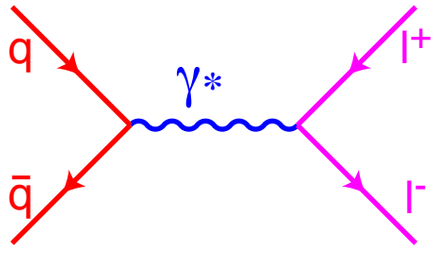
Electromagnetic Processes



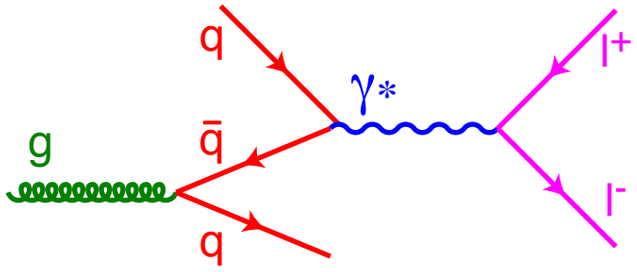
DIS (LO)



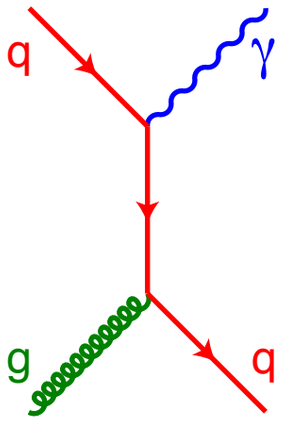
DIS (NLO)



DY (LO)



DY, virtual Compton (NLO)

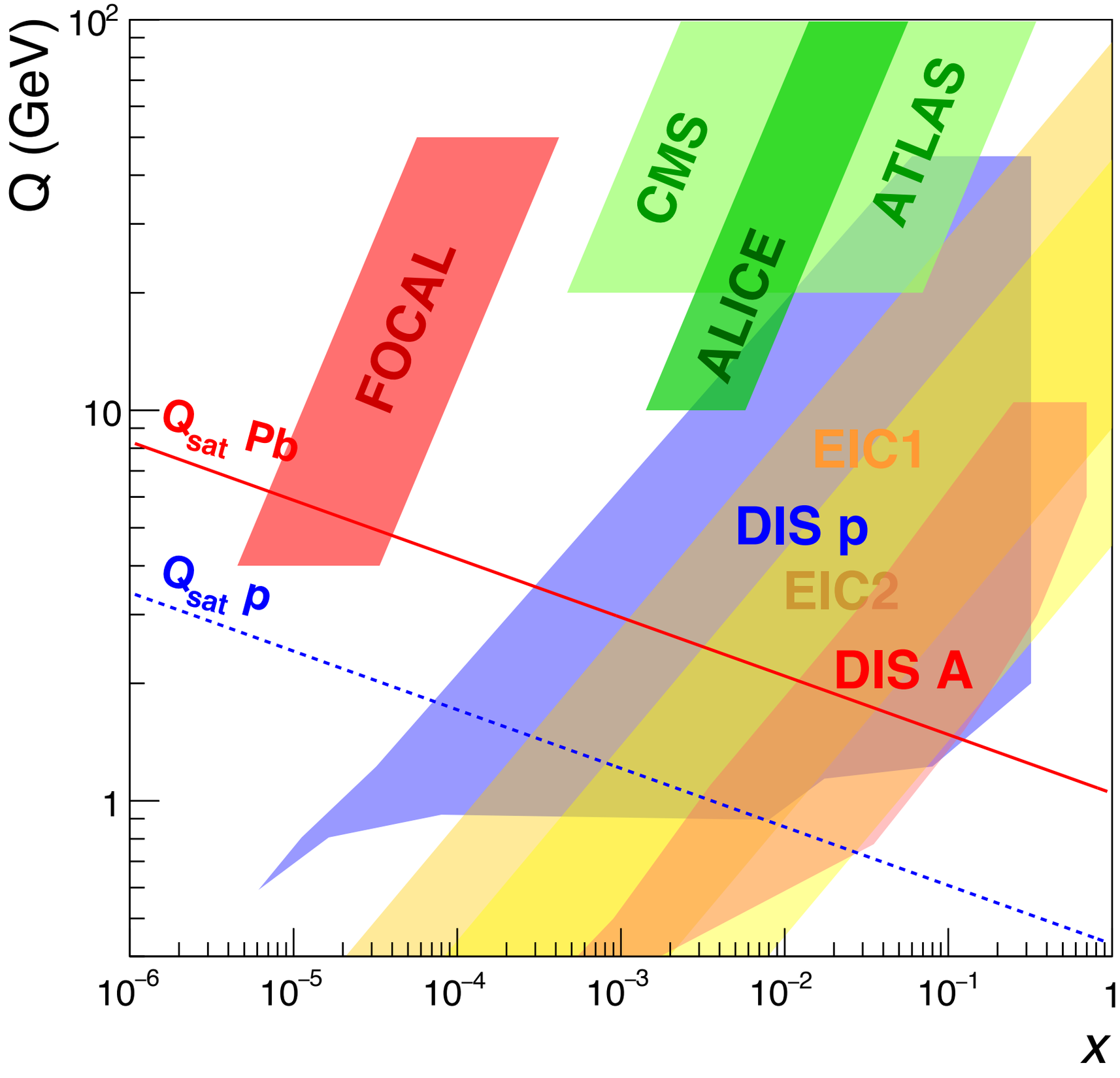


direct-γ, Compton (LO)

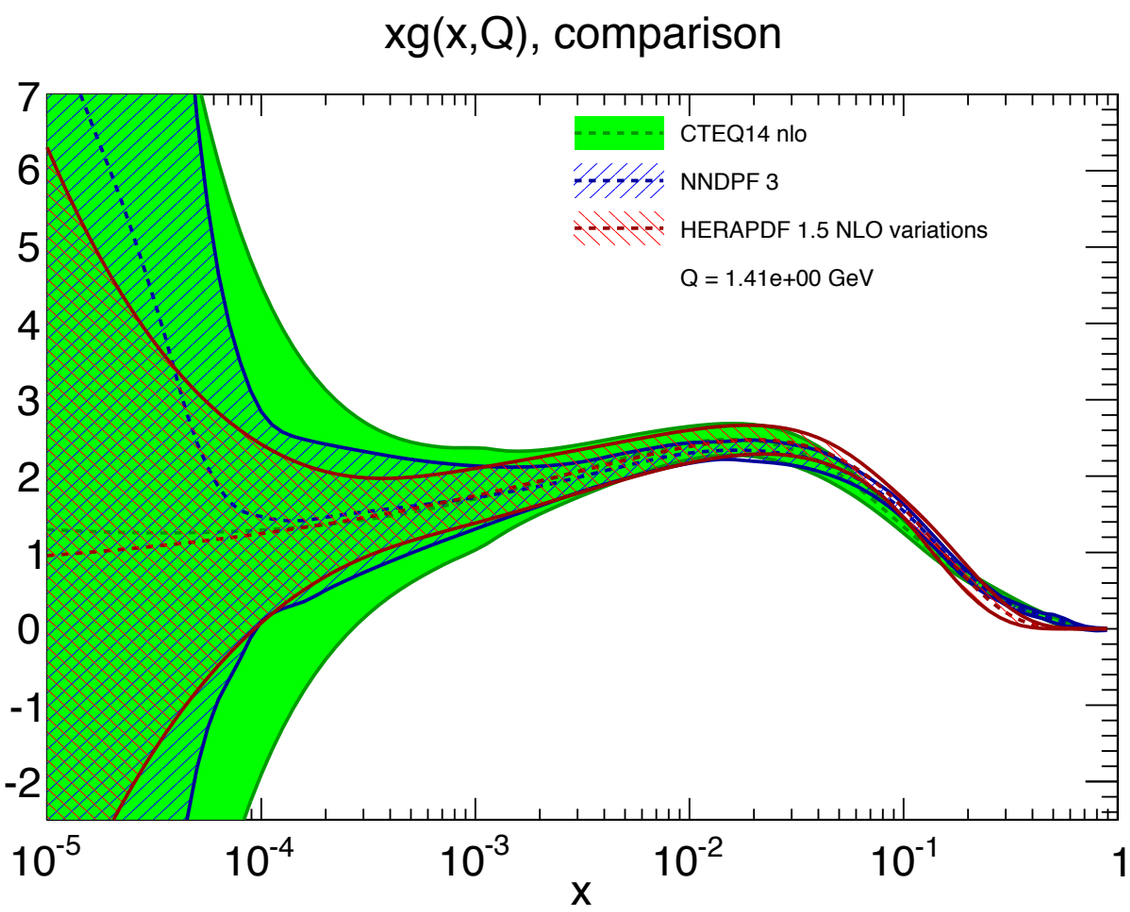
- DIS and Drell-Yan are equivalent processes
  - crossing symmetry
  - sensitivity to gluons only at NLO
    - e.g. virtual qg-Compton
- main disadvantage of DY: very low cross section
  - not accessible in pA

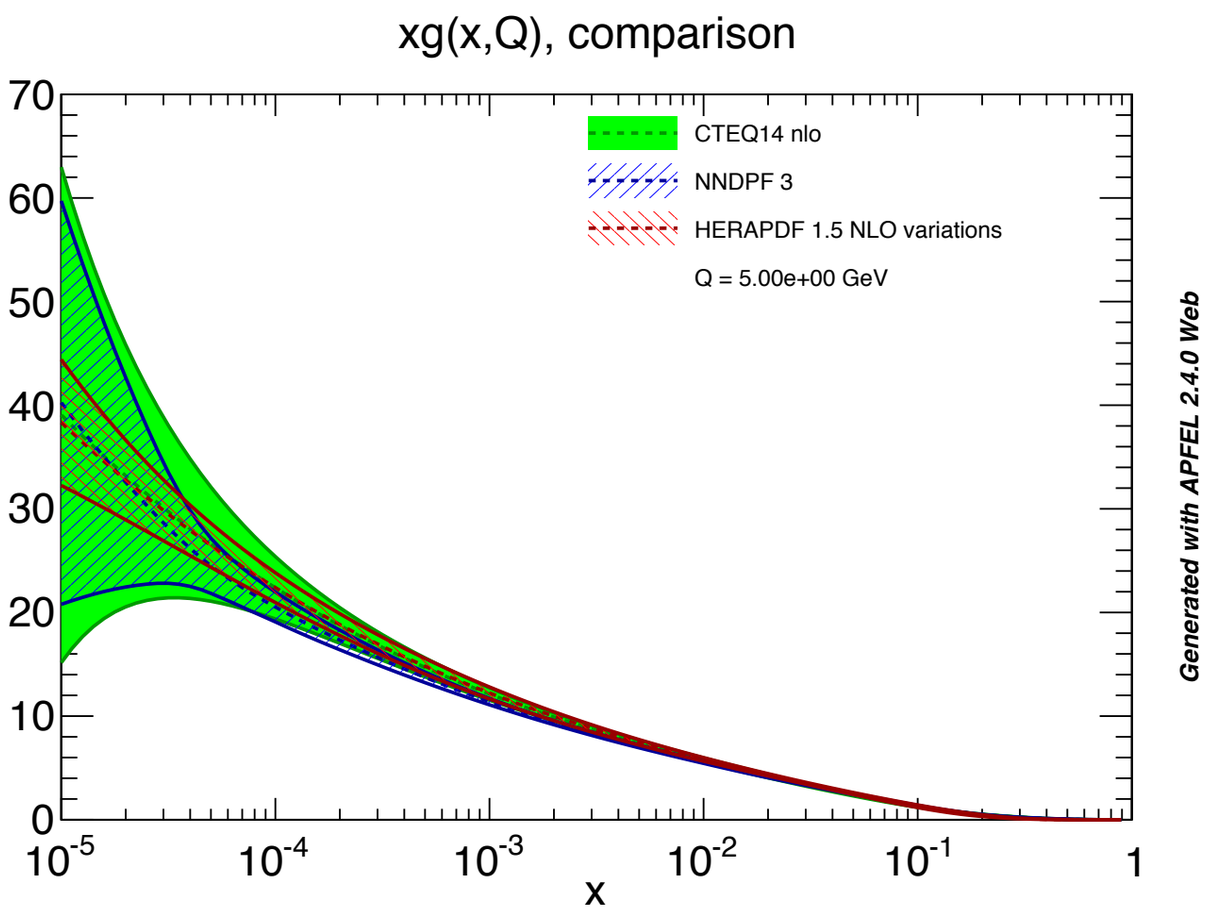
- real photons: sensitivity to gluons at LO, clear kinematic relation
  - higher order corrections?

EM Probes: Kinematic Coverage



Gluon Densities at Low x (Protons)

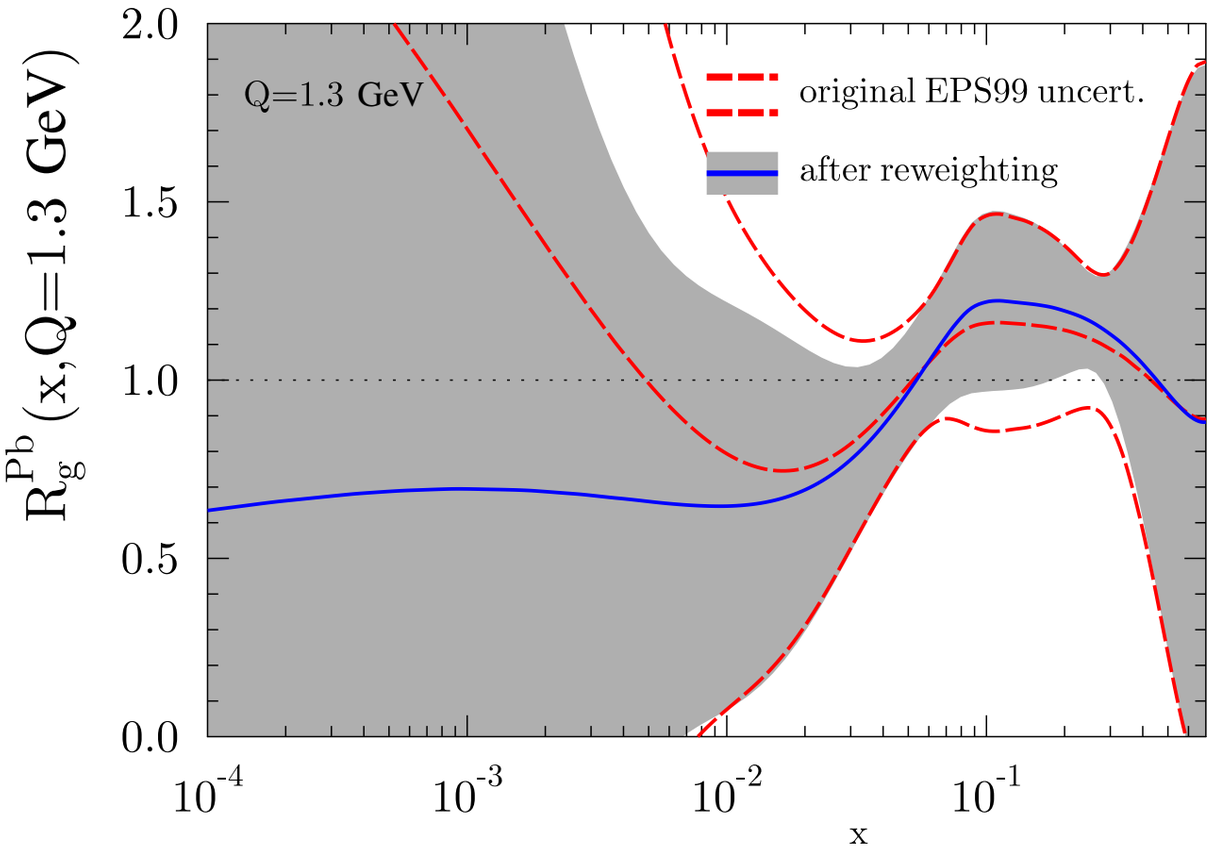


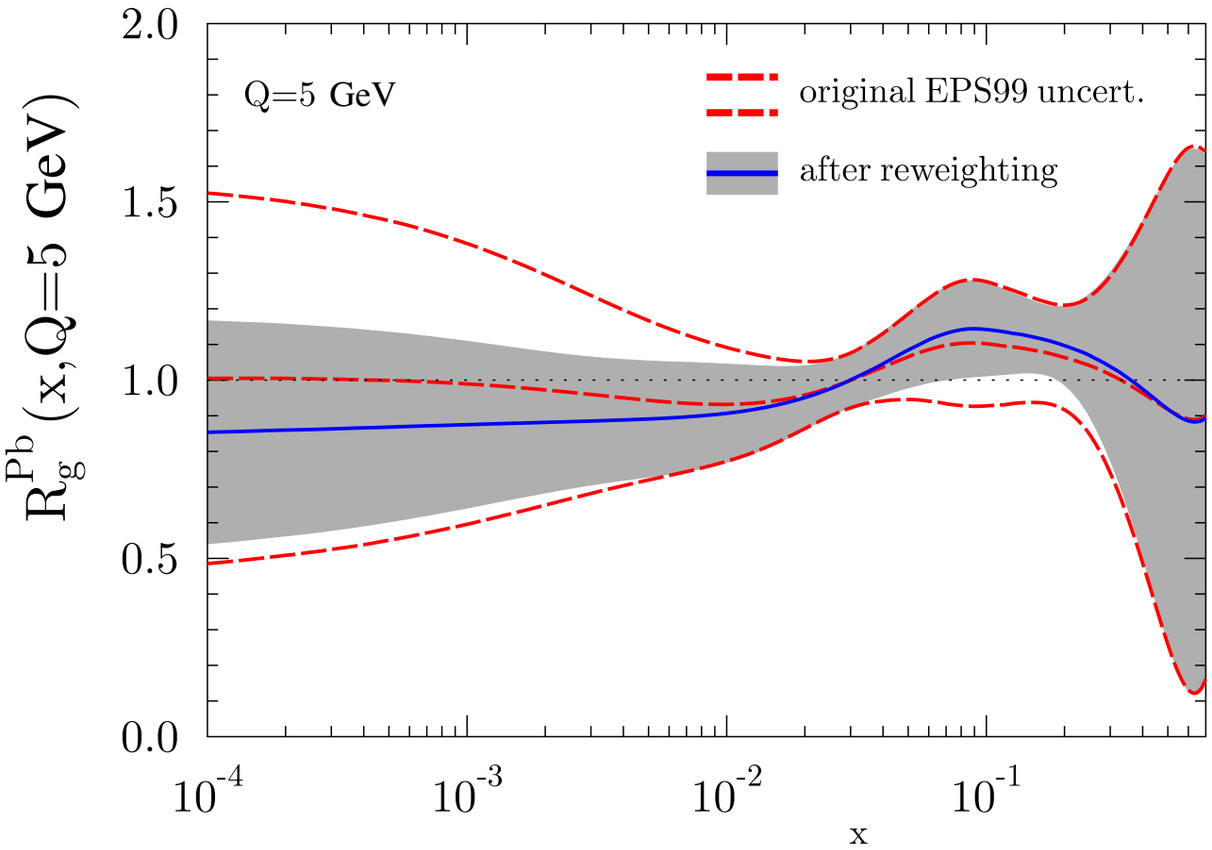


- at Q = 1.41 GeV, g(x) essentially unconstrained for $x < 10^{-4}$
- apparent uncertainty significantly reduced at slightly larger Q (5 GeV)
  - not from more data constraints!
  - strong role of QCD evolution

- careful: we want to test QCD evolution!

Gluon Densities at Low x (Nuclei)

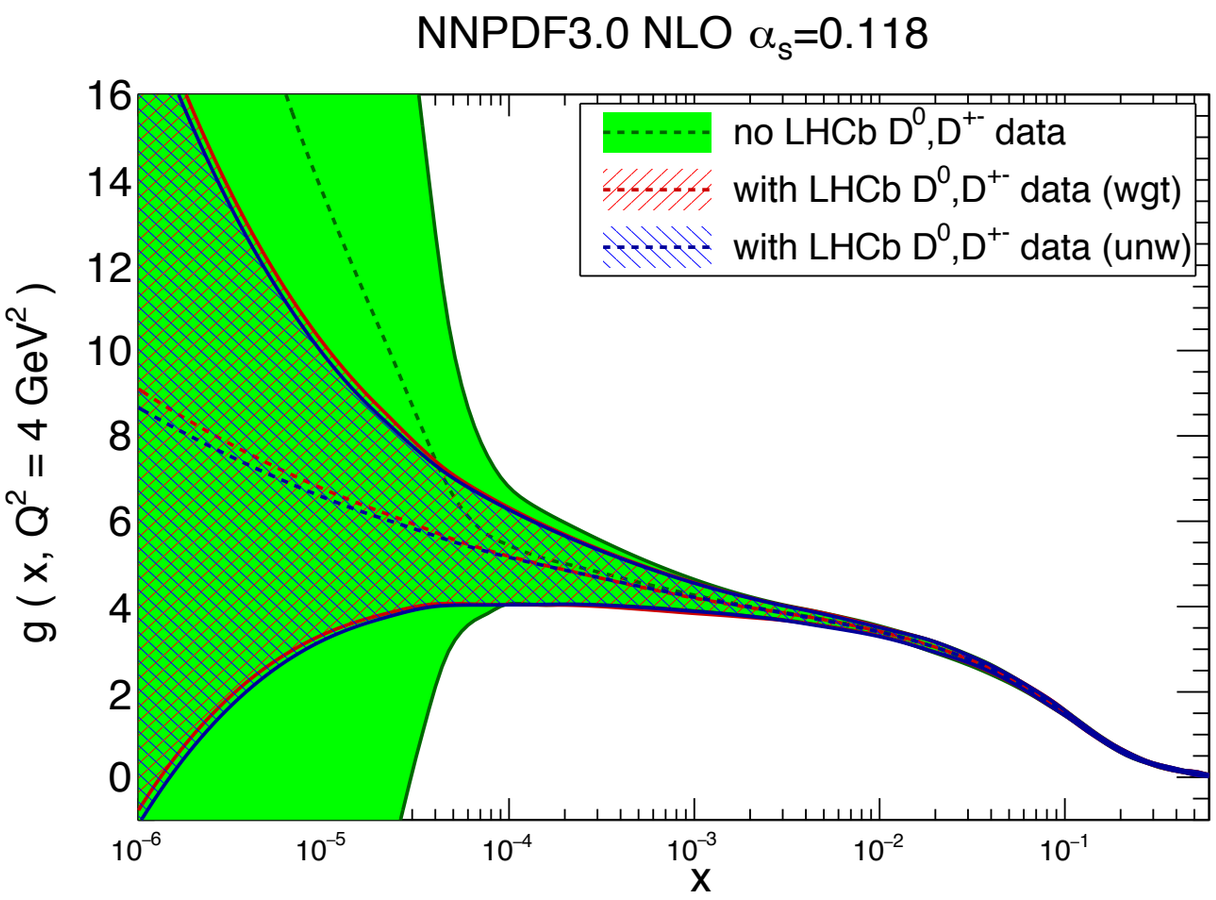


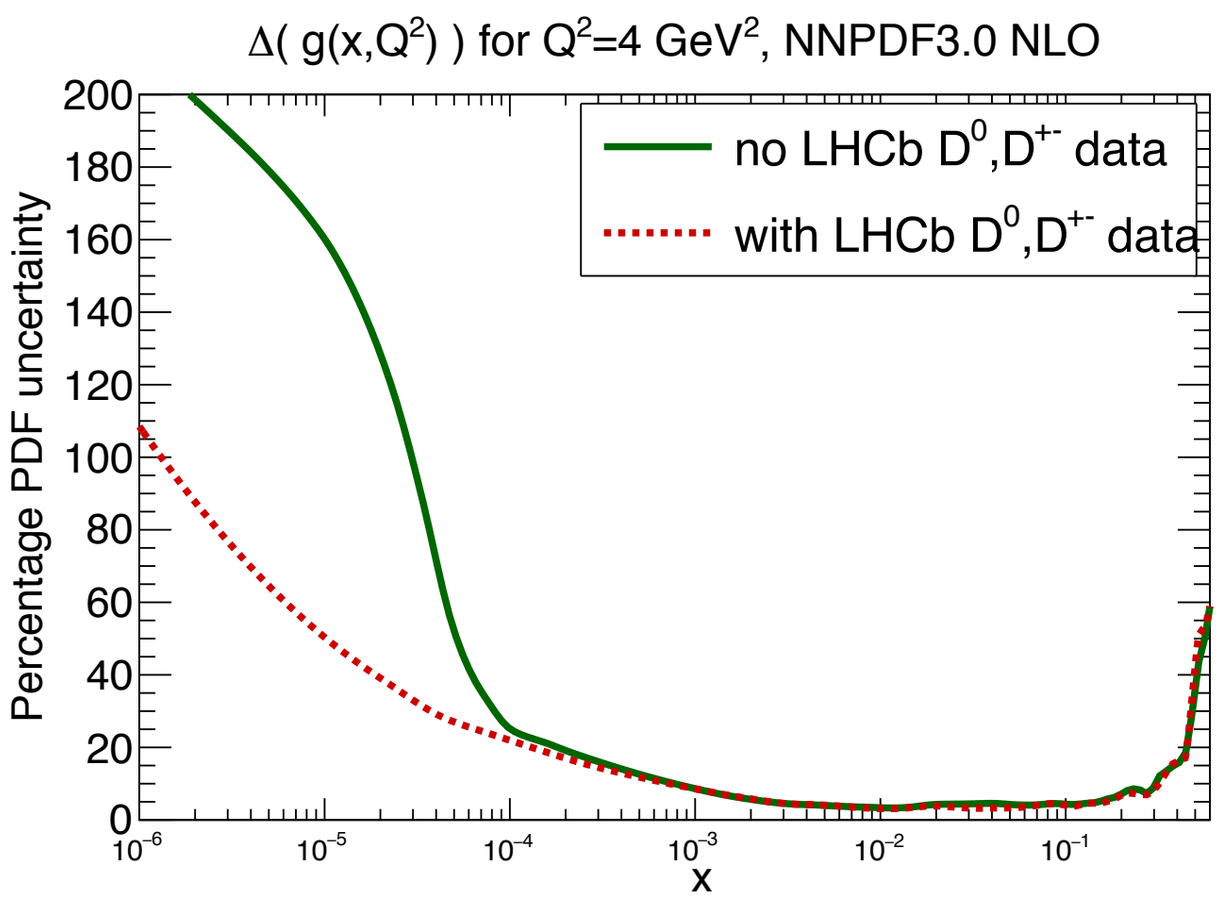


H. Paukkunen, I. Helenius, priv. communication

- at Q = 1.3 GeV, g(x) essentially unconstrained for $x < 10^{-2}$
  - old PDF sets in nuclei did not allow sufficient freedom
  - new parameterisations under way – still not equivalent flexibility as NNPDFs

Impact of Forward Open Charm

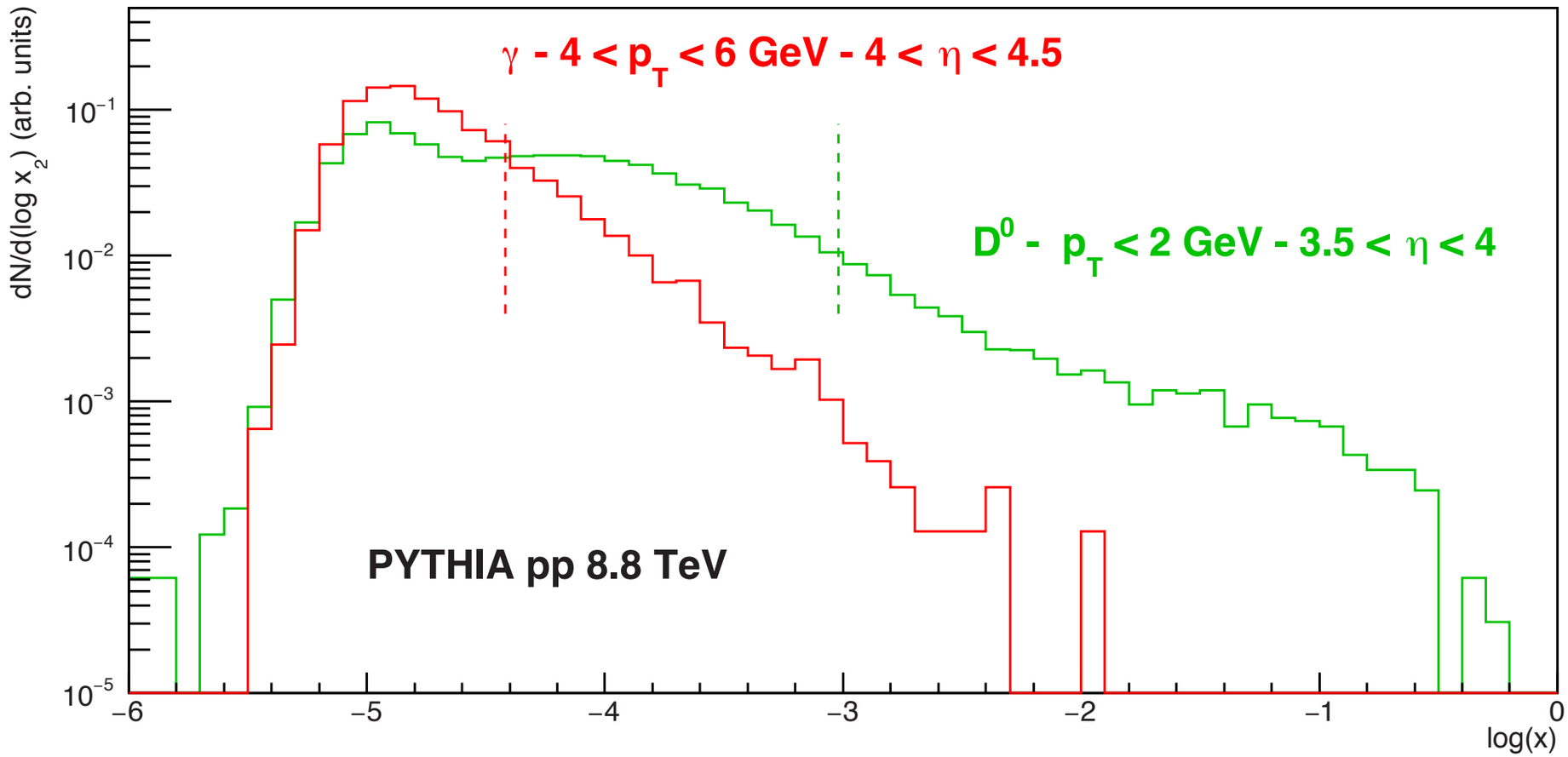




R. Gauld et al., arXiv 1506.08025

- usage of forward D measurements by LHCb can constrain gluon distribution
  - fit uses normalisation at low y, high p_T
- how much of the constraints due to data?

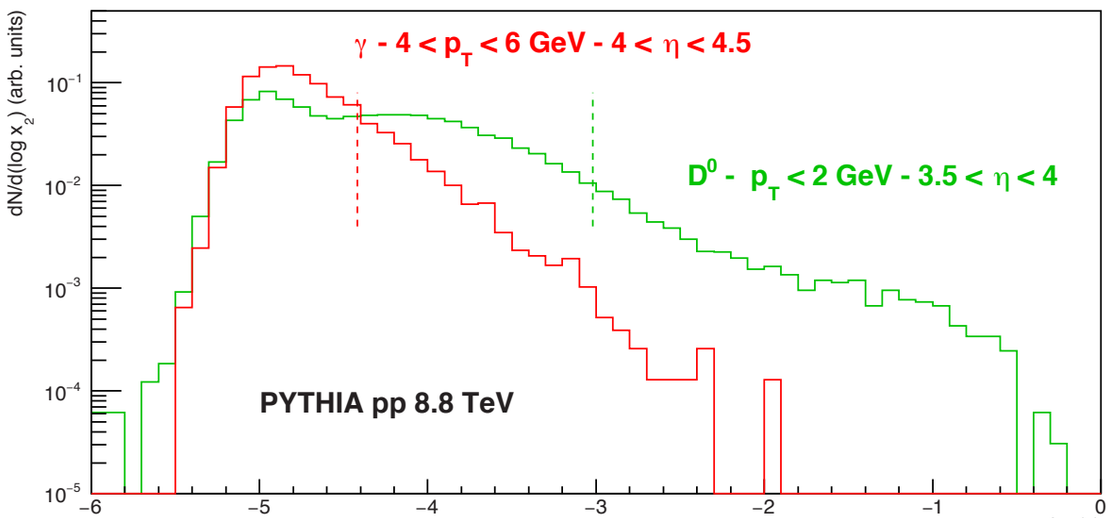
x-Sensitivity

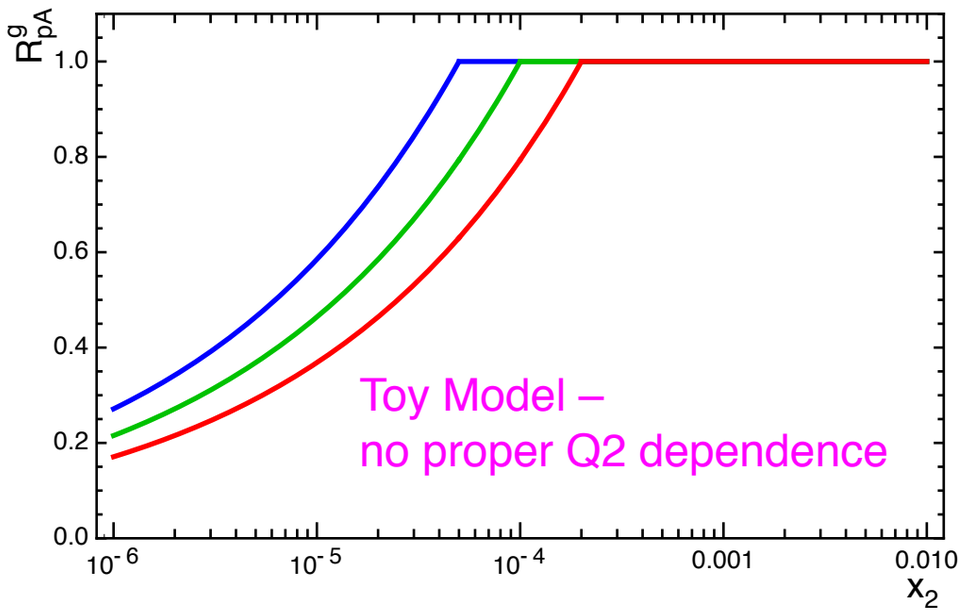


- x_2 distributions for forward production
  - LO production from PYTHIA
  - D^0 (LHCb) vs prompt γ (FoCal)
- apparent maximum at $x \approx 10^{-5}$
  - beware of log(x) scale!
  - significantly larger mean value
- significant advantage of proposed direct photon measurement relative to charm in LHCb

Parameterised Nuclear Modification

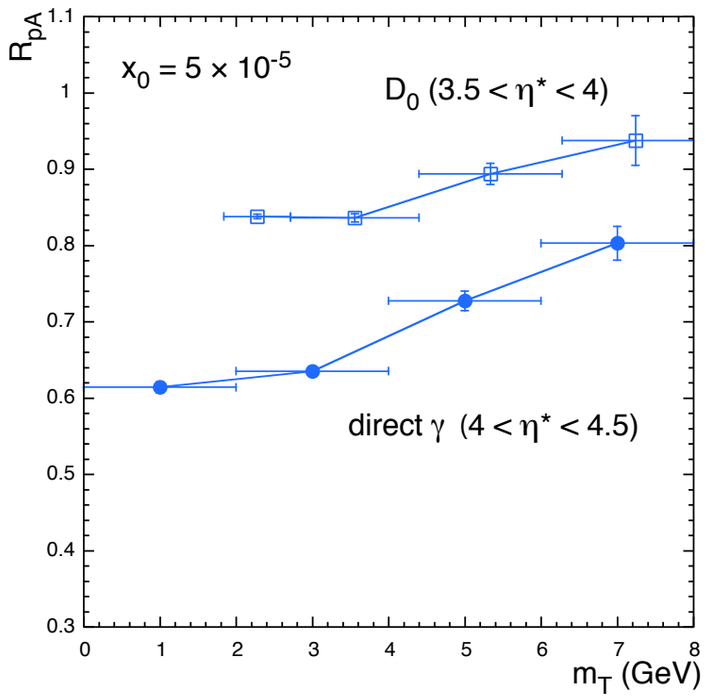
assume nuclear modification of gluon PDFs

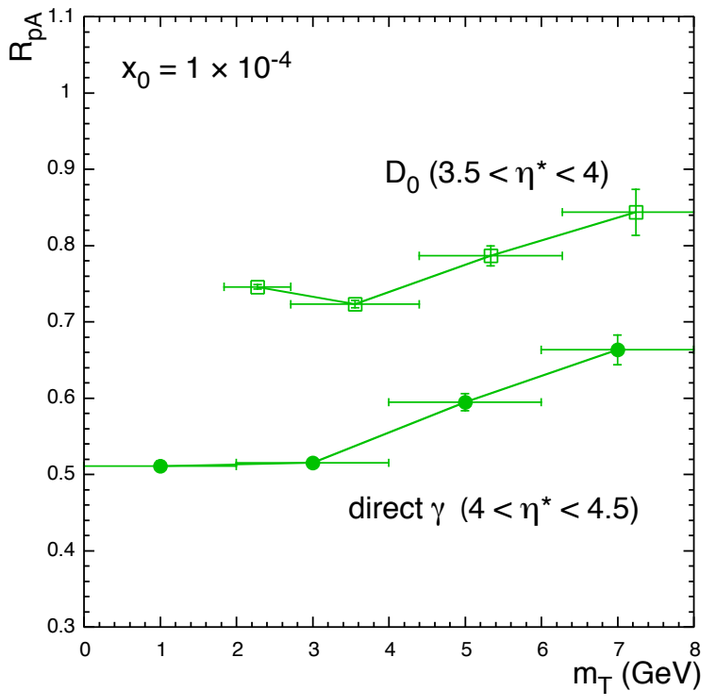


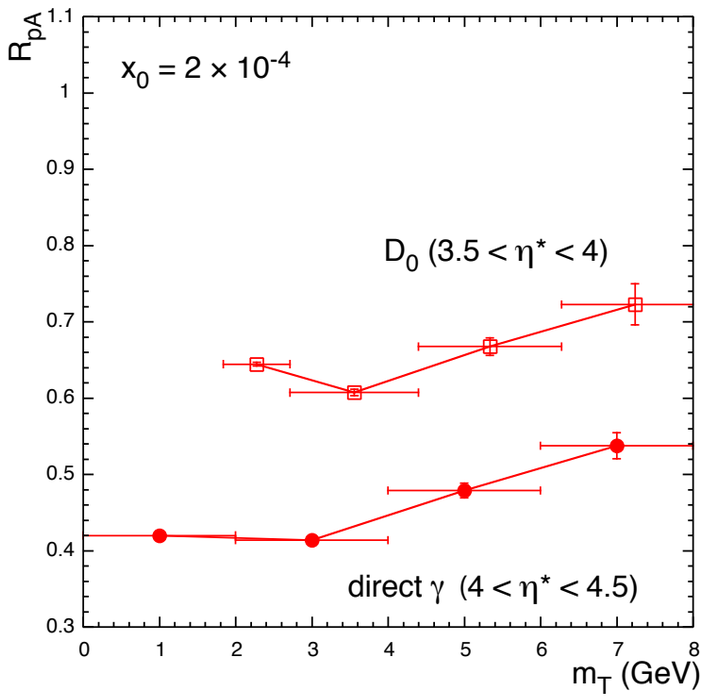


fold with gluon x distribution for a given observable in pp collisions (PYTHIA)

from ratio of integrals obtain nuclear modification of observable







More Realistic Nuclear Modification?

naive recipe to compare gluon density from saturation models:
calculate “effective gluon PDFs” (thanks to Elena Petreska)

$$xG(x,Q^2) = \int^{Q} \frac{d^2k_T}{\pi}\Phi(x,k_T)$$

GBW-model:
$$xG_{\mathrm{GBW}}(x,Q^2) = \frac{N_c}{2\pi^3\alpha_s}\pi R^2 Q_s^2(x)\left[1-\left(1+\frac{Q^2}{Q_s^2(x)}\right)e^{-Q^2/Q_s^2(x)}\right]$$

MV-model ($k_T >> Q_s$):
$$xG_{\mathrm{MV}}(x,Q^2) = \frac{N_c}{4\pi^2\alpha_s}\pi R^2 Q_s^2(x)\log\left(\frac{Q^2}{\Lambda^2}\right)$$

with:
$$Q_{sp}^2(x) = Q_{s0}^2(x)\left(\frac{x_0}{x}\right)^{\lambda}$$

Nuclear Modification of Gluon PDFs

calculate with: $Q^2_{sA}(x) = cA^{1/3}Q^2_{sp}(x)$

$$Q^2_{s0}(x) = 1\,\mathrm{GeV}^2;\;\; x_0 = 3.04 \cdot 10^{-4};\;\; \lambda = 0.288$$

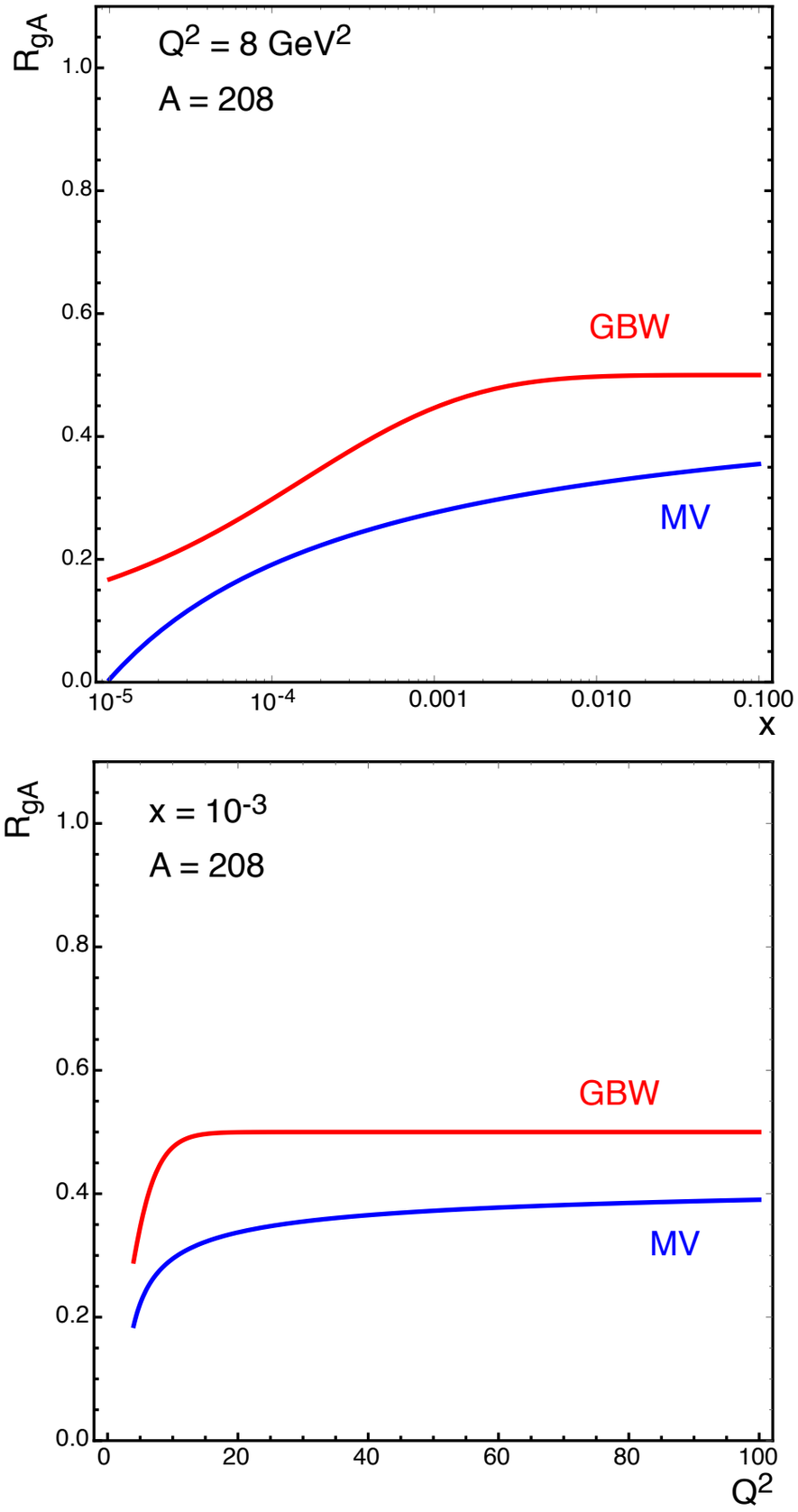
$$c = 0.5$$

limited range of applicability (if at all)

models do not have proper high-x and high-Q^2 limits!

calculations using similar approximations will not be able to properly describe observables with broad x-Q^2-distributions of initial partons

“better” saturation models with correct asymptotic limits available?

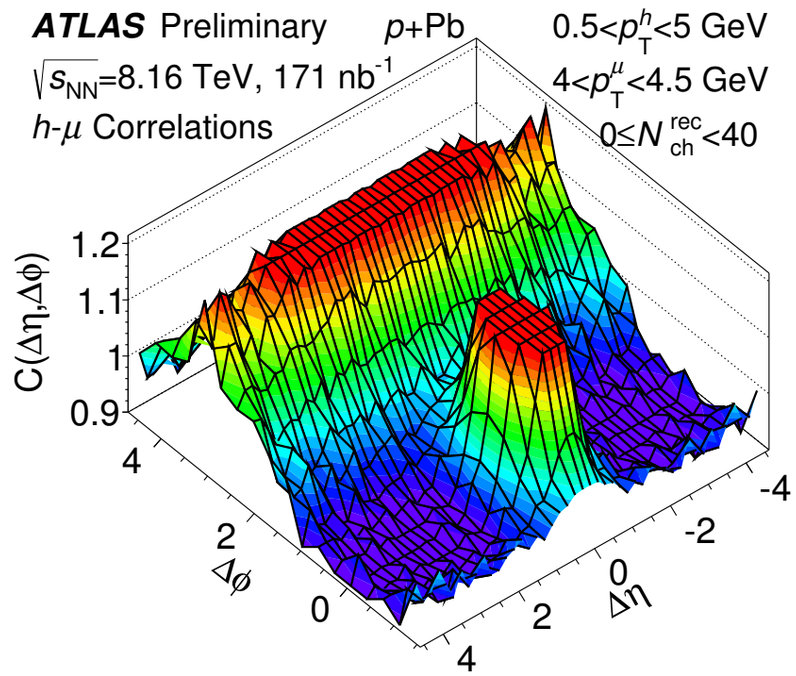


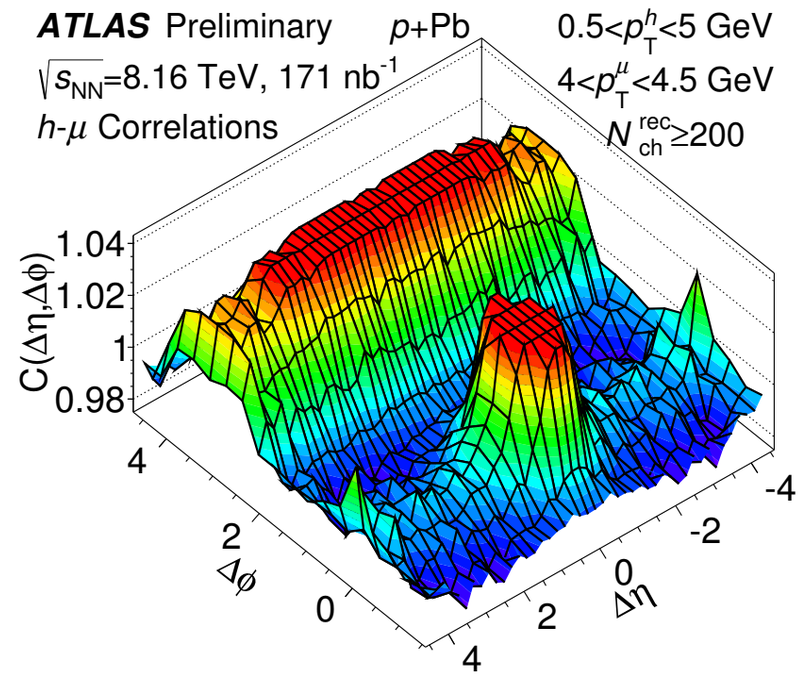
Final State Nuclear Modification of HF in p–Pb?

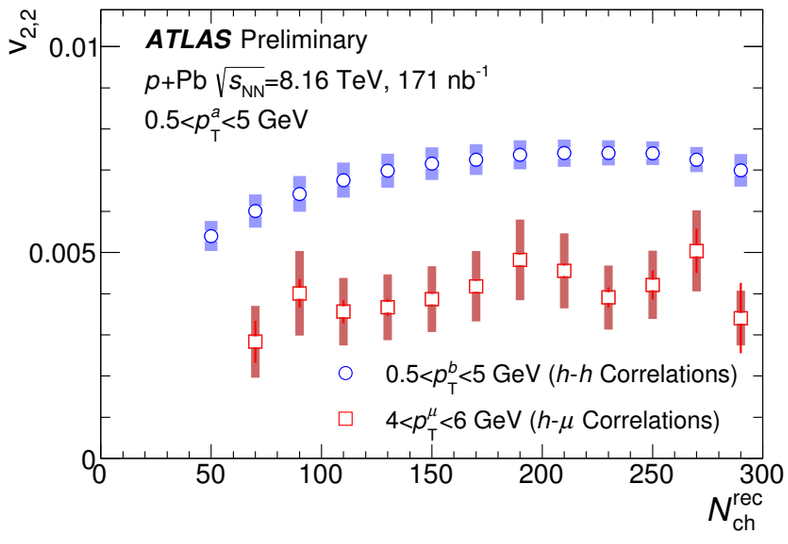
recent results from ATLAS (presented at QM2017): ATLAS-CONF-2017-006

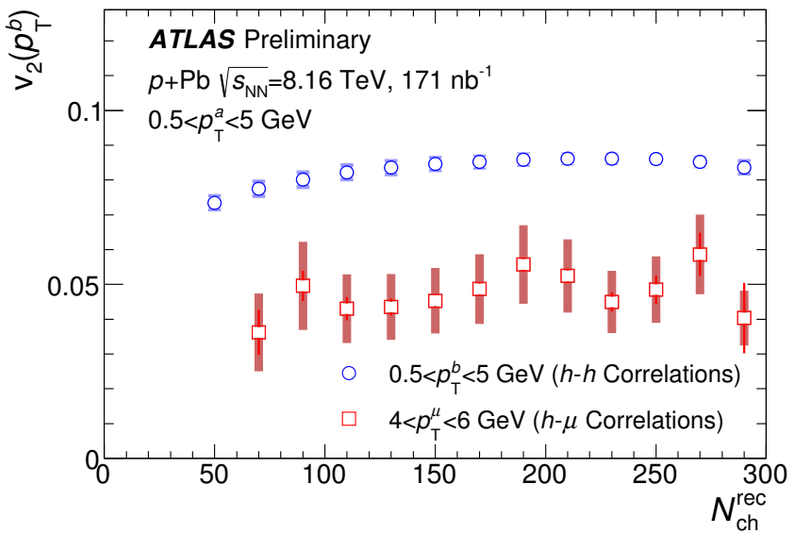
study of h-μ angular correlations,
observe flow-like correlation of muons
in high multiplicity p–Pb (muons dominated by heavy flavour)

heavy flavour suffering final state modification in pPb?
still useful as initial state probe?

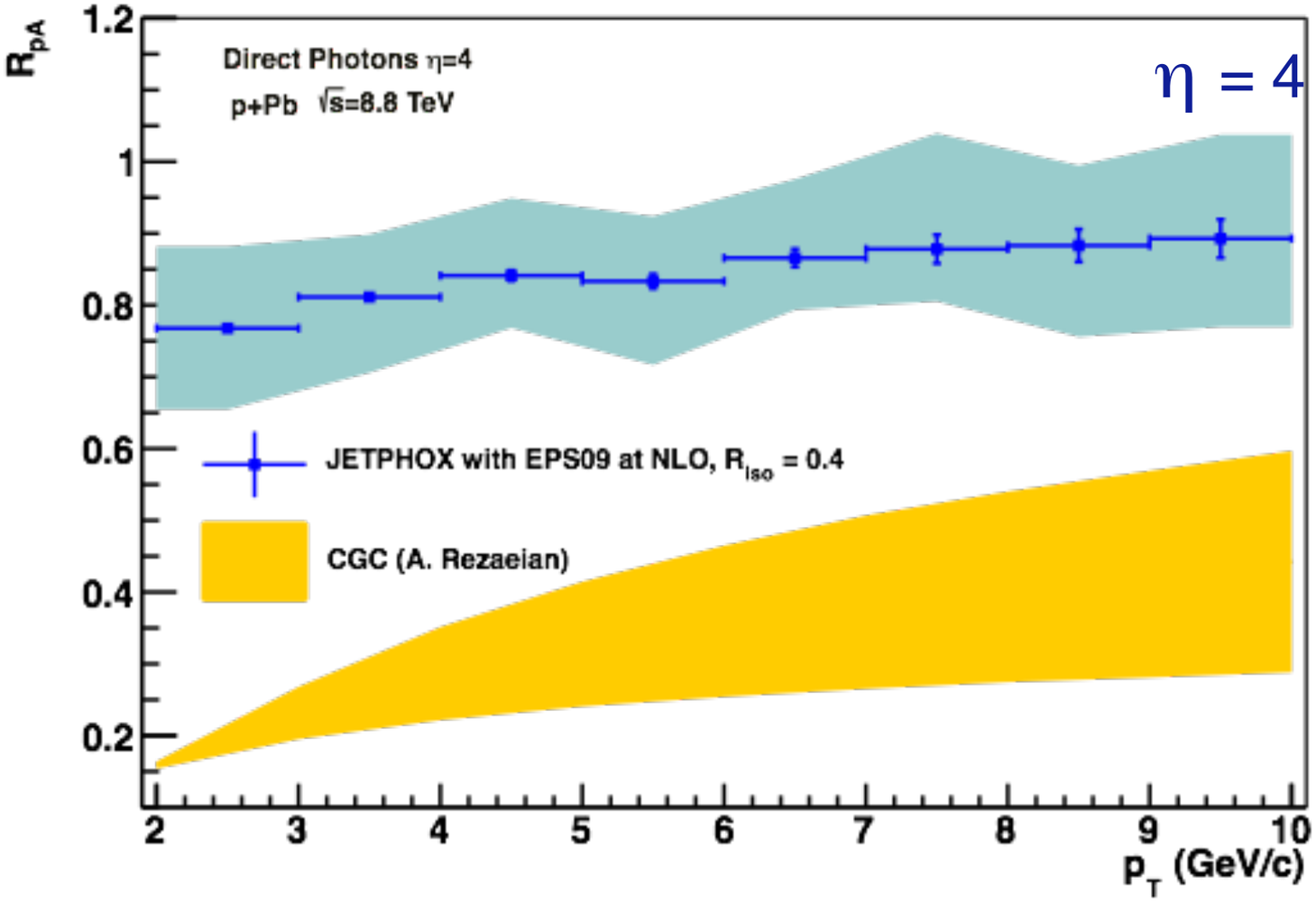








Starting Point Now: nPDF/DGLAP vs CGC



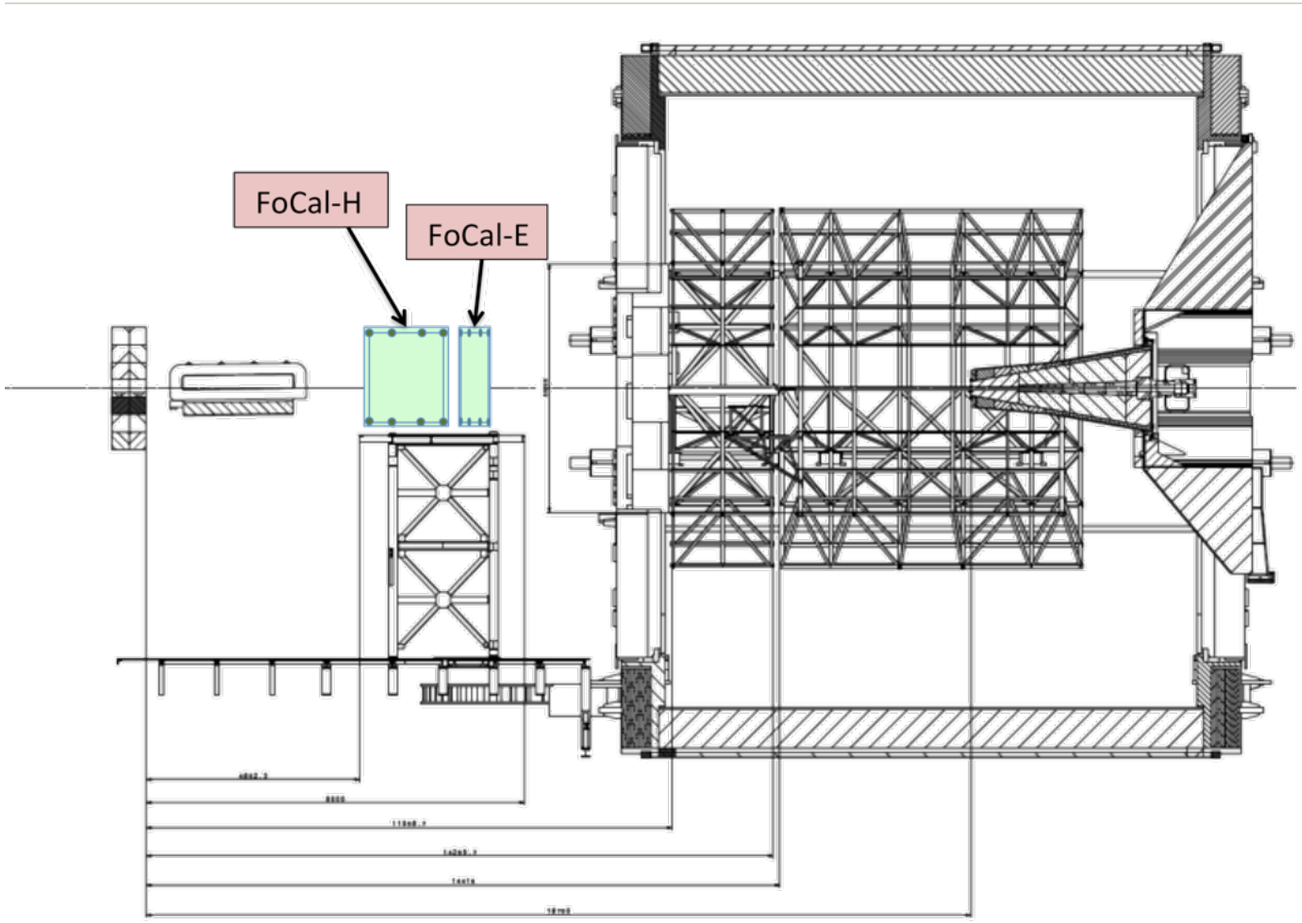
two scenarios for forward γ production in p+A at LHC:

- normal nuclear effects
  linear evolution, shadowing
- saturation/CGC
  running coupling BK evolution

Rezaeian, PLB 718, 1058

- strong suppression in direct γ R_{pA}
  - clean signal for isolated photons
- signals expected at forward η, low-intermediate p_T

FoCal in ALICE



electromagnetic calorimeter for γ and π^0 measurement

preferred scenario:

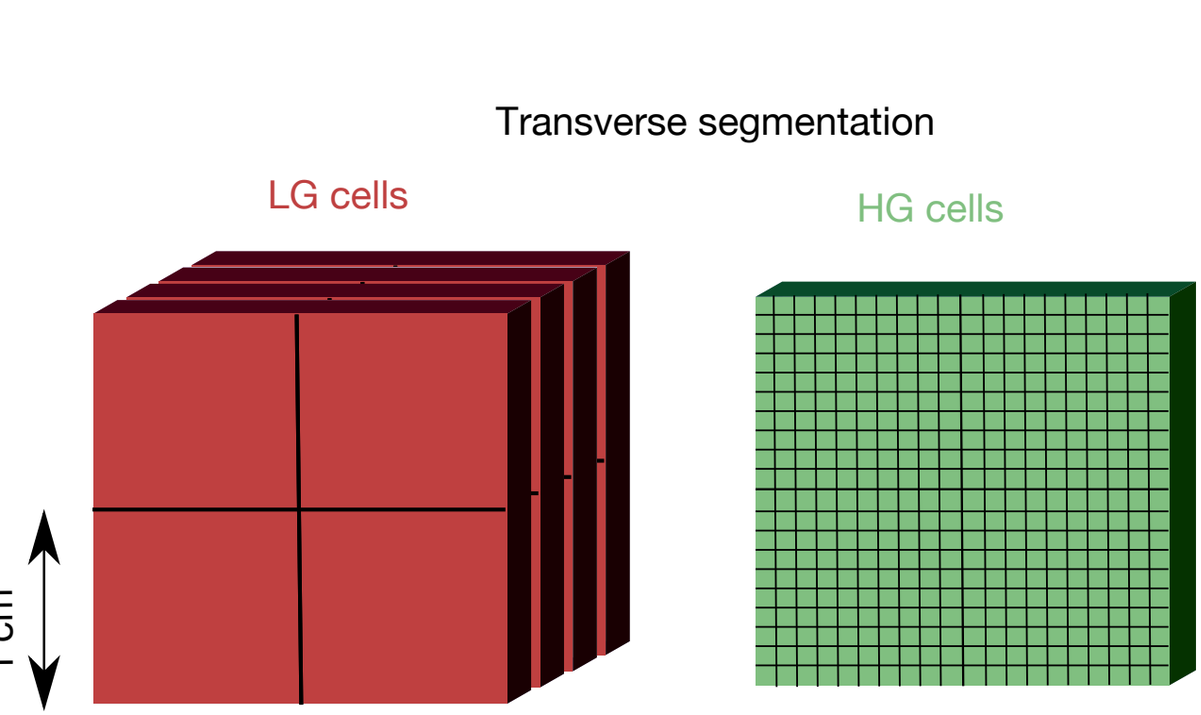
- at $z \approx 7$m (outside magnet)
  $3.3 < \eta < 5.3$
  (space to add hadr. calorimeter)

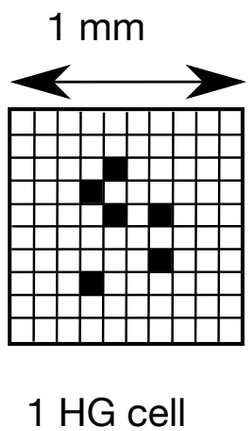
under internal discussion
possible installation in LS3

- main challenge: separate γ/π^0 at high energy
- need small Molière radius, high-granularity read-out
  - Si-W calorimeter, effective granularity $\approx 1\text{mm}^2$

note: two-photon separation from π^0 decay (p_T = 10 GeV/c, y = 4.5, α = 0.5) is d = 2 mm!

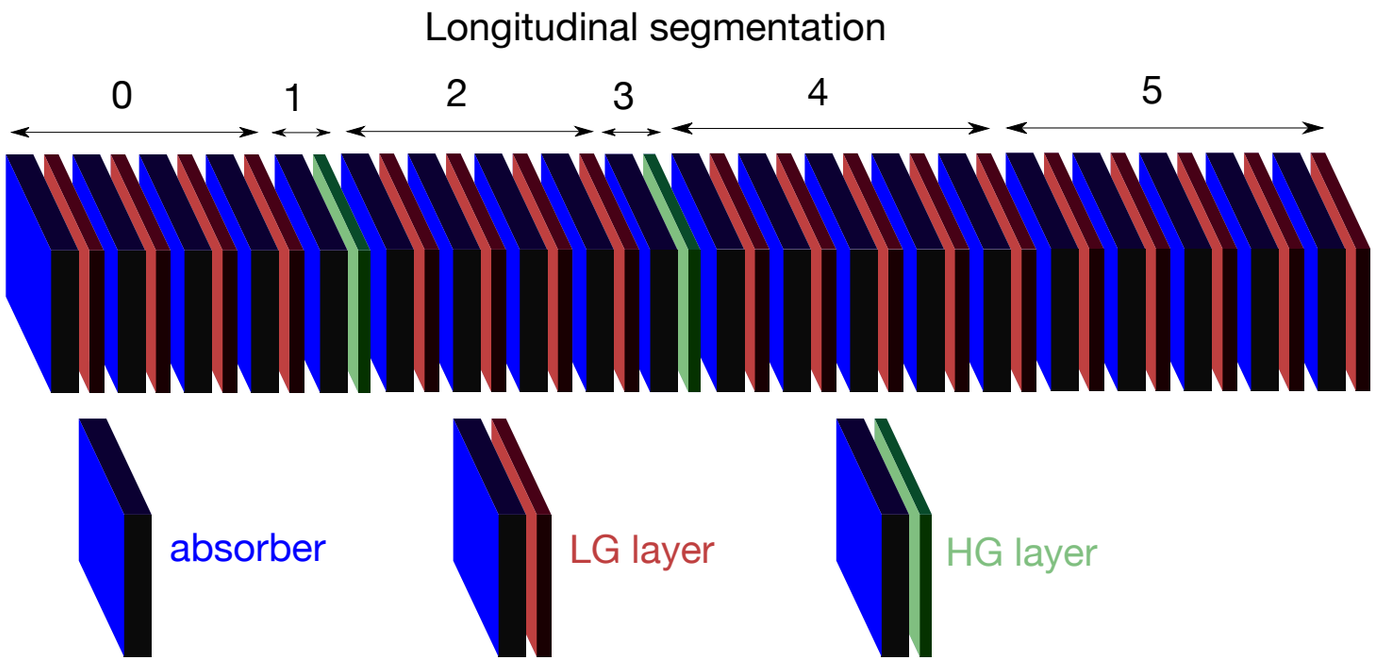
FoCal Strawman Design





studied in performance simulations:

24 layers: W (3.5mm ≈ 1 X0) +
Si-sensors (2 types)
low granularity (LG), Si-pads
high granularity (HG), pixels
(e.g. CMOS-MAPS)



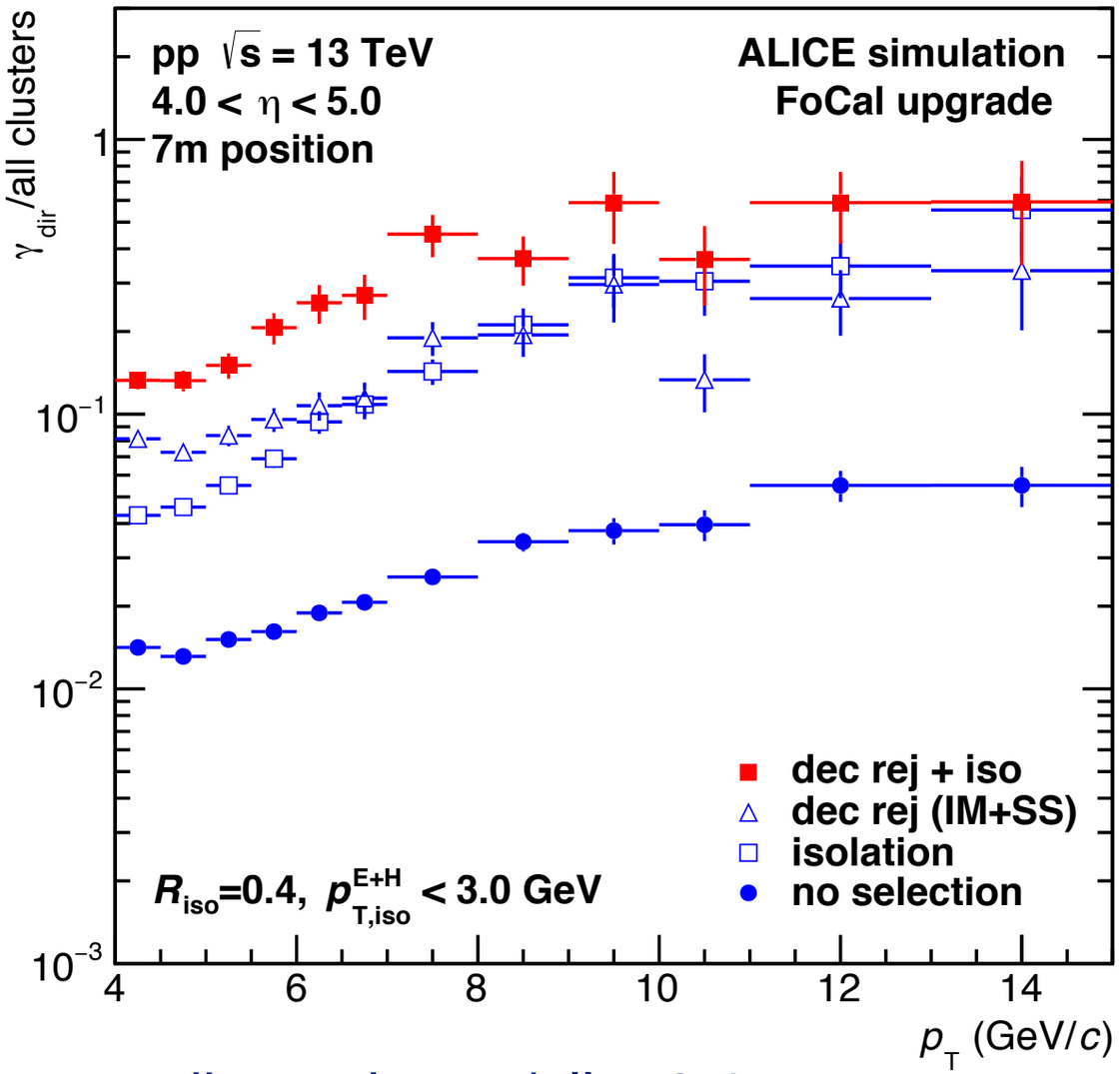
	LG	HG
pixel/pad size	≈ 1 cm^2	≈ 30x30 μm^2
total # pixels/pads	≈ 2.5 x 10^5	≈ 2.5 x 10^9
readout channels	≈ 5 x 10^4	≈ 2 x 10^6

assuming ≈ 1m^2 detector surface

Direct γ Performance in pp

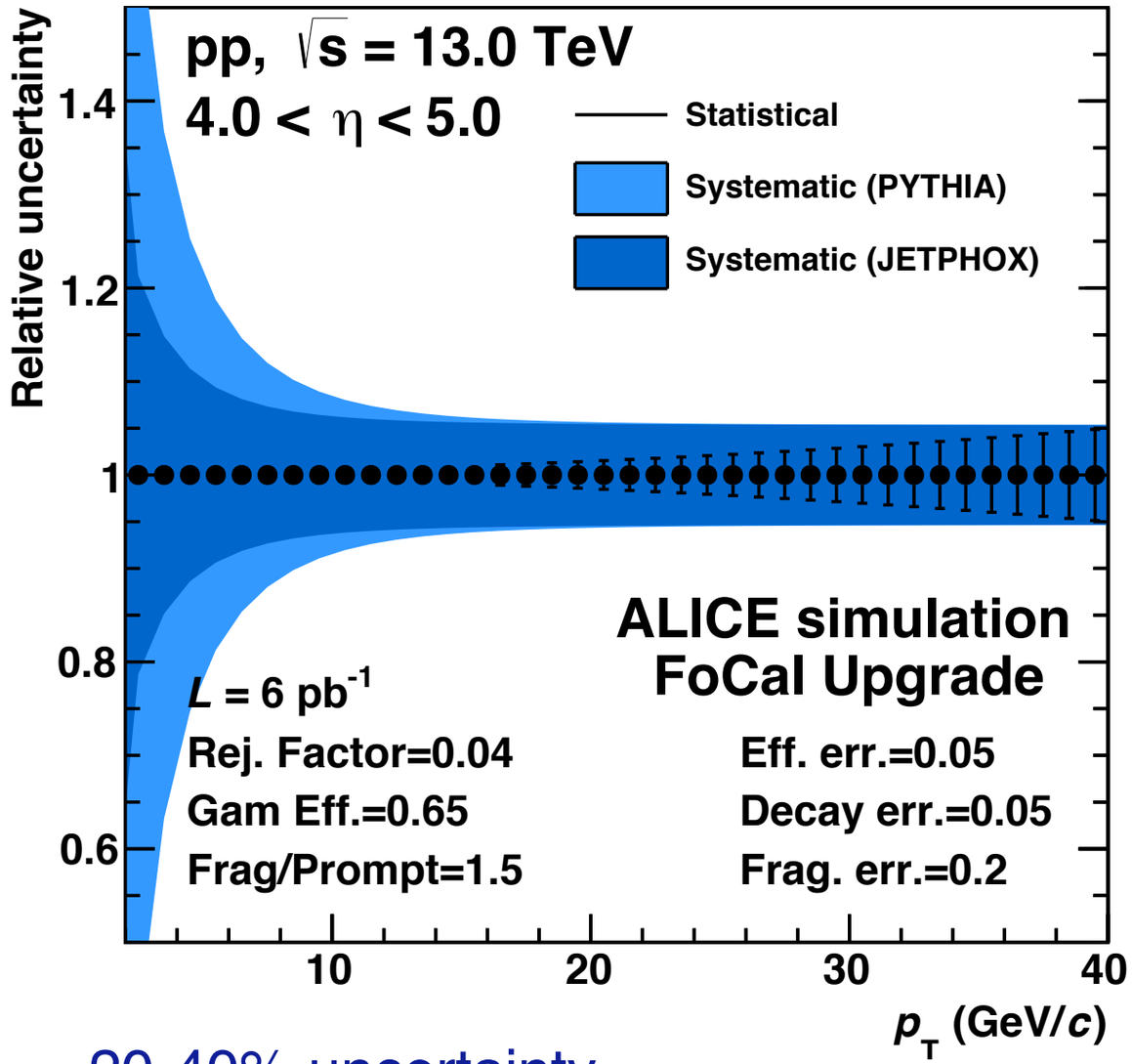
- combined rejection (invariant mass + shower shape, isolation)
- rejection factor ≈25, direct photon efficiency ≈80%
  - largely p_T-independent

Direct γ/all cluster ratio



direct photon/all > 0.1
for p_T > 4 GeV/c

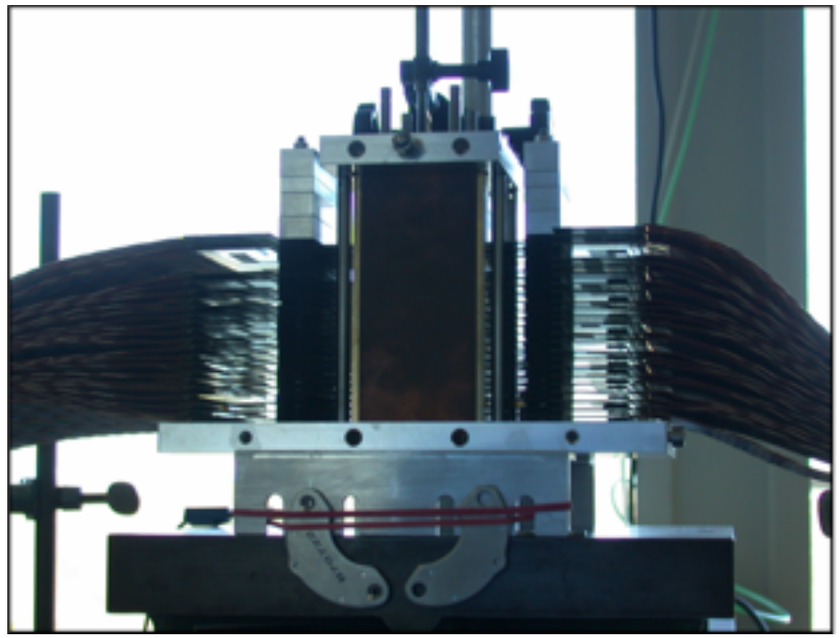
Direct γ uncertainty



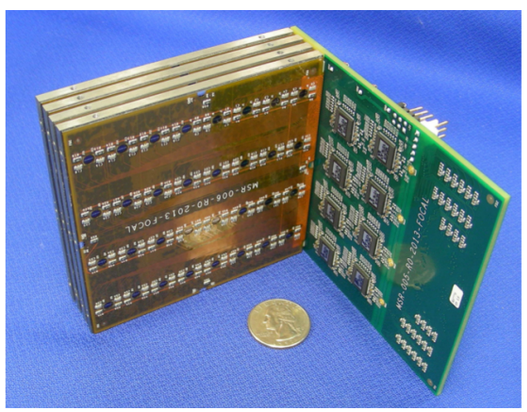
20-40% uncertainty
at p_T = 4 GeV/c
decreases with increasing p_T

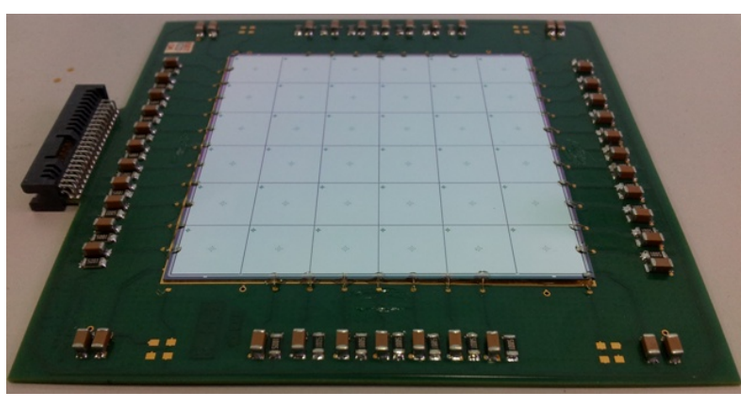
FoCal R&D: Si-W pixel and pad readout

24 layer pixel detector



Pad layer integration



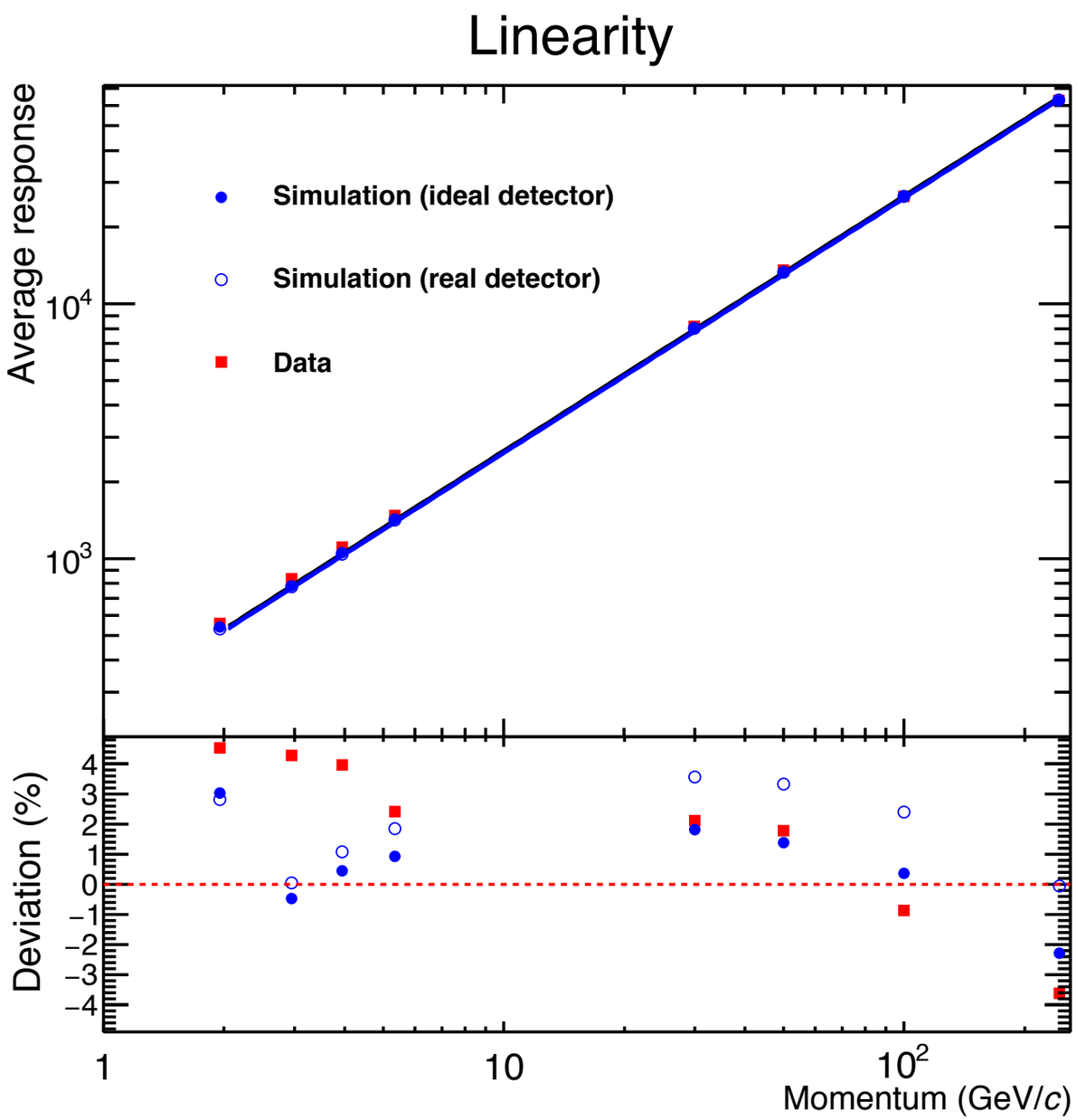


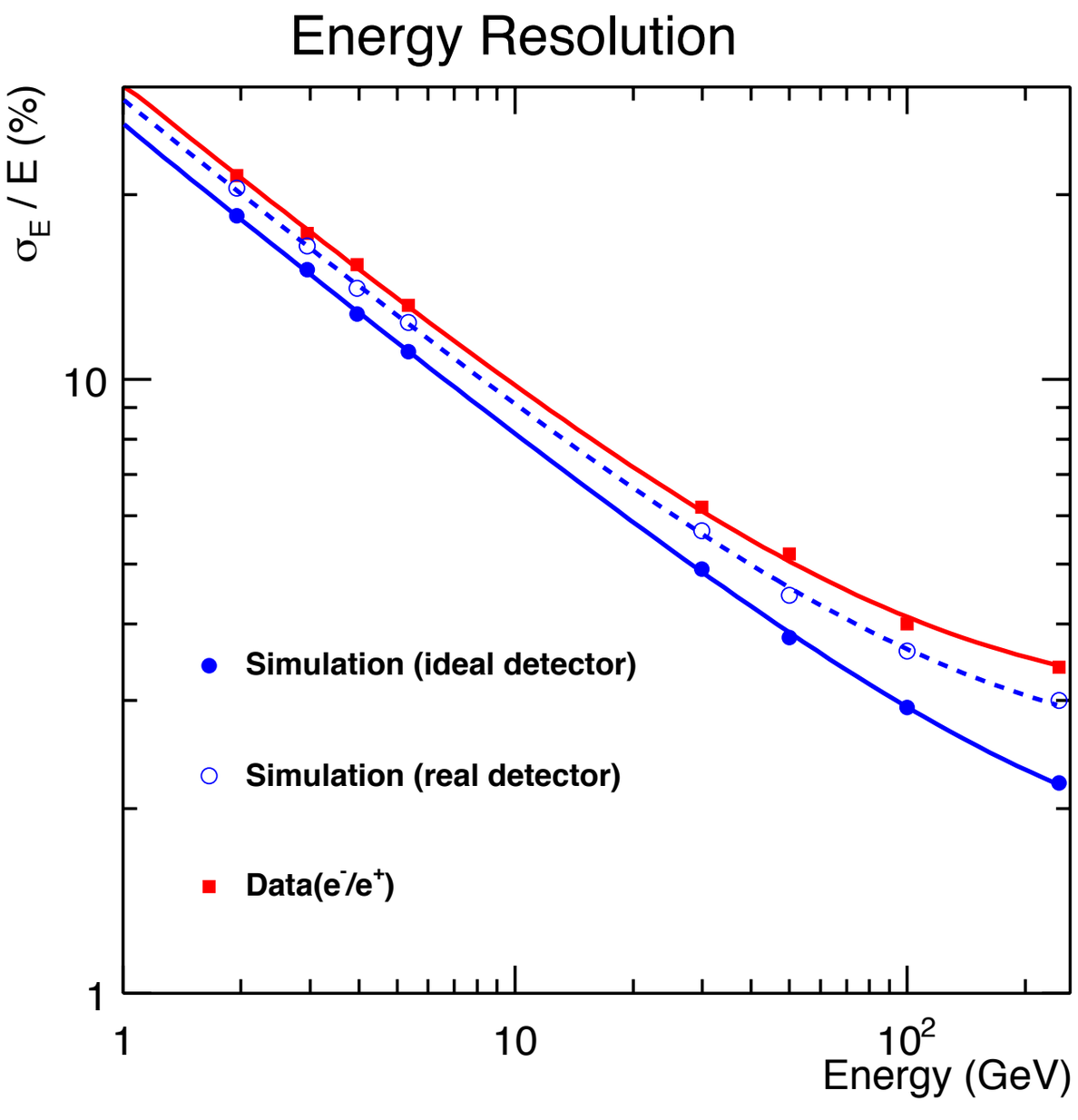
Several groups involved:
- Full prototype with pixel detectors
  - CMOS (MIMOSA) 39M pixels, 30µm pitch
    - use synergy with R&D for ALICE ITS upgrade
  - Full prototype with pad readout

Performed systematic tests:
- Test beam data from 2 to 250 GeV (DESY, PS, SPS)
- Cosmic muons

Utrecht/Nikhef (Netherlands),
Bergen (Norway),
Tsukuba, Nara (Japan),
ORNL (US)

R&D - Energy Linearity and Resolution



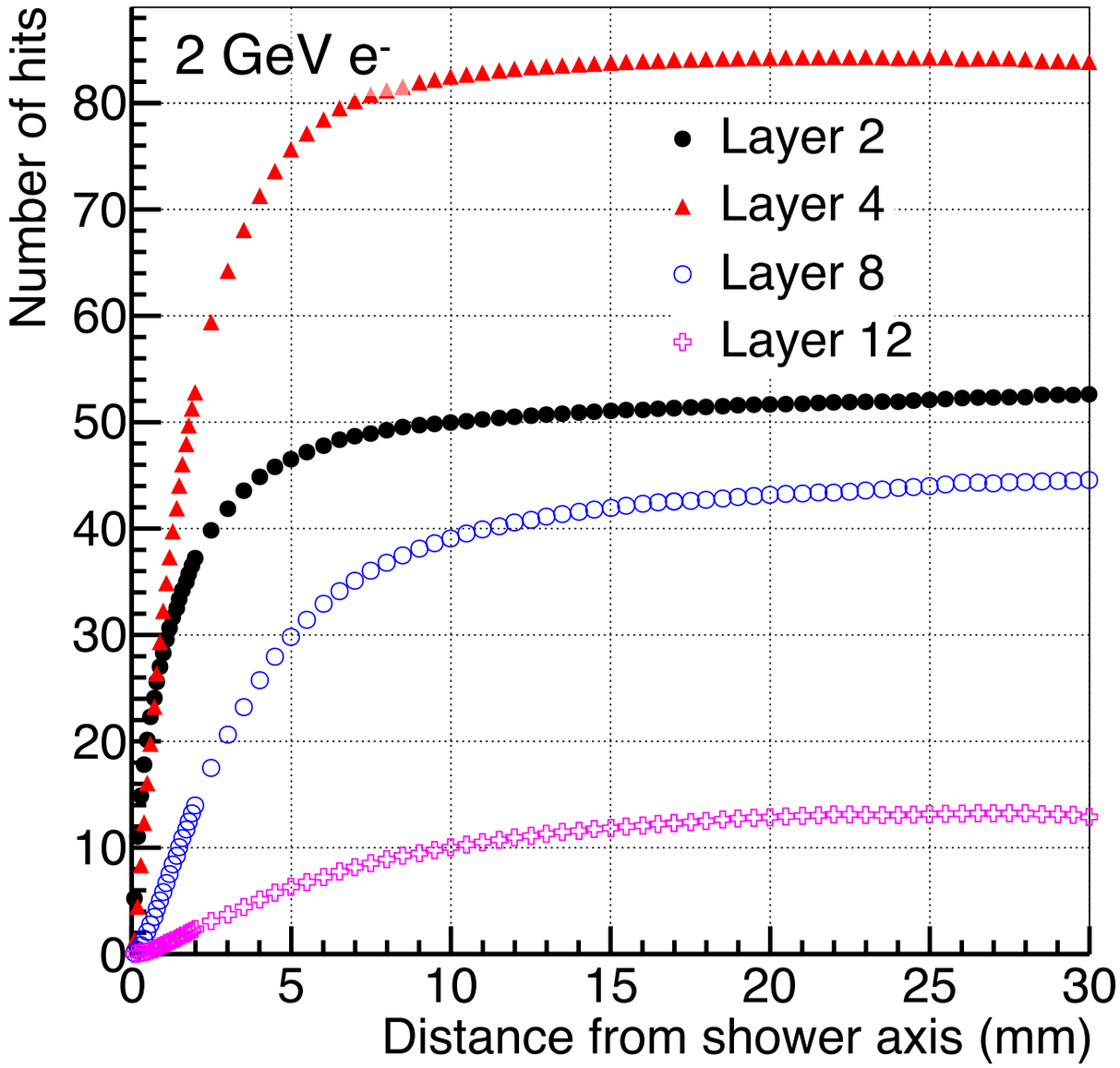


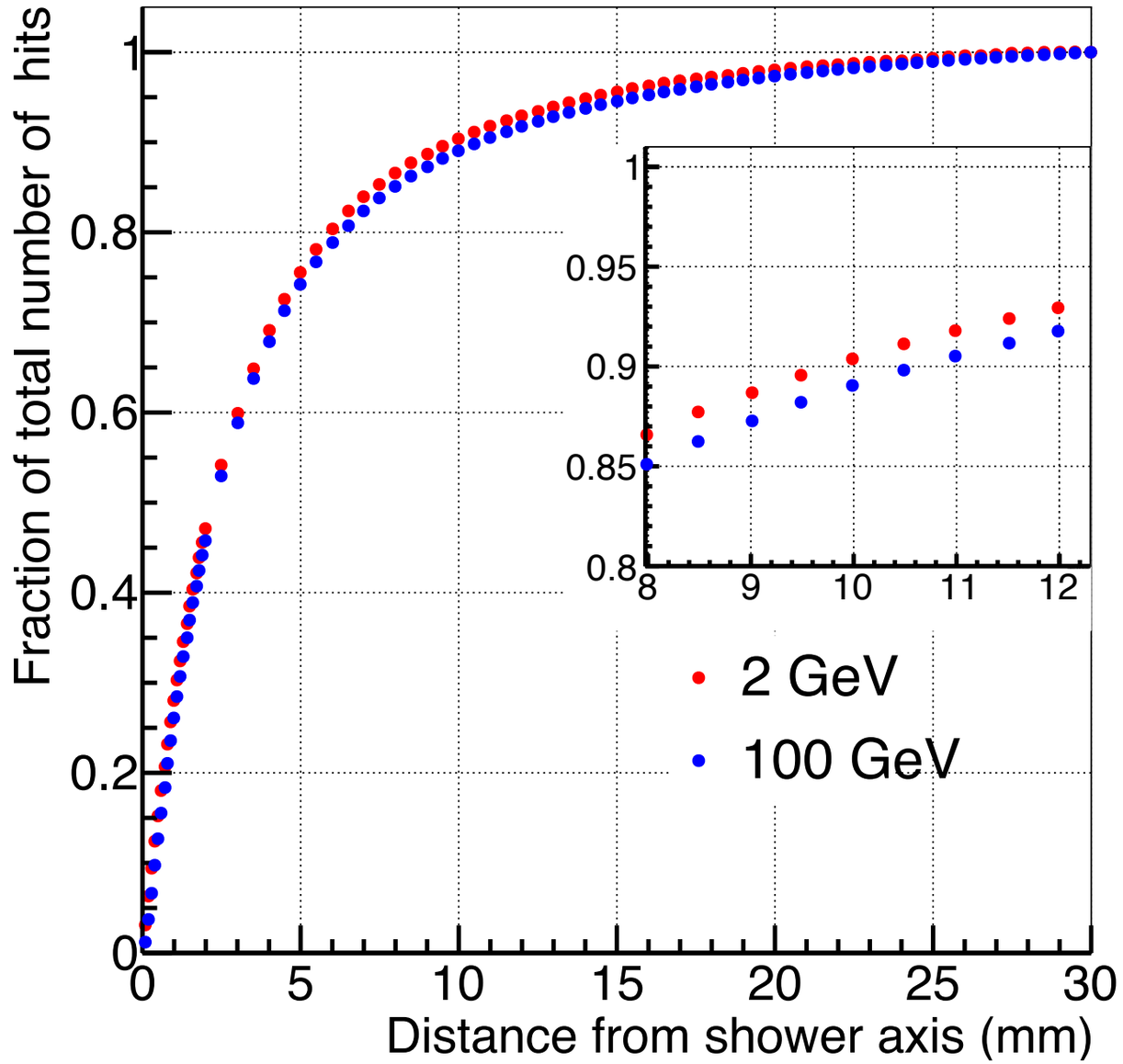
good linearity and energy resolution

- note: different calibration for low and high energy
- possibly still improve calibration
- effects of saturation seen at 244 GeV – to be corrected

proof of principle of digital calorimetry

R&D - Cumulative Lateral Profiles





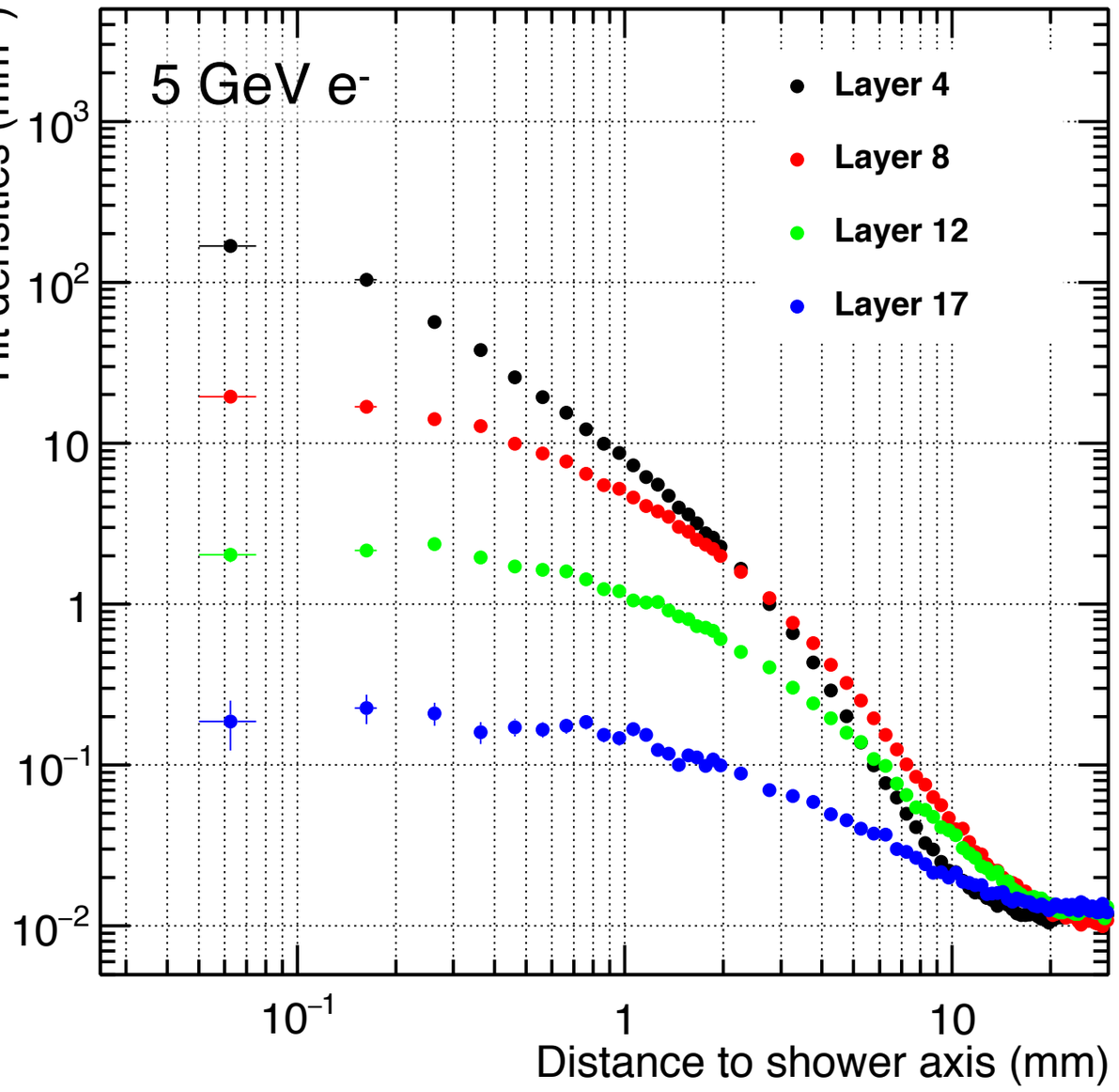
extract cumulative distributions both per layer and integrated

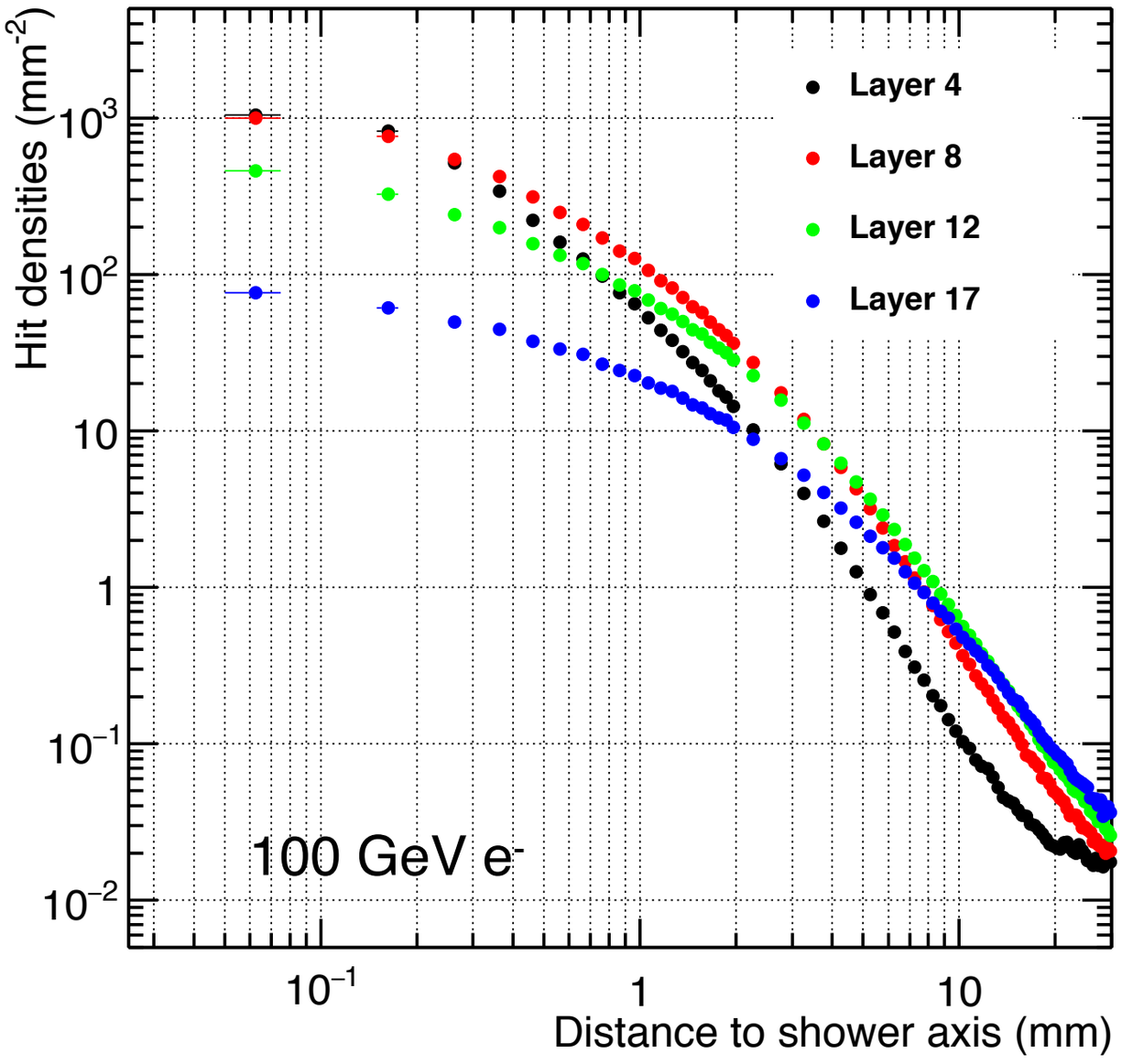
- some lateral leakage at higher energy

small Moliere radius: $R_M \approx 11$mm

≈ 75% of hits within R = 5mm, 50% within R = 3mm, …

R&D - Lateral Profiles





average hit densities as a function of radius $\frac{dN_{\mathrm{hit}}}{dA}(r)$ for different layers

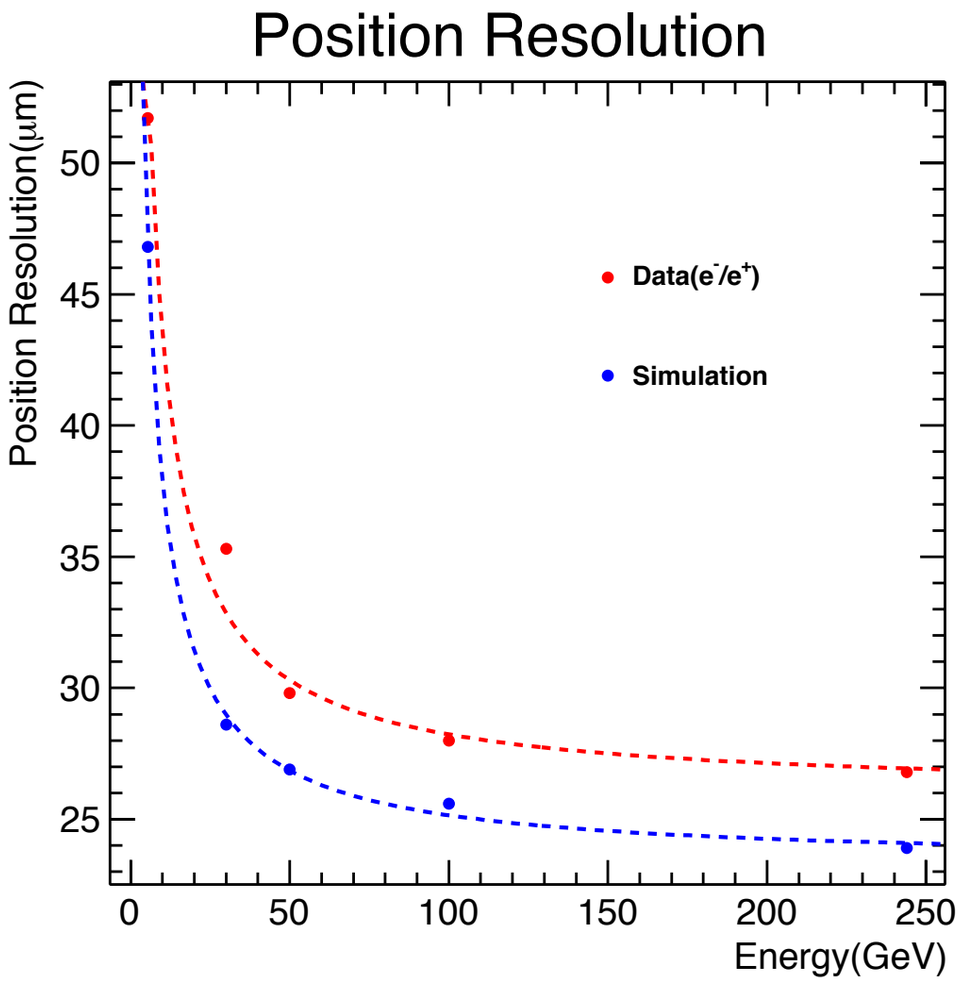
- low energy: early shower max, profiles broaden and decay with depth
- high energy: profiles broaden with depth, increase up to shower max

shower measurements with unprecedented detail!

R&D - Position Resolution and Shower Separation

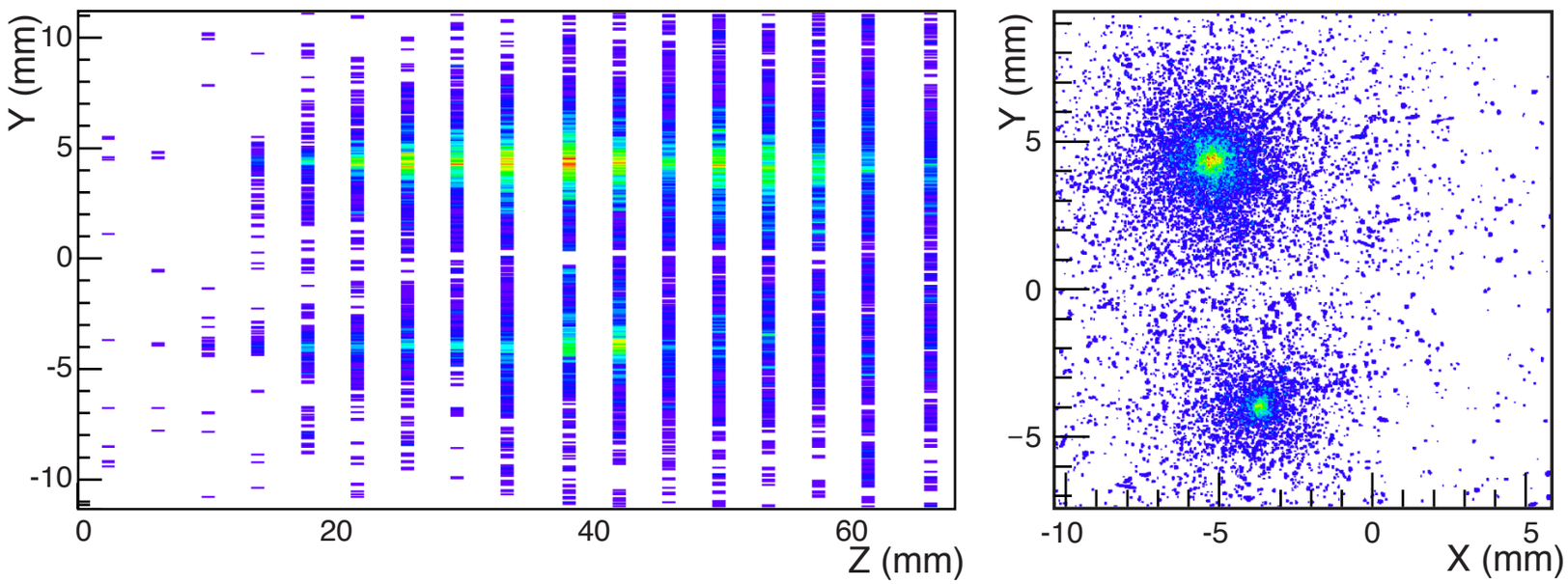
calculate difference of position from
- cluster in layer 0 and
- center of gravity of shower in layers 1 - 23

single shower position resolution obtained from width of residuals



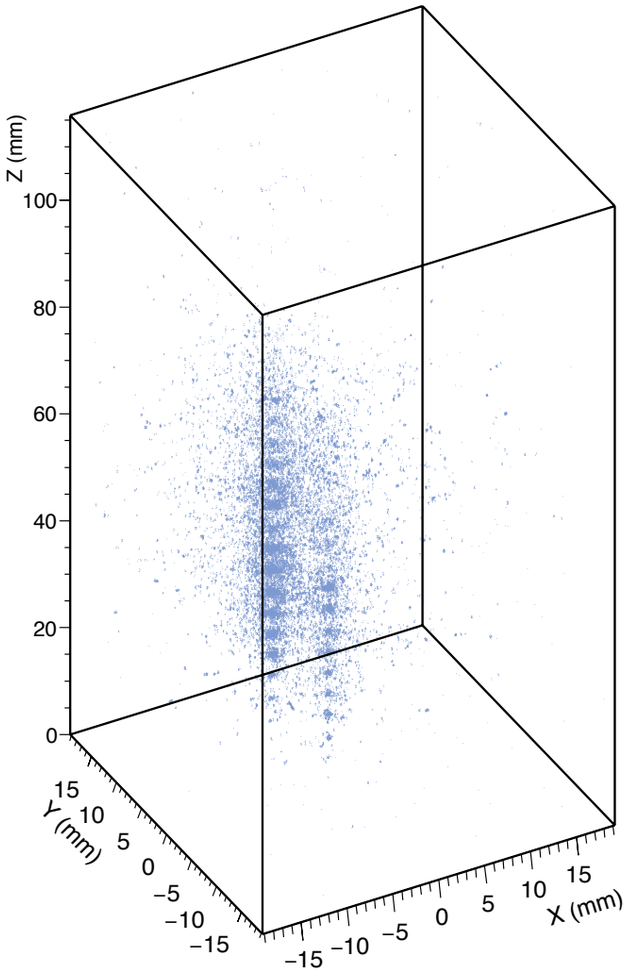
can provide excellent two-shower separation

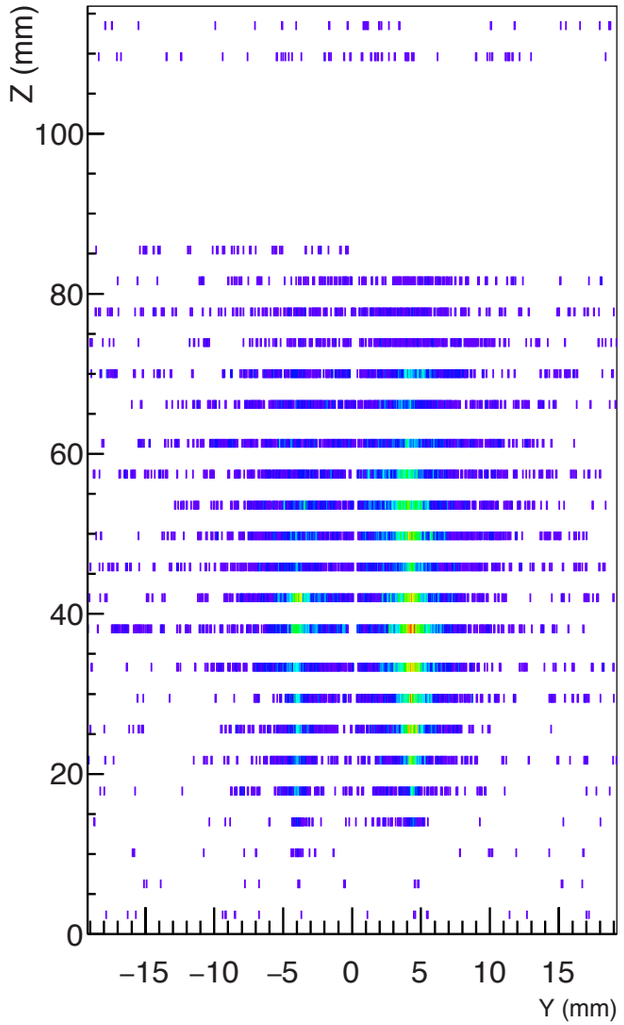
single-event from data: two neighbouring showers

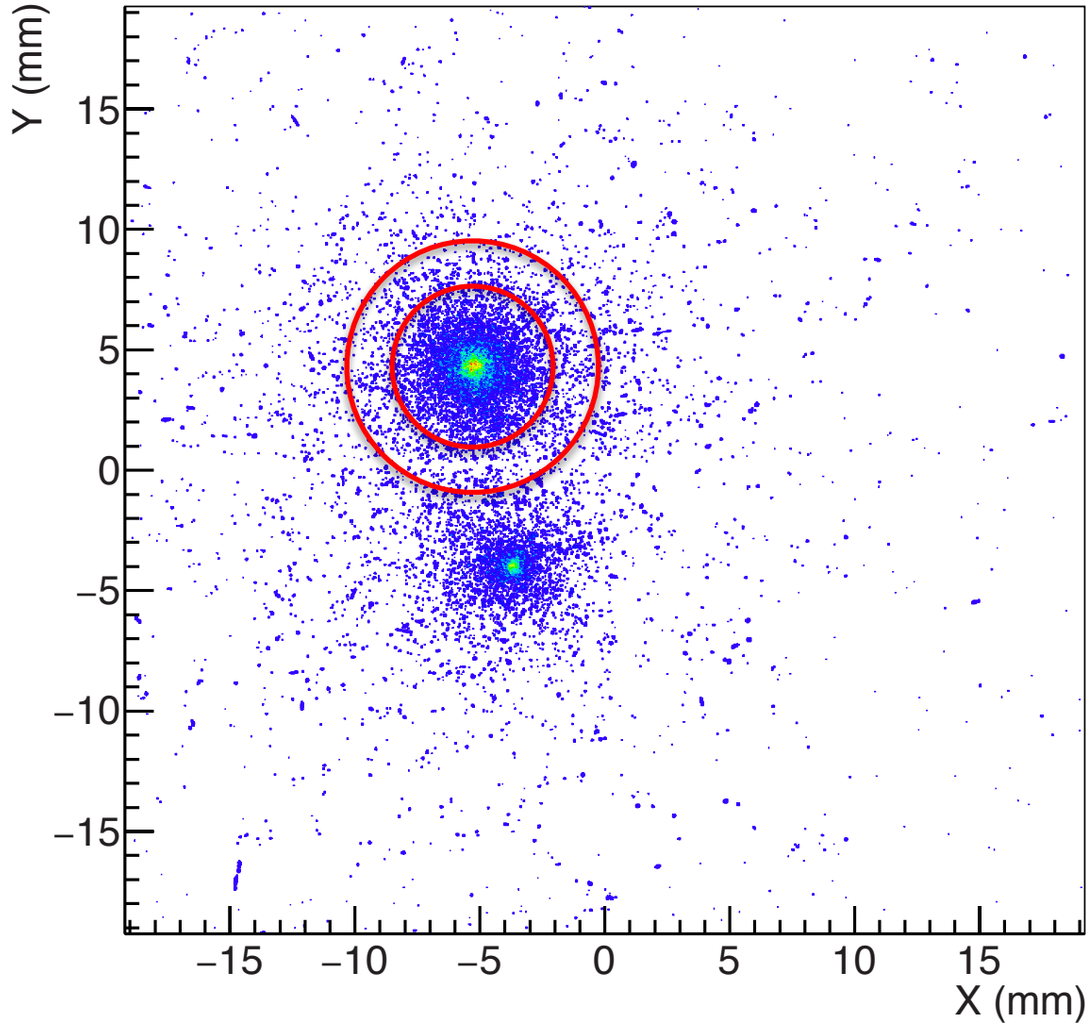


Two Shower Separation

display of single event (with pile-up) from 244 GeV mixed beam





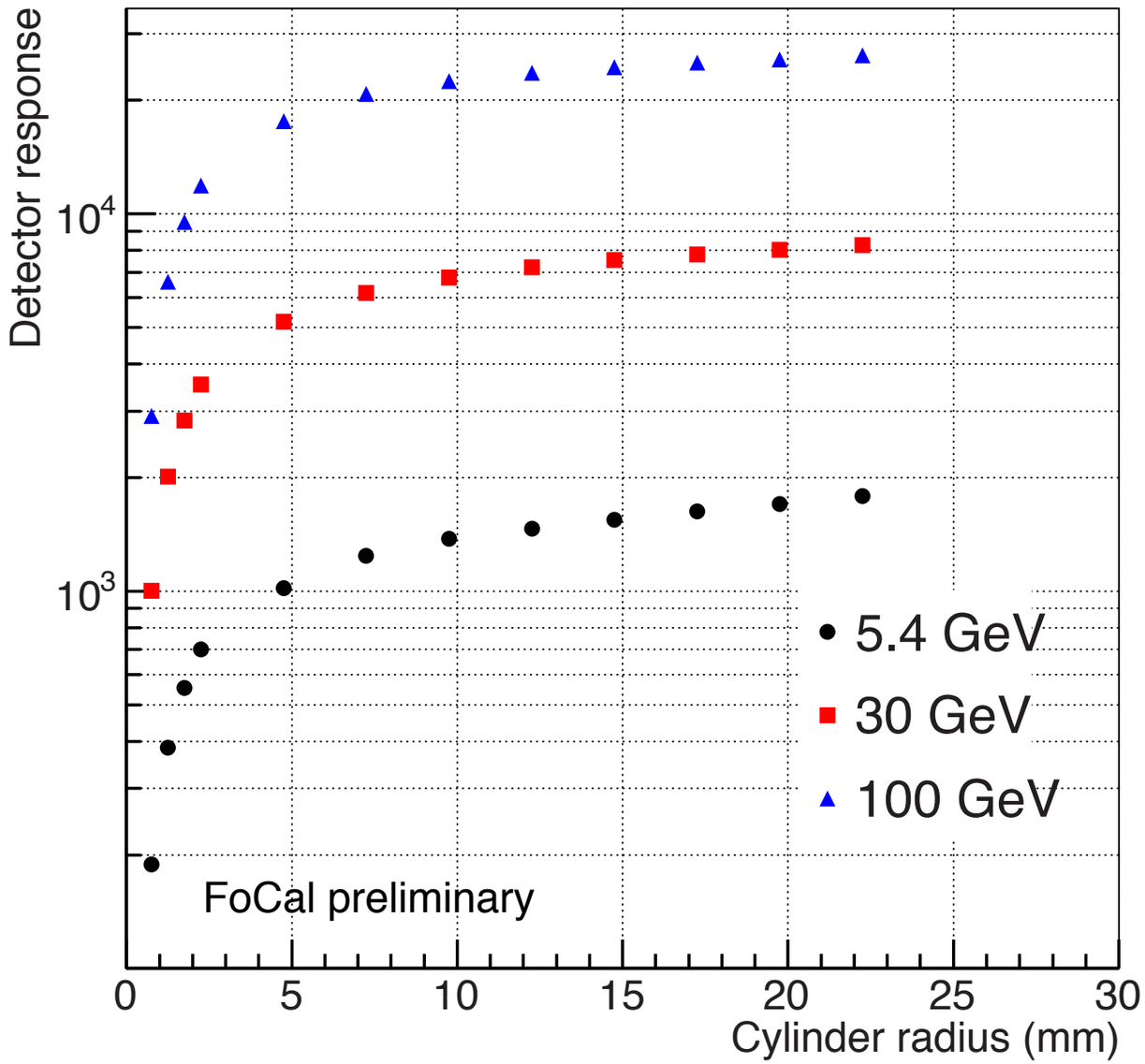


evaluate separation capability: core energy

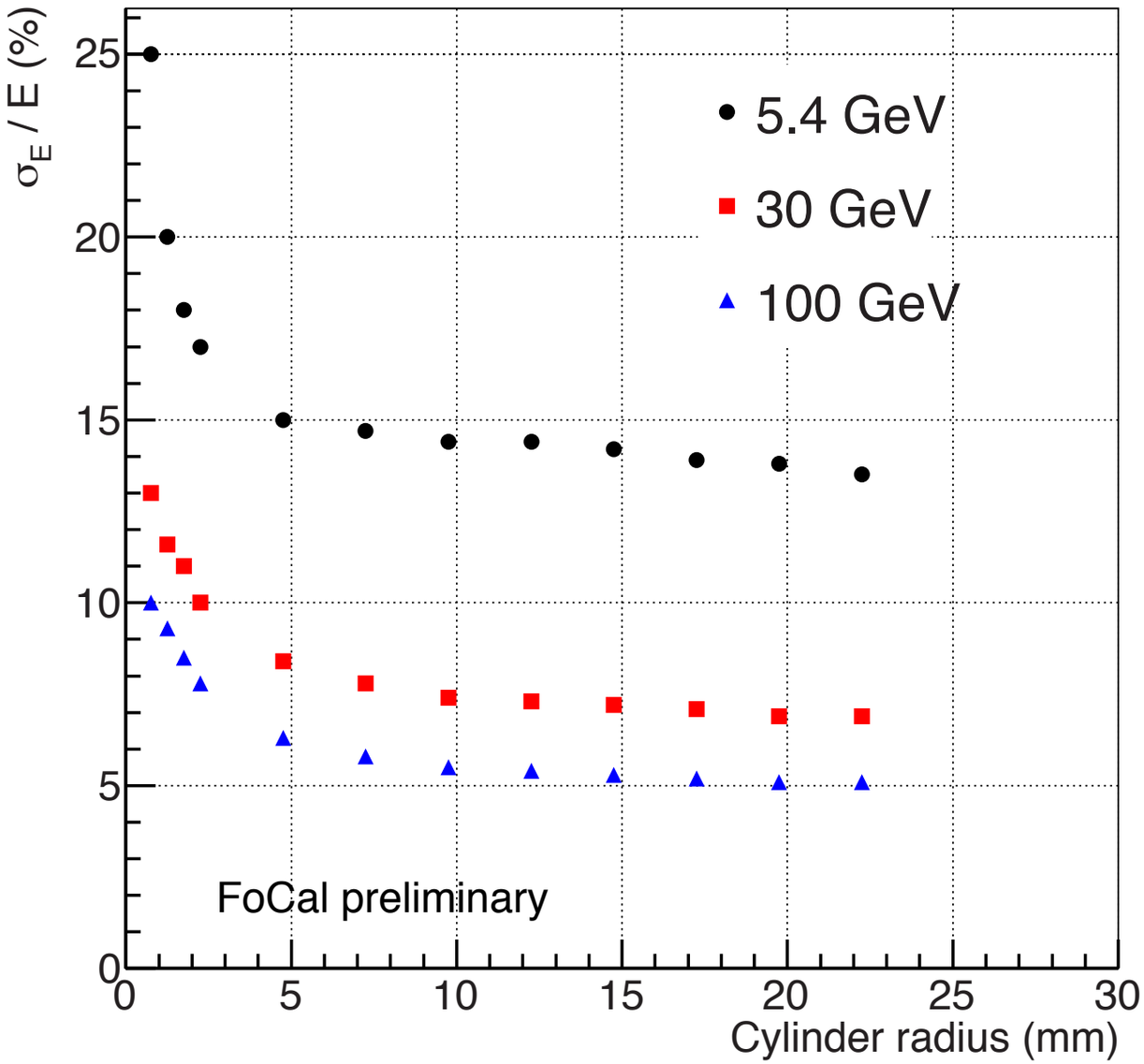
- calculate shower energy in cylinder of finite radius
- study as function of radius

R&D Results: Core Energy

detector response (number of hits)



energy resolution



reasonable energy resolution of pixel calorimeter, sufficient for conceptual design

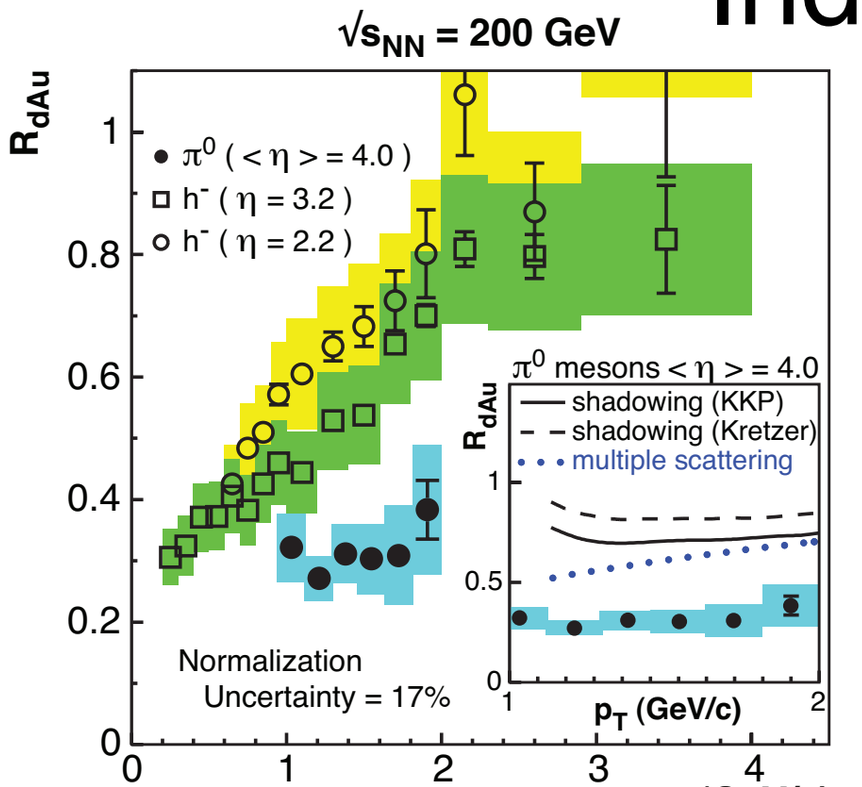
response and resolution for core energy hardly affected down to r = 5mm:
adequate for very high particle density

Summary

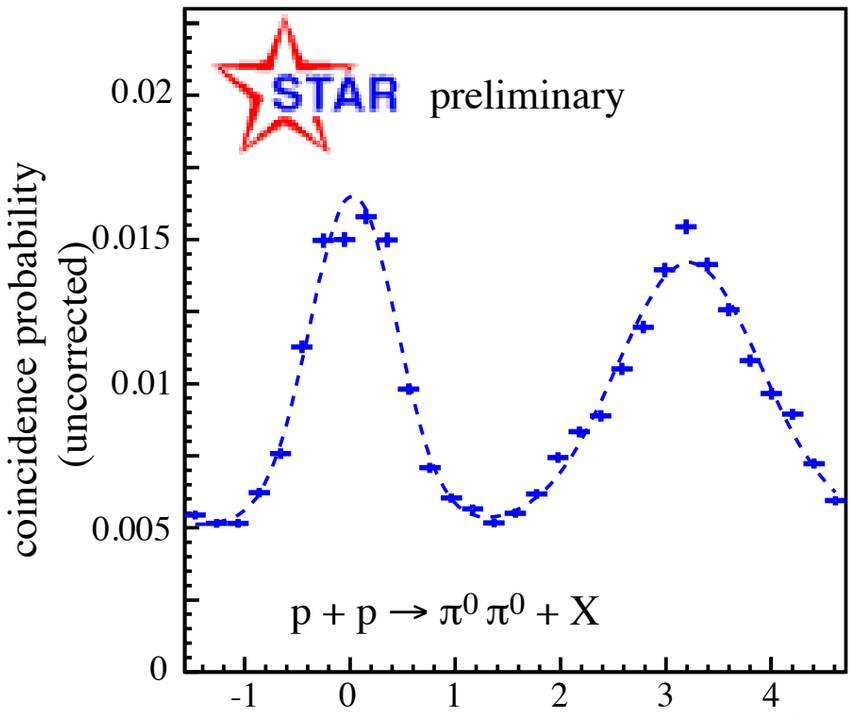
- LHC forward measurements provide unique opportunity for low-x physics
  - hadronic probes inconclusive
    - best bet: open charm (?)
  - advantage of EM probes: sensitivity to initial state, clean production process
  - need better understanding of PDF uncertainties, role of QCD evolution, and saturation models
  - measurement needs detector upgrade at LHC
    - proposed FoCal detector in ALICE
      - opportunity for forward direct photon measurement
      - particle density/kinematics require extremely high granularity: feasible with SiW pixel calorimeter

Backup Slides

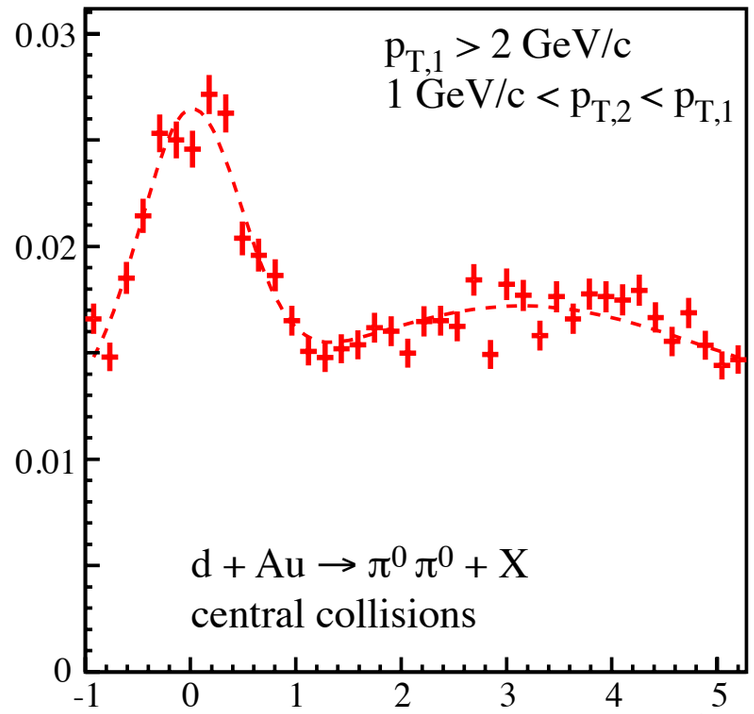
Indications from RHIC



STAR, PRL97, 152302



STAR, Braidot, Ogawa et al.



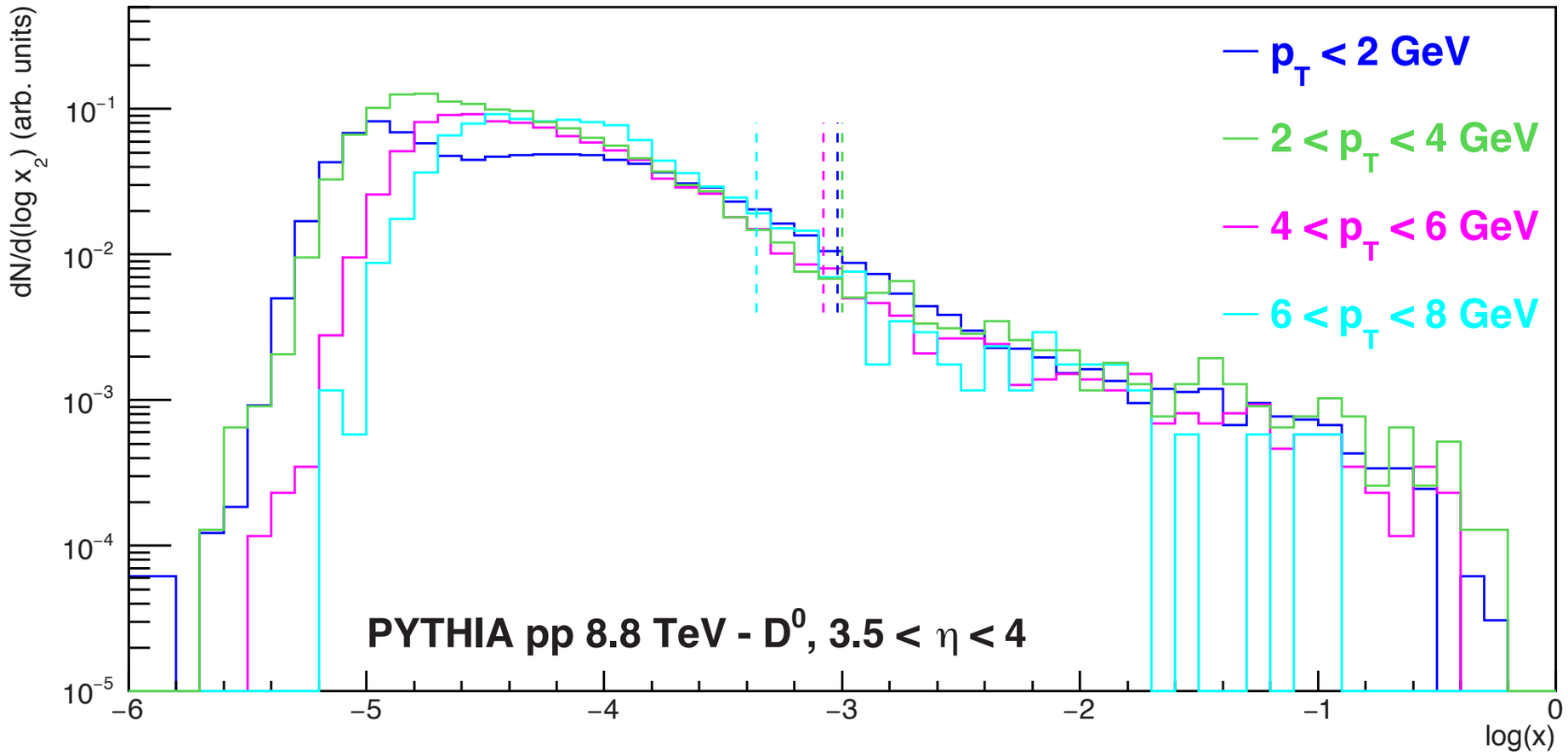
R_{dA}: strong suppression of hadron yield at forward rapidity

di-hadron correlations: broadening/suppression of away-side peak in dAu

$$R_{dA} = \frac{dN/dp_T(dA)}{< N_{coll}(dA) > dN/dp_T(pp)}$$

- qualitatively consistent with CGC, but ...
  - very low p_T, close to kinematic limit, hadron observable (final state interactions)!
- extend p_T and y range (not possible at RHIC)

x-Sensitivity

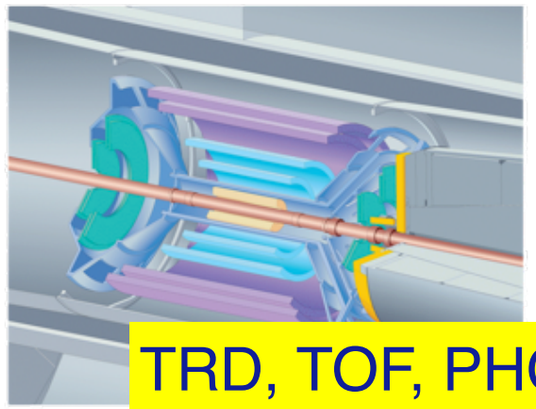


- x_2 distributions for forward charm production
- weak p_T dependence

ALICE Detector & Upgrades

new ITS: high resolution, low material budget

TPC: new GEM readout chambers, pipelined readout



TRD, TOF, PHOS, EMCal, Muon spectrometer: new readout electronics

FoCal project

Upgrade of forward/ trigger detectors (ZDC, VZERO, T0)

new beam pipe: smaller diameter

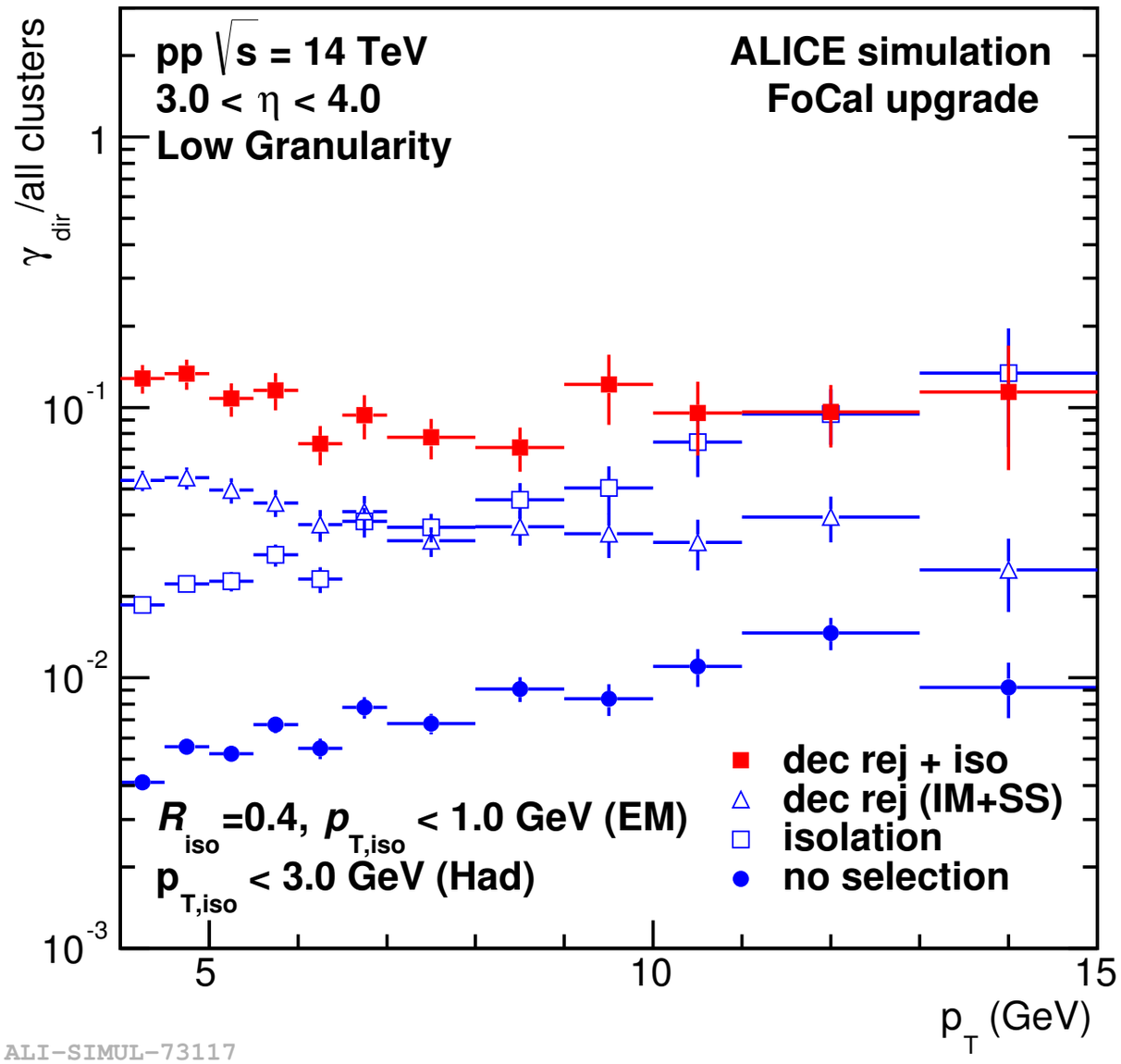
MFT: secondary vertexing for muons

planned for installation in LS2 (2019), Letter of Intent: CERN-LHCC-2012-012

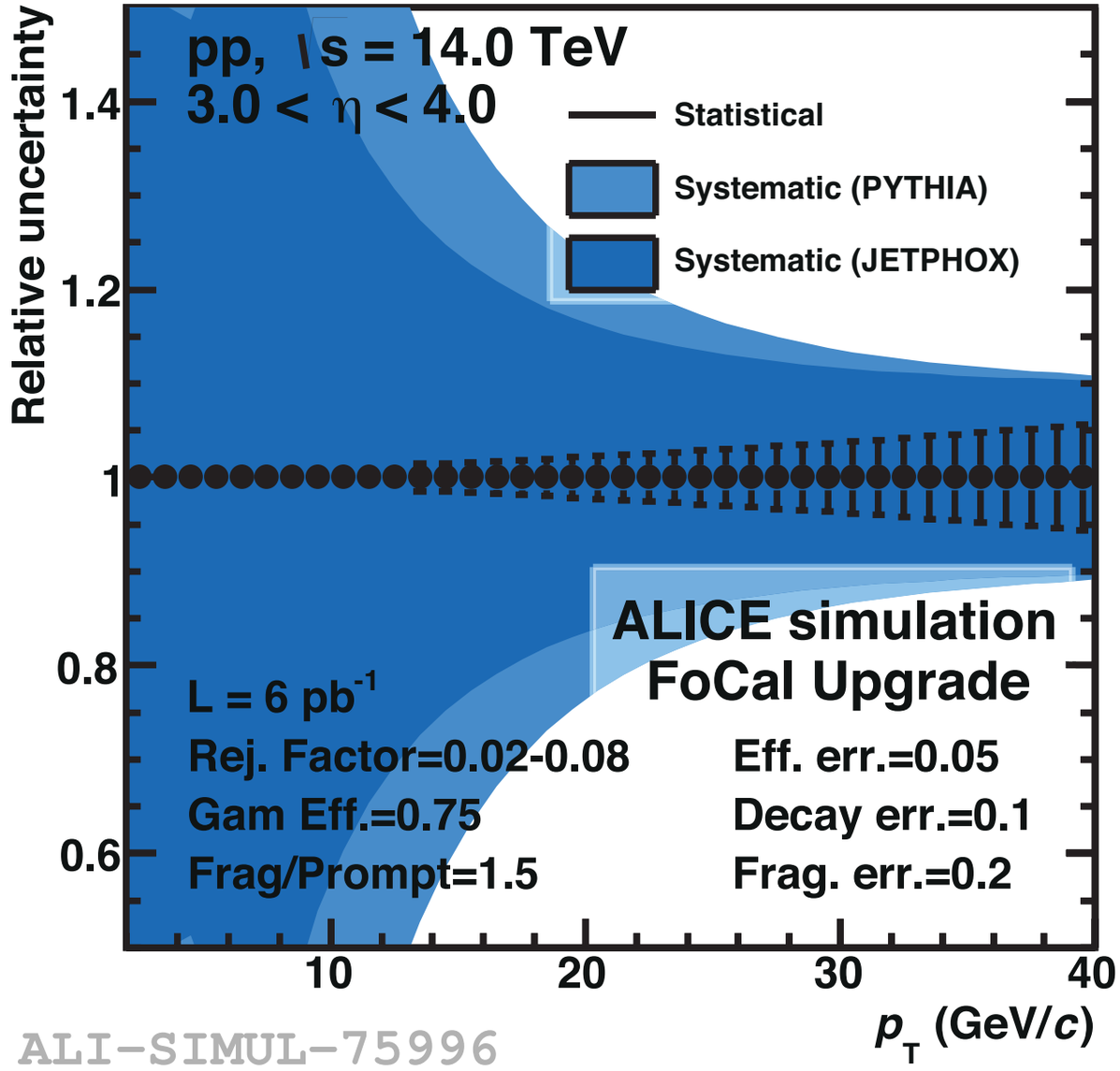
under internal review

ALICE

Low Granularity Measurement



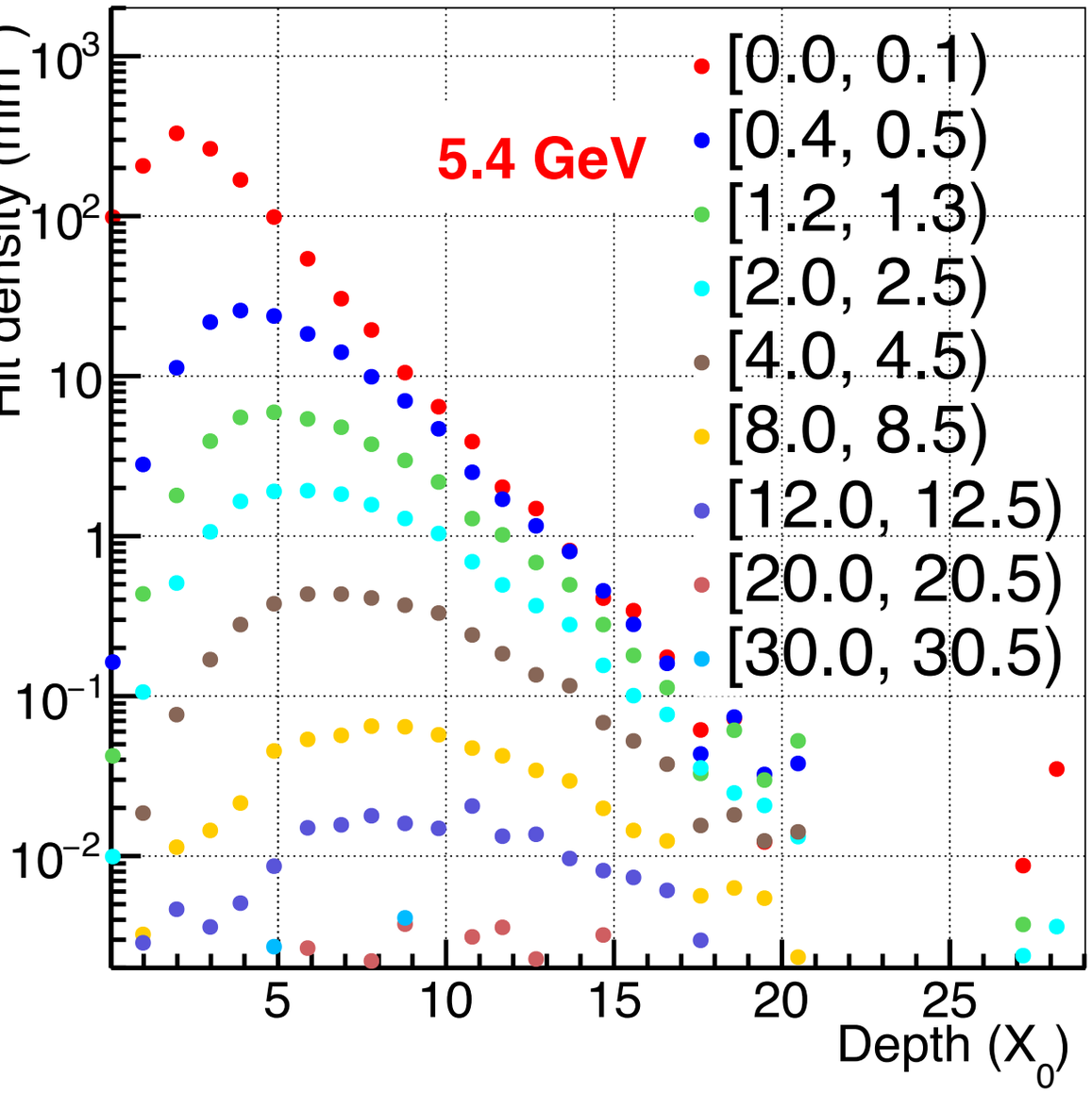
low granularity (1cm2) does not allow efficient decay rejection
direct photon/all ≈ 0.1
for all pT

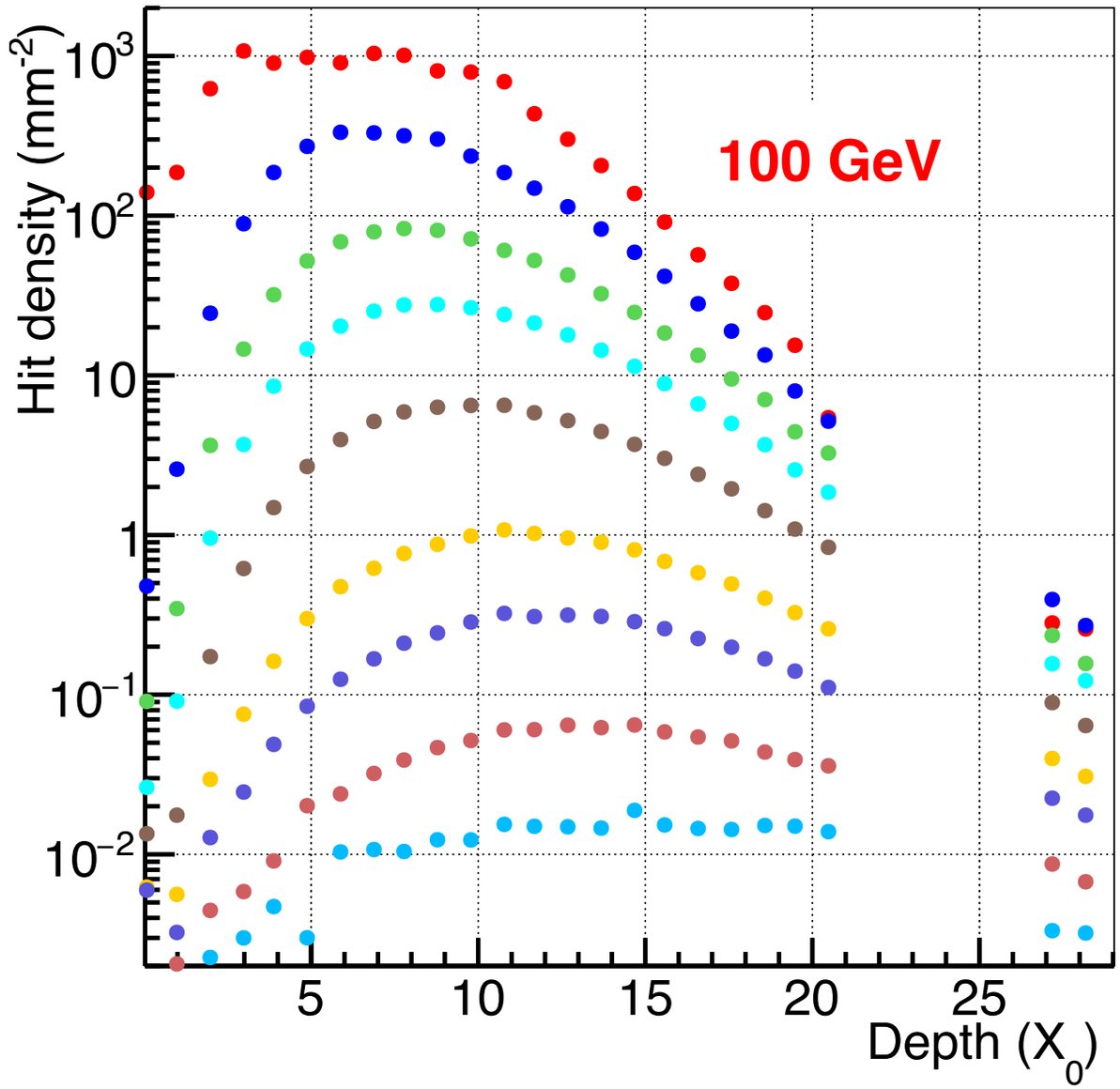


significant measurement not possible at low pT

NB: conditions similar to LHCb

Longitudinal Profiles



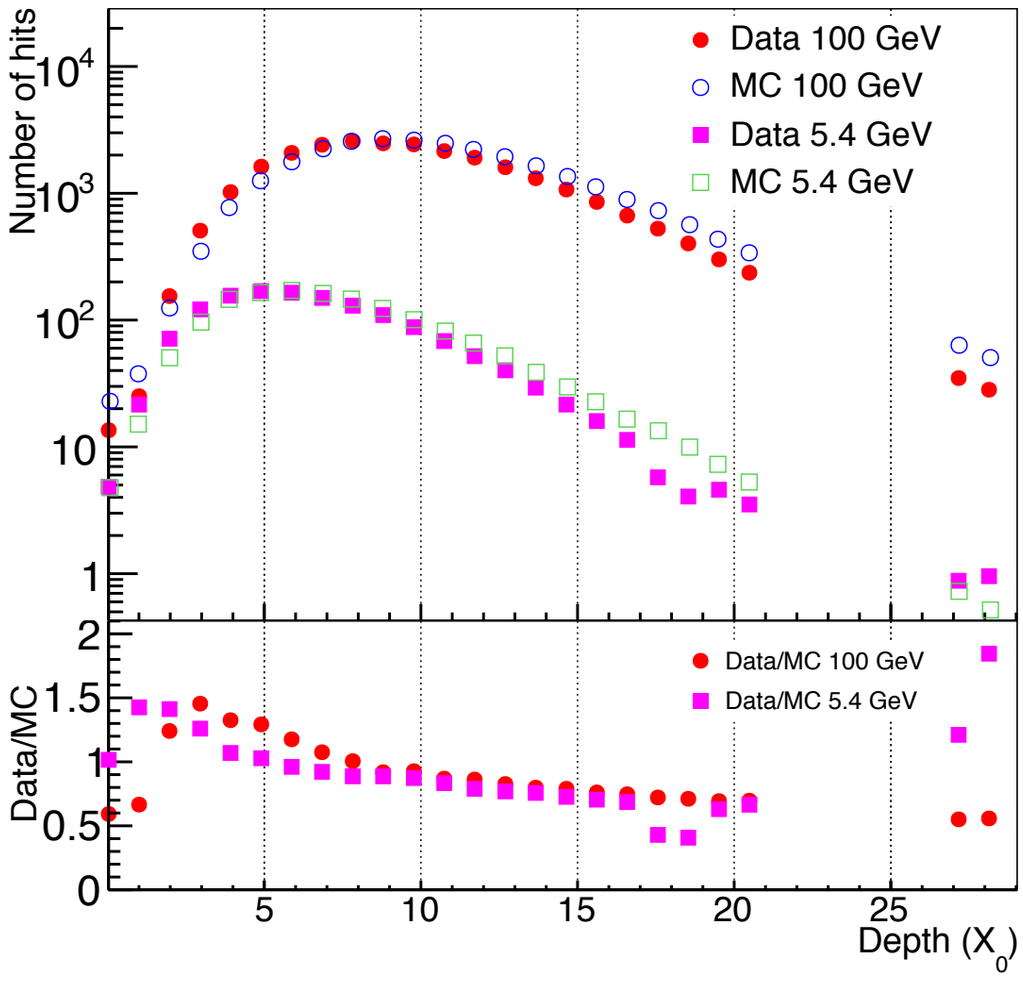


average hit densities as a function of depth for different radial positions

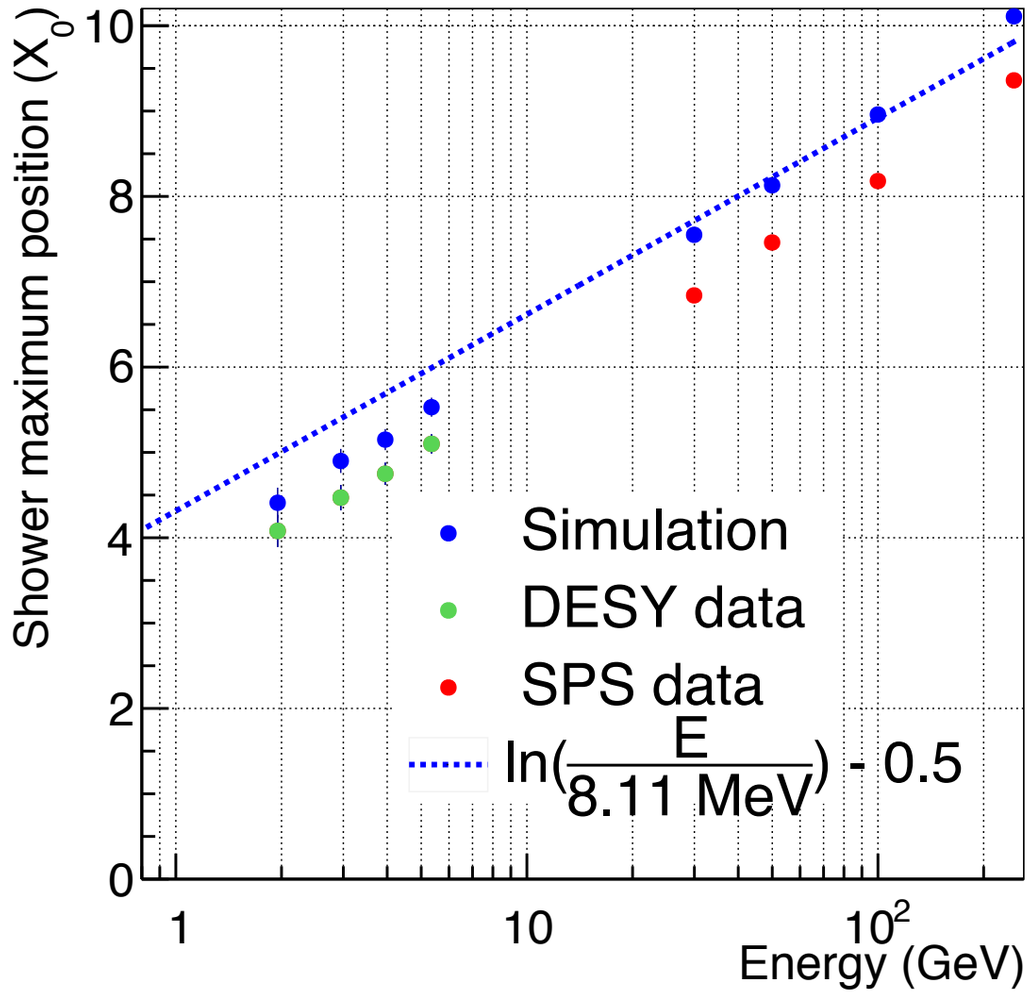
- different view of 3-dimensional info

Longitudinal Profiles - MC Comparison

Longitudinal Profile



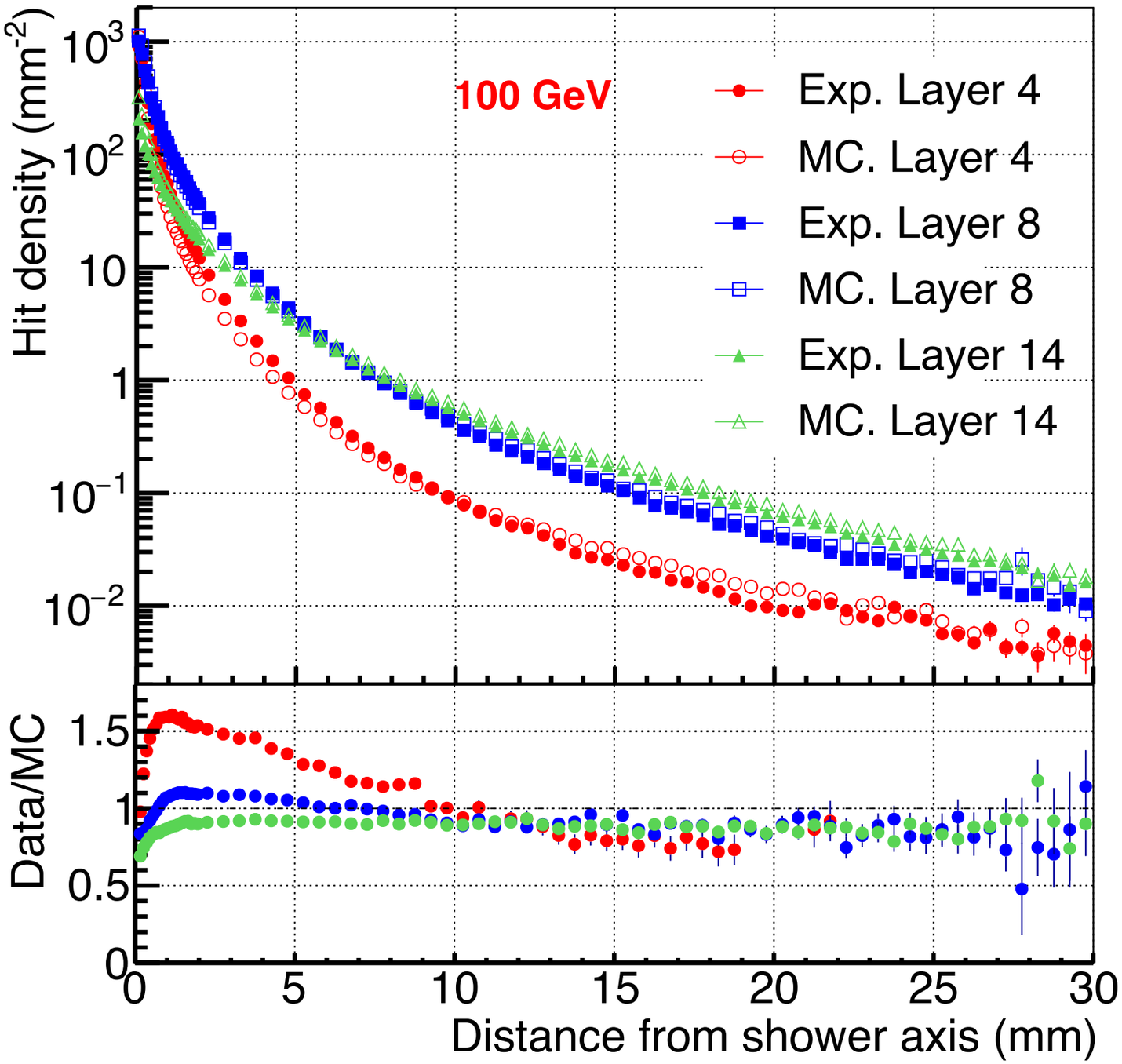
Shower Maximum



significant difference between data and MC

- larger number of hits in data for early layers
- shower maximum reached earlier than in MC
- similar effect observed in CALICE AHCAL!

Lateral Profiles - MC Comparison



also differences to MC in lateral profiles

consistent with difference in longitudinal profiles: larger number of hits in early layers

more details significant?

- narrower profiles?
- drop in hit density in central core?

possible issues: imperfect implementation of charge diffusion in MC?

Elliptic flow from color-dipole orientation in pp and pA collisions

Amir Rezaeian

UTFSM, Valparaiso

In collaboration with Edmond Iancu

RBRC Workshop, BNL, April 26 - 28, 2017



UNIVERSIDAD TECNICA
FEDERICO SANTA MARIA



Centro Científico
Tecnológico
de Valparaíso

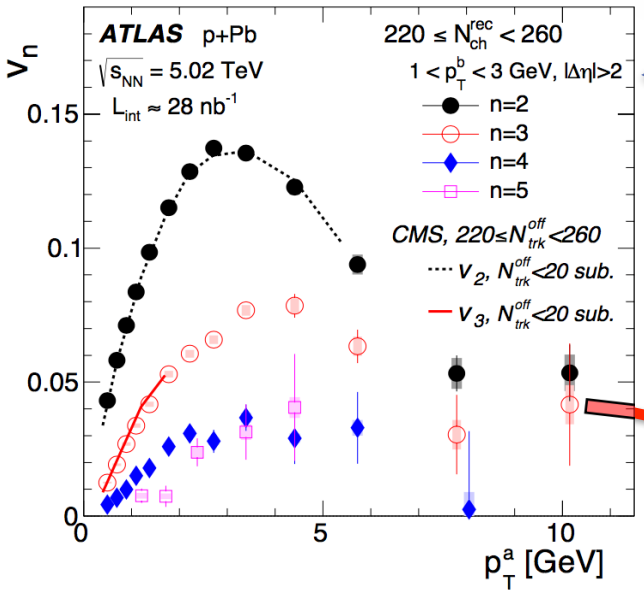
Outline:

- **Motivation**
- **Color dipole orientation in the MV model.**
- **Elliptic flow in pp collisions.**
- **Elliptic flow in pA collisions.**

***This talk is based on*: Iancu and Rezaeian, arXiv:1702.03943; in PRD press**

Can we understand this?

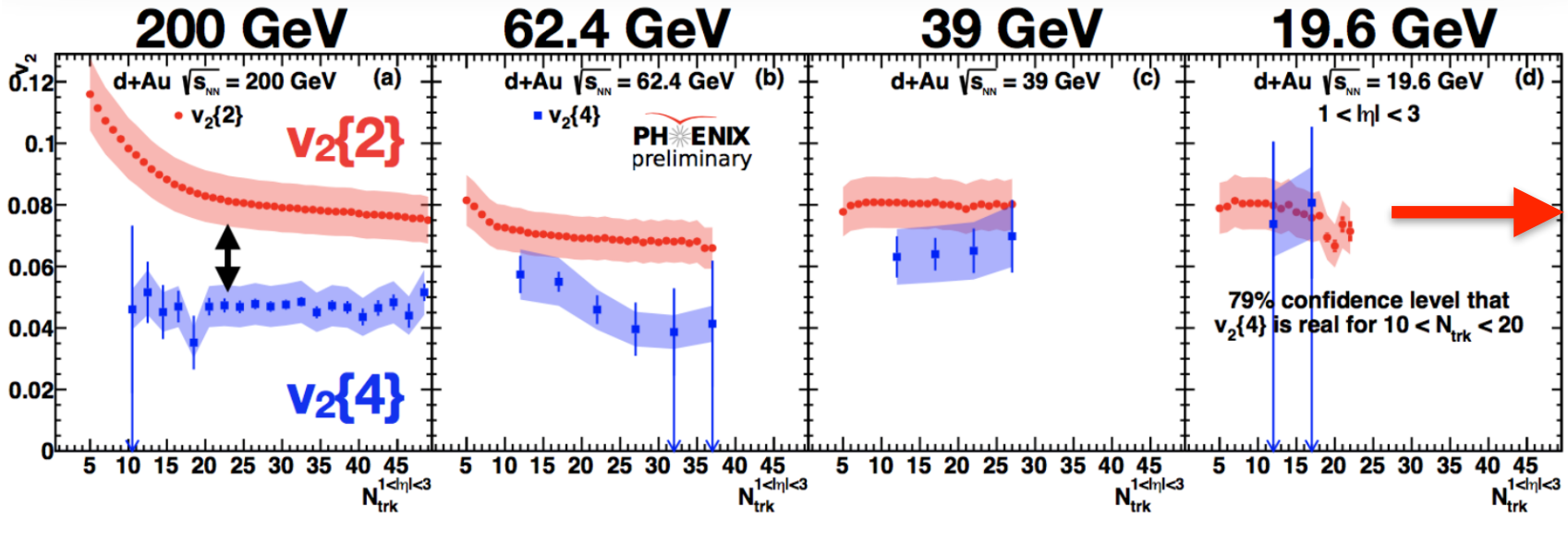
Motivation:



Jiangyong Jia's talk

x~10^{-4}

Is this small-x physics?



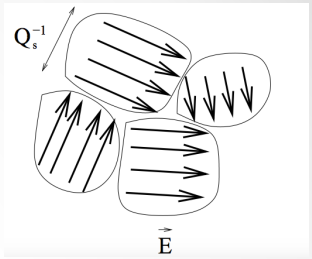
x > 10^{-2}

Different Saturation based mechanisms for elliptic flow

❑ **'Saturation domains' inside a dense hadronic target**

Kovner, Lublinsky, PRD83, 034017 (2011).
Dumitru and Giannini, Nucl. Phys. A933, 212 (2015).
Dumitru and Skokov, Phys. Rev. D91, 074006 (2015).
Dumitru, McLerran, and Skokov, Phys. Lett. B743, 134 (2015).
Lappi, Schenke, Schlichting, and Venugopalan, JHEP 01, 061 (2016).

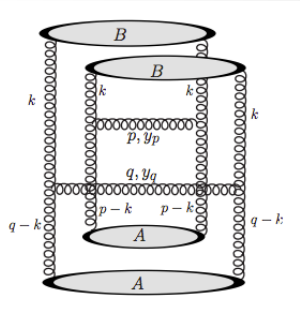
Alex's talk



❑ **Glasma-like & 'IP-Glasma' scenarios**

Schenke, Tribedy, and Venugopalan, Phys. Rev. Lett. 108, 252301 (2012).
Schenke, Tribedy, and Venugopalan, Phys. Rev. C86, 034908 (2012).
Dusling and Venugopalan, Phys. Rev. Lett. 108, 262001 (2012).
Dusling and Venugopalan, Phys. Rev. D87, 094034 (2013).
Dusling, Tribedy, and Venugopalan, Phys. Rev. D93, 014034 (2016).
Kovchegov and Wertepny, Nucl. Phys. A925, 254 (2014).
Schenke and Schlichting, Phys. Rev. C94, 044907 (2016).
Schenke, Schlichting, Tribedy, and Venugopalan, Phys. Rev. Lett. 117, 162301 (2016)

Bjorn's talk
Raju's Talk



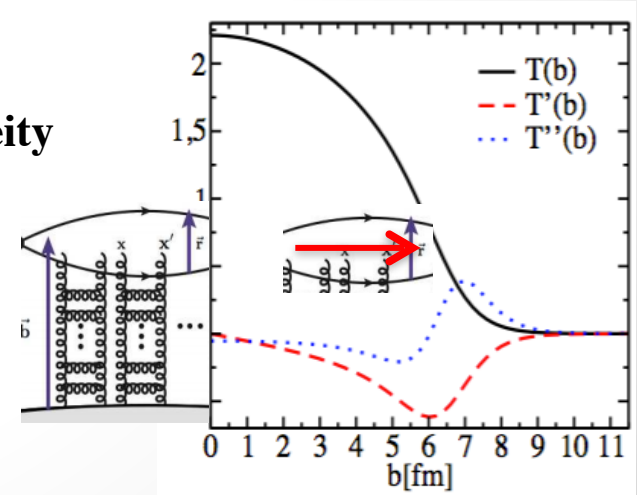
❑ **Spatial variation of partonic density**:

Levin and Rezaeian, Phys. Rev. D84, 034031 (2011).

✓ **'Color-dipole orientation' scenario as a probe of inhomogeneity**

Kopeliovich, Pirner, Rezaeian, and Schmidt, Phys. Rev. D77, 034011 (2008),
Zhou, Phys. Rev. D94, 114017 (2016).
Hagiwara, Hatta, Xiao, and Yuan (2017), 1701.04254.
Iancu and Rezaeian, arXiv:1702.03943; in PRD press. ← **In MV model**

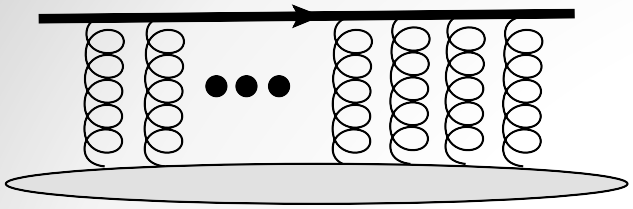
This talk



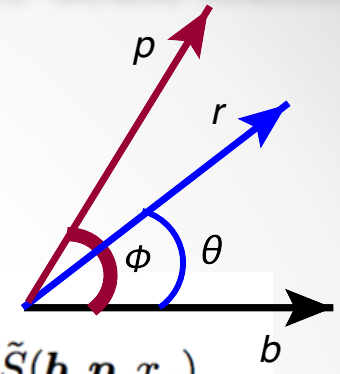
- **The effect is not 1/ N_c suppressed!.**
- **Can generate sizable azimuthal asymmetries already in the absence of fluctuations (it is manifest for the single particle spectrum).**

Color-dipole as an origin of elliptic flow

Color-dipole orientation as an origin of elliptic flow in dilute-dense scatterings



See Edmond's talk

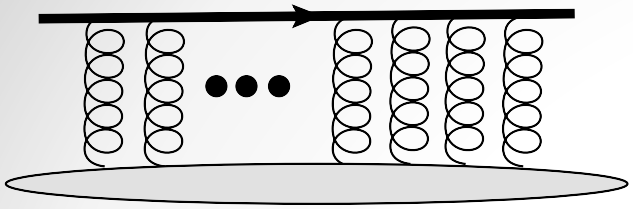


$$\frac{\mathrm{d}\sigma^q(qA\to qX)}{\mathrm{d}\eta\,\mathrm{d}^2\boldsymbol{p}\,\mathrm{d}^2\boldsymbol{b}} = x_p q(x_p)\int\frac{\mathrm{d}^2\boldsymbol{r}}{(2\pi)^2}\,\mathrm{e}^{-\mathrm{i}\boldsymbol{p}\cdot\boldsymbol{r}}S(\boldsymbol{b},\boldsymbol{r},x_g) = \frac{1}{(2\pi)^2}\,x_p q(x_p)\tilde{S}(\boldsymbol{b},\boldsymbol{p},x_g).$$

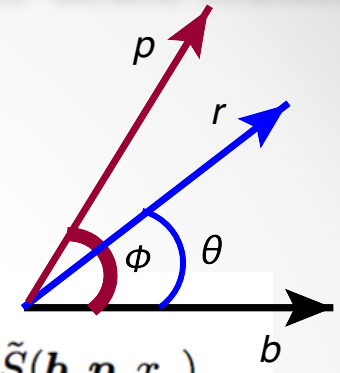
correlations btw **(p, r)** and btw **(r, b)** ⟶ correlations btw **(p, b)**

$$v_n(p,b) \equiv \frac{\int_0^{2\pi}\mathrm{d}\phi\cos(n\phi)\,\frac{\mathrm{d}\sigma^q(qA\to qX)}{\mathrm{d}\eta\mathrm{d}^2\boldsymbol{p}\mathrm{d}^2\boldsymbol{b}}}{\int_0^{2\pi}\mathrm{d}\phi\,\frac{\mathrm{d}\sigma^q(qA\to qX)}{\mathrm{d}\eta\mathrm{d}^2\boldsymbol{p}\mathrm{d}^2\boldsymbol{b}}}$$

Color-dipole orientation as an origin of elliptic flow in dilute-dense scatterings



See Edmond's talk



$$\frac{\mathrm{d}\sigma^q(qA\to qX)}{\mathrm{d}\eta\,\mathrm{d}^2\boldsymbol{p}\,\mathrm{d}^2\boldsymbol{b}} = x_p q(x_p)\int\frac{\mathrm{d}^2\boldsymbol{r}}{(2\pi)^2}\,\mathrm{e}^{-\mathrm{i}\boldsymbol{p}\cdot\boldsymbol{r}}S(\boldsymbol{b},\boldsymbol{r},x_g) = \frac{1}{(2\pi)^2}\,x_p q(x_p)\tilde{S}(\boldsymbol{b},\boldsymbol{p},x_g).$$

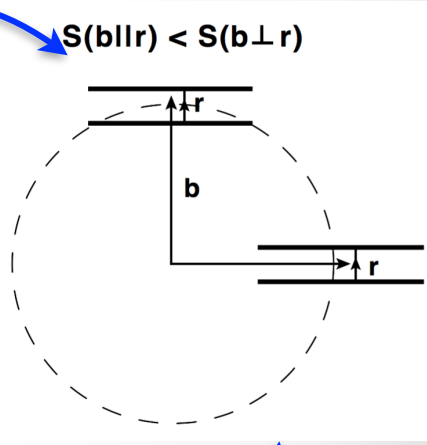
correlations btw **(p, r)** and btw **(r, b)** ⟶ correlations btw **(p, b)**

$$v_n(p,b)\equiv\frac{\int_0^{2\pi}\mathrm{d}\phi\cos(n\phi)\,\frac{\mathrm{d}\sigma^q(qA\to qX)}{\mathrm{d}\eta\mathrm{d}^2\boldsymbol{p}\mathrm{d}^2\boldsymbol{b}}}{\int_0^{2\pi}\mathrm{d}\phi\,\frac{\mathrm{d}\sigma^q(qA\to qX)}{\mathrm{d}\eta\mathrm{d}^2\boldsymbol{p}\mathrm{d}^2\boldsymbol{b}}}$$

$cos(n\Phi)\longrightarrow cos(n\theta)$

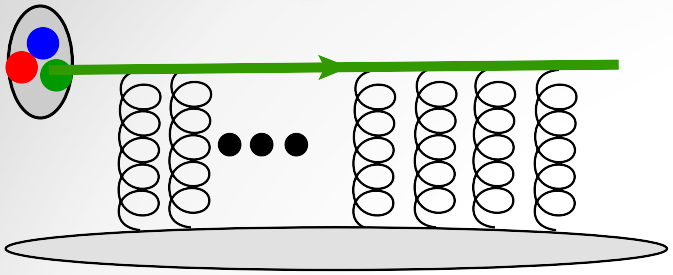
$$v_2(p,b) = -\frac{\int r\mathrm{d}r\mathrm{d}\theta\,\cos(2\theta)\,\mathrm{J}_2(pr)\,S(b,r,\theta)}{\int r\mathrm{d}r\mathrm{d}\theta\,\mathrm{J}_0(pr)\,S(b,r,\theta)},$$

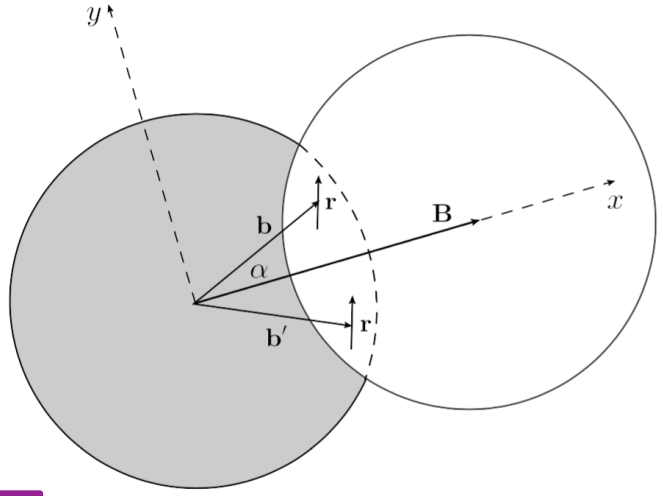
$$v_3(p,b) = -\mathrm{i}\,\frac{\int r\mathrm{d}r\mathrm{d}\theta\,\cos(3\theta)\,\mathrm{J}_3(pr)\,S(b,r,\theta)}{\int r\mathrm{d}r\mathrm{d}\theta\,\mathrm{J}_0(pr)\,S(b,r,\theta)}.$$



- **Spontaneous breaking of rotational symmetry in the transverse plane.**
- $S(\vec{b},\vec{r})\to S(b,r)\longrightarrow v_n=0$ **(Regardless of the shape of projectile)**
- $v_3\neq 0\longrightarrow$ non-zero odderon contribution

Color-dipole orientation: including finite-size effect of the projectile



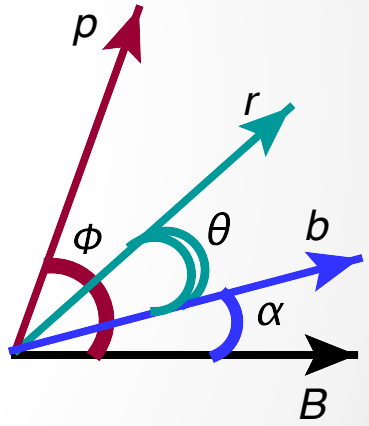


$$\frac{\mathrm{d}\sigma^q(qA\to qX)}{\mathrm{d}\eta\,\mathrm{d}^2\boldsymbol{p}\,\mathrm{d}^2\boldsymbol{B}} = \frac{1}{(2\pi)^2}\int \mathrm{d}^2\boldsymbol{b}\; x_p q(x_p,\boldsymbol{b}-\boldsymbol{B})\,\tilde{S}(\boldsymbol{b},\boldsymbol{p},x_g)$$

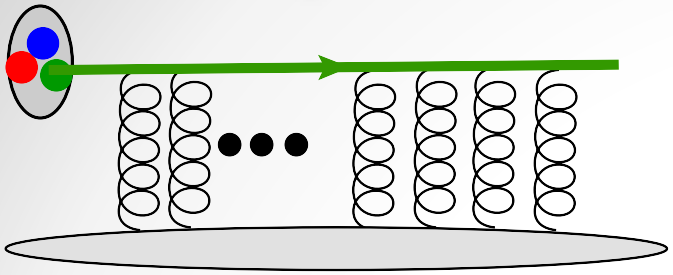
Proton GPD: $x_p q(x_p,\boldsymbol{b}) \simeq x_p q(x_p) f(\boldsymbol{b})$, with $\int \mathrm{d}^2\boldsymbol{b}\, f(\boldsymbol{b}) = 1$

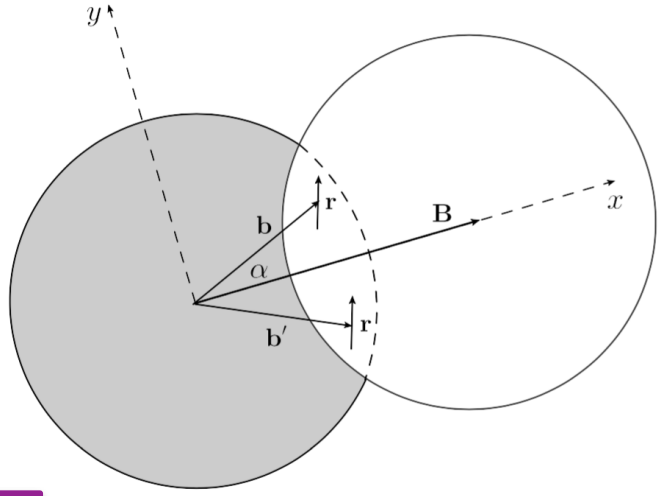
proton distribution is isotropic: $f(\boldsymbol{b}) = f(|\boldsymbol{b}|)$

$$v_n(p,B) \equiv \frac{\int_0^{2\pi}\mathrm{d}\Phi\,\cos(n\Phi)\,\frac{\mathrm{d}\sigma^q(qA\to qX)}{\mathrm{d}\eta\mathrm{d}^2\boldsymbol{p}\mathrm{d}^2\boldsymbol{B}}}{\int_0^{2\pi}\mathrm{d}\Phi\,\frac{\mathrm{d}\sigma^q(qA\to qX)}{\mathrm{d}\eta\mathrm{d}^2\boldsymbol{p}\mathrm{d}^2\boldsymbol{B}}}$$



Color-dipole orientation: including finite-size effect of the projectile



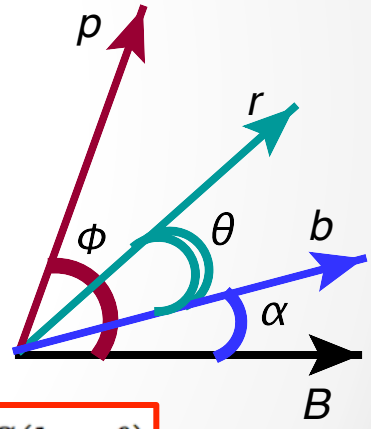


$$\frac{\mathrm{d}\sigma^q(qA\to qX)}{\mathrm{d}\eta\,\mathrm{d}^2\boldsymbol{p}\,\mathrm{d}^2\boldsymbol{B}} = \frac{1}{(2\pi)^2}\int \mathrm{d}^2\boldsymbol{b}\; x_p q(x_p,\boldsymbol{b}-\boldsymbol{B})\,\tilde{S}(\boldsymbol{b},\boldsymbol{p},x_g)$$

Proton GPD: $x_p q(x_p,\boldsymbol{b}) \simeq x_p q(x_p) f(\boldsymbol{b})$, with $\int \mathrm{d}^2\boldsymbol{b}\, f(\boldsymbol{b}) = 1$

proton distribution is isotropic: $f(\boldsymbol{b}) = f(|\boldsymbol{b}|)$

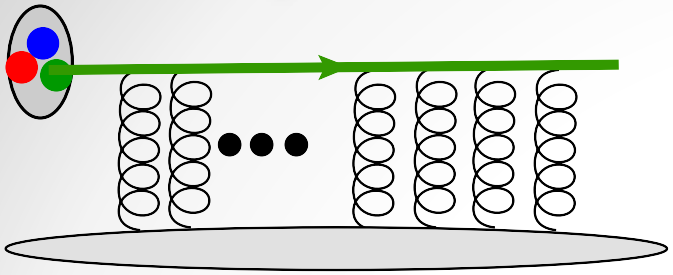
$$v_n(p,B) \equiv \frac{\int_0^{2\pi}\mathrm{d}\Phi\,\cos(n\Phi)\,\frac{\mathrm{d}\sigma^q(qA\to qX)}{\mathrm{d}\eta\mathrm{d}^2\boldsymbol{p}\mathrm{d}^2\boldsymbol{B}}}{\int_0^{2\pi}\mathrm{d}\Phi\,\frac{\mathrm{d}\sigma^q(qA\to qX)}{\mathrm{d}\eta\mathrm{d}^2\boldsymbol{p}\mathrm{d}^2\boldsymbol{B}}} \qquad cos(n\Phi) \longrightarrow cos(n\theta)$$

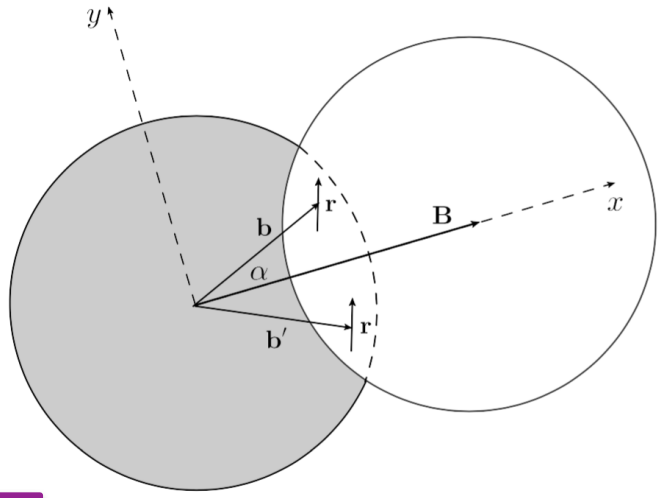


$$v_2(p,B) = -\frac{\int b\mathrm{d}b\mathrm{d}\alpha\,\cos(2\alpha)\,f(|\boldsymbol{b}-\boldsymbol{B}|)\int r\mathrm{d}r\mathrm{d}\theta\,\cos(2\theta)\,\mathrm{J}_2(pr)\,S(b,r,\theta)}{\int b\mathrm{d}b\mathrm{d}\alpha\,f(|\boldsymbol{b}-\boldsymbol{B}|)\int r\mathrm{d}r\mathrm{d}\theta\,\mathrm{J}_0(pr)\,S(b,r,\theta)}$$

$S(\vec{b},\vec{r}) \to S(b,r) \longrightarrow v_n = 0$ **(Regardless of the shape of projectile and target)**

Color-dipole orientation: including finite-size effect of the projectile



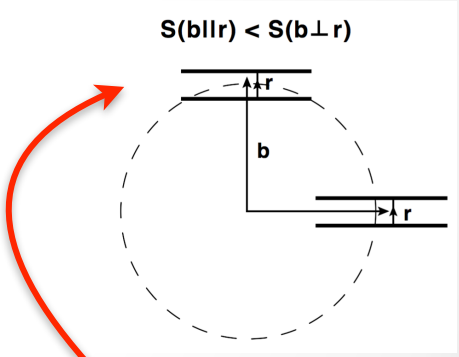


$$\frac{\mathrm{d}\sigma^q(qA\to qX)}{\mathrm{d}\eta\,\mathrm{d}^2\boldsymbol{p}\,\mathrm{d}^2\boldsymbol{B}} = \frac{1}{(2\pi)^2}\int \mathrm{d}^2\boldsymbol{b}\; x_p q(x_p,\boldsymbol{b}-\boldsymbol{B})\,\tilde{S}(\boldsymbol{b},\boldsymbol{p},x_g)$$

Proton GPD: $x_p q(x_p,\boldsymbol{b}) \simeq x_p q(x_p) f(\boldsymbol{b})$, with $\int \mathrm{d}^2\boldsymbol{b}\, f(\boldsymbol{b}) = 1$

proton distribution is isotropic: $f(\boldsymbol{b}) = f(|\boldsymbol{b}|)$

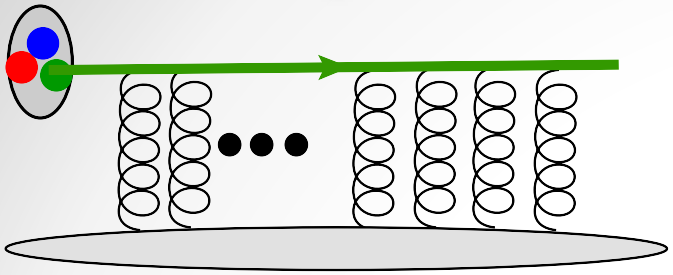
$$v_n(p,B) \equiv \frac{\int_0^{2\pi}\mathrm{d}\Phi\,\cos(n\Phi)\,\frac{\mathrm{d}\sigma^q(qA\to qX)}{\mathrm{d}\eta\mathrm{d}^2\boldsymbol{p}\mathrm{d}^2\boldsymbol{B}}}{\int_0^{2\pi}\mathrm{d}\Phi\,\frac{\mathrm{d}\sigma^q(qA\to qX)}{\mathrm{d}\eta\mathrm{d}^2\boldsymbol{p}\mathrm{d}^2\boldsymbol{B}}} \qquad cos(n\Phi)\longrightarrow cos(n\theta)$$



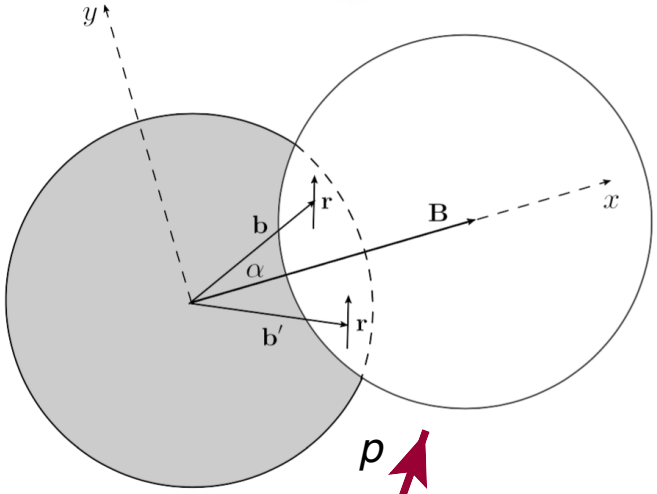
$$v_2(p,B) = -\frac{\int b\mathrm{d}b\mathrm{d}\alpha\,\cos(2\alpha)\,f(|\boldsymbol{b}-\boldsymbol{B}|)\int r\mathrm{d}r\mathrm{d}\theta\,\cos(2\theta)\,\mathrm{J}_2(pr)\,S(b,r,\theta)}{\int b\mathrm{d}b\mathrm{d}\alpha\,f(|\boldsymbol{b}-\boldsymbol{B}|)\int r\mathrm{d}r\mathrm{d}\theta\,\mathrm{J}_0(pr)\,S(b,r,\theta)}$$

- $S(\vec{b},\vec{r}) \to S(b,r) \longrightarrow v_n = 0$ **(Regardless of the shape of projectile and target)**

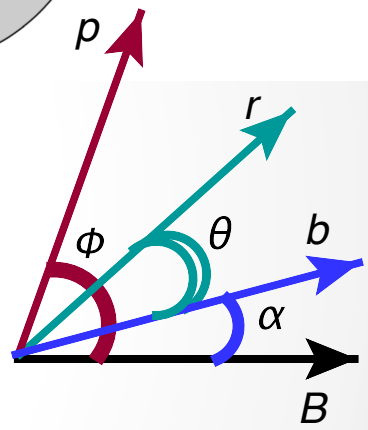
Elliptic flow and eccentricity in dilute-dense scatterings



$$\frac{\mathrm{d}\sigma^q(qA\to qX)}{\mathrm{d}\eta\,\mathrm{d}^2\boldsymbol{p}\,\mathrm{d}^2\boldsymbol{B}} = \frac{1}{(2\pi)^2}\int \mathrm{d}^2\boldsymbol{b}\; x_p q(x_p,\boldsymbol{b}-\boldsymbol{B})\,\tilde{S}(\boldsymbol{b},\boldsymbol{p},x_g)$$



$$v_2(p,B) = -\frac{\int b\mathrm{d}b\mathrm{d}\alpha\,\cos(2\alpha)\,f(|\boldsymbol{b}-\boldsymbol{B}|)\int r\mathrm{d}r\mathrm{d}\theta\,\cos(2\theta)\,\mathrm{J}_2(pr)\,S(b,r,\theta)}{\int b\mathrm{d}b\mathrm{d}\alpha\,f(|\boldsymbol{b}-\boldsymbol{B}|)\int r\mathrm{d}r\mathrm{d}\theta\,\mathrm{J}_0(pr)\,S(b,r,\theta)}$$



- **Eccentricity: is a measure of the projection of the impact parameters of the participants quarks along the direction of their average impact parameter**

$$\varepsilon_2(p,B) = \frac{\langle x^2-y^2\rangle}{\langle x^2+y^2\rangle} = \frac{\langle b^2\cos(2\alpha)\rangle}{\langle b^2\rangle},$$
$$= \frac{\int b\mathrm{d}b\mathrm{d}\alpha\, b^2\cos(2\alpha)\,f(|\boldsymbol{b}-\boldsymbol{B}|)\int r\mathrm{d}r\mathrm{d}\theta\,\mathrm{J}_0(pr)\,S(b,r,\theta)}{\int b\mathrm{d}b\mathrm{d}\alpha\, b^2\,f(|\boldsymbol{b}-\boldsymbol{B}|)\int r\mathrm{d}r\mathrm{d}\theta\,\mathrm{J}_0(pr)\,S(b,r,\theta)}$$

$$\epsilon_2(B=0)=0,\ \epsilon_2(B\to\infty)=1$$

$$v_2(p,B)\propto\epsilon_2(p,B)$$

Color-dipole orientation in the McLerran-Venugopalan model

$$\langle \rho^a(\boldsymbol{x})\rho^b(\boldsymbol{y})\rangle = \delta^{ab}\delta^{(2)}(\boldsymbol{x}-\boldsymbol{y})\mu(\boldsymbol{x})$$

In the original MV model:

$$\mu(\mathbf{b}) = \mu_0, \qquad \tilde{\mu}(\mathbf{q}'+\mathbf{q}) = \delta^{\mathbf{2}}(\mathbf{q}'+\mathbf{q})$$

$$\mu(b) = \mu_0\, \mathrm{e}^{-b^2/4R^2},$$

$$\tilde{\mu}(\Delta) = \int \mathrm{d}^2\boldsymbol{b}\, \mathrm{e}^{-\mathrm{i}\boldsymbol{b}\cdot\boldsymbol{\Delta}}\mu(b) = 4\pi R^2\mu_0\, \mathrm{e}^{-\Delta^2 R^2}$$

μ_0, R : fixed via a fit to the DIS & diffractive DIS data: **Using IP-Sat or bCGC**

$$\langle A_a^-(\boldsymbol{x})A_b^-(\boldsymbol{y})\rangle = \delta^{ab}\gamma(\boldsymbol{x},\boldsymbol{y})$$

$$\gamma(\boldsymbol{x},\boldsymbol{y}) \equiv \int \mathrm{d}^2\boldsymbol{z}\, G(\boldsymbol{x}-\boldsymbol{z})G(\boldsymbol{y}-\boldsymbol{z})\mu(\boldsymbol{z}) = \int \frac{\mathrm{d}^2\boldsymbol{q}}{(2\pi)^2}\frac{\mathrm{d}^2\boldsymbol{q}'}{(2\pi)^2}\, \mathrm{e}^{\mathrm{i}\boldsymbol{q}'\cdot\boldsymbol{x}+\mathrm{i}\boldsymbol{q}\cdot\boldsymbol{y}}\frac{\tilde{\mu}(\boldsymbol{q}'+\boldsymbol{q})}{q'^2q^2}$$

Color-dipole orientation in the McLerran-Venugopalan model

$$\langle \rho^a(\boldsymbol{x})\rho^b(\boldsymbol{y})\rangle \;=\; \delta^{ab}\delta^{(2)}(\boldsymbol{x}-\boldsymbol{y})\mu(\boldsymbol{x})$$

In the original MV model:

$$\mu(\mathbf{b}) = \mu_{\mathbf{0}}, \qquad \tilde{\mu}(\mathbf{q}'+\mathbf{q}) = \delta^{\mathbf{2}}(\mathbf{q}'+\mathbf{q})$$

$$\mu(b) \;=\; \mu_0\, \mathrm{e}^{-b^2/4R^2}\,,$$

$$\tilde{\mu}(\Delta) \;=\; \int \mathrm{d}^2\boldsymbol{b}\, \mathrm{e}^{-\mathrm{i}\boldsymbol{b}\cdot\boldsymbol{\Delta}}\mu(b) = 4\pi R^2\mu_0\, \mathrm{e}^{-\Delta^2 R^2}$$

μ_0, R : fixed via a fit to the DIS & diffractive DIS data.

$$\langle A_a^-(\boldsymbol{x})A_b^-(\boldsymbol{y})\rangle = \delta^{ab}\gamma(\boldsymbol{x},\boldsymbol{y})$$

$$\gamma(\boldsymbol{x},\boldsymbol{y}) \equiv \int \mathrm{d}^2\boldsymbol{z}\, G(\boldsymbol{x}-\boldsymbol{z})G(\boldsymbol{y}-\boldsymbol{z})\mu(\boldsymbol{z}) = \int \frac{\mathrm{d}^2\boldsymbol{q}}{(2\pi)^2}\frac{\mathrm{d}^2\boldsymbol{q}'}{(2\pi)^2}\, \mathrm{e}^{\mathrm{i}\boldsymbol{q}'\cdot\boldsymbol{x}+\mathrm{i}\boldsymbol{q}\cdot\boldsymbol{y}}\, \frac{\tilde{\mu}(\boldsymbol{q}'+\boldsymbol{q})}{q'^2q^2}$$

- **Single-scattering limit:**

Color-dipole orientation in the McLerran-Venugopalan model

$$\langle \rho^a(\boldsymbol{x})\rho^b(\boldsymbol{y})\rangle = \delta^{ab}\delta^{(2)}(\boldsymbol{x}-\boldsymbol{y})\mu(\boldsymbol{x})$$

In the original MV model:

$$\mu(\mathbf{b}) = \mu_0, \qquad \tilde{\mu}(\mathbf{q}'+\mathbf{q}) = \delta^{\mathbf{2}}(\mathbf{q}'+\mathbf{q})$$

$$\mu(b) = \mu_0\, \mathrm{e}^{-b^2/4R^2},$$

$$\tilde{\mu}(\Delta) = \int \mathrm{d}^2\boldsymbol{b}\, \mathrm{e}^{-\mathrm{i}\boldsymbol{b}\cdot\boldsymbol{\Delta}}\mu(b) = 4\pi R^2\mu_0\, \mathrm{e}^{-\Delta^2 R^2}$$

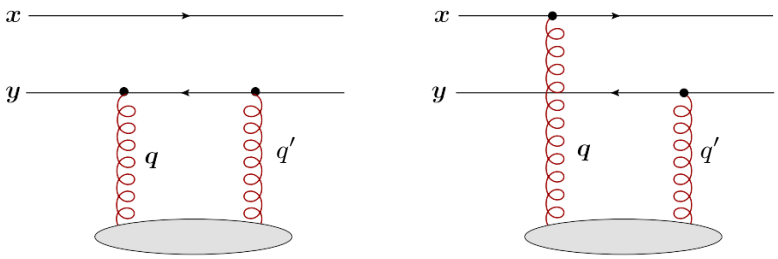
μ_0, R : fixed via a fit to the DIS & diffractive DIS data.

$$\langle A_a^-(\boldsymbol{x})A_b^-(\boldsymbol{y})\rangle = \delta^{ab}\gamma(\boldsymbol{x},\boldsymbol{y})$$

$$\gamma(\boldsymbol{x},\boldsymbol{y}) \equiv \int \mathrm{d}^2\boldsymbol{z}\, G(\boldsymbol{x}-\boldsymbol{z})G(\boldsymbol{y}-\boldsymbol{z})\mu(\boldsymbol{z}) = \int \frac{\mathrm{d}^2\boldsymbol{q}}{(2\pi)^2}\frac{\mathrm{d}^2\boldsymbol{q}'}{(2\pi)^2}\, \mathrm{e}^{\mathrm{i}\boldsymbol{q}'\cdot\boldsymbol{x}+\mathrm{i}\boldsymbol{q}\cdot\boldsymbol{y}}\frac{\tilde{\mu}(\boldsymbol{q}'+\boldsymbol{q})}{q'^2q^2}$$

soft scale ~ 1/R

- **Single-scattering limit:**



$$\mathbf{\Delta = q' + q} \qquad \mathbf{k = (q' - q)/2}$$

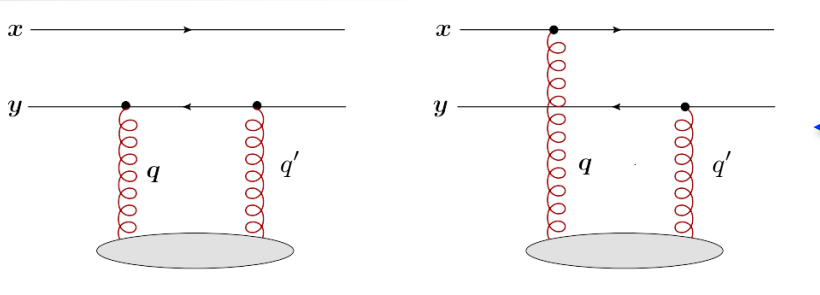
$$\mathbf{r = x - y} \qquad \mathbf{b = (x + y)/2}$$

$$N_{2g}(\boldsymbol{b},\boldsymbol{r}) = \frac{g^2C_F}{2}\int \frac{\mathrm{d}^2\boldsymbol{\Delta}}{(2\pi)^2}\frac{\mathrm{d}^2\boldsymbol{k}}{(2\pi)^2}\frac{\tilde{\mu}(\boldsymbol{\Delta})}{(\boldsymbol{k}+\boldsymbol{\Delta}/2)^2(\boldsymbol{k}-\boldsymbol{\Delta}/2)^2}\, \mathrm{e}^{\mathrm{i}\boldsymbol{\Delta}\cdot\boldsymbol{b}}\left[\mathrm{e}^{\mathrm{i}\boldsymbol{\Delta}\cdot\boldsymbol{r}/2} + \mathrm{e}^{-\mathrm{i}\boldsymbol{\Delta}\cdot\boldsymbol{r}/2} - 2\,\mathrm{e}^{\mathrm{i}\boldsymbol{k}\cdot\boldsymbol{r}}\right]$$

$$\text{If } \tilde{\mu}(\mathbf{\Delta}) = \tilde{\mu}(|\mathbf{\Delta}|) \longrightarrow \mathbf{N_{2g}(b,r)} \propto \mathbf{(b.r)^{2n}} \longrightarrow \mathbf{v_{3,odd} = 0}$$

Elliptic flow in the single scattering approximation

Single-scattering approximation:



$$\Delta = q' + q \qquad k = (q' - q)/2$$

$$r = x - y \qquad b = (x + y)/2$$

$$N_{2g}(\boldsymbol{b},\boldsymbol{r}) = \frac{g^2 C_F}{2}\int \frac{d^2\boldsymbol{\Delta}}{(2\pi)^2}\frac{d^2\boldsymbol{k}}{(2\pi)^2}\frac{\tilde{\mu}(\boldsymbol{\Delta})}{(\boldsymbol{k}+\boldsymbol{\Delta}/2)^2(\boldsymbol{k}-\boldsymbol{\Delta}/2)^2} e^{i\boldsymbol{\Delta}\cdot\boldsymbol{b}}\left[e^{i\boldsymbol{\Delta}\cdot\boldsymbol{r}/2} + e^{-i\boldsymbol{\Delta}\cdot\boldsymbol{r}/2} - 2\,e^{i\boldsymbol{k}\cdot\boldsymbol{r}}\right.$$

$pR \gg 1$ (while $\Delta \lesssim 1/R$)

$$\tilde{S}(\mathbf{b},\mathbf{p}) \simeq -\tilde{N}_{2g}(\mathbf{b},\mathbf{p}) \simeq \frac{g^2 C_F}{p^4}\mu(\mathbf{b})\left[1 - \frac{b^2}{8p^2R^4}\cos(2\phi)\right]$$

$$v_2(p,b) \simeq \frac{\int_{-\pi}^{\pi} d\phi \cos(2\phi)\left[1 - \frac{b^2}{8p^2R^4}\cos(2\phi)\right]}{\int_{-\pi}^{\pi} d\phi \left[1 - \frac{b^2}{8p^2R^4}\cos(2\phi)\right]} = -\frac{b^2}{16p^2R^4}$$

★ **v2=0 at b=0.**

★ **A quark produced via a single scattering has more chances to propagate along a direction which is perpendicular on its impact parameter rather than parallel to it.**

★ **Multiple scatterings will change the sign of v2.**

Color-dipole orientation in the MV model

Adding multiple scattering: → $S(\boldsymbol{b},\boldsymbol{r}) = \exp\{-N_{2g}(\boldsymbol{b},\boldsymbol{r})\}$

$$N_{2g}(\boldsymbol{b},\boldsymbol{r}) = \frac{g^2 C_F}{2}\int \frac{\mathrm{d}^2\boldsymbol{\Delta}}{(2\pi)^2}\frac{\mathrm{d}^2\boldsymbol{k}}{(2\pi)^2}\frac{\tilde{\mu}(\boldsymbol{\Delta})}{(\boldsymbol{k}+\boldsymbol{\Delta}/2)^2(\boldsymbol{k}-\boldsymbol{\Delta}/2)^2}\,\mathrm{e}^{\mathrm{i}\boldsymbol{\Delta}\cdot\boldsymbol{b}}\left[\mathrm{e}^{\mathrm{i}\boldsymbol{\Delta}\cdot\boldsymbol{r}/2}+\mathrm{e}^{-\mathrm{i}\boldsymbol{\Delta}\cdot\boldsymbol{r}/2}-2\,\mathrm{e}^{\mathrm{i}\boldsymbol{k}\cdot\boldsymbol{r}}\right]$$

- In soft multiple scattering regime, $k << 1/r$ and $\Delta \leq 1/R$:

$$N_{2g}(\boldsymbol{b},\boldsymbol{r}) \simeq \frac{g^2 C_F}{2}\,r^i r^j \int \frac{\mathrm{d}^2\boldsymbol{\Delta}}{(2\pi)^2}\frac{\mathrm{d}^2\boldsymbol{k}}{(2\pi)^2}\frac{\left(k^i k^j - \Delta^i\Delta^j/4\right)\tilde{\mu}(\Delta)}{[(\boldsymbol{k}+\boldsymbol{\Delta}/2)^2+m^2][(\boldsymbol{k}-\boldsymbol{\Delta}/2)^2+m^2]}\,\mathrm{e}^{\mathrm{i}\boldsymbol{\Delta}\cdot\boldsymbol{b}}$$

- **Infrared finite at m—> 0:**

'gluon mass' m is needed in order to restrict the phase-space allowed to very soft momenta $k \sim \Lambda_{QCD}$

Color-dipole orientation in the MV model

Adding multiple scattering: → $S(\boldsymbol{b},\boldsymbol{r}) = \exp\{-N_{2g}(\boldsymbol{b},\boldsymbol{r})\}$

$$N_{2g}(\boldsymbol{b},\boldsymbol{r}) = \frac{g^2 C_F}{2}\int \frac{\mathrm{d}^2\boldsymbol{\Delta}}{(2\pi)^2}\frac{\mathrm{d}^2\boldsymbol{k}}{(2\pi)^2}\frac{\tilde{\mu}(\boldsymbol{\Delta})}{(\boldsymbol{k}+\boldsymbol{\Delta}/2)^2(\boldsymbol{k}-\boldsymbol{\Delta}/2)^2}\,\mathrm{e}^{\mathrm{i}\boldsymbol{\Delta}\cdot\boldsymbol{b}}\left[\mathrm{e}^{\mathrm{i}\boldsymbol{\Delta}\cdot\boldsymbol{r}/2}+\mathrm{e}^{-\mathrm{i}\boldsymbol{\Delta}\cdot\boldsymbol{r}/2}-2\,\mathrm{e}^{\mathrm{i}\boldsymbol{k}\cdot\boldsymbol{r}}\right]$$

- In soft multiple scattering regime, $k << 1/r$ and $\Delta \leq 1/R$:

$$N_{2g}(\boldsymbol{b},\boldsymbol{r}) \simeq \frac{g^2 C_F}{2}\,r^i r^j \int \frac{\mathrm{d}^2\boldsymbol{\Delta}}{(2\pi)^2}\frac{\mathrm{d}^2\boldsymbol{k}}{(2\pi)^2}\frac{\left(k^i k^j - \Delta^i\Delta^j/4\right)\tilde{\mu}(\Delta)}{[(\boldsymbol{k}+\boldsymbol{\Delta}/2)^2+m^2][(\boldsymbol{k}-\boldsymbol{\Delta}/2)^2+m^2]}\,\mathrm{e}^{\mathrm{i}\boldsymbol{\Delta}\cdot\boldsymbol{b}}$$

- **UV regularization :**

$$\frac{g^2 C_F}{4}\,r^2\int \frac{\mathrm{d}^2\boldsymbol{\Delta}}{(2\pi)^2}\frac{\mathrm{d}^2\boldsymbol{k}}{(2\pi)^2}\frac{k^2\tilde{\mu}(\Delta)}{(k^2+m^2)^2}\,\mathrm{e}^{\mathrm{i}\boldsymbol{\Delta}\cdot\boldsymbol{b}} \equiv \frac{Q_s^2(b)r^2}{4}\ln\left(\frac{1}{r^2m^2}+\mathrm{e}\right)$$

$$Q_s^2(b) \equiv \alpha_s C_F \mu(b) = Q_{0s}^2\,\mathrm{e}^{-b^2/4R^2}$$

Color-dipole orientation in the MV model

Adding multiple scattering: → $S(\boldsymbol{b},\boldsymbol{r}) = \exp\{-N_{2g}(\boldsymbol{b},\boldsymbol{r})\}$

$$N_{2g}(b,r,\theta) = \mathcal{N}_0(b,r) + \mathcal{N}_\theta(b,r)\cos(2\theta)$$

$$\mathcal{N}_0(b,r) = \frac{Q_s^2(b)r^2}{4}\ln\left(\frac{1}{r^2m^2}+\mathrm{e}\right) + \frac{g^2C_F}{4(2\pi)^2}r^2\int_0^\infty \mathrm{d}\Delta\,\Delta\,\tilde{\mu}(\Delta)\mathrm{J}_0(\Delta b) \times \int_0^\infty \mathrm{d}k\,k\left[\frac{k^2-\Delta^2/4}{(k^2+\Delta^2/4+m^2)\left((k^2+\Delta^2/4+m^2)^2-k^2\Delta^2\right)^{1/2}} - \frac{k^2}{(k^2+m^2)^2}\right]$$

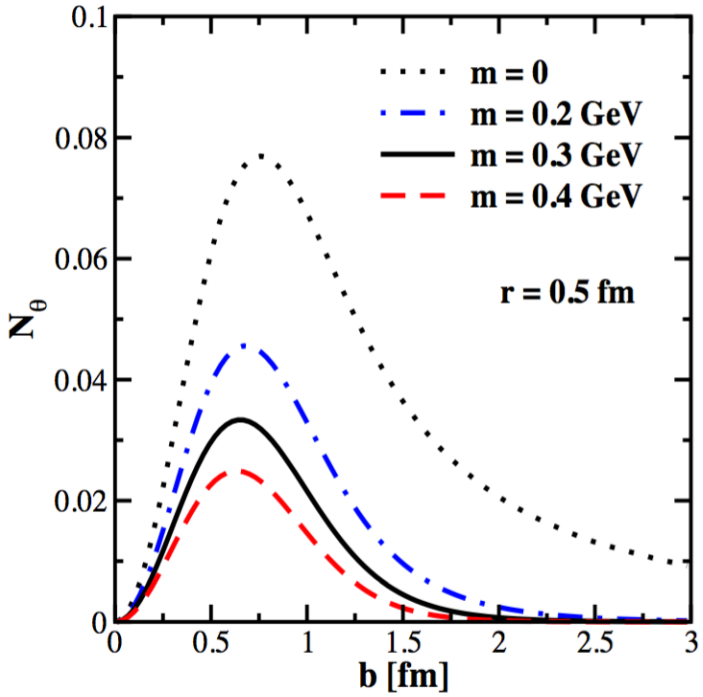
← **Original MV model**

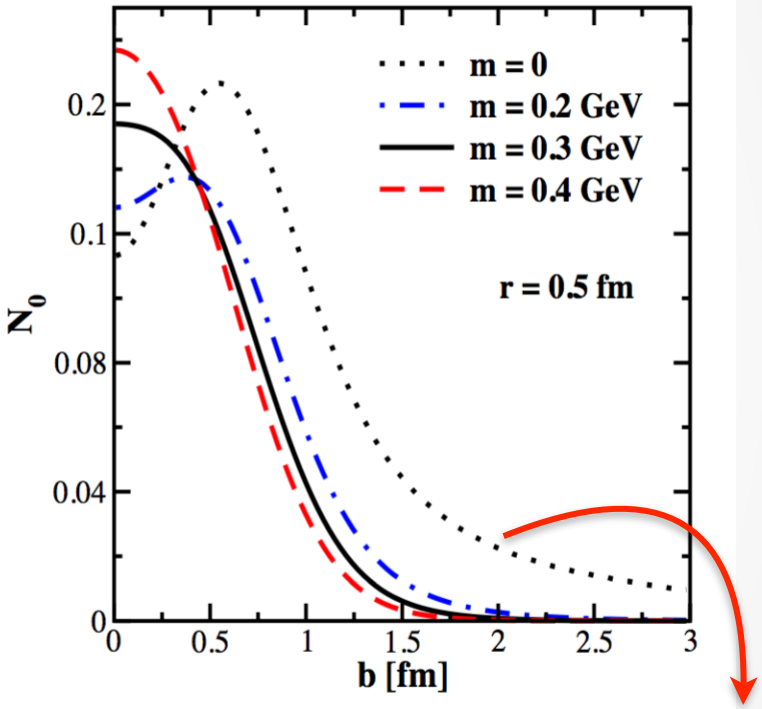
$$\mathcal{N}_\theta(b,r) = \frac{g^2C_F}{4(2\pi)^2}r^2\int_0^\infty \mathrm{d}\Delta\,\Delta\,\tilde{\mu}(\Delta)\mathrm{J}_2(\Delta b)\int_0^\infty \mathrm{d}k\,k\left[\frac{k^2+\Delta^2/4}{(k^2+\Delta^2/4+m^2)\left((k^2+\Delta^2/4+m^2)^2-k^2\Delta^2\right)^{1/2}} + \frac{2}{\Delta^2} - \frac{2\left(k^2+\Delta^2/4+m^2\right)}{\Delta^2\left((k^2+\Delta^2/4+m^2)^2-k^2\Delta^2\right)^{1/2}}\right].$$

Color-dipole orientation in the MV model

Adding multiple scattering: $\rightarrow$ $S(\boldsymbol{b},\boldsymbol{r}) = \exp\{-N_{2g}(\boldsymbol{b},\boldsymbol{r})\}$

$$N_{2g}(b,r,\theta) = \mathcal{N}_0(b,r) + \mathcal{N}_\theta(b,r)\cos(2\theta)$$



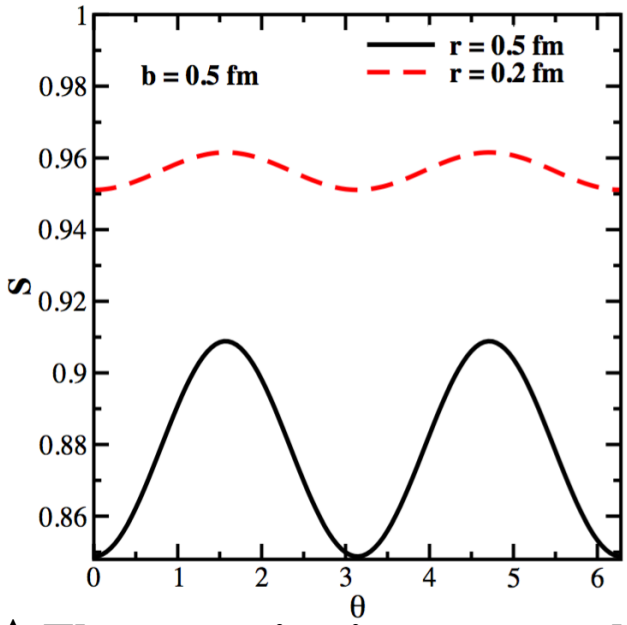


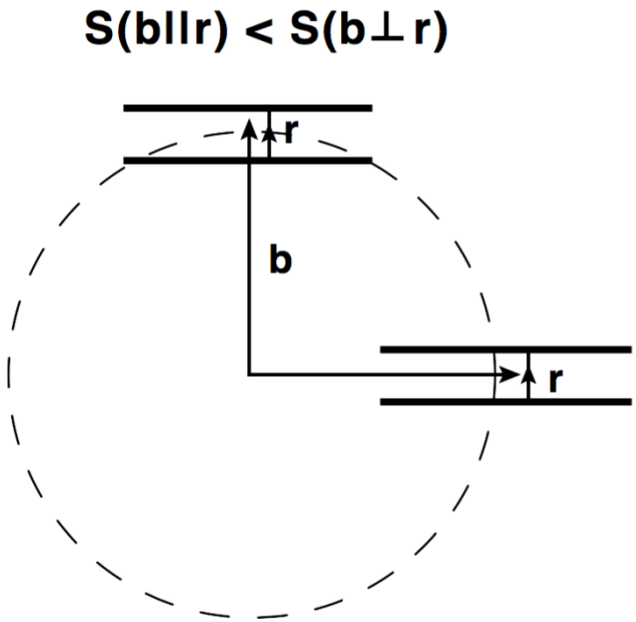
$$\mathcal{N}_\theta(b,r)\Big|_{m=0} = \frac{1}{2}\times\frac{g^2 C_F}{4(2\pi)^2} r^2 \int_0^\infty \mathrm{d}\Delta\,\Delta\,\tilde{\mu}(\Delta)\mathrm{J}_2(\Delta b) = Q_{0s}^2 r^2 \frac{R^2}{b^2}\left[1-\left(1+\frac{b^2}{4R^2}\right)\mathrm{e}^{-\frac{b^2}{4R^2}}\right]$$

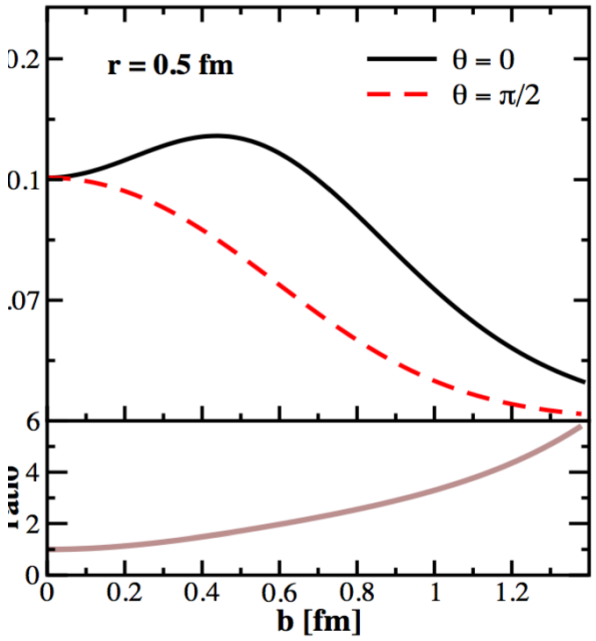
no confinement in the limit $m \to 0$

Color-dipole orientation as an origin of elliptic flow

$$N_{2g}(b,r,\theta) = \mathcal{N}_0(b,r) + \mathcal{N}_\theta(b,r)\cos(2\theta) \qquad S(\boldsymbol{b},\boldsymbol{r}) = \exp\{-N_{2g}(\boldsymbol{b},\boldsymbol{r})\}$$





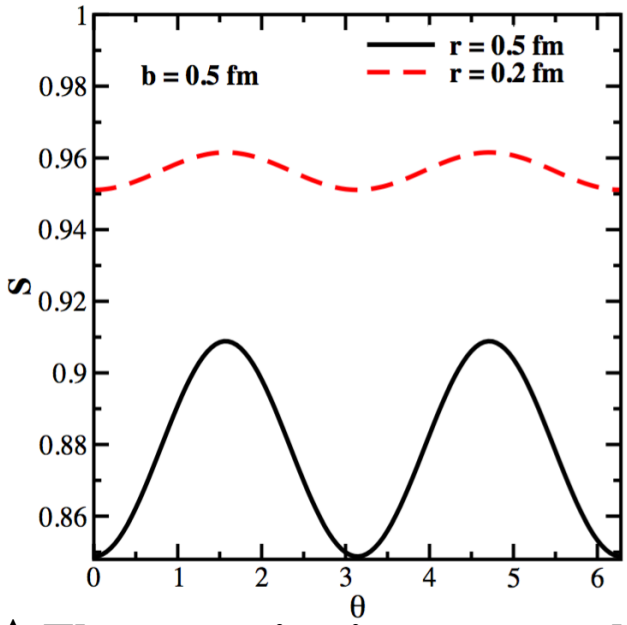


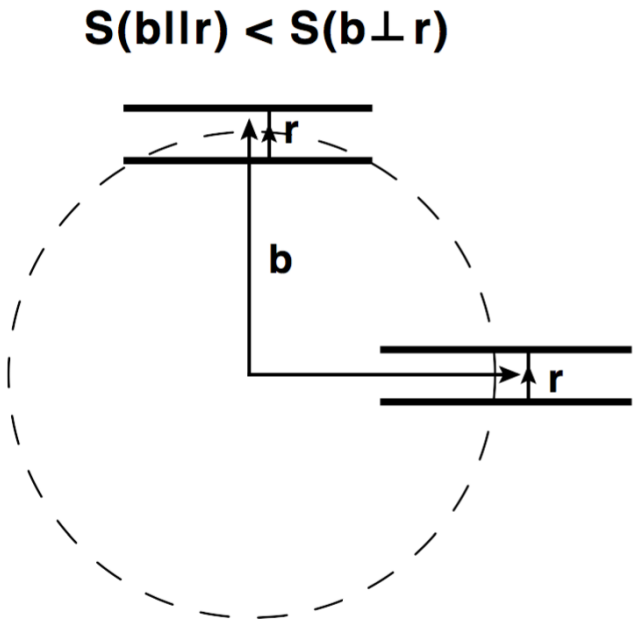
- The scattering is stronger when the dipole orientation is (anti)parallel to its impact parameter ($\theta = 0$ or $\theta = \pi$) than for a dipole perpendicular on b ($\theta = \pi/2$).

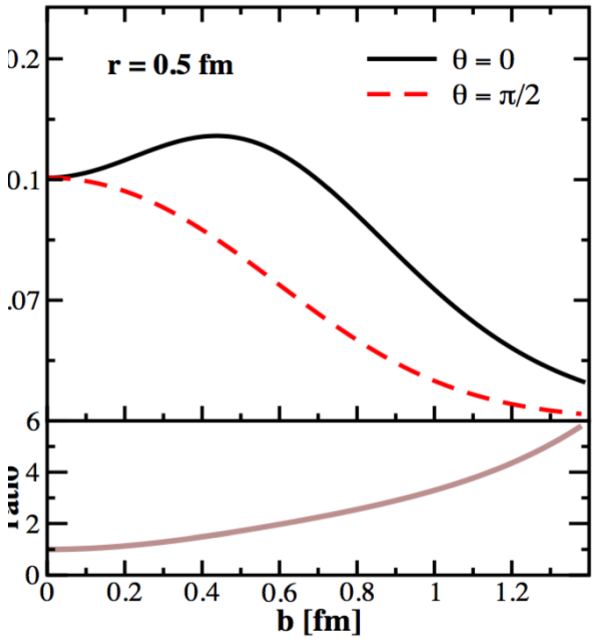
- The difference between 'parallel' and 'perpendicular' scattering increases with the dipole size r and also with the impact parameter b.

Color-dipole orientation as an origin of elliptic flow

$$N_{2g}(b,r,\theta) = \mathcal{N}_0(b,r) + \mathcal{N}_\theta(b,r)\cos(2\theta) \qquad S(\boldsymbol{b},\boldsymbol{r}) = \exp\{-N_{2g}(\boldsymbol{b},\boldsymbol{r})\}$$







✦ **The scattering is stronger when the dipole orientation is (anti)parallel to its impact parameter (θ = 0 or θ = π) than for a dipole perpendicular on b (θ = π/2).**

✦ **The difference between 'parallel' and 'perpendicular' scattering increases with the dipole size r and also with the impact parameter b.**

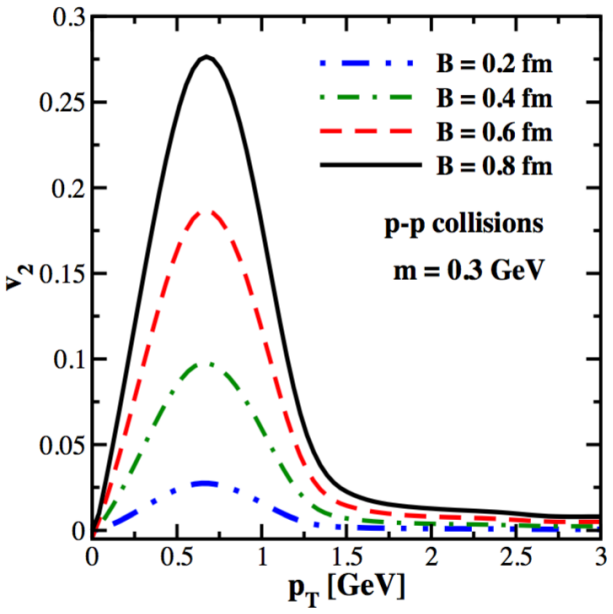
$$v_2(p,b) = -\frac{\int r dr\, e^{-\mathcal{N}_0(b,r)} J_2(pr) \int d\theta\, e^{-\mathcal{N}_\theta(b,r)\cos(2\theta)} \cos(2\theta)}{\int r dr\, e^{-\mathcal{N}_0(b,r)} J_0(pr) \int d\theta\, e^{-\mathcal{N}_\theta(b,r)\cos(2\theta)}}$$

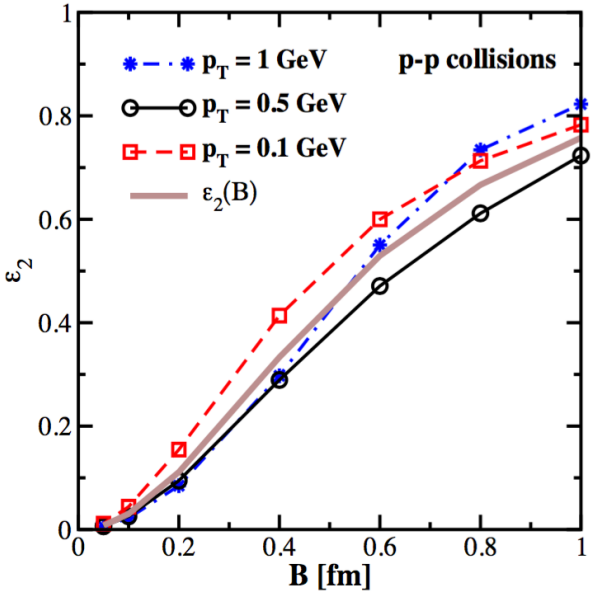
$$= \frac{\int r dr\, e^{-\mathcal{N}_0(b,r)} J_2(pr)\, I_1\left(\mathcal{N}_\theta(b,r)\right)}{\int r dr\, e^{-\mathcal{N}_0(b,r)} J_0(pr)\, I_0\left(\mathcal{N}_\theta(b,r)\right)},$$

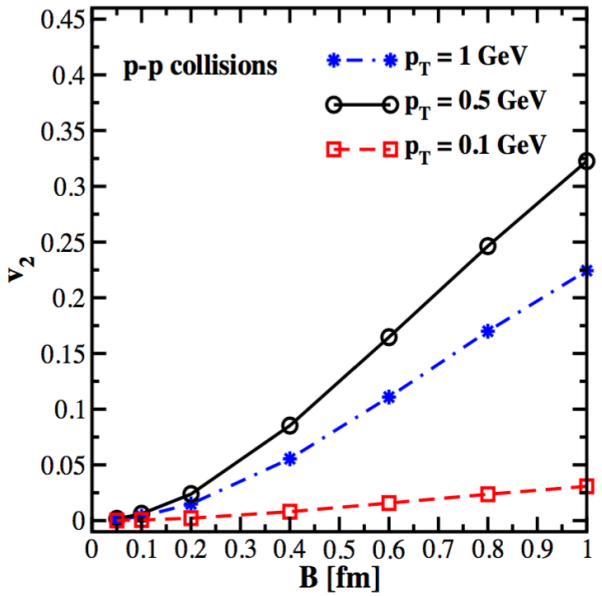
$$N(\mathbf{b}||\mathbf{r}) > \mathbf{N}(\mathbf{b} \perp \mathbf{r})$$

$$\mathcal{N}_\theta > 0 \longrightarrow v_2 > 0$$

Elliptic flow from color-dipole orientation in pp collisions







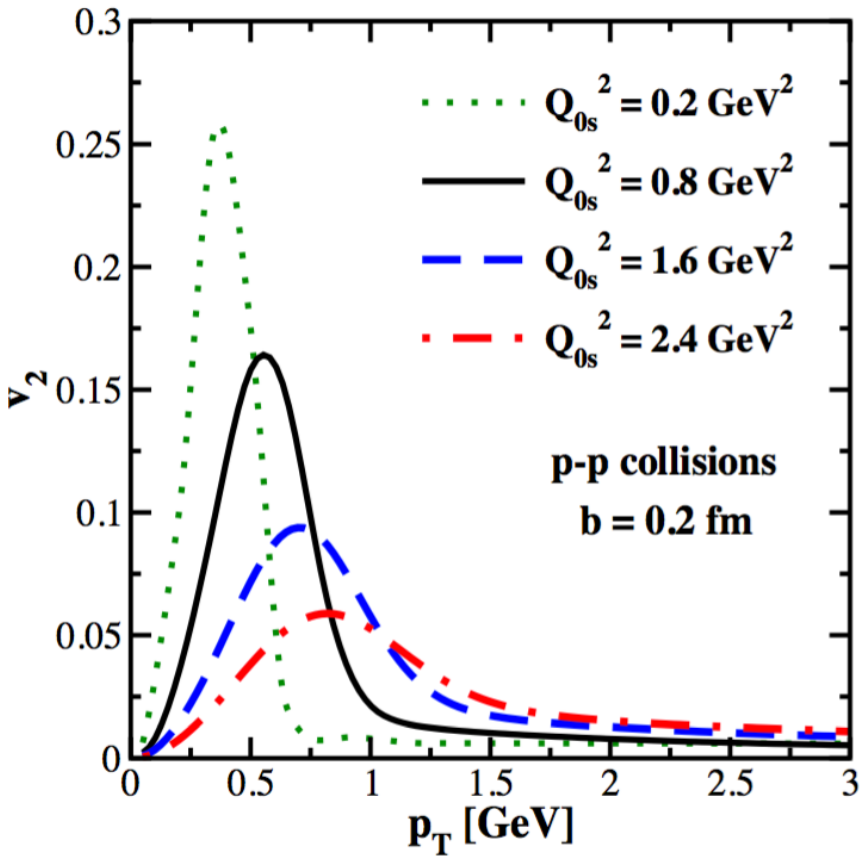
- The strength of v_2 increases with B (and b) since dipole orientation becomes important at large B (and b).
  The typical transverse size of the color charge distribution in the target is $2R \sim 0.6$ fm.

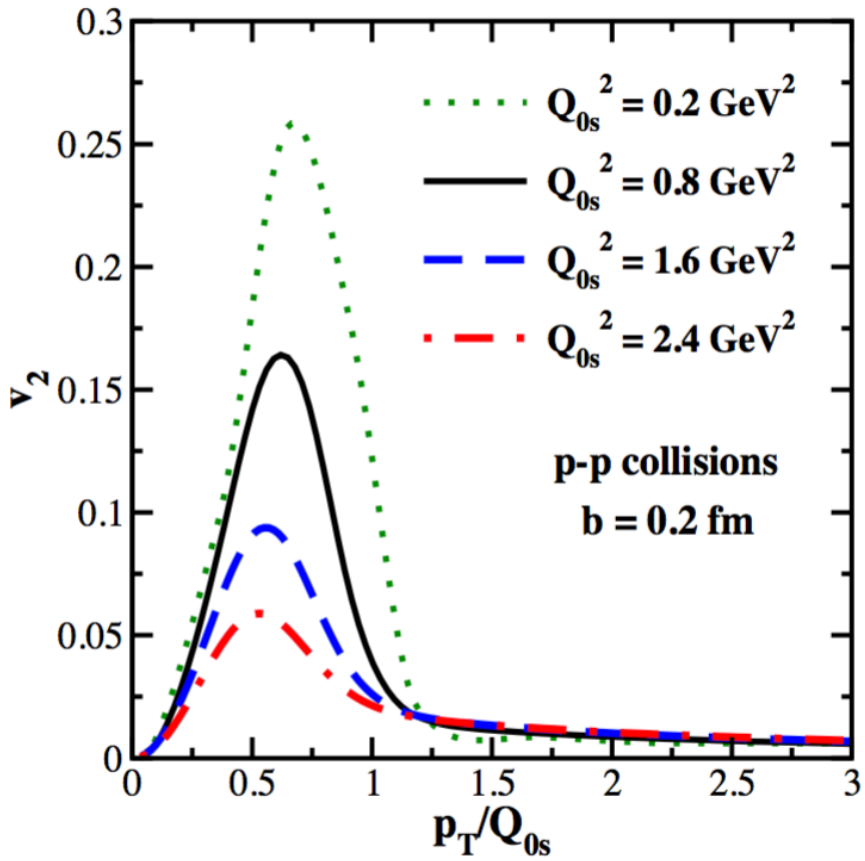
- v_2 and ϵ_2 show a similar trend with B, they monotonously increase with B:

$$v_2(p, B) \propto \epsilon_2(p, B)$$

- $\varepsilon_2(p_T, B)$ is only weakly sensitive to the dipole scattering, since mostly controlled by the geometry.

Scaling property of v_2 with the saturation scale:

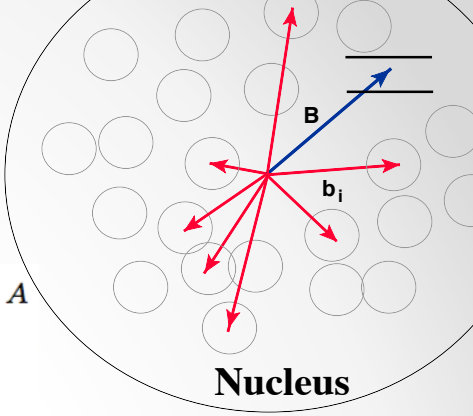




- v_2 develops a peak at a transverse momentum which scales with the saturation momentum in the target.

Dipole-nucleus scattering: the case of a lumpy target :

To include nucleon fluctuations in nucleus:



$$S_A(\boldsymbol{B},\boldsymbol{r}) = \int \prod_{i=1}^{A} \mathrm{d}^2\boldsymbol{b}_i \, T_A(\boldsymbol{b}_i)\, \mathrm{e}^{-\sum_{i=1}^{A} N_{2g}(\boldsymbol{B}-\boldsymbol{b}_i,\boldsymbol{r})} = \left(\int \mathrm{d}^2\boldsymbol{b}\, T_A\left(|\boldsymbol{B}-\boldsymbol{b}|\right)\, \mathrm{e}^{-N_{2g}(\boldsymbol{b},\boldsymbol{r})} \right)^A$$

- **B** to denote the impact parameter of the dipole w.r.t. the center of the nucleus.
- $\mathbf{b_i}$ is the position of the struck nucleon w.r.t. the center of the nucleus.

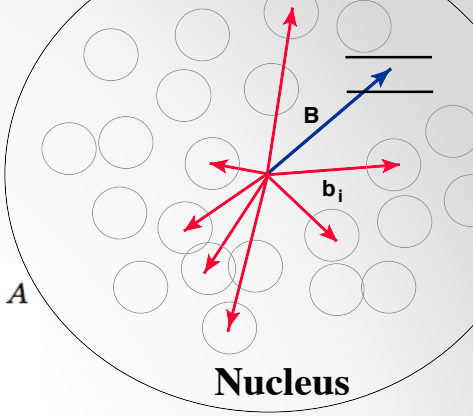
✦ Assuming scattering between the dipole and a *single* nucleon is weak $N_{2g}(\mathbf{b},\mathbf{r}) \ll 1$

$$S_A(\boldsymbol{B},\boldsymbol{r}) \simeq \left(1 - \int \mathrm{d}^2\boldsymbol{b}\, T_A\left(|\boldsymbol{B}-\boldsymbol{b}|\right)\, N_{2g}(\boldsymbol{b},\boldsymbol{r}) \right)^A \simeq \mathrm{e}^{-A N_{2g}^A(\boldsymbol{B},\boldsymbol{r})}$$

$$N_{2g}^A(\boldsymbol{B},\boldsymbol{r}) = \int d^2\boldsymbol{b}\, N_{2g}(\boldsymbol{b},\boldsymbol{r})\, T_A\left(|\boldsymbol{B}-\boldsymbol{b}|\right)$$

Dipole-nucleus scattering: the case of a lumpy target :

To include nucleon fluctuations in nucleus:



$$S_A(\boldsymbol{B},\boldsymbol{r}) = \int \prod_{i=1}^{A} \mathrm{d}^2\boldsymbol{b}_i \, T_A(\boldsymbol{b}_i)\, \mathrm{e}^{-\sum_{i=1}^{A} N_{2g}(\boldsymbol{B}-\boldsymbol{b}_i,\boldsymbol{r})} = \left(\int \mathrm{d}^2\boldsymbol{b}\, T_A\left(|\boldsymbol{B}-\boldsymbol{b}|\right)\, \mathrm{e}^{-N_{2g}(\boldsymbol{b},\boldsymbol{r})} \right)^A$$

- **B** to denote the impact parameter of the dipole w.r.t. the center of the nucleus.
- $\mathbf{b_i}$ is the position of the struck nucleon w.r.t. the center of the nucleus.

✦ Assuming scattering between the dipole and a *single* nucleon is weak $N_{2g}(\mathbf{b},\mathbf{r}) \ll 1$

$$S_A(\boldsymbol{B},\boldsymbol{r}) \simeq \left(1 - \int \mathrm{d}^2\boldsymbol{b}\, T_A\left(|\boldsymbol{B}-\boldsymbol{b}|\right)\, N_{2g}(\boldsymbol{b},\boldsymbol{r})\right)^A \simeq \mathrm{e}^{-A N_{2g}^A(\boldsymbol{B},\boldsymbol{r})}$$

$$N_{2g}^A(\boldsymbol{B},\boldsymbol{r}) = \int d^2\boldsymbol{b}\, N_{2g}(\boldsymbol{b},\boldsymbol{r})\, T_A\left(|\boldsymbol{B}-\boldsymbol{b}|\right)$$

Homogeneous target: $T_A(\mathbf{B}-\mathbf{b}) \simeq \mathbf{T_A(B)}$ ⟶ **No dipole orientation:** $v_n \approx 0$

In central collisions: $v_n \approx 0$

Dipole-nucleus scattering: the case of a lumpy target

$$N_{2g}^{A}(\boldsymbol{B},\boldsymbol{r}) = \int d^2\boldsymbol{b}\, N_{2g}(\boldsymbol{b},\boldsymbol{r})\, T_A\left(|\boldsymbol{B}-\boldsymbol{b}|\right)$$

B >> b:

$$\begin{aligned} T_A(|\boldsymbol{B}-\boldsymbol{b}|) &= \left(1 - b^i\frac{\partial}{\partial B^i} + \frac{1}{2}b^i b^j \frac{\partial^2}{\partial B^i \partial B^j} + \dots\right) T_A\left(|\boldsymbol{B}|\right), \\ &\simeq T_A(B) - \frac{\boldsymbol{b}\cdot\boldsymbol{B}}{B}T_A'(B) + \frac{b^i b^j}{2}\left\{\frac{B^i B^j}{B^2}T_A''(B) + \frac{1}{B}\left(\delta^{ij} - \frac{B^i B^j}{B^2}\right)T_A'(B)\right\} \end{aligned}$$

correlations (**B, b**) and (**b, r**) ⟶ correlations (**B, r**)

$$N_{2g}^{A}(B,r,\theta) = \mathcal{N}_0^A(B,r) + \mathcal{N}_\theta^A(B,r)\cos(2\theta)$$

$$\begin{aligned} \mathcal{N}_0^A(B,r) &= 2\pi \int \mathrm{d}b\, b\, \mathcal{N}_0(b,r)\left\{T_A(B) + \frac{b^2}{4}\left(T_A''(B) + \frac{1}{B}T_A'(B)\right)\right\} \\ \mathcal{N}_\theta^A(B,r) &= \frac{\pi}{4}\int \mathrm{d}b\, b^3\, \mathcal{N}_\theta(b,r)\left(T_A''(B) - \frac{1}{B}T_A'(B)\right). \end{aligned}$$

Dipole-nucleus scattering: the case of a lumpy target

$$N_{2g}^{A}(\boldsymbol{B},\boldsymbol{r}) = \int d^2\boldsymbol{b}\, N_{2g}(\boldsymbol{b},\boldsymbol{r})\, T_A\left(|\boldsymbol{B}-\boldsymbol{b}|\right)$$

B >> b:

$$\begin{aligned} T_A(|\boldsymbol{B}-\boldsymbol{b}|) &= \left(1 - b^i\frac{\partial}{\partial B^i} + \frac{1}{2}b^ib^j\frac{\partial^2}{\partial B^i \partial B^j} + \dots\right) T_A\left(|\boldsymbol{B}|\right), \\ &\simeq T_A(B) - \frac{\boldsymbol{b}\cdot\boldsymbol{B}}{B}T_A'(B) + \frac{b^ib^j}{2}\left\{\frac{B^iB^j}{B^2}T_A''(B) + \frac{1}{B}\left(\delta^{ij} - \frac{B^iB^j}{B^2}\right)T_A'(B)\right\} \end{aligned}$$

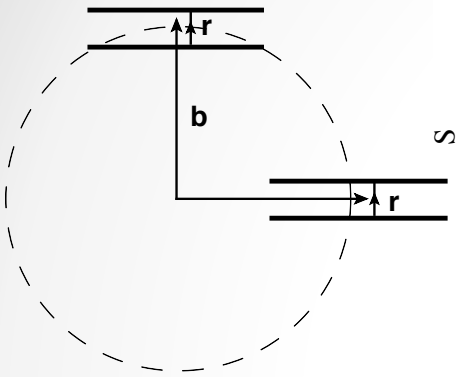
correlations (**B, b**) and (**b, r**) ⟶ correlations (**B, r**)

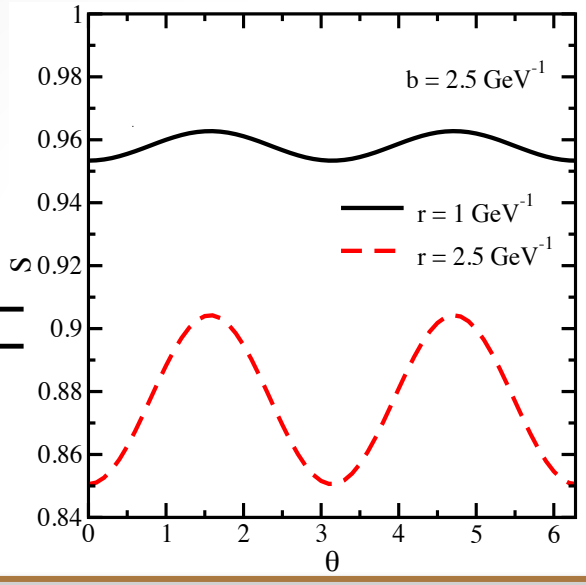
$$N_{2g}^{A}(B,r,\theta) = \mathcal{N}_0^A(B,r) + \mathcal{N}_\theta^A(B,r)\cos(2\theta)$$

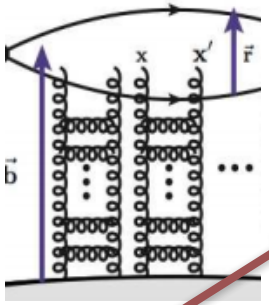
Original MV model

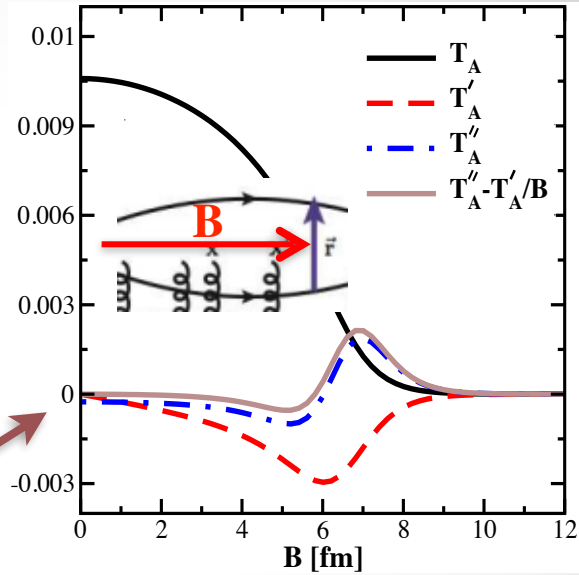
$$\begin{aligned} \mathcal{N}_0^A(B,r) &= \pi R^2 Q_{0s}^2 r^2 \ln\left(\frac{1}{r^2m^2} + \mathrm{e}\right)\left[T_A(B) + R^2\left(T_A''(B) + \frac{1}{B}T_A'(B)\right)\right] \\ &\quad + \frac{\pi}{3}\frac{R^2}{m^2}Q_{0s}^2 r^2\left(T_A''(B) + \frac{1}{B}T_A'(B)\right), \\ \mathcal{N}_\theta^A(B,r) &= \frac{\pi}{6}\frac{R^2}{m^2}Q_{0s}^2 r^2\left(T_A''(B) - \frac{1}{B}T_A'(B)\right). \end{aligned}$$

Elliptic flow as a good probe of the lumpiness of the target









The color-dipole orientation probes the inhomogeneity of the target in the transverse plane.

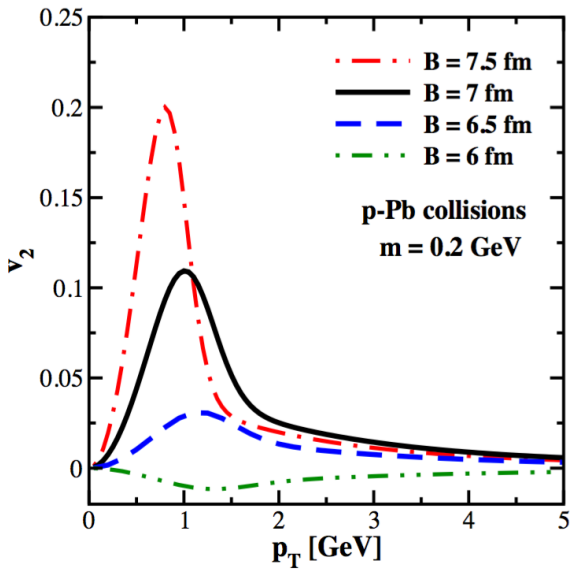
$$N_{2g}^A(B,r,\theta) = \mathcal{N}_0^A(B,r) + \mathcal{N}_\theta^A(B,r)\cos(2\theta),$$

Original MV model

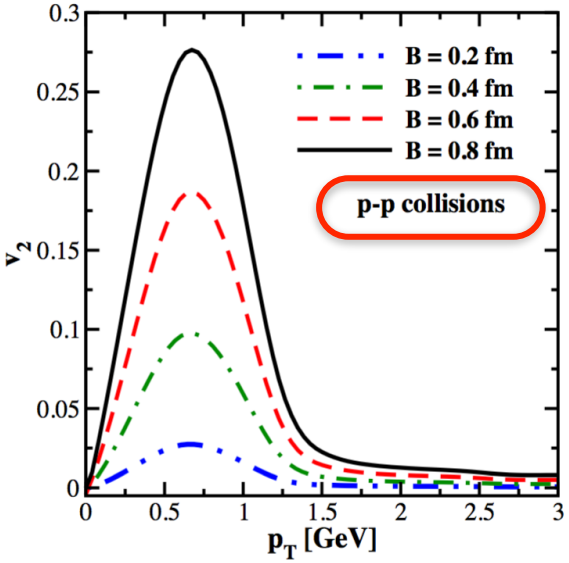
$$\mathcal{N}_0^A(B,r) = \pi R^2 Q_{0s}^2 r^2 \ln\left(\frac{1}{r^2 m^2} + e\right)\left[T_A(B) + R^2\left(T_A''(B) + \frac{1}{B}T_A'(B)\right)\right] + \frac{\pi}{3}\frac{R^2}{m^2}Q_{0s}^2 r^2\left(T_A''(B) + \frac{1}{B}T_A'(B)\right),$$

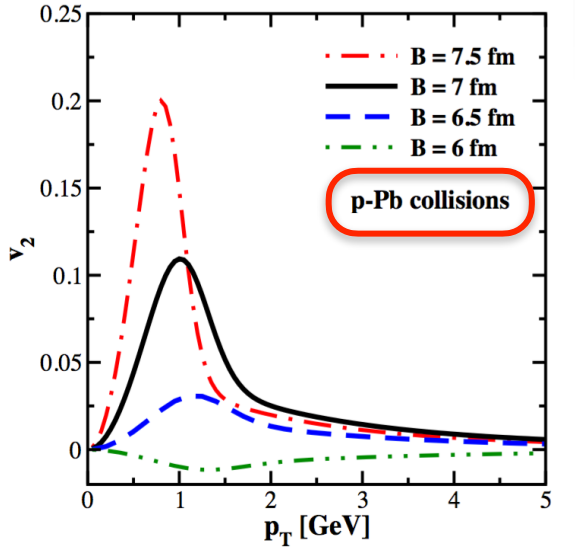
$$\mathcal{N}_\theta^A(B,r) = \frac{\pi}{6}\frac{R^2}{m^2}Q_{0s}^2 r^2\left(T_A''(B) - \frac{1}{B}T_A'(B)\right).$$

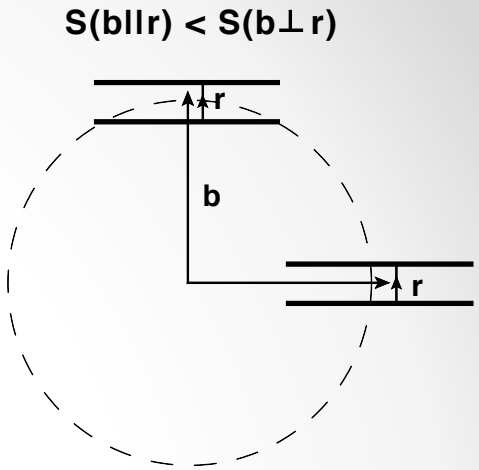
$$v_2(p,B) = \frac{\int r dr\, e^{-A\mathcal{N}_0^A(B,r)}\, J_2(pr)\, I_1\left(A\mathcal{N}_\theta^A(B,r)\right)}{\int r dr\, e^{-A\mathcal{N}_0^A(B,r)}\, J_0(pr)\, I_0\left(A\mathcal{N}_\theta^A(B,r)\right)}.$$



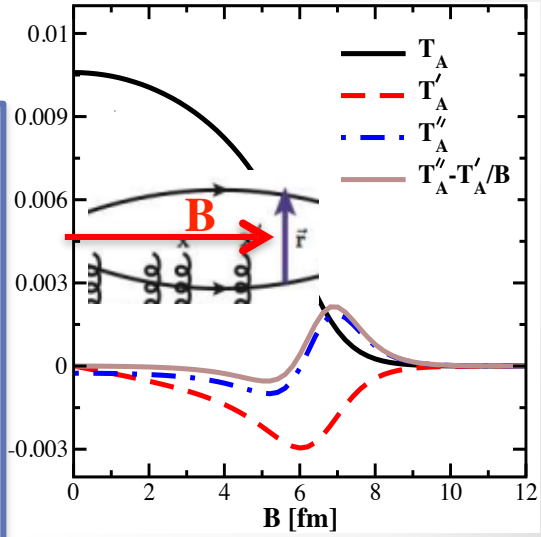
pp v. pA collisions





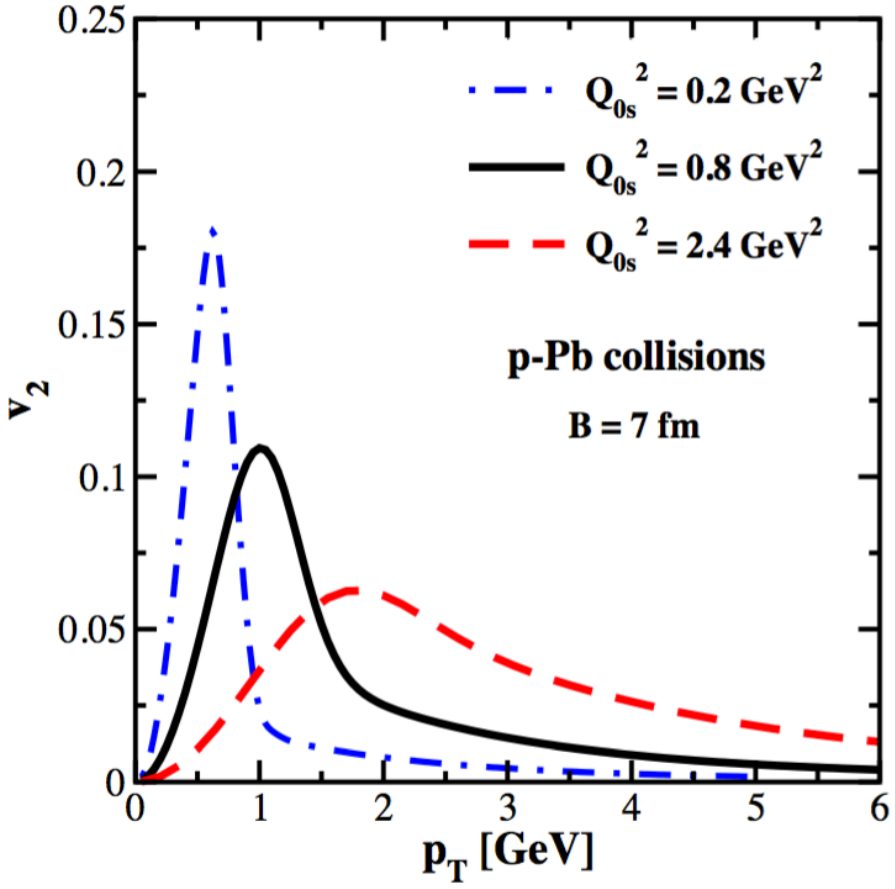


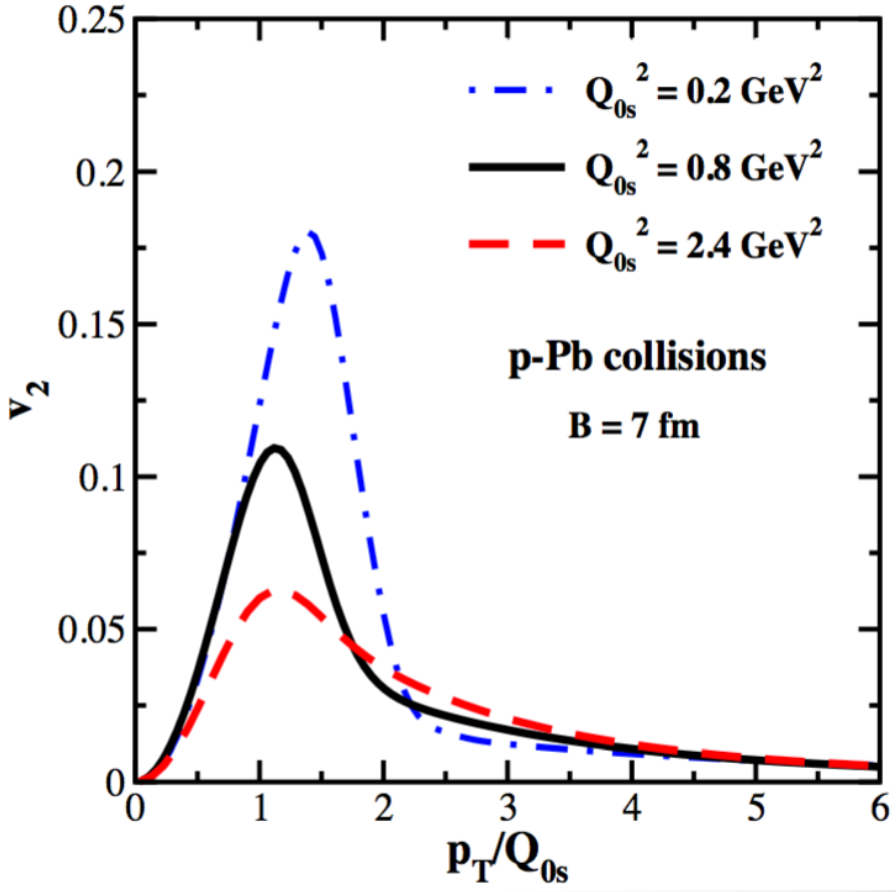
- $v_2 \to 0$ for $p_T \to 0$ or large p_T.
  The angular orientation cannot play any role when either the momentum p_T, or the dipole size r, are too small.
- $v_2 \to 0$ for $b, B \to 0$.
- $v_2(p_{\rm max}) \gtrsim 0.1$ when b or $B \sim$ the typical size for inhomogeneity in the target:
  $b \sim R \gtrsim 0.2$ fm for a proton and $B \sim R_A \gtrsim 6.5$ fm for a large nucleus.



✓The color-dipole orientation (and v_2) probes the inhomogeneity of the target.

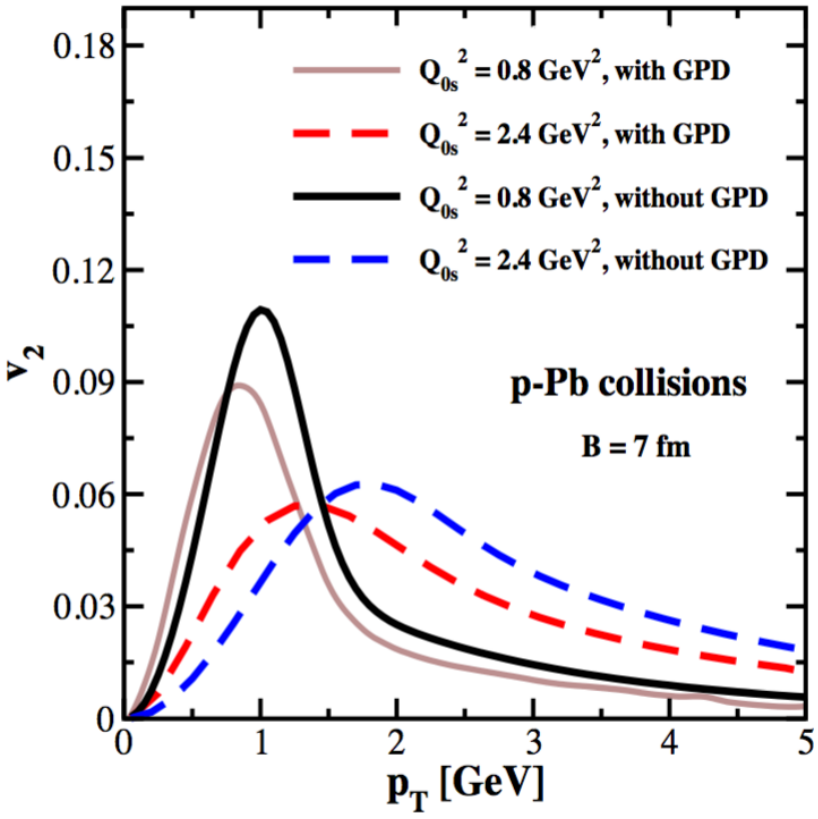
Scaling property of v_2





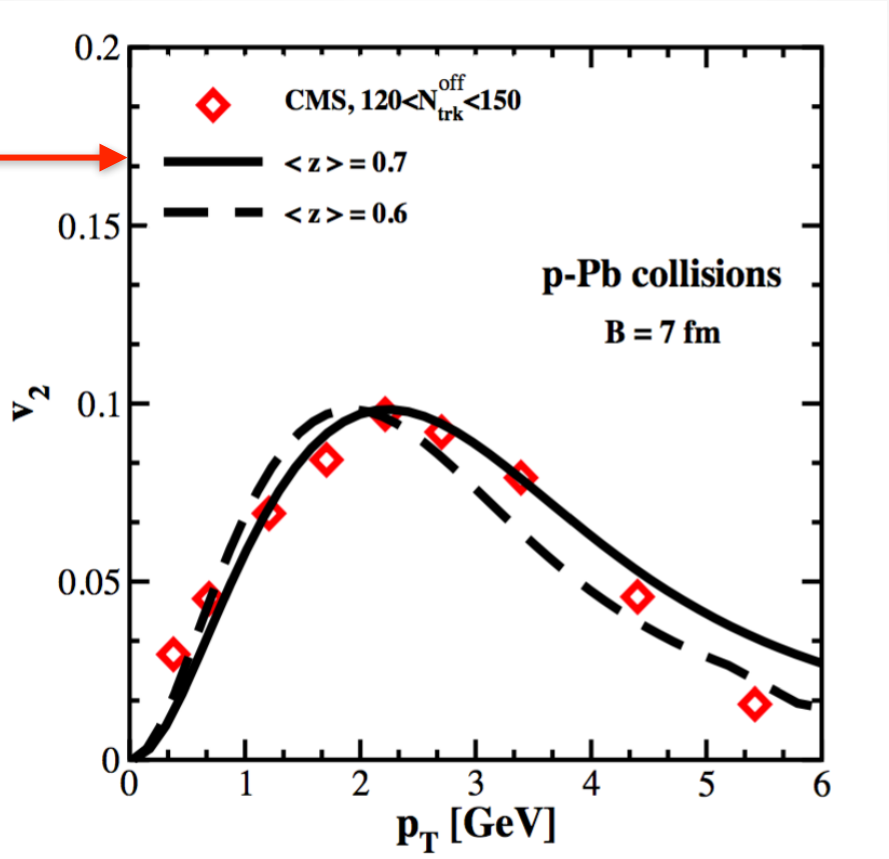
- Similar to pp collisions, v_2 develops a peak at a transverse momentum which scales with the saturation momentum in the target.

Finite-size effect of projectile proton (GPD):



✓ **The finite-size effect of proton is quite small — at most a change of 20% in the value of v_2 at its peak. This is due to the fact that the color-dipole orientation is only important for peripheral collisions.**

$p_{\rm hadron} = \langle z \rangle p_{\rm quark}$



- **Assuming that the final particles are correlated with each other only through the flow correlations with the reaction plane:** $v_2\{4\} = [-c_2\{4\}]^{1/4}$

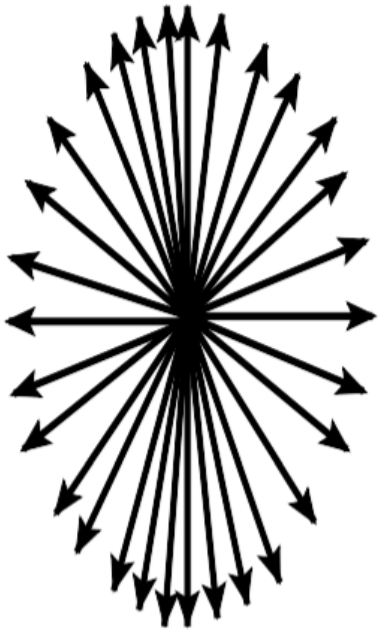
- **We have 3 free parameters:** $R^2 Q_{0s}^2,\ m, B$

From HERA: $R^2 = 2\ \mathbf{GeV}^{-2}$**, For the LHC:** $Q_{0s}^2 = 3\ \mathbf{GeV}^2$

This scenario is not excluded by the current data.

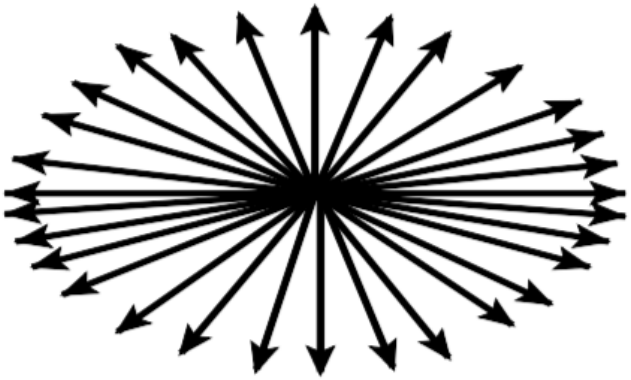
Geometrical picture of pp and pA collisions

$v_2 < 0$



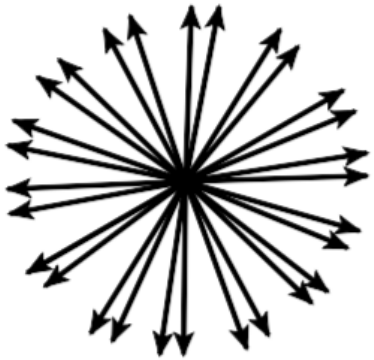
$c_2 > 0$

✓ $v_2 > 0$



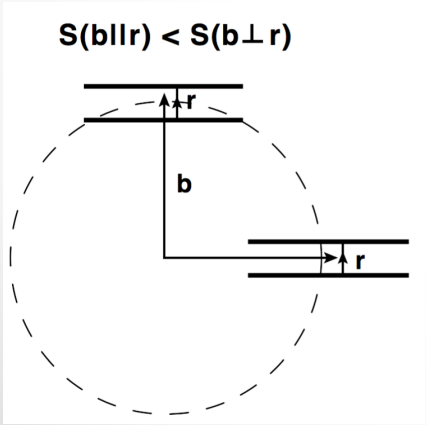
$c_2 > 0$

$v_2 = 0$



$c_2 > 0$

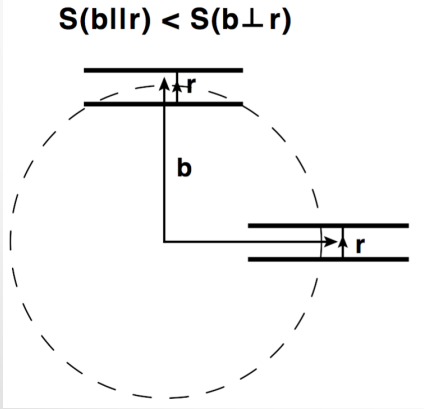
(inspired by Snellings, arXiv:1102.3010)



$N(\mathbf{b}||\mathbf{r}) > \mathbf{N}(\mathbf{b} \perp \mathbf{r}) \longrightarrow \mathcal{N}_\theta > 0 \longrightarrow v_2 > 0$

Such geometrical aspects are clearly reminiscent of the classical discussion of hydrodynamic flow in AA collisions:

- ✓ **AA collisions:** the flow is driven by the 'pressure gradient' (the final state interactions) associated with the spatial asymmetry of the interaction region.
- ✓ **pA (pp) collisions:** the flow is rather a consequence of the angular dependence of the amplitude for dipole scattering.



$$N(\mathbf{b}||\mathbf{r}) > \mathbf{N}(\mathbf{b} \perp \mathbf{r}) \longrightarrow \mathcal{N}_\theta > 0 \longrightarrow v_2 > 0$$

The anisotropy due to the color-dipole orientation mechanism is universal for different processes in dilute-dense scatterings.

There will be the analog of azimuthal anisotropy v_n in DIS and UPC.

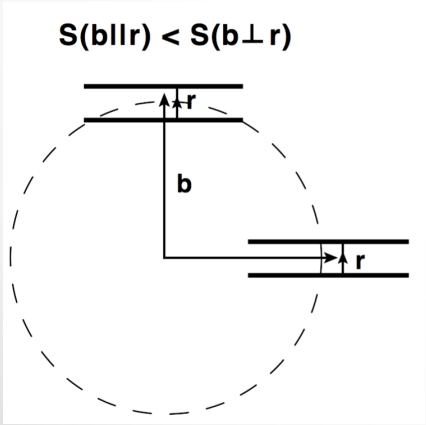
Stay tuned!.



$c_2 > 0$

$c_2 > 0$

$c_2 > 0$



$N(\mathbf{b}||\mathbf{r}) > \mathbf{N}(\mathbf{b} \perp \mathbf{r}) \longrightarrow \mathcal{N}_\theta > 0 \longrightarrow v_2 > 0$

Final remarks:

- *Typical sources of the inhomogeneity:*

1. The target geometry in our scenario (dipole orientation)
It can already be probed by the single inclusive particle spectrum and the effect is NOT suppressed at large N_c. The effect is important for peripheral collisions.

2. Fluctuations in the target gluon distribution (glasma scenario)
Can be probed by 2-particle correlations, and are suppressed at large N_c. The effect is important for central collisions.

Final remarks:

- *Typical sources of the inhomogeneity:*

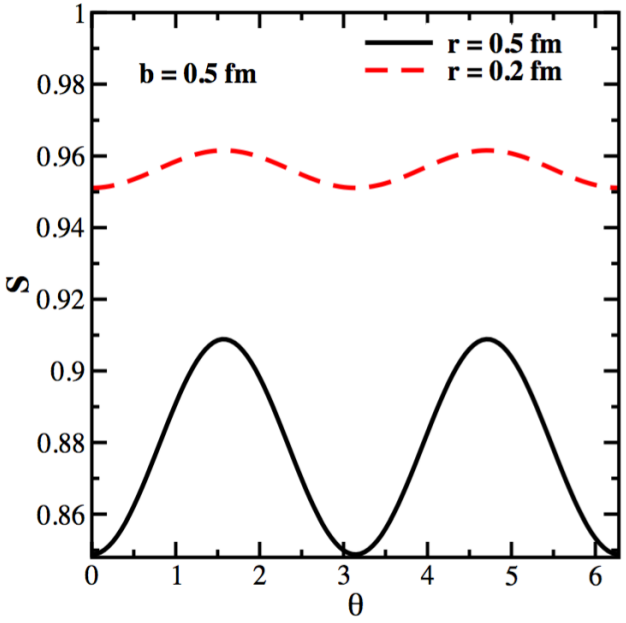
1. The target geometry in our scenario (dipole orientation)
It can already be probed by the single inclusive particle spectrum and the effect is NOT suppressed at large N_c. The effect is important for peripheral collisions.

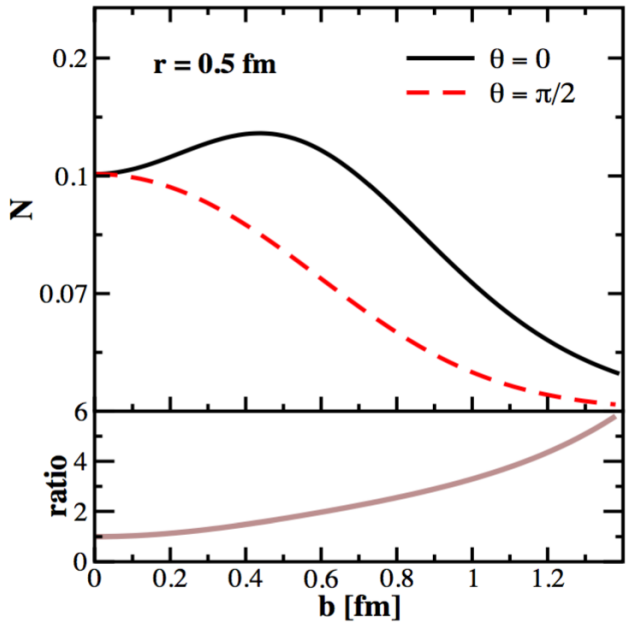
2. Fluctuations in the target gluon distribution (glasma scenario)
Can be probed by 2-particle correlations, and are suppressed at large N_c. The effect is important for central collisions.

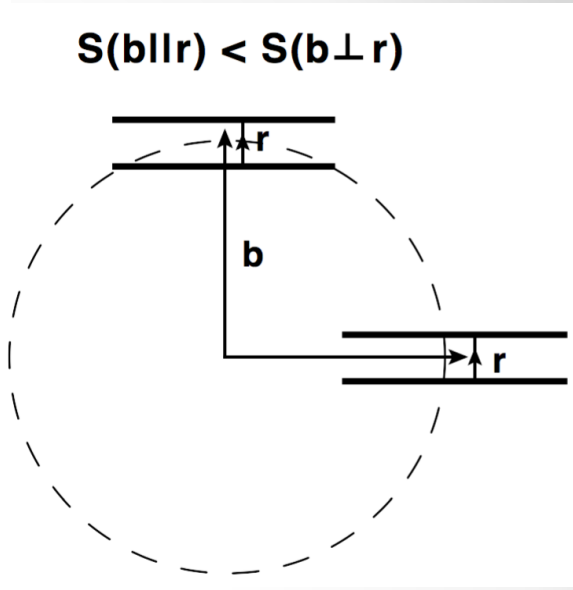
Remains to be studied:
#2 fluctuation can also be probed by the color-dipole orientation.

Backup

$$N_{2g}(b,r,\theta) = \mathcal{N}_0(b,r) + \mathcal{N}_\theta(b,r)\cos(2\theta) \qquad S(\boldsymbol{b},\boldsymbol{r}) = \exp\{-N_{2g}(\boldsymbol{b},\boldsymbol{r})\}$$





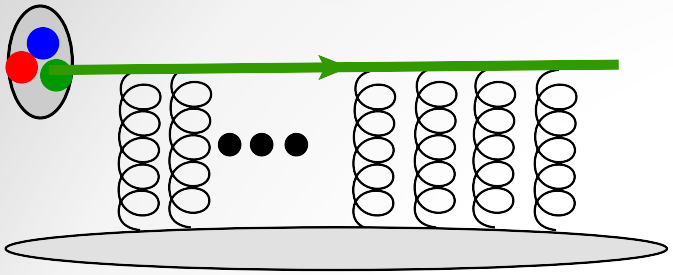


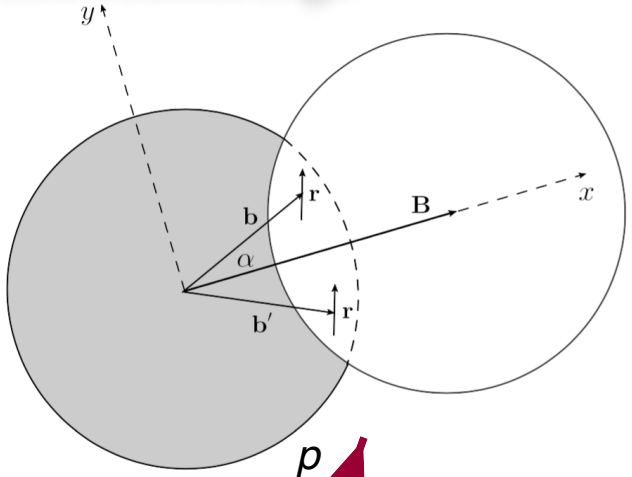
$$N(\mathbf{b}||\mathbf{r}) > \mathbf{N}(\mathbf{b} \perp \mathbf{r})$$
$$\mathcal{N}_\theta > 0 \longrightarrow v_2 > 0$$

Including finite-size effect for the projectile (GPD):

$$v_2(p,B) = \frac{\int b\mathrm{d}b\, \mathrm{e}^{-(b^2+B^2)/4R^2}\, \mathrm{I}_2\left(bB/2R^2\right) \int r\mathrm{d}r\, \mathrm{e}^{-\mathcal{N}_0(b,r)}\, \mathrm{J}_2(pr)\, \mathrm{I}_1\left(\mathcal{N}_\theta(b,r)\right)}{\int b\mathrm{d}b\, \mathrm{e}^{-(b^2+B^2)/4R^2}\, \mathrm{I}_0\left(bB/2R^2\right) \int r\mathrm{d}r\, \mathrm{e}^{-\mathcal{N}_0(b,r)}\, \mathrm{J}_0(pr)\, \mathrm{I}_0\left(\mathcal{N}_\theta(b,r)\right)}.$$

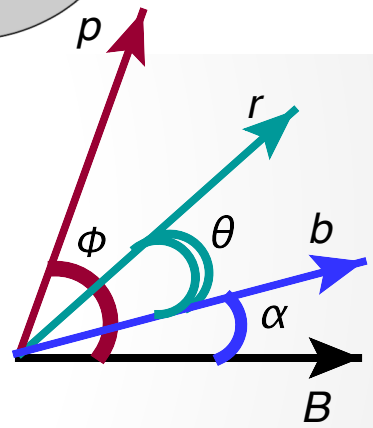
Elliptic flow and eccentricity in dilute-dense scatterings





$$\frac{\mathrm{d}\sigma^q(qA\to qX)}{\mathrm{d}\eta\,\mathrm{d}^2\boldsymbol{p}\,\mathrm{d}^2\boldsymbol{B}}=\frac{1}{(2\pi)^2}\int \mathrm{d}^2\boldsymbol{b}\; x_p q(x_p,\boldsymbol{b}-\boldsymbol{B})\,\tilde{S}(\boldsymbol{b},\boldsymbol{p},x_g)$$

Proton GPD: $x_p q(x_p,\boldsymbol{b})\simeq x_p q(x_p) f(\boldsymbol{b})$, with $\int \mathrm{d}^2\boldsymbol{b}\, f(\boldsymbol{b})=1$



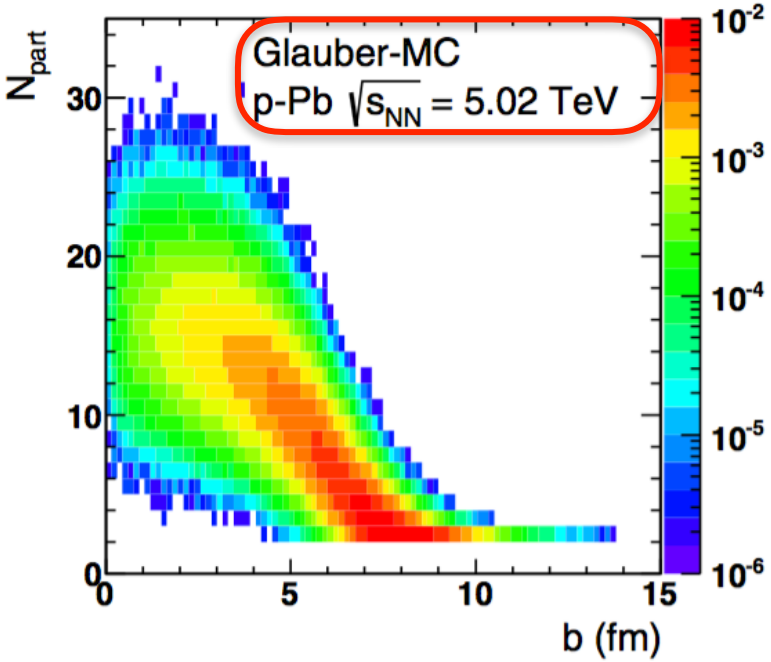
$$\int \frac{\mathrm{d}^2\boldsymbol{p}}{(2\pi)^2}\,\tilde{S}(\boldsymbol{b},\boldsymbol{p})=1 \quad\Longrightarrow\quad \int p\mathrm{d}p\int r\mathrm{d}r\mathrm{d}\theta\,\mathrm{J}_0(pr)\,S(b,r,\theta)=2\pi$$

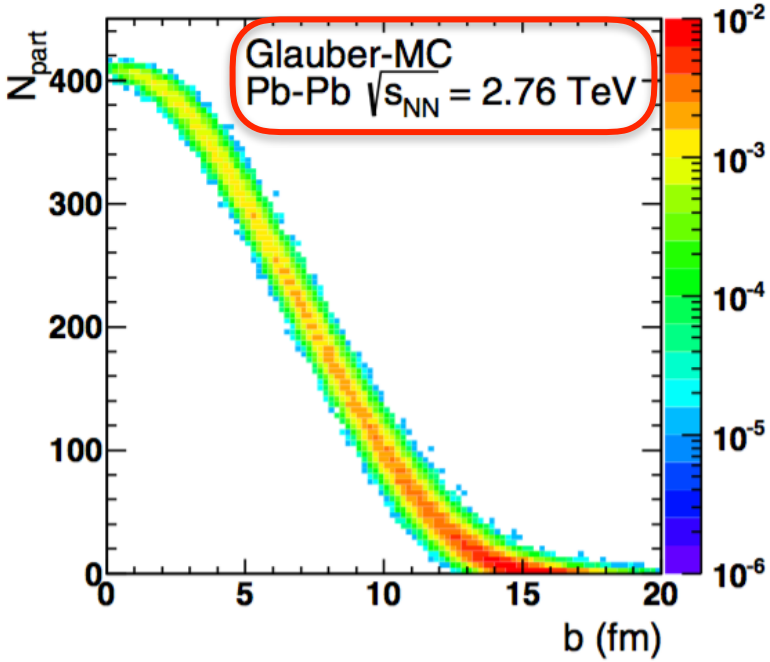
★ **Probability conservation:** **the total probability for the quark to emerge with any momentum must be equal to one.**

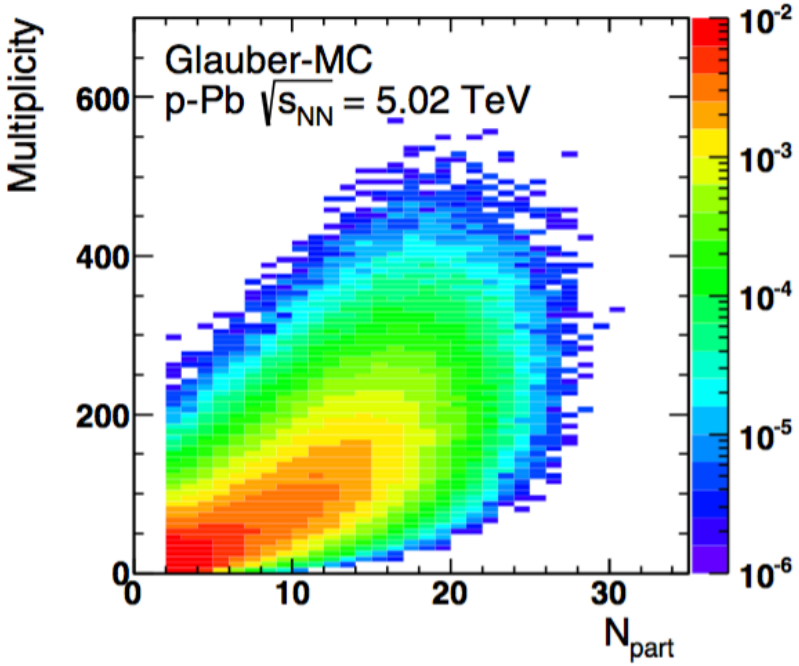
$$\varepsilon_2(B)=\frac{\int b\mathrm{d}b\mathrm{d}\alpha\, b^2\cos(2\alpha)\, f(|\boldsymbol{b}-\boldsymbol{B}|)}{\int b\mathrm{d}b\mathrm{d}\alpha\, b^2\, f(|\boldsymbol{b}-\boldsymbol{B}|)}$$

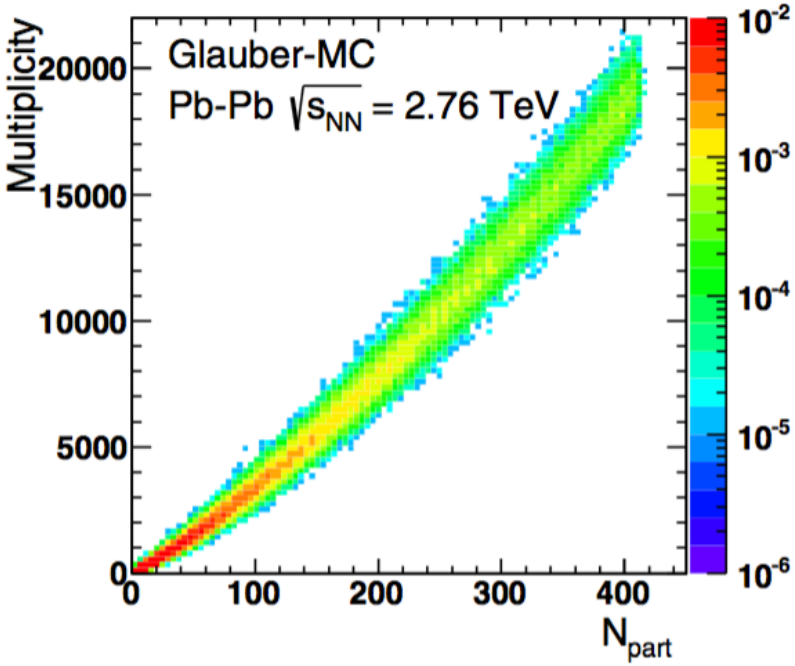
★ **Purely geometrical quantity, without any information about the scattering of the dipole**

$$\epsilon_2(B=0)=0,\ \ \epsilon_2(B\to\infty)=1$$


Glauber-MC
p-Pb $\sqrt{s_{NN}}$ = 5.02 TeV
N_{part}
b (fm)

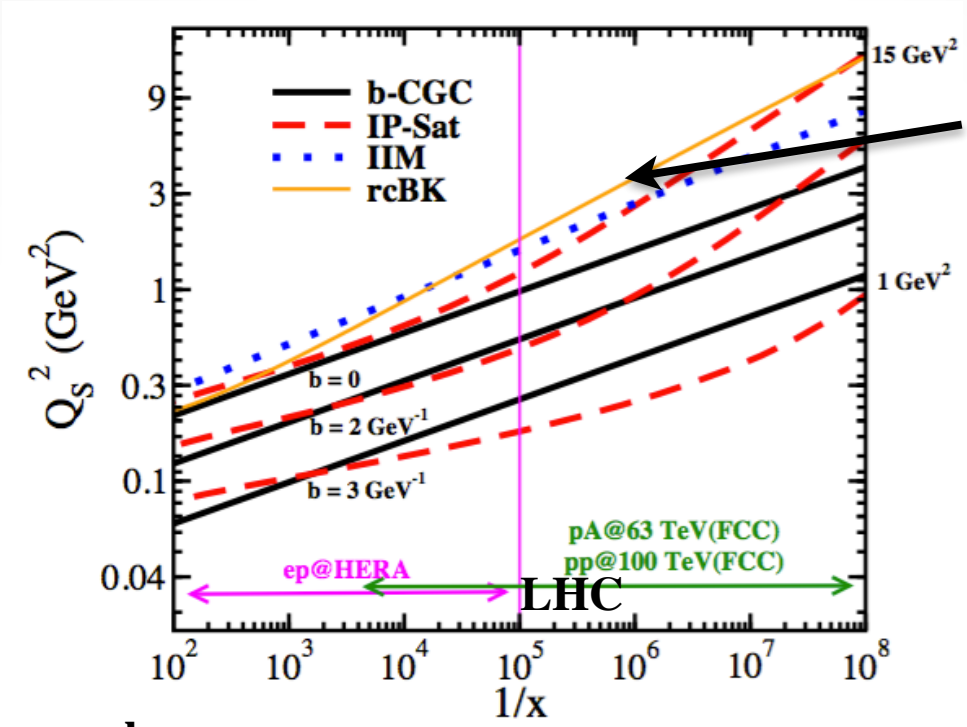

Glauber-MC
Pb-Pb $\sqrt{s_{NN}}$ = 2.76 TeV
N_{part}
b (fm)


Glauber-MC
p-Pb $\sqrt{s_{NN}}$ = 5.02 TeV
Multiplicity
N_{part}


Glauber-MC
Pb-Pb $\sqrt{s_{NN}}$ = 2.76 TeV
Multiplicity
N_{part}

b-dependence of Saturation scale & applicability of the CGC

Rezaeian and Schmidt, arXiv:1307.0825



- **b-independent saturation models significantly overestimate Q_s.**

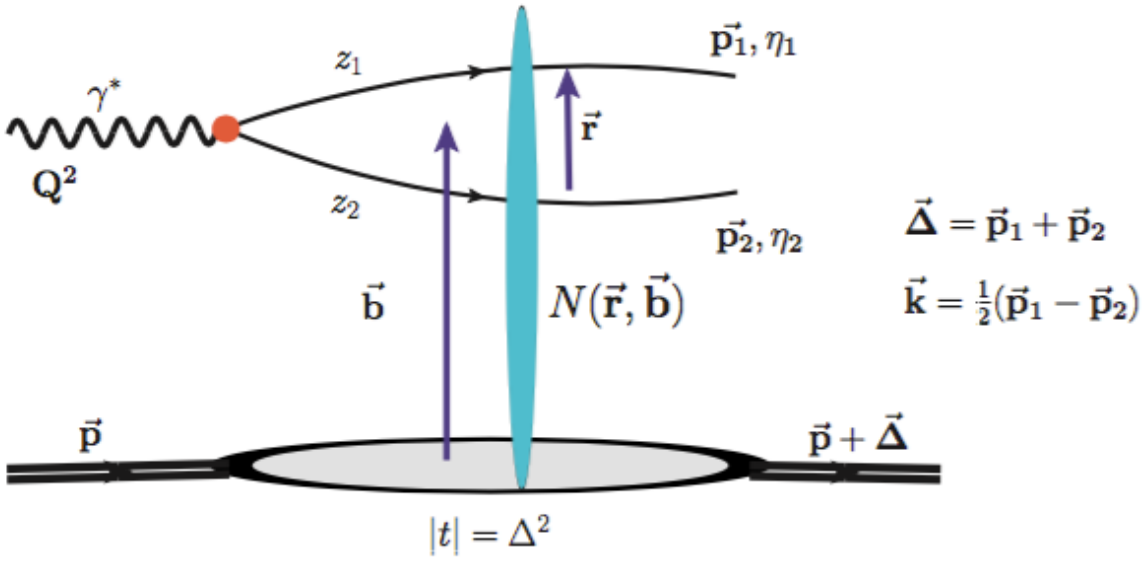
- **Proton saturation scale:**

$$\text{HERA} : Q_s < 1\,\text{GeV}$$
$$\text{LHC} : Q_s \leq 1 - 2\,\text{GeV}$$
$$\text{FCC} : Q_s \leq 2 - 4\,\text{GeV}$$

- **Nuclear saturation scale:** $Q_{sA}^2 \approx A^{1/3} Q_s^2 \approx 6\, Q_s^2$

$$\text{EIC} : Q_{sA} < 2.5\,\text{GeV}$$

Diffractive Dijet production in the CGC: $\gamma^* + p(A) \to q\bar{q} + p(A)$



$$\sigma = \psi^{\gamma}_{q\bar{q}} \otimes \mathcal{N}(\vec{r}, \vec{b}) \otimes \mathcal{N}(\vec{r'}, \vec{b'}) \neq \psi^{\gamma}_{q\bar{q}} \otimes [\mathcal{N}(r, b)]^2$$

$$\left(\frac{d\sigma_{\mathrm{T}}^{\mathrm{dijet}}}{dz_1 dz_2 d^2\mathbf{p}_1 d^2\mathbf{p}_2} \right) = (2\pi)^2 \delta(z_1 + z_2 - 1) N_c \alpha_{em} \sum_f e_f^2 \int \frac{d^2\mathbf{r}}{(2\pi)^2} \int \frac{d^2\mathbf{r}'}{(2\pi)^2} \int \frac{d^2\mathbf{b}}{(2\pi)^2} \int \frac{d^2\mathbf{b}'}{(2\pi)^2}$$

$$\times \, \mathbf{e}^{-\mathbf{i}(\mathbf{b}-\mathbf{b}')\cdot(\mathbf{p}_1+\mathbf{p}_2)} \mathbf{e}^{-\mathbf{i}(\mathbf{r}-\mathbf{r}')\cdot(\mathbf{p}_1-\mathbf{p}_2)/2} \mathcal{N}(\mathbf{r}, \mathbf{b}) \, \mathcal{N}(\mathbf{r}', \mathbf{b}') \, 2[z_1^2 + z_2^2] \, \frac{\mathbf{r}\cdot\mathbf{r}'}{\mathbf{r}^2\mathbf{r}'^2} \, [\varepsilon|\mathbf{r}|K_1(\varepsilon|\mathbf{r}|)] \, \left[\varepsilon|\mathbf{r}'|K_1(\varepsilon|\mathbf{r}'|)\right]$$

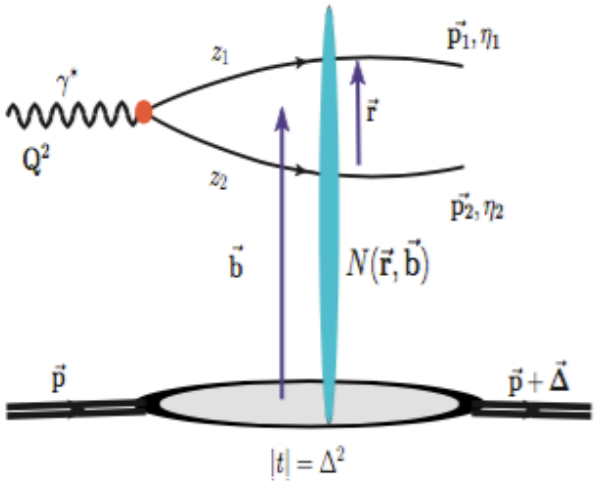
- **Diffractive dijet production is a sensitive probe of the color-dipole orientation.**

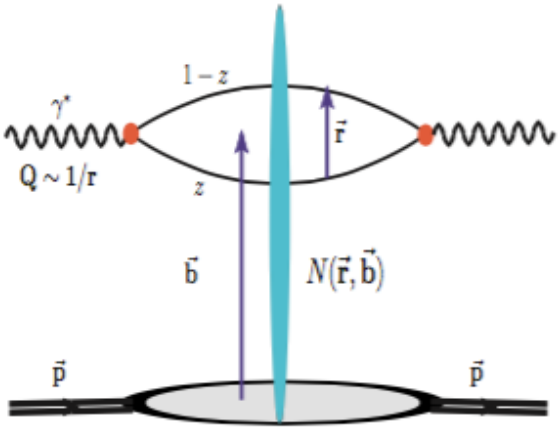
Diffractive dijet v. inclusive dijet in UPC & DIS

Diffractive (averaging over color at amplitude level): $\sigma \propto |\langle \mathcal{M} \rangle_\rho|^2$

Inclusive (averaging over color at cross-section level): $\sigma \propto \langle |\mathcal{M}|^2 \rangle_\rho$

Dominguez, Marquet, Xiao, Yuan, arXiv:1101.0715





Altinoluk, Armesto, Beuf, Rezaeian, arXiv:1511.07452

$$\sigma^{\text{Diffractive dijet}} \propto \psi^{\gamma}_{q\bar{q}} \otimes \mathcal{N}(\vec{r}, \vec{b}) \otimes \mathcal{N}(\vec{r'}, \vec{b'}) \neq \psi^{\gamma}_{q\bar{q}} \otimes [\mathcal{N}(r, b)]^2$$

$$\sigma^{\text{Inclusive dijet}} \propto \psi^{\gamma}_{q\bar{q}} \otimes [\mathcal{N}(\vec{r}, \vec{b}) + S^{\text{Quadrupole}}(\vec{r}, \vec{r\prime}, \vec{b}, \vec{b'})]$$

$$\sigma^{\text{Inclusive DIS}} \propto \psi^{\gamma}_{q\bar{q}} \otimes \mathcal{N}(\vec{r}, \vec{b})$$

- In contrast to inclusive dijet production, diffractive dijet production only depends on the dipole amplitude (not WW gluon distribution) at LO.

Diffractive dijet production as a probe of color-dipole orientation

Inspired by "saturation domain" picture of Kovner & Lublinsky (2011)

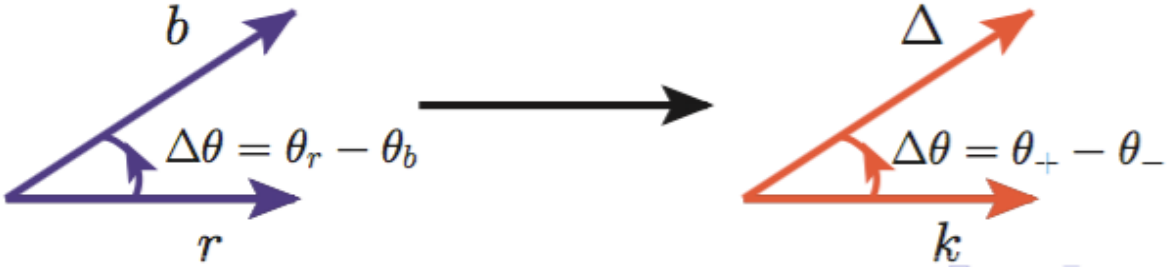
$$\mathcal{N}(\mathbf{r},\mathbf{b}) = \mathcal{N}(r,b,\theta_r-\theta_b) = 1 - e^{-\frac{Q_s^2(b)}{4} r^2 \left(1+\mathbf{A}\cos^2(\theta_r-\theta_b)\right)}$$

θ_r, θ_b are the angles of vectors $\vec{r}$, $\vec{b}$ with respect to a reference vector, respectively. Assuming $Q_s^2 r^2 A/4 \ll 1$:

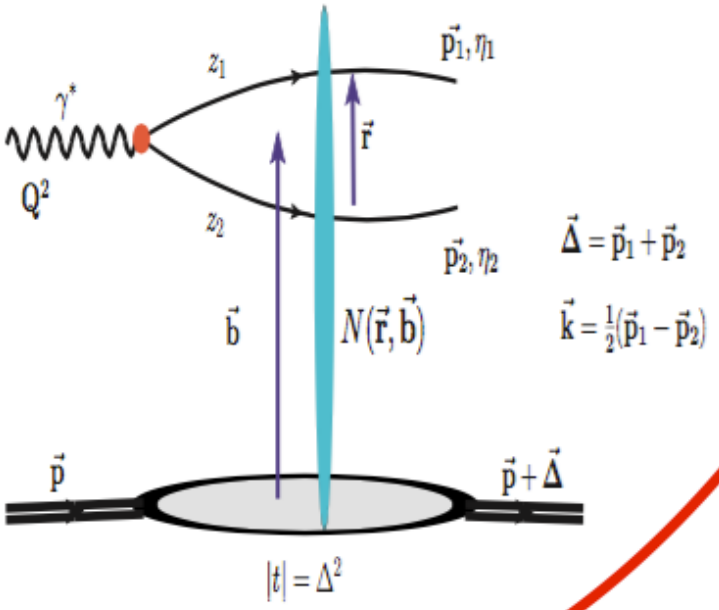
$$\int \frac{d^2\mathbf{r}}{(2\pi)^2} \int \frac{d^2\mathbf{b}}{(2\pi)^2} e^{-i\mathbf{b}\cdot(\mathbf{p}_0+\mathbf{p}_1)} e^{-i\mathbf{r}\cdot(\mathbf{p}_0-\mathbf{p}_1)/2} \mathcal{N}(\mathbf{r},\mathbf{b}) K_0(\varepsilon|\mathbf{r}|) \simeq \int_0^{+\infty} \frac{dr}{2\pi} r \int_0^{+\infty} \frac{db}{2\pi} b\, J_0\left(b|\mathbf{p}_0+\mathbf{p}_1|\right)$$
$$\times \; J_0\left(r\frac{|\mathbf{p}_0-\mathbf{p}_1|}{2}\right) \mathcal{N}(r,b,\theta_- - \theta_+) K_0(\varepsilon r)$$

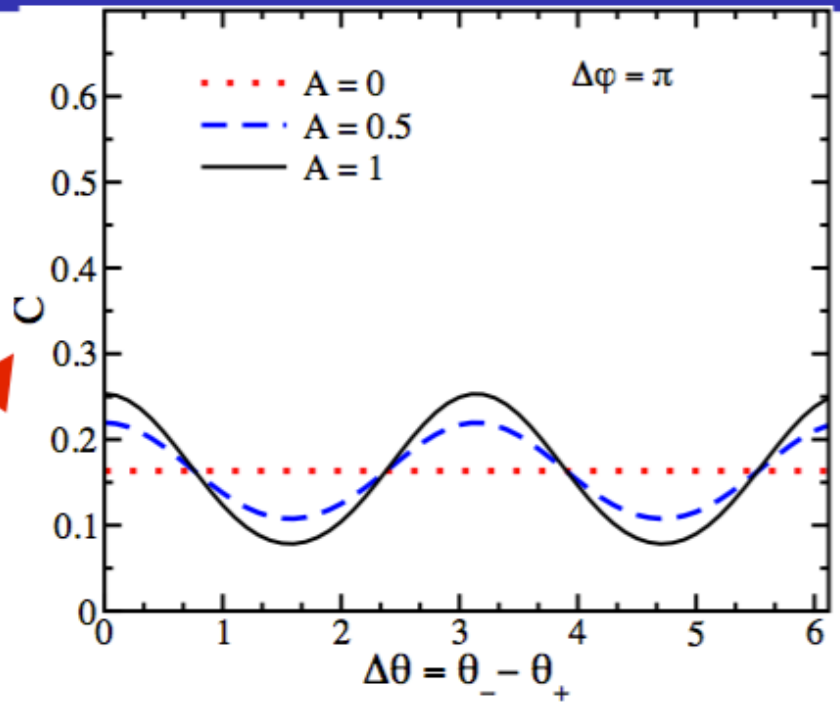
θ_+, θ_- denote the angles of vectors $\vec{\Delta} = \vec{p}_0 + \vec{p}_1$ and $\vec{k} = \frac{1}{2}(\vec{p}_0 - \vec{p}_1)$ with respect to a reference vector, respectively.

- **A nonzero A corresponding to the existence of $\vec{r} - \vec{b}$ correlations in the color dipole amplitude, induces azimuthal correlations between $\vec{\Delta}$ and $\vec{k}$.**



Diffractive dijet production as a probe of color-dipole orientation

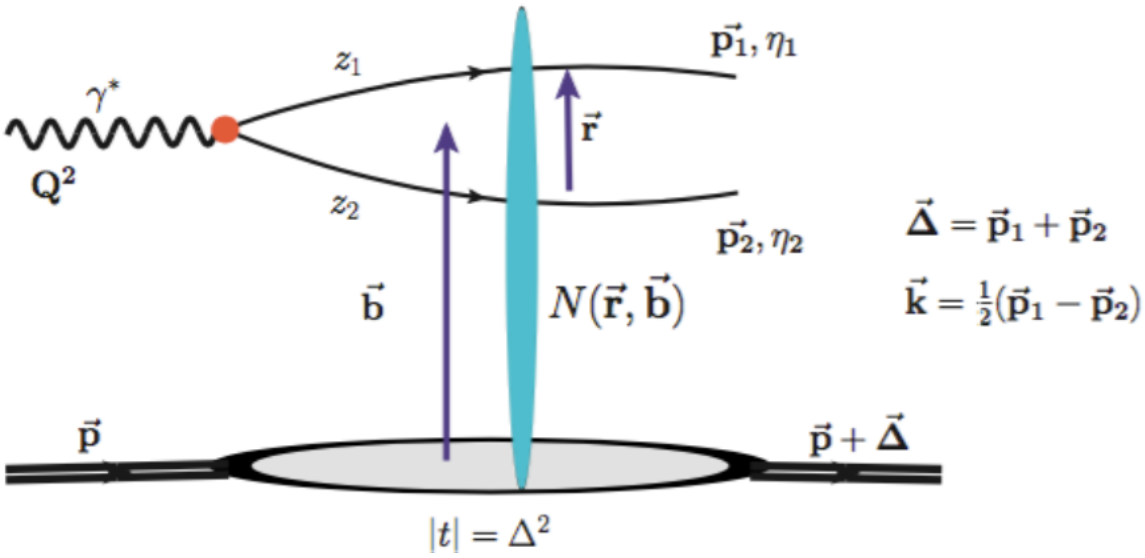




$$C(\Delta\theta) = \frac{d\sigma^{\gamma^* p \to q\bar{q}p}}{d\mathbf{p}_0\, \mathbf{p}_1 d\Delta\theta} \Big/ \int_0^{2\pi} d\Delta\theta \frac{d\sigma^{\gamma^* p \to q\bar{q}p}}{d\mathbf{p}_0\, \mathbf{p}_1 d\Delta\theta}$$

- **A nonzero A corresponding to the existence of $\vec{r} - \vec{b}$ correlations in the color dipole amplitude, induces sizeable azimuthal correlations for dijet between $\vec{\Delta}$ and $\vec{k}$.**

Main conclusion: Small-x gluon tomography in diffractive dijet in UPC



- **Correlations between $\vec{p}_1$, $\vec{p}_2$ probe the effective dipole size $r \approx 1/Q_s(b)$.**
- **Correlation between $\vec{k}, \vec{\Delta}$ probe the color-dipole orientation and correlations between $\vec{r}, \vec{b}$.**
- **t-distribution of the diffractive dijet photo-production probes the inhomogeneity of the target.**

Altinoluk, Armesto, Beuf, and Rezaeian, PLB 758 (2016) 373.
Hatta, Xiao and Yuan, PRL 116 (2016) 202301.

Probing the BFKL dynamics at hadronic colliders

Christophe Royon
University of Kansas, Lawrence, USA

RBRC Workshop, BNL, April 26- 28 2017

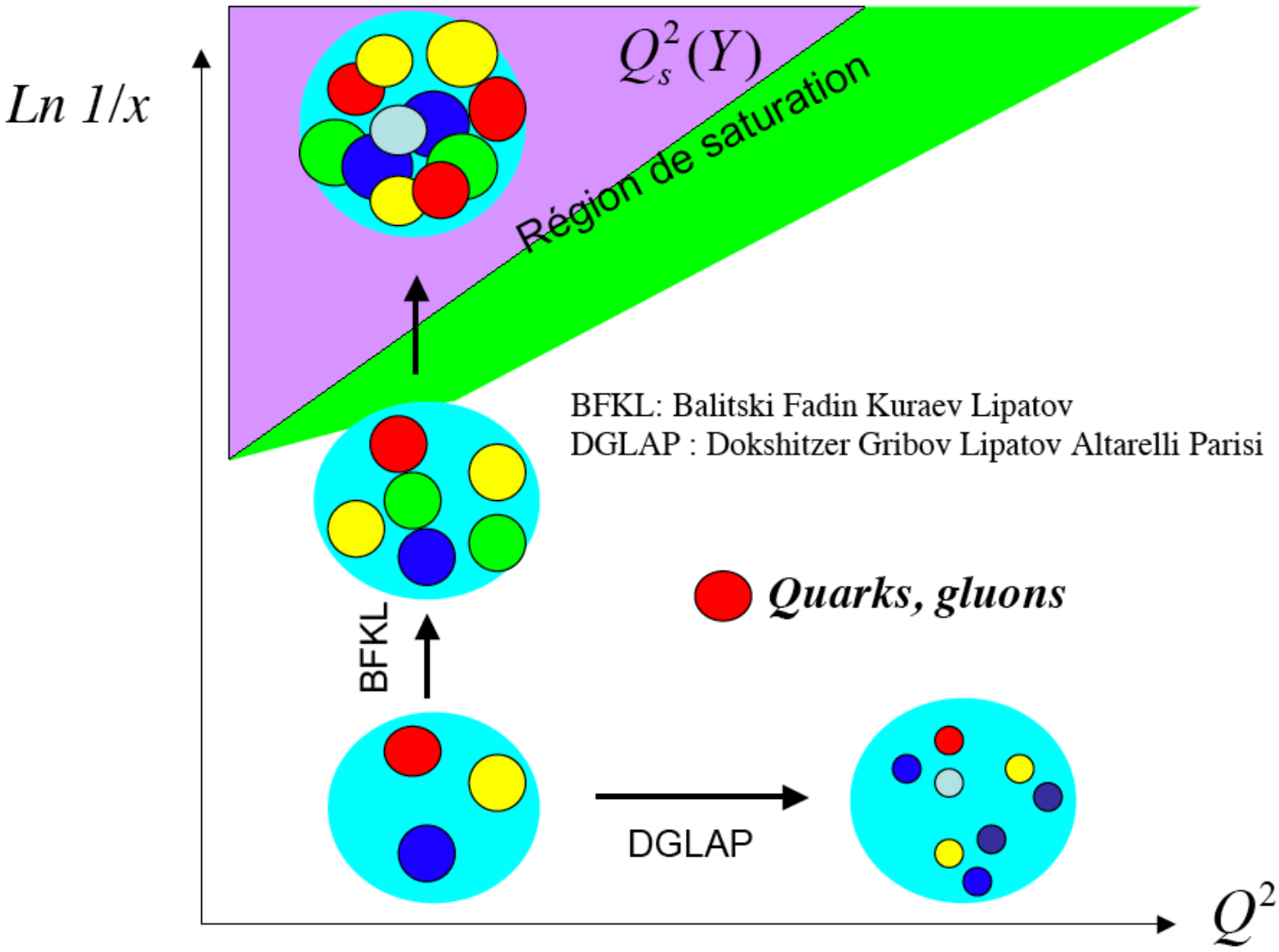
Contents:

- Forward jets at HERA (short reminder)
- Mueller Navelet jet
- Jet veto (atlas measurement)
- Jet gap jet at Tevatron, LHC
- Jet gap jet in diffraction at the LHC

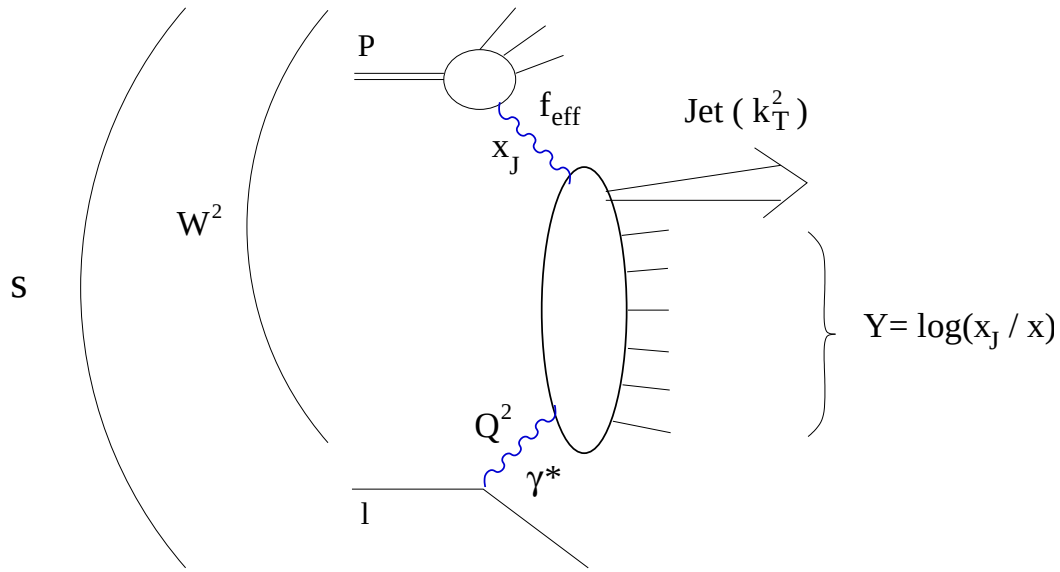
Work done in collaboration with D. Werder, O. Kepka, C. Marquet, R. Peschanski, M. Trzebinski, Y. Hatta, G. Soyez, T. Ueda, R. Zlebcik,...
Work in progress with D. Colferai, F. Deganutti, T. Raben, S. Schlichting

Looking for BFKL/saturation effects

Looking for BFKL effects (x-resummation) at HERA/LHC in dedicated final states



Forward jet measurement at HERA

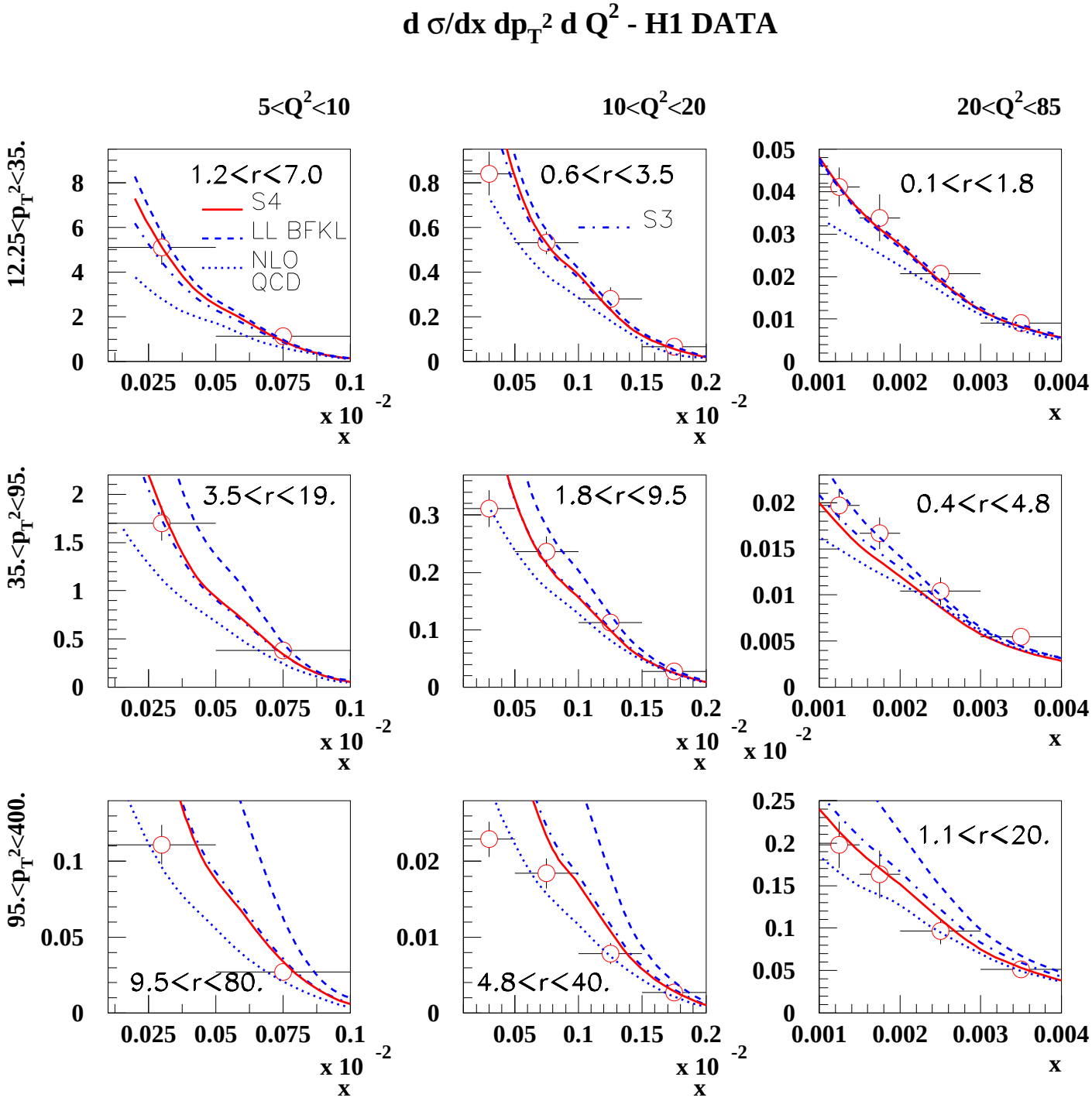


- Full BFKL NLL calculation used for the BFKL kernel, available in S3 and S4 resummation schemes to remove the spurious singularities (modulo the impact factors taken at LL)
- Equation:

$$\frac{d\sigma_{T,L}^{\gamma^* p \to JX}}{dx_J dk_T^2} = \frac{\alpha_s(k_T^2)\alpha_s(Q^2)}{k_T^2 Q^2} \; f_{eff}(x_J, k_T^2)$$
$$\int \frac{d\gamma}{2i\pi} \left(\frac{Q^2}{k_T^2}\right)^{\gamma} \phi_{T,L}^{\gamma}(\gamma) \; e^{\bar{\alpha}(k_T Q)\chi_{eff}[\gamma, \bar{\alpha}(k_T Q)]Y}$$

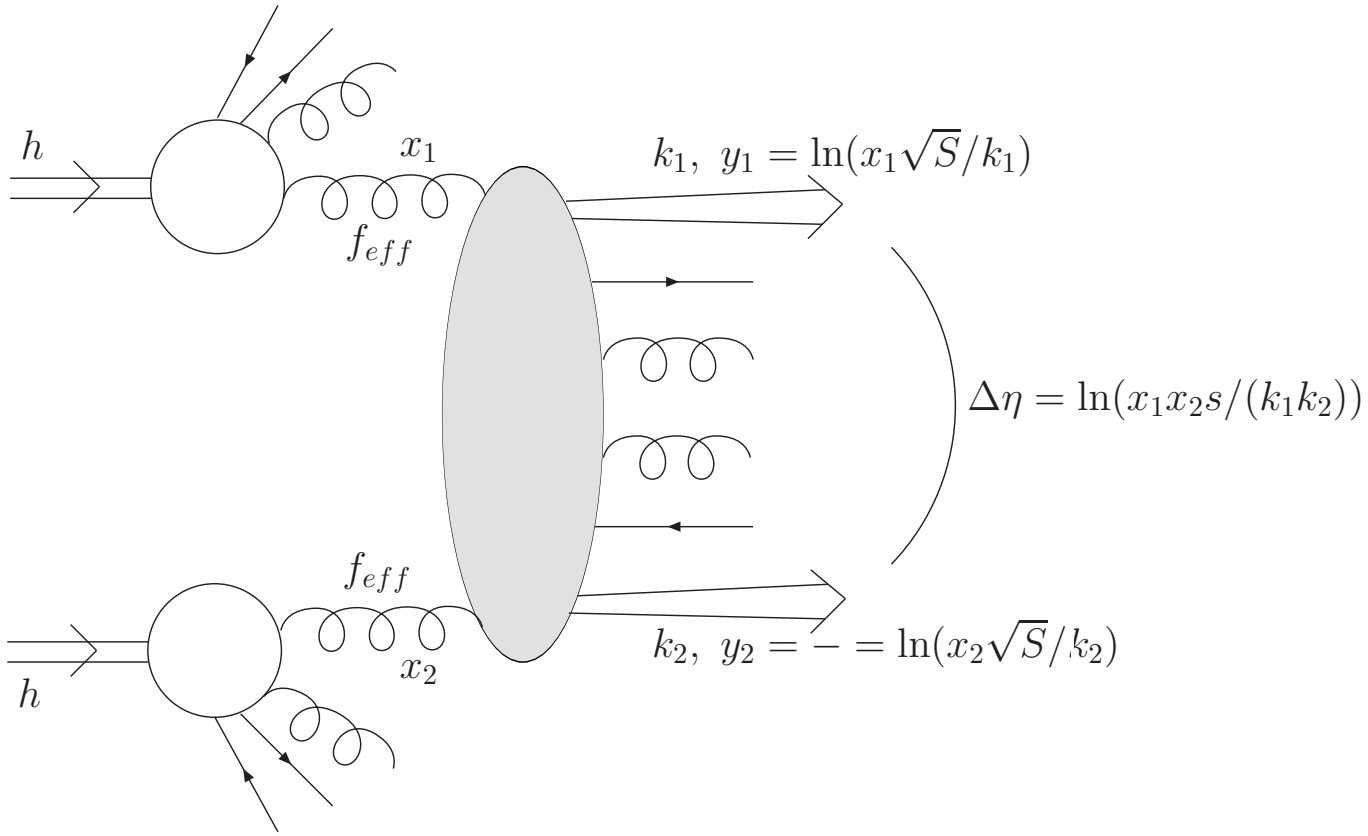
- Implicit equation: $\chi_{eff}(\gamma, \alpha) = \chi_{NLL}(\gamma, \alpha, \chi_{eff}(\gamma, \alpha))$ solved numerically (Nucl. Phys. B 739 (2006) 131; Phys. Lett. B 655 (2007) 236; Eur. Phys. J. C55 (2008) 259)

Comparison with H1 triple differential data



Mueller Navelet jets

Same kind of processes at the Tevatron and the LHC



- Same kind of processes at the Tevatron and the LHC: Mueller Navelet jets
- Study the $\Delta\Phi$ between jets dependence of the cross section:
- See papers by Papa, Murdaca, Wallon, Szymanowski, Ducloue, Sabio-Vera, Chachamis...

Mueller Navelet jets: $\Delta\Phi$ dependence

- Study the $\Delta\Phi$ dependence of the relative cross section
- Relevant variables:

$$\begin{aligned} \Delta\eta &= y_1 - y_2 \\ y &= (y_1 + y_2)/2 \\ Q &= \sqrt{k_1 k_2} \\ R &= k_2/k_1 \end{aligned}$$

- Azimuthal correlation of dijets:

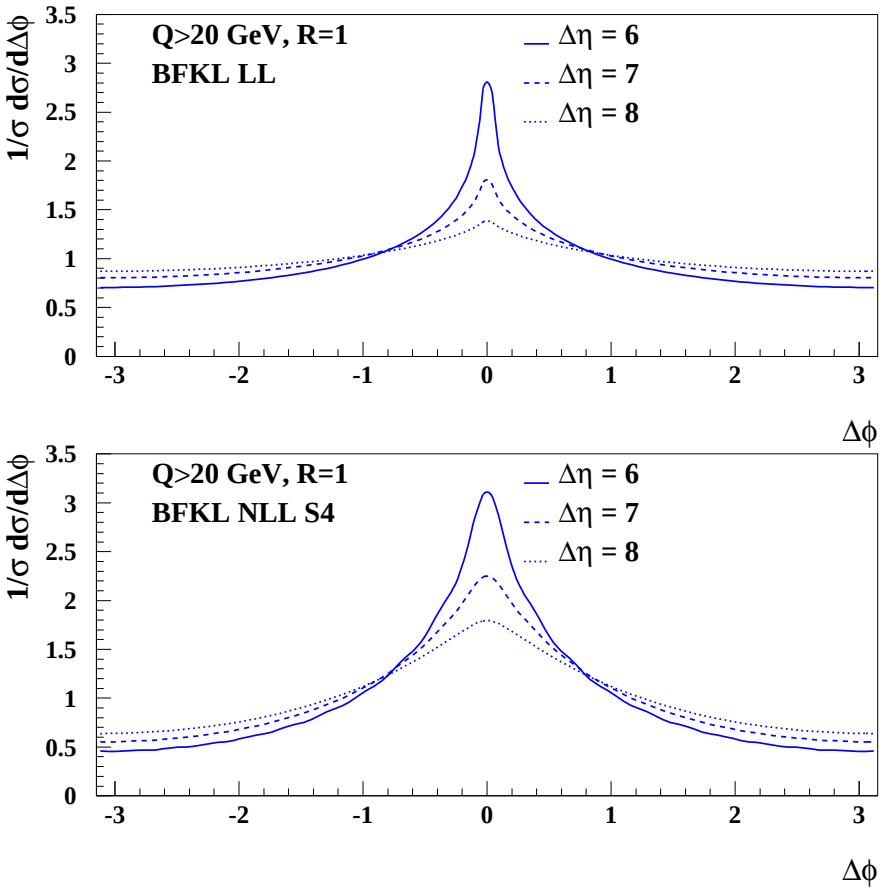
$$2\pi \frac{d\sigma}{d\Delta\eta dR d\Delta\Phi} \Big/ \frac{d\sigma}{d\Delta\eta dR} = 1 + \frac{2}{\sigma_0(\Delta\eta, R)} \sum_{p=1}^{\infty} \sigma_p(\Delta\eta, R) \cos(p\Delta\Phi)$$

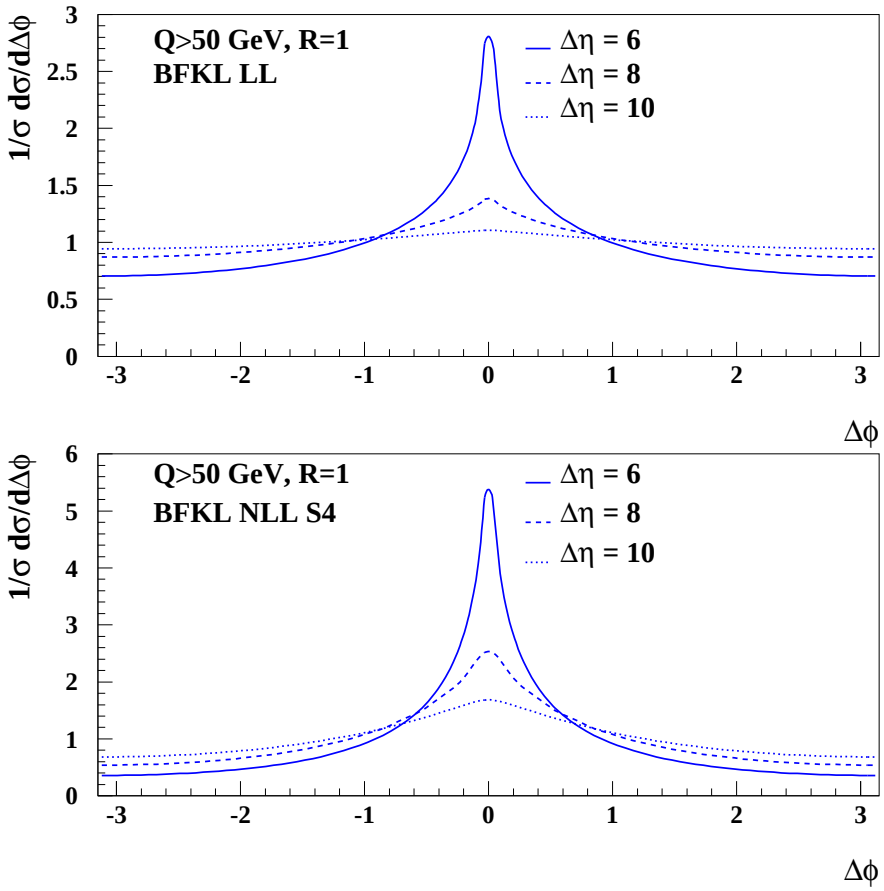
where

$$\sigma_p = \int_{E_T}^{\infty} \frac{dQ}{Q^3} \alpha_s(Q^2/R)\alpha_s(Q^2 R) \left(\int_{y_<}^{y_>} dy x_1 f_{eff}(x_1, Q^2/R) x_2 f_{eff}(x_2, Q^2 R) \right) \int_{1/2-\infty}^{1/2+\infty} \frac{d\gamma}{2i\pi} R^{-2\gamma} \; e^{\bar{\alpha}(Q^2)\chi_{eff}(p)\Delta\eta}$$

Mueller Navelet jets: $\Delta\Phi$ dependence

- $1/\sigma d\sigma/d\Delta\Phi$ spectrum for BFKL LL and BFKL NLL as a function of $\Delta\Phi$ for different values of $\Delta\eta$, scale dependence: $\sim$20%





- C. Marquet, C.R., Phys. Rev. D79 (2009) 034028
- Mueller Navelet jets at NLL and saturation effects: Study in progress with F. Deganutti, T. Raben, S. Schlichtling

Effect of energy conservation on BFKL equation

- BFKL cross section lacks energy-momentum conservation since these effects are higher order corrections
- Following Del Duca-Schmidt, we substitute $\Delta\eta$ by an effective rapidity interval y_{eff}

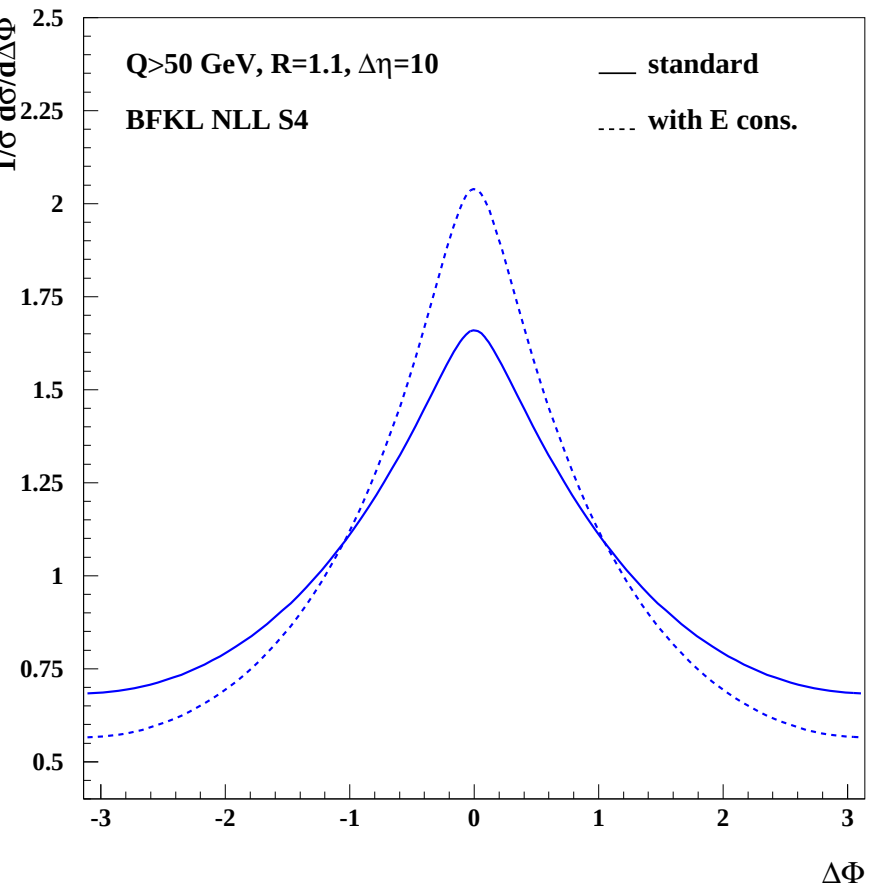
$$y_{eff} = \Delta\eta \left(\int d\phi \cos(p\phi) \frac{d\sigma^{O(\alpha_s^3)}}{d\Delta\eta dy dQ dR d\Delta\Phi} \right) \left(\int d\phi \cos(p\phi) \frac{d\sigma^{LL-BFKL}}{d\Delta\eta dy dQ dR d\Delta\Phi} \right)^{-1}$$

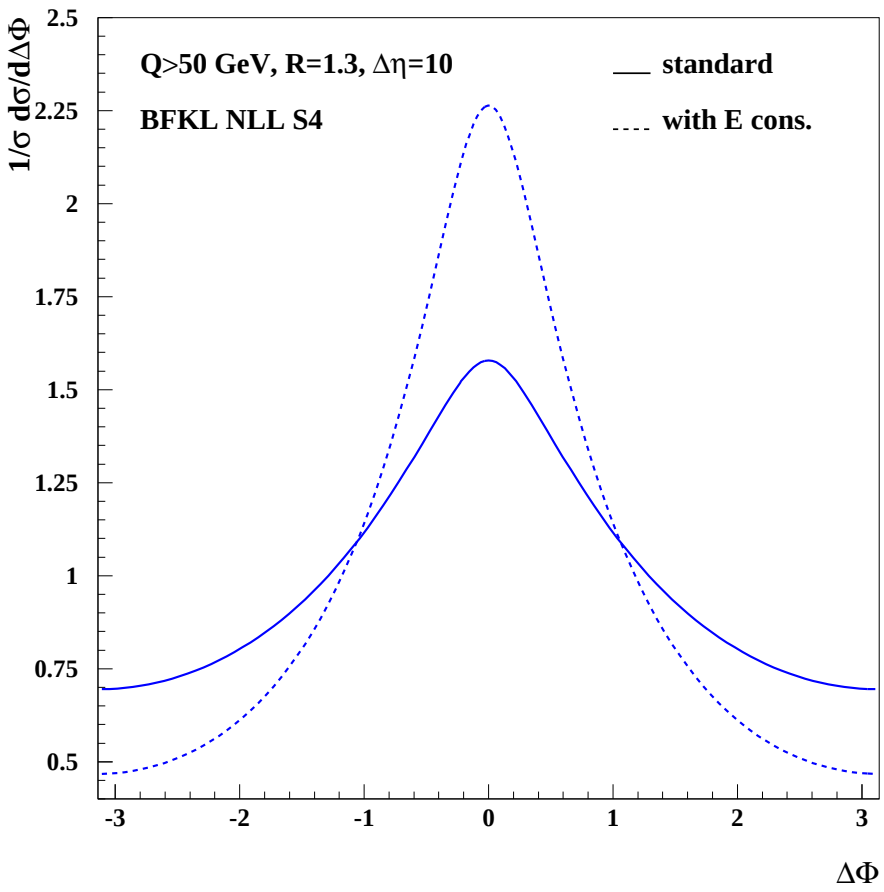
where $d\sigma^{O(\alpha_s^3)}$ is the exact $2 \to 3$ contribution to the $hh \to JXJ$ cross-section at order α_s^3, and $d\sigma^{LL-BFKL}$ is the LL-BFKL result

- To compute $d\sigma^{O(\alpha_s^3)}$, we use the standard jet cone size $R_{cut} = 0.5$ when integrating over the third particle's momentum

Mueller Navelet cross sections: energy conservation effect in BFKL

- Effect of energy conservation on BFKL dynamics
- Large effect if jet p_T ratios not close to 1: goes closer to DGLAP predictions, needs jet p_T ratio $<$ 1.1-1.15





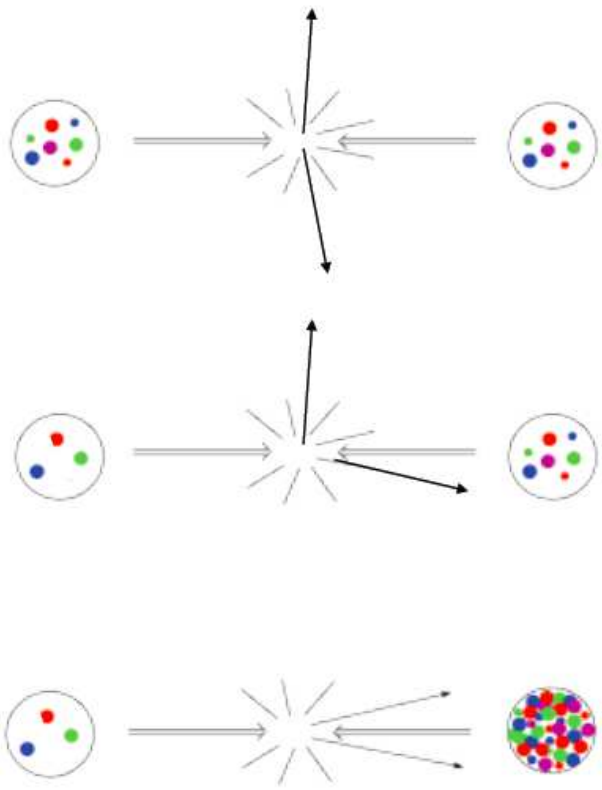
Saturation effects at the LHC: Use pA data

- Saturation effects: need to go to low x, jets as forward as possible on the same side
- Compare pp and pA runs in order to remove many systematics

final state : $k_1, y_1 \qquad k_2, y_2$

$$x_p = \frac{k_1 e^{y_1} + k_2 e^{y_2}}{\sqrt{s}} \qquad x_A = \frac{k_1 e^{-y_1} + k_2 e^{-y_2}}{\sqrt{s}}$$

scanning the wave functions:



$x_p \sim x_A < 1$

central rapidities probe moderate x

x_p increases | x_A ~ unchanged

$x_p \sim 1, x_A < 1$

forward/central doesn't probe much smaller x

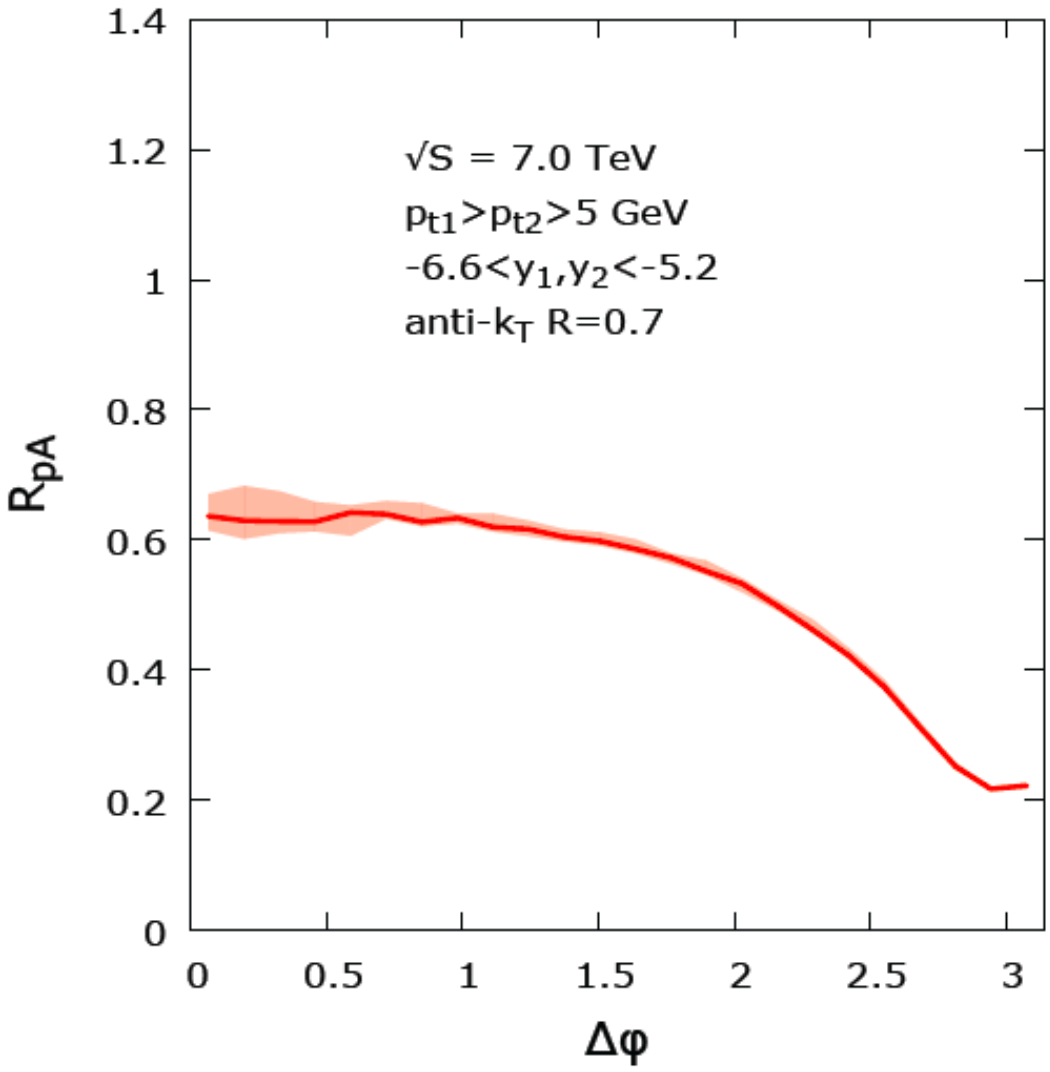
x_p ~ unchanged | x_A decreases

$x_p \sim 1, x_A << 1$

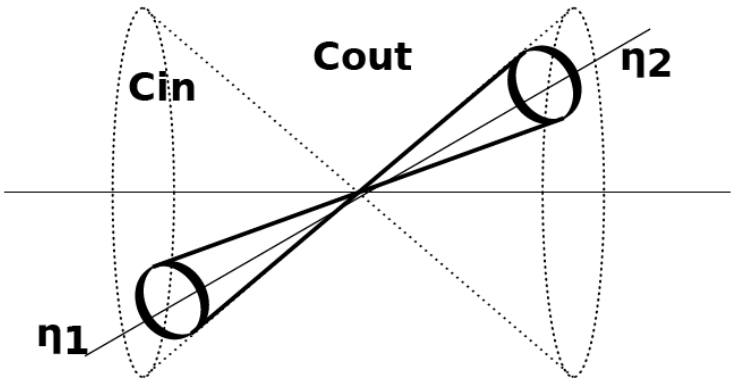
forward rapidities probe small x

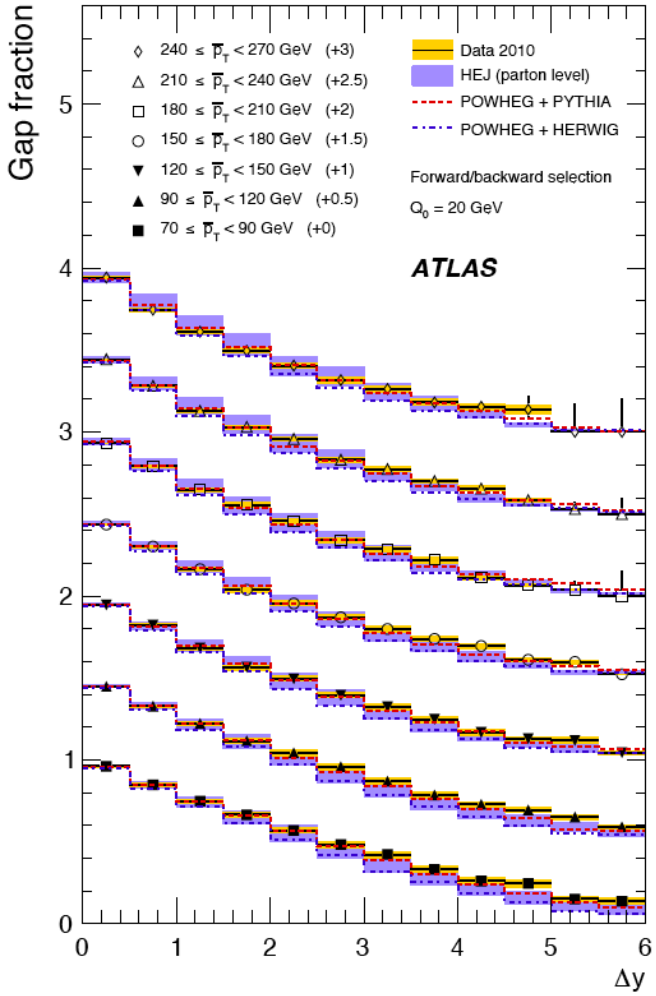
Saturation effects at the LHC

- Suppression factor between pp and pA runs: estimated to be $1/2$ in CASTOR acceptance
- Important to get CASTOR in pA and low lumi pp data
- Study performed by Cyrille Marquet et al.



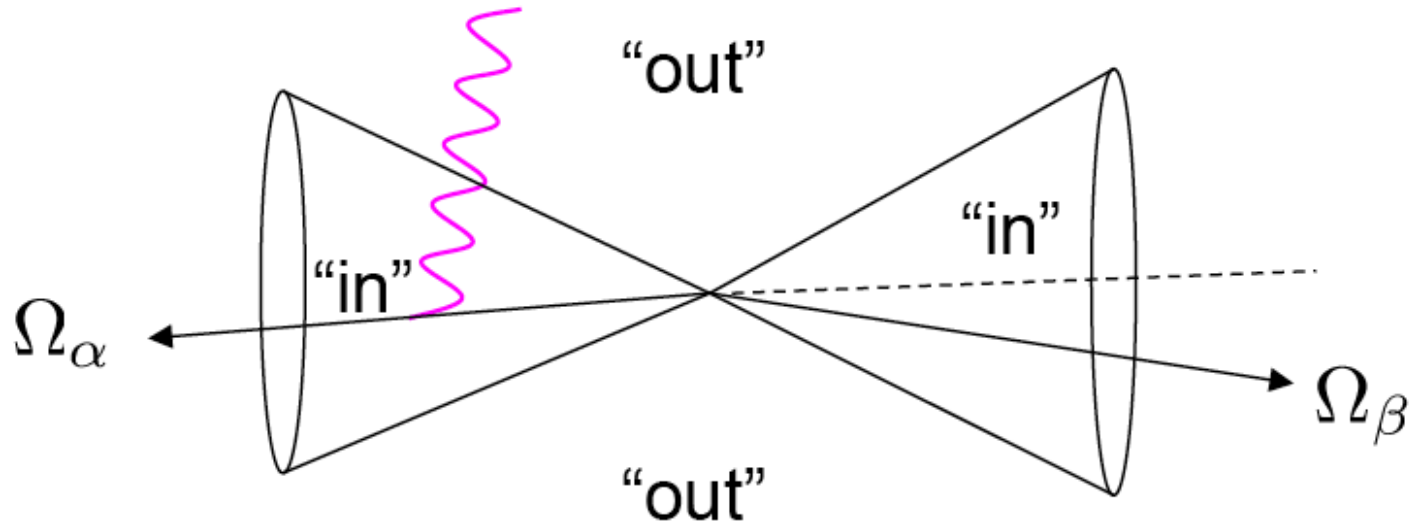
One aside: ATLAS "jet veto" measurement: sign of BFKL?





- Select events with two high p_T jets, well separated in rapidity by Δy
- Veto on additional jet activity (with $k_T > Q_0$, with $Q_0 \gg \Lambda_{QCD}$) between the two jets
- Measure the "gap" fraction: dijet events with veto/total dijet events
- Y.Hatta, C. Marquet, C. Royon, G. Soyez, T. Ueda, D. Werder: Phys.Rev. D87 (2013) 054016

Banfi Marchesini Smye equation



- Compute the probability P_T that the total energy emitted outside the jet cone is less than E_{out}

$$\partial_\tau P_\tau(\Omega_\alpha,\Omega_\beta) = -\int_{C_{out}} \frac{d^2\Omega_\gamma}{4\pi} \frac{1-\cos\theta_{\alpha\beta}}{(1-\cos\theta_{\alpha\gamma})(1-\cos\theta_{\gamma\beta})} P_\tau(\Omega_\alpha,\Omega_\beta)$$
$$+\int_{C_{in}} \frac{d^2\Omega_\gamma}{4\pi} \frac{1-\cos\theta_{\alpha\beta}}{(1-\cos\theta_{\alpha\gamma})(1-\cos\theta_{\gamma\beta})} \Big(P_\tau(\Omega_\alpha,\Omega_\gamma)P_\tau(\Omega_\gamma,\Omega_\beta) - P_\tau(\Omega_\alpha,\Omega_\beta)\Big)$$

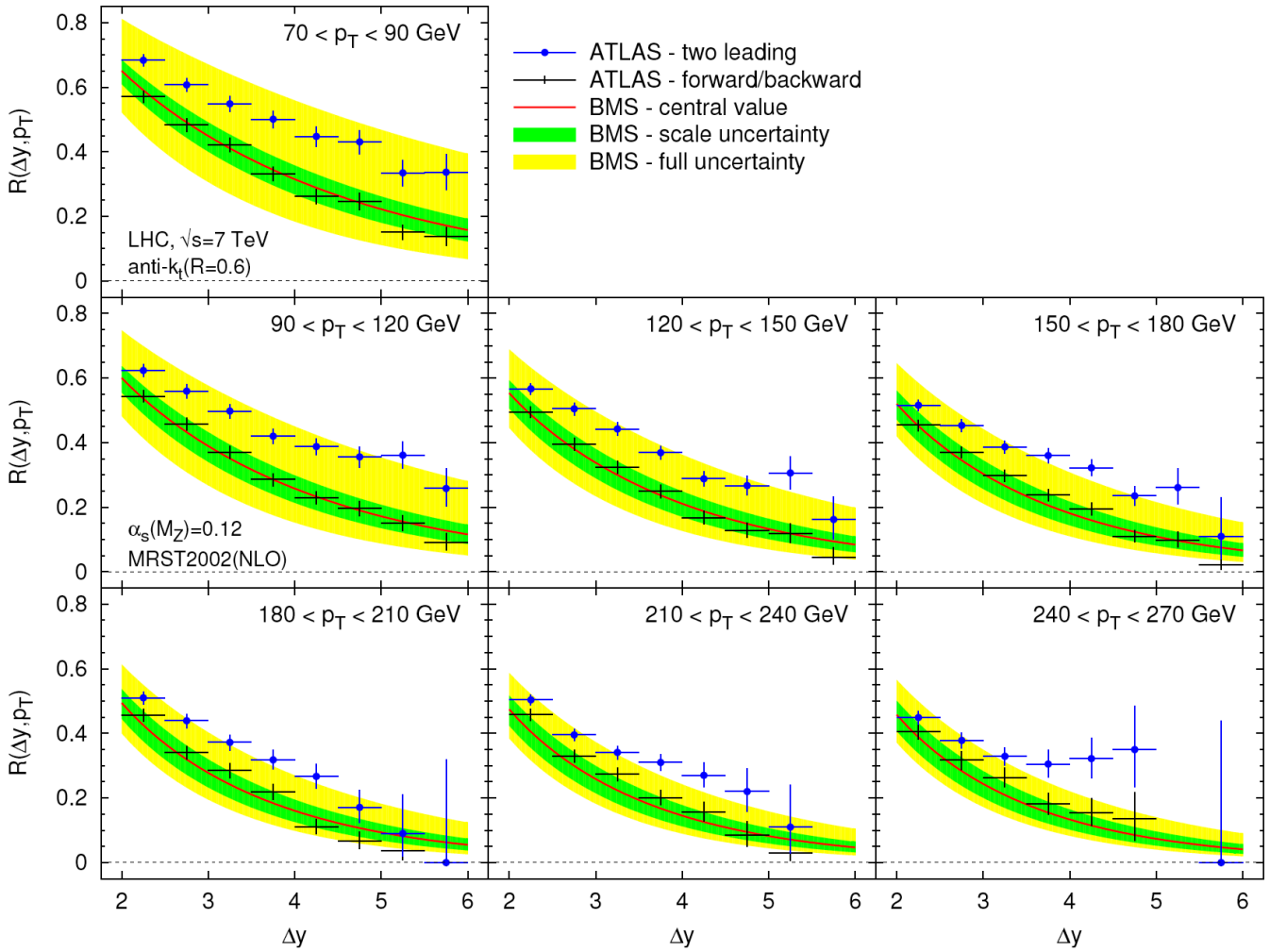
Sudakov logs

non-global logs

differential probability for the soft gluon emission

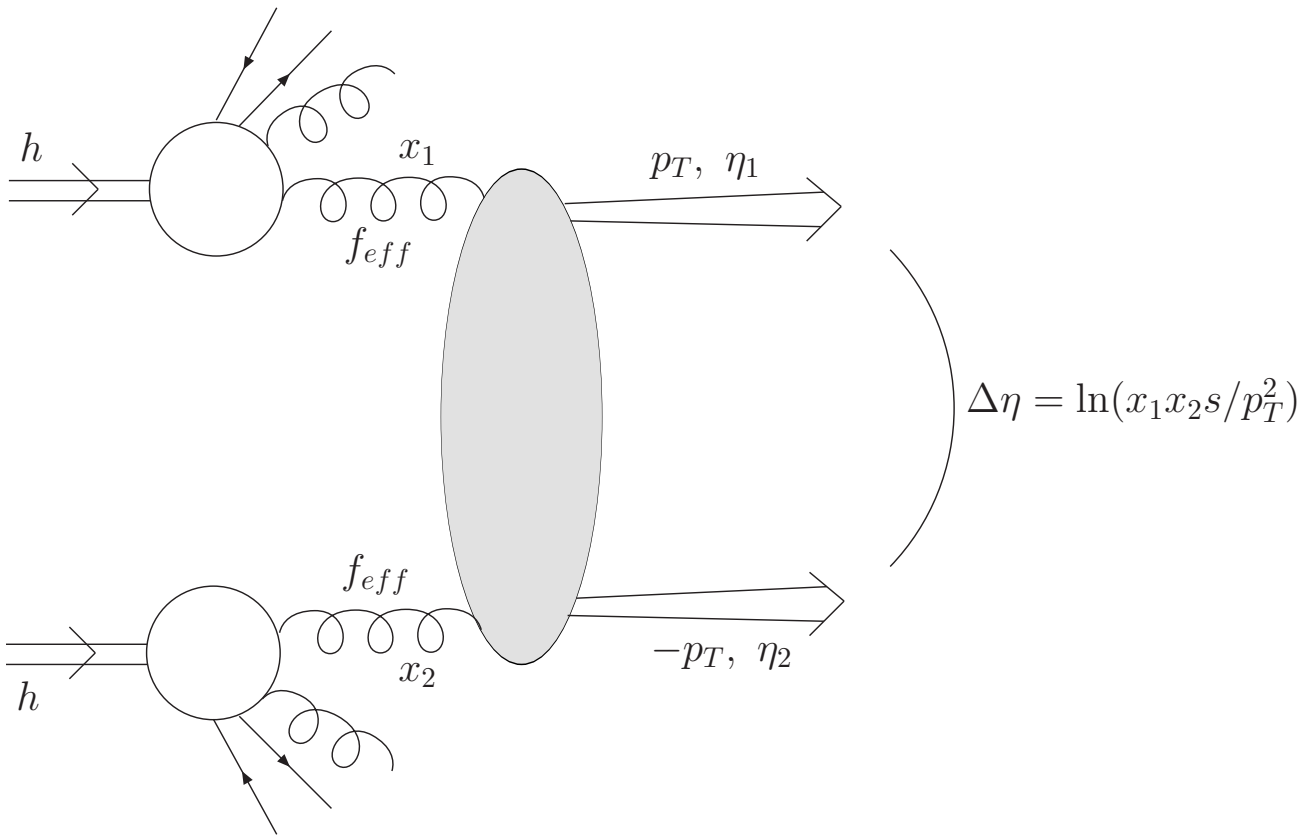
- Numerical solutions are available (Hatta and Ueda, 2009)

Comparison with ATLAS data



- Good agreement between prediction and ATLAS data (black points when the most forward and backward jets are selected and E_{out}=20 GeV)
- Plot as a function of Δy between jets in different jet p_T bins
- Green band: renormalisation and factorisation scale uncertainties (between $2p_T$ and $p_T/2$); yellow band: uncertainties related to sub-leading logs

Jet gap jet cross sections



- Test of BFKL evolution: jet gap jet events, large $\Delta\eta$, same p_T for both jets in BFKL calculation
- Principle: Implementation of BFKL NLL formalism in HERWIG Monte Carlo (Measurement sensitive to jet structure and size, gap size smaller than $\Delta\eta$ between jets)

BFKL formalism

- BFKL jet gap jet cross section: integration over ξ, p_T performed in Herwig event generation

$$\frac{d\sigma^{pp\to XJJY}}{dx_1 dx_2 dp_T^2} = \mathcal{S}\frac{f_{eff}(x_1,p_T^2)f_{eff}(x_2,p_T^2)}{16\pi}\left|A(\Delta\eta,p_T^2)\right|^2$$

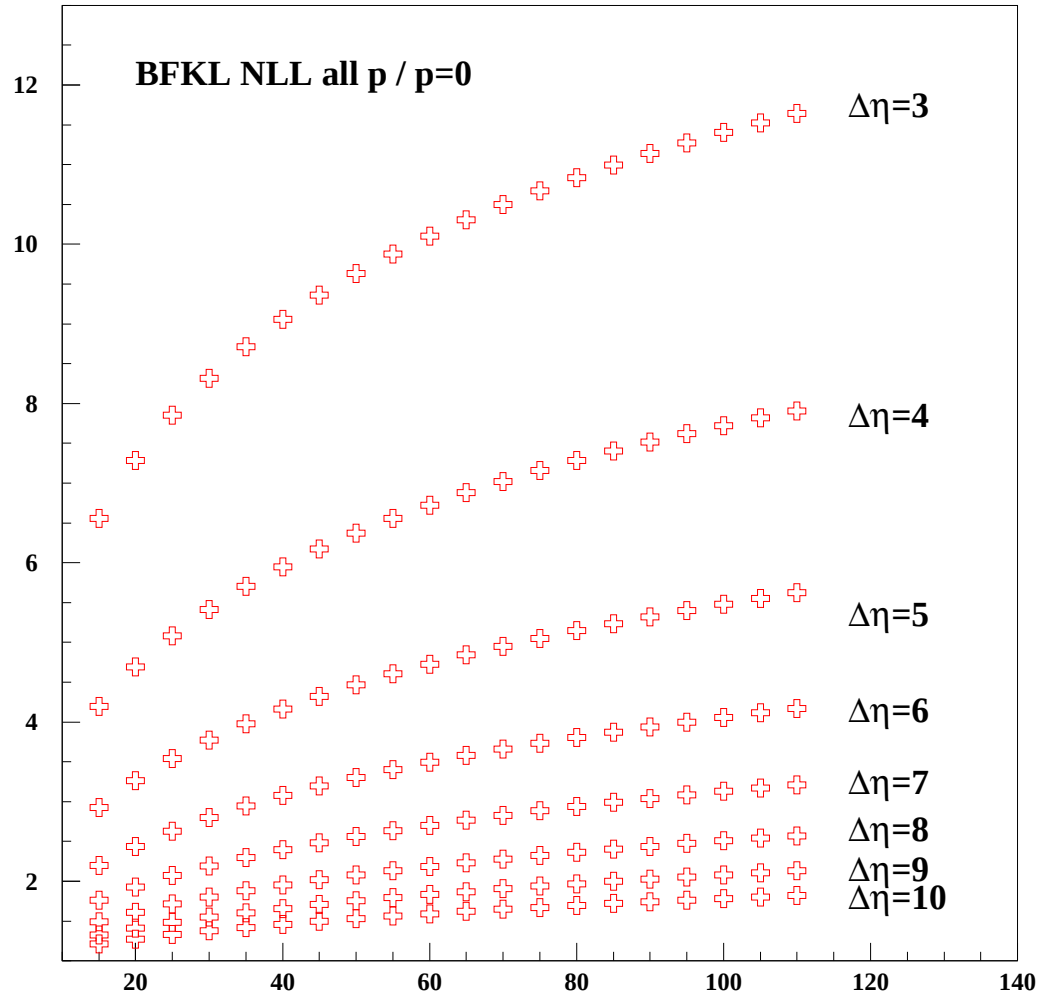
  where S is the survival probability (0.1 at Tevatron, 0.03 at LHC)

$$A(\Delta\eta,p_T^2) = \frac{16N_c\pi\alpha_s^2}{C_F p_T^2}\sum_{p=-\infty}^{\infty}\int\frac{d\gamma}{2i\pi}\frac{[p^2-(\gamma-1/2)^2]}{[(\gamma-1/2)^2-(p-1/2)^2]}\frac{\exp\left\{\frac{\alpha_S N_C}{\pi}\chi_{eff}\Delta\eta\right\}}{[(\gamma-1/2)^2-(p+1/2)^2]}$$

- α_S: 0.17 at LL (constant), running using RGE at NLL
- BFKL effective kernel χ_{eff}: determined numerically, solving the implicit equation: $\chi_{eff} = \chi_{NLL}(\gamma, \bar{\alpha}\ \chi_{eff})$
- S4 resummation scheme used to remove spurious singularities in BFKL NLL kernel
- Implementation in Herwig Monte Carlo: needed to take into account jet size and at parton level the gap size is equal to $\Delta\eta$ between jets
- Herwig MC: Parametrised distribution of $d\sigma/dp_T^2$ fitted to BFKL NLL cross section (2200 points fitted between $10 < p_T < 120$ GeV, $0.1 < \Delta\eta < 10$ with a $\chi^2 \sim 0.1$)

BFKL formalism: resummation over conformal spins

- Study of the ratio $\frac{d\sigma/dp_T(all\ \ p)}{d\sigma/dp_T(p{=}0)}$
- Resummation over p needed: modifies the p_T and $\Delta\eta$ dependences...:

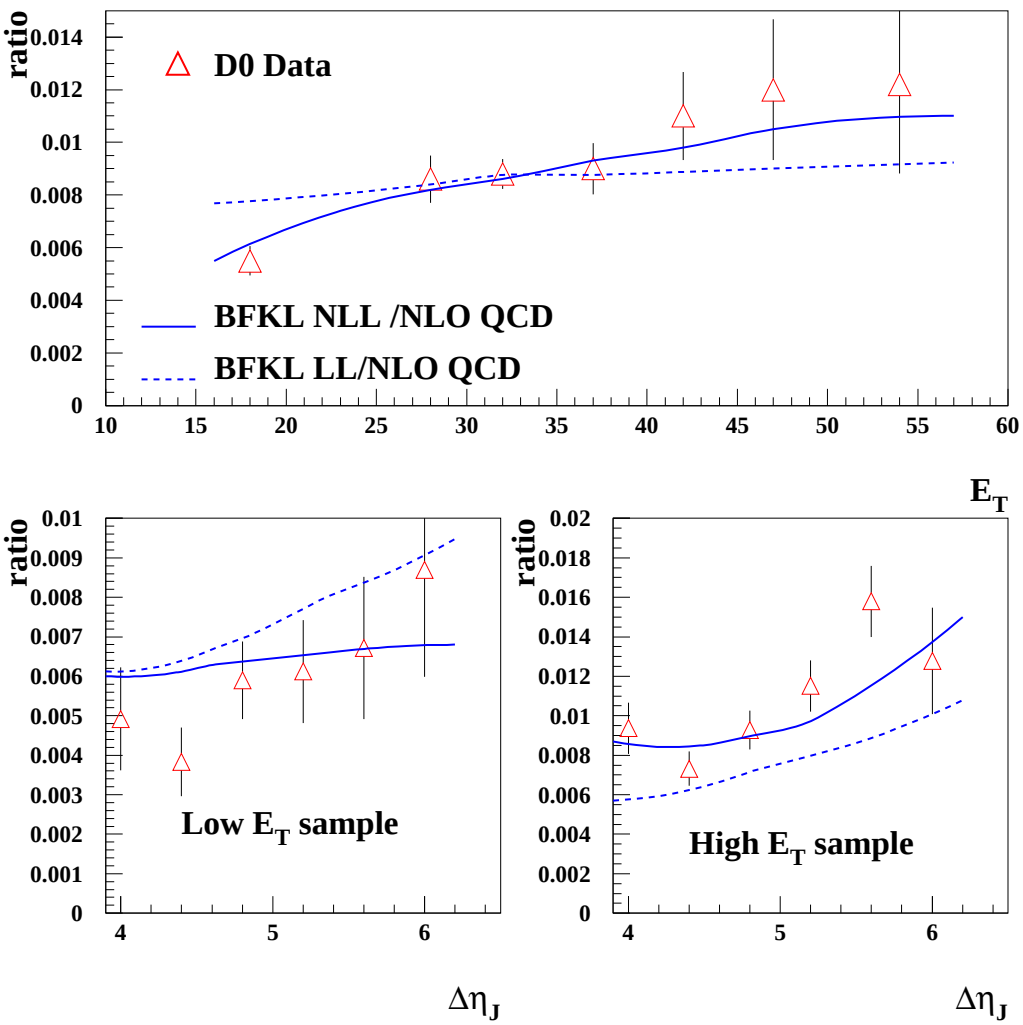


Comparison with D0 data

- D0 measurement: Jet gap jet cross section ratios as a function of second highest E_T jet, or $\Delta\eta$ for the low and high E_T samples, the gap between jets being between -1 and 1 in rapidity
- Comparison with BFKL formalism:

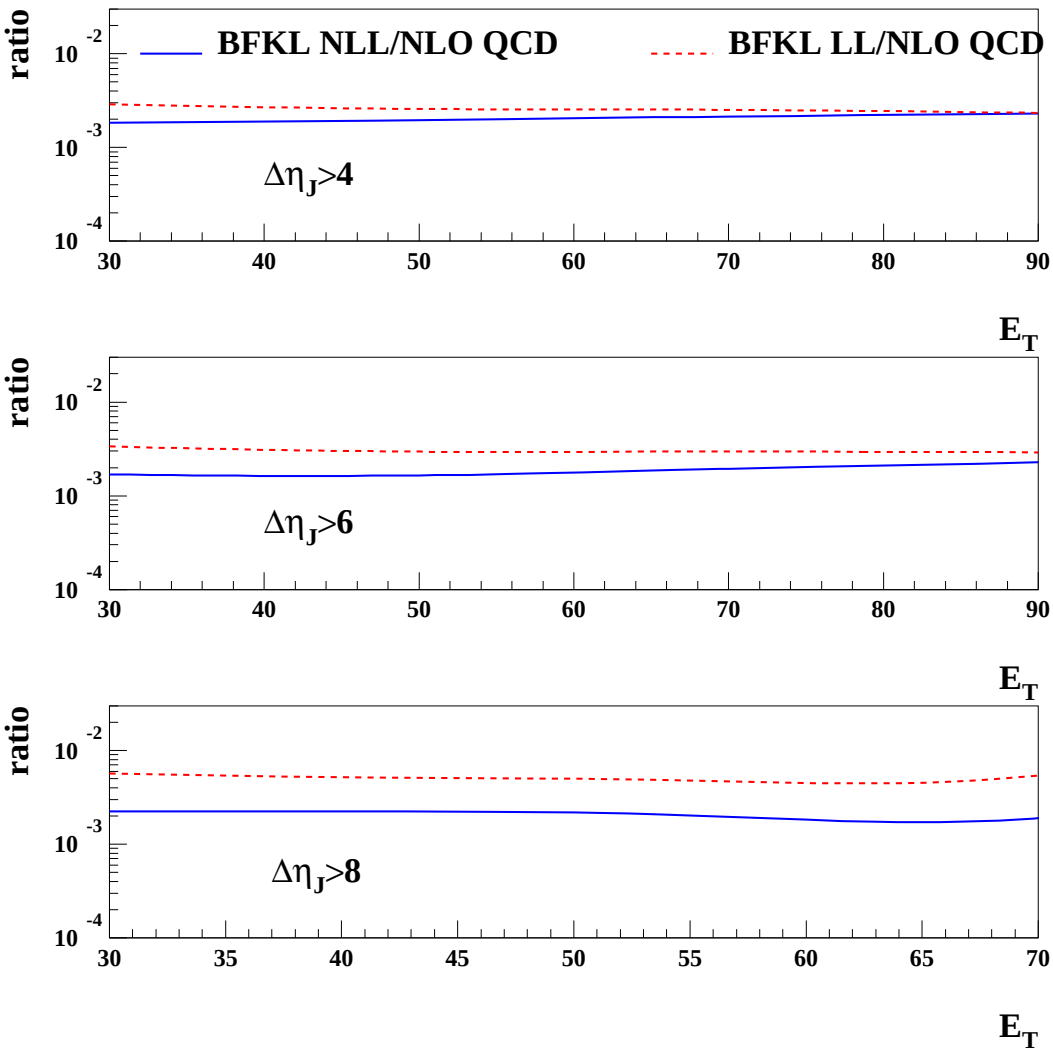
$$Ratio = \frac{BFKL\ NLL\ Herwig}{Dijet\ Herwig} \times \frac{LO\ QCD\ NLOJet++}{NLO\ QCD\ NLOJet++}$$

- Reasonable description using BFKL NLL formalism



Predictions for the LHC

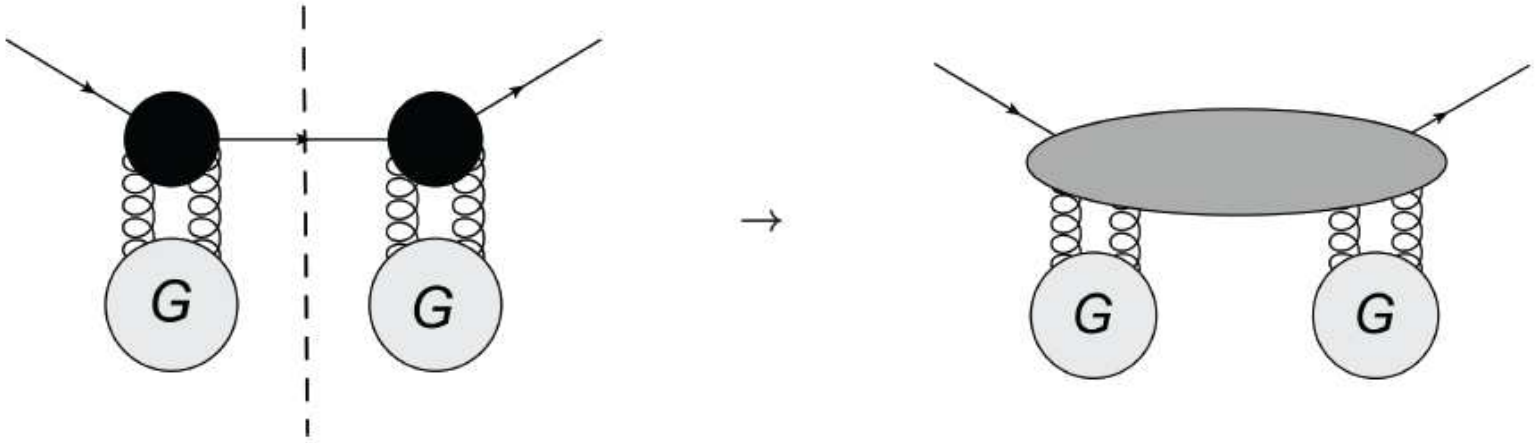
- Weak E_T and $\Delta\eta$ dependence
- Large differences in normalisation between BFKL LL and NLL predictions



- Implementation of BFKL NLL formalism including NLO impact factors
- Work done in collaboration with D. Colferai, F. Deganutti, T. Raben

Full NLL calculation (in progress)

- Combine NLL kernel with NLO impact factors (Hentschinski, Madrigal, Murdaca, Sabio Vera 2014)
- At NLO, impact factors are much more complicated!



•

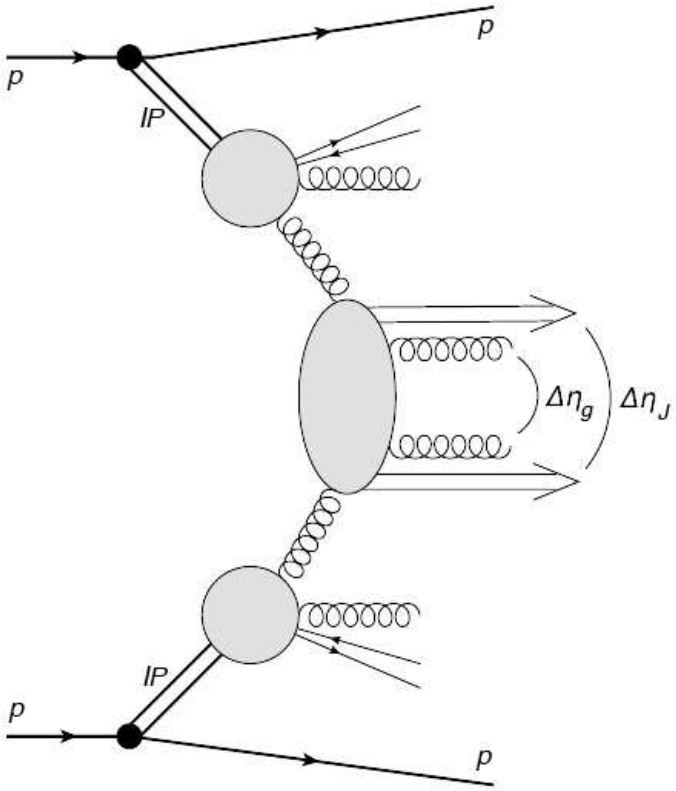
NLL impact factors

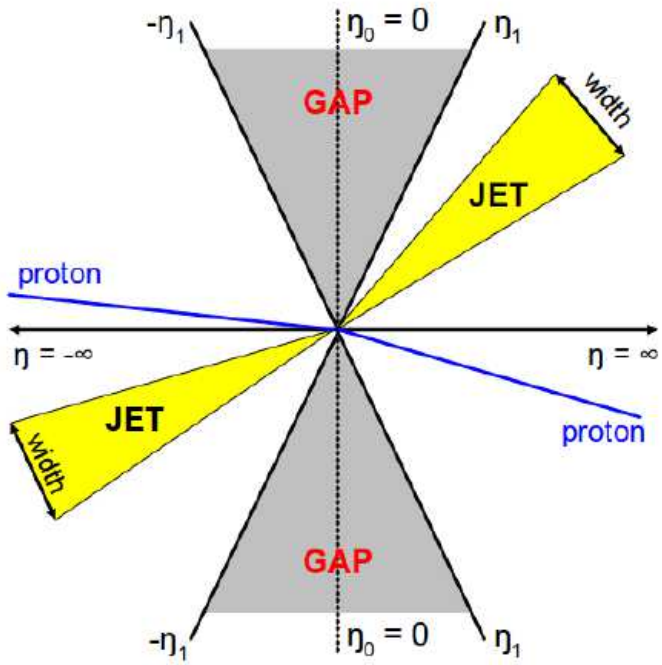
- Mix loop momenta (not factorized)
- Involve jet distributions with two final states
- Contain complicated non-analytic progress
- Work in progress by D. Colferai, F. Daganutti, T. Raben

- Will lead to an improved parametrisation to be omplemented in HERWIG

Jet gap jet events in diffraction

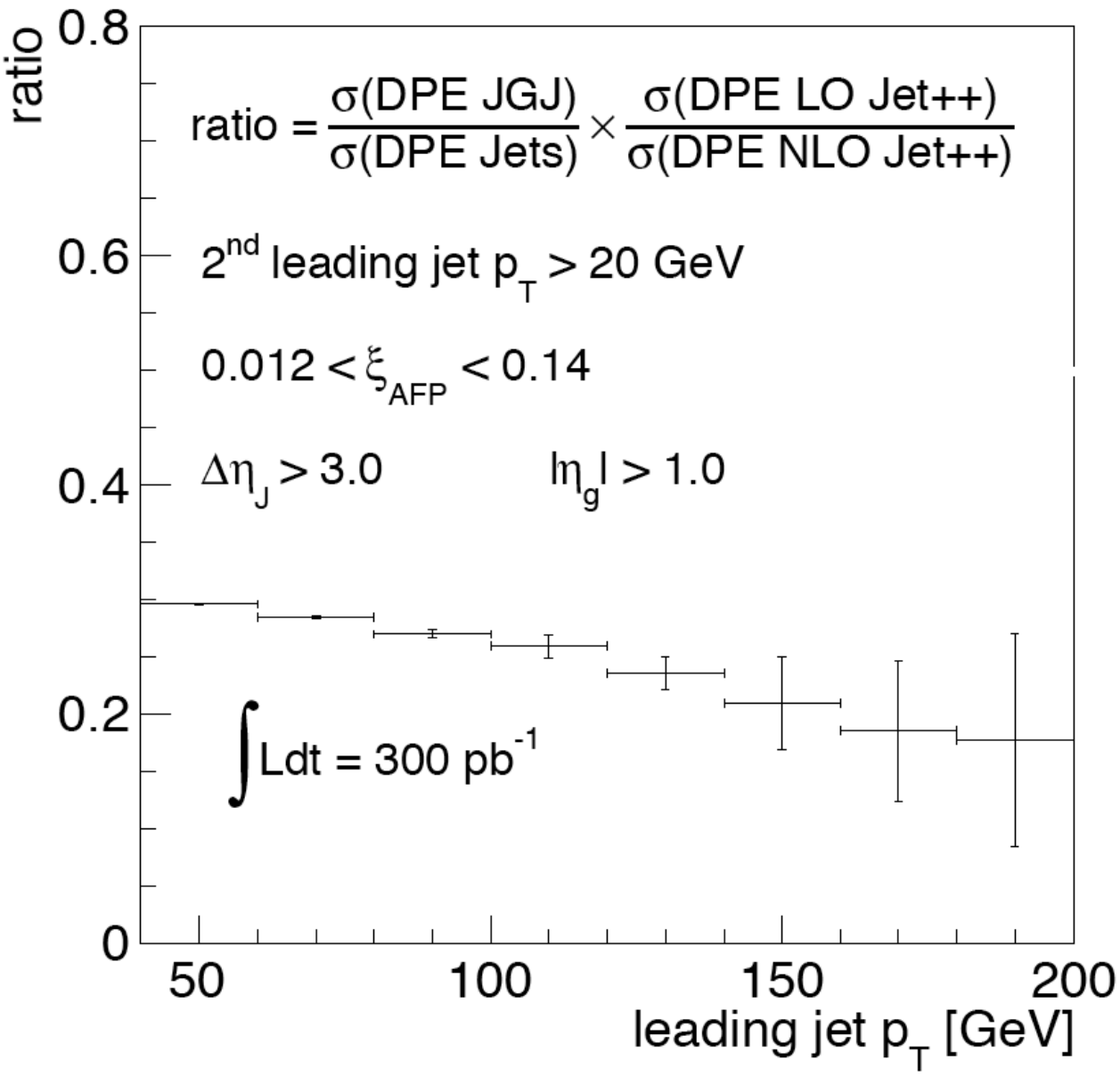
- Study BFKL dynamics using jet gap jet events
- Jet gap jet events in DPE processes: clean process, allows to go to larger $\Delta\eta$ between jets
- Reference: Gaps between jets in double-Pomeron-exchange processes at the LHC, C. Marquet, C. Royon, M. Trzebinski, R. Zlebcik, Phys. Rev. D87 (2013) 3, 034010





Jet gap jet events in diffraction

- Measure the ratio of the jet gap jet to the dijet cross sections: sensitivity to BFKL dynamics
- As an example, study as a function of leading jet p_T
- Advantage: ratio close to 10% (no survival probability), very clean events since jets not "polluted" by remnants)



Conclusion

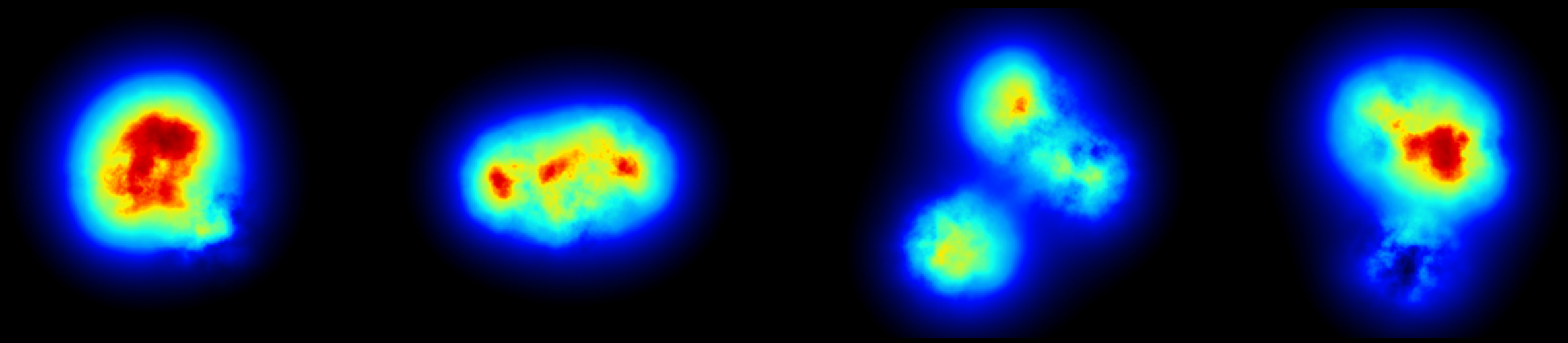
- Full implementation of BFKL NLL kernel for many jet proceeses at HERA, Tevatron and LHC
- Forward jets at HERA: DGLAP NLO fails to describe HERA data, good description of data using BFKL NLL formalism
- Mueller Navelet jets: Larger decorrelation expected for BFKL formalism, unfortunately suffers a lot of higher order corrections, NLL BFKL with saturation in progress
- Jet veto measurements in ATLAS: mainly not related to BFKL resummation effects
- Jet gap jets:
  - NLL BFKL cross section implemented in HERWIG (Kernel)
  - Fair description of D0 and CDF data
  - Full NLL calculation in progress
  - Jet gap jet events in diffraction: clean tests of BFKL, modulo the survival probability (and its depndence on kinematics)

U.S. DEPARTMENT OF ENERGY | Office of Science

BROOKHAVEN NATIONAL LABORATORY

SUBNUCLEONIC FLUCTUATIONS, DIFFRACTION, AND SMALL-X EVOLUTION

Björn Schenke
Brookhaven National Laboratory



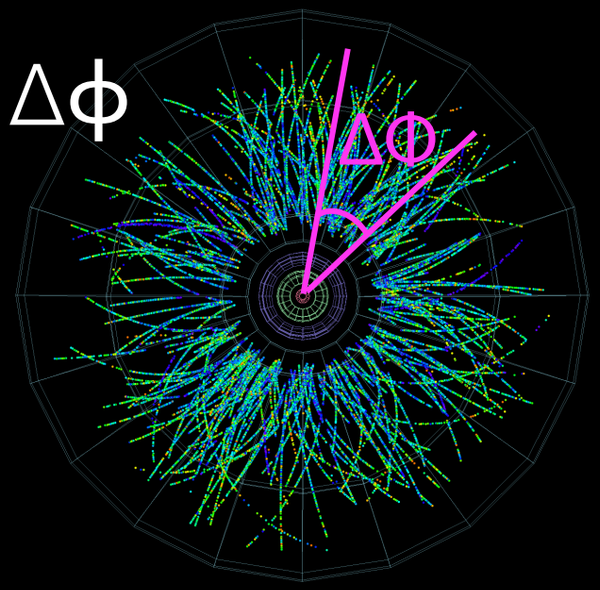
April 26, 2017
Saturation: Recent Developments, New Ideas and Measurements
RBRC Workshop

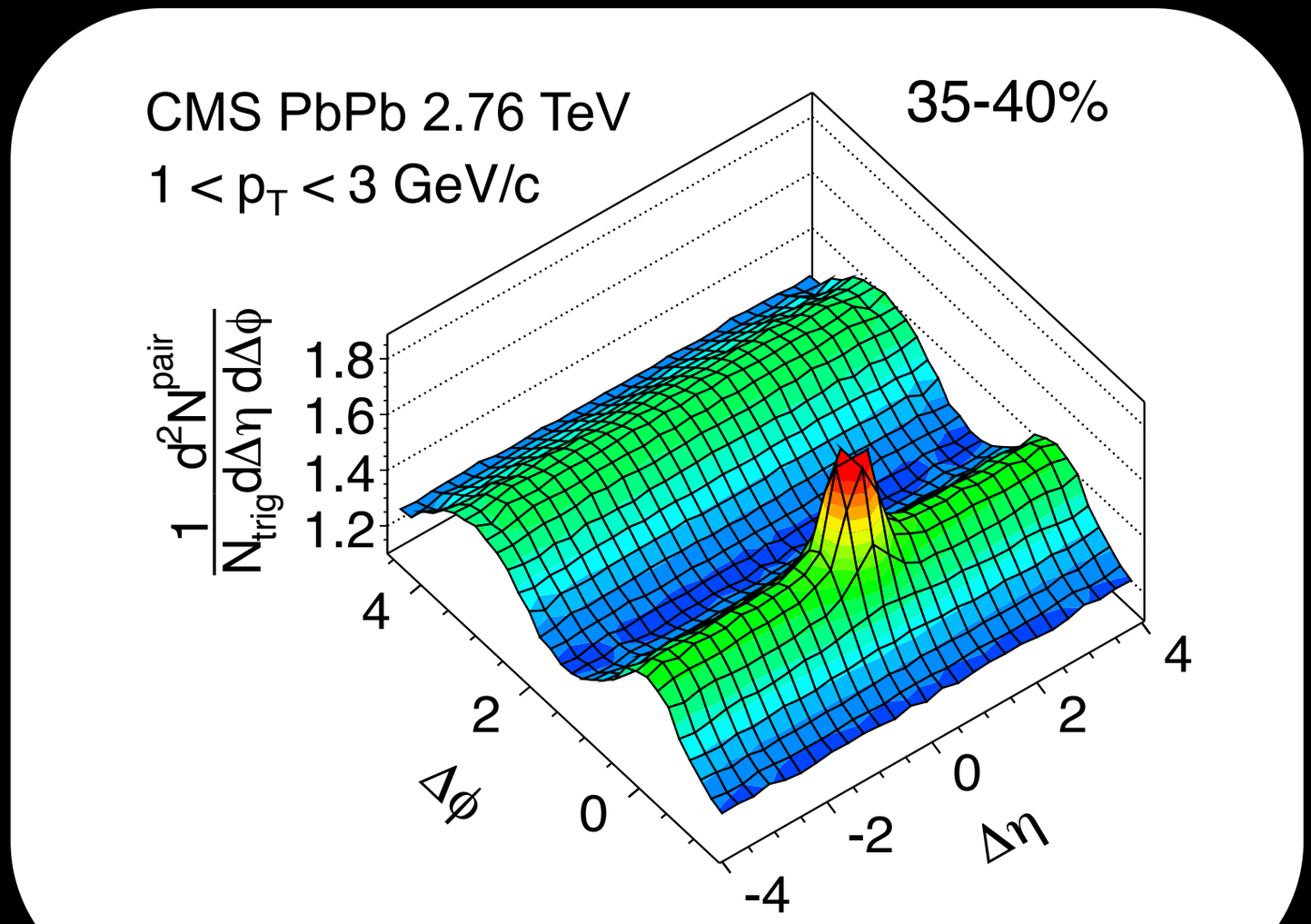
Introduction: Multi-particle correlations

2-particle correlation as a function of $\Delta\eta$ and $\Delta\phi$

$\Delta\eta$: DIFFERENCE IN PSEUDO-RAPIDITY

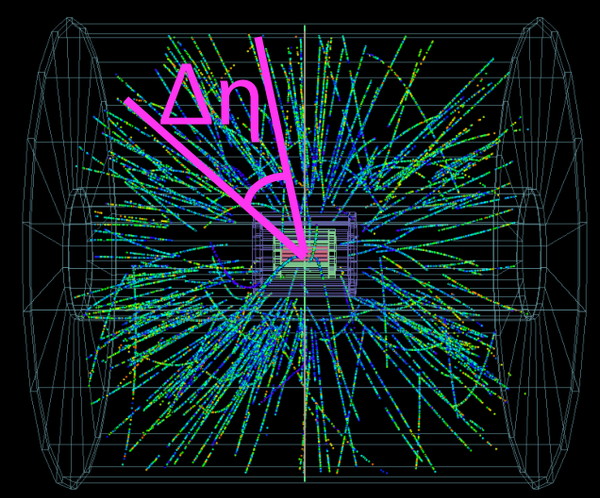
$\Delta\Phi$: DIFFERENCE IN AZIMUTHAL ANGLE





CMS COLL., EUR. PHYS. J. C72 (2012)

$\Delta\Phi$: DIFFERENCE IN AZIMUTHAL ANGLE

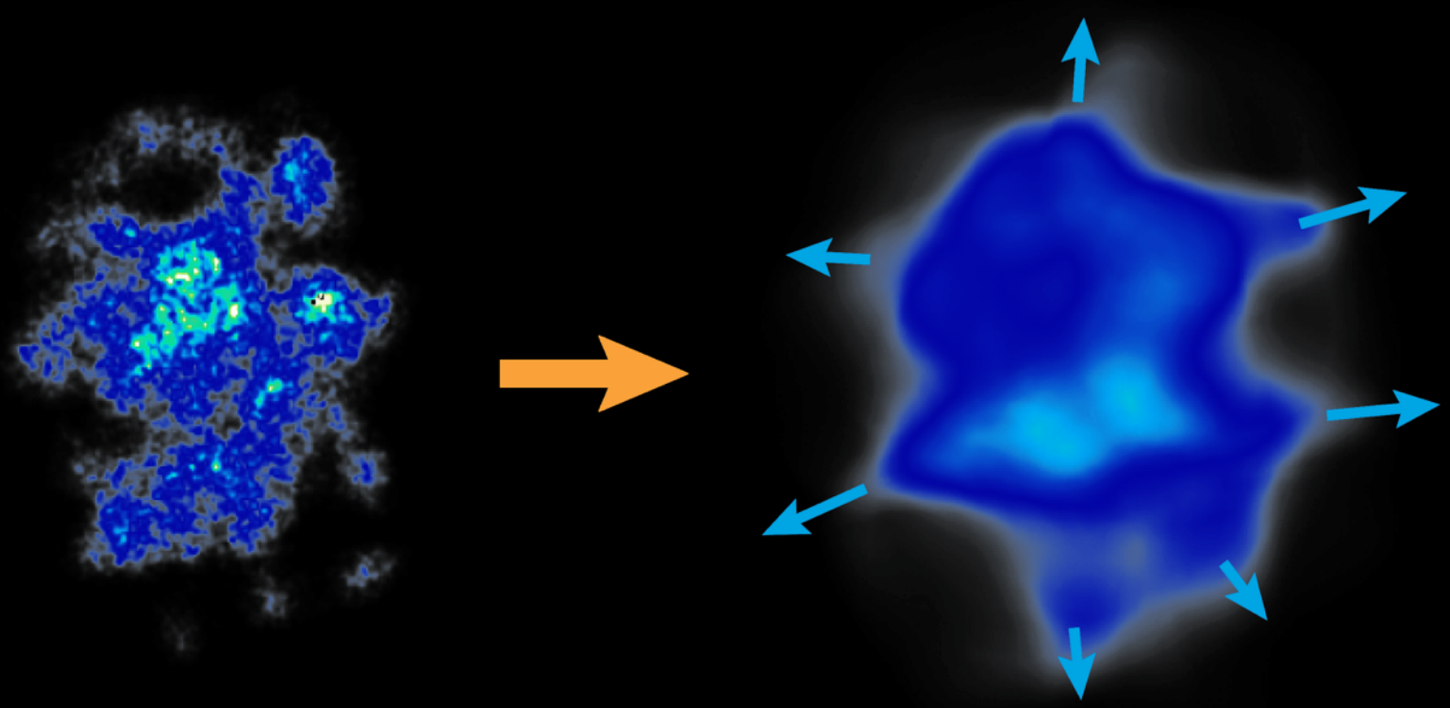


$\Delta\eta$: DIFFERENCE IN PSEUDO-RAPIDITY

Event Displays: © 2012 CERN, ALICE

Interpretation: Strong final state effects

- Long range Δη correlations emerge from early times (causality)
- Azimuthal structure formed by the medium response to the fluctuating initial transverse geometry



Initial energy density distribution

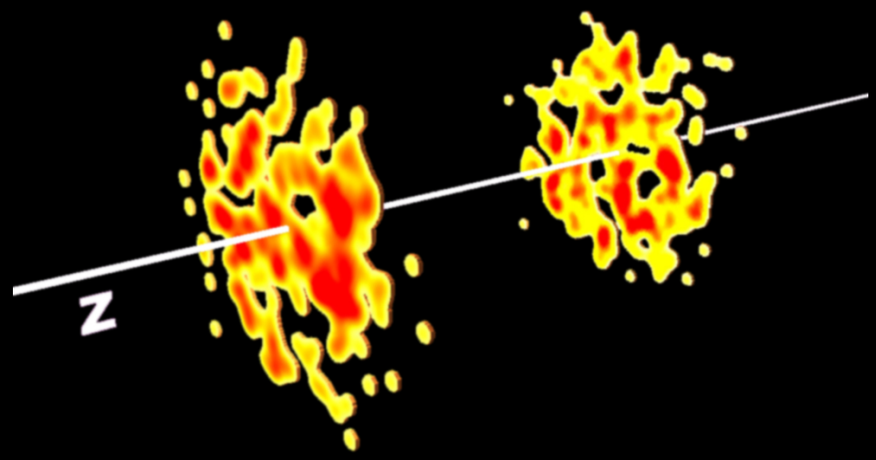
Hydrodynamic expansion

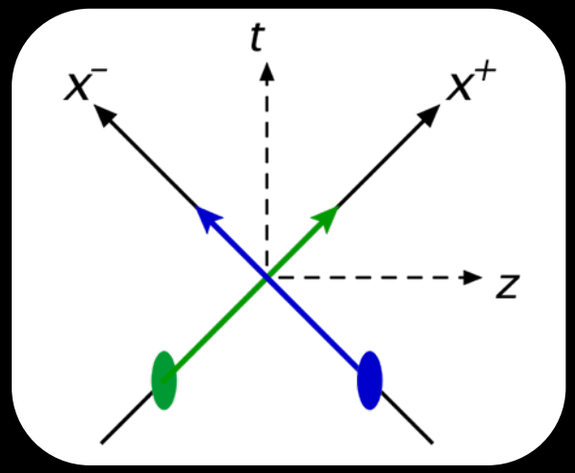
IP-Glasma initial state

B.Schenke, P.Tribedy, R.Venugopalan, PRL108, 252301 (2012), PRC86, 034908 (2012)

Particle production governed by the **Yang Mills equations**

$$[D_\mu, F^{\mu\nu}] = J^\nu$$





Incoming currents

How to determine the incoming currents J^ν:

- IP-Sat model: Parametrize energy and spatial dependence of deep inelastic cross section - fit parameters to HERA data
  Kowalski, Teaney, Phys.Rev. D68 (2003) 114005
- → energy and position dependent saturation scale $Q_s(x, \vec{x})$
- Sample nucleons and color charges $\rho(\vec{x})$ with density ~ $Q_s(x, \vec{x})$

IP-Glasma initial state

B.Schenke, P.Tribedy, R.Venugopalan, PRL108, 252301 (2012)
PRC86, 034908 (2012)

Fields before the collision:

$$A^i_{(1)}(\vec{x}) = -\frac{i}{g} V_{(1)}(\vec{x}) \partial_i V^\dagger_{(1)}(\vec{x}) \text{ with Wilson lines:}$$

$$V_{(1)}(\vec{x}) = P \exp\left(-ig \int dx^- \frac{\rho_{(1)}(x^-, \vec{x})}{\nabla^2 + m^2} \right)$$

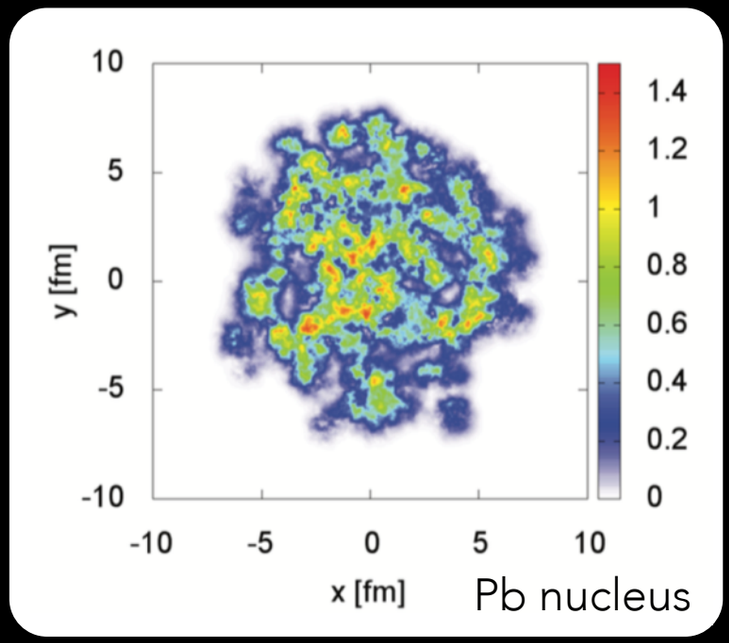
Fields after the collision:

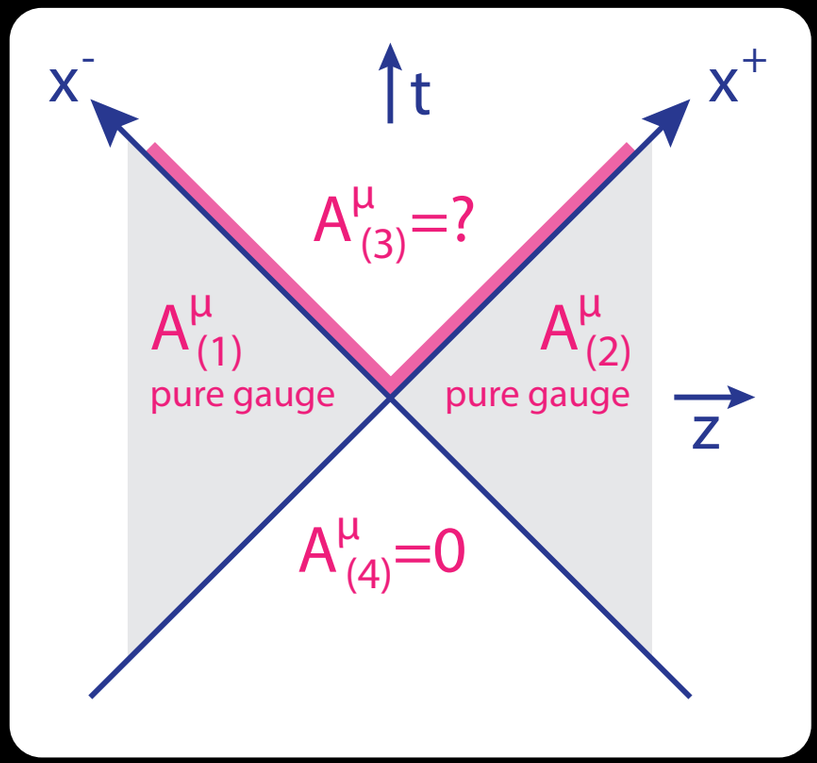
$$A^i_{(3)}|_{\tau=0^+} = A^i_{(1)} + A^i_{(2)}$$

$$A^\eta_{(3)}|_{\tau=0^+} = \frac{ig}{2}[A^i_{(1)}, A^i_{(2)}]$$

Kovner, McLerran, Weigert, Phys. Rev. D52, 6231 (1995)
Krasnitz, Venugopalan, Nucl.Phys. B557 (1999) 237

Trace of Wilson lines

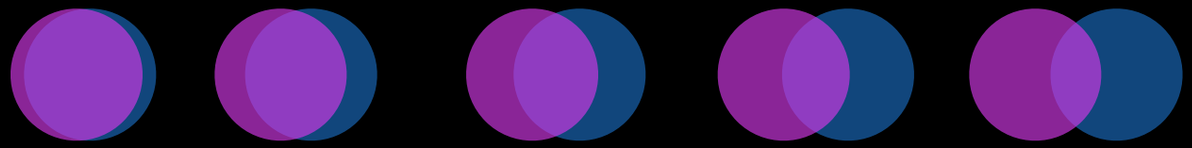


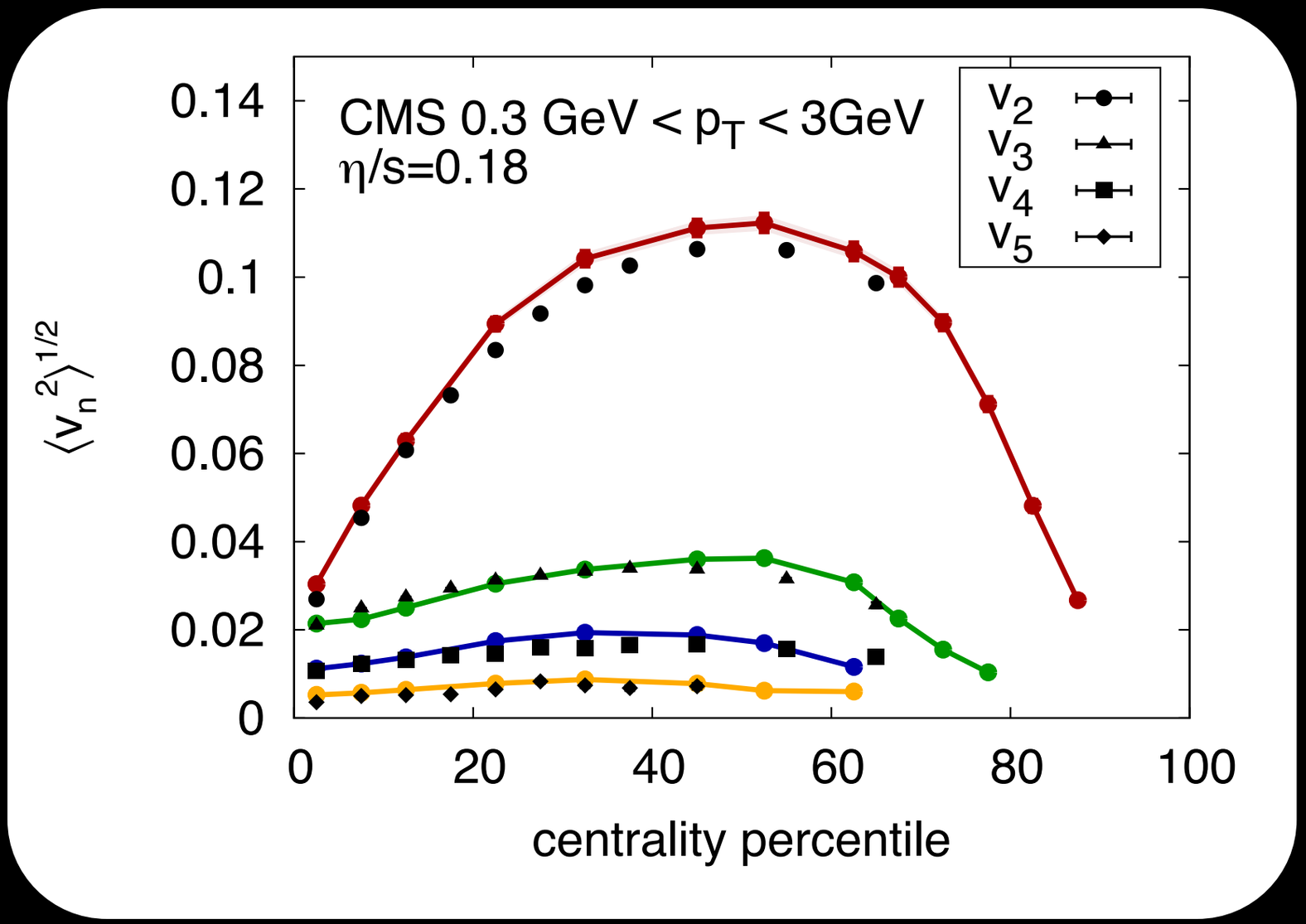


Fields in Schwinger gauge

Heavy ions: v_n from IP-Glasma initial state and MUSIC hydrodynamics

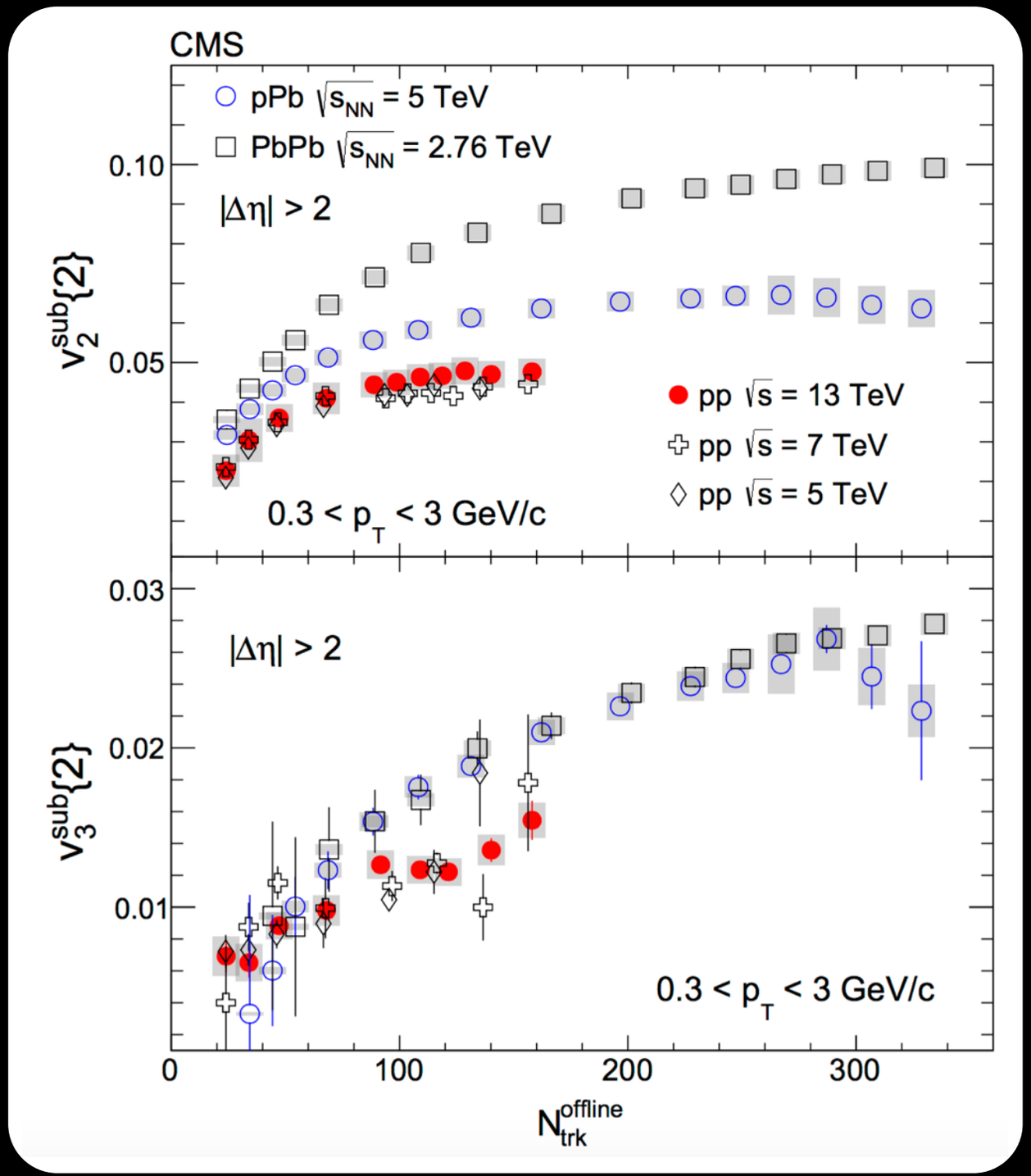
C.Gale, S.Jeon, B.Schenke, P.Tribedy, R.Venugopalan, Phys.Rev.Lett. 110, 012302 (2013)
B. Schenke, R. Venugopalan, Phys.Rev.Lett. 113 (2014) 102301





CMS Collaboration, PRC 87(2013) 014902

v_n in p+p, p+Pb, Pb+Pb Collisions



CMS Collaboration, Phys.Lett. B765 (2017) 193-220

see also:

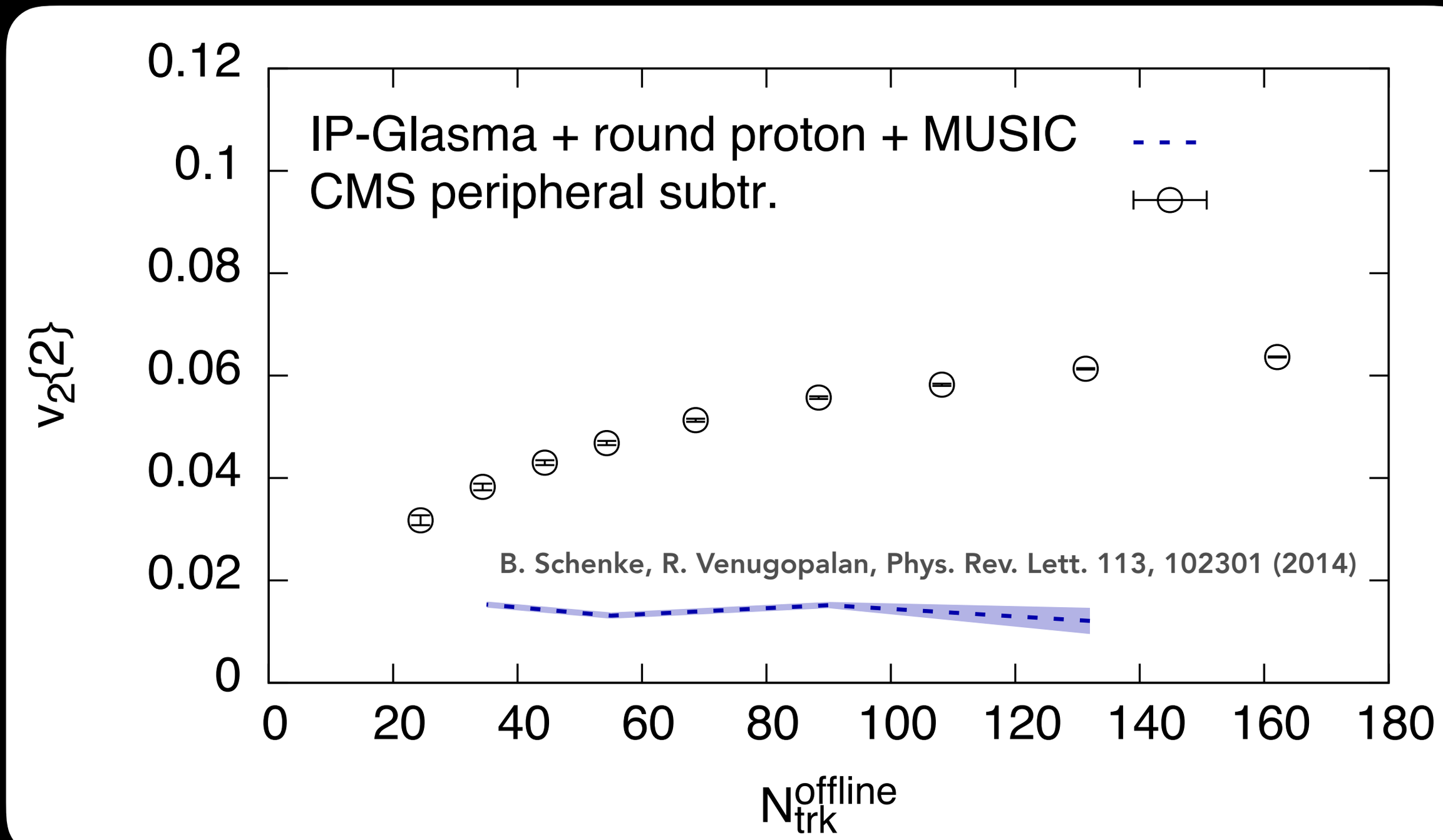
ALICE CollABORATION
Phys. Lett. B719 (2013) 29-41; Phys. Rev. C 90, 054901

ATLAS CollABORATION
Phys. Rev. Lett. 110, 182302 (2013); Phys. Rev. C 90.044906 (2014)

CMS CollABORATION Phys.Rev.Lett. 115, 012301 (2015)

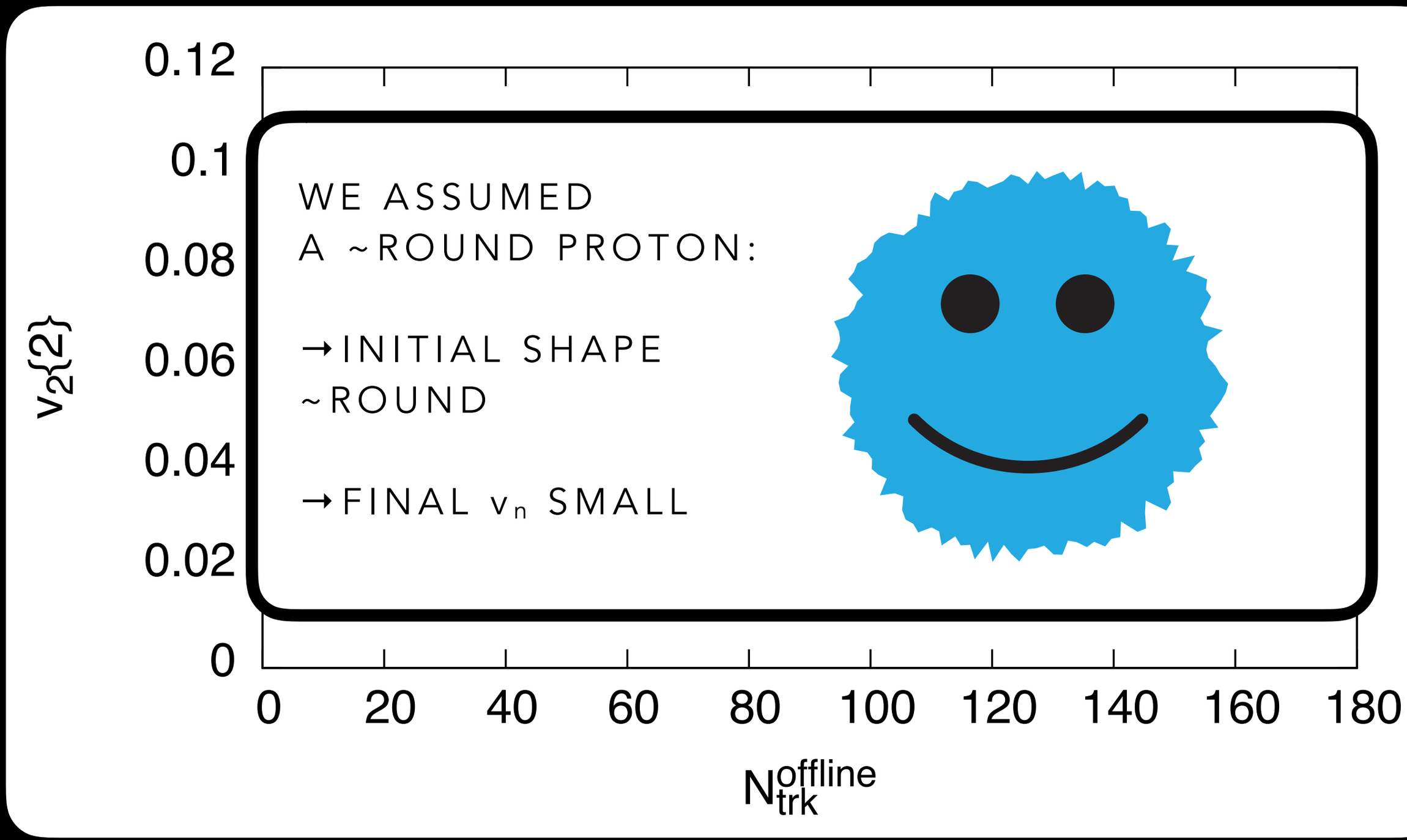
IP-Glasma+MUSIC results

Experimental data: CMS Collaboration, Phys.Lett. B724, 213 (2013)



IP-Glasma+MUSIC results

Experimental data: CMS Collaboration, Phys.Lett. B724, 213 (2013)



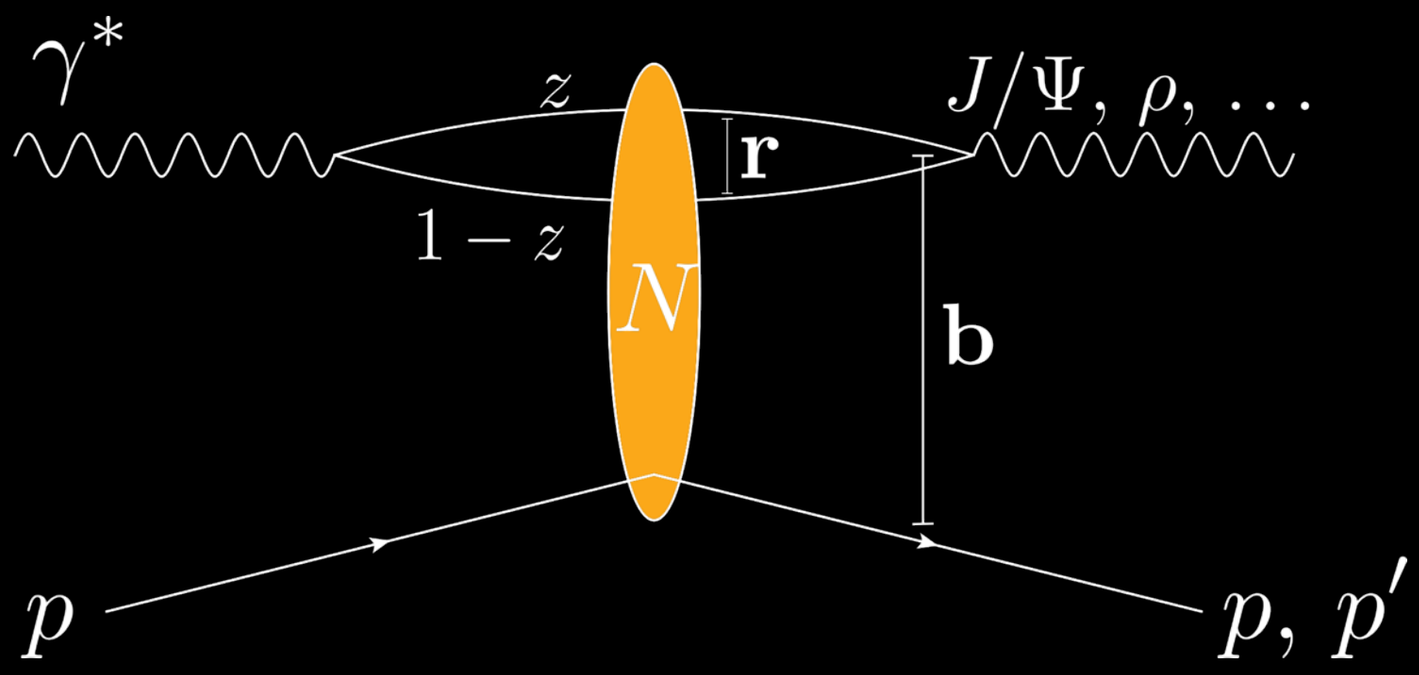
THEORY FRAMEWORK
REQUIRES ADDITIONAL
PROTON SHAPE
FLUCTUATIONS

HOW TO CONSTRAIN THEM?

Diffractive J/Ψ production

H. Mäntysaari, B. Schenke, Phys. Rev. Lett. 117 (2016) 052301; Phys.Rev. D94 (2016) 034042

No exchange of color charge
→Large rapidity gap



Coherent diffraction:
Proton remains intact, Sensitive to average gluon distribution in the proton

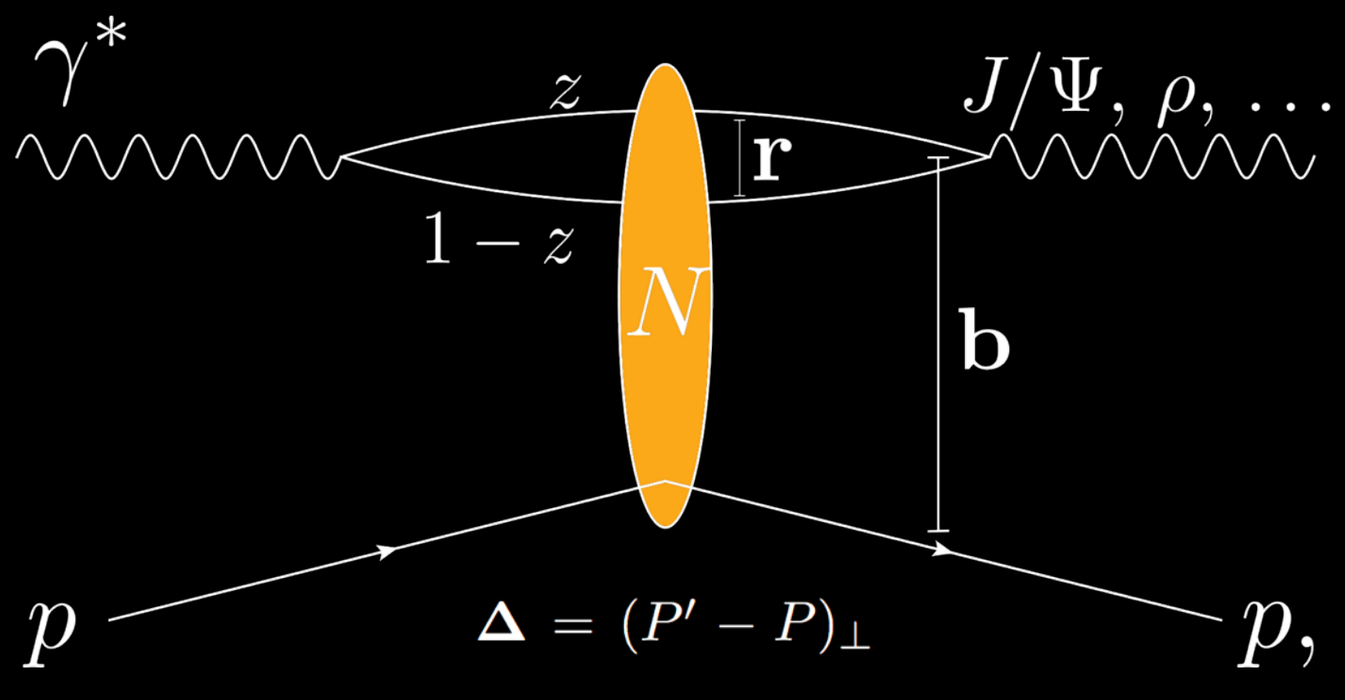
Incoherent diffraction:
Proton breaks up, Sensitive to shape fluctuations

CGC Framework J/Ψ production

H. Mäntysaari, B. Schenke, Phys. Rev. Lett. 117 (2016) 052301; Phys.Rev. D94 (2016) 034042

Diffractive eigenstates are color dipoles at fixed r_T and b_T

see
M. L. Good and W. D. Walker
Phys. Rev. 120 (1960) 1857.



Scattering amplitude

$$\mathcal{A} \sim \int \mathrm{d}^2 b \mathrm{d} z \mathrm{d}^2 r \Psi^* \Psi^V(r, z, Q^2) e^{-ib\cdot\Delta} N(r, x, b)$$

Dipole amplitude N determined in IPsat or IP-Glasma

Averaging over the target

H. Mäntysaari, B. Schenke, Phys. Rev. Lett. 117 (2016) 052301; Phys.Rev. D94 (2016) 034042

COHERENT DIFFRACTION:
TARGET STAYS INTACT

$$\frac{\mathrm{d}\sigma^{\gamma^* p\to Vp}}{\mathrm{d}t} = \frac{1}{16\pi}\left|\left\langle \mathcal{A}^{\gamma^* p\to Vp}(x_{\mathbb{P}}, Q^2, \boldsymbol{\Delta})\right\rangle\right|^2$$

INCOHERENT DIFFRACTION:
TARGET BREAKS UP

$$\frac{\mathrm{d}\sigma^{\gamma^* p\to Vp^*}}{\mathrm{d}t} = \frac{1}{16\pi}\left(\left\langle\left|\mathcal{A}^{\gamma^* p\to Vp}(x_{\mathbb{P}}, Q^2, \boldsymbol{\Delta})\right|^2\right\rangle - \left|\left\langle \mathcal{A}^{\gamma^* p\to Vp}(x_{\mathbb{P}}, Q^2, \boldsymbol{\Delta})\right\rangle\right|^2\right)$$

SENSITIVE TO FLUCTUATIONS!

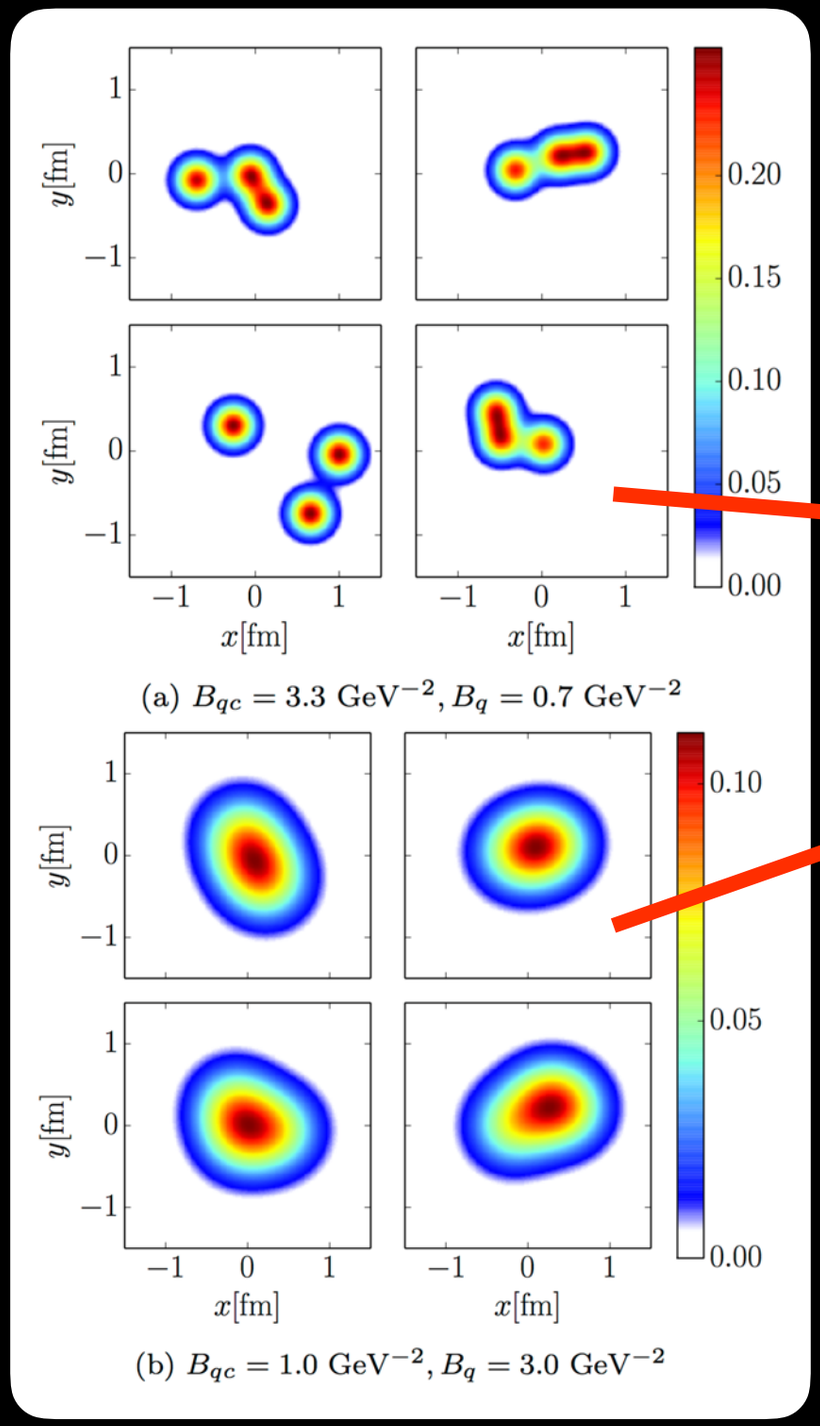
SEE
H. I. MIETTINEN
AND J. PUMPLIN
PHYS. REV. D18 (1978) 1696

Y. V. KOVCHEGOV
AND L. D. MCLERRAN
PHYS. REV. D60 (1999) 054025

A. KOVNER AND
U. A. WIEDEMANN
PHYS. REV. D64 (2001) 114002

Introduce geometric fluctuations

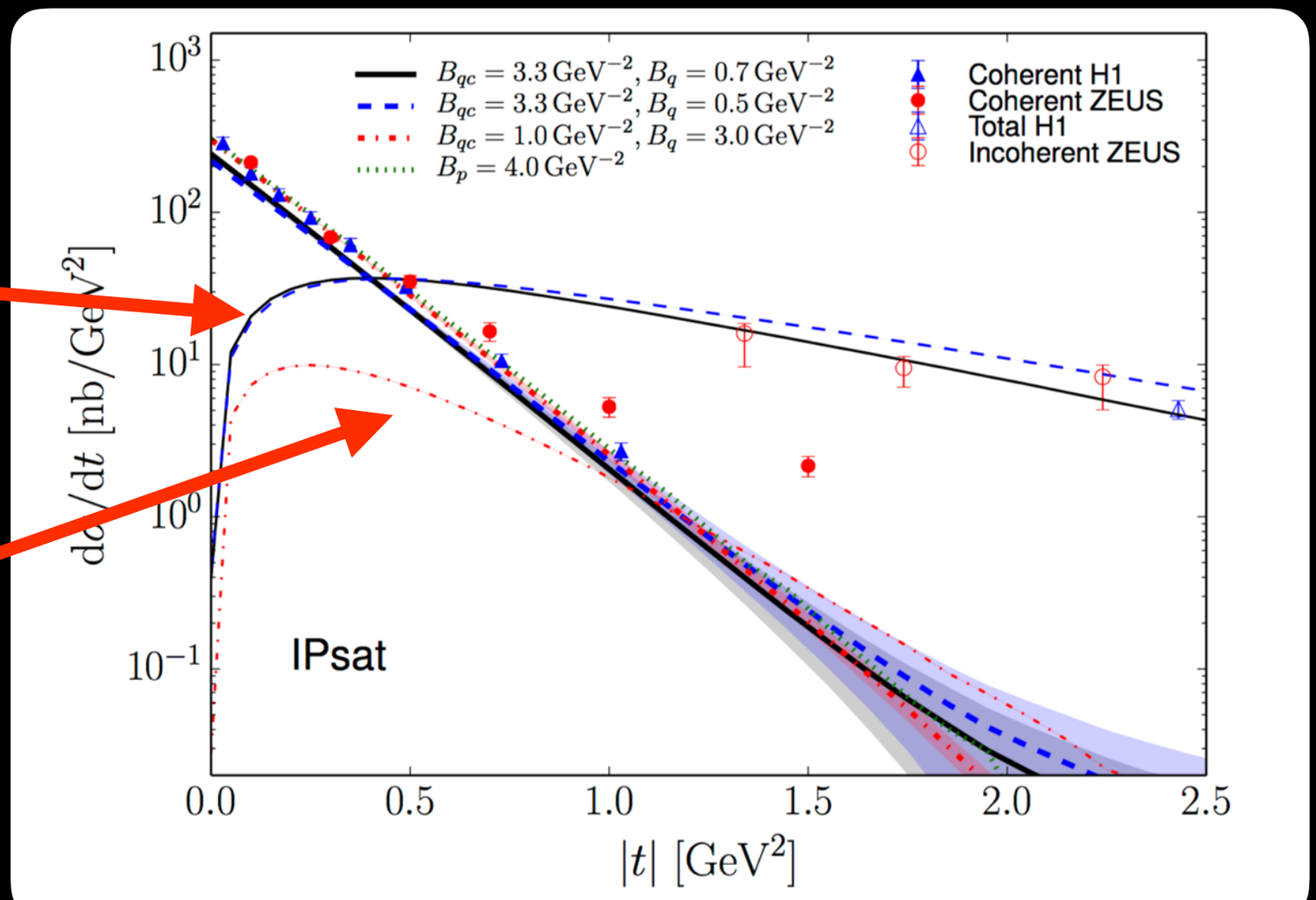
Assume 3 valence quark-like hot spots



(a) $B_{qc} = 3.3\ \mathrm{GeV}^{-2}, B_q = 0.7\ \mathrm{GeV}^{-2}$

(b) $B_{qc} = 1.0\ \mathrm{GeV}^{-2}, B_q = 3.0\ \mathrm{GeV}^{-2}$

H. Mäntysaari, B. Schenke, Phys. Rev. Lett. 117 (2016) 052301
Phys.Rev. D94 (2016) 034042



H1 collaboration, Eur. Phys. J. C46 (2006) 585,
Phys. Lett. B568 (2003) 205
ZEUS collaboration, Eur. Phys. J. C24 (2002) 345
Eur. Phys. J. C26 (2003) 389

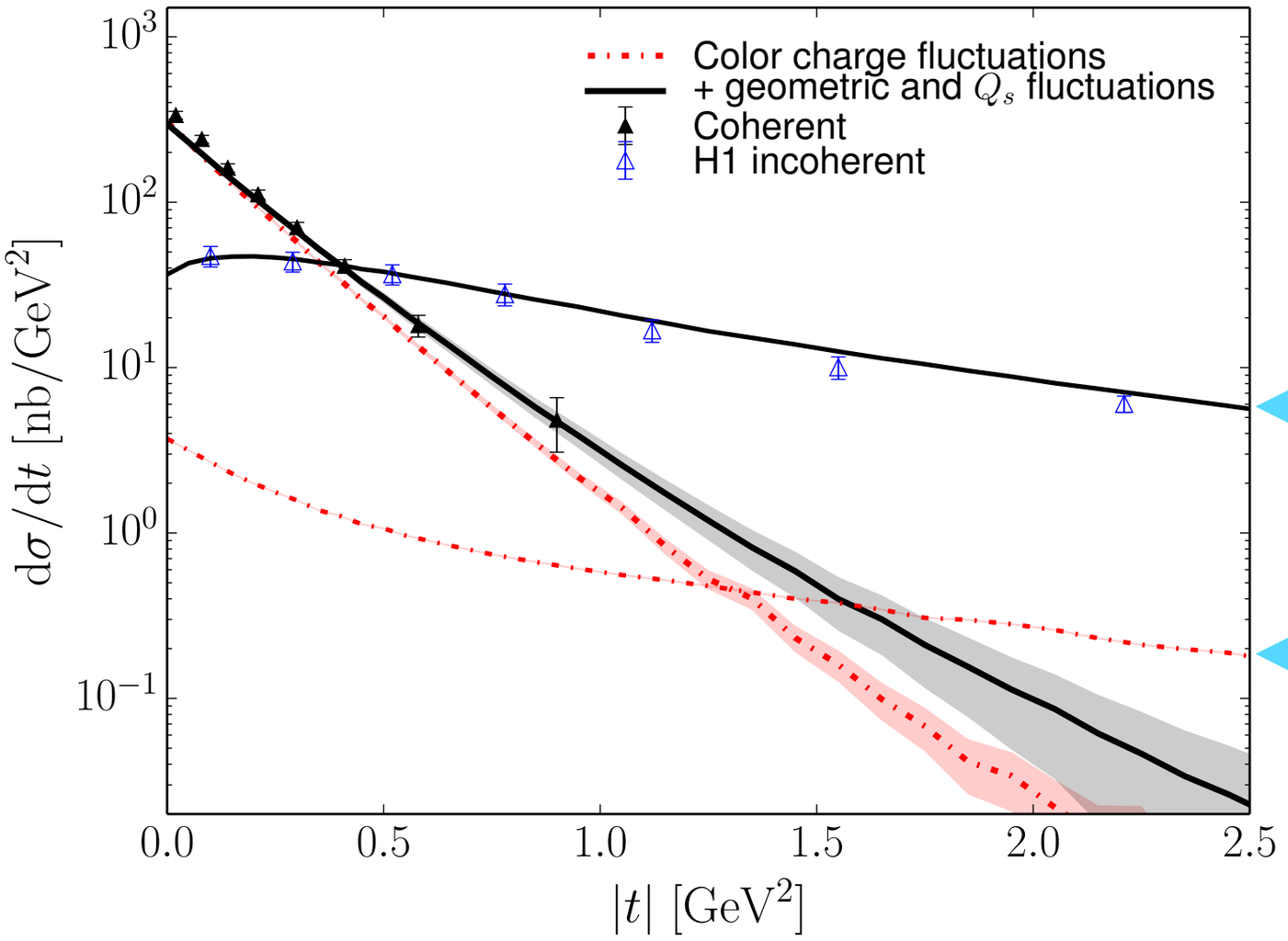
IP-Glasma calculation

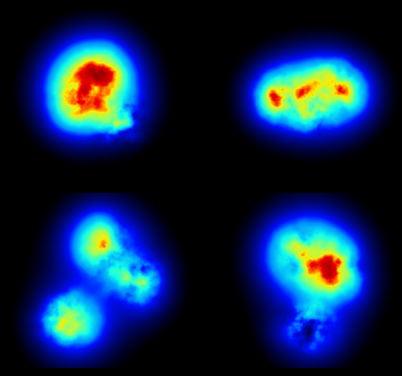
H. Mäntysaari, B. Schenke, Phys. Rev. Lett. 117 (2016) 052301; Phys.Rev. D94 (2016) 034042

Geometric + color charge fluctuations

Wilson lines

Dipole amp.: $N(\vec{r}, x_{\mathbb{P}}, \vec{b}) = N(\vec{x}-\vec{y}, x_{\mathbb{P}}, (\vec{x}+\vec{y})/2) = 1 - \mathrm{Tr} V(\vec{x}) V^{\dagger}(\vec{y})/N_c$





tuned shape fluctuations

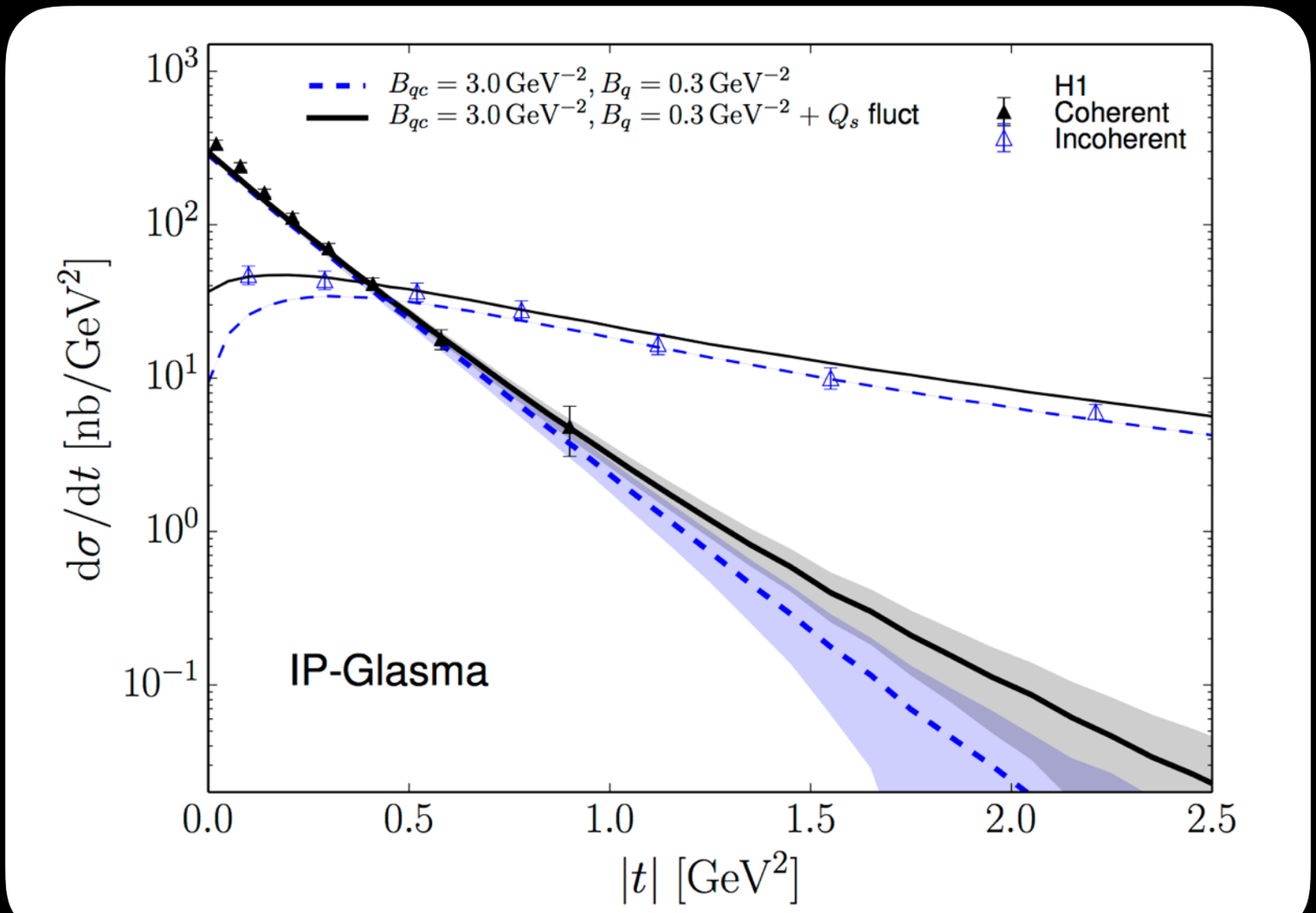
round proton

H1 Collaboration, Eur. Phys. J. C73 (2013) no. 6 2466

Effect of Q_S fluctuations

H. Mäntysaari, B. Schenke, Phys. Rev. Lett. 117 (2016) 052301; Phys.Rev. D94 (2016) 034042

$$P(\ln Q_s^2/\langle Q_s^2\rangle) = \frac{1}{\sqrt{2\pi}\sigma}\exp\left[-\frac{\ln^2 Q_s^2/\langle Q_s^2\rangle}{2\sigma^2}\right]$$

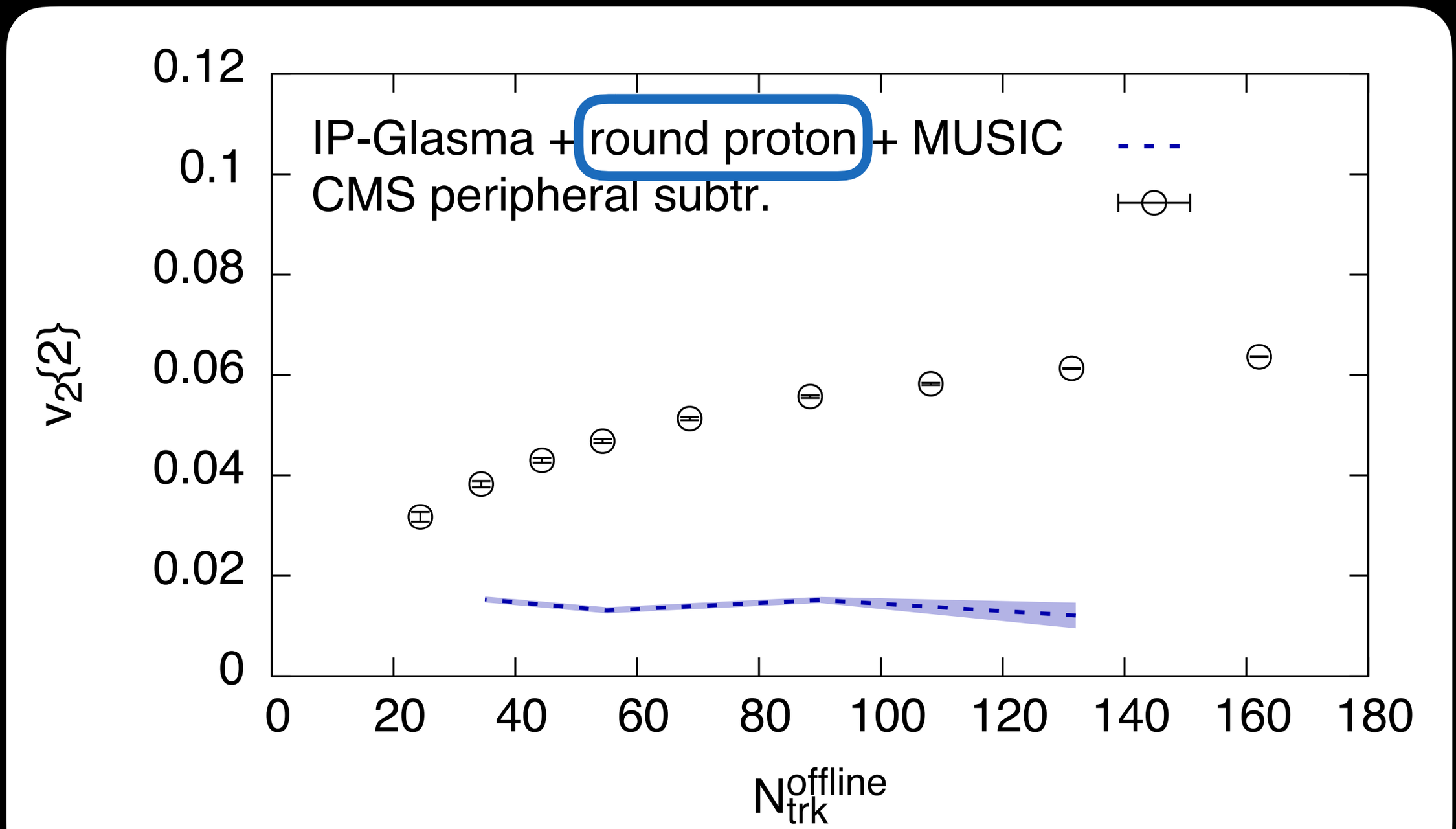


σ=0.5

Experimental data: H1 collaboration, JHEP 1005 (2010) 032

Let's compare to p+Pb data again…

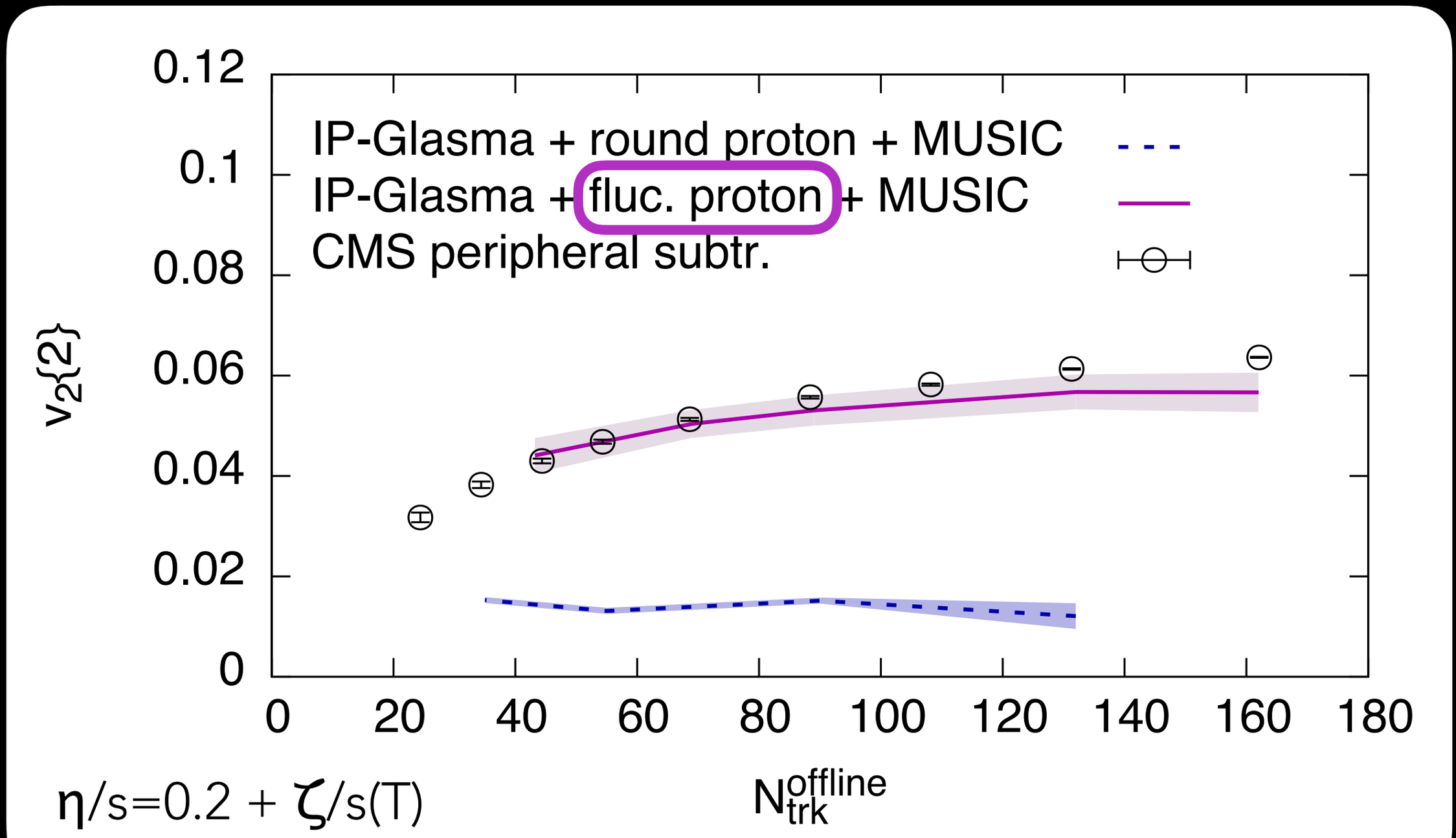
B. Schenke, R. Venugopalan, Phys. Rev. Lett. 113, 102301 (2014)



Experimental data: CMS Collaboration, Phys.Lett. B724, 213 (2013)

Effect of proton shape fluctuations

B. Schenke, R. Venugopalan, Phys. Rev. Lett. 113, 102301 (2014)
H. Mäntysaari, P. Tribedy, B. Schenke, C. Shen, in preparation (2017)



Experimental data: CMS Collaboration, Phys.Lett. B724, 213 (2013)

Subnucleonic fluctuations in large nuclei

H. Mäntysaari, B. Schenke, arXiv:1703.09256

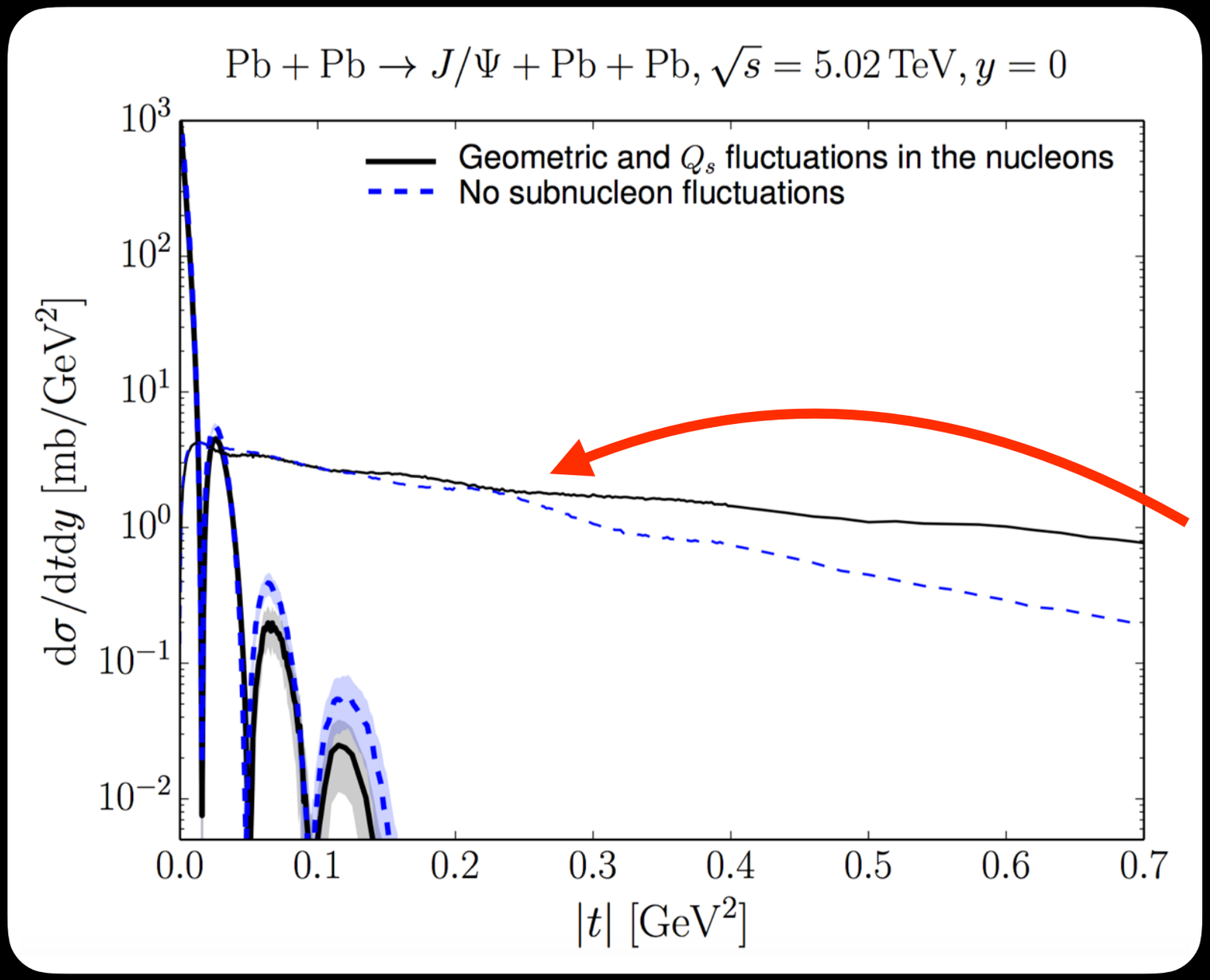
UltraPeripheral heavy ion Collisions (UPC)
At $|b_T| > 2R_A$ one nucleus acts as a photon source

Two sources of fluctuations:
Sample nucleon positions from Woods-Saxon
Sample constituent quark structure for each nucleon

We use the IPsat model for this analysis

Subnucleonic fluctuations in large nuclei

H. Mäntysaari, B. Schenke, arXiv:1703.09256

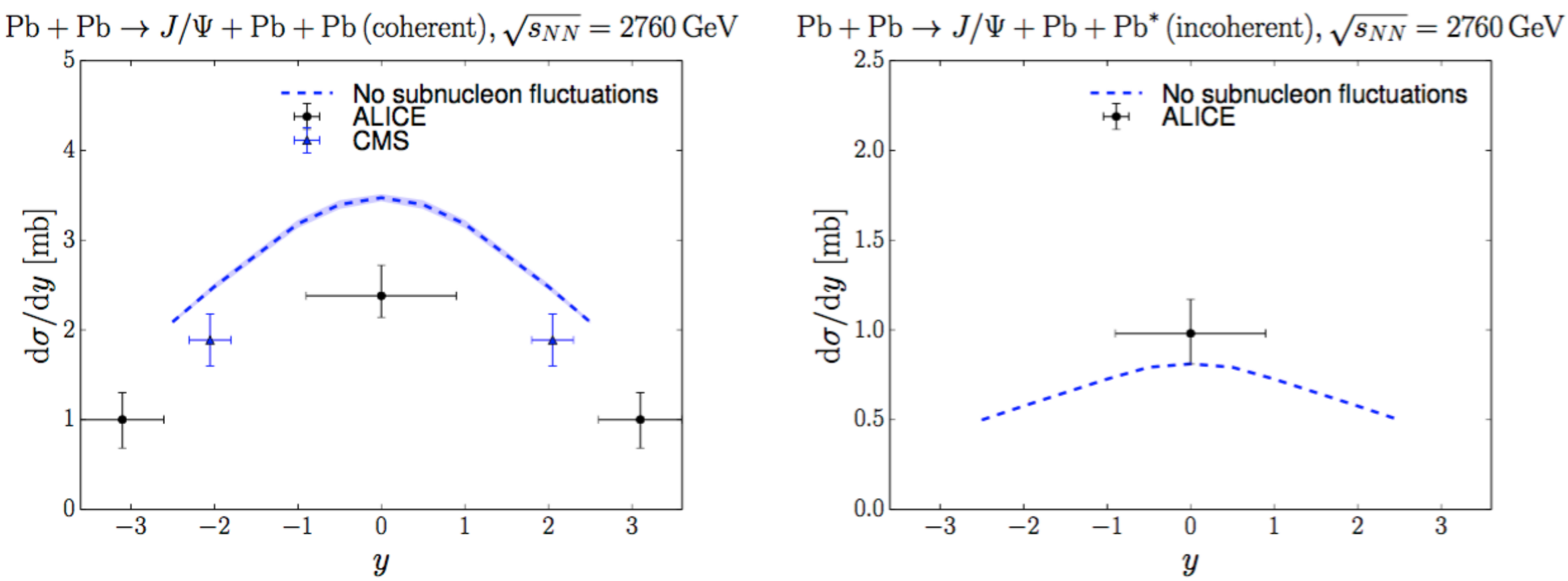


- Small |t|: fluctuations of nucleon positions
- Large |t|: fluctuations at subnucleon scale
- Incoherent slope changes at $|t| \approx 0.25$ GeV^2 → 0.4 fm which is size of hot spots

Coherent: thick lines
Incoherent: thin lines

LHC data - no subnucleonic fluctuations

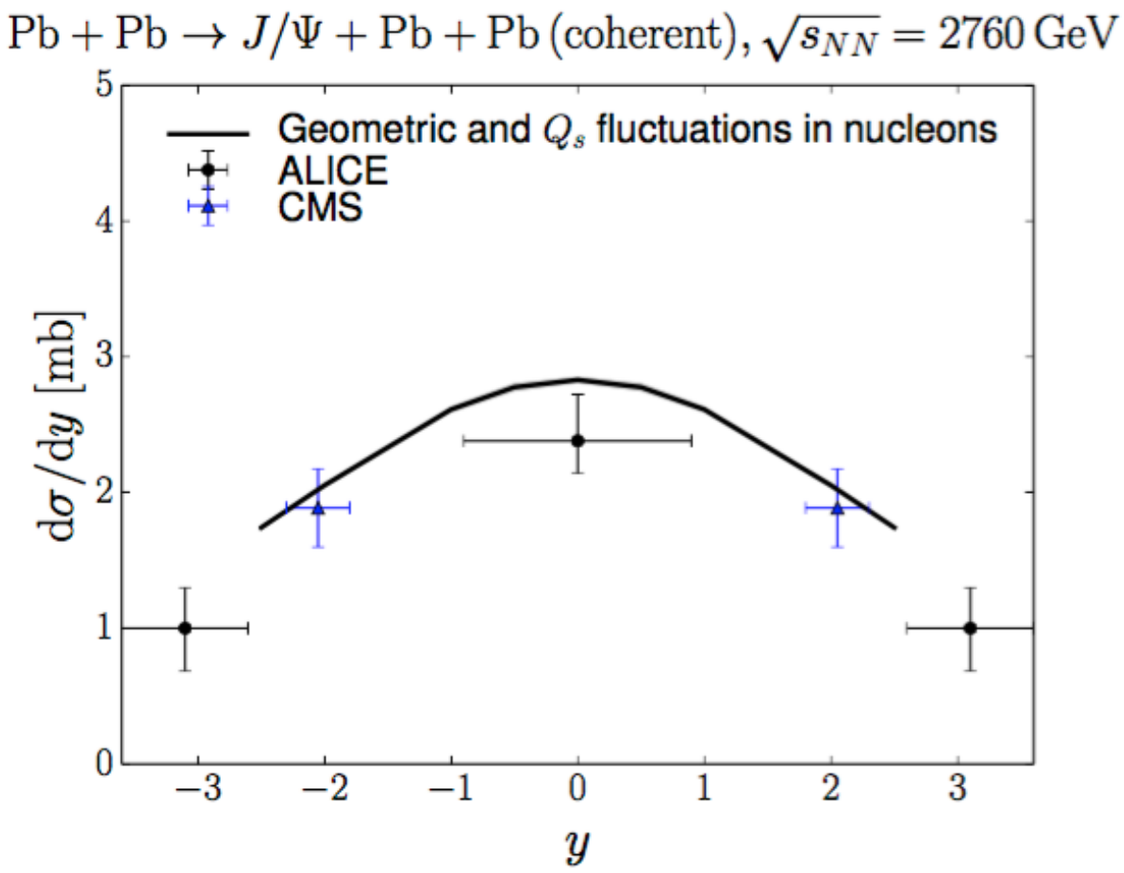
H. Mäntysaari, B. Schenke, arXiv:1703.09256

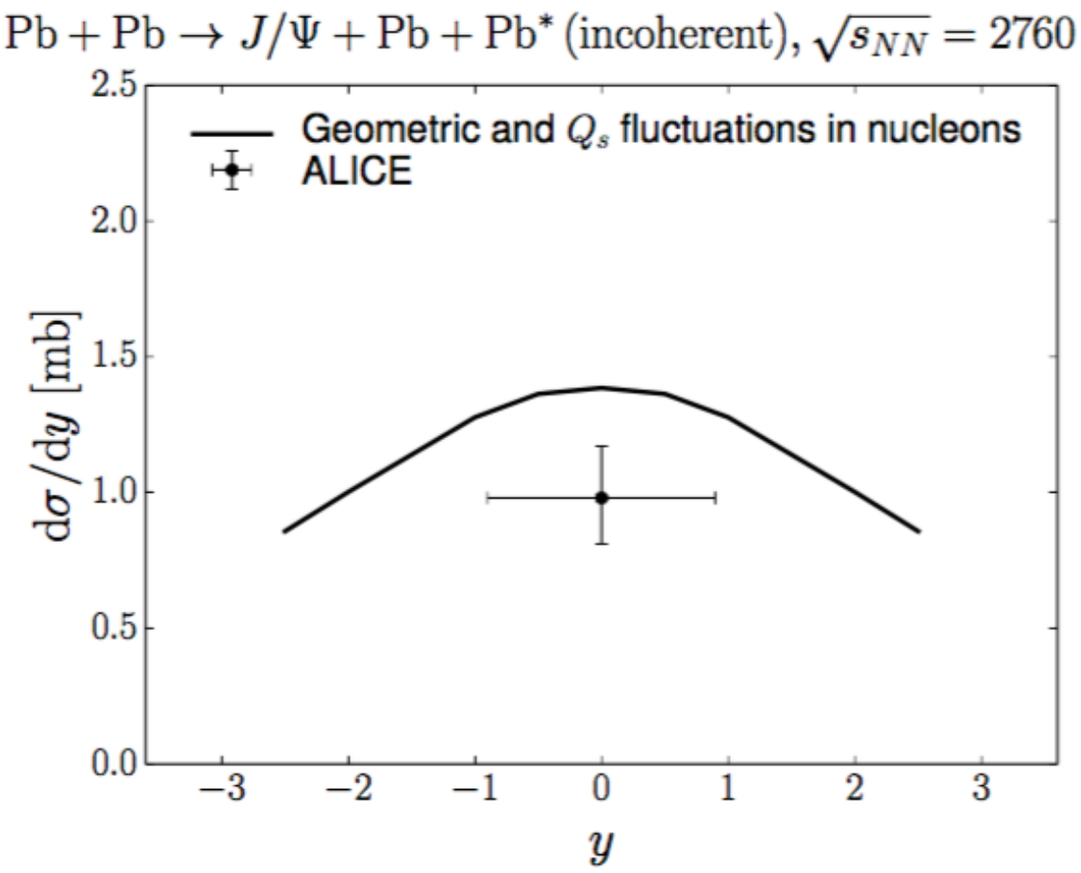


- Only fluctuations of nucleon positions
- Coherent cross section overestimated, incoherent underestimated
- ~ 20-30% normalization uncertainty from the J /Ψ wave function

LHC data - with subnucleonic fluctuations

H. Mäntysaari, B. Schenke, arXiv:1703.09256

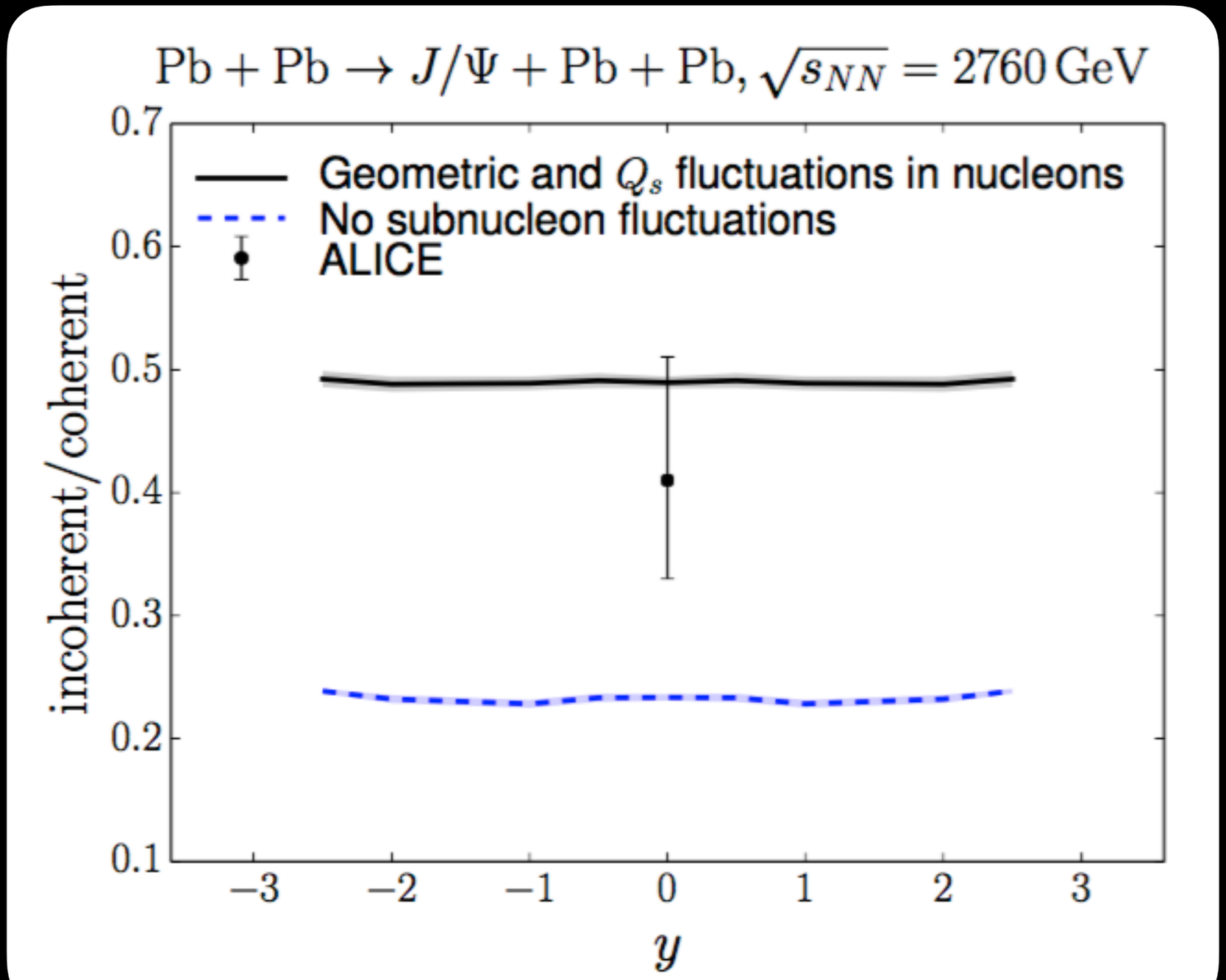




- Same subnucleonic fluctuations as used for protons earlier
- Both cross sections slightly above the data
- ~ 20-30% normalization uncertainty from the J /Ψ wave function

Ratio incoherent/coherent cross sections

H. Mäntysaari, B. Schenke, arXiv:1703.09256



JIMWLK evolution

Replace parametrized x-dependence by renormalization group equation for x-dependence of probability distribution of Wilson lines

$$\partial_y W_y[V(\vec{x})] = \mathcal{H} W_y[V(\vec{x})]$$

with the JIMWLK Hamiltonian

$$\mathcal{H} = -\frac{1}{2}\frac{\alpha_s}{\pi^2}\int_{\vec{x}\vec{y}\vec{z}} \frac{\delta}{\delta A^{c+}(\vec{x})}\left[(1 - V^\dagger(\vec{x})V(\vec{z}))^{ca}(1 - V^\dagger(\vec{y})V(\vec{z}))^{ba}\right.$$
$$\left.\times \frac{(\vec{x}-\vec{z})\cdot(\vec{y}-\vec{z})}{(\vec{x}-\vec{z})^2(\vec{y}-\vec{z})^2}\frac{\delta}{\delta A^{b+}(\vec{y})} W_y[V]\right]$$

J. Jalilian-Marian, A. Kovner, A. Leonidov, H. Weigert, Nucl. Phys. B504, 415 (1997), Phys. Rev. D59, 014014 (1999)
E. Iancu, A. Leonidov, and L. D. McLerran, Nucl. Phys. A692, 583 (2001)
E. Ferreiro, E. Iancu, A. Leonidov, and L. McLerran, Nucl. Phys. A703, 489 (2002)
A. H. Mueller, Phys. Lett. B523, 243 (2001)

Numerical JIMWLK implementation

H. Weigert, Nucl. Phys. A 703, 823 (2002).
T. Lappi and H. Mantysaari, Eur. Phys. J. C 73, 2307 (2013)

Langevin formulation

$$V_{\mathbf{x}}(Y+dY) = \exp\left\{-i\frac{\sqrt{\alpha_s dY}}{\pi}\int_{\mathbf{z}} K_{\mathbf{x}-\mathbf{z}}\cdot(V_{\mathbf{z}}\boldsymbol{\xi}_{\mathbf{z}}V_{\mathbf{z}}^{\dagger})\right\}$$

$$\times V_{\mathbf{x}}(Y)\exp\left\{i\frac{\sqrt{\alpha_s dY}}{\pi}\int_{\mathbf{z}} K_{\mathbf{x}-\mathbf{z}}\cdot\boldsymbol{\xi}_{\mathbf{z}}\right\}$$

$\boldsymbol{\xi}$ is Gaussian noise with zero average and

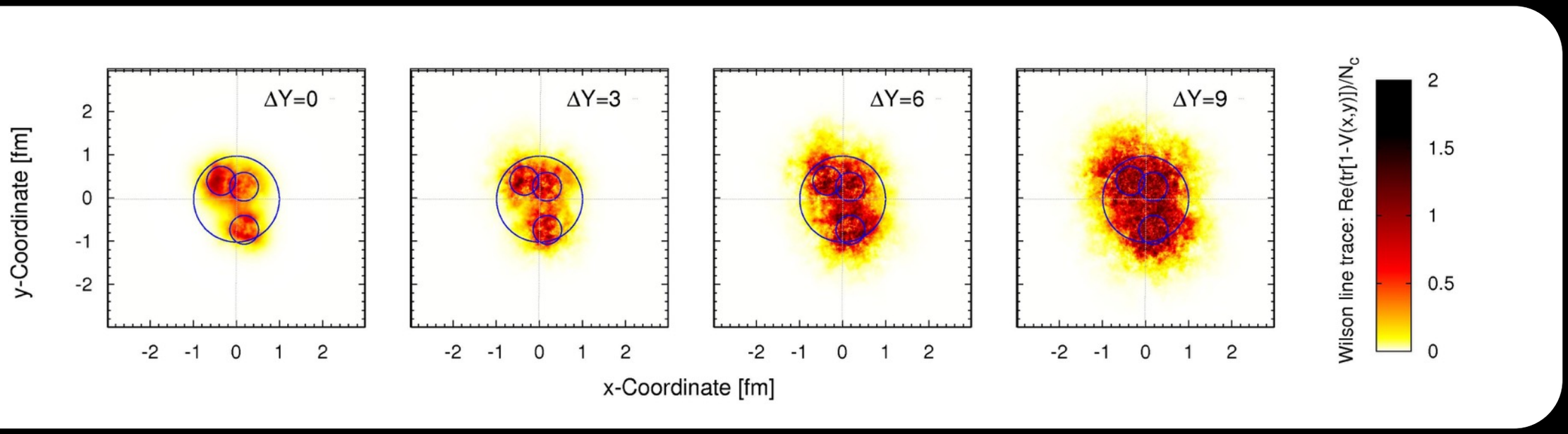
$$\left\langle \xi^a_{\mathbf{x},i}(Y)\xi^b_{\mathbf{y},j}(Y')\right\rangle = \delta^{ab}\delta^{ij}\delta^{(2)}_{\mathbf{xy}}\delta(Y-Y')$$

The JIMWLK Kernel is modified to avoid infrared tails:

$$K^{\mathrm{mod}}_{\mathbf{x}-\mathbf{z}} = m|\mathbf{x}-\mathbf{z}|K_1(m|\mathbf{x}-\mathbf{z}|)\frac{\mathbf{x}-\mathbf{z}}{(\mathbf{x}-\mathbf{z})^2}$$

Shape evolution of the proton

decreasing x, increasing energy



S. Schlichting, B. Schenke, Phys. Lett. B739, 313-319 (2014)

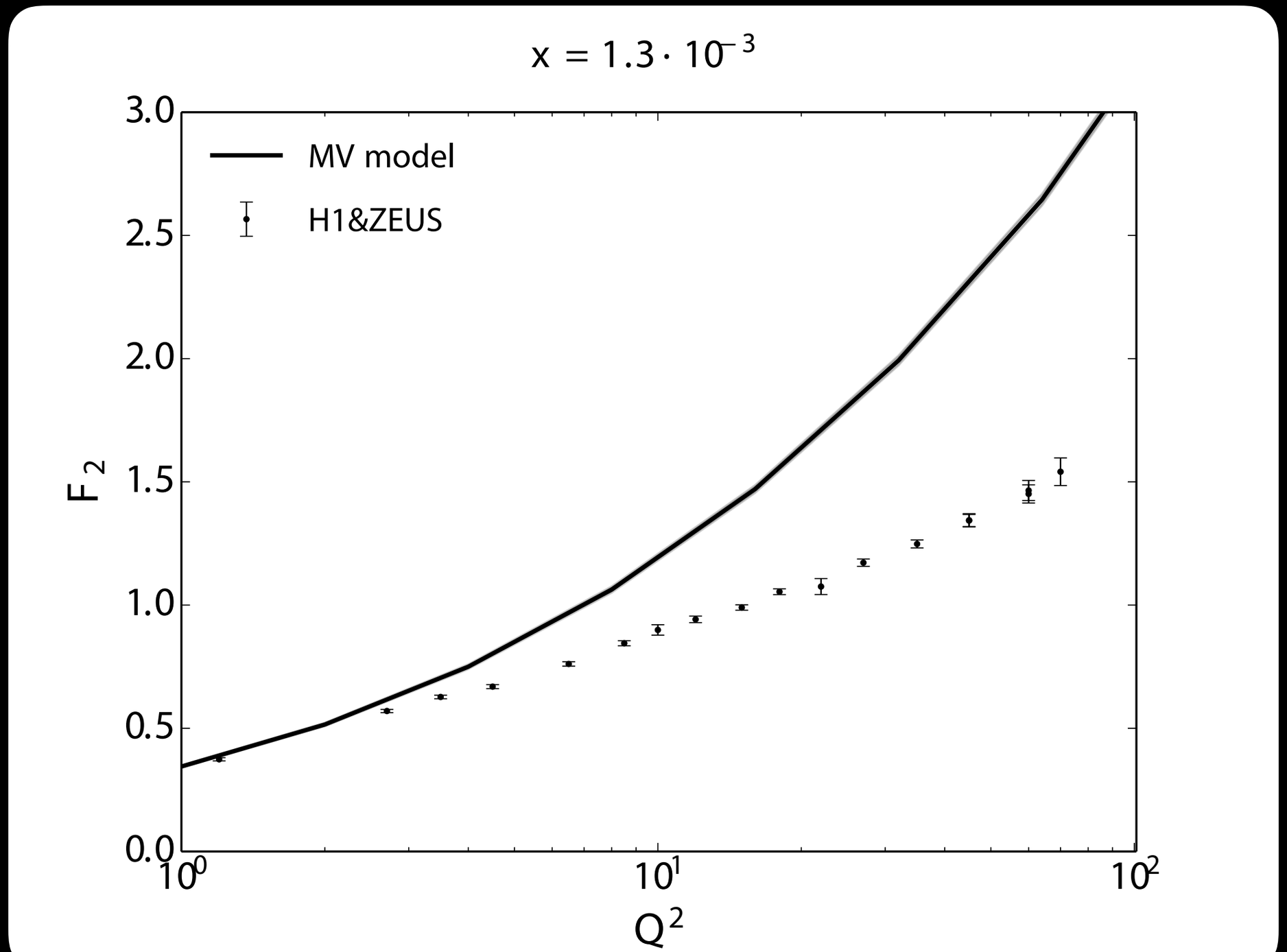
Proton grows with increasing x

Growth is linear with Y when infrared regulator is used

Froissart bound not violated

Q^2 dependence of F_2

H. Mäntysaari, B. Schenke, in preparation



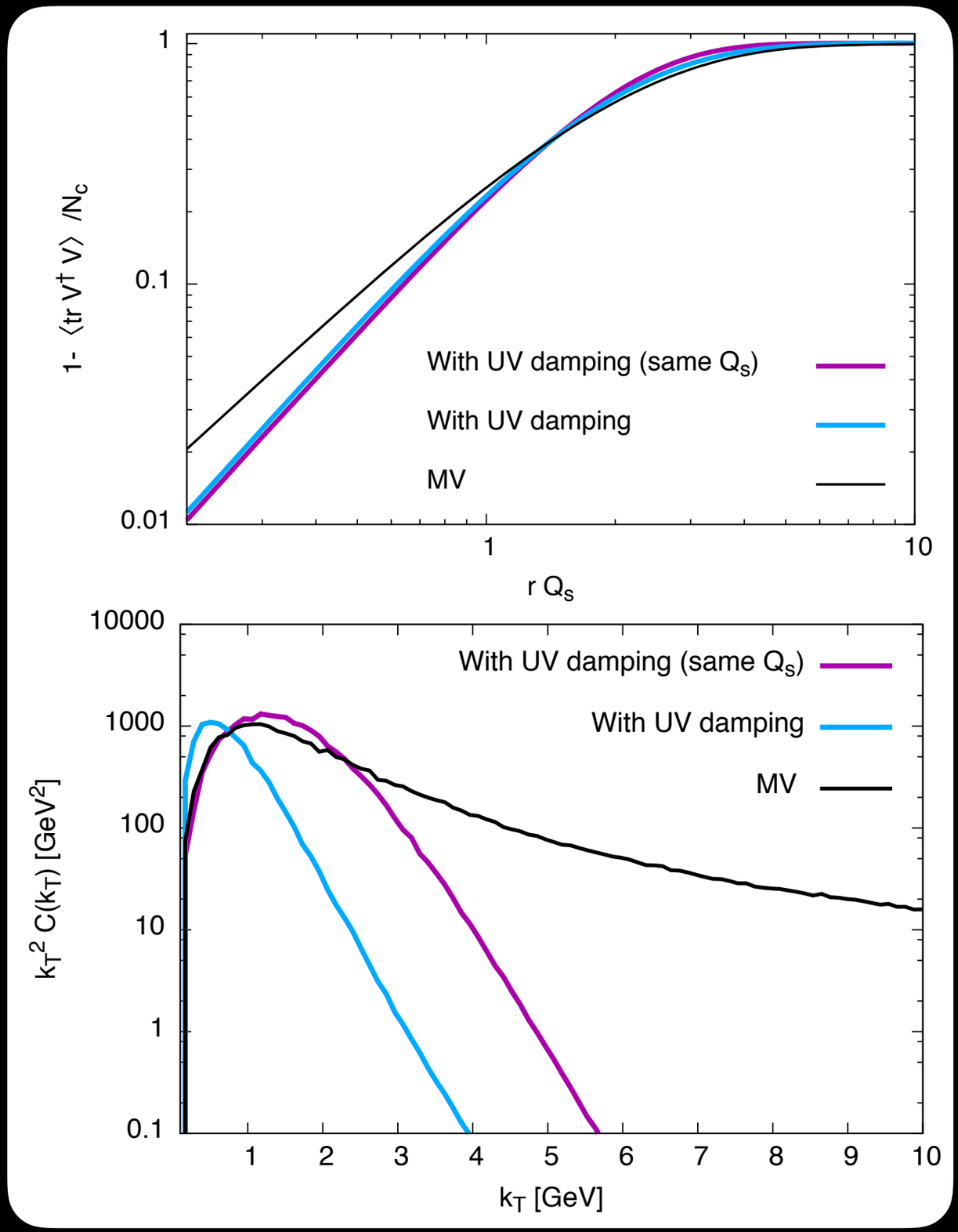
Modifying MV - changing the large k_T tails

H. Mäntysaari, B. Schenke, in preparation

Introduce a UV cutoff:
Filter out high frequency modes in the color charge distribution using FT with exp(- # k_T)

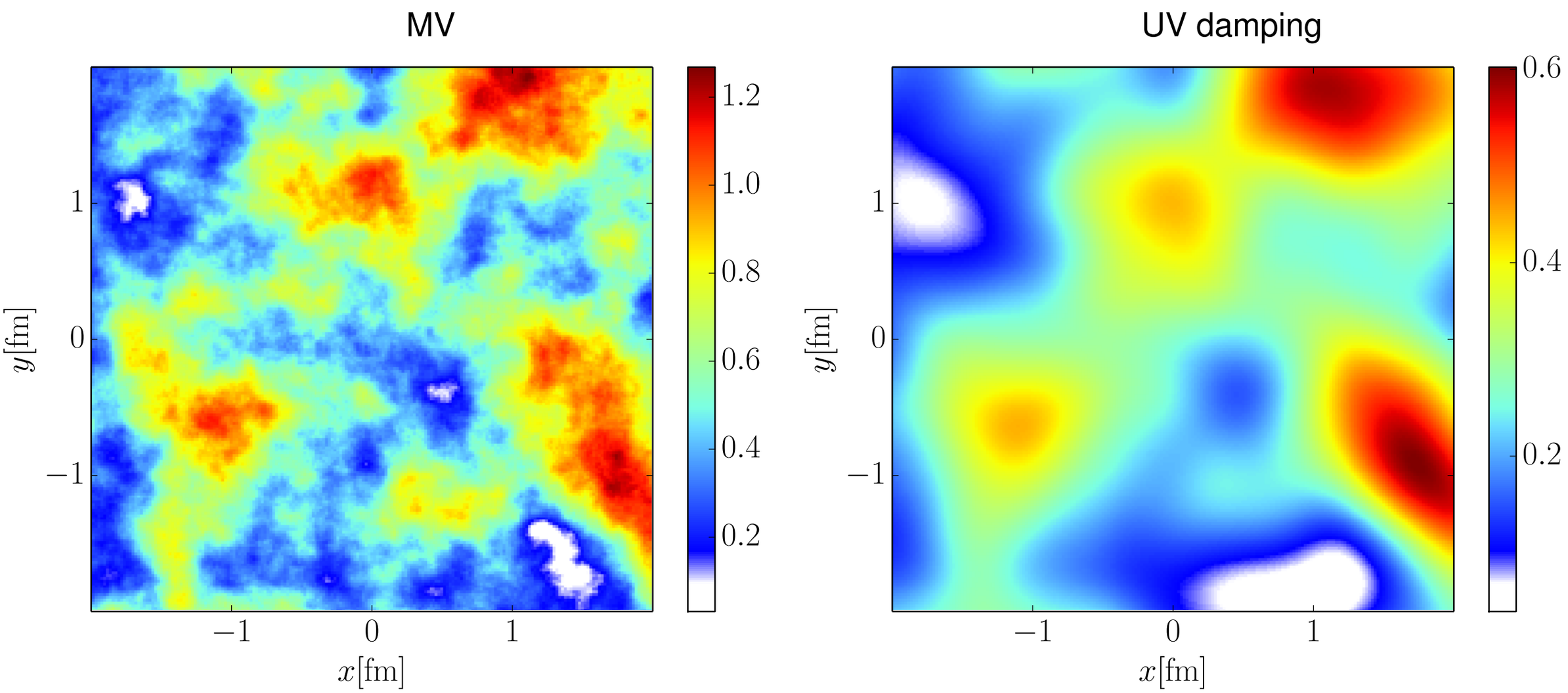
Has similar effect as anomalous dimension in AAMQS

J. L. Albacete, N. Armesto, J.G. Milhano, P. Quiroga Arias, C.A. Salgado
Eur.Phys.J. C71 (2011) 1705



Modifying MV - changing the large k_T tails

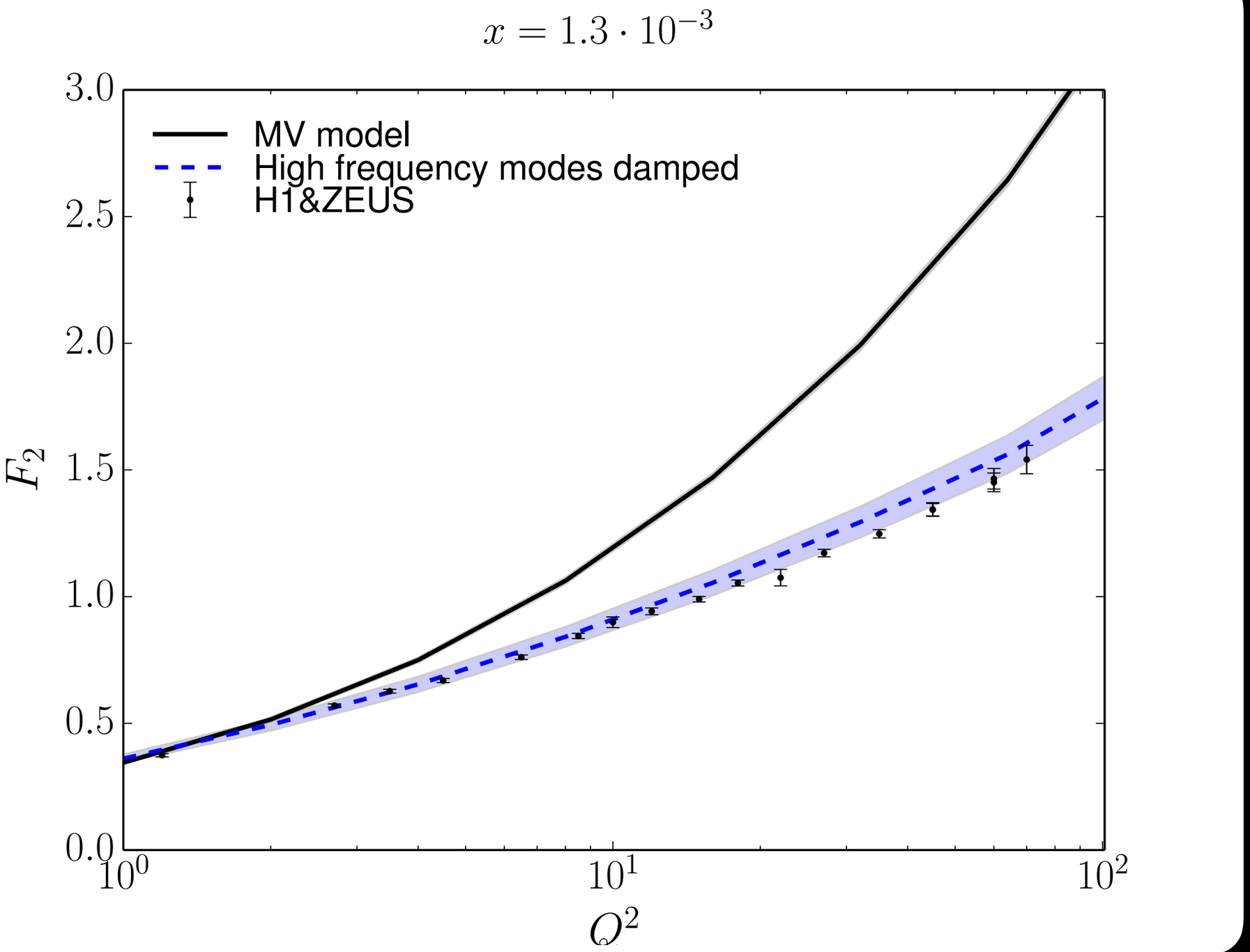
H. Mäntysaari, B. Schenke, in preparation



$$\mathrm{Re}[\mathrm{Tr}(1 - V(\vec{x}))]/N_c$$

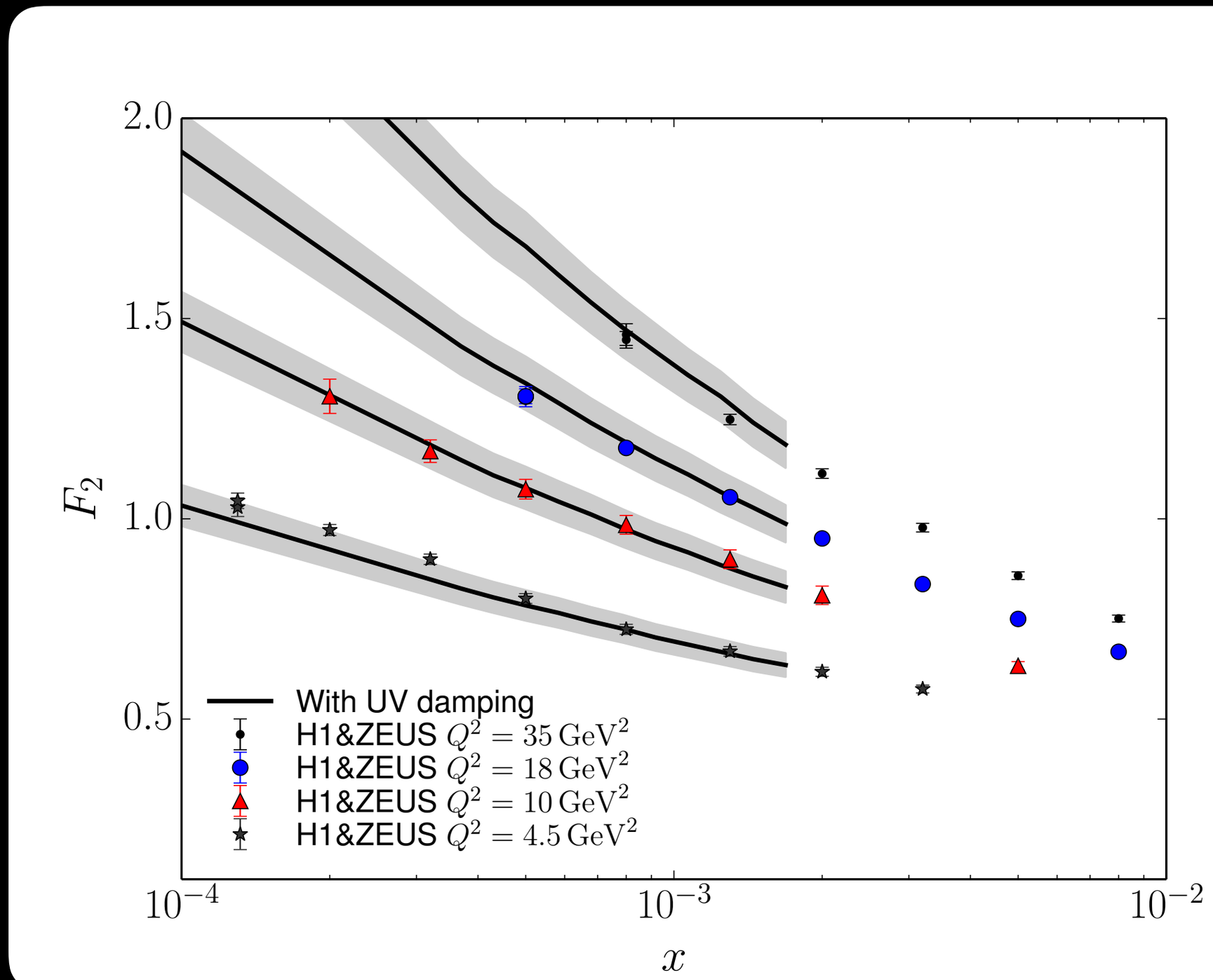
Q^2 dependence of F_2

H. Mäntysaari, B. Schenke, in preparation



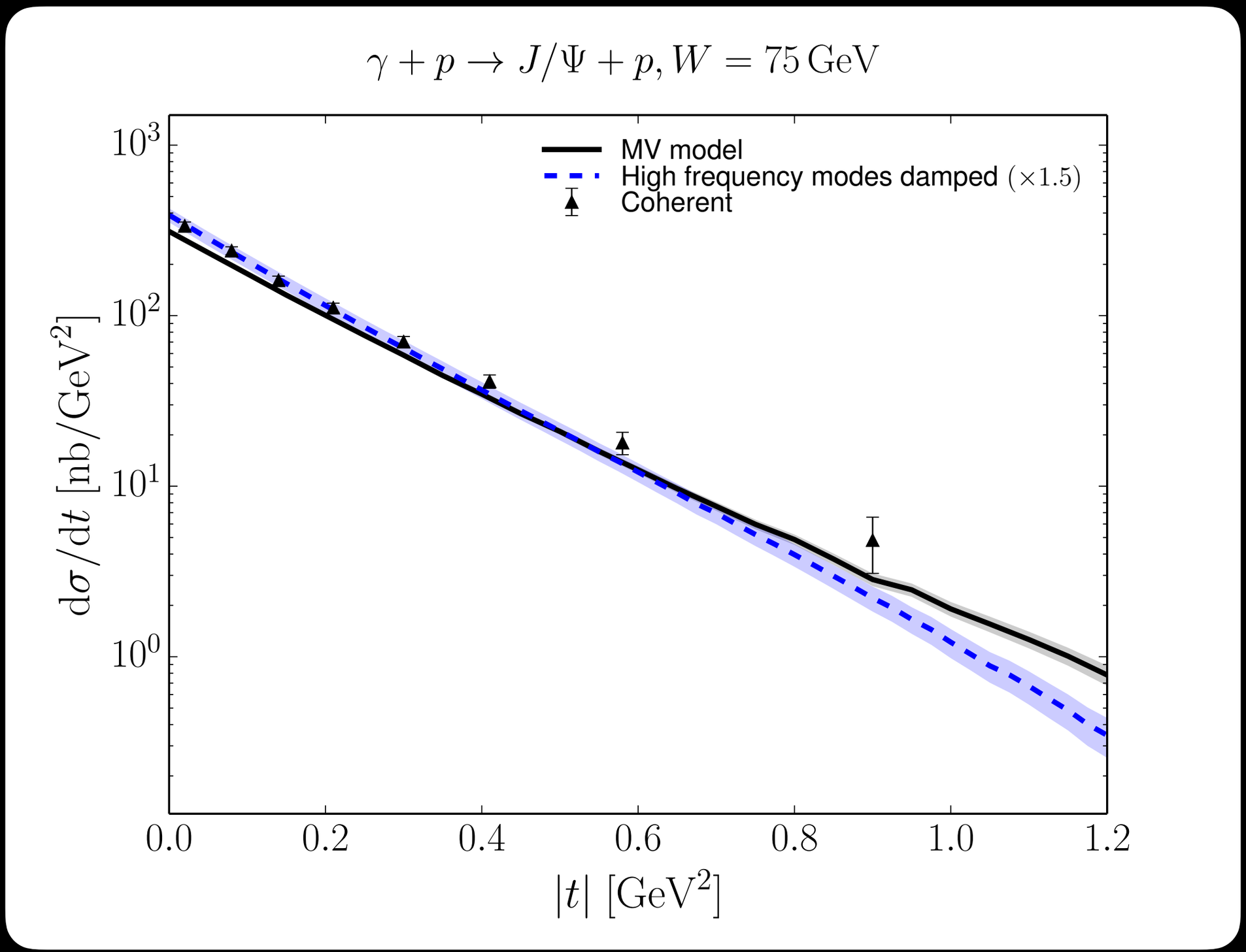
x dependence of F_2 from JIMWLK

H. Mäntysaari, B. Schenke, in preparation



Proton size constrained by diffractive data

H. Mäntysaari, B. Schenke, in preparation



Summary

- Shape fluctuations of the proton's gluon distribution are needed to describe incoherent diffractive vector meson data from HERA

- Constrained fluctuating proton shape compatible with anisotropic flow in p+Pb collisions

- Sub-nucleonic fluctuations also affect incoherent diffractive cross section in ultra-peripheral A+A collisions

- Next step: Go from IPsat to explicit JIMWLK evolution and describe F_2 and diffractive data - Modification of MV initial condition necessary

BACKUP

Why a variance?

H. I. Miettinen and J. PumpLin, Phys. Rev. D18 (1978) 1696

Simple model: Target particle → average optical potential

$$|B\rangle = \sum_k C_k |\psi_k\rangle$$

beam particle

linear comb. of diffractive eigenstates

$$ImT\,|\psi_k\rangle = A_k |\psi_k\rangle$$

Imaginary part of scattering amplitude

Probability for Ψ_k to interact with target

$$\langle B|B\rangle = \sum_k |C_k|^2 = 1$$

Why a variance?

H. I. Miettinen and J. PumpLin, Phys. Rev. D18 (1978) 1696

Total diffractive cross section:

$$\frac{d\sigma_{\rm diff}}{d^2\vec{b}} = \sum_k |\langle\psi_k|ImT|B\rangle|^2 = \sum_k |C_k|^2 A_k^2 = \langle A^2\rangle$$

Elastic scattering amplitude:

$$\langle B|ImT|B\rangle = \sum_k |C_k|^2 A_k = \langle A\rangle$$

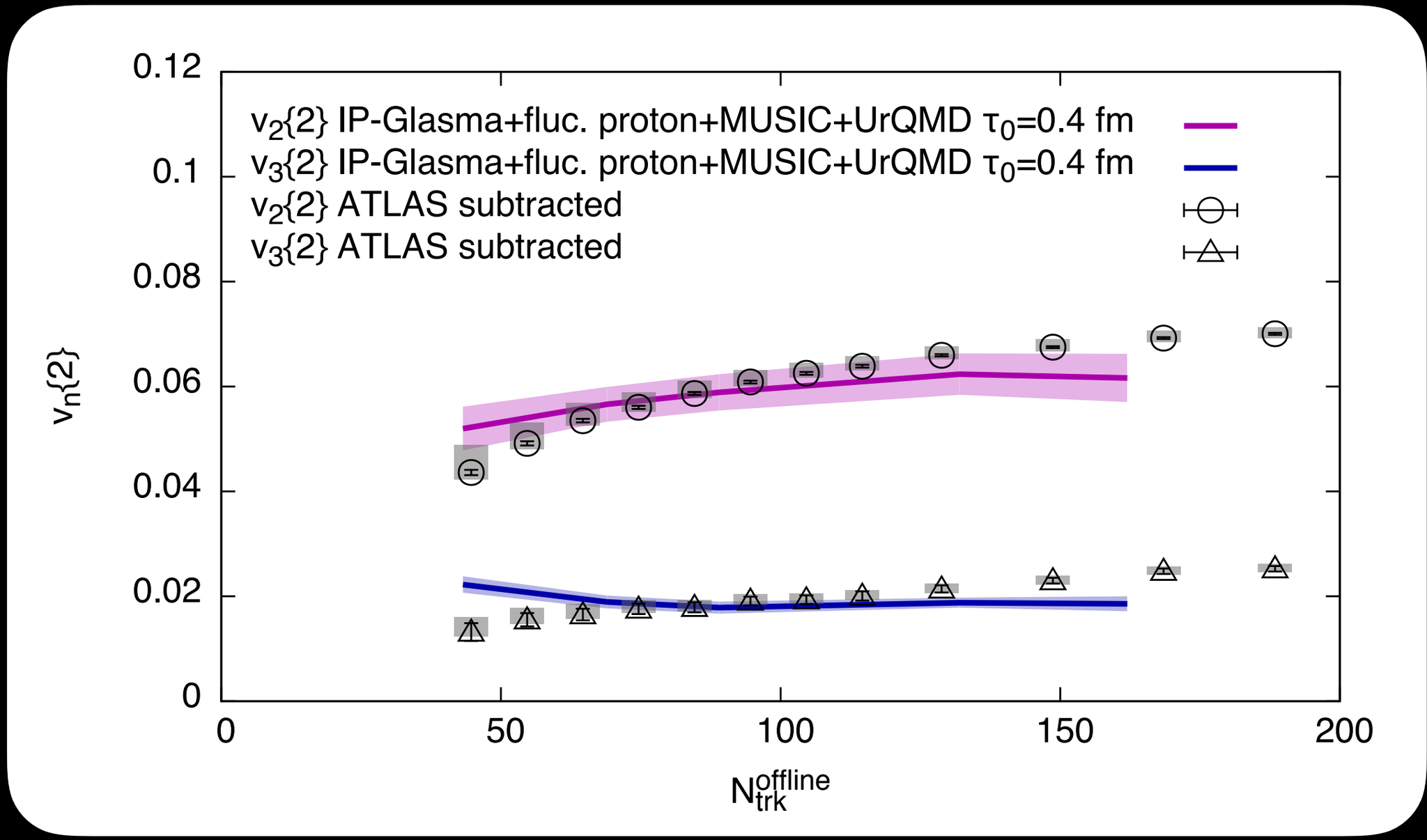
Average over absorption coefficients, weighted according to their probability of occurrence in the particle B

Elastic cross section: $\frac{d\sigma_{\rm el}}{d^2\vec{b}} = \langle A\rangle^2$

Inelastic diffractive cross section: $\frac{d\sigma_{\rm inel}}{d^2\vec{b}} = \langle A^2\rangle - \langle A\rangle^2$

Elliptic and triangular flow

H. Mäntysaari, P. Tribedy, B. Schenke, C. Shen, in preparation (2017)



v_2

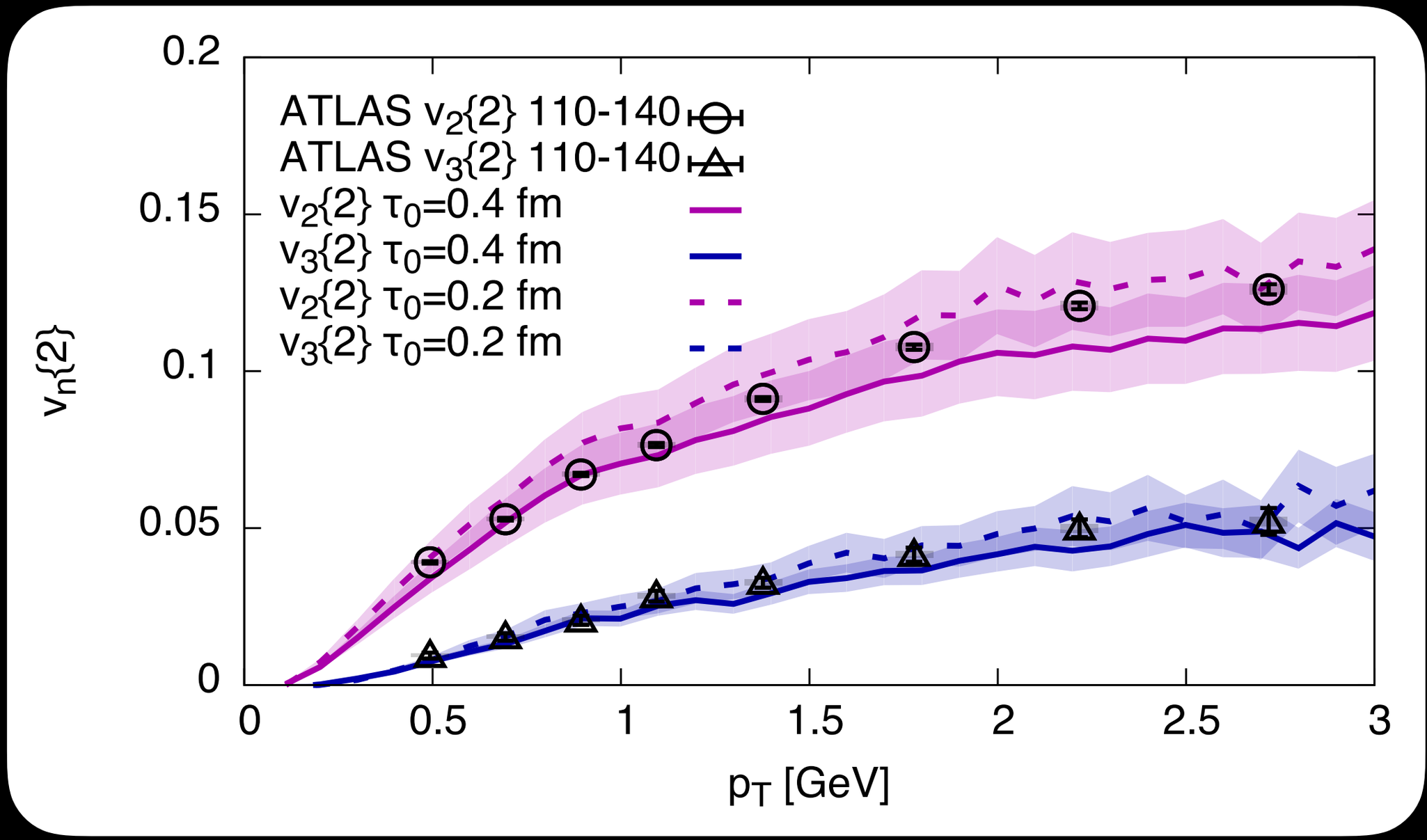
v_3

ATLAS Collaboration, Phys.Rev. C90 (2014) 044906

$\eta/s=0.2 + \zeta/s(T)$

Transverse momentum dependence

H. Mäntysaari, P. Tribedy, B. Schenke, C. Shen, in preparation (2017)



V_2

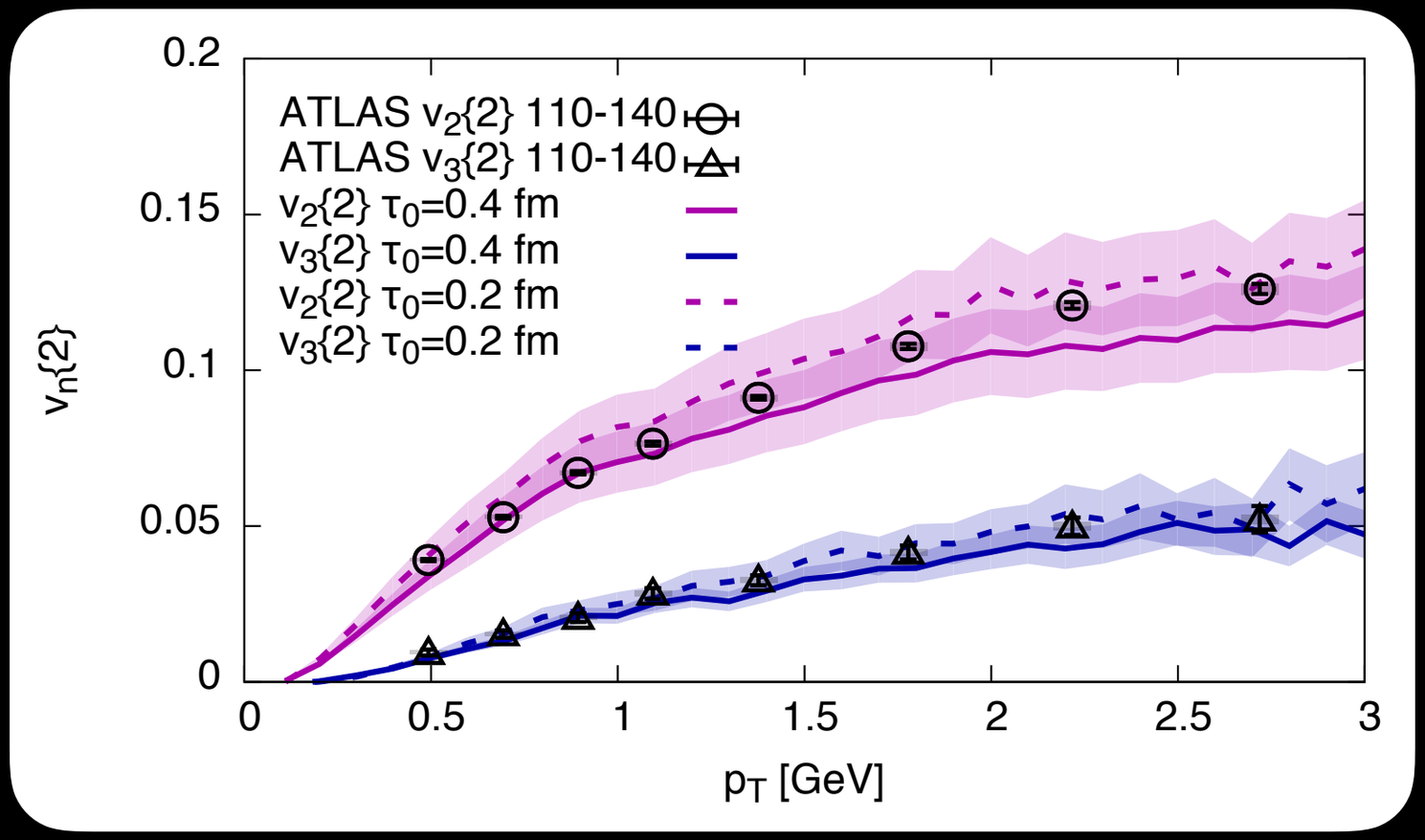
V_3

ATLAS Collaboration, Phys.Rev. C90 (2014) 044906

$\eta/s=0.2 + \zeta/s(T)$

Transverse momentum dependence

H. Mäntysaari, P. Tribedy, B. Schenke, C. Shen, in preparation (2017)



v_2

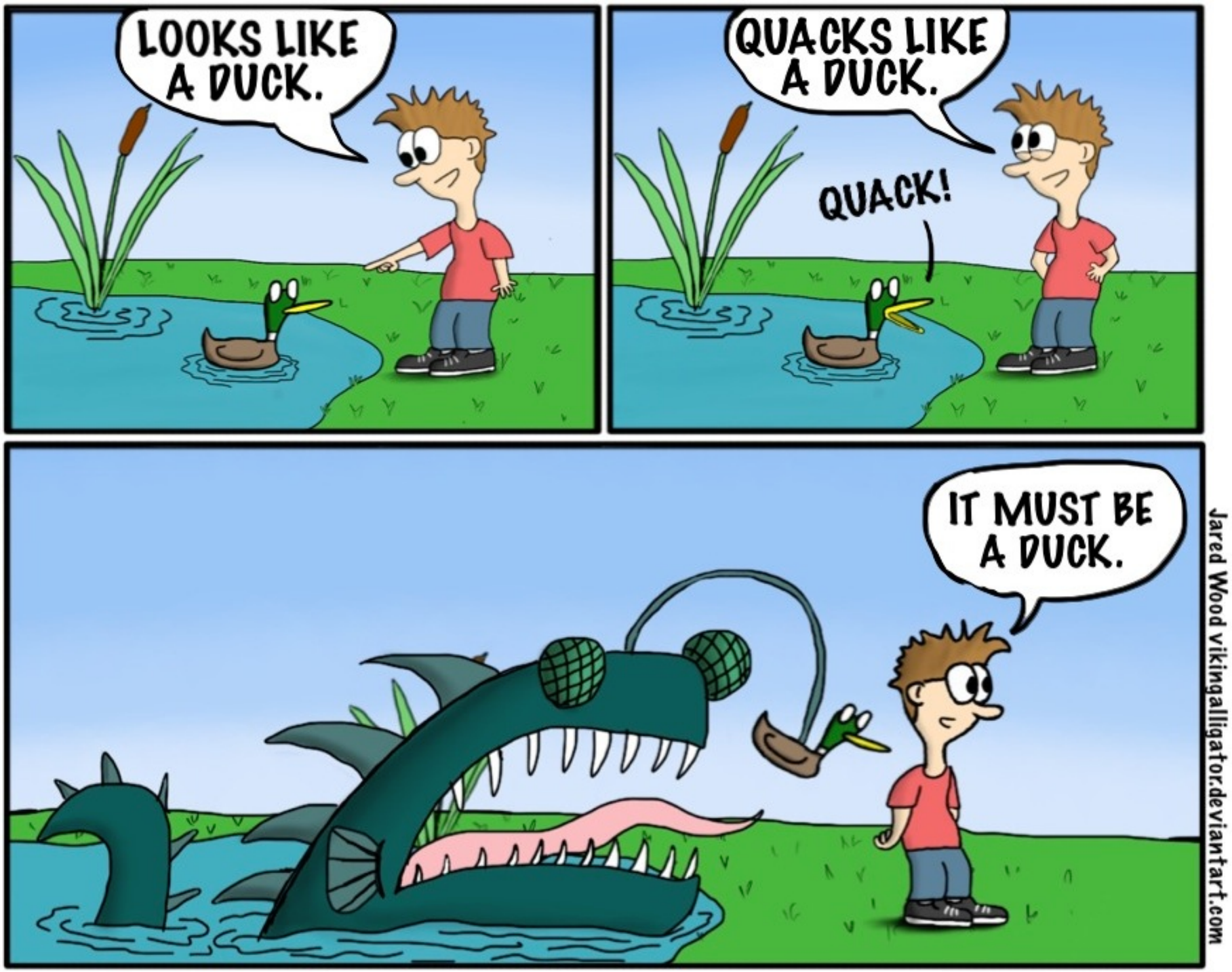
v_3

$\eta/s=0.2 + \zeta/s(T)$

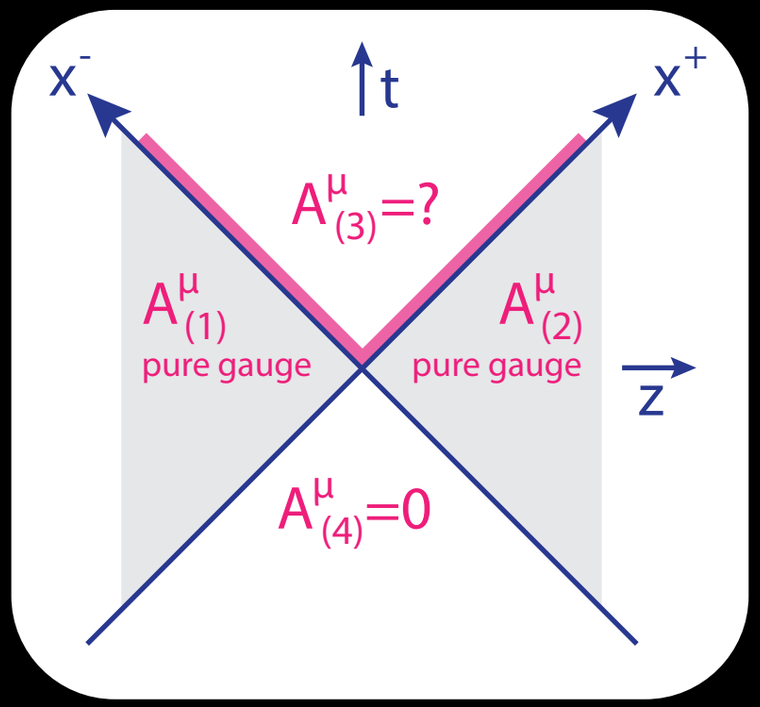
ATLAS Collaboration, Phys.Rev. C90 (2014) 044906

Fair warning: Strong dependence on whether initial shear stress tensor is included and the relaxation time. Viscous corrections can be very large

OTHER EXPLANATIONS



Backing up to the calculation of initial gluon fields



$$A^{i}_{(3)}|_{\tau=0^+} = A^{i}_{(1)} + A^{i}_{(2)}$$

$$A^{\eta}_{(3)}|_{\tau=0^+} = \frac{ig}{2}[A^{i}_{(1)}, A^{i}_{(2)}]$$

Now compute gluon momentum distributions from the fields in Coulomb gauge

Next we analyze the momentum distribution of the produced gluons

There is NO hydrodynamics in what follows, just Yang-Mills

Correlations from the initial state

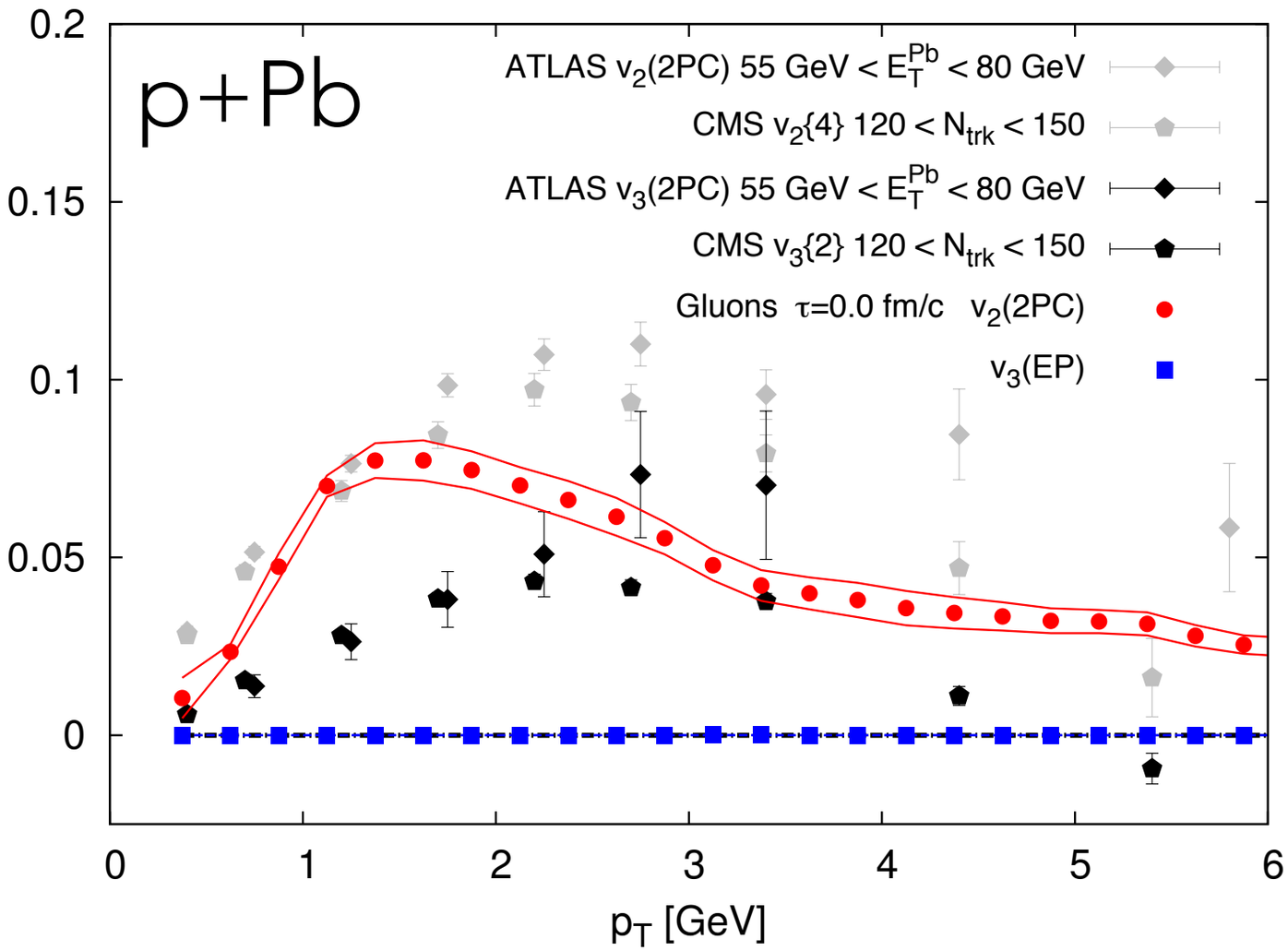
Schenke, Schlichting, Venugopalan, Phys. Lett. B747, 76-82 (2015)

τ=0.0 fm/c

gluons

v2 v3

Fourier harmonics *(event average)*



Significant v_2 at time 0

No odd harmonics for gluons without final state interactions

Correlations from the initial state

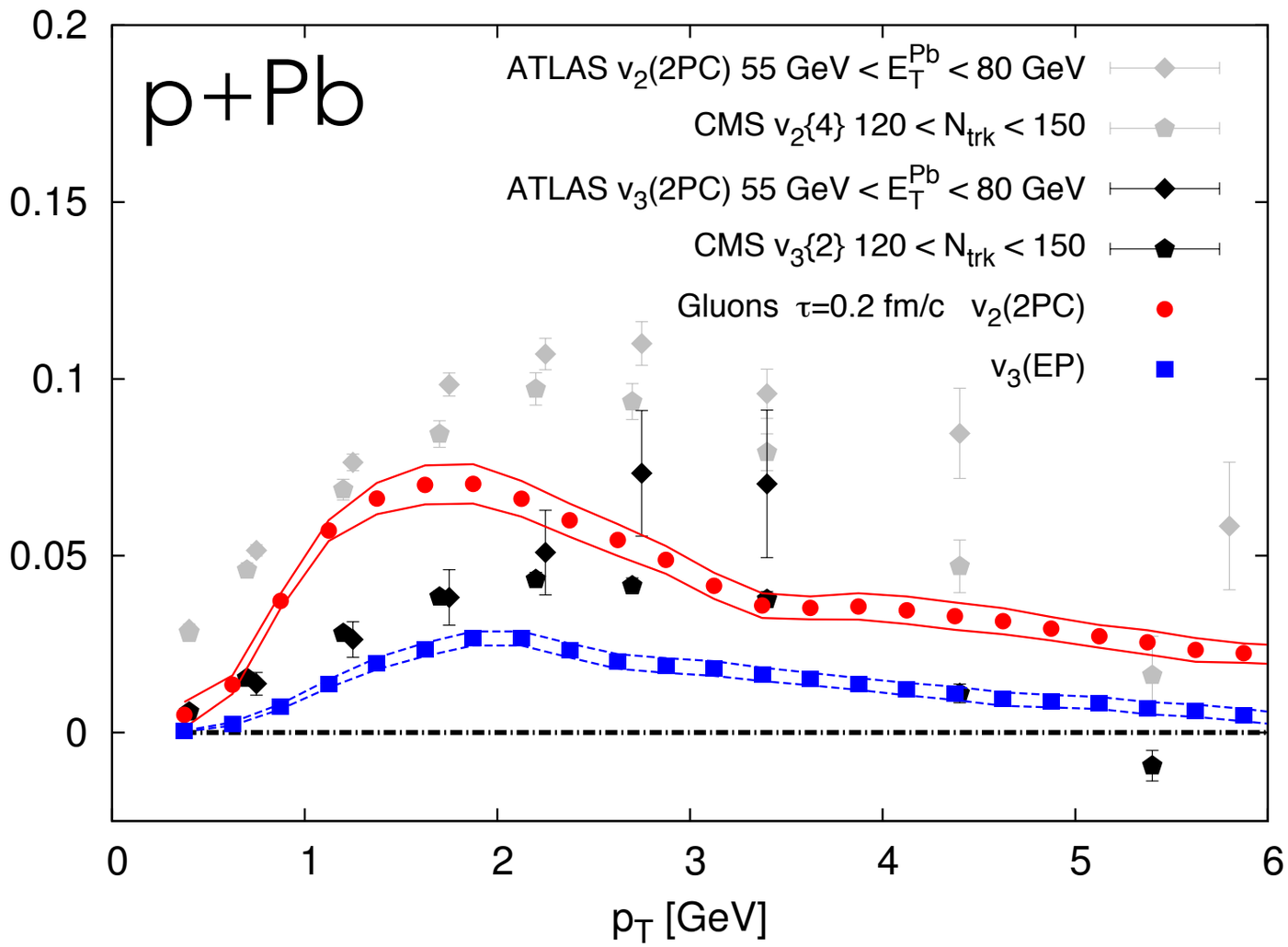
Schenke, Schlichting, Venugopalan, Phys. Lett. B747, 76-82 (2015)

τ=0.2 fm/c

gluons

V2 V3

Fourier harmonics *(event average)*



Correlations from the initial state

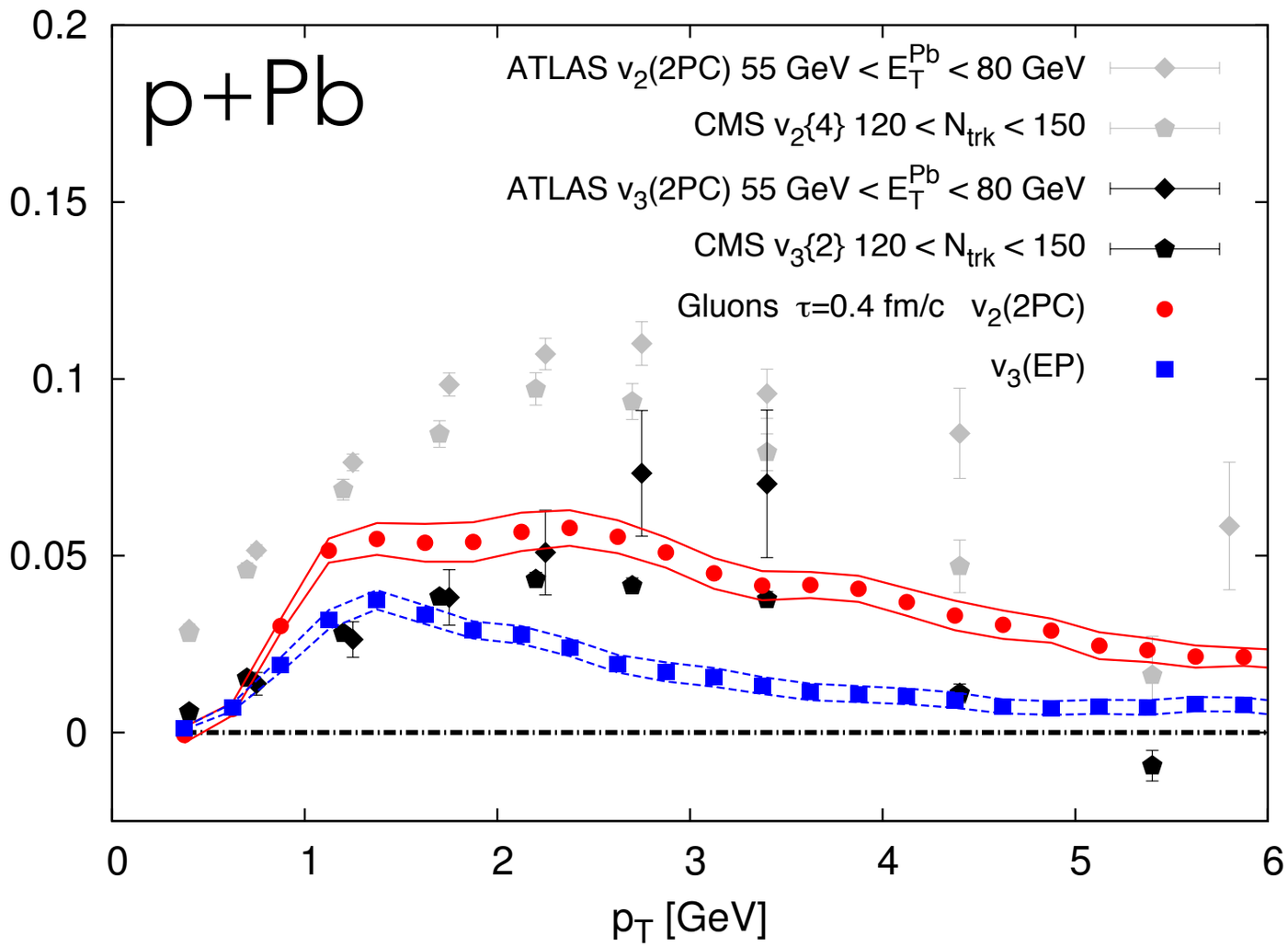
Schenke, Schlichting, Venugopalan, Phys. Lett. B747, 76-82 (2015)

τ=0.4 fm/c

gluons

V2 V3

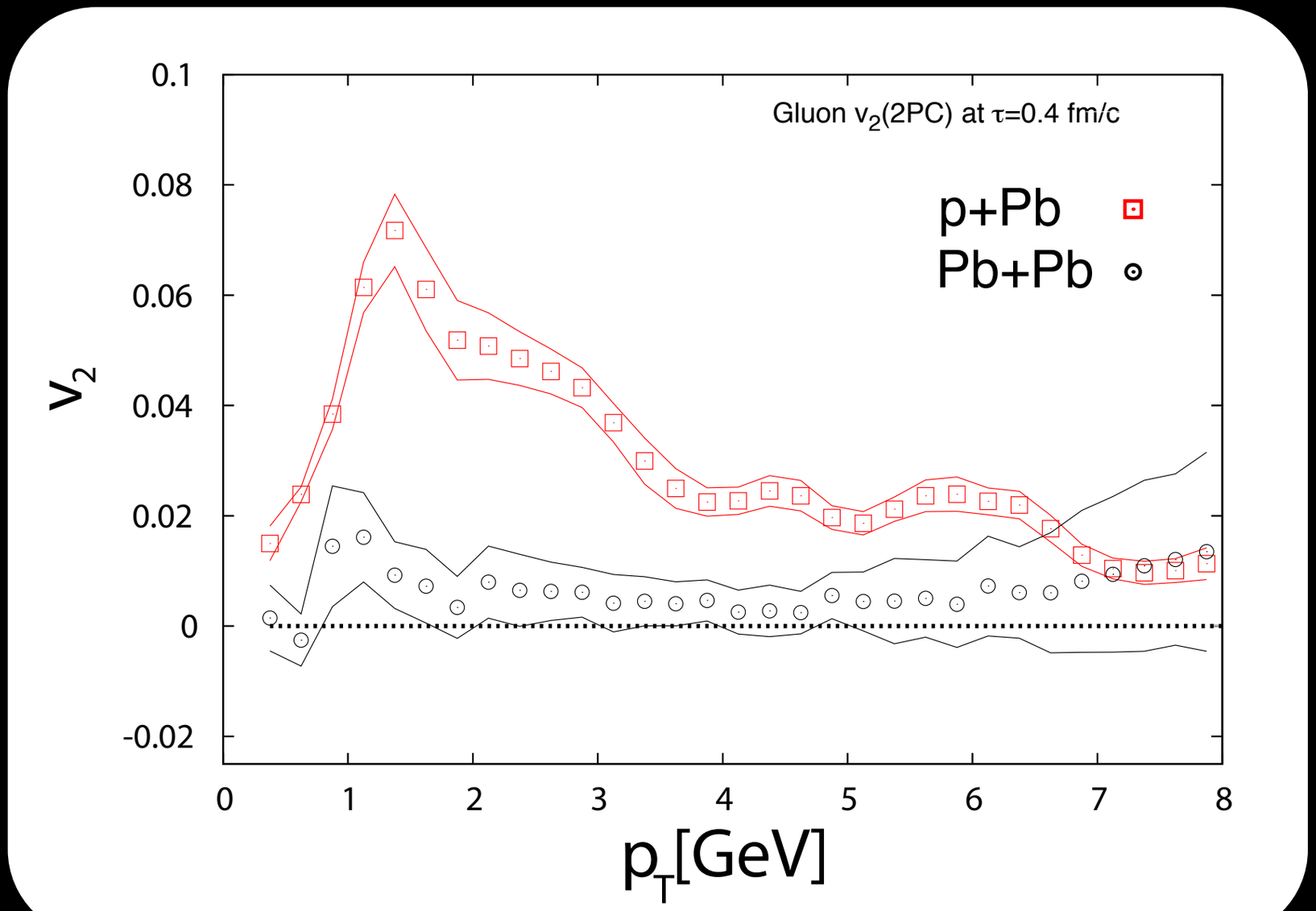
Fourier harmonics *(event average)*

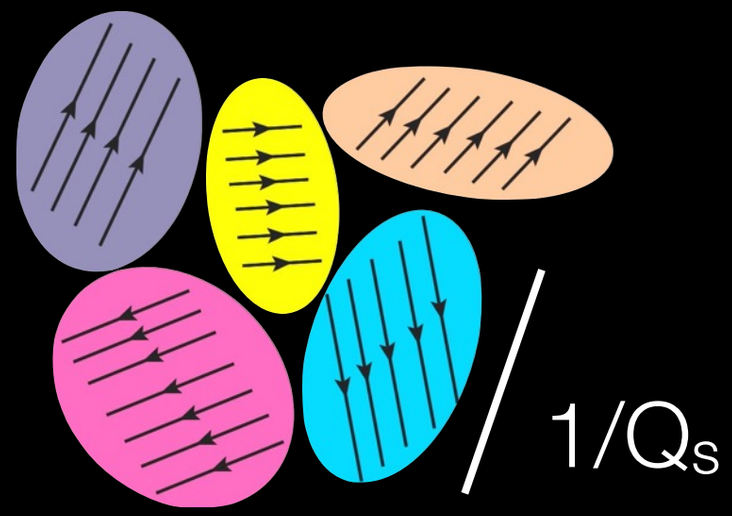


Odd harmonics generated by pre-equilibrium dynamics

Interpretation and system size dependence

Schenke, Schlichting, Venugopalan, Phys. Lett. B747, 76-82 (2015)





Pb+Pb not described in initial state picture. Reason:

Gluons produced from many uncorrelated color field domains

Collective flow in the final state is needed

Many calculations, different approximations

- **Glasma graph approximation:** only two gluon exchange and Gaussian statistics of color charge fluctuations
- **Non-linear Gaussian approximation:** Multi-gluon exchanges and Gaussian statistics
- **Numerical solution:** Solves Yang-Mills equations exactly as we did, includes multiple-gluon exchange, "rescattering"
- Some go beyond classical approximation by including **JIMWLK** evolution which will introduce some non-Gaussian correlations

They all find anisotropies without any hydrodynamics

Some are compared in

T. Lappi, B. Schenke, S. Schlichting, R. Venugopalan, JHEP 1601 (2016) 061

See the review article

K. Dusling, W. Li, B. Schenke, Int. J. Mod. Phys. E25, 1630002 (2016)

So what do we see?

1. Initial momentum correlations

or

2. A reflection of the initial geometry mediated by final state effects?

Observables to tell the difference

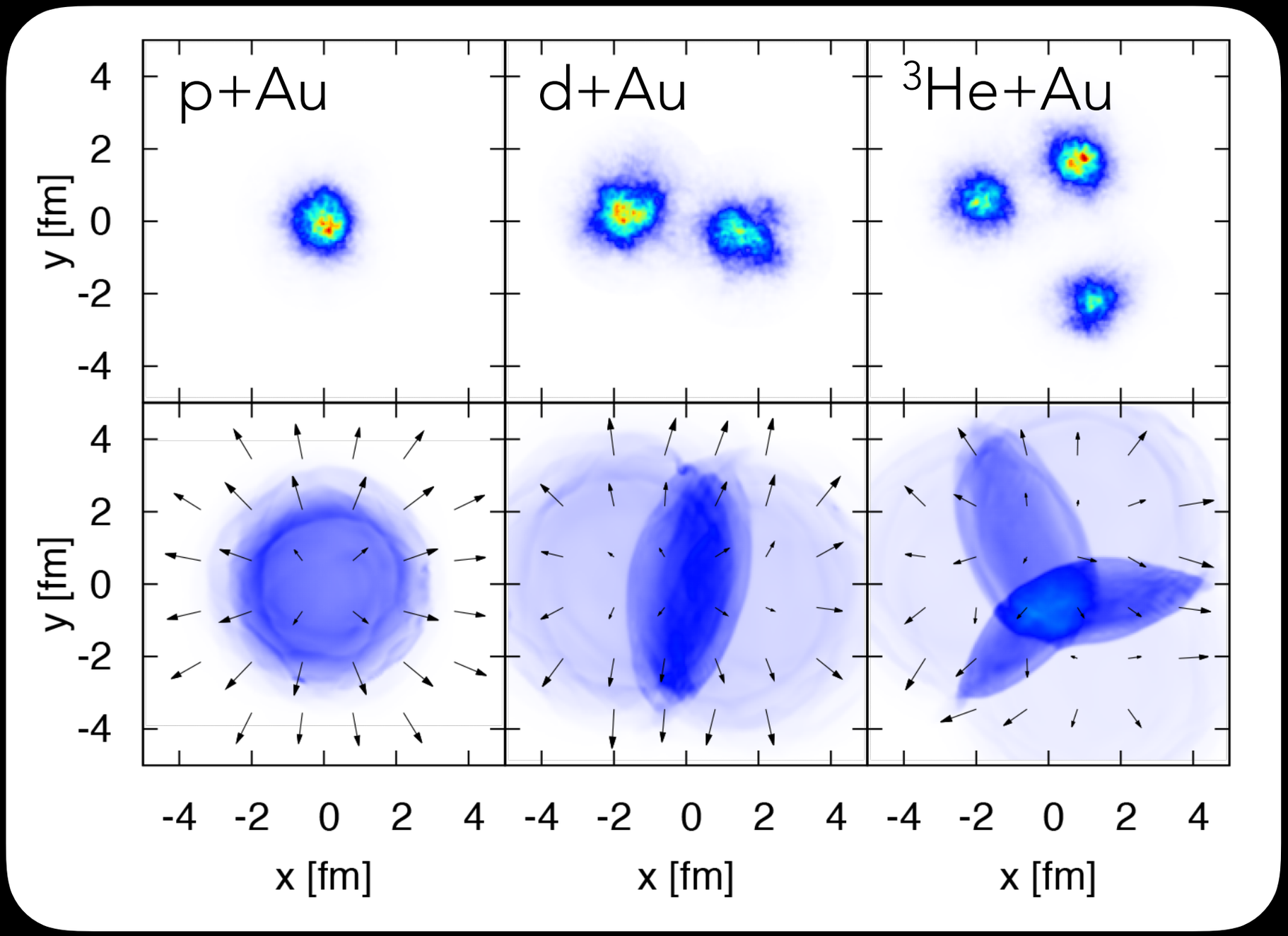
- Different collision systems
- Mass ordering
- Odd harmonics
- Beam energy dependence
- Jet quenching
- Electromagnetic probes
- Sign change of $c_2\{4\}$
- Multi particle (>2) cumulants

Observables to tell the difference

- Different collision systems
- Mass ordering
- Odd harmonics
- Beam energy dependence
- Jet quenching
- Electromagnetic probes
- Sign change of $c_2\{4\}$
- Multi particle (>2) cumulants

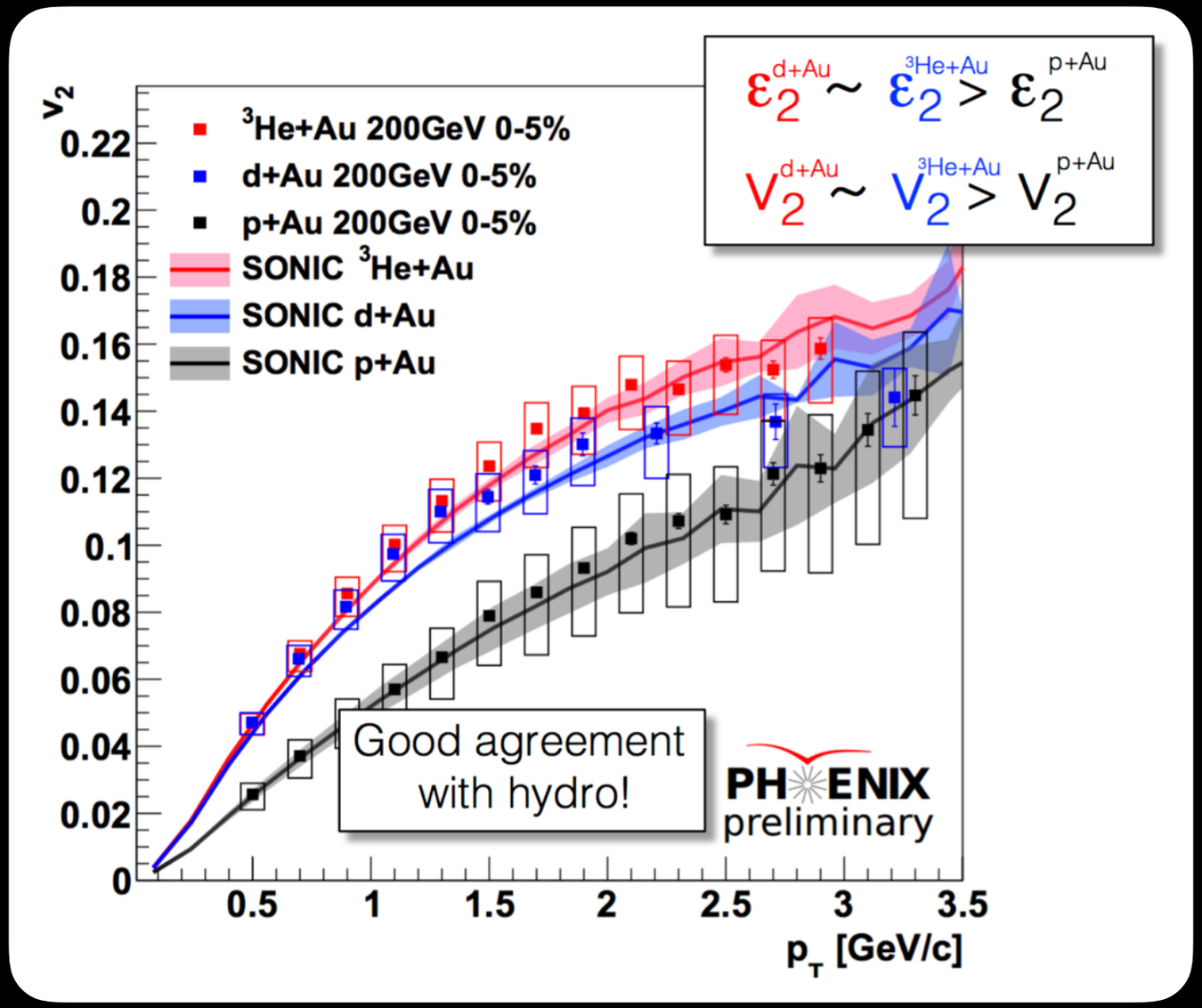
RHIC to the rescue: Different small systems

Different initial shapes lead to different flow harmonics



Different small systems

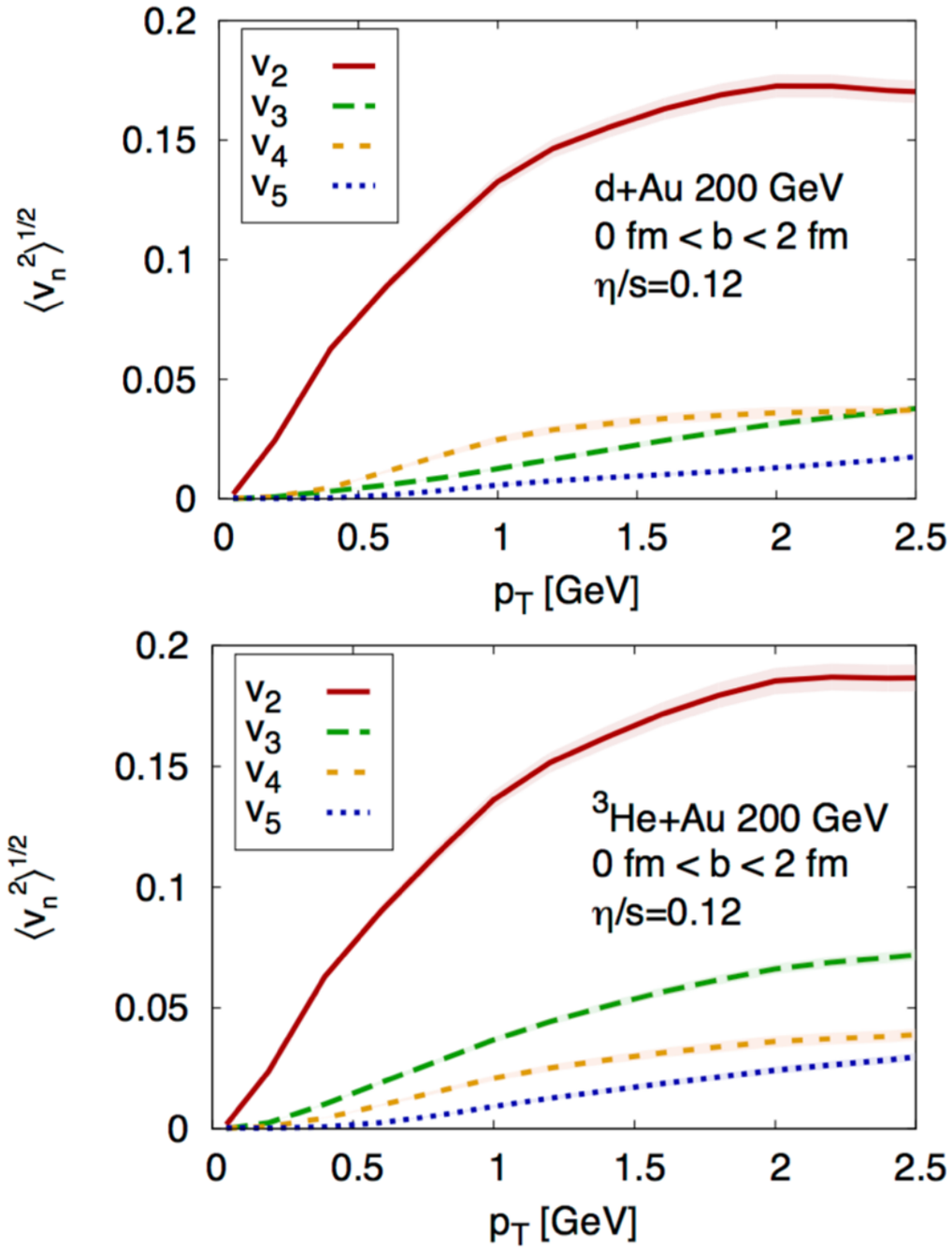
Different initial shapes lead to different flow harmonics



from Javier Orjuela-Koop
for the PHENIX Collaboration
at Initial Stages 2016

d+Au: PHENIX Collaboration, Phys.Rev.Lett. 114 (2015) 192301
^{3}He+Au: PHENIX Collaboration, Phys. Rev. Lett. 115, 142301 (2015)
P. Romatschke, Eur. Phys. J. C 75 (2015) 305

d+Au ^{3}He+Au Hydro Predictions

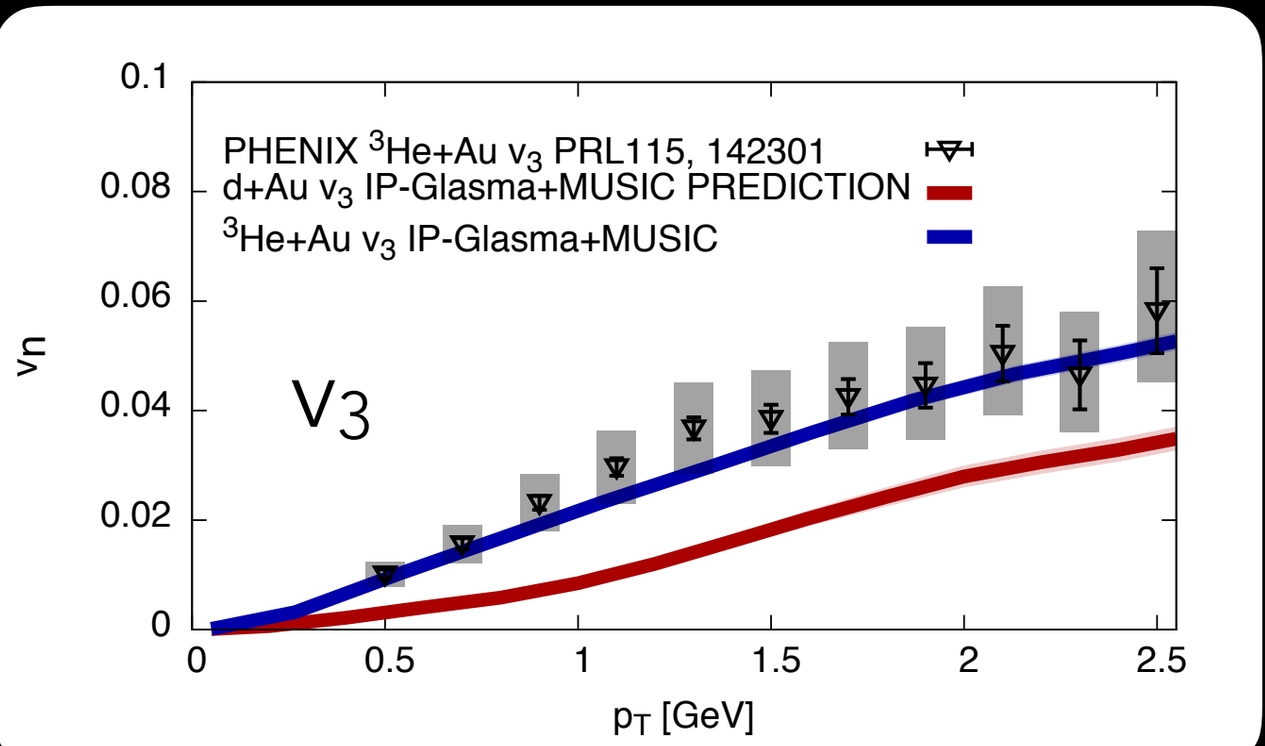


Left: Initial prediction for d+Au and ^{3}He+Au with η/s=0.12

Bottom: adjusted calculation with η/s=0.18

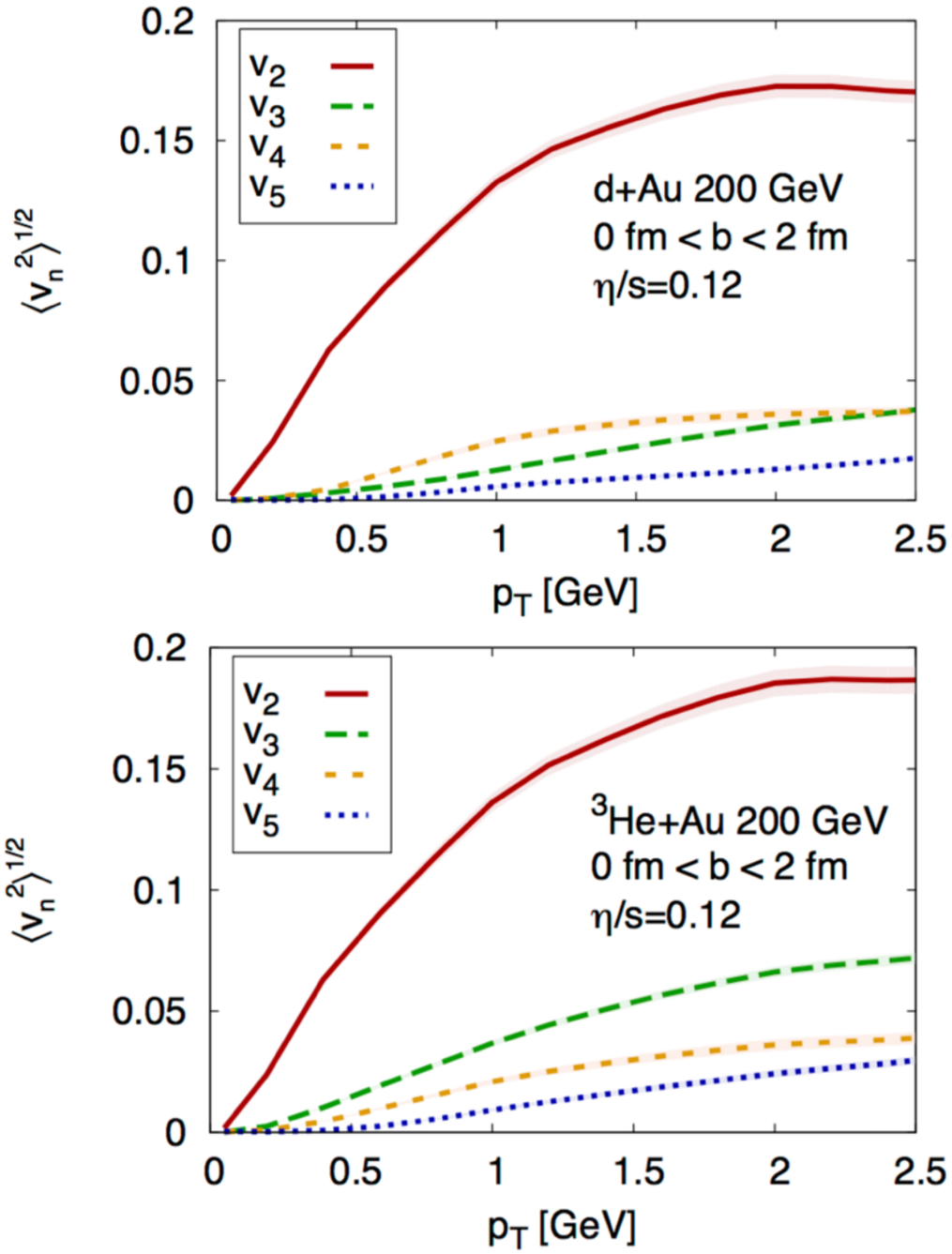
d+Au v_3 is a true prediction

(shown @2015 RHIC&AGS Users' Meeting)



B. Schenke and R. Venugopalan, Nucl. Phys. A 931 (2014) 1039

d+Au ^{3}He+Au Hydro Predictions

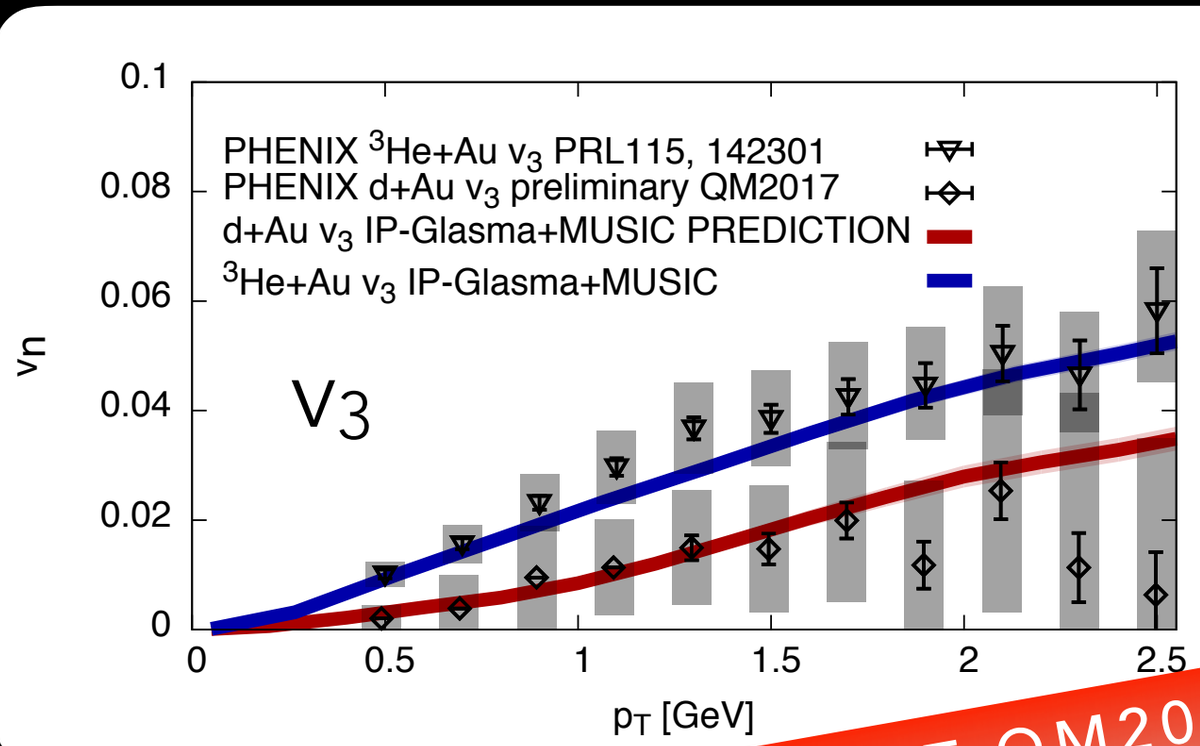


Left: Initial prediction for d+Au and ^{3}He+Au with η/s=0.12

Bottom: adjusted calculation with η/s=0.18

d+Au v_3 is a true prediction

(shown @2015 RHIC&AGS Users' Meeting)



NEW AT QM2017

B. Schenke and R. Venugopalan, Nucl. Phys. A 931 (2014) 1039

Initial state picture

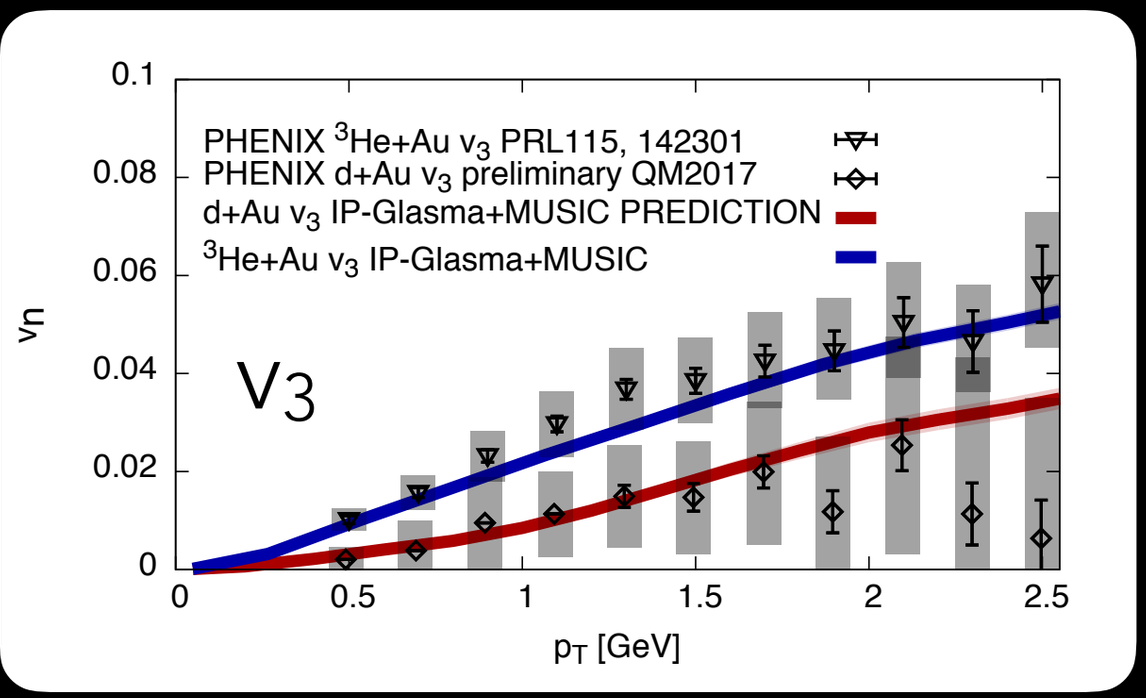
So far there is no initial state calculation comparing different small collision systems

There is no correlation between the harmonics and the initial global eccentricities

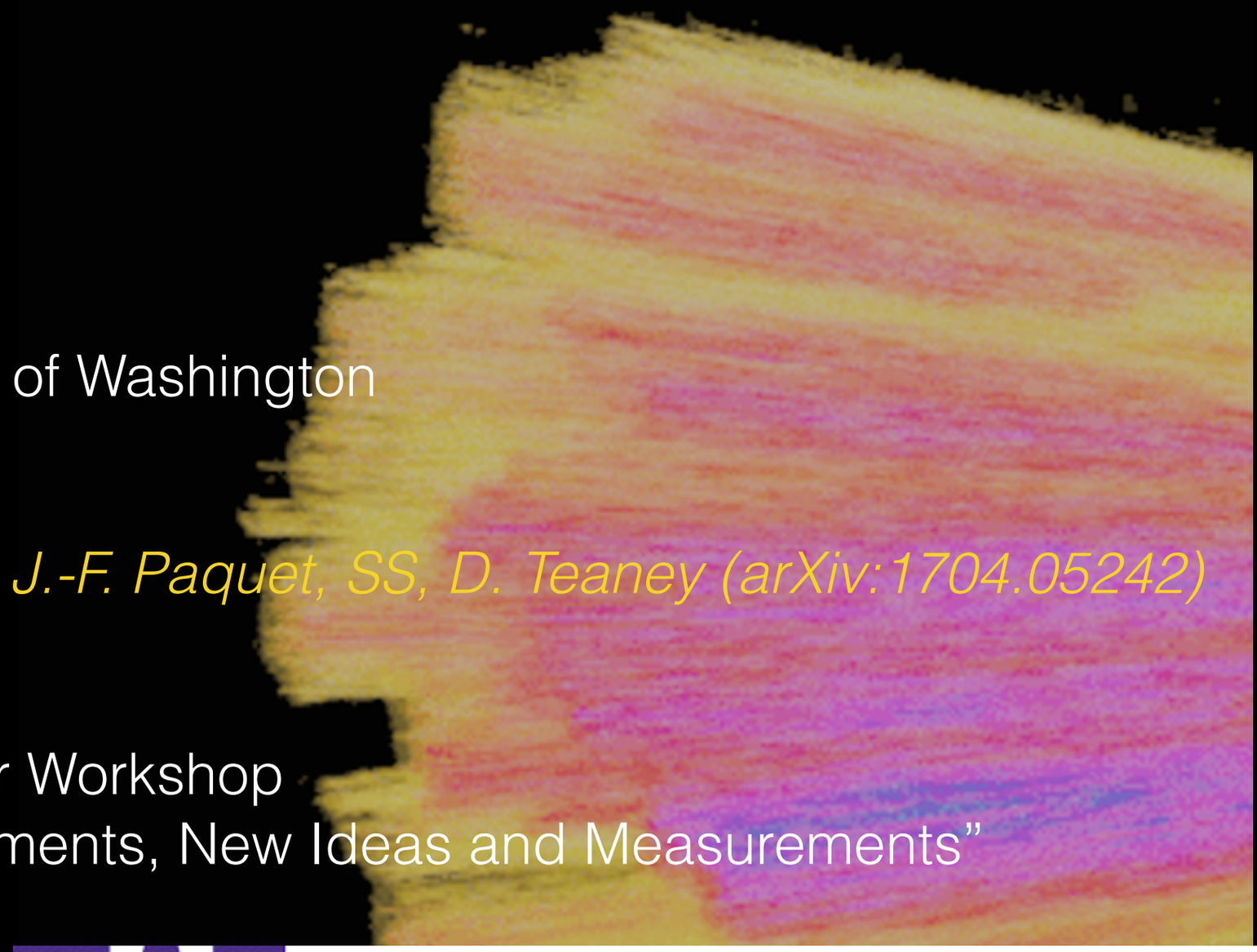
B. Schenke, S. Schlichting, R. Venugopalan, Phys. Lett. B747, 76-82 (2015)

L. McLerran, V. Skokov, arXiv:1611.09870

Difference must have a different origin:
Different multiplicities in the 0-5% bin?



Event-by-event pre-equilibrium dynamics
— from gluon saturation towards the onset of hydrodynamics



Sören Schlichting | University of Washington

Based on
A. Kurkela, A. Mazeliauskas, J.-F. Paquet, SS, D. Teaney (arXiv:1704.05242)
(more in preparation)

RIKEN/BNL Research Center Workshop
“Saturation: Recent Developments, New Ideas and Measurements”
Apr 2017

UNIVERSITY of WASHINGTON

Outline

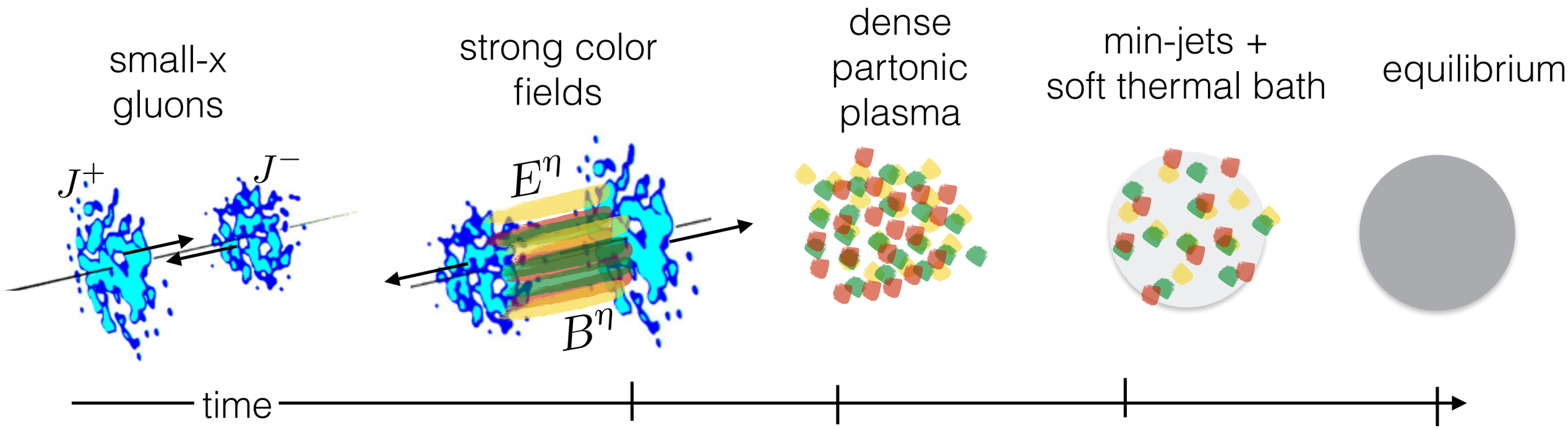
Microscopic early time dynamics & equilibration process

Macroscopic description of equilibration process

Event-by-event simulation of pre-equilibrium dynamics

Conclusions & Outlooks

Early time dynamics & equilibration process



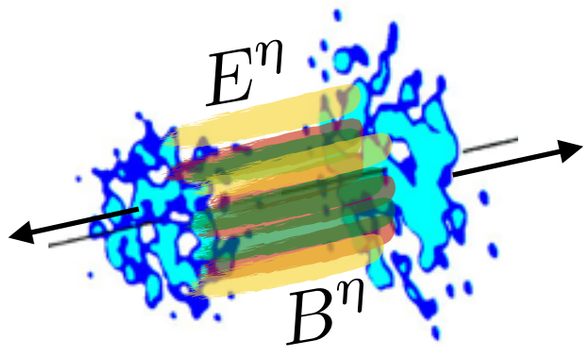
Starting from saturated nuclei before the collisions
sequence of processes that eventually leads to the formation
of an equilibrated QGP

Early time dynamics ($0<\tau<1/Q_s$)

Because of high phase-space density of gluons particle initial particle production and early time dynamics described in terms of classical field theory to leading order

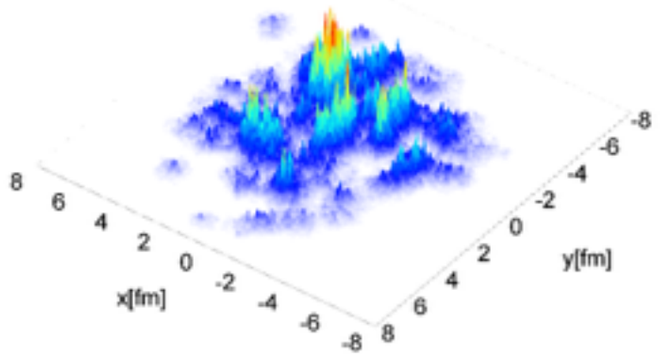
$$D_\mu F^{\mu\nu} = J^\nu$$

Strong boost invariant classical fields E^η, B^η created immediately after the collision



Decoherence of classical fields occurs on a time scale $\tau \sim 1/Q_s$ where quasi-particle description starts to become applicable

-> Basis for microscopic initial state calculations (IP-Glasma)



IP-Glasma

Challenge to understand subsequent equilibration process

- need quantum corrections (beyond NLO)
- effects of plasma instabilities

Equilibration process at weak coupling

Equilibration proceeds as three step process described by "bottom-up" scenario

Baier, Mueller, Schiff, Son PLB502 (2001) 51-58

Phase I: Evolution towards classical-attractor

quasi-particle description becomes applicable

Phase II: Mini-jets undergo a radiative break-up cascade

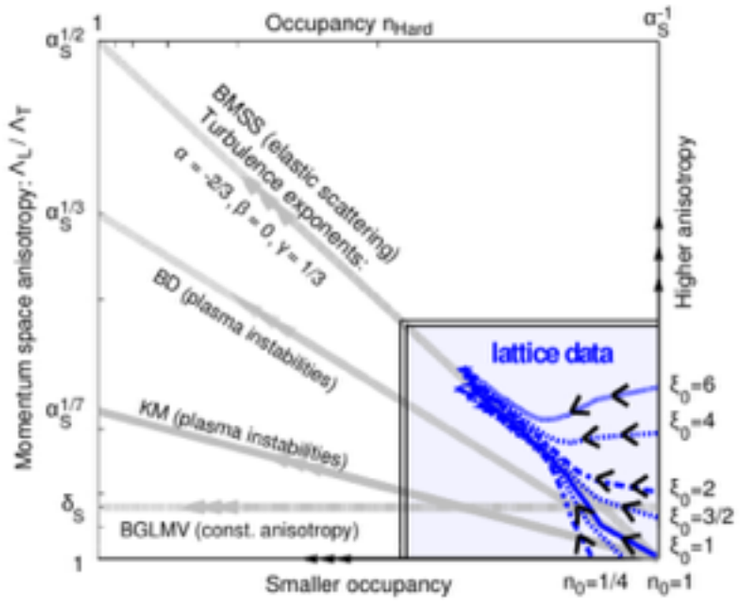
formation of soft thermal bath

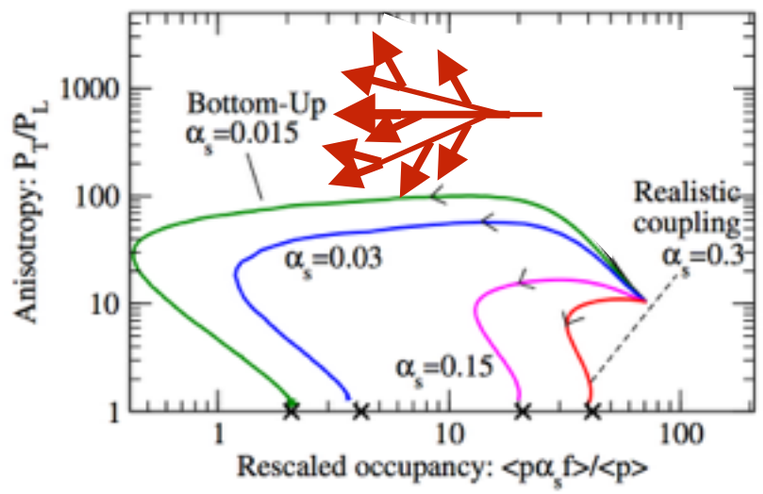
Phase III: Quenching of mini-jets in soft thermal bath

isotropization of plasma

Equilibration time determined by the time-scale for a mini-jet Q_s to loose all its energy

Berges,Boguslavski,SS, Venugopalan, PRD 89 (2014) no.7, 074011





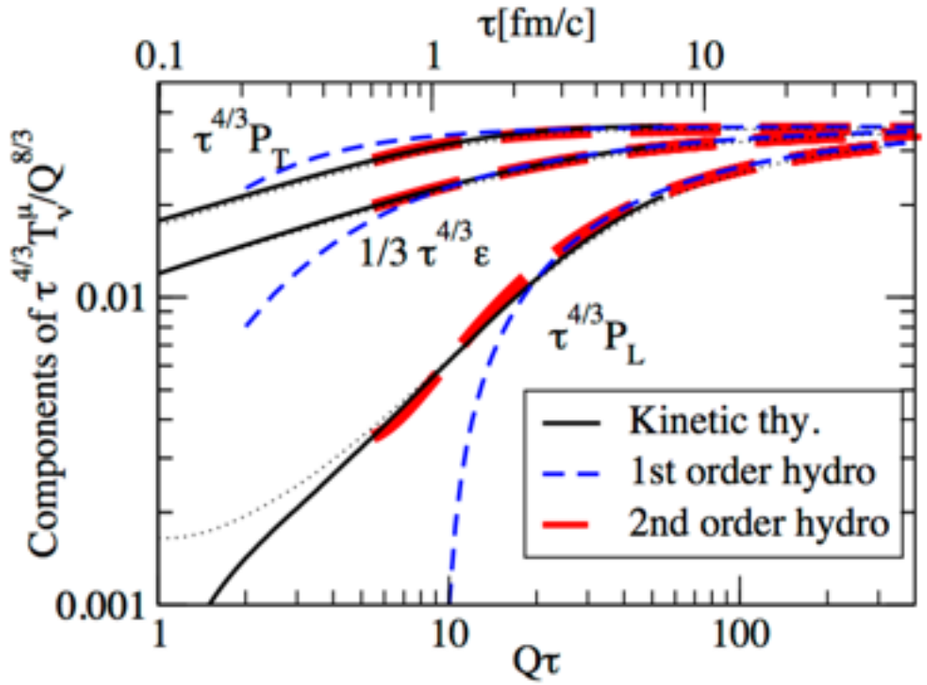
Kurkela, Zhu PRL 115 (2015) 182301

Hydrodynamic behavior

Extrapolations from weak-coupling limit to realistic values of α_s (~0.3) at RHIC & LHC energies yield results consistent with phenomenological estimates

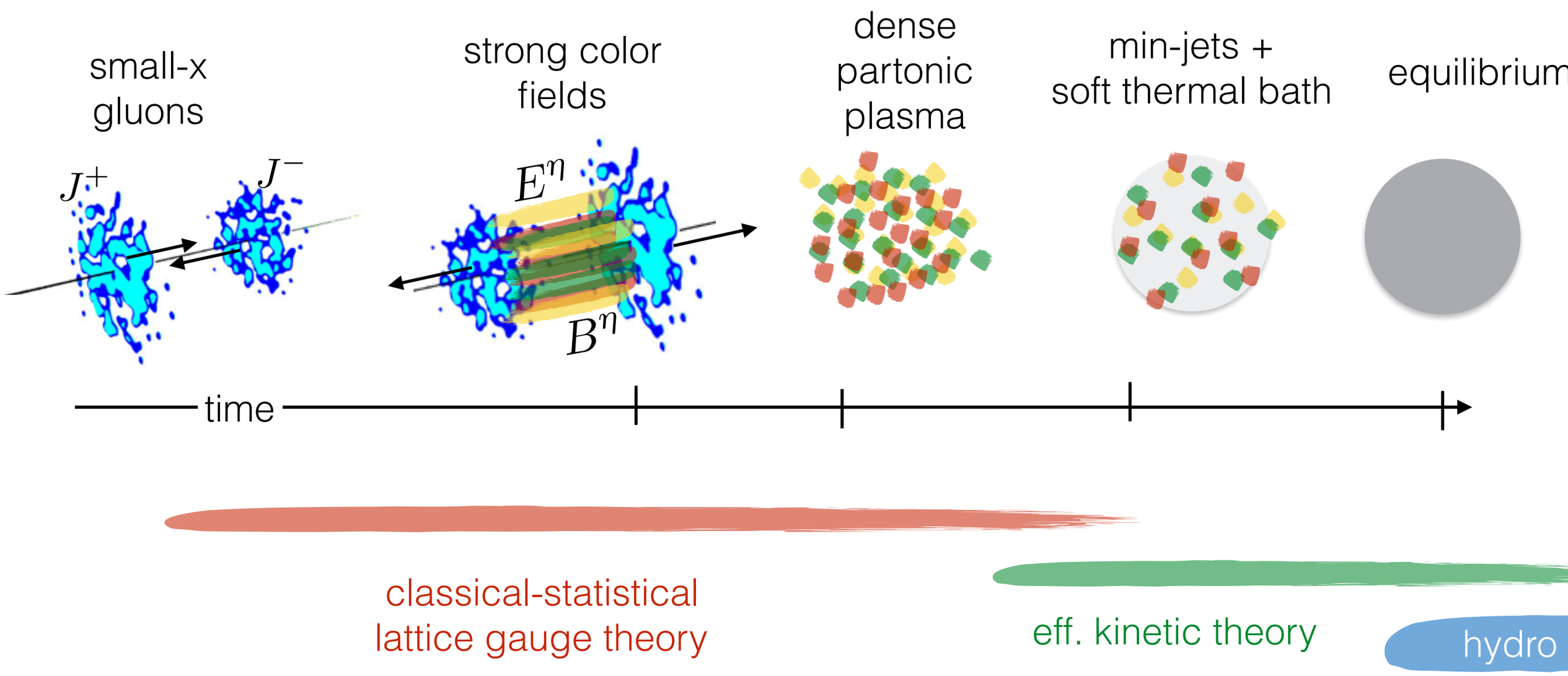
Viscous hydrodynamics applicable on time scales ~1 fm/c

Similar to strong coupling picture viscous hydrodynamics becomes applicable when pressure anisotropies are still O(1)



Kurkela, Zhu PRL 115 (2015) 182301

Early time dynamics & equilibration process



By combination of weak-coupling methods a complete description of early-time dynamics can be achieved

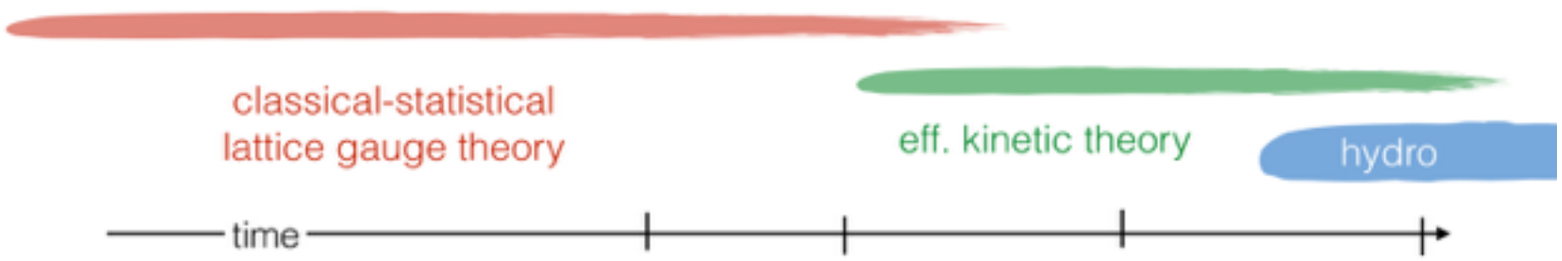
Event-by-event pre-equilibrium dynamics

Goal: Obtain event-by-event initial conditions including weakly coupled pre-equilibrium evolution

-> Eliminate uncertainties in extraction of QGP transport properties due to artificial time scale τ_{Hydro} when hydro simulation starts

Challenge: Different degrees of freedom relevant at different times

classical fields, quasi-particles, energy-momentum tensor



Brute force calculation extremely challenging (CYM f(x,p), 3+2+1D EKT)

Ultimately we are only interested in calculation of energy-momentum tensor

Exploit memory loss to use macroscopic degrees of freedom for description of pre-equilibrium dynamics

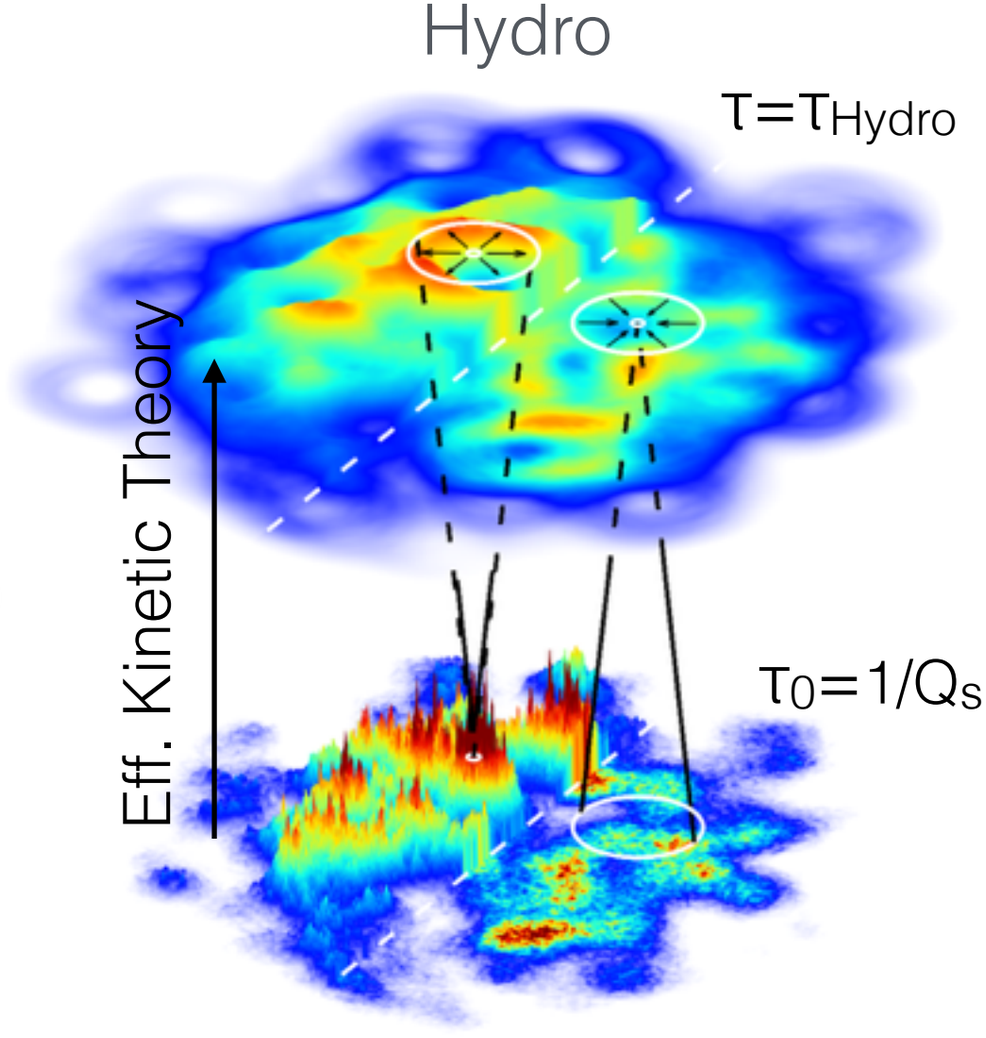
Macroscopic pre-equilibrium evolution

Extract energy-momentum tensor $T^{\mu\nu}(x)$ from classical statistical lattice simulation

Evolve $T^{\mu\nu}$ from initial time $\tau_0 \sim 1/Q_s$ to hydro initialization time τ_{Hydro} using eff. kinetic theory description

Causality restricts contributions to $T^{\mu\nu}(x)$ to be localized from causal disc $|x-x_0| < \tau_{Hydro}-\tau_0$ useful to decompose into a local average $T^{\mu\nu}_{BG}(x)$ and fluctuations $\delta T^{\mu\nu}(x)$

Since in practice size of causal disc is small $\tau_{Hydro}-\tau_0 << R_A$ fluctuations $\delta T^{\mu\nu}(x)$ around local average $T^{\mu\nu}_{BG}(x)$ are small and can be treated in a linearized fashion



Keegan,Kurkela, Mazeliauskas, Teaney JHEP 1608 (2016) 171
Kurkela, Mazeliauskas, Paquet, SS, Teaney (in preparation)

Macroscopic pre-equilibrium evolution

Effective kinetic description needs phase-space distribution $f(\tau, p, x)$

Memory loss: Details of initial phase-space distribution become irrelevant as system approaches local equilibrium

Can describe evolution of $T^{\mu\nu}$ in kinetic theory in terms of a representative phase-space distribution

$$f(\tau, p, x) = f_{BG}(Q_s(x)\tau, p/Q_s(x)) + \delta f(\tau, p, x)$$

where f_{BG} characterizes typical momentum space distribution, and δf can be chosen to represent local fluctuations of initial energy momentum tensor, e.g. energy density $\delta T^{\tau\tau}$ and momentum flow $\delta T^{\tau i}$

Energy perturbations:

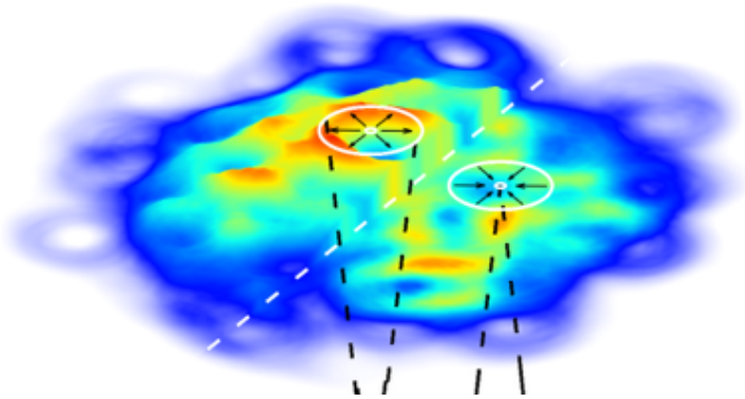
$$\delta f_s(\tau_0, p, x) \propto \frac{\delta T^{\tau\tau}(x)}{T^{\tau\tau}_{BG}(x)} \times \frac{\partial}{\partial Q_s(x)} f_{BG}\Big(\tau_0, p/Q_s(x)\Big)$$

local amplitude

representative form of phase-space distribution

Macroscopic pre-equilibrium evolution

Energy-momentum tensor on the hydro surface can be reconstructed directly from initial conditions according to

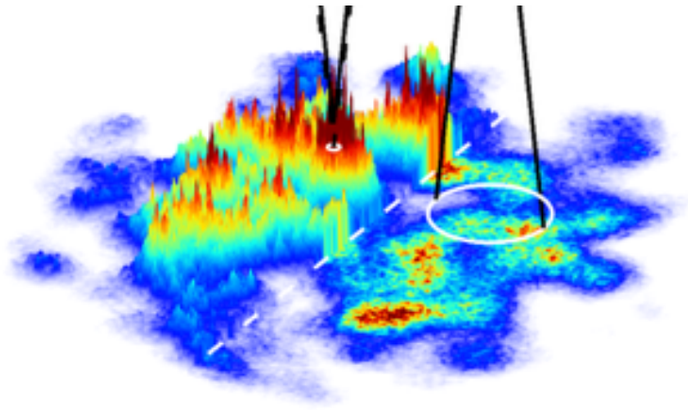


$$T^{\mu\nu}(\tau,x) = T^{\mu\nu}_{BG}\Big(Q_s(x)\tau\Big) + \int_{Disc} G^{\mu\nu}_{\alpha\beta}\Big(\tau,\tau_0,x,x_0,Q_s(x)\Big)\ \delta T^{\alpha\beta}(\tau_0,x_0)$$

non-equilibrium evolution of (local) average background

non-equilibrium Greens function of energy-momentum tensor

Effective kinetic theory simulations only need to be performed once to compute background evolution and Greens functions



Scaling variables

Background evolution and Greens functions still depend on variety of variables, $Q_s(x)$, α_s, …

-> Identify appropriate scaling variables to reduce complexity

Since ultimately evolution will match onto visc. hydrodynamics, check wether hydrodynamics admits scaling solution

1st order hydro: $$T^{\tau\tau}(\tau) = T^{\tau\tau}_{Ideal}(\tau)\left(1 - \frac{8}{3}\frac{\eta/s}{T_{eff}\tau} + ...\right)$$

where $T^{\tau\tau}_{Ideal}(\tau)$ is the Bjorken energy density and $T_{eff} = \tau^{-1/3} \lim_{\tau\to\infty} T(\tau)\tau^{1/3}$

Natural candidate for scaling variable is $x_s = T_{eff}\tau/(\eta/s)$

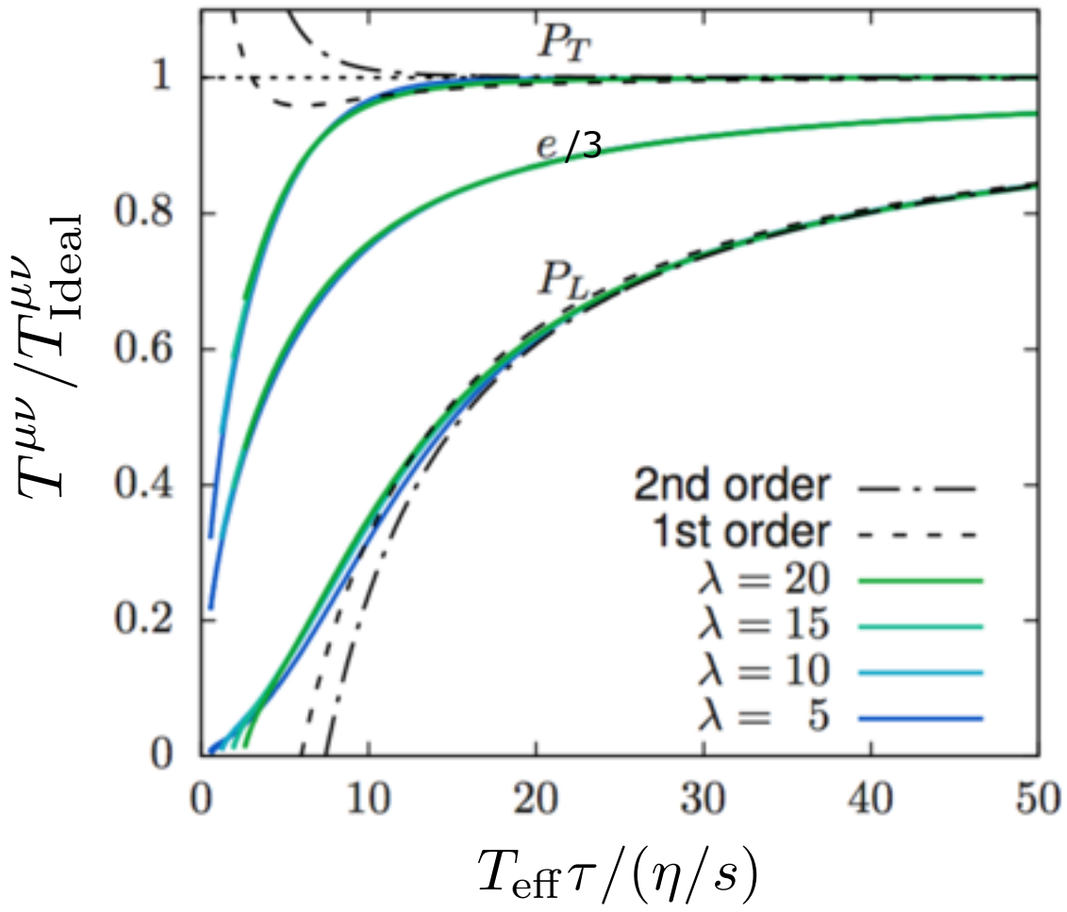
Background — Scaling variables

Numerical simulation of background evolution in effective kinetic theory

$$\left(\partial_\tau - \frac{p_z}{\tau}\right) f(\tau, |\mathbf{p}_\perp|, p_z) = \mathcal{C}[f]$$

$$\mathcal{C}[f] = \underbrace{\mathcal{C}_{2\leftrightarrow 2}[f]}_{\text{}} + \underbrace{\mathcal{C}_{1\leftrightarrow 2}[f]}_{\text{}}$$





Non-equilibrium evolution of background $T^{\mu\nu}$ is a unique function of x_s

Scaling property extends beyond hydrodynamic regime in the relevant range of (large) couplings

Greens functions

Greens functions describe evolution of energy/momentum perturbations on top of a (locally) homogenous boost-invariant background

-> Description of perturbations in Fourier space

Decomposition in a complete basis of tensors leaves a total of 10 independent functions, e.g. for energy perturbations

energy response

$$\tilde{G}^{\tau\tau}_{\tau\tau}(\tau,\tau_0,\mathbf{k}) = \tilde{G}^{s}_{s}(\tau,\tau_0,|\mathbf{k}|)\ ,$$

momentum response

$$\tilde{G}^{\tau i}_{\tau\tau}(\tau,\tau_0,\mathbf{k}) = \frac{\mathbf{k}^i}{|\mathbf{k}|}\tilde{G}^{v}_{s}(\tau,\tau_0,|\mathbf{k}|)\ ,$$

shear stress response

$$\tilde{G}^{ij}_{\tau\tau}(\tau,\tau_0,\mathbf{k}) = \tilde{G}^{t,\delta}_{s}(\tau,\tau_0,|\mathbf{k}|)\ \delta^{ij} + \tilde{G}^{t,k}_{s}(\tau,\tau_0,|\mathbf{k}|)\ \frac{\mathbf{k}^i\mathbf{k}^j}{|\mathbf{k}|^2}\ ;$$

Numerically computed in eff. kinetic theory by solving linearized Boltzmann equation on top of non-equilibrium background

$$\left(\partial_\tau + \frac{i\mathbf{p}_\perp\mathbf{k}_\perp}{p} - \frac{p_z}{\tau}\right)\ \widetilde{\delta f}(\tau,|\mathbf{p}_\perp|,p_z;\ \mathbf{k}_\perp) = \delta\mathcal{C}[f,\widetilde{\delta f}]$$

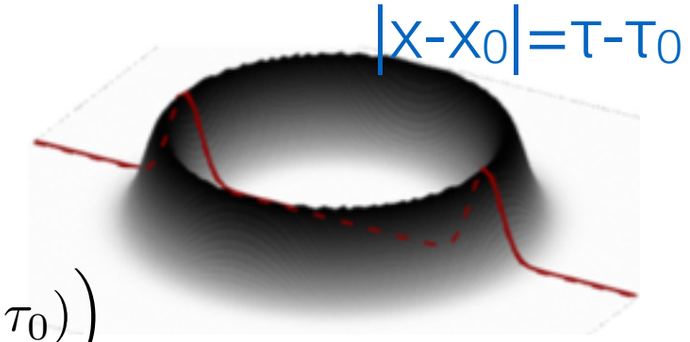
and computing appropriate moments of δf

Greens functions

Free-streaming:

Energy-momentum perturbations propagate as a concentric wave traveling at the speed of light

coordinate space



energy/momentum response:

$$G_s^{s/v}(\tau,\tau_0,\mathbf{x}-\mathbf{x}_0)=\frac{1}{2\pi(\tau-\tau_0)}\delta\Big(|\mathbf{x}-\mathbf{x}_0|-(\tau-\tau_0)\Big)$$

Hydrodynamic response functions in the limit of small wave-number k (τ-τ_0) << 1 and large times x_s>>1:

(c.f. Vredevoogd,Pratt PRC79 (2009) 044915, Keegan,Kurkela, Mazeliauskas, Teaney JHEP 1608 (2016) 171)

energy response: $\tilde{G}_s^s(\tau,\tau_0,k) = \tilde{G}_s^s(\tau,\tau_0,k=0)\left(1-\frac{1}{2}k^2(\tau-\tau_0)^2\ \tilde{s}_s^{(2)}+\ldots\right),$

momentum response: $\tilde{G}_s^v(\tau,\tau_0,k) = \tilde{G}_s^s(\tau,\tau_0,k=0)\left(-ik(\tau-\tau_0)\ \tilde{s}_v^{(1)}+\ldots\right),$

shear response: determined by hydrodynamic constitutive relations

$$\tilde{G}_s^s(\tau,\tau_0,k=0)=\left(\frac{T^{\tau\tau}(\tau_0)}{T^{\tau\tau}(\tau)}\right)\left(\frac{3T^{\tau\tau}(\tau)-T^{\eta}_{\eta}(\tau)}{3T^{\tau\tau}(\tau_0)-T^{\eta}_{\eta}(\tau_0)}\right)$$

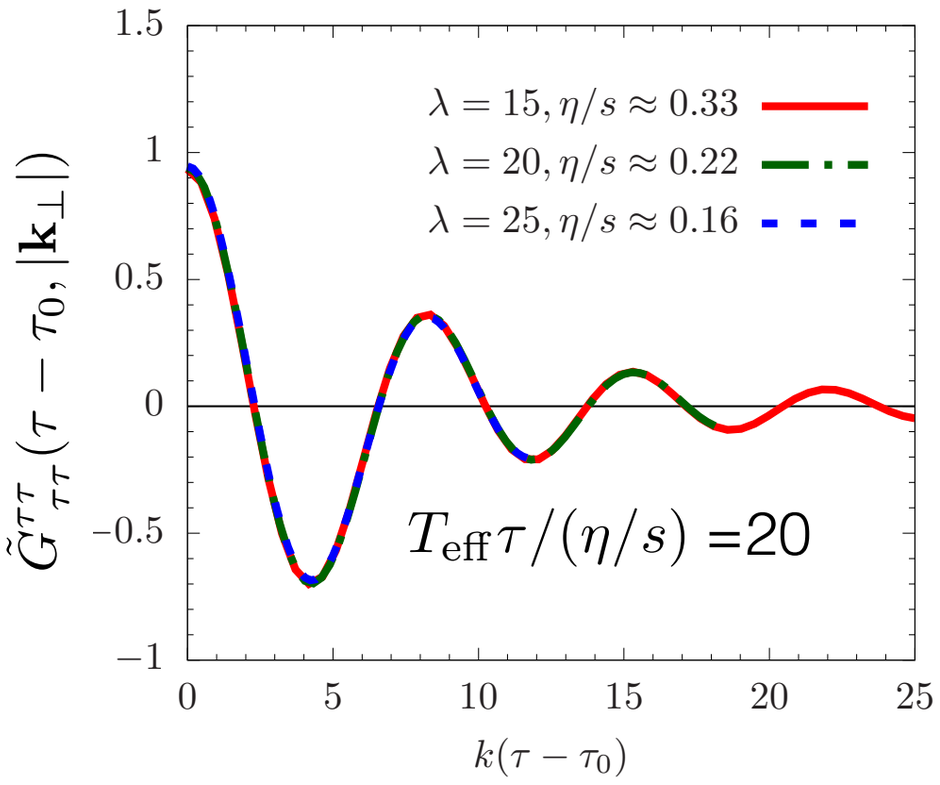
background evolution

$$\tilde{s}_v^{(1)}=\frac{1}{2}\qquad \tilde{s}_s^{(2)}=\frac{1}{2}\left(1+\frac{2}{3x_s}\right)$$

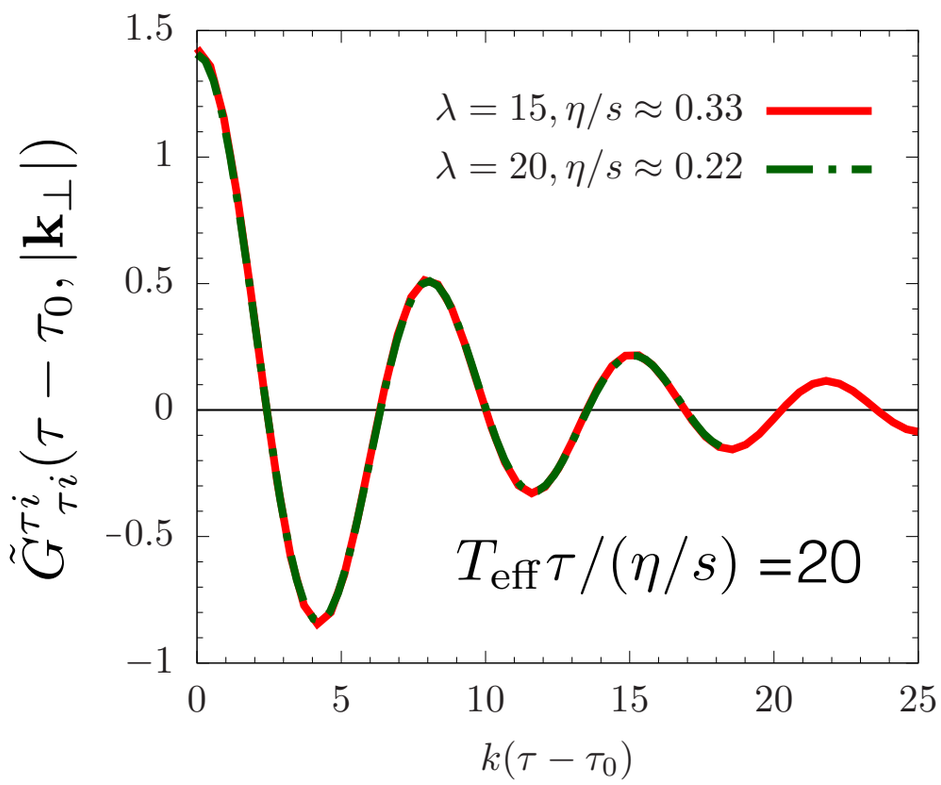
“long wave-length constants”

Greens functions — Scaling variables

Energy response
to energy perturbation



Momentum response
to momentum perturbations



Non-equilibrium Greens functions show universal scaling
in $x_s = T_{eff}\tau/(\eta/s)$ and $k(\tau-\tau_0)$ beyond hydro limit

Satisfy hydrodynamic constitutive relations for sufficiently large times $x_s >> 1$ and long wave-length $k\,(\tau-\tau_0) << 1$

Scaling variables

Scaling properties ensure that pre-equilibrium evolution of energy momentum tensor can be expressed in terms of

Background: $T^{\mu\nu}_{BG}(x_s)$ Greens-functions: $G^{\mu\nu}_{\alpha\beta}\left(x_s, \frac{x-x_0}{\tau-\tau_0}\right)$

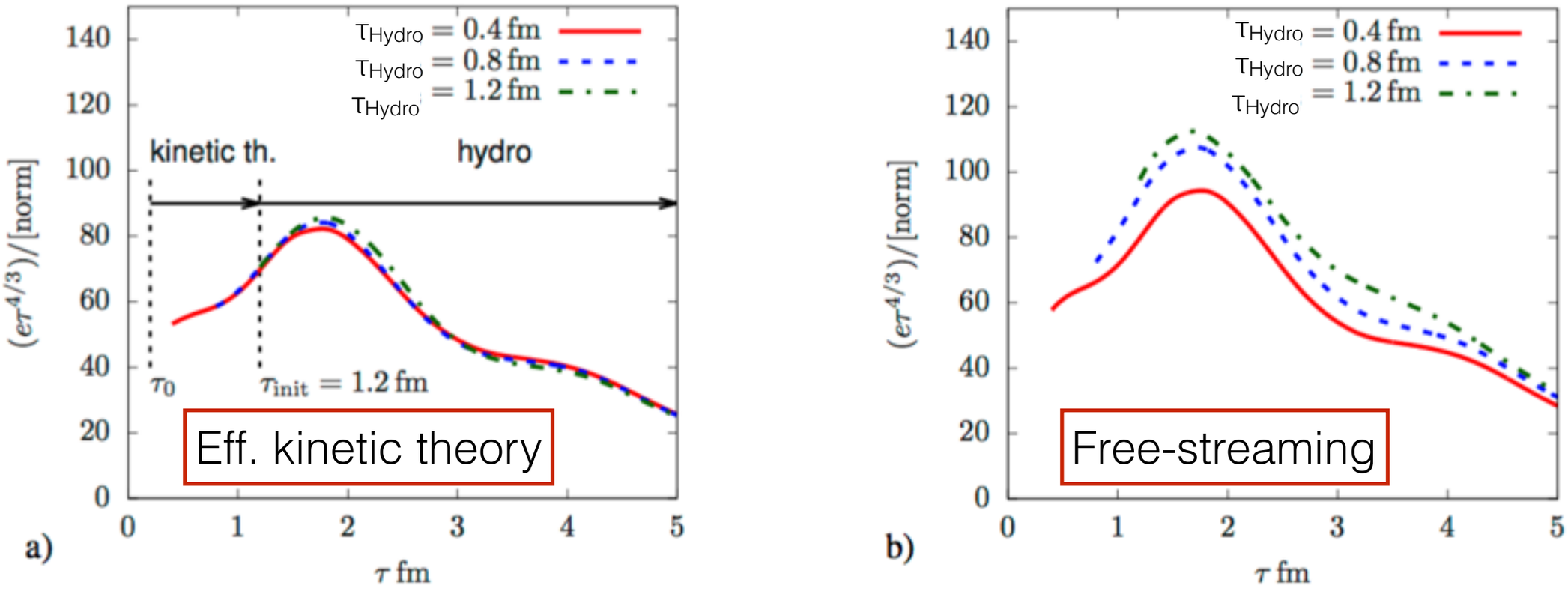
which are computed once and for all in numerical kinetic theory simulation

Since dependence of coupling constant α_s has been re-expressed in terms of physical parameter η/s, can now perform event-by-event simulations for variety of physical parameters

Event-by-event pre-equilibrium evolution

1) Evolve IP-Glasma initial conditions to early time τ_0 = 0.2 fm/c
2) Macroscopic pre-equilibrium evolution to hydro initialization time τ_{Hydro}
3) Hydrodynamic evolution from τ_{Hydro} ($\eta/s = 2/(4\pi)$ | conformal EoS)

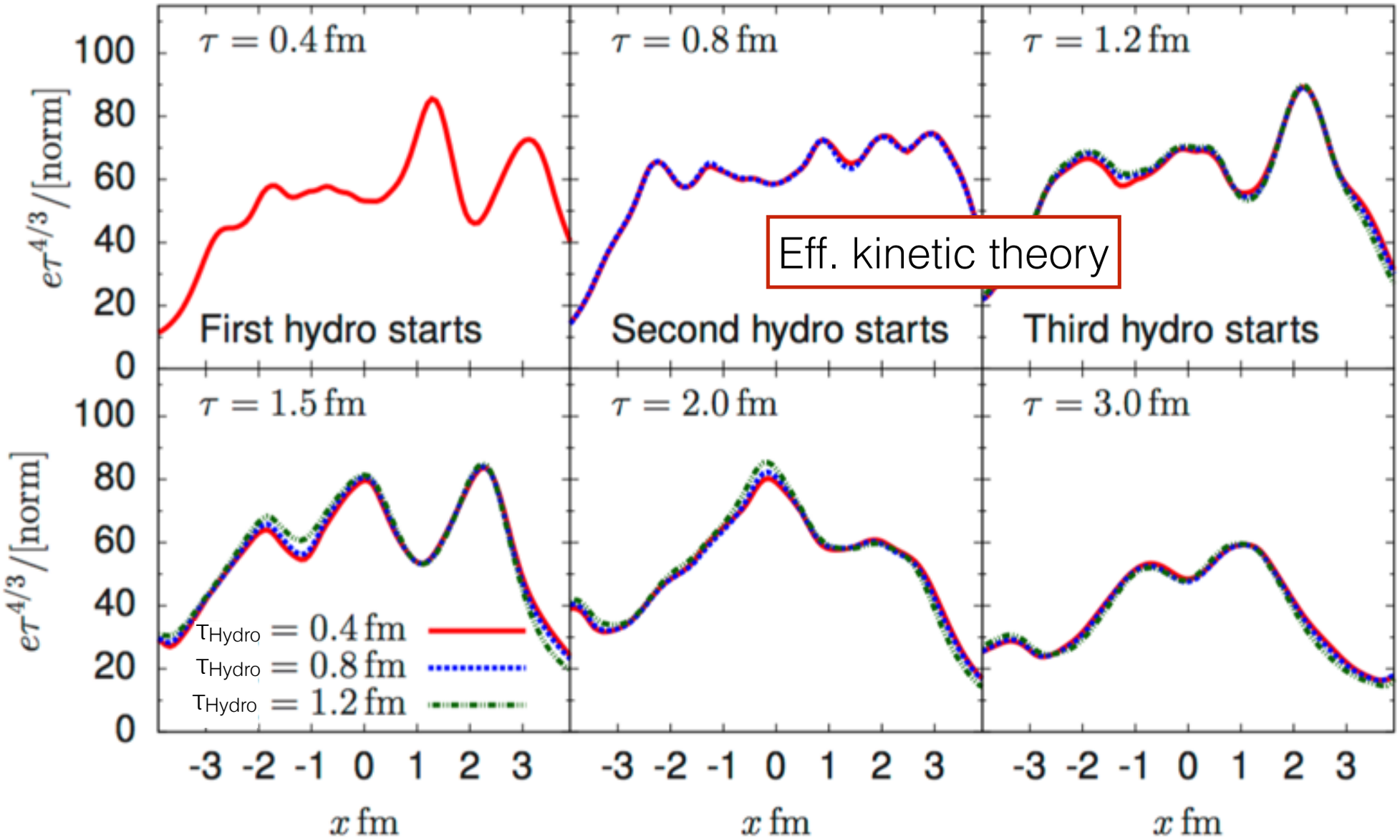
Energy density in the central region of Pb+Pb collision



Consistent description of pre-equilibrium dynamics ensures smooth transition to hydrodynamics at times $\tau > \tau_{Hydro}$

Event-by-event pre-equilibrium evolution

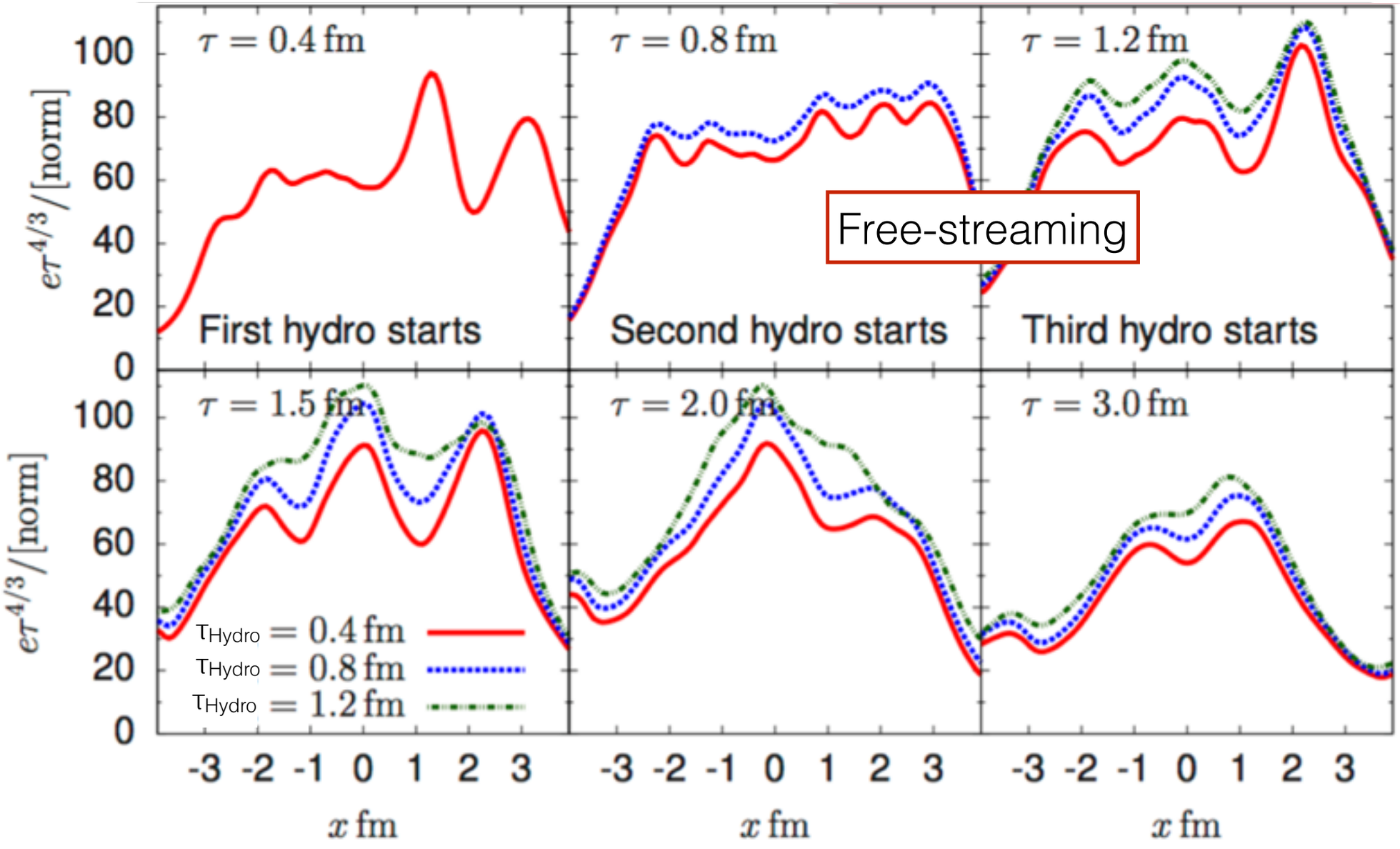
Energy density profile in Pb+Pb collision



No sensitivity to switching time τ_{Hydro} from pre-equilibrium to hydro

Event-by-event pre-equilibrium evolution

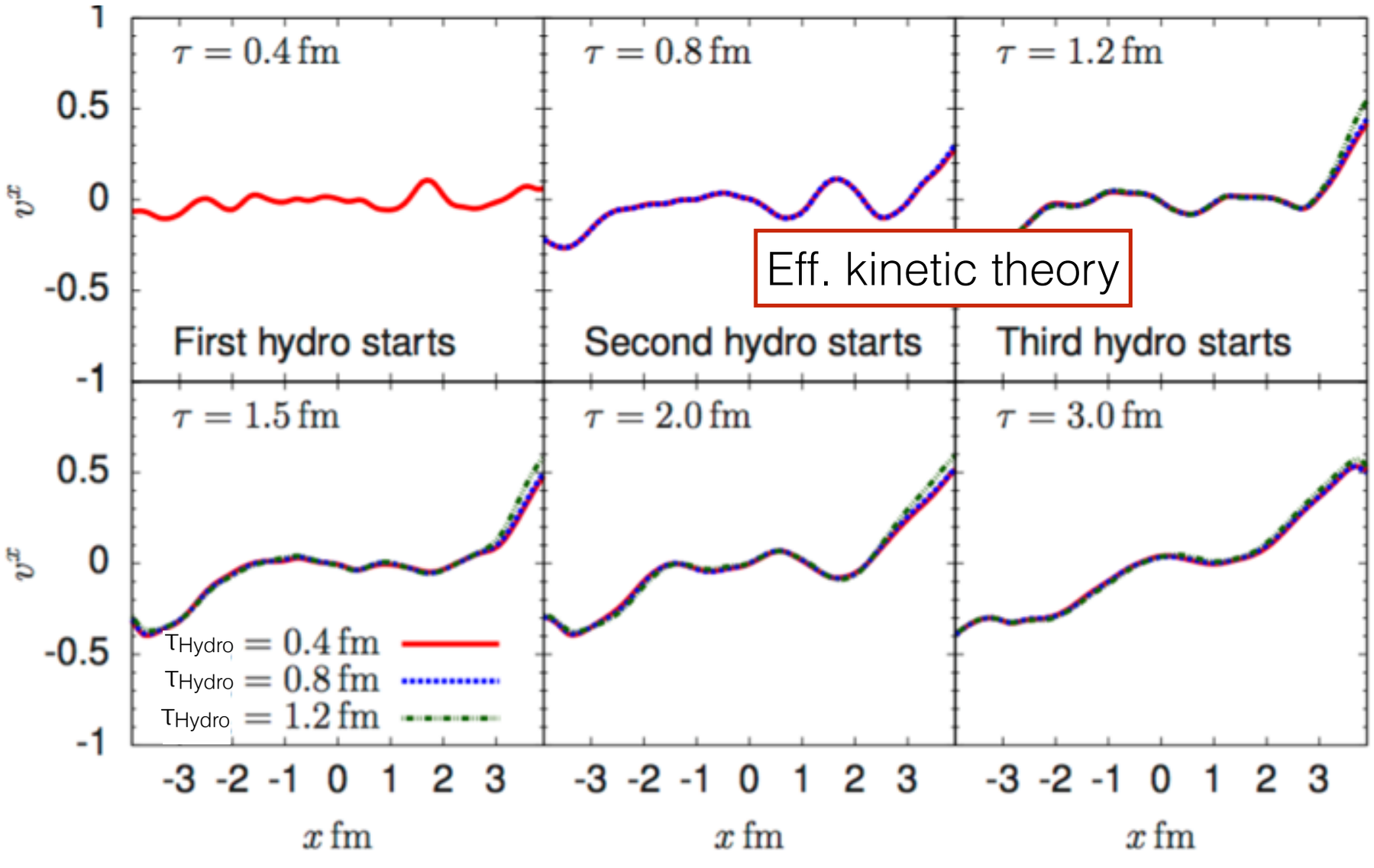
Energy density profile in Pb+Pb collision



Non-trivial result as free-streaming evolution yields similar profiles but incorrect normalization

Event-by-event pre-equilibrium evolution

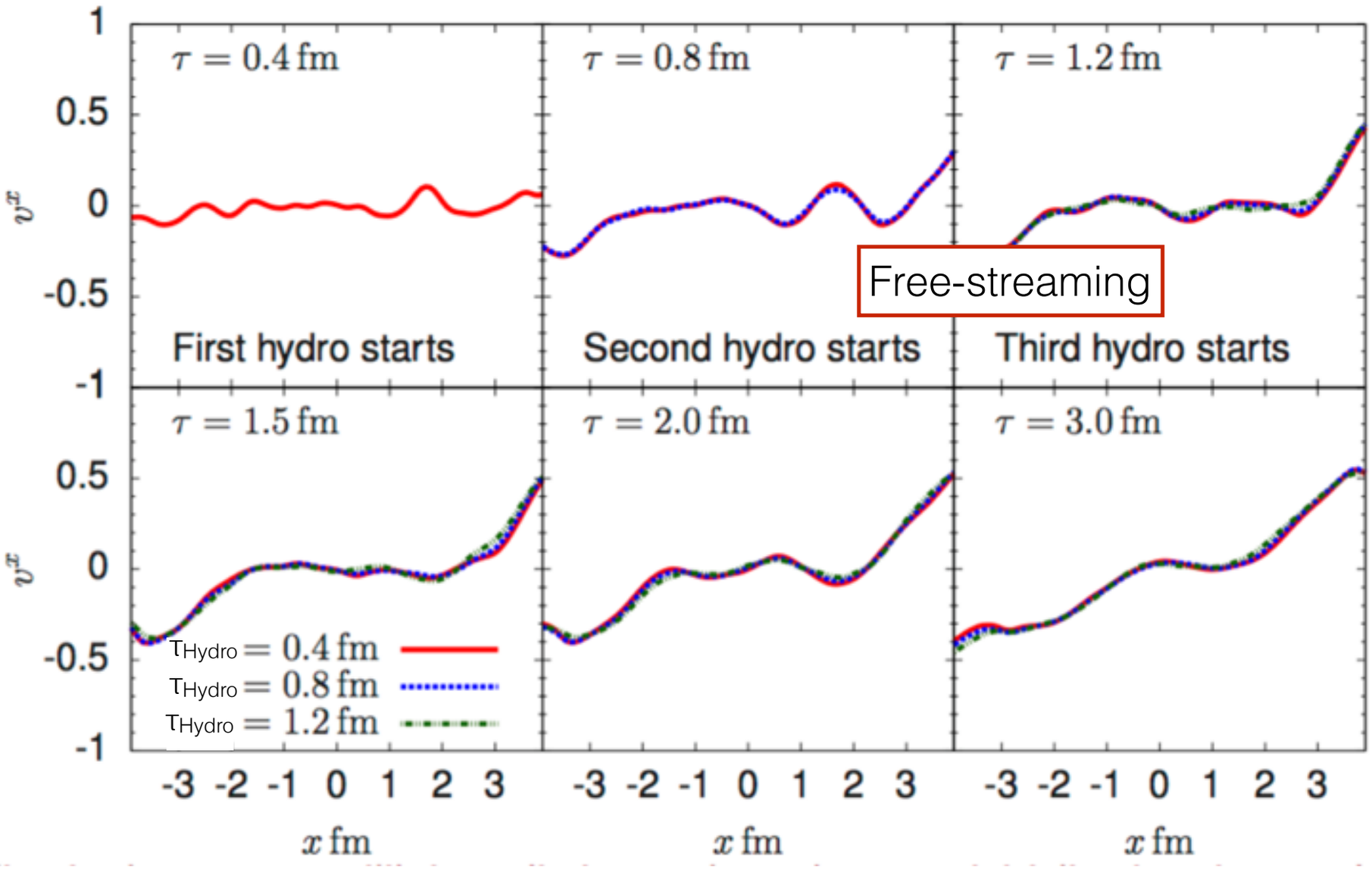
Pre-equilibrium flow profile in Pb+Pb collision:



No sensitivity to switching time τ_{Hydro} from pre-equilibrium to hydro

Event-by-event pre-equilibrium evolution

Pre-equilibrium flow profile in Pb+Pb collision:

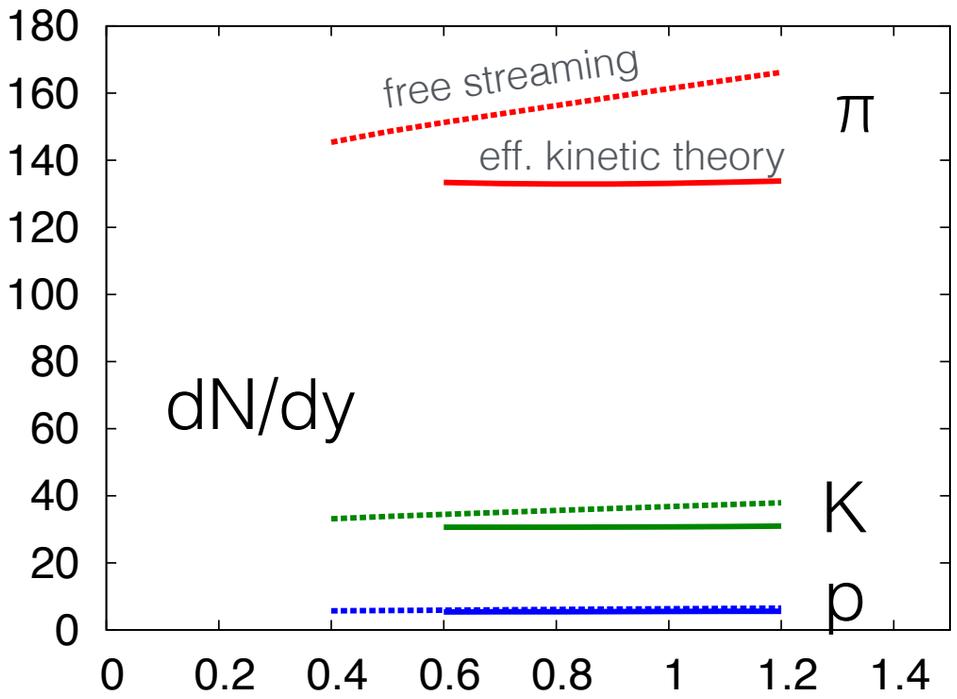


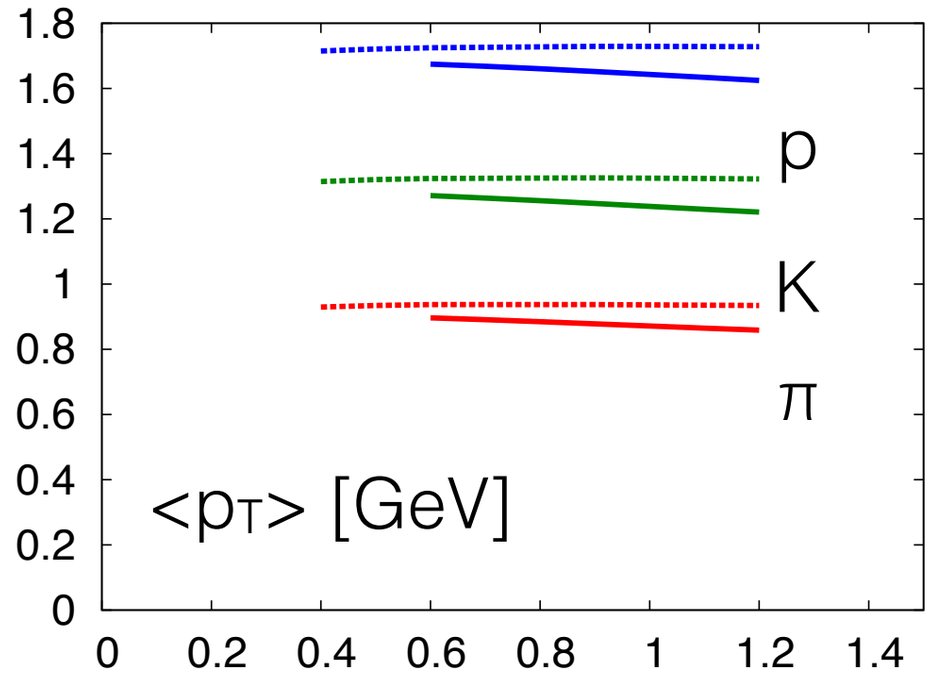
Universality of long wave-length response leads to very similar results for free-streaming and effective kinetic theory

(c.f. Vredevoogd,Pratt PRC79 (2009) 044915, Keegan,Kurkela, Mazeliauskas, Teaney JHEP 1608 (2016) 171)

Event-by-event pre-equilibrium evolution

Hadronic observables in single Pb+Pb event:





Hydro initialization time τ_{Hydro} [fm/c]

Very little to no sensitivity to switching time τ_{Hydro} from pre-equilibrium to hydro for dN/dy, $\langle p_T \rangle$, $\langle v_2 \rangle$, …

Conclusions & Outlook

Significant progress in understanding early time dynamics of heavy-ion collisions from weak-coupling perspective

Development of macroscopic description which enables event-by-event description and can be used in phenomenological modeling of heavy-ion collisions

Description in macroscopic framework is completely general and can be used beyond weak coupling limit

-> Direct comparisons with strong coupling limit should be possible

Several interesting directions beyond bulk phenomenology are starting to be explored

topological transitions, quark production & anomalous transport, photon production

Quark Helicity Evolution at Small x

Matthew D. Sievert



with Yuri Kovchegov



and Daniel Pitonyak

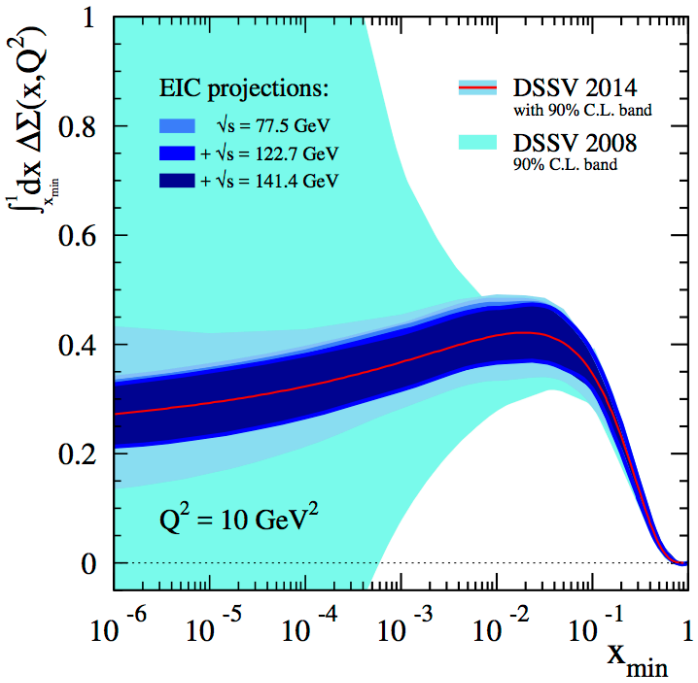


RBRC Workshop: Wed. April 26, 2017

Saturation: Recent Developments, New Ideas, and Measurements

Small-x Enhancement of Quark Polarization

Without Small-x Evolution

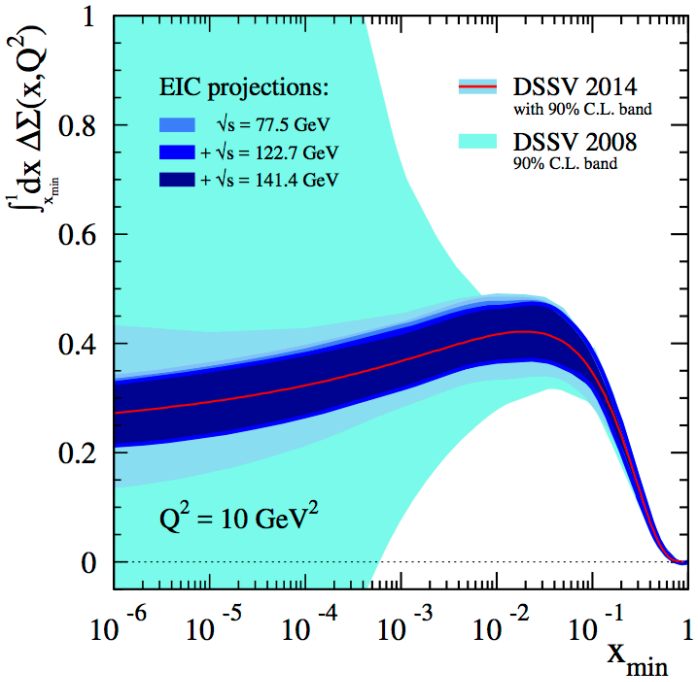


adapted from Aschenauer et al., Phys. Rev. ***D92*** *(2015) no.9 094030*

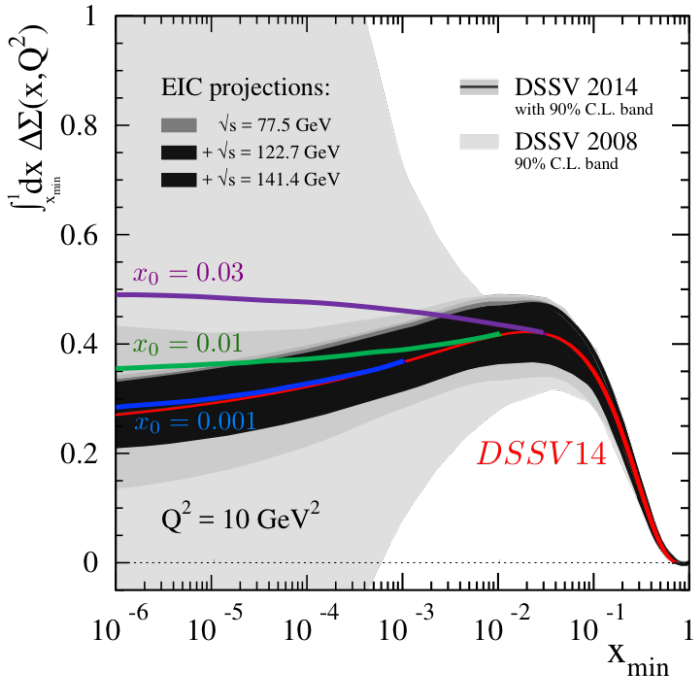
- Quark polarization not well constrained below $x \leq 10^{-2}$

Small-x Enhancement of Quark Polarization

Without Small-x Evolution



With Small-x Evolution



*adapted from Aschenauer et al., Phys. Rev. **D92** (2015) no.9 094030*

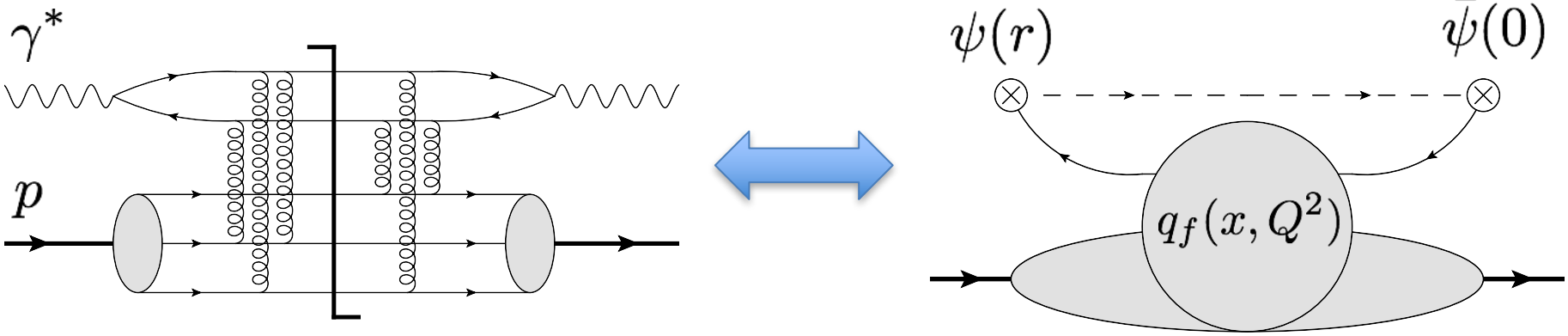
- Quark polarization not well constrained below $x \leq 10^{-2}$
- New small-x evolution can lead to significant enhancement

An Appetizer:

Small-x Evolution of the
Unpolarized Quark Distribution

Unpolarized Cross Sections and PDFs

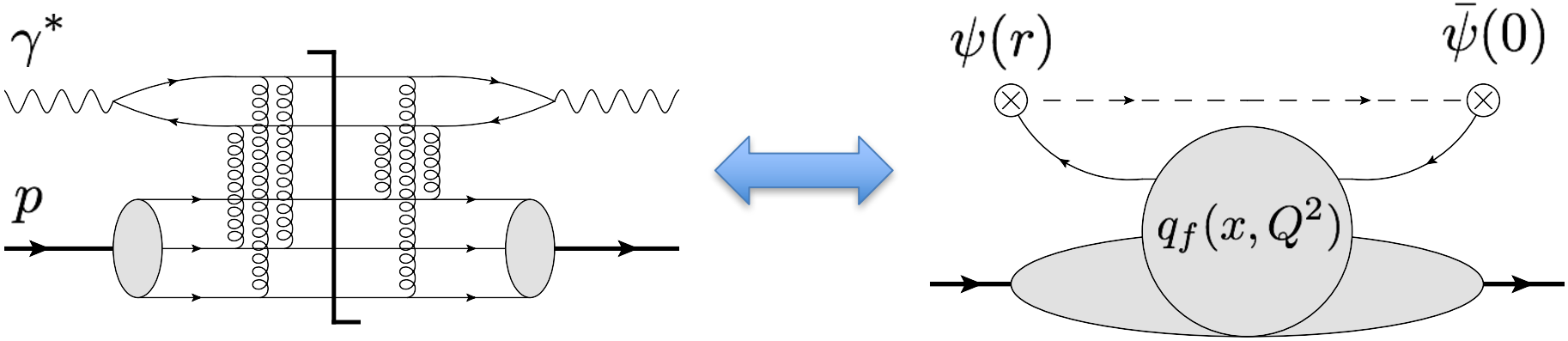
- **Factorization**: One-to-one correspondence between the DIS cross section and the parton distribution functions



$$\frac{Q^2}{4\pi^2\alpha_{EM}}\frac{d\sigma^{(\gamma^* p)}}{dx\,dQ^2} = F_2(x,Q^2) \overset{L.O.}{=} \sum_f e_f^2\, x q_f(x,Q^2)$$

Unpolarized Cross Sections and PDFs

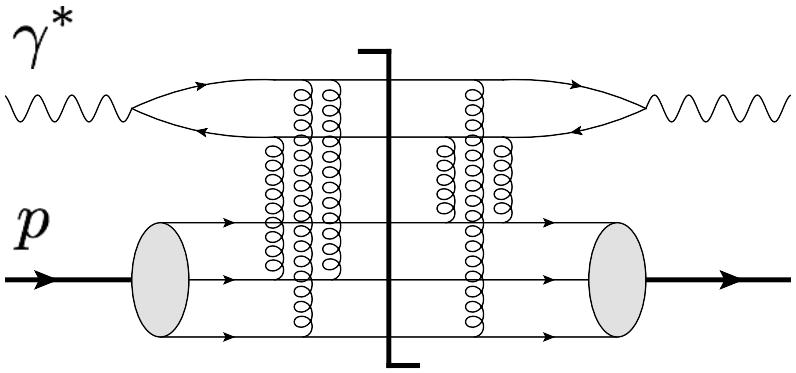
- **Factorization**: One-to-one correspondence between the DIS cross section and the parton distribution functions



$$\frac{Q^2}{4\pi^2\alpha_{EM}}\frac{d\sigma^{(\gamma^* p)}}{dx\,dQ^2} = F_2(x,Q^2) \overset{L.O.}{=} \sum_f e_f^2\, x q_f(x,Q^2)$$

$$\frac{d\sigma^{(\gamma^* p)}}{dx\,dQ^2} \sim \left(\frac{1}{x}\right)^{\alpha_P - 1} \sim x\, q_f(x,Q^2)$$

The Unpolarized Dipole Amplitude



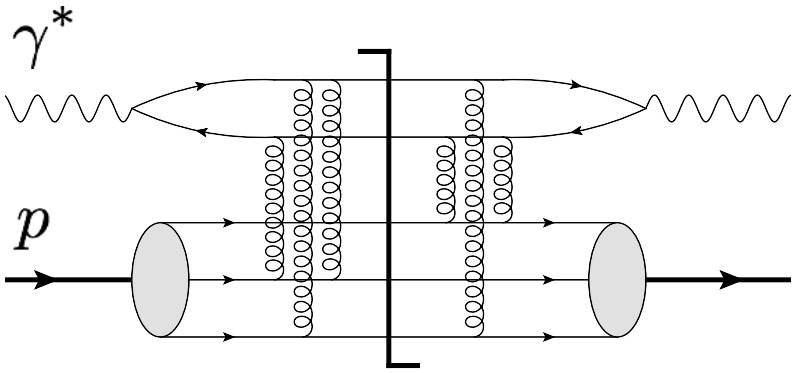
Quark PDF

$$q(x,Q^2) = \int \frac{dr^-}{2\pi}\, e^{ixp^+r^-}\, \langle p|\, \bar{\psi}(0)\, \mathcal{U}[0,r^-]\, \frac{\gamma^+}{2}\, \psi(r^-)\, |p\rangle$$

- The DIS cross section / PDF is expressed in terms of a dipole scattering amplitude amplitude / cross section

$$xq_f(x,Q^2) \overset{L.O.}{=} \frac{Q^2\, N_c}{2\pi^2 \alpha_{EM}} \int \frac{d^2x_{10}\, dz}{4\pi\, z(1-z)} \left[\left|\Psi_{T,f}(x_{10}^2, z)\right|^2 + \left|\Psi_{L,f}(x_{10}^2, z)\right|^2 \right] \int d^2b_{10}\, (1 - S_{10}(zs))$$

The Unpolarized Dipole Amplitude



Quark PDF

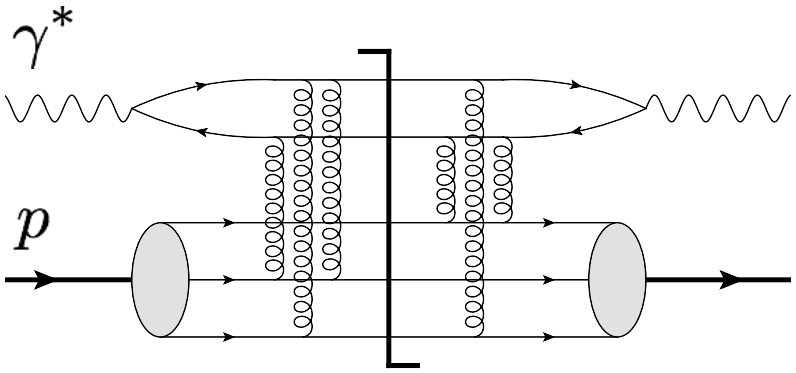
$$q(x,Q^2) = \int \frac{dr^-}{2\pi}\, e^{ixp^+r^-}\, \langle p|\, \bar{\psi}(0)\, \mathcal{U}[0,r^-]\, \frac{\gamma^+}{2}\, \psi(r^-)\, |p\rangle$$

- The DIS cross section / PDF is expressed in terms of a dipole scattering amplitude amplitude / cross section

$$xq_f(x,Q^2) \overset{L.O.}{=} \frac{Q^2\, N_c}{2\pi^2 \alpha_{EM}} \int \frac{d^2x_{10}\, dz}{4\pi\, z(1-z)} \left[\left|\Psi_{T,f}(x_{10}^2, z)\right|^2 + \left|\Psi_{L,f}(x_{10}^2, z)\right|^2 \right] \int d^2b_{10} \boxed{(1 - S_{10}(zs))}$$

$$S_{10}(zs) \equiv \left\langle \frac{1}{N_c} \mathrm{tr}[V_{\underline{x_0}} V^\dagger_{\underline{x_1}}]_{(zs)} \right\rangle = 1 - \frac{1}{2} \frac{d\sigma^{(q^{unp}_{\underline{x_0}}\, \bar{q}^{unp}_{\underline{x_1}})}}{d^2b_{10}}(zs)$$

The Unpolarized Dipole Amplitude



Quark PDF

$$q(x,Q^2) = \int \frac{dr^-}{2\pi}\, e^{ixp^+r^-}\, \langle p|\, \bar{\psi}(0)\, \mathcal{U}[0,r^-]\, \frac{\gamma^+}{2}\, \psi(r^-)\, |p\rangle$$

- The DIS cross section / PDF is expressed in terms of a dipole scattering amplitude amplitude / cross section

$$xq_f(x,Q^2) \overset{L.O.}{=} \frac{Q^2\, N_c}{2\pi^2 \alpha_{EM}} \int \frac{d^2x_{10}\, dz}{4\pi\, z(1-z)} \left[\left|\Psi_{T,f}(x_{10}^2, z)\right|^2 + \left|\Psi_{L,f}(x_{10}^2, z)\right|^2 \right] \int d^2b_{10} \left(1 - S_{10}(zs)\right)$$

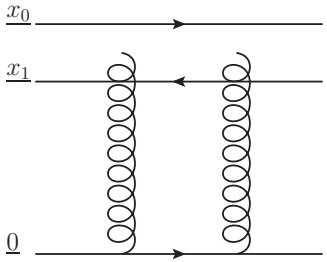
$$S_{10}(zs) \equiv \left\langle \frac{1}{N_c} \mathrm{tr}[V_{\underline{x}_0} V^\dagger_{\underline{x}_1}]_{(zs)} \right\rangle = 1 - \frac{1}{2} \frac{d\sigma^{(q^{unp}_{\underline{x}_0}\, \bar{q}^{unp}_{\underline{x}_1})}}{d^2b_{10}}(zs)$$

Wilson lines: $V_{\underline{x}} = \mathcal{P} \exp\left[ig \int dz^- \hat{A}^+(0^+, z^-, \underline{x}) \right]$

Origins of Unpolarized Evolution

- Initial conditions from the quark target model:

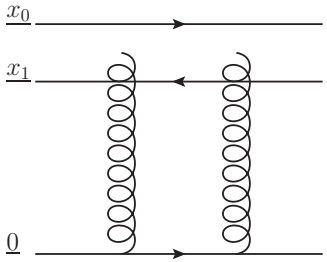
$$S_{10}^{(0)}(zs) = \frac{2\alpha_s^2 C_F}{N_c} \ln^2 \frac{x_{0T}}{x_{1T}}$$



Origins of Unpolarized Evolution

- Initial conditions from the quark target model:

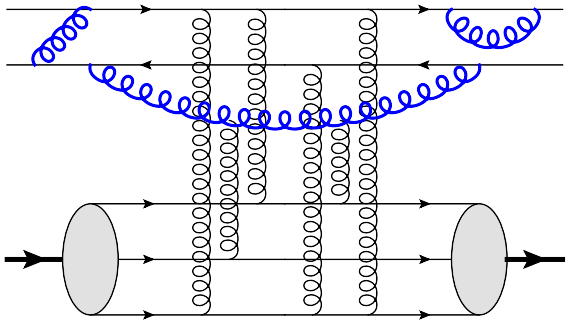
$$S_{10}^{(0)}(zs) = \frac{2\alpha_s^2 C_F}{N_c} \ln^2 \frac{x_{0T}}{x_{1T}}$$



- Soft gluon emission spans the full rapidity interval $Y \sim \ln \frac{s}{\Lambda^2} \sim \ln \frac{1}{x}$

$$\frac{1}{N_c}\mathrm{tr}[V_{\underline{x}_0} V_{\underline{x}_1}^\dagger]_{(zs)} \sim \alpha_s \int_{\frac{\Lambda^2}{s}}^{z} \frac{dz'}{z'} \int d^2x_2 \, \mathcal{K}(\underline{x}_0, \underline{x}_1, \underline{x}_2) \, \mathcal{O}$$

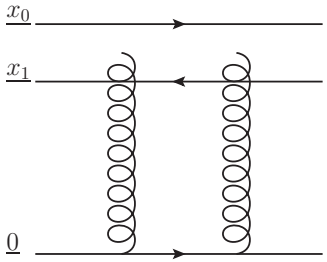
$$\ln \frac{zs}{\Lambda^2}$$



Origins of Unpolarized Evolution

- Initial conditions from the quark target model:

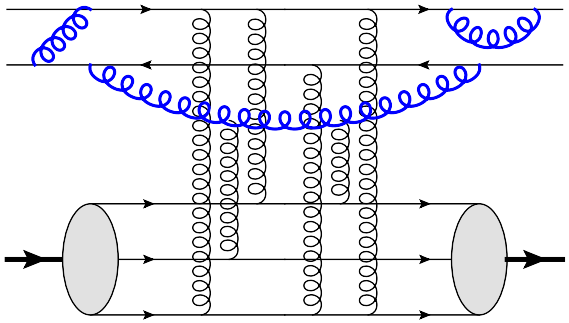
$$S_{10}^{(0)}(zs) = \frac{2\alpha_s^2 C_F}{N_c} \ln^2 \frac{x_{0T}}{x_{1T}}$$



- Soft gluon emission spans the full rapidity interval $Y \sim \ln \frac{s}{\Lambda^2} \sim \ln \frac{1}{x}$

$$\frac{1}{N_c}\mathrm{tr}[V_{\underline{x}_0} V_{\underline{x}_1}^\dagger]_{(zs)} \sim \alpha_s \int_{\frac{\Lambda^2}{s}}^{z} \frac{dz'}{z'} \int d^2x_2\, \mathcal{K}(\underline{x}_0, \underline{x}_1, \underline{x}_2)\, \mathcal{O}$$

$$\ln \frac{zs}{\Lambda^2}$$



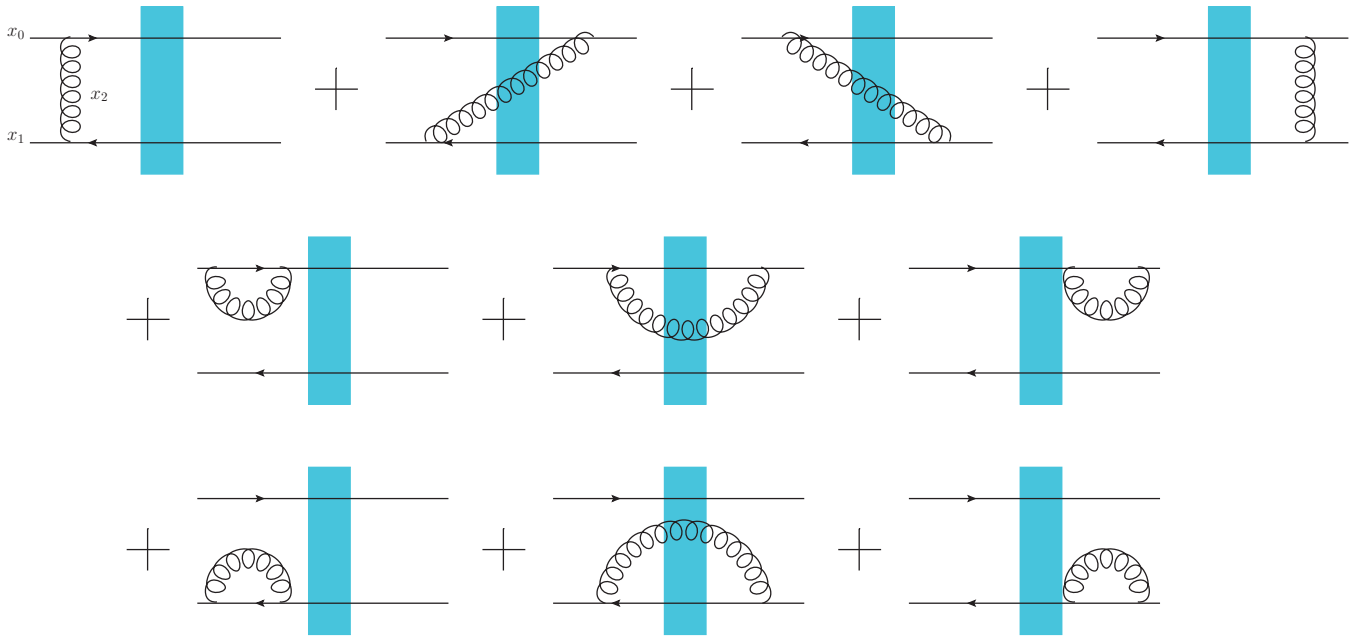
- Successive emissions continue to generate a logarithm of energy if they are ordered longitudinally

$$z \gg z' \gg z'' \gg \cdots$$

- Unpolarized evolution is leading-logarithmic

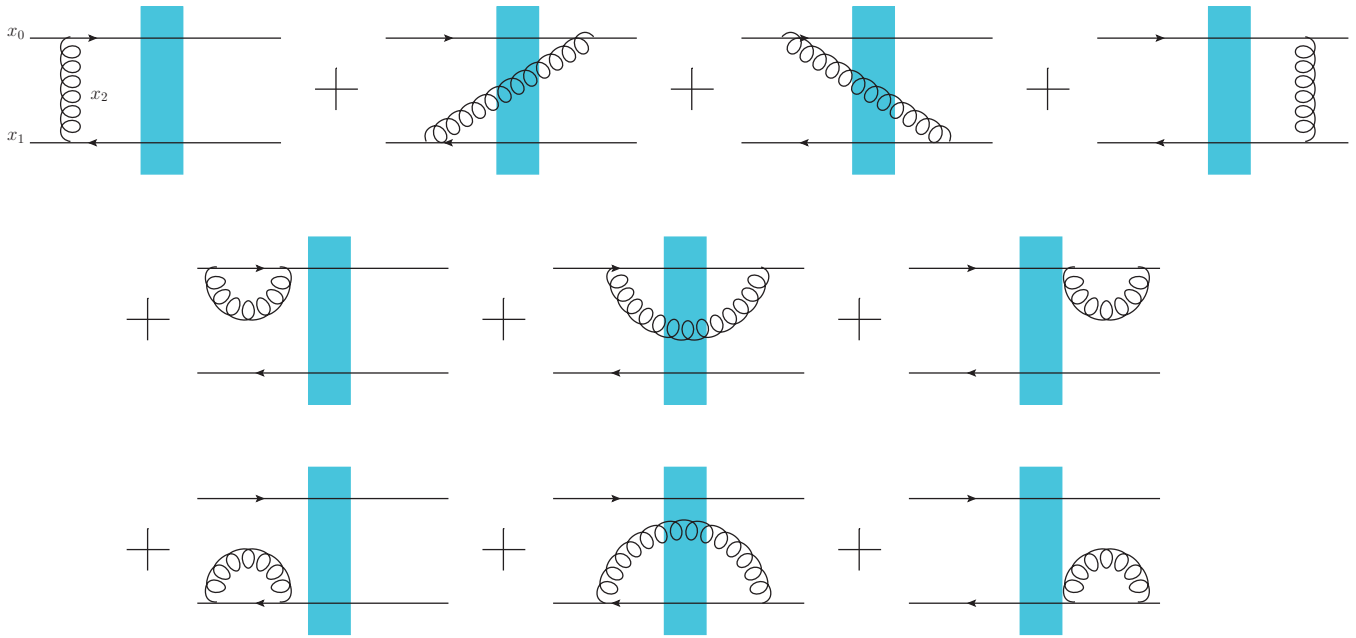
$$\alpha_s \ln \frac{1}{x} \sim 1$$

Unpolarized Small-x Evolution



$$S_{10}(zs) = S_{10}^{(0)}(zs) + \frac{\alpha_s N_c}{2\pi^2} \int_{\frac{\Lambda^2}{s}}^{z} \frac{dz'}{z'} \int d^2x_2 \, \frac{x_{10}^2}{x_{12}^2 \, x_{20}^2} \left[\frac{1}{N_c^2} \left\langle \mathrm{tr}[V_{\underline{x}_2} V_{\underline{x}_1}^\dagger] \, \mathrm{tr}[V_{\underline{x}_0} V_{\underline{x}_2}^\dagger] \right\rangle_{(z's)} - S_{10}(z's) \right]$$

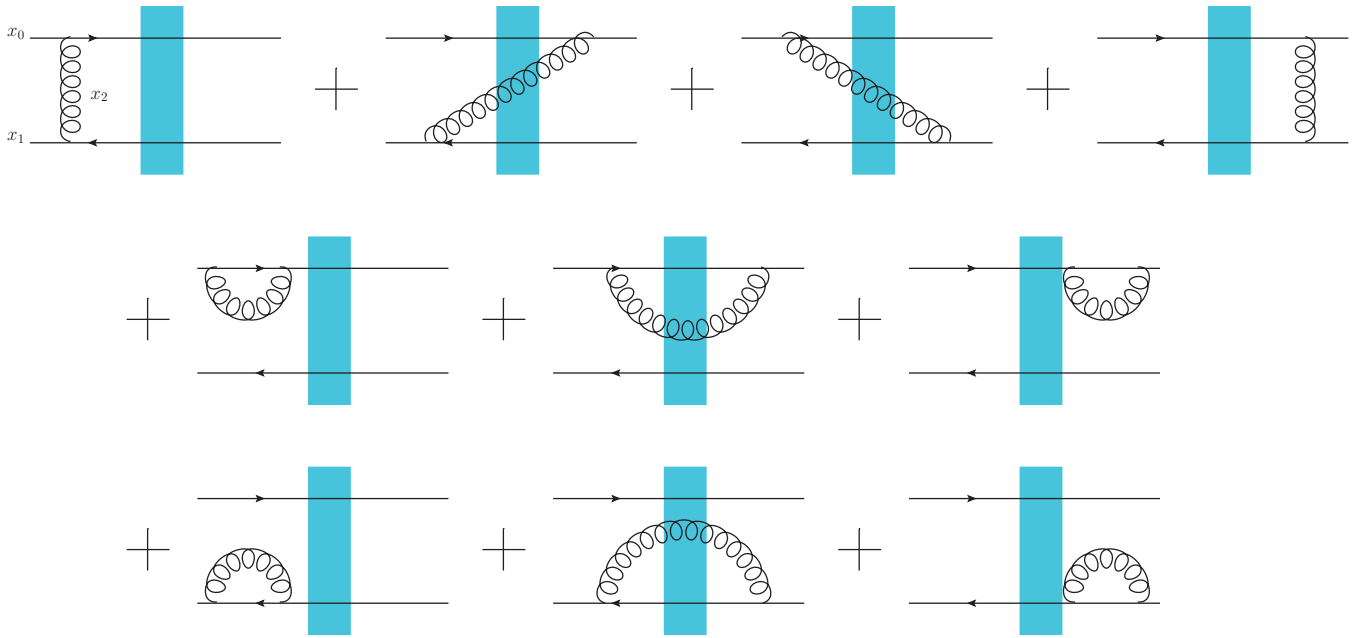
Unpolarized Small-x Evolution



Leading Log

$$S_{10}(zs) = S_{10}^{(0)}(zs) + \boxed{\frac{\alpha_s N_c}{2\pi^2} \int_{\frac{\Lambda^2}{s}}^{z} \frac{dz'}{z'}} \int d^2x_2 \, \frac{x_{10}^2}{x_{12}^2 \, x_{20}^2} \left[\frac{1}{N_c^2} \left\langle \mathrm{tr}[V_{\underline{x}_2} V_{\underline{x}_1}^\dagger] \, \mathrm{tr}[V_{\underline{x}_0} V_{\underline{x}_2}^\dagger] \right\rangle_{(z's)} - S_{10}(z's) \right]$$

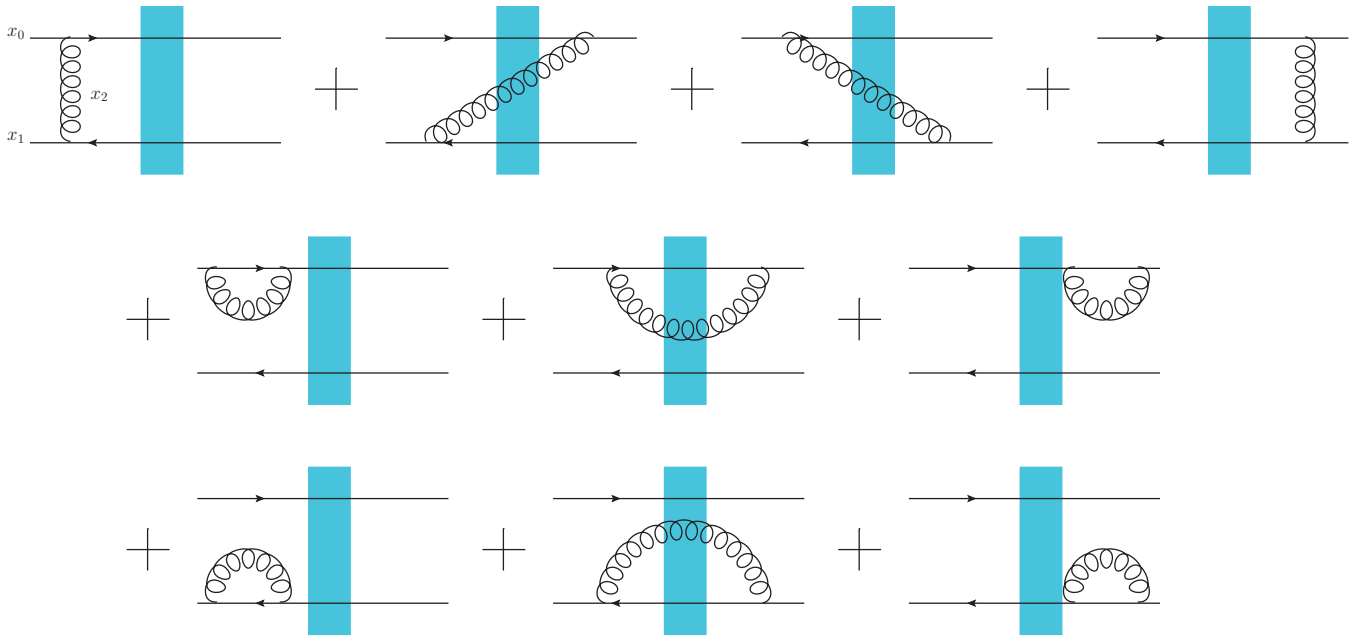
Unpolarized Small-x Evolution



Leading Log **BFKL Kernel**

$$S_{10}(zs) = S_{10}^{(0)}(zs) + \frac{\alpha_s N_c}{2\pi^2} \int_{\frac{\Lambda^2}{s}}^{z} \frac{dz'}{z'} \int d^2x_2 \, \frac{x_{10}^2}{x_{12}^2\, x_{20}^2} \left[\frac{1}{N_c^2} \left\langle \mathrm{tr}[V_{\underline{x}_2} V_{\underline{x}_1}^\dagger] \, \mathrm{tr}[V_{\underline{x}_0} V_{\underline{x}_2}^\dagger] \right\rangle_{(z's)} - S_{10}(z's) \right]$$

Unpolarized Small-x Evolution



Leading Log **BFKL Kernel** **Operator Hierarchy**

$$S_{10}(zs) = S_{10}^{(0)}(zs) + \frac{\alpha_s N_c}{2\pi^2} \int_{\frac{\Lambda^2}{s}}^{z} \frac{dz'}{z'} \int d^2x_2 \, \frac{x_{10}^2}{x_{12}^2\, x_{20}^2} \left[\frac{1}{N_c^2} \left\langle \mathrm{tr}[V_{\underline{x}_2} V_{\underline{x}_1}^\dagger] \, \mathrm{tr}[V_{\underline{x}_0} V_{\underline{x}_2}^\dagger] \right\rangle_{(z's)} - S_{10}(z's) \right]$$

Solution: The Pomeron Intercept

- Operator hierarchy closes in the large-N_c limit (BK)

$$S_{10}(zs) = S_{10}^{(0)}(zs) + \frac{\alpha_s N_c}{2\pi^2} \int_{\frac{\Lambda^2}{s}}^{z} \frac{dz'}{z'} \int d^2x_2 \, \frac{x_{10}^2}{x_{12}^2 \, x_{20}^2} \left[S_{12}(z's) \, S_{20}(z's) - S_{10}(z's) \right]$$

Solution: The Pomeron Intercept

- Operator hierarchy closes in the large-N_c limit (BK)

$$S_{10}(zs) = S_{10}^{(0)}(zs) + \frac{\alpha_s N_c}{2\pi^2} \int_{\frac{\Lambda^2}{s}}^{z} \frac{dz'}{z'} \int d^2x_2 \, \frac{x_{10}^2}{x_{12}^2 \, x_{20}^2} \left[S_{12}(z's) \, S_{20}(z's) - S_{10}(z's) \right]$$

- Dilute / linearized regime (BFKL): $1 - S_{10} \ll 1$

$$S_{10}(zs) = S_{10}^{(0)}(zs) + \frac{\alpha_s N_c}{2\pi^2} \int_{\frac{\Lambda^2}{s}}^{z} \frac{dz'}{z'} \int d^2x_2 \, \frac{x_{10}^2}{x_{12}^2 \, x_{20}^2} \left[S_{12}(z's) + S_{20}(z's) - S_{10}(z's) - 1 \right]$$

Solution: The Pomeron Intercept

- Operator hierarchy closes in the large-N_c limit (BK)

$$S_{10}(zs) = S_{10}^{(0)}(zs) + \frac{\alpha_s N_c}{2\pi^2} \int_{\frac{\Lambda^2}{s}}^{z} \frac{dz'}{z'} \int d^2x_2 \, \frac{x_{10}^2}{x_{12}^2 \, x_{20}^2} \left[S_{12}(z's) \, S_{20}(z's) - S_{10}(z's) \right]$$

- Dilute / linearized regime (BFKL): $1 - S_{10} \ll 1$

$$S_{10}(zs) = S_{10}^{(0)}(zs) + \frac{\alpha_s N_c}{2\pi^2} \int_{\frac{\Lambda^2}{s}}^{z} \frac{dz'}{z'} \int d^2x_2 \, \frac{x_{10}^2}{x_{12}^2 \, x_{20}^2} \left[S_{12}(z's) + S_{20}(z's) - S_{10}(z's) - 1 \right]$$

- Analytic solution by Laplace/Mellin transform (intercept):

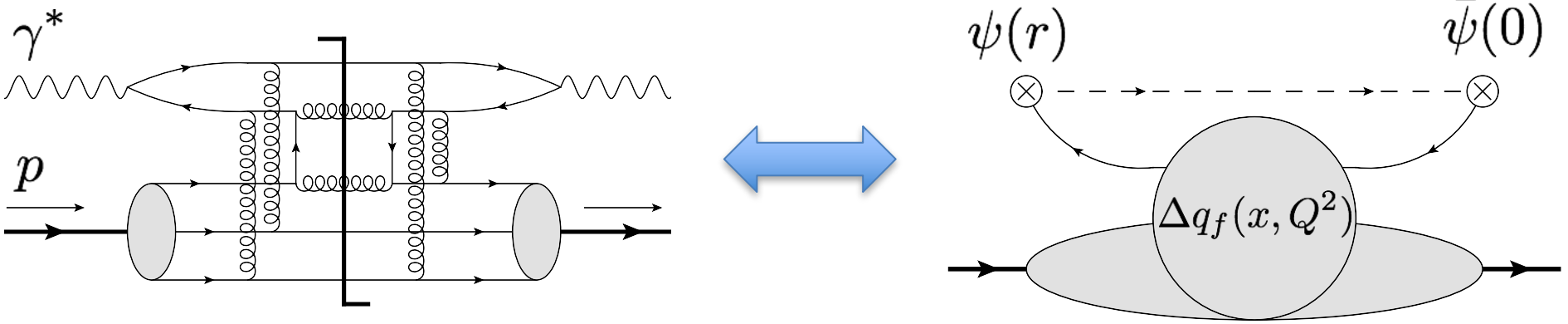
$$x \, q_f(x, Q^2) \sim S_{10}(s = \frac{Q^2}{x}) \sim \left(\frac{1}{x}\right)^{\alpha_P - 1} \qquad \alpha_P - 1 = \frac{4\alpha_s N_c}{\pi} \ln 2$$

The Main Course:

Small-x Evolution of the
Quark Helicity Distribution

Polarized Cross Sections and PDFs

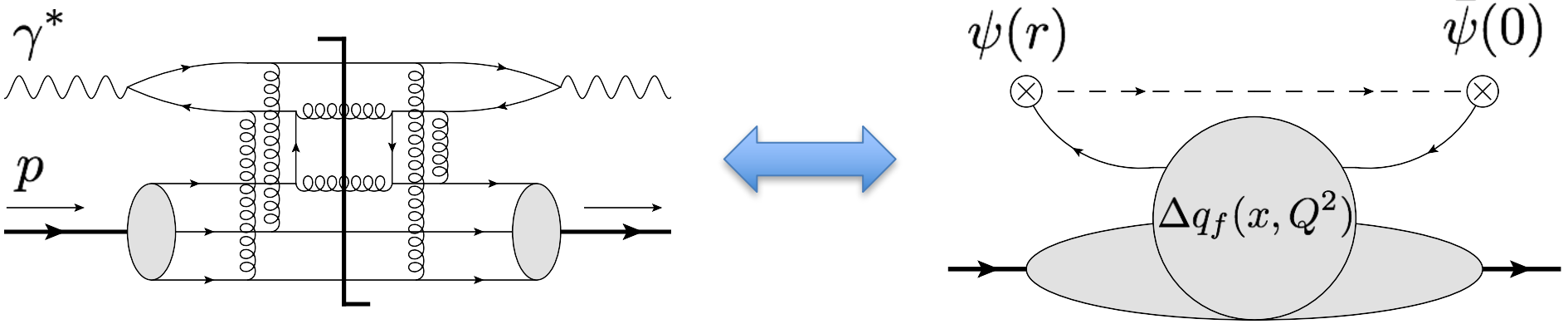
- **Factorization:** One-to-one correspondence between the spin-dependent DIS cross-section and the quark helicity PDF



$$\frac{Q^2}{4\pi^2\alpha_{EM}}\frac{d\,\Delta\sigma^{(\gamma^*\,p)}}{dx\,dQ^2} = 2x\,g_1(x,Q^2) \overset{L.O.}{=} \sum_f e_f^2\,x\Delta q_f(x,Q^2)$$

Polarized Cross Sections and PDFs

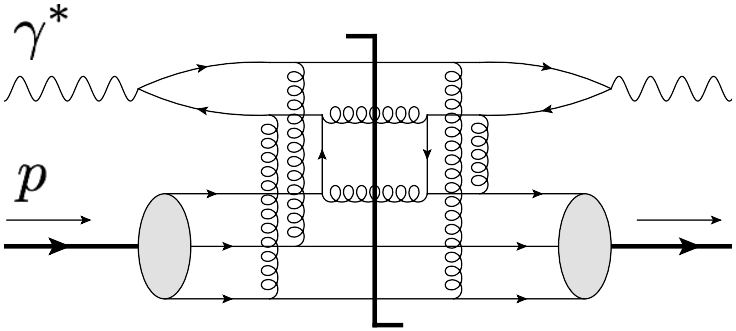
- **Factorization:** One-to-one correspondence between the spin-dependent DIS cross-section and the quark helicity PDF



$$\frac{Q^2}{4\pi^2\alpha_{EM}}\frac{d\,\Delta\sigma^{(\gamma^*\,p)}}{dx\,dQ^2} = 2x\,g_1(x,Q^2) \overset{L.O.}{=} \sum_f e_f^2\,x\Delta q_f(x,Q^2)$$

$$\frac{d\,\Delta\sigma^{(\gamma^*\,p)}}{dx\,dQ^2} \sim \left(\frac{1}{x}\right)^{\alpha_h-1} \sim x\Delta q_f(x,Q^2)$$

The Polarized Dipole Amplitude



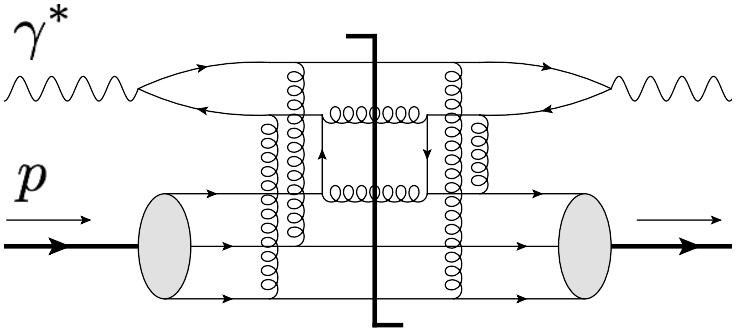
Flavor-Singlet Quark Helicity PDF

$$\Delta q^S(x,Q^2) = \sum_f \int \frac{dr^-}{2\pi}\, e^{ixp^+r^-}\, \langle p|\, \bar{\psi}(0)\, \mathcal{U}[0,r^-]\, \frac{\gamma^+\gamma^5}{2}\, \psi(r^-)\, |p\rangle$$

- The spin-dependent DIS cross-section / hPDF is expressed in terms of a polarized dipole amplitude / cross section

$$x\Delta q^S(x,Q^2) \overset{L.O.}{=} \frac{Q^2\, N_c}{2\pi^2 \alpha_{EM}} \sum_f \int \frac{d^2x_{10}\, dz}{4\pi\, z(1-z)} \left[\left|\Delta\Psi_{T,f}(x_{10}^2,z)\right|^2 + \left|\Delta\Psi_{L,f}(x_{10}^2,z)\right|^2 \right] \int d^2b_{10}\, \frac{1}{zs} G_{10}(zs)$$

The Polarized Dipole Amplitude



Flavor-Singlet Quark Helicity PDF

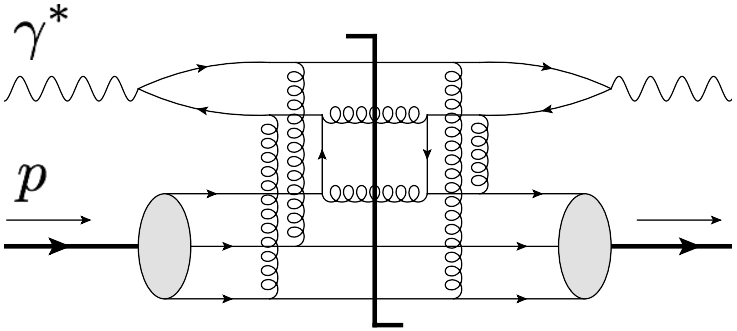
$$\Delta q^S(x,Q^2) = \sum_f \int \frac{dr^-}{2\pi}\, e^{ixp^+r^-}\, \langle p|\, \bar{\psi}(0)\, \mathcal{U}[0,r^-]\, \frac{\gamma^+\gamma^5}{2}\, \psi(r^-)\, |p\rangle$$

- The spin-dependent DIS cross-section / hPDF is expressed in terms of a polarized dipole amplitude / cross section

$$x\Delta q^S(x,Q^2) \overset{L.O.}{=} \frac{Q^2\, N_c}{2\pi^2 \alpha_{EM}} \sum_f \int \frac{d^2x_{10}\, dz}{4\pi\, z(1-z)} \left[\left|\Delta\Psi_{T,f}(x_{10}^2,z)\right|^2 + \left|\Delta\Psi_{L,f}(x_{10}^2,z)\right|^2 \right] \int d^2b_{10}\, \frac{1}{zs} G_{10}(zs)$$

$$\frac{1}{zs} G_{10}(zs) \equiv \left\langle \frac{1}{2N_c} \mathrm{tr}[V_{\underline{x}_0} V^{pol\,\dagger}_{\underline{x}_1}] + c.c. \right\rangle_{(zs)} = -\frac{1}{4} \left(\frac{d\,\Delta\sigma^{(q^{unp}_{\underline{x}_0}\, \bar{q}^{pol}_{\underline{x}_1})}}{d^2b_{10}}(zs) + ch.c. \right)$$

The Polarized Dipole Amplitude



Flavor-Singlet Quark Helicity PDF

$$\Delta q^S(x,Q^2) = \sum_f \int \frac{dr^-}{2\pi}\, e^{ixp^+r^-}\, \langle p|\, \bar\psi(0)\, \mathcal{U}[0,r^-]\, \frac{\gamma^+\gamma^5}{2}\, \psi(r^-)\, |p\rangle$$

- The spin-dependent DIS cross-section / hPDF is expressed in terms of a polarized dipole amplitude / cross section

$$x\Delta q^S(x,Q^2) \overset{L.O.}{=} \frac{Q^2\, N_c}{2\pi^2\alpha_{EM}} \sum_f \int \frac{d^2x_{10}\, dz}{4\pi\, z(1-z)} \left[\left|\Delta\Psi_{T,f}(x_{10}^2,z)\right|^2 + \left|\Delta\Psi_{L,f}(x_{10}^2,z)\right|^2 \right] \int d^2b_{10}\, \frac{1}{zs} G_{10}(zs)$$

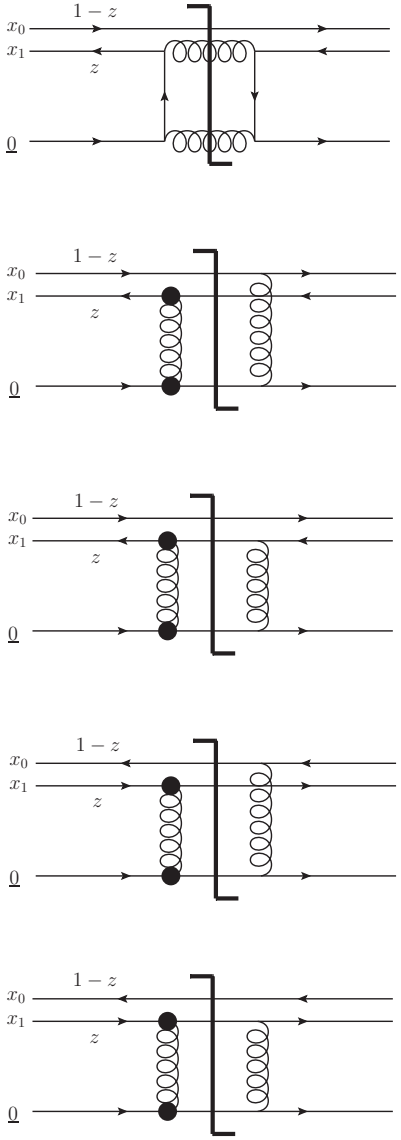
$$\frac{1}{zs} G_{10}(zs) \equiv \left\langle \frac{1}{2N_c} \mathrm{tr}[V_{\underline{x}_0} V^{pol\,\dagger}_{\underline{x}_1}] + c.c. \right\rangle_{(zs)} = -\frac{1}{4} \left(\frac{d\,\Delta\sigma^{(q^{unp}_{\underline{x}_0}\, \bar q^{pol}_{\underline{x}_1})}}{d^2b_{10}}(zs) + ch.c. \right)$$

"Polarized Wilson line"

Helicity Evolution: Initial Conditions

- Initial conditions from the quark target model
  - Quark and sub-eikonal gluon exchange

$$G_{10}^{(0)}(zs) = \frac{\alpha_s^2 C_F}{N_c}\left[\frac{C_F}{x_{1T}^2} - 2\pi\delta^2(\underline{x}_1)\,\ln(zs\,x_{10}^2)\right]$$



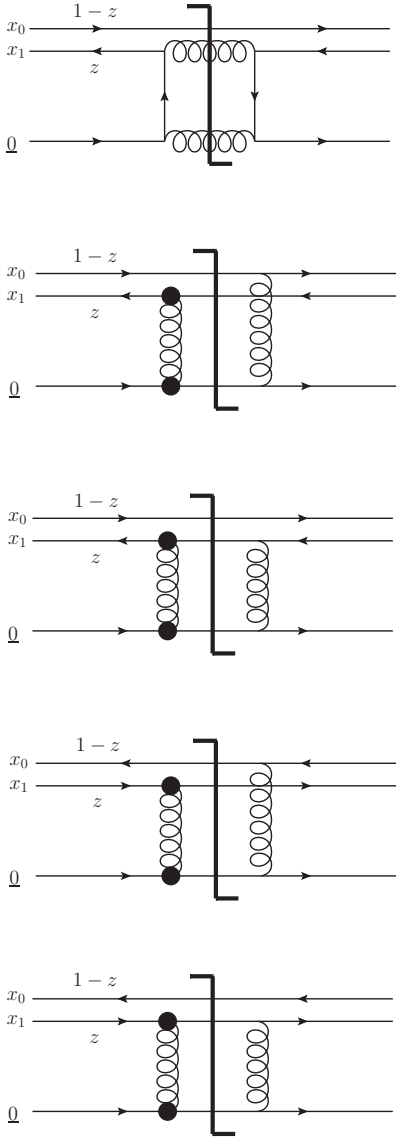
Helicity Evolution: Initial Conditions

- Initial conditions from the quark target model
  - Quark and sub-eikonal gluon exchange

$$G_{10}^{(0)}(zs) = \frac{\alpha_s^2 C_F}{N_c}\left[\frac{C_F}{x_{1T}^2} - 2\pi\delta^2(\underline{x}_1)\,\ln(zs\,x_{10}^2)\right]$$

- Polarization transfer is suppressed at small x
  - Leading term has exactly 1 sub-eikonal exchange

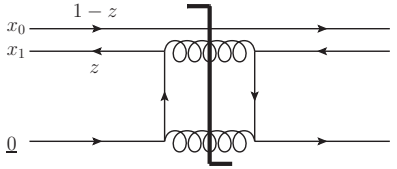
$$\frac{d\,\Delta\sigma^{(q^{unp}_{\underline{x}_0}\,\bar{q}^{pol}_{\underline{x}_1})}}{d^2b_{10}}(zs) \propto \frac{1}{zs}$$

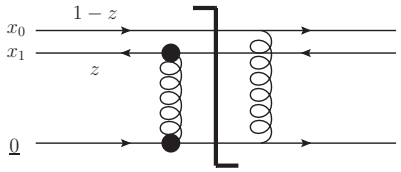


Helicity Evolution: Initial Conditions

- Initial conditions from the quark target model
  - Quark and sub-eikonal gluon exchange

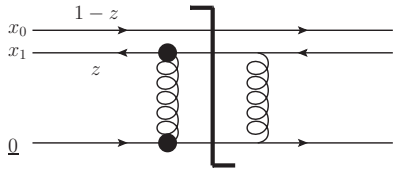
$$G_{10}^{(0)}(zs) = \frac{\alpha_s^2 C_F}{N_c}\left[\frac{C_F}{x_{1T}^2} - 2\pi\delta^2(\underline{x}_1)\,\ln(zs\,x_{10}^2)\right]$$



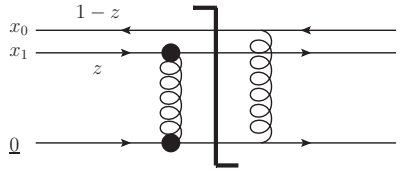


- Polarization transfer is suppressed at small x
  - Leading term has exactly 1 sub-eikonal exchange

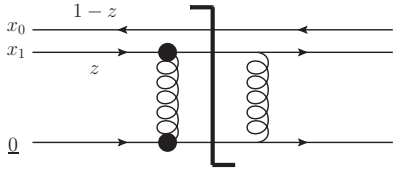
$$\frac{d\,\Delta\sigma^{(q^{unp}_{\underline{x}_0}\,\bar{q}^{pol}_{\underline{x}_1})}}{d^2b_{10}}(zs) \propto \frac{1}{zs}$$



- Include this known scaling in the definition of the polarized dipole amplitude



$$\frac{1}{zs}G_{10}(zs) \equiv \left\langle \frac{1}{2N_c}\mathrm{tr}[V_{\underline{x}_0}V^{pol\,\dagger}_{\underline{x}_1}] + c.c. \right\rangle_{(zs)} = -\frac{1}{4}\left(\frac{d\,\Delta\sigma^{(q^{unp}_{\underline{x}_0}\,\bar{q}^{pol}_{\underline{x}_1})}}{d^2b_{10}}(zs) + ch.c.\right)$$



Origins of Helicity Evolution

- Soft polarized quark and gluon emission spans the full rapidity interval:

$$\int \frac{dz'}{z'} \to \ln \frac{zs}{\Lambda^2}$$

- The polarized line is also sensitive to collinear / short-distance fluctuations:

$$\int \frac{dx_{21}^2}{x_{21}^2} \to \ln \frac{zs}{\Lambda^2}$$

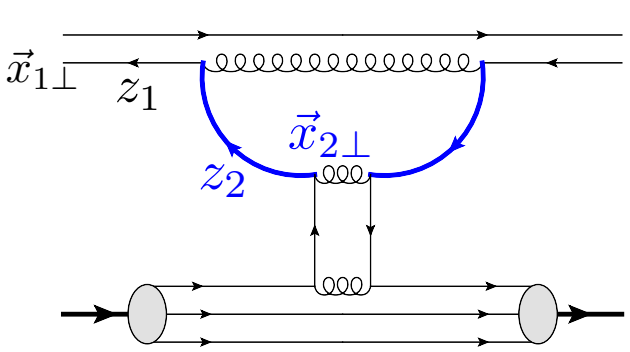
Origins of Helicity Evolution

- Soft polarized quark and gluon emission spans the full rapidity interval:

$$\int \frac{dz'}{z'} \to \ln \frac{zs}{\Lambda^2}$$

- The polarized line is also sensitive to collinear / short-distance fluctuations:

$$\int \frac{dx_{21}^2}{x_{21}^2} \to \ln \frac{zs}{\Lambda^2}$$



$$\underbrace{\left\langle V_1^{pol\,\dagger}(z_1)\right\rangle}_{\sim \frac{1}{z_1 s}} \sim \int \frac{dz_2}{z_2} \int d^2x_2 \left(\frac{\alpha_s C_F}{2\pi^2} \frac{z_2}{z_1} \frac{1}{x_{21}^2}\right) \underbrace{\left\langle V_2^{pol\,\dagger}(z_2)\right\rangle}_{\sim \frac{1}{z_2 s}}$$

$$G_{10}(z_1) \sim \frac{\alpha_s C_F}{2\pi} \underbrace{\int \frac{dz_2}{z_2} \int \frac{dx_{21}^2}{x_{21}^2}}_{\ln^2 \frac{z_1 s}{\Lambda^2}} G_{21}(z_2)$$

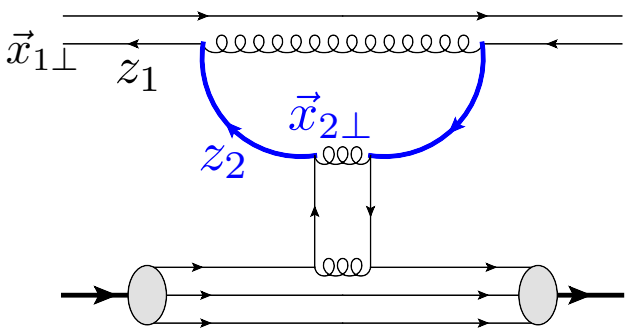
Origins of Helicity Evolution

- Soft polarized quark and gluon emission spans the full rapidity interval:

$$\int \frac{dz'}{z'} \to \ln \frac{zs}{\Lambda^2}$$

- The polarized line is also sensitive to collinear / short-distance fluctuations:

$$\int \frac{dx_{21}^2}{x_{21}^2} \to \ln \frac{zs}{\Lambda^2}$$



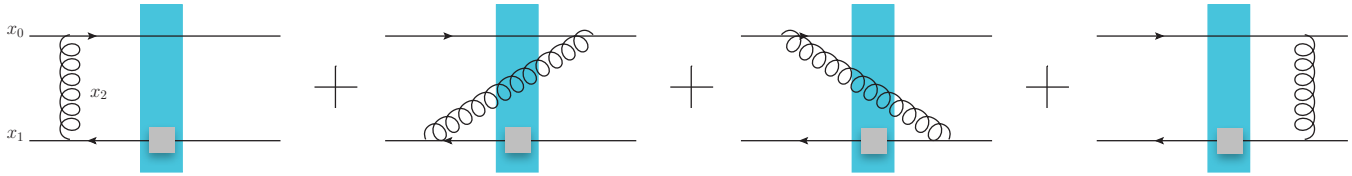
$$\underbrace{\left\langle V_1^{pol\,\dagger}(z_1)\right\rangle}_{\sim \frac{1}{z_1 s}} \sim \int \frac{dz_2}{z_2} \int d^2x_2 \left(\frac{\alpha_s C_F}{2\pi^2} \frac{z_2}{z_1} \frac{1}{x_{21}^2}\right) \underbrace{\left\langle V_2^{pol\,\dagger}(z_2)\right\rangle}_{\sim \frac{1}{z_2 s}}$$

$$G_{10}(z_1) \sim \frac{\alpha_s C_F}{2\pi} \underbrace{\int \frac{dz_2}{z_2} \int \frac{dx_{21}^2}{x_{21}^2}}_{\ln^2 \frac{z_1 s}{\Lambda^2}} G_{21}(z_2)$$

- Helicity evolution is double logarithmic
  - ➢ Stronger than unpolarized evolution!

$$\alpha_s \ln^2 \frac{1}{x} \sim 1$$

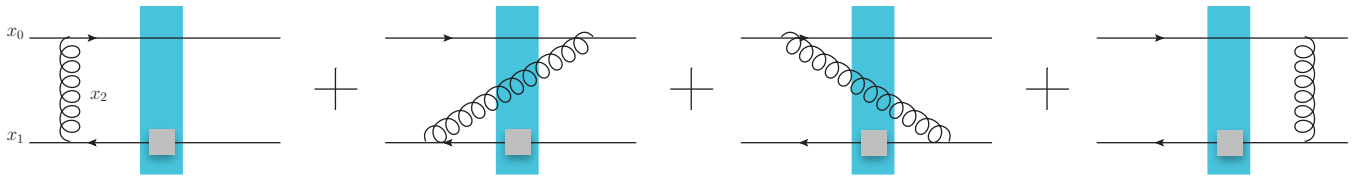
An Example: The Collinear BFKL Sector



$$\sim \int d^2x_2 \frac{(\underline{x_{21}} \cdot \underline{x_{20}})}{x_{21}^2\, x_{20}^2}$$

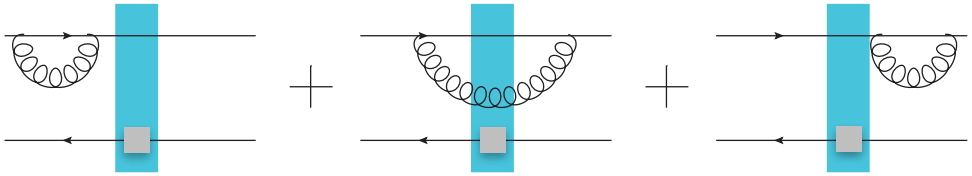
- No collinear logarithms

An Example: The Collinear BFKL Sector



$$\sim \int d^2x_2 \frac{(\underline{x_{21}} \cdot \underline{x_{20}})}{x_{21}^2\, x_{20}^2}$$

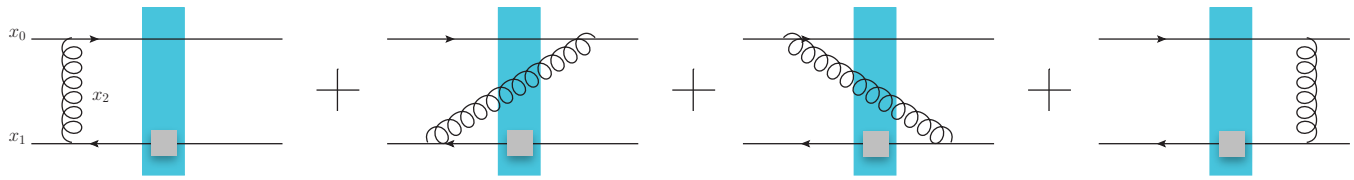
- No collinear logarithms



$$\sim \int d^2x_2 \frac{1}{x_{20}^2} \left[\frac{1}{N_c^2} \left\langle \mathrm{tr}[V_{\underline{x_2}} V_{\underline{x_1}}^{pol\,\dagger}] \, \mathrm{tr}[V_{\underline{x_0}} V_{\underline{x_2}}^{\dagger}] \right\rangle - \frac{1}{N_c} \left\langle \mathrm{tr}[V_{\underline{x_0}} V_{\underline{x_1}}^{pol\,\dagger}] \right\rangle \right]$$

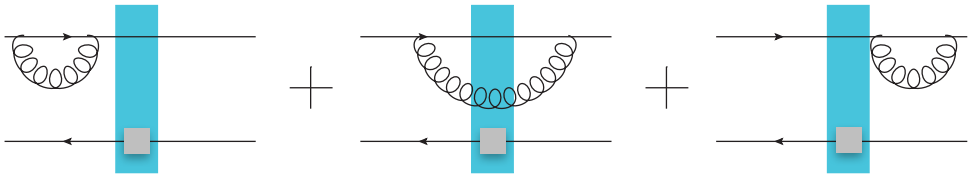
- Collinear enhancement as $\underline{x}_2 \to \underline{x}_0$, but vanishing support due to real-virtual cancellations

An Example: The Collinear BFKL Sector



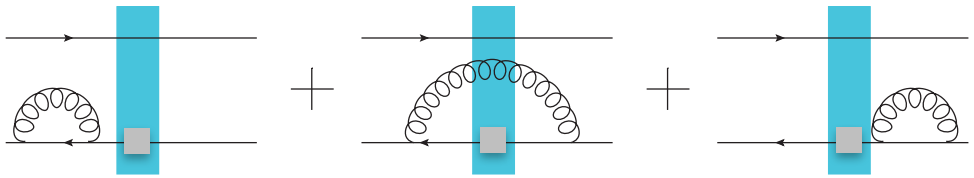
$$\sim \int d^2x_2 \frac{(\underline{x_{21}} \cdot \underline{x_{20}})}{x_{21}^2\, x_{20}^2}$$

- No collinear logarithms



$$\sim \int d^2x_2 \frac{1}{x_{20}^2} \left[\frac{1}{N_c^2} \left\langle \mathrm{tr}[V_{\underline{x_2}} V_{\underline{x_1}}^{pol\,\dagger}] \, \mathrm{tr}[V_{\underline{x_0}} V_{\underline{x_2}}^{\dagger}] \right\rangle - \frac{1}{N_c} \left\langle \mathrm{tr}[V_{\underline{x_0}} V_{\underline{x_1}}^{pol\,\dagger}] \right\rangle \right]$$

- Collinear enhancement as $\underline{x_2} \to \underline{x_0}$, but vanishing support due to real-virtual cancellations



$$\sim \int d^2x_2 \frac{1}{x_{21}^2} \left[\frac{1}{N_c^2} \left\langle \mathrm{tr}[V_{\underline{x_2}} V_{\underline{x_1}}^{pol\,\dagger}] \, \mathrm{tr}[V_{\underline{x_0}} V_{\underline{x_2}}^{\dagger}] \right\rangle - \frac{1}{N_c} \left\langle \mathrm{tr}[V_{\underline{x_0}} V_{\underline{x_1}}^{pol\,\dagger}] \right\rangle \right]$$

- Collinear enhancement as $\underline{x_2} \to \underline{x_1}$, about the distinct polarized line

DLA Ordering for Helicity Evolution

- Because one line of the dipole is polarized, a subset of the BFKL kernel becomes double logarithmic (DLA) for $x_{21}^2 \ll x_{10}^2$

$$\delta G_{10}(zs) = \frac{\alpha_s N_c}{2\pi^2} \int_{\frac{1}{x_{10}^2 s}}^{z} \frac{dz'}{z'} \int_{\frac{1}{z's}}^{x_{10}^2} \frac{d^2x_{21}}{x_{21}^2} \left[\frac{1}{N_c^2} \left\langle\!\!\left\langle \mathrm{tr}[V_{\underline{x}_2} V^{pol\,\dagger}_{\underline{x}_1}] \, \mathrm{tr}[V_{\underline{x}_0} V^{\dagger}_{\underline{x}_2}] \right\rangle\!\!\right\rangle_{(z's)} - \frac{1}{N_c} \left\langle\!\!\left\langle \mathrm{tr}[V_{\underline{x}_0} V^{pol\,\dagger}_{\underline{x}_1}] \right\rangle\!\!\right\rangle_{(z's)} \right]$$

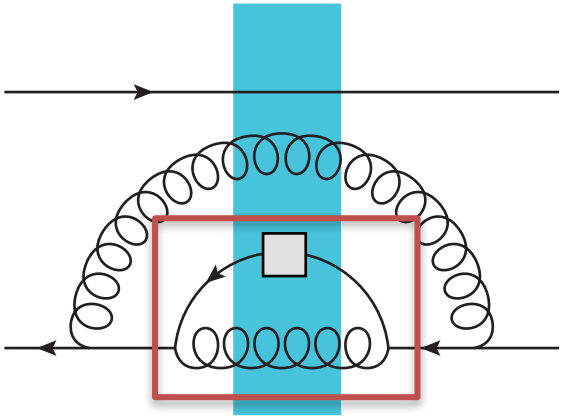
$$\frac{1}{2} \ln^2(zs\, x_{10}^2)$$

DLA Ordering for Helicity Evolution

- Because one line of the dipole is polarized, a subset of the BFKL kernel becomes double logarithmic (DLA) for $x_{21}^2 \ll x_{10}^2$

$$\delta G_{10}(zs) = \frac{\alpha_s N_c}{2\pi^2} \int_{\frac{1}{x_{10}^2 s}}^{z} \frac{dz'}{z'} \int_{\frac{1}{z's}}^{x_{10}^2} \frac{d^2x_{21}}{x_{21}^2} \left[\frac{1}{N_c^2} \left\langle\!\!\left\langle \mathrm{tr}[V_{\underline{x}_2} V_{\underline{x}_1}^{pol\,\dagger}] \, \mathrm{tr}[V_{\underline{x}_0} V_{\underline{x}_2}^{\dagger}] \right\rangle\!\!\right\rangle_{(z's)} - \frac{1}{N_c} \left\langle\!\!\left\langle \mathrm{tr}[V_{\underline{x}_0} V_{\underline{x}_1}^{pol\,\dagger}] \right\rangle\!\!\right\rangle_{(z's)} \right]$$

$$\frac{1}{2} \ln^2(zs\, x_{10}^2)$$



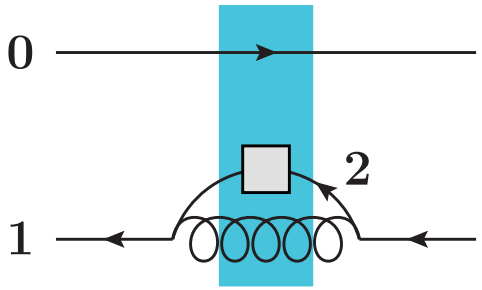
- To continue generating both soft and collinear logs, further evolution must be doubly ordered:

$$z \gg z' \gg z'' \gg \cdots$$

$$z\,\Delta x_T^2 \gg z'\,\Delta x_T'^2 \gg z''\,\Delta x_T''^2 \gg \cdots$$

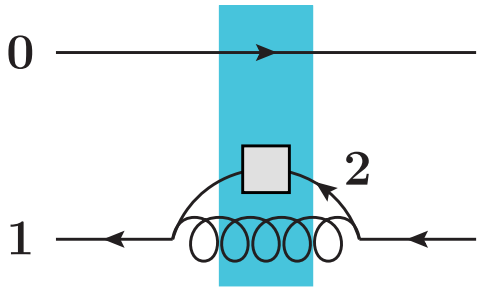
New Contributions: Polarized Quarks

- Emission of a soft polarized (anti)quark is only possible from the polarized line
  - DLA contribution extends over the whole ordered phase space
  - No $x_{21}^2 \ll x_{10}^2$ restriction



New Contributions: Polarized Quarks

- Emission of a soft polarized (anti)quark is only possible from the polarized line
  - DLA contribution extends over the whole ordered phase space
  - No $x_{21}^2 \ll x_{10}^2$ restriction



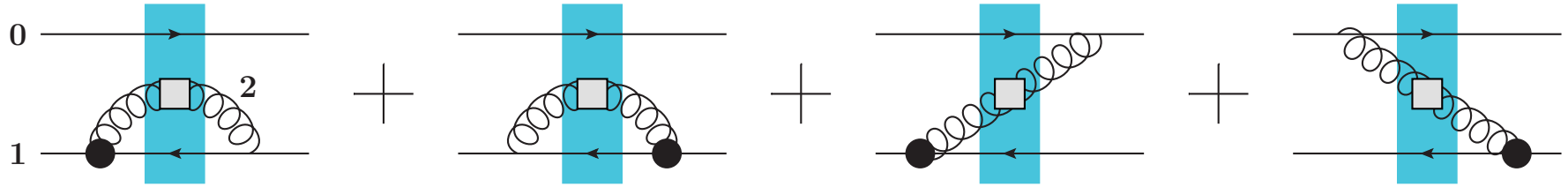
Full phase space

$$\delta G_{10}(zs) = \frac{\alpha_s N_c}{4\pi^2} \int_{\frac{\Lambda^2}{s}}^{z} \frac{dz'}{z'} \int_{\frac{1}{z's}}^{x_{10}^2 \frac{z}{z'}} \frac{d^2x_{21}}{x_{21}^2} \left[\frac{1}{N_c^2} \left\langle\!\!\left\langle \mathrm{tr}[V_{\underline{x}_1} V^{pol\,\dagger}_{\underline{x}_2}] \, \mathrm{tr}[V_{\underline{x}_0} V^{\dagger}_{\underline{x}_1}] \right\rangle\!\!\right\rangle_{(z's)} - \frac{1}{N_c^3} \left\langle\!\!\left\langle \mathrm{tr}[V_{\underline{x}_0} V^{pol\,\dagger}_{\underline{x}_2}] \right\rangle\!\!\right\rangle_{(z's)} \right]$$

$$\ln(zs\,x_{10}^2)\,\ln(zs/\Lambda^2)$$

New Contributions: Polarized Gluons

- Emission of a soft polarized gluon can couple to both lines

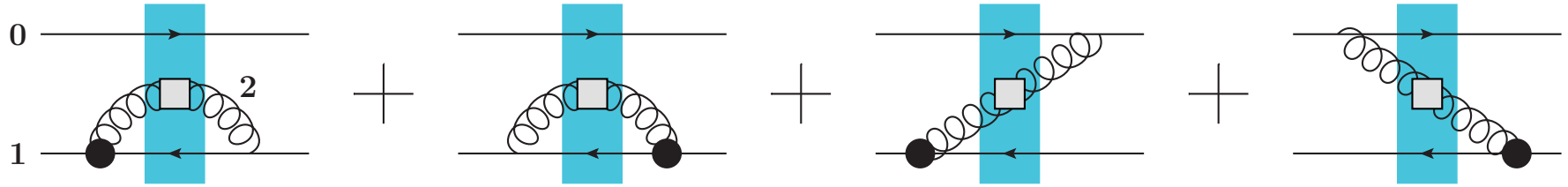


➢ **Ladder (from polarized line only): DLA everywhere**

$$\delta G_{10}(zs) = +\frac{\alpha_s N_c}{2\pi^2}\int_{\frac{\Lambda^2}{s}}^{z}\frac{dz'}{z'}\int_{\frac{1}{z's}}^{x_{10}^2\frac{z}{z'}}\frac{d^2x_{21}}{x_{21}^2}\left[\frac{1}{N_c^2}\left\langle\!\left\langle \mathrm{tr}[t^b V_{\underline{x}_0} t^a V_{\underline{x}_1}^\dagger]\left(U_{\underline{x}_2}^{pol}\right)^{ba}\right\rangle\!\right\rangle_{(z's)}\right]$$

New Contributions: Polarized Gluons

- Emission of a soft polarized gluon can couple to both lines



➢ **Ladder (from polarized line only):** **DLA everywhere**

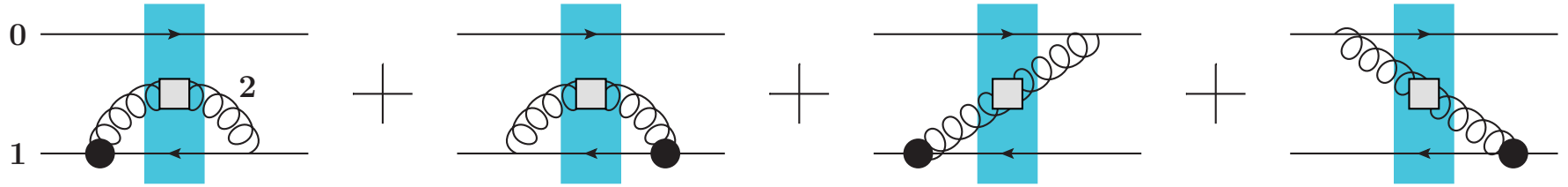
$$\delta G_{10}(zs) = +\frac{\alpha_s N_c}{2\pi^2}\int_{\frac{\Lambda^2}{s}}^{z}\frac{dz'}{z'}\int_{\frac{1}{z's}}^{x_{10}^2\frac{z}{z'}}\frac{d^2x_{21}}{x_{21}^2}\left[\frac{1}{N_c^2}\left\langle\!\left\langle \mathrm{tr}[t^b V_{\underline{x_0}} t^a V_{\underline{x_1}}^\dagger]\left(U_{\underline{x_2}}^{pol}\right)^{ba}\right\rangle\!\right\rangle_{(z's)}\right]$$

➢ **Non-Ladder (across the dipole):** Cancel ladders for $x_{21}^2 \gg x_{10}^2$

$$\delta G_{10}(zs) = -\frac{\alpha_s N_c}{2\pi^2}\int_{\frac{\Lambda^2}{s}}^{z}\frac{dz'}{z'}\int_{\frac{1}{z's}}^{x_{10}^2\frac{z}{z'}} d^2x_2\,\frac{(\underline{x_{21}}\cdot\underline{x_{20}})}{x_{21}^2\,x_{20}^2}\left[\frac{1}{N_c^2}\left\langle\!\left\langle \mathrm{tr}[t^b V_{\underline{x_0}} t^a V_{\underline{x_1}}^\dagger]\left(U_{\underline{x_2}}^{pol}\right)^{ba}\right\rangle\!\right\rangle_{(z's)}\right]$$

New Contributions: Polarized Gluons

- Emission of a soft polarized gluon can couple to both lines



➢ **Ladder (from polarized line only):** **DLA everywhere**

$$\delta G_{10}(zs) = +\frac{\alpha_s N_c}{2\pi^2}\int\limits_{\frac{\Lambda^2}{s}}^{z}\frac{dz'}{z'}\int\limits_{\frac{1}{z's}}^{x_{10}^2\frac{z}{z'}}\frac{d^2x_{21}}{x_{21}^2}\left[\frac{1}{N_c^2}\left\langle\!\left\langle \mathrm{tr}[t^b V_{\underline{x_0}} t^a V_{\underline{x_1}}^\dagger]\left(U_{\underline{x_2}}^{pol}\right)^{ba}\right\rangle\!\right\rangle_{(z's)}\right]$$

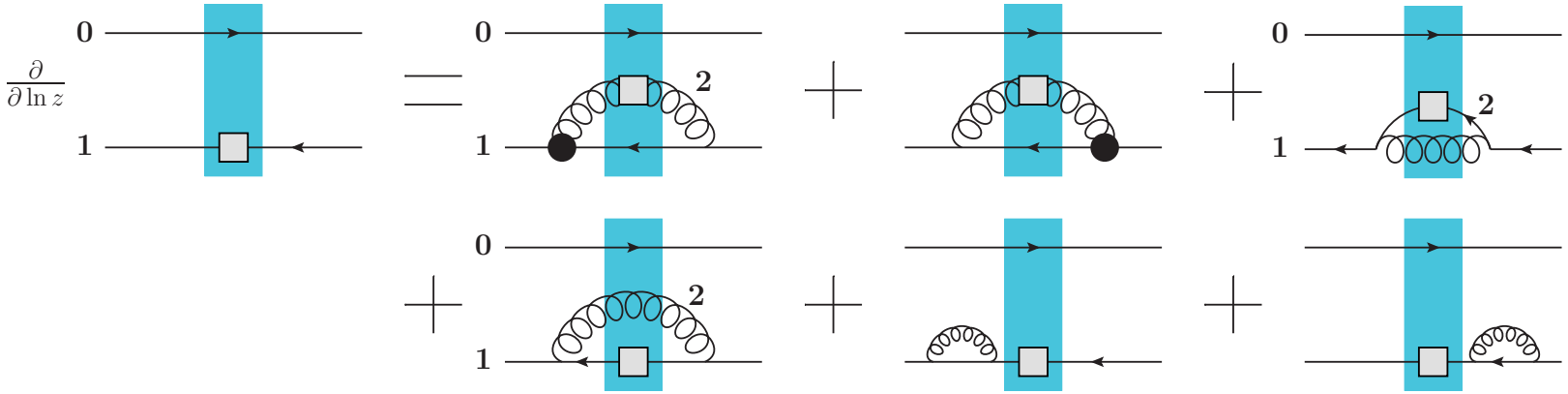
➢ **Non-Ladder (across the dipole):** Cancel ladders for $x_{21}^2 \gg x_{10}^2$

$$\delta G_{10}(zs) = -\frac{\alpha_s N_c}{2\pi^2}\int\limits_{\frac{\Lambda^2}{s}}^{z}\frac{dz'}{z'}\int\limits_{\frac{1}{z's}}^{x_{10}^2\frac{z}{z'}} d^2x_2\,\frac{(\underline{x_{21}}\cdot\underline{x_{20}})}{x_{21}^2\,x_{20}^2}\left[\frac{1}{N_c^2}\left\langle\!\left\langle \mathrm{tr}[t^b V_{\underline{x_0}} t^a V_{\underline{x_1}}^\dagger]\left(U_{\underline{x_2}}^{pol}\right)^{ba}\right\rangle\!\right\rangle_{(z's)}\right]$$

➢ **Limits the DLA phase space** for polarized ladder gluons: $x_{21}^2 \ll x_{10}^2$

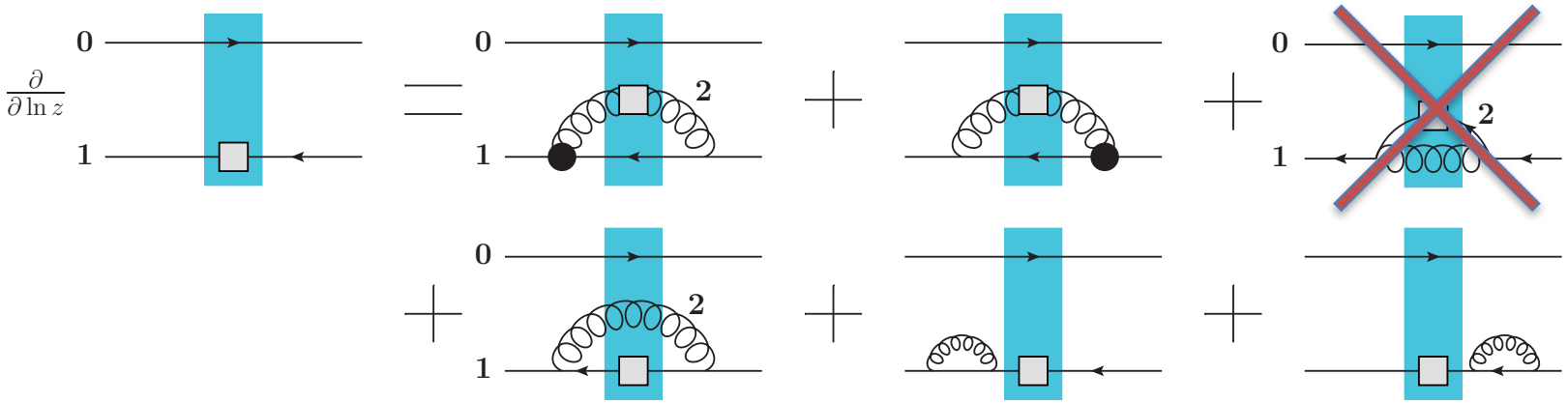
When the Dust Settles

- DLA evolution is only sensitive to fluctuations near the polarized line
  - For all gluon emissions, ladder / non-ladder cancellation limits the DLA to the strongly ordered phase space $x_{21}^2 \ll x_{10}^2$



When the Dust Settles

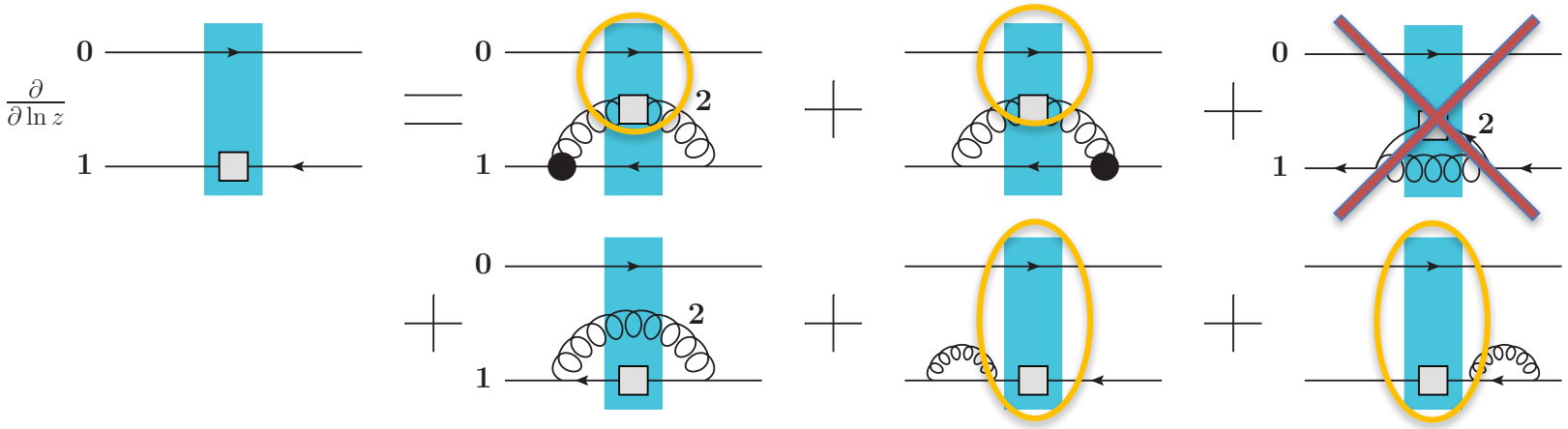
- DLA evolution is only sensitive to fluctuations near the polarized line
  - For all gluon emissions, ladder / non-ladder cancellation limits the DLA to the strongly ordered phase space $x_{21}^2 \ll x_{10}^2$



- The polarized analog of BFKL is the linearized, large-N_c limit

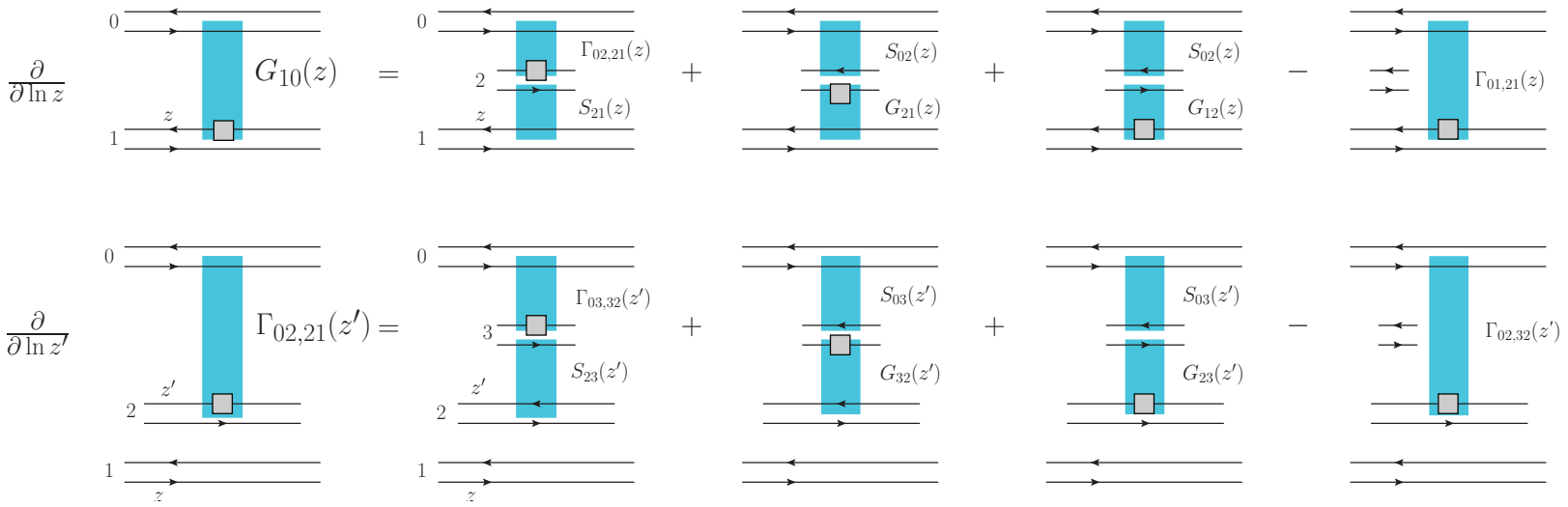
When the Dust Settles

- DLA evolution is only sensitive to fluctuations near the polarized line
  - For all gluon emissions, ladder / non-ladder cancellation limits the DLA to the strongly ordered phase space $x_{21}^2 \ll x_{10}^2$



- The polarized analog of BFKL is the linearized, large-N_c limit
  - There is a nontrivial constraint on the lifetime of large polarized dipoles from their short-lived "neighbor" fluctuations!

Large-N_c Evolution Equations



- The impact-parameter integrated dipole amplitude evolves as:

$$G(x_{10}^2, z) = G^{(0)}(x_{10}^2, z) + \frac{\alpha_s N_c}{2\pi} \int_{\frac{1}{x_{10}^2 s}}^{z} \frac{dz'}{z'} \int_{\frac{1}{z's}}^{x_{10}^2} \frac{dx_{21}^2}{x_{21}^2} \left[\Gamma(x_{10}^2, x_{21}^2, z') + 3G(x_{21}^2, z')\right]$$

$$\Gamma(x_{10}^2, x_{21}^2, z') = G^{(0)}(x_{10}^2, z') + \frac{\alpha_s N_c}{2\pi} \int_{\frac{1}{x_{10}^2 s}}^{z'} \frac{dz''}{z''} \int_{\frac{1}{z''s}}^{\min[x_{10}^2, x_{21}^2 \frac{z'}{z''}]} \frac{dx_{32}^2}{x_{32}^2} \left[\Gamma(x_{10}^2, x_{32}^2, z'') + 3G(x_{32}^2, z'')\right]$$

Up Next: Dessert

Finding a Solution at Small x

The Task at Hand

$$G(x_{10}^2, z) = G^{(0)}(x_{10}^2, z) + \frac{\alpha_s N_c}{2\pi} \int\limits_{\frac{1}{x_{10}^2 s}}^{z} \frac{dz'}{z'} \int\limits_{\frac{1}{z's}}^{x_{10}^2} \frac{dx_{21}^2}{x_{21}^2} \left[\Gamma(x_{10}^2, x_{21}^2, z') + 3G(x_{21}^2, z')\right]$$

$$\Gamma(x_{10}^2, x_{21}^2, z') = G^{(0)}(x_{10}^2, z') + \frac{\alpha_s N_c}{2\pi} \int\limits_{\frac{1}{x_{10}^2 s}}^{z'} \frac{dz''}{z''} \int\limits_{\frac{1}{z''s}}^{\min[x_{10}^2, x_{21}^2 \frac{z'}{z''}]} \frac{dx_{32}^2}{x_{32}^2} \left[\Gamma(x_{10}^2, x_{32}^2, z'') + 3G(x_{32}^2, z'')\right]$$

- Must solve a set of coupled integro-differential equations
  - Neighbor dipole depends on two spatial arguments

The Task at Hand

$$G(x_{10}^2, z) = G^{(0)}(x_{10}^2, z) + \frac{\alpha_s N_c}{2\pi} \int\limits_{\frac{1}{x_{10}^2 s}}^{z} \frac{dz'}{z'} \int\limits_{\frac{1}{z's}}^{x_{10}^2} \frac{dx_{21}^2}{x_{21}^2} \left[\Gamma(x_{10}^2, x_{21}^2, z') + 3G(x_{21}^2, z')\right]$$

$$\Gamma(x_{10}^2, x_{21}^2, z') = G^{(0)}(x_{10}^2, z') + \frac{\alpha_s N_c}{2\pi} \int\limits_{\frac{1}{x_{10}^2 s}}^{z'} \frac{dz''}{z''} \int\limits_{\frac{1}{z''s}}^{\min[x_{10}^2, x_{21}^2 \frac{z'}{z''}]} \frac{dx_{32}^2}{x_{32}^2} \left[\Gamma(x_{10}^2, x_{32}^2, z'') + 3G(x_{32}^2, z'')\right]$$

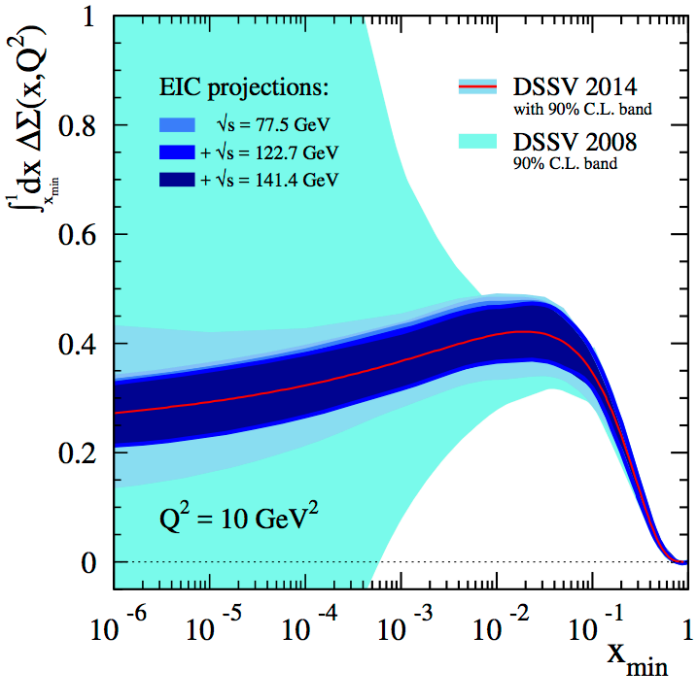
- Must solve a set of coupled integro-differential equations
  - Neighbor dipole depends on two spatial arguments
- Can it be done numerically? Can it be done analytically?
  - What is the helicity intercept at small x?

$$\frac{d\,\Delta\sigma^{(\gamma^* p)}}{dx\,dQ^2} \sim \left(\frac{1}{x}\right)^{\alpha_h - 1} \sim x\Delta q_f(x, Q^2)$$

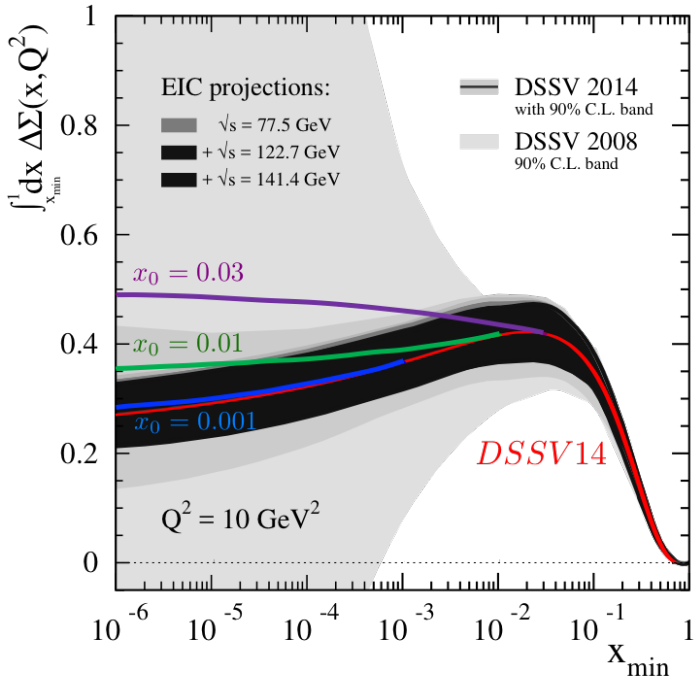
$$\alpha_h = ???$$

Conclusion: A Taste of the Answer

Without Small-x Evolution



With Small-x Evolution



adapted from Aschenauer et al., Phys. Rev. ***D92*** *(2015) no.9 094030*

- Quark helicity at small x receives **strong double-logarithmic enhancement** through the evolution near a polarized Wilson line

Low x physics and prompt neutrino production

Anna Staśto

PennState
Eberly College of Science

RBRC Workshop, Saturation: Recent Developments, New Ideas and Measurements, BNL, April 27, 2017

Outline

- Motivation: ultrahigh energy neutrino astronomy
- Atmospheric neutrinos: conventional and prompt
- Cross section for charm production at forward rapidities: collinear, dipole and k_T factorization calculations
- Calculation of prompt neutrino fluxes

Work in collaboration with

A. Bhattacharya, R. Enberg, Y. S. Jeong, C. S. Kim, M. H. Reno, I. Sarcevic
arXiv:1502.01076, arXiv:1607.00193

Neutrino astronomy

- Universe not transparent to extragalactic photons with energy > 10 TeV
- Weakly interacting: neutrinos can travel large distances without distortion

Interaction lengths (at 1 TeV):

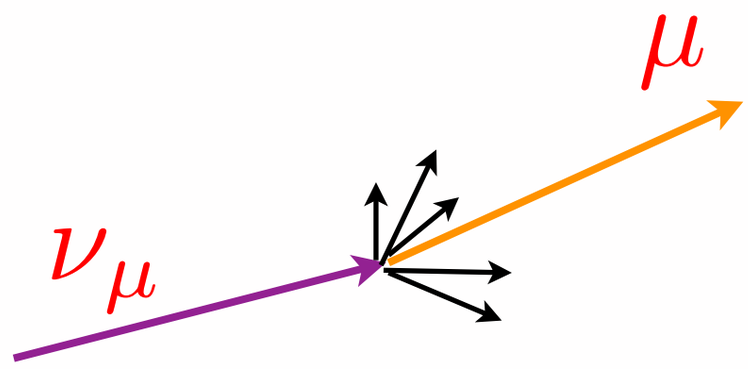
$$\mathcal{L}^{\gamma}_{\rm int} \sim 100\,{\rm g/cm^2}$$

$$\mathcal{L}^{\nu}_{\rm int} \sim 250 \times 10^9\,{\rm g/cm^2}$$

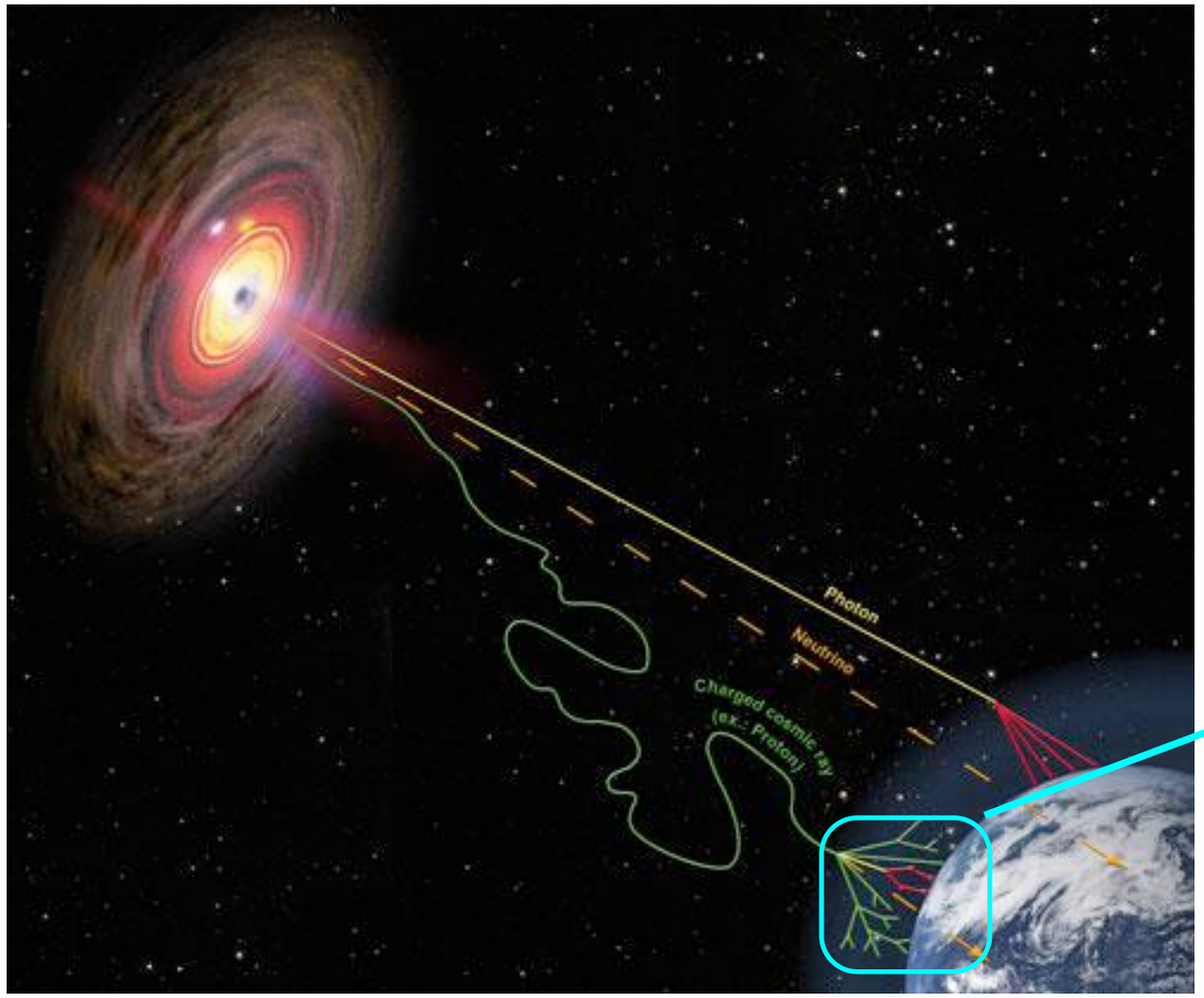
- Trajectories of protons and nuclei are distorted by the magnetic fields
- Neutrinos can point back to their sources

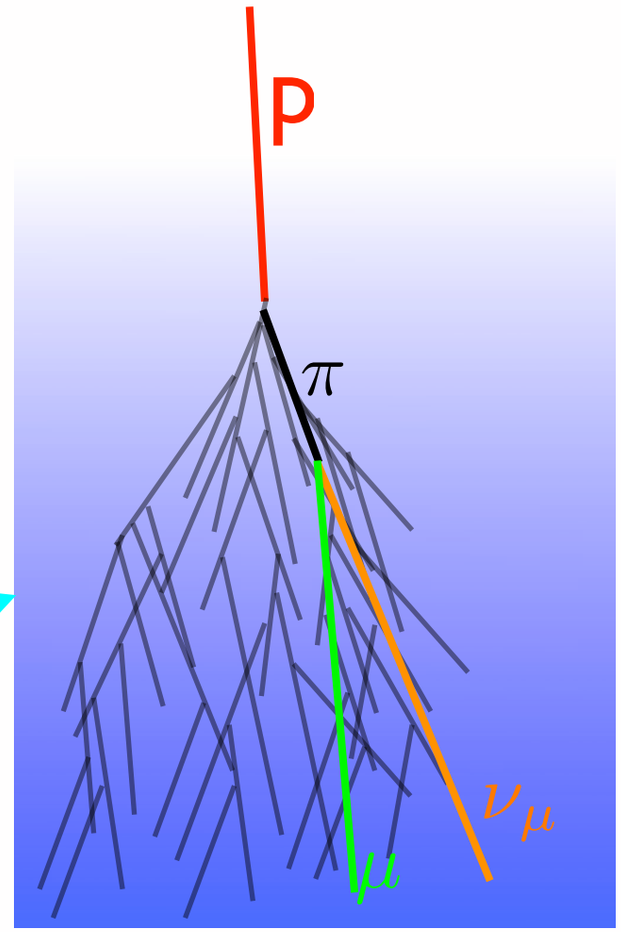
Angular distortion

$$\delta\phi \simeq \frac{0.7^o}{(E_\nu/{\rm TeV})^{0.7}}$$



Atmospheric neutrinos





(credit: www.hap-astroparticle.org/ A. Chantelauze)

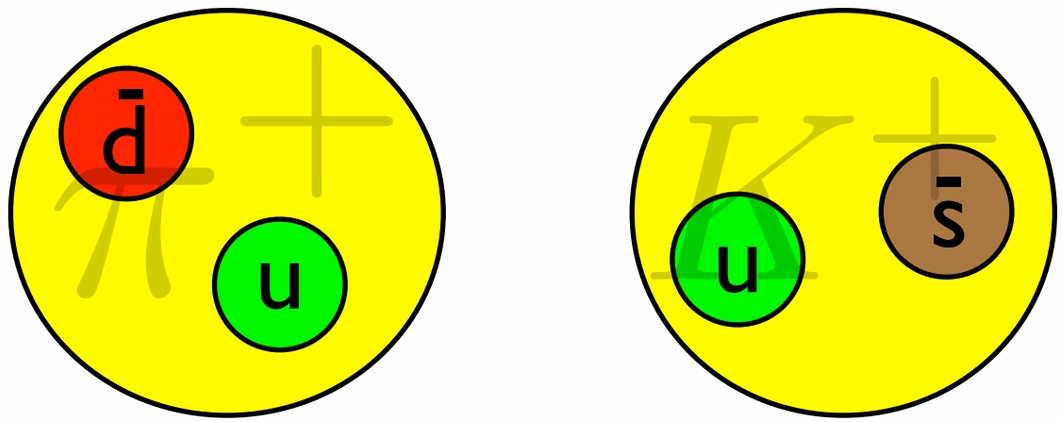
Neutrinos in the atmosphere originate from the interactions of cosmic rays (etc. protons) with nuclei.

$$p + \text{Air} \xrightarrow{\textit{interaction}} \pi, K \xrightarrow{\textit{decay}} \mu, \nu_\mu$$

Atmospheric neutrinos

- *Conventional*: decays of lighter mesons

$\pi^{\pm}, K^{\pm}$



Mean lifetime: $\tau \sim 10^{-8}\ s$

Long lifetime: interaction occurs before decay

$$\mathcal{L}_{\rm int} < \mathcal{L}_{\rm dec}$$

Long-lived mesons loose energy → Steeply falling flux of neutrinos

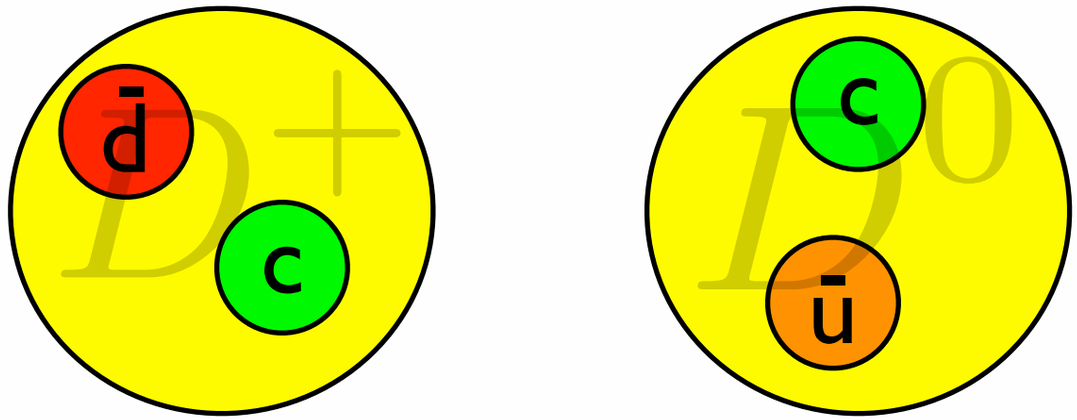
$$\Phi_\nu \sim E_\nu^{-3.7}$$

Prompt neutrinos

- *Prompt*: decays of heavier, charmed or bottom mesons

$D^{\pm}, D^{0}, D_s$

baryon Λ_c



Mean lifetime: $\tau \sim 10^{-12}\ s$

Short lifetime: decay, no interaction

$$\mathcal{L}_{\rm int} > \mathcal{L}_{\rm dec}$$

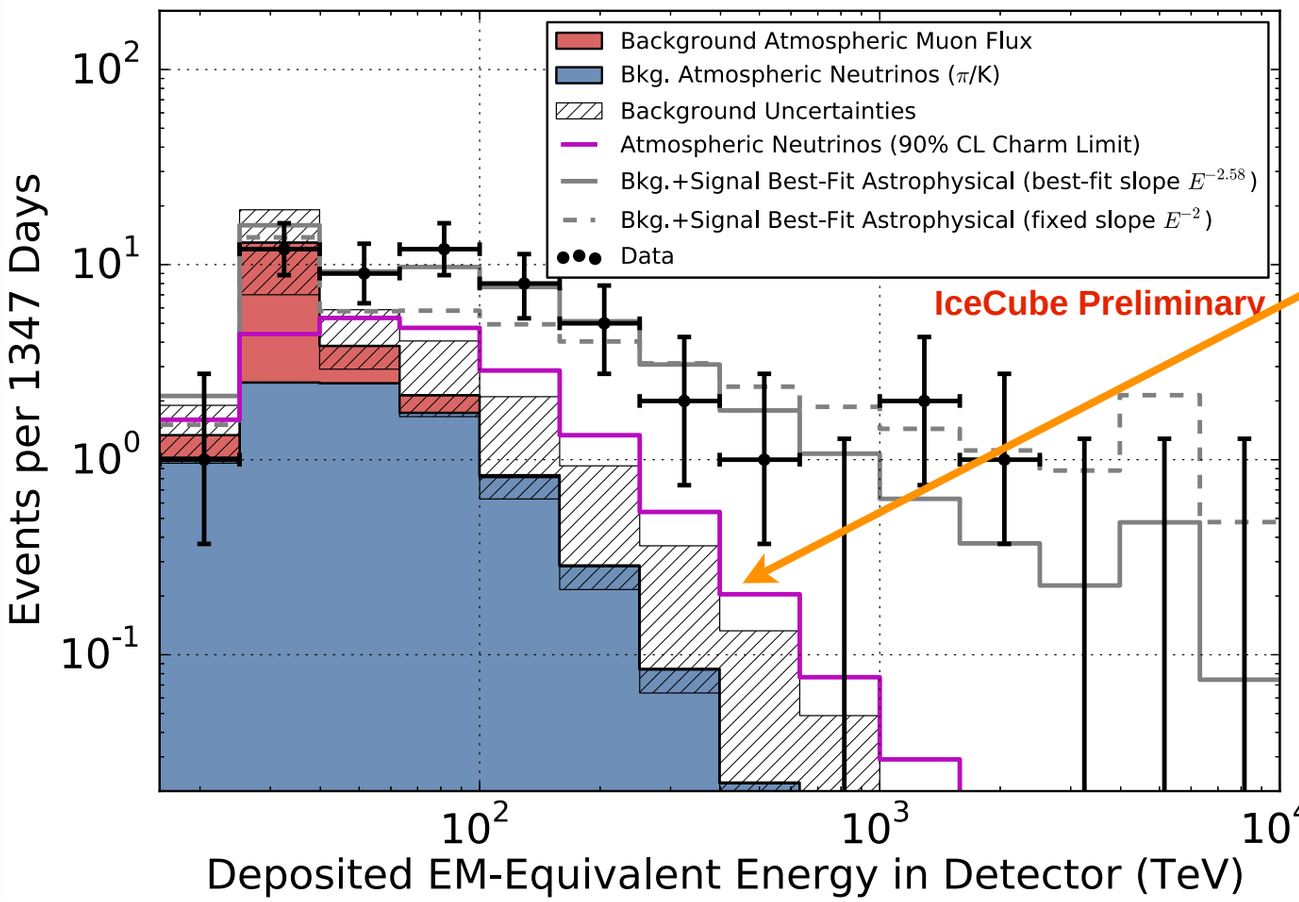
Flat flux, more energy transferred to neutrino

$$\Phi_\nu \sim E_\nu^{-2.7}$$

Motivation

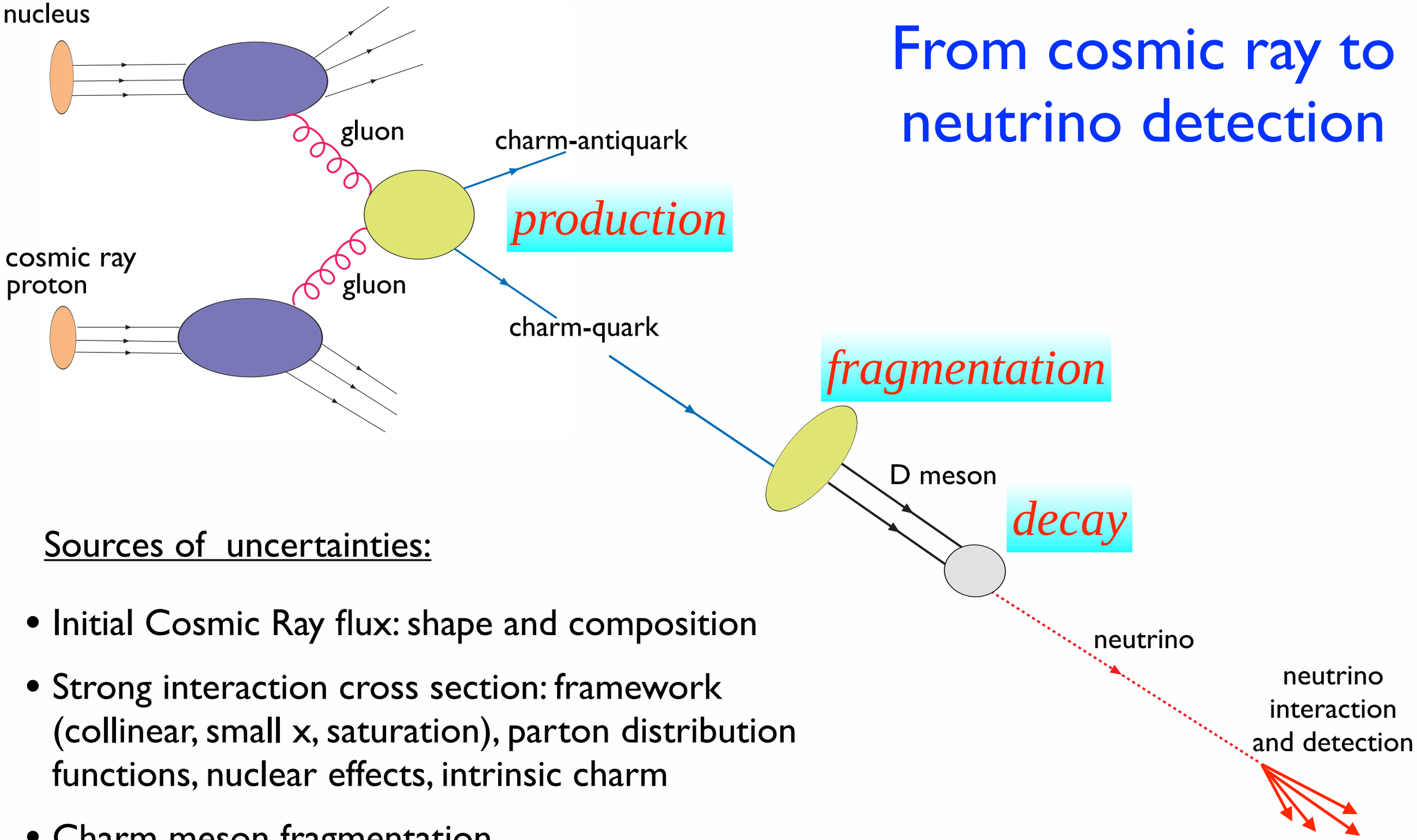
- Prompt neutrino is the background for the astrophysical flux of neutrinos.
- 4 year IceCube data, 1347 days, 54 events, 9 events expected from the background.
- Atmospheric origin excluded with 7 sigma.
- Neutrino production at these range of energies is sensitive to small x physics.

C. Kopper (ICRC2015, arXiv:1510.05223)



prompt contribution

From cosmic ray to neutrino detection



<u>Sources of uncertainties:</u>

- Initial Cosmic Ray flux: shape and composition
- Strong interaction cross section: framework (collinear, small x, saturation), parton distribution functions, nuclear effects, intrinsic charm
- Charm meson fragmentation
- Decay
- Interaction cross section of neutrino

pQCD collinear calculation

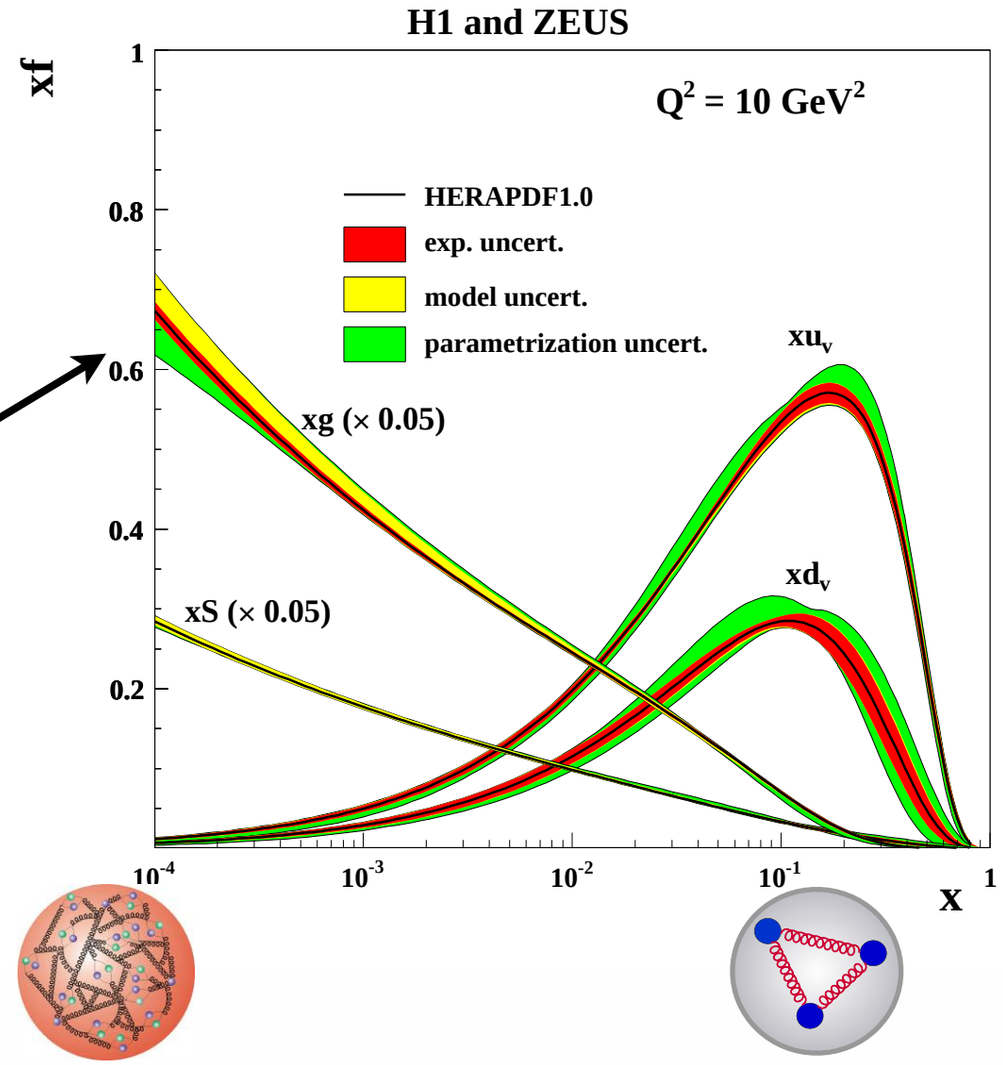
$$\frac{d\sigma^{pp\to c+X}}{dx_F} = \sum_{i,j} f_i(x_1,\mu_F) \otimes \hat{\sigma}_{gg\to c\bar{c}}(\hat{s}, m_c, \mu_F, \mu_R) \otimes f_j(x_2,\mu_F)$$

For the cosmic ray interactions we are interested in the forward production: charm quark is produced with very high fraction of the momentum of the incoming cosmic ray projectile. Other participating gluon will have very small fraction of longitudinal momentum:

$$x_F \simeq \frac{E_c}{E_p} \qquad x_F \gg x_2 \qquad x_2 \sim \frac{M^2_{c\bar{c}}}{x_F s}$$

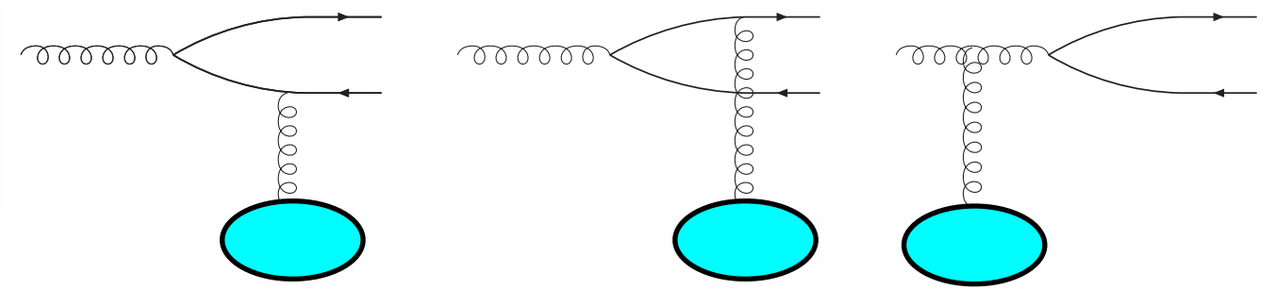
$$s \gg M^2_{c\bar{c}}$$

The cross section is sensitive to the domain of parton densities which are at very small values of x. This is poorly constrained region.



Dipole model calculation

At high energy the production of the heavy quark pair is viewed as interaction of color dipole:



Gluon fluctuation into heavy quark-antiquark pair : color dipole

Interaction of the color dipole with the hadronic target.

Heavy quark cross section in the dipole model:

$$\sigma(pp \to q\bar{q}X) \simeq \int dy\, x_1 g(x_1, M_F)\sigma^{gp\to q\bar{q}X}(x_2, M_R, Q^2 = 0)$$

Partonic cross section:

$$\sigma^{gp\to q\bar{q}X}(x, M_R, Q^2) = \int dz\, d^2\vec{r}\, |\Psi_g^q(z, \vec{r}, M_R, Q^2)|^2 \sigma_d(x, \vec{r})$$

Advantage of this framework: saturation and nuclear effects can be easily included as multiple scattering of the color dipole off the target.

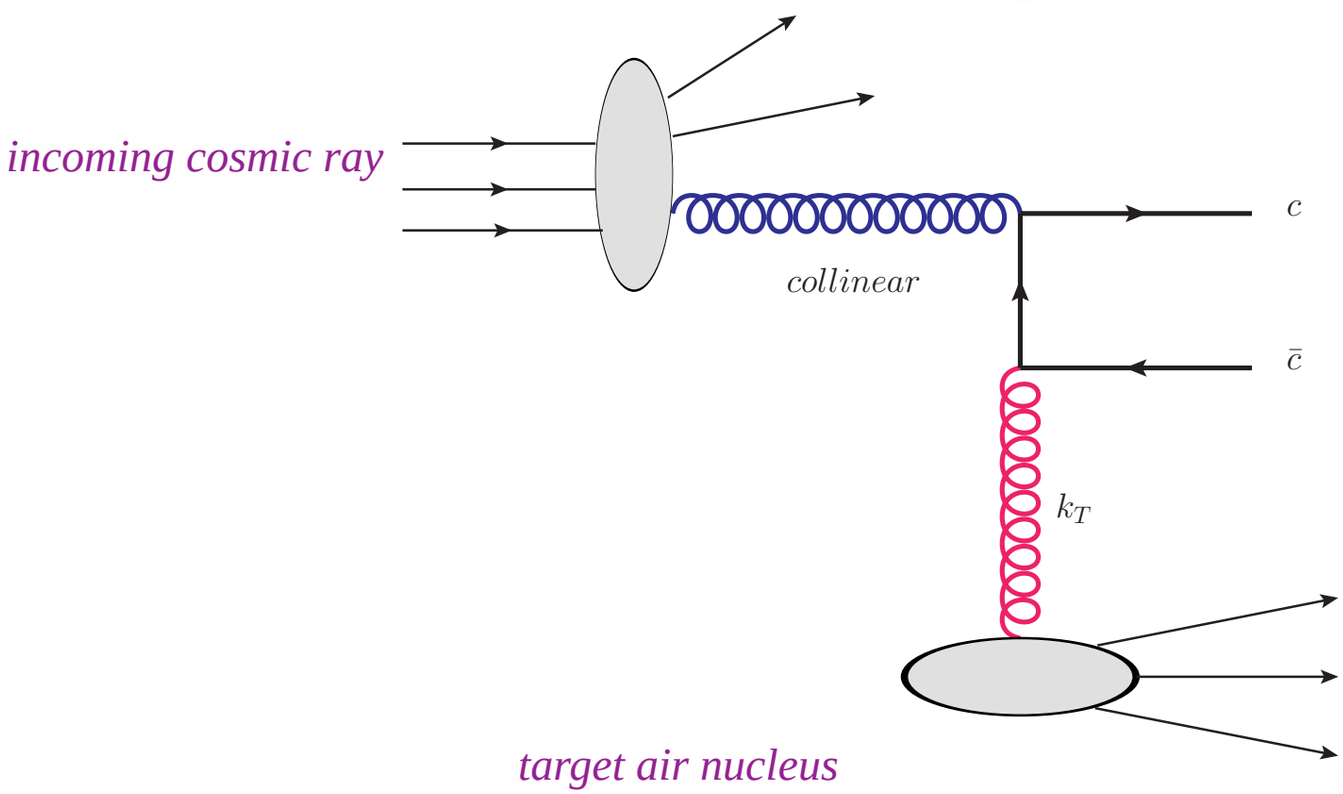
Hybrid k_T factorization calculation

- Use k_T factorization with off-shell gluon and unintegrated parton density.
- Suitable for the high energy - low x regime.
- Since it is forward production, use hybrid calculation: treat large x gluon as collinear, and small x gluon as off-shell.

collinear gluon

$$\sigma(pp \to q\bar{q}X) = \int \frac{dx_1}{x_1}\frac{dx_2}{x_2}\, dz\, dx_F\, \delta(zx_1 - x_F)\, x_1 g(x_1, M_F) \times \int \frac{dk_T^2}{k_T^2}\hat{\sigma}^{\rm off}(z, \hat{s}, k_T) f(x_2, k_T^2)$$

off-shell gluon with k_T dependence



- Unintegrated gluon with small x effects
- Can also include saturation

Hybrid k_T factorization calculation

Unintegrated gluon density obtained from the resummed small x evolution equation with non-linear term:

BFKL term with kinematical constraint

$$f(x,k^2) = \tilde{f}^{(0)}(x,k^2) + \frac{\alpha_s(k^2)N_c}{\pi}k^2\int_x^1\frac{dz}{z}\int_{k_0^2}\frac{dk'^2}{k'^2}\left\{\frac{f(\frac{x}{z},k'^2)\,\Theta(\frac{k^2}{z}-k'^2)-f(\frac{x}{z},k^2)}{|k'^2-k^2|}+\frac{f(\frac{x}{z},k^2)}{|4k'^4+k^4|^{\frac{1}{2}}}\right\}+$$

DGLAP with non-singular splitting

$$+\frac{\alpha_s(k^2)N_c}{\pi}\int_x^1 dz\,\bar{P}_{gg}(z)\int_{k_0^2}^{k^2}\frac{dk'^2}{k'^2}\,f(\frac{x}{z},k'^2)-$$

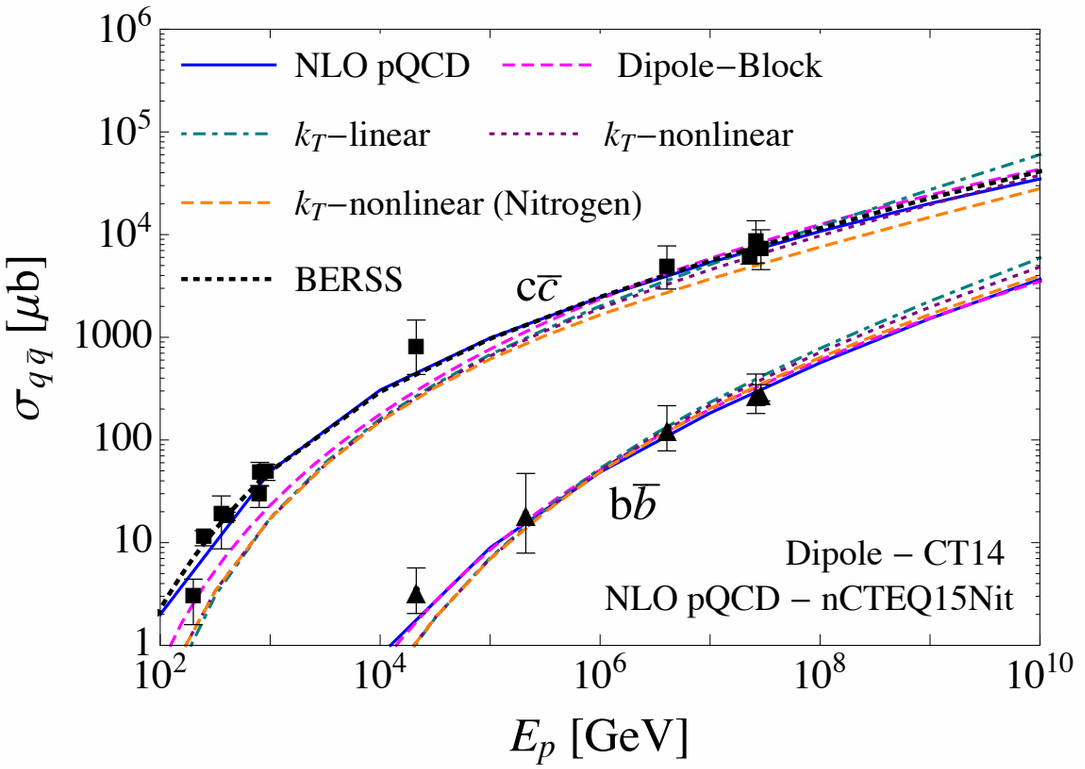
$$-\left(1-k^2\frac{d}{dk^2}\right)^2\frac{k^2}{R^2}\int_x^1\frac{dz}{z}\left[\int_{k^2}^{\infty}\frac{dk'^2}{k'^4}\alpha_s(k'^2)\ln\left(\frac{k'^2}{k^2}\right)f(z,k'^2)\right]^2$$

non-linear term

Nonlinear term responsible for taming the growth of the gluon density
Unintegrated parton density fitted to the inclusive structure function data
(*Kutak-Stasto, Kutak-Sapeta*)

Total charm production cross section

- For pQCD calculation using NLO code by Cacciari, Frixione, Greco, Nason.
- Charm quark mass $m_c = 1.27$ GeV
- Comparison with RHIC and LHC data. Data are extrapolated with NLO QCD from measurements in the limited phase space region.
- All models describe the data very well at high energies.
- Nuclear effects are very small for the total cross section
- k_T factorization suitable for the description at high energy; underestimates the data at lower energy; need additional diagrams there to match to NLO pQCD

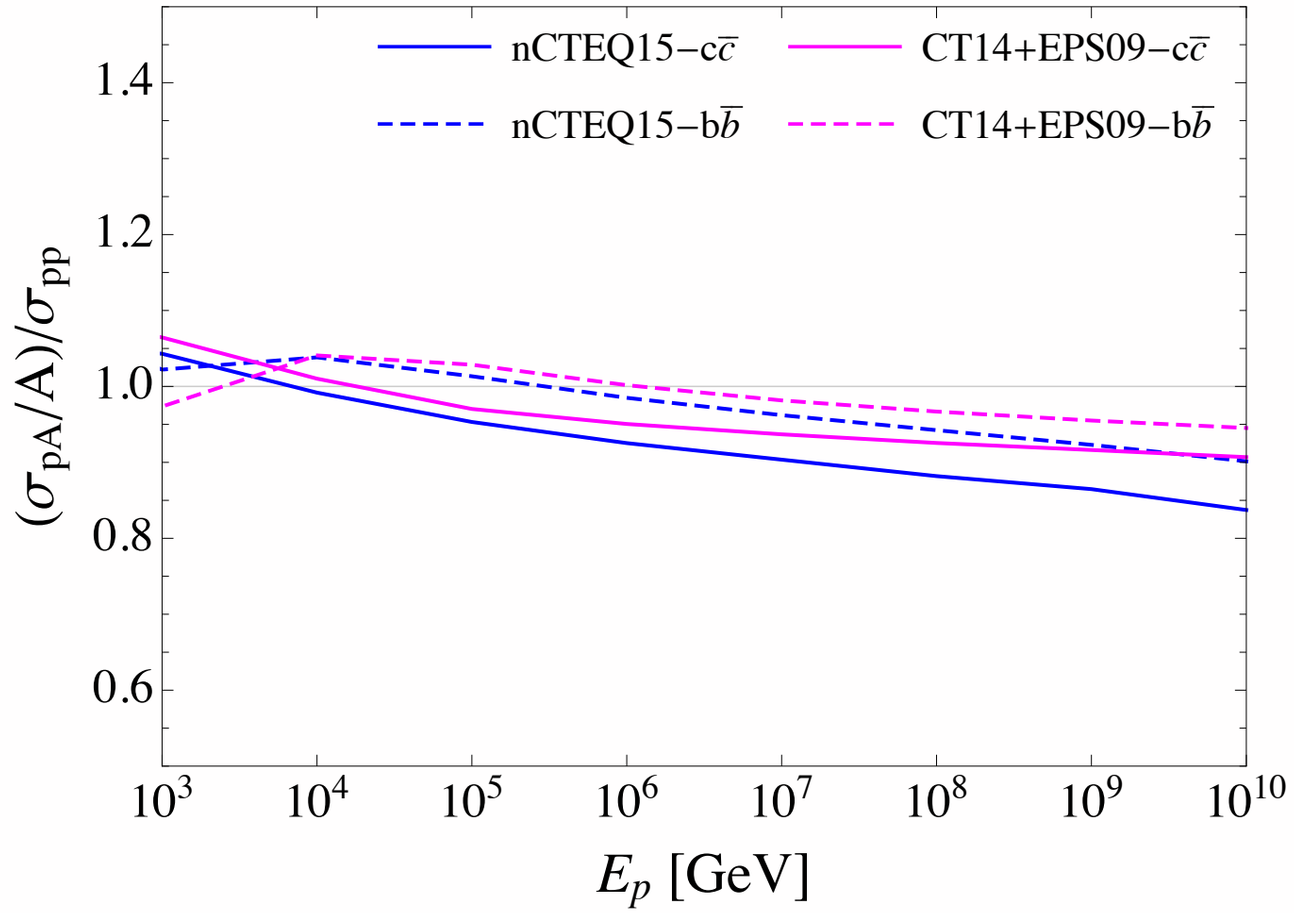


Expt.	$\sqrt{s}$ [TeV]	σ [mb]
PHENIX [31]	0.20	$\mathbf{0.551}^{+0.203}_{-0.231}$ (sys)
STAR [32]	0.20	$\mathbf{0.797} \pm 0.210$ (stat)$^{+0.208}_{-0.295}$ (sys)
ALICE [27]	2.76	$\mathbf{4.8} \pm 0.8$ (stat)$^{+1.0}_{-1.3}$ (sys) ± 0.06 (BR) ± 0.1(frag) ± 0.1 (lum)$^{+2.6}_{-0.4}$ (extrap)
ALICE [27]	7.00	$\mathbf{8.5} \pm 0.5$ (stat)$^{+1.0}_{-2.4}$ (sys) ± 0.1 (BR) ± 0.2(frag) ± 0.3 (lum)$^{+5.0}_{-0.4}$ (extrap)
ATLAS [28]	7.00	$\mathbf{7.13} \pm 0.28$ (stat)$^{+0.90}_{-0.66}$ (sys) ± 0.78 (lum)$^{+3.82}_{-1.90}$ (extrap)
LHCb [30]	7.00	$\mathbf{6.100} \pm 0.930$

Table 1: Total cross-section for $pp(pN) \to c\bar{c}X$ in hadronic collisions, extrapolated based on NLO QCD by the experimental collaborations from charmed hadron production measurements in a limited phase space region.

Nuclear corrections

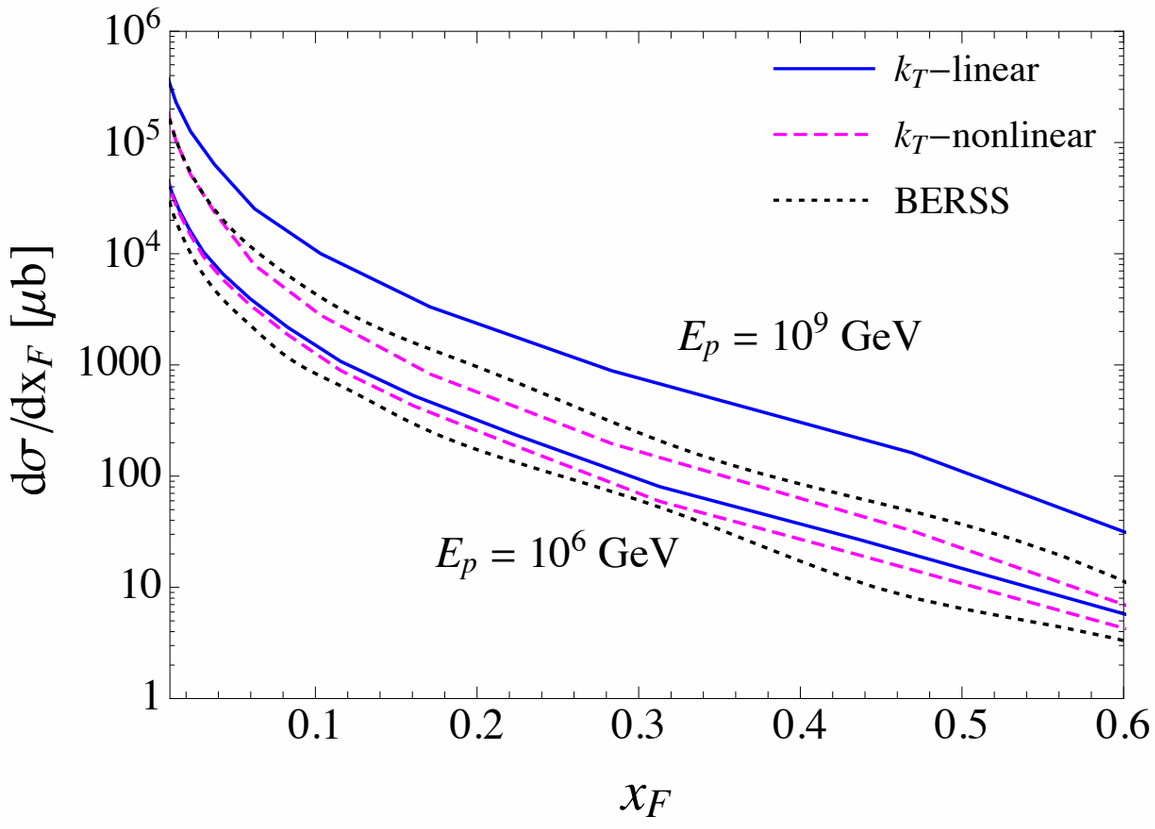
Nuclear modifications to the total charm production cross section are small 5-15%

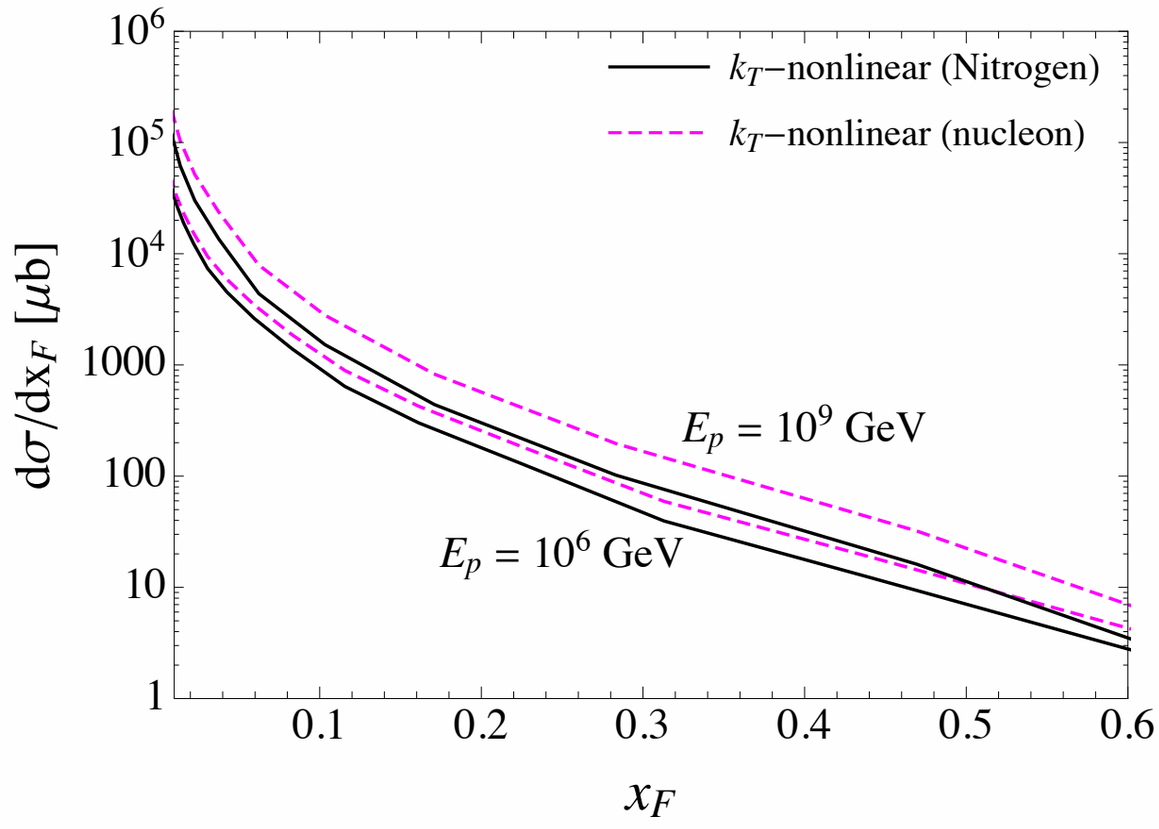


E_p	$\sigma(pp \to c\bar{c}X)$ [μb]		$\sigma(pA \to c\bar{c}X)/A$ [μb]		$[\sigma_{pA}/A]/[\sigma_{pp}]$	
	$M_{F,R} \propto m_T$	$M_{F,R} \propto m_c$	$M_{F,R} \propto m_T$	$M_{F,R} \propto m_c$	$M_{F,R} \propto m_T$	$M_{F,R} \propto m_c$
10^2	1.51	1.87	1.64	1.99	1.09	1.06
10^3	3.84×10^1	4.72×10^1	4.03×10^1	4.92×10^1	1.05	1.04
10^4	2.52×10^2	3.06×10^2	2.52×10^2	3.03×10^2	1.00	0.99
10^5	8.58×10^2	1.03×10^3	8.22×10^2	9.77×10^2	0.96	0.95
10^6	2.25×10^3	2.63×10^3	2.10×10^3	2.43×10^3	0.93	0.92
10^7	5.36×10^3	5.92×10^3	4.90×10^3	5.35×10^3	0.91	0.90
10^8	1.21×10^4	1.23×10^4	1.08×10^4	1.09×10^4	0.89	0.89
10^9	2.67×10^4	2.44×10^4	2.35×10^4	2.11×10^4	0.88	0.86
10^{10}	5.66×10^4	4.67×10^4	4.94×10^4	3.91×10^4	0.87	0.84

Differential charm cross section

Differential charm cross section in proton-nucleon collision as a function of the fraction of the incident beam energy carried by the charm quark.



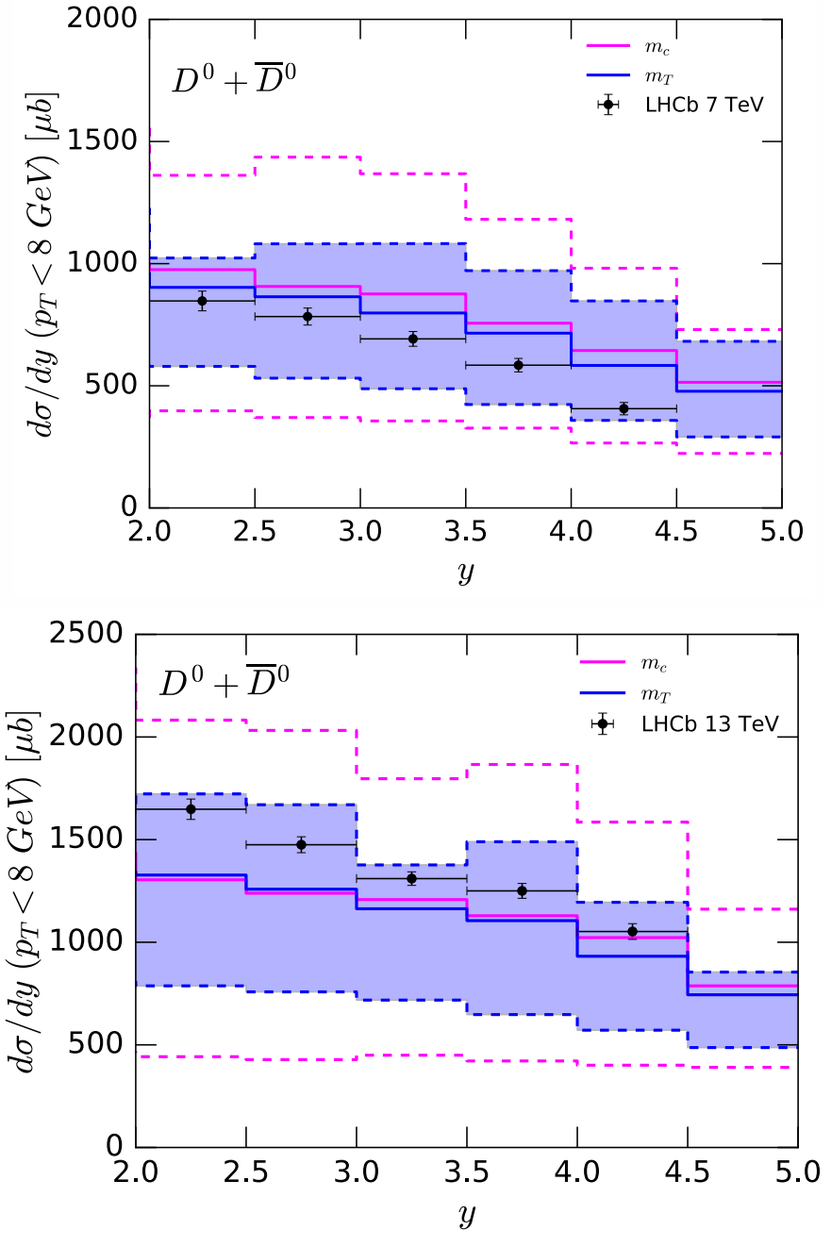


- Parton saturation effects affect the differential cross section more than the integrated cross section.
- Reduction of the cross section, at large energy of the charm quark.
- Nuclear effects in nitrogen are non-negligible at these energies.

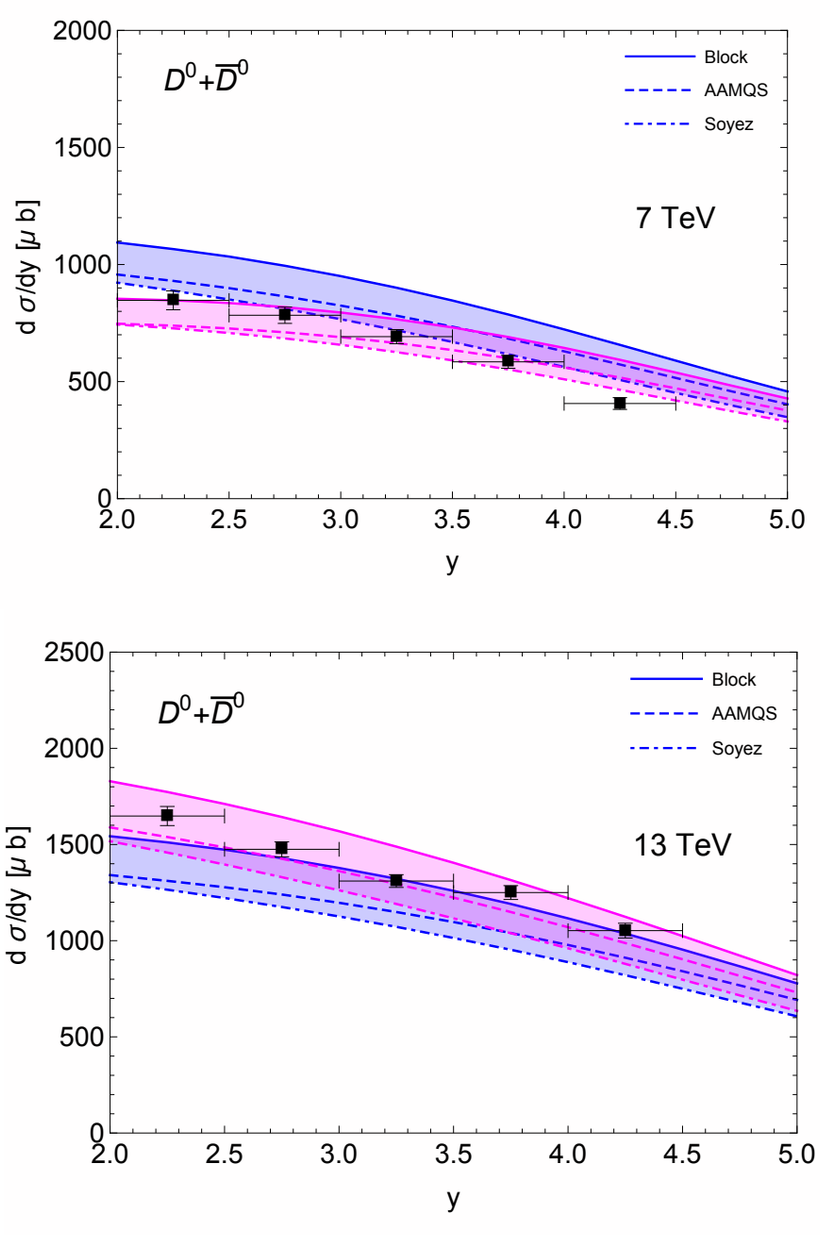
Comparison with LHCb 7 and 13 TeV

Rapidity distributions

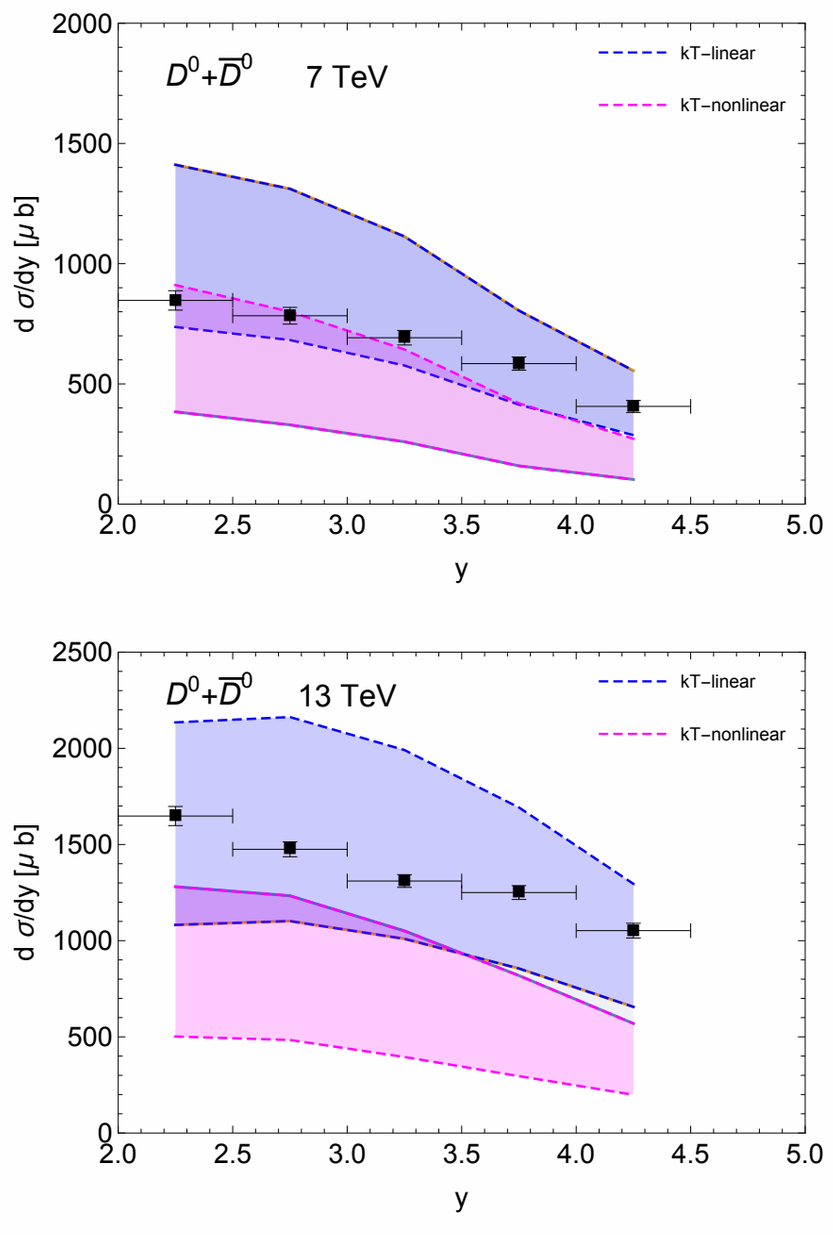
NLO



dipole



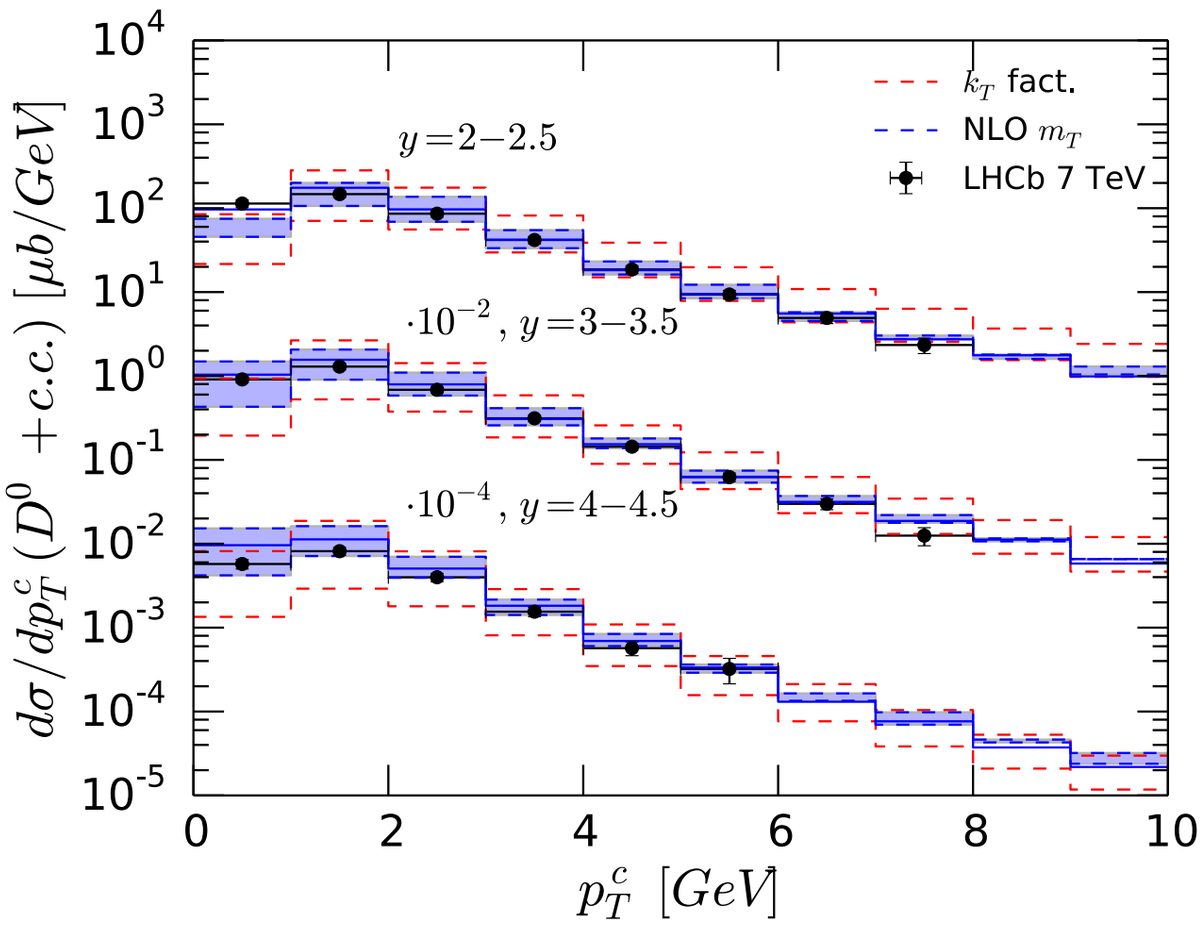
kT

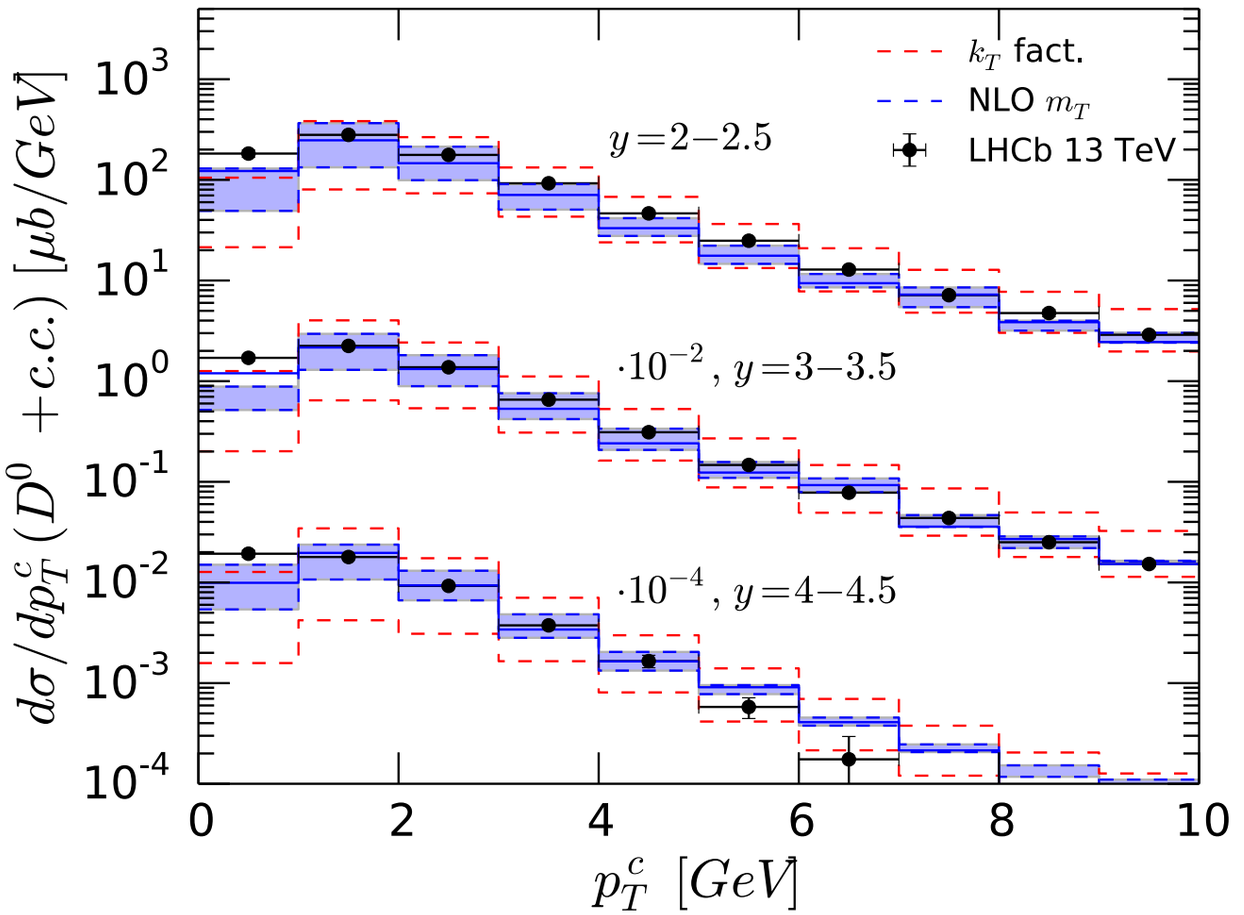


All approaches describe the LHCb data well within the error bands

Comparison with LHCb 7 and 13 TeV

Transverse momentum distributions



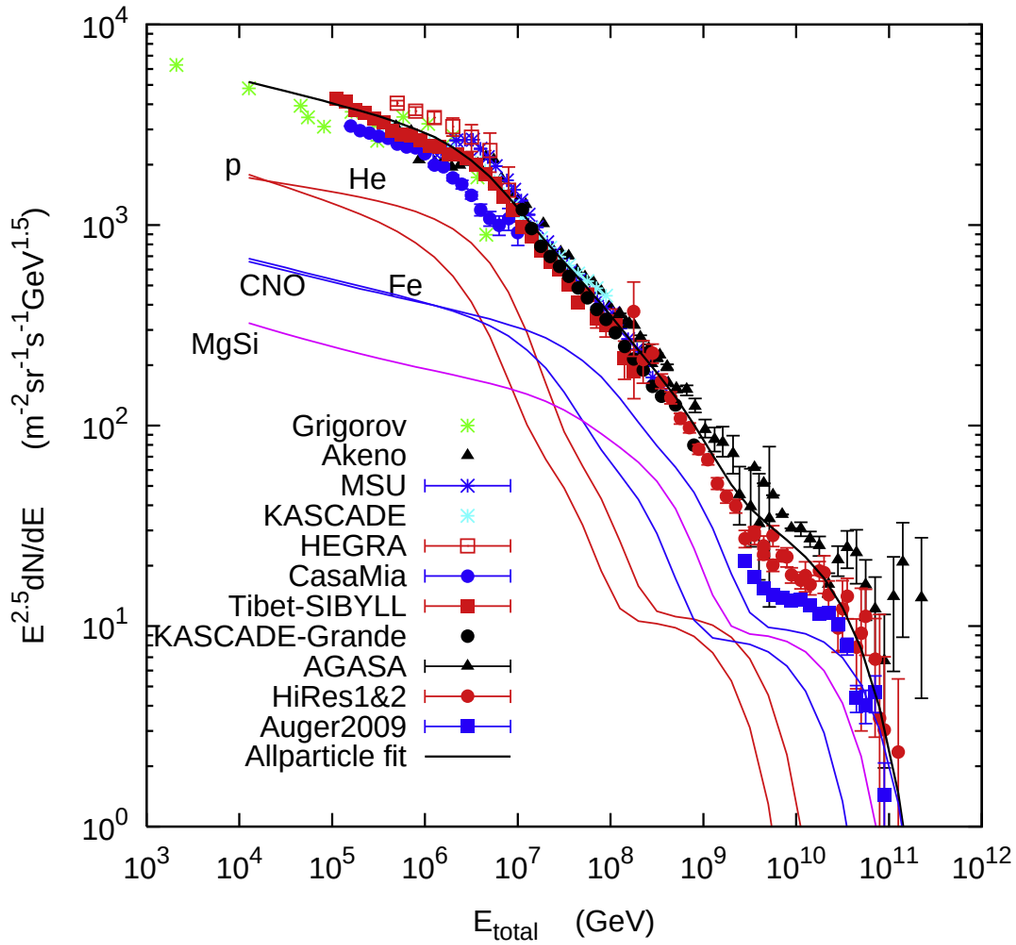


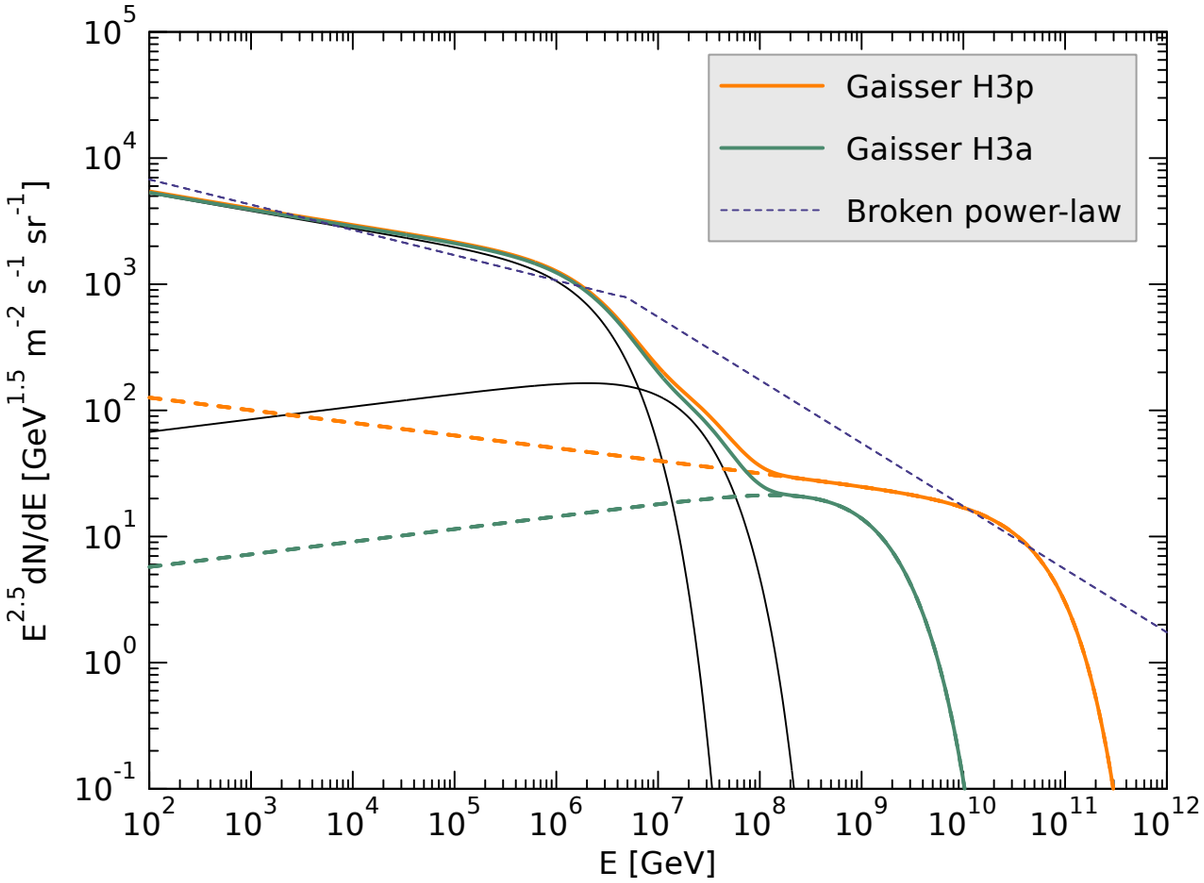
- NLO pQCD and k_T factorization consistent with each other.
- Bands on NLO pQCD calculation correspond to scale variation.
- Two lines in k_T factorization correspond to the saturation/no-saturation calculation.

Cosmic ray flux

Important ingredient for lepton fluxes: initial cosmic ray flux.

Parametrization by Gaisser (2012) with three populations and five nuclei groups:
H,He,CNO,Fe,MgSi





Gaisser,
Astroparticle Physics 35 (2012) 801

Development of air shower: cascade equations

Production of prompt neutrinos:

$$\mathrm{p} \overset{\text{production}}{\longrightarrow} \mathrm{c} \overset{\text{fragmentation}}{\longrightarrow} \mathrm{M} \overset{\text{decay}}{\longrightarrow} \nu$$

where M=$D^{\pm}, D^{0}, D_s, \Lambda_c$

Use set of cascade equations in depth X

$$X = \int_h^{\infty} \rho(h')dh'$$

$$\frac{d\Phi_j}{dX} = -\frac{\Phi_j}{\lambda_j} - \frac{\Phi_j}{\lambda_j^{dec}} + \sum_k \int_E^{\infty} dE_k \frac{\Phi_k(E_k, X)}{\lambda_k(E_k)} \frac{dn_{k\to j}(E; E_k)}{dE}$$

λ_j interaction length and $\lambda_j^{dec} = \gamma c \tau_j \rho(X)$ decay length

$\frac{dn_{k\to j}}{dE}$ production or decay distribution

$$\frac{1}{\sigma_k}\frac{d\sigma_{k\to j}(E, E_k)}{dE} \qquad \frac{1}{\Gamma_k}\frac{d\Gamma_{k\to j}(E, E_k)}{dE}$$

Need to solve these equations simultaneously assuming non-zero initial proton flux.

Development of air shower: cascade equations

Can solve equations numerically or semi-analytically
(assuming factorization of X and E dependence) via Z-moment method

$$\int_E^\infty \mathrm{d}\, E_k \frac{\phi_k(E_k, X)}{\lambda_k(E_k)} \frac{\mathrm{d}n_{k\to j}(E; E_k)}{\mathrm{d}E} \quad \simeq \quad \frac{\phi_k(E, X)}{\lambda_k(E)} Z_{kj}(E)$$

where

$$Z_{kj}(E) = \int_0^1 \frac{\mathrm{d}x_E}{x_E} \frac{\phi_k(E/x_E, 0)}{\phi_k(E, 0)} \frac{\lambda_k(E)}{\lambda_k(E/x_E)} \frac{\mathrm{d}n_{k\to j}(E/x_E)}{\mathrm{d}x_E}$$

$$x_E = \frac{E}{E_k}$$

Then fluxes can be expressed via closed analytical expressions in terms of Z moments.

For example proton flux is:

$$\phi_p(E, X) \simeq \phi_p^0(E) \exp(-X/\Lambda_p) = (dN/dE) \exp(-X/\Lambda_p)$$

$$\Lambda_p = \lambda_p(E)/(1 - Z_{pp}(E))$$

Semi-analytical solutions to lepton fluxes

Lepton fluxes from the decays of the hadrons.
Characteristics of solution depends on the energy range and competition between decay and interactions.

Critical energy at which hadron decay probability is suppressed with respect to the interaction probability

$$E_{\rm crit} \simeq 3.7 - 9.5 \times 10^7 \ \ {\rm GeV}$$

$E < E_{\rm crit}$

$$\phi_\ell^{low}(h) = Z_{h\ell}^{low} \frac{Z_{ph}}{1 - Z_{pp}} \phi_p^0$$

$E > E_{\rm crit}$

$$\phi_\ell^{high}(h) = Z_{h\ell}^{high} \frac{Z_{ph}}{1 - Z_{pp}} \frac{\ln(\Lambda_h/\Lambda_p)}{1 - \Lambda_p/\Lambda_h} \phi_p^0$$

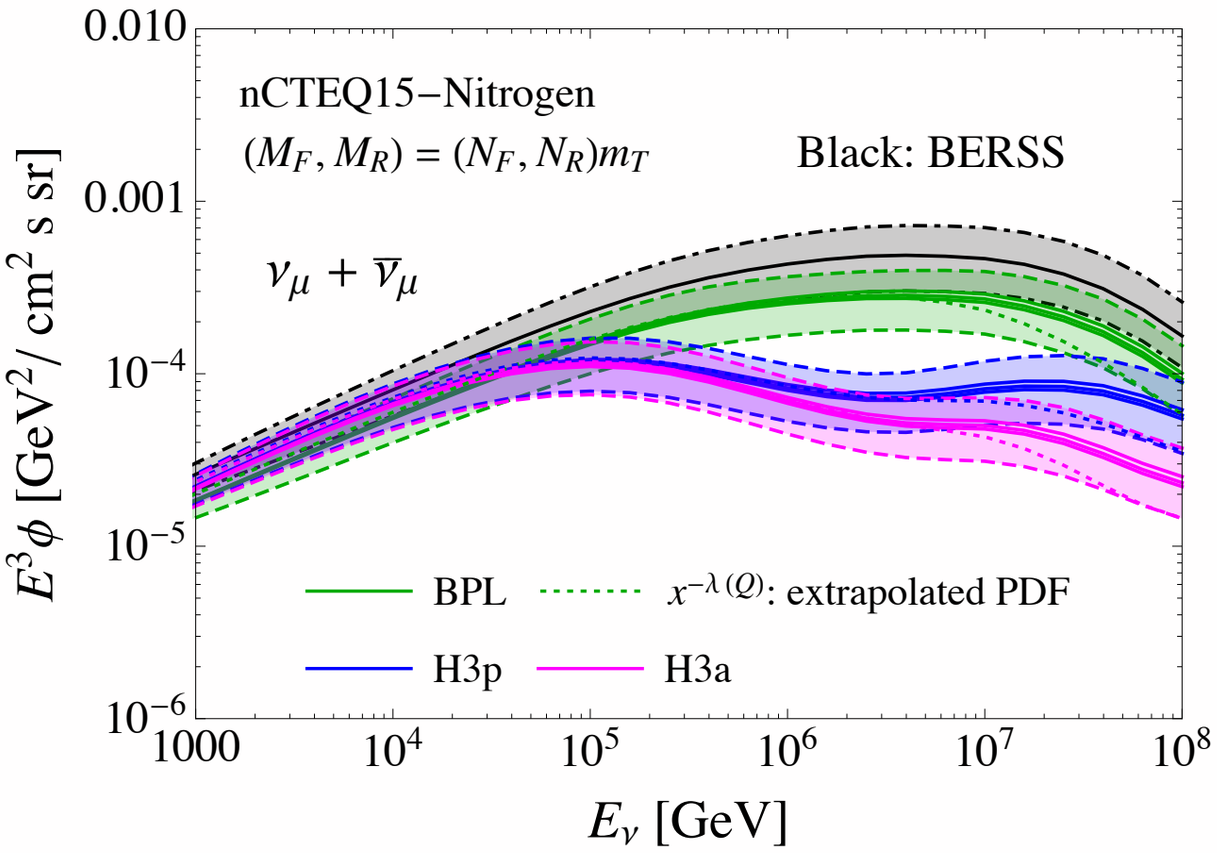
Interpolation:

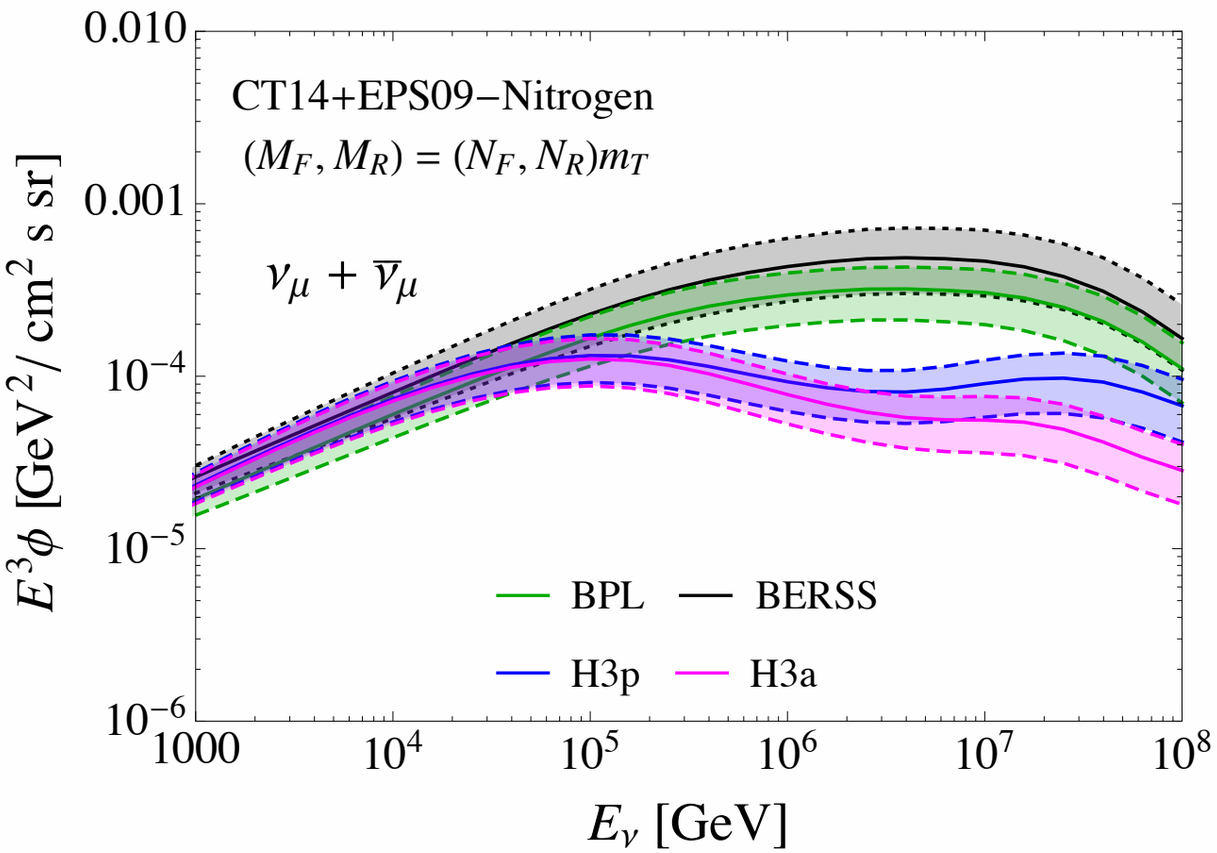
$$\phi_\ell = \sum_h \frac{\phi_\ell^{low}(h)\phi_\ell^{high}(h)}{\phi_\ell^{low}(h) + \phi_\ell^{high}(h)}$$

Above formulae are good approximation to the exact solution of the cascade equations.

Neutrino fluxes

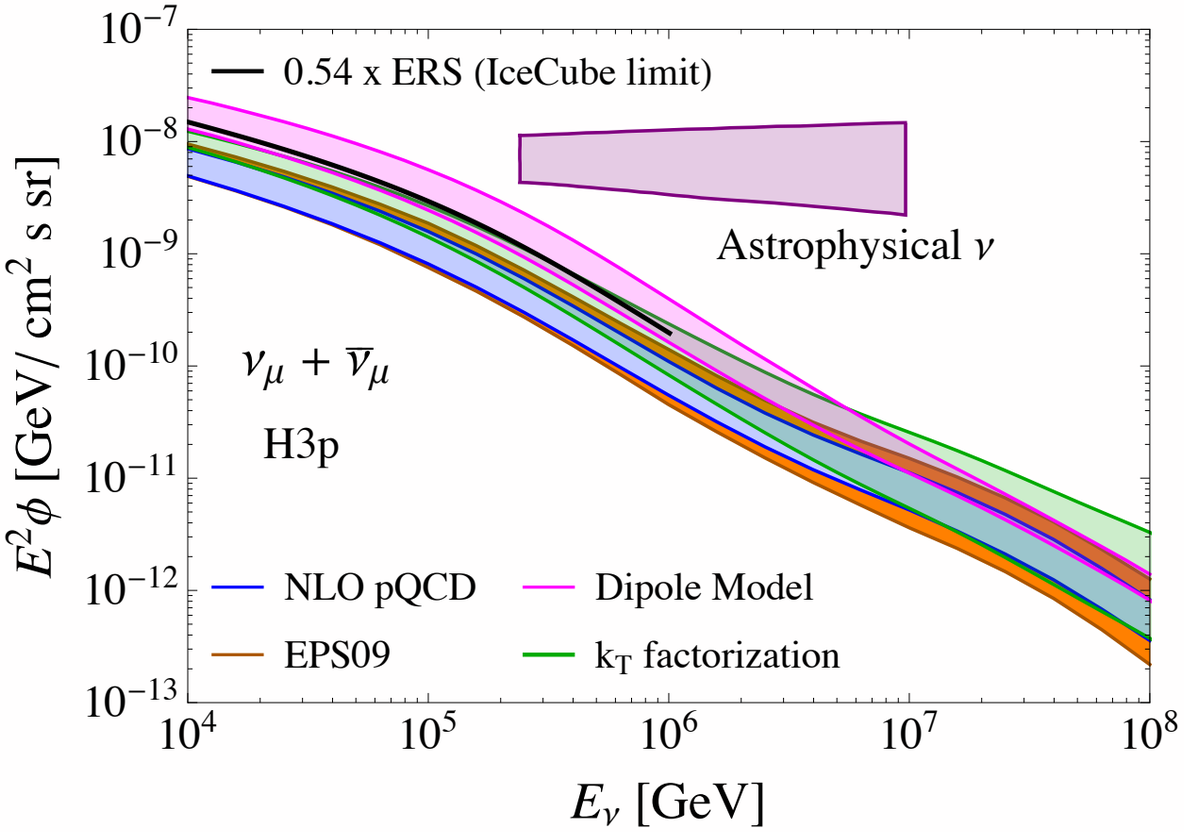
flux of $\nu_\mu + \bar{\nu}_\mu$

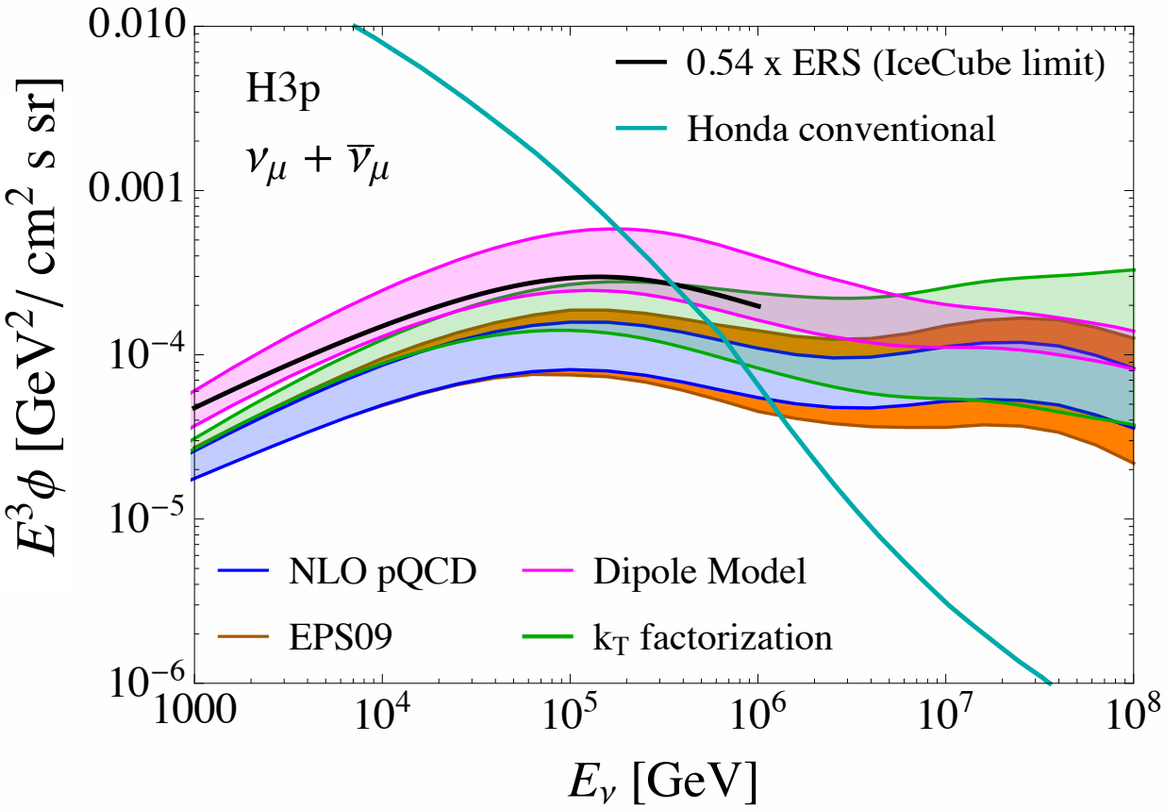




- Significant reduction (factor 2-3) due to the updated cosmic ray spectrum with respect to the broken power law.
- The reduction is in the region of interest, where prompt neutrino component should dominate over the atmospheric one.
- Black band: previous calculation. Bands correspond to the scale variation.
- The updated fragmentation function reduces flux by 20%.
- B hadron contribution increases flux by about 5-10%.
- Nuclear effects: 20-35%.
- Combined effects: reduction by 45% at highest energies.

Predictions and IceCube limit





- IceCube limit on prompt neutrino flux (PoS(ICRC2015)1079).
- NLO perturbative and k_T factorization within the limit.
- Dipole model calculation is in tension with the IceCube limit.
- Overall the flux is well below the astrophysical flux measured by IceCube.

Summary and outlook

- Calculation of the prompt neutrino flux using NLO pQCD and latest PDFs as well as dipole and k_T factorization. Charm cross section matched to LHC and RHIC data.

- Consistent with LHCb data (rapidity and transverse momentum distributions) on forward charm production.

- Updated cosmic ray flux gives lower values (as compared with earlier ERS and BERSS evaluation) for the atmospheric neutrino flux.

- Prompt neutrino component is rather small. Limit on prompt production from IceCube data constraints dipole calculation.

- Nuclear effects in the target. Further reduction of the flux by about 20-35%. Estimate of nuclear corrections within the NLO pQCD consistent with the small x calculation.

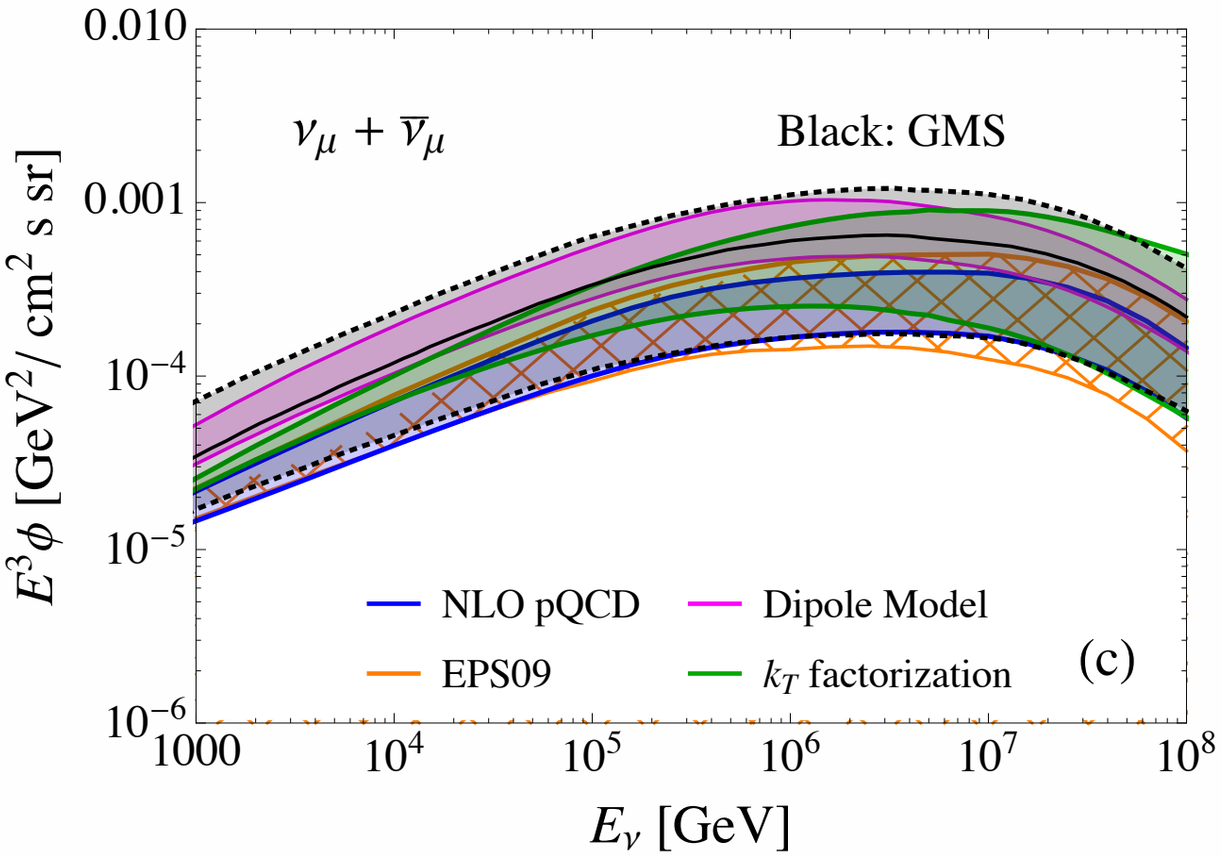
- Small x resummation leads to enhancement, saturation to the reduction of the flux. Dipole model larger than other calculations at low energies, needs improvement.

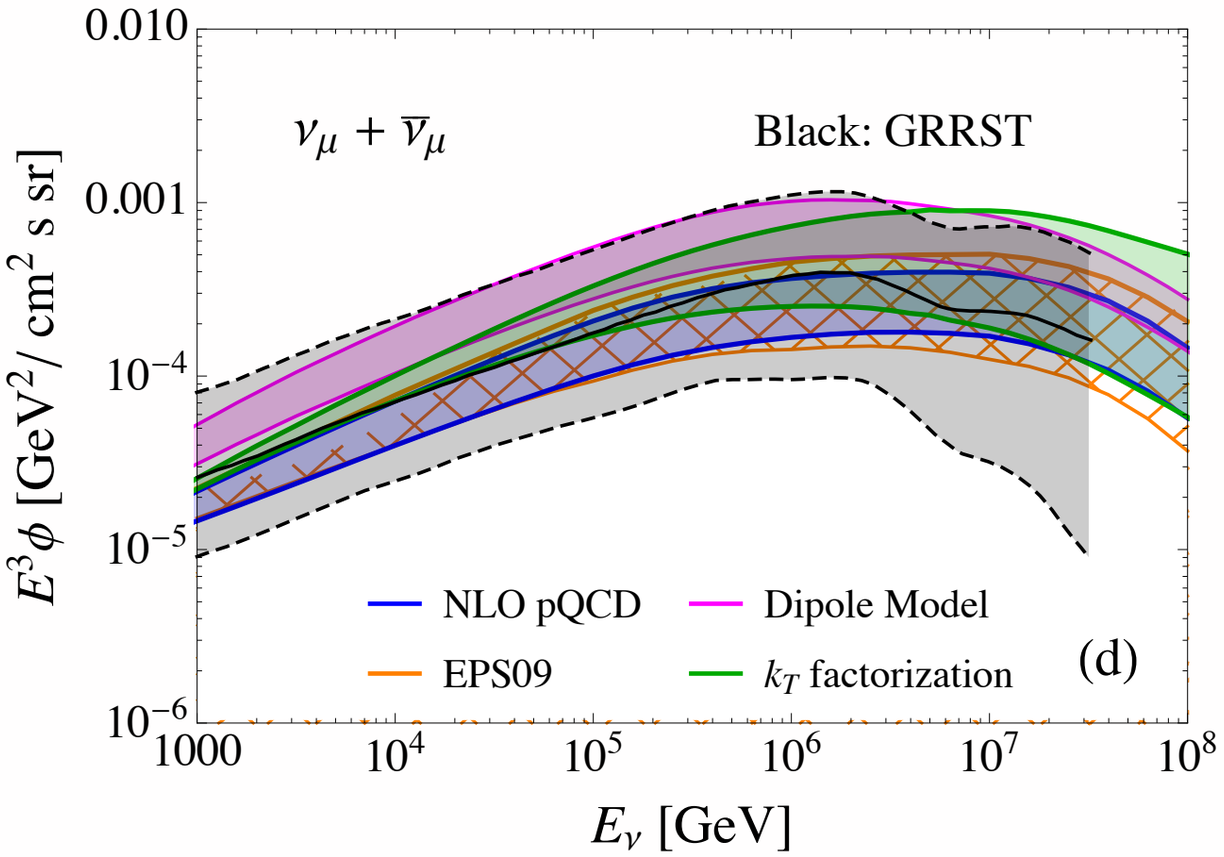
- Other calculations also on the market: consistent but still large uncertainties. Largest uncertainties due to the QCD scale variation, PDF uncertainties and CR flux.

- Outstanding questions: fragmentation (forward production, hadronic-nuclear environment, differences between PYTHIA and fragmentation functions); intrinsic charm.

backup

Neutrino fluxes





Comparison with other calculations:

GMS: Garzelli, Moch, Sigl

GRRST: Gauld, Rojo, Rotolli, Sarkar, Talbert

Consistency within the error bands.

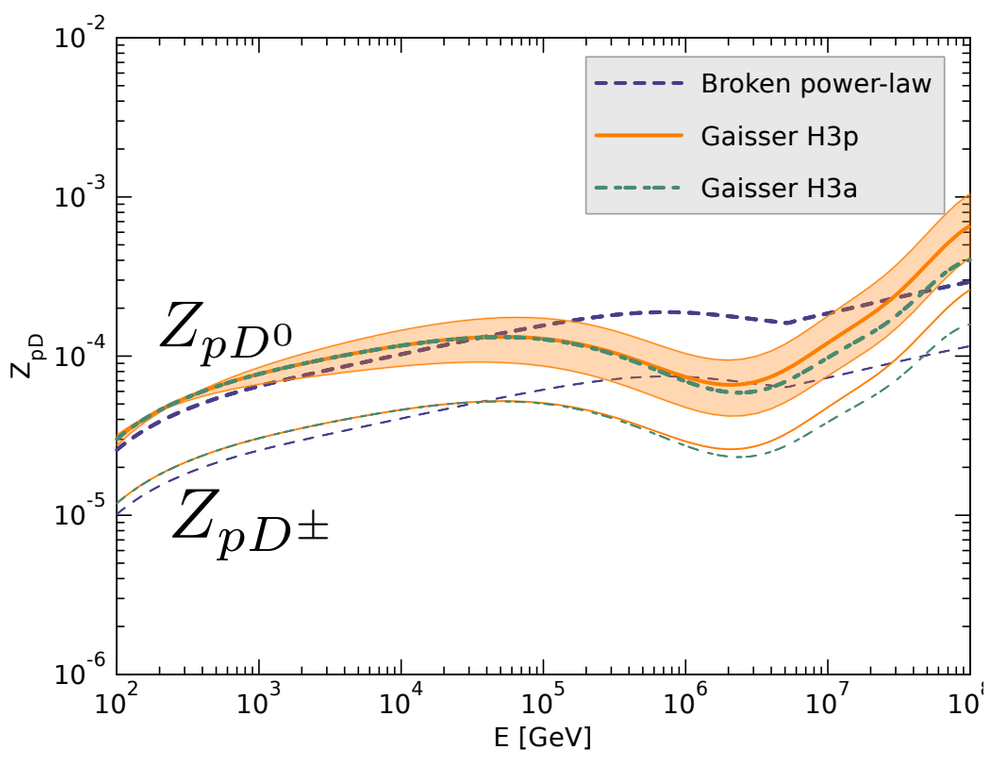
Impact of CR flux on Z moments

Z moments:

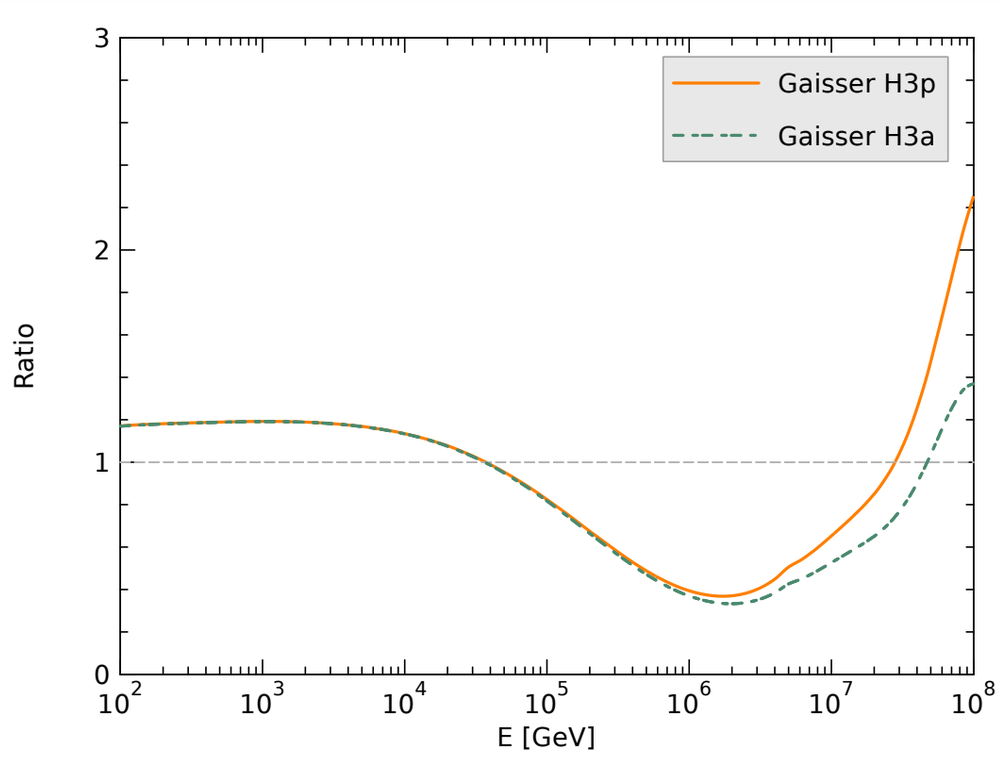
$$Z_{ph}(E_h) = \int_{x_{E_{\rm min}}}^{1} \frac{dx_E}{x_E} \frac{\phi_p^0(E_h/x_E)}{\phi_p^0(E_h)} \frac{1}{\sigma_{pA}(E_h)} \times A \frac{d\sigma}{dx_E}(pN \to hX)$$

Noticeable dip of Z moments as a function of energy. The dip corresponds to the softening of cosmic ray flux due to the change of the population. The energy is reduced because of the inelasticity of the collisions.

$$x_E = \frac{E_{\rm hadron}}{E_{\rm beam}}, \quad \langle x_E \rangle \sim 0.1$$



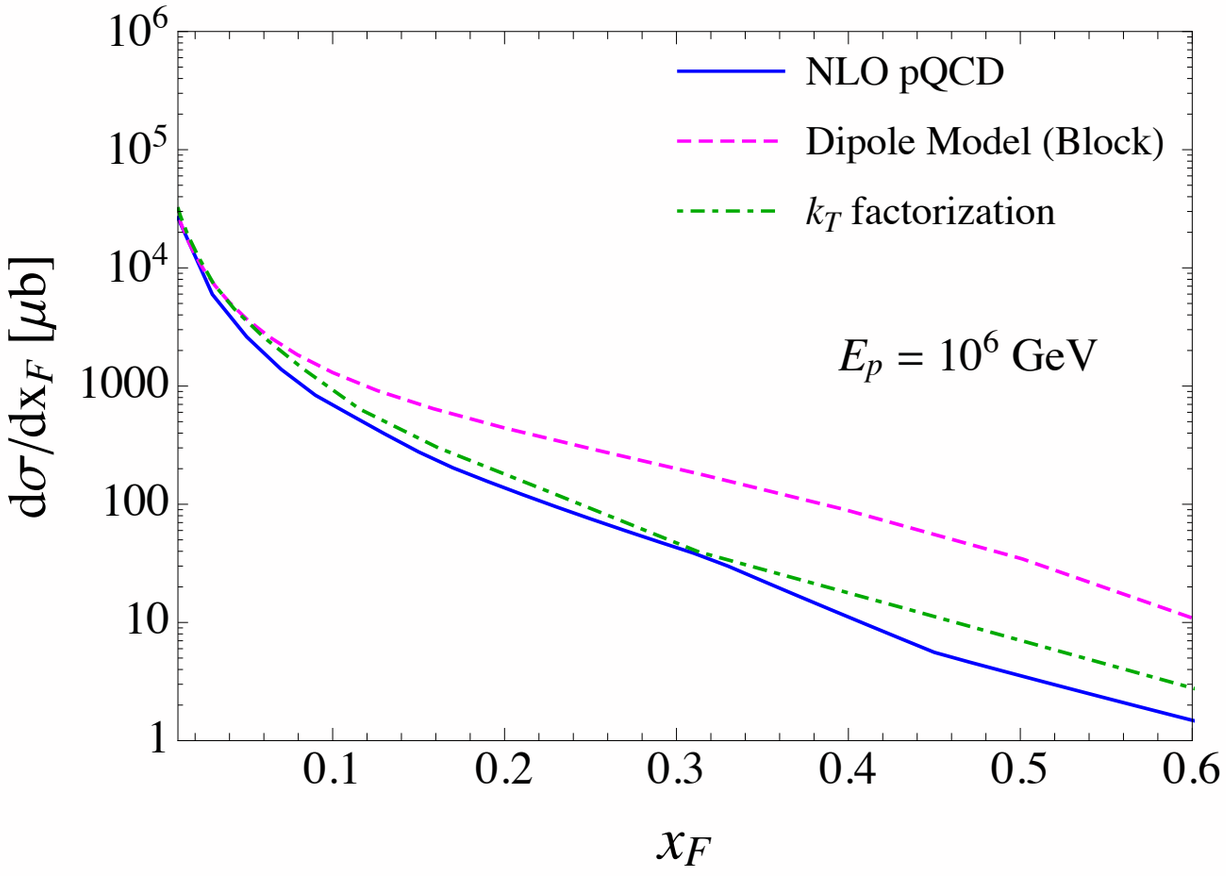
Ratio to the calculation with power law

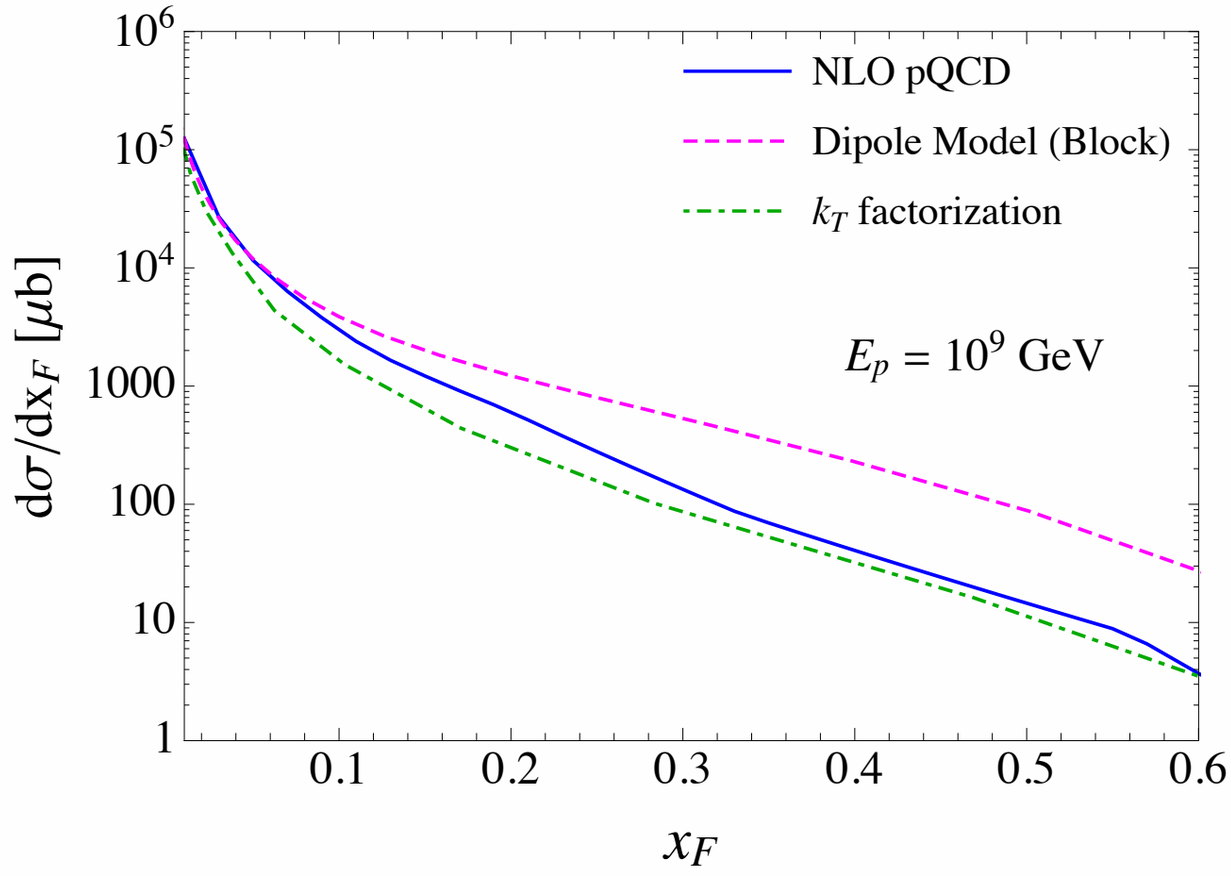


BERSS

Differential charm cross section

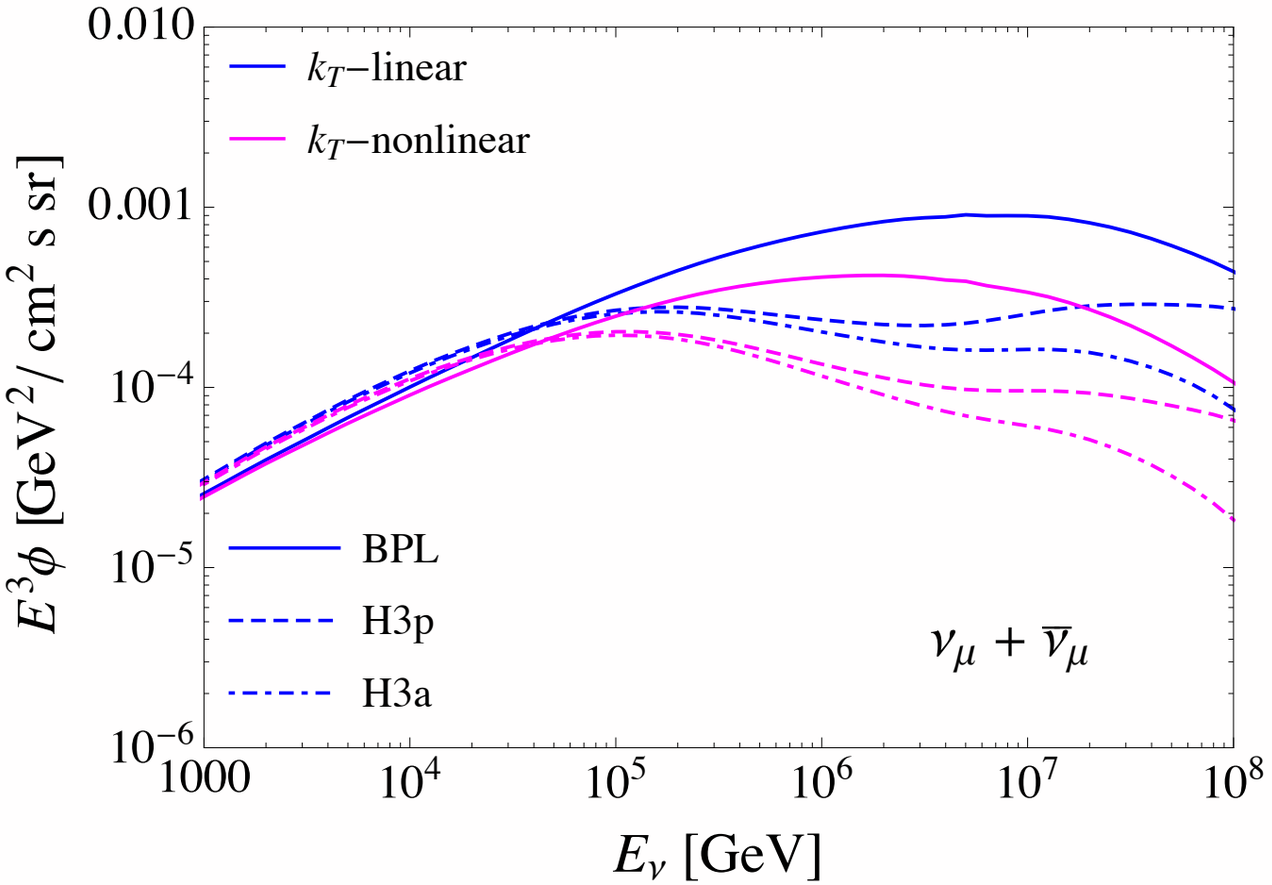
Comparison of NLO pQCD, dipole model, and kT factorization

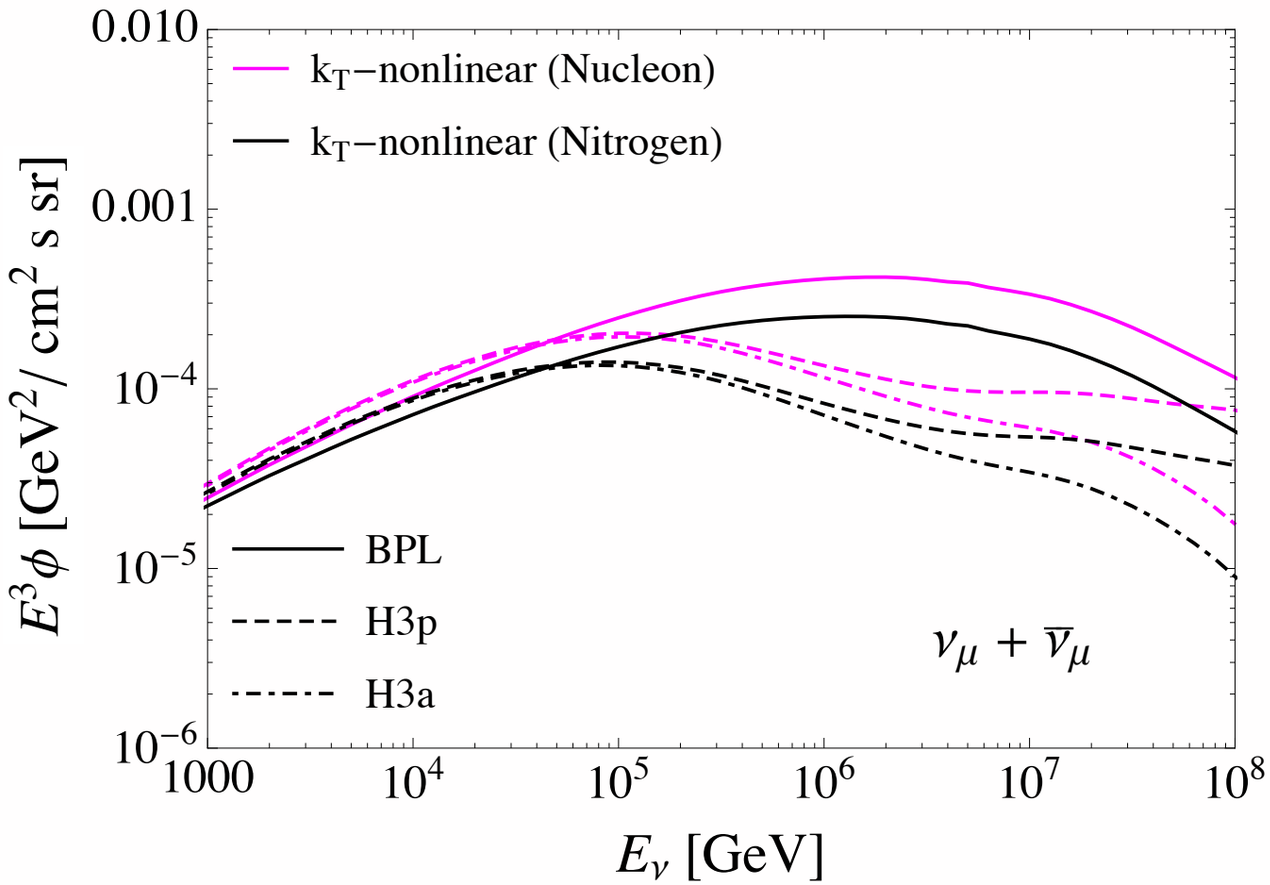




- NLO calculation and kT factorization calculation consistent with each other.
- Dipole calculation systematically above the other two : need for improvements in this model.

Neutrino fluxes



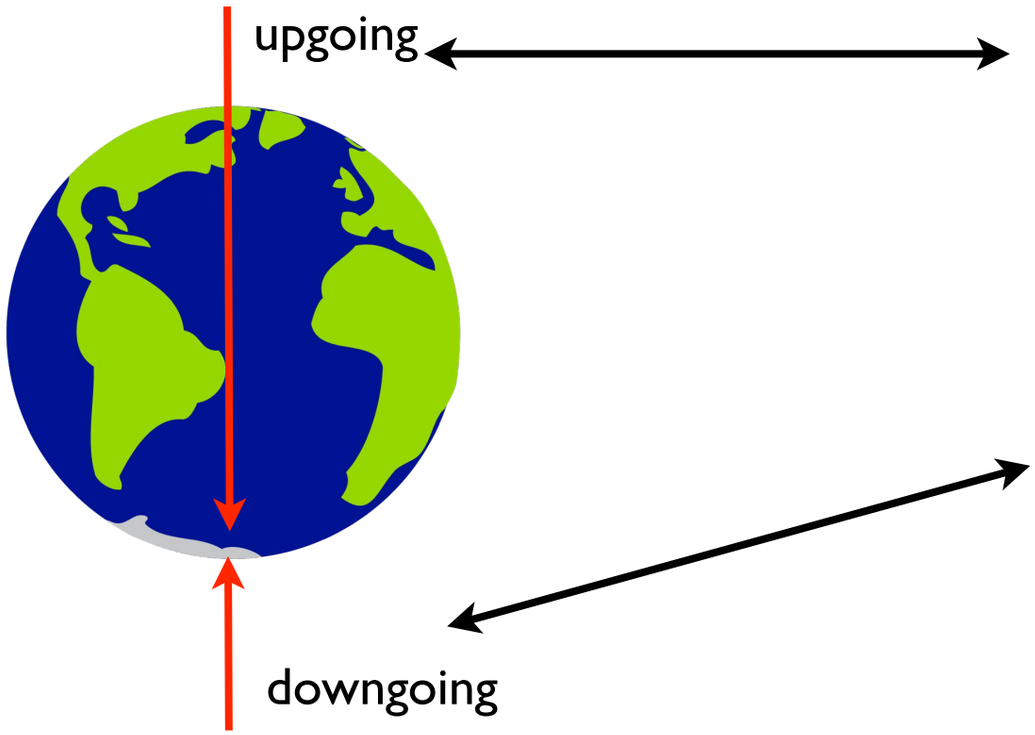


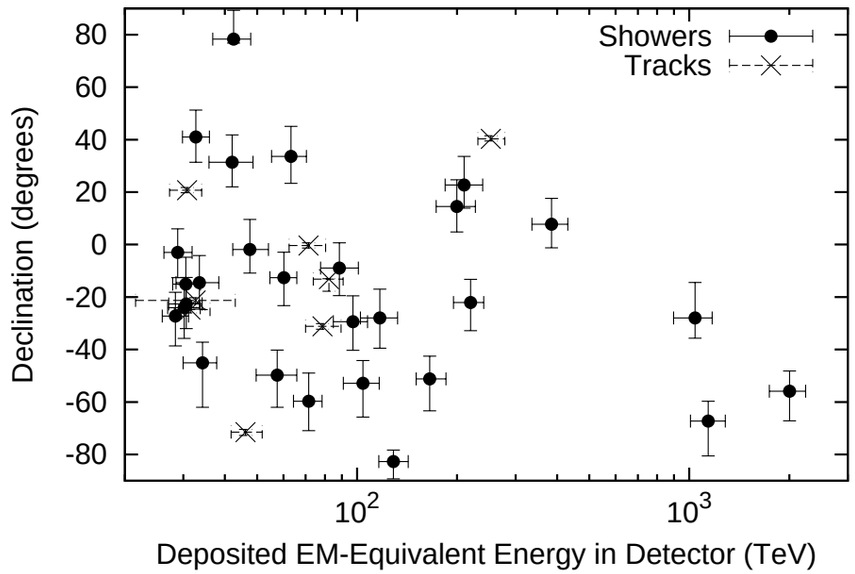
- Sizeable reduction of the flux due to the changes from linear to nonlinear evolution in kT factorization.
- Further reduction of the flux when nuclear effects in nitrogen are included.

IceCube results

IceCube Coll. Phys.Rev.Lett. 113 (2014) 101101; Observation of High-Energy Astrophysical Neutrinos in Three Years of IceCube Data

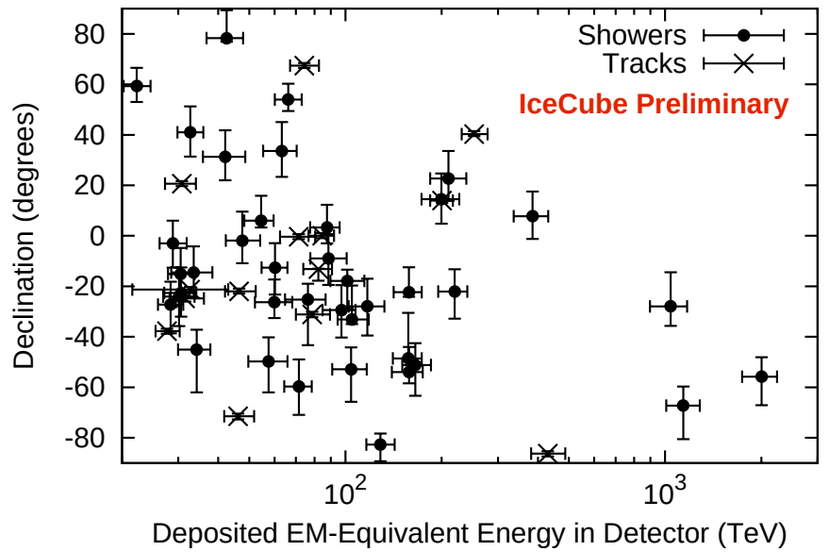
988 day sample, 37 events observed (after selection with entering muon veto) with energies between 30-2000 TeV





4-year data, ICRC2015, arxiv:1510.05223.

1347 day sample, 54 events observed.



Studying gluon saturation and nuclear gluon effects using forward heavy-ion probes and UPCs

Daniel Tapia Takaki

Saturation: Recent developments, New Ideas and measurements
RIKEN BNL Research Center Workshop
April 26, 2017

Plan of this talk

- Highlights from the QM, INT workshop and DIS this year, focusing mainly on experimental measurements/ideas
- Lots of synergies with the EIC program and UPC at RHIC/LHC. Will mention it briefly but this is material for another talk….
- Discussions about new ideas …

INT workshop

Organizers:

Daniel Tapia Takaki
University of Kansas
Daniel.Tapia.Takaki@cern.ch

Carlos Bertulani
Texas A&M University-Commerce
carlos.bertulani@tamuc.edu

Spencer R. Klein
Lawrence Berkeley Laboratory
SRKlein@lbl.gov

Tuomas Lappi
University of Jyvaskykla
tuomas.v.v.lappi@jyu.fi

Mark Strikman
Pennsylvania State University
strikman@phys.psu.edu

Program Coordinator:
Farha Habib
faraway@uw.edu
(206) 685-4286

Application form
For full consideration, please apply by October 31, 2016.

Talks online

Exit report

Visitor Information

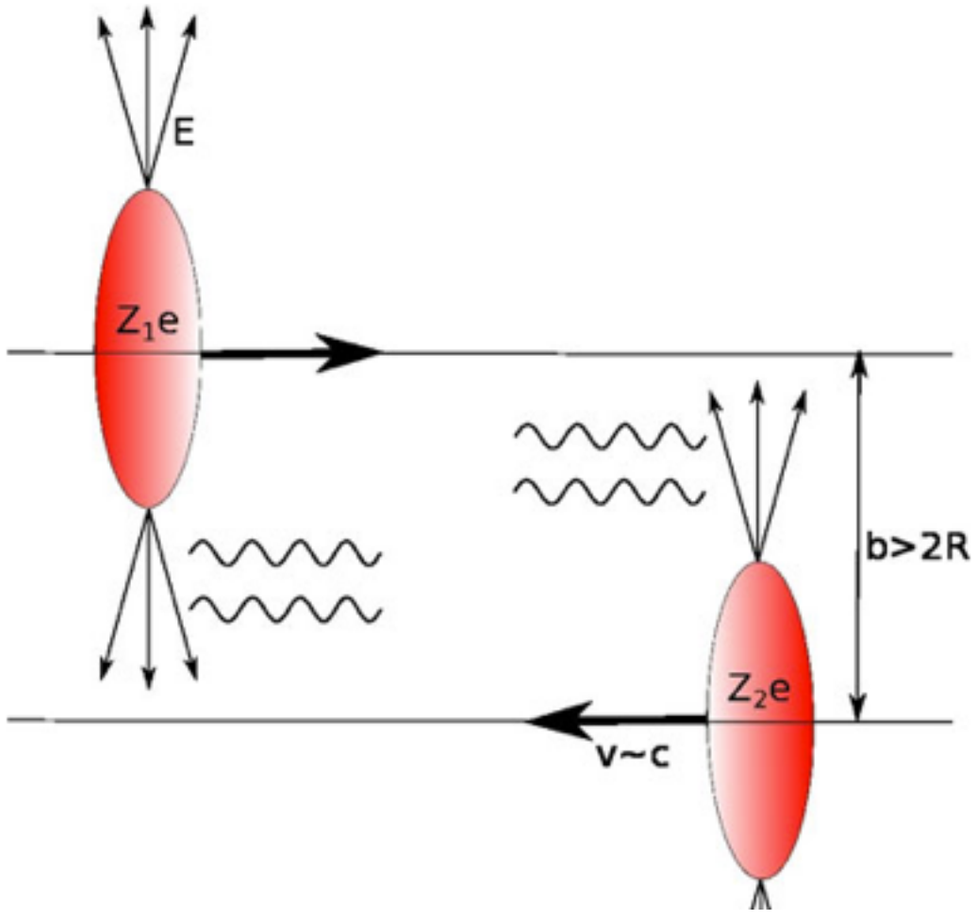
Friends of the INT

Obtain an INT preprint number

INT Workshop INT-17-65W

Probing QCD in Photon-Nucleus Interactions at RHIC and LHC: the Path to EIC

February 13 - 17, 2017



http://www.int.washington.edu/PROGRAMS/17-65w/

DIS 2017



WG2 conveners

Grzegorz Gach — AGH

Anna Staśto — PennState Eberly College of Science

Daniel Tapia Takaki — KU

INT workshop

Organizers

Daniel Tapia Takaki
University of Kansas
Daniel.Tapia.Takaki@cern.ch

Carlos Bertulani
Texas A&M University-Commerce
carlos.bertulani@tamuc.edu

Spencer R. Klein
Lawrence Berkeley Laboratory
SRKlein@lbl.gov

Tuomas Lappi
University of Jyvaskykla
tuomas.v.v.lappi@jyu.fi

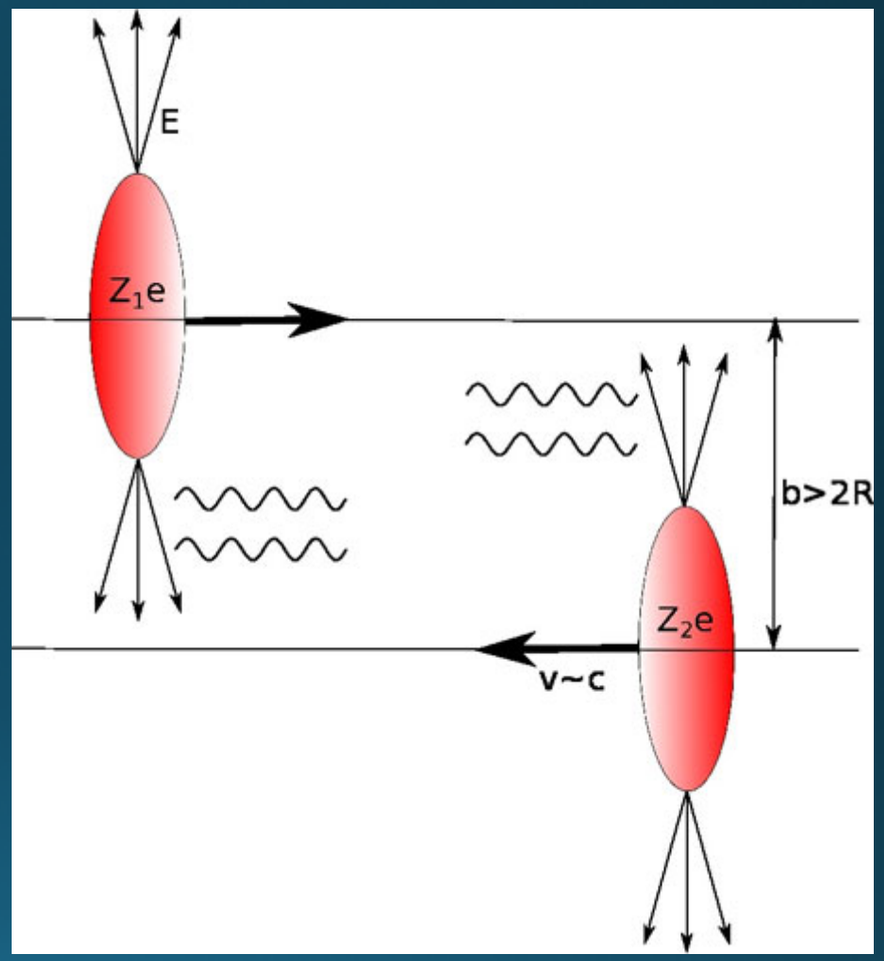
Mark Strikman
Pennsylvania State University
strikman@phys.psu.edu

INT workshop

Overview

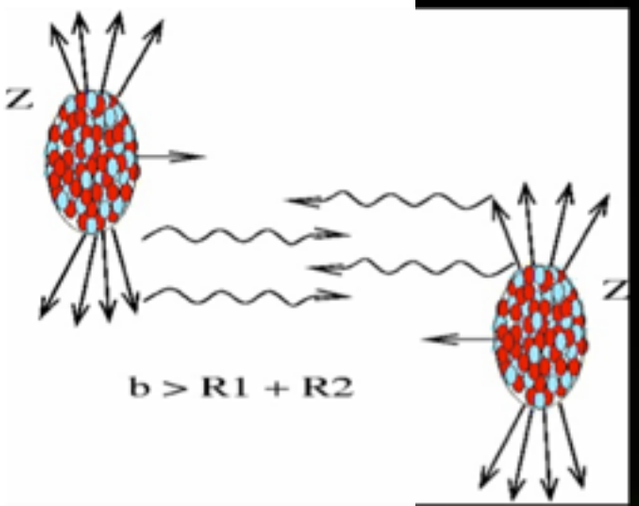
- High-energy photon-nucleon (nucleus) collisions offer us a unique opportunity to study the hadron and photon structure, QCD dynamics and small Bjorken-x gluon dynamics at photon intensities and energies that are unavailable elsewhere

- These interactions can already be studied in a wide energy range from W ~10 GeV (RHIC Au-Au) to W ~ 500 GeV (LHC Pb-Pb) using ultraperipheral collisions at hadronic colliders

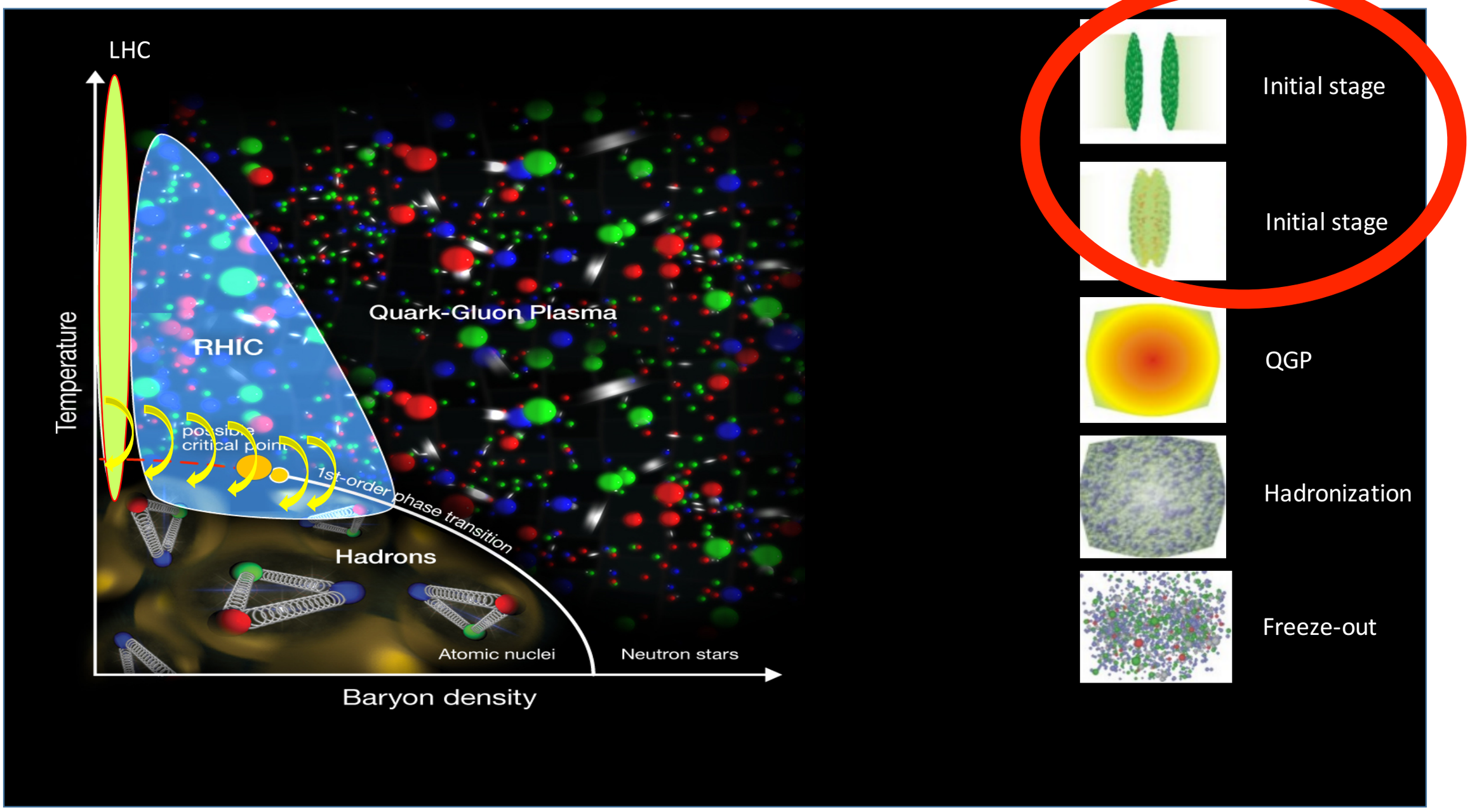


Ultra-peripheral collisions

UPC collisions: shedding light on the proton (pp or p-Pb) or nucleus (Pb-Pb)



Understanding the initial state



the nature of the initial state is one of the most important questions in high-energy nuclear physics

10 UPC studies with heavy ions at the LHC

- *Coherent J/ψ photoproduction in ultra-peripheral Pb-Pb collisions at sNN=2.76 TeV* Phys.Lett. B718 (2013) 1273-1283
- *Charmonium and e+e− pair photoproduction at mid-rapidity in ultra-peripheral Pb-Pb collisions at sNN√=2.76 TeV* Eur.Phys.J. C73 (2013) 11, 2617
- *Exclusive J/ψ photoproduction off protons in ultra-peripheral p-Pb collisions at sNN√=5.02 TeV* Phys.Rev.Lett. 113 (2014) 23, 232504
- *Coherent ρ0 photoproduction in ultra-peripheral Pb-Pb collisions at sNN =2.76 TeV* JHEP 1509 (2015) 095
- *Coherent ψ(2S) photo-production in ultra-peripheral Pb Pb collisions at sNN = 2.76 TeV* Phys.Lett. B751 (2015) 358-370
- *Measurement of an excess in the yield of J/\psi at very low pT in Pb-Pb collisions at sNN = 2.76 TeV* Phys. Rev. Lett.116 (2016) 22, 222301
- *Coherent J/ψ photoproduction in ultra-peripheral Pb-Pb collisions at sNN=2.76 TeV with the CMS detector* CMS-PAS-HIN-12-009. Submitted to PLB
- *Measurement of exclusive Upsilon in pPb collisions at sNN = 5.02 TeV* CMS-PAS-FSQ-13-009
- *Measurement of high-mass dimuon pairs from ultraperipheral lead-lead collisions at sNN =5.02 TeV with the ATLAS detector at the LHC* ATLAS-CONF-2016-025
- Light-by-light scattering in ultra-peripheral Pb+Pb collisions at sNN = 5.02 TeV with the ATLAS detector at the LHC ATLAS-CONF-2016-111

INT workshop

Overview

- ***UPC studies serve as a forerunner of the Electron Ion Collider (EIC) experiments.***
- The top of the energy range in UPCs at LHC is a factor of ten higher than that of the EIC, which offers a unique opportunity to explore this novel kinematic regime.
- At the same time, UPC collisions at RHIC and LHC have their own limitations, since it is not possible to study the Q^2 dependence systematically for most physics processes of interest.

INT workshop

Overview

- Despite the recent experimental progress, work on the theoretical side is clearly not at a similar level to that of inclusive hard scattering.

- ***The goal of this workshop is to identify and discuss the theoretical challenges of photon-induced physics, and how to use this knowledge for physics studies at the EIC.***

INT workshop

Topics (main focus)

- **Current status of nuclear PDFs and developments using photon-nucleus data**
- **Strategies for observing nonlinear and gluon saturation effects in photon - nucleus scattering**
- Progress in understanding heavy quark hadronization in exclusive processes.
- Models for coherent and incoherent soft photon - nucleon / nucleus interactions
- Predictions of the leading twist models, dipole models and CGC models for exclusive gamma-p and gamma A scattering.
- Exotic spectroscopy and searches for new physics

Overview

- **Studying QCD with high energy photon-photon, photon-proton and photon-nuclear interactions at RHIC and LHC**
  - **Searching for saturation effects in the proton**
  - **Nuclear effects at both low and high Bjorken-x**

- **So far, most analyses have been carried out for exclusive VM photoproduction but new studies possible and ongoing dijets, diphotons…**

- **Inclusive photo-nuclear and photon-proton reactions also possible and first studies ongoing**

INT workshop

PDFs

Ramona Vogt (LLNL)
Fred Olness (SMU)
Shunzo Kumano (KEK)

Diffraction, Jets, Saturation, and Dipoles

Beatriz Gay Ducati (UFRGS)
Anna Stasto (PSU)
Guangyao Chen (Iowa State)
Piotr Kotko (PSU)
Wolfgang Schaefer (Cracow)
Amir Rezaeian (Valparaiso)
Heikki Mantysaari (BNL)
Misak Sargsian (FIU)

Shadowing

Vadim Guzey (Petersburg
Leonid Frankfurt (Tel Aviv
Mark Strikman (PSU)
Boris Blok (Technion)

Polarization in UPCs and EIC

Maria Elena Tejeda-Yeomans (Sonora)
John Ralston (Kansas)

Path to EIC

Elke Aschenauer (BNL)
Christian Weiss (JLab)
Michael Lomnitz (LBNL)

Experiments at RHIC and LHC

Jarda Adam (Creighton)
Aaron Angerami (Columbia)
Evgeny Kryshen (Petersburg)
Michael Murray (Kansas)

INT workshop

48 participants at INT

Some selected slides….

DIS 2017

Working Group 2: Low x and Diffraction

9 sessions, 42 talks, 18 experiment, 24 theory/phenomenology

Speakers:

Marcin Guzik
Laurent Forthomme
Alexander Bylinkin
Bartłomiej Rachwał
Jesus G. Contreras Nuno
Frigyes Janos Nemes
Grzegorz Gach
Peter John Bussey
John Dainton
Karel Cerny
Kay Graham
Martin Hentschinski
Jan Cepila
Heikki Mantysaari
Radek Zlebcik
Renaud Boussarie
Yoshitaka Hatta
Oleg Kuprash
Benoit Roland
Gilvan Augusto Alves

Merijn van de Klundert
Jamal Jalilian-Marian
Mirko Serino
Oldrich Kepka
Grigorios Chachamis
Krzysztof Kutak
Agustin Sabio Vera
Victor Fadin
Sergey Bondarenko
Giovanni Antonio Chirilli
Guillaume Beuf
Tibor Zenis
Nestor Armesto Perez
Stephane Munier
Leszek Motyka
Bertrand Ducloue
Ian Balitsky
Elena Petreska
Aleksander Kusina

INT workshop

UPC in parallel with EIC

- UPCs and EIC complementary

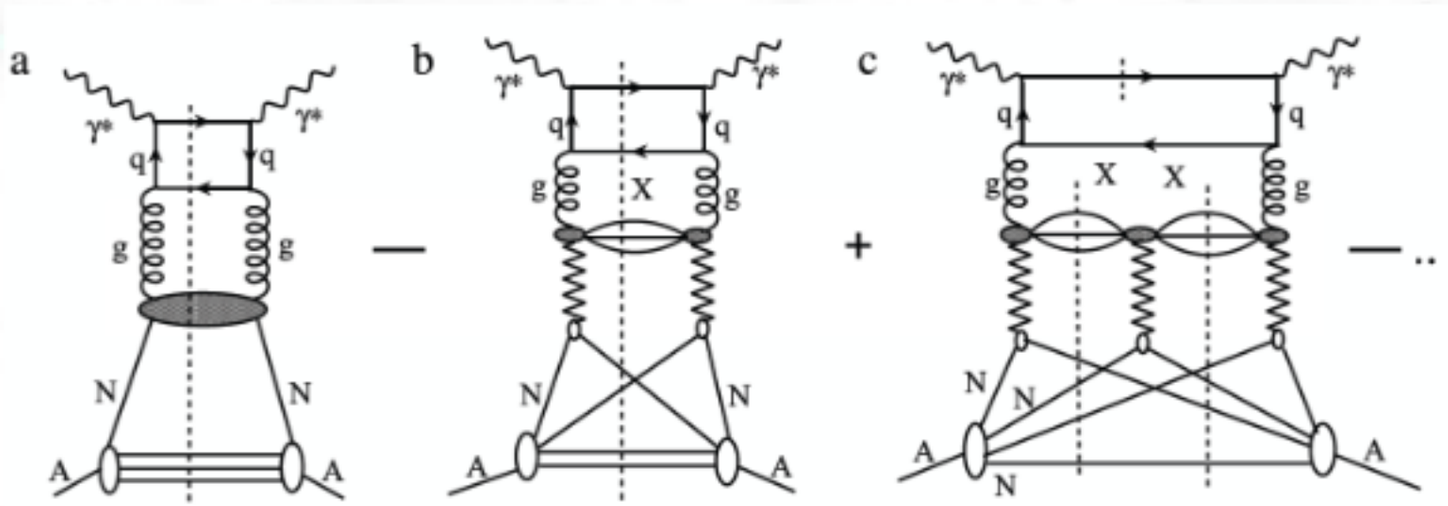
  Highest energy $\leftrightarrow$ control of hard-process kinematics

- Concrete possibilities for "joint" studies

  Mechanism of nuclear shadowing
  Nuclear quarks/gluons at larger x
  Transverse nucleon structure
  Unitarity limit in hard interactions

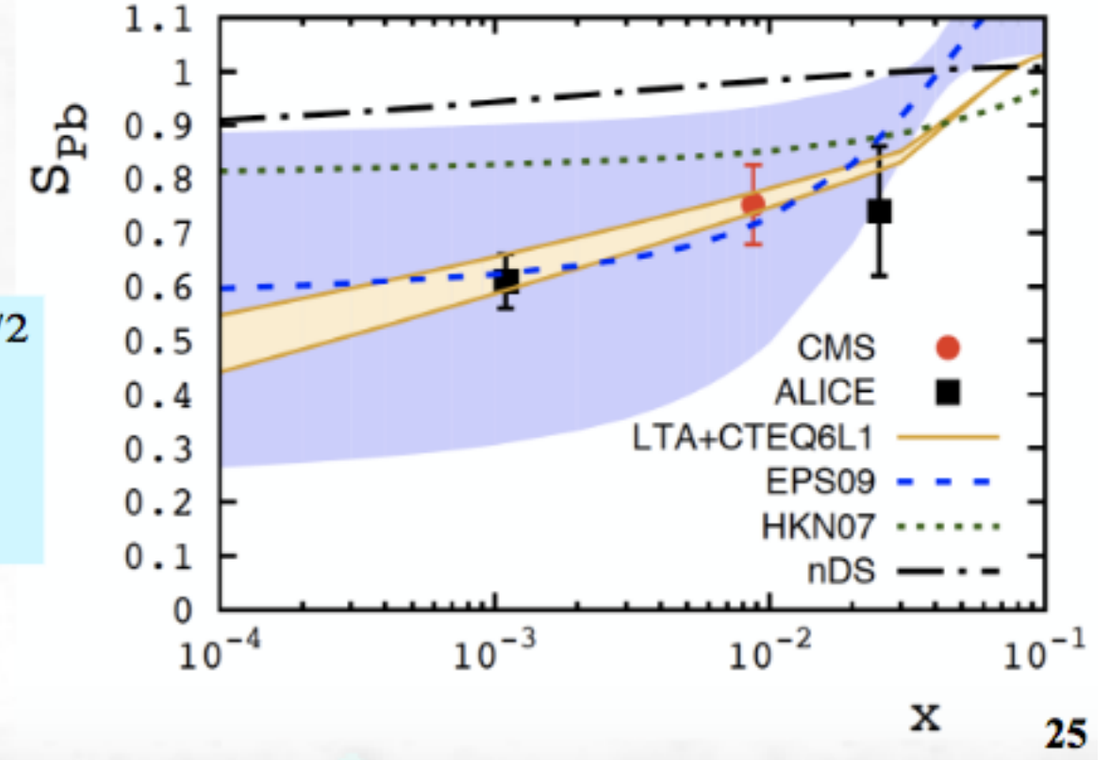
From Christian Weiss' talk

Leading Twist Shadowing Model



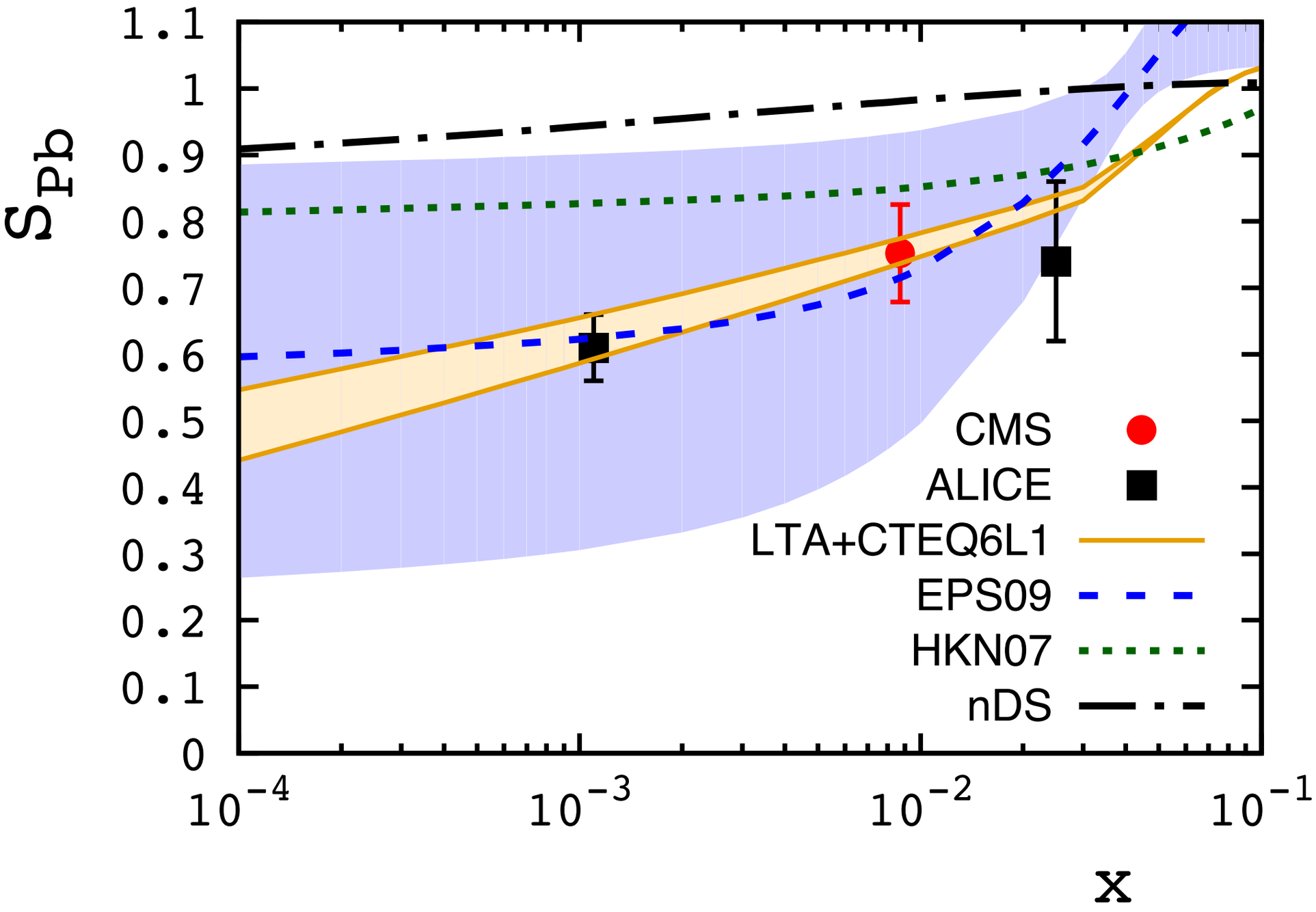
From Vadim Guzey's talk

$$S(W_{\gamma p}) = \left[\frac{\sigma_{\gamma Pb \to J/\psi Pb}}{\sigma^{IA}_{\gamma Pb \to J/\psi Pb}} \right]^{1/2}$$



Nuclear suppression factor in Pb (S)

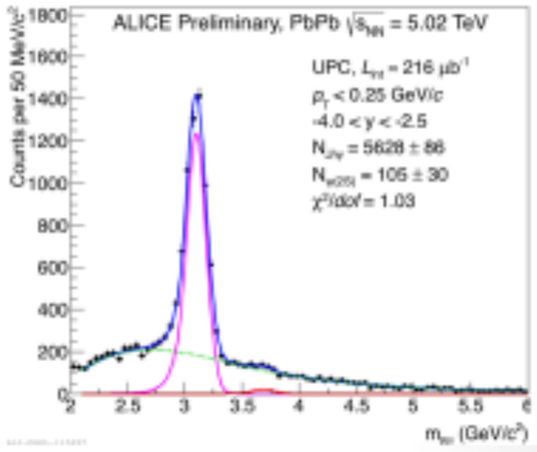
V. Guzey, et al.



Exclusive production of J/ψ and ψ(2S) in Pb+Pb

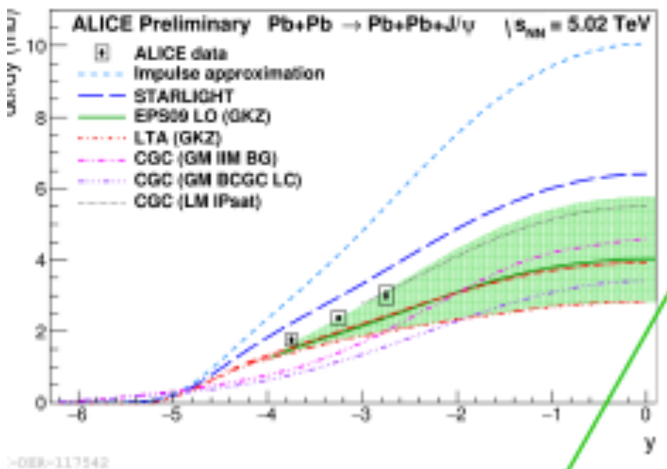
Kay Graham
ALICE

Run 2 data



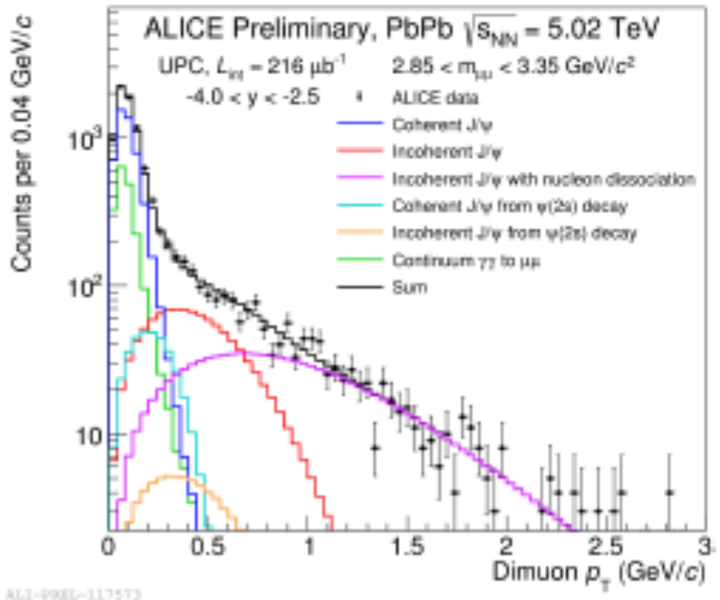
σ(ψ(2s))/σ(J/ψ) ≈0.166 ± 0.011 fits well with H1

data: 0.166 ± 0.007 (stat) ± 0.008 (syst) ± 0.007 (BR) [Phys.Lett.B541:251-264,2002]



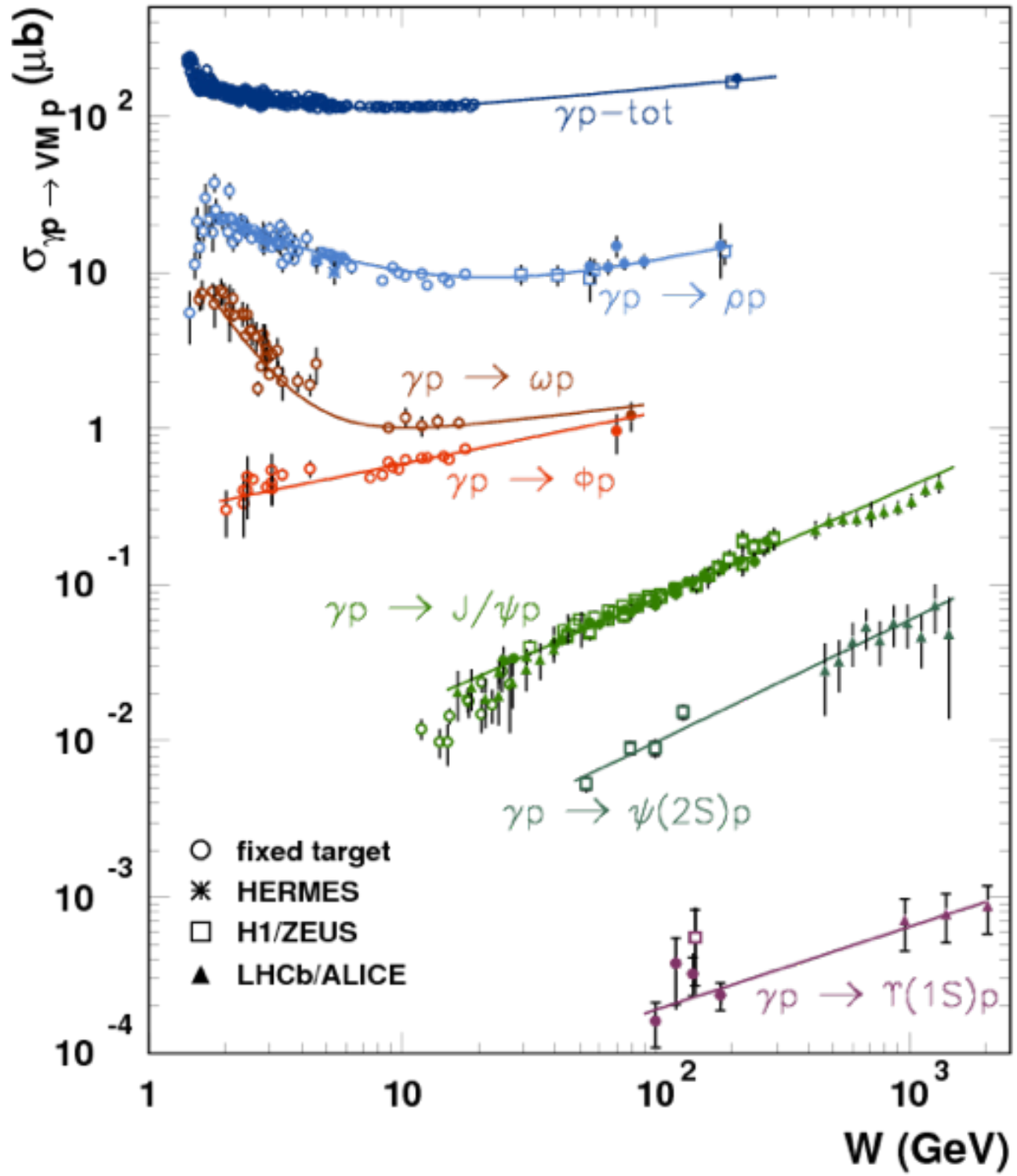
- Impulse approximation: no nuclear effects
- STARLIGHT: VDM + Glauber (Klein, Nystrand *et al* Comput. Phys. Commun. 212 (2017) 258)
- EPS09 L0: EPS09 shadowing (Guzey, Kryshen, Zhalov, PRC93 (2016) 055206)
- LTA: Leading Twist Approximation (Guzey, Kryshen, Zhalov, PRC93 (2016) 055206)
- CGC GM: color dipole model + IIM/BCGC (Goncalves, Machado *et al*, PRC 90 (2014) 015203, JPG 42 (2015) 105001)
- CGC LM: Color dipole model + IPSat (Lappi, H. Mäntysaari, PRC 83 (2011) 065202; 87 (2013) 032201)

Cross section consistent with moderate nuclear gluon shadowing

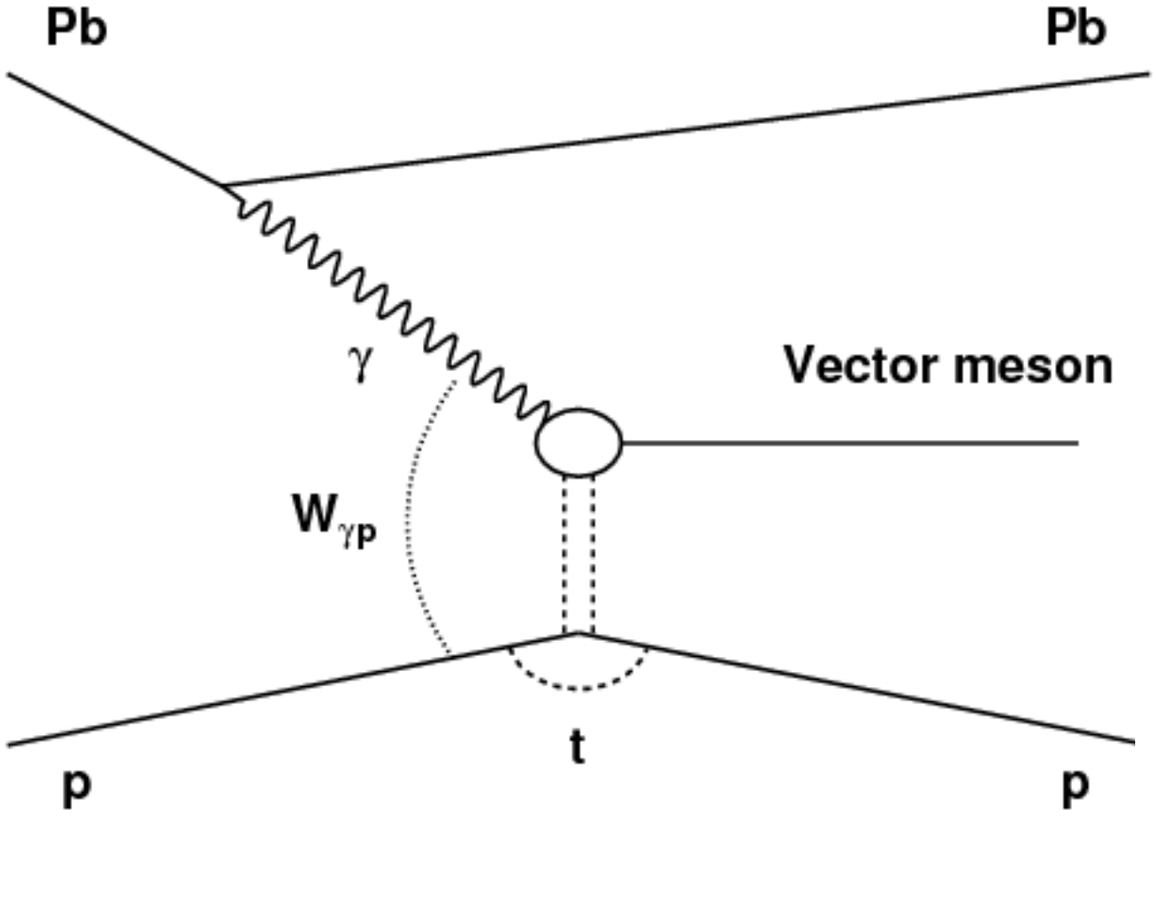


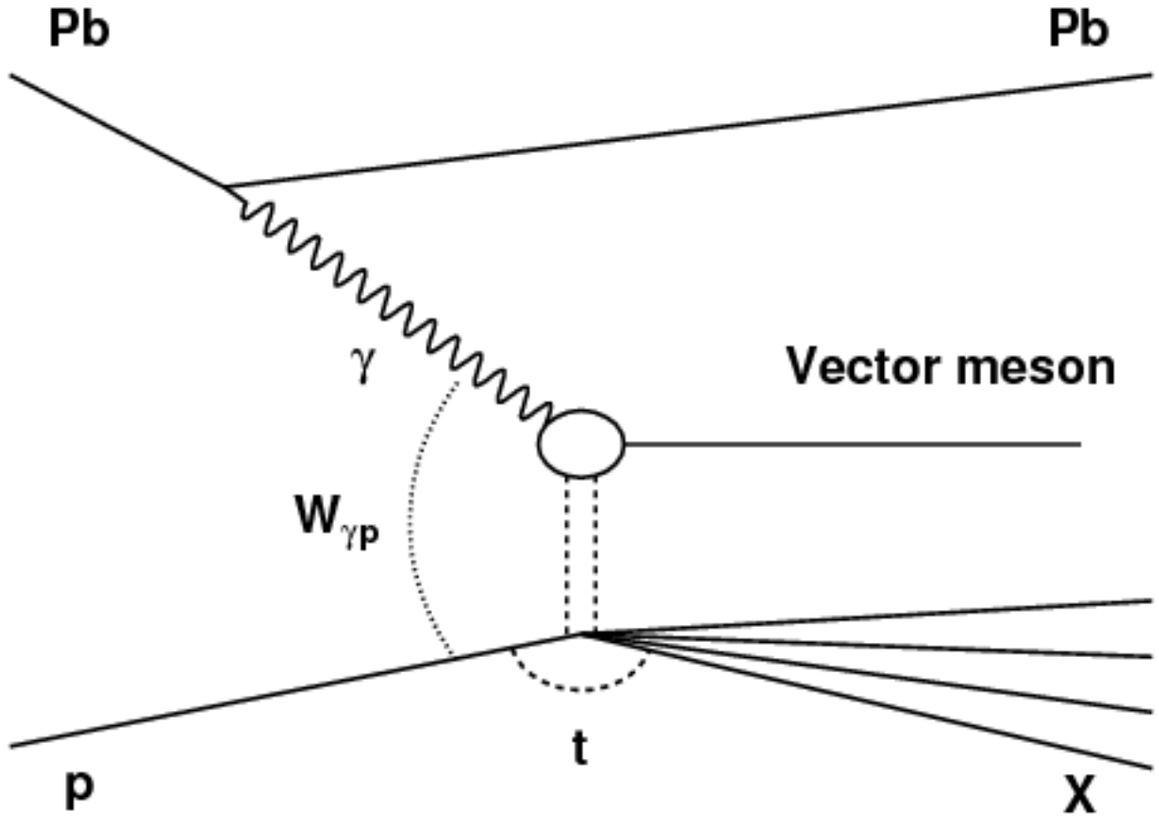
Both nucleon dissociation and incoherent production are needed to describe the data.

VM photoproduction data



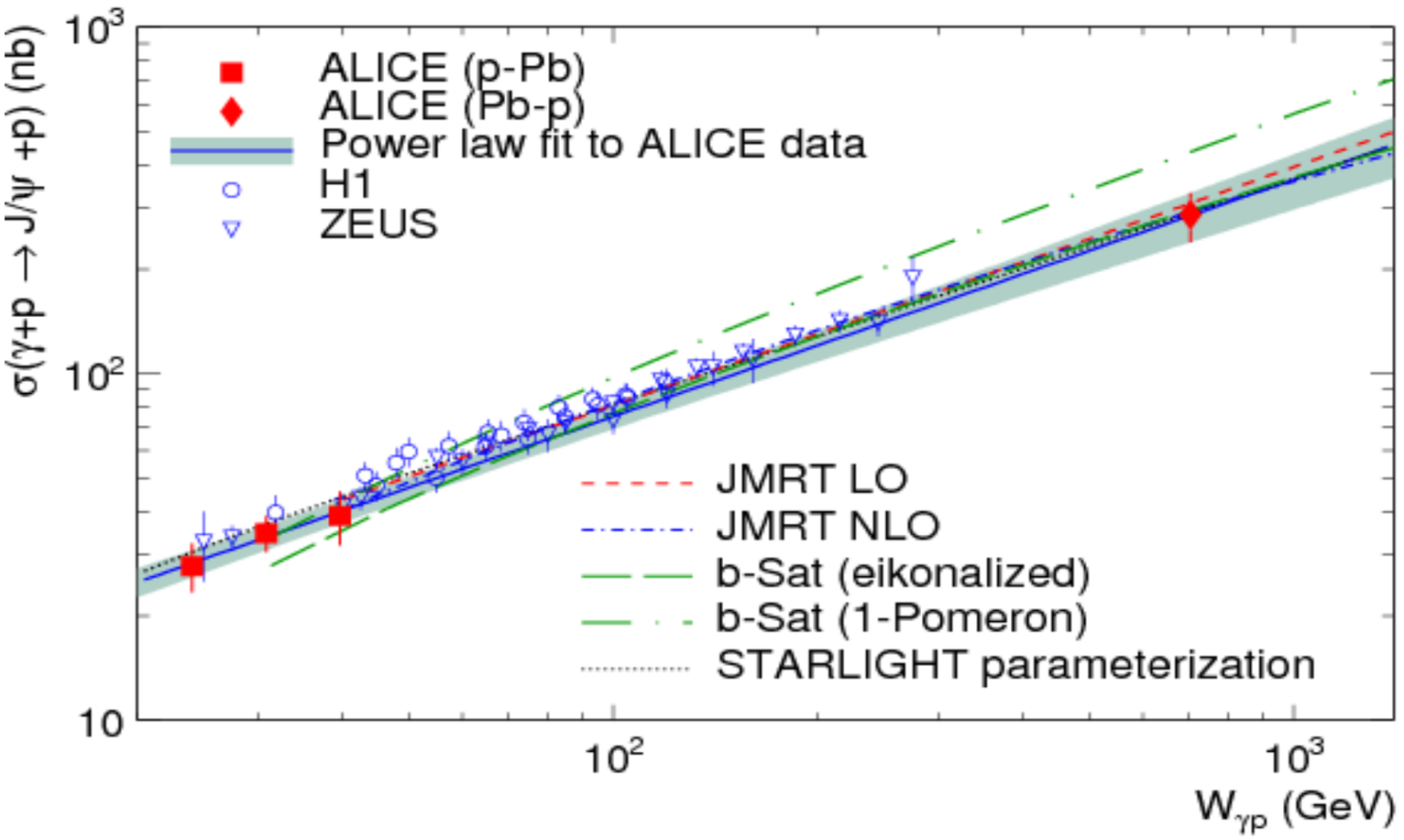
Vector meson photoproduction

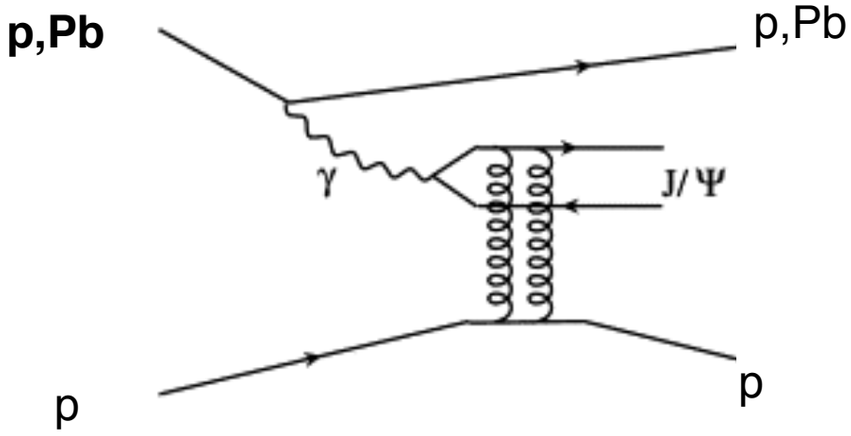




Exclusive J/psi photoproduction

Phys.Rev.Lett. 113 (2014) 23, 232504





$$\frac{d\sigma_{\gamma \mathrm{Pb} \to J/\psi \mathrm{Pb}}(t=0)}{dt} = \frac{16\,\Gamma_{ee}\pi^3}{3\alpha_{em}M_{J/\psi}^5}\left[\alpha_s(Q^2)xG_{\mathrm{Pb}}(x,Q^2)\right]^2$$

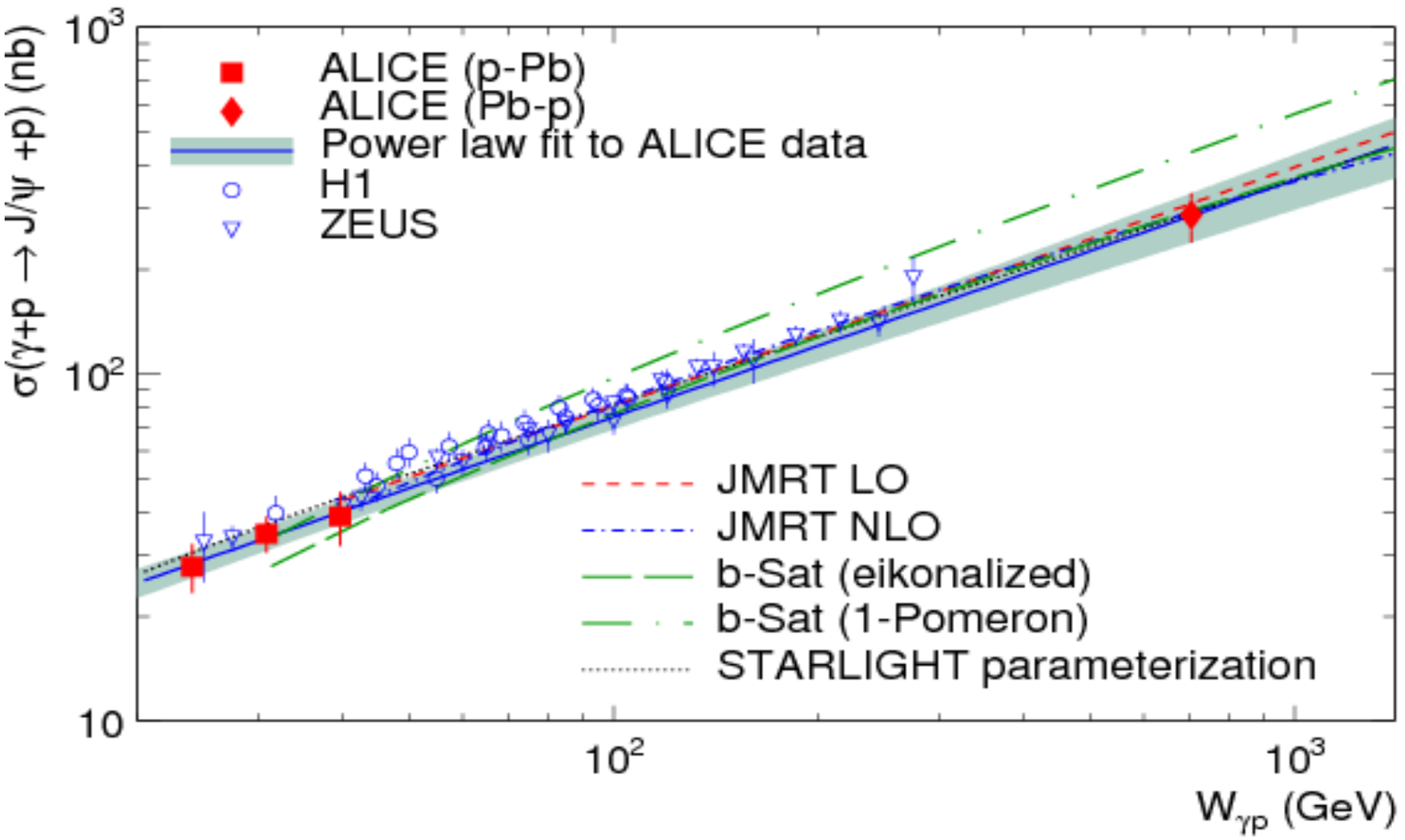
UPC VM in pp, p-Pb is a direct tool to measure saturation

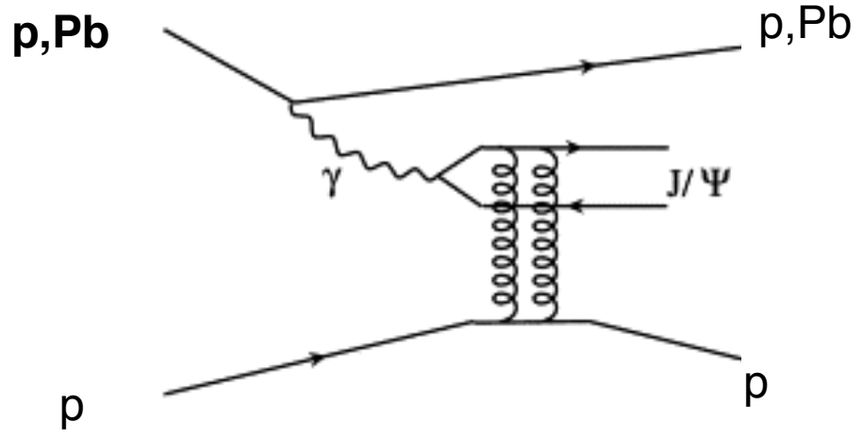
Bjorken $x \sim 10^{-2} - 10^{-5}$

accessible at LHC

Exclusive J/psi photoproduction

Phys.Rev.Lett. 113 (2014) 23, 232504





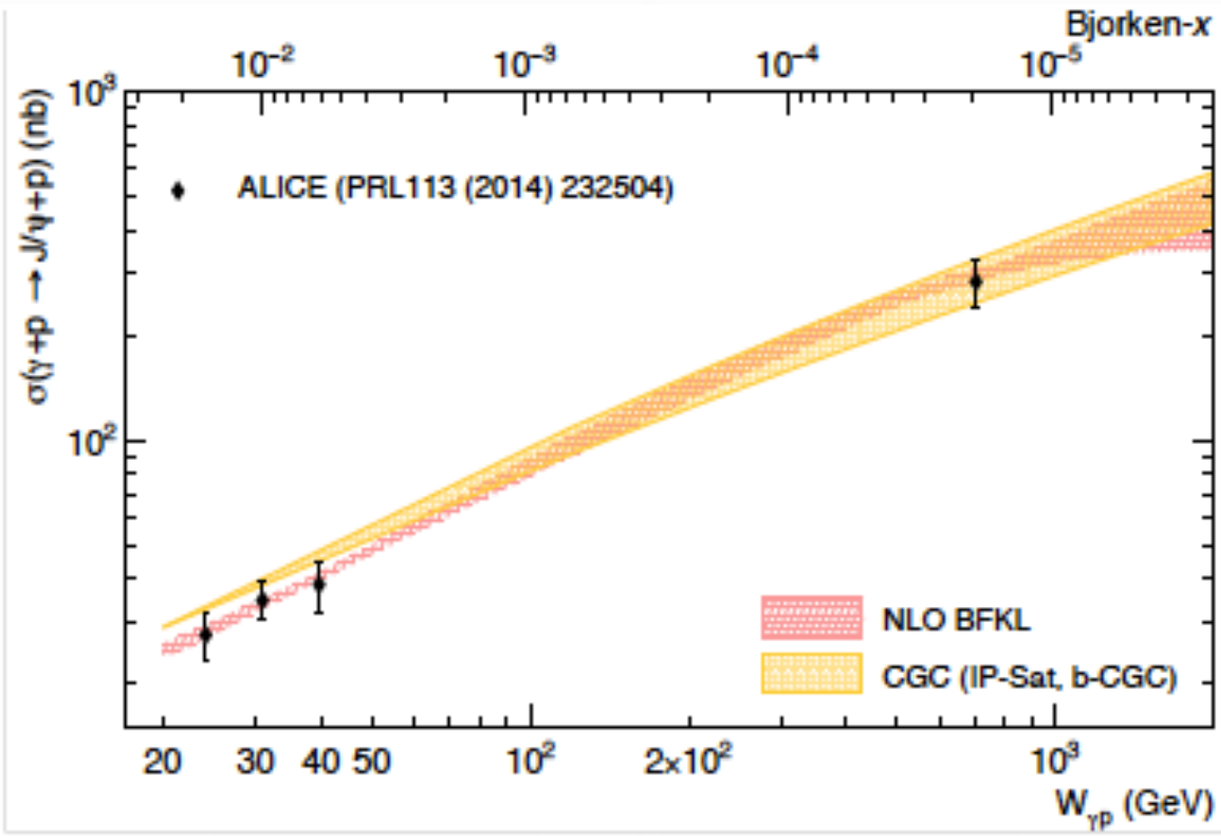
A natural explanation is that no change in the behaviour of the gluon PDF in the proton is observed between HERA and LHC energies" PRL 113 (2014) 232504.

Exclusive J/psi photoproduction

Phys.Rev.Lett. 113 (2014) 23, 232504

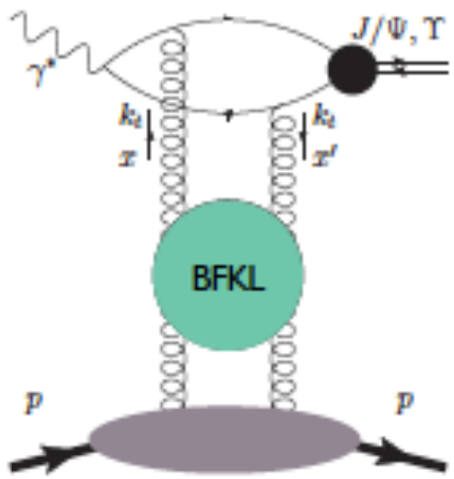
p,Pb

In pPb in ALICE, $W_{\gamma p}$ from 20 GeV to 1.5 TeV



Martin Hentschinski

NLL BFKL calculation - no saturation
Very good description of the data
Approaches with saturation work well too..



WG2: Low x and Diffraction

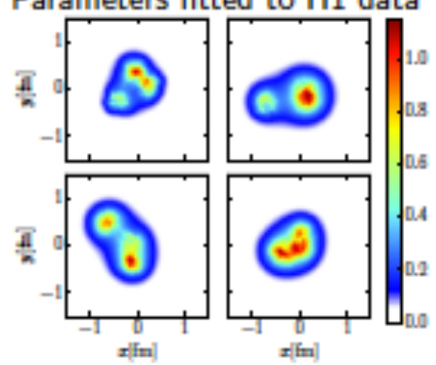
VM exclusive and dissociative production

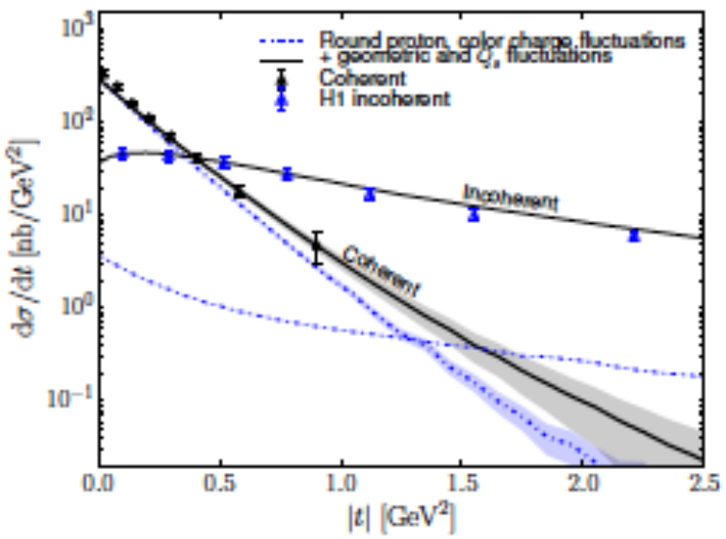
...so we do not know if gluon density *saturates* (yet), but maybe it *fluctuates*?

Heikki Mantysaari

Model the geometric fluctuations of density inside the proton

Parameters fitted to H1 data





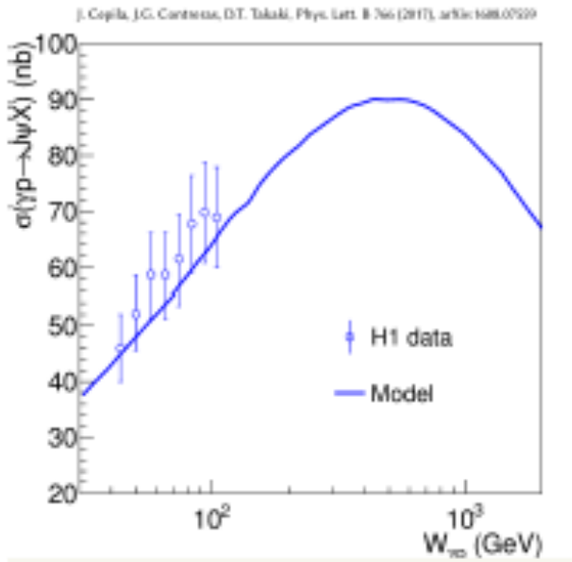
Coherent VM production: target stays intact

$$\frac{d\sigma^{\gamma^* p \to Vp}}{dt} \sim |\langle \mathcal{A}(x, Q^2, t)\rangle|^2$$

Incoherent VM diffraction: target breaks up.

$$\frac{d\sigma^{\gamma^* p \to Vp^*}}{dt} \sim \langle |\mathcal{A}(x, Q^2, t)|^2\rangle - |\langle \mathcal{A}(x, Q^2, t)\rangle|^2$$

Jan Cepila

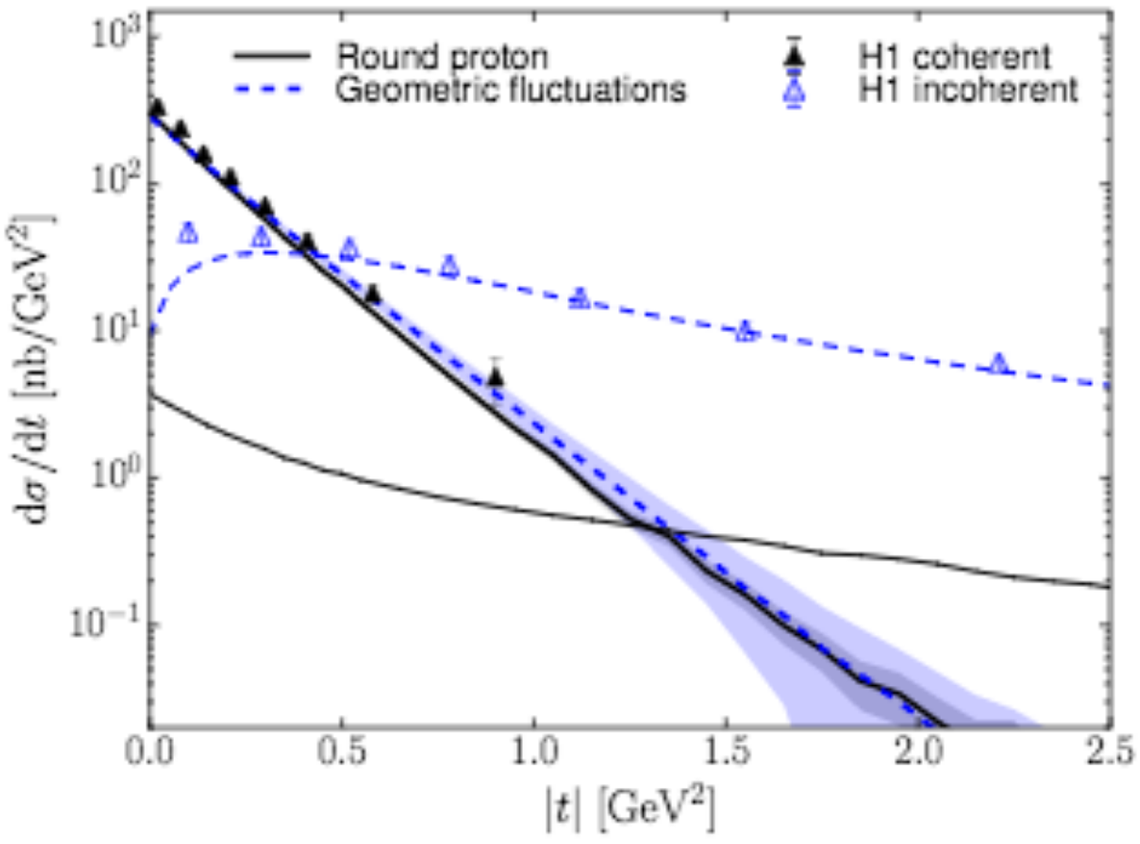


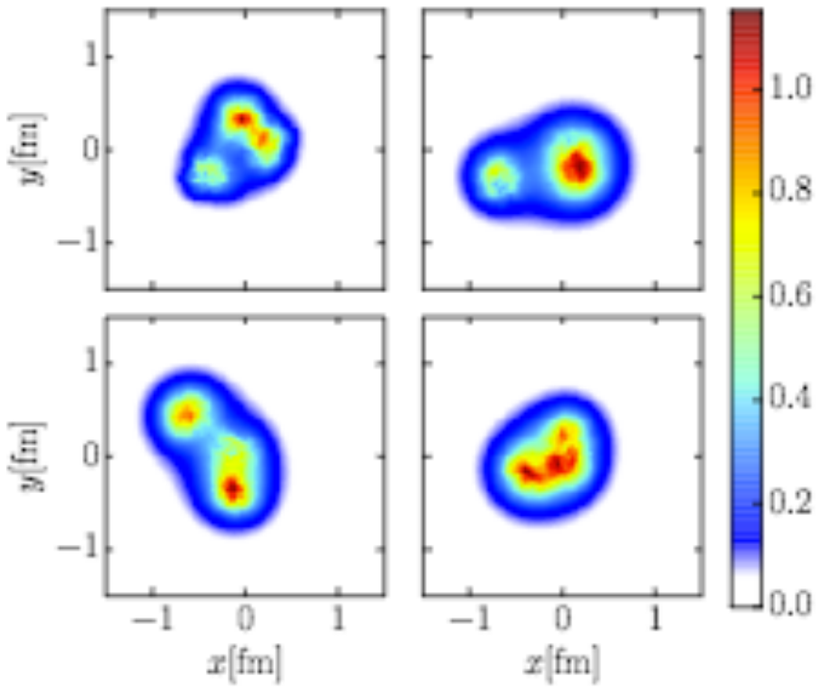
At high energies the incoherent cross section decreases with energy, due to increase and overlap of hotspots

WG2: Low x and Diffraction

IP-Glasma and HERA data

Include color charge fluctuation, parameters fitted to H1 data

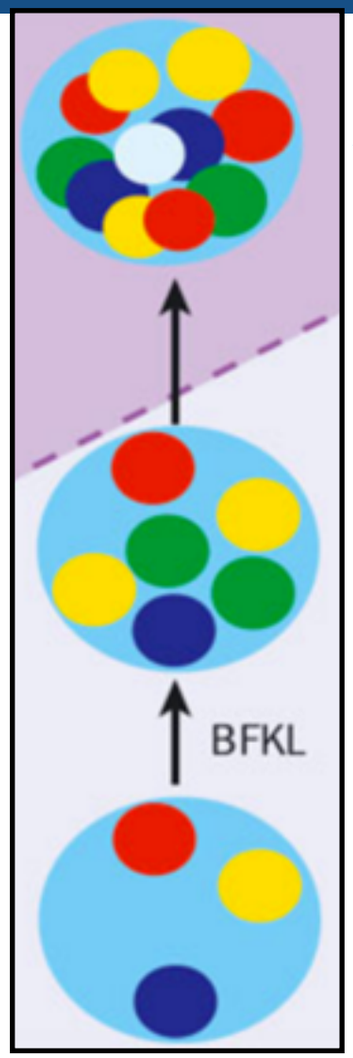


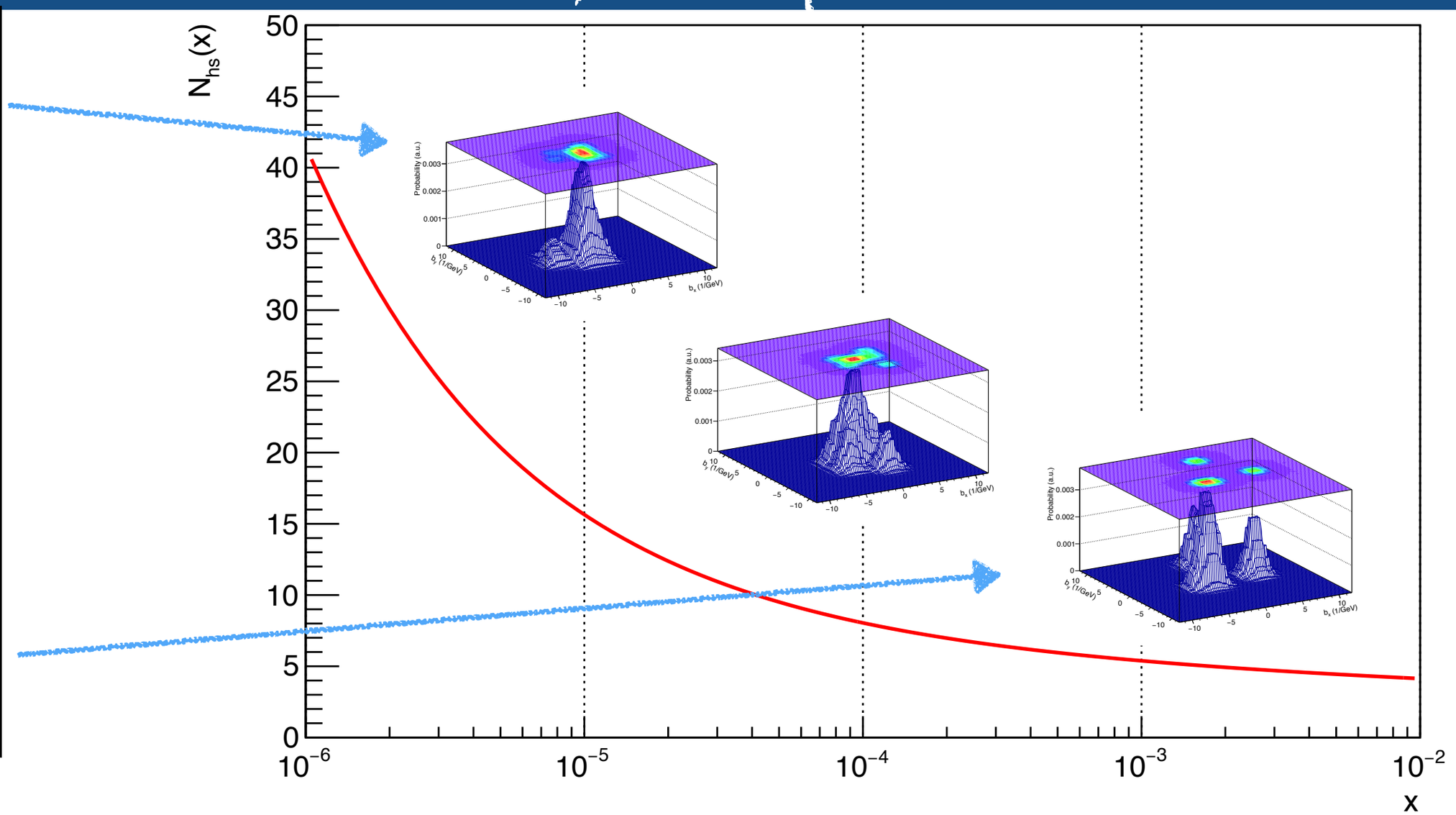


H.M., B. Schenke, PRD94 (2016), 034042

- Initial condition for pA hydro, good description of v_2 and v_3 data!

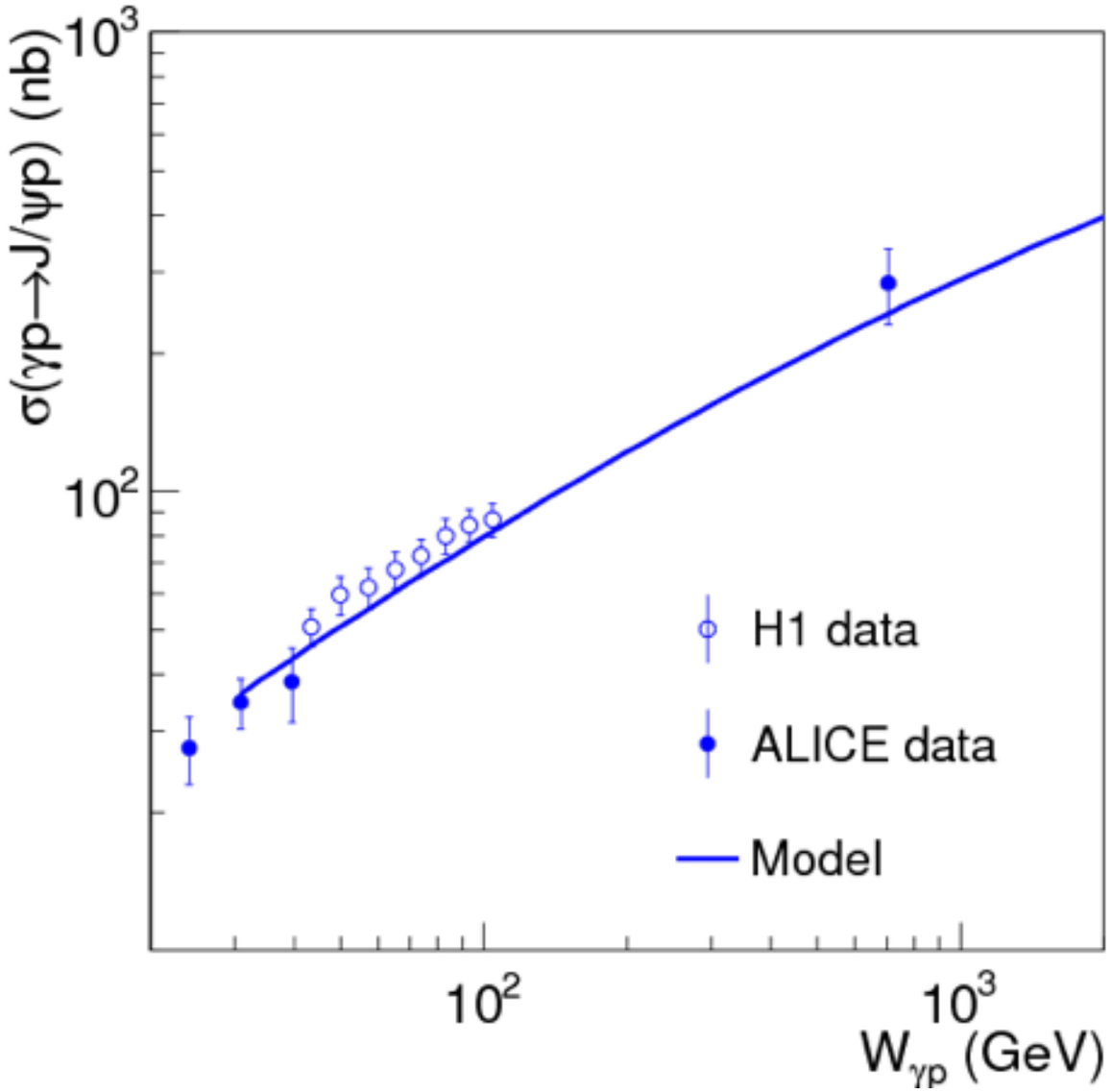
Number of hot spots

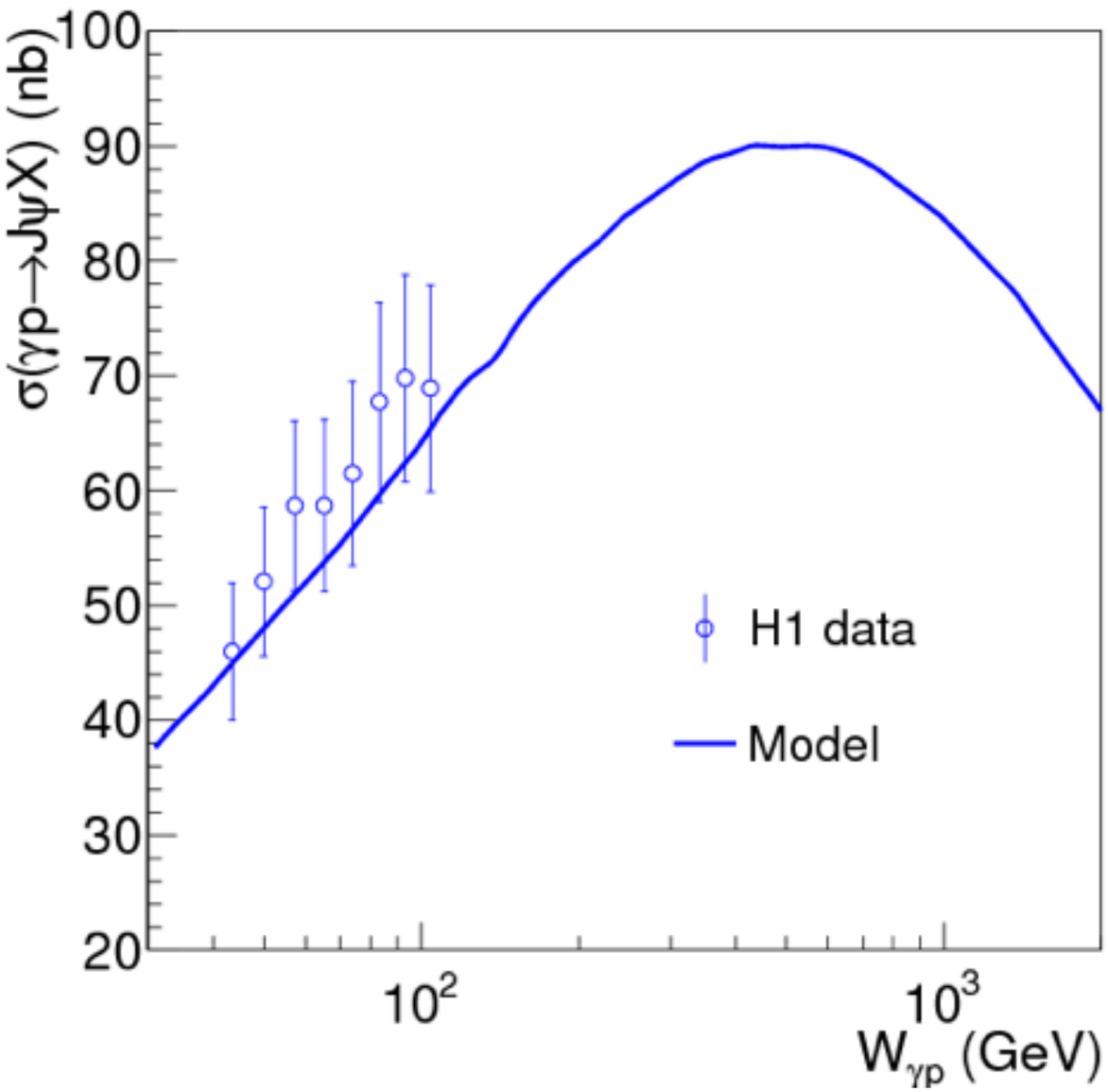




Energy dependence of dissociative photoproduction: ***signature of gluon saturation***

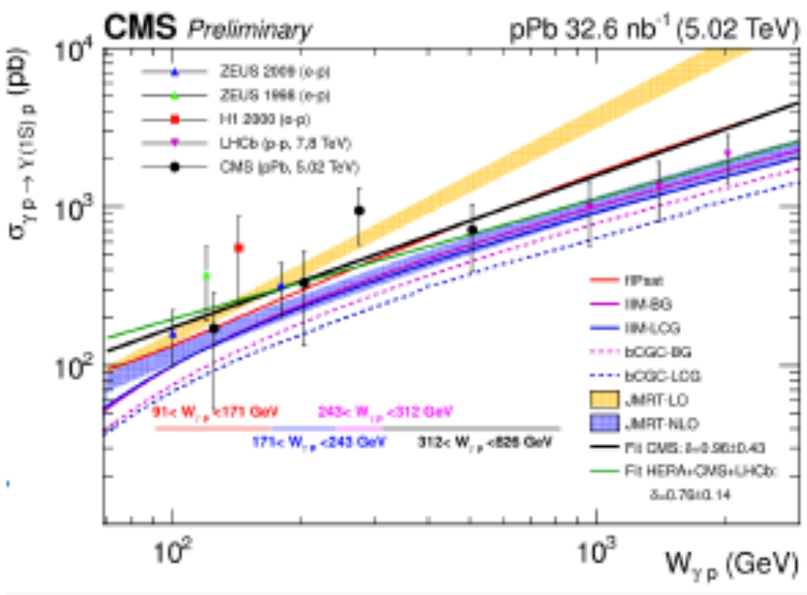
J. Cepina et al. Phys. Lett. B766 (2017) 186-191





Exclusive production of ψ(2s) and ϒ

Alexander Bylinkin
CMS



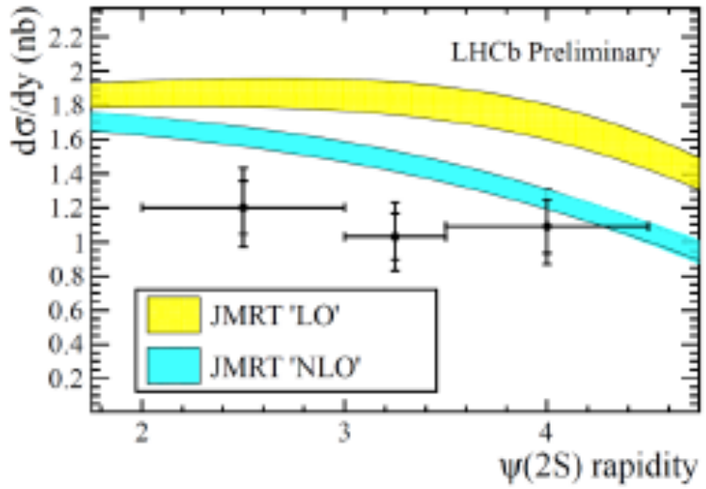
A fit with power-law **A X (W/400)$^{\delta}$** to the CMS data
δ = (0.96 ± 0.43) , A = 655 ± 196
Data compatible with power-law dependence of σ($W_{\gamma p}$), disfavours LO pQCD predictions

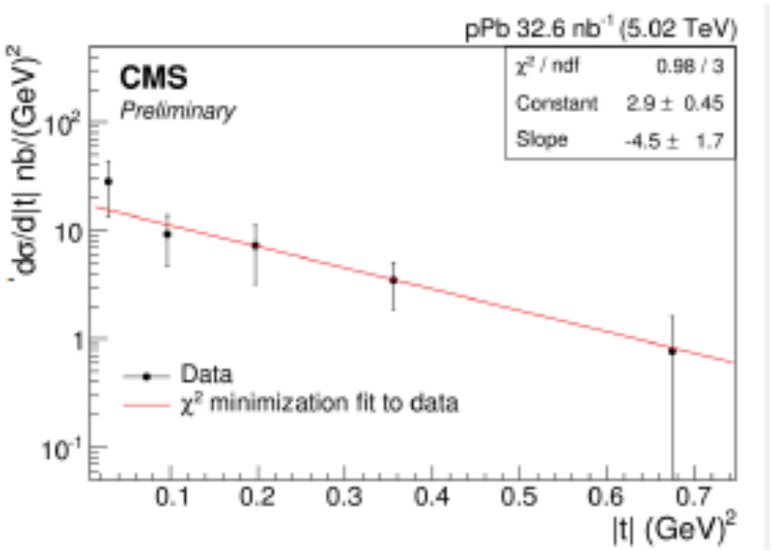
Still missing: energy dependence of t distribution for vector meson

Bartłomiej Rachwał
LHCb

Exclusive production ψ(2s) at 13 TeV

$\sigma_{\psi(2S)\to\mu^+\mu^-}\ (2.0 < \eta(\mu^{\pm}) < 4.5) = 9.4 \pm 1.3(stat) \pm 0.5(sys) \pm 0.4\text{pb}$

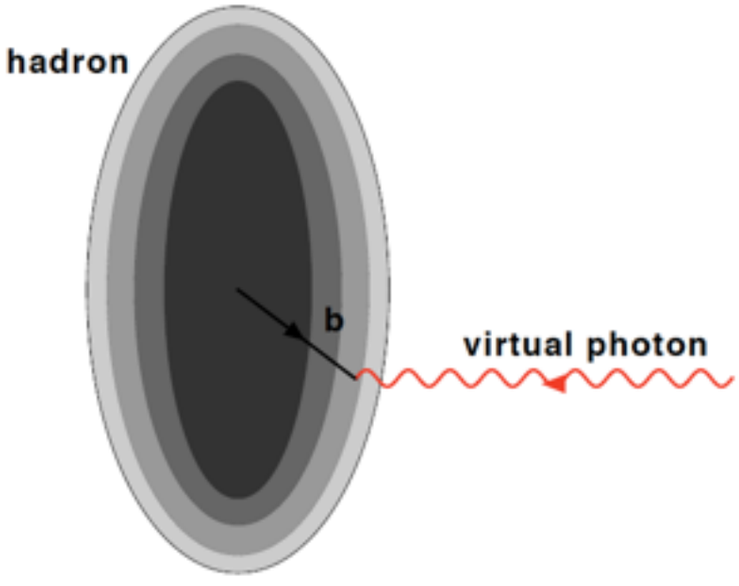


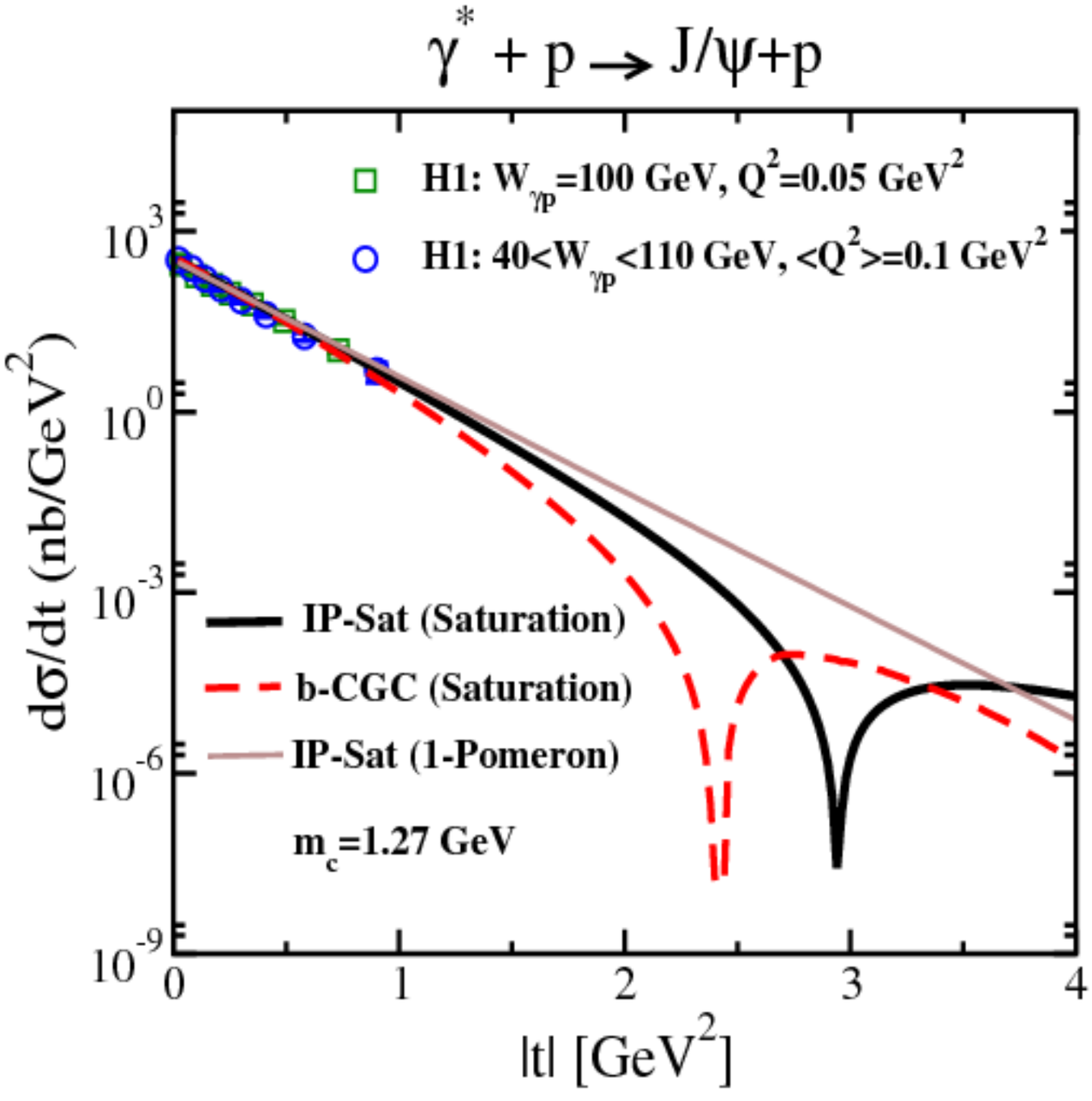


WG2: Low x and Diffraction

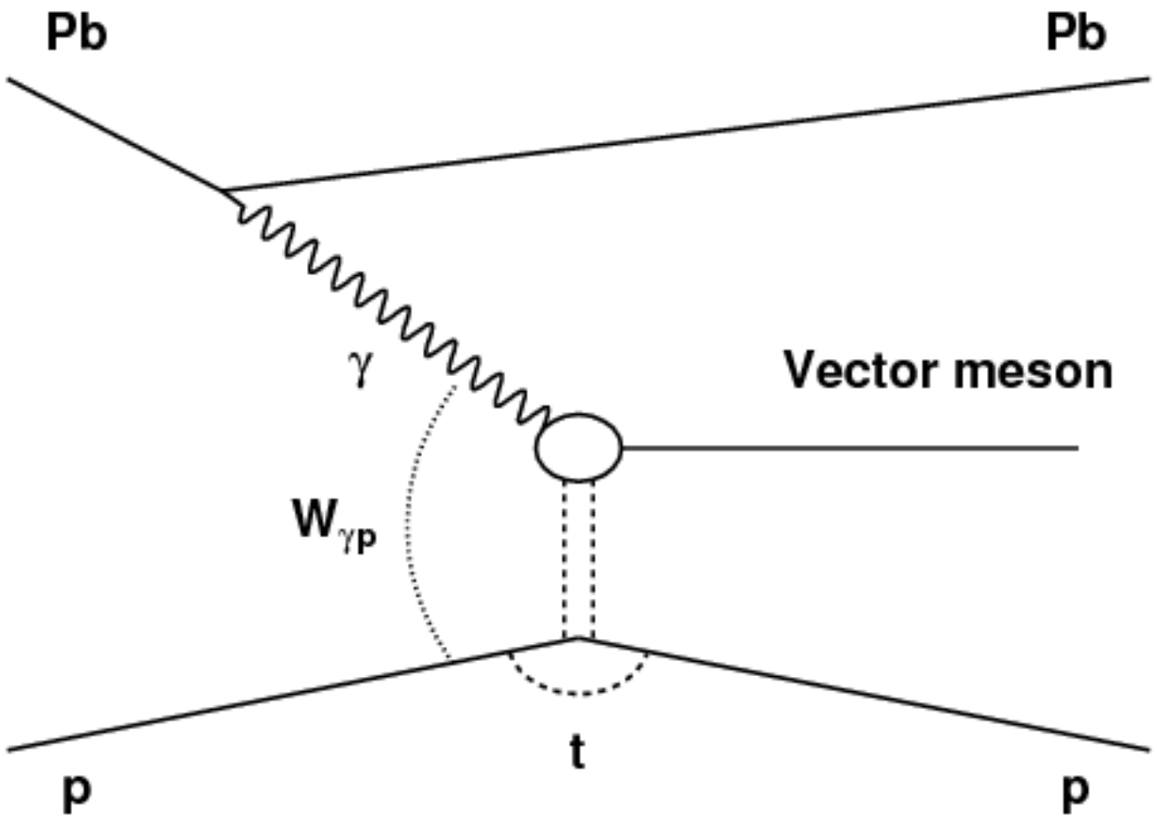
t-distribution

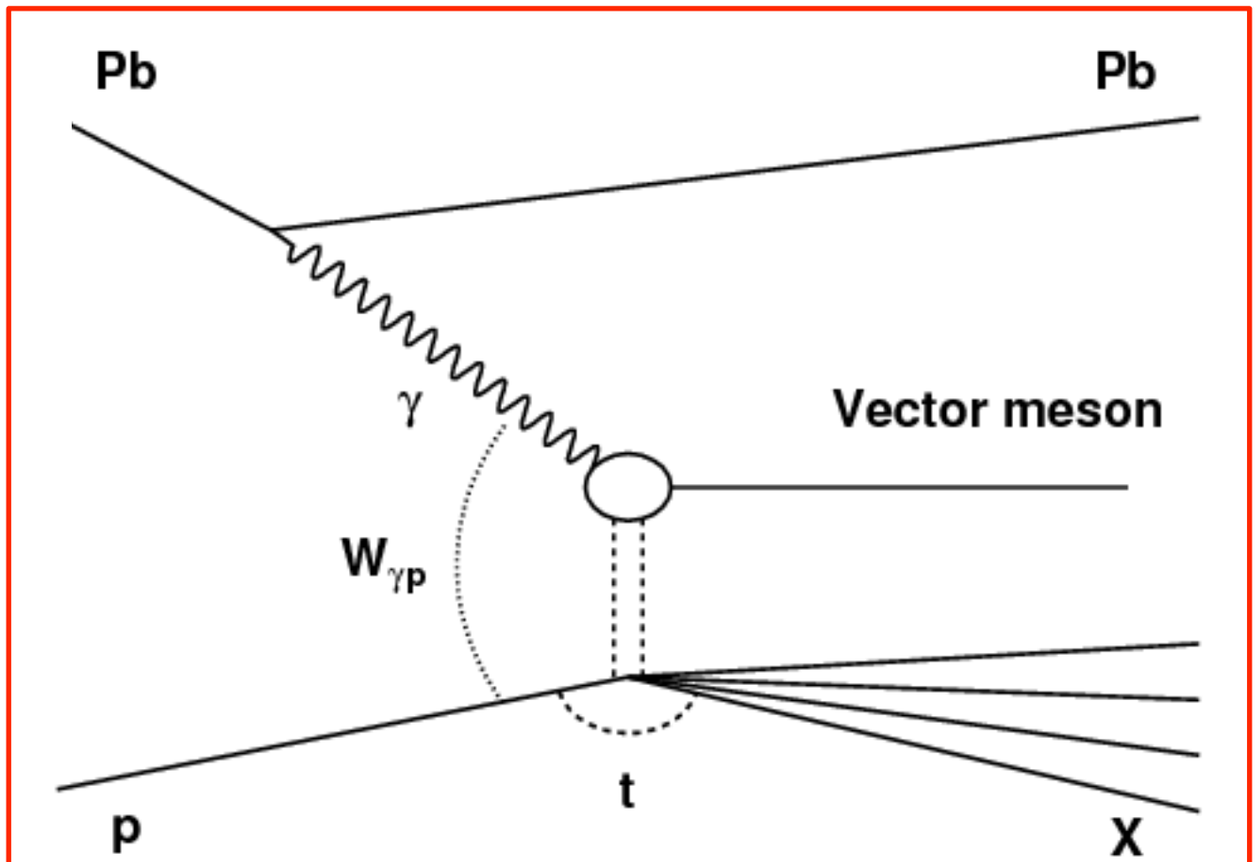
- t-differential measurements give a gluon tranverse mapping of the hadron/ nucleus.



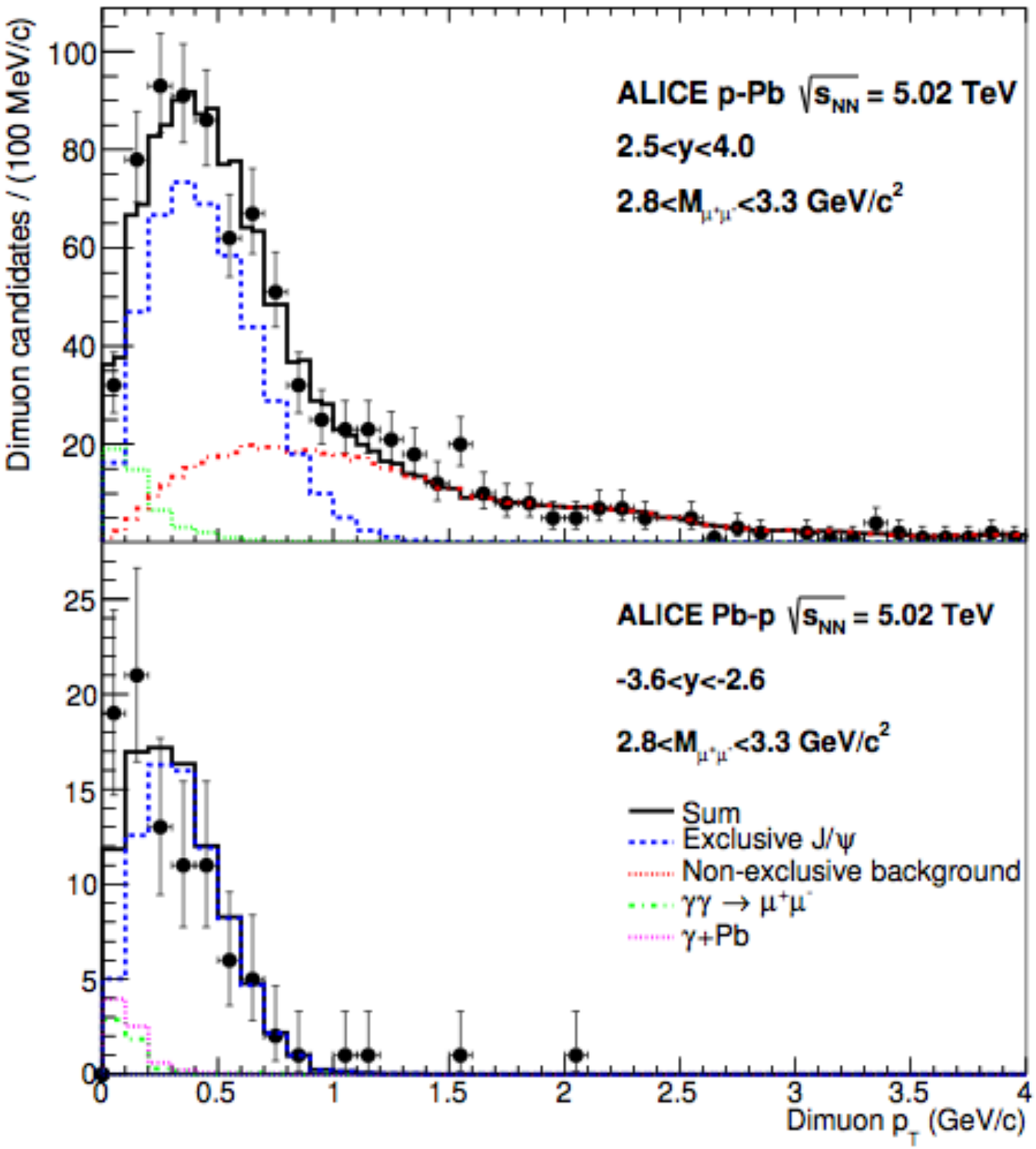


Vector meson photoproduction





Exclusive J/psi in p-Pb



Phys.Rev.Lett. 113 (2014) 23, 232504

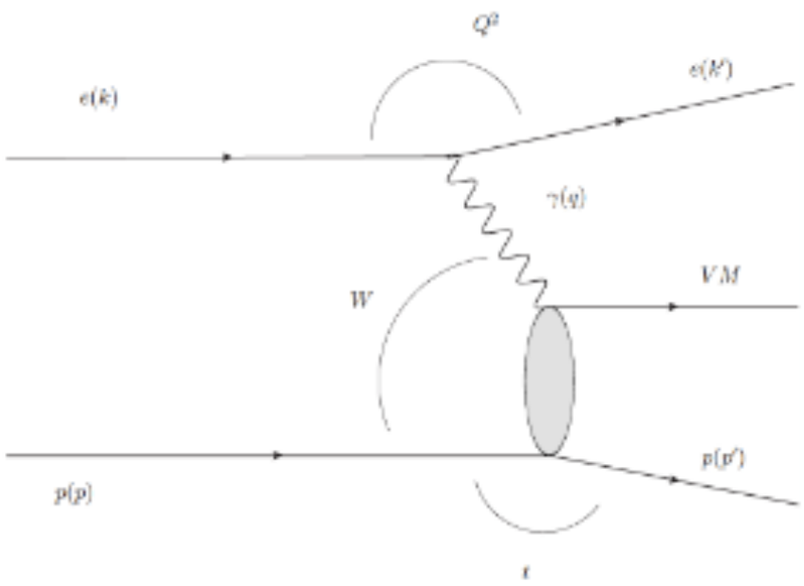
Data well described by templates

Energy dependence is clearly visible

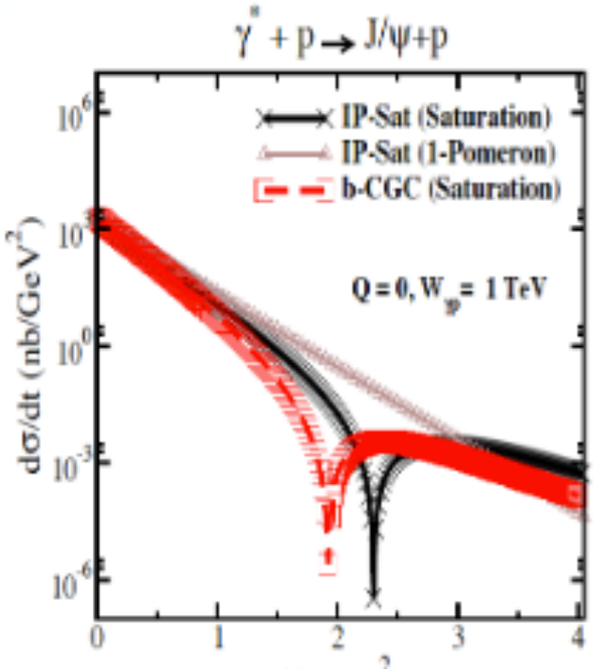
Low W_{gp} energy point
$\langle W_{gp} \rangle \sim 30$ GeV

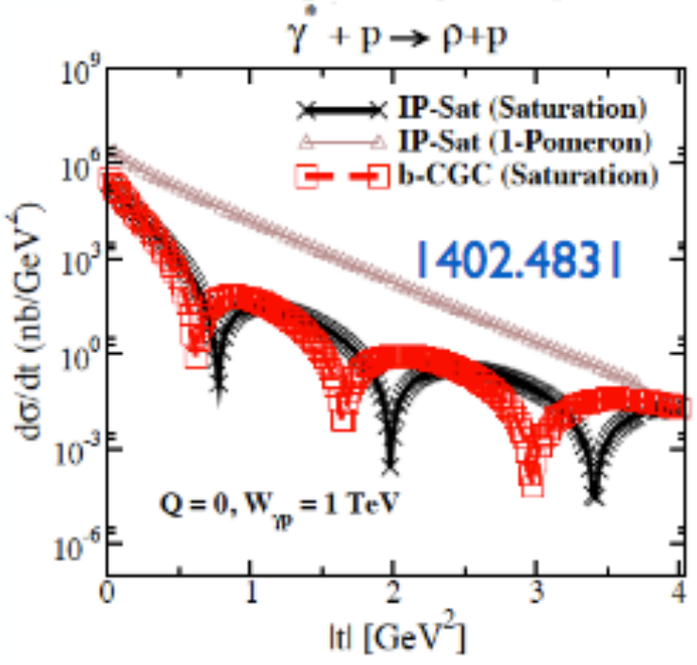
High W_{gp} energy point
$\langle W_{gp} \rangle \sim 700$ GeV

Elastic VM production in ep (III):

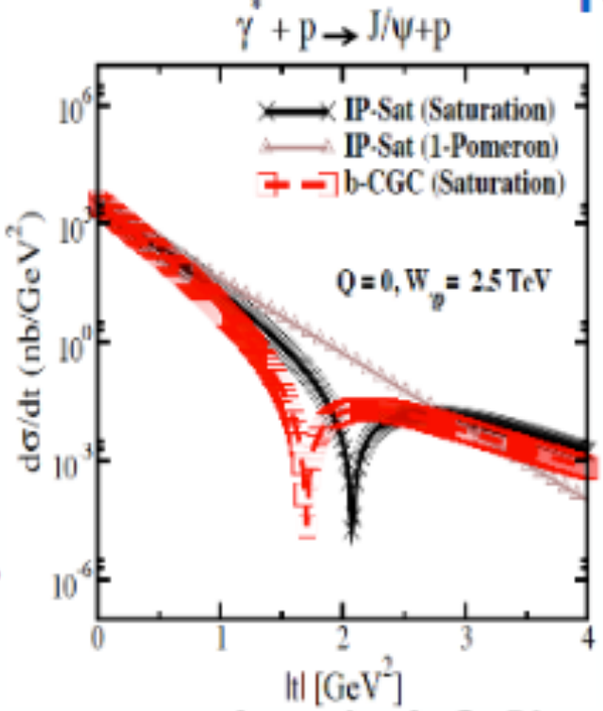


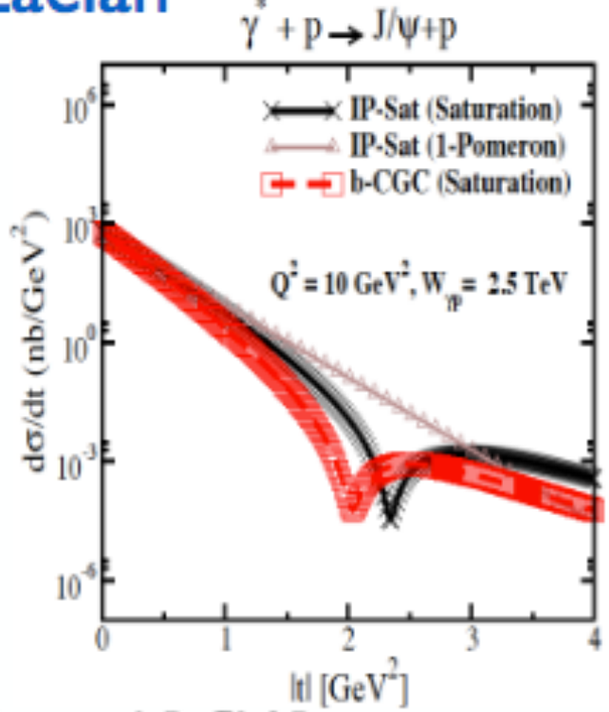
- Position of the dip and its evolution determined by the transverse structure of proton/ nuclei; its shrinking is natural in non-linear evolution towards the black disk (unitarity) limit.





Rezaeian





N.Armesto, 16.01.2017 - Small-x Physics in ep, eA and pA: 3. Physics beyond DGLAP. 17

Vector meson photoproduction in UPC Pb-Pb

Neutron dependence

$$d\sigma(\text{total})/dy = d\sigma(0\text{n}0\text{n})/dy + 2d\sigma(0\text{n}\text{X}\text{n})/dy + d\sigma(\text{X}\text{n}\text{X}\text{n})/dy$$

There is a factor 2 since the neutron and the coherent J/ψ are independent processes (confirmed by data)

Two components:

High-x: **J/ψ and the emitted neutrons: same rapidity hemisphere**

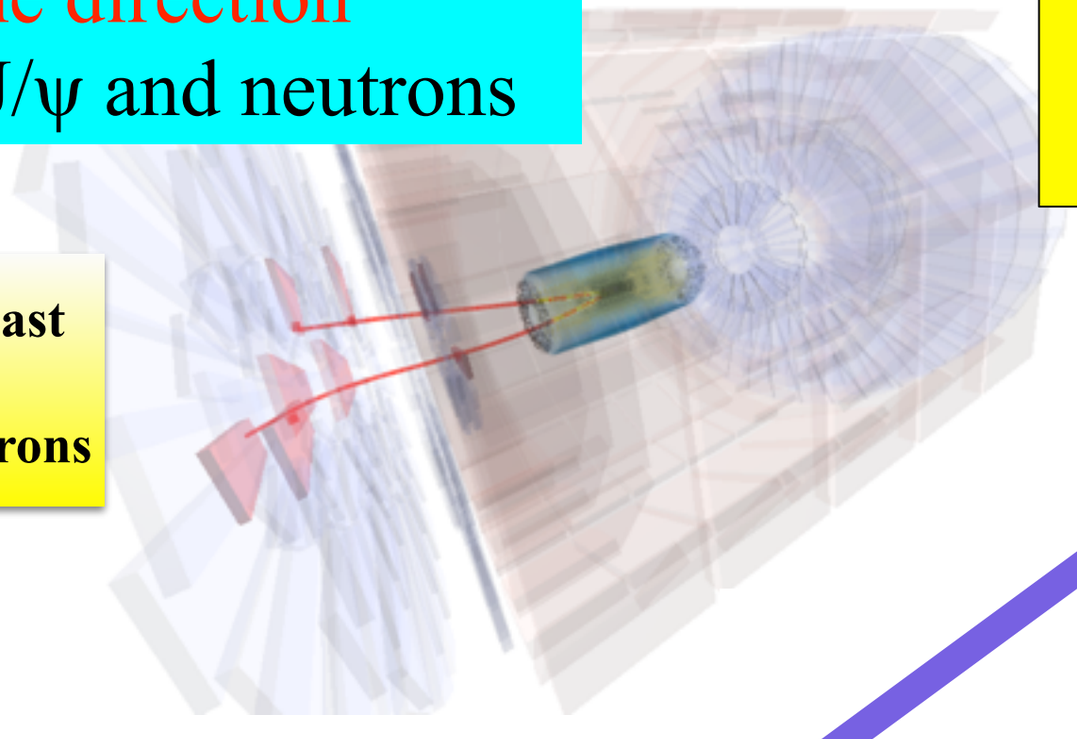
Low-x: **J/ψ and the emitted neutrons: opposite rapidity hemisphere**

Two different type of topologies

Same direction
for J/ψ and neutrons

No neutrons

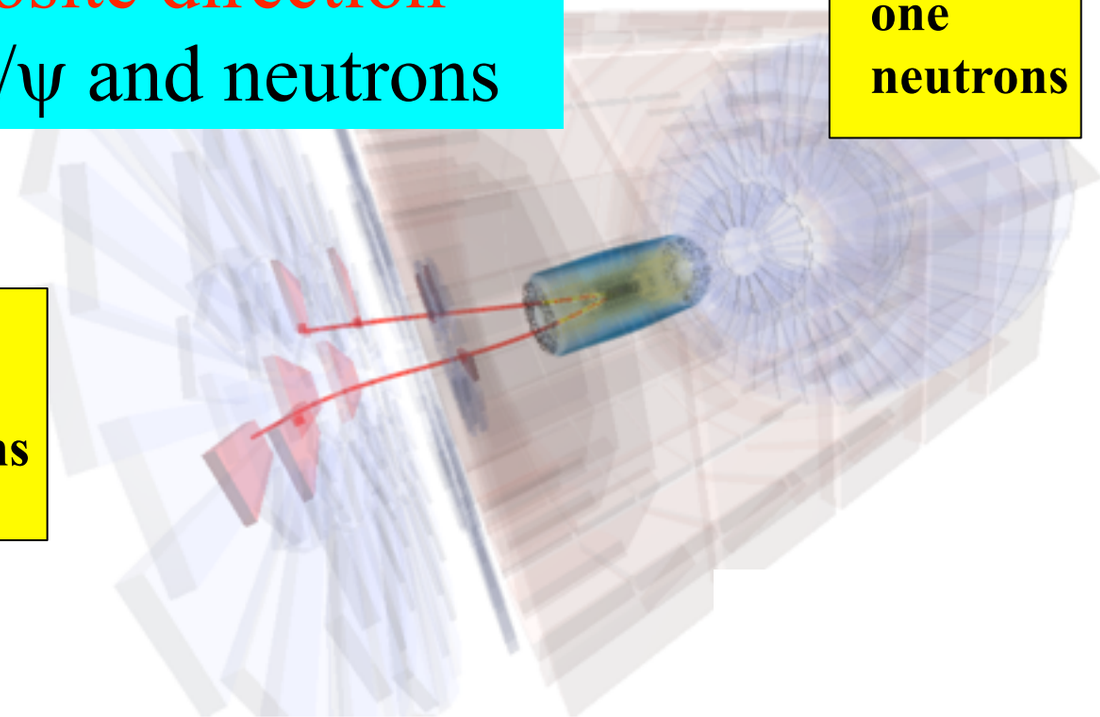
At least one neutrons



Opposite direction
for J/ψ and neutrons

At least one neutrons

No neutrons

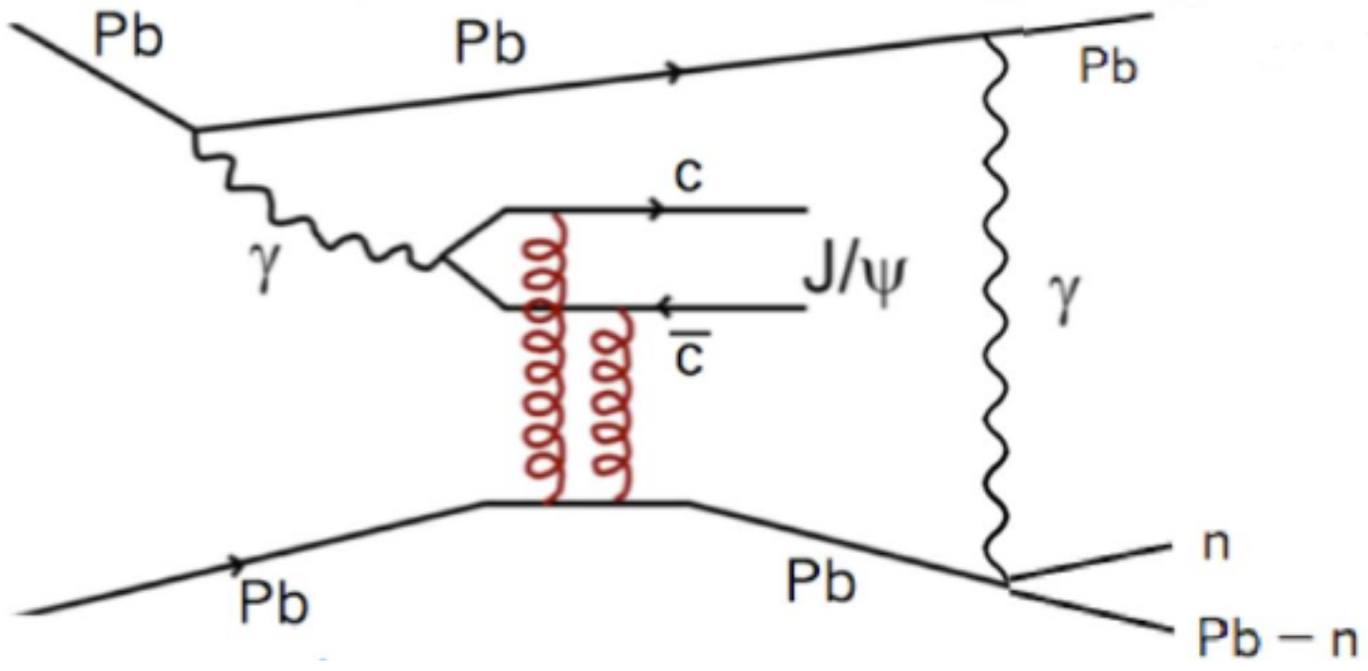


Incoherent photoproduction in UPC Pb-Pb

Total cross section

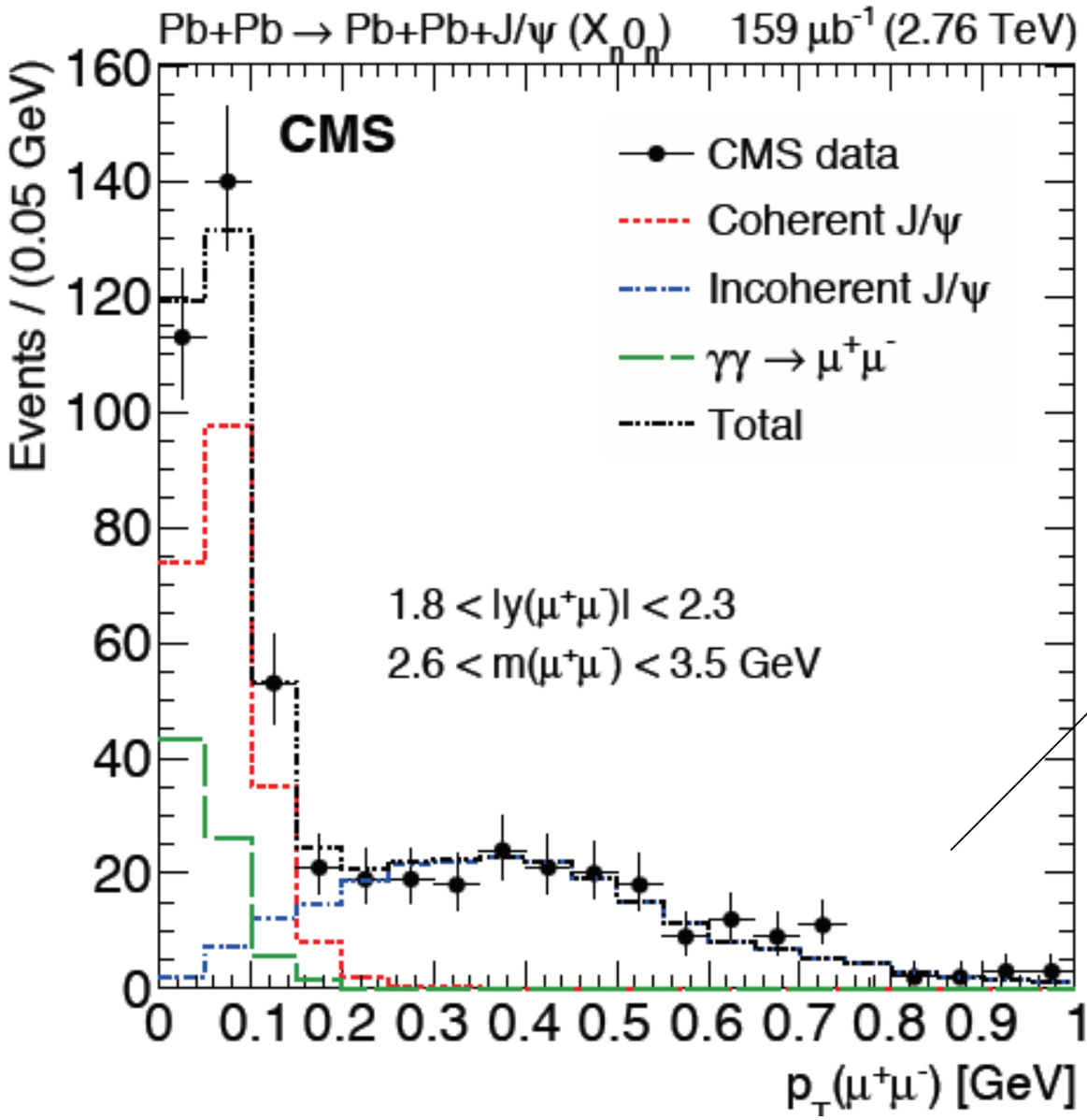
Low W: **x~ 10-2** **High W:** **x~ 10-4**

$$\frac{d\sigma_{\mathrm{PbPb}}(y)}{dy} = N_{\gamma/\mathrm{Pb}}(y, M)\sigma_{\gamma\mathrm{Pb}}(y) + N_{\gamma/\mathrm{Pb}}(-y, M)\sigma_{\gamma\mathrm{Pb}}(-y)$$



Incoherent production is expected to be more sensitive to the photon direction (energy dependence). Here 0nXn and Xn0n will unfold the two x-values

Energy dependence of Incoherent J/ψ



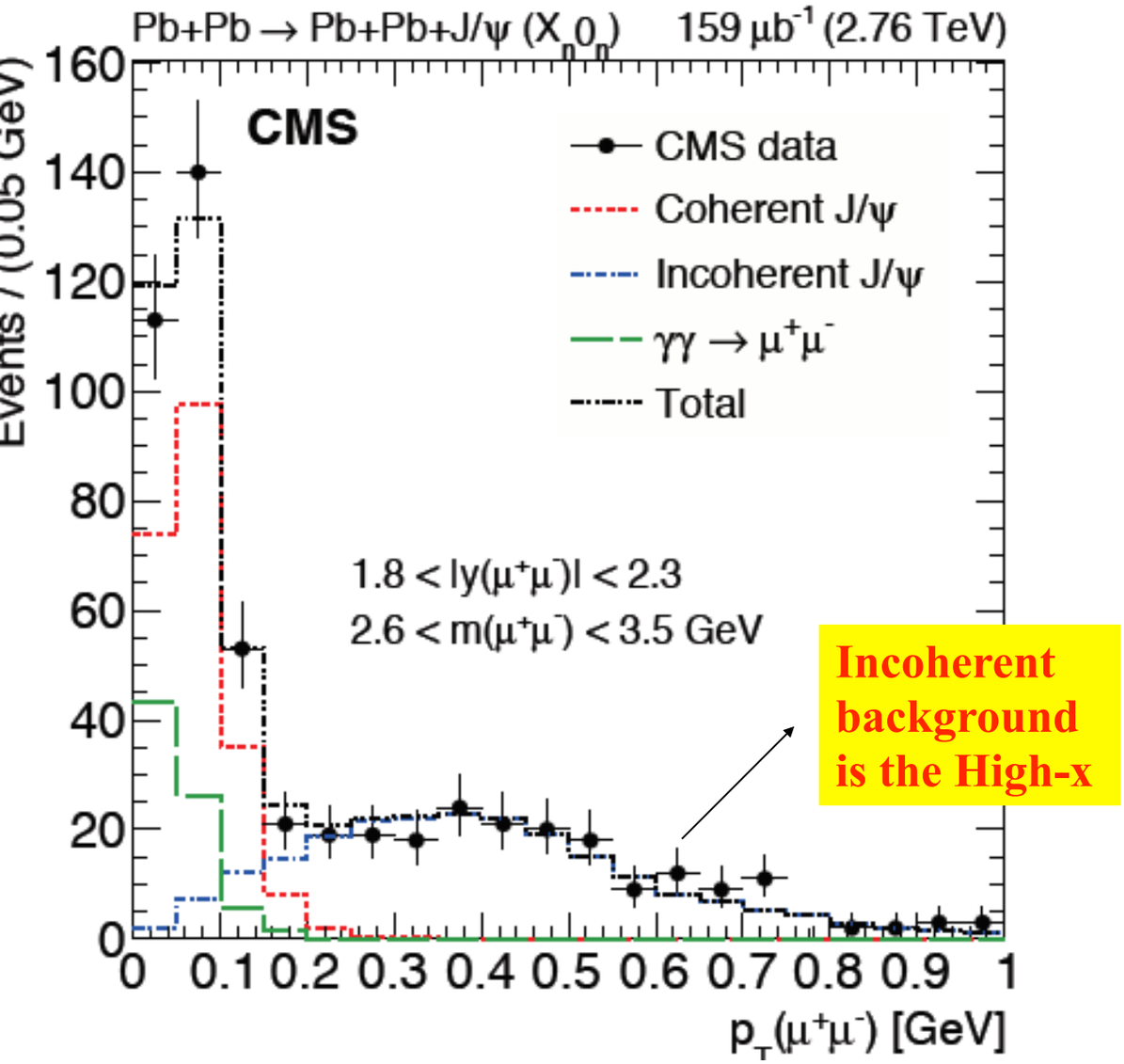
Incoherent background is the High-x region

Incoherent J/ψ background (Xn0n): ***Events are in the High-x region.***

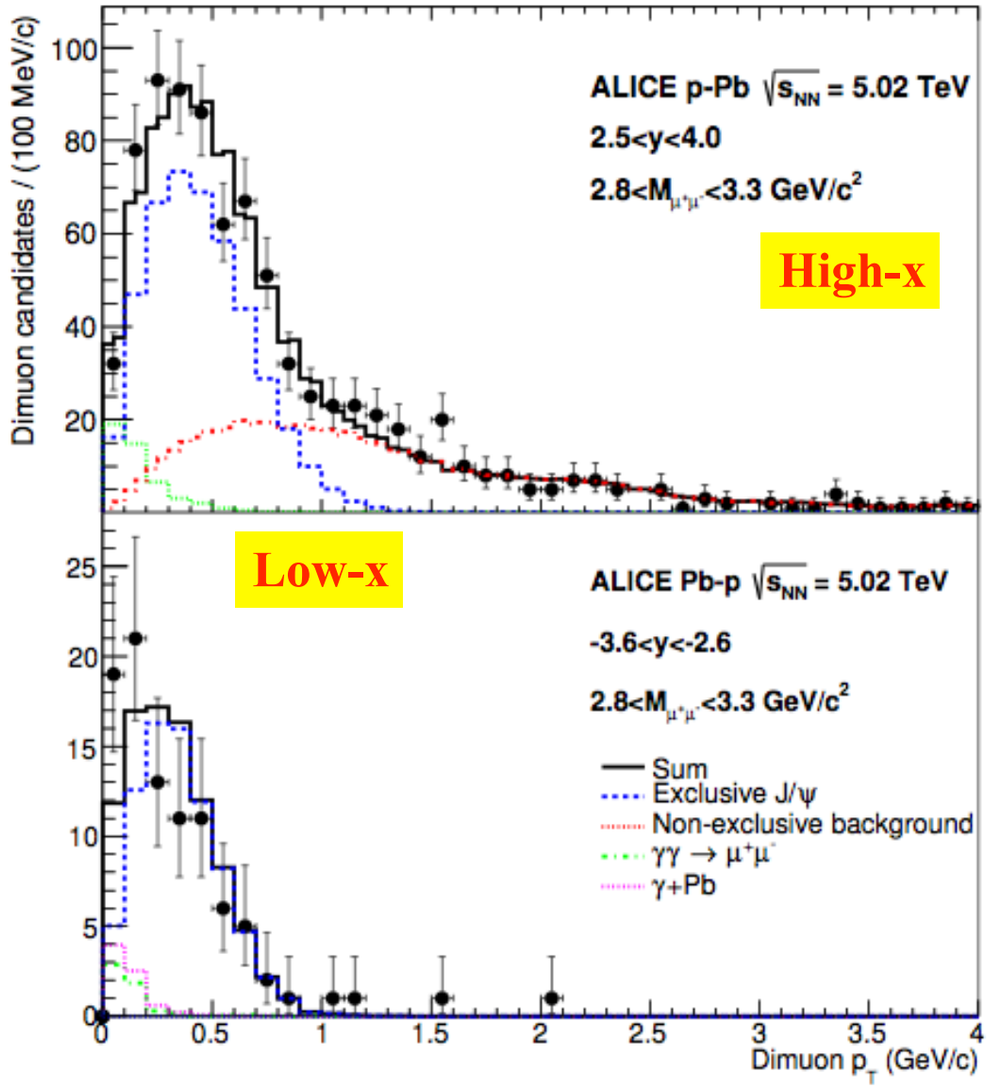
At Low-x, incoherent production is very strongly suppressed wrt to High-x region - First time seen in γ+Pb interactions

Energy dependence of Incoherent J/ψ

γ+Pb interactions



γ+p interactions

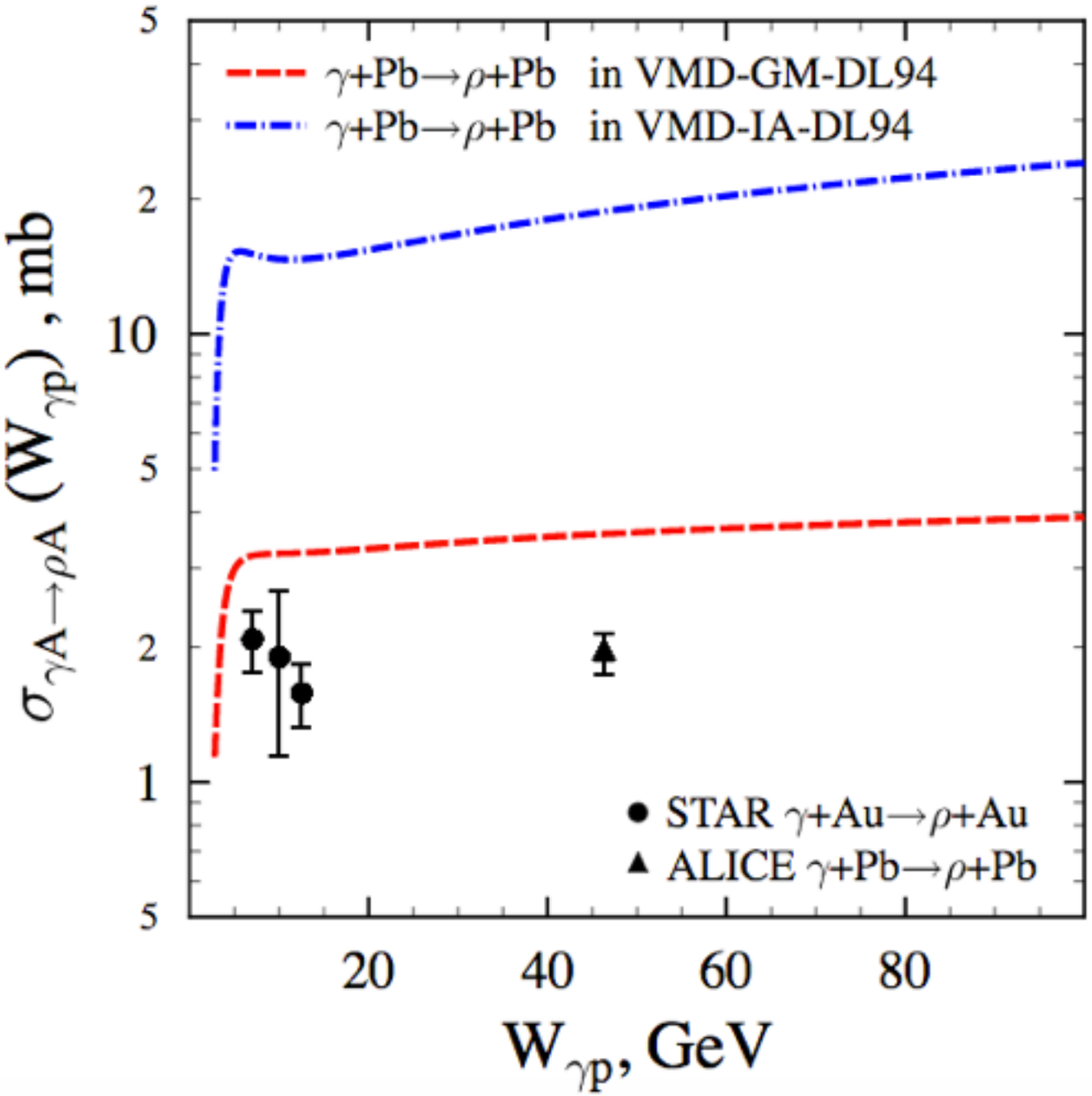


Incoherent J/ψ background (Xn0n): ***Events are in the High-x region. At Low-x incoherent background is heavy suppressed***

In qualitative agreement with ALICE Collaboration. Phys. Rev. Lett. 113 (2014) 23, 232504 (see also J. Cepina et al. Phys. Lett. B766 (2017) 186-191)

Coherent Rho0

ALICE
JHEP 1509 (2015) 095



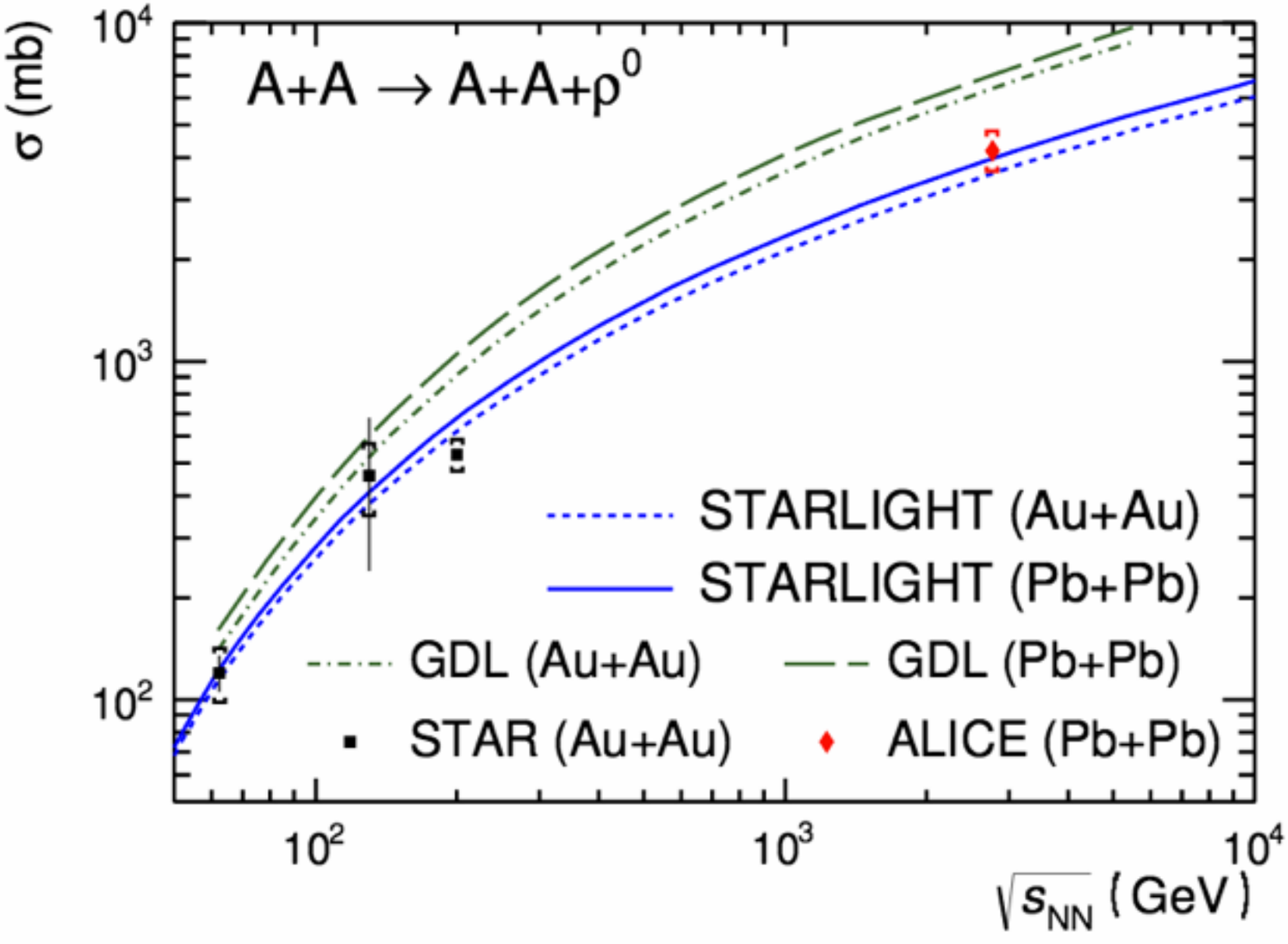
L. Frankfurt et al.
Phys.Lett. B752 (2016) 51-58

Both ALICE and STAR find measured cross section ~40% lower than predicted by Glauber, ….although works fine at fixed-target experiments

Nuclei does not behave like individual nucleons?

Coherent Rho0

JHEP 1509 (2015) 095

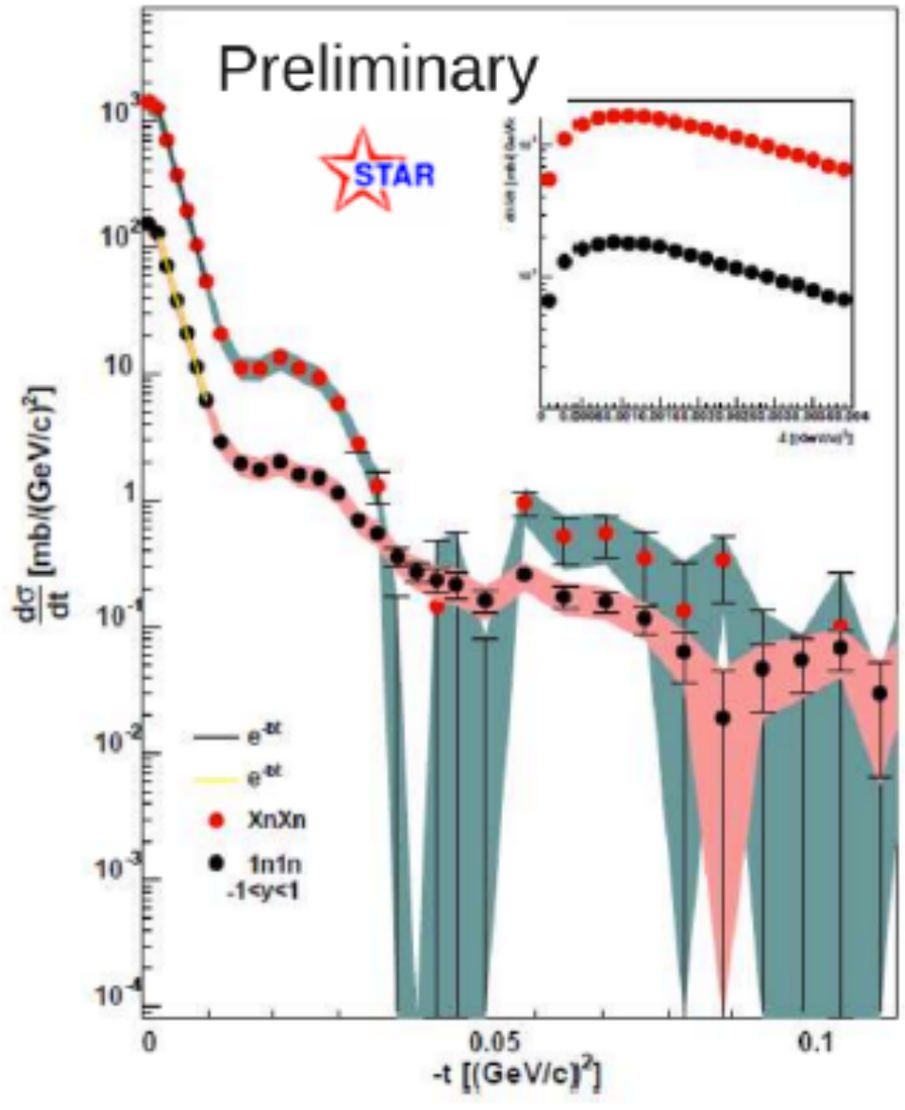


Both ALICE and STAR find measured cross section ~40% lower than predicted by Quantum Glauber, ….although works fine at fixed-target experiments

Nuclei does not behave like individual nucleons?

Coherent ρ^0 cross section

- Characteristic diffraction dips visible, positions:
  - 1^{st} : $-t = 0.018 \pm 0.005$ GeV^{-2}
  - 2^{nd} : $-t = 0.043 \pm 0.01$ GeV^{-2}
- Expected when approaching black disk limit
- Partially washed out due to photon p_T distribution and detector resolution
- Consistent with Normalized nuclear form factor, mVMD-GGM lower by $\sim 1\sigma$
- Interference between the two production nuclei makes downturn at $|t| < 10^{-3}$ GeV^2

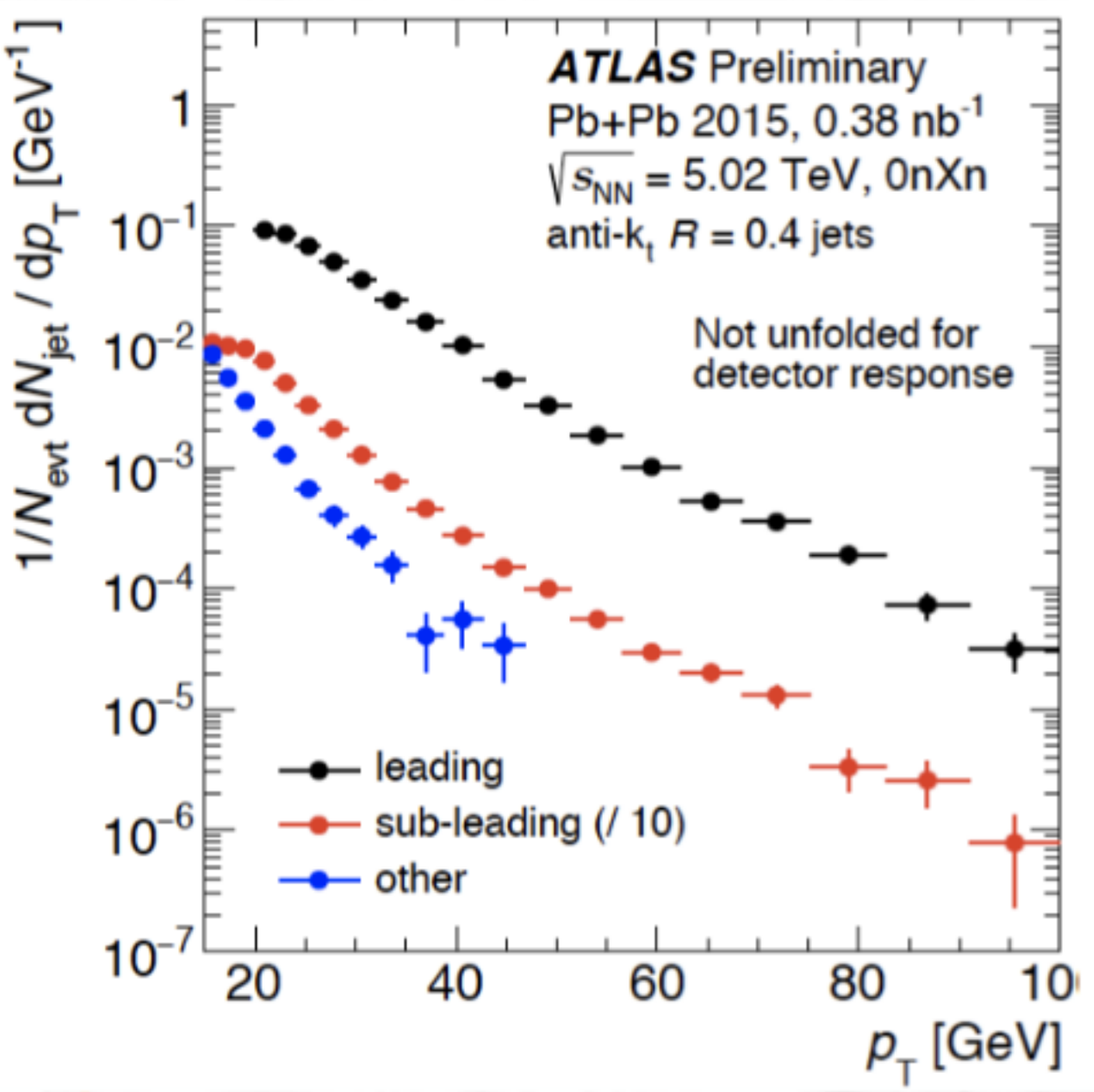


Norm nucl form factor: Atom. Data Nucl. Data Tabl. 36, 495 (1987), mVMD-GGM: Phys. Lett. B 752, 51 (2016), calculations: arXiv:1611.05471

INT workshop

Jets

From
Aaron Angerami's
talk



Measurement Coverage

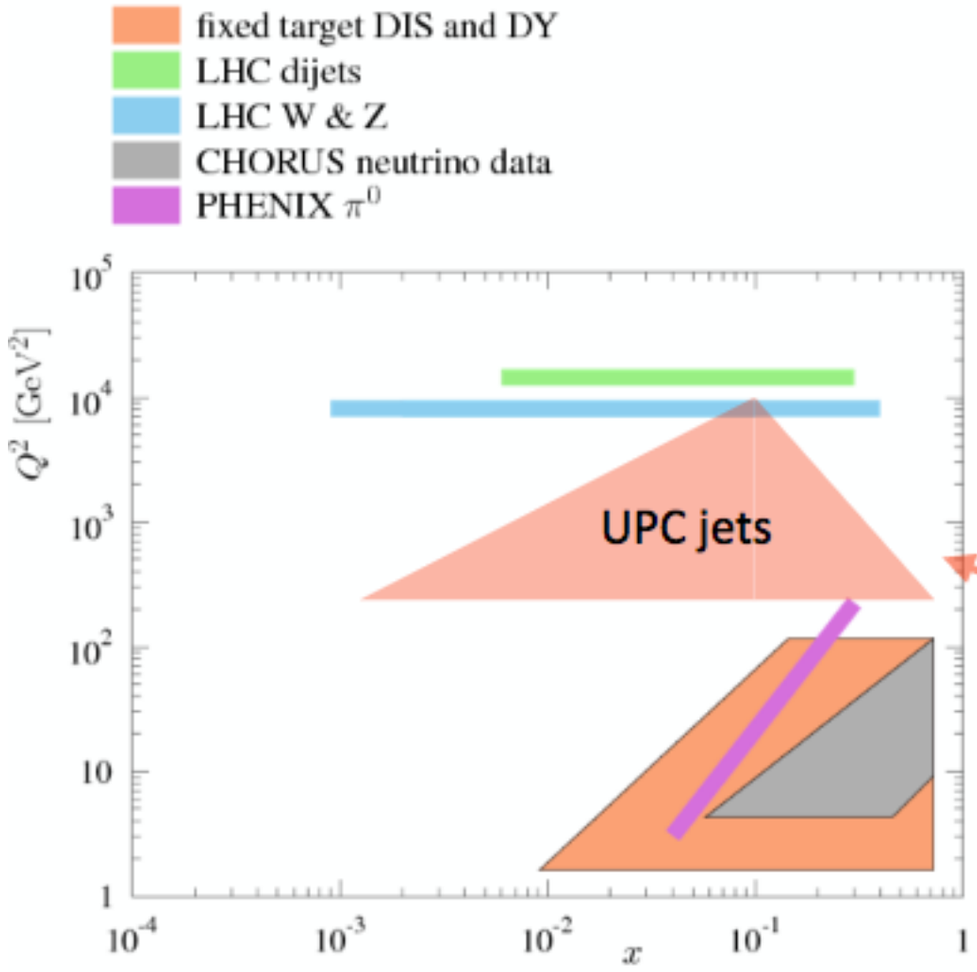
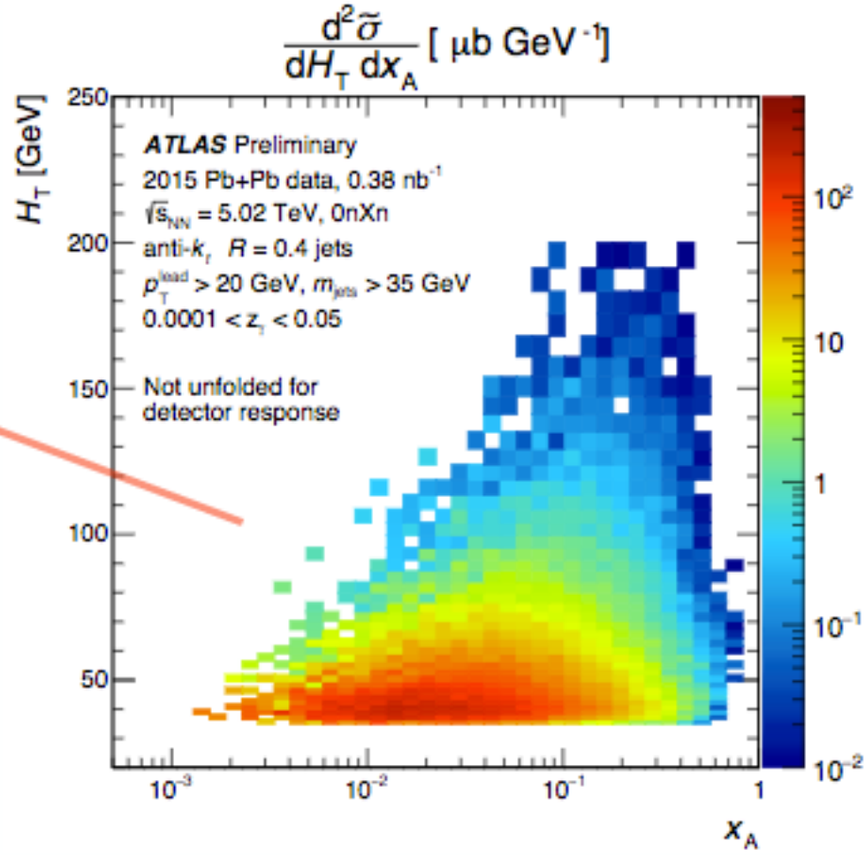


Figure adapted from EPPS16
1612.05741 [hep-ph]

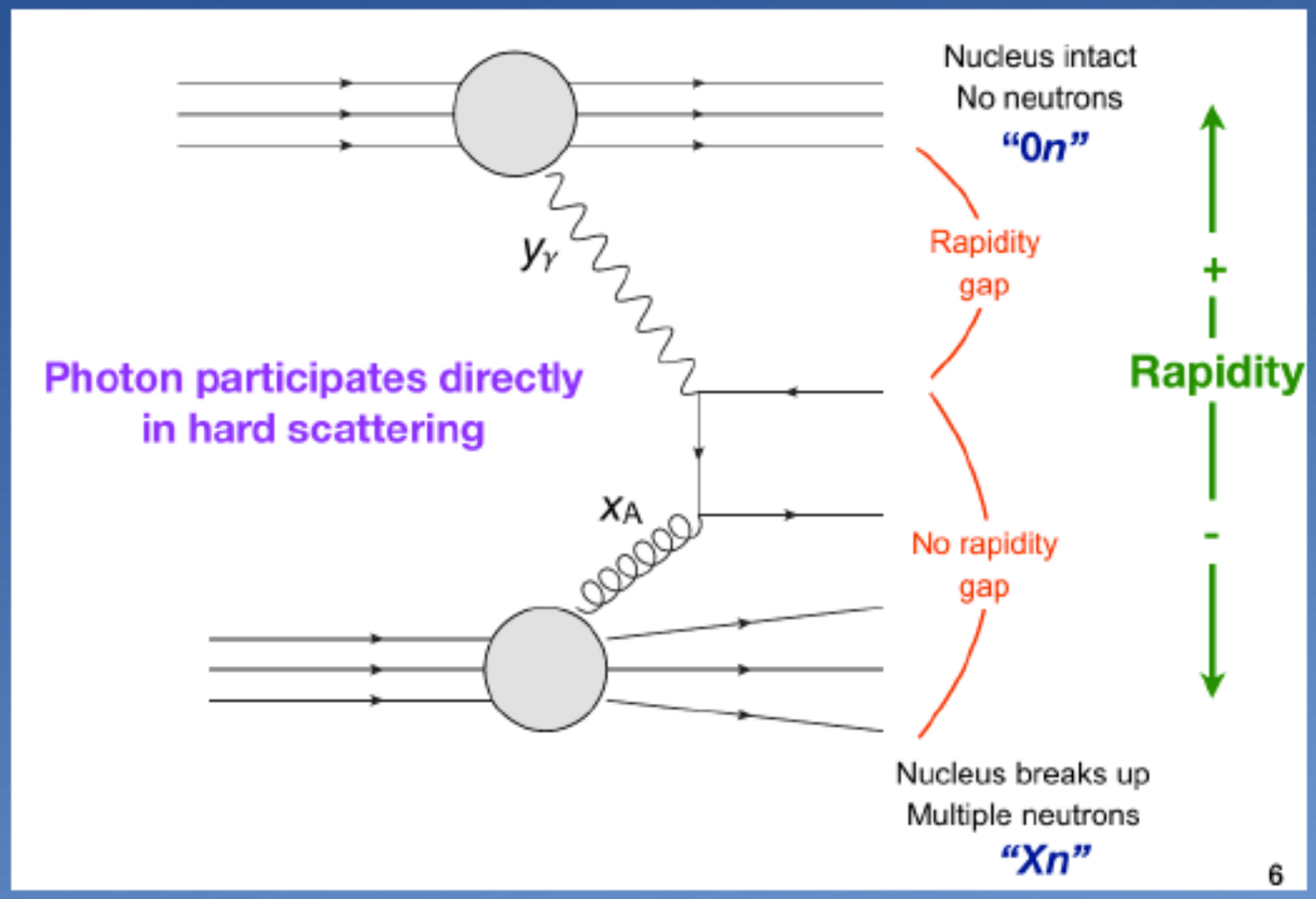


- **ATLAS-CONF-2017-011**

Cross section depends linearly on nuclear PDFs.

Photonuclear jet-production at the LHC

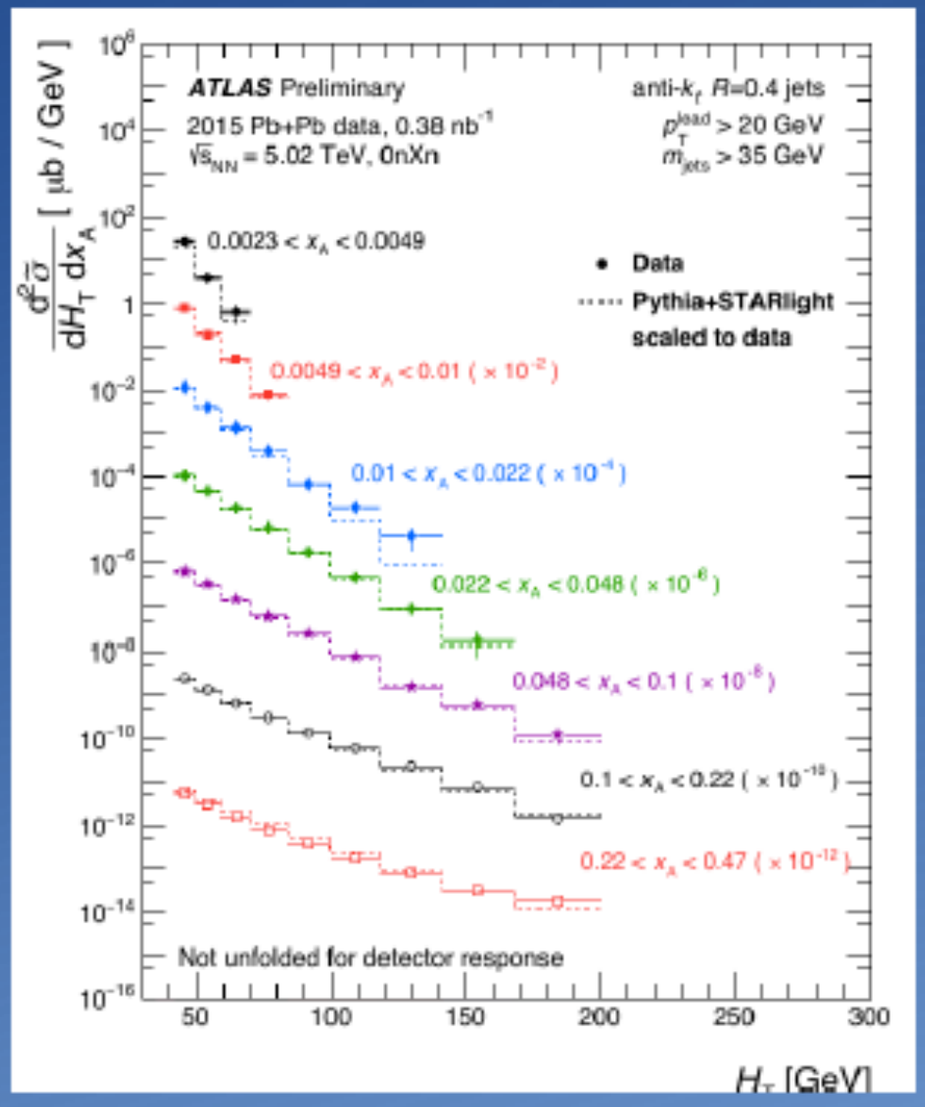
One rapidity gap between photon emitting nucleus and "target" nucleus.



A. Angerami, Quark Matter 2017.

Cross section depends linearly on nuclear PDFs.

Photonuclear jet-production at the LHC



A. Angerami, Atlas Collaboration, Quark Matter 2017.

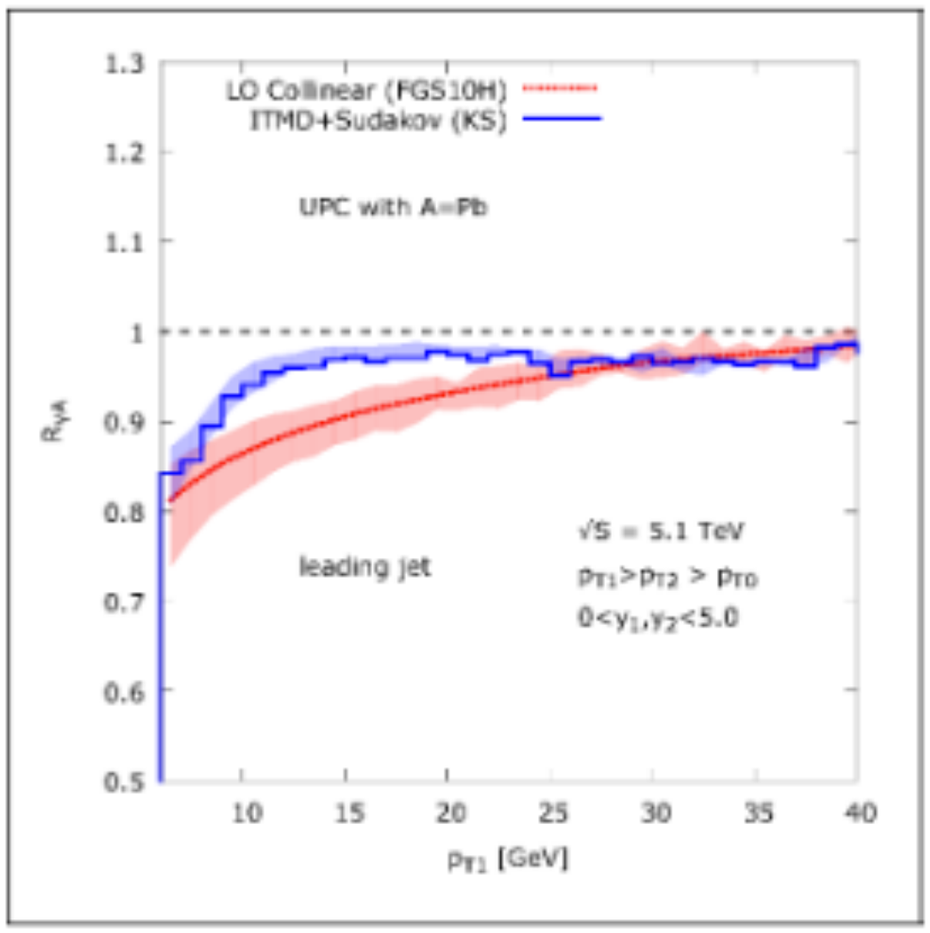
Rather good agreement with Pythia, if photon spectrum is adjusted to that of STARLIGHT (photon spectrum in Pythia is for a lepton beam).

Results for dijets in UPC

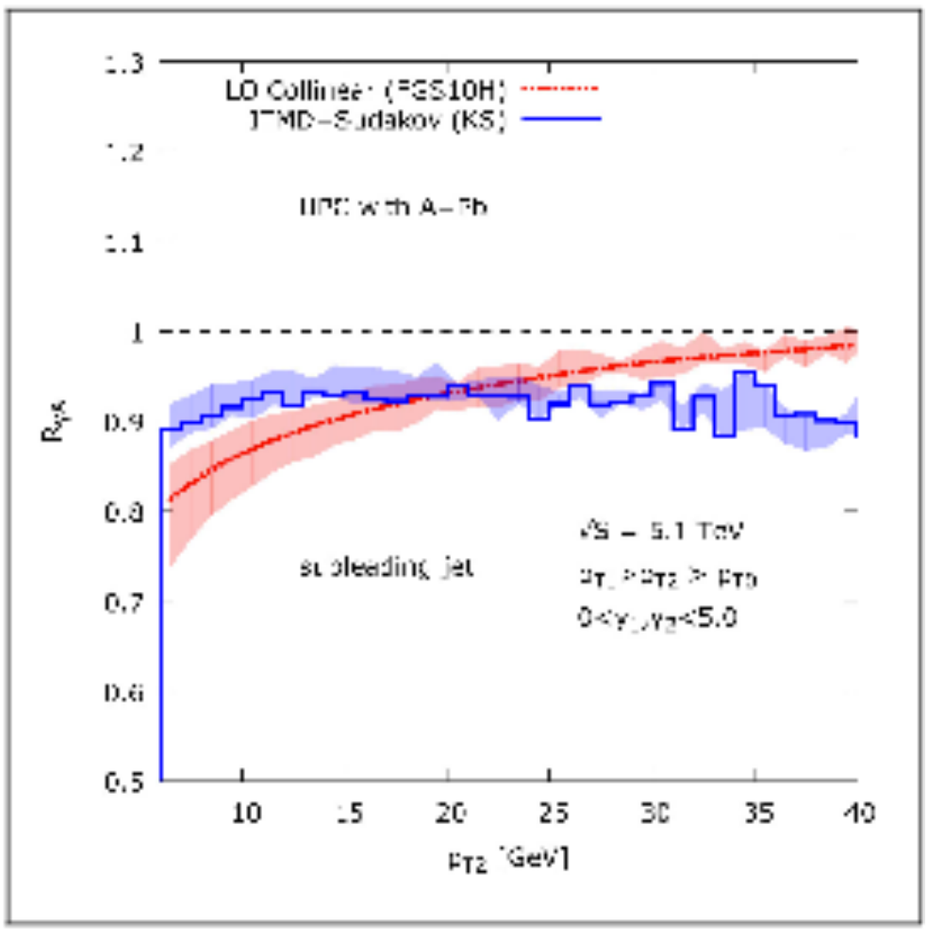
P. Kotko, A. Stasto, M. Strikman

Nuclear modification factor R_{yA}

leading jet p_T

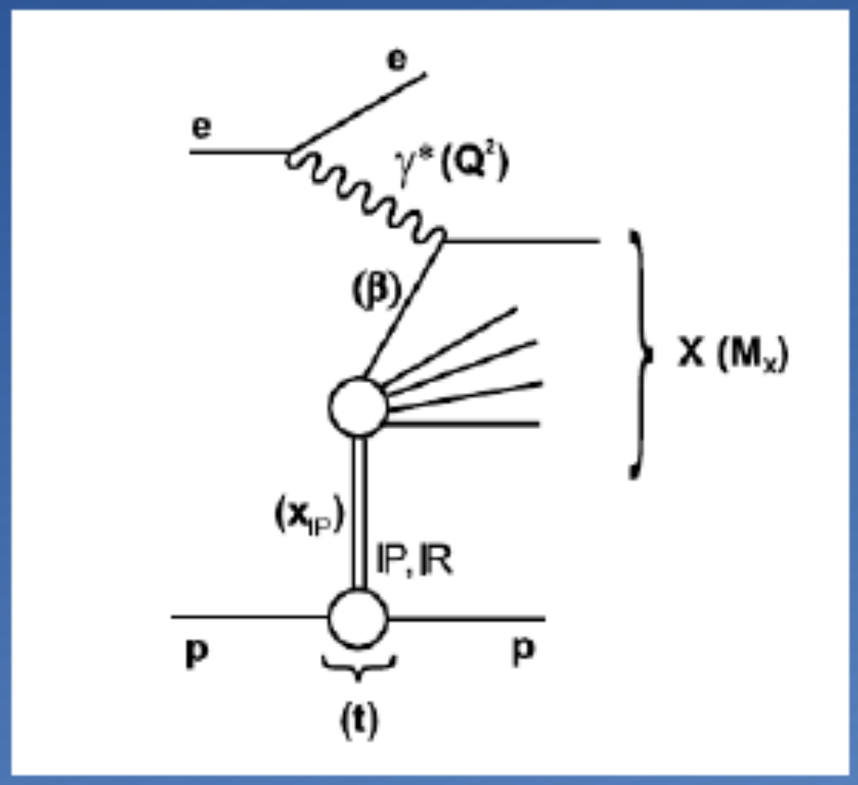


subleading jet p_T



Photonuclear jet-production at the LHC

Photonuclear jets can also be studied in “diffractive” events.



Rapidity gap between both nuclei and the produced state.

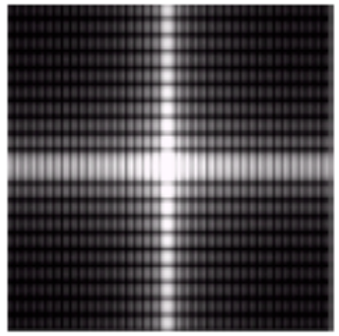
- Has been studied at HERA with proton target.
- Nothing done with nuclear targets.

Diffractive dijets in DIS and UPC

Diffractive VM production, especially t - dependence, can provide with the valuable information about the spatial distribution of the target.

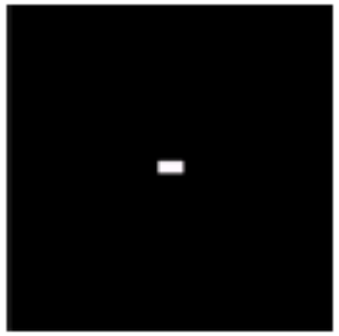
It is similar to image processing:

Fourier image

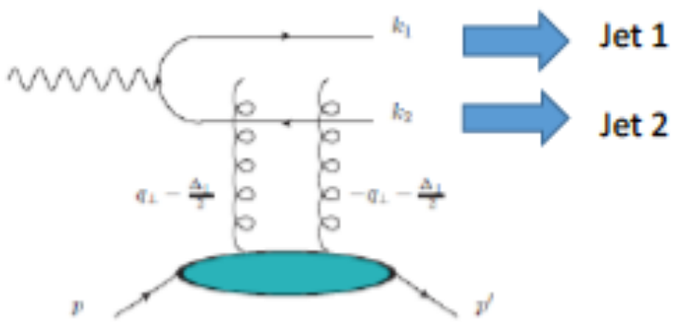


inverse 2-dim FT transform

Real space



Yoshitaka Hatta



Jet 1

Jet 2

$$\vec{\Delta}_\perp = -(\vec{k}_{1\perp} + \vec{k}_{2\perp})$$

Proton recoil momentum

$$\vec{P}_\perp = \frac{1}{2}(\vec{k}_{2\perp} - \vec{k}_{1\perp})$$

Dijet relative momentum

Diffractive dijets provide access to Wigner distribution or Generalized Transverse Momentum Distribution

$$W(x, \vec{k}, \vec{\Delta})$$

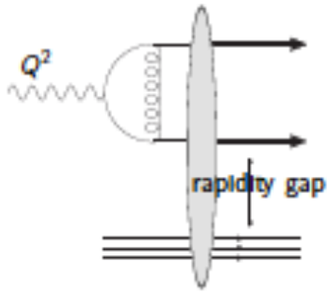
WG2: Low x and Diffraction

Diffractive dijets: higher order calculations

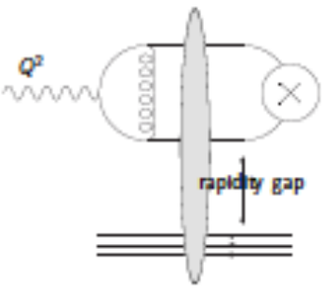
Higher order corrections to diffractive dijets

Renaud Boussarie

Diffractive dijet in CGC formalism at NLO



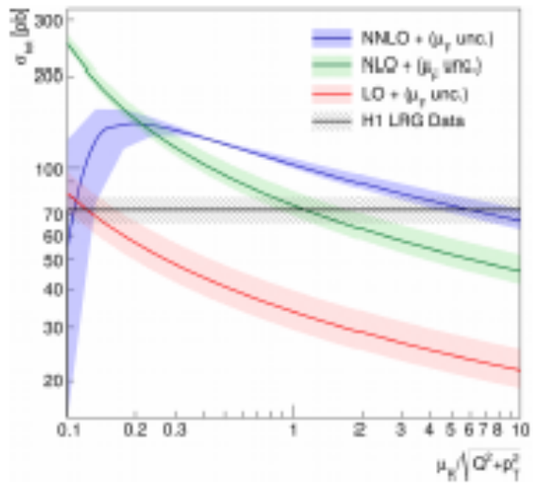
Diffractive VM production in CGC formalism at NLO



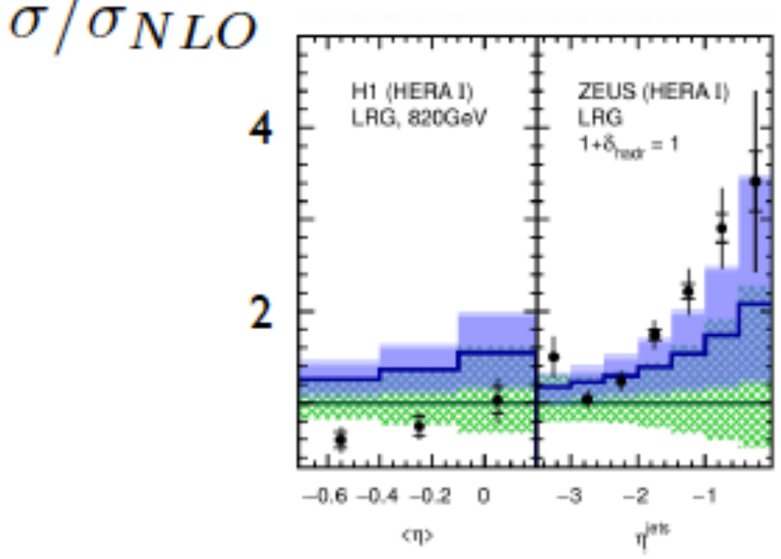
Radek Zlebcik

First study of diffractive dijets in collinear formalism at NNLO!

Renormalization scale dependence



Reduction of the renormalization (and factorization) scale dependence at NNLO

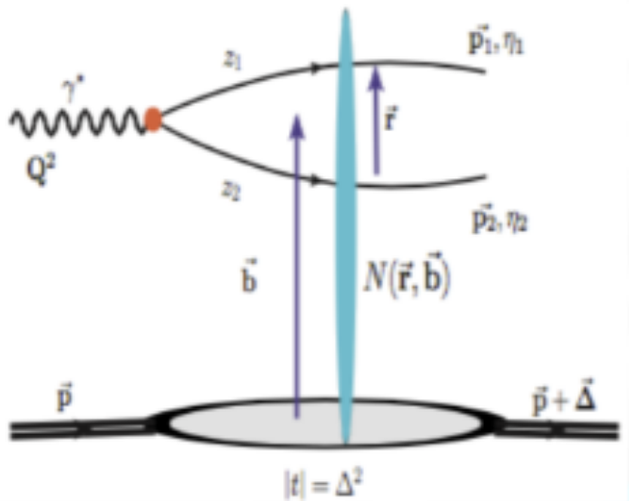


Higher order corrections are large: NNLO substantially higher than NLO for some distributions.
Need more detailed study, NNLO DPDFs?

WG2: Low x and Diffraction

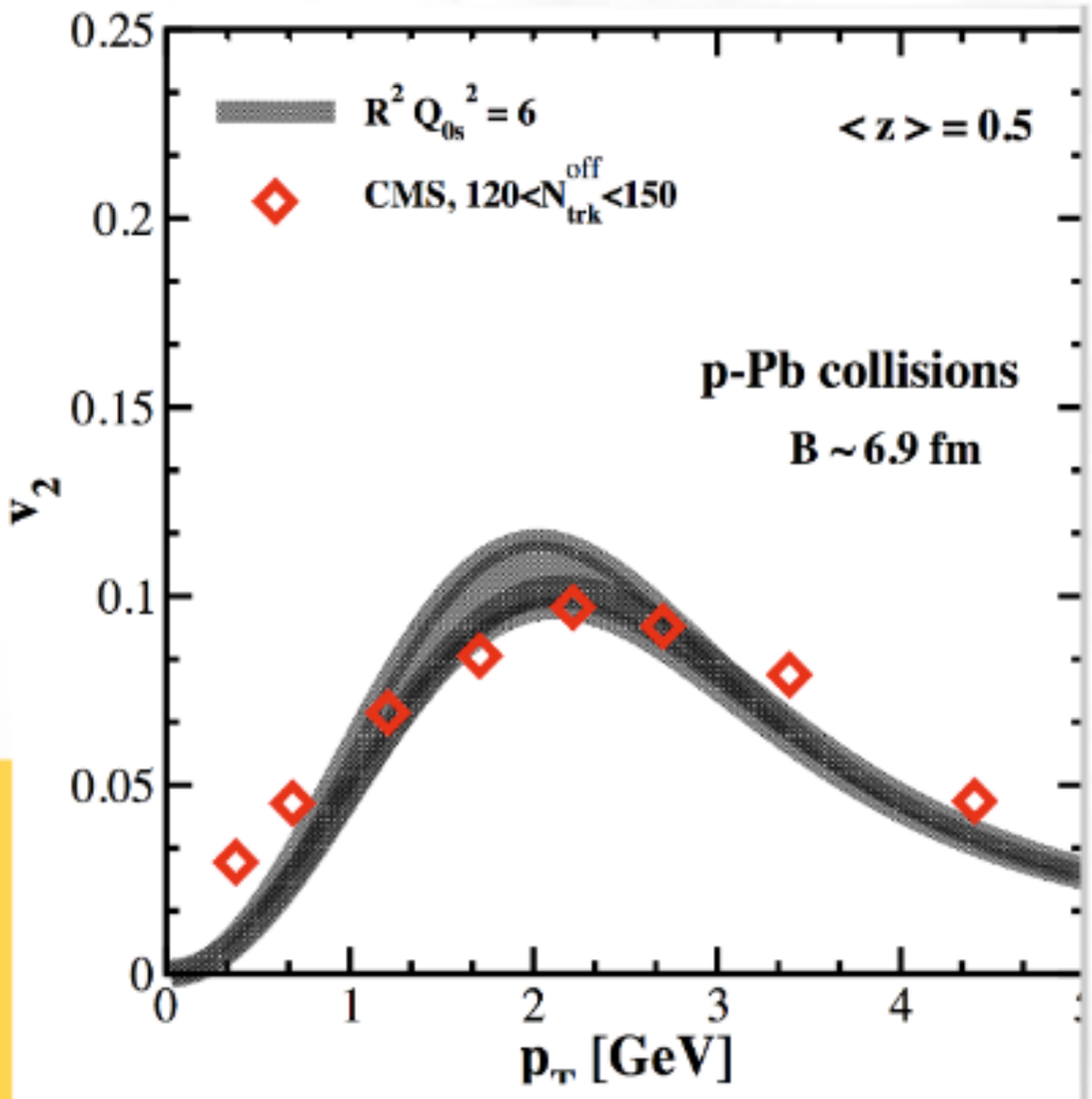
13

Motivation:
Test gluon saturation model

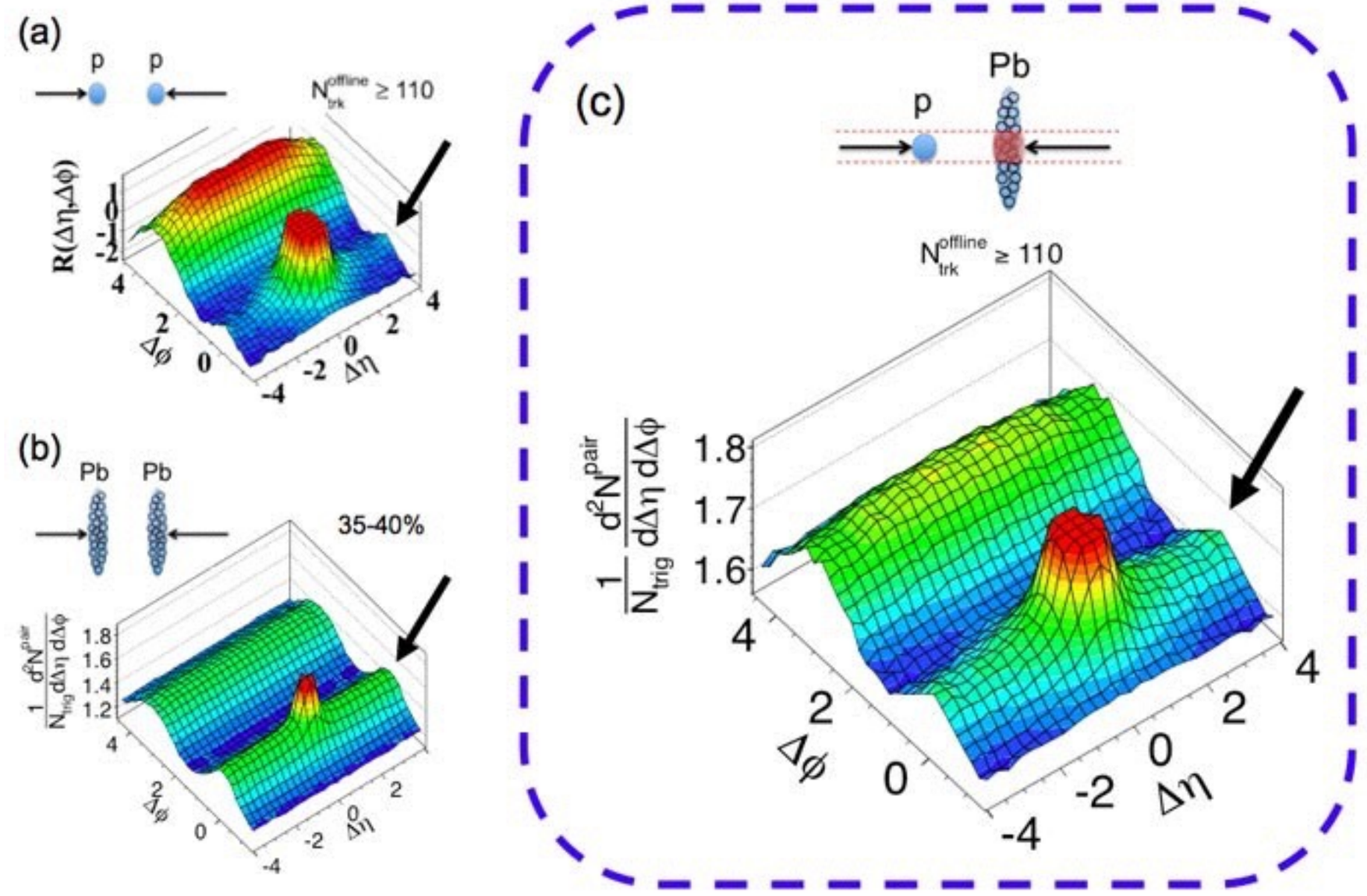


From Amir Rezaeian's talk

Since jet is color neutral, jet production dominated by q-qbar pairs of smaller transverse size with increasing saturation

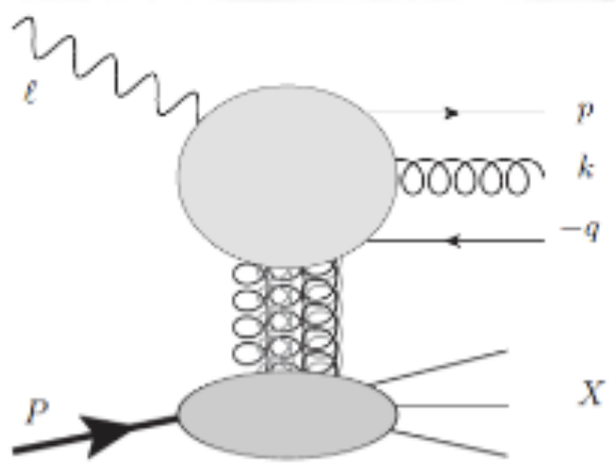


21



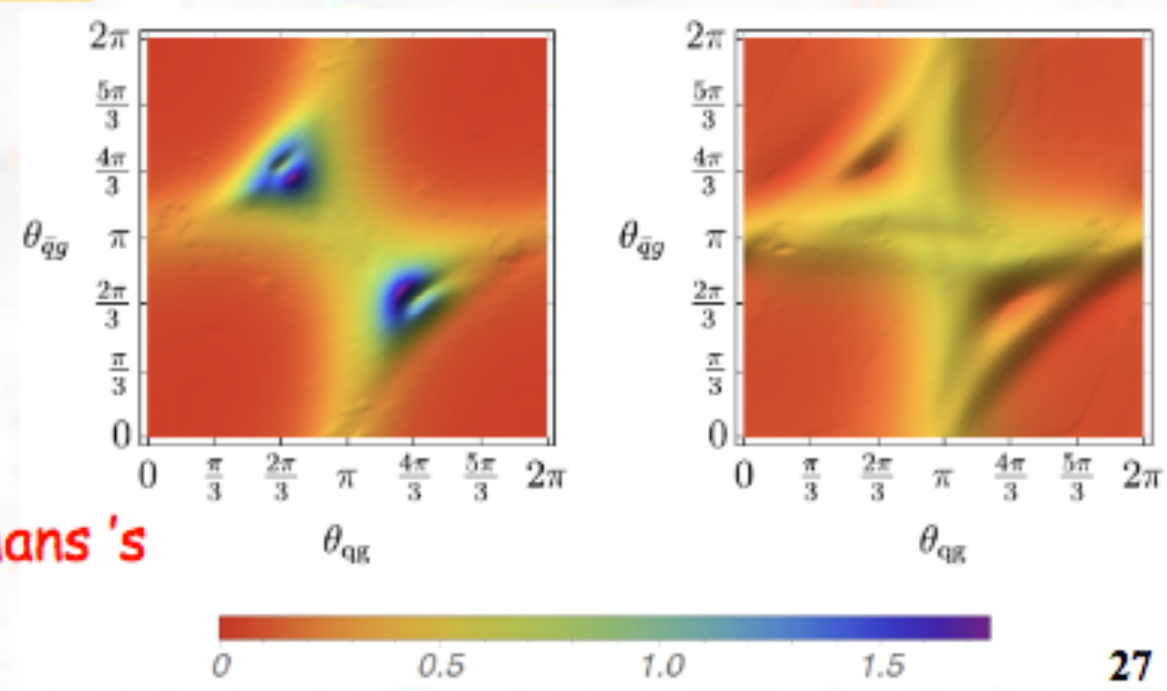
2-particle correlations in UPC collisions?

Polarization in UPCs and EIC



Motivation: use azimuthal angular correlations of 3 partons in inclusive DIS to explore the dynamics of saturated partonic matter

Azimuthal correlations between 3 partons in DIS

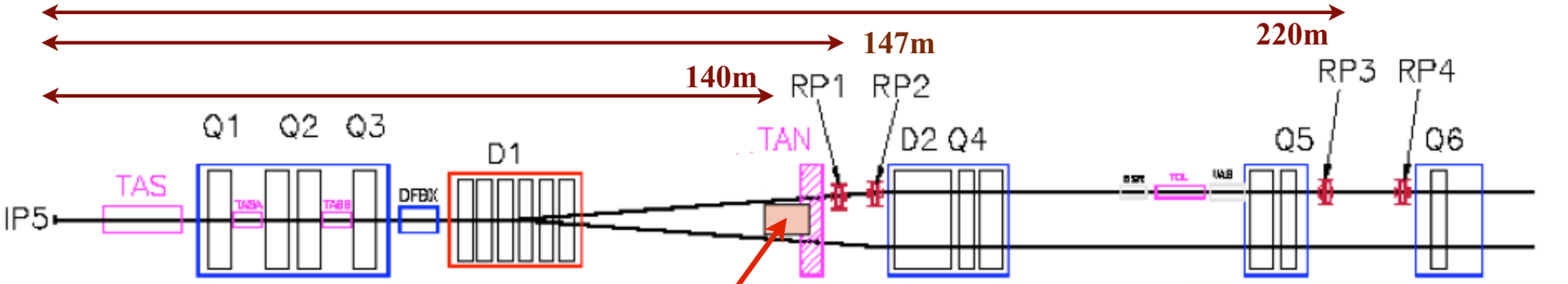


From Maria Elena Tejeda-Yeomans 's talk

27

One more thing …

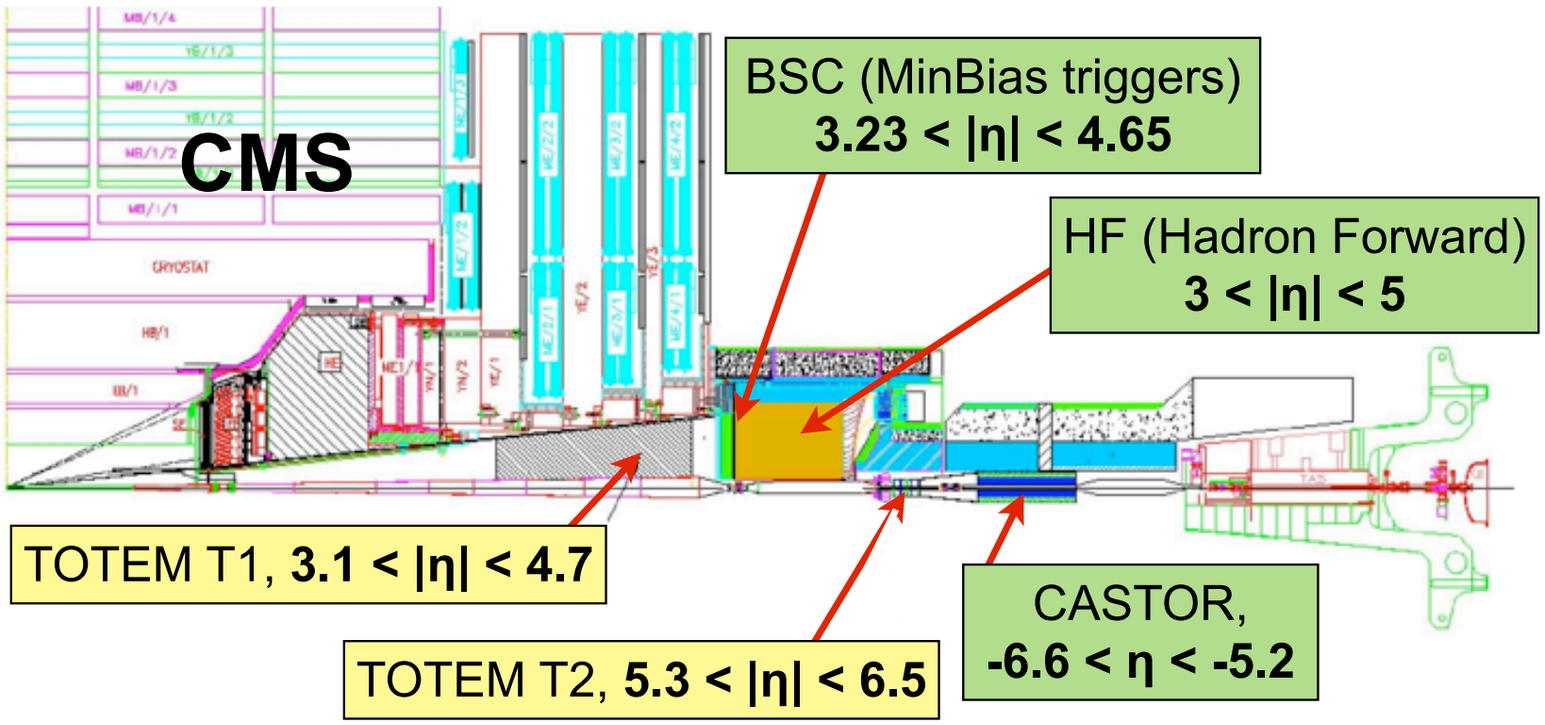
Forward detectors at CMS



Forward Shower Counters
6 < |η| < 8

Zero Degree Calorimeter
|η| > 8.1

TOTEM Roman Pots
±147m, ±220m



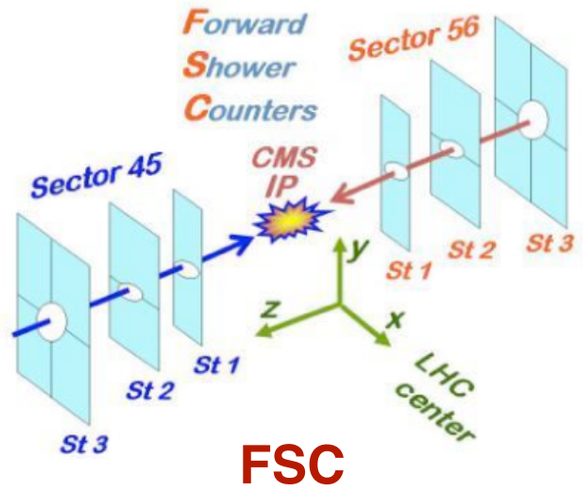
BSC (MinBias triggers)
3.23 < |η| < 4.65

HF (Hadron Forward)
3 < |η| < 5

TOTEM T1, **3.1 < |η| < 4.7**

TOTEM T2, **5.3 < |η| < 6.5**

CASTOR,
-6.6 < η < -5.2

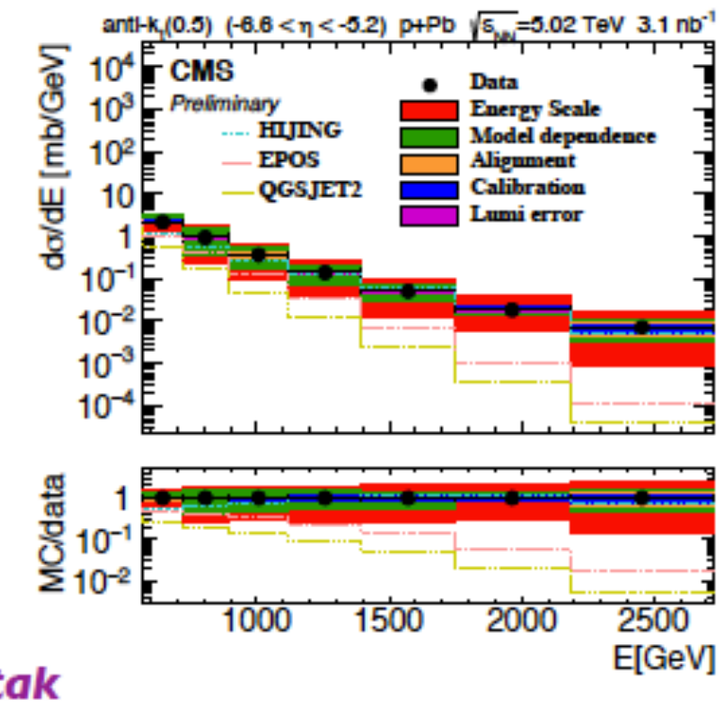


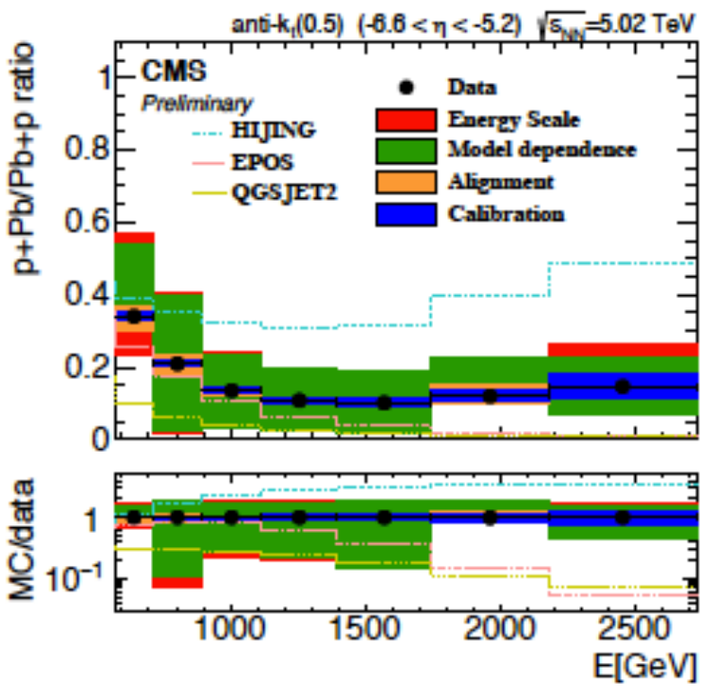
FSC

From DIS 2017 —sensitive to saturation …Not UPCs but possible to use CASTOR in UPC studies in the future

Very forward jets in p+Pb and Pb+p with CASTOR

Merijn van de Klundert
CMS

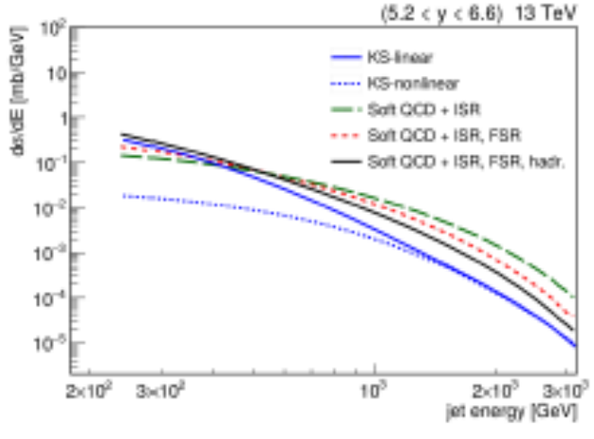




Krzysztof Kutak

Calculation of very forward inclusive jet in pp using formalism
of hybrid factorization for CASTOR kinematics.
Comparison of calculations with and without the gluon saturation.
Strong suppression expected at low transverse momenta even in the proton - proton case.

Very strong suppression of the p+Pb/Pb+p ratio
Caveat: compromised by boost of center of mass frame



WG2: Low x and Diffraction

14

White paper

- Following the INT workshop, a White Paper on photon-nucleus/proton will be prepared

Coordinated by DTT and in preparation…

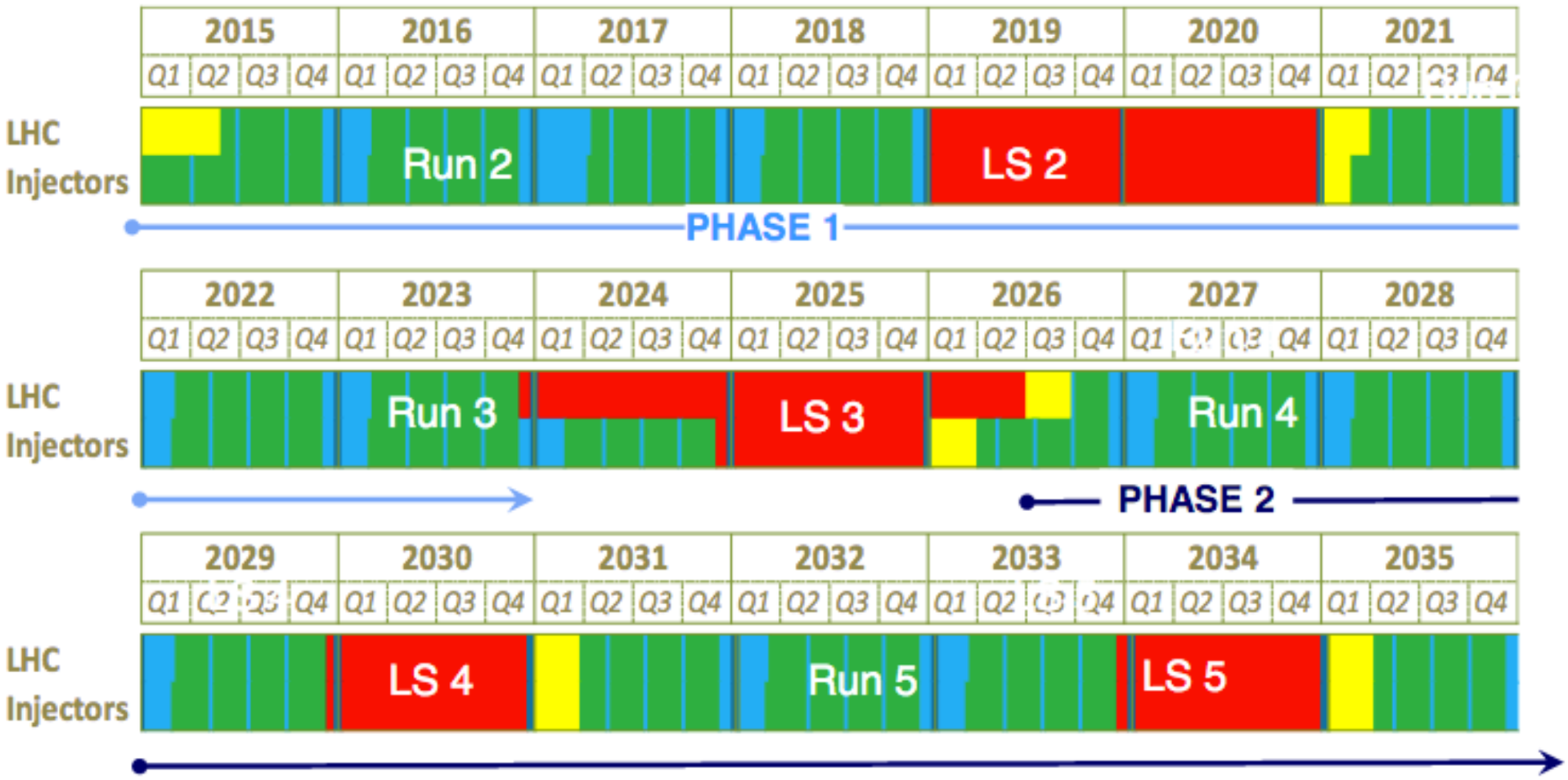
LHC schedule

CERN Yellow Report: *CERN-PH-LPCC-2015-001*

LHC roadmap: according to MTP 2016-2020 V1

LS2 starting in 2019 => 24 months + 3 months BC
LS3 LHC: starting in 2024 => 30 months + 3 months BC
Injectors: in 2025 => 13 months + 3 months BC





Summary and outlook

- **Studying QCD with high energy photon-photon, photon-proton and photon-nuclear interactions at the LHC**
  - **Searching for saturation effects in the proton**
  - **Nuclear effects at both low and high Bjorken-x**

- **So far, most analyses have been carried out for exclusive VM photoproduction but new studies possible for other final states (dijets, double VM, diphoton, etc)**

- **Inclusive photo-nuclear and photon-proton reactions also possible**

Summary and outlook

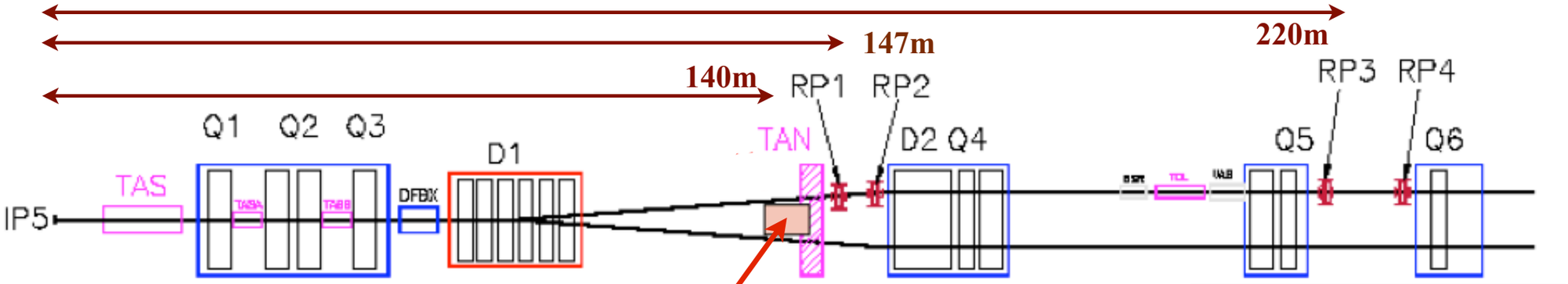
- **UPC studies at RHIC/LHC, some new energy regime. Despite the limitations in terms of statistics and precision, there are lots of synergies with the EIC program**

- **New saturation studies ongoing**

- **Community building around these topics from both the theory and experimental side**

Additional slides

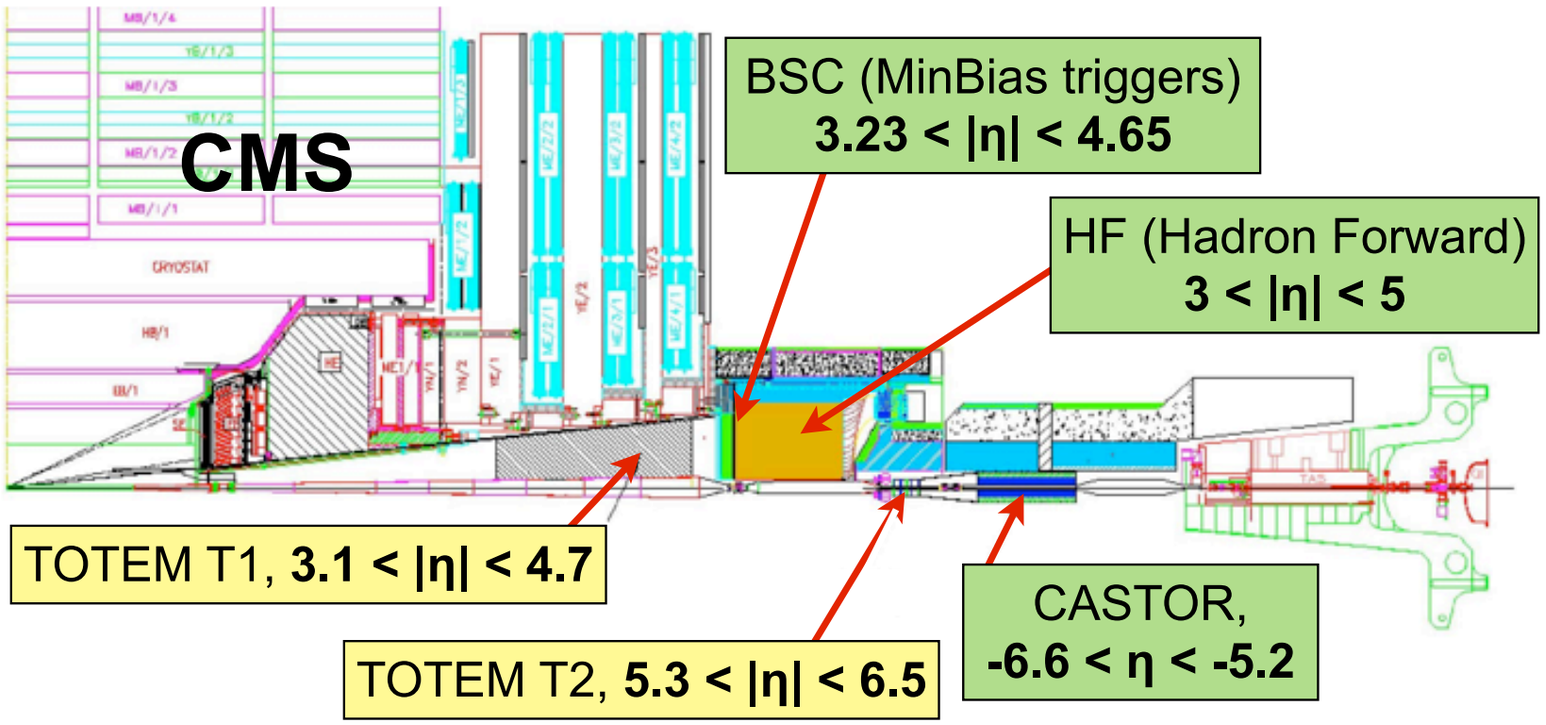
Forward detectors at CMS



Forward Shower Counters
6 < |η| < 8

Zero Degree Calorimeter
|η| > 8.1

TOTEM Roman Pots
±147m, ±220m



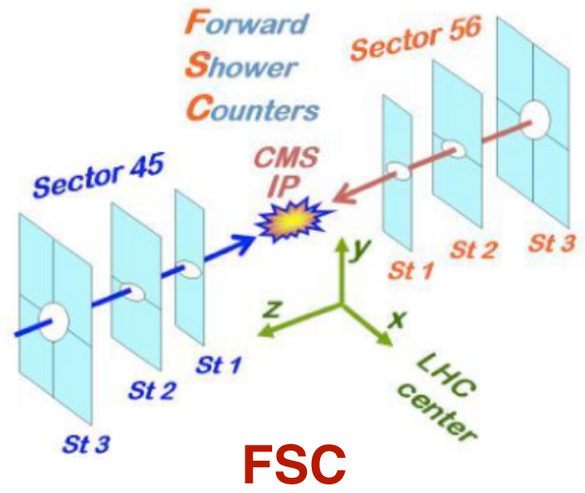
BSC (MinBias triggers)
3.23 < |η| < 4.65

HF (Hadron Forward)
3 < |η| < 5

TOTEM T1, **3.1 < |η| < 4.7**

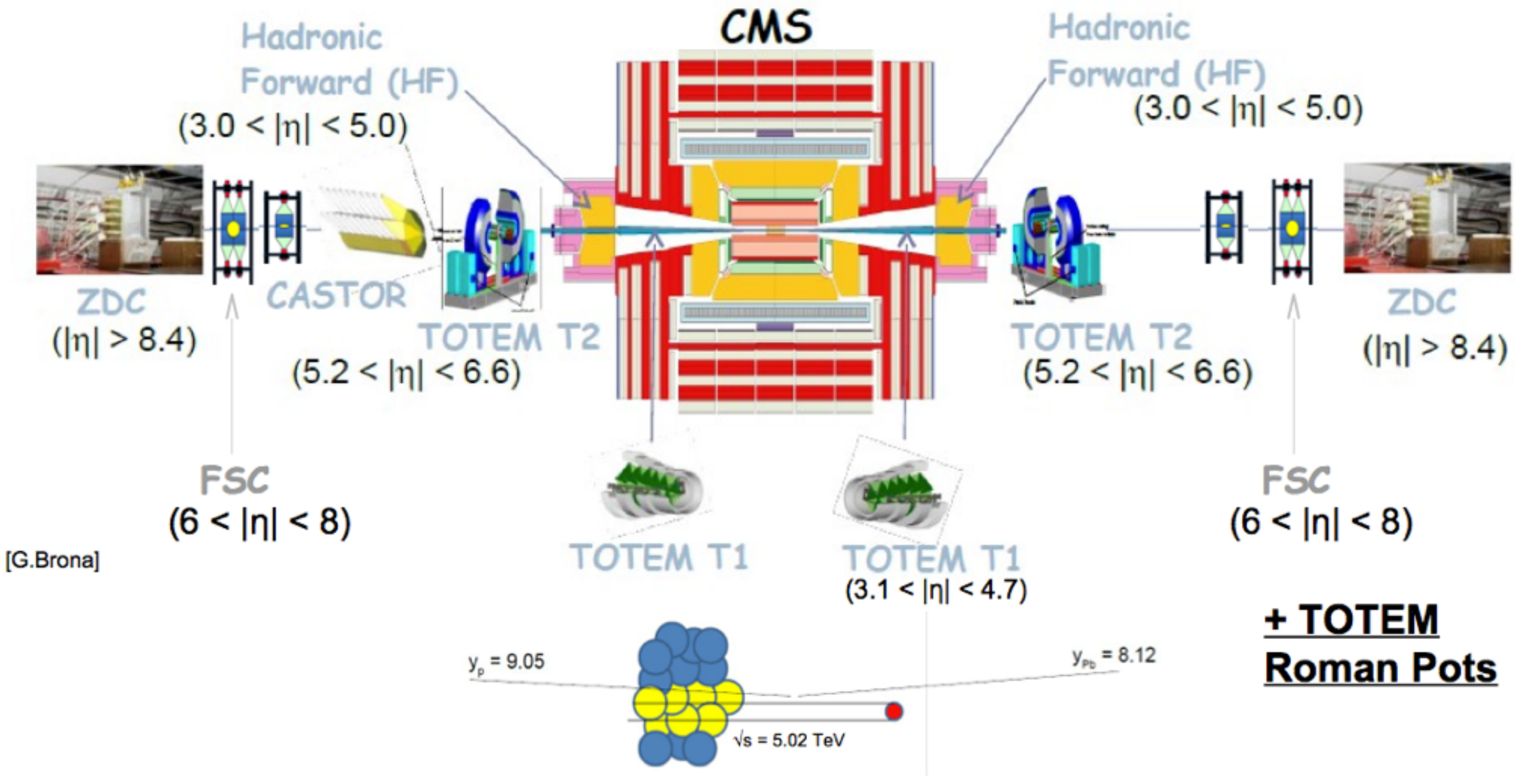
TOTEM T2, **5.3 < |η| < 6.5**

CASTOR,
-6.6 < η < -5.2



FSC

Forward detectors at CMS

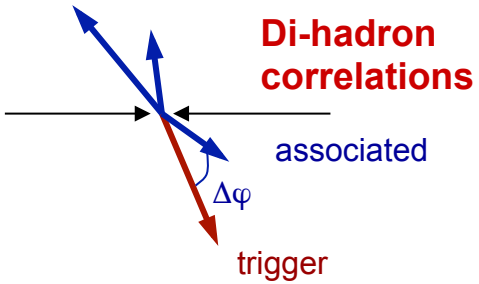


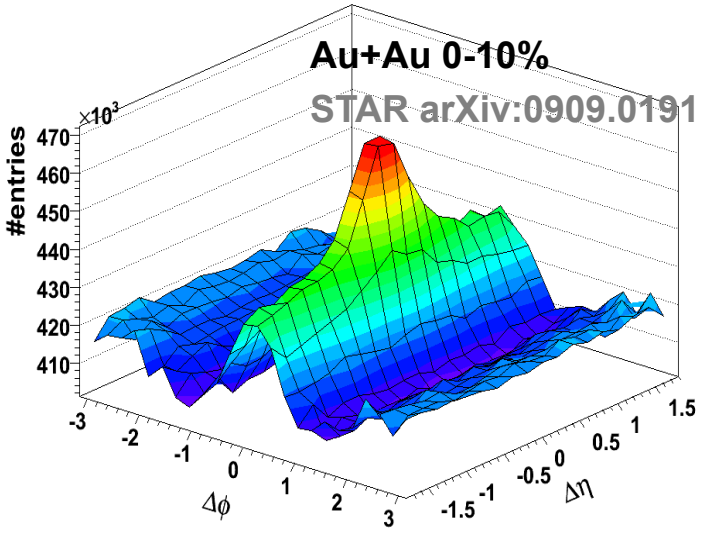
Probing extreme QCD through ridge-like correlations in small systems: status and problems

Raju Venugopalan
Brookhaven National Laboratory

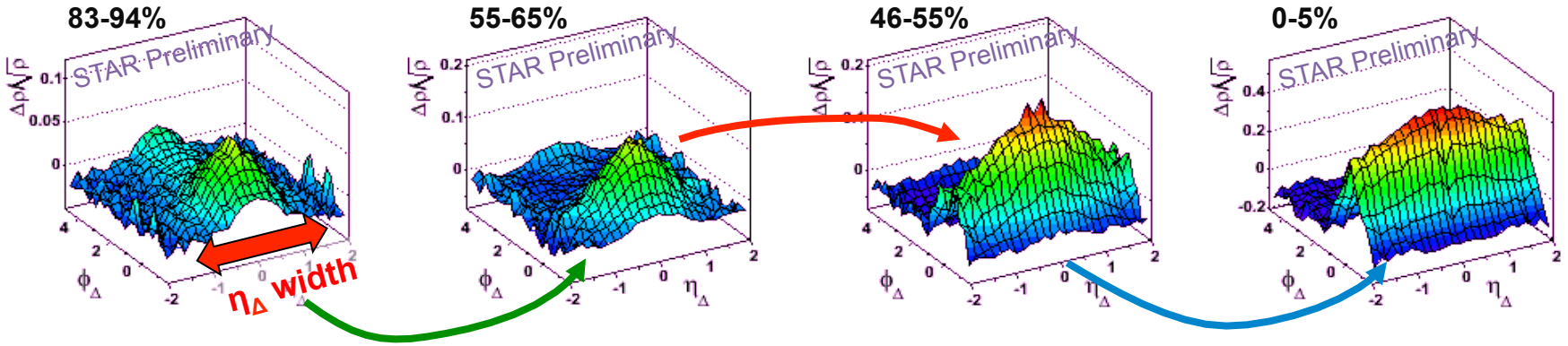
RBRC Saturation Workshop, April 26-28, 2017

The ridge in A+A collisions



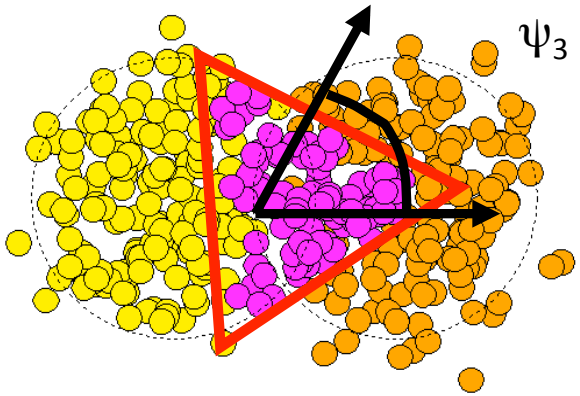


$3 < p_{t,trigger} < 4$ GeV
$p_{t,assoc.} > 2$ GeV

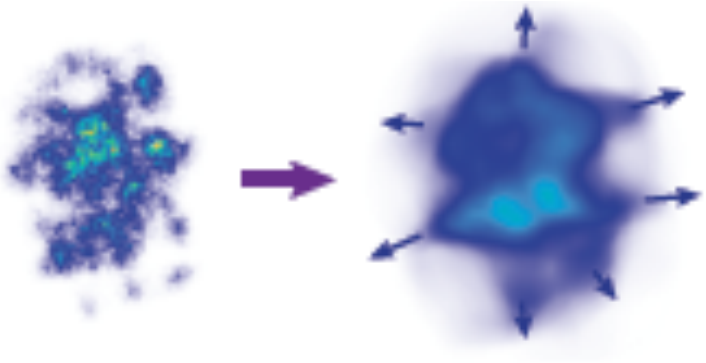


Collimated, long range rapidity correlations:
First seen by RHIC Au+Au experiments: STAR, PHOBOS, PHENIX

The ridge in A+A collisions



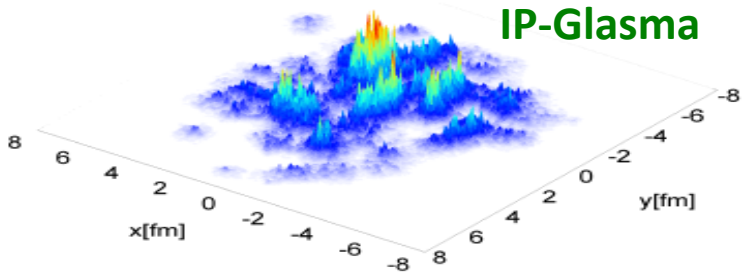
Alver, Roland, PRC81(2010) 054905
Alver, Gombeaud, Luzum, Ollitrault, PRC82 (2010) 03491

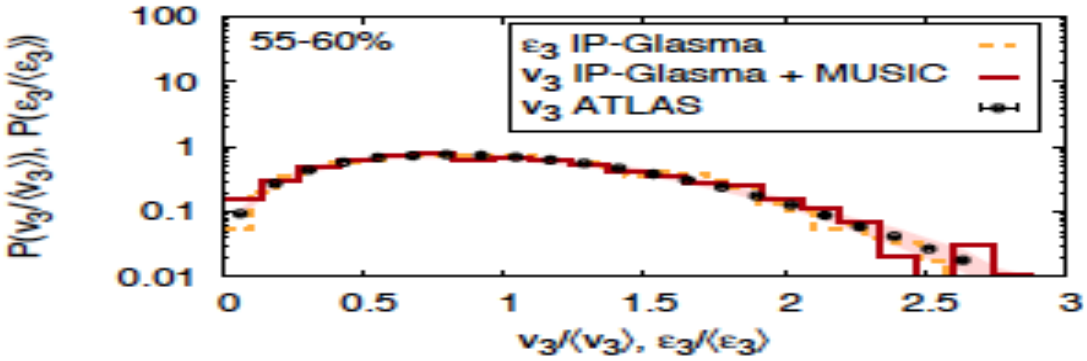


Structure of ridge-correlations can be understood as hydrodynamic flow driven by event-by-event fluctuations in nucleon positions

$$\frac{1}{N_{\rm trig}N_{\rm assoc.}}\frac{d^2N}{d\Delta\Phi} = 1 + V_1\,Cos(\Delta\Phi) + V_2\,Cos(2\Delta\Phi) + \cdots$$

Gale,Jeon,Schenke,Tribedy,Venugopalan, PRL110 (2013) 012302



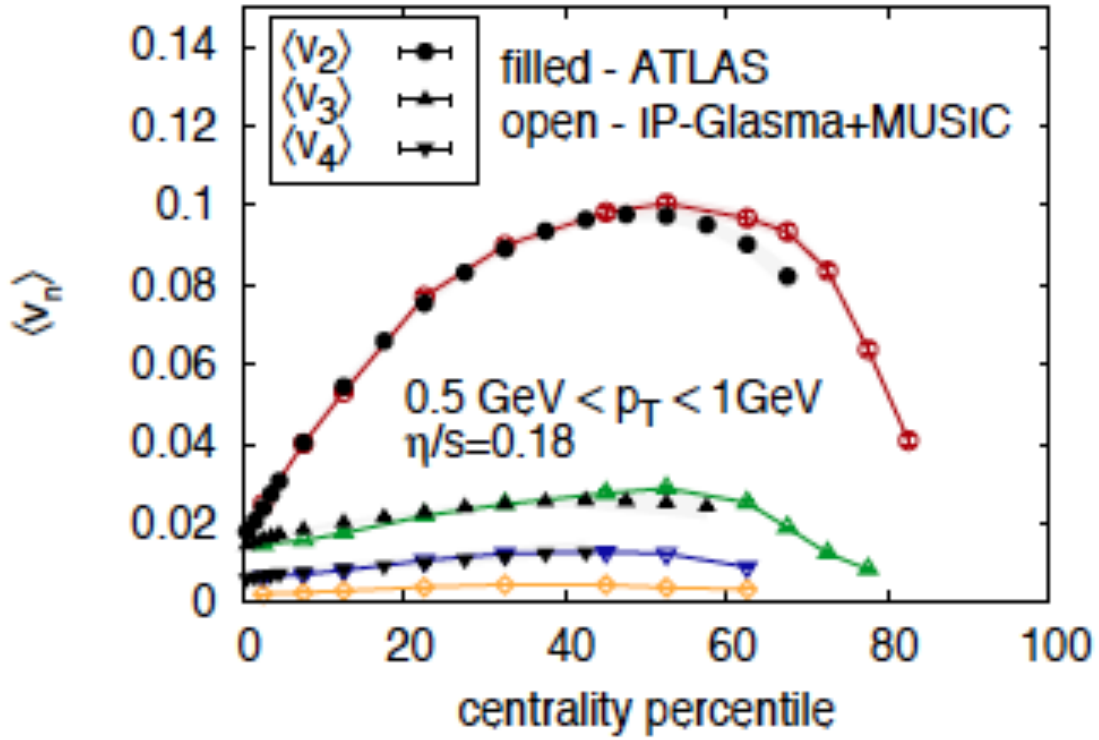


Some evidence of sensitivity of data to sub-nucleon scale fluctuations

What's the smallest sized QGP droplet?

IP-Glasma= initial state
MUSIC=event.by.event. hydro

Schenke, Venugopalan, PRL 113 (2014) 102301



Where does the hydro paradigm break down?

Higher cumulants of elliptic flow

m-particle flow cumulants

$$c_n\{2m\} = \langle\langle e^{in(\phi_1+\cdots\phi_m-\phi_{m+1}-\cdots\phi_{2m})}\rangle\rangle$$

Borghini,Dinh,Ollitrault, nucl-th/0105040

$$v_n\{2\}^2 \equiv c_n\{2\}\,;\; v_n\{4\}^2 \equiv -c_n\{4\}\,;\; v_n\{6\}^6 \equiv c_n\{6\}/4$$

Spatial eccentricities:

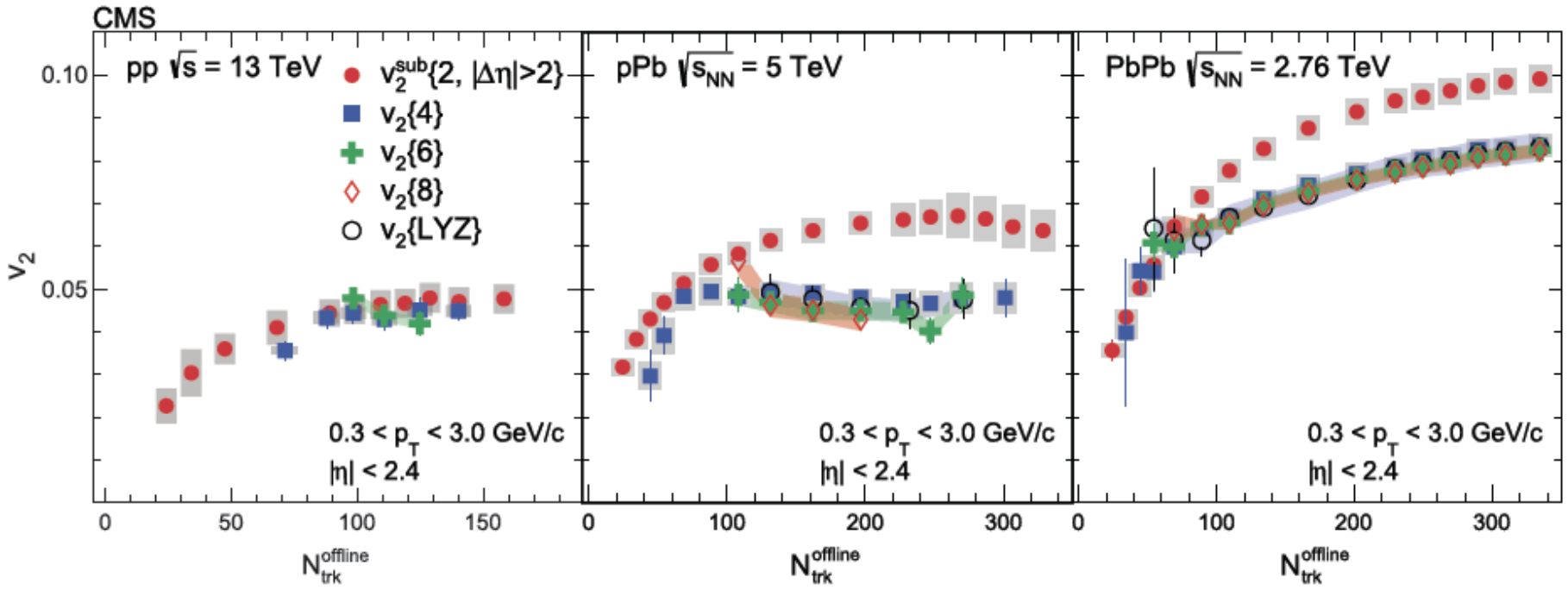
$$\epsilon_n = \frac{1}{< r_\perp^n >} \int d^2r_\perp\, e^{in\phi_r}\, r_\perp^n\, \frac{dN}{dyd^2r_\perp}$$

A number of simple models give $\epsilon_n\{2\} > \epsilon\{4\} = \epsilon\{6\} = \cdots$

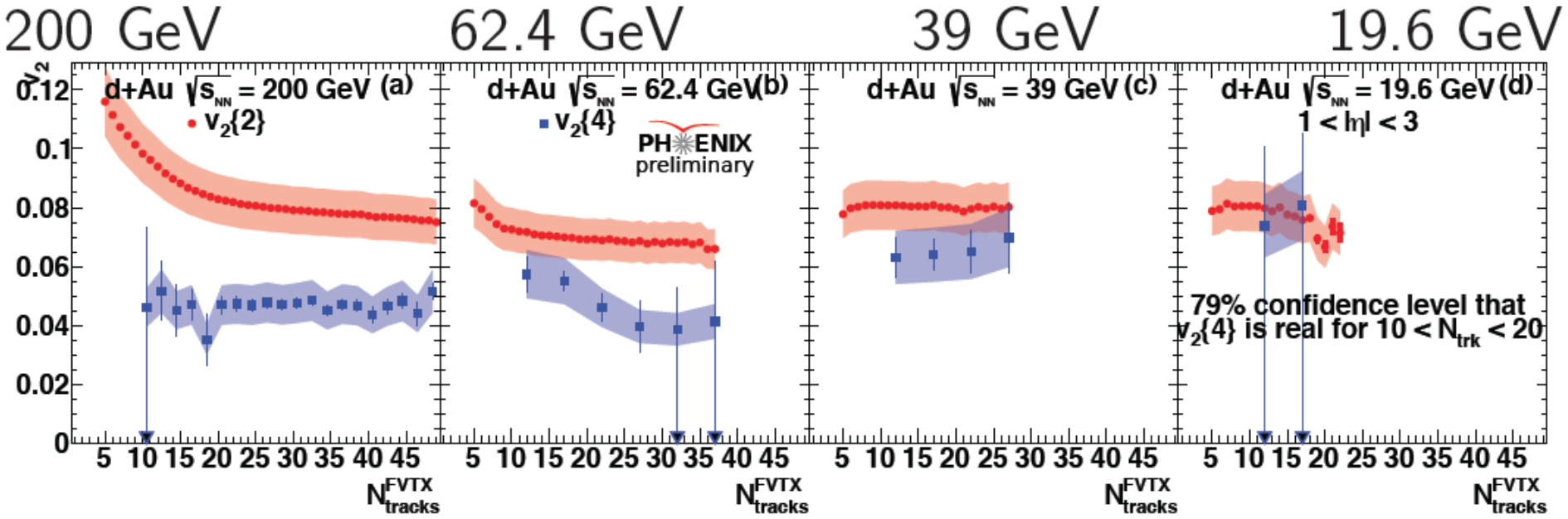
Hydro linear response: $v_n\{m\} \approx c_n\varepsilon_n\{m\}$

Gardim,Grassi,Luzum,Ollitrault, PRC (2012)024908; Niemi,Denicol,Holopainen,Huovinen, PRC87 (2013)054901
Bzdak,Bozek,McLerran, arXiv:1311.7325, Bzdak, Skokov, arXiv: 1312.7349
Li, Ollitrault, arXiv:1312.6555, Basar,Teaney, arXiv:1312.6770

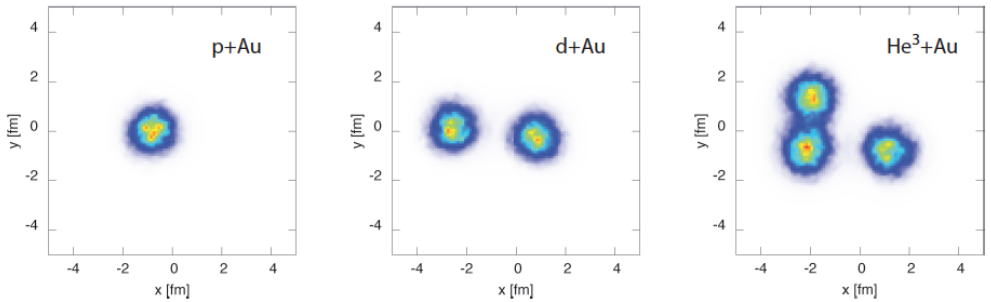
Collectivity across system size

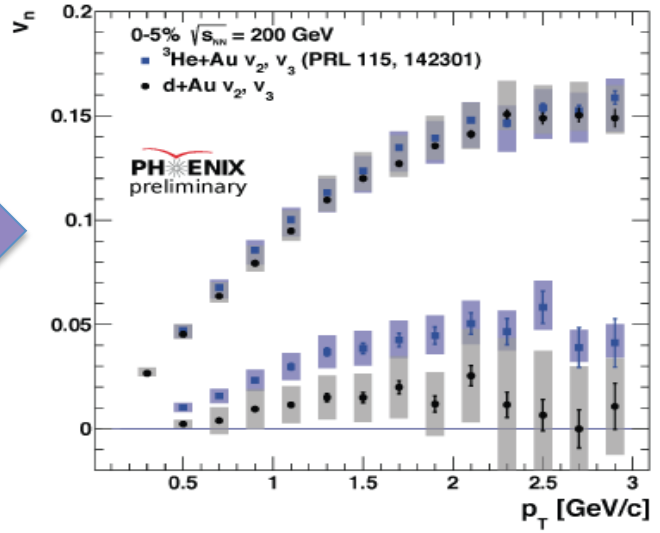


Collectivity across wide energy scales

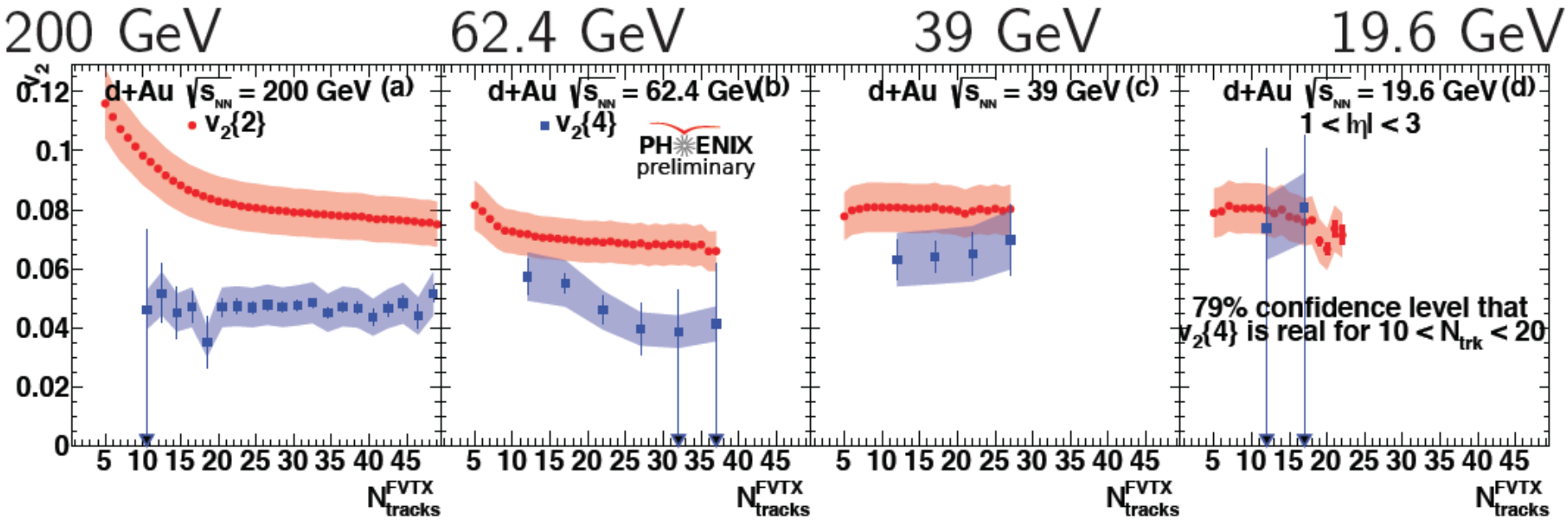


Schenke, RV:1407.7557





Collectivity across wide energy scales



Panta Rhei ?



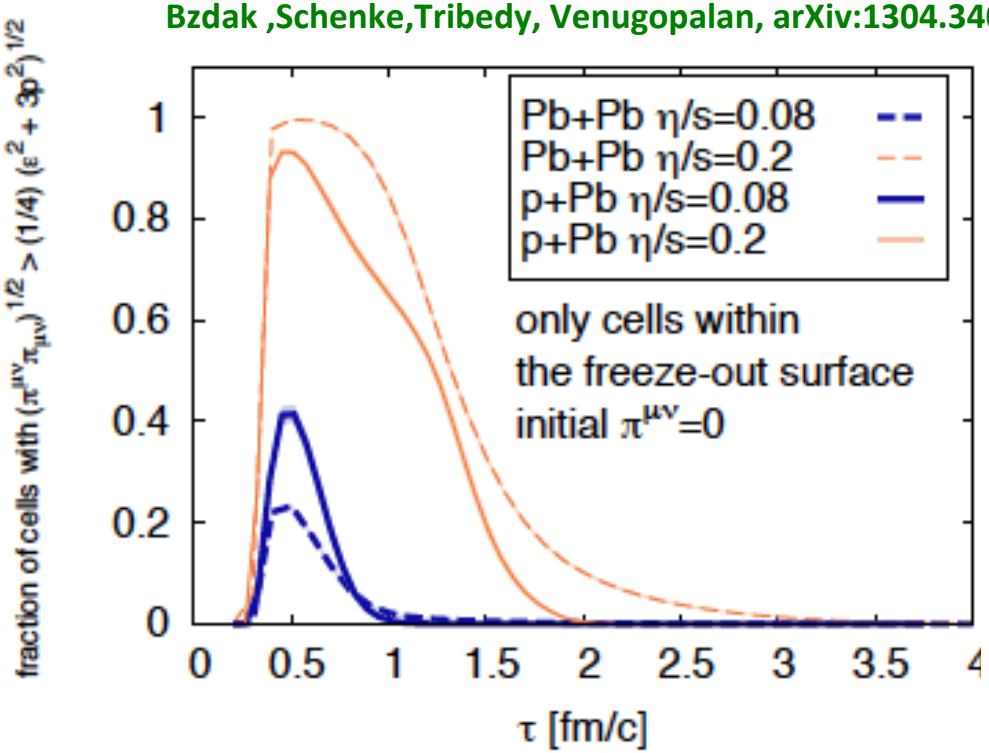
Heraclitus of Ephesus
535-475 BC

Issues with the hydrodynamic paradigm: I

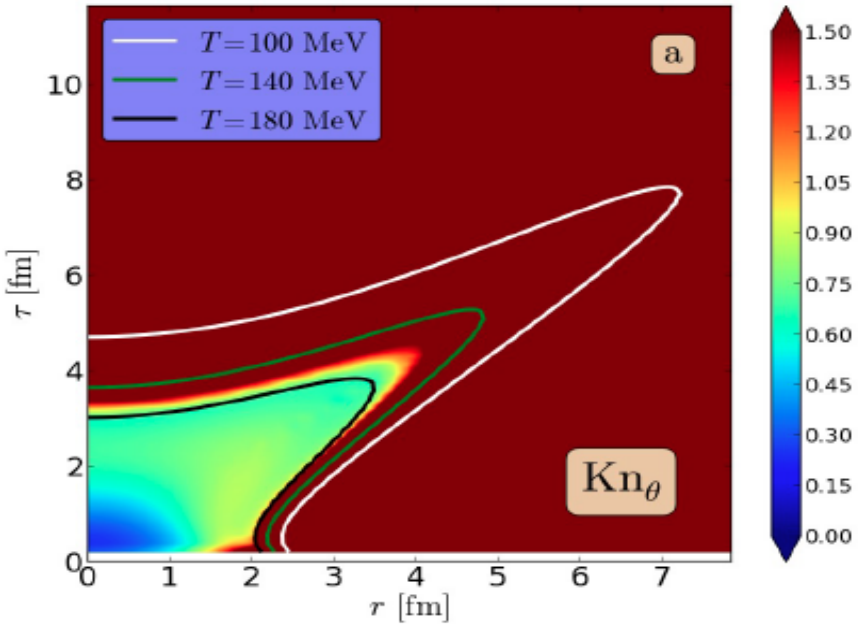
Two frequently used measures: Reynolds # and Knudsen #

$$R^{-1} \propto (\Pi^{\mu\nu}\Pi_{\mu\nu})^{1/2}/(\epsilon^2 + 3P^2)^{1/2} \qquad \mathrm{Kn} = \frac{\tau_\pi}{L} \;\; ; \;\; \tau_\pi \propto \frac{\eta}{sT}$$

Bzdak ,Schenke,Tribedy, Venugopalan, arXiv:1304.3403



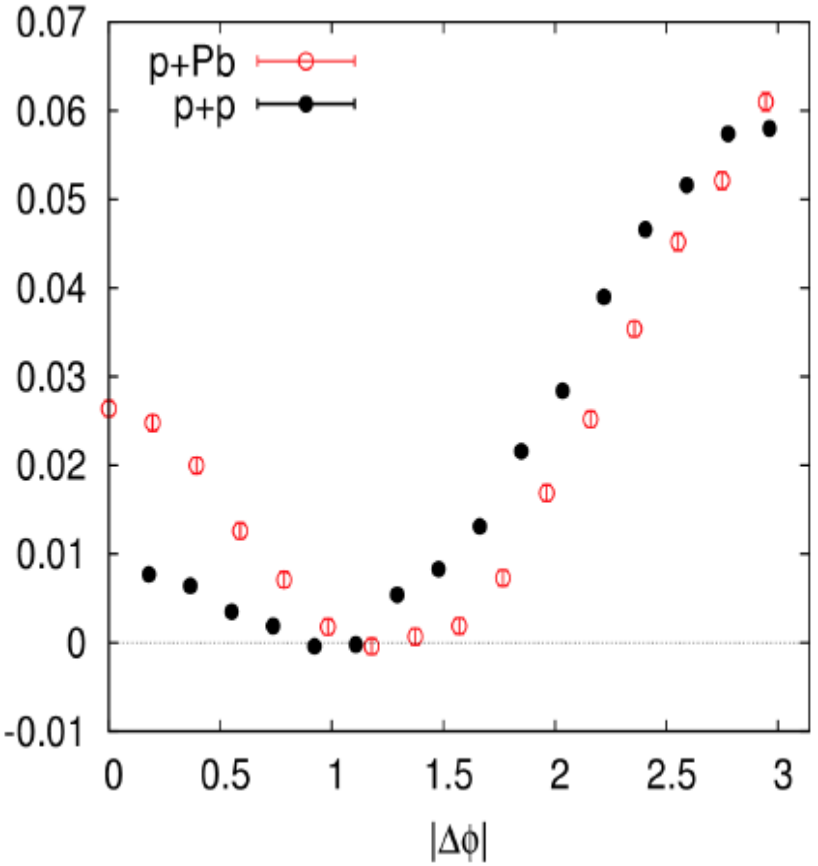
Dumitru,Molnar,Nara,arXiv:0706.2233
Denicol, Niemi, arXiv:1404.7327

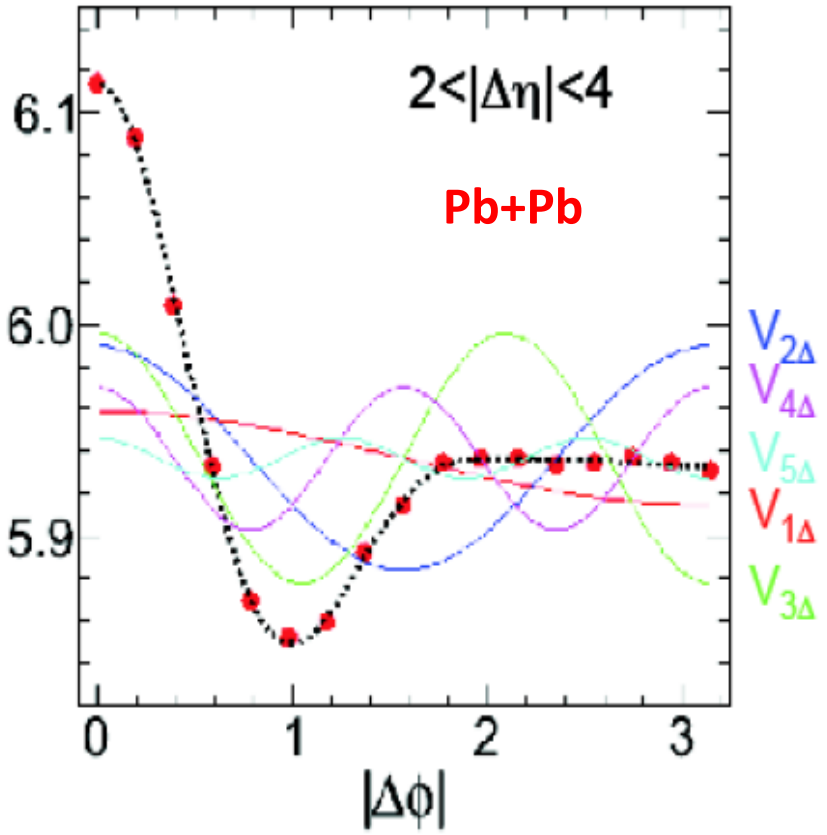


Hydro good for Kn < 0.5,
marginal for K < 1 transient regime;
K > 1 free streaming

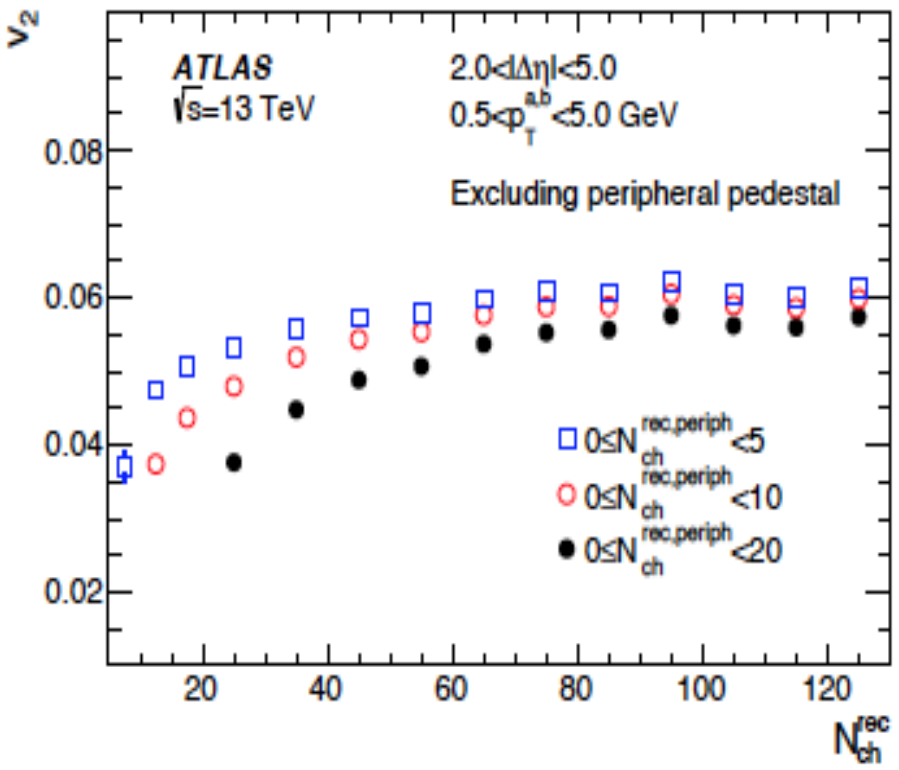
Issues with the hydrodynamic paradigm: II

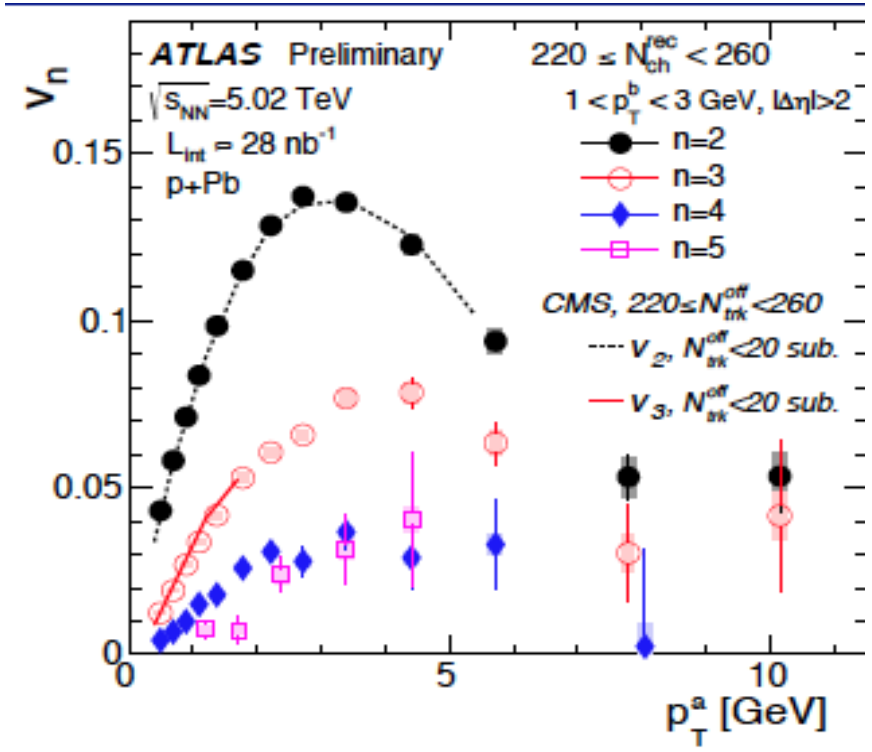
No (mini-) jet quenching seen in the smaller systems





Issues with the hydrodynamic paradigm: III



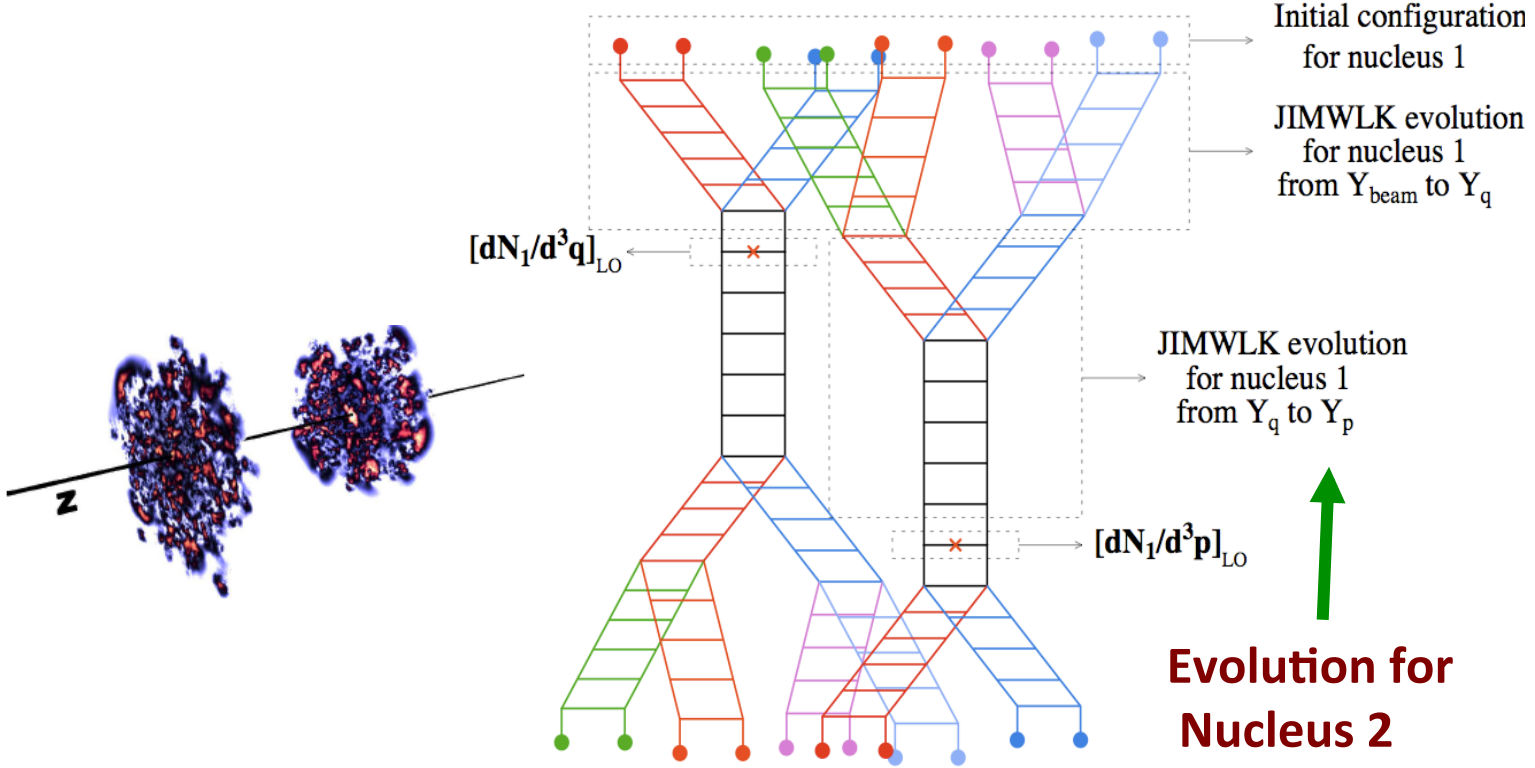


Large anistropies at larger p_T and smaller N_{ch} than one might reconcile with a hydrodynamic description

Can we understand multiparticle correlations in an *ab initio* approach

Two-parton azimuthal correlations in the CGC

Dumitru,Gelis,McLerran,Venugopalan: 0804.3858
Gelis, Lappi, Venugopalan, arXiv: 0807.1306
Dusling,Gelis,Lappi,Venugopalan, arXiv:0911.2720



Evolution for Nucleus 2

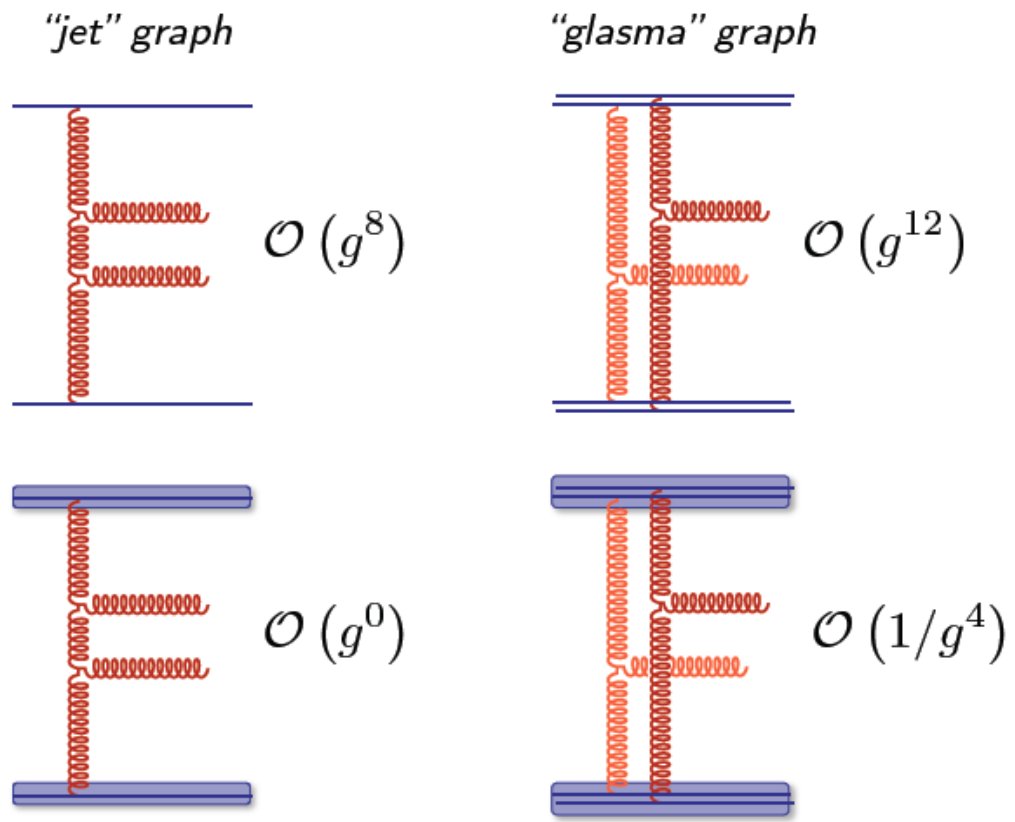
$$\langle \frac{dN_2}{d^3p\, d^3q} \rangle_{\rm LLogs} = \int [d\rho_1][d\rho_2] W_{Y_1}[\rho_1]\, W_{Y_2}[\rho_2]\, \frac{dN}{d^3p}|_{\rm LO}\, \frac{dN}{d^3q}|_{\rm LO}$$

JIMWLK evolution

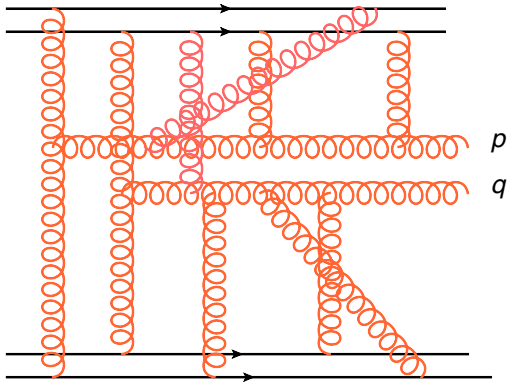
Solution of Yang-Mills for dense-dense systems (as in A+A)

Glasma graph approximation: power counting

Dumitru,Dusling,Gelis,Jalilian-Marian,
Lappi,Venugopalan, PLB697 (2011)21
Dusling,Venugopalan,PRL108 (2012)262001

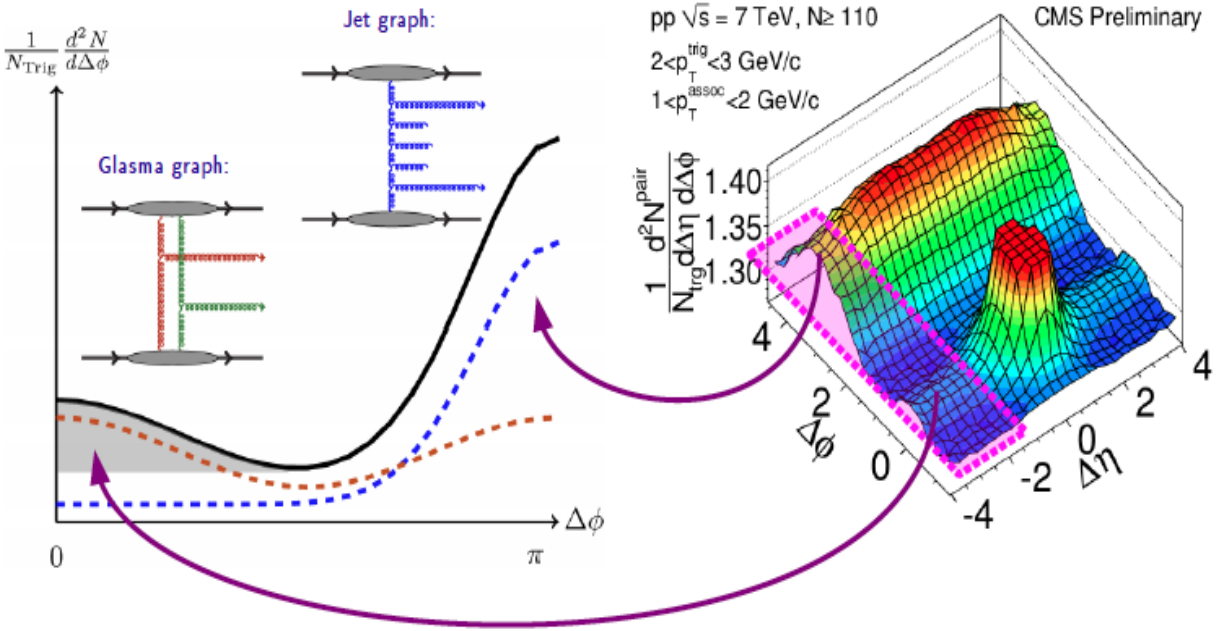


Gluons with $k_T \sim Q_S$ resolve
$n \sim 1/g^2$ color sources
Effective coupling: $g*n \sim 1/g$



Note: neither the Glasma graphs nor the jet graphs include the multiple coherent scatterings resummed by the YM equations…
become important for $p_T < Q_S$

Anatomy of long range collimations



RG evolution of Glasma graphs:

$$C(\mathbf{p},\mathbf{q}) \propto \frac{g^4}{\mathbf{p}_\perp^2\mathbf{q}_\perp^2}\int \mathrm{d}^2\mathbf{k}_{1\perp}\,\Phi_{A_1}^2(y_p,\mathbf{k}_{1\perp})\Phi_{A_2}(y_p,\mathbf{p}_\perp-\mathbf{k}_{1\perp})\Phi_{A_2}(y_q,\mathbf{q}_\perp-\mathbf{k}_{1\perp}) + \text{permutations}$$

Dusling,RV, PRD 87, 051502 (R) (2013); PRD87 (2013) 094034
Dusling,Tribedy,RV,PRD93 (2016) 014034

RG evolution of the mini-jets:

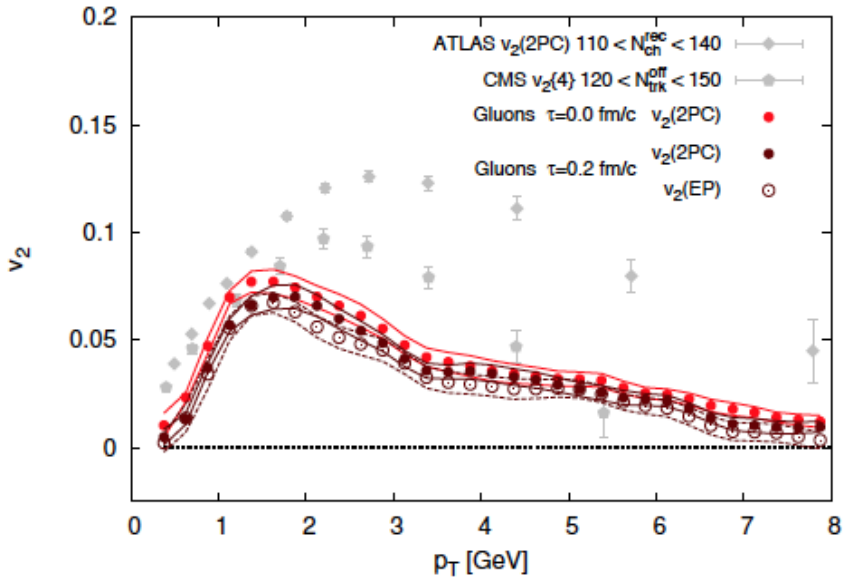
$$C_{\rm dijet}(\mathbf{p},\mathbf{q}) \propto \Phi_A \otimes \Phi_B \otimes G_{\rm BFKL}$$

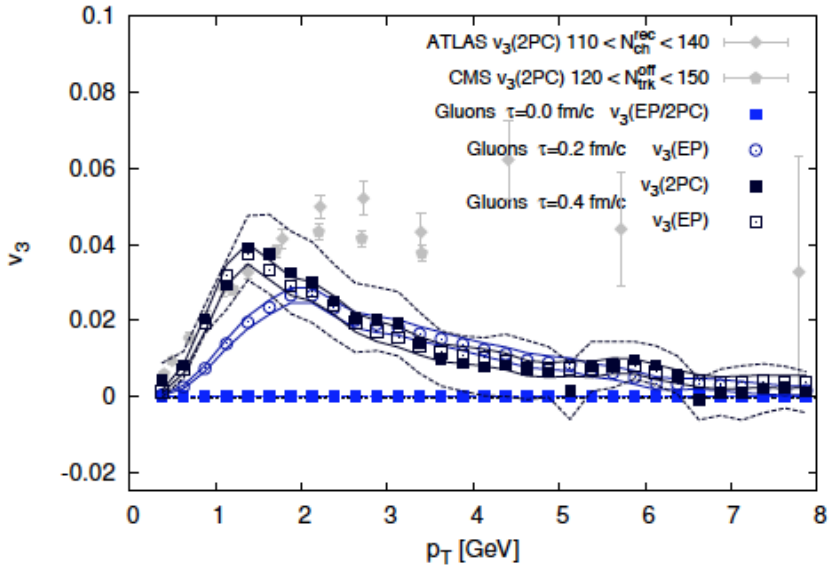
Good agreement with data for $p_T > Q_s$

However no odd harmonics v_3, v_5 in this approximation…

Azimuthal anistropy from Yang-Mills dynamics

Schenke,Schlichting,RV, PLB747(2015)76





See also, Lappi,Srednyak,RV, JHEP1001 (2010)066

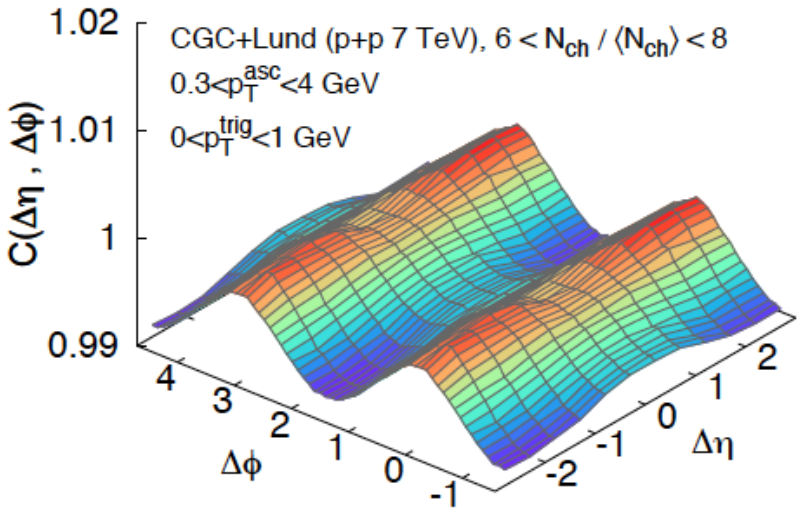
Recent analytical work in dilute-dense approx:
Kovchegov,Wertepny,NPA906 (2013)50
McLerran, Skokov arXiv:1611.09870
Kovner,Lublinsky,Skokov, arXiv:1612.07790

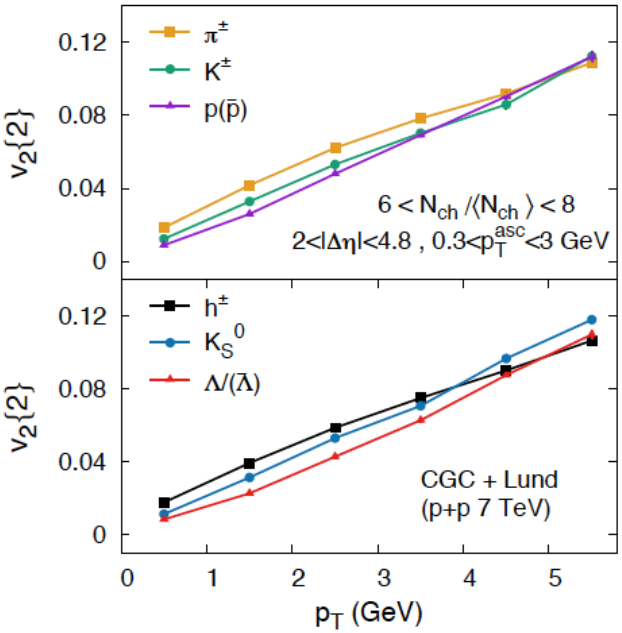
What about 4 and higher particle cumulants from YM dynamics?

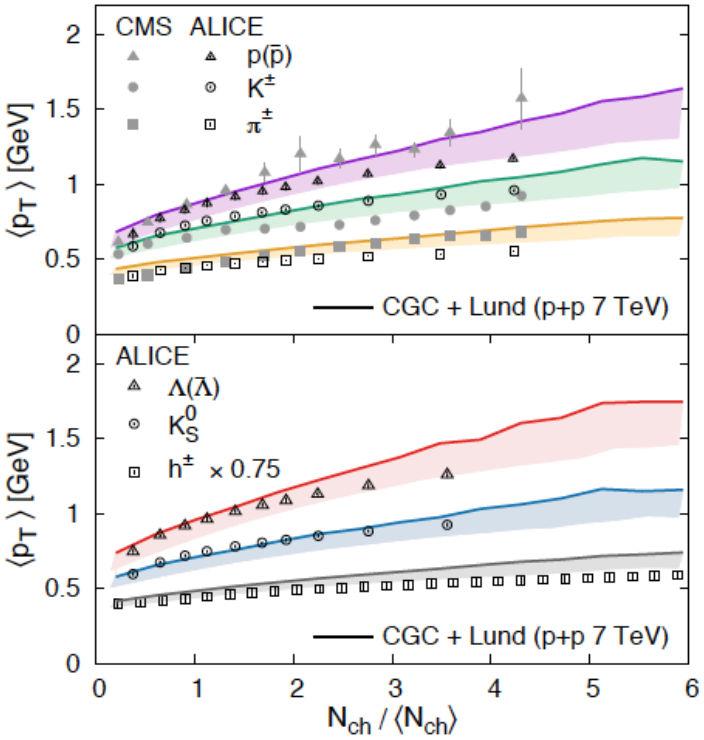
Numerically very challenging to look at rare events – in progress

Schenke,Schlichting,Tribedy,RV

IP-Glasma+Lund fragmentation







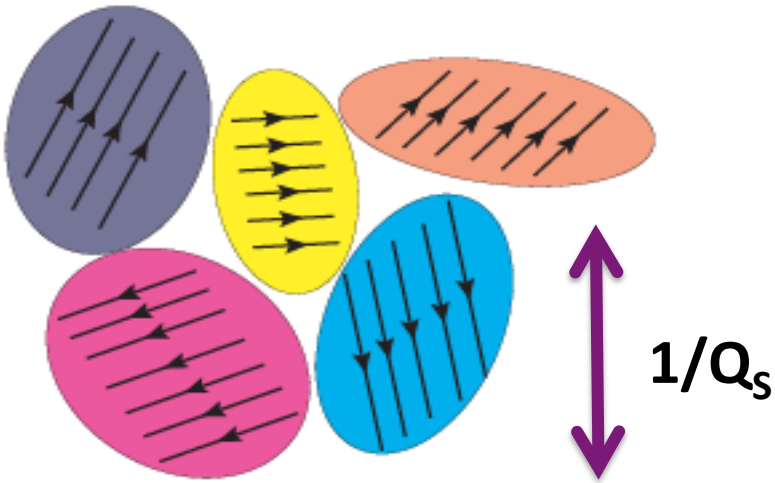
Schenke,Schlichting,Tribedy,RV, PRL117(2016)162301

Pattern of mass splitting of $\langle p_T \rangle$ and v_2 seen in high multiplicity events is reproduced

Tracing azimuthal initial state correlations

Multi-particle correlations from eikonal scattering of partons off color domains in a nuclear target

Kovner,Lublinsky,arXiv:1012.3398,1109.0347
Dumitru,Gianini, arXiv:1406.5781
Dumitru,Skokov,arXiv:1411.6630,
Dumitru,McLerran,Skokov,arXiv:1410.4844



Explore in simple model:

$$\frac{d^2N}{d^2\mathbf{p}_1 d^2\mathbf{p}_2} = \int d^2\mathbf{b}_1 d^2\mathbf{b}_2 \int \frac{d^2\mathbf{k}_1}{(2\pi)^2}\frac{d^2\mathbf{k}_2}{(2\pi)^2} W(\mathbf{b}_1,\mathbf{k}_1,\mathbf{b}_2,\mathbf{k}_2)$$
$$\times \int d^2\mathbf{r}_1 d^2\mathbf{r}_2\, e^{i(\mathbf{p}_1-\mathbf{k}_1)}\, e^{i(\mathbf{p}_2-\mathbf{k}_2)} \langle D\left(\mathbf{b}_1+\frac{\mathbf{r}_1}{2},\mathbf{b}_1-\frac{\mathbf{r}_1}{2}\right) D\left(\mathbf{b}_2+\frac{\mathbf{r}_2}{2},\mathbf{b}_2-\frac{\mathbf{r}_2}{2}\right)\rangle$$

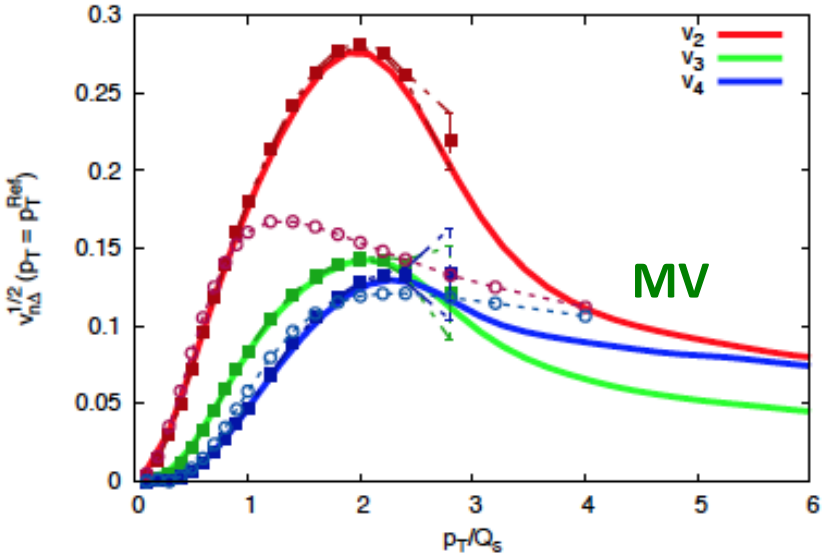
Dipole $D(\mathbf{x},\mathbf{y}) = \frac{1}{N_c}\mathrm{Tr}\left(V(\mathbf{x})V^\dagger(\mathbf{y})\right) \qquad V(\mathbf{x}) = P\exp\left(-ig\int dx^+ A^-(\mathbf{x},x^+)\right)$

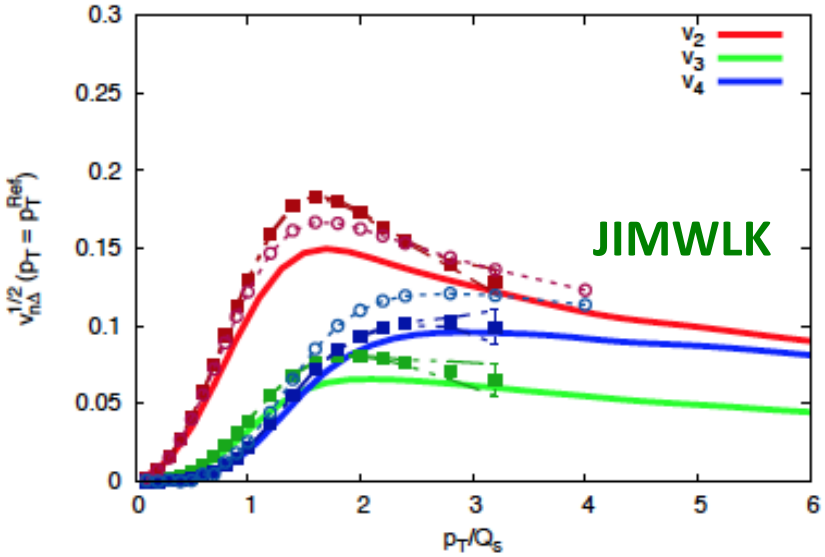
Ansatz: $W(\mathbf{b}_1,\mathbf{k}_1,\mathbf{b}_2,\mathbf{k}_2) = W(\mathbf{b}_1,\mathbf{k}_1)\,W(\mathbf{b}_2,\mathbf{k}_2)$

$W(\mathbf{b},\mathbf{k}) = \exp\left(-\mathbf{b}^2/B - \mathbf{k}^2 B\right)$ **B=transverse area of projectile**

Tracing azimuthal initial state correlations

Lappi, arXiv:1501.05505
Lappi,Schenke,Schlichting,RV, arXiv:1509.03499





What about 4-particle correlations?

$$\frac{d^m N}{\prod_{i=1}^m d^2\mathbf{p_{i\perp}}} = \frac{1}{(4\pi^3 B)^m}\prod_{i=1}^m \int d^2\mathbf{b_i}\int d^2\mathbf{r_i}\; e^{-b_i^2/E}\; e^{-r_i^2/4B} e^{i\mathbf{p_{i\perp}}\cdot\mathbf{r_i}} \left\langle \prod_{j=1}^m D(\mathbf{b_j}+\frac{\mathbf{r_j}}{2},\mathbf{b_j}-\frac{\mathbf{r_j}}{2})\right\rangle$$

$$\kappa_n\{m\} = \int d^2\mathbf{p}_{1\perp}...d^2\mathbf{p}_{m\perp}\frac{d^m N}{\prod_{k=1}^m d^2\mathbf{p}_{k\perp}}\prod_{j=1}^{m/2}\prod_{l=\frac{m}{2}+1}^{m} e^{ni(\phi_j^p-\phi_l^p)}$$

$$c_n\{4\} = \frac{\kappa_n\{4\}}{\kappa_0\{4\}} - 2\left(\frac{\kappa_n\{2\}}{\kappa_0\{2\}}\right)^2$$

First initial state results on $c_n\{4\}$, SC{m,n}
Kevin Dusling's talk at 10:30 am Friday
Dusling,Mace,RV, in preparation

Summary-I

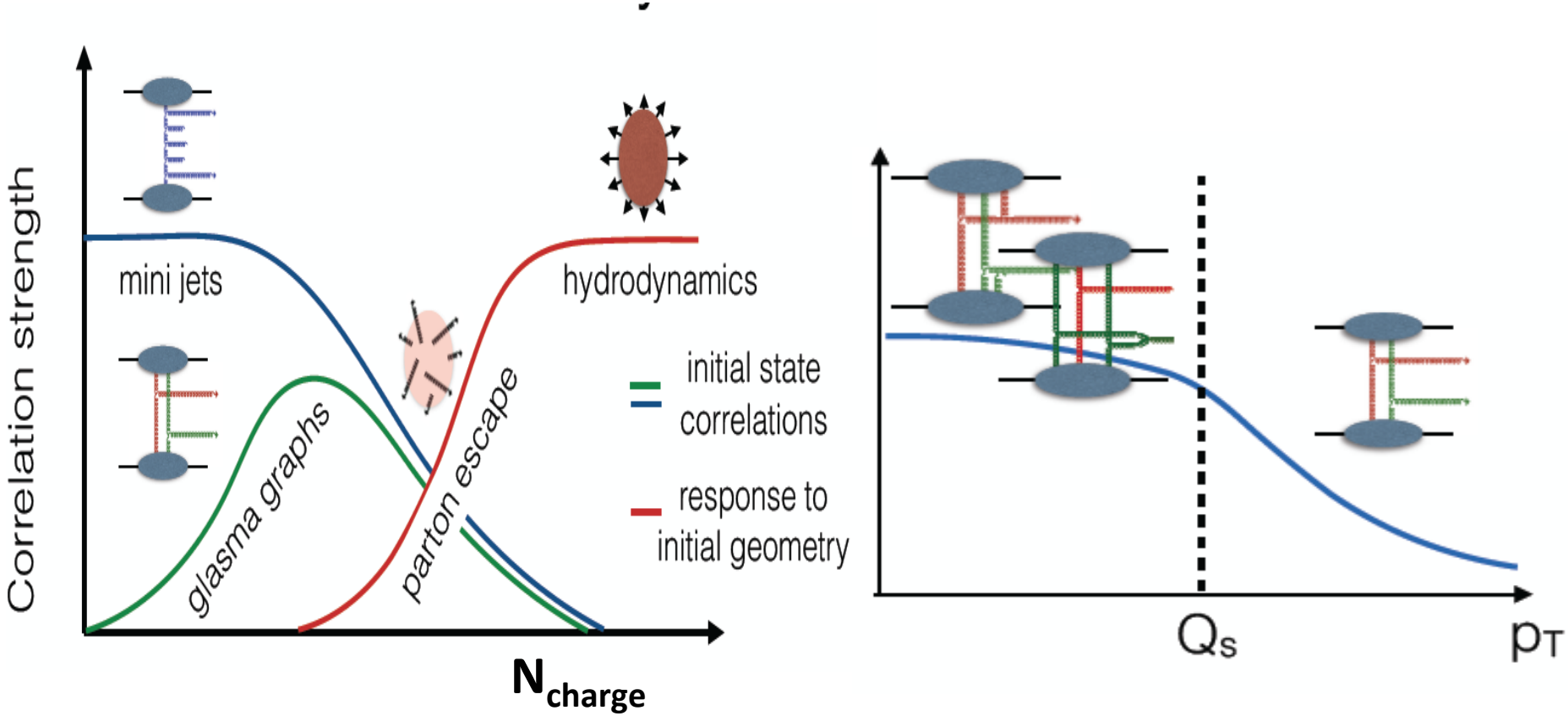
Hydrodynamic paradigm appears to describe
multi-particle correlations even in the smallest systems

There are however puzzling features of the data,
questions about the the validity of hydro, fine tuning of initial conditions (requiring implicitly strong initial state correlations),
⋯ and explanation of anisotropies for p_T > few GeV

Initial state QCD frameworks now also able to explain many features of the data but systematic treatments are still in their infancy

Despite much progress no satisfactory explanation of the data
-- the problem is still wide open

Summary-II



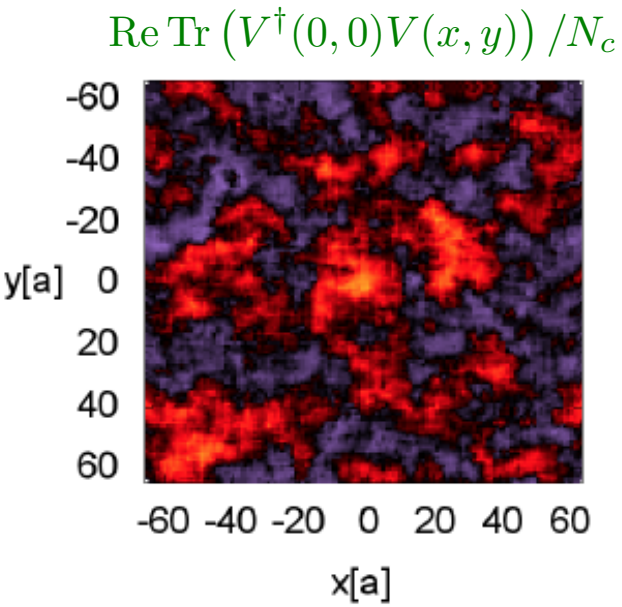
Event engineering across system sizes, energies, and varieties of probes, offers the exciting possibility of exploring dynamical evolution of strongly correlated quark-gluon matter from high occupancy, out of equilibrium, dynamics… to hydrodynamics

Figiures: S. Schlichting at Quark Matter 2015

Thanks for listening!

Higher cumulants from Glasma domains

Dumitru,McLerran,Skokov, 1410.4844



Simple model: express intrinsic higher point correlators as correlators of produced particles with a target field in a color domain, averaged over all orientations of the field.

$$c_2\{2\} = \frac{1}{N_D}\left(\mathcal{A}^2 + \frac{1}{4(N_c^2-1)}\right)$$

$$c_2\{4\} = -\frac{1}{N_D^3}\left(\mathcal{A}^4 - \frac{1}{4(N_c^2-1)^3}\right)$$

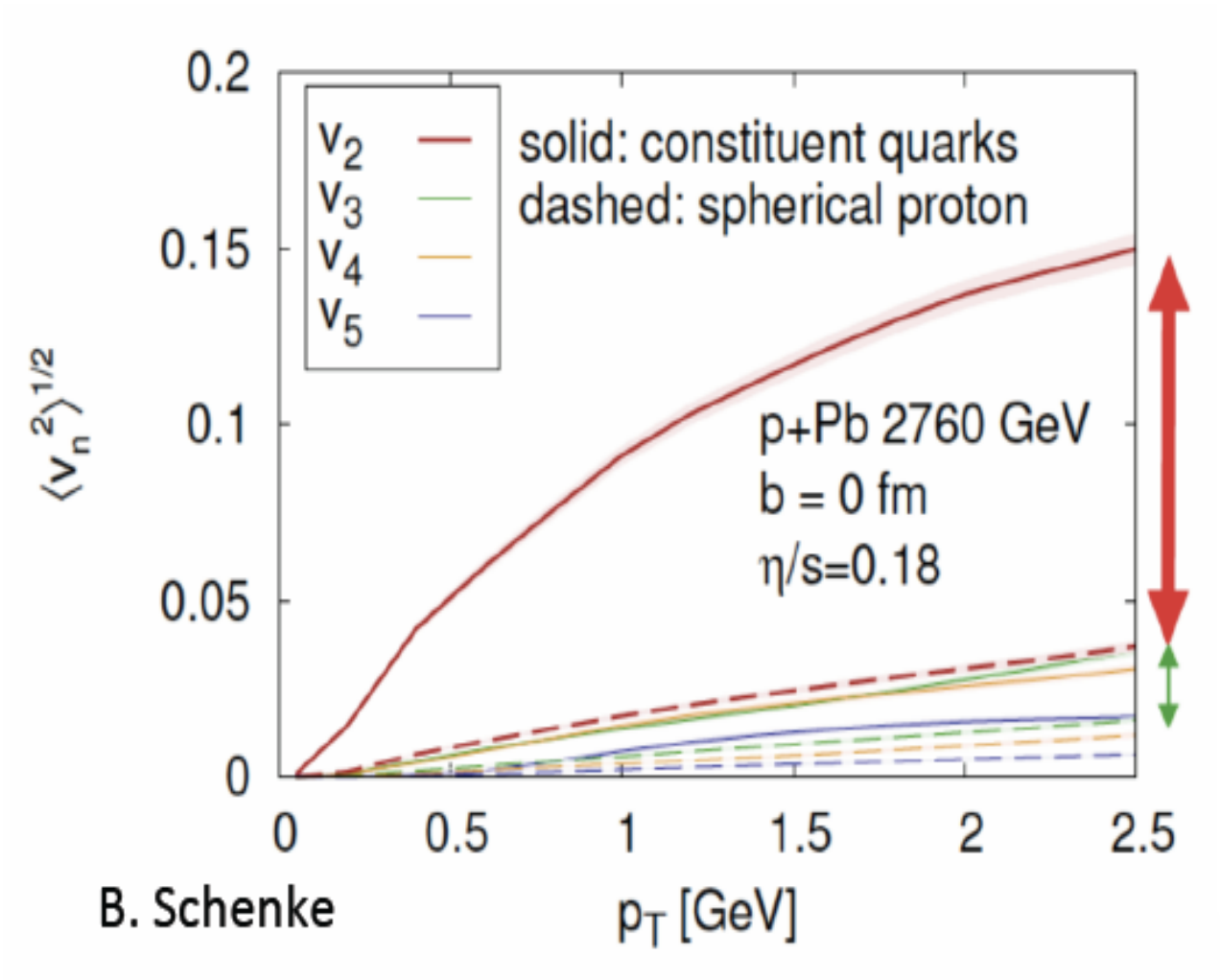
"A" term is the correlation induced between projectile particles due to color field orientation of target (more generically, non-Gaussian correlations)

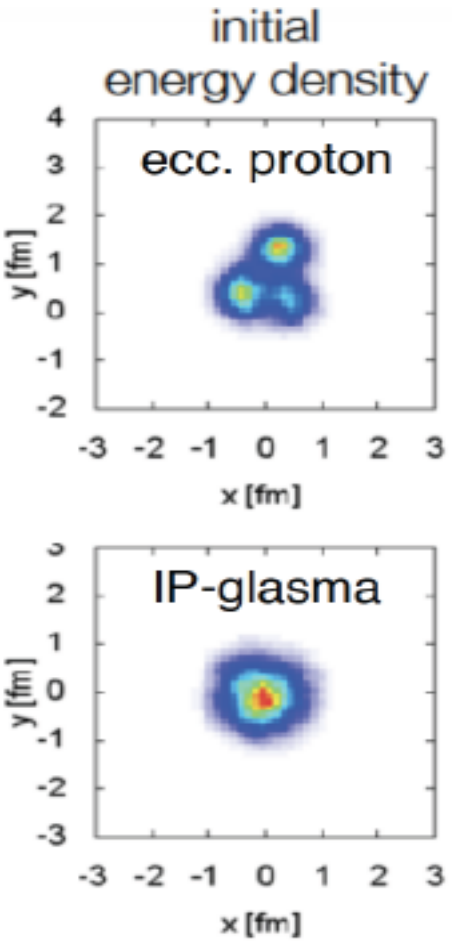
The N_c term is the "connected Glasma graph" (Gaussian correlations)

N_D is # of color domains – few in p+A, several in A+A

Shape matters ?

Schenke,Schlichting, 1407.8458





RBRC Workshop
Saturation: Recent Developments, New Ideas and Measurements

April 26-28, 2017

Physics Department, Large Seminar Room

WEDNESDAY, APRIL 26, 2017

08:30-08:50 REGISTRATION

08:50-09:00 Welcome..... *Workshop Organizers*
09:00-09:30 D. Kharzeev ..... *Deep inelastic scattering as a probe of entanglement*
09:30-10:00 E. Iancu ..... *Particle production in proton-nucleus collisions beyond leading order*

10:00-10:30 COFFEE BREAK (included in attendance)

10:30-11:00 M. Lublinsky..... *From light-cone wave function to NLO JIMWLK*
11:00-11:30 G. Beuf ..... *Full NLO corrections for DIS structure functions in the dipole factorization formalism*
11:30-12:00 B. Schenke ..... *Subnucleonic fluctuations, diffraction, and small-x evolution*

12:00-14:00 LUNCH BREAK (on your own, self-pay)

14:00-14:30 M. Sievert ..... *Quark helicity evolution at small-x*
14:30-15:00 Y. Kovchegov..... *Small-x asymptotics of the quark helicity distribution*

15:00-15:30 COFFEE BREAK (included in attendance)

15:30-16:00 A. Ogawa ..... *Polarized p+A physics at forward rapidity at STAR*
16:00-16:30 T. Peitzmann..... *Opportunities for forward photon measurements in ALICE at the LHC*
16:30-17:00 D. Tapia-Takaki... *Studying gluon saturation and nuclear effects using forward heavy-ion probes and UPCs at LHC*
17:00-17:30 D. Neill ..... *Finding small-x like evolution in QCD final state dynamics: the problem of non-global logarithms*

18:00-20:00 NO HOST DINNER (optional, off-site, self-pay)

THURSDAY, APRIL 27, 2017

09:00-09:30 R. Venugopalan... *Ridge-like correlations in small systems: status and problems*
09:30-10:00 A. Mueller ..... *Transverse momentum broadening and Sudakov effects*

10:00-10:30 COFFEE BREAK (included in attendance)

10:30-11:00 I. Balitsky..... *Higher-twist corrections to gluon TMD factorization*
11:00-11:30 S. Caron-Huot..... *Linear and nonlinear small-x evolution in perturbation theory*
11:30-12:00 C. Royon..... *Forward jets at HERA and Mueller-Navelet and jet gap jet events at Tevatron and LHC*

Back to Contents

12:00-14:00 LUNCH BREAK (on your own, self-pay)

14:00-14:30 K. Fukushima ..... *Particle production in CGC*
14:30-15:00 J. Jia ..... *Flow in small systems*

15:00-15:30 COFFEE BREAK (included in attendance)

15:30-16:00 A. Dumitru..... *Fluctuations of the gluon distribution at small-x: correlation of multiplicity and transverse momentum fluctuations*
16:00-16:30 G. Chirilli..... *Rapidity factorization of high-energy scattering processes at NLO*
16:30-17:00 S. Schlichting..... *Event-by-event pre-equilibrium dynamics – from gluon saturation toward the onset of hydrodynamics*
17:00-17:30 A. Stasto..... *Low-x physics and prompt neutrino production*

18:00-20:00 NO HOST DINNER (optional, off-site, self-pay)

FRIDAY, APRIL 28, 2017

09:00-09:30 P. Newman ..... *Low-x physics and saturation studies for the Large Hadron Electron Collider*
09:30-10:00 A. Kovner ..... *Exploring correlations in the CGC wave function: odd azimuthal anisotropy*

10:00-10:30 COFFEE BREAK (included in attendance)

10:30-11:00 K. Dusling ..... *Collectivity from the initial state: four-particle correlations in proton-nucleus collisions*
11:00-11:30 R. Paatelainen ..... *Toward higher-order accuracy in LCPT*
11:30-12:00 A. Rezaeian ..... *Elliptic flow from color-dipole orientation in pp and pA collisions*

12:00-14:00 LUNCH BREAK (on your own, self-pay)

14:00-15:00 Nuclear Theory/RIKEN Seminar:
S. Caron-Huot..... *Analyticity in Spin and Causality in Conformal Theories*

15:00 END OF WORKSHOP

Back to Contents

Registered Participants

Ian Balitsky	Professor, Jefferson Laboratory / Old Dominion University
Guillaume Beuf	Post-doc, ECT*
Simon Caron-Huot	Assistant Professor, McGill University
Yufen Chen	Researcher, Cornell University
Giovanni Antonio Chirilli	Associate Researcher, University of Regensburg
Adrian Dumitru	Professor, Baruch College, The City University of New York
Kevin Dusling	Associate Editor, American Physical Society
Kenji Fukushima	Professor, The University of Tokyo
Shengli Huang	Research Scientist, Stony Brook University
Edmond Iancu	Directeur de Recherche, Institut de Physique Théorique, Saclay
Jiangyong Jia	Professor, Stony Brook University
Dmitri Kharzeev	Senior Scientist, Brookhaven National Lab & Theory Group Leader, RBRC
Yuri Kovchegov	Professor, Ohio State University
Alexander Kovner	Professor, University of Connecticut
Tuomas Lappi	Research Fellow, University of Jyvaskyla
J.H. Lee	Physicist, Brookhaven National Laboratory
Michael Lublinsky	Professor, Ben Gurion University of the Negev
Mark Mace	Research Assistant, Stony Brook University
Heikki Mäntysaari	Research Associate, Brookhaven National Laboratory
Alfred Mueller	Professor, Columbia University
Duff Neill	Feynman Fellow, Los Alamos National Laboratory
Paul Newman	Professor, University of Birmingham
Akio Ogawa	Scientist, Brookhaven National Laboratory
Risto Paatelainen	Postdoc, University of Jyvaskyla
Zohreh Parsa	Physicist, Brookhaven National Laboratory
Thomas Peitzmann	Professor, Utrecht University/Nikhef
Amir Rezaeian	Assistant Professor, Federico Santa Maria Technical University
Kaushik Roy	Graduate Teaching Assistant, Stony Brook University
Christophe Royon	Professor, University of Kansas
Takao Sakaguchi	Physicist, Brookhaven National Laboratory
Bjoern Schenke	Associate Physicist, Brookhaven National Laboratory
Soeren Schlichting	Research Assistant Professor, University of Washington
Matthew Sievert	Postdoctoral Research Associate, Los Alamos National Laboratory
Vladimir Skokov	Postdoc, RIKE BNL Research Center
Anna Stasto	Associate Professor, Pennsylvania State University
Daniel Tapia Takaki	Assistant Professor, University of Kansas
Andrey Tarasov	Research Associate, Brookhaven National Laboratory
Prithwish Tribedy	Postdoctoral Research Associate, Brookhaven National Laboratory
Thomas Ullrich	Physicist, Brookhaven National Laboratory
Raju Venugopalan	Senior Scientist, Brookhaven National Laboratory
Zhangbu Xu	Senior Scientist, Brookhaven National Laboratory

Back to Contents

RIKEN BNL Research Center Proceedings

Volume 128 – QCD in Finite Temperature and Heavy-Ion Collisions, February 13-15, 2017 – BNL- 113645-2017
Volume 127 – High pT Physics in the RHIC-LHC Era, April 12-15, 2016 – BNL-112446-2016
Volume 126 – RBRC Scientific Review Committee Meeting, April 5-8, 2016 – BNL-112102 -2016
Volume 125 – Lattice Gauge Theories 2016, March 9-11, 2016 – BNL-112316-2016
Volume 124 – Emerging Spin and Transverse Momentum Effects in pp and p+A Collisions, February 8-10, 2016 – BNL-112217-2016
Volume 123 – Opportunities for Exploring Longitudinal Dynamics in Heavy Ion Collisions at RHIC, January 20-22, 2016 – BNL-112139-2016
Volume 122 – Collectivity in Small Colliding Systems with High Multiplicity, March 4-6, 2015 – BNL-107696 -2015
Volume 121 – Theory and Modeling for the Beam Energy Scan: from Exploration to Discovery, February 26-27, 2015 – BNL-107682-2015
Volume 120 – Multi-Hadron and Nonlocal Matrix Elements in Lattice QCD, February 5-6, 2015 – BNL-107603-2015
Volume 119 – Thermal Photons and Dileptons in Heavy-Ion Collisions, August 20-22, 2014 – BNL-106066-2014
Volume 118 – The Approach to Equilibrium in Strongly Interacting Matter, April 2-4, 2014 – BNL-104423-2014
Volume 117 – Lattice Meets Experiment 2013: Beyond the Standard Model, December 5-6, 2013 – BNL-103493-2013
Volume 116 – RBRC Scientific Review Committee Meeting, October 31 - November 1, 2013 – BNL-102596-2013
Volume 115 – Jet Quenching at RHIC vs LHC in Light of Recent dAu vs pPb Controls, April 15-17, 2013 – BNL-100766-2013
Volume 114 – The Physics of p↑+A Collisions at RHIC, January 7-9, 2013 – BNL-99107-2013
Volume 113 – Thermal Radiation Workshop, December 5-7, 2012 – BNL-99088-2013
Volume 112 – RBRC Scientific Review Committee Meeting, November 6-8, 2012 – BNL-99621-2013
Volume 111 – Forward Physics at RHIC, July 30-Aug 1, 2012 – BNL-98400-2012
Volume 110 – P- and CP-odd Effects in Hot and Dense Matter, June 25-27, 2012 – BNL-98398-2012
Volume 109 – New Horizons for Lattice Computations with Chiral Fermions, May 14-18, 2012 – BNL-98392-2012
Volume 108 – Hyperon-Hyperon Interactions and Searches for Exotic Di-Hyperons in Nuclear Collisions, February 29 – March 2, 2012 – BNL-97035-2012
Volume 107 – Future Directions in High Energy QCD, October 20-22, 2011 – BNL-98119-2011
Volume 106 – Fluctuations, Correlations and RHIC Low Energy Runs, October 3-5, 2011 – BNL-96514-2011
Volume 105 – Opportunities for Polarized He-3 in RHIC and EIC, September 28-30, 2011 – BNL-96418-2011
Volume 104 – Brookhaven Summer Program on Quarkonium Production in Elementary and Heavy Ion Collisions, June 6-18, 2011 – BNL-96171-2011
Volume 103 – Opportunities for Drell-Yan Physics at RHIC, May 11-13, 2011 – BNL-95236-2011
Volume 102 – Initial State Fluctuations and Final-State Particle Correlations, February 2-4, 2011 – BNL-94704-2011
Volume 101 – RBRC Scientific Review Committee Meeting, October 27-29, 2010 – BNL-94589-2011
Volume 100 – Summer Program on Nucleon Spin Physics, July 14-27, 2010 – BNL-96163-2011
Volume 99 – The Physics of W and Z Bosons, June 24-25, 2010 – BNL-94287-2010
Volume 98 – Saturation, the Color Glass Condensate and the Glasma: What Have We Learned from RHIC? – May 10-12, 2010 – BNL-94271-2010
Volume 97 – RBRC Scientific Review Committee Meeting, October 21-22, 2009 – BNL-90674-2009
Volume 96 – P- and CP-Odd Effects in Hot and Dense Matter, April 26-30, 2010 – BNL-94237-2010
Volume 95 – Progress in High-pT Physics at RHIC, March 17-19, 2010 – BNL-94214-2010
Volume 94 – Summer Program on Nucleon Spin Physics at LBL, June 1-12, 2009
Volume 93 – PHENIX Spinfest School 2009 at BNL - July 1-31, 2009 – BNL-90343-2009

Back to Contents

Link: PHENIXSpinfestSchool2009@BNL

Volume 92 – PKU-RBRC Workshop on Transverse Spin Physics, June 30 - July 4, 2008, Beijing, China – BNL-81685-2008

Volume 91 – RBRC Scientific Review Committee Meeting, November 17-18, 2008 – BNL-81556-2008

Volume 90 – PHENIX Spinfest School 2008 at BNL, August 4-8, 2008 – BNL-81478-2008

Volume 89 – Understanding QGP through Spectral Functions and Euclidean Correlators, April 23-25, 2008 – BNL-81318-2008

Volume 88 – Hydrodynamics in Heavy Ion Collisions and QCD Equation of State, April 21-22, 2008 – BNL-81307-2008

Volume 87 – RBRC Scientific Review Committee Meeting, November 5-6, 2007 – BNL-79570-2007

Volume 86 – Global Analysis of Polarized Parton Distributions in the RHIC Era, October 8, 2007 – BNL-79457-2007

Volume 85 – Parity-Violating Spin Asymmetries at RHIC-BNL, April 26-27, 2007 – BNL-79146-2007

Volume 84 – Domain Wall Fermions at Ten Years, March 15-17, 2007 – BNL 77857-2007

Volume 83 – QCD in Extreme Conditions, July 31 - August 2, 2006 – BNL-76933-2006

Volume 82 – RHIC Physics in the Context of the Standard Model, June 18-23, 2006 – BNL-76863-2006

Volume 81 – Parton Orbital Angular Momentum (Joint RBRC/University of New Mexico Workshop) February 24-26, 2006 – BNL-75937-2006

Volume 80 – Can We Discover the QCD Critical Point at RHIC?, March 9-10, 2006 – BNL-75692-2006

Volume 79 – Strangeness in Collisions, February 16-17, 2006 – BNL-79763-2008

Volume 78 – Heavy Flavor Productions and Hot/Dense Quark Matter, December 12-14, 2005 – BNL-76915-2006

Volume 77 – RBRC Scientific Review Committee Meeting, October 10-12, 2005 – BNL-52649-2005

Volume 76 – Odderon Searches at RHIC, September 27-29, 2005 – BNL-75092-2005

Volume 75 – Single Spin Asymmetries, June 1-3, 2005 – BNL-74717-2005

Volume 74 – RBRC QCDOC Computer Dedication and Symposium on RBRC QCDOC, May 26, 2005 – BNL-74813-2005

Volume 73 – Jet Correlations at RHIC, March 10-11, 2005 – BNL-73910-2005

Volume 72 – RHIC Spin Collaboration Meetings XXXI, XXXII, XXXIII – BNL-73866-2005

Volume 71 – Classical and Quantum Aspects of the Color Glass Condensate – BNL-73793-2005

Volume 70 – Strongly Coupled Plasmas: Electromagnetic, Nuclear & Atomic – BNL-73867-2005

Volume 69 – RBRC Scientific Review Committee Meeting, November 16-17, 2004 – BNL-73546-2004

Volume 68 – Workshop on the Physics Programme of the RBRC and UKQCD QCDOC Machines – BNL-73604-2004

Volume 67 – High Performance Computing with BlueGene/L and QCDOC Architectures, October 27-28, 2004

Volume 66 – RHIC Spin Collaboration Meeting XXIX, Torino Italy – BNL-73534-2004

Volume 65 – RHIC Spin Collaboration Meetings XXVII, XXVIII, XXX – BNL-73506-2004

Volume 64 – Theory Summer Program on RHIC Physics – BNL-73263-2004

Volume 63 – RHIC Spin Collaboration Meetings XXIV, XXV, XXVI – BNL-72397-2004

Volume 62 – New Discoveries at RHIC, May 14-15, 2004 – BNL-72391-2004

Volume 61 – RIKEN-TODAI Mini Workshop on "Topics in Hadron Physics at RHIC", March 23-24, 2004 – BNL-72336-2004

Volume 60 – Lattice QCD at Finite Temperature and Density – BNL-72083-2004

Volume 59 – RHIC Spin Collaboration Meetings XXI, XXII, XXIII – BNL-72382-2004

Volume 58 – RHIC Spin Collaboration Meeting XX – BNL-71900-2004

Volume 57 – High pt Physics at RHIC, December 2-6, 2003 – BNL-72069-2004

Volume 56 – RBRC Scientific Review Committee Meeting, November 20-21, 2003 – BNL-71899-2003

Volume 55 – Collective Flow and QGP Properties – BNL-71898-2003

Volume 54 – RHIC Spin Collaboration Meetings XVII, XVIII, XIX – BNL-71751-2003

Volume 53 – Theory Studies for Polarized pp Scattering – BNL-71747-2003

Volume 52 – RIKEN School on QCD "Topics on the Proton" – BNL-71694-2003

Volume 51 – RHIC Spin Collaboration Meetings XV, XVI – BNL-71539-2003

Volume 50 – High Performance Computing with QCDOC and BlueGene – BNL-71147-2003

Back to Contents

Volume 49 – RBRC Scientific Review Committee Meeting, November 21-22, 2002 – BNL-52679
Volume 48 – RHIC Spin Collaboration Meeting XIV – BNL-71300-2003
Volume 47 – RHIC Spin Collaboration Meetings XII, XIII – BNL-71118-2003
Volume 46 – Large-Scale Computations in Nuclear Physics using the QCDOC – BNL-52678
Volume 45 – Summer Program: Current and Future Directions at RHIC – BNL-71035
Volume 44 – RHIC Spin Collaboration Meetings VIII, IX, X, XI – BNL-71117-2003
Volume 43 – RIKEN Winter School – Quark-Gluon Structure of the Nucleon and QCD – BNL-52672
Volume 42 – Baryon Dynamics at RHIC – BNL-52669
Volume 41 – Hadron Structure from Lattice QCD – BNL-52674
Volume 40 – Theory Studies for RHIC-Spin – BNL-52662
Volume 39 – RHIC Spin Collaboration Meeting VII – BNL-52659
Volume 38 – RBRC Scientific Review Committee Meeting, November 29-30, 2001 – BNL-52649
Volume 37 – RHIC Spin Collaboration Meeting VI (Part 2) – BNL-52660
Volume 36 – RHIC Spin Collaboration Meeting VI – BNL-52642
Volume 35 – RIKEN Winter School – Quarks, Hadrons and Nuclei – QCD Hard Processes and the Nucleon Spin – BNL-52643
Volume 34 – High Energy QCD: Beyond the Pomeron – BNL-52641
Volume 33 – Spin Physics at RHIC in Year-1 and Beyond – BNL-52635
Volume 32 – RHIC Spin Physics V – BNL-52628
Volume 31 – RHIC Spin Physics III & IV Polarized Partons at High Q^2 Region – BNL-52617
Volume 30 – RBRC Scientific Review Committee Meeting, September 28-29, 2000 – BNL-52603
Volume 29 – Future Transversity Measurements – BNL-52612
Volume 28 – Equilibrium & Non-Equilibrium Aspects of Hot, Dense QCD – BNL-52613
Volume 27 – Predictions and Uncertainties for RHIC Spin Physics & Event Generator for RHIC Spin Physics III – Towards Precision Spin Physics at RHIC – BNL-52596
Volume 26 – Circum-Pan-Pacific RIKEN Symposium on High Energy Spin Physics – BNL-52588
Volume 25 – RHIC Spin – BNL-52581
Volume 24 – Physics Society of Japan Biannual Meeting Symposium on QCD Physics at RIKEN BNL Research Center – BNL-52578
Volume 23 – Coulomb and Pion-Asymmetry Polarimetry and Hadronic Spin Dependence at RHIC Energies – BNL-52589
Volume 22 – OSCAR II: Predictions for RHIC – BNL-52591
Volume 21 – RBRC Scientific Review Committee Meeting, May 27-28, 1999 – BNL-52568
Volume 20 – Gauge-Invariant Variables in Gauge Theories – BNL-52590
Volume 19 – Numerical Algorithms at Non-Zero Chemical Potential – BNL-52573
Volume 18 – Event Generator for RHIC Spin Physics – BNL-52571
Volume 17 – Hard Parton Physics in High-Energy Nuclear Collisions – BNL-52574
Volume 16 – RIKEN Winter School - Structure of Hadrons - Introduction to QCD Hard Processes – BNL-52569
Volume 15 – QCD Phase Transitions – BNL-52561
Volume 14 – Quantum Fields In and Out of Equilibrium – BNL-52560
Volume 13 – Physics of the 1 Teraflop RIKEN-BNL-Columbia QCD Project First Anniversary Celebration – BNL-66299
Volume 12 – Quarkonium Production in Relativistic Nuclear Collisions – BNL-52559
Volume 11 – Event Generator for RHIC Spin Physics – BNL-66116
Volume 10 – Physics of Polarimetry at RHIC – BNL-65926
Volume 9 – High Density Matter in AGS, SPS and RHIC Collisions – BNL-65762
Volume 8 – Fermion Frontiers in Vector Lattice Gauge Theories – BNL-65634
Volume 7 – RHIC Spin Physics – BNL-65615

Back to Contents

Volume 6 – Quarks and Gluons in the Nucleon – BNL-65234
Volume 5 – Color Superconductivity, Instantons and Parity (Non?)-Conservation at High Baryon Density – BNL-65105
Volume 4 – Inauguration Ceremony and Non-Equilibrium Many Body Dynamics – BNL-64912
Volume 3 – Hadron Spin-Flip at RHIC Energies – BNL-64724
Volume 2 – Perturbative QCD as a Probe of Hadron Structure – BNL-64723
Volume 1 – Open Standards for Cascade Models for RHIC – BNL-64722

Back to Contents



Li Keran

Nuclei as heavy as bulls
Through collision
Generate new states of matter.
T.D. Lee

©CCASTA

Organizers:
Tuomas Lappi (U. Jyvaskyla)
Vladimir Skokov (RBRC)
Andrey Tarasov (BNL)
Thomas Ullrich (BNL/Yale U)

RIKEN BNL Research Center
Bldg. 510A, Brookhaven National Laboratory
Upton, NY 11973-5000, USA

April 2017